

DISSERTATION ZUR ERLANGUNG DES DOKTORGRADES
DER FAKULTÄT FÜR CHEMIE UND PHARMAZIE
DER LUDWIG-MAXIMILIANS-UNIVERSITÄT MÜNCHEN

NITROGEN-RICH HIGH ENERGY DENSITY MATERIALS

—

SYNTHESIS, CHARACTERIZATION AND TESTING



VORGELEGT VON

NIKO FISCHER

AUS

AUGSBURG

2012

Erklärung

Diese Dissertation wurde im Sinne von § 7 der Promotionsordnung vom 28. November 2011 von Prof. Dr. Thomas M. Klapötke betreut.

Eidesstattliche Versicherung

Diese Dissertation wurde eigenständig und ohne unerlaubte Hilfe erarbeitet.

München,

.....

(Niko Fischer)

Dissertation eingereicht am: 19.11.2012

1. Gutachter Prof. Dr. Thomas M. Klapötke

2. Gutachter Prof. Dr. Konstantin Karaghiosoff

Mündliche Prüfung am: 13.12.2012

DANKSAGUNG

Nicht nur aus obligatorischen Gründen möchte ich an dieser Stelle zuerst meinem Doktorvater Prof. Dr. Thomas M. Klapötke danken. Er hat sich von Anfang an um finanzielle Unterstützung während meiner Zeit im Arbeitskreis gekümmert und sich zu jeder Tages- (und Nacht-)zeit nicht nur einen Moment Zeit genommen für alle möglichen Belange, mit denen er von mir „belästigt“ wurde. Neben der finanziellen Unterstützung hat er durch seine große Kompetenz im Fachgebiet und bei den „public relations“, wie man heutzutage sagen würde, entscheidend zum Gelingen der Arbeit beigetragen und mir unter anderem die Teilnahme an der Gordon Research Konferenz in den USA im Juni 2012 ermöglicht.

Als nächstes möchte ich Prof. Dr. Konstantin Karaghiosoff für die Übernahme der Zweitkorrektur danken. Vielmehr aber hat Conny meinen größten Dank für seine große Unterstützung nicht nur bei NMR und Einkristallstrukturanalyse, viele hilfreiche Diskussionen und einfach dafür, dass er die Gruppe in guten wie in schlechten Zeiten immer zusammengehalten hat und für (fast) jeden Spaß zu haben ist, verdient. Dass der Conny über die Jahre nicht nur ein guter Vorgesetzter sein, sondern auch – was in dieser Konstellation relativ selten ist – zu einem Freund werden würde, war mir spätestens am zweiten Tag meiner Anwesenheit in der Gruppe klar, als ich von ihm mit den Worten „...das mit dem ‚Sie‘, das lassen wir mal!“ empfangen wurde.

Jörg Stierstorfer gilt mein ganz besonderer Dank für eine ganze Reihe von Dingen: Er hat mich von Anfang meiner Diplomarbeit an und während der ganzen Zeit der Promotion im Arbeitskreis mit Rat und Tat, mit bestem Wissen und Gewissen unterstützt und beim Chef wahrscheinlich nicht nur einmal ein gutes Wort für mich eingelegt. Die Einführung in die Kristallstrukturlösung habe ich ihm zu verdanken. Ohne seine Hilfe (speziell quantenchemische Berechnungen) bei den unzähligen Publikationen und sonstigen Arbeiten, seine große Erfahrung und sein Geschick beim Einreichen von Manuskripten wäre es niemals zu der Fülle an bearbeiteten Projekten und veröffentlichten Manuskripten gekommen. Vor allem aber möchte ich ihm Danke sagen für unsere gute Freundschaft, die sich relativ schnell nach meiner Ankunft im AK eingestellt hat und sich über die Jahre nicht nur in einer super Zusammenarbeit, sondern auch außeruniversitär bei allen möglichen Bergtouren und sonstigen „Stories“ manifestiert hat. Ungefähr das gleiche gilt für Karin Lux, die immer die ganz verzweifelten Fälle von Kristallstrukturen noch gemeistert hat und beim Bergsteigen nie „kleinzukriegen“ war, selbst nicht am Watzmann-Mittelgipfel.

Sämtlichen Mitgliedern des AK möchte ich für eine super Zeit während der letzten vier Jahre danken. Wenns auch mal die eine oder andere Reiberei gegeben hat und ich bis jetzt immer noch nicht alle davon überzeugen hab können, dass Aktien Hell das beste Bier der Welt is, is unser AK glaub ich mal eine von den eingeschworenen Truppen am Campus (Zitat Student: „Schau sie an! Jetzt hocken die Klapötkes scho wieder da unten beim saufen...!“). Trotzdem möchte ich noch einige Leute erwähnen, die mir nicht nur aus den im Folgenden erwähnten Gründen besonders ans Herz gewachsen sind: Susanne Scheutzow möchte ich für die Freundschaft danken, für einige Bergtouren, bei denen sie sich fast jedes mal bis zur völligen Erschöpfung verausgabt hat und natürlich für die inzwischen schon fast langjährige „Squashpartnerschaft“. Vera Hartdegen möchte ich für ihre große Kundentreue bei sämtlichen essbaren Produkten, die die Firma Fischer in den letzten Jahren so hervorgebracht hat, bedanken. Andi Eckart (Der E) für die mit lustigsten Schafkopfrunden, die ich erlebt hab und für seine ganze Art, die nicht nur bei mir immer für gute Laune gesorgt hat. Steffi Schönberger möchte ich danken für ihre offene Art und dass sie mich wenigstens ein bissl von meiner schlechten Eigenschaft, vorurteilsbehaftet zu sein, abgebracht hat. Sebastian Rest, der einiges von seiner Zeit in die Vorbereitung und Durchführung von Koenen-Test und high-speed Kameraaufnahmen gesteckt hat sowie Richard Moll, der mich jedesmal vor meinem Computer gerettet hat, wenns mal wieder nötig war, gebührt ordentlicher Dank. Des weiteren möchte ich mich bei Manuel Joas und Dániel Izsák vom Primary Labor zum ersten für die gute Zusammenarbeit bedanken und zum zweiten, dass der Säck jetzt wieder Fleisch isst und der Manu bis ans Ende seiner Tage ein eingefleischter FC Bayern-Hasser bleiben wird („In Giesing da wern die Leut wenigstens no mitm Maßkrug totg’schlagen.“). Unserer AK-Italienerin Camilla Evangelisti danke ich für die Bereitstellung von so manchem kulinarischen Highlight aus Bella Italia. Ein spezieller Gruß und Dank geht natürlich an die „Insassen“ unseres Labors D3.110, das in meinen Augen (die anderen Labore mögens mir verzeihen) auf Grund seiner gepflegten Musikkultur (Bayern 1, 19-20 h, Bayern Plus 16-19 h: Die guat’ Musik) und seiner guten bis sehr guten Atmosphäre (Laborausflug in die Berge, Laborhalbe...wer hat das schon?) und wie manche behaupten auf Grund seiner guten Ergebnisse, immer noch einen gewissen Sonderstatus einnimmt: Bei meinem Bruder Dennis, mit dem man sich auch manchmal lautstark über alles Mögliche streiten kann, bei Franziska Betzler, mit der ich schon „seit dem ersten Semester“ im selben Labor bin, bei Davin Piercey, auch wenn ich seinen Dreck nicht nur im Labor, sondern seit wir zusammen in einer WG

wohnen auch zu Hause wegputzen muss, und natürlich bei unserem Pfleger bayerischer Kultur und Gemütlichkeit, Alex „Aldi“ Dippold.

Einem weiteren Mitglied unserer Führungsriege, Dr. Burkhard Krumm, möchte ich für die wissenschaftliche Assistenz, für die geteilte Leidenschaft für Vulkane – nicht nur beim Lavafischen auf Hawai‘i – und für die abgewickelten Brennholzgeschäfte bedanken.

Eine weitere sehr wichtige Person, die mir durch Messung von Sensitivitäten und Bestellen von Chemikalien auf der einen Seite viel Zeit gespart hat, auf der anderen Seite aber auch durch Aufhalsen von stundenlangen (!) vor- und nachmittäglichen Ratschunden viel Zeit gekostet hat, ist unser CTA Stefan Huber. Huaber, vielen Dank für die aufmunternden Diskussionen (in 5 min vom Inhalt der AC1 Grundvorlesung bis zur Aussage „...die Ramona Leiß is ja so a zamgsoffene Loas, dassd es gar nimmer kennsch...“) und dass man, wenn man irgendwas wissen wollte (was im AK grad so angesagt is), immer zu Dir kommen konnte. Und wir kommen Dich irgendwann daheim besuchen! (Huaber: „Kommen könnts scho, aber aufmachen werd eich koaner!“)

Bei der besten Sekretärin, die ich kenne, Frau Irene Scheckenbach möchte ich mich für ihre Leidenschaft für Katzen, ihre sonstige Tierliebe und Fürsorge um zwei- und vierbeinige Arbeitskreismitglieder bedanken. Frau Scheckenbach hat sich mit größter Sorgfalt und Mühe um sämtliche Belange gekümmert und mich gegen etwaige feindselige Angriffe anderer Sekretärinnen am Department wacker verteidigt (Augschburger halten halt zamm).

Eine ganze Schar von Bachelor- und Forschungs-Praktikanten sowie einen Hiwi, bei denen ich mich bedanken möchte, zähle ich im Folgenden auf: Tobias Fendt, Robert Greiner, Carina Wiedemann, Tobias Stürzer, Fabian Wehnekamp, Andreas Beil, Stefan Hieke, Manuel Boehm, Sebastian Rappenglück, Marius Reymann, Kristina Peters, Katharina Hüll, Li Gao und Stefan Marchner. Ohne ihre Hilfe, ihre Arbeit im Labor wäre das Vorlegen meiner Dissertation in diesem Umfang innerhalb von dreieinhalb Jahren nicht möglich gewesen. Ich möchte mich bei allen für die ausgesprochen gute Atmosphäre während der Zusammenarbeit und die guten Freundschaften, die daraus entstanden sind, herzlich bedanken!

Was Mitarbeiter der Fakultät angeht bin ich den Leuten von der Analytik, speziell Peter Mayer (NMR-Mayer), Herrn Andres and Frau Breitenstein (Massenspektroskopie) und Frau Käser, Herrn Eicher und Frau Sauerer (Elementaranalyse) zu Dank verpflichtet, dass sie aus den (teilweise nicht gekennzeichneten) explosiven Proben, die richtigen Ergebnisse rausgebracht haben. Dem arbeitskreisinternen X-ray-Team, welches mit der Zeit immer

wieder die Besetzung wechselte, möchte ich besonders für die Mühen, vier Jahre lang aus eingetrockneten Mutterlaugen und von ölverschmierten Objektträgern zu jeder Tages- und Nachtzeit unzählige messbare Kristalle isoliert und vermessen zu haben, meinen besonderen Dank aussprechen.

Ansonsten möchte ich mich bei allen, die in sonst irgendeiner Weise zum Gelingen der Arbeit beigetragen haben und die bisher keine Erwähnung gefunden haben, bedanken einschließlich aller Freunde, die mich auf meinem Weg in München bis hierher begleitet haben.

Neben all den Leuten, die ich während meiner Zeit am Campus Großhadern kennengelernt habe, gibts es noch einige Leute, die hier besondere Erwähnung finden sollen. Ich möchte mich bei meinen Eltern Manfred und Elke-Anita und meinen Brüdern Dirk und Dennis aus Augsburg sowie meiner Verwandtschaft Anton, Hildegard und Benedikt Fischer, Dieter, Elisabeth und Bianca Fröschle aus Uttenhofen und Anton und Josefine Fischer aus Dinkelscherben für die geistige und finanzielle Unterstützung nicht nur während der Zeit meiner Promotion sondern auch schon während des Studiums und überhaupt herzlichst bedanken. Bei der Verwandtschaft konnte und kann man zu jeder Tages- und Nachtzeit und in jedem Zustand hereinschneien und ist immer aufs Beste versorgt und unterhalten worden. Bester Dank gilt auch dem Opa (Anton Fischer), der zu Lebzeiten zusätzlich zu seinen Tagesgeschäften noch die halbe Uni mit Fisch (geräucherte Forellen), Fleisch (speziell Spanferkel und Kesselfleisch) und Wurst (zig Weißwurstfrühstücke und Leberkässchen im AK) versorgt hat. Schade, dass er das Ende der Promotion nicht mehr erlebt hat.

Eine spezielle Volksgruppe, nämlich die Einwohner eines kleinen Dorfes im südlichen Pfaffenwinkel (Staltannen) möchte ich an dieser Stelle besonders erwähnen, da sie mich durch eine Einführung in die Landwirtschaft und eine Eingliederung in die bäuerlichen Strukturen in Südbayern vor einer Existenz als Fachidiot seit nunmehr 16 Jahren mehr als nur bewahrt haben.

Unter allen guten Freunden, bei denen ich mich für die gemeinsame bisherige Zeit bedanken will, fällt mir noch einer ein, der mir in München in der Zeit, seit wir uns kennen zum besten Freund hier geworden ist: Steffen Abt. Ohne die ganzen kleineren oder größeren Abenteuer und sonstigen Lausbubeng'schichten, die ich mit Dir schon mitgemacht hab, weiß ich nicht, ob ichs hier in München überhaupt so lang ausgehalten hätte. Vielen Dank einfach für Alles, wesst scho☺!

TABLE OF CONTENTS

INTRODUCTION	1
HISTORY	1
Before WW I	1
WW I – WW II	1
Recent developments	2
CLASSIFICATION	3
Primary explosives	4
Secondary explosives	5
Propellants	7
Pyrotechnics	7
MOTIVATIONS FOR THE DEVELOPMENT OF MODERN EXPLOSIVES	8
Drawbacks of energetic materials in current use	8
Requirements for modern explosives	8
Advantages of nitrogen-rich compounds over carbon based energetic materials	10
The tetrazole heterocycle as a basis for the synthesis of new high energy density materials (HEDMs)	11
METHODS AND OBJECTIVES	12
Requirements for new HEDMs and methods for their evaluation	12
Scope of the dissertation	13
 CONCLUSION	 16
SECONDARY EXPLOSIVES	16
PRIMARY EXPLOSIVES	24
PROPELLANTS	26
PYROTECHNICS	28
DIAZO TRANSFER REAGENTS	29

APPENDIX

1. N. Fischer, T. M. Klapötke, S. Scheutzow, J. Stierstorfer, Hydrazinium 5-Aminotetrazolate: An Insensitive Energetic Material Containing 83.72% Nitrogen, *Cent. Eur. J. Energetic Mater.* **2008**, 5 (3–4), 3–18 32
2. N. Fischer, T. M. Klapötke, J. Stierstorfer, New Nitriminotetrazoles – Synthesis, Structures and Characterization, *Z. Anorg. Allg. Chem.* **2009**, 635, 271–28148
3. N. Fischer, K. Karaghiosoff, T. M. Klapötke, J. Stierstorfer, New Energetic Materials featuring Tetrazoles and Nitramines – Synthesis, Characterization and Properties, *Z. Anorg. Allg. Chem.* **2010**, 636, 735–749 59
4. N. Fischer, T. M. Klapötke, D. Piercey, S. Scheutzow, J. Stierstorfer, Diaminouronium Nitriminotetrazolates – Thermally Stable Explosives, *Z. Anorg. Allg. Chem.* **2010**, 636, 2357–236374
5. N. Fischer, T. M. Klapötke, F. Martin, J. Stierstorfer, Energetic Materials based on 1-amino-3-nitroguanidine, *New Trends in Research of Energetic Materials, Proceedings of the Seminar*, 13th, Pardubice, Czech Republic, **2010**, 1, 113–12981
6. N. Fischer, T. M. Klapötke, J. Stierstorfer, K. R. Tarantik, 1-Nitratoethyl-5-nitriminotetrazole Derivatives - Shaping Future High Explosives, *New Trends in Research of Energetic Materials, Proceedings of the Seminar*, 13th, Pardubice, Czech Republic, **2010**, 2, 455–467 98
7. N. Fischer, T. M. Klapötke, J. Stierstorfer, Salts of 2-methyl-5-nitraminotetrazole, *New Trends in Research of Energetic Materials, Proceedings of the Seminar*, 13th, Pardubice, Czech Republic, **2010**, 2, 684–698111

8. T. Fendt, N. Fischer, T. M. Klapötke, J. Stierstorfer, N-Rich Salts of 2-Methyl-5-nitraminotetrazole: Secondary Explosives with Low Sensitivities, *Inorg. Chem.* **2011**, *50*, 1447–1458126
9. N. Fischer, T. M. Klapötke, J. Stierstorfer, Calcium 5-Nitriminotetrazolate – A Green Replacement for Lead Azide in Priming Charges, *J. Energetic Mater.* **2011**, *29(1)*, 61–74 138
10. N. Fischer, T. M. Klapötke, J. Stierstorfer, Energetic Nitrogen-Rich Salts of 1-(2-Hydroxyethyl)-5-nitriminotetrazole, *Eur. J. Inorg. Chem.* **2011**, 4471–4480152
11. N. Fischer, T. M. Klapötke, J. Stierstorfer, Explosives Based on Diaminourea, *Propellants Explos. Pyrotech.* **2011**, *36*, 225–232162
12. N. Fischer, T. M. Klapötke, J. Stierstorfer, Hydrazinium Nitriminotetrazolates, *Z. Anorg. Allg. Chem.* **2011**, *637*, 1273–1276170
13. N. Fischer, T. M. Klapötke, Kristina Peters, Magdalena Rusan, J. Stierstorfer, Alkaline Earth Metal Salts of 5,5'-Bistetrazole – from Academical Interest to Practical Application, *Z. Anorg. Allg. Chem.* **2011**, *637*, 1693–1701174
14. N. Fischer, T. M. Klapötke, J. Stierstorfer, C. Wiedemann, 1-Nitratoethyl-5-nitriminotetrazole derivatives – Shaping future high explosives, *Polyhedron* **2011**, *30(14)*, 2374–2386 183
15. N. Fischer, T. M. Klapötke, J. Stierstorfer, The Hydroxylammonium Cation in Tetrazole based Energetic Materials, *New Trends in Research of Energetic Materials, Proceedings of the Seminar*, 14th, Pardubice, Czech Republic **2011**, *1*, 128–156196

16.	M. Boehm, D. Fischer, N. Fischer, T. M. Klapötke, S. Scheutzow, J. Stierstorfer, Experimentally determined Detonation Velocities of new Secondary Explosives, <i>New Trends in Research of Energetic Materials, Proceedings of the Seminar</i> , 14 th , Pardubice, Czech Republic 2011 , 2, 513–521	225
17.	N. Fischer, T. M. Klapötke, J. Stierstorfer, E. N. Wiedemann, Highly sensitive 3,5-Diazidotriazole and the binary C ₂ N ₉ ⁻ -anion, <i>New Trends in Research of Energetic Materials, Proceedings of the Seminar</i> , 14 th , Pardubice, Czech Republic 2011 , 2, 637–645	234
18.	N. Fischer, D. Izsák, T. M. Klapötke, S. Rappenglück, J. Stierstorfer, Nitrogen-Rich 5,5'-Bistetrazolates and their Potential Use in Propellant Systems: A Comprehensive Study, <i>Chem. Eur. J.</i> 2012 , 18(13), 4051–4062	244
19.	N. Fischer, T. M. Klapötke, D. Piercey, J. Stierstorfer, Hydroxylammonium 5-Nitriminotetrazolates, <i>Z. Anorg. Allg. Chem.</i> 2012 , 638, 302–310	256
20.	N. Fischer, E. D. Goddard-Borger, R. Greiner, T. M. Klapötke, B. W. Skelton, J. Stierstorfer, Sensitivities of Some Imidazole-1-sulfonyl Azide Salts, <i>J. Org. Chem.</i> 2012 , 77, 1760–1764	265
21.	N. Fischer, K. Hüll, T. M. Klapötke, J. Stierstorfer, G. Laus, M. Hummel, C. Froschauer, K. Wurst, H. Schottenberger, 5,5'-Azoxytetrazolates – a new nitrogen-rich dianion and its comparison to 5,5'-azotetrazolate, <i>Dalton Trans.</i> 2012 , 41(36), 11201–11211	270
22.	N. Fischer, D. Fischer, T. M. Klapötke, D. G. Piercey, J. Stierstorfer, Pushing the limits of energetic materials – the synthesis and characterization of dihydroxylammonium 5,5'-bistetrazole-1,1'-diolate, <i>J. Mater. Chem.</i> 2012 , 22, 20418–20422	281

23. N. Fischer, T. M. Klapötke, J. Stierstorfer, 1-Amino-3-nitroguanidine (ANQ) in High-performance Ionic Energetic Materials, *Z. Naturforsch. B* **2012**, 67(6), 573—588 286
24. N. Fischer, T. M. Klapötke, J. Stierstorfer, V. Kahlenberg, G. Laus, H. Schottenberger, K. Wurst, Synthesis and Crystal Structures of New 5,5'-azotetrazolates, *Crystals* **2012**, 2, 127–136302
25. N. Fischer, T. M. Klapötke, K. Lux, F. A. Martin, J. Stierstorfer, Inorganic Amino-Nitro-Guanidinium Derivatives, *Crystals* **2012**, 2, 675–689312
26. N. Fischer, T. M. Klapötke, J. Stierstorfer, TKX50 – The revolution in RDX Replacements, *New Trends in Research of Energetic Materials, Proceedings of the Seminar*, 15th, Pardubice, Czech Republic **2012**, 1, 130–141 327
27. N. Fischer, T. M. Klapötke, S. Rappenglück, J. Stierstorfer, The Reactivity of 5-Cyanotetrazole towards Water and Hydroxylamine, *Chempluschem* **2012**, 77(10), 877–888 339
28. N. Fischer, K. Hüll, T. M. Klapötke, J. Stierstorfer, Synthesis and Characterization of the New Heterocycle 5-(4-Amino-1,2,4-triazol-3-on-5'-yl)-1*H*-tetrazole and Some Ionic Nitrogen-rich Derivatives, *J. Heterocycl. Chem.* **2012**, in press 351
29. N. Fischer, T. M. Klapötke, M. Reymann, J. Stierstorfer, Nitrogen-Rich Salts of 5,5'-Bis(1-hydroxytetrazole) – Energetic Materials Combining Low Sensitivities with High Thermal Stability, *Eur. J. Inorg. Chem.* **2012**, in press362
30. N. Fischer, M. Joas, T. M. Klapötke, J. Stierstorfer, T. Stürzer, Transition metal complexes of 3-amino-1-nitroguanidine as laser ignitable primary explosives – structures and properties, *Inorg. Chem.* **2012**, submitted378

31.	N. Fischer, L. Gao, T. M. Klapötke, J. Stierstorfer, Energetic Salts of 5,5'-Bis(2-hydroxytetrazole) in a Comparison to 5,5'-Bis(1-hydroxytetrazole) Derivatives, <i>Polyhedron</i> 2012 , submitted	405
32.	N. Fischer, T. M. Klapötke, S. Marchner, M. Reymann, M. Rusan, S. Scheutzow, J. Stierstorfer, A Selection of Alkali and Alkaline Earth Metal Salts of 5,5'-Bis(1-hydroxytetrazole) in Pyrotechnic Compositions, <i>Propellants Explos. Pyrotech.</i> 2012 , in press	425
	BIBLIOGRAPHY	437

Für meinen Großvater Anton Fischer

INTRODUCTION

HISTORY

Before WW I

Due to their more or less controllable release of energy in various forms, energetic materials themselves as well as their utilization for military and civil operations have always attracted peoples interest since the discovery of the first energetic composition, which happened to be the accidental invention of black powder by Chinese alchemists as early as 220 BC. Apart from this invention – the knowledge about the mentioned composition of 75 % potassium nitrate, 10 % sulfur and 15 % charcoal did not make its way to Europe until the middle ages – blackpowder was independently found by the German monk Berthold Schwartz in 1320, who also studied its energetic properties. The upcoming industrial revolution in the middle of the 19th century, which involved difficult mining and tunneling operations, however, necessitated the use of a more powerful explosive, which was found by the invention of nitroglycerin. Although the name of Alfred Nobel to most of the people is principally associated with nitroglycerin, it was discovered by an Italian, Ascanio Sobrero, in 1846. The main advantage of nitroglycerin over blackpowder is the combination of the oxidizer and the fuel in the same molecule, causing its superior explosive performance. After the repeated occurrence of severe explosions during its manufacturing – amongst others, Alfred Nobel's brother Emil was killed in 1864 – safety aspects of explosives were more and more discussed leading to the invention of "guhr dynamite", a mixture of nitroglycerin with an absorbant clay, "Kieselguhr", in 1867. Further improvements were made by mixing nitroglycerin (NG) with nitrocellulose (NC), a nitrate ester of cellulose, which was discovered at about the same time as nitroglycerine, to form a gel named gelatine dynamite.

WW I – WW II

The growing use of explosives in coal mining still brought a corresponding increase on the number of gas and dust explosions with appalling casualty totals mandating replacement of the used explosives, which led to the discovery of modern explosives such as picric acid or TNT. While picric acid was suffering from substantial drawbacks like the formation of highly sensitive heavy metal picrates in shells – picric acid is a comparatively corrosive acid – TNT, which was firstly prepared by Wilbrand in 1863, was safer to handle, replaced picric acid and became the standard explosive for all armies during World War I by 1914. Furthermore, nitroguanidine (NQ), which was first prepared by Jouselin in 1877, was used during WW I in a mixture with NC as flashless propellant. However, storage problems based on decomposition of the mixture also ruled out the further use of this composition and led to the inauguration of major research programs after WW I to find new, more powerful explosives. The search resulted in the investigation of the explosive performances of PETN (pentaerythritol tetranitrate) and RDX (1,3,5-trinitro-1,3,5-triazacyclohexane) both of which were already known compounds firstly prepared at the end of the 19th century for medicinal purposes. PETN was less used in WW II than RDX because of its high sensitivities and poor

chemical stability. The sensitivity problem of PETN therefore was overcome by mixing it with 50 w-% TNT (Pentolite), which noticeably decreased the explosive performance.

Recent developments

For decades before RDX became a standard explosive in WW II, it could not be produced on a larger scale due to the lack of an inexpensive and attractive synthetic procedure. However, no substantial improvements were made in the manufacture of RDX until 1940, when Bachmann developed a process for the synthesis with the greatest yield. Bachmann's product was known as Type B RDX containing a constant impurity level of 8-12%. After discovering the chemical nature and the explosive properties of this impurity, the new, better performing high explosive, HMX (1,3,5,7-tetranitro-1,3,5,7-tetraazacyclooctane) was developed, which was available since the end of WW II. In 1952 a mixture called "Octol", consisting of 75 % HMX and 25 % TNT was developed, which again shows the need of desensitization of the newly developed explosives. Another approach to make the handling of these materials safer, is embedding the crystalline materials into a rubber-like polymeric matrix, resulting in the development of so called polymer bound explosives (PBX). They mainly contain HMX, which was plasticized using Teflon as the binder in the 1960s, but also RDX and/or PETN containing mixtures using styrene and butadiene based binder systems have been developed and are known as "Semtex". While in the beginnings inert, non-energetic binders such as polystyrene were used, the trend was to replace inert binders by energetic binders, which in most cases are based on covalent azides or nitrates as for instance GAP (glycidyl azide polymer) or polyGLYN (Poly(glycidyl nitrate)). Later, the use of plasticizers as e. g. NENAs (alkylated nitrateethyl nitramines) for PBX was introduced based on the findings, that PBXs containing energetic binders are more sensitive to impact compared to traditional explosive compositions. The addition of plasticizers has reduced the sensitivity of PBXs whilst improving its processability and mechanical properties. The most recent developments in energetic materials concentrate on the synthesis of compounds with either outstanding thermal or mechanical stability or a very high explosive performance. Examples of highly thermal materials are HNS (hexanitrostilbene), which was produced by Shipp in 1966 or TATB (1,3,5-trinitro-2,4,6-triaminobenzene) (Adkins and Norris, 1978), the later of which additional to being highly thermally stable also shows very low sensitivities. Another example of a highly energetic compound with low sensitivities, which shows autocatalytic behavior during decomposition, was first reported in 1905 as NTO (5-nitro-1,2,4-triazole-3-one), but it was not until 1987, that Lee, Chapman and Coburn reported its explosive properties. Trends in the development of highly energetic materials in the late 20th century have seen the isolation and explosive characterization of highly cage strained nitro- and nitramino-substituted molecules such as CL-20 (2,4,6,8,10,12-hexanitro-2,4,6,8,10,12-hexaazaisowurtzitane, HNIW), which was found by Arnie Nielsen in 1987 or ONC (octanitrocubane), developed by Eaton and co-workers in 1997. The research into energetic materials, which, based on a high hydrogen to carbon atom ratio, release a large amount of gas per mass unit led to molecular structures like HNF (hydrazinium nitroformate), which was mainly developed in The Netherlands, or ADN, the majority of research of which has taken place in Russia, the USA and Sweden. Since it has a high oxygen content, ADN is a promising, chlorine free replacement for ammonium

perchlorate as an oxidizer in composite propellants. Figure 1 shows a selection of modern explosives introduced in the last section.

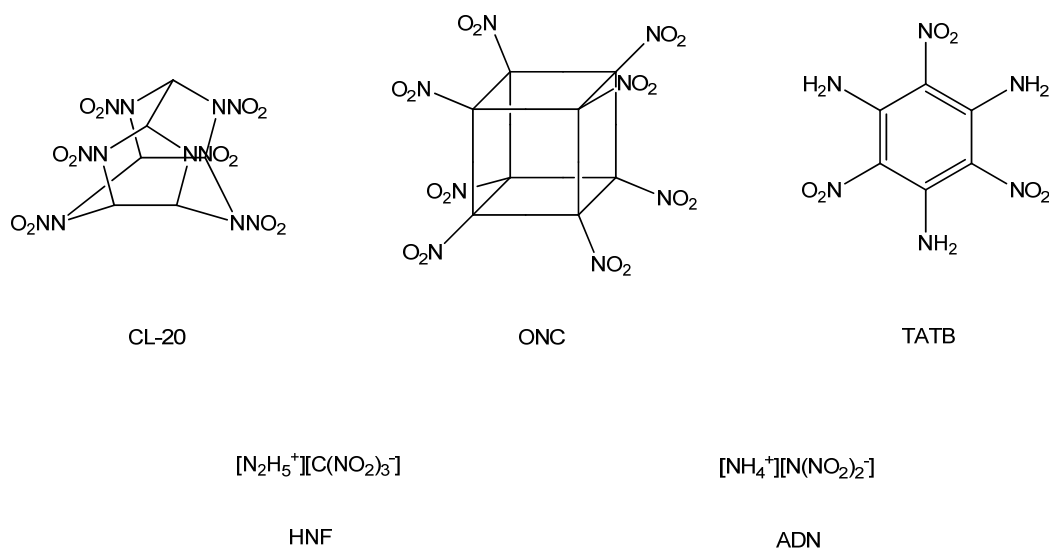


Figure 1. Examples of modern energetic materials: 2,4,6,8,10,12-hexanitro-2,4,6,8,10,12-hexaazaisowurtzitane (CL-20), octanitrocubane (ONC), 1,3,5-trinitro-2,4,6-triaminobenzene (TATB), hydrazinium nitroformate (HNF) and ammonium dinitramide (ADN)

CLASSIFICATION

If the entirety of energetic materials has to be classified, firstly there is the question, on which basis we want to separate them into various classes. Energetic materials have been classified by many chemists throughout the 20th century. One systematic approach to the relationship between the explosive properties and the chemical nature of various compounds was undertaken by Plets in 1953, who classified materials upon the presence of definite structural groupings such as peroxides and ozonides, chlorates and perchlorates, nitro- and nitrato-moieties, azides and azo-bridges, fulminates or acetylenes and acetylides. However, this classification does not give any information on the explosive performance or behavior of a compound, so that nowadays the classification based on performance and uses of materials is practiced. According to this way of classification, there are primary explosives, secondary explosives for both civil and military applications, propellants and pyrotechnics, whereas propellants itself can be separated into propellant charges and rocket propellants (figure 2). Also there is a vast variety of different applications for pyrotechnic mixtures, which will be discussed later on.

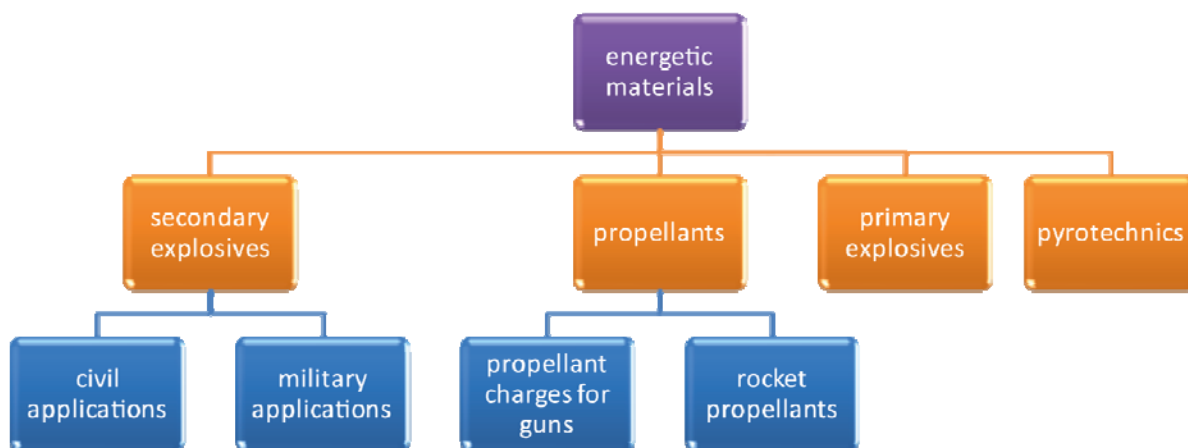


Figure 2. *Classification of energetic materials based on their performance and use*

Primary Explosives

Primary explosives, unlike secondary explosives, detonate when they are subjected to heat and shock and since they are producing a shockwave, they are used to set off the less sensitive charge (main charge, secondary explosive) of an explosive device. They undergo a very fast deflagration to detonation transition (DDT) and are therefore used in initiating devices. Primary explosives have a high degree of sensitivity towards shock, friction, electrostatic discharge or thermal stress and explode whether they are confined or unconfined. To test the behaviour of a material upon thermal stress, the “hot needle test” can be applied. Here, the material is fixed on a solid surface by means of an adhesive tape and slightly compressed. Melting through the adhesive tape with a very hot needle results in a detonation of the sample, if it can be classified as a real primary explosive. Although their decomposition is highly exothermic as exemplified by the decomposition of lead azide, $\text{Pb}(\text{N}_3)_2$, to one mole equivalent of elemental lead (Pb) and three mole equivalents of gaseous dinitrogen (N_2), their detonation velocities are comparatively low in a typical range of $3500\text{--}5500\text{ ms}^{-1}$. However, if a newly developed material is sufficiently sensitive towards impact and/or friction, it may also be regarded as a primary explosive, even if a detonation velocity of more than 5500 m s^{-1} or no deflagration to detonation transition in the unconfined state is observed. Typical primary explosives, that are widely used include the mentioned lead azide (LA) as well as lead styphnate (LS), 5,7-dinitro-[2,1,3]-benzoxadiazol-4-olate 3-oxide potassium salt (KDNP) or the lesser used mercury fulminate (MF) (figure 3).

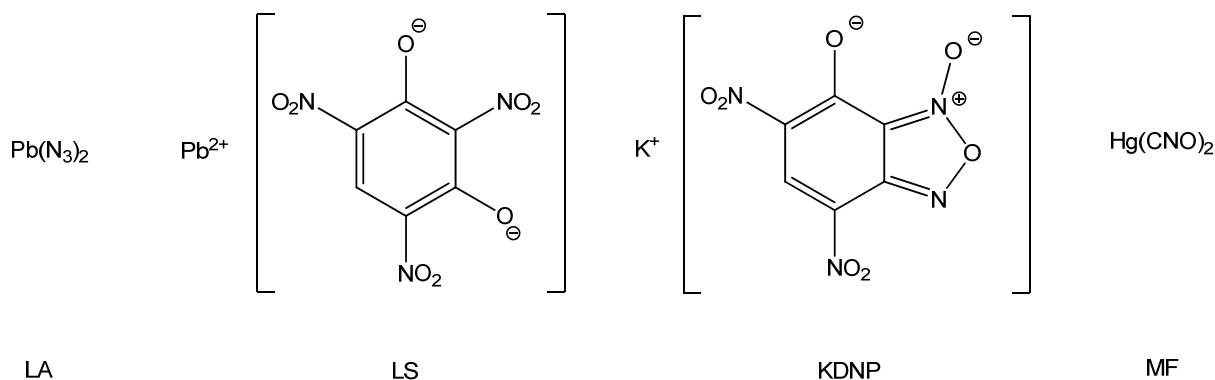


Figure 3. Formerly and recently used primary explosives: Lead azide (LA), lead styphnate (LS), 5,7-dinitro-[2,1,3]-benzoxadiazol-4-olate 3-oxide potassium salt (KDNP) and mercury fulminate (MF)

Secondary Explosives

Secondary explosives differ from primary explosives in that they cannot be detonated readily but need the shockwave produced by a primary explosive to be initiated. Generally speaking, secondary explosives are less sensitive and have detonation velocities of around 5500 ms^{-1} up into the vicinity of $10'000 \text{ ms}^{-1}$. After initiation, the secondary explosive almost instantaneously dissociates into atoms, which recombine to lower heat of formation products like N_2 , CO , CO_2 , H_2O and H_2 evolving a considerable amount of gas. This process generates a shockwave of high brisance, which promotes the reaction front through the unreacted material before the pressure of the exerted gas takes its effect to the environment. Examples for widely known and commonly used secondary explosives are TNT, RDX, HMX, NG, NC and NQ (figure 4).

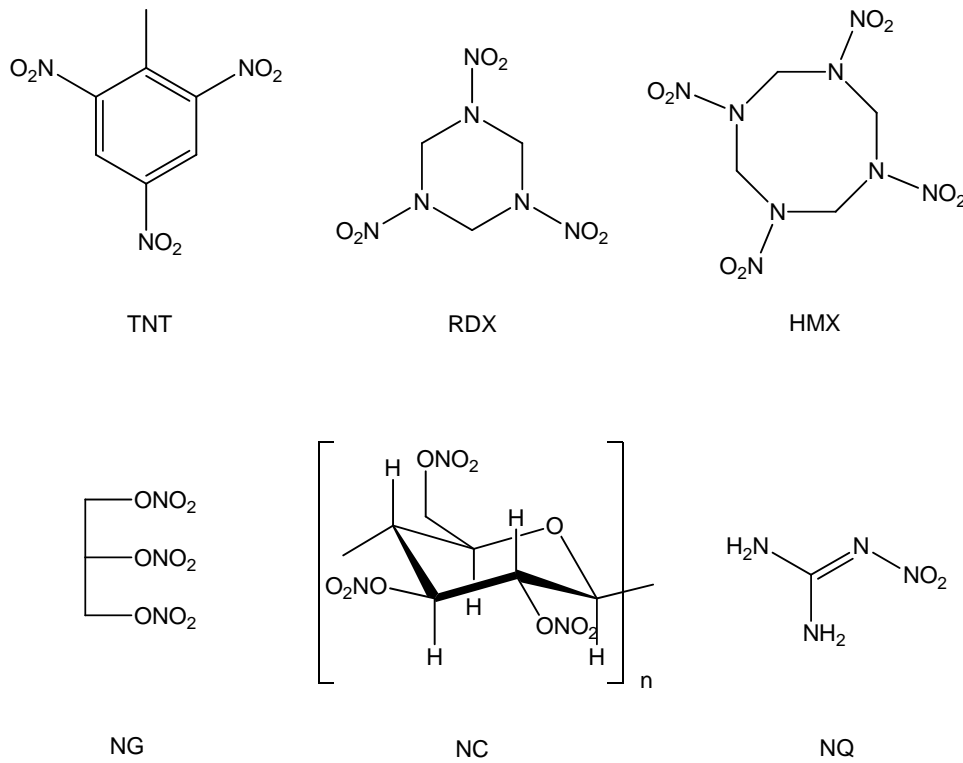


Figure 4. Commonly used secondary explosives: 2,4,6-trinitrotoluene (TNT), 1,3,5-trinitro-1,3,5-triazacyclohexane (RDX), 1,3,5,7-tetranitro-1,3,5,7-tetraazacyclooctane (HMX), nitroglycerin (NG), nitrocellulose (NC) and nitroguanidine (NQ).

Important parameters for the characterization of a secondary explosive are its detonation velocity (D), detonation pressure (P) and heat of explosion (Q) besides the less important parameters of the explosion temperature (T) and the volume of gas released per kg of explosive (V). The performance of an explosive therefore cannot be described by only one parameter. A further important term for the characterization of a charge is the brisance (B), which describes the destructive fragmentation effect on its immediate vicinity. The brisance B depends on the loading density (ρ) of the charge, the specific energy (F) and the detonation velocity (D):

$$B = \rho F D \quad (1)$$

Here, the specific energy of an explosive can be calculated according to the general equation of state for gases:

$$F = p_e V = n R T \quad (2)$$

p_e is the maximum pressure through the explosion, V is the volume of detonation gases, n is the number of moles of gas formed by the explosion per kg of explosive R is the gas constant and T is the temperature of explosion. In contrast to secondary explosives, the specific energy of propellant charges is lower due to a lower combustion temperature, which is desirable to avoid gun barrel erosion.

Propellants

Generally, the largest difference between primary or secondary explosives and propellants is, that propellants only burn, they do not explode. Basically there are two main classes of propellants, which are propellant charges and rocket propellants. Propellant charges can be either single base propellants based on NC, which are used in weapons from pistols to artillery weapons, or the better performing double-base propellant charges, mainly used in pistols and mortars. The disadvantage of double-base formulations containing NC and NG is their high combustion temperature, which leads to enhanced gun barrel erosion and the possible appearance of a muzzle flash after partial explosion of the combustion gases upon contact with air. To overcome the mentioned problems, triple-based formulations (NC+NG+NQ) are used, particularly in large caliber tanks and NAVY weapons, however, the performance of a triple-base powder does not reach that of a double base powder. The second main class of propellants are rocket propellants. Compared to the above introduced propellant charges, rocket propellants have lower burning rates. The most important parameter for the characterization of rocket propellants is the specific impulse I_{sp} , which is the change of the impulse per mass unit of the propellant. It shows the effective velocity of the combustion gases when leaving the nozzle. Generally, two types of rocket propellants, solid and liquid propellants, can be distinguished. Solid propellants can be either double-base propellants, which are based on NC/NG or composite propellants, where a crystalline oxidizer (e.g. ammonium perchlorate) is embedded in a polymeric binder matrix (e.g. hydroxy-terminated polybutadiene, HTPB, polymerized with a diisocyanate) which contains the propellant fuel (e.g. Al). Liquid rocket propellants themselves can also be categorized into mono- and bipropellants depending on the number of ingredients used. Monopropellants necessarily need to be endothermic compounds, which decompose to deliver the required thrust in the absence of oxygen. An example is the decomposition of hydrazine N_2H_4 into one mole equivalent of dinitrogen N_2 and two mole equivalents of dihydrogen H_2 . Other monopropellants used are hydrogen peroxide, isopropyl nitrate or nitromethane. However, the energy content and the specific impulse of monopropellants is relatively small, so that they are only used in small missiles or small satellites. Bipropellants consist of an oxidizer and a fuel, which are stored in separated tanks. If combining the two liquids results in self ignition within 20 ms, the mixture is called hypergolic, whereas non-hypergolic mixtures need to be ignited first. The advantages of hypergolic mixtures such as the system MMH (monomethylhydrazine) and HNO_3/N_2O_4 , which practically is the only hypergolic propellant system used today, is that the ignition definitely occurs, which is important for weapon systems such as intercontinental rockets or the reignition of upper stages of launch vehicles in space, and a once ignited combustion can easily be interrupted by turning off the supply of one the components.

Pyrotechnics

The last field of energetic materials to be categorized are pyrotechnics, which are solid mixtures containing the oxidizer and a fuel, beside, depending on the intended use, a binder, a propellant charge, a colorant as well as smoke or noise generating additives. Regarding their reaction speeds, pyrotechnics are located between explosives, which reveal the highest reaction speeds, and propellants. They can be used as either heat generating, smoke

generating or light generating pyrotechnics, whereas the entire electromagnetic spectrum reaching from IR to near UV-Vis can be covered depending on its composition. Commonly used oxidizers are nitrates, perchlorates or chromates, whereas metals such as magnesium, boron or silicon serve as fuel. Coloring agents like barium or lithium and strontium salts for green and red light emission respectively, can be added for mixtures emitting in the visible range of the electromagnetic spectrum. For the development of night vision devices new pyrotechnic formulations emitting in the near infrared (NIR) region of the electromagnetic spectrum are of major interest. The mainly used spectral region for night vision detection is in the range of 700 to 1000 nm. NIR pyrotechnics find therefore application in clandestine night operations and are used for instance as hand-held signal flares or parachute flares to illuminate large areas or aiding in emergency landings of aircrafts. IR illuminants are specified by radiometric measurements, whereas the most important parameters are the radiant intensity and the concealment index, which give information about the quantity of emitted light as well as its spectral purity.

MOTIVATIONS FOR THE DEVELOPMENT OF MODERN EXPLOSIVES

Drawbacks of energetic materials in current use

Many of the energetic materials, primary as well as secondary explosives, pyrotechnics or propellants, which are in use today, suffer from manifold drawbacks, such as high toxicity or high sensitivity, which makes intensive research in possible replacements necessary, like several examples show. Primary explosives such as the widely used lead azide, are based on heavy metals bearing energetic counterions. Lead as well as cadmium or mercury all are highly toxic to the human as well as other organisms by complexing and/or inhibiting vital enzymes causing multiple disfunction of organs. Therefore, heavy metal free primary explosives based on other metals such as zinc or iron, or even metal-free compounds are of major interest. Also in the field of secondary explosives widely used RDX reveals hazards like the toxicity for plants, microorganisms and microbes of the explosive itself as well as of its degradation and decomposition products, which contain nitramines and nitrosamines. RDX itself is toxic to organisms at the base of the food chain such as earthworms and also TNT and its degradation products are ecologically toxic. The use of barium salts as colorants in pyrotechnic mixtures needs to be banned due to its toxicity to the nervous system. Pyrotechnical mixtures moreover oftentimes contain perchlorates as oxidizers. Perchlorate has an ionic radius similar to that of the iodide anion causing an inhibition of the iodide storage in the thyroid gland and a resulting decrease of thyroxine synthesis. For the same reason, perchlorate also needs to be replaced from rocket propellants, where it is used as the oxidizer in composite propellants. Further its chlorine containing decomposition products (mainly HCl) hold considerable contribution to ozone depletion if released in the upper atmosphere, where they cannot be washed out by precipitation.

Requirements for modern explosives

Beside the toxicity of energetic materials in current use, which has been shown in a couple of examples, the high sensitivity of many materials certainly is a major concern which shows the

need to develop and synthesize safer alternatives not only for this reason. The disposal of unreacted energetic material (UXOs = unexploded ordnance) in recent times plays a more and more important role. Safer and less toxic energetic materials will help to minimize the ecological risks as well as the risks to human life when disposing of UXOs. The historical disposal of waste explosive compositions by dumping them into the sea was banned by the United Nations in 1994 and due to an increase in environmental awareness, also burning or detonating them in an open bonfire will soon be banned since it is environmentally unacceptable. Next to the mentioned ecotoxicological and sensitivity concerns, improved physicochemical properties of newly developed energetic materials are desired, which are detonation parameters and stabilities exceeding those of commonly used RDX next to a variety of chemical properties. The detonation velocity should exceed 9000 ms^{-1} and the detonation pressure should be higher than 380 kbar. The heat of explosion found for RDX is roughly 6200 kJ kg^{-1} , which also needs to be outperformed. The thermal stability of a newly synthesized material should exceed 180°C , which also makes sure, that a shell sitting in the direct sun at high air temperatures can still securely be handled. Beside that, a high long term thermal stability is required for the safe storage of explosives even at elevated temperatures without decomposition of the energetic material. The sensitivities towards outer stimuli, which are impact, friction and electrostatic discharge of the benchmark RDX are 7 J (IS), 120 N (FS) and 0.20 J (ESD). For a safe synthesis, handling and disposal of energetic materials, higher values for all sensitivities are wanted. The required properties for new energetic materials as RDX replacements are summarized in table 1.

Table 1. *Desired properties of new nitrogen-rich highly energetic compounds*

performance	detonation velocity detonation pressure heat of explosion	$D > 9000 \text{ m s}^{-1}$ $P > 380 \text{ kbar}$ $Q > 6200 \text{ kJ kg}^{-1}$
stability	thermal stability impact sensitivity friction sensitivity electrostatic sensitivity	$T_{\text{dec.}} \geq 180^\circ\text{C}$ $IS > 7 \text{ J}$ $FS > 120 \text{ N}$ $ESD > 0.2 \text{ J}$
chemicall properties	hydrolytically stable, compatible with binder and plasticizer, low water solubility ^a (or non-toxic), smoke-free combustion, long-term stable (> 15 years under normal conditions)	

^a low octanol-water partition coefficient

Unfortunately for newly synthesized energetic materials oftentimes a mutual exclusivity of high performance and low sensitivities is observed, which means that high performing compounds are often unstable and insensitive materials have a low detonation performance. This makes the development of acceptable replacements for commonly used explosives a great challenge especially if considering, that a low budget large scale industrial synthesis, which oftentimes cannot be examined on a laboratory scale, is desired. Next to a high performance and a low sensitivity, a newly synthesized material should be hydrolytically stable, so that it does not need to be stored under anhydrous conditions to prevent

decomposition upon contact with moisture, which also involves its long-term stability under normal conditions (>15 years). The compatibility with binder systems and plasticizers needs to be proved in order to assess its suitability in formulations. To avoid contamination of ground water, a very low water solubility is required, as exemplified by a high octanol-water partition coefficient. Last but not least, the material ideally combusts smoke free to keep the signature of its decomposition products as low as possible.

Advantages of nitrogen-rich compounds over carbon based energetic materials

Most of the currently used high explosives such as TNT, RDX or HMX derive most of their energy from the oxidation of their carbon backbone to CO and CO₂ respectively. Modern developments as exemplified in the synthesis of CL-20 additionally utilize the release of a considerable amount of energy from their ring or cage strain, when decomposing into low heat of formation products such as CO₂ and H₂O. Due to increasing environmental concerns, a rethinking in the last decades, however, made the development of energetic materials based on nitrogen-rich compounds more and more popular since they mainly decompose into environmentally benign N₂. Unlike caged and cyclic nitramines, nitrogen-rich materials derive their energy from the formation of the highly stable N–N-triple bond after decomposition since they contain a large number of inherently energetic N–N-single and N=N-double bonds. The extraordinary stability of the N₂ molecule and therefore the high enthalpies of formation of high nitrogen compounds can be explained after looking at the average element-element bond energies per 2-electron bond between single, double and triple bonded carbon, nitrogen or oxygen atoms (figure 5). While the average bond energies per 2-electron bond for a C–C bond decrease with increasing bond order, the energies for a N–N-bond increase.

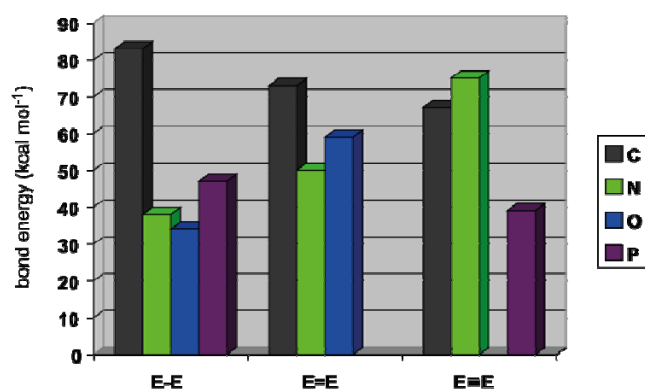


Figure 5. Average element-element bond energies per 2-electron bond (in kcal mol⁻¹)

This means, that the overall bond energy for a N–N bond increases disproportionately high compared to the bond order, while for a C–C-bond it increases disproportionately low. A C–C-triple bond therefore does not reveal a bond energy, which is three times as high as for a C–C-single bond, whereas for nitrogen it is more than three times as high (figure 6).

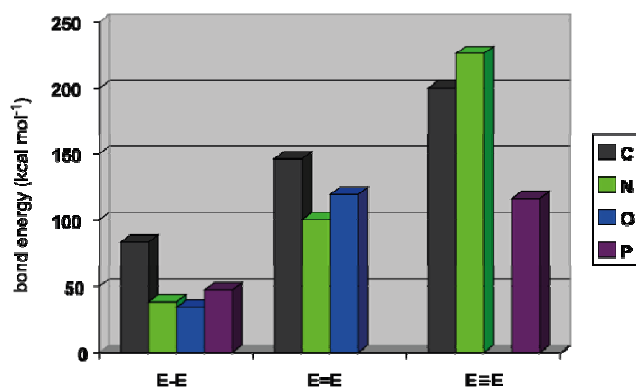


Figure 6. Bond energies for C–C, N–N, O–O and P–P single, double and triple bonds (in kcal mol⁻¹)

The reason for the particular stability of the N–N-triple bond in comparison to carbon can be found in the small size of the N atoms, resulting in a better overlapping of orbitals, and also as a result of the different hybridization of N and C in N₂ in comparison with HCCH, in which the N–N σ -bond in N₂ has a considerably higher p-character than the C–C-bond in acetylene does.

The tetrazole heterocycle as a basis for the synthesis of new new high energy density materials (HEDMs)

The search for new compounds with a high nitrogen content certainly cannot end at all-nitrogen compounds (N = 100%), since N₂ is the only all-nitrogen compound (known today), which is stable under normal conditions (1 atm, 298 K). The formation of open chain molecules with a large number of N–N single and double bonds, however is thermodynamically not favorable, so that an additional stabilization is needed, which can be found in the formation of a π -electronic system. Therefore, nitrogen-rich azoles such as triazoles, tetrazoles and pentazoles come into consideration. While triazoles, due to their lower nitrogen content reveal lower heats of formation and pentazoles are kinetically too labile and have to be stabilized by bulky substituents, which again decrease their nitrogen-content, the tetrazole heterocycle occupies the middleground of the stability versus high performance continuum due to their endothermicity and kinetic stability. Additionally, the ring strain of the heterocycle contributes to the high heat of formation of tetrazole based energetic materials. The carbon atom at position 5 ensures the tailorability with energetic substituents such as –NO₂, =N–NO₂ or other tetrazole cycles. Oxygen containing substituents improve the oxygen balance Ω of the compound, which is a percentage representation of a compound's ability to oxidize all carbon and hydrogen in the molecule to carbon dioxide and water, respectively without using outer oxygen sources. When an oxygen balance is at or near zero, explosive performances are high, however significant deviation into either a negative (fuel rich) or positive (oxygen rich) oxygen balance leads to a loss of performance. The high nitrogen content of tetrazole based high compounds, beside being environmentally friendly through the release of molecular dinitrogen, also is a desirable feature in the gun propellant sector. The use of propellant charges with high carbon contents leads to increased gun barrel erosion due to the formation of iron carbide especially if compositions with high combustion temperatures are used. The research for new propellant charges is therefore focused on

materials, which burn with lower temperatures and have a highest possible N_2/CO ratio of their combustion gases, since the iron nitride, which is formed on the inner surface of the gun barrel has a higher melting point compared to iron carbide and therefore builds a protective layer, which helps to increase the life span of the used facilities. The requirement of a high thermal stability of new energetic materials can be fulfilled by tetrazole based compounds, since they are stabilized by their π -electronic system. Additional thermostability can be achieved by the formation of ionic compounds, which in the case of tetrazoles can be reached after abstraction of the proton(s), the acidity of which depends on the substituents on the tetrazole ring, but in most of the cases is sufficiently high enough to be abstracted with nitrogen-rich bases such as guanidine derivatives. The formation of ionic compounds also increases the density of the energetic material due to the presence of ionic attractive forces in the solid state. A high density beside a high positive heat of formation and an oxygen balance close to zero is one of the most important parameters, if high detonation performances are desired. The density mainly is influenced by the substituents of the tetrazole ring, which in the case of oxygen containing side groups such as nitro or hydroxyl groups results in the increased formation of nitro-nitro interactions and hydrogen bonds to tighten the ionic network in the crystal.

METHODS AND OBJECTIVES

Requirements for new HEDMs and methods for their evaluation

As already mentioned above, the most important requirement for new HEDMs first of all is a high performance, which is based on a high density, a high heat of formation and a balanced oxygen content. The heats of formation were either calculated from the heats of combustion of the materials in bomb calorimetric measurements or theoretical using quantum chemical calculations, whereas the densities were obtained from single crystal X-ray diffraction measurements. A further important parameter for suitable replacements of in use high explosives is a sufficient thermostability, which examined by conducting differential scanning calorimetric measurements, where the samples were heated until decomposition with a linear heating rate of $5\text{ }^{\circ}\text{C min}^{-1}$. Here it is important, not to use too high heating rates, which would lead to misinterpretations of the decomposition temperatures, since the decomposition temperature of a material increases with increasing heating rate in a DSC measurement. Also it is important to report the absolute onset temperatures, when a DSC curve is analysed, which means to find the point, where the first deviation of the DSC curve changes its sign to positive. To assess the long term stability of a compound, RADEX experiments were carried out. Here, the sample is heated to $75\text{ }^{\circ}\text{C}$ for a period of 48 h and analysed spectroscopically as well as by elemental analysis after the experiment. The long term thermal stability is an important parameter, which needs to be fulfilled to assure the safe handling of a material, even if sitting in the desert under direct sun light or to evaluate the storage stability of an explosive over an extended period of time at elevated temperatures. Beside the sensitivity to thermal stress, the sensitivities to mechanical stimuli must not exceed a certain value. These values can be determined by the use of a drophammer in case of measuring the impact sensitivity. In this test, the sample (approx. 40 mg) is placed in a plunger assembly consisting of two steel

rollers, a hollow steel collar and a centring ring for fixation. The assembly is placed onto a small anvil, which is then hit with a steel block, the weight and dropping height of which can exactly be determined. From these values the maximum energy in Joules at which 1 out of 6 trials to initiate the sample was successful, can be calculated. To determine the sensitivity towards friction, the sample is placed onto a rough porcelain plate, which is then fixed on the moving plate of the friction apparatus. The friction force between the porcelain plate and a static porcelain peg, which is attached to an arm, is determined by using different weights, which can be put onto the arm in different distances to the porcelain peg. Electrostatic discharge often is a reason for accidental explosion and therefore, the sensitivities towards it need to be determined. This can be achieved by applying different spark energies to a sample, which is placed in a small plastic holder slipped over the conductive piston of the electrical grounding. The spark energies can be varied by applying different voltages and variable capacitive resistances. If a newly synthesized HEDM has performance values exceeding those of commonly used RDX, is comparatively insensitive and reveals a sufficient thermostability, the toxicity of the material is assessed by subjecting solutions of different concentration of the sample to a marine luminescent bacterium, *Vibrio fischeri*. The advantage of the use of this luminescent bacterial strain is, that the decrease of living organisms can easily be detected by the decrease in luminescence of the sample, which allows conclusions on the toxicity of the material.

Although the detonation performance of most of the new HEDMs presented in this work was calculated from their energy of formation, their density and sum formula, using the EXPLO5 computer code (different versions) also larger scale safety and/or performance test were carried out. The detonation velocity for instance can also be determined experimentally by filling the sample into a plastic tube (length: 100 mm, inner diameter: 14 mm), which serves as confinement and igniting it with a commercially available detonator. The progress of the detonation wave, which essentially is the detonation velocity, is measured using optical fiber technique. A test essentially for assessing the transport safety of a sample in case of fire, when the material is stored in a confined vessel, is the steel sleeve test (Koenen Test). In this test the substance is filled into a steel sleeve (internal diameter: 24 mm, length: 75 mm, wall thickness: 0.5 mm, $V = 25$ mL) up to a height of 15 mm beneath the top edge and then the sleeve is closed with a nozzle plate. Nozzle plates are available with an orifice of 1.0 – 20 mm. The sleeve is then heated simultaneously by four Bunsen burners and the maximum critical diameter at which the pressure increase on burning and the subsequent explosion destroys the sleeve into at least four pieces, is determined. Another test on the behavior of an energetic material in an open fire is the so called fast cook-off test, where the sample, which is stored in an unconfined vessel, is placed in an open container filled with saw dust, which is soaked with kerosene. After ignition of the saw dust and following ignition of the sample, it ideally only burns down without exploding. This behavior is desirable for any secondary explosive, but is not expected if testing a primary explosive.

Scope of the dissertation

The dissertation “Nitrogen-rich High Energy Density Materials – Synthesis, Characterization and Testing” encompasses a broad scope of new materials for use as primary and secondary

explosives as well as propellant charges and in pyrotechnical application. In the following, a reference to the respective publication(s) is added using a number in squared brackets referring to the publication list, which is given in the table of contents or the bibliography. The biggest part of the thesis is dealing with the synthesis and characterization of new secondary explosives as RDX replacements. The development of new HEDMs with high performance, guaranteed through high enthalpies of formation and high densities, combined with high thermal stabilities, was exemplified in the synthesis of various nitrogen rich salts of 5,5'-bis(1-hydroxytetrazole) and 5,5'-bis(2-hydroxytetrazole) [22, 26, 29, 31] as well as compounds based on 5-nitriminotetrazole [2, 4, 12]. The aspect of high density as a requirement was further delved into by characterizing a scope of nitrogen-rich, energetic hydroxylammonium salts [15, 19], which emerged to have outstandingly high densities among salts containing other energetic cations. To decrease the sensitivities of the aforementioned 5-nitriminotetrazoles by introduction of an alkyl- or functionalized alkyl substituent, methylated, hydroxyethylated, nitratoethylated or other differently *N*-substituted nitrimino- and aminotetrazole derivatives were investigated [3, 6, 7, 8, 10, 14]. The versatile reactivity of the cyano functionality in 5-cyanotetrazole leading to the formation of carboxamide- and carboxamide oxime substituted tetrazoles as well as the formation of a new tetrazol-triazole based heterocycle was studied in two contributions [27, 28]. For the investigation of a potential use as propellant charges, ionic 5,5'-bistetrazolates [18] as well as hydrazinium 5-aminotetrazolate [1] with extraordinary high nitrogen contents were synthesized and characterized. Additionally, synthesized ionic derivatives of diaminourea may contribute to this topic [11]. Today, triaminoguanidinium 5,5'-azotetrazolate (TAGzT) is a compound under recent investigation as ingredient for propellant charges. Here the comparison of TAGzT with nitrogen-rich salts of the newly introduced 5,5'-bis-azoxytetrazole, which due to *N*-oxidation at the azo-bridge has an improved oxygen balance, was undertaken [21]. A mixed aminated and nitrated guanidine derivative, 3-amino-1-nitroguanidine and its utilization for new high energy density materials was examined by the synthesis of various nitrogen-rich salts containing the 3-amino-1-nitroguanidinium cation [5, 23] as well as inorganic salts thereof, which have potential to be used as starting materials [25]. Also efforts in the characterization of new primary explosives based on diazidotriazole [17], 5-nitriminotetrazol [9] or 3-amino-1-nitroguanidine complexes, which were investigated upon their possible laser ignitability, were made [30]. If these complexes are insensitive towards impact and friction and can easily be ignited by a short, but highly energetic laser pulse with a specific wave length, the probability of being accidentally ignited, which oftentimes happened while handling commonly used impact and friction sensitive primary explosives, can be reduced. In the field of tetrazole compounds used for pyrotechnical applications, alkaline earth metal salts of 5,5'-bistetrazole [13] as well as alkali and alkaline earth metal salts of 5,5'-bis(1-hydroxytetrazole) [32] were synthesized and their use in various pyrotechnical compositions was investigated. To assess the suitability of the fibre optic technique as a method to experimentally determine detonation velocities, a variety of energetic materials, which have been prepared in our research group were used in the experimental setup described in respective publication [16]. Last but not least, also a contribution to the development of safer reactants in organic syntheses was published after investigation of safer alternatives to the diazo-transfer reagent imidazol-1-sulfonyl azide,

which is widely used to convert covalent organic amines to the respective azides as starting materials in [1+3]-dipolar cycloadditions [20].

References (introduction)

1. J. Akhavan, The Chemistry of Explosives, 3rd ed., The Royal Society of Chemistry, Cambridge, UK, **2011** and references therein.
2. T. M. Klapötke, Chemistry of High-Energy Materials, de Gruyter, Berlin, New York, **2011** and references therein.

CONCLUSION

During the course of this dissertation, a broad variety of energetic materials based on nitrogen-rich molecules encompassing new primary and secondary explosives as well as materials with possible applications in the propellants and pyrotechnics sector was examined. Beside a smaller number of unpublished results, 169 compounds were synthesized and fully characterized. The solid state structure of 155 (92 %) of the described compounds additionally was determined by single crystal X-ray diffraction. The uppermost part (98, 58 %) of the described materials was characterized with regard to their possible application in the secondary explosives sector, as it is shown in figure 7. The remaining fraction can be divided into potential primary explosives (22, 13 %), propellants (18, 11 %) and colorants for pyrotechnics (7, 4 %). The remaining 24 compounds (14 %), which cannot be classified as either of the described energetic materials served as intermediates, reagents or have other applications. A reference to the corresponding publication as listed in the end of the introduction of this work or in the bibliography is given in squared brackets for each class of compounds in the respective section.

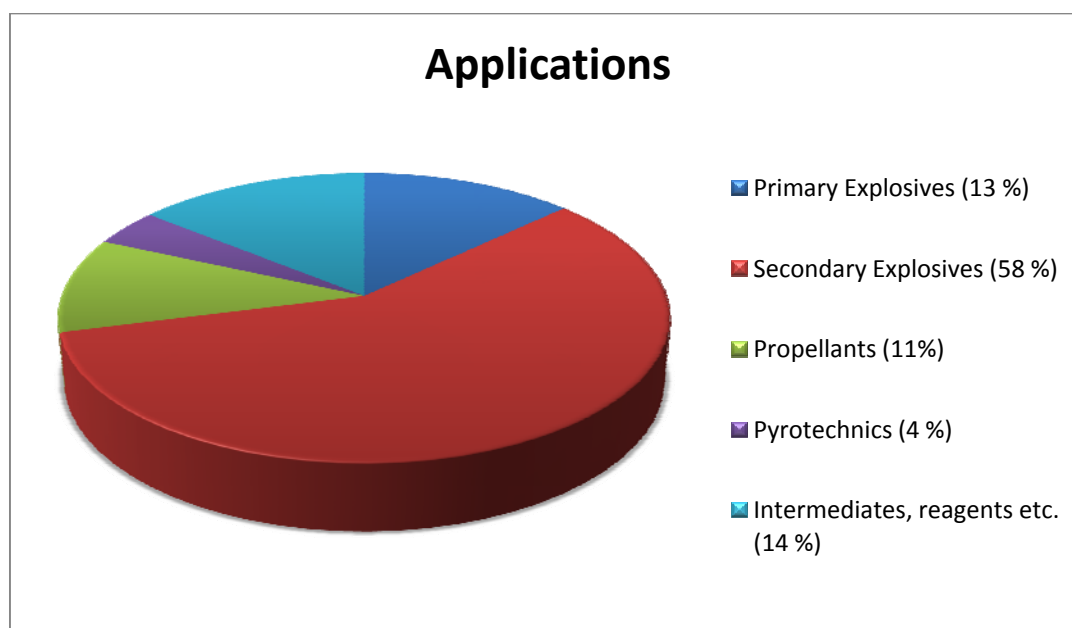


Figure 7. *Classification of investigated energetic materials*

SECONDARY EXPLOSIVES

Starting with the achievements made in the synthesis and characterization of the largest class of energetic materials, which are new secondary explosives, table 2 gives an overview on materials with a detonation performance better or comparable to this observed for RDX. Since different versions of the computer program EXPLO5 (V5.02-V5.05) were used for the calculation of the detonation parameters of the mentioned compounds throughout the last four years, also different values for the detonation parameters of RDX, although the same heat of

formation, density and sum formula was used as input information, was obtained. For a better comparison, the detonation parameters of the best performing compounds were recalculated with the latest version (EXPLO5.05) available in November 2012 and compared to the values obtained for the commonly used high explosives 2,4,6-TNT, RDX, β -HMX and ϵ -CL-20 (table 2, figure 17).

In summary, 16 compounds with detonation parameters comparable or better than those of RDX were characterized. They belong to the substance classes of nitrogen-rich salts of substituted and unsubstituted 5-nitriminotetrazoles, 3-amino-1-nitroguanidine and nitrogen-rich salts thereof, a diaminourea salt as well as salts of 5,5'-bis(1-hydroxytetrazole) and 5,5'-bis(2-hydroxytetrazole).

Diaminouronium 2-methyl-5-nitraminotetrazolate (**1**) (figure 8) is the best performing compound in a series of nitrogen-rich salts of 2-methyl-5-nitraminotetrazole [8]. Bearing in mind, that the triaminoguanidinium salts of 1-methyl-5-nitriminotetrazole, due to its good explosive performance, is already in an upscaling process for further investigations as RDX replacements, the nitrogen-rich salts of 2-methyl-5-nitraminotetrazole were prepared and characterized.

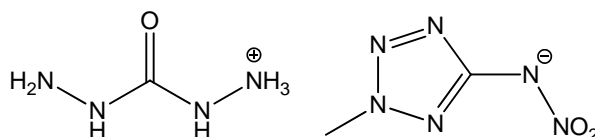


Figure 8. Lewis structure of diaminouronium 2-methyl-5-nitraminotetrazolate (DAU-2-MeATNO₂, **1**)

The 2-methyl-5-nitraminotetrazolate anion has a higher positive heat of formation $\Delta_f H^\circ(s)$ than the 1-methyl-5-nitriminotetrazolate anion, which promises better detonation parameters for its salts as compared to its 1-methylated sister compounds. The major drawback of the synthesis is the low yield of 2-methyl-5-aminotetrazole after methylation of 5-aminotetrazole with dimethyl sulfate in aqueous media, which, following a procedure of Finnegan et al.¹ proceeds in a yield of only 7 %, with 1-methyl-5-aminotetrazole as the major product. By changing the solvent to DMF, the temperature of the reaction could be raised resulting in the isolation of 2-methyl-5-aminotetrazole in up to 29 % yield, which is the thermodynamic product of the reaction (figure 9).

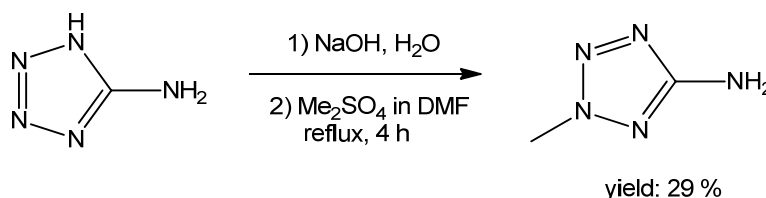


Figure 9. Methylation of 5-aminotetrazole in DMF

Another diaminouronium salt, diaminouronium nitrate (**2**) (figure 10), which can be synthesized from cheap starting materials is an easily accessible compound, however the crystallization from water or mixtures of water and alcohols is inhibited [11]. The crystals for

X-ray diffraction were obtained after repeated (several days!) cooling of the mixture and scratching the walls of the flask with a glass rod. Its detonation parameters are not superior to RDX, but it burns smokeless, without residues and self-containing, if unconfined.

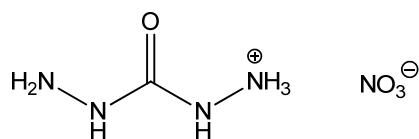


Figure 10. Lewis structure of diaminouronium nitrate (DAU-NO₃, **2**)

To complete the row of unsubstituted 5-nitriminotetrazolates listed in table 2, the monohydrazinium salt of 5-nitriminotetrazole (**3**) [12] as well as the mono- (**5**) and dihydroxylammonium salt (**6**) [19] thereof have to be mentioned. Their Lewis structures are shown in figure 11. All salts reveal a fairly good explosive performance (the dihydroxylammonium salt **6** although crystallizing as a hemihydrate), their sensitivities against impact and/or friction however are higher than the sensitivities of RDX, which disqualifies them as suitable replacements. Also the thermal stability of **3**, **5** and **6** is not superior to that of RDX.

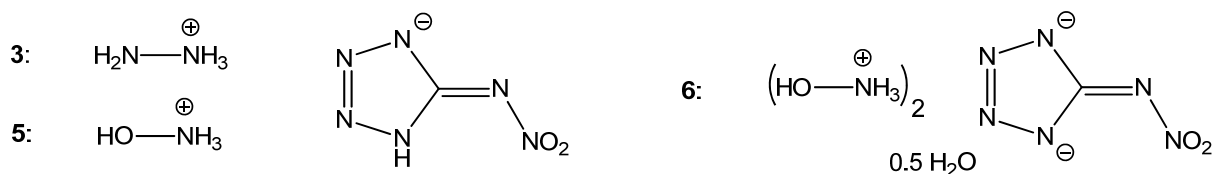


Figure 11. Lewis structure of monohydrazinium 5-nitriminotetrazolate (HyHATNO₂, **3**), monohydroxylammonium 5-nitriminotetrazolate (HxHATNO₂, **5**) and dihydroxylammonium 5-nitriminotetrazolate hemihydrate (Hx₂ATNO₂ · 0.5 H₂O, **6**)

The hydroxylammonium salt of the 1-(2-nitratoethyl)-substituted 5-nitriminotetrazole (**4**) (figure 12) suffers from the same disadvantages, which are high sensitivities and a relatively poor thermal stability [14]. The class of nitrogen-rich 1-(2-nitratoethyl)-5-nitriminotetrazolates was synthesized due to its good oxygen-balance and the anticipated good detonation parameters, which indeed were observed. 1-(2-Nitratoethyl)- as well as 1-(2-hydroxyethyl)-5-nitriminotetrazole and 1-(2-nitratoethyl)-5-aminotetrazolium nitrate are products from the nitration of 1-(2-hydroxyethyl)-5-aminotetrazole with 100 % nitric acid. Depending on the excess of nitric acid used, the three products are formed in different ratios and can be separated upon their different water solubility. In an attempt to isolate diaminouronium 1-(2-nitratoethyl)-5-nitriminotetrazolate, the nitrimino moiety was reduced by the base diaminourea (carbonyl dihydrazide) resulting in the formation of 1-(2-nitratoethyl)-5-aminotetrazole, which is shown in figure 12.

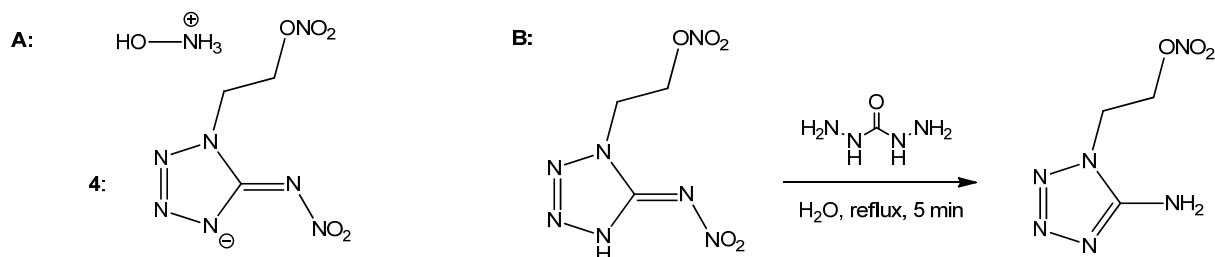


Figure 12. **A:** Lewis structure of hydroxylammonium 1-(2-nitratoethyl)-5-nitriminotetrazolate (Hx-1-EtONO₂-ATNO₂, **4**); **B:** Reduction of 1-(2-nitratoethyl)-5-nitriminotetrazole to 1-(2-nitratoethyl)-5-aminotetrazole by diaminourea

The best performing secondary explosive, which was synthesized and characterized is the dihydroxylammonium salt of 5,5'-bis(1-hydroxytetrazole) (**7**) (TKX-50) (figure 13) [22]. Fulfilling all requirements for a greener replacement of RDX, this material outperforms not only the commonly used high explosives RDX and HMX, which due to their simple and cheap preparation are widely used. It reveals detonation parameters, that even exceed those of CL-20, a caged nitramine with a calculated detonation velocity in the vicinity of 9500 ms⁻¹, which is not yet used because of its expensive, multi-step synthesis.

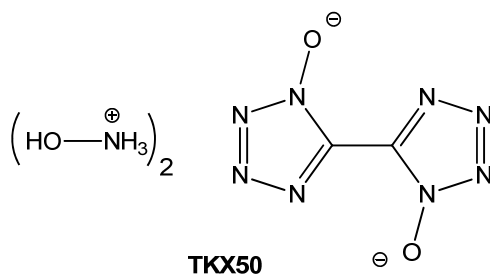


Figure 13. Lewis structure of dihydroxylammonium 5,5'-bis(tetrazole-1-oxide), (TKX-50, **7**)

The aspect of a “greener” replacement for RDX, beside its high nitrogen content resulting in the predominant formation of N₂ after its deflagration or detonation, was proved by a toxicity study, which revealed a toxicity for TKX-50 slightly lower than that of RDX. The luminescent bacterial strain *Vibrio fischeri* was utilized, which is representative for a broad variety of aquatic life. The detonation performance of the material was tested in a small-scale reactivity test (SSRT), where TKX-50 showed a performance superior to RDX and comparable to that of HMX. The long-term thermal stability was proved in a RADEX experiment, where the material easily withstood a temperature of 75 °C for 48 h. Even higher temperatures of 150 °C did not lead to decomposition after two days. The thermal stability of the material at a heating rate of 5 °C in a DSC measurement is 220 °C, which is even slightly higher than that of RDX. For safety testing, the material was proved in a fast cook-off test. In this unconfined case, TKX-50 burns down without detonation. The Koenen test (confined case), where a hole diameter of 10 mm was applied, resulted in a fragmentation of the steel tube. The synthesis of the free acid 5,5'-bis(1-hydroxytetrazole) involves the isolation and further processing of the highly friction and impact sensitive intermediate diazidoglyoxime. This problem was solved by developing a five-step four-pot synthesis to isolate its dihydroxylammonium salt (TKX-50). The improved synthesis involves a combined procedure to form and cyclize diazidoglyoxime in solution without isolation. By either using DMF or

NMP for the chloro-azido exchange of dichloroglyoxime and sodium azide, the dimethylammonium salt or the free acid is obtained after treatment of the mixture containing diazidoglyoxime with HCl gas in diethylether. The isolated dimethylammonium salt, in case of using DMF as the solvent, is directly converted to TKX-50 by the addition of hydroxylammonium chloride, and the free acid 5,5'-bis(1-hydroxytetrazole), if using NMP, first has to be converted into the disodium salt by the addition of NaOH. The isolated disodium salt can be converted into TKX-50 again using hydroxylammonium chloride.

Also other nitrogen-rich salts of this anion, namely the dihydrazinium (**11**) as well as the 5-aminotetrazolium (**12**) and the 1,5-diaminotetrazolium salt (**13**) (figure 14) show performances, which qualify them for suitable RDX replacements [29]. However, their performances as well as their sensitivities do not reach the values, which were found for TKX-50.

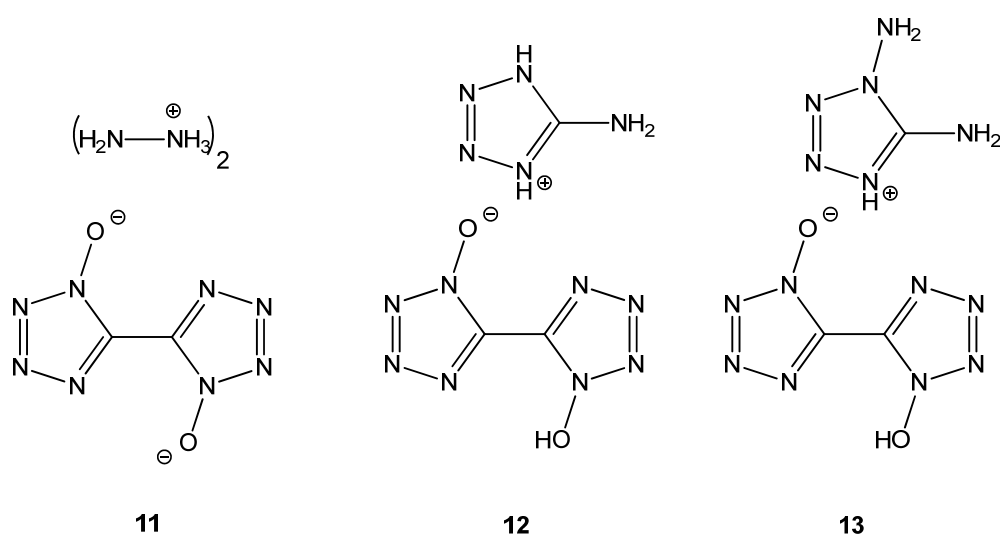


Figure 14. Lewis structures of dihydrazinium 5,5'-bis(tetrazole-1-oxide) (Hy₂-1-BTO, **11**), 5-aminotetrazolium 5,5'-bis(tetrazole-1-oxide) (AT-1-BTOH, **12**) and 1,5-diaminotetrazolium 5,5'-bis(tetrazole-1-oxide) (DAT-1-BTOH, **13**)

Table 2. *Energetic properties and detonation parameters of 1–8.*

	1	2	3	4	5	6	7	8
Formula	$C_3H_{10}N_{10}O_3$	$CH_7N_5O_4$	$CH_6N_8O_2$	$C_3H_8N_8O_6$	$CH_5N_7O_3$	$CH_9N_8O_{4.5}$	$C_2H_8N_{10}O_4$	$CH_5N_5O_2$
FW [g mol ⁻¹]	234.18	153.12	162.21	252.15	163.13	205.16	236.15	119.08
IS [J] ^a	5	9	3	3	2	10	20	20
FS [N] ^b	168	288	56	60	40	80	120	144
ESD-test [J] ^c	0.50	0.60	0.40	0.15	0.30	0.30	0.10	0.15
N [%] ^d	59.8	45.7	69.1	44.4	60.1	54.6	59.3	58.8
Ω [%] ^e	-54.7	-15.7	-29.6	-25.4	-14.7	-20.3	-27.1	-33.6
T_{dec} [°C] ^f	195	242	188	148	172	166	221	184
Density [g cm ⁻³] ^g	1.730	1.782	1.680	1.796	1.785	1.771	1.915	1.722
$\Delta_f H_m^\circ$ [kJ mol ⁻¹] ^h	345	-180	380	257	290	80	447	77
$\Delta_f U^\circ$ [kJ kg ⁻¹] ⁱ	1596	-1048	2464	1125	1895	520	2006	770

Detonation parameters calculated with EXPLO5.05:

$-\Delta_E U^\circ$ [kJ kg ⁻¹] ^j	4891	5048	5592	6347	6114	5759	6025	4915
T_E [K] ^k	3205	3396	3776	4220	4205	3754	3954	3318
p_{C-J} [kbar] ^l	306	335	321	364	371	362	424	308
D [m s ⁻¹] ^m	8734	8902	8926	9035	9238	9244	9698	8731
Gas vol. [L kg ⁻¹] ⁿ	831	910	876	787	853	923	846	878

^a impact sensitivity (BAM drophammer, 1 of 6); ^b friction sensitivity (BAM friction tester, 1 of 6); ^c electrostatic discharge device (OZM); ^d nitrogen content; ^e oxygen balance; ^f decomposition temperature from DSC ($\beta = 5$ °C); ^g estimated from X-ray diffraction; ^h calculated (CBS-4M) heat of formation; ⁱ calculated energy of formation; ^j energy of explosion; ^k explosion temperature; ^l detonation pressure; ^m detonation velocity; ⁿ assuming only gaseous products.

Table 2 (contd.). *Energetic properties and detonation parameters of 9–16.*

	9	10	11	12	13	14	15	16
Formula	$CH_6N_6O_5$	$CH_8N_8O_7$	$C_2H_{10}N_{12}O_2$	$C_3H_5N_{13}O_2$	$C_3H_6N_{14}O_2$	$C_2H_2N_8O_2$	$C_2H_8N_{10}O_4$	$C_4H_{12}N_{18}O_6$
FW [g mol ⁻¹]	182.10	244.12	234.18	255.20	270.22	170.09	236.15	408.26
IS [J] ^a	10	10	9	4	2	3	3	10
FS [N] ^b	120	40	252	72	160	5	60	48
ESD-test [J] ^c	0.50	0.10	0.10	0.30	0.35	0.03	0.26	1.5
N [%] ^d	46.2	45.9	71.8	71.4	65.4	65.9	59.3	61.8
Ω [%] ^e	0.0	+6.6	-47.8	-40.8	-41.5	-28.2	-27.1	-31.4
T_{dec} [°C] ^f	130	108	220	224	170	165	172	163
Density [g cm ⁻³] ^g	1.905	1.850	1.725	1.839	1.828	1.953	1.822	1.832
$\Delta_f H_m^\circ$ [kJ mol ⁻¹] ^h	22	0	678	911	991	560	391	1044
$\Delta_f U^\circ$ [kJ kg ⁻¹] ⁱ	237	112	3020	3667	3767	3377	1770	2666

Detonation parameters calculated with EXPLO5.05:

$-\Delta_E U^\circ$ [kJ kg ⁻¹] ^j	6196	5635	5415	5576	5625	5854	5790	6135
T_E [K] ^k	4181	3975	3433	4009	3970	4396	3869	4129
p_{C-J} [kbar] ^l	426	376	340	358	361	409	372	382
D [m s ⁻¹] ^m	9550	9171	9159	9097	9160	9364	9264	9350
Gas vol. [L kg ⁻¹] ⁿ	858	871	863	760	774	721	847	816

^a impact sensitivity (BAM drophammer, 1 of 6); ^b friction sensitivity (BAM friction tester, 1 of 6); ^c electrostatic discharge device (OZM); ^d nitrogen content; ^e oxygen balance; ^f decomposition temperature from DSC ($\beta = 5$ °C); ^g estimated from X-ray diffraction; ^h calculated (CBS-4M) heat of formation; ⁱ calculated energy of formation; ^j Energy of explosion; ^k explosion temperature; ^l detonation pressure; ^m detonation velocity; ⁿ assuming only gaseous products.

Table 2 (contd.). *Energetic properties and detonation parameters of commonly used high explosives*

	2,4,6-TNT	RDX	β-HMX	ϵ-CL-20
Formula	C ₇ H ₅ N ₃ O ₆	C ₃ H ₆ N ₆ O ₆	C ₄ H ₈ N ₈ O ₈	C ₆ H ₆ N ₁₂ O ₁₂
FW [g mol ⁻¹]	227.13	222.12	296.16	438.19
IS [J] ^a	15	7	7	4
FS [N] ^b	353	120	112	48
ESD-test [J] ^c	—	0.20	0.20	0.13
N [%] ^d	18.5	37.8	37.8	38.3
Ω [%] ^e	-74.0	-21.6	-21.6	-11.0
T _{dec.} [°C] ^f	290	210	279	215
Density [g cm ⁻³] ^g	1.713	1.858	1.944	2.083
$\Delta_f H_m^\circ$ [kJ mol ⁻¹] ^h	-56	86	116	365
$\Delta_f U^\circ$ [kJ kg ⁻¹] ⁱ	-168	489	493	919
<i>Detonation parameters calculated with EXPLO5.05:</i>				
$-\Delta_f U^\circ$ [kJ kg ⁻¹] ^j	5258	6190	6185	6406
T _E [K] ^k	3663	4232	4185	4616
p _{C-J} [kbar] ^l	235	380	415	467
D [m s ⁻¹] ^m	7459	8983	9221	9455
Gas vol. [L kg ⁻¹] ⁿ	569	734	729	666

^a impact sensitivity (BAM drophammer, 1 of 6); ^b friction sensitivity (BAM friction tester, 1 of 6); ^c electrostatic discharge device (OZM); ^d nitrogen content; ^e oxygen balance; ^f decomposition temperature from DSC ($\beta = 5$ °C); ^g estimated from X-ray diffraction; ^h calculated (CBS-4M) heat of formation; ⁱ calculated energy of formation; ^j energy of explosion; ^k explosion temperature; ^l detonation pressure; ^m detonation velocity; ⁿ assuming only gaseous products.

A class of compounds, which is strongly related to the nitrogen-rich salts of 5,5'-bis(1-hydroxytetrazole) are the respective salts of 5,5'-bis(2-hydroxytetrazole) [31]. These materials were synthesized expecting characteristics, which are comparable to those of their sister compounds which are oxidized in position 1 of the tetrazole ring. The free acid 5,5'-bis(2-hydroxytetrazole) (**14**) reveals a density of 1.953 g cm⁻³, which promised high densities for its nitrogen-rich salts, too. Indeed, the densities and hence, the explosive performance of the free acid **14** as well as its dihydroxylammonium salt (**15**) and the bis-(3-amino-1-nitroguanidinium) salt (**16**) (figure 15) is high and exceeds the values for RDX. The densities given in the manuscript, unlike for all other compounds, were measured at room temperature. The reported detonation parameters supposingly are even higher if using densities, which are determined at -100 °C. The mentioned examples unfortunately reveal lower thermal stabilities and higher sensitivities compared to the respective nitrogen-rich salts of 5,5'-bis(1-hydroxytetrazole).

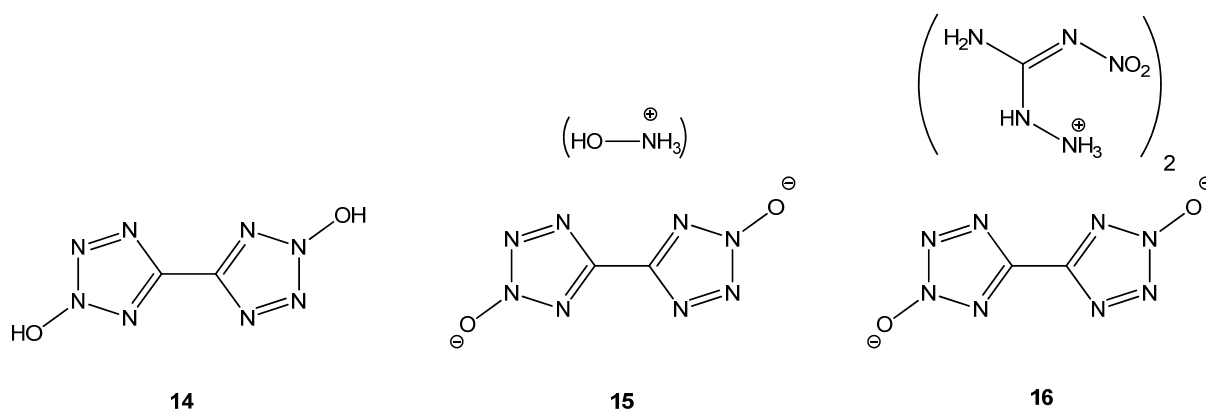


Figure 15. Lewis structures of 5,5'-bis(2-hydroxytetrazole) (2-BTO, **14**), dihydroxylammonium 5,5'-bis(tetrazole-2-oxide) (Hx₂-2-BTO, **15**) and bis(3-amino-1-nitroguanidinium) 5,5'-bis(tetrazole-2-oxide) (ANQ₂-2-BTO, **16**)

A group of energetic materials, which is not based on the tetrazole heterocycle, is 3-amino-1-nitroguanidine (**8**) (ANQ), its nitrate (**9**) and dinitramide salt (**10**), which crystallizes as a monohydrate (figure 16) [23]. Since promising higher densities compared to other guanidinium based nitrogen-rich salts such as guanidinium, aminoguanidinium, di- and triaminoguanidinium salts were observed, this mixed aminated and nitrated guanidine derivative was utilized as a cation in the synthesis of new energetic materials. The high densities and therefore also the excellent explosive performance of compounds containing the ANQ⁺-cation was exemplified in the synthesis of **9** and **10**. Unfortunately, all compounds bearing the ANQ⁺-cation lack thermal and mechanical stability in an extend, which disqualifies these compounds as thermally stable RDX replacements. A reason for the poor thermal stability of these salts could be a lowering of the C-N bond order in the hydrazine moiety of the molecule upon protonation. This was evidenced by comparing the mentioned bond length in unprotonated ANQ and the ANQ⁺-cation.

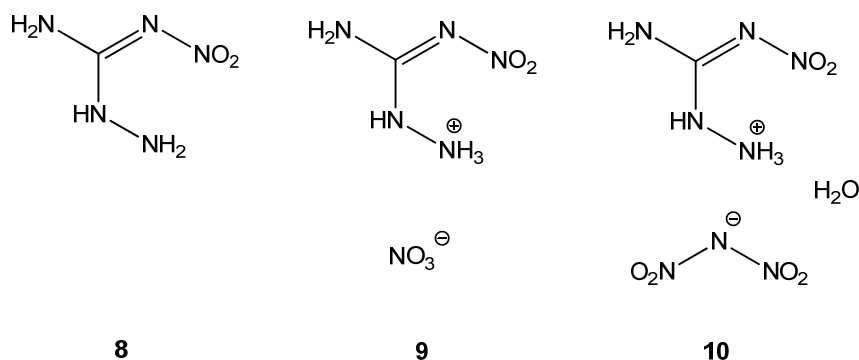


Figure 16. Lewis structures of 3-amino-1-nitroguanidine (ANQ, **8**), 3-amino-1-nitroguanidinium nitrate (ANQ-NO₃, **9**) and 3-amino-1-nitroguanidinium dinitramide monohydrate (ANQ-DN · H₂O, **10**)

To point out the most important parameter, a diagram of the detonation velocities of all compounds contained in table 2 including the high explosives TNT, RDX, HMX and CL-20 for comparison is shown in figure 17.

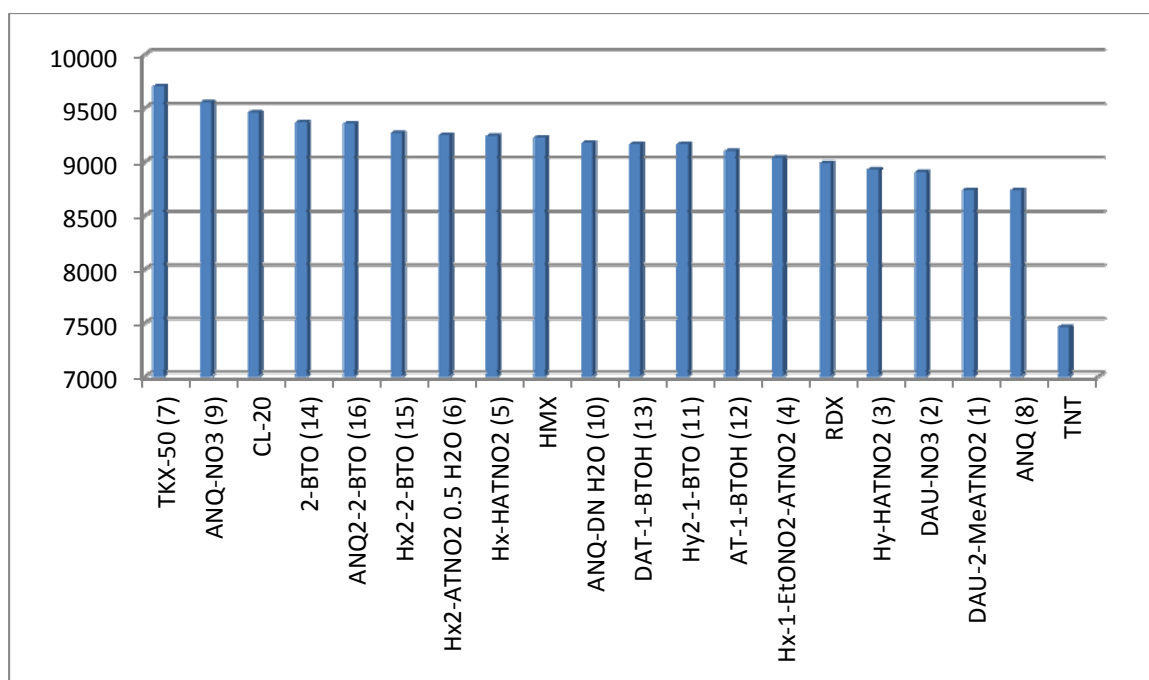


Figure 17. Detonation velocities in m s^{-1} of **1–16** as well as of 2,4,6-TNT, RDX, β -HMX and ϵ -CL-20

PRIMARY EXPLOSIVES

In the sector of new primary explosives, two contributions are of major importance. Firstly, a row of Co^{II} , Ni^{II} , Cu^{II} , Zn^{II} and Ag^{I} containing complexes of neutral 3-amino-1-nitroguanidine with energetic anions such as nitrate, perchlorate and dinitramide were synthesized and fully characterized [30]. Three of the mentioned complexes were successfully initiated upon irradiation with a short laser pulse (100 μs) of 940 nm wavelength. The field of laser ignitable primary explosives is a very recent development in the search for safer and also less toxic alternatives to the commonly used highly sensitive lead, cadmium or mercury containing azides or styphnates (2,4,6-trinitroresorcinates). If these compounds reveal a sufficient thermal as well as mechanical stability, the risk of an accidental initiation can be minimized, since they can only be initiated by laser radiation, ideally of a particular wavelength. $[\text{Co}^{\text{II}}(\text{ANQ})_2(\text{H}_2\text{O})_2](\text{ClO}_4)_2$ (**17**), $[\text{Cu}^{\text{II}}(\text{ANQ})_2(\text{ClO}_4)_2](\text{H}_2\text{O})_2$ (**18**) and $[\text{Ag}^{\text{I}}(\text{ANQ})_2]\text{ClO}_4$ (**19**) (figure 18, 19) were the candidates, which could be successfully initiated under the described conditions, however, their impact and friction sensitivities are comparatively low (table 3).

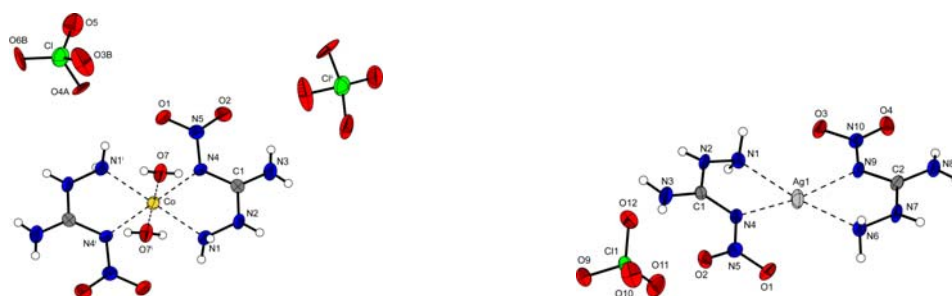


Figure 18. Molecular moieties of $[\text{Co}^{\text{II}}(\text{ANQ})_2(\text{H}_2\text{O})_2](\text{ClO}_4)_2$ (**17**, left) and $[\text{Ag}^{\text{I}}(\text{ANQ})_2]\text{ClO}_4$ (**19**, right).

After measuring the UV-Vis-NIR spectra of the solid samples, we could conclude, that there is no relationship between the optical absorption properties of the complexes and their photosensitivity towards pulsed laser irradiation, since the complexes did not equally absorb (**19** did not absorb at all) at the wavelength of the used laser radiation (940 nm). On the other hand, a thermal initiation can also be excluded, since complexes with a very poor thermal stability ($[\text{Cu}^{\text{II}}(\text{ANQ})_2(\text{NO}_3)_2]$, $T_{\text{dec}} = 77^\circ\text{C}$, figure 19) showed no response in the initiation experiment.

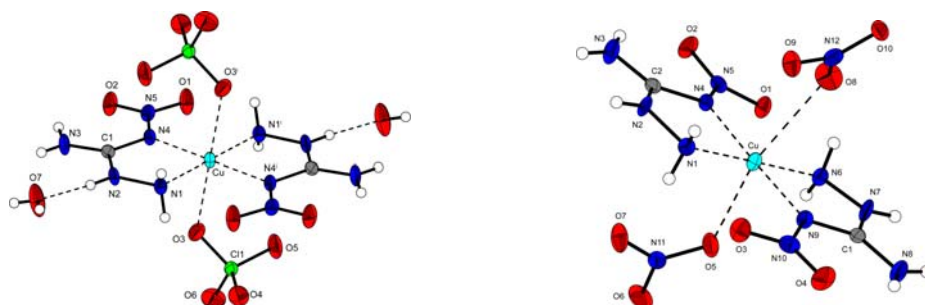


Figure 19. Molecular moieties of $[\text{Cu}^{\text{II}}(\text{ANQ})_2(\text{ClO}_4)_2](\text{H}_2\text{O})_2$ (**18**, left) and $[\text{Cu}^{\text{II}}(\text{ANQ})_2(\text{NO}_3)_2]$.

The fact that only perchlorate compounds and no nitrates could be initiated fits to the literature claimed initiation mechanism² where an active ClO_4^\cdot radical is formed by a one-electron transfer from the perchlorate anion to the metal cation induced by the laser beam. Other trends, which were observed during this study were a higher decomposition temperature of the Ni^{II} -complexes as compared to the corresponding Co^{II} - and Zn^{II} -complexes. Cu^{II} -complexes revealed the lowest thermal stability. Also, chloride and perchlorate containing complexes have higher decomposition temperatures as the corresponding nitrates or dinitramides.

Table 3. Sensitivities and thermal behavior of **17–19**.

	<i>IS (J)</i>	<i>FS (N)</i>	<i>ESD (J)</i>	<i>T_{dehydr} (°C)</i>	<i>T_{dec} (°C)</i>
17	3	10	0.03	170 ^a	176
18	<1	16	0.50	120	134
19	<1	<5	0.01	- ^b	148

^a decomposition (exothermic) occurs immediately after dehydration (endothermic); ^b no crystal water contained

A second approach in the synthesis of highly thermally stable, green primary explosives is the investigation of calcium 5-nitriminotetrazolate (**20**) [9]. Its decomposition temperature of 360 °C makes it a suitable replacement for lead azide, which is used as a priming charge for the initiation of the highly thermally stable HNS (hexanitrostilbene, $T_{\text{dec}} = 318$ °C) for mining (figure 20).

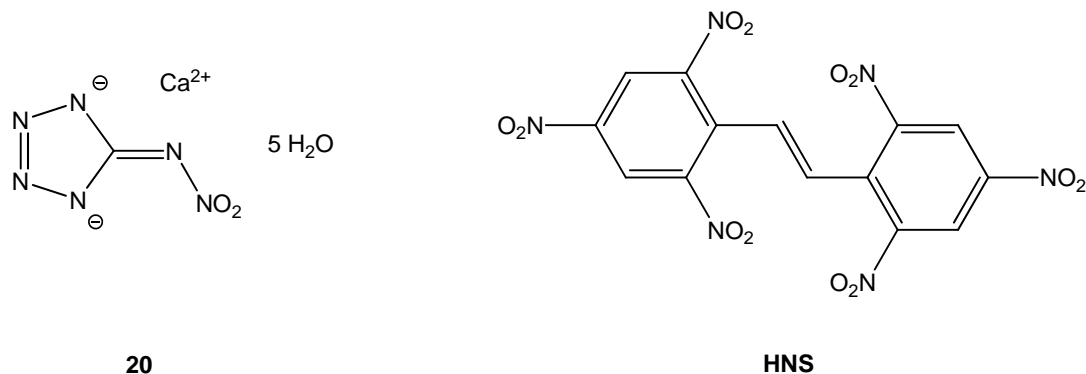


Figure 20. Lewis structures of Calcium 5-nitriminotetrazolate pentahydrate (**20**) and hexanitrostilbene (HNS).

20 crystallizes as a pentahydrate with sensitivities of 75 J (IS) and 240 N (FS) and can be dehydrated at 200 °C in 48 h resulting in an increase in sensitivity (5 J (IS), 112 N (FS)). Its calculated explosion enthalpy of -4632 kJ kg^{-1} exceeds this of commonly used $\text{Pb}(\text{N}_3)_2$ ($\Delta H_{\text{Ex}}^\circ = -1638 \text{ kJ kg}^{-1}$). To assess its ability to initiate HNS, which requires primary explosives with performances equal or greater than that of silver azide for initiation, 2.0 g of HNS was filled in a copper tube, which was topped with 0.5 g of **20**. The calcium salt was initiated with a commercially available igniter resulting in a successful initiation of the HNS.

PROPELLANTS

Materials with an extraordinary high nitrogen content and appropriate thermal and mechanical stability are candidates for use as rocket or gun propellants. The nitrogen-rich salts of 5,5'-bistetrazole were investigated and their use as gun propellant ingredients was examined [18]. Their high nitrogen contents of 68.6–83.1 % ensure a high N_2/CO ratio of the combustion gases which is advantageous considering the problems of gun barrel erosion due to formation of iron carbide. Despite their high nitrogen contents they reveal thermal stabilities higher than 200 °C while being comparatively insensitive. The impact sensitivities are in a range between 10 J (dihydroxylammonium salt) and 40 J (dihydrazinium, bis-guanidinium and bis-aminoguanidinium salt) and the friction sensitivities are spread over a range between 240 N (dihydroxylammonium salt) and >360 N (diammonium salt and bis-guanidinium salt). Their performance in gun propellant formulations was evaluated by calculating the combustion temperature T_c , the maximum pressure p_{max} , the specific energy f_E , the co-volume b_E and the N_2/CO ratio of the combustion gases, which are important parameters for gun propellant formulations, under isochoric conditions. The best performing formulation (**21**-HN2) contains the dihydrazinium salt of 5,5'-bistetrazole (**21**) and is

compared to a formulation HN2 (high nitrogen 2), which contains triaminoguanidinium 5,5'-azotetrazolate (TAGzT) as a high nitrogen fuel instead (figure 21).

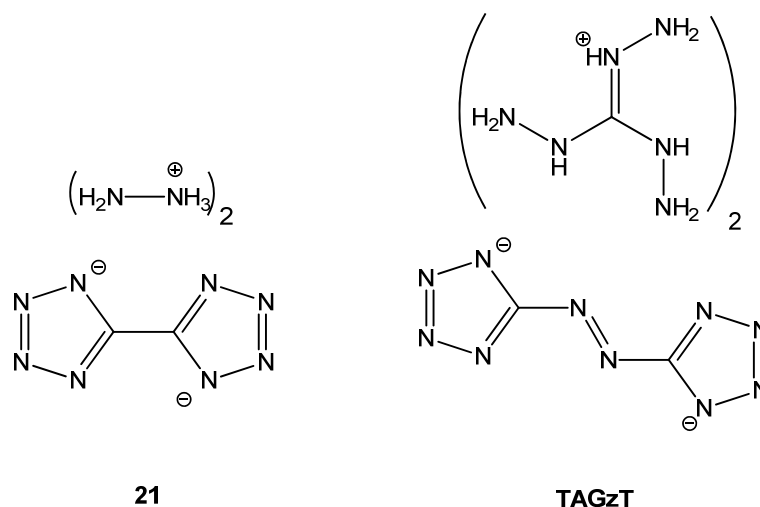


Figure 21. Lewis structures of dihydrazinium 5,5'-bistetrazolate (**21**) and bis-triaminoguanidinium 5,5'-azotetrazolate (**TAGzT**)

The composition of the formulations is as follows: RDX//TAGzT/**21**//FOX-12//CAB//BDNPA/F//NC = 40//20//16//12//8//4, where FOX-12 is guanyluronium dinitramide, CAB is cellulose acetate butyrate and BDNPA/F is a 1:1 mixture of bis(2,2-dinitroprop-1-yl)acetal and -formal. The results are gathered in table 4.

Table 4. Combustion parameters of HN2 and **21**-HN2 under isochoric conditions

	T_c (K)	p_{\max} (bar)	f_E (kJ kg ⁻¹)	b_E (cm ³ g ⁻¹)	N ₂ /CO
HN2	2735	2848	1.088	1.181	1.05
21-HN2	2738	2910	1.111	1.183	1.06

Another alternative for TAGzT in gun propellant formulations are nitrogen-rich salts of 5,5'-azoxy-bistetrazole [21]. While the 5,5'-azotetrazolate anion is formed after adding KMnO₄ to a solution of sodium 5-aminotetrazolate³, the 5,5'-azoxybistetrazole anion can be isolated after adding sodium 5-aminotetrazolate to a solution of KMnO₄ (figure 22).

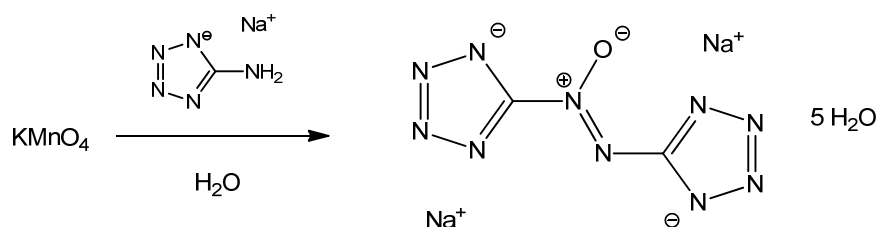


Figure 22. Formation of disodium 5,5'-azoxybistetrazolate pentahydrate from sodium 5-aminotetrazolate and potassium permanganate

The formation of the newly synthesized anion proceeds via a suggested mechanism involving the formation of 5-hydroxylaminotetrazole and 5-nitrosotetrazole and following condensation. The advantages of 5,5'-azoxybistetrazolates over 5,5'-azotetrazolates are a higher stability towards acids. This was proved by the isolation and structural characterization of a compound containing monodeprotonated 5,5'-azoxybistetrazole and additionally in an experiment adding 0.5 and 1.0 equivalents of 2M HCl to aqueous solutions of the disodium salts of 5,5'-azotetrazole and 5,5'-azoxytetrazole. The diammonium and the dihydroxylammonium salts of the new anion have better thermal stabilities compared to their non-oxidized analogs and furthermore a better explosive performance due to a better oxygen balance Ω after oxidation of the azo-bridge. Exemplarily, the detonation parameters of dihydroxylammonium 5,5'-azoxytetrazolate dihydrate (**22**) including the specific impulse, which is the most important parameter for materials in use as rocket propellants, are summarized in table 5 and compared to the energetic properties of the respective dihydroxylammonium 5,5'-azotetrazolate. The specific impulse was calculated assuming isobaric condition at a chamber pressure of 60 bar. Both compounds crystallize as dihydrates.

Table 5. *Energetic properties of **22** and dihydroxylammonium 5,5'-azotetrazolate dihydrate ($Hx_2zT \cdot 2 H_2O$)*

	22 · 2 H₂O	Hx₂zT · 2 H₂O
Formula	C ₂ H ₁₂ N ₁₂ O ₅	C ₂ H ₁₂ N ₁₂ O ₄
FW [g mol ⁻¹]	284.1	268.11
IS [J] ^a	30	25
FS [N] ^b	160	192
ESD-test [J] ^c	0.25	0.30
N [%] ^d	59.1	62.7
Ω [%] ^e	-28.2	-35.8
T _{dec.} [°C] ^f	175	130
Density [g cm ⁻³] ^g	1.596	1.615
$\Delta_f H_m^\circ$ [kJ mol ⁻¹] ^h	+80.0	+94.0
$\Delta_f U^\circ$ [kJ kg ⁻¹] ⁱ	+406	+478
<i>Detonation parameters calculated with EXPLO5.05:</i>		
$-\Delta_E U^\circ$ [kJ kg ⁻¹] ^j	4723	4271
T _E [K] ^k	3309	3020
p _{C-J} [kbar] ^l	258	254
D [m s ⁻¹] ^m	8224	8200
Gas vol. [L kg ⁻¹] ⁿ	893	892
I _s [s] ^o	234	218

^a impact sensitivity (BAM drophammer, 1 of 6); ^b friction sensitivity (BAM friction tester, 1 of 6); ^c electrostatic discharge device (OZM); ^d nitrogen content; ^e oxygen balance; ^f decomposition temperature from DSC ($\beta = 5^\circ\text{C}$); ^g estimated from X-ray diffraction; ^h calculated (CBS-4M) heat of formation; ⁱ calculated energy of formation; ^j energy of explosion; ^k explosion temperature; ^l detonation pressure; ^m detonation velocity; ⁿ assuming only gaseous products; ^o specific impulse calculated at isobaric (60 bar, frozen expansion) rocket conditions.

PYROTECHNICS

In the field of coloring agents for pyrotechnical formulation, amongst other salts, the alkaline earth metal salts strontium (**23**) and barium 5,5'-bistetrazolate (**24**) (figure 23) for red and green light emitting formulations were investigated [13].

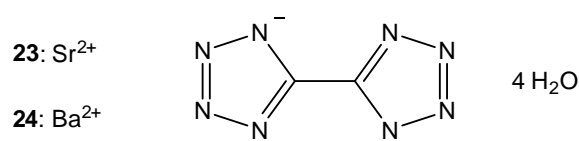


Figure 23. Lewis structures of strontium- (**23**) and barium 5,5'-bistetrazolate (**24**)

The formulation with the best color performance (COMP1) as evaluated by subjective impression, contains 35 % of **23**, 40 % NH_4NO_3 , 18 % Mg and 7 % VAAR (vinyl alcohol acetate resin, a binder). With regard to the formation of smoke, which preferably should be avoided to reduce the signature of the ignited mixture, the best performing formulation (COMP2) contained 40 % of **24**, 44 % NH_4NO_3 , 9 % B and 7 % VAAR. The flame colors of both formulations are shown in figure 24.



Figure 24. Flame colors of COMP1 and COMP2

The decomposition temperatures of all investigated alkaline earth metal salts of 5,5'-bistetrazole (Be-Ba) are higher than 400 °C. Another trend observed in this row is a rapidly decreasing water solubility with increasing molecular weight of the cation. In this context, the beryllium salt plays a special role, since, against expectations from the above mentioned trend, its solubility in water is comparable to that of the barium salt. A possible explanation for this behavior could be the same argumentation as it is applied for diagonal relationships in the periodic table saying that lithium salts behave like magnesium salts rather than the other alkali metal salts or beryllium salts behave like aluminum salts rather than other alkaline earth metal salts because of the similar charge to diameter ratio of the diagonally related ions.

DIAZO TRANSFER REAGENTS

A large part of compounds, which in figure 7 is listed under intermediates, reagents etc. is a class of ionic imidazole-1-sulfonyl azides bearing different anions [20]. Neutral imidazole-1-sulfonyl azide, which under ambient conditions is a liquid, as well as its solid hydrochloride

salt are used as diazotransfer reagents to convert organic amines into azides. Several accidents worldwide, which happened when drying or handling these extremely friction and impact sensitive reagents, gave reason to put efforts in finding safer alternatives. These alternatives were found in the hydrogensulfate salt (**25**) as well as the tetrafluoroborate salt (**26**) of imidazole-1-sulfonyl azide (figure 24).

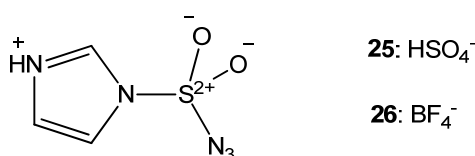


Figure 24. Lewis structures of 3-azidosulfonyl-3H-imidazol-1-ium hydrogen sulfate (**25**) and 3-azidosulfonyl-3H-imidazol-1-ium tetrafluoroborate (**26**)

Compared to the neutral species and its hydrochloride salt, these compounds also have higher decomposition temperatures, which makes it safer to dry the materials since they often have to be used in dry solvents. The efficiency of the newly synthesized salts **25** and **26** in a diazotransfer reaction converting p-amino benzoic acid to p-azidobenzoic acid was found to be equal to the efficiency of the neutral species or its hydrochloride salt respectively. Another major concern, which necessitated an alternative to the neutral species and its hydrochloride salt is their poor shelf stability. Imidazole-1-sulfonyl azide and its hydrochloride decompose on standing at ambient conditions releasing hydrazoic acid, which results in the formation of a brown, viscous liquid of doubtful composition and presumably with high sensitivities. The hydrogensulfate salt **25** and to greater extent the tetrafluoroborate salt **26** can be stored under ambient conditions for several months without decomposition. The sensitivity data as well as the decomposition temperatures of the discussed compounds are gathered in table 6.

Table 6. Sensitivity data and decomposition temperatures of imidazole-1-sulfonyl azide (ImSO_2N_3) and selected salts thereof

	<i>IS (J)</i>	<i>FS (N)</i>	<i>ESD (J)</i>	<i>T_{dec} (°C)</i>
ImSO_2N_3	<1	72	-	112
$\text{ImSO}_2\text{N}_3 \cdot \text{HCl}$	6	240	0.50	102
$\text{ImSO}_2\text{N}_3 \cdot \text{H}_2\text{SO}_4$ (25)	40	240	0.30	131
$\text{ImSO}_2\text{N}_3 \cdot \text{HBF}_4$ (26)	40	240	0.50	146

References (conclusion)

- ¹ R. A. Henry, W. G. Finnegan, *J. Am. Chem. Soc.* **1954**, 76, 923-926.
- ² I. A. Ugryumov, M. A. Ilyushin, I. V. Tselinskii, A. S. Kozlov, *Russ. J. Appl. Chem.* **2003**, 76(3), 439-441.
- ³ J. Thiele, *Justus Liebigs Ann. Chem.*, **1889**, 303, 57-75.

APPENDIX

The following appendix contains a full list of manuscripts, which were published within the scope of this dissertation. These manuscripts have almost completely been published in peer-reviewed journals and are subject to copyrights, therefore they have been reproduced with permission of the corresponding publisher. Furthermore a bibliography is attached. The publications are listed chronologically according to the year of publication without changing the format of the respective scientific journal. Supporting information of the respective publications is not printed in this thesis but available via the web pages of the publishers. If additional information is published in the internet, a link is given in the articles under “supporting information” or “supplementary information”.



Hydrazinium 5-Aminotetrazolate: an Insensitive Energetic Material Containing 83.72% Nitrogen

Niko FISCHER, Thomas M. KLAPÖTKE*,
Susanne SCHEUTZOW and Jörg STIERSTORFER

*Munich, Department of Chemistry and Biochemistry,
Ludwig-Maximilian University Munich*

**E-mail: tmk@cup.uni-muenchen.de*

Abstract: Hydrazinium 5-aminotetrazolate (**2**) was synthesized via two facile routes. Both the reaction of 5-amino-1*H*-tetrazole (**1**) with hydrazine hydrate in aqueous solution and the reaction of **1** with diluted hydrazine solution in THF yield **2** in excellent purities and yields. **2** was characterized comprehensively by X-ray diffraction, IR, Raman and multinuclear NMR spectroscopy, mass spectrometry, elemental analysis and differential scanning calorimetry. The heat of formation was calculated (CMS-4M) using the atomization method to be 373 kJ mol⁻¹. With this value and the X-ray density several detonation parameter (heats of explosion, detonation pressure, detonation velocity, explosion temperature) were calculated with the EXPLO5 computer software. An incredible high value (9516 m s⁻¹) was obtained for the detonation velocity. Therefore experimentally tests to determine the velocity of detonation were performed. In addition the use of **2** in solid propellant compositions was calculated and tested in combination with oxidizers, e.g. ammonium dinitramide. Lastly the sensitivities towards impact, friction and electrostatic discharge were determined with the BAM drophammer, friction tester and an ESD machine.

Keywords: hydrazines, tetrazoles, crystal structure, energetic materials, sensitivities

Introduction

The investigation of energetic, non-nuclear materials for military and space application has been a long term goal in our research group [1]. One approach is the synthesis of high-nitrogen salts which combine a positive heat of formation

($\Delta_f H > 0$) and therefore high explosive and propulsive power with relatively high thermal stability and low volatility and therefore low inhalation toxicity [2, 3]. Future energetic materials should be insensitive, e.g. towards impact, friction and electrical discharge. Usually salts with a nitrogen content above 80% show definite sensitivities. However, these values strongly depend on the constitution of the atoms and cannot be correlated to the nitrogen content. Figure 1 gives an overview about selected CHN compounds based on tetrazoles with their N-content and the determined impact sensitivities. As a matter of principle electron-rich tetrazoles and tetrazolates show lower sensitivities than those, which are bonded to electron withdrawing groups. This is the reason that **1** as well as **2** are insensitive towards impact [4]. In contrast 1*H*-tetrazole and hydrazinium 5,5'-azotetrazolate show increased impact sensitivities of 1 J and 4 J, respectively [5, 6]. The bistetrazoles HBT (**4**) and H₂bta (**8**) are characterized by moderate impact sensitivities of 30 J [7, 8]. However, 1,5-bistetrazole (**6**) is extremely sensitive towards impact and friction, which can be lowered by deprotonation, e.g. forming ammonium 1,5-bistetrazolate (**7**) [9]. Extremely sensitive are salts of 5-azidotetrazolate, e.g. guanidinium 5-azidotetrazolate (**9**) [10].

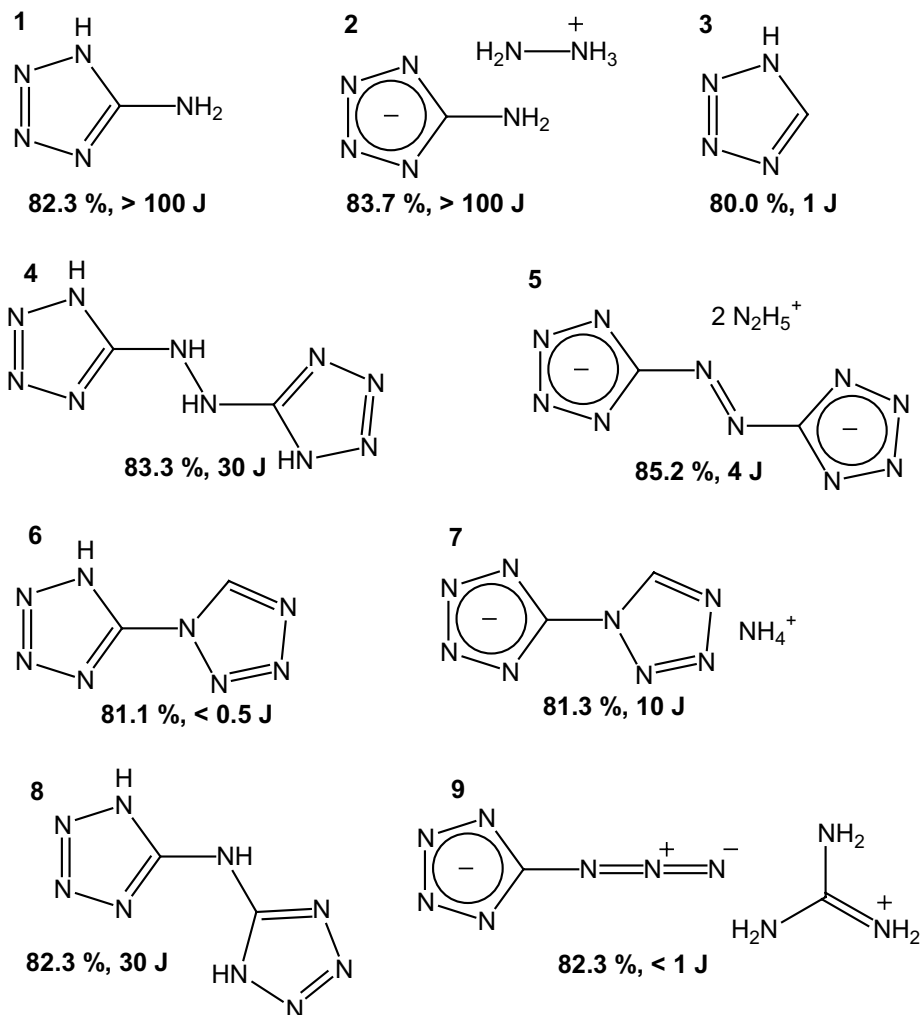


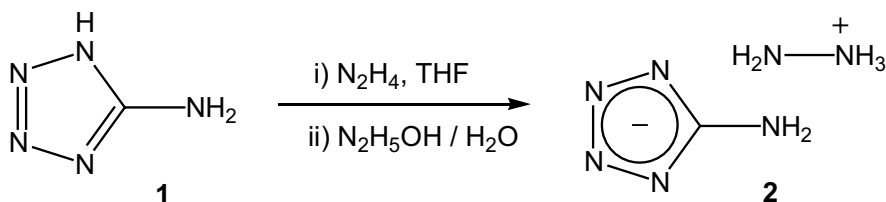
Figure 1. Tetrazole derivatives with a nitrogen content above 80%. **1:** 5-amino-1*H*-tetrazole, **2:** hydrazinium 5-aminotetrazolate, **3:** 1*H*-tetrazole, **4:** BTH, bis(1*H*-tetrazolyl)hydrazine, **5:** hydrazinium azotetrazolate, **6:** 1,5-bistetrazole, **7:** ammonium 1,5-bistetrazolate, **8:** H₂bta, 5,5'-bis(1*H*-tetrazolyl)amine, **9:** guanidinium 5-azidotetrazolate.

The motivation of this study is the insensitivity of **2** in combination with an extraordinarily high calculated detonation pressure and velocity, even succeeding those of HMX. Here we report on an easy one-step synthesis of hydrazinium

aminotetrazolate (**2**), a full characterization as well as its detonation and propulsion parameters.

Synthesis

Hydrazinium 5-aminotetrazolate can be synthesized via two facile routes. (i) The synthesis under exclusion of water by the reaction of 5-amino-1*H*-tetrazole (**1**) with hydrazine in THF yields **2** in high purity and yield. **2** is recrystallized from hot ethanol yielding colorless needle shaped crystals which can be washed with diethyl ether. (ii) Also possible is the reaction of **1** or its monohydrate with hydrazine hydrate in water or in alcoholic (MeOH, EtOH) solutions.



Scheme 1. Two synthetic protocols of the formation of hydrazinium 5-aminotetrazolate (**2**).

Structure

A suitable single crystal was picked from the crystallization mixture, mounted in Kel-F oil and transferred to the N₂ stream of an Oxford Xcalibur3 diffractometer with a Spellman generator (voltage 50 kV, current 40 mA) and a KappaCCD detector. The data collection was performed using the CrysAlis CCD software [11], the data reduction with the CrysAlis RED software [12]. The structure was solved with SIR-92, refined with SHELXL-97 [13] and finally checked using the PLATON software [14]. All programs are implemented in the WinGX suite [15]. The non-hydrogen atoms were refined anisotropically and the hydrogen atoms were located and freely refined. The absorption was corrected by a SCALE3 ABSPACK multi-scan method [16]. All relevant data and parameters of the X-ray measurements and refinements are given in Table 1. Further information on the crystal-structure determinations have been deposited as cif file [17] with the Cambridge Crystallographic Data Centre [18] as supplementary publication No. 697710.

Table 1. X-ray data and parameter for **2**

	2
Formula	CH ₇ N ₇
Form. weight [g mol ⁻¹]	117.14
Crystal system	orthorhombic
Space Group	<i>P</i> 2 ₁ 2 ₁ 2 (No. 18)
Color / Habit	colorless needles
Size, mm	0.04 x 0.09 x 0.09
<i>a</i> [Å]	9.7179(6)
<i>b</i> [Å]	13.5958(8)
<i>c</i> [Å]	3.8056(3)
<i>V</i> [Å ³]	502.81(6)
<i>Z</i>	4
ρ _{calc.} [g cm ⁻³]	1.547
μ [mm ⁻¹]	0.122
<i>F</i> (000)	248
λ _{MoKα} [Å]	0.71073
<i>T</i> [K]	200
Theta Min-Max [°]	3.7, 31.5
Dataset	-9:14; -19:19; -5:5
Reflection collected	3815
Independent reflection	1013
<i>R</i> _{int}	0.065
Observed reflection	522
No. parameters	101
<i>R</i> ₁ (obs)	0.0398
w <i>R</i> ₂ (all data)	0.0778
GooF	0.85
Min/Max Resd. [e/ Å ³]	-0.26, 0.20
Device type	Oxford Xcalibur CCD
Solution	SIR-92
Refinement	SHELXL-97
Absorption correction	multi-scan
CCDC No.	697710

Hydrazinium 5-aminotetrazolate (**2**) crystallizes as correctly published in 1958 [19] in the chiral orthorhombic space group *P*2₁2₁2 with four molecules in the unit cell. However, in the previously solved structure no hydrogen atoms

have been located. Therefore a short reinvestigation is given in this work. The density of **2** was calculated to be 1.547 g cm^{-3} . The planar tetrazolate ring system, which can be seen in Figure 2 is comparable to other 5-aminotetrazolates e.g. triaminoguanidinium 5-aminotetrazolate or alkali 5-aminotetrazolate salts in the literature [20, 21]. The bond lengths and angles are also in the range of those found in neutral 5-aminotetrazole monohydrate [4]. The NH_2 protons of the anion do not follow the planarity of the ring system and are angulated showing torsion angles of $\text{N1-C1-N5-H5a} = 31.32(16)^\circ$ and $\text{N4-C1-N5-H5b} = 24.07(15)^\circ$. The hydrazine bond with an distance of $1.455(3) \text{ \AA}$ fits exactly to value observed for other tetrazole hydrazinium structures in literature, e.g. dihydrazinium bis(tetrazolato)hydrazine [23] and dihydrazinium azotetrazolate [24].

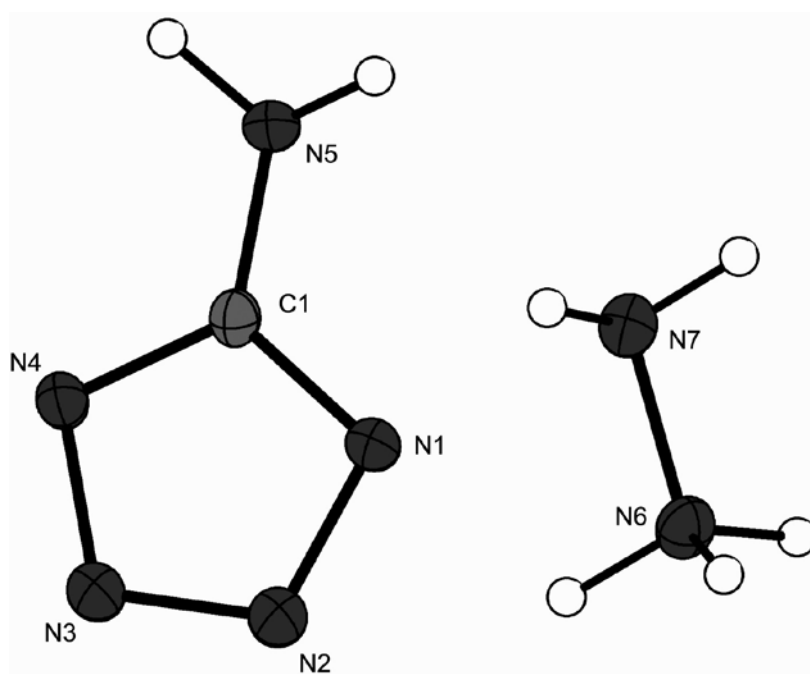


Figure 2. Formula unit of **2** with its labelling scheme. Hydrogen atoms shown as spheres of arbitrary radius and thermal displacements set at 50% probability.

2 forms an extensive hydrogen bond network, which could be the reason for the stability and low sensitivities. All nitrogen atoms of the anions (depicted in Figure 3) as well of the hydrazinium cations participate in hydrogen bonds.

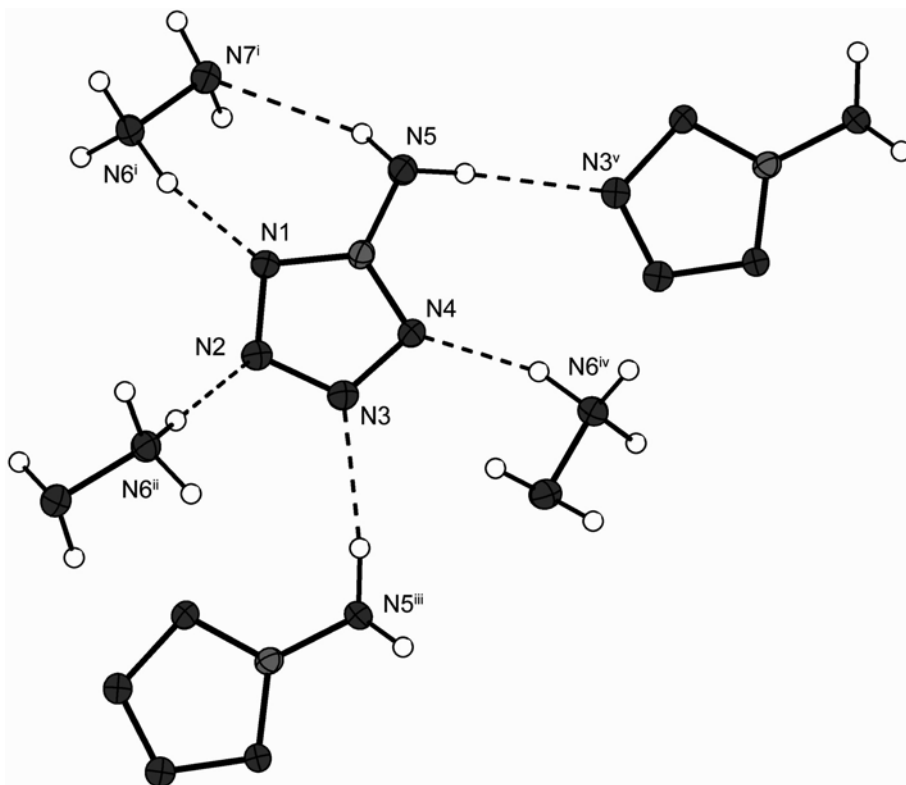


Figure 3. View of the hydrogen bonds of one 5-aminotetrazolate anion. i: $x, y, 1+z$; ii: $1-x, -y, z$; iii: $-0.5+x, 0.5-y, 1-z$; iv: $1.5-x, 0.5+y, -z$; v: $0.5+x, 0.5-y, 1-z$.

Detonation experiments

Theoretical calculations

The enthalpies and free energies of formation were calculated using the CBS-4M method [25, 26] implemented in G03W [27] combined with the atomization energy procedure [28-30]. The lattice energies were estimated according to Jenkins et al. [31-33]. For compound **2** the following energies and enthalpies of formation were calculated:

$$\Delta_f H^\circ(\mathbf{2}, s) = +373.2 \text{ kJ mol}^{-1},$$

$$\Delta_f U(\mathbf{2}, s) = +3333.6 \text{ kJ kg}^{-1}.$$

The detonation parameters were calculated using the EXPLO5 computer program [34]. The program is based on the chemical equilibrium, steady-state

model of detonation. It uses the Becker-Kistiakowsky-Wilson's equation of state (BKW EOS) for gaseous detonation products and Cowan-Fickett's equation of state for solid carbon [35-39]. The calculation of the equilibrium composition of the detonation products is done by applying modified White, Johnson and Dantzig's free energy minimization technique. The program is designed to enable the calculation of detonation parameters at the CJ point. The BKW equation in the following form was used with the BKWN set of parameters (α , β , κ , θ) as stated below the equations and X_i being the mol fraction of i -th gaseous product, k_i is the molar covolume of the i -th gaseous product [35-39]:

$$pV / RT = 1 + xe^{\beta x} \quad x = (\kappa \sum X_i k_i) / [V(T + \theta)]^\alpha$$

$$\alpha = 0.5, \beta = 0.176, \kappa = 14.71, \theta = 6620.$$

The detonation parameters calculated with the EXPLO5 program using the experimentally determined density (X-ray) are summarized in Table 2.

Table 2. Calculated detonation parameters for compound **2**

	$[\text{N}_2\text{H}_5]^+[\text{CH}_2\text{N}_5]^-$ (2)
ρ / g cm ⁻³	1.547
Ω / %	-75.1
Q_v / kJ kg ⁻¹	-4295
T_{ex} / K	2759
P / kbar	296
D / m s ⁻¹	9516
V_0 / L kg ⁻¹	959

ρ = density, Ω = oxygen balance, Q_v = heat of detonation, T_{ex} = detonation temperature, P = detonation pressure, D = detonation velocity, V_0 = Volume of detonation gases bar.

Experimental study

In order to evaluate the detonation velocity and the initiation properties of compound **2** experimentally, it was prepared on a 100 g scale. The detonation velocity tests were performed in an OZM laboratory detonation chamber (model KV-250). The measurement of the detonation velocity was performed using the OZM detonating velocity measuring system EXPLOMET-FO-2000. The use of the fiber optic technique insures excellent electrical noise immunity (Figure 4). The system used had five independent timers measuring the time intervals (in μs) between the illumination of two adjacent optical probes and calculated the velocity of detonation (m s⁻¹). The WinExplomet software package was used to transfer the results to a PC via a serial interface. For the detonation velocity

measurement a 14 mm PE tube was equipped with two optical fibers in a distance of 2 cm. The amount of compound **2** used for the test was 15 g. The compound was loaded into the PE tube and manually compressed with ca. 50 N. As a booster charge 2 g of nitropenta (PETN) were added on top and carefully compressed manually using ca. 20 N force. Initiation was achieved with an electrically ignited (40 V, 5 A) PETN-SAcN detonator (1 g PETN, 0.2 g silver acetylide nitrate).

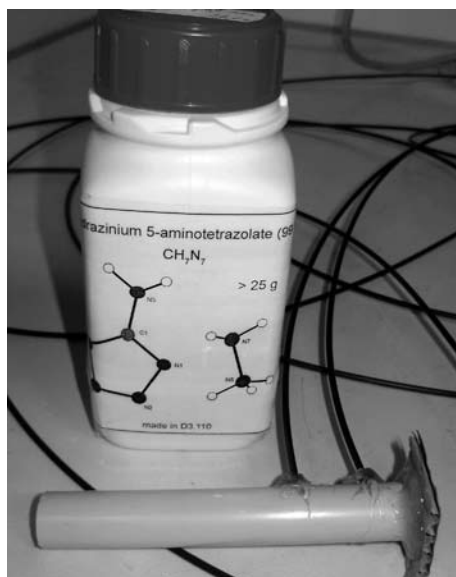


Figure 4. Setup for the determination of the velocity of detonation showing a plastic tube filled with **2**.

Although initiation of the detonator and the booster charge were achieved without any problems, compound **2** could not be initiated using this set up. This clearly shows the insensitivity of compound **2** towards initiation even when a PETN booster charge was used. Although one could try to initiate with a RDX booster charge, for practical applications the use of a detonator that has already been filled is always preferred.

Specific impulse

Energetic materials are most commonly used in either high explosives (HE) or propellant formulations. Whereas the performance of HEs can be related to heat of explosion (Q), detonation pressure (P) and detonation velocity (D), the performance of rocket/missile propellants is best characterized by their specific

impulse (I_{sp}) [2b]. Moreover, for gun propellants, erosivity is an additional concern and lower reaction temperatures and a high N_2/CO ratio of the reaction gases are desirable [40]. Equally important, an increase of the I_{sp} of only 20 s would be expected to increase the payload or range by ca. 100%. Moreover, smokeless combustion, which is an inherent feature of high-nitrogen compounds, is not only of environmental but particularly of strategic interest since location of the gun, missile or rocket is much more difficult.

In order to evaluate the properties of compound **2** as a potential energetic component in gun or missile propellants we calculated the specific impulses and combustion temperatures under isobaric conditions at 45 and 70 bar, representative for rocket and gun propellants, using the EXPLO5 code [35-39].

Table 3 summarizes the computed isobaric combustion temperatures (T_c , the lower the better for gun-propellants), the specific impulses (I_{sp}) and the molar N_2/CO ratios for mixtures of **2** with ADN and three typical conventional gun-propellants (single-, double-, triple-base) at 70 bar.

Table 3. Computed propulsion parameters for formulations of **2** with ADN and for single-, double- and triple-base propellants for comparison

O	F	ρ / g cm ⁻³	Ω / %	T_c / K	I_{sp} / s	N_2/CO
ADN ^a	Hy-At					
10	90	1.573	-65.0	1863	227	9.6
20	80	1.599	-55.0	1922	229	9.2
30	70	1.625	-44.9	2110	236	4.6
40	60	1.651	-34.8	2377	246	5.2
50	50	1.678	-24.7	2653	254	6.3
60	40	1.704	-14.6	2916	260	8.7
70	30	1.730	-4.5	3091	261	17.7
80	20	1.756	+5.6	2954	250	88.8
90	10	1.782	+15.7	2570	229	1440.0
NC ^b		1.66	-30.2	2750	232	0.3
NC ^b /NG (50:50)		1.63	-13.3	3287	248	0.7
NC ^b /NG ^c /NQ ^d (25:25:50)		1.70	-22.0	2663	235	1.4

^a ADN, ammonium dinitramide; ^b NC-13.3 (N content 13.3%); ^c NG, nitroglycerine; ^d NQ, nitroguanidine.

Whereas single-base propellants are used in all guns from pistols to artillery weapons, the more powerful (see I_{sp}) double-base propellants are commonly used in pistols and mortars [41]. The disadvantage of double-base propellants is the excessive erosion of the gun barrel (see N_2/CO ratio) by the much higher

flame temperatures, and the presence of a muzzle flash (fuel-air explosion of the combustion products). In order to reduce erosion and muzzle flash, triple-base propellants with up to 50% nitroguanidine are used in tank guns, large calibre guns and naval guns. However, the performance of triple-base propellants is lower than that of double-base propellants. A formulation of **2** with ADN (**2**:ADN = 40:60) shows a relatively low combustion temperature (comparable to single- and triple-base propellants), with excellent molar N₂/CO ratios (which are usually 0.5 for conventional propellants). The computed specific impulse for such a mixture make a possible application of **2** as promising energetic component in erosion-reduced gun propellants very interesting.

Table 4 summarized the propulsion parameters for formulations of **2** with ADN at 45 bar pressure and for a stoichiometric formulation of AP/Al which is presently used in large booster motors (e.g. ARIANE5, Space Shuttle).

Table 4. Computed propulsion parameters for formulations of **2** with ADN and for an AP/Al formulation for comparison

O	F	ρ / g cm ⁻³	Ω / %	T _c / K	I _{sp} / s
ADN ^a	Hy-At				
10	90	1.573	-65.0	1857	220
20	80	1.599	-55.0	1909	221
30	70	1.625	-44.9	2106	229
40	60	1.651	-34.8	2375	238
50	50	1.678	-24.7	2648	245
60	40	1.704	-14.6	2903	251
70	30	1.730	-4.5	3063	251
80	20	1.756	+5.6	2932	240
90	10	1.782	+15.7	2563	221
AP ^b	Al ^c				
70	30	2.178	-2.9	4199	232

^a ADN, ammonium dinitramide; ^b ammonium perchlorate, ^c aluminum.

A 60:40 mixture of **2** with ADN possesses a calculated specific impulse of 251 s which is ca. 20 s higher than that of a mixture of AP/Al commonly used in solid state boosters.

In conclusion, compound **2** is a new high nitrogen salt which may be suitable as a very powerful, low-erosion, smokeless (no signature) and environmentally benign high-nitrogen ingredient for gun-propellants and solid boosters.

Experimental part

CAUTION! Although hydrazinium 5-aminotetrazolate is an insensitive compound and we never had problems in synthesis proper protective measures such as plastic spatulas, leather jacket, helmet, Kevlar® gloves and earthened shoes should be used when working on larger scales.

5-Aminotetrazole (97%) was received from Aldrich, N_2H_4 (1M) in THF from Fluka and hydrazinium hydrate from Merck. Melting points were measured with a Linseis PT10 DSC [41] and checked with a Büchi Melting Point B-450 apparatus (uncorrected). DSC measurements were performed at a heating rate of $5\text{ }^\circ\text{C min}^{-1}$ in closed aluminum sample pans with a $1\text{ }\mu\text{m}$ hole in the top for gas release under a nitrogen flow of 20 mL min^{-1} with an empty identical aluminum sample pan as a reference. NMR spectra were recorded with a Jeol Eclipse 270, Jeol EX 400 or a Jeol Eclipse 400 instrument. All chemical shifts are quoted in ppm relative to TMS (^1H , ^{13}C) and MeNO_2 (^{14}N , ^{15}N). Infrared (IR) spectra were recorded using a Perkin-Elmer Spektrum One FT-IR instrument [42]. Transmittance values are qualitatively described as “very strong” (vs), “strong” (s), “medium” (m) and “weak” (w). Raman spectra were measured using a Perkin-Elmer Spektrum 2000R NIR FT-Raman instrument equipped with a Nd:YAG laser (1064 nm). The intensities are reported as percentages of the most intense peak and are given in parentheses. Elemental analyses were performed with a Netsch Simultaneous Thermal Analyzer STA 429.

Method 1: 5-Aminotetrazole (42.54 g, 0.5 mol) was suspended in 300 mL of THF (dry, over mol. sieves) and the suspension was heated to $50\text{ }^\circ\text{C}$. Hydrazine (1M in THF, 500 mL, 0.5 mol) was added in small portions under vigorous stirring. Insoluble hydrazinium 5-aminotetrazolate formed instantaneously as a white, flocculent precipitate in quantitative yields. After being stirred for further 5 minutes, the solid was filtered off and dried. The crude product was recrystallized from hot ethanol.

Method 2: 5-Aminotetrazole (42.54 g, 0.5 mol) was suspended in 100 mL water and heated to $50\text{ }^\circ\text{C}$. Hydrazinium hydrate (25.03 g, 0.5 mol) was added dropwise to the suspension until the 5-aminotetrazole was completely deprotonated and the solution was clear. The water was removed under reduced pressure and the crude product was recrystallized from ethanol.

DSC ($5\text{ }^\circ\text{C min}^{-1}$, $^\circ\text{C}$): $118 - 122\text{ }^\circ\text{C}$ (m.p.), $186\text{ }^\circ\text{C}$ (dec.); IR (KBr, cm^{-1}): $\tilde{\nu} = 3405$ (vs), 3351 (vs), 3290 (vs), 3195 (s), 2964 (s), 2721 (s), 2160 (m), 1630 (s), 1522 (s), 1442 (m), 1232 (m), 1106 (s), 1083 (s), 961 (m), 939 (m), 756 (w), 658 (w), 558 (w); Raman (1064 nm, 400 mW, $25\text{ }^\circ\text{C}$, cm^{-1}): $\tilde{\nu} = 3286$ (17), 3181 (21), 1630 (14), 1523 (56), 1452 (17), 1235 (55), 1116 (32), 1085

(30), 1064 (100), 1009 (17), 962 (22), 941 (30), 758 (29), 427 (25), 229 (30); ^1H NMR ($[\text{d}_6]$ -DMSO, 25 °C, ppm) δ : 7.43 (s); ^{13}C NMR ($[\text{d}_6]$ -DMSO, 25 °C, ppm) δ : 161.5(CN₄); ^{15}N NMR ($[\text{d}_6]$ -DMSO, 25 °C) δ = -8.0 (N1), -116.4 (N2), -332.0 (H₂N-NH₃⁺), -342.4 (N5); m/z (FAB⁺): 33 (100); m/z (FAB⁻): 84 (100); EA (CH₇N₇, 117.11): calcd.: C 10.26, H 6.02, N 83.72; found: C 10.65, H 5.72, N 83.85; BAM drophammer: 100 J; friction tester: >360 N, ESD: 3.0 J, Flame test: low flammable.

Acknowledgements

Financial support of this work by the Ludwig-Maximilian University of Munich (LMU), the Fonds der Chemischen Industrie (FCI), the European Research Office (ERO) of the U.S. Army Research Laboratory (ARL) and ARDEC (Armament Research, Development and Engineering Center) under contract nos. N 62558-05-C-0027, R&D 1284-CH-01, R&D 1285-CH-01, 9939-AN-01 & W911NF-07-1-0569 and the Bundeswehr Research Institute for Materials, Explosives, Fuels and Lubricants (WIWEB) under contract nos. E/E210/4D004/X5143 & E/E210/7D002/ 4F088 is gratefully acknowledged. The authors acknowledge collaborations Dr. M. Krupka (OZM Research, Czech Republic) in the development of new testing and evaluation methods for energetic materials and with Dr. M. Sucasca (Brodarski Institute, Croatia) in the development of new computational codes to predict the detonation parameters of high-nitrogen explosives. We are indebted to and thank Dr. Betsy M. Rice (ARL, Aberdeen, Proving Ground, MD) for many helpful and inspired discussions and support of our work.

References

- [1] (a) Klapötke T.M., Stierstorfer J., Nitration Products of 5-Amino-1H-Tetrazole and Methyl-5-Amino-1H-Tetrazoles - Structures and Properties of Promising Energetic Materials, *Helv. Chim. Acta*, **2007**, 90, 2132-2150; (b) Klapötke T.M., Steemann F.X., Sucasca M., Computed Thermodynamic and Explosive Properties of 1-Azido-2-Nitro-2-Azapropene (ANAP), *Propellants Explos., Pyrotech.*, **2008**, 33, 213-218; (c) Crawford M.-J., Evers J., Göbel M., Klapötke T.M., Mayer P., Oehlinger G., Welch J.M., γ -FOX 7: Structure of a High Energy Density Material Immediately Prior to Decomposition, *Propellants, Explos., Pyrotech.*, **2007**, 32, 478-495; (d) Karaghiosoff K., Klapötke T.M., Mayer P., Miró Sabaté C., Penger A., Welch J.M., Salts of Methylated 5-Aminotetrazoles with Energetic Anions, *Inorg. Chem.*, **2008**, 47(3), 1007-1019; (e) Klapötke T.M., Stierstorfer J., Synthesis and Characterization of the Energetic Compounds Aminoguanidinium-, Triaminoguanidinium- and

- Azidoformamidinium Perchlorate, *Centr. Europ. J. Energ. Mater.*, **2008**, 5(1), 13-30; (f) Klapötke T.M., Miró Sabaté C., Nitrogen-Rich Tetrazolium Azotetrazolate salts: A New Family of Insensitive Energetic Materials, *Chem. Mater.*, **2008**, 20(5), 1750-1763; (g) Klapötke T.M., Stierstorfer J., Triaminoguanidinium Dinitramide-Calculations, Synthesis and Characterization of Promising Energetic Materials, *Phys. Chem. Chem. Phys.*, **2008**, 10, 4340-4346; (h) Stierstorfer J., Klapötke T.M., Hammerl A., Chapman R.D., 5-Azido-1H-Tetrazole – Improved Synthesis, Crystal Structure and Sensitivity Data, *Z. Anorg. Allg. Chem.*, **2008**, 634, 1051-1057; (i) Klapötke T.M., Stierstorfer J., Wallek A.U., Nitrogen-Rich Salts of 1-Methyl-5-Nitriminotetrazolate: an Auspicious Class of Thermally Stable Energetic Materials, *Chem. Mater.*, **2008**, 20, 4519-4530; (j) Darwich C., Klapötke T.M., Miró Sabaté C., 1,2,4-Triazolium-Cation-Based Energetic Salts, *Chem. Eur. J.*, **2008**, 14, 5756-5771.
- [2] (a) Klapötke T.M., New Nitrogen-Rich High Explosives, in: *Structure and Bonding*, Vol. 125/2007: High Energy Density Compounds, T.M. Klapötke (vol. editor), Mingos D.M.P. (series editor), Springer, Berlin/Heidelberg **2007**, 85; (b) Klapötke T.M., Tetrazole for the Safe Detonation, *Nachrichten aus der Chemie*, **2008**, 56, 645-648.
- [3] Singh R.P., Gao H., Meshri D.T., Shreeve J.M., Nitrogen-Rich Heterocycles, in: *Structure and Bonding*, Vol. 125/2007: High Energy Density Compounds, Klapötke T.M. (vol. editor), Mingos D.M.P. (series editor), Springer, Berlin/Heidelberg **2007**, 35.
- [4] Ernst V., Klapötke T.M., Stierstorfer J., Alkali Salts of 5-Aminotetrazole: Structures and Properties, *Z. Anorg. Allg. Chem.*, **2007**, 633, 879-887.
- [5] Klapötke T.M., Stein M., Stierstorfer J., Salts of 1H-Tetrazole, *Z. Anorg. Allg. Chem.*, **2008**, in press.
- [6] (a) Hiskey M., Hammerl A., Holl G., Klapötke T.M., Polborn K., Stierstorfer J., Weigand J.J., Azidoformamidinium and Guanidinium 5,5'-Azotetrazolate Salts, *Chem. Mater.*, **2005**, 17, 3784-3793; (b) Hammerl A., Holl G., Klapötke T. M., Mayer P., Nöth H., Piotrowski H., Warchhold M., Salts of 5,5'-Azotetrazolate, *Eur. J. Inorg. Chem.*, **2002**, 4, 834-845.
- [7] Klapötke T.M., Miró Sabaté C., Bistetrazoles: Nitrogen-Rich, High-Performing, Insensitive Energetic Compounds, *Chem. Mater.*, **2008**, 20(11), 3629-3637.
- [8] Klapötke T.M., Mayer P., Stierstorfer J., Weigand J.J., Bistetrazolylamines - Synthesis and Characterization, *J. Mat. Chem.*, **2008**, accepted.
- [9] Klapötke T.M., Stierstorfer J., Recent Developments on Energetic Materials based on 5-Aminotetrazole, *New Trends in Research of Energetic Materials, Proc. of the 11th Seminar*, Pardubice, Czech Republic, **2008**, 1, 278-298.
- [10] Klapötke T.M., Stierstorfer J., *The CN₇ Anion. Gordon Research Conference*, **2008**, Tilton, NH, USA.
- [11] CrysAlis CCD, Oxford Diffraction Ltd., Version 1.171.27p5 beta (release 01-04-2005 CrysAlis171.NET), **2005**.
- [12] CrysAlis RED, Oxford Diffraction Ltd., Version 1.171.27p5 beta (release 01-04-

- 2005 CrysAlis171.NET), **2005**.
- [13] Altomare A., Cascarano G., Giacovazzo C., Guagliardi A., Completion and Refinement of Crystal Structures with SIR92, *J. Appl. Cryst.*, **1993**, 26, 343-350.
- [14] Sheldrick G.M., SHELXL-97, *Program for the Refinement of Crystal Structures*. University of Göttingen, Germany, **1997**.
- [15] Spek A.L., PLATON, A Multipurpose Crystallographic Tool, Utrecht University, Utrecht, The Netherlands, **1999**.
- [16] Farrugia L.J., Wingx Suite for Small Molecule Single Crystal Crystallography, *J. Appl. Cryst.*, **1999**, 32, 837-838.
- [17] SCALE3 ABSPACK - An Oxford Diffraction program (1.0.4,gui:1.0.3) (C) **2005**, Oxford Diffraction Ltd.
- [18] Hall S.R., Allen F.H., Brown I. D., The Crystallographic Information File (CIF): A New Standard Archive File for Crystallography, *Acta Crystallogr. A*, **1991**, 47, 655-685.
- [19] Crystallographic data for the structure(s) have been deposited with the Cambridge Crystallographic Data Centre. Copies of the data can be obtained free of charge on application to The Director, CCDC, 12 Union Road, Cambridge CB2 1EZ, UK (Fax: int.code_(1223)336-033; e-mail for inquiry: fileserv@ccdc.cam.ac.uk; e-mail for deposition: deposit-@ccdc.cam.ac.uk)
- [20] Bryden J.H., The Crystal Structure of the Hydrazine Salt of 5-Aminotetrazole, *Acta Cryst.*, **1958**, 11, 31-37.
- [21] Bracuti A.J., Troup J.M., Extine M.W.. Structure of Bis(1,2,3-Triaminoguanidinium) Bis(5-Aminotetrazolate) Monohydrate, *Acta Crystallogr. C*, **1986**, 42, 505-506.
- [22] Bray D.D., White J.G., Refinement of the Structure of 5-Aminotetrazole Monohydrate. *Acta Crystallogr. B*, **1979**, 35, 3089-3091.
- [23] Hammerl A., Holl G., Kaiser M., Klapötke T.M., Piotrowski H., Nitrogen Rich Materials: Salts of N,N'-Bistetrazolatohydrazine, *Z. Anorg. Allg. Chem.*, **2003**, 629, 2117-2121.
- [24] Hammerl A., Holl G., Kaiser M., Klapötke T.M., Nöth H., Ticmanis U., Warchhold M., [N₂H₅]⁺2[N₄C-N:N-CN₄]²⁻: A New High Nitrogen High Energetic Material, *Inorg. Chem.*, **2001**, 40, 3570-3575.
- [25] Ochterski J.W., Petersson G.A., Montgomery J.A. Jr., A Complete Basis Set Model Chemistry. V. Extensions to Six or More Heavy Atoms, *J. Chem. Phys.*, **1996**, 104, 2598-2619.
- [26] Montgomery J.A. Jr., Frisch M.J., Ochterski J.W., Petersson G.A., A Complete Basis Set Model Chemistry. VII. Use of the Minimum Population Localization Method, *J. Chem. Phys.*, **2000**, 112, 6532-6542.
- [27] Frisch M.J. et al., Gaussian 03, Revision B04, Gaussian Inc., Wallingford, CT, **2004**.
- [28] Curtiss L.A., Raghavachari K., Redfern P.C., Pople J.A., Assesment of Gaussian-2 and Density Functional Theories for the Computation of Enthalpies of Formation, *J. Chem. Phys.*, **1997**, 106(3), 1063-1079.
- [29] Byrd E.F.C., Rice B.M., Improved Prediction of Heats of Formation of Energetic

- Materials Using Quantum Mechanical Calculations, *J. Phys. Chem. A*, **2006**, *110*(3), 1005-1013.
- [30] Rice B.M., Pai S.V., Hare J., Predicting Heats of Formation of Energetic Materials Using Quantum Mechanical Calculations, *Combustion and Flame* **1999**, *118*(3), 445-458.
- [31] Jenkins H.D.B., Roobottom H.K., Passmore J., Glasser L., Relationships Among Ionic Lattice Energies, Molecular (Formula Unit) Volumes and Thermochemical Radii. *Inorg. Chem.*, **1999**, *38*(16), 3609-3620.
- [32] Jenkins H.D.B., Tudela D., Glasser L., Lattice Potential Energy Estimation for Complex Ionic Salts from Density Measurements, *ibid.*, **2002**, *41*(9), 2364-2367.
- [33] Jenkins H.D.B., Glasser L., Ionic Hydrates MpX_qnH_2O : Lattice Energy and Standard Enthalpy of formation Estimation, *ibid.*, **2002**, *41*(17), 4378-4388.
- [34] Sućeska M., *EXPLO5 program*, Zagreb, Croatia, **2005**.
- [35] Sućeska M., Calculation of Detonation Parameters by EXPLO5 Computer Program, *Materials Science Forum*, **2004**, 465-466, 325-330.
- [36] Sućeska M., Calculation of Detonation Properties of C-H-N-O Explosives, *Propellants, Explos., Pyrotech.*, **1991**, *16*, 197-202.
- [37] Sućeska M., Evaluation of Detonation Energy from EXPLO5 Computer Code Results, *ibid.*, **1999**, *24*, 280-285.
- [38] Hobbs M.L., Baer M.R., Calibration of the BKW-EOS with a Large Product Species Data Base and Measured C-J Properties, *Proc. of the 10th Symp. (International) on Detonation*, ONR 33395-12, Boston, MA, July 12-16, **1993**, p. 409.
- [39] Doherty R.M., Novel Energetic Materials for Emerging Needs, *9th -IWCP on Novel Energetic Materials and Applications*, Lerici (Pisa), Italy, September 14-18, **2003**.
- [40] *The Chemistry of Explosives*, 2nd edn., J. Akhavan, RSC Press (Cambridge) **2004**.
- [41] <http://www.linseis.com>
- [42] <http://www.perkin-elmer.com>

New Nitriminotetrazoles – Synthesis, Structures and Characterization

Niko Fischer,^[a] Thomas M. Klapötke,^{*[a]} and Jörg Stierstorfer^[a]

Keywords: Energetic Materials; Tetrazoles; Crystal structures; Detonation parameters; Sensitivities

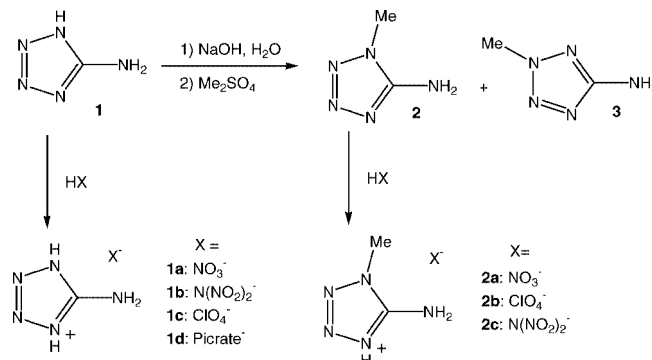
Abstract. The reactions of 5-nitriminotetrazole (**4**) with 1-methyl-5-aminotetrazole (**2**) as well as 2-methyl-5-aminotetrazole (**3**) were investigated. In the first reaction **2** was protonated yielding 1-methyl-5-aminotetrazolium 5-nitrimino-1*H*-tetrazolate monohydrate (**7**). In the latter case no protonation could be observed and a co-crystallization of 5-nitraminotetrazole and 2-methyl-5-aminotetrazole was obtained. In this compound a new tautomer of **4** could be found. Both products were determined by low temperature single crystal X-ray diffraction, IR, Raman and multinuclear (¹H, ¹³C, ¹⁵N) NMR spectroscopy, elemental analysis as well as differential scanning calorimetry. In addition the heats of formation were calculated using experimentally obtained heats of combustion.

With these and the X-ray densities several detonation parameter were computed using the EXPLO5 software. In addition the sensitivities towards impact, friction and electrostatic discharge were determined. Further, two crystal structures of the important starting materials in energetic research 5-nitriminotetrazole monohydrate (**4**·H₂O) and 1-methyl-5-nitriminotetrazolemonohydrate (**5**·H₂O) are presented and compared with the water-free compounds. The heats of formation of **4**, **4**·H₂O, **5**, **5**·H₂O have been calculated by the atomization method using the CBS basis set. Inclusion of crystal water decrease heats of formation about 265 kJ mol⁻¹. Also the influence of crystal water on sensitivities (impact, friction, electrostatic discharge) but also performance is discussed.

Introduction

The development of new energetic heterocyclic compounds has attracted considerable interest in recent years [1]. Generally the class of *energetic materials* is divided into two main groups, according to their different applications in military and civil sectors. These main groups are explosives and propellants. Due to their qualification profile the materials have to meet specific characteristics. Important criteria for the group of explosives are the detonation velocity v_D and the detonation pressure p_{C-J} . But also another criteria such as high densities ρ and large endothermic heats of formations ($\Delta_f H^\circ$) are required for effective energetic materials. In addition, new explosives should be cheap to synthesize, stable towards temperature, storable for long periods and of course safe to handle. Especially the syntheses and application of energetic nitrogen rich heterocyclic based salts is in the focus of many research programs worldwide [2–7]. Energetic materials based on salts often have advantages over non-ionic molecules since these salts tend to exhibit lower vapour pressure and higher densities than neutral derivatives. Tetrazoles, such as 5-amino-1*H*-tetrazole (**1**) have the outstanding property of often combining high densities, high heats of formation and high nitrogen con-

tents with low sensitivities and good thermal stabilities due to their aromatic rings system. Recently we described the synthesis and characterization of several highly energetic 5-aminotetrazolium salts, such as the nitrate [8, 9], dinitramide [10], perchlorate [11], and picrate [12]. Monomethylation of **1** [13] (or an alkali metal salt of it) is known to yield a mixture of 1-methyl-5-aminotetrazole (**2**) and 2-methyl-5-aminotetrazole (**3**) with the first one as the favoured isomer [14]. Both of these isomers also may be protonated by strong mineral acids, which has been already done using classic energetic and oxidizing anions such as ClO₄⁻, NO₃⁻, and N(NO₂)₂⁻ (Scheme 1) [15, 5h]. Salts of 5-nitrimino- or 5-nitramino-tetrazoles are of special interest because they combine both the oxidizer and energetic nitrogen-rich backbone in one molecule. We recently reported the syntheses, characterization and X-ray structures of the simple compounds 5-nitriminotetrazole (**4**), 1-methyl-5-ni-



Scheme 1. Synthesis of energetic 5-aminotetrazolium and 1-methyl-5-aminotetrazolium salts.

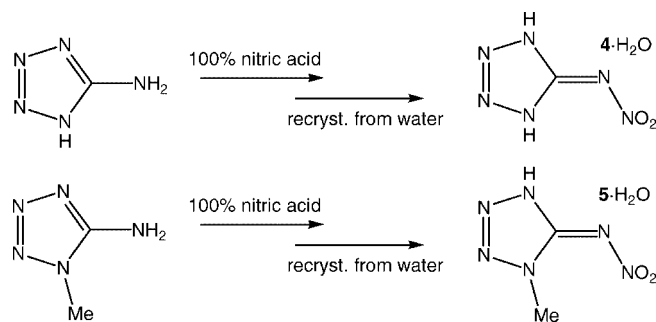
* Prof. Dr. T. M. Klapötke
E-Mail: tmk@cup.uni-muenchen.de
[a] Department of Chemistry and Biochemistry
Energetic Materials Research
Ludwig-Maximilian University
Butenandtstr. 5–13(D)
81377 München, Germany

triminotetrazole (**5**) and 2-methyl-5-nitraminotetrazole (**6**) [16]. **4–6** are popular starting materials in syntheses of new energetic materials. In this work the unknown structures of the monohydrates of **4** and **5** are presented. Since **4** as well as **5** are strong acids (**4** was characterized as a dibasic acid with pK_a values of 2.5 and 6.1) [17], they have also been used to form energetic nitrogen rich salts. Also the combination of two tetrazole derivatives (forming tetrazolium tetrazolates) is possible, which was shown by the formation of 5-aminotetrazolium 5-nitriminotetrazolate [2a]. Here we report on the reactions and products of 5-nitriminotetrazole in combination with 1-methyl- and 2-methyl-5-aminotetrazole.

Results and Discussion

Synthesis

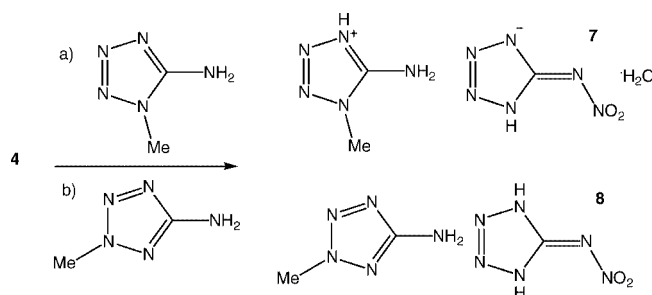
5-Nitriminotetrazole and 1-methyl-5-nitriminotetrazole were synthesized according to our recently described synthesis by the nitration of 5-amino-1*H*-tetrazole and 1-methyl-5-aminotetrazole using 100 % nitric acid (Scheme 2) [16]. Recrystallization from solvents such as ethanol, diethyl ether, acetone, THF, and also nitric acid yields water free crystals of **4** and **5**. Recrystallization from pure water yielded the monohydrates **4**·H₂O and **5**·H₂O. The compounds are neither hygroscopic nor sensitive towards light and air. However, the crystal water is being completely lost by simple standing at room temperature in an open vessel for a few weeks.



Scheme 2. Nitration of 5-aminotetrazole and 1-methyl-5-aminotetrazole.

The synthesis of 1-methylaminotetrazolium nitriminotetrazolate (**7**) and 2-methyl-5-aminotetrazole·5-nitriminotetrazole (**8**) was performed according to Scheme 3. 5-Nitriminotetrazole was dissolved in water and the 1-methyl-5-aminotetrazole and 2-methylaminotetrazole, respectively, was added. After heating the mixture and removing the solvent, both have been recrystallized from ethanol in good yields 77 % (**7**), 81 % (**8**). As shown in many studies, tetrazoles behave as weak bases [18–20]. They are protonated only in the media whose acidity can be described by the empiric scales of acidity function. In the case of weak bases the pK_{BH^+} value is a suitable criterion for the basicity. To the best of our knowledge, we could not find exact values for

1-methyl- and 2-methyl-5-aminotetrazole. However values are given for 1-methyl-5*H*-tetrazole ($\text{pK}_{\text{BH}^+} = -3.00$) and 2-methyl-5*H*-tetrazole (-3.25) as well as 1-methyl-5-aryl-tetrazole (-2.50) and 2-methyl-5-aryl-tetrazole (-3.27), which show that latter molecule is the weaker base and can therefore harder be protonated [21]. Also in DMSO solution no protonation is obtained, which can be seen clearly in the ¹³C NMR spectrum.



Scheme 3. Products of the reaction of 5-nitriminotetrazole with 1-methyl-5-aminotetrazole and 2-methyl-5-aminotetrazole, respectively.

Structures

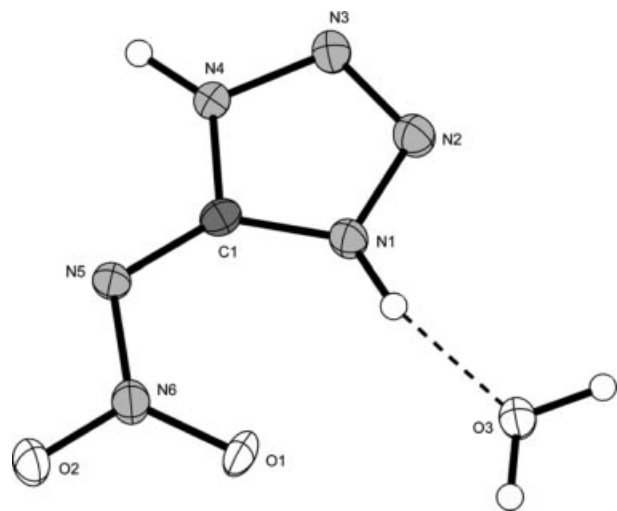
X-ray Diffraction Studies

Suitable single crystals of **4**·H₂O, **5**·H₂O, **7** and **8** were picked from the crystallization mixture and mounted in Kel-F oil on a glass fiber, which was transferred to the N₂ stream of Oxford Xcalibur3 diffractometer with a Spellman generator (voltage 50 kV, current 40 mA) and a KappaCCD detector. The data collection was performed using the Crys-Alis CCD software [22], the data reduction with the Crys-Alis RED software [23]. The structures were solved with Sir-92 (**4**·H₂O, **7**, **8**) [24], and SHELXS-97 (**7**) [25], refined with SHELXL-97 [26] and finally checked using the PLATON software [27], integrated in the WINGX software suite [28]. The non-hydrogen atoms were refined anisotropically and the hydrogen atoms were located and freely refined. The absorptions were corrected by a SCALE3 ABSPACK multi-scan method [29]. All relevant data and parameters of the X-ray measurements and refinements are given in Table 1. Further information on the crystal-structure determinations have been deposited with the Cambridge Crystallographic Data Centre [30] as supplementary publication No. 652904 (**4**·H₂O), 652905 (**5**·H₂O), 705789 (**7**) and 705790 (**8**).

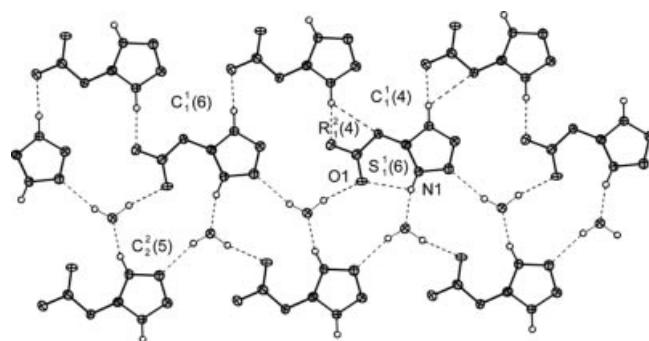
5-Nitriminotetrazole monohydrate (**4**·H₂O) crystallizes in agreement to its water-free analogue in the monoclinic space group *P*2₁/*c* with four molecules in the unit cell. The density of 1.808 g cm^{−3} is lower than that of water-free **4** (1.867 g cm^{−3}). However, the molecular geometry is very similar to that of **4**. Again both hydrogen atoms are located at the tetrazole ring. The nitrimine group follows the planarity (C1–N5–N6–O1 = $-1.1(2)^\circ$) and is fixed by an intramolecular H-bond (S1,1(6), N1–H1···O1: 0.90(2),

Table 1. Crystallographic data and parameter

	4 · H₂O	5 · H₂O	7	8
Formula	CH ₄ N ₆ O ₃	C ₂ H ₆ N ₆ O ₃	C ₃ H ₉ N ₁₁ O ₃	C ₃ H ₇ N ₁₁ O ₂
Form. Mass /g · mol ⁻¹	148.10	162.13	247.21	229.20
Crystal system	monoclinic	monoclinic	monoclinic	monoclinic
Space Group	<i>P</i> 2 ₁ / <i>c</i> (No. 14)	<i>P</i> 2 ₁ / <i>n</i> (No. 14)	<i>P</i> 2 ₁ / <i>c</i> (No. 14)	<i>P</i> 2 ₁ / <i>c</i> (No. 14)
Color / Habit	colorless rods	colorless rods	colorless rods	colorless rods
Size /mm	0.11 x 0.16 x 0.18	0.08 x 0.13 x 0.17	0.06 x 0.14 x 0.17	0.05 x 0.10 x 0.10
<i>a</i> /Å	8.4443(5)	9.8838(6)	7.1470(6)	14.7640(6)
<i>b</i> /Å	8.7433(5)	5.4265(3)	7.3979(6)	9.1430(6)
<i>c</i> /Å	7.4478(4)	12.3380(7)	19.8509(2)	6.810(1)
β /°	98.395(5)	97.888(6)	100.291(7)	92.161(7)
<i>V</i> /Å ³	543.99(5)	655.48(7)	1032.69(15)	918.61(18)
<i>Z</i>	4	4	4	4
$\rho_{\text{calc.}}$ /g · cm ⁻³	1.808	1.643	1.590	1.657
μ /mm ⁻¹	0.168	0.148	0.137	0.139
<i>F</i> (000)	304	336	512	472
$\lambda_{\text{MoK}\alpha}$ /Å	0.71073	0.71073	0.71073	0.71073
<i>T</i> /K	100	200	200	200
τ min-max /°	4.1, 26.3	4.1, 25.8	4.3, 25.5	3.7, 26.0
Dataset <i>h</i> ; <i>k</i> ; <i>l</i>	−10; 7; −8; 10; −7; 9	−12; 11; −4; 6; −15; 14	−8; 8; −8; 8; −24; 23	−18; 18; −11; 11; −8; 5
Reflect. coll.	2833	3141	9653	4640
Independ. refl.	1096	1249	1912	1804
<i>R</i> _{int}	0.025	0.039	0.029	0.041
Reflection obs.	672	691	1777	1003
No. parameters	107	124	190	173
<i>R</i> ₁ (obs)	0.0326	0.0356	0.0432	0.0321
<i>wR</i> ₂ (all data)	0.0746	0.0740	0.1180	0.0716
<i>S</i>	0.88	0.81	1.14	0.85
Resd. Dens. /e · Å ⁻³	−0.29, 0.17	−0.24, 0.19	−0.22, 0.23	−0.19, 0.15
Device type	Oxford Xcalibur3 CCD	Oxford Xcalibur3 CCD	Oxford Xcalibur3 CCD	Oxford Xcalibur3 CCD
Solution	SIR-92	SHELXS-97	SIR-92	SIR-92
Refinement	SHELXL-97	SHELXL-97	SHELXL-97	SHELXL-97
Absorpt. corr.	multi-scan	multi-scan	multi-scan	multi-scan
CCDC	652904	652905	705789	705790

**Figure 1.** Molecular moiety of **4 · H₂O**. Ellipsoids of non-hydrogen atoms are drawn at the 50 % probability level.

2.23(2), 2.588(2) Å, 103(1)°). The C1–N5 bond length is 1.340(2) Å, which is closer to a C=N double bond (1.28 Å) than a C–N single bond (1.46 Å) [31] where as the nitramine bond N5–N6 is considerably longer (1.363(1) Å). The exact bond lengths and angles of both compounds are given in Table 2 and 3.



furcated hydrogen bond with the graph set **R2,1(4)** can be detected including the nitrime atoms N5 and O2 as double acceptor system.

The molecular structure of 1-methyl-5-nitriminotetrazole monohydrate (**5**·H₂O) is shown in Figure 3. It crystallizes in the monoclinic space group *P*2₁/*n* with four molecules in the unit cell. The density of 1.643 g cm^{−3} is also lower than this observed for water-free **5** (1.755 g cm^{−3}), which crystallizes orthorhombic (*P*2₁2₁2₁). The molecular geometry is similar to this observed for water-free **5**. Again the nitro group is only slightly shifted out from the tetrazole ring plane (N4–C1–N5–O1 = 10.9(3)°, but also directed by the intramolecular H-bond N1–H1···O1 (0.96(2), 2.26(2), 2.621(2) Å, 101(2)°). The water molecule is coordinated via the H-bond N4–H4···O3 (0.96(3), 1.67(3), 2.607(2), 165(3)°) to the proton located at ring nitrogen atom N4.

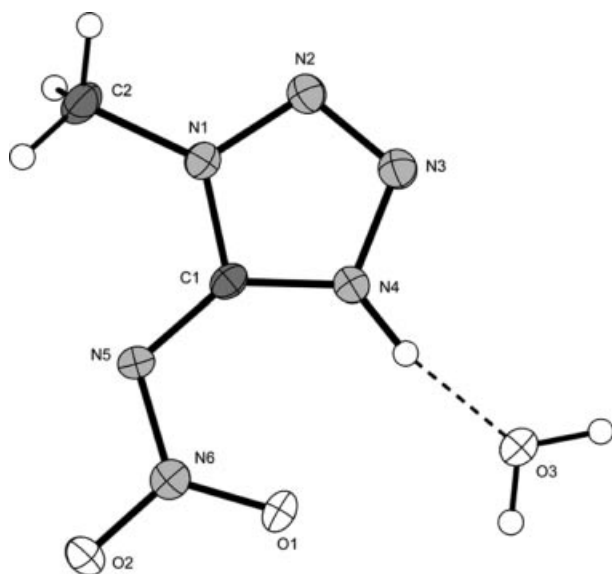


Figure 3. Molecular moiety of **5**·H₂O. Ellipsoids of non-hydrogen atoms are drawn at the 50 % probability level.

In accordance to the water-free structure of **5**, also in the packing of **5**·H₂O the formation of an 3-dim network can be observed. In Figure 4 the hydrogen bonds are depicted. Only the ring nitrogen atoms N1 participate in the hydrogen bonds. In addition nitrogen atom N5 is takes part in a weak hydrogen bond. This may be a reason for the lower density observed in this structure.

1-Methylaminotetrazolium 5-nitriminotetrazolate hydrate (**7**) crystallizes in the monoclinic space group *P*2₁/*c* with a calculated density of 1.590 g cm^{−3}. The complete molecular moiety is build planar and depicted in Figure 5. The coordination of the 1-methyl-5-aminotetrazolium cation is in agreement with those observed for e.g. 1-methyl-5-aminotetrazolium nitrate or dinitramide [5h, 5f]. Within the 5-nitriminotetrazolate anions a intramolecular hydrogen bond (N4–H4···O2 = 0.89(2), 2.32(2), 2.661(2) Å, 102(2)°, graph set **S1,1(6)**) stabilizes the planar structure, which was also observed in the structures of **4** and **4**·H₂O.

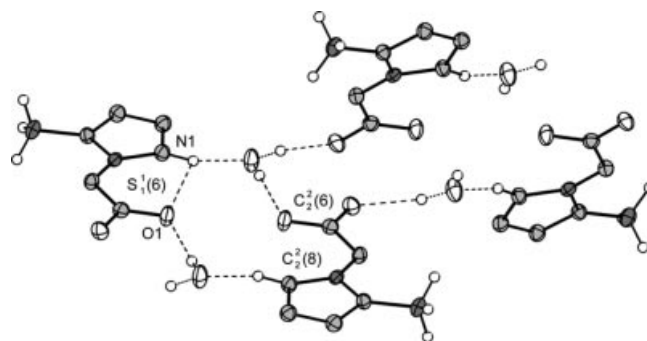


Figure 4. View on the hydrogen bond network in the layers of **5**·H₂O.

Selected hydrogen bonds /Å, °: O3–H3A···O1ⁱ = 0.83(3), 2.07(3), 2.895(2), 172(2); O3–H3B···O2ⁱⁱ = 0.91(3), 1.95(3), 2.836(2), 165(2); O3–H3B···N5ⁱⁱⁱ = 0.91(3), 2.56(3), 3.296(2), 139(2); (i) 2–x, –y, 1–z; (ii) 0.5+x, 0.5–y, 0.5+z.

Table 2. Bond lengths /Å of **4**, **4**·H₂O, **8**, **5** and **5**·H₂O.

Atoms	4	4 ·H ₂ O	8	5	5 ·H ₂ O
O2–N6	1.234(1)	1.251(2)	1.228(2)	1.234(2)	1.224(2)
O1–N6	1.237(1)	1.249(2)	1.228(2)	1.266(2)	1.217(2)
N1–N2	1.358(1)	1.362(2)	1.355(2)	1.355(2)	1.327(2)
N1–C1	1.341(1)	1.340(2)	1.325(2)	1.345(2)	1.325(2)
N4–C1	1.336(1)	1.337(2)	1.318(2)	1.338(2)	1.339(2)
N4–N3	1.352(1)	1.351(2)	1.370(2)	1.364(2)	1.321(2)
N2–N3	1.278(1)	1.280(2)	1.286(2)	1.284(2)	1.318(2)
N5–N6	1.363(1)	1.335(2)	1.343(2)	1.338(2)	1.379(2)
N5–C1	1.341(1)	1.350(2)	1.386(2)	1.346(2)	1.397(2)
N1–C2				1.455(2)	1.459(2)

Table 3. Bond angles /° of **4**, **4**·H₂O, **8**, **5** and **5**·H₂O.

Atoms	4	4 ·H ₂ O	8	5	5 ·H ₂ O
N2–N1–C1	109.87(9)	109.1(1)	107.9(1)	110.4(1)	110.4(2)
C1–N4–N3	110.5(1)	110.7(1)	103.7(1)	110.2(1)	110.2(2)
N1–N2–N3	107.97(9)	108.7(1)	105.9(1)	107.8(1)	107.8(2)
N6–N5–C1	115.43(9)	115.0(1)	122.0(2)	115.7(1)	114.9(2)
N2–N3–N4	107.73(9)	107.2(1)	112.1(1)	107.7(1)	107.7(2)
O1–N6–O2	123.5(1)	121.3(2)	125.8(2)	121.6(1)	121.4(2)
O1–N6–N5	122.07(9)	122.8(1)	118.9(2)	121.9(1)	123.0(2)
O2–N6–N5	114.44(9)	116.0(1)	115.3(2)	116.5(1)	115.6(2)
N4–C1–N1	103.9(1)	104.4(2)	110.5(2)	103.9(1)	103.8(2)
N4–C1–N5	121.4(1)	120.1(2)	120.1(2)	136.9(1)	137.1(2)
N1–C1–N5	134.6(1)	135.4(2)	129.4(2)	119.2(1)	119.1(2)

The packing of **7** is characterized by the formation of layers along the b axis. The layers have distances of ca. 3.25 Å. Within the layers a distinctive hydrogen bond network is formed which is illustrated in Figure 6. Several graph sets, e.g. **S1,1(6)**, **R2,1(4)**, **R2,2(8)**, **R2,2(10)**, **R4,4(10)**, **C1,2(6)**, **C2,2(5)**, **C2,2(5)** and **C2,2(8)** are drawn.

2-Methylaminotetrazole·5-nitriminotetrazole (**8**) crystallizes in the monoclinic space group *P*2₁/*c* with a higher calculated density of 1.657 g cm^{−3} in comparison to **7**. As previously described the reaction of 5-nitriminotetrazole with 2-methyl-5-aminotetrazole does not yield in the formation of a salt. Again the complete molecular moiety, which is depicted in Figure 7, is build planar. The structure of the

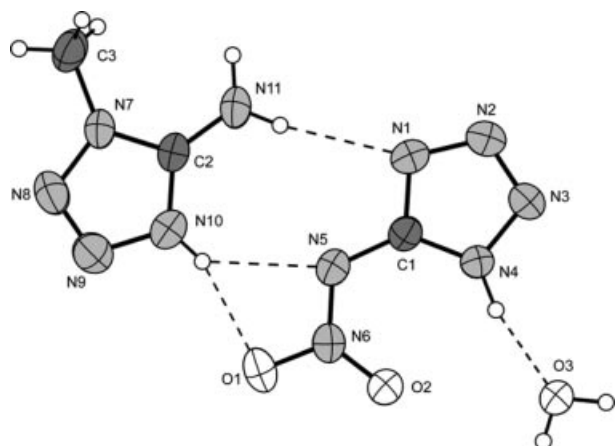


Figure 5. Molecular moiety of **7**. Ellipsoids of non-hydrogen atoms are drawn at the 50 % probability level.

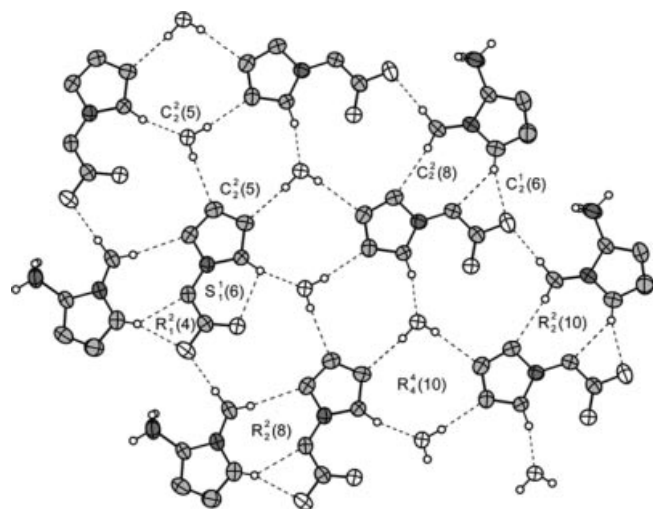


Figure 6. Hydrogen bonding in the layers of **7**.

Selected hydrogen bonds /Å, °: N4–H1 \cdots O3 = 0.89(2), 1.86(2), 2.733(2), 167(2); N11–H3 \cdots N1 = 0.83(2), 2.32(2), 3.137(2), 172(2); N11–H3 \cdots N5 = 0.83(2), 2.62(2), 3.242(2), 133(2), N11–H4 \cdots O1ⁱ = 0.90(3), 1.97(3), 2.865(2), 174(2); N11–H4 \cdots N6ⁱ = 0.90(3), 2.66(3), 3.479(2), 152(2); N10–H2 \cdots O1 = 0.80(2), 2.13(2), 2.903(2), 162(2); N10–H2 \cdots N5 = 0.80(2), 2.27(3), 2.925(2), 140(2); N10–H2 \cdots N6 = 0.80(2), 2.62(3), 3.408(2), 169(2); O3–H8 \cdots N3ⁱⁱ = 0.85(3), 2.10(3), 2.941(2), 170(2); O3–H9 \cdots N2ⁱⁱⁱ = 0.79(3), 2.21(3), 2.977(2), 164(2); (i) $x, 1+y, z$ (ii) $1-x, -0.5+y, -0.5-z$; (iii) $x, -1+y, z$.

2-methyl-5-aminotetrazole molecule is in agreement with this observed for 2-methyl-5-aminotetrazole described by Bryden [33]. However, the structure of the 5-nitraminotetrazole is observed in a special way. The bond lengths and angles are listed in Table 2 and 3. Whereas in the structure of **4** and **4**·H₂O both hydrogen atoms are located at the tetrazole ring (N1 and N4), in this structure the second hydrogen atom is connected at the atom N5. This yields to an elongation of the C1–N5 bond length (1.385 Å vs. 1.340(2) Å in **4**), which is now closer to a C–N single bond than a C=N double bond. With this we observed the first constitution isomer of **4**, which should be named “5-nitramino-1*H*-tetrazole”.

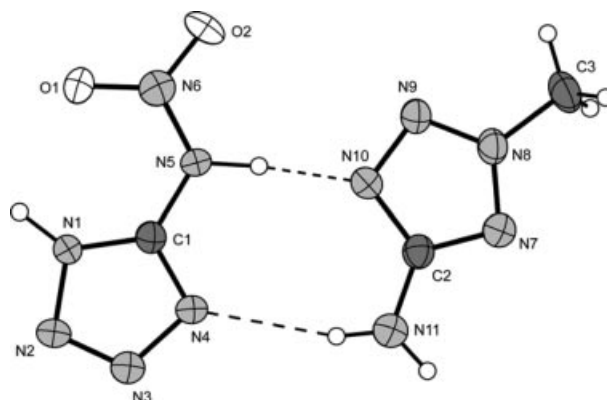


Figure 7. Molecular moiety of **8**. Ellipsoids of non-hydrogen atoms are drawn at the 50 % probability level.

Again an intramolecular hydrogen bond (N4–H4 \cdots O2 = 0.96(2), 2.24(2), 2.629(2) Å, 103(1)°, graph set **S1,1(6)**) appear in the structure of this 5-nitraminotetrazole and the nitro group follows the planarity of the ring plane (N4–C1–N5–O2 = –2.5(2) Å. A reason for the formation of this isomer is the strong hydrogen bond network, which is observed in the packing of **8**. Again a layer structure (distances ca. 3.12 Å) is formed. A view on one layer is shown in Figure 8, whereby important graph sets are drawn (**S1,1(6)**, **R2,2(8)**, **C2,2(8)**, **C2,2(8)** and **C1,1(4)**). Due to the three chain graph sets, alternating tapes are formed. This tapes are connected by an “hydrophobic zipper”, which is build by the methyl groups of 2-methyl-5-aminotetrazole.

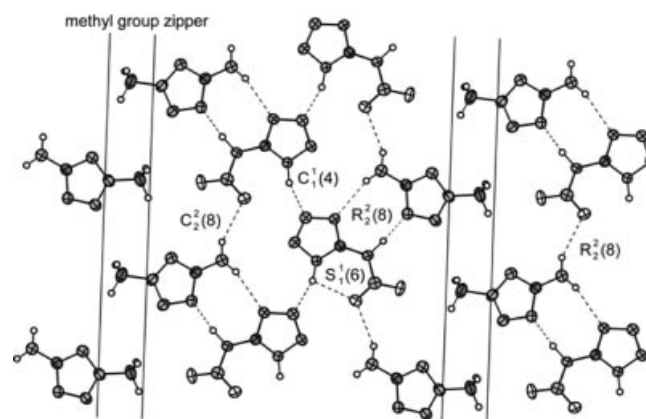


Figure 8. Hydrogen bonding in the layers of **8**.

Selected hydrogen bonds /Å, °: N5–H5 \cdots N10 = 1.00(2), 1.73(2), 2.719(2), 174(2); N11–H11A \cdots O2ⁱ = 0.88(2), 2.32(2), 3.124(2), 152(2); N1–H1 \cdots N3ⁱⁱ = 0.96(2), 1.81(2), 2.738(2), 160(2); (i) $x, 1.5-y, 0.5+z$ (ii) $1-x, 0.5+y, 1.5-z$.

Energetic Properties

Differential Scanning Calorimetry

Differential scanning calorimetry (DSC) measurements to determine the melt- and decomposition temperatures of **4**·H₂O, **5**·H₂O, **7** and **8** (~1.5 mg of each energetic material) were performed in covered Al-containers containing a

hole in the lid with a nitrogen flow of 20 mL/min on a Linseis PT10 DSC [34] calibrated by standard pure indium and zinc at a heating rate of 5 °C min⁻¹. The DSC plots in Figure 9 show the thermal behavior of **7** and **8** in the 50–400 °C temperature range. Temperatures are given as onset temperatures. Interestingly, the thermograms of **4**·H₂O and **5**·H₂O are similar to the curves of **4** and **5** [16]. The compounds exhibit the same decomposition temperatures of 122 and 125 °C as their water-free analogues. The crystal water is being lost slowly over the complete heating phase and could not have been detected in the DSC. Interestingly, although the water molecules participate in several strong hydrogen bonds, they have been lost already by long standing at room temperature. This is in contrast to other tetrazole monohydrates, e.g. 5-aminotetrazole monohydrate or *bis*(1*H*-tetrazol-5-yl)amine monohydrate (H₂bta·H₂O) [35] in which temperatures above 100 °C and reduced pressures are required to remove crystal water. **7** decomposes at temperatures above 138 °C. Even more interesting is the curve of **8**. The formation of the tautomeric form of **4** yields to an increase of the decomposition temperature of 36 °C to 158 °C. This is in contrast to all expectations, since tetrazolates usually have higher decomposition temperatures compared to their neutral analogues.

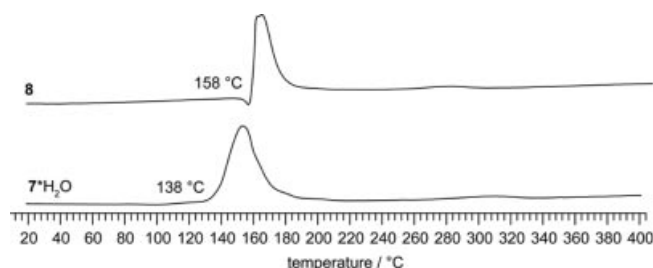


Figure 9. DSC thermograms of compounds **7**–**8** (heating rate of 5 deg·min⁻¹)

Heat of Formations

In bomb calorimetric measurements nitrogen-rich highly energetic compounds, such as **4** and **5**, tend to burn incompletely due to the trend of explosion. Oftentimes wrong heats of combustion ($\Delta_c H$) and finally wrong heats of formation ($\Delta_f H^\circ$) are obtained. Therefore the heats of formation of **4** and **5** [16] as well as of **4**·H₂O and **5**·H₂O have been computed on the same level for better comparison. All calculations were carried out using the Gaussian G03W (revision B.03) program package [36]. The enthalpies (H) and free energies (G) were calculated using the complete basis set (CBS) method described by Petersson and coworkers in order to obtain very accurate values. The CBS models use the known asymptotic convergence of pair natural orbital expressions to extrapolate from calculations using a finite basis set to the estimated complete basis set limit. CBS-4 begins with a HF/3-21G(d) geometry optimization; the zero point energy is computed at the same level. It then

uses a large basis set SCF calculation as a base energy, and a MP2/6-31+G calculation with a CBS extrapolation to correct the energy through second order. A MP4(SDQ)/6-31+(d,p) calculation is used to approximate higher order contributions. To verify the CBS-4M results of the monohydrates **4**·H₂O and **5**·H₂O C₁ optimizations and frequency analyses were performed at B3LYP/cc-pVDZ level of theory. In both cases stable minima with NIMAG = 0 were obtained. In this study we applied the modified CBS-4M method (M referring to the use of minimal population localization) which is a re-parametrized version of the original CBS-4 method and also includes some additional empirical corrections [37, 38]. The enthalpies of the gas-phase species M were computed according to the atomization energy method (eq. 1) [39].

$$\Delta_f H^\circ_{(g, M, 298)} = H_{(Molecule, 298)} - \Sigma H^\circ_{(Atoms, 298)} + \Sigma \Delta_f H^\circ_{(Atoms, 298)} \quad (1)$$

From the gas-phase enthalpies of formation $\Delta_f H^\circ(g)$ (**4**: 398 kJ mol⁻¹, **4**·H₂O: 128 kJ mol⁻¹, **5**: 362 kJ mol⁻¹ and **5**·H₂O: 97 kJ mol⁻¹), the enthalpies of the solid state can be calculated using the enthalpies of sublimation by the equation:

$$\Delta_f H^\circ(s) = \Delta_f H^\circ(g) - (\Delta_{sub} H) \quad (2)$$

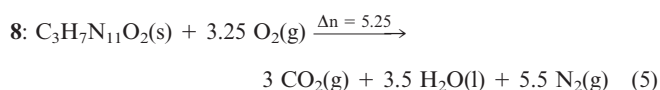
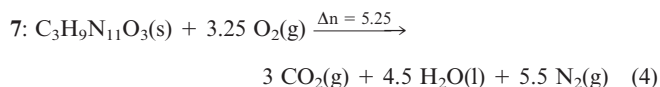
For a solid compound the enthalpy of sublimation ($\Delta_{sub} H$) can be approximated on the basis of TROUTON's rule [40] if the melting temperature, in our case the decomposition temperature (T_m in K) is known:

$$\Delta_{sub} H \cdot [J \text{ mol}^{-1}] = 188 T_m [K] \quad (3)$$

With the known enthalpies of formation of carbon dioxide ($\Delta_f H^\circ_{298}(\text{CO}_2(g)) = -394 \text{ kJ mol}^{-1}$) and water ($\Delta_f H^\circ_{298}(\text{H}_2\text{O}(g)) = -242 \text{ kJ mol}^{-1}$) the enthalpies of formation of **4** (322 kJ mol⁻¹), **4**·H₂O (54 kJ mol⁻¹), **5** (287 kJ mol⁻¹) and **5**·H₂O (22 kJ mol⁻¹) have been calculated. Only the value of **5** is in good agreement with those (**4**: 264 kJ mol⁻¹, **5**: 260 kJ mol⁻¹) measured by bomb calorimetry in literature [16]. Differences of $\Delta(\Delta_f H^\circ(\textbf{4}) - \Delta_f H^\circ(\textbf{4} \cdot \text{H}_2\text{O})) = 268 \text{ kJ mol}$ and $\Delta(\Delta_f H^\circ(\textbf{5}) - \Delta_f H^\circ(\textbf{5} \cdot \text{H}_2\text{O})) = 265 \text{ kJ mol}$ can be calculated. This differences are in agreement to measured heats of formations of H₂O (g: -242 kJ mol⁻¹, l: 286 kJ mol⁻¹).

The heats of combustion of compounds **7** and **8** were determined experimentally using a Parr 1356 bomb calorimeter (static jacket) equipped with a Parr 1108CL oxygen bomb [41]. To achieve better combustion, the samples (ca. 200 mg) were pressed with a defined amount of benzoic acid (ca. 800 mg) forming a tablet, and a Parr 45C10 alloy fuse wire was used for ignition. In all measurements, a correction of 2.3 cal/cm wire burned has been applied and the bomb was examined for evidence of noncombusted carbon after each run. A Parr 1755 printer was furnished with the Parr 1356 calorimeter to produce a permanent record of all

activities within the calorimeter. The reported values are the average of three separate measurements. The calorimeter was calibrated by combustion of certified benzoic acid (SRM, 39i, NIST) in an oxygen atmosphere at a pressure of 3.05 MPa. The experimental results of the constant volume combustion energy ($\Delta_c U$) of the compounds are summarized in Table 4. The standard molar enthalpy of combustion ($\Delta_c H^\circ$) was derived from $\Delta_c H^\circ = \Delta_c U + \Delta n RT$ ($\Delta n = \Delta n_i$ (products, g) – Δn_i (reactants, g); Δn_i is the total molar amount of gases in the products or reactants). The enthalpy of formation, $\Delta_f H^\circ$, for each of the compounds was calculated at 298.15 K using Hess' law and the following combustion reactions:



The heats of formation of the combustion products H_2O (l) (-286 kJ mol^{-1}) and CO_2 (g) (-394 kJ mol^{-1}) were obtained from the literature [42, 43]. The final heats of formation of **7** and **8** have been calculated to be 122 kJ mol^{-1} (**7**) and 444 kJ mol^{-1} (**8**). By comparing these values again the influence of inclusion of crystal water can be seen. However, 2-methyl substituted tetrazoles have mostly more positive $\Delta_f H^\circ$ than their 1-methyl homologues [16].

From the determined energies of formation and X-ray densities, various thermochemical properties have been calculated using the EXPLO5 software (see below) and are summarized in Table 4. The energy of formation ($\Delta_f U^\circ_{298}$) can easily be obtained from the following equation.

$$\Delta_f U^\circ = \Delta_f H^\circ - \Delta n RT \quad (\Delta n \text{ being the change of moles of gaseous components}) \quad (6)$$

Sensitivities

For initial safety testing, the impact and friction sensitivities as well as the electrostatic sensitivity were determined [44]. The impact sensitivity tests were carried out according to STANAG 4489 [45] modified according to instruction [46] using a BAM (Bundesanstalt für Materialforschung) [47] drophammer [48]. The friction sensitivity tests were carried out according to STANAG 4487 [49] modified according to instruction [50] using the BAM friction tester. The detailed values are summarized in Table 4. The impact sensitivity of **4**· H_2O (9 J) and **5**· H_2O (19 J) is significantly lower compared to their water free analogues (**4**: 1.5 J, **5**: 12.5 J). Whereas **4** is classified [51] as *very sensitive* and is considered to the class of primary explosives, **4**· H_2O is classified as *sensitive* and is comparable to famous secondary explosives like RDX (8 J) and HMX (7 J). Compounds **7** (3 J) and **8** (4 J) are highly sensitive towards impact. The same trends are observed regarding the friction sensitivity.

Whereas **4** is extremely sensitive towards friction (8 N), **4**· H_2O is significantly lower. Interestingly, again a lower ratio is observed in the testing of **5** (160 N) and **5**· H_2O (320 N). Again neutral **8** is more sensitive towards friction (72 N) and is classified as *very sensitive* in contrast to **7** (144 N), which is classified “only” as *sensitive*.

The electrostatic sensitivity tests were carried out using an electric spark tester ESD 2010EN (OZM Research) operating with the “Winspark 1.15 software package” [52]. The values of **4** (0.20 J), **4**· H_2O (0.38 J), **5** (0.28 J) and **5**· H_2O (0.35 J) vary only in a small range. These values are in agreement to those observed for commonly used secondary explosives like RDX (0.2 J) and also found in other nitramine compounds [53]. Primary explosives like $\text{Pb}(\text{N}_3)_2$ (0.005 J) have much lower values. The electrical spark sensitivities of **7** (1.50 J) and **8** (0.46 J) were determined to be significantly higher. It should be mentioned that the test towards electrical discharge strongly depends on the particle size and shape. Although we tried to use fine crystalline materials (1–100 μm) a guarantee for the determined values can not be given.

Detonation Parameter

The calculation of the detonation parameters was performed with the program package EXPLO5 (version 5.02) [54]. The program is based on the chemical equilibrium, steady-state model of detonation. It uses the Becker-Kistiakowsky-Wilson's equation of state (BKW EOS) for gaseous detonation products and Cowan-Fickett's equation of state for solid carbon [55, 56]. The calculation of the equilibrium composition of the detonation products is done by applying modified White, Johnson and Dantzig's free energy minimization technique. The program is designed to enable the calculation of detonation parameters at the CJ point. The BKW equation in the following form was used with the BKWN set of parameters (α , β , κ , θ) as stated below the equations and X_i being the mol fraction of i -th gaseous product, k_i is the molar covolume of the i -th gaseous product:

$$pV/RT = 1 + xe^{\beta x} x = (\kappa \sum X_i k_i) / [V(T + \theta)]^\alpha \quad (7)$$

$$\alpha = 0.5, \beta = 0.176, \kappa = 14.71, \theta = 6620.$$

The detonation parameters calculated with the EXPLO5 program using the experimentally determined densities and previously discussed heats of formation are summarized in Table 4. The re-calculated detonation parameter of compound **4**, which one of the most powerful non-nuclear explosives up to date, show very promising values exceeding these of TNT, RDX and in part even those of HMX. The most important criterias of high explosives are the detonation velocity ($v_{\text{Det.}}$ = **4**: 9450, TNT: 7000, RDX: 8796, HMX: 9100 m s^{-1}), the detonation pressure ($p_{\text{Det.}}$ = **4**: 394, RDX: 299 kbar) and the energy of explosion ($\Delta_E U_m^\circ$ = **4**: 5746, RDX: -5902 kJ kg^{-1}). The influence of the inclusion

Table 4. Sensitivities, energetic properties and detonation parameter.

	4	4 · H ₂ O	5	5 · H ₂ O	7	8
Formula	CH ₂ N ₆ O ₂	CH ₄ N ₆ O ₃	C ₂ H ₄ N ₆ O ₂	C ₂ H ₆ N ₆ O ₃	C ₃ H ₉ N ₁₁ O ₃	C ₃ H ₇ N ₁₁ O ₂
Molecular Mass /g · mol ⁻¹	130.09	148.10	144.11	162.13	247.18	229.16
Impact sensitivity /I ^{a)}	1.5	9	12.5	19	3	2
Friction sensitivity /N ^{b)}	8	140	160	320	144	72
ESD-test /J	0.19	0.38	0.28	0.35	1.50	0.46
N /% ^{c)}	64.61	51.84	58.32	57.15	62.33	67.23
O /% ^{d)}	-12.30	-10.8	-44.41	-39.5	-48.5	-52.4
T _{dec.} /°C ^{e)}	122	122	125	125	139	159
Density /g · cm ⁻³ f)	1.867	1.808	1.755	1.643	1.590	1.657
-ΔU _{comb} /cal · g ⁻¹ g)	—	—	—	—	2514	2749
Δ _f H _m ^o /kJ · mol ⁻¹ h)	322	54	287	22	122	444
Δ _f U ^o /kJ · kg ⁻¹ i)	2574	472	2096	250	611	2047
calculated values by EXPLO5:						
-Δ _E U ^o /kJ · kg ⁻¹ j)	5746	5003	5382	4669	3716	4347
T _E /K ^{k)}	4563	3861	3900	3425	2889	3266
p /kbar ^{l)}	394	323	299	239	208	247
D /m · s ⁻¹ m)	9450	8849	8464	7894	7619	8093
Gas vol. /L · kg ⁻¹ n)	800	838	783	832	834	801

a,b) BAM methods; c) Nitrogen content; d) Oxygen balance; e) Temperature of decomposition by DSC (β = 5 °C); f) estimated from a structure determination; g) Experimental (constant volume) combustion energy; h) Molar enthalpy of formation; i) Energy of formation; j) Energy of Explosion; k) Explosion temperature; l) Detonation pressure; m) Detonation velocity; n) Assuming only gaseous products.

of water and also the lower density can be seen on the lower values, except for the amount of decomposition gases, of 4 · H₂O and 5 · H₂O, which are significantly lower than those of 4 and 5. Compounds 7 and 8 are only moderate in detonation performance, which may be a reason of the lower densities. However, both have better calculated detonation criteria than still used TNT.

¹⁵N NMR Spectroscopy

Mostly, ¹⁴N NMR spectroscopy is not suitable to characterize tetrazole derivatives, since the peaks observed are extremely broad due to the quadrupole moment of the ¹⁴N core. However, ¹⁵N NMR spectroscopy is a valuable method to identify tetrazoles, tetrazolates or tetrazolium salts. ¹⁵N NMR spectra of 7 and 8 were measured in *d*₆-DMSO and are depicted in Figure 10. The chemical shifts are given in ppm with respect to MeNO₂ as external standard. The assignments were done by evaluating the ¹⁵N-¹H coupling constants and by comparison with literature [16, 5a]. However, the correct assignments are hard to find, since several peaks are located at the same chemical shift. In both spectra the ¹J coupling of the primary amine nitrogen atoms N5 at -337.4 and 340.5 ppm, respectively, to the hydrogen atoms could not be observed. As a matter of principle, nitrogen atoms N2 and N3 are shifted most to lower fields due to the two neighbored nitrogen atoms in the tetrazole ring. Atom N1 as well as N4 with one neighboring nitrogen atom and one carbon atom is shifted higher fields. The chemical shifts of the 5-nitriminotetrazole molecule are in agreement to those observed for 5-nitriminotetrazole in literature [16]. This is a further proof that also in solution no deprotonation is obtained. The chemical

shifts of the nitro groups are located at -23.6 (7) and -24.9 (8) ppm.

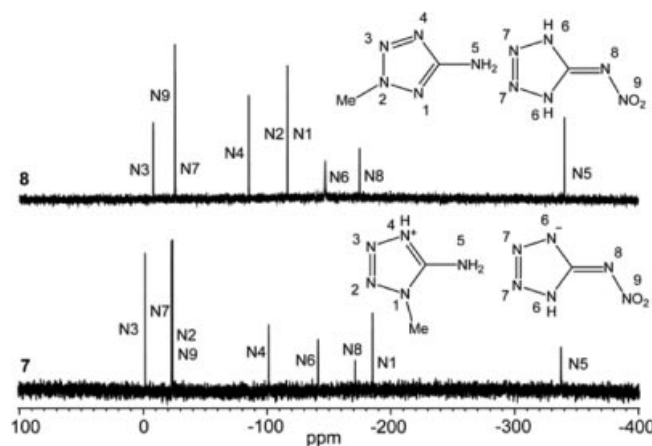


Figure 10. ¹⁵N NMR spectra of 7 and 8. Chemical shifts are given with respect to Me-NO₂. 7: δ = -1.5 (N7), -22.8 (N7), -23.6 (N9 / N2, q, ³J_{N-H} = 1.4 Hz), -101.2 (N4), -141.0 (N6), -170 (N8), -185 (N1, q, ²J_{N-H} = 1.9 Hz), -337.4 (N5); 8: δ = -7.4 (N3, q, ³J_{N-H} = 1.8 Hz), -24.9 (N9), -25.2 (N7), -84.9 (N4), -116.1 (N2 / N1, m), -146.7 (N6), -174.5 (N8), -340.5 (N5).

Conclusions

From this combined experimental and theoretical work the following conclusions can be drawn:

- The reaction of 5-nitriminotetrazole (4) with 1-methyl-5-aminotetrazole (2) as well as 2-methyl-5-aminotetrazole (3) resulted in two different products. In the first case the salt 1-methyl-5-aminotetrazolium 5-nitriminotetrazolate monohydrate (7) is obtained. In the second reaction a co-

crystallization product (**8**) was obtained. In this compound, the first constitution isomer of 5-nitriminotetrazole could have been stabilized by strong hydrogen bonds. In this molecule, which should be named 5-nitraminotetrazole only one hydrogen atom is located at the tetrazole ring. Both compounds were fully characterized, e.g. X-ray structures, multinuclear NMR, vibrational spectroscopy, bomb calorimetry, DSC, sensitivities, calculation of detonation parameter.

- The crystal structures of 5-nitriminotetrazole monohydrate (**4**·H₂O) and 1-methyl-5-nitriminotetrazole monohydrate (**5**·H₂O) are presented. Both crystal packing have, although possessing more hydrogen bonds, lower densities as their water-free analogues.

- The decreased sensitivities (impact, friction, electrical discharge) and detonation parameter of **4**·H₂O and **5**·H₂O have been compared with the water-free compounds.

- The heats of formation of the monohydrates **4**·H₂O (54 kJ mol⁻¹) and **5**·H₂O (22 kJ mol⁻¹) are *ca.* 265 kJ mol⁻¹ lower than those of the water-free analogues.

Experimental Section

All reagents and solvents were used as received (Sigma-Aldrich, Fluka, Acros Organics) if not stated otherwise. 5-Aminotetrazole (97 %) was purchased from Aldrich. Melting points were measured with a Perkin-Elmer Pyris6 DSC, using heating rates of 5°/min. Otherwise melting points were determined with a Büchi Melting Point B-450 apparatus and are not corrected. ¹H and ¹³C spectra were recorded with a JEOL Eclipse 270, JEOL EX 400 or a JEOL Eclipse 400 instrument. All chemical shifts are quoted in ppm relative to TMS (¹H, ¹³C). Infrared (IR) spectra were recorded using a Perkin-Elmer Spektrum One FT-IR instrument. Raman spectra were measured using a Perkin-Elmer Spektrum 2000R NIR FT-Raman instrument equipped with a Nd:YAG laser (1064 nm). Elemental Analyses were performed with a Netsch STA 429 simultaneous thermal analyzer. Bomb Calorimetry was done, using a Parr 1356 Bomb calorimeter with a Parr 1108CL oxygen bomb. The sensitivity data were performed using a BAM drophammer and a BAM friction tester. The electrostatic sensitivity tests were carried out using an electric spark tester ESD 2010EN (OZM Research) operating with the "Winspark 1.15 software package".

CAUTION! The prepared tetrazoles **4–8** are energetic compounds with increased sensitivities against heat, impact and friction. Although we had no problems in synthesis, proper protective measures (safety glasses, face shield, leather coat, earthened equipment and shoes, Kevlar® gloves and ear plugs) should be used especially during work on **4**.

5-Nitriminotetrazole monohydrate (4a): A small amount of **4** was dissolved in water and left for crystallization. After one day colorless rods were obtained. **EA** (CH₄N₆O₃, 148.10): calcd.: C 8.22, H 2.72, N 56.75 %; found: C 8.26, H 2.49, N 57.15 %.

DSC (5 °C min⁻¹, °C): 122–124 °C (dec.); **IR** (KBr, cm⁻¹): $\tilde{\nu}$ = 3538 (m), 3463 (m), 3070 (w), 2930 (w), 2670 (w), 1614 (s), 1591 (s), 1508 (m), 1451 (m), 1355 (s), 1320 (vs), 1259 (s), 1242 (s), 1120 (w), 1062 (m), 1016 (w), 993 (m), 910 (w), 879 (w), 846 (m), 777 (m), 755 (w), 727 (w), 655 (w); **Raman** (1064 nm, 350 mW, 25 °C, cm⁻¹): $\tilde{\nu}$ = 1635 (10), 1585 (62), 1556 (12), 1423 (87), 1372 (7),

1305 (6), 1251 (11), 1083 (15), 1065 (17), 1017 (100), 989 (37), 855 (11), 758 (34), 732 (0), 492 (22), 418 (30), 358 (9), 237 (25), 172 (30); **BAM** drophammer: > 9 J; friction tester: >140 N, ESD: > 0.38 J.

1-Methyl-5-nitriminotetrazole monohydrate (5a): A small amount of **5** was dissolved in warm water and left for crystallization. After one day colorless crystals were obtained. **EA** (C₂H₆N₆O₃, 162.11): calcd.: C 14.82, H 3.73, N 51.84 %; found: C 14.60, H 3.51, N 52.11 %.

DSC (5 °C min⁻¹, °C): 124–126 °C (dec.); **IR** (KBr, cm⁻¹): $\tilde{\nu}$ = 3568 (w), 3443 (w), 3084 (m), 3049 (m), 2879 (m), 2634 (w), 1727 (w), 1700 (w), 1591 (vs), 1515 (s), 1498 (s), 1455 (s), 1411 (m), 1400 (m), 1330 (s), 1307 (s), 1213 (vs), 1135 (m), 1065 (m), 1038 (s), 970 (s), 812 (m), 778 (m), 753 (m), 716 (s), 686 (w), 669 (m); **Raman** (1064 nm, 350 mW, 25 °C, cm⁻¹): $\tilde{\nu}$ = 3034 (10), 3014 (15), 2958 (36), 1582 (95), 1469 (24), 1418 (79), 1340 (12), 1275 (40), 1231 (27), 1088 (19), 1056 (38), 1044 (100), 984 (22), 880 (25), 761 (53), 693 (50), 682 (23), 495 (35), 454 (16), 300 (36), 270 (21), 247 (27), 166 (23); **BAM** drophammer: > 19 J; friction tester: >320 N; **ESD**: > 0.35 J.

1-Methyl-5-aminotetrazolium 5-nitriminotetrazolate monohydrate (7): 5-Nitriminotetrazole (**4**) (650.4 mg, 5 mmol) was dissolved in 10 mL of water and 1-methyl-5-aminotetrazole (495.5 mg, 5 mmol) was added to the solution. It was heated to 60 °C, until the 1-methyl-5-aminotetrazole was completely dissolved. After evaporation of the water in vacuum, a poorly water-soluble white powder was obtained, which could be recrystallized from ethanol to give 952 mg (3.85 mmol, 77 %) 1-methylaminotetrazolium nitriminotetrazolate. **EA** (C₃H₉N₁₁O₃, 247.18): calcd.: C 14.58, H 3.67, N 62.33 %; found: C 13.78, H 2.95, N 61.41 %.

DSC (5 °C min⁻¹, °C): 138 °C (dec.); **IR** (KBr, cm⁻¹): $\tilde{\nu}$ = 3464 (s), 3367 (s), 3112 (s), 2870 (m), 1698 (vs), 1641 (m), 1548 (s), 1447 (s), 1357 (s), 1328 (s), 1227 (m), 1156 (m), 1076 (m), 1061 (m), 1028 (m), 1001 (w), 968 (w), 876 (w), 833 (w), 777 (w), 748 (w), 696 (w), 559 (m), 493 (w); **Raman** (1064 nm, 350 mW, 25 °C, cm⁻¹): $\tilde{\nu}$ = 3150 (11), 2952 (31), 2572 (5), 1661 (13), 1594 (19), 1412 (13), 1320 (29), 1279 (22), 1119 (18), 1046 (9), 973 (8), 788 (100), 680 (18), 478 (10), 313 (27), 219 (17); ¹H NMR (DMSO-*d*₆, 25 °C, ppm) δ : 6.83 (s, NH₂), 3.66 (s, CH₃); ¹³C NMR (DMSO-*d*₆, 25 °C, ppm) δ : 156.1 (1-MeAT⁺), 153.5 (HATNO₂⁻), 32.1 (CH₃); **m/z** (FAB⁺): 100.1 [1-MeAT]⁺; **m/z** (FAB⁻): 129.1 [ATNO₂]⁻; **BAM** drophammer: >3 J; friction tester: >144 N, **ESD**: > 1.50 J.

2-Methyl-5-aminotetrazole 5-nitriminotetrazole (8): 5-Nitriminotetrazole (**4**) (1.30 g, 10 mmol) was dissolved in 20 mL of water and 2-methylaminotetrazole (991 mg, 10 mmol) was added. The suspension was heated to 60 °C, which did not result in a clear solution, but the solution showed certain opalescence. The water was removed in a rotary evaporator and the remaining solid was recrystallized from methanol. The crystals were washed with water and pentane to give 1.86 g (7.1 mmol, 81 %) of the 2-methylaminotetrazole 5-nitriminotetrazole adduct **8**. **EA** (C₃H₉N₁₁O₃, 229.16): calcd.: C 15.72, H 3.08, N 67.23; found: C 16.04, H 3.09, N 67.01.

DSC (5 °C min⁻¹, °C): 158 °C (dec.); **IR** (KBr, cm⁻¹): $\tilde{\nu}$ = 3450 (s), 3341 (s), 3112 (m), 2883 (m), 2705 (m), 2608 (m), 1628 (s), 1554 (m), 1516 (m), 1438 (w), 1405 (w), 1365 (m), 1330 (s), 1310 (vs), 1258 (m), 1194 (m), 1103 (m), 1097 (m), 1058 (m), 1002 (w), 917 (w), 830 (w), 755 (w), 728 (m), 652 (w), 472 (w); **Raman** (1064 nm, 350 mW, 25 °C, cm⁻¹): $\tilde{\nu}$ = 3040 (19), 3027 (17), 2965 (58), 1623 (37), 1570 (72), 1437 (25), 1380 (100), 1262 (44), 1197 (28), 1142

(16), 1097 (49), 1018 (92), 648 (60), 460 (34), 390 (28), 347 (24), 316 (30), 211 (21), 171 (21); ^1H NMR (DMSO- d_6 , 25 °C, ppm) δ : 9.56 (s, NH), 4.06 (s, CH₃); ^{13}C NMR (DMSO- d_6 , 25 °C, ppm) δ : 167.7 (2-MeAt), 153.3 (H₂AtNO₂), 39.3 (CH₃); m/z (FAB⁺): 100.1 [2-MeAt]⁺; m/z (FAB⁻): 129.1 [AtNO₂]⁻; m/z (DCI⁺): 229.2 [M]⁺, 131.2 [AtNO₂+H]⁺, 100.1 [2-MeAt+H]⁺; BAM drophammer: >2 J; friction tester: >72 N, ESD: > 0.46 J.

Acknowledgement

Financial support of this work by the Ludwig-Maximilian University of Munich (LMU), the Fonds der Chemischen Industrie (FCI), the European Research Office (ERO) of the U.S. Army Research Laboratory (ARL) and ARDEC (Armament Research, Development and Engineering Center) under contract nos. N 62558-05-C-0027, R&D 1284-CH-01, R&D 1285-CH-01, 9939-AN-01, W911NF-07-1-0569, W911NF-08-1-0372 and W911NF-08-1-0380 and the Bundeswehr Research Institute for Materials, Explosives, Fuels and Lubricants (WIWEB) under contract nos. E/E210/4D004/X5143 & E/E210/7D002/4F088 is gratefully acknowledged. The authors acknowledge collaborations Dr. M. Krupka (OZM Research, Czech Republic) in the development of new testing and evaluation methods for energetic materials and with Dr. M. Sucasca (Brodarski Institute, Croatia) in the development of new computational codes to predict the detonation parameters of high-nitrogen explosives. We are indebted to and thank Dr. Betsy M. Rice (ARL, Aberdeen, Proving Ground, MD) and Dr. Gary Chen (ARDEC, Picatinny Arsenal, NJ) for many helpful and inspired discussions and support of our work.

References

- [1] a) T. M. Klapötke, in *Moderne Anorganische Chemie*, E. Riedel (Hrsg.), 3. Edn, Walter de Gruyter, Berlin, New York, **2007**, 99–104; b) R. P. Singh, R. D. Verma, D. T. Meshri, J. M. Shreeve, *Ang. Chem. Int. Ed.* **2006**, 45(22), 3584; c) T. M. Klapötke, in *High Energy Density Materials*, T. M. Klapötke (Hrsg.), Springer, Berlin, Heidelberg, **2007**, 85–122; d) B. Rice, E. F. C. Byrd and W. D. Mattson, in *High Energy Density Materials*, T. M. Klapötke (Hrsg.), Springer, Berlin, Heidelberg, **2007**, 153–194.
- [2] a) H. Xue, H. Gao, B. Twamley, J. M. Shreeve, *Chem. Mater.* **2007**, 19, 1731–1739; b) H. Xue, Y. Gao, B. Twamley, J. M. Shreeve, *Chem. Mater.* **2005**, 17, 191–198; c) H. Xue, S. W. Arritt, B. Twamley, J. M. Shreeve, *Inorg. Chem.* **2004**, 43, 7972–7977; d) Y. Gao, S. W. Arritt, B. Twamley, J. M. Shreeve, *Inorg. Chem.* **2005**, 44, 1704–1712; e) C. F. Ye, J. M. Shreeve, *Chem. Commun.* **2005**, 2570–2572; f) H. Xue, Y. Gao, B. Twamley, J. M. Shreeve, *Inorg. Chem.* **2005**, 44, 5068–5072; g) H. Xue, B. Twamley, J. M. Shreeve, *J. Mater. Chem.* **2005**, 15, 3459–3465; h) H. Xue, Y. Gao, B. Twamley, J. M. Shreeve, *Inorg. Chem.* **2005**, 44, 7009–7013; i) C. M. Jin, C. F. Ye, C. Piekarski, B. Twamley, J. M. Shreeve, *Eur. J. Inorg. Chem.* **2005**, 18, 3760–3767; j) H. Xue, H. X. Gao, B. Twamley, J. M. Shreeve, *Eur. J. Inorg. Chem.* **2006**, 15, 2959–2965; k) H. Gao, C. Ye, R. W. Winter, G. L. Gard, M. E. Sitzmann, J. M. Shreeve, *Eur. J. Inorg. Chem.* **2006**, 15, 3221–3226; l) Y. Gao, C. F. Ye, B. Twamley, J. M. Shreeve, *Chem. Eur. J.* **2006**, 12, 9010–9018; m) H. Gao, R. Wang, B. Twamley, M. A. Hiskey, J. M. Shreeve, *Chem. Commun.* **2006**, 4007–4009.
- [3] a) M. X. Zhang, P. E. Eaton, R. D. Gilardi, *Angew. Chem., Int. Ed.* **2000**, 39, 401–404; b) D. E. Chavez, M. A. Hiskey, R. D. Gilardi, *Angew. Chem., Int. Ed.* **2000**, 39, 1791–1793; c) D. E. Chavez, M. A. Hiskey, R. D. Gilardi, *Org. Lett.* **2004**, 6, 2889–2891.
- [4] a) G. Drake, T. Hawkins, A. Brand, L. Hall, M. McKay, A. Vij, I. Ismail, *Propellants, Explos., Pyrotech.* **2003**, 28 (4), 174–180; b) G. Kaplan, G. Drake, K. Tollison, L. Hall, T. Hawkins, *J. Heterocycl. Chem.* **2005**, 42, 19–27; c) G. W. Drake, T. M. Hawkins, J. Boatz, L. Hall, A. Vij, *Propellants, Explos., Pyrotech.* **2005**, 30 (2), 156–163.
- [5] a) T. M. Klapötke, J. Stierstorfer, A. U. Wallek, *Chem. Mater.* **2008**, 20, 4519–4530; b) C. Darwich, T. M. Klapötke, C. Miró Sabaté, *Chemistry – A. Europ. J.* **2008**, 14, 5756–5771; c) T. M. Klapötke, J. Stierstorfer, *Phys. Chem. Chem. Phys.* **2008**, 10, 4340–4346; d) T. M. Klapötke, P. Mayer, C. Miró Sabaté, J. M. Welch, N. Wiegand, *Inorg. Chem.* **2008**, 47(13), 6014–6027; e) T. M. Klapötke, C. Miró Sabaté, *Chem. Mater.* **2008**, 20(5), 1750–1763; f) Thomas M. Klapötke, J. Stierstorfer, *Eur. J. Inorg. Chem.* **2008**, 4055–4062; g) M. Hiskey, A. Hammerl, G. Holl, T. M. Klapötke, K. Polborn, J. Stierstorfer, J. J. Weigand, *Chem. Mater.* **2005**, 17, 3784–3793; h) K. Karaghiosoff, T. M. Klapötke, P. Mayer, C. Miró Sabaté, A. Penger, J. M. Welch, *Inorg. Chem.* **2008**, 47, 1007–1019.
- [6] a) A. J. Bellamy, S. J. Ward, P. Golding, *Propellants, Explos., Pyrotech.* **2002**, 27(2), 59–61; b) A. J. Bellamy, S. J. Ward, P. Golding, *Propellants, Explos., Pyrotech.* **2002**, 27(2), 49–58; c) A. J. Bellamy, P. Golding, *Centr. Europ. J. Energ. Mat.* **2007**, 4(3), 33–57.
- [7] a) K. O. Christe, *Propellants, Explos., Pyrotech.* **2007**, 32, 194–204; b) C. B. Jones, R. Haiges, T. Schroer, K. O. Christe, *Angew. Chem. Int. Ed.* **2006**, 45, 4981–4984; c) K. O. Christe, W. W. Wilson, J. A. Sheehy, J. A. Boatz, *Angew. Chem. Int. Ed.* **1999**, 38, 2004–2009.
- [8] R. Stollé, *Ber. Dtsch. Chem. Ges.* **1929**, 62, 1118.
- [9] M. v. Denffer, T. M. Klapötke, G. Kramer, G. Spieß, J. M. Welch, G. Heeb, *Propellants Explos. Pyrotech.* **2005**, 30(3), 191–195.
- [10] a) T. M. Klapötke, J. Stierstorfer, *Dalton Transactions*, **2008**, accepted; b) V. P. Sinditskii, A. I. Levshenkov, V. Y. Egorshv, V. V. Serushkin, *New Trends in Research of Energetic Materials, Proceedings of the Seminar, 7th*, Pardubice, Czech Republic, 2004, 2, 649–658; c) H. R. Blomquist, *U.S. patent* **1999**, US 6004410, A 19991221; d) C. J. Hinshaw, R. B. Wardle, T. K. Highsmith, *U.S. patent* **1998**, US 5741998, A 19980421.
- [11] T. M. Klapötke, C. M. Sabaté, J. Stierstorfer, *Z. Anorg. Allg. Chem.* **2008**, 634, 1867–1874.
- [12] T. M. Klapötke, C. Miró Sabaté, *Z. Anorg. Allg. Chem.* **2008**, 634, 1017–1024.
- [13] J. Thiele, *Liebigs Ann.* **1892**, 270, 1–63.
- [14] R. J. Spear, *Aust. J. Chem.* **1984**, 37, 2453–2468.
- [15] a) J. A. Garrison, R. M. Herbst, *J. Org. Chem.* **1957**, 22, 278–283; b) A. S. Lyakhov, S. V. Voitekhovich, L. S. Ivashkevich, P. N. Gaponik, *Acta Crystallogr.* **2005**, E61, o3645–o3647.
- [16] T. M. Klapötke, J. Stierstorfer, *Helv. Chim. Acta* **2007**, 90, 2132–2150.
- [17] R. M. Herbst, J. A. Garrison, *J. Org. Chem.* **1953**, 18, 941–945.
- [18] R. E. Trifonov, V. A. Ostrovskii, *Russ. J. Org. Chem.* **2006**, 42, 1585–1605.
- [19] A. A. A. Boraei, *J. Chem. Eng. Data* **2001**, 46, 939–943.
- [20] P. Ochlin, A. Murphy, S. Helf, *J. Am. Chem. Soc.* **1954**, 76, 1451–1453.
- [21] V. A. Ostrovskii, G. I. Koldobskii, R. E. Trifonov, in “*Comprehensive Heterocyclic Chemistry III*”, Volume 6, V. V. Zhdankin, A. R. Katritzky (Ed.), Elsevier, **2008**, p. 301.
- [22] CrysAlis CCD, Oxford Diffraction Ltd., Version 1.171.27p5 beta (release 01-04-2005 CrysAlis171.NET).
- [23] CrysAlis RED, Oxford Diffraction Ltd., Version 1.171.27p5 beta (release 01-04-2005 CrysAlis171.NET).
- [24] A. Altomare, G. Cascarano, C. Giacovazzo, A. Guagliardi, *J. Appl. Cryst.* **1993**, 26, 343.
- [25] G. M. Sheldrick SHELXS-97, Program for Crystal Structure Solution, Universität Göttingen, **1997**.

- [26] G. M. Sheldrick, SHELXL-97. Program for the Refinement of Crystal Structures. University of Göttingen, Germany, **1997**.
- [27] A. L. Spek, PLATON, A Multipurpose Crystallographic Tool, Utrecht University, Utrecht, The Netherlands, 1999.
- [28] L. J. Farrugia, *J. Appl. Cryst.* **1999**, *32*, 837–838.
- [29] SCALE3 ABSPACK – An Oxford Diffraction program (1.0.4.gui:1.0.3) (C) 2005 Oxford Diffraction Ltd.
- [30] Crystallographic data for the structure(s) have been deposited with the Cambridge Crystallographic Data Centre. Copies of the data can be obtained free of charge on application to The Director, CCDC, 12 Union Road, Cambridge CB2 1EZ, UK (Fax: int.code(1223)336-033; e-mail for inquiry: file-serv@ccdc.cam.ac.uk; e-mail for deposition: deposit@ccdc.cam.ac.uk)
- [31] N. Wiberg, in *Lehrbuch der Anorganischen Chemie / Holleman-Wiberg*, 101. Ed., de Gruyter, Berlin, **1995**, p. 1842.
- [32] J. Bernstein, R. E. Davis, L. Shimon, N.-L. Chang, *Angew. Chem. Int. Ed.* **1995**, *34*, 1555–1573.
- [33] J. H. Bryden, *Acta Crystallogr.* **1956**, *9*, 874–878.
- [34] <http://www.linseis.com>
- [35] T. M. Klapötke, P. Mayer, J. Stierstorfer, J. J. Weigand, *J. Mat. Chem.* **2008**, accepted.
- [36] Gaussian 03, Revision B0.4, M. J. Frisch, G. W. Trucks, H. B. Schlegel, G. E. Scuseria, M. A. Robb, J. R. Cheeseman, J. A. Montgomery, Jr., T. Vreven, K. N. Kudin, J. C. Burant, J. M. Millam, S. S. Iyengar, J. Tomasi, V. Barone, B. Mennucci, M. Cossi, G. Scalmani, N. Rega, G. A. Petersson, H. Nakatsuji, M. Hada, M. Ehara, K. Toyota, R. Fukuda, J. Hasegawa, M. Ishida, T. Nakajima, Y. Honda, O. Kitao, H. Nakai, M. Klene, X. Li, J. E. Knox, H. P. Hratchian, J. B. Cross, C. Adamo, J. Jaramillo, R. Gomperts, R. E. Stratmann, O. Yazyev, A. J. Austin, R. Cammi, C. Pomelli, J. W. Ochterski, P. Y. Ayala, K. Morokuma, G. A. Voth, P. Salvador, J. J. Dannenberg, V. G. Zakrzewski, S. Dapprich, A. D. Daniels, M. C. Strain, O. Farkas, D. K. Malick, A. D. Rabuck, K. Raghavachari, J. B. Foresman, J. V. Ortiz, Q. Cui, A. G. Baboul, S. Clifford, J. Cioslowski, B. B. Stefanov, G. Liu, A. Liashenko, P. Piskorz, I. Komaromi, R. L. Martin, D. J. Fox, T. Keith, M. A. Al-Laham, C. Y. Peng, A. Nanayakkara, M. Challacombe, P. M. W. Gill, B. Johnson, W. Chen, M. W. Wong, C. Gonzalez, and J. A. Pople, Gaussian, Inc., Pittsburgh PA, **2004**.
- [37] J. W. Ochterski, G. A. Petersson, J. A. Montgomery Jr., *J. Chem. Phys.* **1996**, *104*, 2598–2619.
- [38] J. A. Montgomery Jr., M. J. Frisch, J. W. Ochterski, G. A. Petersson, *J. Chem. Phys.* **2000**, *112*, 6532–6542.
- [39] E. F. Byrd, B. M. Rice, *J. Phys. Chem.* **2006**, *110*, 1005–1013; B. M. Rice, S. V. Pai, J. Hare, *Combust. Flame* **1999**, *118*, 445–458.
- [40] M. S. Westwell, M. S. Searle, D. J. Wales, D. H. Williams, *J. Am. Chem. Soc.* **1995**, *117*, 5013–5015.
- [41] <http://www.parrinst.de>
- [42] N. Wiberg, in *Lehrbuch der Anorganischen Chemie / Holleman-Wiberg*, 101. Ed., de Gruyter, Berlin, **1995**, p. 51.
- [43] N. Wiberg, in *Lehrbuch der Anorganischen Chemie / Holleman-Wiberg*, 101. Ed., de Gruyter, Berlin, **1995**, p. 141.
- [44] M. Sućeska, *Test Methods for Explosives*, Springer, New York 1995, p. 21 (impact), p. 27 (friction).
- [45] *NATO standardization agreement (STANAG) on explosives, impact sensitivity tests*, no. 4489, Ed. 1, Sept. 17, 1999.
- [46] *WIWEB-Standardarbeitsanweisung 4-5.1.02, Ermittlung der Explosionsgefährlichkeit, hier der Schlagempfindlichkeit mit dem Fallhammer*, Nov. 8, 2002.
- [47] <http://www.bam.de>
- [48] <http://www.reichel-partner.de/>
- [49] *NATO standardization agreement (STANAG) on explosive, friction sensitivity tests*, no. 4487, Ed. 1, Aug. 22, 2002.
- [50] *WIWEB-Standardarbeitsanweisung 4-5.1.03, Ermittlung der Explosionsgefährlichkeit oder der Reibeempfindlichkeit mit dem Reibeapparat*, Nov. 8, 2002.
- [51] impact: Insensitive > 40 J, less sensitive ≥ 35 J, sensitive ≥ 4 , very sensitive ≤ 3 J; friction: Insensitive > 360 N, less sensitive = 360 N, sensitive < 360 N a. > 80 N, very sensitive ≤ 80 N, extreme sensitive ≤ 10 N; According to the UN Recommendations on the Transport of Dangerous Goods (+) indicates: not safe for transport.
- [52] a) S. Zeman, V. Pelikán, J. Majzlík, *Centr. Eur. J. Energy. Mat.* **2006**, *3*, 45–51; b) D. Skinner, D. Olson, A. Block-Bolten, *Propellants, Explos., Pyrotech.* **1997**, *23*, 34–42; c) OZM research, Czech Republic, <http://www.ozm.cz/testing-instruments/pdf/TI-SmallSpark.pdf>.
- [53] S. Zeman, V. Pelikan, J. Majzlík, *Cent. Europ. J. Energ. Mater.* **2006**, *3*(3), 27–44.
- [54] M. Sućeska, EXPLO5 program, Zagreb, Croatia, **2005**.
- [55] a) M. Sućeska, *Mater. Sci. Forum* **2004**, *465–466*, 325–330; b) M. Sućeska, *Propellants, Explos., Pyrotech.* **1991**, *16*, 197–202; c) M. Sućeska, *Propellants, Explos., Pyrotech.* **1999**, *24*, 280–285.
- [56] M. L. Hobbs, M. R. Baer, *Proc. of the 10th Symp. on Detonation*, ONR 33395-12, Boston, MA, July 12–16, **1993**, p. 409.

Received: October 27, 2008

New Energetic Materials featuring Tetrazoles and Nitramines – Synthesis, Characterization and Properties

Niko Fischer,^[a] Konstantin Karaghiosoff,^[a] Thomas M. Klapötke,^{*[a]} and Jörg Stierstorfer^[a]

Dedicated to Dr. Klaus Römer on the Occasion of His 70th Birthday

Keywords: Energetic materials; Tetrazoles; X-ray diffraction; Detonation parameters; Sensitivities; NMR spectroscopy

Abstract. The alkylation of 2-nitro-2-azapropyl chloride (**2**) and deprotonated 5-amino-1*H*-tetrazole (**3**), 1*H*-tetrazole (**4**), 5-nitrimino-1,4*H*-tetrazole (**5**), 1-methyl-5-nitrimino-4*H*-tetrazole (**6**) and 2-methyl-5-nitraminotetrazole (**7**) afforded the products 1-(2-nitro-2-azapropyl)-5-aminotetrazole (**8**), 1-(2-nitro-2-azapropyl)-5*H*-tetrazole (**9**), 1-(2-nitro-2-azapropyl)-5-nitriminotetrazole·H₂O (**10a**), 1-(2-nitro-2-azapropyl)-5-nitriminotetrazole·EtOH (**10b**), 1,5-*bis*(2-nitro-2-azapropyl)-5-nitraminotetrazole (**11**), 1-methyl-5-(2-nitro-2-azapropyl)-5-nitraminotetrazole (**12**), 1-methyl-4-(2-nitro-2-azapropyl)-5-nitraminotetrazole (**13**), 1-methyl-5-(2-nitro-2-azapropyl)-5-aminotetrazole (**14**) and 2-methyl-5-(2-nitro-2-azapropyl)-5-nitraminotetrazole (**15**). In addition, the reaction of potassium 1-methyl-5-nitriminotetrazolate with

dimethyl sulfate was investigated yielding 1,4-dimethyl-5-nitriminotetrazole (**16**). All products (**8**–**16**) were determined by low temperature single X-ray diffraction. A comprehensive characterization and description of the chemical properties (IR, Raman, and multinuclear (¹H, ¹³C and ¹⁵N) NMR spectroscopy, mass spectrometry, elemental analysis and differential scanning calorimetry) is given. The heats of formation were calculated by heats of combustion measured using bomb calorimetry. With these values and the X-ray densities, several detonation parameters (e.g. detonation pressure, detonation velocity, heat of explosion) were computed by the EXPLO5 software. In addition, the sensitivities towards impact, friction and electrical discharge were determined.

Introduction

The synthesis of energetic, non-nuclear materials [1] for possible military or civil application has been a long term goal in our research group [2]. The standards for new energetic materials are high positive heat of formation, high detonation velocity and pressure, high thermal stability and low sensitivity towards external forces like impact, friction or electrostatic discharge. Of particular interest are high-nitrogen compounds (e.g. tetrazoles) in combination with energetic substituents such as nitro groups (*R*–NO₂) [3, 4], nitrate esters (*R*–O–NO₂) [5], azide groups (*R*–N₃) [6] or nitramine functionalities (*R*₂N–NO₂) [7, 8]. Also the formation of tetrazolium salts with oxygen rich counter anions such as NO₃[–] [9, 10] or N(NO₂)₂[–] [11, 12] are in the focus of our research, since these compounds have balanced oxygen contents. We recently reported on the synthesis and characterization of 2-(2-nitro-2-azapropyl)-5-nitrotetrazole [13], which has an appropriate oxygen balance similar to that of RDX (hexogen). The oxygen balance indicates the relative amount of oxygen available for the following ideal combustion reactions without adding *outer* oxygen: car-

bon to carbon dioxide, hydrogen to water, nitrogen to dinitrogen and sulfur to sulfur dioxide. The oxygen balance of CHNSO compounds can be easily calculated by the equation: $\Omega \text{ \%} = (w\text{O} - 2xC - 1/2y\text{H} - 2z\text{S}) \cdot 1600/M$. (*w*: number of oxygen atoms, *x*: number of carbon atoms, *y*: number of hydrogen atoms, *z*: number of sulfur atoms, *M*: molecular weight). In this work, we report on the synthesis of new neutral energetic materials combining tetrazole moieties with the 2-nitro-2-azapropyl substituent.

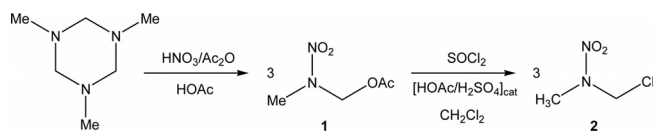
Results and Discussion

The preparative route to 2-nitro-2-azapropyl chloride (**2**) [14] is divided into two steps, shown in Scheme 1. The first step is the nitration of 1,3,5-trimethylhexahydro-1,3,5-triazine forming 2-nitro-2-azapropyl acetate (**1**) [15]. To a mixture of fuming nitric acid and acetic anhydride, 1,3,5-trimethylhexahydro-1,3,5-triazine, dissolved in glacial acetic acid, is added. Because of the strong exothermicity of the reaction it is necessary to control the temperature (70–75 °C) vigilantly. Otherwise, the reaction may run out of control resulting in further rise of the temperature and formation of highly explosive undesirable nitration products.

Compound **1** has to be converted into the 2-nitro-2-azapropyl chloride (**2**) since a leaving group is desired. Therefore, 2-nitro-2-azapropyl acetate is heated under reflux with thionyl

* Prof. Dr. T. M. Klapötke
E-Mail: tmk@cup.uni-muenchen.de

[a] Energetic Materials Research
Department of Chemistry and Biochemistry
Ludwig-Maximilian-University Munich
Butenandstr. 5–13
81377 Munich, Germany



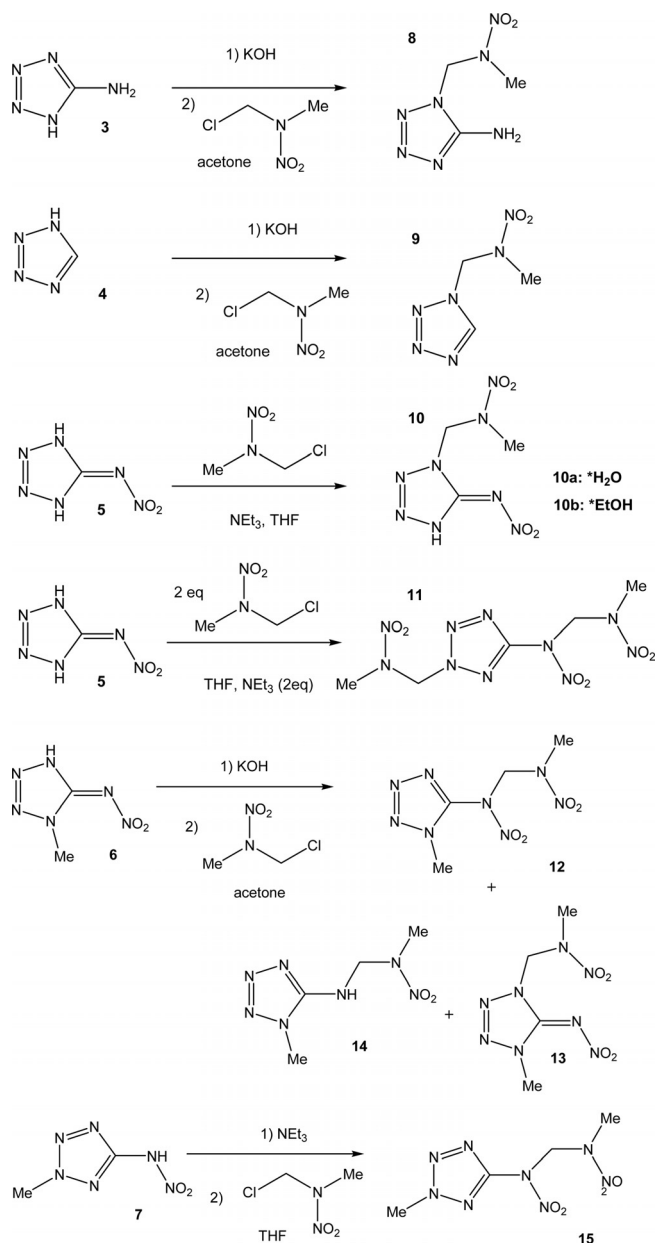
Scheme 1. Synthesis of 2-nitro-2-azapropyl chloride (**2**).

chloride in dichloromethane (DCM). Small amounts of acetic acid and sulfuric acid are used as catalysts.

The tetrazole derivatives **8–15** were synthesized according to Scheme 2. The starting tetrazoles were either purchased commercially [5-amino-1*H*-tetrazole (**3**)] or synthesized according to procedures described in literature (1*H*-tetrazole (**4**) [16, 5-nitriminotetrazole (**5**), 1-methyl-5-nitrimino-tetrazole (**6**), 2-methyl-5-nitraminotetrazole (**7**) 7a]. For the S_N1 -like mechanism, one nitrogen atom of the tetrazole moiety serves as nucleophile, which can be either the nitrogen atoms N1 and N2 or the nitrogen atom N5 of 5-aminotetrazole or different 5-nitriminotetrazoles. For increasing the nucleophilicity of the tetrazole moiety, it has to be activated, which is achieved by deprotonation of the tetrazole or the nitriminotetrazole, respectively, either with alkali metal bases or triethylamine. Polar and aprotic solvents such as acetone and tetrahydrofuran are favored. In case of using an alkali metal salt as starting material, the reaction has to be carried out in suspension. The advantage of carrying out the reaction with the help of triethylamine is the low solubility of the formed triethylammonium chloride in acetone and THF, so that the chloride is removed from the reaction mixture and the progress of the reaction can be observed with the formation of a white precipitate.

1-(2-Nitro-2-azapropyl)-5-aminotetrazole (**8**) was synthesized by stirring a mixture of potassium 5-aminotetrazolate and 2-nitro-2-azapropyl chloride in acetone overnight. The potassium salt of 5-aminotetrazole was synthesized according to literature [17] using aqueous KOH solution and recrystallized from pure ethanol. 1-(2-Nitro-2-azapropyl)-5*H*-tetrazole (**9**) was prepared analogously to **8** by using potassium tetrazolate [16]. 1-(2-Nitro-2-azapropyl)-5-nitriminotetrazole (**10**) could successfully be synthesized by using the monodeprotonated potassium salt of 5-nitriminotetrazole as suspension in acetone or neutral **5** with NEt₃ in THF. After the addition of **2**, the mixture was stirred at room temperature overnight without being refluxed. It is important, that the potassium salt is used in more than double excess. In any case the potassium salt and the 2-nitro-2-azapropyl chloride were used in equimolar amounts, it was not possible to isolate one single product, but always a mixture of **10** and 2,5-bis(2-nitro-2-azapropyl)-nitriminotetrazole (**11**). Compound **10** could not be obtained crystalline without inclusion of any solvent. Recrystallization from water or wet methanol afforded the monohydrate **10a**, recrystallization from ethanol afforded the inclusion of one molecule ethanol (**10b**). Compound **11** is synthesized best by stirring two equivalents of **2** with **5**, which was deprotonated in situ by two equivalents of triethylamine.

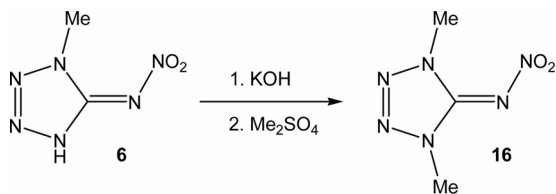
The reaction of potassium 1-methyl-5-nitriminotetrazolate [18] with **2** ended in three products. The main product 1-methyl-5-(2-nitro-2-azapropyl)-nitraminotetrazole (**12**) was



Scheme 2. Synthesis of 2-nitro-2-azapropyl-tetrazoles **8–15**.

obtained in ~60 % yield. The isomer 1-methyl-4-(2-nitro-2-azapropyl)-5-nitriminotetrazole (**13**) was obtained only in very low yields and was detected due to its different crystal shape, while crystal picking of **12**. A third product (~12 %) 1-methyl-5-(2-nitro-2-azapropyl)-5-aminotetrazole (**14**) was obtained as colorless crystals by allowing the mother liquor to stand for a few days. The mechanism of the formation of **14** has not been clarified yet. The coupling reaction of **2** and **7** was carried out as suspension reaction with THF as solvent and one equivalent of triethylamine as base. After filtration and evaporation 2-methyl-5-(2-nitro-2-azapropyl)-nitramino-tetrazole (**15**) was obtained in 94 % yield. The synthesis using the potassium salt of 2-methyl-5-nitraminotetrazole yielded a yellow oil, which could not be recrystallized.

As previously described, alkylation of compound **6** with 2-nitro-2-azapropyl chloride gave three different products. Therefore the alkylation of deprotonated **6** was investigated additionally by the reaction of potassium 1-methyl-5-nitraminotetrazolate and dimethyl sulfate (Scheme 3). In contrast to the previously described alkylation of **6**, only one product [1,4-dimethyl-5-nitriminotetrazole (**16**)] could be isolated in high yields (~85 %).



Scheme 3. Synthesis of 1,4-dimethyl-5-nitriminotetrazole (**16**).

Crystal Structures

Suitable single crystals of **8–16** were picked from the crystallization mixture, mounted in Kel-F oil and transferred to the N₂ stream of an Oxford Xcalibur3 diffractometer with a Spellman

generator (voltage 50 kV, current 40 mA) and a KappaCCD detector. The data collection was performed using the CrysAlis CCD software [19], the data reduction with the CrysAlis RED software [20]. The structures were solved with SIR-92 (**8–12**, **14**, **15**) [21], and SHELXS-97 (**13**, **16**) [22], refined with SHELXL-97 [23] and finally checked using the PLATON software [24], integrated in the WINGX software suite [25]. The non-hydrogen atoms were refined anisotropically and the hydrogen atoms were located and freely refined. In the case of the chiral space groups in **9** and **11**, the “Friedel” pairs were merged. The absorptions were corrected by a SCALE3 AB-SPACK multi-scan method [26]. All relevant data and parameters of the X-ray measurements and refinements are given in Table 1 and Table 2. Further information on the crystal-structure determinations have been deposited with the Cambridge Crystallographic Data Centre [27] as supplementary publication No. 652906 (**8**), 703983 (**9**), 703979 (**10a**), 703978 (**10b**), 703984 (**11**), 652908 (**12**), 652907 (**13**), 703982 (**14**), 703980 (**15**) and 703981 (**16**).

1-(2-Nitro-2-azapropyl)-5-aminotetrazole (**8**) crystallizes in the monoclinic space group *P*2₁/*c* with four molecules in the unit cell. The molecular moiety is depicted in Figure 1. The density of 1.628 g·cm^{−3} is higher than that of 5-aminotetrazole

Table 1. Crystallographic data and parameters of compounds **8–11**.

	8	9	10a	10b	11
Formula	C ₃ H ₇ N ₇ O ₂	C ₃ H ₆ N ₆ O ₂	C ₃ H ₈ N ₈ O ₅	C ₅ H ₁₂ N ₈ O ₅	C ₅ H ₁₀ N ₁₀ O ₆
FW /g·mol ^{−1}	173.16	158.14	236.17	264.20	306.23
Crystal system	monoclinic	monoclinic	monoclinic	monoclinic	monoclinic
Space Group	<i>P</i> 2 ₁ / <i>c</i> (No. 14)	<i>P</i> 2 ₁ (No. 4)	<i>P</i> 2 ₁ / <i>c</i> (No. 14)	<i>P</i> 2 ₁ / <i>c</i> (No. 14)	<i>P</i> 2 ₁ (No. 4)
Color / Habit	colorless rods	colorless plates	colorless rods	colorless rods	colorless needles
Size /mm	0.04 × 0.12 × 0.14	0.06 × 0.10 × 0.15	0.16 × 0.18 × 0.25	0.09 × 0.13 × 0.14	0.05 × 0.06 × 0.14
<i>a</i> /Å	8.6244(4)	6.0193(3)	6.3626(3)	5.6304(4)	9.175(1)
<i>b</i> /Å	6.8715(4)	6.4786(3)	22.1364(8)	24.810(2)	6.177(1)
<i>c</i> /Å	12.0481(6)	8.4598(4)	6.9804(3)	8.5116(6)	11.171(2)
α /°	90	90	90	90	90
β /°	98.263(4)	98.952(5)	13.982(6)	109.103(6)	90.38(1)
γ /°	90	90	90	90	90
<i>V</i> /Å ³	706.59(6)	325.89(3)	898.28(8)	1123.52(14)	633.09(17)
<i>Z</i>	4	2	4	4	2
$\rho_{\text{calcd.}}$ /g·cm ^{−3}	1.628	1.612	1.746	1.562	1.606
μ /mm ^{−1}	0.136	0.136	0.160	0.137	0.144
<i>F</i> (000)	360	164	488	552	316
$\lambda_{\text{Mo-K}\alpha}$ /Å	0.71073	0.71073	0.71073	0.71073	0.71073
<i>T</i> /K	200	200	200	200	200
τ min–max /°	3.9, 26.0	3.9, 32.4	4.0, 26.2	3.8, 25.3	3.8, 30.1
Dataset <i>h</i> ; <i>k</i> ; <i>l</i>	−10:10; −8:7; −11:14	−8:9; −9:9; −12:12	−7:7; −26:27; −8:3	−6:6; −29:29; −10:10	−12:12; −8:8; −15:15
Reflect. coll.	3508	4877	4690	10537	8408
Independ. refl.	1379	1206	1792	2032	2007
<i>R</i> _{int}	0.049	0.021	0.018	0.036	0.050
Reflection obs.	743	1042	1343	1398	1034
No. parameters	137	124	177	193	208
<i>R</i> ₁ (obs)	0.0323	0.0251	0.0371	0.0487	0.0318
<i>wR</i> ₂ (all data)	0.0742	0.0656	0.1057	0.1557	0.0698
<i>S</i>	0.82	1.08	1.09	1.07	0.91
Resd. Dens. /e·Å ^{−3}	−0.16, 0.18	−0.19, 0.24	−0.43, 0.41	−0.39, 0.91	−0.17, 0.18
Device type	Oxford Xcalibur3 CCD	Oxford Xcalibur3 CCD	Oxford Xcalibur3 CCD	Oxford Xcalibur3 CCD	Oxford Xcalibur3 CCD
Solution	SIR-92	SIR-92	SIR-92	SIR-92	SIR-92
Refinement	SHELXL-97	SHELXL-97	SHELXL-97	SHELXL-97	SHELXL-97
Absorpt. corr.	multi-scan	multi-scan	multi-scan	multi-scan	multi-scan
CCDC	652906	703983	703979	703978	703984

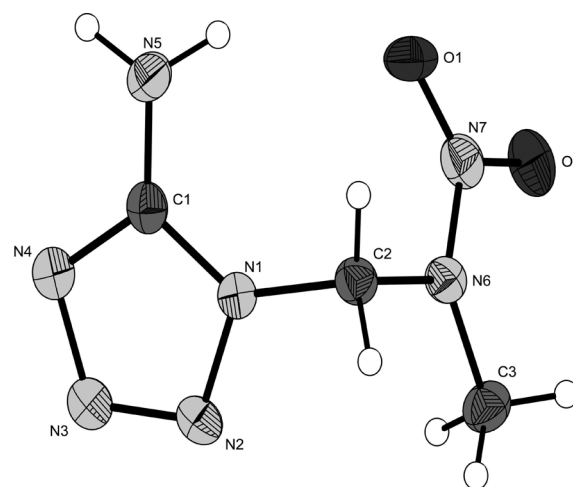
Table 2. Crystallographic data and parameters of compounds **12**–**16**.

	12	13	14	15	16
Formula	C ₄ H ₈ N ₈ O ₄	C ₄ H ₈ N ₈ O ₄	C ₄ H ₉ N ₇ O ₂	C ₄ H ₈ N ₈ O ₄	C ₃ H ₆ N ₆ O ₂
FW /g·mol ^{−1}	232.18	232.18	187.18	232.18	158.12
Crystal system	monoclinic	orthorhombic	monoclinic	monoclinic	orthorhombic
Space Group	<i>P2</i> ₁ / <i>c</i> (No. 14)	<i>Pbca</i> (No. 61)	<i>P2</i> ₁ / <i>c</i> (No. 14)	<i>P2</i> ₁ / <i>c</i> (No. 14)	<i>Pbca</i> (No. 61)
Color / Habit	colorless rods	colorless blocks	colorless rods	colorless rods	colorless blocks
Size /mm	0.06 × 0.15 × 0.20	0.05 × 0.05 × 0.07	0.09 × 0.13 × 0.16	0.08 × 0.11 × 0.12	0.03 × 0.14 × 0.15
<i>a</i> /Å	11.1953(6)	9.413(2)	5.8461(3)	9.2526(5)	14.2278(5)
<i>b</i> /Å	9.3248(4)	9.225(2)	18.4860(7)	11.3617(6)	6.1607(2)
<i>c</i> /Å	9.9411(4)	21.355(4)	8.0667(4)	9.5915(6)	31.200(1)
α /°	90	90	90	90	90
β /°	111.217(5)	90	110.769(5)	106.156(6)	90
γ /°	90	90	90	90	90
<i>V</i> /Å ³	967.45(8)	1854.5(6)	815.13(7)	968.49(10)	2734.81(16)
<i>Z</i>	4	8	4	4	16
$\rho_{\text{calcd.}}$ /g·cm ^{−3}	1.594	1.663	1.525	1.592	1.536
μ /mm ^{−1}	0.140	0.146	0.125	0.140	0.129
<i>F</i> (000)	480	960	392	480	1312
$\lambda_{\text{Mo-K}\alpha}$ /Å	0.71073	0.71073	0.71073	0.71073	0.71073
<i>T</i> /K	200	200	200	200	100
τ min–max /°	3.9, 26.0	3.6, 26.0	3.9, 26.0	4.0, 26.0	3.8, 26.0
Dataset <i>h</i> ; <i>k</i> ; <i>l</i>	−8:13; −7:11; −12:12	−11:8; −10:11; −26:18	−7:6; −21:22; −8:9	−10:11; −14:10; −11:10	−17:17; −7:7; −38:38
Reflect. coll.	4064	8975	4004	4883	25785
Independ. refl.	1890	1814	1580	1890	2676
<i>R</i> _{int}	0.026	0.147	0.041	0.027	0.080
Reflection obs.	1125	643	1085	1146	1386
No. parameters	177	177	154	177	247
<i>R</i> ₁ (obs)	0.0342	0.0415	0.043	0.0349	0.0369
<i>wR</i> ₂ (all data)	0.0757	0.0917	0.0884	0.0904	0.0893
<i>S</i>	0.89	0.78	1.01	0.94	0.98
Resd. Dens. /e·Å ^{−3}	−0.24, 0.20	−0.29, 0.24	−0.20, 0.21	−0.22, 0.22	−0.25, 0.17
Device type	Oxford Xcalibur3 CCD	Oxford Xcalibur3 CCD	Oxford Xcalibur3 CCD	Oxford Xcalibur3 CCD	Oxford Xcalibur3 CCD
Solution	SIR-92	SHELXS-97	SIR-92	SIR-92	SHELXS-97
Refinement	SHELXL-97	SHELXL-97	SHELXL-97	SHELXL-97	SHELXL-97
Absorpt. corr.	multi-scan	multi-scan	multi-scan	multi-scan	multi-scan
CCDC	652908	652907	703982	703980	703981

monohydrate (3·H₂O) [31]. Bond lengths can be found in Table 3 and are similar to those of 3·H₂O. As a matter of course, the tetrazole ring is planar, (as observed in all structures in this work) building an aromatic 6 π ring system. The distance C1–N5 [1.341(2) Å] is significantly shorter than that of a typical C–N single bond. The protons at the primary amine N5 are twisted only slightly (15–20 °) out of the ring plane. The N1–C2 bond length of 1.459(2) Å follows exactly the distance of C–N single bonds. The nitrogen atom N6 is surrounded nearly trigonal planar, whereby also the nitro oxygen atoms lay in this plane. A weak intramolecular hydrogen bond is found between the atoms N5 and O1 [N5–H5B···O1: 0.89(2), 2.49(2), 3.165(2) Å, 134(3)°].

The packing of **8** is characterized by a wave like pattern, which can be seen in Figure 2. This motif is fixed by the strong hydrogen bond N5–H5a···N4ⁱ [0.90(2), 2.10(2), 2.987(2) Å, 169(2)°; (i) = 2−*x*, −*y*, 2−*z*].

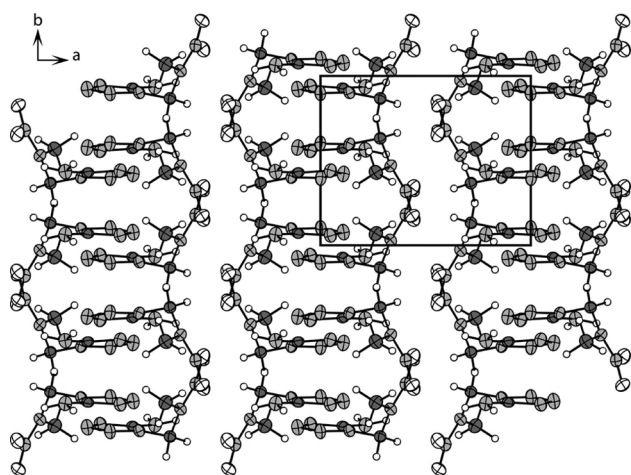
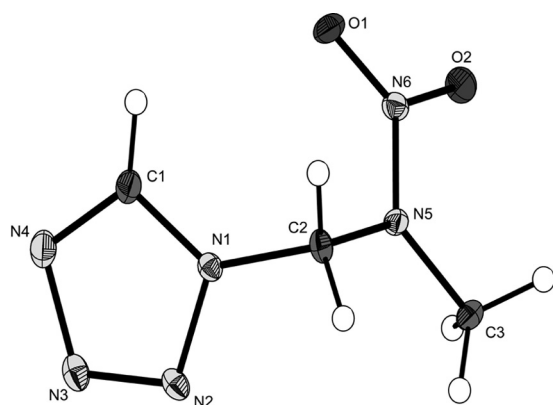
1-(2-Nitro-2-azapropyl)-tetrazole (**9**) crystallizes in the chiral monoclinic space group *P2*₁ with two molecules in the unit cell. The density of 1.612 g·cm^{−3} is only slightly lower than that of **8**, although no classical hydrogen bonds can be formed. However, the proton located at the carbon atom C1 is forming a weak non-classical hydrogen bond [C1–H1···N4ⁱ: 0.92(2),

**Figure 1.** Molecular moiety of **8**. Ellipsoids of non-hydrogen atoms are drawn at the 50 % probability level.

2.66(2), 3.534(2) Å, 160(2)°; (i) 1−*x*, 0.5+*y*, 1−*z*]. The molecular structure (Figure 3) is similar to that of **8**. Again, the nitrogen atom N5 is enclosed trigonal planar [torsion angle C2–N5–N6–O2 = 178.6(1)°].

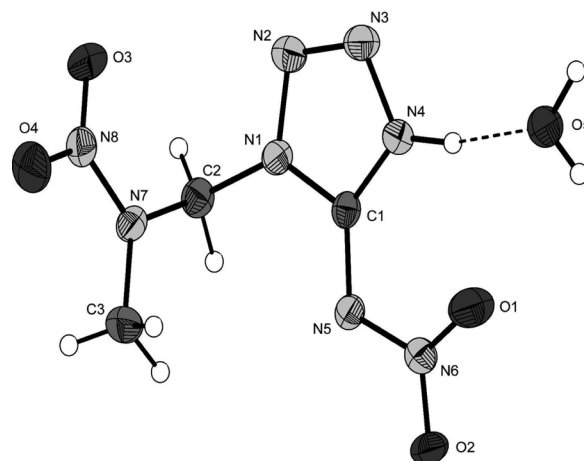
Table 3. Bond lengths /Å of compounds **8–16**.

Atoms	8	9	10·H₂O	10·EtOH	11	12	13	14	15	16
N1–N2	1.371(2)	1.351(2)	1.370(2)	1.364(3)	1.331(3)	1.345(2)	1.363(3)	1.365(2)	1.326(2)	1.358(2)
N2–N3	1.294(2)	1.295(2)	1.268(2)	1.279(3)	1.318(3)	1.311(2)	1.285(3)	1.292(2)	1.311(2)	1.282(2)
N3–N4	1.360(2)	1.373(2)	1.360(2)	1.355(3)	1.319(3)	1.362(2)	1.365(3)	1.366(2)	1.320(2)	1.354(2)
N5–N6			1.350(2)	1.358(3)	1.381(3)	1.395(2)	1.371(3)		1.403(2)	1.350(2)
N6–O1			1.243(2)	1.247(3)	1.219(3)	1.220(2)	1.252(3)		1.216(2)	1.241(2)
N6–O2			1.220(2)	1.225(3)	1.219(3)	1.223(2)	1.236(3)		1.214(2)	1.236(2)
N1–C1	1.339(2)	1.335(2)	1.356(2)	1.348(3)	1.320(3)	1.334(2)	1.354(4)	1.336(2)	1.318(2)	1.337(3)
N4–C1	1.330(2)	1.317(2)	1.335(2)	1.344(4)	1.334(3)	1.315(2)	1.348(4)	1.333(2)	1.336(2)	1.340(2)
N5–C1	1.341(2)		1.341(2)	1.341(3)	1.392(3)	1.399(2)	1.327(4)	1.353(2)	1.399(2)	1.347(3)
N1(4,5)–C2(3)	1.459(2)	1.464(2)	1.461(2)	1.463(3)	1.457(3)	1.458(2)	1.479(4)	1.436(3)	1.459(2)	1.454(3)
N1–Me						1.460(2)	1.464(5)	1.455(3)	1.456(2)	1.458(3)
C2(3)–N(NO ₂)Me	1.445(2)	1.442(2)	1.438(2)	1.435(3)	1.439(3)	1.448(2)	1.434(4)	1.462(3)	1.440(2)	
N–NO ₂	1.358(2)	1.340(1)	1.355(2)	1.355(3)	1.337(3)	1.347(2)	1.365(4)	1.344(2)	1.348(2)	
N(NO ₂)–Me	1.468(2)	1.458(2)	1.457(2)	1.457(4)	1.457(3)	1.458(2)	1.460(5)	1.454(2)	1.446(3)	
N(Me)–O1(3)	1.233(2)	1.241(1)	1.229(2)	1.227(3)	1.230(2)	1.240(2)	1.239(3)	1.243(2)	1.234(2)	
N(Me)–O2(4)	1.231(2)	1.233(1)	1.228(2)	1.229(3)	1.236(2)	1.233(2)	1.230(3)	1.236(2)	1.218(2)	

**Figure 2.** View on the packing of **8** along the *b* axis. One unit cell is marked.**Figure 3.** Molecular moiety of **9**. Ellipsoids of non-hydrogen atoms are drawn at the 50 % probability level.

1-(2-Nitro-2-azapropyl)-5-nitrimino-1*H*-tetrazole (**10**) was only obtained crystalline with one molecule of water or ethanol, as shown in Figure 4 and Figure 5. Both crystallize with densi-

ties of 1.746 g·cm^{−3} (**10**·H₂O) and 1.562 g·cm^{−3} (**10**·EtOH) in the space group *P2₁/c* with four molecules in the unit cell. The molecular structures are very similar and in good agreement to those of other 1-substituted 5-nitrimino-tetrazoles, e.g. 1-methyl-5-nitriminotetrazole. The 2-nitro-2-azapropyl substituent follows the structure found in **8** and **9**. The remaining ring proton forms a very strong hydrogen bond to the crystal water ([N4–H4···O5: 0.90(3), 1.77(3), 2.673(2) Å, 168(3)°] and also to the ethanol oxygen atom [N4–H4···O5: 0.89(4), 1.79(4), 2.648(3) Å, 161(4)°], respectively. This may explain that the solvent free compound was only obtained as colorless oil. The hydroxyl group of the ethanol forms on his part a strong hydrogen bond to one of the nitro oxygen atoms of a neighbored molecule [O5–H5···O1ⁱ: 0.93(5), 2.01(5), 2.930(3) Å, 168(4)°; (i) 1–*x*, 1–*y*, 1–*z*]. Also the water hydrogen atoms form strong hydrogen bonds to the atoms O2 and N5 of different neighbored molecules, which is a reason for the relatively high density observed for this compound.

**Figure 4.** Molecular moiety of **10**·H₂O. Ellipsoids of non-hydrogen atoms are drawn at the 50 % probability level. Marked hydrogen bond: N4–H4···O5: 0.94(3), 1.77(3), 2.691(2) Å, 166(2)°.

2,5-Bis(2-nitro-2-azapropyl)-5-nitraminotetrazole (**11**) crystallizes in the monoclinic space group *P2₁* with two molecules

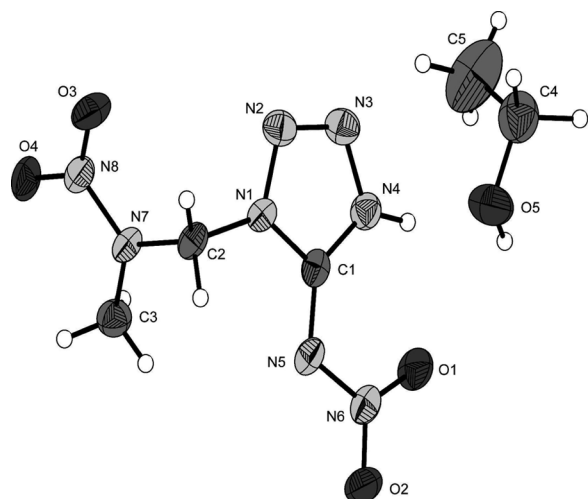


Figure 5. Molecular moiety of **10**-EtOH. Ellipsoids of non-hydrogen atoms are drawn at the 50 % probability level.

in the unit cell. No classical or non-classical hydrogen bonds can be found in the packing of **11**. However, the resulting density of $1.606 \text{ g}\cdot\text{cm}^{-3}$ is in the range of the other structures discussed in this work. The molecular moiety is shown in Figure 6. Interestingly, alkylation takes place at the nitrogen atoms N2 and N5. The structure of both 2-nitro-2-aza-propyl chains is nearly the same.

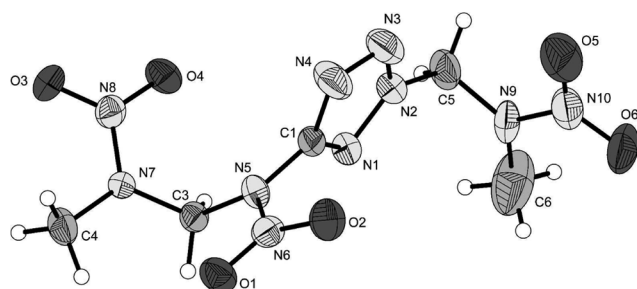


Figure 6. Molecular moiety of **11**. Ellipsoids of non-hydrogen atoms are drawn at the 50 % probability level. Selected distances not given in Table 3: N9–N10 = 1.353(3), N9–C4 = 1.424(4), N9–C5 = 1.435(4), N10–O5 = 1.213(3), N10–O6 = 1.220(3), C4–N2 = 1.455(4).

The alkylation products of 1-methyl-5-nitriminotetrazole **12** and **13** crystallize in common space groups (**12**: $P2_1/c$, **13**: $Pbca$). The molecular structures (Figure 7 and Figure 8) show significant differences. Whereas in **12** the nitro group is strongly twisted out of the ring plane [torsion angle N1–C1–N5–N6 = $-75.6(2)^\circ$] it is less twisted [N1–C1–N5–N6 = $39.3(6)^\circ$] in **13**. Also the C1–N5 bond lengths differ obviously. In the structure of **12** this bond of $1.399(2) \text{ \AA}$ is closer to a C–N single bond, whereas in **13** a distance [$1.327(4) \text{ \AA}$] closer to a C=N double bond is observed. The density of **13** ($1.663 \text{ g}\cdot\text{cm}^{-3}$) is significantly higher than that of **12** ($1.594 \text{ g}\cdot\text{cm}^{-3}$). It might be a general trend that 1,4-substituted nitriminotetrazoles have higher densities than 1,5-substituted ones, which also can be observed by comparing 1,4-dimethyl-

5-nitriminotetrazole (**15**, $1.536 \text{ g}\cdot\text{cm}^{-3}$) with 1,5-dimethyl-5-nitriminotetrazole ([**7c**, $1.522 \text{ g}\cdot\text{cm}^{-3}$).

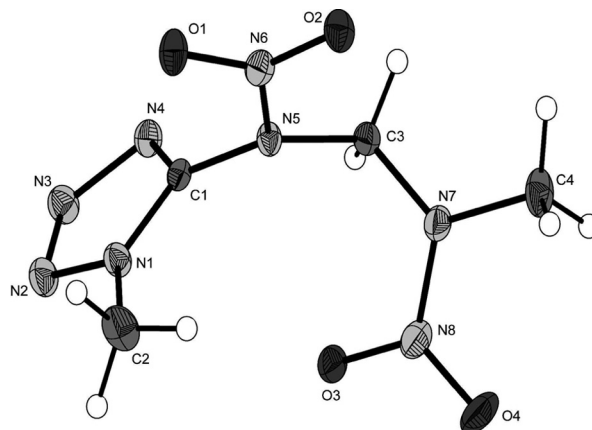


Figure 7. Molecular moiety of **12**. Ellipsoids of non-hydrogen atoms are drawn at the 50 % probability level.

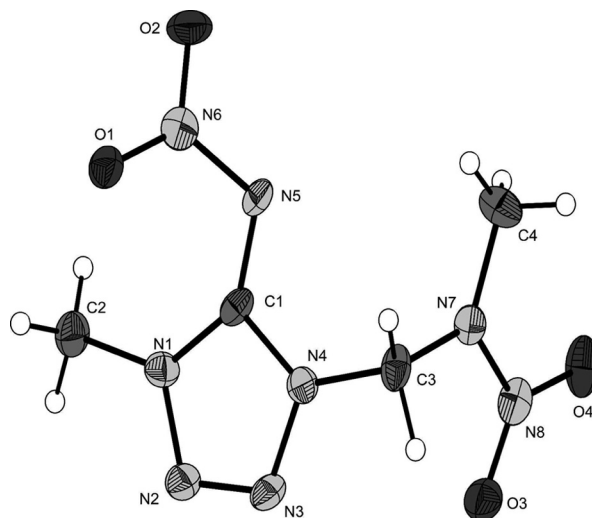


Figure 8. Molecular moiety of **13**. Ellipsoids of non-hydrogen atoms are drawn at the 50 % probability level.

The lowest density observed in this work was calculated for 1-methyl-5-(2-nitro-2-azapropyl)-5-aminotetrazole (**14**) ($1.525 \text{ g}\cdot\text{cm}^{-3}$), which crystallizes in the monoclinic space group $P2_1/c$ with four molecules in the unit cell. The 2-nitro-2-azapropyl unit bonded [N5–C3 = $1.454(3) \text{ \AA}$] at nitrogen atom N5 follows the constitution observed for the other structures discussed in this work. The tetrazole part in Figure 9 resembles the structure of 1-methyl-5-aminotetrazole and its salts. The C1–N5 bond length of $1.347(3) \text{ \AA}$ is similar to this observed for **8**.

2-Methyl-5-(2-nitro-2-azapropyl)-5-nitraminotetrazole (**15**) crystallizes in the monoclinic space group $P2_1/c$ with four molecules in the unit cell. The density of $1.592 \text{ g}\cdot\text{cm}^{-3}$ is similar to that observed for the corresponding 1-methyl compound **12** ($1.596 \text{ g}\cdot\text{cm}^{-3}$). The molecular moiety is shown in Figure 10. The left part is in agreement to the structure observed for

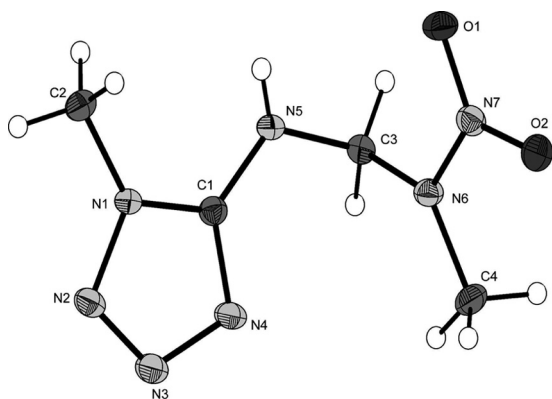


Figure 9. Molecular moiety of **14**. Ellipsoids of non-hydrogen atoms are drawn at the 50 % probability level.

2-methyl-5-aminotetrazole described by Bryden [31]. The N5–C1 bond length of 1.399(2) Å is also comparable to that of **12**. Therefore, compound **15** should be described as a “5-nitraminotetrazole”.

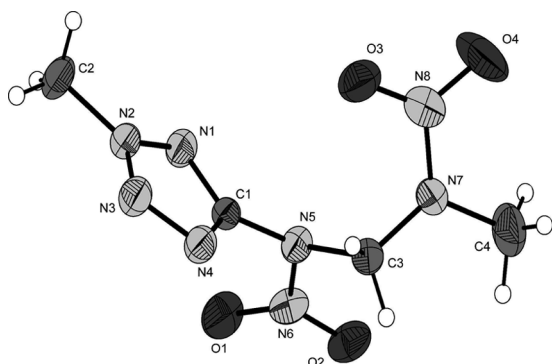


Figure 10. Molecular moiety of **15**. Ellipsoids of non-hydrogen atoms are drawn at the 50 % probability level.

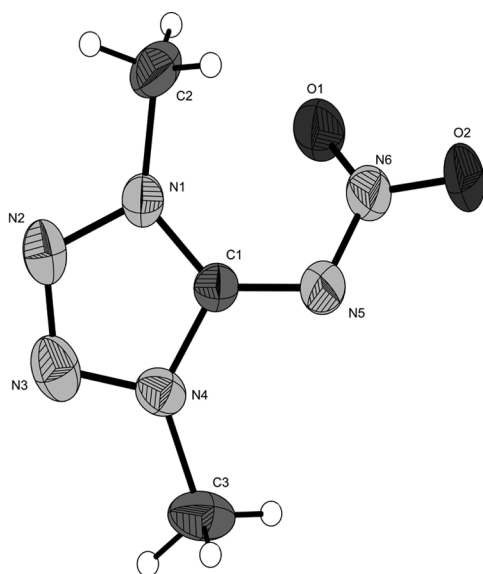


Figure 11. Molecular moiety of **16**. Ellipsoids of non-hydrogen atoms are drawn at the 50 % probability level.

1,4-Dimethyl-5-nitriminotetrazole (**16**) crystallizes in the orthorhombic space group *Pbca* with 16 molecules in the unit cell. In Figure 11 only one molecular moiety is shown.

Both methyl groups are bonded with the same distance of 1.458(3) Å (N1–C2) and 1.454(3) Å (N4–C3) to the tetrazole nitrogen atoms. The C1–N5 bond length of 1.341(2) Å is closer to a C=N double bond, which legitimates the nomenclature “nitrimine”. The nitrimine group is strongly twisted out of the ring plane forming a torsion angle N4–C1–N5–N6 of 142.9(2)°. Since no hydrogen bonds can be formed the observed density of 1.536 g·cm^{−3} is low in comparison with other 5-nitriminotetrazoles. For comparison, 5-nitriminotetrazole and 1-methyl-5-nitrimino-tetrazole show densities of 1.894 g·cm^{−3} and 1.716 g·cm^{−3}, respectively.

Spectroscopy

Multinuclear NMR Spectroscopy

Compounds **8–12** as well as **14** and **15** were investigated by using ¹H, ¹³C{¹H}, and ¹⁵N or ¹⁵N{¹H} NMR spectroscopy. The chemical shifts are given with respect to TMS (¹H, ¹³C) as well as MeNO₂ (¹⁴N, ¹⁵N) as external standards. All spectra were measured in [D₆]DMSO.

¹H NMR: Compared to the starting material **2**, all proton signals of the methylene group of **8–15** are strongly shifted downfield because of the coordination of the 2-nitro-2-azapropyl moiety to the electron withdrawing tetrazole ring system. They exhibit values of 6.06 (**12**) to 6.81 ppm (**11**). Compound **11** contains two of the 2-nitro-2-azapropyl groups attached to the tetrazole ring. One exception from that rule is **14**, in which the 2-nitro-2-azapropyl moiety is attached to the 5-amino group of 1-methyl-5-aminotetrazole with a chemical shift of 5.21 ppm for CH₂ protons and a C–H coupling constant of 6.3 Hz. The same applies for the methyl group of the 2-nitro-2-azapropyl moiety with chemical shifts of 3.47 ppm to 3.55 ppm for **9–15**. The methyl group of **8** is shifted upfield to 3.13 ppm. The aromatic proton of **9** (9.58 ppm) is slightly shifted downfield compared to 1*H*-tetrazole. The methyl protons directly attached to the tetrazole ring in **12**, **14** and **15** exhibit chemical shifts of 4.03 ppm, 3.71 ppm and 4.49 ppm, which is downfield of the chemical shifts for 1-methyl-5-aminotetrazole (3.69 ppm) and 2-methyl-5-aminotetrazole (4.07 ppm) respectively. In addition, for **10**·H₂O and **10**·EtOH the signals of water and ethanol can be seen with chemical shifts according to those for H₂O and EtOH as residual solvents in DMSO.

¹³C NMR: The aromatic tetrazole carbon atoms exhibits chemical shifts between 145.2 (**9**) and 159.5 ppm (**11**), with the trend to downfield shifted signals for the 2-substituted tetrazoles **11** and **15** of 159.5 and 159.1 ppm, respectively, and upfield shifted signals for the 1-substituted compounds **12** and **14** of 150.6 and 155.7 ppm as well as for the unsubstituted compound **9** (145.2 ppm). Comparison of **8** and **10** allows the conclusion, that nitration of the 5-amino group at the tetrazole results in a significant upfield shift of the cyclic carbon atom (**8**: 156.2 ppm, **10**: 151.4 ppm). The chemical shifts for the methyl-

ene and the methyl group of the 2-nitro-2-azapropyl moiety are in the expected range of 59.6 to 67.4 ppm for the methylene group and 39.0 to 39.9 ppm for the methyl group, which are almost identical to the chemical shifts observed for the starting material, however slightly shifted downfield.

^{15}N NMR spectra of compounds **8–12**, as well as **14** and **15** can be seen in Figure 12. Although the ^{15}N NMR spectrum of **8** was measured proton decoupled, all seven nitrogen atoms of **8** could clearly be assigned according to the ^{15}N NMR of 1-methyl-5-aminotetrazole [32]. Nitrogen atoms N3 (6.9 ppm)

and N2 (−26.6 ppm) are shifted most to lower field because of two neighboring nitrogen atoms in the tetrazole ring. Atom N4 with one neighboring nitrogen atom and one carbon atom is shifted to −94.7 ppm, whereas the two nitrogen atoms neighbored by two carbon atoms, N1 and N6, are shifted to −176.2 ppm and −205.3 ppm with the higher shift for the nitramine nitrogen. The electron rich 5-amino-group is found at −335.9 ppm and the nitro group of the nitramine at −30.0 ppm.

A similar explanation also applies to the ^{15}N NMR spectra of **9–12** and **14** as well as **15**. Proton coupled ^{15}N NMR spectra

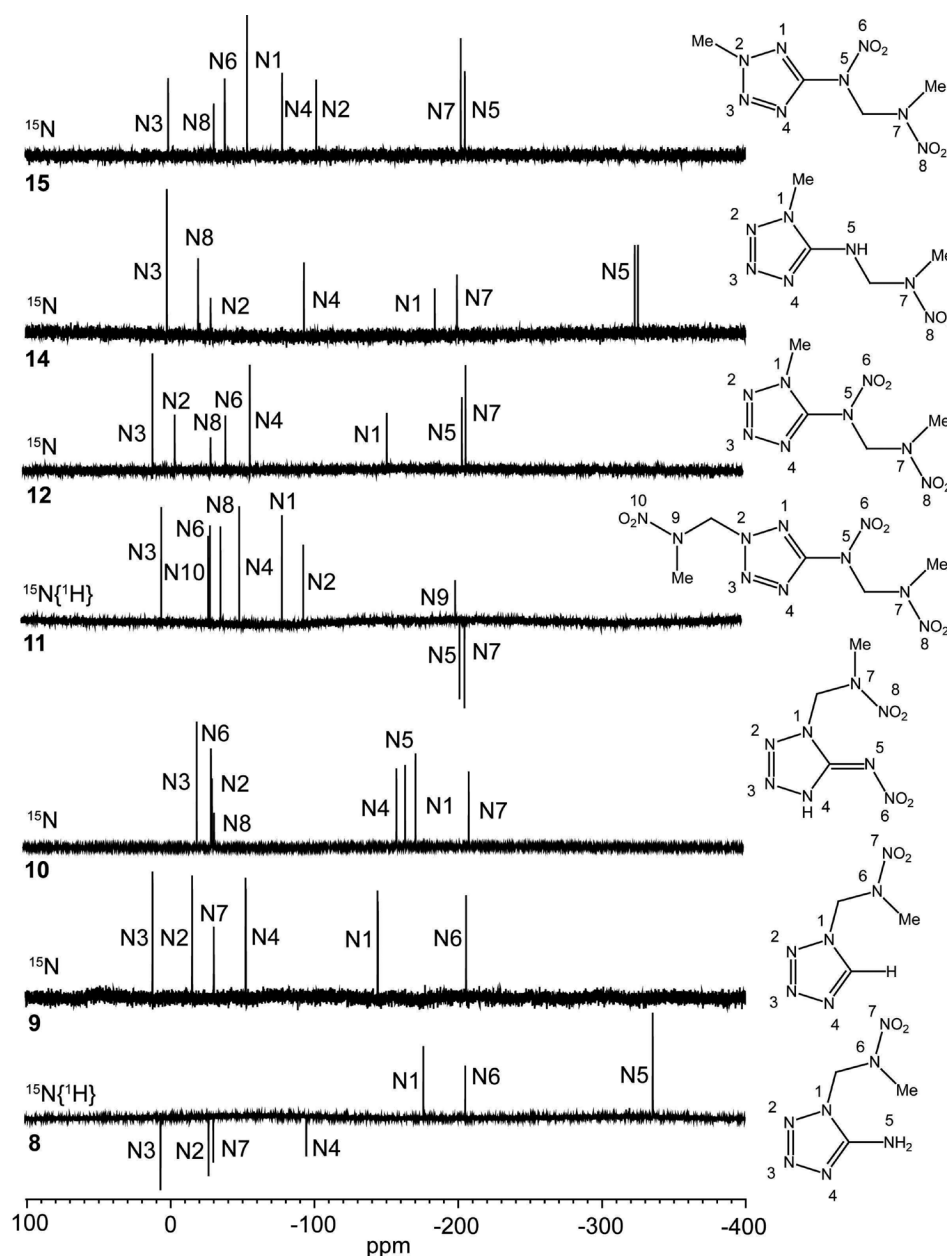


Figure 12. ^{15}N NMR spectra of **8**, **9**, **10**·H₂O, **11**, **12**, **14** and **15** measured in $[D_6]DMSO$. δ : **8** = 6.9 (N3), −26.6 (N2), −30.0 (N7), −94.7 (N4), −176.2 (N1), −205.3 (N6), −333.9 (N5); **9** = 12.2 (N3), −15.3 (N2), −30.4 (N7), −52.6 (N4), −144.3 (N1), −205.9 (N6); **10**·H₂O = −20.2 (N3), −30.1 (N6), −30.8 (N2), −32.2 (N8), −159.1 (N4), −165.1 (N5), −172.4 (N1), −209.4 (N7); **11** = 2.9 (N3), −29.7 (N10), −30.9 (N6), −38.2 (N8), −51.2 (N4), −80.9 (N1), −95.7 (N2), −201.3 (N9), −204.2 (N5), −207.8 (N7); **12** = 9.9 (N3), −5.5 (N2), −30.4 (N8), −40.8 (N6), −57.8 (N4), −152.7 (N1), −205.0 (N7), −207.5 (N5); **14** = 1.3 (N3), −20.3 (N2), −29.0 (N8), −93.8 (N4), −184.5 (N4), −199.9 (N1), −324.4 (N5); **15** = 1.4 (N3), −30.4 (N8), −37.9 (N6), −53.4 (N4), −77.9 (N1), −101.6 (N2), −202.1 (N5), −204.9 (N7).

troscopy is more suitable for alkyl-substituted tetrazoles, since the assignments can be performed by evaluating the 2J and 3J ^{15}N – ^1H coupling constants. Interestingly, in the case of the 2-nitro-2-azapropyl substituent only the 3J coupling (triplet, ca. 1.5 Hz) can be observed significantly, whereas the 2J coupling is hard to detect. All spectra are in agreement with similar ones found for 1- and 2-methyl-5-nitraminotetrazole [7a]. There are strong similarities between the NMR spectra of **12**, **14**, and **15**, which only differ in the position of the methyl group (**12** and **15**) or concerning the nitro group at N5 (**12** and **14**). In all spectra, N3 is shifted downfield [9.9 ppm (**12**), 1.3 ppm (**14**), and 1.4 ppm (**15**)]. The resonance of the nitrogen core N2 strongly varies depending on the substitution of the tetrazole ring. It exhibits chemical shifts of -5.5 ppm (**12**) and -20.3 ppm (**14**) for the 1-substituted tetrazoles and is shifted to -101.6 ppm in the case of **15**, where the tetrazole ring is substituted in position 2. The chemical shifts of nitrogen atom N4 range from -53.4 ppm in **15** to -93.8 ppm in **14**, where it splits up into a doublet with a coupling constant of $^3J_{\text{NH}} = 2.2$ Hz because of the coupling with the remaining proton of the 5-amino group. N4 in **12** can be assigned to the resonance at -57.8 ppm. The resonance of the 5-amino group in compound **14** exhibits a doublet with $^1J_{\text{N-H}} = 94$ Hz at -324.4 ppm.

Vibrational Spectroscopy

Also vibrational spectroscopy, such as IR and Raman spectroscopy is adequate to identify substituted 5-amino- as well as 5-nitriminotetrazoles. All absorptions measured were assigned according to commonly observed absorptions described in literature [33–35].

The infrared and Raman spectra of **8–15** are mainly determined by the stretching and deformation vibrations of aliphatic methylene and methyl groups, nitro groups and vibrations of the tetrazole ring. The bands of the C–H stretching vibrations are located in the range of 3055 – 2837 cm^{-1} , whereas, three or four bands can be distinguished in all cases. Stretching and deformation vibrations of the tetrazole ring can be assigned to one distinct band, which is located within the range of 1020 – 1025 cm^{-1} and two or three further absorptions in the range from 1038 cm^{-1} to 1147 cm^{-1} . Apart from that, a different absorption of the tetrazole moiety is observed between 1265 cm^{-1} and 1320 cm^{-1} . The most characteristic absorptions, however, derive from the nitro groups. Compounds **8**, **9** and **15** exhibit one set of absorptions each, which are located

at 1297 cm^{-1} and 1521 cm^{-1} (**8**), 1281 cm^{-1} and 1533 cm^{-1} (**9**) and 1300 cm^{-1} and 1600 cm^{-1} (**15**). Compounds **10**· H_2O , **12** and **14**, having two nitro groups each, exhibit two sets of absorptions: 1265 cm^{-1} , 1525 cm^{-1} , 1295 cm^{-1} and 1577 cm^{-1} (**10**· H_2O), 1266 cm^{-1} , 1530 cm^{-1} , 1288 cm^{-1} , 1584 cm^{-1} (**12**) and 1261 cm^{-1} , 1531 cm^{-1} , 1282 cm^{-1} and 1585 cm^{-1} (**14**). For compound **11**, even three sets of nitro group absorptions can be seen according to the three nitramine units contained in the molecule. The absorptions are located in the same range given for the nitro groups discussed above. For compound **8**, the stretching and deformation vibration of the 5-amino group can be assigned additionally at 3424 cm^{-1} and 1646 cm^{-1} , respectively. The vibrations of the molecular units of **10**· H_2O and **10**· EtOH are almost equal and therefore not discussed separately. The most obvious difference is the O–H stretching vibration of the water molecule in the monohydrate **10**· H_2O at 3484 cm^{-1} and the O–H stretching vibration of the ethanol hydroxy group in **10**· H_2O at 3540 cm^{-1} . Compound **9**, additionally, exhibits absorption bands for the $\text{C}_{\text{ring}}\text{–H}$ stretching and the deformation vibration at 3128 and 1479 cm^{-1} , respectively.

Mass Spectrometry

Mass spectra of the neutral compounds **8–15** were measured either in EI, DEI, FAB or ESI technique. All compounds measured could be clearly identified by the molecule peak $[\text{M} + \text{H}]^+$. Further fragments visible in all mass spectra are the 2-nitro-2-azapropyl fragment at m/z 89 and the azide moiety resulting from the cleavage of the tetrazole ring at m/z 43. In the cases of **8**, **12** and **14**, the remaining fragment $[\text{M} - \text{NNO}_2]^+$ can be seen at m/z 99.1, 157.2 and 112.1 respectively. The tetrazole ring $[\text{CHN}_4]^+$ at m/z 69.1 can be observed in the spectra of **8**, **9** and **12**. Often, the loss of one or even two nitro groups is observed, which exemplarily is discussed for compound **11**:

The molecule peak $[\text{M} + \text{H}]^+$ is observed at m/z 307.2. The successive cleavage of the three bonds, depicted in Figure 13, leads to three fragments at m/z 260.2 $[\text{M} - \text{NO}_2]^+$, 215.2 $[\text{M} + \text{H} - 2\text{NO}_2]^+$ and m/z 186.2 $[\text{M} + \text{H} - \text{CH}_3\text{NNO}_2 - \text{NO}_2]^+$. Different pathways are shown in the second and third fragmentation (B), (C). The loss of a nitro group and the cleavage of the C–N bond in position 5 of the tetrazole ring leads to the fragments at m/z 111.1 $[\text{CN}_4\text{CH}_2\text{NCH}_3]^+$ and m/z 57.1 $[\text{CH}_3\text{NCH}_2]^+$. Finally, the 2-nitro-2-azapropyl moiety is sepa-

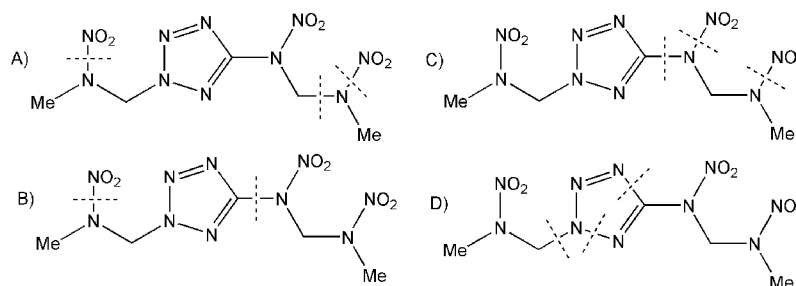


Figure 13. Possible fragmentation pattern of cleaving in the mass spectrum of **11**.

rated and the tetrazole ring is further fragmented (D) to yield the peaks at m/z 89.1 $[\text{CH}_3\text{NNO}_2\text{CH}_2]^+$ and at m/z 43.1 $[\text{N}_3]^+$.

Energetic Properties

Differential Scanning Calorimetry

Differential scanning calorimetry (DSC) measurements to determine the melting and decomposition temperatures of **8**–**15** (~1.5 mg of each energetic material) were performed in covered aluminum containers containing a hole in the lid with a nitrogen flow of $20 \text{ mL}\cdot\text{min}^{-1}$ with a Linseis PT10 DSC at a heating rate of $5 \text{ }^\circ\text{C}\cdot\text{min}^{-1}$. The DSC plots in Figure 14 show the thermal behavior in the 20–400 $^\circ\text{C}$ temperature range. Temperatures are given as onset temperatures.

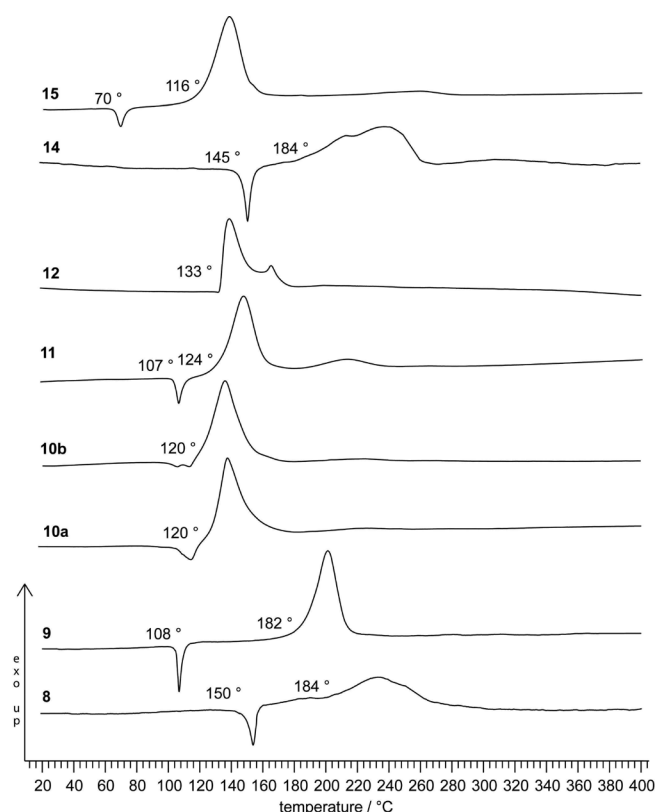


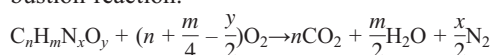
Figure 14. DSC thermograms (exo-up) of compounds **8**–**12**, as well as **14** and **15** (heating rates: $5 \text{ }^\circ\text{C}\cdot\text{min}^{-1}$).

The examined samples of **8**–**12**, as well as **14** and **15** exhibit decomposition temperatures between 116 $^\circ\text{C}$ and 184 $^\circ\text{C}$. Apart from compound **12**, all compounds melt before decomposition and therefore have a definite liquidity range, which ranges e.g. for **9** more than 70 $^\circ\text{C}$ from melting to decomposition. The highest decomposition temperatures of 184 $^\circ\text{C}$ belong to **8** and **14**, which are the two 5-aminotetrazole derivatives. The amino group attached to the tetrazole ring stabilizes the compounds relative to those connected to the nitramine unit. All nitriminotetrazole compounds **10**·H₂O, **10**·EtOH **11**, **12**, and **15** have decomposition temperatures, which are far below those of **8**, **9** and **14**. Comparing the two isomers **12**

and **15**, the decomposition of **12** at 133 $^\circ\text{C}$ starts very precisely, whereas the decomposition peak of molten **15** is observed very broad. Also its melting point is observed much lower at 70 $^\circ\text{C}$, which is the lowest melting point observed in this chapter.

Bomb Calorimetry

The heats of combustion of compounds **8**–**15** were determined experimentally using a Parr 1356 bomb calorimeter. The enthalpy of formation, $\Delta_f H^\circ$, for each of the compounds was calculated at 298.15 K using Hess' law and the following combustion reaction.



The heats of formation of the combustion products H₂O(l) (−286 kJ·mol^{−1}) and CO₂(g) (−394 kJ·mol^{−1}) were obtained from the literature [38, 39]. The values for $\Delta_f H^\circ$ as well as those for $\Delta_c H^\circ$ are summarized in Table 4. The heats of formation for the synthesized compounds are in a broad range from even exothermic (−639 kJ·mol^{−1}, **10**·EtOH) to strongly endothermic (+383 kJ·mol^{−1}, **8**). The other tetrazole derivatives are all formed endothermically ($\Delta_f H^\circ$ **9** = 286, **10**·H₂O = 18, **11** = 296, **12** = 254, **14** = 121, **15** = 333 kJ·mol^{−1}).

The difference of isomers **15** and **12** is 81 kJ·mol^{−1}. The values for **10**·H₂O and **10**·EtOH are lower due to water or ethanol solvate molecules contained. Considering the molar heat of formation of gaseous water of 242 kJ·mol^{−1}, the value for **10**·H₂O is in the range of the other compounds. From the experimentally determined heats of formation and X-ray densities, various thermochemical properties have been calculated using the EXPLO5 software (see below) and are summarized in Table 4.

Sensitivities

For initial safety testing, the impact (RDX = 8 J, Pb(N₃)₂ = 4 J) and friction sensitivities (RDX = 120 N, Pb(N₃)₂ = 1 N) as well as the electrostatic sensitivity were determined.[40–46] The detailed values are summarized in Table 4. The only compound containing three nitramine groups (**11**) stands out with its low impact sensitivity of 2 J. The compounds containing two nitramine groups, one directly connected to the tetrazole ring and a second within the 2-nitro-2-azapropyl moiety fill the range between 5 J and 12 J, which are the methylated isomers **12** (5 J) and **15** (8 J) and on the other hand the unsubstituted homologues **10**·H₂O (12 J) and **10**·EtOH (10 J), which prospectively should be more sensitive, but as they crystallize with one molecule of water and ethanol respectively, the sensitivities are lower. Tetrazole **9** has a moderate sensitivity of 15 J, whereas **8** and **14** are completely insensitive. The friction sensitivities vary from moderately sensitive to insensitive. Again, the molecules containing a nitriminotetrazole moiety are more sensitive. The electrostatic sensitivity tests were carried out using an electric spark tester ESD 2010EN (OZM Research) operating with the “Winspark 1.15 software package” [47]. The electrical spark sensitivities on crystalline material

Table 4. Physico-chemical properties of compounds **8–12** as well as **14** and **15**.

	8	9	10·H₂O	10·EtOH	11	12	14	15
Formula	C ₃ H ₇ N ₇ O ₂	C ₃ H ₆ N ₆ O ₂	C ₃ H ₈ N ₈ O ₅	C ₅ H ₁₂ N ₈ O ₅	C ₅ H ₁₀ N ₁₀ O ₆	C ₄ H ₈ N ₈ O ₄	C ₄ H ₉ N ₇ O ₂	C ₄ H ₈ N ₈ O ₄
Mol. Mass /g·mol ⁻¹	173.13	158.14	236.15	264.20	306.20	232.16	187.16	232.16
Impact sensitivity /J ^{a)}	> 100	15	12	10	2	5	40	8
Friction sensitivity /N ^{b)}	120	128	144	84	108	240	120	96
ESD-test /J	0.22	1.45	1.04	0.75	0.50	0.20	0.60	0.065
N /% ^{c)}	56.63	53.15	47.45	42.41	45.74	48.27	52.39	48.27
Ω /% ^{d)}	-69.3	-70.8	-33.8	-66.6	-47.0	-55.1	-89.8	-55.1
T _{dec.} /K ^{e)}	457	467	393	393	397	406	465	389
Density /g·cm ⁻³ f)	1.628	1.612	1.746	1.562	1.606	1.663	1.525	1.592
-ΔU _{comb.} /cal·g ⁻¹ g)	3547	3520	2380	2760	2892	3068	3812	3149
-ΔH _{comb.} /kJ·mol ⁻¹ h)	2564	2324	2342	3044	3694	2972	2982	3051
Δ _f H _m /kJ·mol ⁻¹ i)	383	286	18	-639	296	254	121	333
-Δ _E U /kJ·kg ⁻¹ j)	5368	5341	4971	2374	5470	5285	3775	5569
T _E /K ^{k)}	3554	3494	3594	2025	3905	3695	2644	3882
p _{C-J} /kbar ^{l)}	273	247	281	138	245	254	194	243
V _{Det.} /m·s ⁻¹ m)	8467	8085	8311	6408	7936	7977	7542	7902
Gas vol. /L·kg ⁻¹ n)	802	776	822	804	791	780	798	783

a) BAM drophammer [Ref. 40–44], grain size (75–150 μm); b) BAM friction tester [Ref. 40, 43–46], grain size (75–150 μm); c) Nitrogen content; d) Oxygen balance; e) Temperature of decomposition by DSC ($\beta = 5$ K); f) estimated from a structure determination; g) Experimental (constant volume) combustion energy; h) Experimental molar enthalpy of combustion; i) Molar enthalpy of formation; j) Energy of Explosion; k) Explosion temperature; l) Detonation pressure. m) Detonation velocity; n) Assuming only gaseous products.

were determined to be 0.22 J (**8**), 1.45 J (**9**), 1.04 J (**10·H₂O**), 0.75 J (**10·EtOH**), 0.50 J (**11**), 0.20 J (**12**), 0.60 J (**14**) and 0.07 J (**15**). Except for the methyl-substituted compounds **12** and **15**, all have values lower than commonly primary explosives (Pb(N₃)₂: 0.005 J) and secondary explosives (RDX: 0.2 J). It should be mentioned that the test towards electrical discharge strongly depends on the particle size and shape. Although we tried to use fine crystalline materials (75–125 μm) a guarantee for the determined values (especially value of **15**) cannot be given.

Detonation Parameters

The calculation of the detonation parameters was performed with the program package EXPLO5 (version 5.02) [48, 49, 50]. Among the investigated compounds **8**, **9** and **10·H₂O** reveal detonation velocities significantly higher than 8000 m·s⁻¹. Although showing detonation pressures of $p_{C-J} = 273$ (**8**), 247 (**9**), and 281 kbar (**10·H₂O**) and an explosion temperature of more than 3500 K, the performance data are lower than those of RDX ($p_{C-J} = 346$ kbar, $V_{Det.} = 8936$ m·s⁻¹, $\Delta_E U = -6043$ kJ·kg⁻¹). The detonation velocities of **10·EtOH**, **11**, **12**, **14**, and **15** are below $V_{Det.} = 8000$ m·s⁻¹, but, however, succeeding easily the detonation parameter of TNT. A reason for the lower p_{C-J} and $V_{Det.}$, in comparison to those of RDX, are the low densities observed for **8–15**. The explosion temperatures seem to be associated with the amount of nitramine moieties contained in the molecule. The explosion temperature of **11**, containing three nitramine units almost reaches 4000 K (3905 K). The value of the highest explosion temperature is also associated with a very high explosion energy of 5470 kJ·kg⁻¹. The explosion temperature of **14**, which is the methylated 5-aminotetrazole derivative is low (2644 K). The remaining values are spread over the range between 2700 K and 3700 K (except from **10·EtOH**) with the trend to higher

temperatures for nitriminotetrazole derivatives (**12**: 3695 K; **15**: 3664 K).

Conclusions

From this experimental study the following conclusions can be drawn:

1-(2-Nitro-2-azapropyl)-5-aminotetrazole (**8**), 1-(2-nitro-2-azapropyl)-5H-tetrazole (**9**), 1-(2-nitro-2-azapropyl)-5-nitriminotetrazole (**10·H₂O**, **10·EtOH**), 2,5-bis(2-nitro-2-azapropyl)-5-nitraminotetrazole (**11**), 1-methyl-5-(2-nitro-2-azapropyl)-5-nitraminotetrazole (**12**), 1-methyl-4-(2-nitro-2-azapropyl)-5-nitriminotetrazole (**13**), 1-methyl-5-(2-nitro-2-azapropyl)-5-aminotetrazole (**14**) and 2-methyl-5-(2-nitro-2-azapropyl)-nitraminotetrazole (**15**) could be synthesized, mostly in good yields from deprotonated 5-amino-1H-tetrazole (**3**), 1H-tetrazole (**4**), 5-nitriminotetrazole (**5**), 1-methyl-5-nitriminotetrazole (**6**) and 2-methyl-5-nitramino-tetrazole (**7**), respectively.

1,4-Dimethyl-5-nitriminotetrazole (**16**) was synthesized by methylation of potassium 1-methyl-5-nitriminotetrazolate with dimethyl sulfate.

The crystal structures of **8–16** were determined by low-temperature single-crystal X-ray diffraction. The compounds crystallize in common space groups ($P2_1/c$: **8**, **10·H₂O**, **10·EtOH**, **12**, **14** and **15**; $P2_1$: **9** and **11**; $Pbca$: **13** and **16**) with densities between 1.52 and 1.75 g·cm⁻³. In addition **8–15** were characterized comprehensively by vibrational spectroscopy (IR and Raman), multinuclear (¹H, ¹³C, ¹⁴N and ¹⁵N) NMR spectroscopy, mass spectrometry, elemental analysis and differential scanning calorimetry.

The thermal behavior of **8–15** was investigated by DSC measurements. The decomposition temperatures reach from 116 °C (**15**) to 184 °C (**8**, **14**).

The sensitivities towards impact, friction and electrical discharge of compounds **8–16** were determined by using the

BAM drophammer and friction tester as well as a small scale electrical discharge tester. The values are mostly lower than those of commonly used secondary explosives such as RDX or HMX. The most sensitive compound is **11**. The impact sensitivities range from 2 to 100 J. Most of the compounds are only moderately sensitive towards friction. The sensitivity towards electrical discharge, of course, strongly depends on the particle sizes and range from 0.07–1.45 J.

The heats of formation $\Delta_f H^\circ$ were calculated using heats of combustion obtained from bomb calorimetric measurements. All compounds, except for **10**-EtOH ($-639 \text{ kJ}\cdot\text{mol}^{-1}$) are formed endothermically with values between $18 \text{ kJ}\cdot\text{mol}^{-1}$ (**10**-H₂O) and $383 \text{ kJ}\cdot\text{mol}^{-1}$ (**8**).

By using $\Delta_f H^\circ$ and the maximum densities obtained from XRD several detonation parameter (heat of explosion, explosion temperature, detonation pressure and velocity) were computed with the EXPLO5 software. The highest detonation pressures (273 and 281 kbar) as well as velocities (8467 and 8311 $\text{m}\cdot\text{s}^{-1}$) were calculated for compounds **8** as well as **10**-H₂O.

Experimental Section

CAUTION! The prepared tetrazoles **8–16** and their starting materials are energetic compounds with increased sensitivities against heat, impact and friction. Although we had no problems in synthesis, proper protective measures (safety glasses, face shield, leather coat, earthened equipment and shoes, Kevlar® gloves and ear plugs) should be used during work on **8–16**.

2-Nitro-2-azapropyl acetate (1): The reaction was carried out according to modified procedure described in the literature [15]. A 500 mL three-necked reaction flask equipped with a thermometer and a dropping funnel was charged with acetic anhydride (88 mL, 936 mmol) and cooled to 0 °C with an ice bath. Fuming nitric acid (28 mL, 666 mmol) was slowly added taking care, that the temperature did not exceed 5 °C for the reaction is somewhat exothermic. To the reaction mixture a solution of 1,3,5-trimethylhexahydro-1,3,5-triazine (25.2 mL, 184 mmol) in glacial acetic acid (25 mL, 436 mmol) was added drop wise within 1 hour before it was heated under reflux to 70–75 °C for 1 hour. The mixture was allowed to cool down to room temperature, water (100 mL) was added and it was extracted with dichloromethane (8 × 25 mL). Either the organic or the aqueous phase was nearly neutralized (pH 6) with ammonium carbonate, the organic phase was washed with water (100 mL) and the combined aqueous phases were again extracted with dichloromethane (4 × 25 mL). The organic phases were dried with magnesium sulfate, the solvent was removed in a rotary evaporator and the crude product was distilled under reduced pressure (3 mbar, 89 °C) to give 50.20 g (61 % yield) of 2-nitro-2-azapropyl acetate as a colorless liquid. **IR** (KBr): $\tilde{\nu}$ = 3482 (w), 2996 (m), 2955 (m), 1751 (vs), 1547 (vs), 1470 (s), 1431 (s), 1630 (s), 1393 (s), 1369 (s), 1301 (s), 1214 (s), 1126 (m), 1017 (s), 958 (s), 857 (m), 829 (m), 770 (m), 681 (m), 647 (w), 603 (m), 495 (m) cm^{-1} . **¹H NMR** (CDCl_3 , 25 °C): δ = 5.68 (s, CH₂), 3.41 (s, H₃C–N(NO₂)), 2.09 (s, H₃C–C(O)O). **¹³C NMR** (CDCl_3 , 25 °C): δ = 170.6 (C(O)CH₃), 72.8 (CH₂), 38.6 (H₃C–N(NO₂)), 20.6 (C(O)CH₃).

2-Nitro-2-azapropyl chloride (2): The reaction was carried out according to modified procedure described in the literature [15]. A 250 mL reaction flask was charged with 2-nitro-2-azapropyl acetate (24.7 g, 167 mmol), glacial acetic acid (0.7 mL, 12.3 mmol), conc. H₂SO₄ (2 drops), and dichloromethane (35 mL). Thionyl chloride

(23.4 g, 334 mmol) was added dropwise over a period of 90 minutes. Afterwards, the mixture was heated to 40–45 °C under reflux for 1 hour, before the solvent was removed under reduced pressure. For purification the pale yellow oil was distilled in vacuo (2 mbar, 48 °C) to give 2-nitro-2-azapropyl chloride (18.14 g, 87 % yield) as a colorless liquid. **¹H NMR** (CDCl_3 , 25 °C): δ = 5.60 (s, CH₂), 3.38 (s, H₃C–N(NO₂)). **¹³C NMR** (CDCl_3 , 25 °C): δ = 60.4 (CH₂Cl), 37.6 (CH₃).

1-(2-Nitro-2-azapropyl)-5-aminotetrazole (8): 5-Amino-tetrazole (17.0 g, 200 mmol) was suspended in a solution of water (100 mL) and KOH (13.2 g, 200 mmol, 85 %). The suspension was heated to 50 °C and 5-aminotetrazole dissolved. Evaporation of the solvent gave potassium-5-aminotetrazolate in quantitative yields. The pale yellow solid can be recrystallized from water/ethanol with 92 % yield (22.7 g). Potassium 5-aminotetrazolate (7.39 g, 60 mmol) was suspended in acetone (50 mL) and the 2-nitro-2-azapropyl chloride (8.22 g, 66 mmol) was slowly added through a dropping funnel. The suspension was stirred overnight, filtered off and the solid was washed with warm acetone. The solvent was removed in a rotary evaporator and a yellowish solid remained, which was recrystallized from hot ethanol to give 6.02 g of **8** (58 % yield). ($\text{C}_3\text{H}_7\text{N}_7\text{O}_2$, 173.13) calcd.: C 20.81, H 4.08, N 56.63 %; found: C 22.14, H 4.25, N 55.09 %; **DSC** (T_{onset} , 5 °C·min^{−1}): 147–153 °C (mp.), 184 °C (dec.). **IR** (KBr): $\tilde{\nu}$ = 3424 (s), 3300 (m), 3134 (m), 3097 (m), 2721 (s), 1646 (s), 1579 (s), 1521 (vs), 1472 (m), 1446 (m), 1424 (m), 1387 (w), 1354 (m), 1297 (s), 1261 (s), 1206 (s), 1116 (m), 1074 (m), 1021 (m), 992 (m), 927 (w), 846 (w), 795 (m), 764 (m), 740 (w), 719 (w), 680 (m), 654 (m), 604 (w), 485 (w) cm^{-1} ; **Raman** (1064 nm, 400 mW, 25 °C): $\tilde{\nu}$ = 3038 (36), 2995 (42), 2964 (36), 1648 (10), 1582 (14), 1529 (10), 1443 (27), 1424 (21), 1356 (23), 1318 (29), 1262 (50), 1128 (18), 1094 (14), 1070 (14), 1021 (15), 928 (17), 849 (100), 793 (57), 655 (14), 603 (22), 445 (27), 398 (23), 304 (19), 235 (27) cm^{-1} . **¹H NMR** ($[D_6]DMSO$, 25 °C): δ = 6.98 (s, NH₂), 6.14 (s, CH₂), 3.13 (s, CH₃). **¹³C NMR** ($[D_6]DMSO$, 25 °C): δ = 156.2 (CN₄), 59.6 (CH₂), 39.4 (s, CH₃). **¹⁵N NMR** ($[D_6]DMSO$, 25 °C): δ = 6.9 (N3), −26.6 (N2), −30.0 (N7), −94.7 (N4), −176.2 (N1), −205.3 (N6), −333.9 (N5); **MS**: m/z (DEI): 173.1 [M]⁺; **impact sensitivity**: > 100 J (neg.); **friction sensitivity**: > 120 N; **ESD**: > 0.22 J; **RADEX** (130 °C, 50 h): no decomposition.

1-(2-Nitro-2-azapropyl)-tetrazole (9): 1H-Tetrazole (701 mg, 10 mmol) was suspended in a solution of KOH (85 %, 660 mg, 10 mmol) in water (15 mL). Tetrazole dissolved and after evaporation of the water under reduced pressure, the potassium tetrazolate formed as a colorless solid. Potassium tetrazolate was directly suspended in acetone (20 mL) without being recrystallized. To this suspension 2-nitro-2-azapropyl chloride (1.245 g, 10 mmol), which was previously dissolved in acetone (few milliliters) was added drop wise. After being stirred overnight, the suspension was heated to reflux for 1 hour and filtered off afterwards. Acetone was removed under reduced pressure and the remaining solid was recrystallized from ethanol to give 1.17 g (74 % yield) **9** as colorless crystals. ($\text{C}_3\text{H}_6\text{N}_6\text{O}_2$, 158.12) calcd.: C 22.79, H 3.82, N 53.15 %; found: C 22.71, H 3.57, N 52.47 %; **DSC** (T_{onset} , 5 °C·min^{−1}): 108 °C (mp.), 182 °C (dec.). **IR** (KBr): $\tilde{\nu}$ = 3450 (vs), 3128 (m), 3051 (w), 1634 (m), 1533 (m), 1479 (m), 1383 (w), 1341 (w), 1303 (m), 1281 (m), 1168 (m), 1096 (m), 1038 (w), 959 (w), 885 (w), 854 (w), 766 (m), 750 (m), 718 (w), 672 (m), 614 (m) cm^{-1} ; **Raman** (1064 nm, 350 mW, 25 °C): $\tilde{\nu}$ = 3127 (33), 3050 (37), 3003 (65), 2959 (36), 1529 (22), 1478 (26), 1448 (33), 1428 (35), 1410 (37), 1374 (27), 1335 (31), 1294 (53), 1264 (34), 1169 (36), 1095 (36), 1038 (29), 1012 (61), 852 (100), 750 (33), 641 (27), 613 (38), 444 (31), 407 (24), 352 (24), 265 (24), 209 (19) cm^{-1} . **¹H NMR** ($[D_6]DMSO$, 25 °C): δ = 9.58 (s, N₄CH), 6.46 (s, CH₂), 3.52 (s, CH₃).

^{13}C NMR ($[D_6]DMSO$, 25 °C): δ = 145.2 (CN_4), 61.9 (CH_2), 39.5 (CH_3). **^{15}N NMR** ($[D_6]DMSO$, 25 °C): δ = 12.2 (N_3), –15.3 (N_2), –30.4 (N_6), –52.6 (N_4), –144.3 (N_1), –205.9 (N_5); **MS**: m/z (FAB^+): 159.2 [$\text{M} + \text{H}$] $^+$; **impact sensitivity**: > 15 J; **friction sensitivity**: > 128 N; **ESD**: > 1.45 J.

1-(2-Nitro-2-azapropyl)-5-nitriminotetrazole monohydrate (10·H₂O): 5-Nitrimino-1,4*H*-tetrazole (4.43 g, 34 mmol) was suspended in an ethanol solution of KOH (85 %, 2.25 g, 34 mmol) and stirred for 15 minutes. The suspension was filtered off, the solid dried to give 5.27 g (31.5 mmol, 92 %) of potassium 5-nitriminotetrazolate. The salt was suspended in THF (50 mL) and 2-nitro-2-azapropyl chloride (1.87 g, 15 mmol), previously dissolved in THF (25 mL), was added drop wise. The suspension was stirred at room temperature overnight and the remaining solid, consisting of potassium 5-nitriminotetrazolate and potassium chloride, was filtered off. THF was removed from the filtrate under reduced pressure, the remaining colorless oil was dissolved in a small amount of water/ethanol for recrystallization to give **10·H₂O** as colorless crystals in 22 % yield (783 mg, 3.3 mmol). ($\text{C}_5\text{H}_8\text{N}_8\text{O}_5$, 236.15) calcd.: C 15.26, H 3.41, N 47.45 %; found: C 15.74, H 3.67, N 47.59 %; **DSC** (T_{onset} , 5 °C·min $^{-1}$): 112–118 °C (mp.), 120 °C (dec.). **IR** (KBr): $\tilde{\nu}$ = 3484 (m), 3049 (w), 1577 (vs), 1554 (s), 1525 (m), 1450 (m), 1408 (m), 1337 (m), 1295 (s), 1265 (s), 1201 (m), 1135 (m), 1113 (w), 1083 (m), 1022 (m), 1007 (m), 916 (m), 799 (m), 765 (m), 746 (m), 686 (w), 673 (w), 643 (m), 607 (m) cm $^{-1}$; **Raman** (1064 nm, 300 mW, 25 °C): $\tilde{\nu}$ = 3051 (37), 2995 (66), 2962 (43), 1585 (58), 1560 (22), 1526 (55), 1441 (31), 1424 (45), 1400 (42), 1293 (49), 1264 (100), 1133 (11), 1059 (28), 1009 (40), 987 (46), 883 (24), 869 (41), 850 (68), 758 (50), 748 (36), 707 (28), 604 (34), 496 (33), 421 (22), 394 (24), 318 (25), 257 (46), 239 (28) cm $^{-1}$. **^1H NMR** ($[D_6]DMSO$, 25 °C): δ = 9.78 (s, NH), 6.12 (s, CH_2), 3.50 (s, CH_3), 3.43 (s, H_2O). **^{13}C NMR** ($[D_6]DMSO$, 25 °C): δ = 151.4 (CN_4), 61.2 (CH_2), 39.8 (CH_3). **^{15}N NMR** ($[D_6]DMSO$, 25 °C): δ = –20.2 (N_3), –30.1 (NO_2 , N_6), –30.8 (N_2 , t, $^3J_{\text{N-H}}$ = 1.5 Hz), –32.2 (NO_2 , N_8 , m), –159.1 (N_4), –165.1 (N_5), –172.4 (N_1), –209.4 (N_7); **MS**: m/z (FAB^+): 219.2 [$\text{M} + \text{H}$] $^+$; **impact sensitivity**: > 12 J; **friction sensitivity**: > 144 N; **ESD**: > 1.04 J.

1-(2-Nitro-2-azapropyl)-5-nitriminotetrazole·EtOH (10·EtOH): 5-Nitrimino-1,4*H*-tetrazole (3.96 g, 30.5 mmol) was dissolved in THF (50 mL) and triethylamine (3.08 g, 30.5 mmol) was slowly added to the solution. A colorless precipitate, which immediately formed, disappeared after a few seconds. 2-Nitro-2-azapropyl chloride (1.87 g, 15 mmol) was dissolved in THF (25 mL) and slowly added through a dropping funnel over a period of 1 hour. A colorless, crystalline precipitate of triethylammonium chloride formed. The reaction was stirred overnight, the precipitate was filtered off and the solvent was removed from the filtrate. A pale yellow oil remained, which was dried under vacuum and taken up in ethanol for recrystallization to give 1.76 g of **10·EtOH** as colorless crystals (22 % yield). The product achieved from the reaction crystallizes with one equivalent of ethanol as solvate as X-ray single crystal structure studies showed. ($\text{C}_5\text{H}_{12}\text{N}_8\text{O}_5$, 264.20) calcd.: C 22.73, H 4.58, N 42.41 %; found: C 20.32, H 4.13, N 43.79 %; **DSC** (T_{onset} , 5 °C·min $^{-1}$): 112–118 °C (mp.), 120 °C (dec.). **IR** (KBr): $\tilde{\nu}$ = 3540 (s), 3488 (s), 3051 (m), 2826 (m), 2737 (m), 2663 (m), 1634 (m), 1586 (vs), 1525 (vs), 1442 (m), 1497 (vs), 1439 (s), 1397 (m), 1356 (s), 1311 (s), 1283 (s), 1260 (s), 1207 (s), 1108 (w), 1057 (m), 1007 (s), 927 (m), 884 (w), 777 (m), 761 (m), 748 (m), 705 (m), 602 (m), 576 (m), 475 (w) cm $^{-1}$; **Raman** (1064 nm, 300 mW, 25 °C): $\tilde{\nu}$ = 3072 (14), 3005 (37), 2970 (36), 2927 (30), 1571 (100), 1453 (37), 1416 (48), 1260 (80), 1056 (30), 1035 (32), 1064 (100), 984 (44), 876 (32), 850 (61), 757 (71), 709 (24), 604 (14), 487 (25), 252 (32) cm $^{-1}$. **^1H NMR** ($[D_6]DMSO$, 25 °C): δ = 9.78 (s, NH),

6.12 (s, CH_2), 3.50 (s, CH_3), 3.44 (q, J = 6.8 Hz, CH_2OH), 1.05 (t, J = 6.8 Hz, CH_3). **^{13}C NMR** ($[D_6]DMSO$, 25 °C): δ = 151.4 (CN_4), 61.2 (CH_2), 56.6 (CH_2OH), 39.8 (CH_3), 19.0 ($\text{CH}_3\text{CH}_2\text{OH}$); **MS**: m/z (FAB^+): 219.2 [$\text{M} + \text{H}$] $^+$; **impact sensitivity**: > 10 J; **friction sensitivity**: > 84 N; **ESD**: > 0.75 J.

2,5-(Bis(2-nitro-2-azapropyl)-nitriminotetrazole (11): 5-Nitrimino-1,4*H*-tetrazole (1.30 g, 10 mmol) was dissolved in THF (40 mL) and triethylamine (2.02 g, 20 mmol) was added dropwise. A colorless precipitate, which formed at first, dissolved again after a few seconds. 2-Nitro-2-azapropyl chloride was dissolved in THF (10 mL) and slowly added to the reaction mixture through a dropping funnel. A colorless precipitate of triethylammonium chloride started to form. The mixture was further stirred overnight, the precipitate was filtered off and the solvent was evaporated from the filtrate to give a yellow, viscous oil. After a few hours, in the oil, the product started to crystallize. The oil/crystal-mixture was vigorously stirred with a small amount of ethanol for 2 hours and a colorless crystalline product could be filtered off. It was recrystallized from ethanol to give 1.27 g (42 % yield) of **11**. ($\text{C}_5\text{H}_{10}\text{N}_{10}\text{O}_6$, 306.20) calcd.: C 19.61, H 3.29, N 45.74 %; found: C 19.81, H 3.26, N 46.85 %; **DSC** (T_{onset} , 5 °C·min $^{-1}$): 107 °C (mp.), 124 °C (dec.). **IR** (KBr): $\tilde{\nu}$ = 3448 (m), 3048 (m), 2999 (w), 2960 (w), 1577 (vs), 1553 (vs), 1449 (s), 1408 (s), 1295 (vs), 1267 (vs), 1201 (s), 1135 (s), 1114 (m), 1083 (s), 1023 (s), 943 (m), 917 (s), 852 (w), 799 (s), 766 (s), 746 (s), 686 (m), 674 (m), 643 (s), 608 (s), 460 (w), 419 (m) cm $^{-1}$; **Raman** (1064 nm, 350 mW, 25 °C): $\tilde{\nu}$ = 3050 (52), 3000 (57), 2962 (44), 2900 (13), 1588 (14), 1559 (20), 1526 (78), 1449 (29), 1401 (34), 1345 (24), 1294 (64), 1269 (33), 1010 (50), 943 (17), 919 (18), 869 (85), 855 (100), 606 (29), 460 (19), 422 (18), 385 (14), 316 (19), 239 (30) cm $^{-1}$. **^1H NMR** ($[D_6]DMSO$, 25 °C): δ = 6.81 (s, 2- CH_2), 6.10 (s, 5- CH_2), 3.55 (s, 5- $\text{H}_3\text{CN}(\text{NO}_2)$), 3.47 (s, 2- $\text{H}_3\text{CN}(\text{NO}_2)$). **^{13}C NMR** ($[D_6]DMSO$, 25 °C): δ = 159.5 (CN_4), 67.4 (5- CH_2), 67.0 (2- CH_2), 39.8 (5- $\text{H}_3\text{CN}(\text{NO}_2)$), 39.4 (2- $\text{H}_3\text{CN}(\text{NO}_2)$). **^{15}N NMR** ($[D_6]DMSO$, 25 °C): δ = 2.9 (N_3), –29.7 (NO_2 , N_{10}), –30.9 (NO_2 , N_6), –38.2 (NO_2 , N_8), –51.2 (N_4), –80.9 (N_1), –95.7 (N_2), –201.3 ($\text{NNO}_2(9)$), –204.2 (NNO_2 , N_5), –207.8 (NNO_2 , N_7); **MS**: m/z (FAB^+): 307.2 [$\text{M} + \text{H}$] $^+$; **impact sensitivity**: > 2 J; **friction sensitivity**: > 108 N; **ESD**: > 0.50 J.

1-Methyl-5-(2-nitro-2-azapropyl)-nitriminotetrazole (12): 1-Methyl-5-nitrimino-4*H*-tetrazole (4.32 g, 30 mmol) was dissolved in a KOH solution (prepared from 1.98 g KOH (85 %) and 50 mL of water), the water was evaporated and potassium 1-methyl-5-nitriminotetrazolate (5.47 g, 30 mmol) was used for the coupling reaction with 2-nitro-2-azapropyl chloride without recrystallization. The potassium salt was suspended in acetone (25 mL) and 2-nitro-2-azapropyl chloride (4.11 g, 33 mmol), dissolved in acetone (10 mL), was added drop wise to the suspension. The mixture was stirred overnight, heated under reflux for 90 minutes and filtered off. The solvent was removed from the filtrate in vacuo which afforded more than 7 g of a yellow oil. The oil was taken up in hot ethanol and recrystallized, which yielded 4.18 g (60 % yield) of **12** as colorless crystals. In the crystallization mixture also a few crystals of **13** were detected. ($\text{C}_4\text{H}_8\text{N}_8\text{O}_4$, 232.16) calcd.: C 20.69, H 3.47, N 48.27 %; found: C 20.23, H 2.86, N 47.62 %; **DSC** (T_{onset} , 5 °C·min $^{-1}$): 133 °C (dec.). **IR** (KBr): $\tilde{\nu}$ = 3432 (m), 3051 (w), 3034 (w), 1584 (vs), 1530 (s), 1480 (m), 1449 (m), 1408 (m), 1390 (m), 1288 (vs), 1266 (s), 1123 (m), 1092 (m), 1015 (m), 913 (m), 855 (w), 766 (m), 748 (m), 700 (m), 659 (w), 643 (m), 604 (m) cm $^{-1}$; **Raman** (1064 nm, 350 mW, 25 °C): $\tilde{\nu}$ = 3035 (21), 2970 (45), 1545 (39), 1449 (14), 1414 (23), 1309 (23), 1264 (23), 988 (12), 916 (12), 857 (93), 799 (20), 700 (37), 660 (16), 644 (10), 606 (26), 491 (20), 474 (24), 388 (12), 303 (13), 176 (12) cm $^{-1}$. **^1H NMR** ($[D_6]DMSO$, 25 °C): δ = 6.06 (s, CH_2), 4.03 (s, $\text{H}_3\text{CN}(\text{NO}_2)$), 3.51 (s, CH_3).

¹³C NMR (*[D₆]DMSO*, 25 °C): δ = 150.6 (CN₄), 67.6 (CH₂), 39.9 (H₃CN(NO₂)), 34.7 (CH₃). **¹⁵N NMR** (*[D₆]DMSO*, 25 °C): δ = 9.9 (N3), −5.5 (N2, q, $^3J_{\text{N-H}}$ = 1.9 Hz), −30.4 (N8, NO₂), −40.8 (N6, NO₂), −57.8 (N4), −152.7 (N1, q, $^2J_{\text{N-H}}$ = 2.3 Hz), −295.0 (N7), −207.5 (N5); **MS**: *m/z* (DEI⁺): 233.3 [M + H]⁺; **impact sensitivity**: > 5 J; **friction sensitivity**: > 240 N; **ESD**: > 0.20 J.

1-Methyl-4-(2-nitro-2-azapropyl)-aminotetrazole (14): The coupling reaction of potassium 1-methyl-5-nitriminotetrazolate and **2** in acetone (described above) delivered 1-methyl-5-NAP-nitriminotetrazole (**12**), but also 1-methyl-5-NAP-aminotetrazole. It could be separated from **12** due to its different solubility in ethanol. **14** was obtained from the mother liquor in 12 % yield (0.68 g). (C₄H₉N₇O₂, 187.16) calcd.: C 25.67, H 4.85, N 52.39 %; found: C 25.71, H 4.84, N 52.51 %; **DSC** (*T_{onset}*: 5 °C·min^{−1}): 142–147 °C (mp.), 184 °C (dec.). **IR** (KBr): $\tilde{\nu}$ = 3262 (m), 3122 (m), 3040 (m), 1617 (vs), 1500 (vs), 1450 (s), 1343 (m), 1300 (vs), 1288 (s), 1248 (vs), 1226 (m), 1082 (m), 1041 (m), 1021 (m), 1002 (m), 843 (m), 768 (m), 742 (w), 668 (m), 653 (m), 619 (w), 562 (m) cm^{−1}; **Raman** (1064 nm, 350 mW, 25 °C): $\tilde{\nu}$ = 3055 (30), 3027 (30), 2952 (65), 1605 (39), 1467 (31), 1450 (39), 1342 (21), 1306 (54), 1244 (35), 1116 (33), 1081 (18), 1000 (61), 843 (90), 780 (100), 664 (23), 620 (16), 563 (13), 423 (21), 253 (36), 181 (21) cm^{−1}. **¹H NMR** (*[D₆]DMSO*, 25 °C): δ = 8.09 (t, J = 6.3 Hz, NH), 5.21 (d, J = 6.3 Hz, CH₂), 3.71 (s, CH₃), 3.53 (s, H₃CN(NO₂)). **¹³C NMR** (*[D₆]DMSO*, 25 °C): δ = 155.7 (CN₄), 60.8 (CH₂), 39.0 (H₃CN(NO₂)), 32.4 (CH₃). **¹⁵N NMR** (*[D₆]DMSO*, 25 °C): δ = 1.3 (s, N3), −20.3 (s, N2), −29.0 (m, $^3J_{\text{N-H}}$ = 2.5 Hz, NO₂), −93.8 (d, $^3J_{\text{N-H}}$ = 2.2 Hz, N4), −184.5 (t, $^2J_{\text{N-H}}$ = 2.2 Hz, N1), −199.9 (s, NNO₂), −324.4 (d, $^1J_{\text{N-H}}$ = 94 Hz, NH); **MS**: *m/z* (FAB⁺): 188.2 [M + H]⁺; **impact sensitivity**: > 40 J; **friction sensitivity**: > 120 N; **ESD**: 0.60 J.

2-Methyl-5-(2-nitro-2-azapropyl)-nitriminotetrazole (15): 2-Methyl-5-nitraminotetrazolate (4.32 g, 30 mmol) was suspended in THF (25 mL) and triethylamine (3.04 g, 30 mmol) was added. A colorless precipitate, which first was formed, disappeared within half a minute. 2-nitro-2-azapropyl chloride (3.74 g, 30 mmol), dissolved in THF (10 mL), was added drop wise. The mixture was stirred at room temperature overnight, filtered off and the solvent was removed from the filtrate. The remaining yellow oil was suspended in pentane (30 mL) and stirred vigorously. After a few minutes all the oil was converted into fine, crystalline material, which was filtered off (6.55 g, 94 % yield) and recrystallized from ethanol/methanol. (C₂H₃KN₆O₂, 182.18) calcd.: C 20.69, H 3.47, N 48.27 %; found: C 21.71, H 3.81, N 47.08 %; **DSC** (*T_{onset}*: 5 °C·min^{−1}): 68–78 °C (mp.), 116 °C (dec.). **IR** (KBr): $\tilde{\nu}$ = 3435 (m), 3043 (m), 1585 (vs), 1531 (vs), 1467 (s), 1458 (s), 1441 (m), 1412 (m), 1397 (s), 1365 (w), 1304 (s), 1282 (s), 1261 (s), 1214 (m), 1195 (m), 1147 (m), 1066 (m), 1048 (m), 1025 (m), 911 (m), 855 (w), 800 (m), 769 (m), 749 (m), 704 (w), 663 (m), 649 (m), 602 (m), 494 (w), 453 (w) cm^{−1}; **Raman** (1064 nm, 350 mW, 25 °C): $\tilde{\nu}$ = 3043 (30), 2994 (43), 2969 (91), 2875 (15), 2837 (9), 1592 (15), 1517 (59), 1457 (20), 1402 (25), 1366 (23), 1337 (18), 1291 (68), 1214 (10), 1197 (15), 1146 (6), 1067 (8), 1046 (26), 1018 (73), 915 (16), 857 (100), 799 (13), 751 (5), 704 (28), 763 (12), 751 (12), 603 (23), 495 (11), 464 (32), 394 (30), 374 (11), 327 (13), 308 (22), 243 (13), 221 (14) cm^{−1}. **¹H NMR** (*[D₆]DMSO*, 25 °C): δ = 6.09 (s, CH₂), 4.49 (s, CH₃), 3.47 (s, CH₃NNO₂). **¹³C NMR** (*[D₆]DMSO*, 25 °C): δ = 159.1 (CN₄), 67.1 (CH₂), 41.2 (CH₃), 39.7 (CH₃NNO₂). **¹⁵N NMR** (*[D₆]DMSO*, 25 °C): δ = 1.4 (N3, q, $^3J_{\text{N-H}}$ = 1.5 Hz), −30.4 (N8), −37.9 (N6), −53.4 (N4), −77.9 (N1, q, $^3J_{\text{N-H}}$ = 1.8 Hz), −101.6 (N2, q, $^2J_{\text{N-H}}$ = 2.4 Hz), −202.1 (N5, t, $^2J_{\text{N-H}}$ = 1.9 Hz), −204.9 (N7); **MS**: *m/z* (DEI⁺): 233.3 [M + H]⁺; **impact sensitivity**: > 8 J; **friction sensitivity**: > 96 N; **ESD**: > 0.07 J.

1,4-Dimethyl-5-nitriminotetrazole (16): 1-Methyl-5-nitriminotetrazole (1.44 g, 10 mmol) was deprotonated using an aqueous KOH solu-

tion (40 mL, 570 mg, 10 mmol). To this, dimethyl sulfate was added drop wise at 60 °C and the mixture was heated under reflux for three hours. Afterwards, the solvent was reduced by half and the product was extracted using CH₂Cl₂ (2 × 30 mL). After evaporating the solvent, the crude product was recrystallized from hot water yielding 1.34 g colorless crystals (85 % yield). (C₃H₆N₆O₂, 158.12) calcd.: C 22.79, H 3.82, N 53.15 %; found: C 23.10, H 3.84, N 52.99 %; **DSC** (*T_{onset}*: 5 °C·min^{−1}): 85 °C (mp.), 200 °C (dec.). **IR** (KBr): $\tilde{\nu}$ = 3029 (w), 2442 (w), 2265 (w), 2115 (w), 1685 (w), 1664 (s), 1495 (m), 1436 (s), 1412 (m), 1376 (s), 1352 (m), 1258 (vs, br), 1229 (vs), 1115 (m), 1049 (m), 1007 (s), 918 (w), 874 (w), 791 (s), 774 (s), 750 (m), 676 (s) cm^{−1}; **Raman** (1064 nm, 200 mW, 25 °C): $\tilde{\nu}$ = 3032 (31), 2964 (93), 1568 (81), 1467 (26), 1439 (27), 1415 (46), 1378 (38), 1353 (41), 1278 (17), 1232 (15), 1050 (18), 1010 (62), 876 (11), 796 (31), 775 (11), 752 (38), 621 (100), 522 (7), 482 (29), 349 (10), 283 (33), 209 (13), 161 (15) cm^{−1}. **¹H NMR** (*[D₆]DMSO*, 25 °C): δ = 3.78 (s, 3 H, CH₃). **¹³C NMR** (*[D₆]DMSO*, 25 °C): δ = 39.7 (CH₃), 168.0 (CN₄). **¹⁴N NMR** (*[D₆]DMSO*, 25 °C): δ = −19.6 (NO₂). **¹⁵N NMR** (*[D₆]DMSO*, 25 °C): δ = −359.4 (N7, NH₄⁺), −149.3 (N5), −111.8 (C2, $^2J_{\text{N-H}}$ = 2.1 Hz), −93.8 (N1, $^3J_{\text{N-H}}$ = 1.8 Hz), −63.9 (N4), −15.4 (N6, NO₂), −6.4 (N3, $^3J_{\text{N-H}}$ = 1.8 Hz); **MS**: *m/z* (DEI): 158(34) [M]⁺, 112(58) [M − NO₂]⁺, 89(10), 83 (6) [M − NO₂ − 2CH₃]⁺, 70(5), 69(10), 57(8), 56(20), 55(12), 53(7), 46 (6) [NO₂]⁺, 45(24), 43 (100) [HN₃]⁺, 42 (12) [N₃]⁺, 41(11), 28(35) [N₂]⁺, 18(23), 15(34) [CH₃]⁺; **impact sensitivity**: > 30 J; **friction sensitivity**: > 360 N.

Acknowledgement

Financial support of this work by the Ludwig-Maximilian University of Munich (LMU), the European Research Office (ERO) of the U.S. Army Research Laboratory (ARL), the Armament Research, Development and Engineering Center (ARDEC) and the Strategic Environmental Research and Development Program (SERDP) under contract nos. W911NF-09-2-0018 (ARL), W911NF-09-1-0120 (ARDEC), W011NF-09-1-0056 (ARDEC) and 10 WPSEED01-002 / WP-1765 (SERDP) is gratefully acknowledged. The authors acknowledge collaborations with Dr. Mila Krupka (OZM Research, Czech Republic) in the development of new testing and evaluation methods for energetic materials and with Dr. Muhamed Sucasca (Brodarski Institute, Croatia) in the development of new computational codes to predict the detonation and propulsion parameters of novel explosives. We are indebted to and thank Drs. Betsy M. Rice and Brad Forch (ARL, Aberdeen, Proving Ground, MD) and Mr. Gary Chen (ARDEC, Picatinny Arsenal, NJ) for many helpful and inspired discussions and support of our work. The authors also acknowledge financial support by CECD.

References

- [1] a) T. M. Klapötke, in *Moderne Anorganische Chemie* (Ed.: E. Riedel), vol. 3, Aufl., Walter de Gruyter, Berlin, New York, **2007**, pp. 99–104; b) R. P. Singh, R. D. Verma, D. T. Meshri, J. M. Shreeve, *Angew. Chem. Int. Ed.* **2006**, *45*, 3584; c) T. M. Klapötke, in *High Energy Density Materials* (Ed.: T. M. Klapötke), Springer, Berlin, Heidelberg, **2007**, pp. 85–122; d) R. D. Chapman, in: *High Energy Density Materials* (Ed.: T. M. Klapötke), Springer, Berlin, Heidelberg, **2007**, p. 123–152.
- [2] a) G. Geisberger, T. M. Klapötke, J. Stierstorfer, *Eur. J. Inorg. Chem.* **2007**, *30*, 4743–4750; b) T. M. Klapötke, J. Stierstorfer, *Centr. Eur. J. Energ. Mater.* **2008**, *5*, 13–30; J. Akhavan, *The Chemistry of Explosives*, 2nd ed. London, RSC press, **2004**; c) M. Hiskey, A. Hammerl, G. Holl, T. M. Klapötke, K. Polborn, J. Stierstorfer, J. J. Weigand, *Chem. Mater.* **2005**, *17*, 3784–3793; d) T. M. Klapötke, P. Mayer, J. Stierstorfer, J. J. Weigand, *J. Ma-*

- ter. *Chem.* **2008**, *18*, 5248–5258; e) G. Steinhäuser, T. M. Klapötke, *Angew. Chem. Int. Ed.* **2008**, *47*, 3330; f) T. M. Klapötke, J. Stierstorfer, K. R. Tarantik, I. Thoma, *Z. Anorg. Allg. Chem.* **2008**, *634*, 2777–2784.
- [3] a) T. M. Klapötke, C. M. Sabaté, J. Stierstorfer, *New J. Chem.* **2009**, *33*, 136–147; b) T. M. Klapötke, C. M. Sabaté, *Dalton Trans.* **2009**, *10*, , 1835–1841.
- [4] G. Holl, T. M. Klapötke, K. Polborn, C. Rienäcker, *Propellants Explos. Pyrotech.* **2003**, *28*, 153–156.
- [5] K. Karaghiosoff, T. M. Klapötke, A. Michailovski, H. Nöth, M. Suter, *Propellants Explos. Pyrotech.* **2003**, *28*, 1–6.
- [6] a) J. Stierstorfer, T. M. Klapötke, A. Hammerl, B. Chapman, *Z. Anorg. Allg. Chem.* **2008**, *634*, 1051–1057; b) A. Hammerl, T. M. Klapötke, H. Nöth, M. Warchhold, G. Holl, *Propellants Explos. Pyrotech.* **2003**, *28*, 165–173; c) D. Adam, K. Karaghiosoff, G. Holl, M. Kaiser, T. M. Klapötke, *Propellants Explos. Pyrotech.* **2002**, *27*, 7–11.
- [7] a) M. Klapötke, J. Stierstorfer, *Helv. Chim. Acta* **2007**, *90*, 2132–2150; b) T. M. Klapötke, J. Stierstorfer, A. U. Wallek, *Chem. Mater.* **2008**, *20*, 4519–4530; c) S. Berger, K. Karaghiosoff, T. M. Klapötke, P. Mayer, H. Piotrowski, K. Polborn, R. L. Willer, J. J. Weigand, *J. Org. Chem.* **2006**, *71*, 1295–1305.
- [8] J. Geith, G. Holl, T. M. Klapötke, J. J. Weigand, *Combust. Flame* **2004**, *139*, 358; J. Geith, T. M. Klapötke, J. J. Weigand, G. Holl, *Propellants Explos. Pyrotech.* **2004**, *29*, 3–8.
- [9] a) M. Denffer, T. M. Klapötke, G. Kramer, G. Spiess, J. M. Welch, G. Heeb, *Propellants Explos. Pyrotech.* **2005**, *30*, 191–195; b) G. Ma, Z. Zhang, J. Zhang, K. Yu, *Thermochim. Acta* **2004**, *423*, 137–141.
- [10] K. Karaghiosoff, T. M. Klapötke, P. Mayer, C. M. Sabaté, A. Penger, J. M. Welch, *Inorg. Chem.* **2008**, *47*, 1007–1019.
- [11] K. O. Christie, W. W. Wilson, M. A. Petrie, H. H. Michels, J. C. Bottaro, R. Gilardi, *Inorg. Chem.* **1996**, *35*, 5068–5071.
- [12] a) T. M. Klapötke, J. Stierstorfer, *Phys. Chem. Chem. Phys.* **2008**, *10*, 4340–4346; b) T. M. Klapötke, J. Stierstorfer, *Eur. J. Inorg. Chem.* **2008**, *26*, 4055–4062.
- [13] R. Boese, T. M. Klapötke, P. Mayer, V. Verma, *Propellants Explos. Pyrotech.* **2006**, *31*, 263–268.
- [14] G. A. Gareev, L. P. Kirillova, V. M. Shul'gina, S. R. Buzilova, L. P. Vologdina, L. I. Vereshchagin, *J. Org. Chem. USSR (Engl. Transl.)* **1988**, *24*, 2003–2007.
- [15] J. Denkstein, V. Kaderabek, *Collect. Czech. Commun.* **1960**, *25*, 2334–2340.
- [16] T. M. Klapötke, M. Stein, J. Stierstorfer, *Z. Anorg. Allg. Chem.* **2008**, *634*, 1711–1723.
- [17] V. Ernst, T. M. Klapötke, J. Stierstorfer, *Z. Anorg. Allg. Chem.* **2007**, *633*, 879–887.
- [18] T. M. Klapötke, H. Radies, J. Stierstorfer, *Z. Naturforsch.* **2007**, *62b*, 1343–1352.
- [19] *CrysAlis CCD*, Version 1.171.27p5 beta (release 01–04–2005 CrysAlis171.NET), Oxford Diffraction Ltd., **2005**.
- [20] *CrysAlis RED*, Version 1.171.27p5 beta (release 01–04–2005 CrysAlis171.NET), Oxford Diffraction Ltd., **2005**.
- [21] A. Altomare, G. Cascarano, C. Giacovazzo, A. Guagliardi, *SIR-92*, A program for crystal structure solution; *J. Appl. Crystallogr.* **1993**, *26*, 343.
- [22] G. M. Sheldrick *SHELXS-97*, Program for Crystal Structure Solution, University of Göttingen, Germany, **1997**.
- [23] G. M. Sheldrick, *SHELXL-97*, Program for the Refinement of Crystal Structures. University of Göttingen, Germany, **1997**.
- [24] A. L. Spek, *PLATON*, A Multipurpose Crystallographic Tool, Utrecht University, Utrecht, The Netherlands, **1999**.
- [25] L. J. Farrugia, *J. Appl. Crystallogr.* **1999**, *32*, 837–838.
- [26] *SCALE3 ABSPACK* - An Oxford Diffraction program (1.0.4.gui:1.0.3), Oxford Diffraction Ltd., **2005**.
- [27] Crystallographic data for the structures have been deposited with the Cambridge Crystallographic Data Centre. Copies of the data can be obtained free of charge on application to The Director, CCDC, 12 Union Road, Cambridge CB2 1EZ, UK (Fax: +44-1223-336-033; E-mail for inquiry: fileserv@ccdc.cam.ac.uk; E-Mail for deposition: deposit-@ccdc.cam.ac.uk).
- [28] D. O. Bray, J. G. White, *Acta Crystallogr., Sect. B* **1979**, *35*, 3089–3091.
- [29] K. Karaghiosoff, T. M. Klapötke, P. Mayer, H. Piotrowski, K. Polborn, R. L. Willer, J. J. Weigand, *J. Org. Chem.* **2005**, *71*, 1295.
- [30] J. J. Weigand, Dissertation, Ludwig-Maximilians-University Munich, **2005**.
- [31] J. H. Bryden, *Acta Crystallogr.* **1956**, *9*, 874–878.
- [32] J. M. Welch, Dissertation, Ludwig-Maximilians-University Munich, **2008**.
- [33] M. Tremblay, *Can. J. Chem.* **1965**, *43*, 1154–1157.
- [34] J. Svetlik, A. Martvon, J. Lesko, *Chem. Papers* **1979**, *33*, 521.
- [35] M. Hesse, H. Meier, B. Zeeh, *Spektroskopische Methoden in der organischen Chemie*, 7th ed., Thieme, Stuttgart, New York, **2005**.
- [36] <http://www.linseis.com>.
- [37] <http://www.parrinst.de>.
- [38] N. Wiberg, in *Lehrbuch der Anorganischen Chemie / Holleman-Wiberg*, 101. Ed., de Gruyter, Berlin, **1995**, p. 51.
- [39] N. Wiberg, in *Lehrbuch der Anorganischen Chemie / Holleman-Wiberg*, 101. Ed., de Gruyter, Berlin, **1995**, p. 141.
- [40] M. Sućeska, *Test Methods for Explosives*, Springer, New York **1995**, p. 21 (impact), p. 27 (friction).
- [41] *NATO standardization agreement (STANAG) on explosives, impact sensitivity tests*, no. 4489, Ed. 1, Sept. 17, **1999**.
- [42] *WIWEB-Standardarbeitsanweisung 4–5.1.02, Ermittlung der Explosionsgefährlichkeit, hier der Schlagempfindlichkeit mit dem Fallhammer*, Nov. 8, **2002**.
- [43] <http://www.bam.de>.
- [44] <http://www.reichel-partner.de/>.
- [45] *NATO standardization agreement (STANAG) on explosive, friction sensitivity tests*, no. 4487, Ed. 1, Aug. 22, **2002**.
- [46] *WIWEB-Standardarbeitsanweisung 4–5.1.03, Ermittlung der Explosionsgefährlichkeit oder der Reibeempfindlichkeit mit dem Reibeapparat*, Nov. 8, **2002**.
- [47] a) S. Zeman, V. Pelikán, J. Majzlík, *Centr. Eur. J. Energy Mater.* **2006**, *3*, 45–51; b) D. Skinner, D. Olson, A. Block-Bolten, *Propellants Explos. Pyrotech.* **1997**, *22*, 34–42; c) OZM research, Czech Republic, <http://www.ozm.cz/testing-instruments/pdf/TI-SmallSpark.pdf>.
- [48] M. Sućeska, *EXPLO5*, Zagreb, Croatia, **2005**.
- [49] a) M. Sućeska, *Mater. Science Forum* **2004**, *465–466*, 325–330; b) M. Sućeska, *Propellants Explos. Pyrotech.* **1991**, *16*, 197–202; c) M. Sućeska, *Propellants Explos. Pyrotech.* **1999**, *24*, 280–285.
- [50] M. L. Hobbs, M. R. Baer, *Proc. of the 10th Symp. on Detonation*, ONR 33395–12, Boston, MA, July 12–16, **1993**, p. 409.

Received: November 16, 2009
Published Online: January 27, 2010

Diaminouronium Nitriminotetrazolates – Thermally Stable Explosives

Niko Fischer,^[a] Thomas M. Klapötke,^{*[a]} Davin Piercey,^[a] Susanne Scheutzw,^[a] and Jörg Stierstorfer^[a]

In Memory of Professor Herbert Schumann

Keywords: X-ray diffraction; Detonation parameters; Energetic materials; Sensitivities; Tetrazoles; NMR spectroscopy

Abstract. Diaminouronium 5-nitriminotetrazolate (**1**) and diaminouronium 1-methyl-5-nitrimino-tetrazolate (**2**) were synthesized by the reaction of diaminourea with 5-nitriminotetrazole (**3**) and 1-methyl-5-nitriminotetrazole (**4**), respectively. The energetic compounds **1** and **2** were fully characterized by single-crystal X-ray diffraction, NMR spectroscopy, IR- and Raman spectroscopy as well as DSC measure-

ments. The sensitivities towards impact, friction and electrical discharge were determined. Several detonation parameters (e.g. heat of explosion, detonation velocity) were computed by the EXPLO5 computer code based on calculated (CBS-4M) heats of formation and X-ray densities. In addition, the detonation velocity of **1** was experimentally determined and compared to the computed values.

Introduction

Nitrogen rich materials play an important role in the design of new energetic materials for use in propellants, explosives, and pyrotechnics [1]. For a nitrogen rich material to find practical application as a high explosive it needs to have high thermal and mechanical stabilities, while at the same time satisfying the increasing demand for higher performing (high detonation velocity, pressure and heat of explosion) materials. Unfortunately, in many cases high performance and low sensitivity appear to be mutually exclusive; many high performing materials are not stable enough to find practical use [2] and many materials with the desired sensitivity do not have the performance requirements of a material to replace a commonly-used explosive [3]. This trend is exemplified in the range of five-membered azoles from pyrazole to pentazole, where pyrazole is not used in energetics due to low performance, and the few pentazole derivatives known are highly unstable [4]. One of the most promising heterocyclic backbones for the preparation of high-performing energetics is the tetrazole ring.

Having high heats of formation resulting from the nitrogen-nitrogen bonds, ring strain, and high density, the tetrazole ring has allowed the preparation of high performing primary [5] and secondary [6] explosives, illustrating the dynamic nature of the tetrazole ring; depending on the ring substituents and anion/cation pairing, tetrazole based energetics can span the

spectrum of sensitivity from insensitive to highly sensitive (primary explosives). Additionally, due to their aromatic ring, tetrazoles are generally thermally stable. Of the tetrazoles suitable for use in secondary explosives, nitriminotetrazolates are one of the most promising due to high thermal stability [7].

Apart from the high heats of formation, for a molecule or salt to be a high-performing energetic, a high oxygen balance is required. The oxygen balance is given in percent and represents the amount of oxygen with respect to the molar mass of the molecule, which is necessary to convert all of its non-oxidizing content to their respective oxides and is easily calculated by the equation $\Omega (\%) = (wO - 2xC - 1/2yH - 2zS) \cdot 1600/M$ (w : number of oxygen atoms, x : number of carbon atoms, y : number of hydrogen atoms, z : number of sulfur atoms). Previous work with nitriminotetrazoles and especially alkylated nitriminotetrazoles [7], has led to compounds with high performance despite negative oxygen balances. The use of oxygen-containing cations with nitriminotetrazoles to improve the oxygen balance of the final nitriminotetrazolate salts is a previously unexplored field. In this work we describe the synthesis and properties of two new energetic nitriminotetrazoles containing the diaminouronium cation.

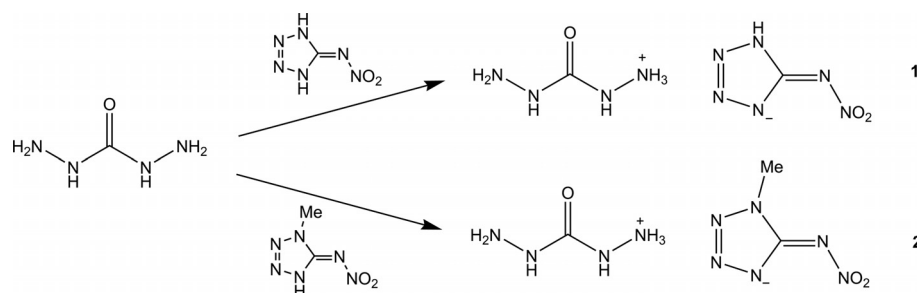
Results and Discussion

Synthesis

The synthetic routes to compounds **1** and **2** are depicted in Scheme 1. As they are both ionic species, they are accessible by facile Brønsted acid base chemistry. An aqueous solution of diaminourea, which is readily soluble in water, is reacted with an equimolar amount of 5-nitriminotetrazole or 1-methyl-5-nitriminotetrazole respectively, which also were dissolved in warm water prior to addition.

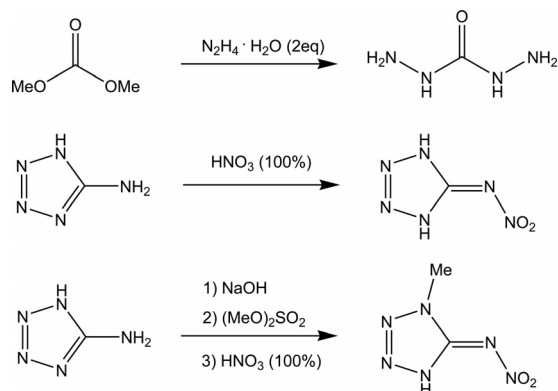
* Prof. Dr. T. M. Klapötke
Fax: +49-89-2180-77492
E-Mail: tmk@cup.uni-muenchen.de

[a] Department of Chemistry
Energetic Materials Research
Ludwig-Maximilian University
Butenandtstr. 5–13 (D)
81377 München, Germany



Scheme 1. Synthesis of **1** and **2** via Brønsted acid base chemistry.

Diaminourrea as well as 5-nitriminotetrazole and 1-methyl-5-nitriminotetrazole were synthesized according to literature procedure [8, 9] which can be seen in Scheme 2. Hydrazinolysis of dimethylcarbonate in aqueous solution leads to diaminourrea, whereas the acidic methylated and unmethylated nitriminotetrazoles are obtained by methylation of 5-aminotetrazole using sodium hydroxide and dimethyl sulfate and following nitration with fuming nitric acid or direct nitration of 5-aminotetrazole respectively.



Scheme 2. Synthesis of the starting materials.

Crystal Structures

The single-crystal X-ray diffraction data was collected using an Oxford Xcalibur3 diffractometer with a Spellman generator (voltage 50 kV, current 40 mA) and a KappaCCD detector. The data collection was undertaken using the CrysAlis CCD software [10] and the data reduction was performed with the CrysAlis Red software [10]. The structure was solved with SIR-92 [11] and refined with SHELXL-97 [12] implemented in the program package WinGX [13] and finally checked using Platon [14]. Due to the chiral space groups in both structure, the *Friedel pairs* were merged. In all structures potential hydrogen atoms have been observed and freely refined. Selected data and parameters from the X-ray data collection and refinement are given in Table 1. Further information regarding the crystal-structure determination have been deposited with the Cambridge Crystallographic Data Centre [15] as supplementary publication Nos CCDC-779254 (**1**) and -779255 (**2**).

Table 1. X-ray data and parameters.

	1	2
Formula	C ₂ H ₈ N ₁₀ O ₃	C ₃ H ₁₀ N ₁₀ O ₃
Form. weight /g·mol ⁻¹	220.18	234.12
Crystal system	monoclinic	orthorhombic
Space group	<i>Pn</i> (No. 7)	<i>P2₁2₁2₁</i> (No. 19)
Color / Habit	colorless rods	colorless plates
Size /mm	0.08 × 0.26 × 0.28	0.06 × 0.18 × 0.20
<i>a</i> /Å	3.7569(2)	4.9434(2)
<i>b</i> /Å	12.3854(6)	13.6462(6)
<i>c</i> /Å	8.7087(5)	14.5469(6)
α /°	90	90
β /°	92.106(5)	90
γ /°	90	90
<i>V</i> /Å ³	404.95(4)	981.21(7)
<i>Z</i>	2	4
$\rho_{\text{calcd.}}$ /g·cm ⁻³	1.806	1.585
μ /mm ⁻¹	0.159	0.136
<i>F</i> (000)	228	488
$\lambda_{\text{Mo-K}\alpha}$ /Å	0.71073	0.71073
<i>T</i> /K	173	173
θ Min-Max /°	4.7, 26.0	4.3, 25.5
Dataset	–5:4; –18:15; –9:13	–6:5; –18:16; –19:18
Reflections collected	2072	5910
Independent reflections	1095	1807
<i>R</i> _{int}	0.0244	0.0374
Observed reflections	995	1354
No. parameters	168	185
<i>R</i> ₁ (obs)	0.0265	0.0311
<i>wR</i> ₂ (all data)	0.0548	0.0526
<i>S</i>	0.965	0.840
Resd. dens. /e·Å ⁻³	–0.18, 0.15	–0.19, 0.15
Device type	Oxford Xcalibur3 CCD	Oxford Xcalibur3 CCD
Solution	SIR-92	SIR-92
Refinement	SHELXL-97	SHELXL-97
Absorption correction	multi-scan	multi-scan
CCDC	779254	779255–

Diaminouronium 5-nitriminotetrazolate (**1**) crystallizes in the monoclinic chiral space group *Pn*. Its density of 1.806 g·cm⁻³ is quite high in comparison with other tetrazolate salts [16]. The molecular unit is shown in Figure 1. The structure of the 5-nitriminotetrazolate anion is comparable to that found in corresponding copper(II) salts [17]. Bond lengths are given in Table 2. The diaminouronium cation follows the structure described e.g. for diaminouronium 5-(4-amino-1,2,5-oxadiazol-3-yl)tetrazolate [18].

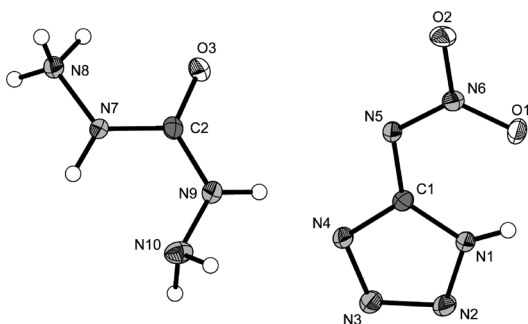


Figure 1. Molecular unit of diamouronium 5-nitriminotetrazolate (**1**). Ellipsoids of non-hydrogen atoms are drawn at the 50 % probability level.

Table 2. Bond lengths and bond angles of **1** and **2**.

atoms	1	2
O1–N6	1.240(2)	1.249(2)
O2–N6	1.269(2)	1.276(2)
N5–N6	1.313(2)	1.315(2)
N5–C1	1.377(3)	1.372(3)
N1–C1	1.338(3)	1.346(3)
N4–C1	1.330(3)	1.341(3)
N1–N2	1.347(3)	1.347(2)
N2–N3	1.298(2)	1.297(3)
N3–N4	1.355(3)	1.370(2)
N1–C2	1.459(3)	1.459(3)
O3–C2(3)	1.244(2)	1.235(3)
N7–N8	1.419(2)	1.407(3)
N7–C2(3)	1.386(2)	1.346(3)
N9–N10	1.417(3)	1.422(3)
N9–C2(3)	1.331(3)	1.338(3)

The packing is strongly influenced by an intense hydrogen-bond network. The formation of all intramolecular (graph sets [19] DAU^+ : $2 \times \text{S}(1,1(5))$; graph set HAtNO_2^- : $\text{S}(1,1(6))$) as well as of selected intermolecular hydrogen bonds is shown in Figure 2.

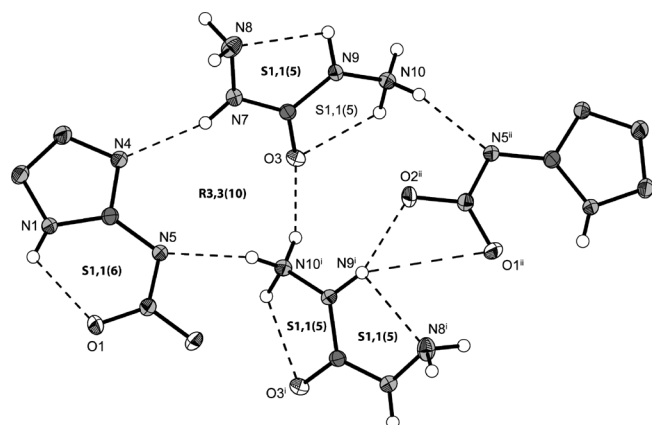


Figure 2. View on selected hydrogen bonds in the structure of **1**. Symmetry codes (i) $-0.5+x, 1-y, 0.5+z$; (ii) $0.5+x, 1-y, -0.5+z$.

Diaminouronium 1-methyl-5-nitriminotetrazolate (**2**) crystallizes in the orthorhombic chiral space group $P2_12_12_1$. Its density of 1.585 g cm^{-3} is significantly lower than that of **1**, how-

ever, it is in the range of other 1-methyl-5-nitriminotetrazolate salts with nitrogen-rich counter cations [7]. The anions are planar [$\angle(\text{O1-N6-C1-N4}) = 1.22(2)^\circ$] and show comparable bond lengths and angles to copper(II) 1-methyl-5-nitriminotetrazolates in the literature [20] (Figure 3).

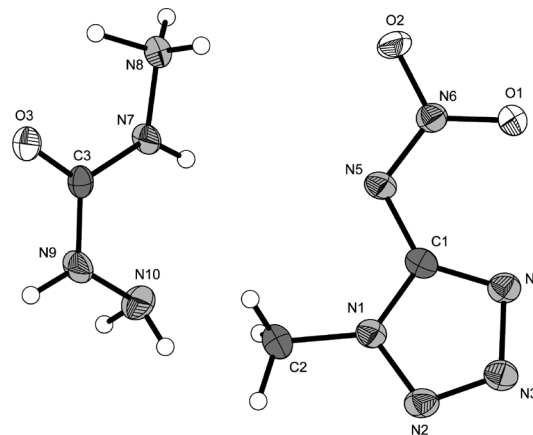


Figure 3. Molecular unit of diamouronium 1-methyl-5-nitriminotetrazolate (**2**). Ellipsoids of non-hydrogen atoms are drawn at the 50 % probability level.

The structure of **2** also shows an intense hydrogen-bond network. All of the hydrogen atoms of the diaminouronium cations are involved in hydrogen bridges, which are shown in Figure 4.

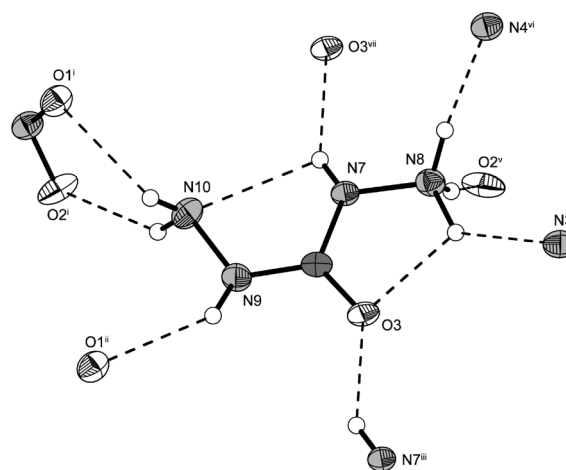


Figure 4. View on the hydrogen bridges of one diaminouronium cation in the structure of **2**. Symmetry codes (i) $2-x, 0.5+y, 0.5-z$; (ii) $1-x, 0.5+y, 0.5-z$; (iii) $-1+x, y, z$; (iv) $0.5-x, -y, 0.5+z$; (v) $-1+x, y, z$; (vi) $1.5-x, -y, 0.5+z$ (vii) $1+x, y, z$.

Spectroscopy

Both compounds described were investigated using ^1H and ^{13}C NMR spectroscopy. For better comparison with literature values, all spectra were measured using $[D_6]\text{DMSO}$ as solvent and all chemical shifts are given with respect to TMS (^1H , ^{13}C).

To identify the specified compounds NMR spectroscopy, especially carbon NMR spectra are a valuable method since the spectra are dominated by only two or three signals, respec-

tively. The signals for the ring carbon atoms in **1** and **2** can be found at 158.0 ppm (**1**) and 157.6 ppm (**2**). Hence, no shift of this signal in the anionic species is observed due to the methylation of the tetrazole ring. The signal of the carbon atom of the carbonyl moiety of the cation is observed at around 159.5 ppm. An additional methyl signal at 33.0 ppm for the methylated nitriminotetrazolate can be assigned and its position is in accordance with values found in literature [7].

IR and Raman spectroscopy is also suitable for the identification of the described nitriminotetrazolate salts. IR and Raman spectra of both compounds were measured and the absorptions were assigned according to commonly observed values found in literature [7, 21–23]. The range between 3550 and 3230 cm⁻¹ is mainly determined by the N–H stretching vibrations of the diaminouronium cation. For the methylated compound **2** the symmetric C–H stretching vibration of the methyl group can nicely be observed in the Raman spectrum at 2957 cm⁻¹. Another characteristic IR absorption is the C=O stretching vibration of the cation at 1692 cm⁻¹ in both cases. The tetrazole ring system itself exhibits stretching and deformation vibrations that can be detected as a set of signals lying in the range from 1031 cm⁻¹ to 1637 cm⁻¹ with a C=N stretching vibration between 1617 and 1637 cm⁻¹.

Sensitivities and Thermal Behavior

The impact sensitivity tests were carried out according to STANAG 4489 [24] modified instruction [25] using a BAM (Bundesanstalt für Materialforschung) drophammer [26]. The friction sensitivity tests were carried out according to STANAG 4487 [27] modified instruction [28] using the BAM friction tester. The classification of the tested compounds results from the “UN Recommendations on the Transport of Dangerous Goods” [29]. All compounds were tested upon the sensitivity towards electrical discharge using the Electric Spark Tester ESD 2010 EN [30]. The values for the impact sensitivities could be determined to 5 J (**2**) and 3 J (**3**) and therefore both compounds have to be classified as “sensitive” and very “sensitive” towards impact. The same classification applies to the friction sensitivity. With values of 108 N (**1**) and 160 N (**2**) both nitriminotetrazolate salts are sensitive towards friction. Compared to the triaminoguanidinium salt of 1-methyl-5-nitriminotetrazole, which was formerly investigated by our research group [7] and exhibits values of 6 J and 240 N, the diaminouronium salt is more sensitive especially towards friction. The sensitivities towards electrical discharge were determined to be 0.20 J (**2**) and 0.15 J (**3**).

Differential scanning calorimetry (DSC) measurements to determine the melt- and decomposition temperatures of **1** and **2** (about 1.5 mg of each energetic material) were performed in covered Al-containers with a hole (0.1 mm) in the lid for gas release and a nitrogen flow of 20 mL per minute with a Linseis PT 10 DSC [31] calibrated by standard pure indium and zinc at a heating rate of 5 °C·min⁻¹. The decomposition temperatures are given as absolute onset temperatures and both compounds decompose at around 200 °C with a slightly higher value for methylated **2** (204 °C) compared to 198 °C for unmethylated **1**. Compared to triaminoguanidinium (210 °C) and

diaminoguanidinium 1-methyl-5-nitriminotetrazolate (208 °C), where the oxo (= O) moiety of the cation is exchanged by a hydrazo (= NH–NH₂) and an imino (= NH) moiety respectively, there is not a significant difference in thermal stability.

Theoretical Calculations

All calculations were carried out using the Gaussian G03W (revision B.03) program package [32]. The enthalpies (H) and free energies (G) were calculated using the complete basis set (CBS) method of *Petersson* and co-workers in order to obtain very accurate energies. The CBS models use the known asymptotic convergence of pair natural orbital expressions to extrapolate from calculations using a finite basis set to the estimated complete basis set limit. CBS-4 begins with a HF/3-21G(d) geometry optimization; the zero point energy is computed at the same level. It then uses a large basis set SCF calculation as a base energy, and a MP2/6-31+G calculation with a CBS extrapolation to correct the energy through second order. A MP4(SDQ)/6-31+(d,p) calculation is used to approximate higher order contributions. In this study we applied the modified CBS-4M method (M referring to the use of minimal population localization) which is a re-parametrized version of the original CBS-4 method and also includes some additional empirical corrections [33]. The enthalpies of the gas-phase species M were computed according to the atomization energy method [Equation (1)] (Table 3, Table 4, and Table 5) [34].

$$\Delta_f H^\circ_{(g, M, 298)} = H_{(Molecule, 298)} - \sum H^\circ_{(Atoms, 298)} + \sum \Delta_f H^\circ_{(Atoms, 298)} \quad (1)$$

Table 3. CBS-4M results.

	point group	$-H^{298}$ /a.u.	NIMAG
DAU ⁺	C _s	335.795706	0
HAtNO ₂ ⁻	C _s	516.973495	0
1MeAtNO ₂ ⁻	C ₁	556.194636	0
H		0.500991	0
C		37.786156	0
N		54.522462	0
O		74.991202	0

Table 4. Literature values for atomic $\Delta_f H^\circ_{298}$ /kcal·mol⁻¹.

	NIST [35]
H	52.1
C	171.3
N	113.0
O	59.6

Table 5. Enthalpies of the gas-phase species M.

M	Formula	$\Delta_f H^\circ_{(g, M)}$ /kcal·mol ⁻¹
DAU ⁺	CH ₇ N ₄ O	155.6
HAtNO ₂ ⁻	CHN ₆ O ₂	35.9
1MeAtNO ₂ ⁻	C ₂ H ₃ N ₆ O ₂	166.3

Table 6. Molecular volumes.

	V_M /Å ³	V_M /nm ³
DAU ⁺	81	0.081
HAtNO ₂ ⁻	121	0.121
1MeAtNO ₂ ⁻	164	0.164

The solid state energy of formations (Table 8) of **1** and **2**, the lattice energy (U_L) and lattice enthalpy (ΔH_L) (Table 7) were calculated from the corresponding molecular volumes (Table 6) according to the equations provided by Jenkins [36]. With the calculated lattice enthalpy (Table 7) the gas-phase enthalpy of formation (Table 5) was converted into the solid state (standard conditions) enthalpy of formation (Table 8). These molar standard enthalpies of formation (ΔH_m) were used to calculate the molar solid state energies of formation (ΔU_m) according to Equation (2) (Table 8).

Table 7. Lattice energies and lattice enthalpies.

	V_M / nm^3	$U_L / \text{kJ} \cdot \text{mol}^{-1}$	$\Delta H_L / \text{kJ} \cdot \text{mol}^{-1}$	$\Delta H_L / \text{kcal} \cdot \text{mol}^{-1}$
1	0.202	503.6	507.1	121.1
2	0.245	478.7	482.2	115.2

$$\Delta U_m = \Delta H_m - \Delta n RT \quad (2)$$

(Δn being the change of moles of gaseous components)

Detonation Parameters

The calculation of the detonation parameters was performed with the program package EXPLO5 (version 5.04) [37]. The program is based on the chemical equilibrium, steady-state model of detonation. It uses the Becker–Kistiakowsky–Wilson's equation of state (BKW EOS) for gaseous detonation products and Cowan–Fickett's equation of state for solid carbon. The calculation of the equilibrium composition of the detonation products is done by applying modified White, Johnson and Dantzig's free energy minimization technique. The program is designed to enable the calculation of detonation parameters at the CJ point. The BKW equation in the following form was used with the BKWN set of parameters (α , β , κ , θ) as stated below the equations and X_i being the mol fraction of i -th gaseous product, k_i is the molar covolume of the i -th gaseous product [38]:

$$pV / RT = 1 + xe^{\beta x} \quad x = (\kappa \sum X_i k_i) / [V(T + \theta)]^\alpha$$

$$\alpha = 0.5, \beta = 0.176, \kappa = 14.71, \theta = 6620.$$

The detonation parameters calculated with the EXPLO5 program (V5.04) of compounds **1** and **2** using the experimentally determined densities (X-ray) are summarized in Table 9 and compared to the values calculated for the triaminoguanidinium 1-methyl-5-nitriminotetrazolate and commonly used RDX.

Due to the much higher crystal density, the value for the detonation velocity for the parent compound **1** ($8979 \text{ m} \cdot \text{s}^{-1}$) exceeds the one of methylated **2** ($8127 \text{ m} \cdot \text{s}^{-1}$) by far and is even slightly higher when compared to RDX. The detonation pressures, how-

ever, only differ slightly. Again, a comparison of **2** to the triaminoguanidinium salt of 1-methyl-5-nitriminotetrazole seems to be appropriate since both compounds only differ by one isobal moiety which is the hydrazo ($= \text{NH}-\text{NH}_2$) moiety in the case of the triaminoguanidinium salt and the oxo ($= \text{O}$) moiety in **2**. There is only one value, which is in the same range for both compounds, which is the explosion energy ($-4895 \text{ kJ} \cdot \text{kg}^{-1}$ (**2**), $-4888 \text{ kJ} \cdot \text{kg}^{-1}$ (TAG-1-MeATNO₂)). Not only the detonation velocity, but also the detonation pressure of the triaminoguanidinium salt is substantially higher than for the diaminouronium salt **2**, even though having a slightly lower crystal density and a lower oxygen balance. In summary, the 5-nitriminotetrazolate salt **1** shows much better performance than its methylated sister compound **2**. Further, the exchange of the triaminoguanidinium cation by the diaminouronium cation does not improve the detonation performance in case of the 1-methyl-5-nitriminotetrazolate anion, although one would expect a higher performance for oxygen containing cations such as the diaminouronium cation. The reason, why we observe inverse behavior might be the connectivity of the oxygen in the cation. In the case of diaminourea, it is connected to a carbon atom, which therefore is already partially oxidized and does not release as much energy as a carbon atom with a lower oxidation state. Probably, oxygen containing cations involving a nitro functionality such as the aminonitroguanidinium cation lead to a better performance of the materials containing the respective anions investigated in this work.

Velocity of Detonation Test

In order to evaluate the detonation velocity of **1** experimentally, compound **1** was prepared on a 50 g scale. The detonation velocity tests were performed in an OZM laboratory detonation chamber (model KV-250). The measurement of the detonation velocity was performed using the OZM detonating velocity measuring system EXPLOMET-FO-2000. The use of the fiber optic technique ensures excellent electrical noise immunity. For the detonation velocity measurement a PE tube with an inner diameter of 14 mm was used, which was equipped with three optical fibers with a distance of 17 mm between them. The amount of compound **1** used for the test was 11.6 g resulting in a density of $0.699 \text{ g} \cdot \text{cm}^{-3}$. The compound was loaded into the PE tube and manually compressed with a force of ca. 30 N. As a booster charge 0.30 g of nitropenta (PETN) were added on top and carefully compressed manually using ca. 20 n force. Initiation was achieved with an electrically ignited detonator containing PETN and RDX (ORICA, DYNADET C2–25MS). To evaluate the used method, the same setup was employed for measuring the detonation velocity of RDX under the same conditions. 14.4 g of RDX were filled into the tube ($\rho = 0.869 \text{ g} \cdot \text{cm}^{-3}$) and for best

Table 8. Solid state enthalpies and energies of formation ($\Delta_f U^\circ$).

	$\Delta_f H^\circ(\text{s}) / \text{kcal} \cdot \text{mol}^{-1}$	$\Delta_f H^\circ(\text{s}) / \text{kJ} \cdot \text{mol}^{-1}$	Δn	$\Delta_f U^\circ(\text{s}) / \text{kJ} \cdot \text{mol}^{-1}$	$M / \text{g} \cdot \text{mol}^{-1}$	$\Delta_f U^\circ(\text{s}) / \text{kJ} \cdot \text{kg}^{-1}$
1	70.4	294.6	10.5	320.7	220.20	1456.3
2	80.1	335.4	11.5	363.9	234.23	1553.7

comparison of the measured values, also 0.30 g of PETN were added on top of the RDX. The results of the measurement can be seen in Table 10. The measured values between fiber 1 and 2 and between 2 and 3 were averaged and compared to the values computed with the EXPLO5 (version 5.04) software [37]. The recorded values for both measurements (RDX as well as compound **1**) are in surprisingly good agreement with the computed values and differ by less than 200 m·s⁻¹ for compound **1** and only 41 m·s⁻¹ for RDX.

Table 9. Detonation parameters.

	1	2	TAG-1-MeATNO ₂	RDX
ρ / g·cm ⁻³ ^{a)}	1.81	1.59	1.57	1.80
Ω / % ^{b)}	-36.3	-54.7	-64.5	-21.6
$\Delta_{\text{Ex}} U^\circ$ / kJ·kg ⁻¹ ^{c)}	-4848	-4850	-4781	-6125
T_{det} / K ^{d)}	3335	3246	3091	4236
P_{CJ} / kbar ^{e)}	337	252	255	349
$V_{\text{Det.}}$ / m·s ⁻¹ ^{f)}	8979	8172	8309	8748
V_o / L·kg ⁻¹ ^{g)}	848	832	847	739

a) X-ray density. b) Oxygen balance. c) Energy of explosion. d) Detonation temperature. e) Detonation pressure. f) Detonation velocity. g) Volume of explosion gases assuming only gaseous products.

Table 10. Calculated and measured detonation velocities of **1** and RDX.

	1	RDX
mass / g	11.6	14.4
density / g·cm ⁻³	0.699	0.869
$V_{\text{det, exp.}}$ / m·s ⁻¹	4384	5339
$V_{\text{det, theor.}}$ / m·s ⁻¹	4568	5370

Conclusions

From this combined theoretical and experimental study the following conclusions can be drawn:

Diaminouronium nitriminotetrazolate (**1**) and diaminouronium 1-methyl nitriminotetrazolate (**2**) were prepared in high yield and purity from the corresponding nitriminotetrazole and diaminourea.

The crystal structures of **1** and **2** were determined by low-temperature single-crystal X-ray diffraction. The compounds crystallize in the space groups *Pn* and *P2₁2₁2₁* with densities of 1.806 and 1.585 g·cm⁻³ respectively. Additionally both compounds were fully characterized by vibrational spectroscopy (IR and Raman) ¹H and ¹³C NMR spectroscopy, mass spectrometry, and elemental analysis.

Thermal stabilities of **1** and **2** were investigated by DSC and decompose at 198 and 204 °C respectively.

The sensitivities towards friction, impact and electrostatic discharge were investigated by BAM methods. Compounds **1** and **2** were found to have impact sensitivities of 5 J and 3 J respectively, friction sensitivities of 108 N and 160 N respectively, and ESD sensitivities of 0.2 J and 0.15 J respectively. These are within the range of commonly-used high explosives such as RDX.

Using calculated heats of formation and experimentally obtained crystal densities the detonation parameters (heat of ex-

plosion, explosion temperature, detonation pressure and velocity) were calculated. Compound **1** has a detonation velocity of 8979 m·s⁻¹ and a detonation pressure of 337 kbar. Compound **2** has a detonation velocity of 8172 m·s⁻¹ and a detonation pressure of 252 kbar.

Experimental Section

Caution! Methylated and unmethylated 5-nitriminotetrazole and their salts are energetic materials with increased sensitivities towards shock and friction. Therefore, proper safety precautions (safety glass, face shield, earthened equipment and shoes, Kevlar® gloves and ear plugs) have to be applied while synthesizing and handling the described compounds.

All chemicals and solvents were employed as received (Sigma–Aldrich, Fluka, Acros). ¹H and ¹³C spectra were recorded using a JEOL Eclipse 270, JEOL EX 400 or a JEOL Eclipse 400 instrument. The chemical shifts quoted in ppm in the text refer to typical standards such as tetramethylsilane (¹H, ¹³C). To determine the melting and decomposition temperatures of the described compounds, a Linseis PT 10 DSC (heating rate 5 °C·min⁻¹) was used. Infrared spectra were measured using a Perkin–Elmer Spectrum One FT-IR spectrometer as KBr pellets. Raman spectra were recorded with a Bruker MultiRAM Raman Sample Compartment D418 equipped with a Nd-YAG-Laser (1064 nm) and a LN-Ge diode as detector. Mass spectra of the described compounds were measured with a JEOL MStation JMS 700 using FAB technique. To measure elemental analyses a Netsch STA 429 simultaneous thermal analyzer was employed.

Diaminouronium 5-nitriminotetrazolate (**1**)

5-Nitriminotetrazole (0.89 g, 6.85 mmol) was dissolved in a few milliliters of water and added to a solution of diaminourea (0.62 g, 6.85 mmol). The mixture was warmed, stirred at elevated temperature for ten minutes and the solvent was removed under vacuum. The colorless solid residue was recrystallized from ethanol to yield 1.96 g (6.10 mmol, 89 %) of **1** as a colorless crystalline material.

DSC (5 °C·min⁻¹): 180 °C (m.p.), 198 °C (dec.). **IR** (KBr): $\tilde{\nu}$ = 3550 (s), 3414 (vs), 3234 (s), 2321 (w), 2024 (w), 1692 (s), 1637 (s), 1617 (vs), 1543 (m), 1512 (s), 1441 (m), 1385 (m), 1326 (s), 1229 (m), 1136 (s), 1110 (m), 1089 (m), 1062 (m), 1031 (m), 1006 (w), 963 (m), 921 (w), 870 (w), 773 (m), 746 (m), 696 (m), 623 (s), 570 (m), 482 (m) cm⁻¹; **Raman** (1064 nm, 250 mW, 25 °C, cm⁻¹): $\tilde{\nu}$ = 1542 (100), 1447 (4), 1390 (8), 1340 (2), 1327 (32), 1232 (4), 1150 (9), 1112 (3), 1081 (7), 1030 (42), 1017 (60), 962 (2), 921 (5), 875 (6), 748 (2), 741 (14), 578 (5), 486 (7), 430 (2), 420 (14), 384 (9), 252 (10) cm⁻¹. **¹H NMR** ([D₆]DMSO, 25 °C) δ = 8.56 (s, 8 H, -NH -NH₂, -NH₃⁺). **¹³C NMR** ([D₆]DMSO, 25 °C) δ = 159.3 (C(O)(NHNH₂)(NHNH₃⁺)), 158.0 (CN₄); *m/z* (FAB⁺): 91.1 [C(O)(N₂H₃)₂+H⁺]; **MS** *m/z* (FAB⁻): 129.0 [ATNO₂⁻]; **EA** (C₂H₈N₁₀O₃, 220.15): calcd.: C 10.91, H 3.66, N 63.62 %; found: C 11.19, H 3.78, N 63.42 %; **BAM drophammer**: 5 J; friction tester: 108 N; ESD: 0.20 J (at grain size 500–1000 μm).

Diaminouronium 1-methyl-5-nitriminotetrazolate (**2**)

1-Methyl-5-nitriminotetrazole (1.44 g, 10.0 mmol) was dissolved in a few milliliters of warm water and added to a solution of diaminourea (0.90 g, 10.0 mmol). The mixture was heated to reflux for one minute and the solvent was removed under vacuum afterwards. The colorless solid residue was recrystallized from an ethanol/water mixture. Yield: 2.15 g (9.20 mmol, 92 %).

DSC (5 °C·min⁻¹): 163 °C (m.p.), 204 °C (dec.). **IR** (KBr): $\tilde{\nu}$ = 3415 (s), 3371 (s), 3355 (s), 3326 (s), 3306 (s), 3230 (m), 3139 (m), 2956 (m), 2666 (m), 2019 (w), 1692 (s), 1619 (s), 1515 (s), 1466 (s), 1425 (m), 1411 (m), 1383 (s), 1324 (vs), 1295 (m), 1279 (m), 1240 (m), 1177 (m), 1163 (m), 1117 (m), 1108 (m), 1052 (w), 1032 (m), 989 (w), 960 (w), 928 (w), 881 (w), 774 (w), 752 (w), 740 (w), 691 (w), 636 (w), 581 (w) cm⁻¹; **Raman** (1064 nm, 400 mW, 25 °C, cm⁻¹): $\tilde{\nu}$ = 3326 (5), 3140 (3), 3008 (2), 2957 (13), 1690 (7), 1636 (2), 1504 (91), 1465 (27), 1411 (12), 1371 (5), 1322 (8), 1301 (36), 1240 (3), 1179 (9), 1109 (29), 1052 (5), 1033 (100), 992 (5), 961 (10), 883 (11), 776 (2), 754 (9), 693 (17), 585 (7), 498 (9), 454 (4), 377 (8), 294 (20), 240 (7), 216 (5) cm⁻¹. **¹H NMR** ([D₆]DMSO, 25 °C) δ = 7.79 (s, 7 H, -NH₂), -NH₃⁺, 3.67 (s, 3 H, -CH₃). **¹³C NMR** ([D₆]DMSO, 25 °C, ppm) δ = 159.6 (C(O)(NHNH₂)(NHNH₃⁺)), 157.6 (CN₄), 33.1 (CH₃); **MS** *m/z* (FAB⁺): 91.1 [C(O)(N₂H₃)₂+H⁺]; *m/z* (FAB⁻): 143.0 [1-MeATNO₂]⁻; **EA** (C₃H₁₀N₁₀O₃, 234.18): calcd.: C 15.39, H 4.30, N 59.81 %; found: C 15.30, H 4.07, N 59.98 %; **BAM drophammer**: 3 J; friction tester: 160 N; ESD: 0.15 J (at grain size 100–500 µm).

Acknowledgement

Financial support of this work by the Ludwig-Maximilian University of Munich (LMU), the U.S. Army Research Laboratory (ARL), the Armament Research, Development and Engineering Center (ARDEC), the Strategic Environmental Research and Development Program (SERDP) and the Office of Naval Research (ONR Global, title: "Synthesis and Characterization of New High Energy Dense Oxidizers (HEDO) - NICOP Effort") under contract nos. W911NF-09-2-0018 (ARL), W911NF-09-1-0120 (ARDEC), W011NF-09-1-0056 (ARDEC) and 10 WPSEED01-002 / WP-1765 (SERDP) is gratefully acknowledged. The authors acknowledge collaborations with Dr. Mila Krupka (OZM Research, Czech Republic) in the development of new testing and evaluation methods for energetic materials and with Dr. Muhamed Sucesca (Brodarski Institute, Croatia) in the development of new computational codes to predict the detonation and propulsion parameters of novel explosives. We are indebted to and thank Drs. Betsy M. Rice and Brad Forch (ARL, Aberdeen, Proving Ground, MD) and Mr. Gary Chen (ARDEC, Picatinny Arsenal, NJ) for many helpful and inspired discussions and support of our work.

References

- [1] L. V. De Yong, G. Campanella, *J. Hazard. Mater.* **1989**, *21*, 125.
- [2] T. M. Klapötke, J. Stierstorfer, *J. Am. Chem. Soc.* **2009**, *131*, 1122.
- [3] A. K. Sikder, N. Sikder, *J. Hazard. Mater.* **2004**, *A112*, 1.
- [4] P. Carlqvist, H. Ostmark, T. Brinck, *J. Phys. Chem. A* **2004**, *108*, 7463.
- [5] M. H. V. Huynh, M. A. Hiskey, T. J. Meyer, M. Wetzler, *Proc. Natl. Acad. Sci. USA* **2006**, *103*, 5409–5412.
- [6] N. Fischer, T. M. Klapötke, S. Scheutzwow, J. Stierstorfer, *Cent. Eur. J. Energetic Mater.* **2008**, *5*, 3.
- [7] T. M. Klapötke, J. Stierstorfer, A. U. Wallek, *Chem. Mater.* **2008**, *20*, 4519.
- [8] Z. Li, W. Zhu, J. Yu, X. Ma, Z. Lu, S. Xiao, *Synth. Commun.* **2006**, *36*, 2613.
- [9] T. M. Klapötke, J. Stierstorfer, *Helv. Chim. Acta* **2007**, *90*, 2132.
- [10] *CrysAlis RED*, Oxford Diffraction Ltd., Version 1.171.27p5 beta (release 01–04–2005 CrysAlis171.NET).
- [11] A. Altomare, G. Cascarano, C. Giacovazzo, A. Guagliardi, *Appl. Crystallogr.* **1993**, *26*, 343.
- [12] G. M. Sheldrick, *SHELXL-97*, Program for the Refinement of Crystal Structures, University of Göttingen, Germany, **1994**.
- [13] L. Farrugia, *J. Appl. Crystallogr.* **1999**, *32*, 837–838.
- [14] A. L. Spek, *Platon*, A Multipurpose Crystallographic Tool, Utrecht University, Utrecht, The Netherlands, **1999**.
- [15] Crystallographic data for the structures have been deposited with the Cambridge Crystallographic Data Centre. Copies of the data can be obtained free of charge on application to The Director, CCDC, 12 Union Road, Cambridge CB2 1EZ, UK (Fax: +44-1223-336-033; E-Mail for inquiry: fileserv@ccdc.cam.ac.uk; E-Mail for deposition: deposit@ccdc.cam.ac.uk).
- [16] J. Stierstorfer, Dissertation, Energetic Materials based on 5-Aminotetrazole, Ludwig-Maximilians-Universität München, **2009**.
- [17] T. M. Klapötke, J. Stierstorfer, B. Weber, *Inorg. Chim. Acta* **2009**, *362*, 2311–2320.
- [18] R. Wang, Y. Guo, Z. Zeng, B. Twamley, J. M. Shreeve, *Chem. Eur. J.* **2009**, *15*, 2625.
- [19] J. Bernstein, R. E. Davis, L. Shimoni, N.-L. Chang, *Angew. Chem. Int. Ed. Engl.* **1995**, *34*, 1555.
- [20] G. Geisberger, T. M. Klapötke, J. Stierstorfer, *Eur. J. Inorg. Chem.* **2007**, *30*, 4743–4750.
- [21] M. Tremblay, *Can. J. Chem.* **1965**, *43*, 1154.
- [22] J. Svetlik, A. Martvon, J. Lesko, *Chem. Papers* **1979**, *33*, 521.
- [23] M. Hesse, H. Meier, B. Zeeh, *Spektroskopische Methoden in der organischen Chemie*, 7th ed., Thieme, Stuttgart, New York, **2005**.
- [24] NATO standardization agreement (STANAG) on explosives, *impact sensitivity tests*, no. 4489, 1st ed., Sept. 17, **1999**.
- [25] WIWEB-Standardarbeitsanweisung 4–5.1.02, *Ermittlung der Explosionsgefährlichkeit*, hier der Schlagempfindlichkeit mit dem Fallhammer, Nov. 8, **2002**.
- [26] <http://www.bam.de>.
- [27] NATO standardization agreement (STANAG) on explosive, *friction sensitivity tests*, no. 4487, 1st ed., Aug. 22, **2002**.
- [28] WIWEB-Standardarbeitsanweisung 4–5.1.03, *Ermittlung der Explosionsgefährlichkeit oder der Reibeempfindlichkeit mit dem Reibeapparat*, Nov. 8, **2002**.
- [29] Impact: Insensitive > 40 J, less sensitive ≤ 35 J, sensitive ≥ 4 J, very sensitive ≤ 3 J; friction: Insensitive > 360 N, less sensitive = 360 N, sensitive < 360 N a. > 80 N, very sensitive ≤ 80 N, extreme sensitive ≤ 10 N; According to the UN Recommendations on the Transport of Dangerous Goods (+) indicates: not safe for transport.
- [30] <http://www.ozm.cz>.
- [31] <http://www.linseis.com>.
- [32] M. J. Frisch et al., *Gaussian 03*, Revision B04, Gaussian Inc., Wallingford, CT, **2004**.
- [33] a) J. W. Ochterski, G. A. Petersson, J. A. Montgomery Jr., *J. Chem. Phys.* **1996**, *104*, 2598; b) J. A. Montgomery Jr., M. J. Frisch, J. W. Ochterski, G. A. Petersson, *J. Chem. Phys.* **2000**, *112*, 6532.
- [34] a) L. A. Curtiss, K. Raghavachari, P. C. Redfern, J. A. Pople, *J. Chem. Phys.* **1997**, *106*, 1063; b) E. F. C. Byrd, B. M. Rice, *J. Phys. Chem. A* **2006**, *110*, 1005; c) B. M. Rice, S. V. Pai, J. Hare, *Comb. Flame* **1999**, *118*, 445.
- [35] P. J. Linstrom, W. G. Mallard, Eds., *NIST Chemistry WebBook*, NIST Standard Reference Database Number 69, June **2005**, National Institute of Standards and Technology, Gaithersburg MD, 20899 (<http://webbook.nist.gov>).
- [36] a) H. D. B. Jenkins, H. K. Roobottom, J. Passmore, L. Glasser, *Inorg. Chem.* **1999**, *38*, 3609; b) H. D. B. Jenkins, D. Tudela, L. Glasser, *Inorg. Chem.* **2002**, *41*, 2364.
- [37] M. Sućeska, *EXPLO5.04* program, Zagreb, Croatia, **2010**.
- [38] a) M. Sućeska, *Materials Science Forum*, **2004**, 465–466, 325; b) M. Sućeska, *Propellants Explos. Pyrotech.* **1991**, *16*, 197; c) M. Sućeska, *Propellants Explos. Pyrotech.* **1999**, *24*, 280; d) M. L. Hobbs, M. R. Baer, *Proc. of the 10th Symp. (International) on Detonation*, ONR 33395–12, Boston, MA, July 12–16, **1993**, p. 409.

Received: June 2, 2010
Published Online: August 16, 2010

Energetic Materials based on 1-Amino-3-nitroguanidine

Niko Fischer, Thomas M. Klapötke, Franz A. Martin and Jörg Stierstorfer

Energetic Materials Research, Department of Chemistry
University of Munich (LMU), Butenandtstr. 5-13, D-81377, Germany

finch@cup.uni-muenchen.de

Abstract:

1-Amino-3-nitroguanidine (2) was synthesized by hydrazinolysis of nitroguanidine (1). Due to its basicity, it can be protonated by energetic compounds bearing an acidic proton. The chloride (3) and perchlorate (5) salts of 1-amino-3-nitroguanidine were synthesized by protonation of 2 with dilute hydrochloric acid and perchloric acid, respectively. 5-Nitrimino-1,4H-tetrazole was used to synthesize the nitriminotetrazolate salt (9). 5-Nitrimino-1,4H-tetrazole was obtained by reacting 5-amino-1H-tetrazole with 100% HNO_3 . Furthermore, the dinitramide (6) salt of 1-amino-3-nitroguanidine was synthesized by metathesis reaction of silver dinitramide and 1-amino-3-nitroguanidinium chloride (3). The dinitroguanidinate salt (8) was synthesized by protonation of 2 with dinitroguanidine. Dinitroguanidine was prepared by nitroguanidine in anhydrous nitric acid N_2O_5 . All compounds were fully characterized by single crystal X-ray diffraction, vibrational spectroscopy (IR and Raman), multinuclear NMR spectroscopy, elemental analysis and DSC measurements. The heats of formation of 2, 6, 8 and 9 were calculated using the atomization method based on CBS-4M enthalpies. With these values and the experimental (X-ray) densities several detonation parameters such as the detonation pressure, velocity, energy and temperature were computed using the EXPLO5 code. In addition, the sensitivities towards impact, friction and electrical discharge were tested using the BAM drophammer, friction tester as well as a small scale electrical discharge device.

Keywords: 1-Amino-3-nitroguanidine; Energetic Materials; Crystal Structures; Detonation Parameters; Sensitivities.

1 Introduction

The synthesis of new energetic, non-nuclear materials ^[1] for military and space application has been a long term goal in our research group. ^[2] Some of our current challenges are (a) new *green* high explosives replacing commonly used toxic compounds; (b) N-rich components in propellant systems. (c) Smokeless and nontoxic colorants for pyrotechnical applications.

Several approaches are being pursued to provide new energetic materials to meet the challenges of the future. Approaches are the synthesis of all-nitrogen ^[3], nitrogen-rich and nitrogen-oxygen-rich energetic materials. ^[4]

Nitroguanidine, $\text{HN}=\text{C}(\text{NH}_2)\text{NHNO}_2$, was first prepared by Jousselein ^[5] by dissolving guanidine nitrate in concentrated sulfuric acid, when the compound separated upon dilution with water. It is used principally as an ingredient in explosive and propellant formulations. Thiele prepared nitrosoguanidine as well as aminoguanidine, $\text{HN}=\text{C}(\text{NH}_2)\text{NHNH}_2$, by reduction of nitroguanidine. ^[6] The introduction of a one further amino group to nitroguanidine yielding 3-amino-1-nitroguanidine by a hydrazinolysis reaction has the advantage of lowering the pK_B value of 1-amino-3-nitroguanidine ^[7] with respect to nitroguanidine so that it can be protonated in aqueous solution and therefore used as an energetic cation. However, strong

acids are required to protonate it. Due to the presence of the nitro group, the alkaline character of 1-amino-3-nitroguanidine is not as pronounced as for the corresponding 1-aminoguanidine. In this work, we report on the synthesis and characterization of energetic salts and also intermediate compounds of 1-amino-3-nitroguanidine such as the perchlorate (**5**), the dinitramide (**6**), the dinitroguanidinate (**8**) and the nitriminotetrazolate (**9**). All target molecules described herein are summarized in Figure 1.

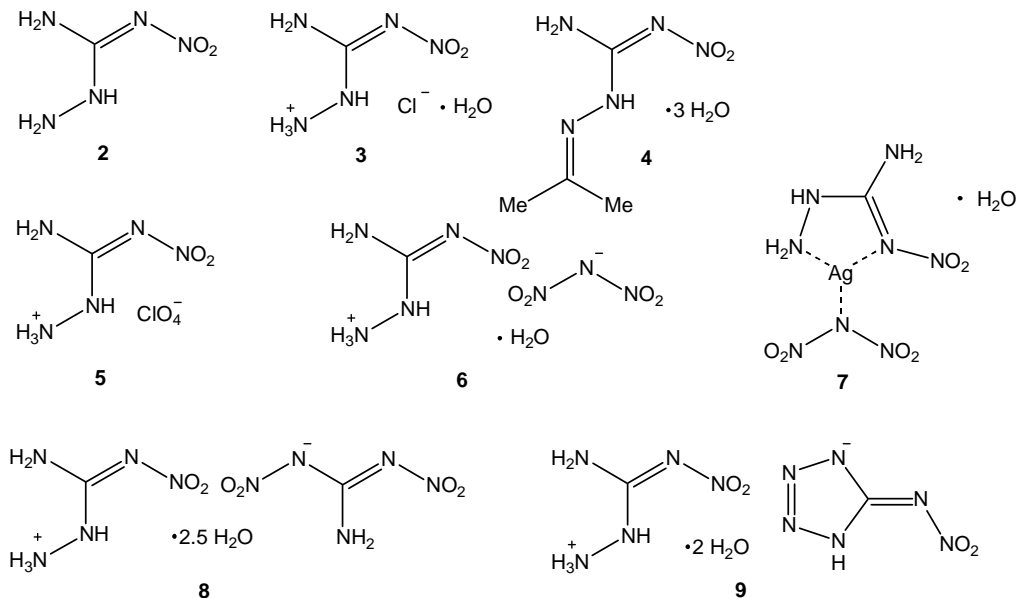
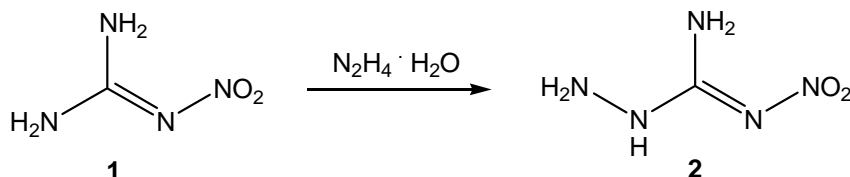


Figure 1: Target molecules 2–9.

2 Results and discussion

a) 1-Amino-3-nitroguanidine (**2**)

Aminonitroguanidine (**2**) was synthesized in aqueous solution employing a hydrazinolysis reaction of commercially available nitroguanidine (**1**), whereas it is important to control the temperature accurately.^[8] The product itself shows fairly poor solubility in water and therefore can be recrystallized from hot water.



Scheme 1. Hydrazinolysis of nitroguanidine

Single crystals were obtained from an acidic aqueous media. **2** crystallizes in the monoclinic space group $P2_1/c$ with 8 molecules in the unit cell. Figure 2 represents half of the

asymmetric unit. The relatively high density of 1.767 g cm^{-3} is a consequence of several strong hydrogen-bonds. **2** crystallizes in a layer like structure, in which the layers are formed by the H-bond modes depicted in Figure 3.

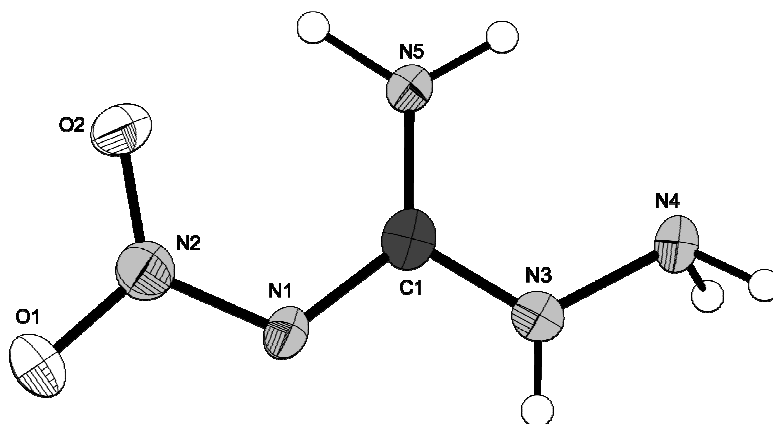


Figure 2: Molecular structure of compound **2**.

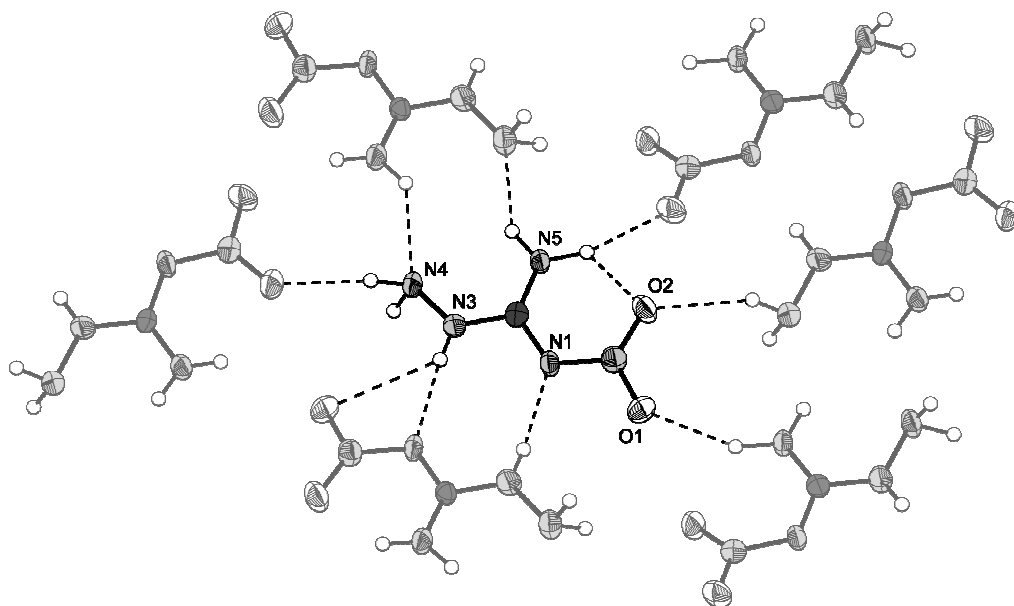
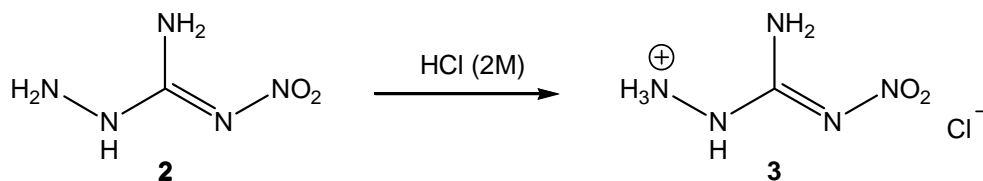


Figure 3: Hydrogen-bonding of one ANG molecule.

b) 1-Amino-3-nitroguanidinium chloride (3**)**

ANG can be protonated by non-oxidizing strong acids such as hydrochloric acid and perchloric acid by the reaction of equimolar amounts at higher temperatures (60°C). The corresponding reaction of ANG with nitric acid yielded 1-nitroguanidine.

1-Amino-3-nitroguanidinium chloride (**3**) was synthesized by simple protonation of the ANG unit with 2M hydrochloric acid. As expected, it is protonated at N3, which is the nitrogen at the hydrazine moiety of **3**.



Scheme 2. Formation of ANG hydrochloride

The hydrochloride **3** was prepared as an intermediate compound on the way to the synthesis of the aminonitroguanidinium dinitramide. It crystallizes with one molecule of water per unit cell. The molecular structure is shown in Figure 3.

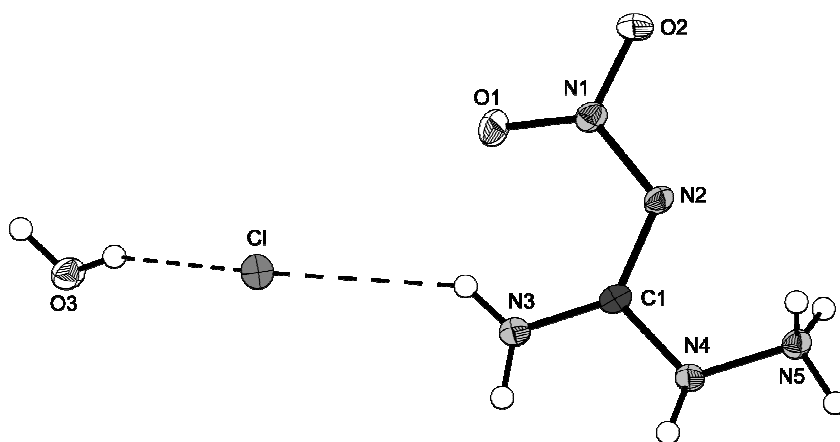
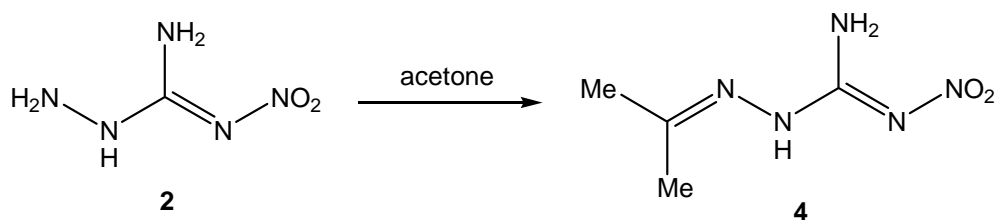


Figure 4: Molecular Structure of compound 3.

c) 1-Amino-3-nitroguanidine-1-isopropylidene hydrazone (4)



Scheme 3. Formation of ANG isopropylidene hydrazone

Recrystallization from polar solvents such as H_2O or wet alcohols containing traces of acetone ended in the formation of hydrazone **4** as its trihydrate. Compound **4** crystallizes in the triclinic space group $P\bar{1}$ with 2 molecules in the unit cell and a lower density of 1.388 g cm^{-3} compared with **2**. The condensation reaction of the hydrazine moiety of **2** with a ketone such as acetone shows the strongly nucleophilic character of aminonitroguanidine. Its molecular structure can be seen in Figure 4.

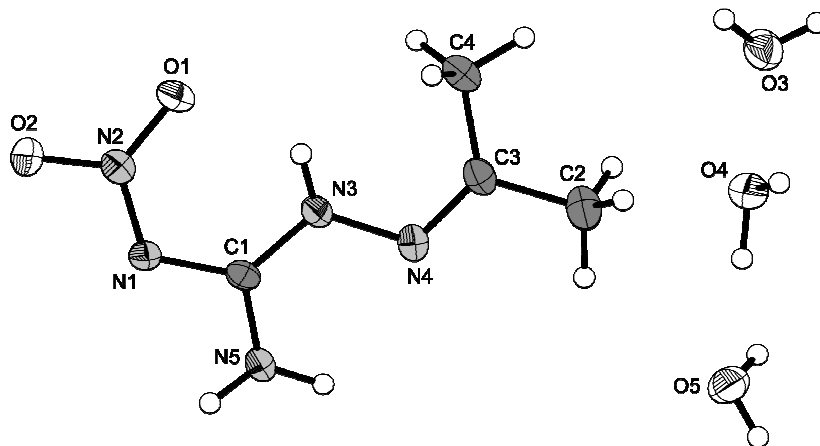
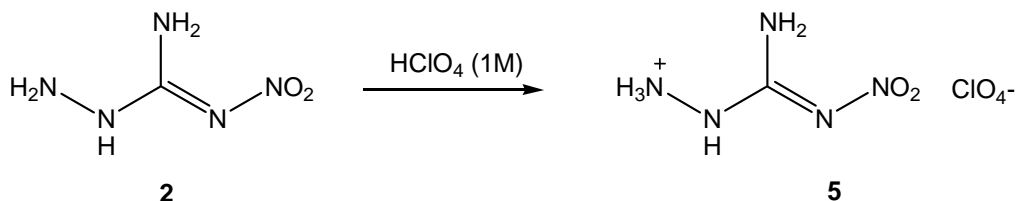


Figure 5: Molecular structure of compound **4**.

d) 1-Amino-3-nitroguanidinium perchlorate (5)

Similar to the synthesis of **3**, also the perchlorate salt **5** was obtained by facile protonation of **2** with dilute perchloric acid in equimolar amounts. Crystals suitable for X-ray measurements were obtained directly from the reaction mixture without any further recrystallization.



Scheme 4. Formation of aminonitroguanidinium perchlorate (**5**)

The molecular structure of **5** is depicted in Figure 5. It is the only aminonitroguanidine containing compound crystallizing without any crystal water so far. Again the structure of the cation is strongly influenced by the intramolecular H-bridge N5–H5a...O2 described by the graph set S(1,1)6. The bond lengths of ANG, **3**, **4** and **5** are listed in Table 1. The bond length show similar values in the neutral as well as in the protonated examples.

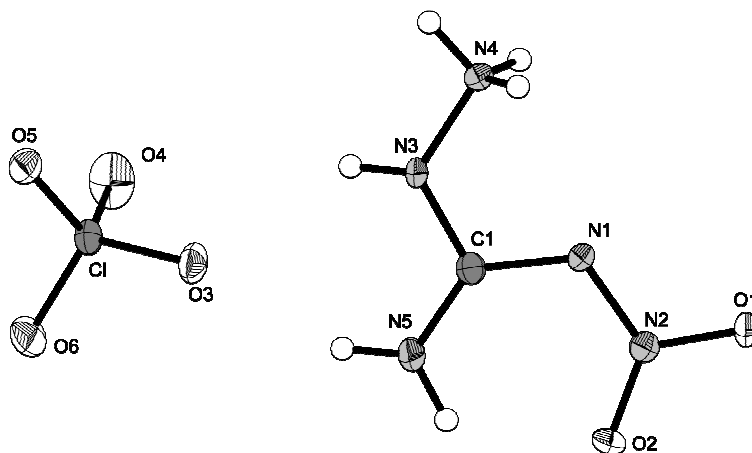


Figure 6: Molecular structure of compound 5.

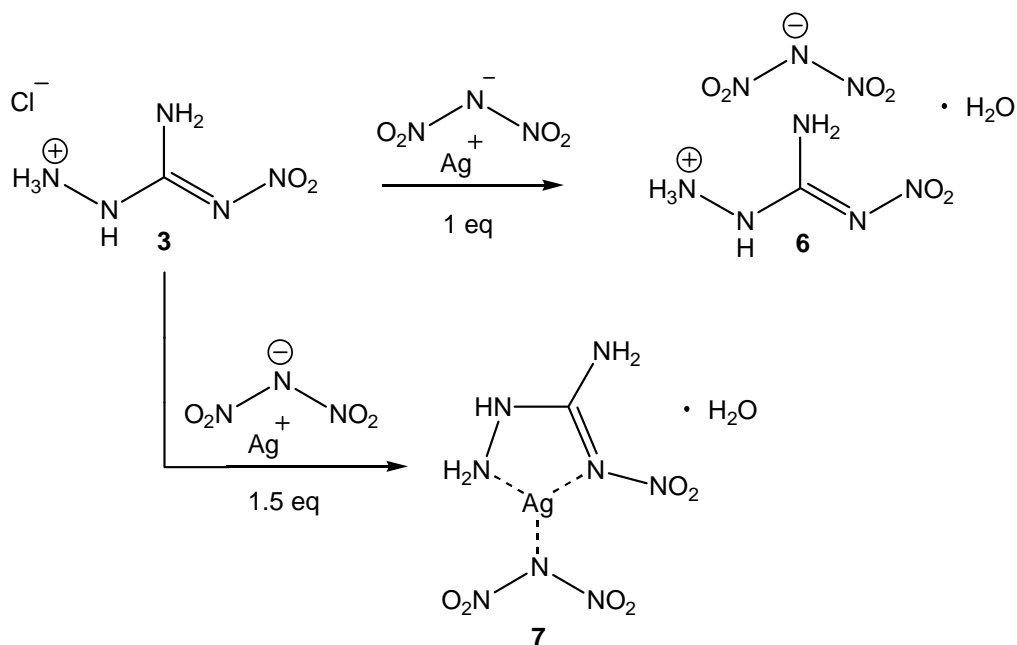
Table 1: Selected bond lengths of compounds 2, 3, 4 and 5

atoms A–B	2	3	4	5
O1–N2	1.242(2)	1.2337(18)	1.2511(17)	1.247(2)
O2–N2	1.238(2)	1.2336(18)	1.2544(16)	1.239(2)
N1–N2	1.333(3)	1.3609(18)	1.3333(18)	1.338(2)
N1–C1	1.356(2)	1.3374(19)	1.3729(14)	1.348(3)
N3–C1	1.303(2)	1.3672(19)	1.3345(18)	1.355(3)
N3–N4	1.410(2)	1.422(2)	1.3943(18)	1.408(2)
N5–C1	1.320(2)	1.317(2)	1.3133(18)	1.306(3)

e) 1-Amino-3-nitroguanidinium dinitramide (6) and silver (1-amino-3-nitroguanidine) dinitramide (7)

Both, compound **6** and the coordination compound **7** were obtained during the reaction of **3** with silver dinitramide. The silver dinitramide was prepared according to literature as acetonitrile adduct, dissolved in very little acetonitrile and then added to an aqueous solution of **3**. First an excess of 1.5 equivalents of silver dinitramide was used resulting in the crystallization of silver dinitramide with the silver cation coordinated to an aminonitroguanidine ligand.

To avoid the inclusion of one equivalent of silver, both, the hydrochloride **3** and silver dinitramide were reacted in equimolar amounts, whereas the silver dinitramide, dissolved in acetonitrile was added dropwise to the solution of **3** in water. To ensure the completeness of the reaction, the mixture was further heated to 35 °C for 2 h under the exclusion of light before being filtered off resulting in the formation of **6**. Both compounds **6** and **7** crystallize with one molecule of water in the unit cell. Their molecular structures are shown in Figure 6 and 7, respectively.



Scheme 5. Formation 3-amino-1-nitroguanidinium dinitramide monohydrate (**6**) and an ANG silver dinitramide complex.

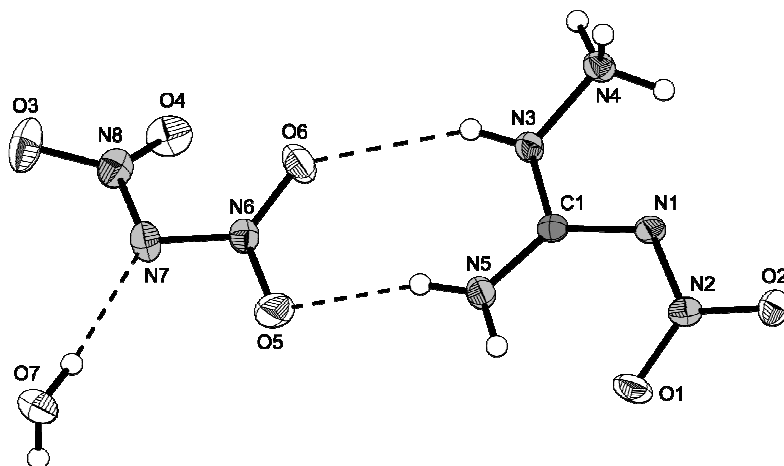


Figure 7: Molecular structure of compound **6**.

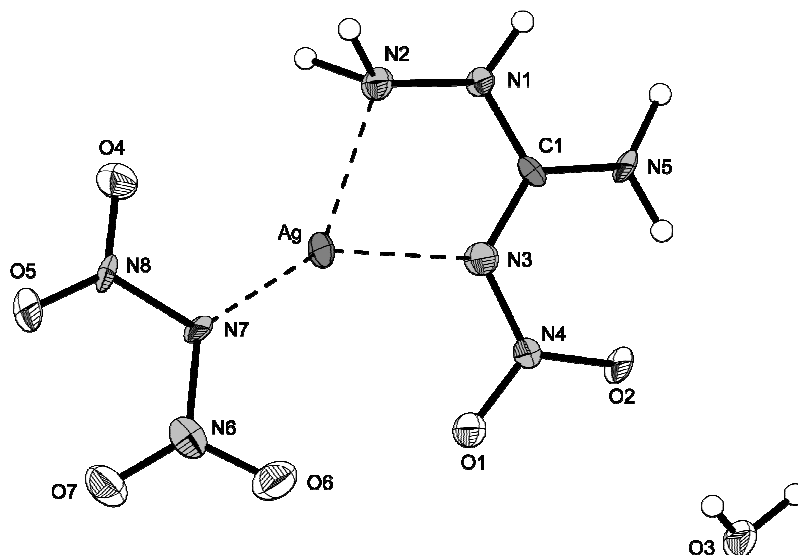
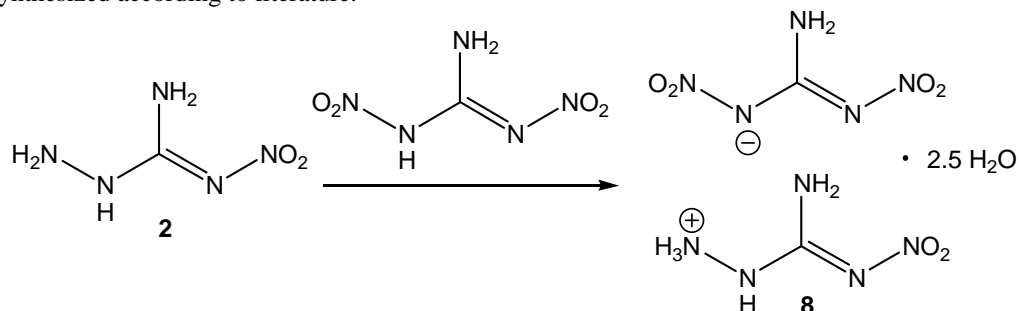


Figure 8: Molecular structure of compound 7.

e) 1-Amino-3-nitroguanidinium dinitroguanidinate (8)

From a facile Brønsted acid base reaction of an aqueous solution of **2** with an aqueous solution of dinitroguanidine the ionic product **8** could be isolated. It crystallizes directly from the reaction mixture with two and a half molecules of water per unit cell. Dinitroguanidine was synthesized according to literature.^[9]



Scheme 6. Protonation of ANG by dinitroguanidine.

Interestingly, the exchange of one amino group in **2** by a nitro group lowers the pK_a value of the compound by a step, which is just large enough to protonate **2** in aqueous solution. The molecular moiety of **8** is depicted in Figure 8.

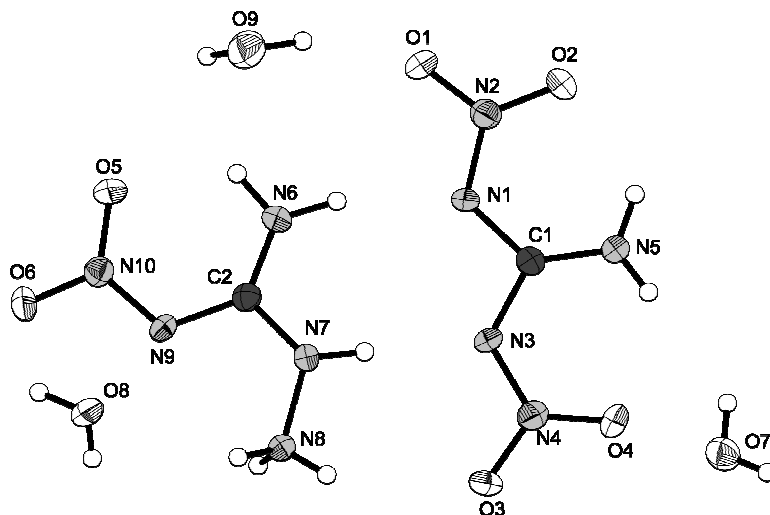
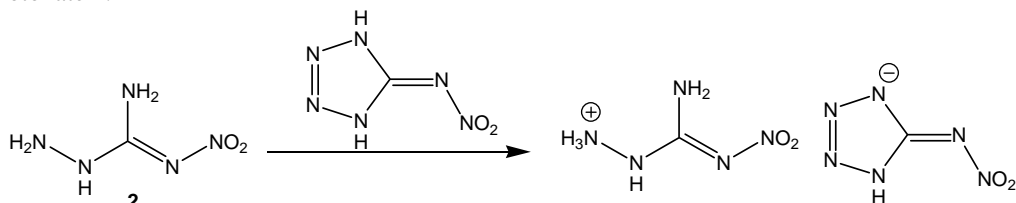


Figure 9: Molecular Structure of compound 8.

f) 1-Amino-3-nitroguanidinium nitriminotetrazolate (9)

5-Nitriminotetrazole shows pK_s values of 2.5 and 6.1 ^[10] and can therefore be used to protonate **2**.



Scheme 7. Formation of 3-amino-1-nitroguanidinium 5-nitriminotetrazolate dihydrate (**9**).

Since the reaction was carried out in aqueous solution, the product again crystallizes containing crystal water. Single crystals were obtained from a water/ethanol mixture. **9** as its dihydrate crystallizes in the monoclinic space group $P2_1/c$ with 4 molecules in the unit cell and a density of 1.726 g cm^{-3} . Its molecular structure is shown in Figure 9.

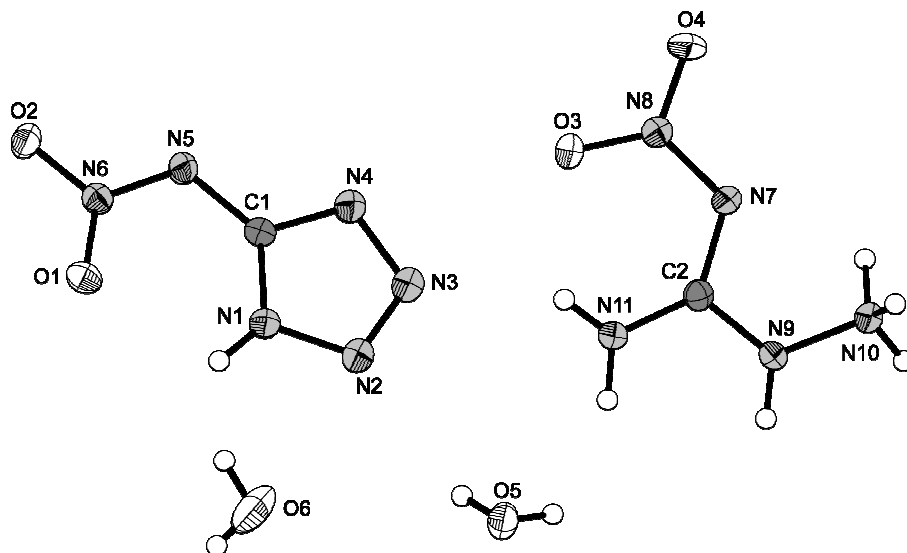


Figure 10: Molecular structure of compound **9**.

2.1 Sensitivities and thermal stability

The impact sensitivity tests were carried out according to STANAG 4489^[11] modified instruction^[12] using a BAM (Bundesanstalt für Materialforschung) drophammer.^[13] The friction sensitivity tests were carried out according to STANAG 4487^[14] modified instruction^[15] using the BAM friction tester. The classification of the tested compounds results from the “UN Recommendations on the Transport of Dangerous Goods”.^[16] Additionally all compounds were tested upon the sensitivity towards electrical discharge using the Electric Spark Tester ESD 2010 EN.^[17] All sensitivities of compounds **2** and **5–9** were determined by the above described procedures. Beside from the silver complex **7** and the perchlorate salt **5**, the impact sensitivities of all the other ANG salts including ANG itself have to be classified as sensitive and are in the range of 5 J (**9**) to 20 J (**2**). As expected the salts **5** and **7** stand out with a very low value of 1 J and 2 J respectively and therefore are classified as very sensitive. Also the friction sensitivity of **5** and **7** are higher (20 N, 7 N) than for the other ANG compounds described. Even without the silver cation, the dinitramide **6** is the most sensitive compound towards friction (40 N, very sensitive), whereas **2**, **8** and **9** show lower sensitivities of 144 N, 288 N and 96 N respectively. Towards electrostatic discharge, the determined sensitivity values do not differ very much. Values can be found from 0.1 J (**6**, **7**) up to 0.4 J (**9**). All sensitivity data as well as decomposition temperatures can be found in Table 2.

Differential scanning calorimetry (DSC) measurements to determine the melt- and decomposition temperatures of **2**, **3** and **5–7** (about 1.5 mg of each energetic material) were performed in covered Al-containers containing a hole in the lid and a nitrogen flow of 20 mL per minute on a Linseis PT 10 DSC^[18] calibrated by standard pure indium and zinc at a heating rate of 5 °C min⁻¹. The most temperature stable of the described energetic materials is the free base ANG itself. It decomposes in a two step mechanism, which could be due to the loss of an amino group first and then decomposition of the remaining nitroguanidine starting at 184 °C and the second step at 200 °C. For the ionic species **5–9** decomposition temperatures are significantly lower ranging from 108 °C (**5–7**) to 136 °C for **9**. Additionally, the loss of crystal water of **6–9** can be observed in the DSC curves as endothermic peaks between 66 °C (**6**) and 79 °C (**8**).

Table 2: Sensitivities and thermal behaviour of 2–9

	IS (J)	FS (N)	ESD (J)	T _{dec} (°C)	T _{dehydr} (°C)
2	20	144	0.15	184	–
5	1	20	0.15	108	–
6	10	40	0.1	108	66
7	2	7	0.1	108	71
8	12	288	0.2	118	79
9	5	96	0.4	136	76

2.2 Detonation Parameters

The detonation parameters were calculated using the program EXPLO5 V5.02.^[19] The program is based on the steady-state model of equilibrium detonation and uses Becker-Kistiakowsky-Wilson's equation of state (BKW E.O.S) for gaseous detonation products and Cowan-Fickett E.O.S. for solid carbon.^[20] The calculation of the equilibrium composition of the detonation products is done by applying modified White, Johnson and Dantzig's free energy minimization technique. The program is designed to enable the calculation of detonation parameters at the CJ point. The BKW equation in the following form was used with the BKWN set of parameters (α , β , κ , θ) as stated below the equations and X_i being the mol fraction of i -th gaseous product, k_i is the molar covolume of the i -th gaseous product.^[21]

$$pV / RT = 1 + x e^{\beta x} \quad x = (\kappa \sum X_i k_i) / [V(T + \theta)]^\alpha$$

$$\alpha = 0.5, \beta = 0.176, \kappa = 14.71, \theta = 6620.$$

The calculations were performed for ANG, its dinitramide monohydrate, the dinitroguanidinate·2.5 H₂O and the nitriminotetrazolate using the maximum densities according to the crystal structures. Additionally the explosion performance parameters of the water free dinitramide assuming the same density as for the monohydrate were calculated. The calculated heats of formation of **6–9** are positive throughout all of the compounds with values ranging from only slightly positive 24.9 kJ mol^{−1} due to the crystal water inclosed. For the dinitramide **6** 365.2 kJ mol^{−1} were calculated, an astonishingly high value, although it is a monohydrate. According to this, the heat of formation for the water free dinitramide is even higher reaching 606.8 kJ mol^{−1}. All calculated values for the heats and energies of formation can be found in Table 3.

Table 3: Calculated heats of formation and energies of formation.

	$\Delta_f H^\circ(s) /$ kcal mol ^{−1}	$\Delta_f H^\circ(s) /$ kJ mol ^{−1}	Δn	$\Delta_f U^\circ(s) /$ kJ mol ^{−1}	M / g mol ^{−1}	$\Delta_f U^\circ(s) /$ kJ kg ^{−1}
ANG (2)	18.4	76.9	−6	91.8	119.11	770.4
6·H₂O	87.2	365.2	−11.5	393.7	244.12	1612.9
6	144.9	606.8	−10	631.6	226.12	2793.2
8·2.5H₂O	6.0	24.9	−16.5	65.8	313.09	210.3
9·2H₂O	18.2	76.0	−14	110.7	285.18	388.2

Having a look at the explosive performance parameters shown in Table 4 the dinitramide **6** stands out with its very high detonation velocity and pressure of 9694 ms^{-1} and 406 kbar for the monohydrate and even higher values for the water free dinitramide of 9840 ms^{-1} and a detonation pressure of 427 kbar due to the high density of 1.85 g cm^{-3} . It reveals an even positive oxygen balance, which gives the possibility of using it in a formulation with a binder for desensitizing it without losing performance. ANG as free base and the dinitroguanidinate **8** show detonation velocities around 9000 ms^{-1} and therefore still perform better than commonly used RDX.

Table 4: Calculated explosive performance parameters using EXPLO5 code.

	ANG	6·H ₂ O	6	8·2.5H ₂ O	9·2H ₂ O
$\rho / \text{g cm}^{-3}$	1.767	1.850	1.850 (est.)	1.705	1.726
$\Omega / \%$	−33.59	6.55	7.08	−13.11	−19.63
$Q_v / \text{kJ kg}^{-1}$	−4934	−7009	−7493	−6133	−5288
T_{ex} / K	3436	4784	5262	4165	3802
P / kbar	323	406	427	335	315
$D / \text{m s}^{-1}$	8977	9694	9840	9084	8787
$V_0 / \text{L kg}^{-1}$	890	874	846	921	894

3 Experimental part

1-Amino-3-nitroguanidine (2)

Commercially available nitroguanidine (25 g, 192 mmol) are dispensed in 250 mL of water and the mixture is heated to 55 °C. Hydrazine hydrate (10.5 mL, 216 mmol) is added dropwise over a period of 15 min and the temperature is kept at 55 °C for further 15 min under constant stirring. After the mixture turned to a clear, orange solution, it is cooled down to room temperature in an ice bath and the reaction is quenched with conc. hydrochloric acid (pH 7). 1-Amino-3-nitroguanidine starts to precipitate after the solution has been cooled down to 4 °C overnight. The product is separated by filtration and recrystallized from hot water. Yield: 10.3 g (86 mmol, 45 %).

DSC (5 °C min^{−1}): 184 °C (dec. 1), 200 °C (dec. 2); IR (KBr, cm^{−1}): $\tilde{\nu}$ = 3551 (s), 3411 (s), 3234 (s), 2025 (w), 1692 (m), 1637 (s), 1616 (vs), 1545 (m), 1502 (m), 1443 (m), 1384 (m), 1329 (m), 1134 (m), 1108 (m), 1088 (m), 1031 (m), 1005 (w), 963 (w), 870 (w), 772 (w), 745 (w), 696 (w), 622 (m), 571 (w), 482 (m); Raman (1064 nm, 200 mW, 25 °C, cm^{−1}): $\tilde{\nu}$ = 3319 (4), 3255 (13), 1659 (5), 1616 (4), 1580 (32), 1381 (13), 1287 (32), 1190 (5), 1111 (39), 1019 (5), 961 (100), 770 (27), 483 (30), 419 (33), 378 (10), 248 (13); ¹H NMR (DMSO-*d*₆, 25 °C, ppm) δ : 9.29 (s, 1H, NH), 8.23 (s, 1H, C–NH_AH_B), 7.52 (s, 1H, C–NH_AH_B), 4.64 (s, 2H, N–NH₂); ¹³C NMR (DMSO-*d*₆, 25 °C, ppm) δ : 161.5 (C(NNO₂)(N₂H₄)(NH₂)); ¹⁵N NMR (DMSO-*d*₆, 25 °C, ppm) δ : −13.3 (NO₂), −146.3 (NNO₂), −276.4 (NH), −301.8 (C–NH₂), −327.9 (N–NH₂); *m/z* (FAB[−]): 117.99 [M–H[−]]; EA (CH₅N₅O₂, 119.08) calc.: C 10.09, H 4.23, N 58.81 %; found: C 10.51, H 4.32, N 58.90 %; BAM drophammer: 20 J; friction tester: 144 N (neg.); ESD: 0.15 J.

1-Amino-3-nitroguanidinium chloride monohydrate (3)

3 was synthesized as an intermediate product for the synthesis of 1-amino-3-nitroguanidinium dinitramide (**6**). Therefore **2** (2.38 g, 20.0 mmol) was suspended in 2M HCl

(10 mL, 20 mmol), the mixture was heated to 60°C and the water was removed in vacuo. The residue was recrystallized from ethanol/water to yield 2.80 g (18.0 mmol, 90 %) of **3** as a white powder.

1-Amino-3-nitroguanidine isopropylidene hydrazone trihydrate (**4**)

4 was crystallized from a reaction vessel containing 1-amino-3-nitroguanidine dissolved in an ethanol/water mixture with a small amount of acetone.

1-Amino-3-nitroguanidinium perchlorate (**5**)

2 (1.19 g, 10 mmol) was dissolved in 1M HClO₄ (20 mL, 20 mmol) under moderate heating to 60°C. **5** crystallizes from the clear solution in colorless blocks. Yield: 4.16 g, 18.9 mmol, 95 %).

DSC (5 °C min⁻¹): 108 °C (dec.); IR (ATR, cm⁻¹): $\tilde{\nu}$ = 3387 (m), 3293 (m), 3084 (m, br), 3008 (m, br), 2891 (m, br), 2753 (m, br), 2686 (m, br), 2168 (w), 1705 (m), 1634 (m), 1559 (m), 1484 (m), 1450 (m), 1373 (m, br), 1270 (m, br), 1089 (vs, br), 1019 (s, br), 930 (s), 785 (m), 687 (w); Raman (1064 nm, 400 mW, 25 °C, cm⁻¹): $\tilde{\nu}$ = 3336 (3), 1623 (6), 1572 (10), 1491 (14), 1264 (28), 1159 (9), 1107 (10), 1038 (4), 1001 (11), 933 (100), 799 (25), 634 (35), 472 (15), 453 (17), 436 (8), 359 (32), 285 (9); ¹H NMR (DMSO-*d*₆, 25 °C, ppm) δ : 9.03 (s, NH-NH₃), 8.37 (s, NH₂); ¹³C NMR (DMSO-*d*₆, 25 °C, ppm) δ : 159.0 (C(NNO₂)(N₂H₃)(NH₂)); m/z (FAB⁺): 120.1 [C(NNO₂)(N₂H₃)(NH₂)+H⁺]; m/z (FAB⁻): 98.9 [ClO₄⁻]; EA (CH₆ClN₅O₆, 219.54): calc.: C 5.47, H 2.75, N 31.90 %; found: C 5.70, H 2.80, N 31.28 %; BAM drophammer: 1 J; friction tester: 20 N (neg.); ESD: 0.15 J.

1-Amino-3-nitroguanidinium dinitramide monohydrate (**6**)

10 mmol of silver dinitramide acetonitrile adduct was prepared according to literature.^[22] 1-amino-3-nitroguanidinium chloride (**3**) (1.47 g, 9.4 mmol) was dissolved in 10 mL of boiling water. After cooling down the solution to about 60°C, the silver dinitramide acetonitrile adduct, dissolved in 5 mL of acetonitrile was added dropwise to the solution. After complete addition, the mixture was stirred under the exclusion of light at 35°C for further 2 h. The mixture was cooled down to 5°C in a fridge and then filtrated. **6** crystallizes from the clear filtrate in colorless blocks. Yield: 1.34 g (5.5 mmol, 59 %).

DSC (5 °C min⁻¹): 66 °C (dehydr.), 108 °C (dec.); IR (ATR, cm⁻¹): $\tilde{\nu}$ = 3535 (w), 3413 (m), 3296 (m), 3121 (m), 2736 (m), 1633 (m), 1579 (m), 1508 (m), 1467 (m), 1429 (m), 1387 (m), 1324 (w), 1265 (m), 1167 (s), 1037 (m), 994 (m), 905 (m), 823 (w), 783 (w), 760 (m), 740 (w); Raman (1064 nm, 400 mW, 25 °C, cm⁻¹): $\tilde{\nu}$ = 3333 (4), 3133 (4), 1574 (24), 1528 (20), 1491 (27), 1426 (17), 1397 (23), 1340 (90), 1331 (84), 1320 (100), 1258 (78), 1199 (19), 1182 (22), 1161 (21), 1105 (6), 1035 (45), 993 (11), 964 (31), 920 (40), 826 (95), 805 (54), 762 (12), 622 (43), 497 (44), 442 (23), 362 (21), 316 (12), 298 (16), 252 (7); ¹H NMR (DMSO-*d*₆, 25 °C, ppm) δ : 8.37 (s, 1H, NH), 6.90 (s, 5H, -NH₂, -NH₃⁺); ¹³C NMR (DMSO-*d*₆, 25 °C, ppm) δ : 159.2 (C(NNO₂)(N₂H₄)(NH₂)); ¹⁴N NMR (DMSO-*d*₆, 25 °C, ppm) δ : -10.2 (N(NO₂)₂), -15.2 (N-NO₂); m/z (FAB⁺): 119.9 [C(NNO₂)(N₂H₃)(NH₂)+H⁺]; m/z (FAB⁻): 106.1 [N(NO₂)₂]; EA (CH₈N₈O₇, 244.12): calc.: C 4.92, H 3.30, N 45.90 %; found: C 4.74, H 3.23, N 44.40 %; BAM drophammer: 10 J; friction tester: 40 N (neg.); ESD: 0.10 J.

Silver (1-amino-3-nitroguanidine) dinitramide monohydrate (7)

The same amount of silver dinitramide (10 mmol) as used for the preparation of **6** was dissolved in little water and a solution of **3** (1.00 g, 6.4 mmol), previously boiled and cooled to 60 °C, was added at once. A white precipitate forms immediately and is filtered off. **7** crystallizes from the filtrate within a few minutes as colorless needles in almost quantitative yield.

DSC (5 °C min⁻¹): 71 °C (dehydr.), 108 °C (dec.); IR (KBr, cm⁻¹): $\tilde{\nu}$ = 3398 (m), 3304 (m), 3218 (m), 1671 (m), 1622 (m), 1580 (m), 1539 (s), 1431 (s), 1344 (m), 1297 (s), 1205 (vs), 1176 (vs), 1108 (w), 1031 (s), 951 (w), 827 (w), 761 (w), 732 (w), 706 (w), 594 (w), 484 (w), 470 (w); Raman (1064 nm, 400 mW, 25 °C, cm⁻¹): $\tilde{\nu}$ = 3330 (13), 3246 (23), 1968 (6), 1616 (10), 1539 (34), 1517 (49), 1466 (14), 1405 (12), 1329 (100), 1263 (61), 1211 (12), 1183 (37), 1116 (8), 992 (38), 975 (40), 929 (55), 829 (69), 801 (39), 757 (10), 746 (12), 727 (6), 629 (57), 592 (14), 471 (37), 443 (18), 386 (38), 305 (25); ¹H NMR (DMSO-*d*₆, 25 °C, ppm) δ : 9.31 (s, 1H, NH), 8.19 (s, 1H, C–NH_AH_B), 7.69 (s, 1H, C–NH_AH_B), 4.76 (s, 2H, N–NH₂), 3.36 (s, 2H, H₂O); ¹³C NMR (DMSO-*d*₆, 25 °C, ppm) δ : 160.9 (C(NNO₂)(N₂H₄)(NH₂)); ¹⁴N NMR (DMSO-*d*₆, 25 °C, ppm) δ : –11.0 (NO₂), –14.5 (NNO₂); *m/z* (FAB⁺): 120.1 [C(NNO₂)(N₂H₃)(NH₂)+H⁺], 107.0 [Ag⁺]; *m/z* (FAB[–]): 106.0 [N(NO₂)₂][–]; EA (AgCH₇N₈O₇, 244.12): calc.: C 3.42, H 2.01, N 31.93 %; found: C 3.31, H 1.80, N 31.61 %; BAM drophammer: 2 J; friction tester: 7 N; ESD: 0.10 J.

1-Amino-3-nitroguanidinium dinitroguanidinate (8)

Dinitroguanidine (1.49 g, 10 mmol) was dissolved in 10 mL of hot water and poured onto neat **2** (1.19 g, 10 mmol). The suspension was heated until no precipitate was observed any more and then filtrated. The filtrate shows evolution of gas and turns to light yellow. A yellow, amorphous precipitate started to form, which was filtered off again. From the mother liquor, **8** precipitates in colorless blocks on standing for a few minutes. Yield: 1.85 g (5.9 mmol, 59%).

DSC (5 °C min⁻¹): 79 °C (dehydr.), 118 °C (dec.); IR (KBr, cm⁻¹): $\tilde{\nu}$ = 3605 (m), 3409 (s), 3377 (s), 3205 (m), 2672 (m), 1619 (s), 1492 (m), 1384 (m), 1357 (m), 1259 (vs), 1218 (vs), 1150 (m), 1112 (m), 1063 (m), 974 (w), 915 (w), 785 (m), 764 (w), 720 (w), 680 (m), 636 (m), 589 (w), 550 (w); Raman (1064 nm, 500 mW, 25 °C, cm⁻¹): $\tilde{\nu}$ = 3440 (5), 3199 (9), 1609 (15), 1578 (15), 1456 (22), 1370 (38), 1310 (5), 1254 (19), 1191 (35), 1154 (100), 1060 (24), 977 (54), 917 (8), 792 (32), 631 (14), 553 (22), 554 (6), 352 (24), 231 (13); ¹H NMR (DMSO-*d*₆, 25 °C, ppm) δ : 9.74 (s), 9.52 (s), 8.59 (s), 8.14 (s), 5.30 (s); ¹³C NMR (DMSO-*d*₆, 25 °C, ppm) δ : 160.3 (C(NNO₂)(N₂H₄)(NH₂)), 159.5 (C(NH₂)(N–NO₂)₂); ¹⁴N NMR (DMSO-*d*₆, 25 °C, ppm) δ : –14.5 (NNO₂), –18.7 (C(NNO₂)₂); *m/z* (FAB⁺): 120.1 [C(NNO₂)(N₂H₃)(NH₂) + H⁺]; *m/z* (FAB[–]): 147.9 [C(NH₂)(N–NO₂)₂][–]; EA (C₂H₁₃N₁₀O_{8.5}, 313.09): calc.: C 7.67, H 4.18, N 44.72 %; found: C 7.90, H 4.20, N 45.43 %; BAM drophammer: 12 J; friction tester: 288 N; ESD: 0.20 J.

1-Amino-3-nitroguanidinium 5-nitriminotetrazolate (9)

2 (1.19 g, 10 mmol) is dissolved in a few milliliters of boiling water. The solution is cooled down to 70 °C and then a solution of 5-nitriminotetrazole (1.63 g, 11 mmol) is added slowly. The solvent is removed in vacuum and the residue recrystallized from an ethanol/water mixture. Yield: 2.17 g (7.6 mmol, 76%).

DSC (5 °C min⁻¹): 136 °C (dec.); IR (KBr, cm⁻¹): $\tilde{\nu}$ = 3358 (vs), 3126 (s), 2939 (s), 2736 (s, br), 1658 (s), 1591 (s), 1531 (s), 1489 (s), 1436 (s), 1384 (s), 1313 (s), 1267 (s), 1210 (s), 1167 (m), 1144 (m), 1117 (m), 1087 (m), 1042 (s), 918 (w), 870 (w), 789 (w), 738 (w), 638 (m), 489 (w), 457 (w); Raman (1064 nm, 300 mW, 25 °C, cm⁻¹): $\tilde{\nu}$ = 3908 (2), 3701 (2), 3355

(3), 3106 (3), 1581 (2), 1534 (100), 1437 (2), 1382 (3), 1315 (25), 1272 (6), 1144 (5), 1030 (34), 1010 (16), 925 (5), 874 (4), 799 (5), 757 (3), 630 (5), 457 (3), 415 (3), 376 (2), 251 (3), 113 (4), 85 (31); ^1H NMR (DMSO- d_6 , 25 °C, ppm) δ : 8.15 (s, NH), 7.13 (NH₂); ^{13}C NMR (DMSO- d_6 , 25 °C, ppm) δ : 160.7 (C(NNO₂)(N₂H₃)(NH₂)), 154.7 (CN₄); m/z (FAB⁺): 120.15 [C(NNO₂)(NH₂)(NHNH₂)+H⁺]; m/z (FAB⁻): 129.1 [HATNO₂⁻]; EA (C₂H₁₁N₁₁O₆, 281.15): calc.: C 8.42, H 3.89, N 54.03 %; found: C 8.51, H 3.85, N 54.01 %; BAM drophammer: 5 J; friction tester: 96 N (neg.); ESD: 0.4 J.

4 Conclusion

From the experimental study of energetic materials based on 1-amino-3-nitroguanidine the following conclusions can be drawn:

- 3-Amino-1-nitroguanidine can be easily prepared by the reaction of 1-nitroguanidine and hydrazine hydrate.
- 1-Amino-3-nitroguanidine can be protonated using moderate to strong non-oxidizing Brønsted acids such as hydrochloric acid, perchloric acid, dinitroguanidine or 5-nitriminotetrazole.
- The hydrochloride of 1-amino-3-nitroguanidine can be utilized in metathesis reactions with silver salts of nitrogen/oxygen rich anions. Here we reported on the synthesis of aminonitroguanidinium dinitramide.
- Upon the easy formation of the isopropylidene hydrazone, which was built in the presence of traces of acetone we could show the very nucleophilic character of 1-amino-3-nitroguanidine.
- The crystal structures of **2–9** were determined using low temperature single crystal diffraction.
- A comprehensive characterization of the physico-chemical properties and sensitivities of **2–9** is given.
- Promising detonation parameters were calculated especially for **6**, although a monohydrate, compared to common explosives like TNT and RDX. The outstanding performance (calculated values: $p_{CJ} = 406$ kbar; $D = 9694$ m s⁻¹) qualifies it for further investigations concerning special military applications.

Acknowledgment

Financial support of this work by the Ludwig-Maximilian University of Munich (LMU), the European Research Office (ERO) of the U.S. Army Research Laboratory (ARL), the Armament Research, Development and Engineering Center (ARDEC) and the Strategic Environmental Research and Development Program (SERDP) under contract nos. W911NF-09-2-0018 (ARL), W911NF-09-1-0120 (ARDEC), W011NF-09-1-0056 (ARDEC) and 10 WPSEED01-002 / WP-1765 (SERDP) is gratefully acknowledged. The authors acknowledge collaborations with Dr. Mila Krupka (OZM Research, Czech Republic) in the development of new testing and evaluation methods for energetic materials and with Dr. Muhamed Sucasca (Brodarski Institute, Croatia) in the development of new computational codes to predict the detonation and propulsion parameters of novel explosives. We are indebted to and thank Drs. Betsy M. Rice and Brad Forch (ARL, Aberdeen, Proving Ground, MD) and Mr. Gary Chen (ARDEC, Picatinny Arsenal, NJ) for many helpful and inspired discussions and support of our work. The authors thank Mr. Stefan Huber for the sensitivity measurements as well as Mr. Alexander Penger and Tom Altenburg for providing DNQ.

References

- [1] a) T. M. Klapötke, in *Moderne Anorganische Chemie*, E. Riedel (Hrsg.), 3. Aufl., Walter de Gruyter, Berlin, New York, **2007**, 99–104. b) R. P. Singh, R. D. Verma, D. T. Meshri, J. M. Shreeve, *Ang. Chem. Int. Ed.* **2006**, 45(22), 3584. c) T. M. Klapötke, in *High Energy Density Materials*, T. M. Klapötke (Hrsg.), Springer, Berlin, Heidelberg, **2007**, 85–122. d) R. D. Chapman, in *High Energy Density Materials*, T. M. Klapötke (Hrsg.), Springer, Berlin, Heidelberg, **2007**, 123–152.
- [2] a) J. Stierstorfer, *dissertation*, Ludwig-Maximilians-Universität München, **2009**, ; b) J. J. Weigand, *dissertation*, Ludwig-Maximilians-Universität München, **2005**; c) <http://www.cup.uni-muenchen.de/ac/klapoetke/index>
- [3] a) M. Tobita, R. J. Bartlett, Structure and Stability of N6 Isomers and Their Spectroscopic Characteristics, *J. Phys. Chem. A* **2001**, 105(16), 4107–4113. b) S. A. Perera, R. J. Bartlett, Coupled-cluster calculations of Raman intensities and their application to N4 and N5. *Chem. Phys. Let.* **1999**, 314(3,4), 381–387. c) W. J. Lauderdale, J. F. Stanton, R. J. Bartlett, Stability and energetics of metastable molecules: tetraazatetrahedrane (N4), hexaazabenzene (N6), and octaazacubane (N8), *J. Phys. Chem.* **1992**, 96(3), 1173–1178. b) T. M. Klapötke, *J. Mol. Struct.* **2000**, 499, 99–104. c) T. M. Klapötke, R. D. Harcourt, *J. Mol. Struct.* **2001**, 541, 237–242.
- [4] a) A. Hammerl, G. Holl, M. Kaiser, T. M. Klapötke, P. Mayer, H. Nöth, H. Piotrowski, M. Suter, New hydrazinium salts of 5,5'- azotetrazolate, *Z. Naturforsch. B*, **2001**, 56(9), 857–870. b) A. Hammerl, G. Holl, M. Kaiser, T. M. Klapötke, P. Mayer, H. Piotrowski, M. Vogt, Martin. Methylated ammonium and hydrazinium salts of 5,5'- azotetrazolate. *Z. Naturforsch. B*, **2001**, 56(9), 847–856.
- [5] a) E.-H. Jousselin, *Compt. rend.* **1879**, 88, 1087; b) G. Pellizzari, *Guzz. chim. ital.* **1891**, 21, 405; c) A. Stettbacher, Nitroguanidine, preparation and properties, *Nitrocellulose* **1936**, 7, 141–145.
- [6] (a) J. Thiele *Liebigs Ann.* **1892**, 270, 1; (b) C. F. Boehringer & Söhne, *J. Chem. Soc.* **1906**, 90, 637; (c) T. Ewan, J. H. J. Young, *J. Soc. Chem. Ind.* **1921**, 40, 109; (d) T. L. Davis, *J. Am. Chem. Soc.* **1922**, 44, 868 ; (e) W. Davis, S. Abrams, *Proc. Am. Acad. Arts Sci.* **1926**, 61, 437.
- [7] R. Phillips, J. F. Williams, *J. Am. Chem. Soc.*, **1928**, 50, 2465–2470
- [8] J. A. Castillo-Meléndez, B. T. Golding, *Synthesis* **2004**, 10, 1655–1663.
- [9] A. A. Astrat'yev, D. V. Dashko, L. L. Kuznetsov, *Russ. J. Org. Chem.* **2003**, 39, 537–548.
- [10] R. M. Herbst, J. A. Garrison, *J. Org. Chem.* **1953**, 18, 941.
- [11] NATO standardization agreement (STANAG) on explosives, impact sensitivity tests, no. 4489, 1st ed., Sept. 17, **1999**.
- [12] WIWEB-Standardarbeitsanweisung 4-5.1.02, Ermittlung der Explosionsgefährlichkeit, hier der Schlagempfindlichkeit mit dem Fallhammer, Nov. 8, **2002**.
- [13] <http://www.bam.de>.
- [14] NATO standardization agreement (STANAG) on explosive, friction sensitivity tests, no. 4487, 1st ed., Aug. 22, **2002**.

- [15] WIWEB-Standardarbeitsanweisung 4-5.1.03, Ermittlung der Explosionsgefährlichkeit oder der Reibeempfindlichkeit mit dem Reibeapparat, Nov. 8, **2002**.
- [16] Impact: insensitive > 40 J, less sensitive g 35 J, sensitive g 4 J, very sensitive e 3 J. Friction: insensitive > 360 N, less sensitive) 360 N, sensitive < 360 N a.> 80 N, very sensitive e 80 N, extremely sensitive e 10 N. According to the UN Recommendations on the Transport of Dangerous Goods, (+) indicates not safe for transport.
- [17] <http://www.ozm.cz>
- [18] <http://www.linseis.com>
- [19] (a) M. Sucasca, EXPLO5.V2, Computer program for calculation of detonation parameters. *Proceedings of the 32nd Int. Annual Conference of ICT*, July 3–6, **2001**, Karlsruhe, Germany, pp 110–111. (b) Sucasca, M. *Proceedings of 30th Int. Annual Conference of ICT*, June 29–July 2, **1999**, Karlsruhe, Germany, 50/1.
- [20] M. Sucasca, *Propellants, Explos., Pyrotech.* **1991**, 16 (4), 197–202.
- [21] M. Sucasca, *Mater. Sci. Forum* **2004**, 465–466, 325–330. (b) Sucasca, M. *Propellants, Explos., Pyrotech.* **1999**, 24, 280–285. (c) Hobbs, M. L.; Baer, M. R. *Proceedings of the 10th Symp. (International) on Detonation*, ONR 33395-12, Boston, MA, July 12–16, **1993**, p 409.
- [22] T. M. Klapötke, B. Krumm, M. Scherr, First structural characterization of solvate-free silver dinitramide, $\text{Ag}[\text{N}(\text{NO}_2)_2]$, *Dalton Transactions* **2008**, 43, 5876–5878.

1-Nitratoethyl-5-nitriminotetrazole derivatives – Shaping future high explosives

Niko Fischer, Thomas M. Klapötke, Jörg Stierstorfer and Karina R. Tarantik

Energetic Materials Research, Department of Chemistry,
University of Munich (LMU), Butenandtstr. 5-13, D-81377, Germany

tmk@cup.uni-muenchen.de

Abstract:

1-(2-Nitratoethyl)-5-nitriminotetrazole (1) was formed by the reaction of 1-(2-hydroxyethyl)-5-aminotetrazole and 100% HNO₃. The former one was obtained by alkylation of 5-amino-1H-tetrazole. The byproduct 1-(2-nitratoethyl)-5-aminotetrazolium nitrate (2) has also been characterized and is compared to compound 1. Nitrogen-rich salts such as ammonium (5), guanidinium (6), aminoguanidinium (7) and triaminoguanidinium (8) 1-(2-nitratoethyl)-5-nitriminotetrazolate were prepared by facile deprotonation or metathesis reactions. Most of the compounds were fully characterized by single crystal X-ray diffraction, vibrational spectroscopy (IR and Raman), multinuclear NMR spectroscopy, elemental analysis and DSC measurements. The heats of formation of 1, 2 and 5–8 were calculated by the atomization method based on CBS-4M enthalpies. With these values and the X-ray densities several detonation parameters such as the detonation pressure, velocity, energy and temperature were computed using the EXPLO5 code. In addition the sensitivities towards impact, friction and electrical discharge were tested using the BAM drop-hammer, a friction tester as well as a small scale electrical discharge device.

Keywords: 1-(2-Nitratoethyl)-5-nitriminotetrazole; High-Explosives; Crystal Structures; Detonation Parameters.

1 Introduction

Tetrazoles have the outstanding property of often combining high nitrogen content and high positive heat of formation with good thermal stability, owing to their aromatic ring system. Of particular interest are tetrazoles, which exhibit energetic nitrogen-oxygen-containing functional groups, such as nitro groups (R–NO₂),^[1, 2] nitrate esters (R–O–NO₂),^[3] or nitramine functionalities (R₂N–NO₂).^[4, 5] Also, the formation of tetrazolium salts with oxygen-rich counter anions such as NO₃[–]^[6, 7] or (NO₂)₂[–]^[8, 9] are the focus of research because these compounds have balanced oxygen contents. 5-Nitriminotetrazoles have been known for a long time, as they can be obtained by facile synthetic routes.^[10] 1-Substituted 5-nitriminotetrazoles, such as 1-methyl-5-nitriminotetrazole and 1-ethyl-5-nitriminotetrazole, were first described in 1957.^[11] Also various N-alkylations of 5-aminotetrazoles, which involve different alkylation reagents such as methyl iodide, dimethyl- and diethyl sulfate and chloroethanol have been known to literature.^[12] Here we report on different reaction products of the nitration of 1-(2-hydroxyethyl)-5-aminotetrazole with nitric acid. Using 65% nitric acid, the 5-aminotetrazole moiety is protonated to give 1-(2-hydroxyethyl)-5-amino-tetrazolium nitrate^[13]. Using 100% nitric acid, three different possible nitration products can be observed, since the amino group in **1** can be nitrated as well as the hydroxyl group in the side chain (Figure 1).

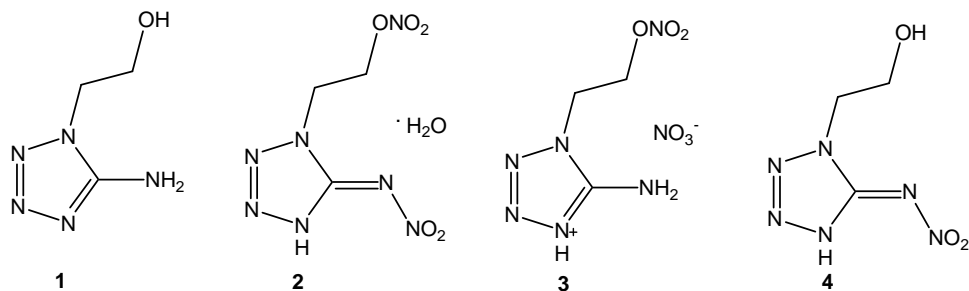


Figure 1: Different products of the reaction of **1** with nitric acid

The focus in this work is the comparison of the energetic properties of two of the above described nitration products (**2** and **3**), which is of special interest as they could be separated as two isomeric forms.

2 Results and discussion

2.1 Synthesis

1 was synthesized reacting the sodium salt of 5-amino-1H-tetrazole with 2-chloroethanol in aqueous solution under reflux conditions. Beside from **1**, also 2-(2-hydroxyethyl)-5-aminotetrazole can be isolated from this reaction^[12]. Treating **1** with fuming nitric acid at 0 °C overnight affords the O-nitrated compound **3** as well as the double N- and O-nitrated product **2**, which have the same formula since **2** crystallizes as a monohydrate. They can be separated from each other by recrystallization due to the different solubility in water. Even a third nitration product, 1-(2-hydroxyethyl)-5-nitriminotetrazole (**4**) could be observed in the reaction mixture and was detected by NMR spectroscopy when less than the required amount of fuming nitric acid was used.

Furthermore four nitrogen rich salts of **2** were synthesized, which are the ammonium (**5**), the guanidinium (**6**), the aminoguanidinium (**7**) and the triaminoguanidinium (**8**) salts. The Lewis structures of **5** - **8** are drawn in Figure 2.

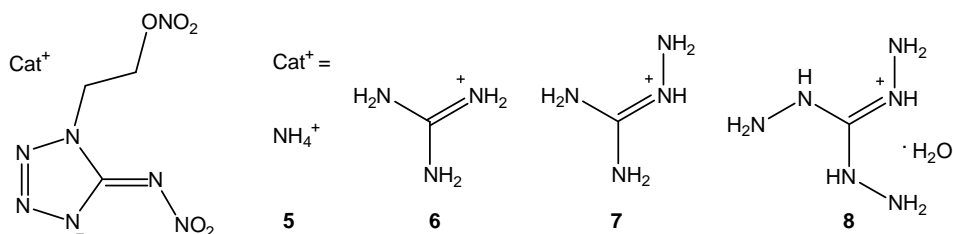


Figure 2: The nitrogen rich salts of **2** presented in this work

The syntheses of **5**–**8** are based on facile acid/base reactions using aqueous ammonia solution, guanidinium carbonate and aminoguanidinium carbonate, respectively. In the case of **6** and **7** they were dissolved in a suspension of **2**, whereas carbon dioxide was expelled by moderate heating to 40°C.

The triaminoguanidinium salt could not be synthesized by a hydrazinolysis reaction of **7** and two equivalents of hydrazine in dioxane, because the hydrazine reduced the nitrate ester moiety and only the triaminoguanidinium salt of **4** could be isolated. Reacting the free acid **2** with the free base triaminoguanidine instead resulted in a successful synthesis of **8**. Free triaminoguanidine was synthesized reacting a suspension of triaminoguanidinium chloride in water under N₂ with 1 equivalent of sodium hydroxide. It separates from the reaction mixture upon addition of DMF as white solid.

2.2 Molecular structures

To determine the molecular structures of **2**, **3** and **5–8** in the crystalline state an Oxford Xcalibur3 diffractometer with a Spellman generator (voltage 50 kV, current 40 mA) and a KappaCCD detector was used. The data collection was performed using the CrysAlis CCD software,^[14] the data reductions with the CrysAlis RED software.^[15] The solution of all structures were performed using SIR-92,^[16] and SHELXS-97,^[17] and SHELXL-97^[18] implemented in the WinGX software package^[19] and finally checked with the PLATON software.^[20] In all crystal structures the hydrogen atoms were located and refined. The absorptions were corrected with the SCALE3 ABSPACK multi-scan method.^[21]

Selected data and parameter of the X-ray determinations are given in Table 1. The data of **2** was adopted from the literature.^[13]

Table 1: X-ray data and parameters.

	2	3	5	6	7	8
Formula	C ₃ H ₇ N ₇ O ₆	C ₃ H ₇ N ₇ O ₆	C ₃ H ₈ N ₈ O ₅	C ₄ H ₁₀ N ₁₀ O ₅	C ₄ H ₁₁ N ₁₁ O ₅	C ₄ H ₁₃ N ₁₃ O ₆
Form. weight [g mol ⁻¹]	237.16	237.16	236.17	278.22	248.25	341.29
Crystal system	Triclinic	Monoclinic	Orthorhombic	Orthorhombic	Monoclinic	Monoclinic
Space Group	<i>P</i> -1	<i>P</i> 2 ₁ / <i>c</i>	<i>P</i> 2 ₁ 2 ₁ 2 ₁	<i>P</i> ca2 ₁	<i>P</i> 2 ₁ / <i>c</i>	<i>C</i> c
Color / Habit	colorless plates	colorless blocks	colorless rods	colorless plates	colorless blocks	colorless block
Size [mm]	0.03 x 0.10 x 0.10	0.35 x 0.25 x 0.20	0.11 x 0.11 x 0.18	0.35 x 0.32 x 0.02	0.25 x 0.20 x 0.10	0.40 x 0.30 x 0.25
<i>a</i> [Å]	6.324(1)	23.499(2)	5.3372(2)	6.4067(4)	4.7075(2)	12.011(5)
<i>b</i> [Å]	7.198(1)	5.5543(5)	7.2473(3)	14.9629(8)	10.7539(4)	7.0212(3)
<i>c</i> [Å]	10.711(2)	14.3477(13)	23.9611(8)	11.3562(5)	22.7782(10)	16.6414(7)
α [°]	82.99(2)	90	90	90	90	90
β [°]	82.73(2)	102.769(9)	90	90	92.757(4)	95.896(4)
γ [°]	66.52(2)	90	90	90	90	90
<i>V</i> [Å ³]	442.22(15)	1826.3(3)	926.82(6)	1088.64(10)	1151.79(8)	1395.98(10)
<i>Z</i>	2	8	4	4	4	4
ρ_{calc} [g cm ⁻³]	1.781	1.725	1.693	1.697	1.691	1.624
μ [mm ⁻¹]	0.168	0.163	0.155	0.151	0.150	0.145
<i>F</i> (000)	244	976	488	576	608	712
$\lambda_{\text{MoK}\alpha}$ [Å]	0.7107(3)	0.7107(3)	0.7107(3)	0.7107(3)	0.7107(3)	0.7107(3)
<i>T</i> [K]	200(2)	200(2)	173(2)	173(2)	173(2)	173(2)
θ Min–Max [°]	4.4, 26.0	3.8, 28.8	4.2, 33.6	4.2, 26.5	4.2, 28.9	4.3, 26.0
Dataset	–7: 7 ; –8:8 ; –13:13	–22: 28 ; –6: 6 ; –17:13	–6:7 ; –10:10 ; –36:36	–4:8 ; –18:16 ; –14:13	–5:5 ; –14:14 ; –30:27	–14:14 ; –8:8 ; –20:20
Reflections collected	4503	7383	7455	2915	8790	9909
Independent reflections	1723	3561	1978	1892	2664	2734
<i>R</i> _{int}	0.040	0.0258	0.045	0.032	0.037	0.025
Observed reflections	1293	2270	1173	1182	1582	2450
Parameters	173	313	177	212	225	268
<i>R</i> ₁ (obs)	0.0658	0.0345	0.0387	0.0360	0.0355	0.0283
<i>wR</i> ₂ (all data)	0.1971	0.0745	0.0786	0.0549	0.0697	0.0659
Goof	1.14	0.88	0.83	0.77	0.82	1.00
Resd. Dens. [e/ Å ³]	–0.61, 1.13	–0.21, 0.21	–0.20, 0.30	–0.19, 0.17	–0.22, 0.18	–0.19, 0.24
Device type	Oxford Xcalibur3 CCD	Oxford Xcalibur3 CCD	Oxford Xcalibur3 CCD	Oxford Xcalibur3 CCD	Oxford Xcalibur3 CCD	Oxford Xcalibur3 CCD
Solution	SIR-92	SIR-92	SHELXS-97	SHELXS-97	SHELXS-97	SHELXS-97
Refinement	SHELXL-97	SHELXL-97	SHELXL-97	SHELXL-97	SHELXL-97	SHELXL-97
Absorption correction	multi-scan	multi-scan	multi-scan	multi-scan	multi-scan	multi-scan

Figure 3 shows the molecular structure of 1-(2-nitratoethyl)-5-nitriminotetrazole monohydrate (**2**), which crystallizes in the triclinic space group $P\bar{1}$. The density is 1.781 g cm^{-3} . This may be a reason of the intensive hydrogen bond network shown in Figure 4.

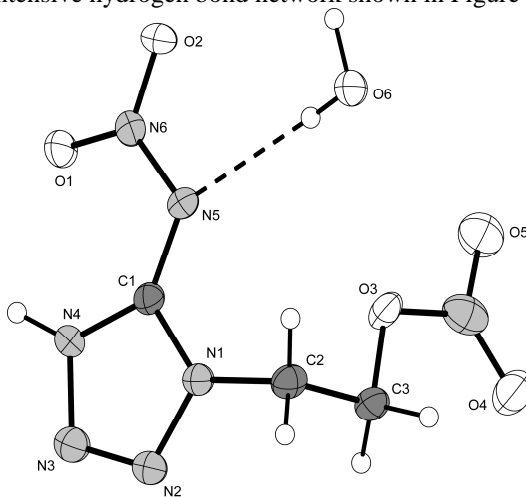


Figure 3: Molecular structure of **2**. Thermal ellipsoids represent the 50% probability level.

All atoms of the crystal water molecules participate in strong H-bond interactions connected to three different 5-nitriminotetrazole moieties, which is shown in Figure 4. Particularly, the formation of $C_1^1(6)$ chains can be observed.

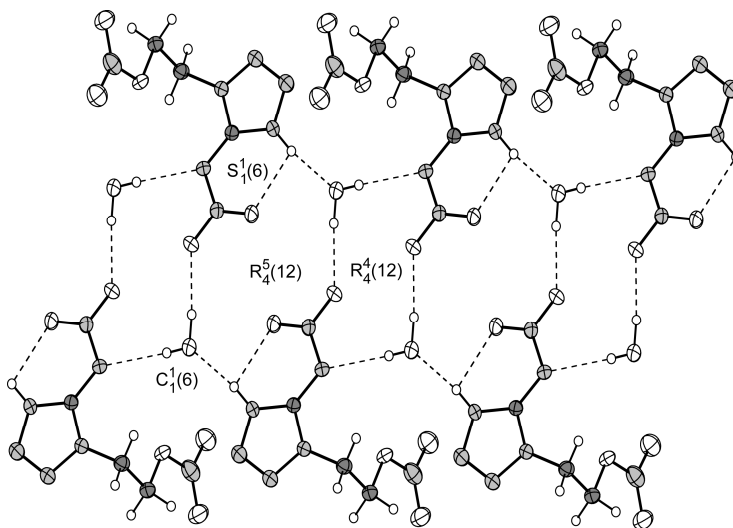


Figure 4: H-bonding in the structure of **2**. Four graph sets are marked. Selected hydrogen bonds (\AA , $^\circ$): $\text{N4-H4}\cdots\text{O6}^{\text{i}} = 0.87(4), 1.81(5), 2.678(4), 170(4)$; $\text{O6-H6A}\cdots\text{N5} = 0.78(6), 2.19(6), 2.946(4), 166(5)$; $\text{O6-H6A}\cdots\text{O2} = 0.78(6), 2.56(5), 3.080(4), 126(4)$; $\text{O6-H6B}\cdots\text{O2}^{\text{ii}} = 0.94(5), 2.01(5), 2.951(4), 174(4)$; (i) $x, -1+y, z$; (ii) $1-x, 1-y, 1-z$.

Crystals of 1-(2-nitratoethyl)-5-aminotetrazolium nitrate (**3**) were obtained from the mother liquor of **2**.

The molecular unit of **3** is depicted in Figure 5. The salt **3** crystallizes in the monoclinic space group $P2_1/c$ with eight molecular units per unit cell. Compared to **2** ($442.2(2) \text{ \AA}^3$) the cell volume of **3** is much larger with $1826.3(3) \text{ \AA}^3$. The calculated density of 1.725 g cm^{-3} of **3** is slightly lower than the one of **2** (1.781 g cm^{-3}).^[13]

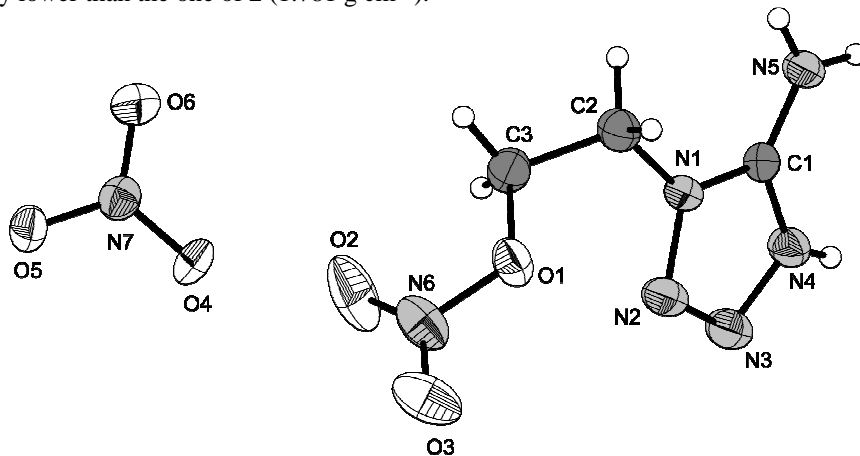


Figure 5: Molecular unit of **3**. Hydrogen atoms shown as spheres of arbitrary radius and ellipsoids are drawn at a 50% probability level.

The bond lengths angles in **2** and **3** are very similar. However, the packing differs. In **2** alternation layers formed by hydrogen bonds and alkyl chain interactions and in **3** layers containing the amine and nitrate moieties connected by hydrogen bonds can be distinguished.

Compounds **5–8** crystallize in the orthorhombic and monoclinic space groups $P2_12_12_1$ (**5**), $Pca2_1$ (**6**), $P2_1/c$ (**7**) and Cc (**8**) with densities lying in a narrow range between 1.624 g cm^{-3} (**8**) to 1.697 g cm^{-3} (**6**) and four molecules in a unit cell for each structure determined. Except from **8**, which crystallizes as monohydrate, all other nitrogen rich salts **5–7** were obtained as water-free compounds.

The five membered ring of the tetrazole moiety reveals planar geometry indicated by the torsion angle $N1-N2-N3-N4 = 0.09(16)^\circ$ in **7** and up to $0.6(3)^\circ$ in **6**. The nitramine unit is slightly twisted out of the tetrazole ring plane in **5** ($N4-C1-N5-N6 = 10.2(3)^\circ$) and **6** ($N4-C1-N5-N6 = -8.9(5)^\circ$), whereas it is sitting almost inside the plane in **7** ($N4-C1-N5-N6 = -1.8(2)^\circ$) and **8** ($N4-C1-N5-N6 = 0.3(3)^\circ$). The bond distances within the anion of **5–8** are comparable to those found in **2**.^[13]

The most interesting difference in the structures of **5–8** is the arrangement of the nitra-toethyl moiety within the asymmetric unit, that can be characterized by the torsion angles $C1-N1-C2-C3$, $N1-C2-C3-O3$ and $C2-C3-O3-N7$. In **6**, **7** and **8** torsion angle $C1-N1-C2-C3$ is positive ($117.9(4)^\circ$, $96.61(18)^\circ$ and $77.4(2)^\circ$) and therefore the nitra-toethyl moiety lies above the tetrazole ring (if $C1-N1-N2-N3-N4$ counted clockwise). In contrast for **5**, the same angle is negative ($-79.2(3)^\circ$) and the nitra-toethyl moiety switched to the other side of the tetrazole ring. Combination of the torsion angles $N1-C2-C3-O3 = 65.89(18)^\circ$ and $C2-C3-O3-N7 = -90.09(16)^\circ$ in **7** leads to a geometry, where the nitrate ester is inclined towards the tetrazole ring, which is not the case for **5**, **6** and **8**.

The ammonium salt **5** is stabilized by various H-bonds between H8a and N4ⁱ [(i) $x, 1+y, z$], H8c and N4, H8c and O2 and H8b and O1. Also the structures of **6**, **7** and **8** is stabilized by hydrogen bonds between the guanidinium hydrogen atoms H8b and H10a and the nitramine oxygen atoms O1 and O2 respectively in **6**. The same argumentation applies to the aminoguanidinium hydrogen atoms in **7**, where H10 has a contact distance to O2 of $d(\text{H10}-\text{O2}^{\text{i}}) = 2.029(15) \text{ \AA}$ [(i) $1+x, y, z$]. The triaminoguanidinium salt is additionally stabilized by hydrogen bonds involving the hydrogen atoms of the crystal water, which are for instance $d(\text{H6a}-\text{N4}^{\text{i}}) = 1.83(4) \text{ \AA}$ [(i) $-1/2+x, 1/2+y, z$] and $d(\text{H6b}-\text{O5}^{\text{ii}}) = 2.16(3) \text{ \AA}$ [(ii) $x, -1+y, z$].

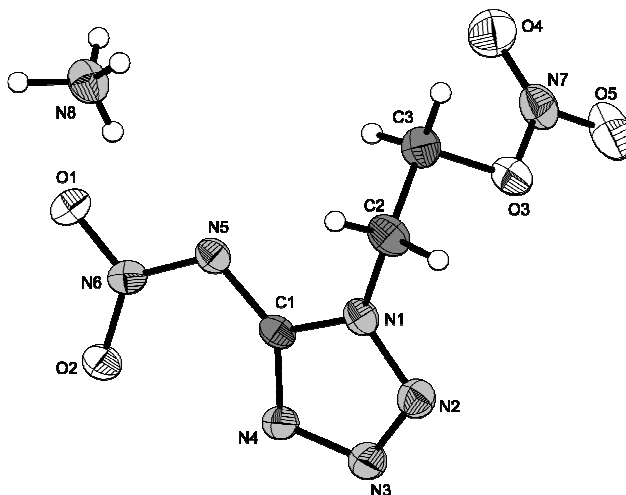


Figure 6: Molecular unit of **5**. Hydrogen atoms shown as spheres of arbitrary radius and thermal displacements set at 50 % probability.

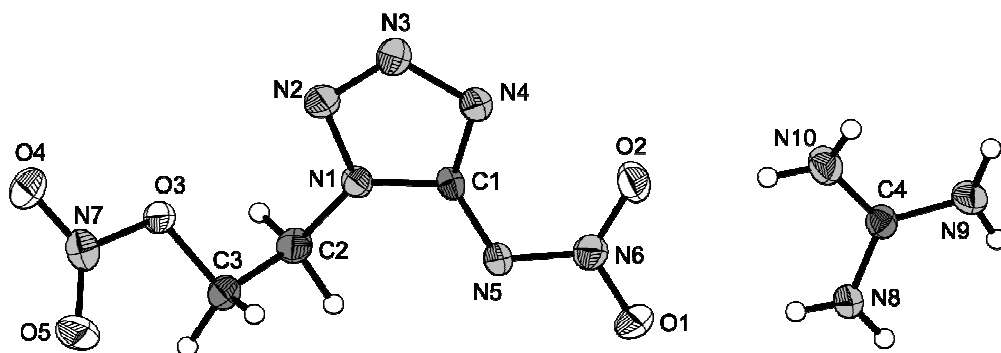


Figure 7: Molecular unit of **6**. Hydrogen atoms shown as spheres of arbitrary radius and thermal displacements set at 50 % probability.

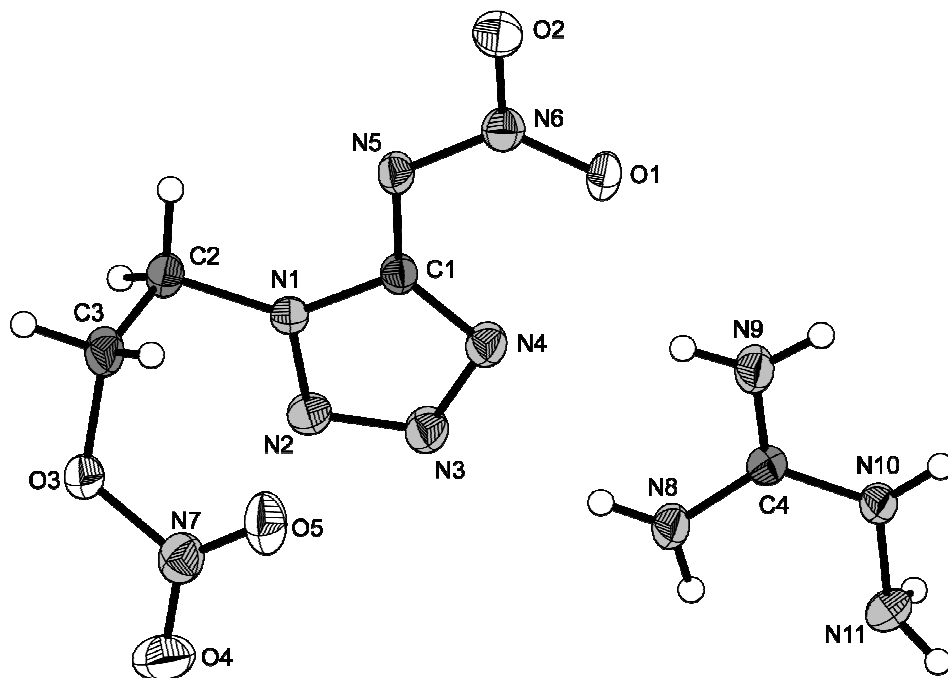


Figure 8: Molecular unit of 7. Hydrogen atoms shown as spheres of arbitrary radius and thermal displacements set at 50 % probability.

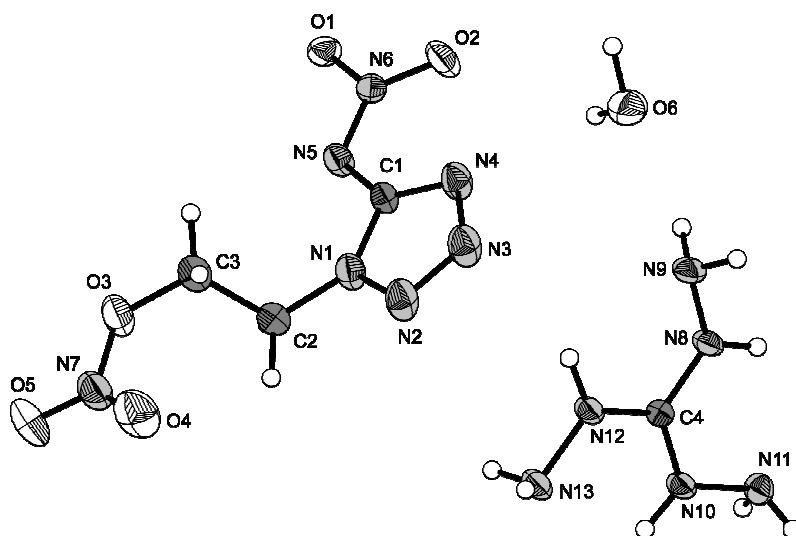


Figure 9: Molecular unit of 8. Hydrogen atoms shown as spheres of arbitrary radius and thermal displacements set at 50 % probability.

2.3 Sensitivities and thermal stability

The impact sensitivity tests were carried out according to STANAG 4489^[22] modified instruction^[23] using a BAM (Bundesanstalt für Materialforschung) drophammer.^[24] The friction sensitivity tests were carried out according to STANAG 4487^[25] modified instruction^[26] using the BAM friction tester. The classification of the tested compounds results from the “UN Recommendations on the Transport of Dangerous Goods”.^[27] Additionally all compounds were tested upon the sensitivity towards electrical discharge using the Electric Spark Tester ESD 2010 EN^[28]. Differential scanning calorimetry (DSC) measurements to determine the melt- and decomposition temperatures of **2**, **3** and **5–7** (about 1.5 mg of each energetic material) were performed in covered Al-containers containing a hole in the lid and a nitrogen flow of 20 mL per minute on a Linseis PT 10 DSC^[29] calibrated by standard pure indium and zinc at a heating rate of 5°C min⁻¹.

The free acid **2** and nitrate salt **3** have to be classified as sensitive towards impact. The determined values are 25 J (**2**) and 10 J (**3**), respectively. Against expectations **2** is only less sensitive towards friction (360 N), whereas the nitrate salt shows similar sensitivity to the nitrogen rich salts **6**, **7** and **8** and is classified as sensitive (160 N). The nitrogen rich salts **5**, **6**, **7** and **8** reveal impact sensitivities with values of 10 J (**5**), 7 J (**6**), 5 J (**7**) and 10 J (**8**). Upon the UN Recommendations on the Transport of Dangerous Goods” they have to be classified as sensitive. The same applies to the friction sensitivities with values of 120 N (**6**), 108 N (**7**) and 96 N (**8**). Only the ammonium salt reveals a value (240 N) higher than that of **6**, **7** and **8**. No general trend in sensitivities can be observed here, which is due to the relatively low values in the very lower range of the scale. Sensitivities towards electrical discharge are scattered over a relatively small area of 0.1 J (**7**) to 0.15 J (**6**, **8**) and 0.35 J (**5**). Generally speaking, the ammonium salt is the least sensitive of the nitrogen rich salts having also the lowest nitrogen content of the four compounds **5–8**. It also has the highest decomposition temperature (180°C) making it the favoured compound in possible applications as high explosive.

For **5–8** the decomposition temperatures show a trend often observed for high nitrogen compounds: The higher the nitrogen content, the lower the decomposition temperature. For the remaining salts they can be found between 130°C (**8**) and 160°C (**6**) with the diaminoguanidinium salt in between (150°C). As expected the decomposition temperature of the neutral 1-(2-nitratoethyl)-5-nitriminotetrazole (**2**) can be found below the ones for its ionic correspondents (128°C). Also the nitrate salt **3** decomposes at a relatively low temperature of 137°C. None of the described compounds has a large liquidity range as decomposition starts immediately after melting. For **8**, no melting point could be detected, however, it can be dehydrated at 54°C.

2.4 Detonation parameters

The detonation parameters were calculated using the program EXPLO5 V5.02.^[30] The program is based on the steady-state model of equilibrium detonation and uses Becker-Kistiakowsky-Wilson’s equation of state (BKW E.O.S) for gaseous detonation products and Cowan-Fickett E.O.S. for solid carbon.^[31] The calculation of the equilibrium composition of the detonation products is done by applying modified White, Johnson and Dantzig’s free energy minimization technique. The program is designed to enable the calculation of detonation parameters at the CJ point. The BKW equation in the following form was used with the BKWN set of parameters (α , β , κ , θ) as stated below the equations and X_i being the mol fraction of i -th gaseous product, k_i is the molar covolume of the i -th gaseous product:^[32]

$$pV / RT = 1 + x e^{\beta x} \quad x = (\kappa \sum X_i k_i) / [V (T + \theta)]^\alpha$$

$$\alpha = 0.5, \beta = 0.176, \kappa = 14.71, \theta = 6620.$$

The calculations were performed using the maximum densities according to the crystal structures.

Not only the lowest sensitivity data but also regarding the detonation velocities pressures, the ammonium salt ($v_d = 8460 \text{ ms}^{-1}$, $p_d = 287 \text{ kbar}$) is the favourite compound amongst **5–8** as it has the least negative oxygen balance. The detonation velocities and pressures of the isomers **2** and **3** are higher, than the one discussed above. Directly compared to each other, the molar energy of formation is higher for the nitrate salt (78 kJ mol^{-1}), than for the nitramine monohydrate (-24 kJ mol^{-1}) due to the strongly negative term for the formation of one equivalent of water. Therefore also the explosion energy and the detonation temperature are higher for **3**. Detonation velocities of **2** and **3** are in the same range of about 8700 ms^{-1} . Compared to the free acid **2**, the detonation parameters of **6–8** exhibit fairly bad values of 8139 ms^{-1} (**6**) to 8402 ms^{-1} (**8**) for the detonation velocity and 265 kbar (**6**) to 276 kbar (**7**) for the detonation pressure. Also the detonation temperatures of **6–8** are significantly lower (around 3600 K) compared to those of **2**, **3** and **5**. All sensitivities, as well as physical properties and detonation parameters of **2**, **3** and **5–8** are summarized in Table 2.

Table 2: Explosive and detonation parameters.

	2	3	5	6	7	8	RDX
Formula	$\text{C}_3\text{H}_7\text{N}_7\text{O}_6$	$\text{C}_3\text{H}_7\text{N}_7\text{O}_6$	$\text{C}_3\text{H}_8\text{N}_8\text{O}_5$	$\text{C}_4\text{H}_{10}\text{N}_{10}\text{O}_5$	$\text{C}_4\text{H}_{11}\text{N}_{11}\text{O}_5$	$\text{C}_4\text{H}_{13}\text{N}_{13}\text{O}_6$	$\text{C}_3\text{H}_7\text{N}_7\text{O}_6$
FW / g mol ⁻¹	237.16	237.16	236.14	278.19	293.20	341.25	222.12
IS / J	25	10	10	7	5	10	7.5
FS / N	360	160	240	120	108	96	120
ESD / J	0.25	0.40	0.35	0.15	0.10	0.15	0.1–0.2
N / %	44.75	41.35	47.45	50.35	52.55	53.36	37.8
Ω / %	-23.61	-23.61	-33.87	-46.01	-46.38	-44.54	-21.6
T _{Dec.} / °C	128	137	180	160	150	130	210
ρ / g cm ⁻³	1.781	1.725	1.692	1.697	1.691	1.624	1.80
Δ _f H _m ^o / kJ mol ⁻¹	-24	78	204	160	267	251	70
Δ _f U ^o / kJ kg ⁻¹	4	432	974	688	1024	855	417
EXPLOS values:							
-Δ _{Ex} U ^o / kJ kg ⁻¹	5415	5783	5712	4949	5143	5197	6038
T _{det} / K	4000	4208	4022	3546	3610	3540	4368
P _{CJ} / kbar	321	307	287	265	276	268	341
V _{Det.} / m s ⁻¹	8712	8637	8460	8139	8327	8402	8906
V _o / L kg ⁻¹	807	815	828	811	824	870	793

3 Experimental part

3.1 1-(2-Nitratoethyl)-5-nitriminotetrazole monohydrate (**2**)

To a cooled solution of nitric acid (20 mL, 100%) was added portion wise 1-(2-hydroxyethyl)-5-aminotetrazole (**1**) (25 mmol). The solution was stirred for 12 h at room temperature and then poured onto ice. The solvent was removed under high vacuum to obtain the crude product, which was washed until it became free of acid. Recrystallization from very dilute HNO_3 gave colorless **2** (2.46 g, 45% yield).

DSC ($5 \text{ }^\circ\text{C min}^{-1}$, $^\circ\text{C}$): 128°C (dec.); IR (KBr, cm^{-1}): $\tilde{\nu} = 3571$ (m), 3374 (s, br), 3127 (s, br), 3016 (s), 2961 (s), 2648 (m), 2067 (w), 1690 (m), 1643 (s), 1583 (s), 1496 (s), 1448 (s), 1384 (s), 1312 (s), 1283 (s), 1250 (s), 1141 (m), 1031 (s), 978 (m), 892 (m), 846 (m), 779 (m), 755 (m), 720 (m), 678 (w), 649 (w), 579 (vw), 565 (vw), 543 (vw), 522 (vw), 504 (vw); Raman (1064 nm , 200 mW , $25 \text{ }^\circ\text{C}$, cm^{-1}): $\tilde{\nu} = 3020$ (31), 2979 (69), 1621 (26), 1584 (100), 1508 (39), 1452 (43), 1422 (86), 1316 (38), 1279 (75), 1263 (78), 1247 (70), 1159 (21), 1084 (25), 1038

(56), 996 (40), 881 (37), 849 (31), 758 (92), 706 (25), 662 (38), 567 (33), 493 (48), 446 (26), 353 (32), 312 (55), 237 (41), 209 (37), 175 (42); ^1H NMR (DMSO- d_6 , 25 °C, ppm) δ : 8.18 (s, 1H, NH), 4.88 (t, $^3J = 5$ Hz, 2H, CH_2), 3.76 (t, $^3J = 5$ Hz, 2H, CH_2); ^{13}C NMR (DMSO- d_6 , 25 °C, ppm) δ : 151.1 (CN_4), 48.7 (CH_2), 41.6 (CH_2); EA ($\text{C}_3\text{H}_5\text{N}_7\text{O}_4$, 219.12): calc.: C 16.44, H 2.30, N 44.75 %; found: C 16.31, H 2.62, N 44.55; BAM drophammer: 25 J; friction tester: 360 N (neg.); ESD: 0.25 J.

3.2 1-(2-Nitratoethyl)-5-aminotetrazolium nitrate (3)

This compound was obtained during the reaction of 1-(2-hydroxyethyl)-5-aminotetrazole with nitric acid (100 %). It is a byproduct in the synthesis of 1-(2-nitratoethyl)-5-nitriminotetrazole monohydrate (2) and could be isolated from the mother liquor of the recrystallization of 2. Yield: 8 %.

DSC (5 °C min^{-1} , °C): 137°C (dec.); IR (ATR, cm^{-1}): $\tilde{\nu} = 3347$ (m), 3158 (w), 2920 (m), 2853 (w), 2363 (m), 2337 (w), 1690 (m), 1636 (s), 1581 (m), 1548 (w), 1532 (w), 1493 (m), 1447 (m), 1407 (m), 1372 (m), 1341 (m), 1310 (m), 1283 (s), 1241 (m), 1145 (vw), 1060 (w), 1042 (w), 1018 (w), 976 (w), 946 (vw), 894 (w), 871 (w), 852 (w), 843 (w), 778 (vw), 756 (w), 724 (w), 672 (vw), 625 (w); Raman (1064 nm, 200 mW, 25 °C, cm^{-1}): $\tilde{\nu} = 3243$ (4), 3031 (17), 2982 (41), 2966 (19), 1684 (6), 1638 (9), 1598 (7), 1562 (3), 1503 (10), 1455 (13), 1433 (12), 1380 (14), 1290 (18), 1228 (5), 1144 (5), 1048 (100), 950 (5), 860 (7), 845 (17), 768 (38), 717 (12), 673 (9), 639 (10), 571 (19), 535 (4), 493 (4), 444 (7), 414 (8), 333 (6), 306 (5), 284 (5), 248 (8), 208 (5). ^1H NMR (DMSO- d_6 , 25 °C, ppm) δ : 8.76 (s, 2H, NH_2), 4.86 (t, $^3J = 4.9$ Hz, 2H, CH_2), 4.51 (t, $^3J = 4.9$ Hz, 2H, CH_2). ^{13}C NMR (DMSO- d_6 , 25 °C, ppm) δ : 167.6 (CN_4), 59.5 (CH_2ONO_2), 55.3 (NCH_2). ^{14}N NMR (DMSO- d_6 , 25 °C, ppm) δ : -15 (NNO_2), -44 (ONNO_2). ^{15}N NMR (DMSO- d_6 , 25 °C, ppm) δ : -5.7 (N3), -14.8 (NO_3), -25.5 (N2 , $^3J(^1\text{H}, ^{15}\text{N}) = 1.6$ Hz), -43.6 (t, ONO_2 , $^3J(^1\text{H}, ^{15}\text{N}) = 3.3$ Hz), -116.5 (N4), -180.7 (N1), -332.7 (N5). EA ($\text{C}_3\text{H}_7\text{N}_7\text{O}_6$, 237.13): calc.: C 15.20; H 2.98; N 41.35 %; found: C 15.08; H 3.24; N 41.32 %. BAM drophammer: 10 J; friction tester: 160 N; ESD: 0.40 J.

3.3 Guanidinium 1-(2-nitratoethyl)-5-nitriminotetrazolate (6)

1-(2-Nitratoethyl)-5-nitriminotetrazole monohydrate (2.37 g, 10 mmol) is suspended in a few milliliters of water and a suspension of guanidinium carbonate (0.90 g, 5 mmol) in water is added slowly. The mixture is heated to 40°C and then filtrated. The solvent is removed in vacuum and the residue recrystallized from water/ethanol. Yield: 2.10 g (7.55 mmol, 76%).

DSC (5 °C min^{-1} , °C): 160°C (dec.); IR (KBr, cm^{-1}): $\tilde{\nu} = 3552$ (s), 3400 (s), 3238 (m), 3169 (s), 2891 (w), 2298 (w), 2049 (m), 1974 (w), 1666 (vs), 1619 (vs), 1496 (s), 1446 (s), 1427 (m), 1373 (s), 1303 (s), 1283 (s), 1265 (s), 1170 (m), 1117 (m), 1040 (m), 1028 (m), 995 (m), 907 (m), 878 (m), 861 (m), 776 (m), 759 (m), 739 (w), 714 (m), 673 (w), 620 (m), 576 (w), 543 (w), 519 (w), 503 (w), 479 (w); Raman (1064 nm, 200 mW, 25 °C, cm^{-1}): $\tilde{\nu} = 3009$ (4), 2972 (8), 1510 (100), 1373 (3), 1340 (20), 1274 (7), 1162 (4), 1110 (14), 1066 (4), 1034 (49), 993 (6), 974 (7), 895 (4), 845 (6), 745 (12), 629 (5), 582 (8), 506 (4), 489 (3), 439 (4), 385 (3), 258 (9); ^1H NMR (DMSO- d_6 , 25 °C, ppm) δ : 6.94 (s, 6H, NH_2), 4.87 (t, 2H, CH_2), 4.45 (t, 2H, CH_2); ^{13}C NMR (DMSO- d_6 , 25 °C, ppm) δ : 158.4 (C_{Gua}), 157.7 (CN_4), 70.8 (CH_2ONO_2), 43.7 (CH_2N); m/z (FAB^+): 60.1 [$\text{C}(\text{NH}_2)_3^+$]; m/z (FAB^-): 218.0 [$\text{EtONO}_2\text{ATNO}_2$]; EA ($\text{C}_3\text{H}_9\text{N}_9\text{O}_2$, 203.16): calc.: C 17.27, H 3.62, N 50.35 %; found: C 17.59, H 3.81, N 50.07 %; BAM drophammer: 7 J; friction tester: 120 N (neg.); ESD: >0.15 J.

3.4 Aminoguanidinium-2-methyl-5-nitriminotetrazolate (7)

1-(2-Nitratoethyl)-5-nitriminotetrazole monohydrate (2.37 g, 10 mmol) is suspended in a few milliliters of water and a suspension of aminoguanidinium bicarbonate (1.36 g, 10 mmol)

in water is added slowly. The mixture is heated to 40°C and then filtrated. The solvent is removed in vacuum and the residue recrystallized from water/ethanol. Yield: 2.25 g (7.68 mmol, 77%).

DSC (5 °C min⁻¹, °C): 150°C (dec.); IR (KBr, cm⁻¹): $\tilde{\nu}$ = 3930 (w), 3552 (s), 3415 (vs, br), 3168 (s), 3007 (m), 2970 (m), 2893 (m), 2139 (m), 1864 (w), 1777 (m), 1632 (vs), 1545 (m), 1509 (s), 1453 (s), 1428 (s), 1414 (m), 1368 (s), 1338 (s), 1283 (s), 1233 (s), 1108 (s), 1064 (m), 1032 (s), 1011 (s), 935 (m), 895 (m), 877 (s), 844 (s), 773 (m), 742 (m), 704 (w), 676 (s), 607 (s), 488 (s); Raman (1064 nm, 200 mW, 25 °C, cm⁻¹): $\tilde{\nu}$ = 3009 (4), 2972 (8), 1510 (100), 1372 (4), 1341 (20), 1275 (6), 1161 (3), 1111 (14), 1065 (3), 1034 (49), 993 (5), 974 (8), 845 (6), 745 (11), 630 (5), 583 (7), 590 (4), 540 (4), 385 (3), 258 (9), 201 (4); ¹H NMR (DMSO-*d*₆, 25 °C, ppm) δ : 8.58 (s, 1H, C_{AG}NH), 7.25 (s, 2H, C_{AG}(NHH)₂), 6.77 (s, 2H, C_{AG}(NHH)₂), 4.87 (t, 2H, CH₂ONO₂), 4.70 (s, 2H, NNH₂), 4.45 (t, 2H, NCH₂); ¹³C NMR (DMSO-*d*₆, 25 °C, ppm) δ : 158.3 (C_{Gau}), 157.7 (CN₄), 70.8 (CH₂ONO₂), 43.7 (CH₂N); m/z (FAB⁺): 75.1 [C(NHNH₂)(NH₂)₂⁺]; m/z (FAB⁻): 217.9 [EtONO₂ATNO₂]; EA (C₃H₁₀N₁₀O₂, 218.18): calc.: C 16.39, H 3.78, N 52.55 %; found: C 16.63, H 4.00, N 52.07 %; BAM drophammer: 5 J; friction tester: 108 N (neg.); ESD: 0.1 J.

3.5 Triaminoguanidinium 1-(2-nitratoethyl)-5-nitriminotetrazolate (8)

In a 100 mL schlenk flask triaminoguanidinium chloride (4.64 g, 33 mmol) is suspended in 6 mL of water under nitrogen. Sodium hydroxide (1.32 g, 33 mmol), previously dissolved in 4 mL of water, is added. After all triaminoguanidinium chloride has been dissolved, 20 mL of N,N'-dimethylformamide is added and the mixture is cooled in an ice bath, where triaminoguanidine starts to precipitate. It is isolated in a schlenk frit and transferred (1.04 g, 10 mmol) to a flask containing a suspension of 1-(2-Nitratoethyl)-5-nitriminotetrazole (2.37 g, 10 mmol) as a suspension in 10 mL of water. The mixture is stirred until clear, filtrated and the solvent removed in vacuo. After 7 crystallized from the solution, it was filtered off, washed with cold ethanol and diethyl ether and dried.

DSC (5 °C min⁻¹, °C): 54°C (dehydr.), 130°C (dec.); IR (KBr, cm⁻¹): $\tilde{\nu}$ = 3923 (w), 3644 (m), 3340 (s), 3320 (s), 3212 (s), 2348 (w), 1685 (vs), 1636 (s), 1507 (s), 1457 (m), 1433 (m), 1388 (m), 1330 (s), 1281 (s), 1204 (m), 1182 (m), 1129 (m), 1105 (m), 1057 (m), 998 (m), 979 (m), 954 (m), 888 (m), 861 (m), 772 (w), 755 (w), 741 (w), 654 (m), 640 (m), 608 (m), 556 (m); Raman (1064 nm, 500 mW, 25 °C, cm⁻¹): $\tilde{\nu}$ = 3340 (11), 3295 (14), 3244 (14), 3013 (5), 2970 (15), 1685 (4), 1633 (3), 1561 (2), 1505 (100), 1436 (4), 1394 (4), 1339 (19), 1278 (11), 1107 (9), 1060 (8), 1030 (43), 975 (2), 892 (10), 744 (8), 609 (2), 492 (7), 265 (6); ¹H NMR (DMSO-*d*₆, 25 °C, ppm) δ : 8.55 (s, 3H, C_{TAG}NH), 4.83 (t, 2H, CH₂ONO₂), 4.45 (s, 6H, NNH₂), 4.41 (t, 2H, NCH₂); ¹³C NMR (DMSO-*d*₆, 25 °C, ppm) δ : 159.1 (C_{TAG}), 157.2 (CN₄), 70.3 (CH₂ONO₂), 43.2 (CH₂N); m/z (FAB⁺): 105.1 [C(NHNH₂)₃⁺]; m/z (FAB⁻): 218.0 [EtONO₂ATNO₂]; EA (C₃H₁₀N₁₀O₂, 218.18): calc.: C 14.86, H 4.05, N 56.33 %; found: C 14.21, H 4.25, N 53.50 %; BAM drophammer: 10 J; friction tester: 96 N (neg.); ESD: 0.15 J.

Acknowledgments

Financial support of this work by the Ludwig-Maximilian University of Munich (LMU), the European Research Office (ERO) of the U.S. Army Research Laboratory (ARL), the Armament Research, Development and Engineering Center (ARDEC) and the Strategic Environmental Research and Development Program (SERDP) under contract nos. W911NF-09-2-0018 (ARL), W911NF-09-1-0120 (ARDEC), W011NF-09-1-0056 (ARDEC) and 10 WPSEED01-002 / WP-1765 (SERDP) is gratefully acknowledged. The authors acknowledge collaborations with Dr. Mila Krupka (OZM Research, Czech Republic) in the development of new testing and evaluation methods for energetic materials and with Dr. Muhamed

Sucesca (Brodarski Institute, Croatia) in the development of new computational codes to predict the detonation and propulsion parameters of novel explosives. We are indebted to and thank Drs. Betsy M. Rice and Brad Forch (ARL, Aberdeen, Proving Ground, MD) and Mr. Gary Chen (ARDEC, Picatinny Arsenal, NJ) for many helpful and inspired discussions and support of our work. The authors are indebted to and thank Mr. Stefan Huber for performing the sensitivity tests.

References

- [1] a) T. M. Klapötke, C. M. Sabate, J. Stierstorfer, *New J. Chem.* **2008**, DOI: 10.1039/b812529e; b) T. M. Klapötke, C. M. Sabate, *Dalton Trans.* **2009**, 1835–1841.
- [2] G. Holl, T. M. Klapötke, K. Polborn, C. Rienäcker, *Propellants Explos. Pyrotech.* **2003**, 28, 153–156.
- [3] K. Karaghiosoff, T. M. Klapötke, A. Michailovski, H. Nöth, M. Suter, *Propellants Explos. Pyrotech.* **2003**, 28, 1–6.
- [4] a) T. M. Klapötke, J. Stierstorfer, *Helv. Chim. Acta* 2007, 90, 2132–2150; b) T. M. Klapötke, J. Stierstorfer, A. U. Wallek, *Chem. Mater.* **2008**, 20, 4519–4530; c) S. Berger, K. Karaghiosoff, T. M. Klapötke, P. Mayer, H. Piotrowski, K. Polborn, R. L. Willer, J. J. Weigand, *J. Org. Chem.* **2006**, 71, 1295–1305.
- [5] J. Geith, G. Holl, T. M. Klapötke, J. J. Weigand, *Combust. Flame* **2004**, 139, 358–366; J. Geith, T. M. Klapötke, J. J. Weigand, G. Holl, *Propellants Explos. Pyrotech.* **2004**, 29, 3–8.
- [6] a) M. von Denffer, T. M. Klapötke, G. Kramer, G. Spiess, J. M. Welch, G. Heeb, *Propellants Explos. Pyrotech.* **2005**, 30, 191–195; b) G. Ma, Z. Zhang, J. Zhang, K. Yu, *Thermochim. Acta* **2004**, 423, 137–141.
- [7] K. Karaghiosoff, T. M. Klapötke, P. Mayer, C. M. Sabate, A. Penger, J. M. Welch, *Inorg. Chem.* **2008**, 47, 1007–1019.
- [8] K. O. Christe, W.W. Wilson, M. A. Petrie, H. H. Michels, J. C. Bottaro, R. Gilardi, *Inorg. Chem.* **1996**, 35, 5068–5071.
- [9] a) T. M. Klapötke, J. Stierstorfer, *Phys. Chem. Chem. Phys.* **2008**, 10, 4340–4346; b) T. M. Klapötke, J. Stierstorfer, *Eur. J. Inorg. Chem.* **2008**, 4055–4062.
- [10] E. Lieber, E. Sherman, R. A. Henry, J. Cohen, *J. Am. Chem. Soc.* **1951**, 73, 2327–2329.
- [11] J. A. Garrison, R. M. Herbst, *J. Org. Chem.* **1957**, 22, 278–283.
- [12] R. A. Henry, W. G. Finnegan, *J. Am. Chem. Soc.* **1954**, 76, 923–926.
- [13] T. M. Klapötke, J. Stierstorfer, K. R. Tarantik: New Energetic Materials: Functionalized 1-Ethyl-5-aminotetrazoles and 1-Ethyl-5-nitriminotetrazoles, *Chem. Eur. J.* **2009**, 15, 5775–5792.
- [14] *CrysAlis CCD*, Version 1.171.27p5 beta; Oxford Diffraction Ltd.
- [15] *CrysAlis RED*, Version 1.171.27p5 beta; Oxford Diffraction Ltd.
- [16] Altomare, A.; Cascarano, G.; Giacovazzo, C.; Guagliardi, A. *J. Appl. Crystallogr.* **1993**, 26, 343.
- [17] Sheldrick, G. M. *SHELXS-97, Program for Crystal Structure Solution*; University of Goettingen: Goettingen, Germany, **1997**.

- [18] Sheldrick, G. M. *Shelxl-97, Program for the Refinement of Crystal Structures*; University of Goettingen: Goettingen, Germany, **1994**.
- [19] Farrugia, L. J. *J. Appl. Crystallogr.* **1999**, 32, 837–838.
- [20] Spek, A. L. *PLATON, A Multipurpose Crystallographic Tool*; Utrecht, The Netherlands, **1999**.
- [21] SCALE3 ABSPACK-An Oxford Diffraction program; Oxford Diffraction Ltd., 2005.
- [22] NATO standardization agreement (STANAG) on explosives, impact sensitivity tests, no. 4489, 1st ed., Sept. 17, **1999**.
- [23] WIWEB-Standardarbeitsanweisung 4-5.1.02, Ermittlung der Explosionsgefährlichkeit, hier der Schlagempfindlichkeit mit dem Fallhammer, Nov. 8, **2002**.
- [24] <http://www.bam.de>.
- [25] NATO standardization agreement (STANAG) on explosive, friction sensitivity tests, no. 4487, 1st ed., Aug. 22, **2002**.
- [26] WIWEB-Standardarbeitsanweisung 4-5.1.03, Ermittlung der Explosionsgefährlichkeit oder der Reibeempfindlichkeit mit dem Reibeapparat, Nov. 8, **2002**.
- [27] Impact: insensitive > 40 J, less sensitive g 35 J, sensitive g 4 J, very sensitive e 3 J. Friction: insensitive > 360 N, less sensitive) 360 N, sensitive < 360 N a.> 80 N, very sensitive e 80 N, extremely sensitive e 10 N. According to the UN Recommendations on the Transport of Dangerous Goods, (+) indicates not safe for transport.
- [28] <http://www.ozm.cz>
- [29] <http://www.linseis.com>
- [30] a) Suceska, M., EXPLO5.V2, Computer program for calculation of detonation parameters. *Proceedings of the 32nd Int. Annual Conference of ICT*, July 3-6, **2001**, Karlsruhe, Germany, pp 110–111. (b) Suceska, M. *Proceedings of 30th Int. Annual Conference of ICT*, June 29-July 2, **1999**, Karlsruhe, Germany, 50/1.
- [31] Suceska, M. *Propellants, Explos., Pyrotech.* **1991**, 16 (4), 197–202.
- [32] a) Suceska, M. *Mater. Sci. Forum* **2004**, 465-466, 325–330. (b) Suceska, M. *Propellants, Explos., Pyrotech.* **1999**, 24, 280–285. (c) Hobbs, M. L.; Baer, M. R. *Proceedings of the 10th Symp. (International) on Detonation*, ONR 33395-12, Boston, MA, July 12–16, **1993**; p 409.

Salts of 2-methyl-5-nitraminotetrazolate – Low sensitivity secondary explosives

Niko Fischer, Thomas M. Klapötke and Jörg Stierstorfer

Energetic Materials Research, Department of Chemistry,
University of Munich (LMU), Butenandtstr. 5-13, D-81377, Germany

tmk@cup.uni-muenchen.de

Abstract:

2-Methyl-5-nitraminotetrazole (**1**) was formed by nitration of 2-methyl-5-aminotetrazole. 2-Methyl-5-aminotetrazole was obtained by methylation of sodium 5-aminotetrazolate. Nitrogen-rich salts such as guanidinium (**2**), 1-aminoguanidinium (**3**), 1,3-diaminoguanidinium (**4**), 1,3,5-triamino-guanidinium (**5**), azidoformamidinium 2-methyl-5-nitriminotetrazolate (**6**) as well as an urea adduct (**7**) were prepared by facile deprotonation or metathesis reactions. All compounds were fully characterized by single crystal X-ray diffraction, vibrational spectroscopy (IR and Raman), multinuclear NMR spectroscopy, elemental analysis and DSC measurements. The heats of formation of **2–7** were calculated using the atomization method based on CBS-4M enthalpies. With these values and the experimental (X-ray) densities several detonation parameters such as the detonation pressure, velocity, energy and temperature were computed using the EXPLO5 code. In addition, the sensitivities towards impact, friction and electrical discharge were tested using the BAM drop hammer, a friction tester as well as a small scale electrical discharge device.

Keywords: 2-Methyl-5-nitraminotetrazolate; Secondary Explosives; Crystal Structures; Detonation Parameters; Sensitivities.

1 Introduction

The development of high-energy-density materials (HEDM) ^[1] is an ongoing area of interest in our research group. ^[2] Generally the class of HEDMs is divided into two main groups, according to their different applications in military and civil sectors. These main groups are explosives and propellants. Due to their qualification profile the materials have to meet specific characteristics. Important criteria for the group of explosives are the detonation velocity v_D and the detonation pressure p_{CJ} . Thereby the focus lies on the synthesis of compounds, which feature values as high as possible for both magnitudes, to reach maximum performance. Another critical parameter is the density ρ of the explosive, because the detonation pressure is directly proportional to the squared density ρ^2 . In contrast the detonation velocity depends on the molar quantity N of formed gaseous products and also on the density. Also high, endothermic heats of formations ($\Delta_f H^\circ$) are required for effective energetic materials. ^[3] Moreover the new explosive should be cheap to synthesize, stable towards temperature, storable for long periods and of course safe to handle. For safety reasons it only should detonate under specific conditions. Increasing environmental concerns over the last few years also raised the requirements of HEDMs, and new replacements for the commonly used toxic RDX are wanted. ^[4] Therefore explosives containing high nitrogen contents are in the focus, because of the environmentally benign dinitrogen N_2 molecule as the reaction product. ^[5] To prepare new energetic materials often tetrazoles, ^[6] tetrazolates ^[7] and tetrazolium ^[8,9] salts are used since they are

mostly endothermic compounds with a high nitrogen content. In addition these compounds are considered mostly less toxic, easy to handle due to their high kinetic and thermal stability and easy to prepare. Disadvantage of tetrazolates and tetrazolium compounds are the possible contamination of ground water since these ionic structures feature a high solubility. On the other side, they show mostly high densities and stabilities based on their lattice energy. The formation of ionic structures is a popular approach for the synthesis of new energetic materials. It is hard to fulfill all requirements for new energetic materials. However, the compounds described in this work are N-rich salts of the anion 2-methyl-5-nitraminotetrazolate. In accordance to its 1-substituted sister compound, it is a valuable energetic anion, due to the combination of the nitrogen-rich backbone as a fuel and the nitro group as an oxidizer. The nitration of the amino group in 5-aminotetrazole (Figure 1) leads to an increased energetic character as well as higher sensitivities compared to 5-aminotetrazole and improves the oxygen balance. The methyl group attached to the tetrazole ring system lowers the sensitivity in comparison to non-methylated 5-nitriminotetrazole. Furthermore, deprotonation of 2-methyl-5-nitraminotetrazole affords more suitable compounds with higher decomposition temperatures. For this reason 2-methyl-5-nitriminotetrazolate anions are convenient components for new ionic energetic materials.

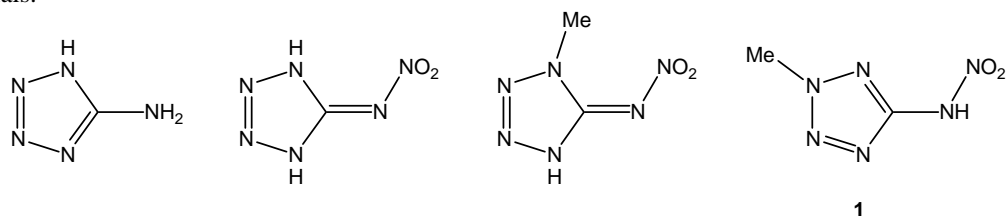


Figure 1: 5-Aminotetrazole (5-AT), 5-nitriminotetrazole, 1-methyl-5-nitriminotetrazole and 2-methyl-5-nitraminotetrazole (**1**).

According to the performance in energetic salts the same requirements have to be applied for the cations of the energetic material. Therefore 2-methyl-5-nitraminotetrazolate salts containing nitrogen rich cations are in the focus of this study. We recently synthesized the ammonium 2-methyl-5-nitraminotetrazolate^[10] as well as several 1-methyl-5-nitrimino-tetrazolate salts.^[11] The ammonium ion is very popular due to its environmental compatibility and its structure containing only nitrogen and hydrogen atoms. Following this approach different guanidinium salts of **2** were synthesized and are presented in this work. Guanidine chemistry has extended over a period of more than 100 years, and many useful compounds have been identified. The spectrum of uses of these compounds is highly diverse, ranging from biologically active molecules to highly energetic materials, thus indicating the manifold usability of the guanidine moiety as building block.^[12] Figure 2 gives an overview over the new nitrogen rich salts and adducts of 2-methyl-5-nitraminotetrazole presented in this work.

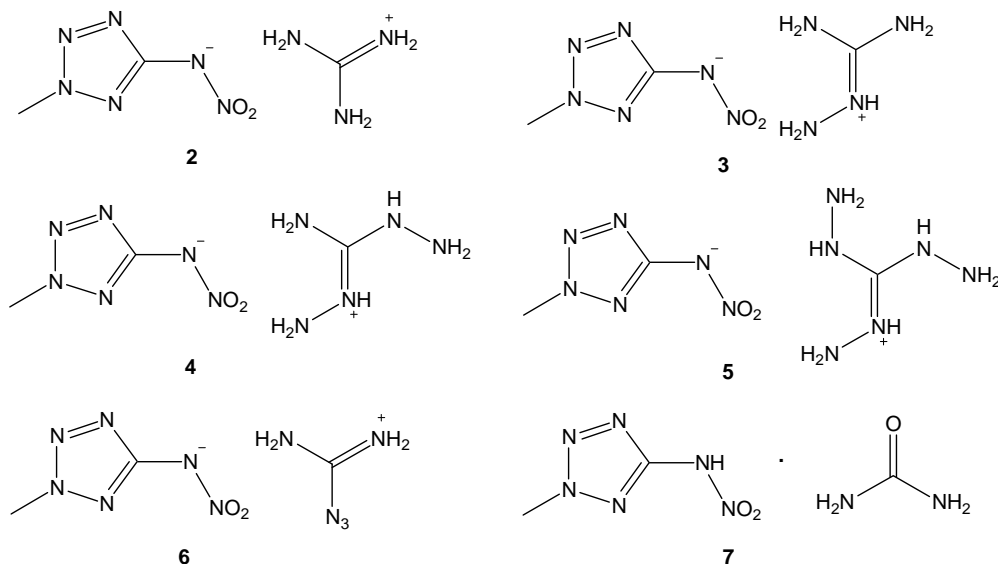
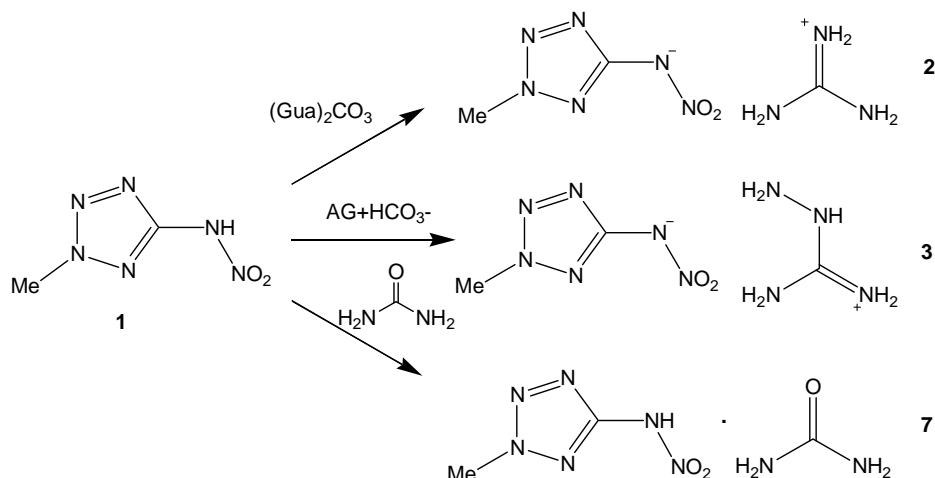


Figure 2: Target molecules presented in this work: guanidinium 2-methyl-5-nitraminotetrazolate (2), 1-aminoguanidinium 2-methyl-5-nitraminotetrazolate (3), 1,3-diaminoguanidinium 2-methyl-5-nitraminotetrazolate (4), 1,3,5-triaminoguanidinium 2-methyl-5-nitraminotetrazolate (5), azidoformamidinium 2-methyl-5-nitraminotetrazolate (6) and urea*2-methyl-5-nitraminotetrazole (7).

2 Results and discussion

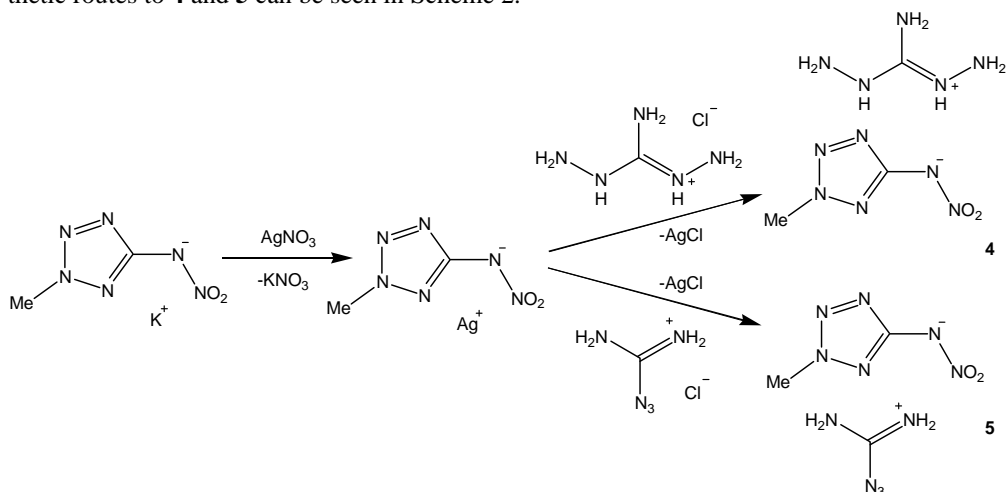
2.1 Synthesis

Scheme 1 shows the synthesis of the guanidinium (2) and 1-aminoguanidinium (3) salt of 2-methyl-5-nitraminotetrazole (1) as well as the formation of the urea adduct of 1. All synthetic routes shown are based on simple Brønstedt acid-base reactions. 2 and 3 were formed by reacting the free acid 1 with guanidinium carbonate and aminoguanidinium carbonate respectively, whereas the formation of gaseous CO_2 , which can be expelled from the reaction mixture by moderate warming of the solutions, is utilized. The urea adduct 7 is a cocrystallization product, which was obtained by the reaction of 1 with an aqueous solution of urea.



Scheme 1. Syntheses of compounds **2**, **3** and **7** via Brønsted acid-base reactions.

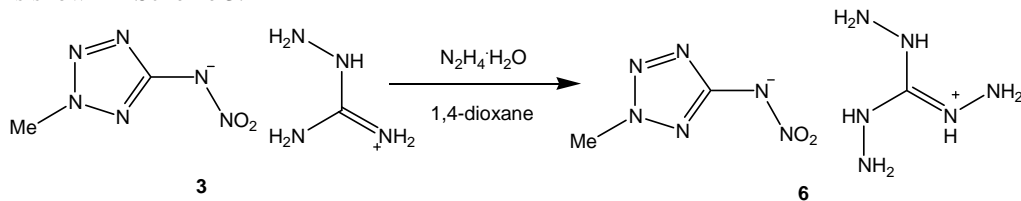
The reaction products 1,3-diaminoguanidinium 2-methyl-5-nitraminotetrazolate (**4**) and azidoformamidinium 2-methyl-5-nitraminotetrazolate (**5**) were obtained by metathesis reactions using the silver 2-methyl-5-nitraminotetrazolate as an intermediate. It was prepared from potassium 2-methyl-5-nitraminotetrazolate and silver nitrate in aqueous solution and after being separated from the reaction mixture as poorly soluble white salt, it was further reacted with diaminoguanidinium chloride and azidoformamidinium chloride, which was prepared by the reaction of aminoguanidinium chloride with 1 eq of NaNO_2 and HCl , followed by a recrystallization from water/ethanol, respectively to yield the above described salts **4** and **5**. The synthetic routes to **4** and **5** can be seen in Scheme 2.



Scheme 2. Synthetic routes to **4** and **5** via silver 2-methyl-5-nitraminotetrazolate

For the synthesis of the triaminoguanidinium 2-methyl-5-nitraminotetrazolate (**6**), the hydrazinolysis reaction of the aminoguanidinium salt **3** was employed. Therefore **3** was heated

with hydrazine hydroxide in 1,4-dioxane under the release of ammonia. The reaction procedure is shown in Scheme 3.



Scheme 3. Synthesis of **6** via hydrazinolysis of **3**.

Beside from the synthetic routes to the compounds **2–7**, that are shown above, a different way via the potassium salt of **1** and the corresponding guanidinium perchlorates and azidoformamidinium perchlorate respectively can be considered, where the reaction is driven by the low solubility of potassium perchlorate. Although this route seems to be more practicable than the syntheses, that involve intermediates like silver salts, that have to be isolated first, appropriate safety measures have to be applied due to the high sensitivity of the guanidinium and azidoformamidinium perchlorates used as starting material.

2.2 Molecular structures

To determine the molecular structures of **2–7** in the crystalline state an Oxford Xcalibur3 diffractometer with a Spellman generator (voltage 50 kV, current 40 mA) and a KappaCCD detector was used. The data collection was performed using the CrysAlis CCD software,^[13] the data reductions with the CrysAlis RED software.^[14] The solution of all structures were performed using SIR-92,^[15] and SHELXS-97,^[16] and SHELXL-97^[17] implemented in the WinGX software package^[18] and finally checked with the PLATON software.^[24] In all crystal structures the hydrogen atoms were located and refined. The absorptions were corrected with the SCALE3 ABSPACK multi-scan method.^[20] Selected data and parameter of the X-ray determinations are given in Table 1.

2-Methyl-5-nitriminotetrazole and its crystal structure were recently investigated and published by our research group.^[21] Its structure is different compared to the molecular structures of the anions in the investigated 2-methyl-5-nitriminotetrazolate salts. The position of the nitramine group to the tetrazole ring plane differs significantly since there are various hydrogen bonds influencing this building block.

Compounds **2–7** crystallize in the monoclinic and triclinic space groups $P2_1$ (**2**), $P-1$ (**3** and **5**), $P2_1/c$ (**4**) and $P2_1/n$ (**6** and **7**) with densities lying in a range from 1.567 g cm^{-3} (**4**) to 1.632 g cm^{-3} (**2**). The bond distances between N1, N2, N3 and N4 vary from 1.30 to 1.33 Å, which fits between the bond lengths of a N–N single bond (1.45 Å) and an N=N double bond (1.25 Å)^[22]. Furthermore the torsion angles C1–N2–N3–N4 are nearly located to 0° ($0.3(3)^\circ$ for **2** to $-0.24(14)^\circ$ for **5**) implying a π -aromatic system. Also the bond lengths C1–N1 and C1–N4 are located between the bond lengths of a C–N single (1.47 Å) and a C=N double bond (1.22 Å)^[23], whereas the distance between N2 and the exocyclic carbon atom C2 is in the range of a C–N single bond (1.452(2) (**3**) to 1.462(4) (**2**)). The nitro group of the nitramine unit is more or less strongly twisted out of the tetrazole ring plane indicated by a N1–C1–N5–N6 torsion angle between $-1.2(5)^\circ$ for **2** and up to $30.3(2)^\circ$ for the triaminoguanidinium salt **5**.

Table 1: X-ray data and parameters.

	2		3		4		5		6		7		
Formula	C ₃ H ₉ N ₉ O ₂		C ₃ H ₁₀ N ₁₀ O ₂		C ₃ H ₁₁ N ₁₁ O ₂		C ₃ H ₁₂ N ₁₂ O ₂		C ₃ H ₇ N ₁₁ O ₂		C ₃ H ₈ N ₈ O ₃		
Form. weight [g mol ⁻¹]	203.16		218.21		234.24		248.25		229.20		204.17		
Crystal system	Monoclinic		Triclinic		Monoclinic		Triclinic		Monoclinic		Monoclinic		
Space Group	P2 ₁		P-1		P2 ₁ /c		P-1		P2 ₁ /n		P2 ₁ /n		
Color / Habit	colorless rods		colorless rods		colorless plates		colorless rods		colorless rods		colorless plates		
Size [mm]	0.05 x	0.12 x	0.12 x	0.15 x	0.10 x	0.25 x	0.25 x	0.16 x	0.25 x	0.14 x	0.15 x	0.40 x	0.35 x
	0.15		0.24				0.25		0.22		0.13		
<i>a</i> [Å]	3.6562(3)		3.7828(4)		17.4021(14)		6.9170(4)		7.6150(10)		7.5867(5)		
<i>b</i> [Å]	8.1552(8)		8.5095(8)		8.3403(7)		7.5831(5)		13.7932(14)		7.3684(7)		
<i>c</i> [Å]	13.9458(11)		14.1651(14)		14.7111(13)		11.0147(7)		9.5095(10)		15.3282(9)		
α [°]	90		91.281(8)		90.00		97.315(5)		90		90.00		
β [°]	95.919 (8)		95.299(8)		111.581(9)		106.030(5)		103.988(14)		95.764(6)		
γ [°]	90		96.743(8)		90.00		104.979(5)		90		90.00		
<i>V</i> [Å ³]	413.61(6)		450.63(8)		1985.5(3)		523.99(6)		969.2(2)		852.54(11)		
<i>Z</i>	2		2		8		2		4		4		
$\rho_{\text{calc.}}$ [g cm ⁻³]	1.632		1.608		1.567		1.573		1.571		1.591		
μ [mm ⁻¹]	0.136		0.134		0.065		0.131		0.132		0.138		
<i>F</i> (000)	212		228		488		260		472		424		
$\lambda_{\text{MoK}\alpha}$ [Å]	0.7107(3)		0.7107(3)		0.7107(3)		0.7107(3)		0.7107(3)		0.7107(3)		
<i>T</i> [K]	200(2)		173(2)		173(2)		173(2)		173(2)		173(2)		
θ Min-Max [°]	4.41, 28.29		4.34, 32.36		4.24, 33.41		4.1997, 32.35		4.26, 28.78		4.17, 28.76		
Dataset	-4:3; -4:10; -		-4:4; -10:8; -		-19:21; -7:10; -		-8:8; -9: 9; -		-9:5; -15:16; -		-9:6; -9:5; -		
	17:16		16:17		15:18		13: 13		10:11		15:18		
Reflections collected	1703		3303		5007		5352		3581		3063		
Independent reflections	988		1768		1948		2062		1797		1611		
<i>R</i> _{int}	0.028		0.024		0.025		0.018		0.027		0.029		
Observed reflections	756		1119		1377		1650		1097		1067		
Parameters	151		176		189		202		173		159		
<i>R</i> ₁ (obs)	0.0371		0.0320		0.0328		0.0289		0.0352		0.0375		
<i>wR</i> ₂ (all data)	0.0767		0.0710		0.0759		0.0773		0.0700		0.0856		
GooF	0.92		0.83		0.90		1.04		0.82		0.88		
Resd. Dens. [e/Å ³]	-0.24, 0.26		-0.22, 0.15		-0.12, 0.08		-0.23, 0.17		-0.21, 0.18		-0.22, 0.21		
Device type	Oxford	Xcali-	Oxford	Xcali-	Oxford	Xcalibur3	Oxford	Xcalibur3	Oxford	Xcali-	Oxford	Xcali-	
	bur3	bur3	bur3	bur3	bur3	CCD	bur3	CCD	bur3	bur3	bur3	bur3	
	CCD	CCD	CCD	CCD	CCD		CCD		CCD	CCD	CCD	CCD	
Solution	SHELXS-97		SHELXS-97		SHELXS-97		SHELXS-97		SHELXS-97		SHELXS-97		
Refinement	SHELXL-97		SHELXL-97		SHELXL-97		SHELXL-97		SHELXL-97		SHELXL-97		
Absorption correction	multi-scan		multi-scan		multi-scan		multi-scan		multi-scan		multi-scan		

The distances between C1 and N5 are closer to a C–N single bond than to a C=N double bond (1.377(2) Å for **4** to 1.388(2) Å for **3**), which justifies the nomenclature nitraminetetrazolate rather than nitriminetetrazolate. The C–N distances in the cations match the typical values found in literature for guanidinium nitrate^[24] and guanidinium chloride^[25], exhibiting a bond order between a single and a double bond. The N–N bond orders of the aminoguanidinium, diaminoguanidinium and triaminoguanidinium cation are close to a N–N single bond with distances between 1.406(2) Å (**2**) and 1.4191 (17) Å for N9–N10 in **5**. The azidoformamidinium cation is not planar (torsion angle = N8–N7–C3–N11 16.1(3)°) and angulated (angle N8–N7–C3 = 114.49(15)°) and the bond distances are very similar to those found in azidoformamidinium chloride.^[26] The urea moiety in **7** reveals the geometry of urea itself, as it is not protonated but only an adduct, whereas the C–O bond distance is slightly larger (1.225(2) Å) than a classic C=O double bond (1.19 Å)^[27] due to a very strong H-bond formed between H5 and O3 (1.57(2) Å).

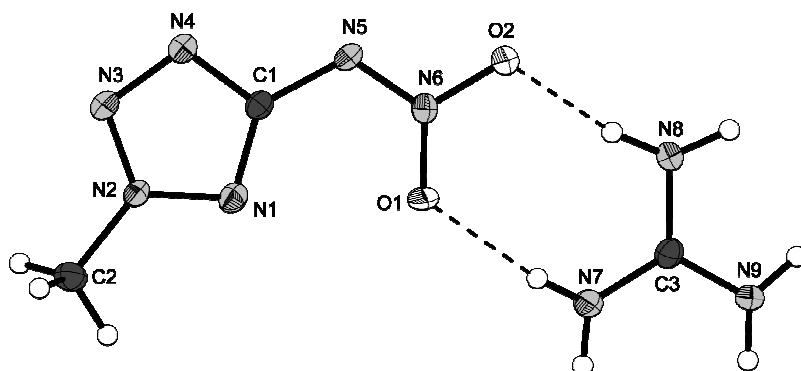


Figure 3: Molecular Structure of compound 2.

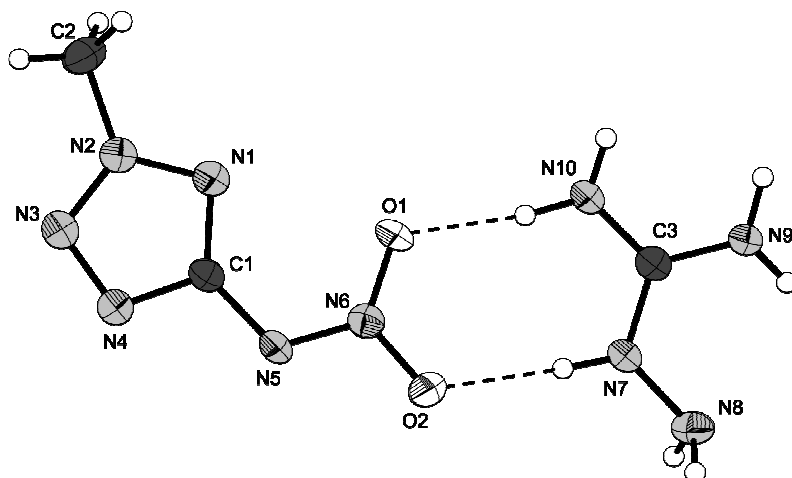


Figure 4: Molecular Structure of compound 3.

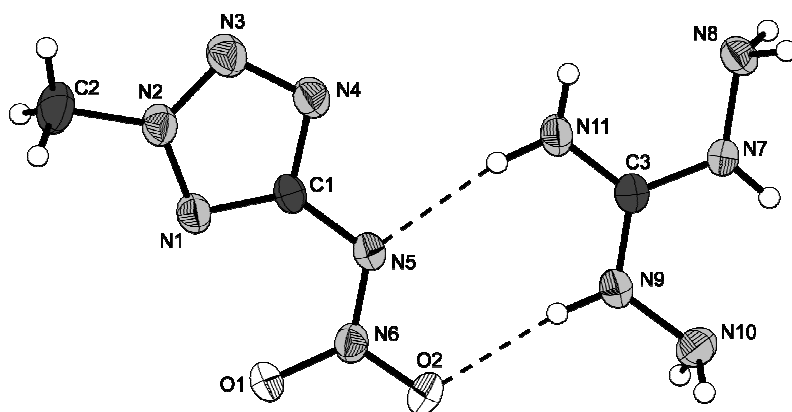


Figure 5: Molecular Structure of compound 4.

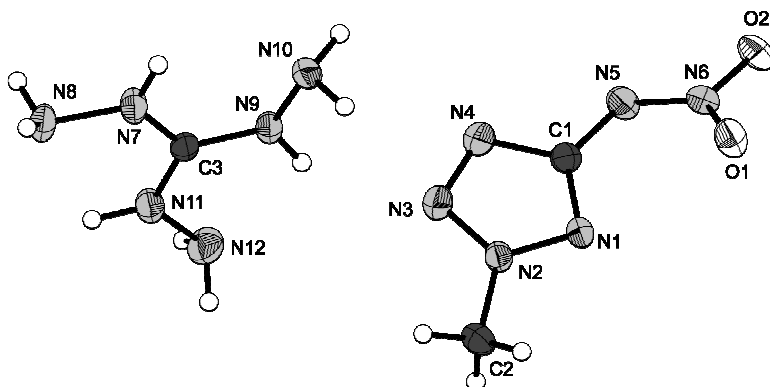


Figure 6: Molecular Structure of compound 5.

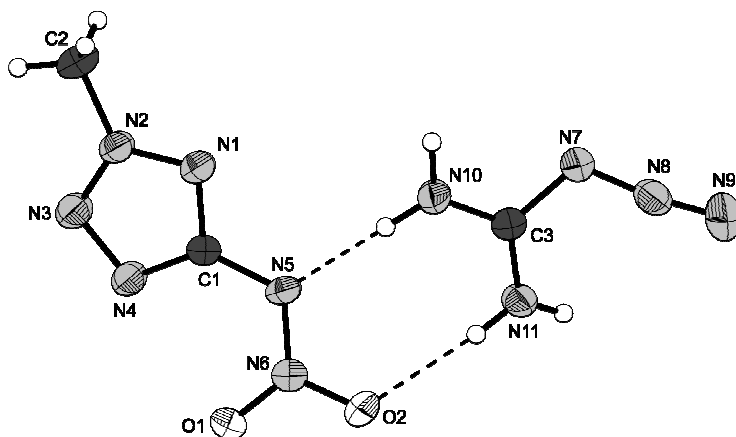


Figure 7: Molecular Structure of compound 6.

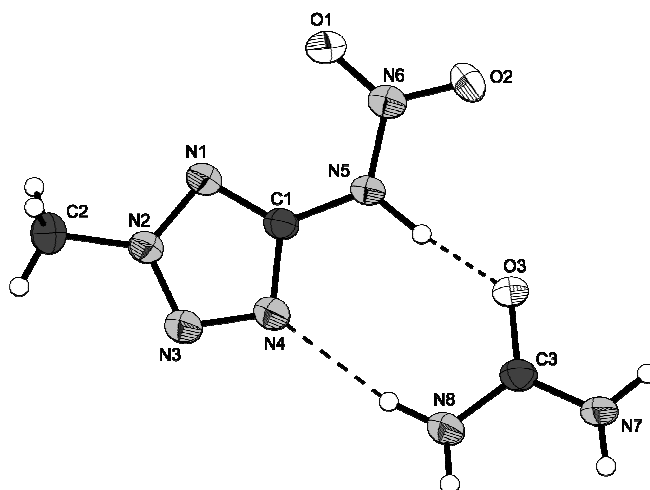


Figure 8: Molecular Structure of compound 7.

2.3 Sensitivities and thermal stability

The impact sensitivity tests were carried out according to STANAG 4489^[28] modified instruction^[29] using a BAM (Bundesanstalt für Materialforschung) drophammer.^[30] The friction sensitivity tests were carried out according to STANAG 4487^[31] modified instruction^[32] using the BAM friction tester. The classification of the tested compounds results from the “UN Recommendations on the Transport of Dangerous Goods”.^[33] Additionally all compounds were tested upon the sensitivity towards electrical discharge using the Electric Spark Tester ESD 2010 EN^[34]. Beside from the impact sensitivity of **6** (3 J), which has to be classified as very sensitive, the sensitivities of all other compounds **1–5** and **7** are in the range of 6 J to 30 J and therefore have to be classified as sensitive towards friction. The guanidinium salt **2** stands out with a relatively low sensitivity of 30 J. The same classification applies to the friction sensitivities. Again, the azidoformamidinium salt **6** has to be classified as very sensitive with a value of 72 N, whereas the remaining compounds **1–5** and **7** are classified as sensitive having values in a range from 120 N to 288 N. Concerning the sensitivities towards electrical discharge, all tested materials **1–7** have values of about 0.2 J, whereas the compounds could not be detonated but started to decompose upon treatment with the specified electrical energy. The explicit sensitivity data can be seen in Table 2.

Differential scanning calorimetry (DSC) measurements to determine the melt- and decomposition temperatures of **2–7** (about 1.5 mg of each energetic material) were performed in covered Al-containers containing a hole in the lid and a nitrogen flow of 20 mL per minute on a Linseis PT 10 DSC^[35] calibrated by standard pure indium and zinc at a heating rate of 5°C min⁻¹. The decomposition temperatures are in a range from 148°C for **6** to 212°C for **2**. Compared to the 1-methyl-derivatives, the 2-methyl-derivatives decompose at lower temperature. Also the melting points of the corresponding 2-methyl-derivatives are lower^[11]. **2**, **3** and **4** reach decomposition temperatures of more than 200 °C. With rising nitrogen content, the thermal stability drops, which can be seen at the values for **5** (143 °C) and **6** (148 °C). The decomposition of the adduct **7** takes place in two separate processes, which can be observed at 158 °C and 190 °C belonging to the decomposition of 2-methyl-5-nitraminotetrazole and urea.

2.4 Detonation Parameters

The detonation parameters were calculated using the program EXPLO5 V5.02.^[36] The program is based on the steady-state model of equilibrium detonation and uses Becker-Kistiakowsky-Wilson’s equation of state (BKW E.O.S) for gaseous detonation products and Cowan-Fickett E.O.S. for solid carbon.^[37] The calculation of the equilibrium composition of the detonation products is done by applying modified White, Johnson and Dantzig’s free energy minimization technique. The program is designed to enable the calculation of detonation parameters at the CJ point. The BKW equation in the following form was used with the BKWN set of parameters (α , β , κ , θ) as stated below the equations and X_i being the mol fraction of i -th gaseous product, k_i is the molar covolume of the i -th gaseous product:^[38]

$$pV / RT = 1 + x e^{\beta x} \quad x = (\kappa \sum X_i k_i) / [V(T + \theta)]^\alpha$$

$$\alpha = 0.5, \beta = 0.176, \kappa = 14.71, \theta = 6620.$$

The calculations were performed using the maximum densities according to the crystal structures. The most promising compound concerning the detonation velocity and pressure discussed here is the triaminoguanidinium salt **5** with values of $v_d = 8827 \text{ ms}^{-1}$ for the detonation velocity and a detonation pressure of $p_{CJ} = 277 \text{ kbar}$ since the values are closest to those of

commonly used RDX (royal demolition explosive; $p_{CJ} = 340$ kbar, $v_d = 8882$ m s⁻¹). The detonation velocities and pressures of **1–4**, **6** and **7** are slightly lower than those of RDX ranging from $v_d = 7806$ m s⁻¹ (**7**) to $v_d = 8603$ m s⁻¹ (**4**). Due to their lower nitrogen content and molar amount of gaseous reaction products, compounds **2–4**, **6** and **7** do not reach the level of **5** in terms of detonation pressure and velocity. However, the molar amount of gaseous reaction products is subject to only small variations (**2**: 844, **3**: 861, **4**: 876, **5**: 888, **6**: 806, **7**: 822 L kg⁻¹) which are funded in the different detonation temperatures (**2**: 2907, **3**: 3039, **4**: 3170, **5**: 3249, **6**: 3887, **7**: 3179 K).

Compared to the nitrogen-rich salts of the 1-methyl-5-nitriminotetrazole, which recently were synthesized in our research group ^[11], the detonation velocities and pressures of the 2-methyl-derivatives are slightly higher with larger differences for the guanidinium and aminoguanidinium salts and smaller differences for the diaminoguanidinium and triaminoguanidinium salts. Also the heats of explosion and the explosion temperatures are higher than those of the 1-methyl-derivatives. The molar amount of gaseous products, however is nearly in the same range due to the same molecular weights.

Table 2. Explosive and detonation parameters.

	G 2MNAT	AG 2MNAT	DAG 2MNAT	TAG 2MNAT	AF 2MNAT	Uro 2MNAT	RDX
Formula	C ₃ H ₆ N ₉ O ₂	C ₃ H ₁₀ N ₁₀ O ₂	C ₃ H ₁₁ N ₁₁ O ₂	C ₃ H ₁₂ N ₁₂ O ₂	C ₃ H ₇ N ₁₁ O ₂	C ₃ H ₈ N ₈ O ₃	C ₃ H ₆ N ₆ O ₇
FW / g mol ⁻¹	203.17	218.23	233.11	248.27	229.16	204.19	222.12
IS / J	30	6	10	6	3	10	7.5
FS / N	192	120	160	120	72	288	120
ESD / J	0.2	0.2	0.16	0.18	0.2	0.2	0.1 - 0.2
N / %	62.1	64.2	66.1	67.72	67.23	54.89	37.8
Δ / %	-66.9	-66.0	-65.2	-64.5	-52.36	-54.9	-21.6
T _{Dec.} / °C	212	210	203	188	148	158	210
ρ / g cm ⁻³	1.632	1.608	1.567	1.573	1.571	1.591	1.80
Δ _t H _m ^o / kJ mol ⁻¹	255	366	479	587	687	120	70
Δ _t U ^o / kJ kg ⁻¹	1378	1801	2182	2496	3105	701	417
EXPLQ5 values:							
Δ _{Ex} U ^o / kJ kg ⁻¹	-4148	-4454	-4733	-4959	-5381	-4370	-6038
T _{det} / K	2907	3039	3170	3249	3887	3179	4368
P _{CJ} / kbar	250	260	262	277	258	224	341
V _{Det.} / m s ⁻¹	8300	8495	8603	8827	8290	7806	8906
V _o / L kg ⁻¹	844	861	876	888	806	822	793

3 Experimental part

3.1 Guanidinium-2-methyl-5-nitraminotetrazolate (2)

2-Methyl-5-nitraminotetrazole (1.44 g, 10 mmol) is suspended in a few milliliters of water and a suspension of guanidinium carbonate (0.90 g, 5 mmol) in water is added slowly. The mixture is heated to 40°C and then filtrated. The solvent is removed in vacuum and the residue recrystallized from ethanol. Yield: 1.73 g (8.52 mmol, 85%).

DSC (5 °C min⁻¹, °C): 176°C (m.p.), 212°C (dec.); IR (KBr, cm⁻¹): $\tilde{\nu} = 3423$ (s), 3342 (s), 3276 (s, br), 3173 (s), 2790 (m), 1927 (w), 1694 (vs), 1662 (s), 1488 (s), 1422 (s), 1355 (s), 1217 (m), 1099 (m), 1037 (m), 990 (w), 893 (w), 766 (w), 632 (m, br), 528 (m); Raman (1064 nm, 500 mW, 25 °C, cm⁻¹): $\tilde{\nu} = 3202$ (2), 2963 (9), 1490 (100), 1404 (6), 1375 (4), 1339 (3), 1224 (4), 1101 (2), 1039 (36), 1015 (45), 896 (2), 743 (5), 705 (8), 539 (4), 450 (9), 398 (4), 349 (3) 207 (5), 145 (3), 129 (15), 91 (31); ¹H NMR (DMSO-*d*₆, 25 °C, ppm) δ: 7.03 (s, 6H, NH₂), 4.20 (CH₃); ¹³C NMR (DMSO-*d*₆, 25 °C, ppm) δ: 168.4 (CN₄), 158.6 (C(NH₂)₃), 39.7 (CH₃); m/z (FAB⁺): 60.1 [C(NH₂)₃⁺]; m/z (FAB⁻): 143.0 [2-MeATNO₂⁻]; EA (C₃H₉N₉O₂,

203.16): calc.: C 17.74, H 4.47, N 62.05 %; found: C 17.86, H 4.84, N 61.39 %; BAM drophammer: >30 J; friction tester: >192 N (neg.); ESD: >0.2 J.

3.2 Aminoguanidinium-2-methyl-5-nitriminotetrazolate (3)

2-Methyl-5-nitraminotetrazole (4.32 g, 30 mmol) is suspended in few milliliters of water and then a suspension of aminoguanidinium bicarbonate (4.08 g, 30 mmol) in water is added slowly. The mixture is heated to 40°C and then filtrated. The solvent is removed in vacuum and the residue then recrystallized from an ethanol/water mixture to yield 5.24 g (24.0 mmol, 80%).

DSC (5 °C min⁻¹, °C): 146°C (m.p.), 210°C (dec.); IR (KBr, cm⁻¹): $\tilde{\nu}$ = 3902 (w), 3463 (s), 3336 (s, br), 3238 (s, br), 3113 (s, br), 2831 (m), 2426 (m), 2237 (m), 1950 (w), 1927 (w), 1840 (w), 1776 (w), 1693 (s), 1639 (s), 1598 (m), 1548 (m), 1488 (s), 1401 (vs), 1374 (s), 1358 (s), 1337 (s), 1278 (s), 1221 (s), 1184 (m), 1099 (s), 1061 (s), 1037 (s), 893 (m), 760 (m), 706 (m), 557 (s); Raman (1064 nm, 500 mW, 25 °C, cm⁻¹): $\tilde{\nu}$ = 2963 (3), 1491 (100), 1404 (5), 1372 (2), 1346 (2), 1221 (3), 1039 (15), 1011 (26), 962 (5), 895 (3), 740 (4), 703 (6), 529 (3), 446 (4), 405 (3), 345 (3), 200 (5), 141 (3), 113 (22), 83 (13); ¹H NMR (DMSO-*d*₆, 25 °C, ppm) δ : 7.34 (s, 5H, C-NH₂, NH-NH₂), 4.70 (s, 2H, NH₂NH), 4.20 (CH₃); ¹³C NMR (DMSO-*d*₆, 25 °C, ppm) δ : 168.4 (CN₄), 159.4 (C(NHNH₂)(NH₂)₂), 39.7 (CH₃); m/z (FAB⁺): 75.1 [C(NHNH₂)(NH₂)₂⁺]; m/z (FAB⁻): 143.0 [2-MeATNO₂⁻]; EA (C₃H₁₀N₁₀O₂, 218.18): calc.: C 16.52, H 4.62, N 64.20 %; found: C 16.92, H 5.05, N 62.57 %; BAM drophammer: >6 J; friction tester: >120 N (neg.); ESD: >0.2 J.

3.3 Diaminoguanidinium-2-methyl-5-nitraminoetrazolate (4)

2-Methyl-5-nitraminotetrazole (1.98 g, 13.74 mmol) is dissolved in a solution of potassium hydroxide in 20 mL of water and an aqueous solution of silver nitrate (13.74 mmol, 2.33 g) is added. The colorless and fluffy precipitate is filtered off and directly given to a solution of diaminoguanidinium chloride (1.73 g, 13.78 mmol) in 50 mL of water. The suspension is stirred under exclusion of light for 20 minutes, filtered off and the solvent of the clear solution is removed in vacuo. The residue is recrystallized from ethanol. Yield: 1.98 g (8.49 mmol, 62%).

DSC (5 °C min⁻¹, °C): 138°C (m.p.), 203°C (dec.); IR (KBr, cm⁻¹): $\tilde{\nu}$ = 3737 (w), 3457 (s), 3353 (s), 3310 (vs), 3098 (s), 2376 (w), 2284 (w), 2105 (w), 1990 (w), 1957 (w), 1679 (vs, br), 1639 (s), 1567 (m), 1545 (m), 1489 (s), 1385 (s), 1324 (s, br), 1276 (s), 1213 (s), 1182 (s), 1099 (s), 1037 (s), 976 (s), 890 (m), 773 (m), 756 (m), 744 (w), 706 (m), 673 (m), 562 (m), 468 (m); Raman (1064 nm, 500 mW, 25 °C, cm⁻¹): $\tilde{\nu}$ = 2956 (3), 1590 (100), 1443 (3), 1376 (4), 1216 (3), 1101 (4), 1038 (9), 1012 (39), 932 (3), 893 (4), 746 (9), 718 (6), 547 (3), 447 (5), 402 (3), 341 (6), 188 (7), 126 (4), 107 (5), 81 (42); ¹H NMR (DMSO-*d*₆, 25 °C, ppm) δ : 8.62 (s, 2H, NH-NH₂), 7.17 (s, 2H, C-NH₂), 4.58 (s, 4H, NH₂NH), 4.16 (CH₃); ¹³C NMR (DMSO-*d*₆, 25 °C, ppm) δ : 168.4 (CN₄), 160.3 (C(NHNH₂)₂(NH₂)), 39.6 (CH₃); m/z (FAB⁺): 90.1 [C(NHNH₂)₂(NH₂)⁺]; m/z (FAB⁻): 143.0 [2-MeATNO₂⁻]; EA (C₃H₉N₉O₂, 203.16): calc.: C 15.45, H 4.75, N 66.07 %; found: C 15.75, H 4.77, N 65.63 %; BAM drophammer: >10 J; friction tester: 160 N (neg.); ESD: 0.16 J.

3.4 Triaminoguanidinium-2-methyl-5-nitraminotetrazolate (5)

Aminoguanidinium 2-methyl-5-nitraminotetrazolate (1.89 g, 8.7 mmol) is suspended in 20 mL of 1,4-dioxane and hydrazine hydrate (0.96 g, 19.1 mmol) is added dropwise. The solution is heated to 90°C for 5 h in a constant nitrogen flow. As soon as ammonia is no longer evolved from the reaction mixture the solution is cooled down and the solvent is removed in vacuum. The residue is recrystallized from ethanol to give 1.71 g (6.89 mmol, 88%).

DSC (5 °C min⁻¹, °C): 143°C (m.p.), 188°C (dec.); IR (KBr, cm⁻¹): $\tilde{\nu}$ = 3484 (s), 3336 (s, br), 3155 (s, br), 2950 (s), 2801 (s), 2670 (s), 2456 (s), 2379 (m), 2158 (m), 1667 (vs, br), 1595 (s, br), 1521 (m), 1484 (s), 1454 (s), 1321 (s), 1298 (s), 1235 (m), 1158 (s), 1120 (s), 1090 (s), 995 (s), 970 (s), 916 (m, br), 789 (s), 755 (m), 742 (s), 679 (s), 622 (s), 544 (s, br); Raman (1064 nm, 500 mW, 25 °C, cm⁻¹): $\tilde{\nu}$ = 3318 (6), 3218 (3), 2962 (3), 1545 (2), 1481 (100), 1449 (4), 1389 (9), 1360 (3), 1213 (3), 1131 (2), 1096 (3), 1061 (4), 1017 (50), 886 (7), 767 (6), 706 (8), 678 (2), 456 (4), 396 (8), 344 (2), 259 (3), 172 (4), 143 (13); ¹H NMR (DMSO-*d*₆, 25 °C, ppm) δ : 8.59 (s, 3H, NHNH₂), 4.50 (s, 6H, NHNH₂), 4.18 (CH₃); ¹³C NMR (DMSO-*d*₆, 25 °C, ppm) δ : 168.8 (CN₄), 159.6 (C(NHNH₂)₃), 39.6 (CH₃); m/z (FAB⁺): 105.1 [C(NHNH₂)₃⁺]; m/z (FAB⁻): 142.9 [2-MeATNO₂⁻]; EA (C₃H₁₂N₁₂O₂, 248.21): calc.: C 14.52, H 4.87, N 67.72 %; found: C 14.85, H 4.94, N 67.38 %; BAM drophammer: 6 J; friction tester: 120 N (neg.); ESD: 0.18 J.

3.5 Azidoformamidinium-2-methyl-5-nitraminoetrazolate (6)

Potassium 2-methyl-5-nitraminotetrazolate (1.82 g, 10 mmol) was prepared by dissolving 2-methyl-5-nitraminotetrazole (1.44 g, 10 mmol) in a solution of potassium hydroxide (85%, 0.66 g, 10 mmol) in 20 milliliters of water. The resulting solution was added to a solution of silver nitrate (1.70 g, 10 mmol) in 10 mL of water, while the reaction vessel was kept in darkness. Silver 2-methyl-5-nitraminotetrazolate precipitated instantaneously, the suspension was centrifuged and the aqueous layer pipetted off. It was washed with three portions of water (50 mL each) and suspended in 25 mL of water afterwards. Azidoformamidinium chloride (1.15 g, 9.5 mmol) was dissolved in 10 mL of water and added to the suspension. Silver chloride started to precipitate and the suspension was stirred in darkness for further 30 minutes at 30°C. The precipitate was filtered off, the water was removed in vacuo and the remaining solid recrystallized from an ethanol/water mixture to yield 1.28 g (5.58 mmol, 56%) of azidoformamidinium 2-methyl-5-nitraminotetrazolate as colorless crystals.

DSC (5 °C min⁻¹, °C): 115°C (m.p.), 148°C (dec.); IR (KBr, cm⁻¹): $\tilde{\nu}$ = 3264 (m), 3029 (m), 2783 (w), 2446 (w), 2185 (vs), 2121 (w), 1931 (w), 1698 (s), 1476 (vs), 1401 (vs), 1366 (vs), 1337 (s), 1287 (m), 1232 (m), 1180 (w), 1120 (m), 1098 (m), 1035 (w), 909 (w), 880 (w), 841 (w), 773 (w), 764 (w), 748 (w), 704 (m), 690 (m), 677 (m), 536 (w), 509 (m), 481 (w); Raman (1064 nm, 500 mW, 25 °C, cm⁻¹): $\tilde{\nu}$ = 3034 (2), 2970 (14), 2185 (14), 2123 (3), 1473 (100), 1418 (10), 1360 (5), 1232 (3), 1183 (7), 1143 (5), 1123 (2), 1098 (2), 547 (3), 1026 (78), 911 (8), 883 (4), 765 (5), 708 (7), 510 (5), 484 (3), 464 (8), 395 (5), 321 (10), 214 (4); ¹H NMR (DMSO-*d*₆, 25 °C, ppm) δ : 6.40 (s, 4H, NH₂), 4.36 (s, 3H, CH₃); ¹³C NMR (DMSO-*d*₆, 25 °C, ppm) δ : 168.4 (CN₄), 158.7 (C(N₃)₂(NH₂)₂), 40.4 (CH₃); m/z (FAB⁺): 86.1 [C(N₃)(NH₂)₂⁺]; m/z (FAB⁻): 143.0 [2-MeATNO₂⁻]; EA (C₃H₇N₁₁O₂, 229.16): calc.: C 15.72, H 3.08, N 67.23 %; found: C 15.72, H 3.10, N 67.03 %; BAM drophammer: 3 J; friction tester: 72 N; ESD: 0.20 J.

3.6 Urea · 2-methyl-5-nitraminotetrazole (7)

2-Methyl-5-nitraminotetrazole (1.44 g, 10 mmol) is suspended in a few milliliters of water and a solution of urea (0.60 g, 10 mmol) in water is added. The solvent of the clear solution is removed in vacuum and the residue then recrystallized from an ethanol/water mixture. Yield: 1.95 g (9.55 mmol, 96%).

DSC (5 °C min⁻¹, °C): 158°C, 190°C (dec.); IR (KBr, cm⁻¹): $\tilde{\nu}$ = 3437 (s, br), 3346 (s, br), 2804 (w), 2642 (w), 2184 (w), 1670 (vs, br), 1465 (s), 1384 (m), 1330 (m), 1279 (m), 1209 (m), 1153 (m), 1050 (m), 1016 (m), 863 (w), 787 (w), 736 (m), 618 (w), 573 (m), 558 (m); Raman (1064 nm, 130 mW, 25 °C, cm⁻¹): $\tilde{\nu}$ = 3437 (2), 3329 (8), 3239 (4), 3124 (2), 2967 (6), 2330 (3), 2130 (1), 1650 (6), 1626 (2), 1538 (11), 1363 (3), 1281 (3), 1176 (5), 1047 (2), 1011

(100), 698 (4), 548 (17), 432 (2), 370 (2), 329 (1), 132 (17), 102 (74), 84 (5); ^1H NMR (DMSO- d_6 , 25 °C, ppm) δ : 6.99 (s, 1H, NH), 5.78 (s, 4H, NH_2), 4.30 (CH_3); ^{13}C NMR (DMSO- d_6 , 25 °C, ppm) δ : 160.7 ($\text{C}(\text{O})(\text{NH}_2)_2$), 158.6 (CN_4), 40.6 (CH_3); m/z (FAB $^+$): 60.1 [$\text{C}(\text{O})(\text{NH}_2)_2^+$]; m/z (FAB $^-$): 143.0 [2-MeATNO_2^-]; EA ($\text{C}_3\text{H}_8\text{N}_8\text{O}_3$, 204.15): calc.: C 17.65, H 3.95, N 54.89 %; found: C 18.60, H 5.48, N 48.59 %; BAM drophammer: 10 J; friction tester: 288 N (neg.); ESD: 0.2 J.

4 Conclusion

From the experimental study of N-rich 2-methyl-5-nitriminotetrazolate salts the following conclusions can be drawn:

- 2-Methyl-5-nitriminotetrazole can be easily deprotonated in aqueous solution using alkali hydroxides forming the corresponding alkali salts in nearly quantitative yields. These form the silver salt by the reaction with AgNO_3 in aqueous solutions.
- The nitrogen-rich 2-methyl-5-nitriminotetrazolate salts **2–7** can easily be obtained via Brønstedt acid-base reactions using the guanidinium carbonates or metathesis reactions using silver 2-methyl-5-nitriminotetrazolate and the guanidinium chlorides in aqueous solution with high yields and good purity. The triaminoguanidinium salt **5** was synthesized via the hydrazinolysis of the aminoguanidinium salt **3**. The products can be recrystallized from water/ethanol mixtures resulting in colorless crystals.
- The crystal structures of **2–7** were determined using low temperature single crystal diffraction.
- A comprehensive characterization of the physico-chemical properties and sensitivities of **2–7** is given. Although the salts are energetic materials with high nitrogen contents, they show good stabilities towards friction and impact and a good thermal stability.
- Promising detonation parameters were calculated for **2–7** compared to common explosives like TNT and RDX. The performance (calculated values: $p_{\text{CJ}} = 277$ kbar; $v_d = 8827$ m s $^{-1}$) of triaminoguanidinium 2-methyl-5-nitriminotetrazolate (**7**) qualifies it for further investigations concerning military applications.

Acknowledgment

Financial support of this work by the Ludwig-Maximilian University of Munich (LMU), the European Research Office (ERO) of the U.S. Army Research Laboratory (ARL), the Armament Research, Development and Engineering Center (ARDEC) and the Strategic Environmental Research and Development Program (SERDP) under contract nos. W911NF-09-2-0018 (ARL), W911NF-09-1-0120 (ARDEC), W011NF-09-1-0056 (ARDEC) and 10 WPSEED01-002 / WP-1765 (SERDP) is gratefully acknowledged. The authors acknowledge collaborations with Dr. Mila Krupka (OZM Research, Czech Republic) in the development of new testing and evaluation methods for energetic materials and with Dr. Muhamed Sucasca (Brodarski Institute, Croatia) in the development of new computational codes to predict the detonation and propulsion parameters of novel explosives. We are indebted to and thank Drs. Betsy M. Rice and Brad Forch (ARL, Aberdeen, Proving Ground, MD) and Mr. Gary Chen (ARDEC, Picatinny Arsenal, NJ) for many helpful and inspired discussions and support of our work.

References

- [1] (a) Klapötke, T. M.; in *Moderne Anorganische Chemie*, Riedel E., 3rd ed., Walter de Gruyter, Berlin, New York, **2007**, 99-104. (b) Singh, R. P.; Verma, R. D.; Meshri, D. T.; Shreeve, J. M. *Ang. Chem. Int. Ed.* **2006**, 45(22), 3584. (c) Chapman, R. D., in *High Energy Density Materials*, Klapötke T. M.; Springer, Berlin, Heidelberg, **2007**, 123-152.
- [2] Klapötke, T. M.; in *High Energy Density Materials*, Klapötke, T. M.; Springer, Berlin, Heidelberg, **2007**, 85-122.
- [3] Chavez, D. E.; Hiskey, M. A.; Gilardi, R. D. *Angew. Chem.* **2000**, 112, 1861; *Angew. Chem., Int. Ed.* **2000**, 39, 1791.
- [4] Hurley, M.; Klapötke, T. M.; *SERDP, Technical Symposium & Workshop*, **2007**, Dec 4-6, United States, Washington DC.
- [5] (a) Hammerl, A.; Hiskey, M. A.; Holl, G.; Klapötke, T. M.; Polborn, K.; Stierstorfer, J.; Weigand, J. J. *Chem. Mat.* **2005**, 17, 3784-3793. (b) Hammerl, A.; Holl, G.; Klapötke, T. M.; Meyer, P.; Nöth, H.; Piotrowski, H.; Warchhold, M. *Eur. J. Inorg. Chem.* **2004**, 4, 834-845. (c) Hammerl, A.; Klapötke, T. M.; Nöth, H.; Warchhold, M. *Inorg. Chem.* **2001**, 40, 3570-3575. (d) Klapötke, T. M.; Mayer, P.; Schulz, A.; Weigand, J. J. *J. Am. Chem. Soc.* **2005**, 127, 2032-2033.
- [6] Klapötke, T. M.; Meyer, P.; Schulz, A.; Weigand, J. J. *Propellants, Explos., Pyrotech.* **2004**, 29(6), 325-332.
- [7] Ye, C.; Xiao, J.-C.; Twamley, B.; Shreeve, J. M. *Chem. Comm.* **2005**, 21, 2750-2752.
- [8] Galvez-Ruiz, J. C.; Holl, G.; Karaghiosoff, K.; Klapötke, T. M.; Löhnwitz, K.; Mayer, P.; Nöth, H.; Polborn, K.; Rohbogner, C. J.; Suter, M.; Weigand, J. J. *Inorg. Chem.* **2005**, 44(14), 4237-4253.
- [9] Xue, H.; Twamley, B.; Shreeve, J. M. *Inorg. Chem.* **2004**, 43(25), 7972-7977.
- [10] Klapötke, T. M.; Laub H. A.; Stierstorfer, J. *Propellants Explos. Pyrotech.* **2008**, 33, 421.
- [11] Klapötke, T. M.; Wallek A. U.; Stierstorfer J. *Chem. Mater.* **2008**, 20, 4519-4530.
- [12] (a) Fukumoto, S.; Imamiya, E.; Kusumoto, K.; Fujiwara, S.; Watanabe, T.; Shiraishi, M. *J. Med. Chem.* **2002**, 45 (14), 3009-3021. (b) Jedidi, I.; Therond, P.; Zarev, S.; Cosson, C.; Couturier, M.; Massot, C.; Jore, D.; Gardes-Albert, M.; Legrand, A.; Bonnefondt-Rousselot, D.; *Biochemistry* **2003**, 42 (38), 11356-11365. (c) Schug, K. A.; Lindner, W. *Chem. Rev.* **2005**, 105 (1), 67-114. (d) Nineham, A. W. *Chem. Rev.* **1955**, 55 (2), 355-483. (e) Brotherton, T. K.; Lynn, J. W. *Chem. Rev.* **1959**, 59 (5), 841-883. (f) Neutz, J.; Grosshardt, O.; Schäufele, S.; Schnuppler, H.; Schweikert, W. *Propellants, Explos., Pyrotech.* **2003**, 28 (4), 181-188. (g) Wingborg, N.; Latypov, N. *Propellants, Explos., Pyrotech.* **2003**, 28 (6), 314-318.
- [13] CrysAlis CCD, Oxford Diffraction Ltd., Version 1.171.27p5 beta
- [14] CrysAlis RED, Oxford Diffraction Ltd., Version 1.171.27p5 beta
- [15] Altomare, A.; Cascarano, G.; Giacovazzo, C.; Guagliardi, A.; SIR-92, *J. Appl. Cryst.* **1993**, 26, 343.
- [16] Sheldrick, G. M. *SHELXS-97, Program for Crystal Structure Solution*, University of Göttingen, Germany **1997**.
- [17] Sheldrick, G. M. **1994**, Shelxl-97, Program for the Refinement of Crystal Structures. University of Göttingen, Germany.
- [18] Farrugia, L. J. *J. Appl. Cryst.* **1999**, 32, 837-838.

- [19] Spek, A. L. *PLATON, A Multipurpose Crystallographic Tool*, Utrecht, The Netherlands, **1999**.
- [20] SCALE3 ABSPACK – An Oxford Diffraction program, **2005** Oxford Diffraction Ltd.
- [21] Klapötke, T. M., Stierstorfer J. *Helv. Chim. Acta* **2007**, 90, 2132.
- [22] N=N values and N=N values from: International tables for X-ray crystallography; Kluwer Academic Publisher: Dordrecht, The Netherlands, **1992**, Vol. C.
- [23] Wiberg, N. in *Lehrbuch der Anorganischen Chemie / Holleman-Wiberg*, 101st ed., Walter de Gruyter, Berlin, **1995**, 1842.
- [24] Akella, A.; Keszler, D. A. *Acta Cryst.* **1994**, C50, 1974-1976.
- [25] Bryden, J. H. *Acta Cryst.* **1957**, 10, 677-680.
- [26] Henke, H.; Barnighausen H. *Acta Crystallogr.* **1972**, 28B, 1100.
- [27] Wiberg, N. in *Lehrbuch der Anorganischen Chemie / Holleman-Wiberg*, 102nd ed., Walter de Gruyter, Berlin, **2007**, 1842.
- [28] NATO standardization agreement (STANAG) on explosives, *impact sensitivity tests*, no. 4489, 1st ed., Sept. 17, 1999.
- [29] WIWEB-Standardarbeitsanweisung 4-5.1.02, Ermittlung der Explosionsgefährlichkeit, hier der Schlagempfindlichkeit mit dem Fallhammer, Nov. 8, **2002**.
- [30] <http://www.bam.de>
- [31] NATO standardization agreement (STANAG) on explosive, *friction sensitivity tests*, no. 4487, 1st ed., Aug. 22, **2002**.
- [32] WIWEB-Standardarbeitsanweisung 4-5.1.03, Ermittlung der Explosionsgefährlichkeit oder der Reibeempfindlichkeit mit dem Reibeapparat, Nov. 8, **2002**.
- [33] Impact: Insensitive > 40 J, less sensitive ≥ 35 J, sensitive ≥ 4 J, very sensitive ≤ 3 J; friction: Insensitive > 360 N, less sensitive = 360 N, sensitive < 360 N a. > 80 N, very sensitive ≤ 80 N, extreme sensitive ≤ 10 N; According to the UN Recommendations on the Transport of Dangerous Goods (+) indicates: not safe for transport.
- [34] <http://www.ozm.cz>
- [35] <http://www.linseis.com>
- [36] a) Sucéska, M., EXPLO5.V2, Computer program for calculation of detonation parameters, *Proc. of 32nd Int. Annual Conference of ICT*, July 3-6, Karlsruhe, German, **2001**, pp. 110-111. b) Sucéska, M., *Proc. of 30th Int. Annual Conference of ICT*, June 29-July 2, Karlsruhe, Germany, **1999**, 50/1.
- [37] Sucéska, M., *Propellants, Explos., Pyrotech.* **1991**, 16(4), 197-202.
- [38] a) Sućeska, M., *Materials Science Forum*, **2004**, 465-466, 325-330. b) Sućeska, M. *Propellants, Explos., Pyrotech.* **1999**, 24, 280-285. c) Hobbs, M. L.; Baer, M. R.; *Proc. of the 10th Symp. (International) on Detonation*, ONR 33395-12, Boston, MA, July 12-16, **1993**, p. 409.

N-Rich Salts of 2-Methyl-5-nitraminotetrazole: Secondary Explosives with Low Sensitivities[†]

Tobias Fendt, Niko Fischer, Thomas M. Klapötke,* and Jörg Stierstorfer

Energetic Materials Research, Department of Chemistry, University of Munich (LMU), Butenandtstrasse 5-13, D-81377, Germany

Received September 29, 2010

2-Methyl-5-nitraminotetrazole (**1**) was formed by nitration of 2-methyl-5-aminotetrazole. 2-Methyl-5-aminotetrazole was obtained by an improved synthesis starting from sodium 5-aminotetrazolate, which is methylated with dimethyl sulfate in dimethyl formamide giving 2-methyl-5-aminotetrazole in 29% yield. Nitrogen-rich salts such as guanidinium (**2**), 1-aminoguanidinium (**3**), 1,3-diamino-guanidinium (**4**), 1,3,5-triamino-guanidinium (**5**), azidoformamidinium (**6**), hydrazinium (**7**), diaminouronium 2-methyl-5-nitraminotetrazolate (**8**), as well as an urea adduct (**9**), were prepared by facile deprotonation or metathesis reactions. Diaminourrea was synthesized by hydrazinolysis of dimethyl carbonate with hydrazine hydrate. All compounds were fully characterized by vibrational spectroscopy (IR and Raman), multinuclear NMR spectroscopy, elemental analysis, and differential scanning calorimetry (DSC) measurements. The crystal structures of **2–6**, **8**, and **9** could be determined using single crystal X-ray diffraction. The heats of formation of **2–9** were calculated using the atomization method based on CBS-4M enthalpies. With these values and the experimental (X-ray) densities several detonation parameters such as the detonation pressure, velocity, energy, and temperature were computed using the EXPLO5 code. In addition, the sensitivities toward impact, friction, and electrical discharge were tested using the BAM drop hammer, BAM friction tester, as well as a small scale electrical discharge device.

Introduction

The development of new high-energy-density materials (HEDMs)¹ with improved performance and decreased sensitivity is one of the main goals in our research group.² Generally, the class of HEDMs is divided into two main groups, according to their different applications in military and civil sectors. These main groups are explosives and propellants. Because of their qualification profile the materials have to meet specific characteristics. Important criteria for the group of explosives are the detonation velocity V_{det} and the detonation pressure p_{CJ} . Thereby the focus lies on the synthesis of compounds which feature values as high as possible for both magnitudes to reach maximum performance. Another critical parameter is the density ρ of the explosive, because the detonation pressure is directly proportional to the squared

density ρ^2 . In contrast the detonation velocity depends on the molar quantity N of formed gaseous products and also on the density. Also high, endothermic heats of formation ($\Delta_f H^\circ$) are required for effective energetic materials.³ Unfortunately, performance and sensitivity are often mutually exclusive parameters. Moreover, the new explosive should be cheap to synthesize, stable toward temperature, storable for long periods, and of course safe to handle. One way of counteracting the mutual exclusivity between sensitivity and performance is the use of systems with great possibility to form hydrogen bonds, which stabilize the material. In this regard, nitrogen-rich compounds will have many electronegative atoms available for hydrogen bonding and azole- (in particular tetrazole)-based energetic materials have attracted considerable attention since they tend to show a good compromise between high energy content, high chemical/thermal stability, and low sensitivity. Also increasing environmental concerns over the past few years raised the requirements of HEDMs, and new replacements for the commonly used toxic RDX are wanted.⁴ Therefore explosives containing high nitrogen contents are in the focus because of the

[†] Dedicated to Prof. Dr. Hansgeorg Schnöckel on the Occasion of His 70th Birthday

*To whom correspondence should be addressed. E-mail: tmk@cup.uni-muenchen.de. Phone: +49 2180 77491. Fax: +49 2180 77492.

(1) (a) Klapötke, T. M. In *Moderne Anorganische Chemie*, 3rd ed.; Riedel, E., Ed.; Walter de Gruyter: Berlin, Germany, 2007; pp 99–104. (b) Singh, R. P.; Verma, R. D.; Meshri, D. T.; Shreeve, J. M. *Angew. Chem., Int. Ed.* **2006**, 45(22), 3584. (c) Chapman, R. D. In *High Energy Density Materials*; Klapötke, T. M., Ed.; Springer: Berlin, Germany, 2007; pp 123–152.

(2) Klapötke, T. M. In *High Energy Density Materials*; Klapötke, T. M., Ed.; Springer: Berlin, Germany, 2007; pp 85–122.

(3) Chavez, D. E.; Hiskey, M. A.; Gilardi, R. D. *Angew. Chem.* **2000**, 112, 1861. Chavez, D. E.; Hiskey, M. A.; Gilardi, R. D. *Angew. Chem., Int. Ed.* **2000**, 39, 1791.

(4) Hurley, M.; Klapötke, T. M. *SERDP, Technical Symposium & Workshop*, Dec 4–6, 2007, Washington, DC.

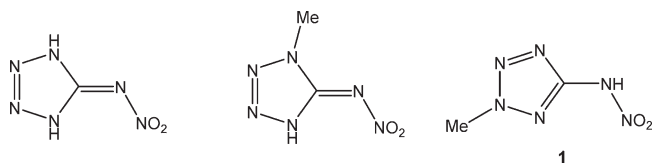


Figure 1. 5-Nitriminotetrazole, 1-methyl-5-nitriminotetrazole, and 2-methyl-5-nitraminotetrazole.

environmentally benign dinitrogen N_2 molecule as the main reaction product.⁵ To prepare new energetic materials often tetrazoles,⁶ tetrazolates,⁷ and tetrazolium^{8,9} salts are used since they are mostly endothermic compounds with a high nitrogen content. In addition, these compounds are considered mostly less toxic, easy to handle because of their high kinetic and thermal stability, and easy to prepare. A disadvantage of tetrazolates and tetrazolium compounds is the possible contamination of groundwater since these ionic structures feature a high solubility. On the other side, they show mostly high densities and stabilities based on their lattice energy. Therefore, formation of ionic structures is a popular approach for the synthesis of new energetic materials. It is hard to fulfill all requirements for new energetic materials. However, the compounds described in this work are N-rich salts of 2-methyl-5-nitraminotetrazole (**1**). In accordance to its 1-substituted sister compound, it serves, if deprotonated, as a valuable energetic anion, because of the combination of the nitrogen-rich backbone as a fuel and the nitramine group as an oxidizer. Nitramine moieties are often used in the synthesis of new energetic materials since they increase the oxygen balance of the molecule and therefore lead to a better performance.^{10–14} The methyl group attached to the tetrazole ring system lowers the sensitivity in comparison to non-methylated 5-nitriminotetrazole (Figure 1).

Furthermore, deprotonation of **1** affords more suitable compounds with higher decomposition temperatures compared to protonated **1**. For this reason 2-methyl-5-nitraminotetrazolate anions are convenient components for new ionic energetic materials. According to the performance in energetic salts the same requirements have to be

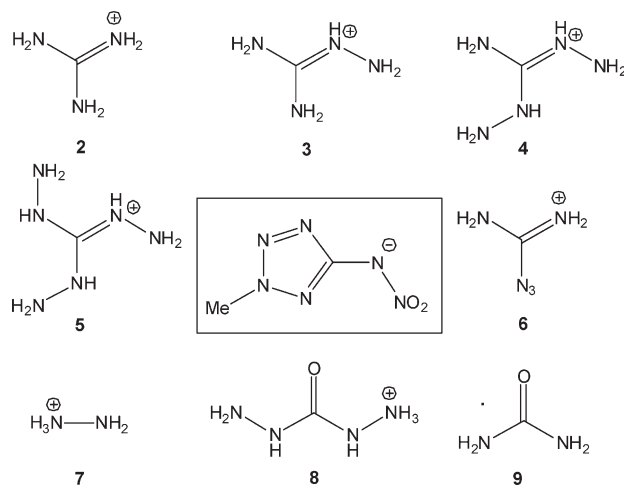


Figure 2. Target molecules presented in this work: guanidinium 2-methyl-5-nitraminotetrazolate (**2**), 1-aminoguanidinium 2-methyl-5-nitraminotetrazolate (**3**), 1,3-diaminoguanidinium 2-methyl-5-nitraminotetrazolate (**4**), 1,3,5-triaminoguanidinium 2-methyl-5-nitraminotetrazolate (**5**), azidoformamidinium 2-methyl-5-nitraminotetrazolate (**6**), hydrazinium 2-methyl-5-nitraminotetrazolate (**7**), diaminouronium 2-methyl-5-nitraminotetrazolate (**8**), and urea 2-methyl-5-nitraminotetrazolate (**9**).

applied for the cations of the energetic material. Besides the ammonium salt of 2-methyl-5-nitraminotetrazolate¹⁵ and the 2-methyl-5-*N*-(2-nitro-2-azapropyl)-nitraminotetrazole,¹⁰ to also mention a covalent derivative of 2-methyl-5-nitraminotetrazole, only very little about the chemistry of 2-methyl-5-nitraminotetrazole is known in the literature so far. In 2008, we reported on the synthesis and full characterization of nitrogen-rich salts of 1-methyl-5-nitriminotetrazole.¹⁶ Following this approach different nitrogen-rich salts of 2-methyl-5-nitraminotetrazole were synthesized and are presented in this work (Figure 2).

Experimental Section

Caution! 2-Methyl-5-nitriminotetrazole and its salts are energetic materials with increased sensitivities toward shock and friction. Therefore, proper security precautions (safety glass, face shield, earthened equipment and shoes, Kevlar gloves, and ear plugs) have to be applied while synthesizing and handling the described compounds. Specifically, compounds described having the azido group are extremely sensitive and have to be handled very carefully.

All chemicals and solvents were employed as received (Sigma-Aldrich, Fluka, Acros). 1H , ^{13}C , and ^{15}N NMR spectra were recorded using a JEOL Eclipse 270, JEOL EX 400 or a JEOL Eclipse 400 instrument. The chemical shifts quoted in parts per million (ppm) in the text refer to typical standards such as tetramethylsilane (1H , ^{13}C) and nitromethane (^{15}N). To determine the melting points of the described compounds a Linseis PT 10 DSC (heating rate $5^\circ C\ min^{-1}$) was used. Infrared spectra were measured using a Perkin-Elmer Spectrum One FT-IR spectrometer as KBr pellets. Raman spectra were recorded on a Bruker Multi-RAM Raman Sample Compartment D418 equipped with a Nd:YAG-Laser (1064 nm) and a LN-Ge diode as detector. Mass spectra of the described compounds were measured at a JEOL MStation JMS 700 using either DEI or FAB technique. To measure elemental analyses a Netsch STA 429 simultaneous thermal analyzer was employed.

(16) Klapötke, T. M.; Wallek, A. U.; Stierstorfer, J. *Chem. Mater.* **2008**, *20*, 4519–4530.

- (5) (a) Hammerl, A.; Hiskey, M. A.; Holl, G.; Klapötke, T. M.; Polborn, K.; Stierstorfer, J.; Weigand, J. J. *Chem. Mater.* **2005**, *17*, 3784–3793. (b) Hammerl, A.; Holl, G.; Klapötke, T. M.; Meyer, P.; Nöth, H.; Piotrowski, H.; Warchhold, M. *Eur. J. Inorg. Chem.* **2004**, *4*, 834–845. (c) Hammerl, A.; Klapötke, T. M.; Nöth, H.; Warchhold, M. *Inorg. Chem.* **2001**, *40*, 3570–3575. (d) Klapötke, T. M.; Mayer, P.; Schulz, A.; Weigand, J. J. *J. Am. Chem. Soc.* **2005**, *127*, 2032–2033.
- (6) Klapötke, T. M.; Meyer, P.; Schulz, A.; Weigand, J. J. *Propellants, Explos., Pyrotech.* **2004**, *29*(6), 325–332.
- (7) Ye, C.; Xiao, J.-C.; Twamley, B.; Shreeve, J. M. *Chem. Commun.* **2005**, *21*, 2750–2752.
- (8) Galvez-Ruiz, J. C.; Holl, G.; Karaghiosoff, K.; Klapötke, T. M.; Löhnwitz, K.; Mayer, P.; Nöth, H.; Polborn, K.; Rohbogner, C. J.; Suter, M.; Weigand, J. J. *Inorg. Chem.* **2005**, *44*(14), 4237–4253.
- (9) Xue, H.; Twamley, B.; Shreeve, J. M. *Inorg. Chem.* **2004**, *43*(25), 7972–7977.
- (10) Fischer, N.; Karaghiosoff, K.; Klapötke, T. M.; Stierstorfer, J. Z. *Anorg. Allg. Chem.* **2010**, *636*, 735–749.
- (11) Fischer, N.; Klapötke, T. M.; Stierstorfer, J. Z. *Anorg. Allg. Chem.* **2009**, *635*, 271–281.
- (12) Holl, G.; Karaghiosoff, K.; Klapötke, T. M.; Michailowski, A. *Acta Crystallogr., Sect. C* **2002**, *58*(9), 580–581.
- (13) Boese, R.; Hammerl, A.; Harris, K.; Klapötke, T. M. *Cent. Eur. J. Energ. Mater.* **2005**, *2*(2), 29–44.
- (14) Klapötke, T. M.; Krumm, B.; Steemann, F. X. *Propellants, Explos., Pyrotech.* **2009**, *34*(1), 13–23.
- (15) Klapötke, T. M.; Laub, H. A.; Stierstorfer, J. *Propellants, Explos., Pyrotech.* **2008**, *33*, 421.

Diaminourea, 2-methyl-5-nitraminotetrazole as well as its potassium salt were prepared according to literature.^{17–19} Azidoformamidinium chloride was prepared by the reaction of aminoguanidinium chloride with 1 equiv of NaNO₂ and HCl, followed by a recrystallization from water/ethanol. Aminoguanidinium chloride was synthesized by neutralization of commercially available aminoguanidinium bicarbonate with 2 N hydrochloric acid followed by recrystallization from water/ethanol. 5-Aminotetrazole, guanidinium carbonate, aminoguanidinium bicarbonate, as well as diaminoguanidinium chloride, were used as commercially available.

2-Methyl-5-aminotetrazole. 5-Aminotetrazole (15.3 g, 180 mmol) is dissolved in a solution containing sodium hydroxide (7.20 g, 180 mmol) in approximately 200 mL of water. The solvent is removed in vacuum, and the residue is suspended in 200 mL of dimethyl formamide. The mixture is heated to reflux and dimethyl sulfate (11.4 g, 90 mmol) is added dropwise to the refluxing suspension by means of a dropping funnel within 15 min. The mixture is then refluxed for 4 h, and then 100 mL of water is added. After being further refluxed for 1 h, the solvent is removed in vacuum, and the residue is extracted with a mixture of ethanol and acetone (1:1 v/v). The combined filtrates are evaporated, and 2-methyl-5-aminotetrazole is extracted from the mixture of isomers with boiling benzene. The benzene is removed from the filtrates in vacuum, and the crude material can be recrystallized from the same solvent to give 2-methyl-5-aminotetrazole in 29% (5.20 g, 52 mmol) yield.

¹H NMR (DMSO-*d*₆, 25 °C, ppm) δ : 5.92 (s, 2H, NH₂), 4.06 (CH₃); ¹³C NMR (DMSO-*d*₆, 25 °C, ppm) δ : 167.7 (CN₄), 39.4 (CH₃).

Guanidinium-2-methyl-5-nitraminotetrazolate (2). 2-Methyl-5-nitraminotetrazole (1.44 g, 10 mmol) is suspended in a few milliliters of water, and a suspension of guanidinium carbonate (0.90 g, 5 mmol) in water is added slowly. The mixture is heated to 40 °C and then filtrated. The solvent is removed in vacuum, and the residue recrystallized from ethanol. Yield: 1.73 g (8.52 mmol, 85%).

DSC (5 °C min⁻¹, °C): 176 °C (m.p.), 212 °C (dec.); IR (KBr, cm⁻¹): $\tilde{\nu}$ = 3423 (s), 3342 (s), 3276 (s, br), 3173 (s), 2790 (m), 1927 (w), 1694 (vs), 1662 (s), 1488 (s), 1422 (s), 1355 (s), 1217 (m), 1099 (m), 1037 (m), 990 (w), 893 (w), 766 (w), 632 (m, br), 528 (m); Raman (1064 nm, 500 mW, 25 °C, cm⁻¹): $\tilde{\nu}$ = 3202 (2), 2963 (9), 1490 (100), 1404 (6), 1375 (4), 1339 (3), 1224 (4), 1101 (2), 1039 (36), 1015 (45), 896 (2), 743 (5), 705 (8), 539 (4), 450 (9), 398 (4), 349 (3), 207 (5), 145 (3), 129 (15), 91 (31); ¹H NMR (DMSO-*d*₆, 25 °C, ppm) δ : 7.03 (s, 6H, NH₂), 4.20 (CH₃); ¹³C NMR (DMSO-*d*₆, 25 °C, ppm) δ : 168.4 (CN₄), 158.6 (C(NH₂)₃), 39.7 (CH₃); *m/z* (FAB⁺): 60.1 [C(NH₂)₃⁺]; *m/z* (FAB⁻): 143.0 [2-Me-ATNO₂⁻]; EA (C₃H₉N₅O₂, 203.16): calcd: C 17.74, H 4.47, N 62.05%; found: C 17.86, H 4.84, N 61.39%; BAM drophammer: 30 J; friction tester: 192 N; ESD: 0.2 J.

Aminoguanidinium-2-methyl-5-nitraminotetrazolate (3). 2-Methyl-5-nitraminotetrazole (4.32 g, 30 mmol) is suspended in a few milliliters of water, and then a suspension of aminoguanidinium bicarbonate (4.08 g, 30 mmol) in water is added slowly. The mixture is heated to 40 °C and then filtrated. The solvent is removed in vacuum, and the residue then recrystallized from an ethanol/water mixture to yield 5.24 g (24.0 mmol, 80%).

DSC (5 °C min⁻¹, °C): 146 °C (m.p.), 210 °C (dec.); IR (KBr, cm⁻¹): $\tilde{\nu}$ = 3463 (s), 3336 (s, br), 3238 (s, br), 3113 (s, br), 2831 (m), 2426 (m), 2237 (m), 1950 (w), 1927 (w), 1840 (w), 1776 (w), 1693 (s), 1639 (s), 1598 (m), 1548 (m), 1488 (s), 1401 (vs), 1374 (s), 1358 (s), 1337 (s), 1278 (s), 1221 (s), 1184 (m), 1099 (s), 1061 (s), 1037 (s), 893 (m), 760 (m), 706 (m), 557 (s); Raman (1064 nm,

500 mW, 25 °C, cm⁻¹): $\tilde{\nu}$ = 2963 (3), 1491 (100), 1404 (5), 1372 (2), 1346 (2), 1221 (3), 1039 (15), 1011 (26), 962 (5), 895 (3), 740 (4), 703 (6), 529 (3), 446 (4), 405 (3), 345 (3), 200 (5), 141 (3), 113 (22), 83 (13); ¹H NMR (DMSO-*d*₆, 25 °C, ppm) δ : 7.34 (s, 5H, C–NH₂, NH–NH₂), 4.70 (s, 2H, NH₂NH), 4.20 (CH₃); ¹³C NMR (DMSO-*d*₆, 25 °C, ppm) δ : 168.4 (CN₄), 159.4 (C(NH–NH₂)(NH₂)₂), 39.7 (CH₃); *m/z* (FAB⁺): 75.1 [C(NHNH₂)(NH₂)₂⁺]; *m/z* (FAB⁻): 143.0 [2-MeATNO₂⁻]; EA (C₃H₁₀N₁₀O₂, 218.18): calcd: C 16.52, H 4.62, N 64.20%; found: C 16.73, H 5.01, N 63.88%; BAM drophammer: 6 J; friction tester: 120 N; ESD: 0.2 J.

Diaminoguanidinium-2-methyl-5-nitraminotetrazolate (4). 2-Methyl-5-nitraminotetrazole (1.98 g, 13.74 mmol) is dissolved in a solution of potassium hydroxide in 20 mL of water and an aqueous solution of silver nitrate (13.74 mmol, 2.33 g) is added. The colorless and fluffy precipitate is filtered off and directly given to a solution of diaminoguanidinium chloride (1.73 g, 13.78 mmol) in 50 mL of water. The suspension is stirred under exclusion of light for 20 min, filtered off, and the solvent of the clear solution is removed in vacuo. The residue is recrystallized from ethanol. Yield: 1.98 g (8.49 mmol, 62%).

DSC (5 °C min⁻¹, °C): 138 °C (m.p.), 203 °C (dec.); IR (KBr, cm⁻¹): $\tilde{\nu}$ = 3457 (s), 3353 (s), 3310 (vs), 3098 (s), 2376 (w), 2284 (w), 2105 (w), 1990 (w), 1957 (w), 1679 (vs, br), 1639 (s), 1567 (m), 1545 (m), 1489 (s), 1385 (s), 1324 (s, br), 1276 (s), 1213 (s), 1182 (s), 1099 (s), 1037 (s), 976 (s), 890 (m), 773 (m), 756 (m), 744 (w), 706 (m), 673 (m), 562 (m), 468 (m); Raman (1064 nm, 500 mW, 25 °C, cm⁻¹): $\tilde{\nu}$ = 2956 (3), 1590 (100), 1443 (3), 1376 (4), 1216 (3), 1101 (4), 1038 (9), 1012 (39), 932 (3), 893 (4), 746 (9), 718 (6), 547 (3), 447 (5), 402 (3), 341 (6), 188 (7), 126 (4), 107 (5), 81 (42); ¹H NMR (DMSO-*d*₆, 25 °C, ppm) δ : 8.62 (s, 2H, NH–NH₂), 7.17 (s, 2H, C–NH₂), 4.58 (s, 4H, NH₂NH), 4.16 (CH₃); ¹³C NMR (DMSO-*d*₆, 25 °C, ppm) δ : 168.4 (CN₄), 160.3 (C(NH–NH₂)₂(NH₂)), 39.6 (CH₃); *m/z* (FAB⁺): 90.1 [C(NHNH₂)₂(NH₂)⁺]; *m/z* (FAB⁻): 143.0 [2-MeATNO₂⁻]; EA (C₃H₉N₉O₂, 203.16): calcd: C 15.45, H 4.75, N 66.07%; found: C 15.71, H 4.83, N 65.79%; BAM drophammer: 10 J; friction tester: 160 N; ESD: 0.16 J.

Triaminoguanidinium-2-methyl-5-nitraminotetrazolate (5). Aminoguanidinium 2-methyl-5-nitraminotetrazolate (1.89 g, 8.7 mmol) is suspended in 20 mL of 1,4-dioxane and hydrazine hydrate (0.96 g, 19.1 mmol) is added dropwise. The solution is heated to 90 °C for 5 h in a constant nitrogen flow. As soon as ammonia is no longer evolved from the reaction mixture, the solution is cooled down, and the solvent is removed in vacuum. The residue is recrystallized from ethanol to give 1.71 g (6.89 mmol, 88%).

DSC (5 °C min⁻¹, °C): 143 °C (m.p.), 188 °C (dec.); IR (KBr, cm⁻¹): $\tilde{\nu}$ = 3484 (s), 3336 (s, br), 3155 (s, br), 2950 (s), 2801 (s), 2670 (s), 2456 (s), 2379 (m), 2158 (m), 1667 (vs, br), 1595 (s, br), 1521 (m), 1484 (s), 1454 (s), 1321 (s), 1298 (s), 1235 (m), 1158 (s), 1120 (s), 1090 (s), 995 (s), 970 (s), 916 (m, br), 789 (s), 755 (m), 742 (s), 679 (s), 622 (s), 544 (s, br); Raman (1064 nm, 500 mW, 25 °C, cm⁻¹): $\tilde{\nu}$ = 3318 (6), 3218 (3), 2962 (3), 1545 (2), 1481 (100), 1449 (4), 1389 (9), 1360 (3), 1213 (3), 1131 (2), 1096 (3), 1061 (4), 1017 (50), 886 (7), 767 (6), 706 (8), 678 (2), 456 (4), 396 (8), 344 (2), 259 (3), 172 (4), 143 (13); ¹H NMR (DMSO-*d*₆, 25 °C, ppm) δ : 8.59 (s, 3H, NH–NH₂), 4.50 (s, 6H, NHNHNH₂), 4.18 (CH₃); ¹³C NMR (DMSO-*d*₆, 25 °C, ppm) δ : 168.8 (CN₄), 159.6 (C(NH–NH₂)₃), 39.6 (CH₃); *m/z* (FAB⁺): 105.1 [C(NHNH₂)₃⁺]; *m/z* (FAB⁻): 142.9 [2-MeATNO₂⁻]; EA (C₃H₁₂N₁₂O₂, 248.21): calcd: C 14.52, H 4.87, N 67.72%; found: C 14.85, H 4.94, N 67.38%; BAM drophammer: 6 J; friction tester: 120 N; ESD: 0.18 J.

Azidoformamidinium-2-methyl-5-nitraminotetrazolate (6). Potassium 2-methyl-5-nitraminotetrazolate (1.82 g, 10 mmol) was prepared by dissolving 2-methyl-5-nitraminotetrazole (1.44 g, 10 mmol) in a solution of potassium hydroxide (85%, 0.66 g, 10 mmol) in 20 mL of water. The resulting solution was added to a solution of silver nitrate (1.70 g, 10 mmol) in 10 mL of water, while the reaction vessel was kept in darkness. Silver

(17) Klapötke, T. M.; Stierstorfer, J. *Helv. Chim. Acta* **2007**, *90*, 2132–2150.

(18) Klapötke, T. M.; Radies, H.; Stierstorfer, J. *Z. Naturforsch.* **2007**, *62b*, 1343–1352.

(19) Li, Z.; Zhu, W.; Yu, J.; Ma, X.; Lu, Z.; Xiao, S. *Synth. Commun.* **2006**, *36*, 2613–2619.

2-methyl-5-nitraminotetrazolate precipitated instantaneously, the suspension was centrifuged, and the aqueous layer pipetted off. It was washed with three portions of water (50 mL each) and suspended in 25 mL of water afterward. Azidoformamidinium chloride (1.15 g, 9.5 mmol) was dissolved in 10 mL of water and added to the suspension. Silver chloride started to precipitate, and the suspension was stirred in darkness for further 30 min at 30 °C. The precipitate was filtered off, the water was removed in vacuo, and the remaining solid recrystallized from an ethanol/water mixture to yield 1.28 g (5.58 mmol, 56%) of azidoformamidinium 2-methyl-5-nitraminotetrazolate as colorless crystals.

DSC (5 °C min⁻¹, °C): 115 °C (m.p.), 148 °C (dec.); IR (KBr, cm⁻¹): $\tilde{\nu}$ = 3264 (m), 3029 (m), 2783 (w), 2446 (w), 2185 (vs), 2121 (w), 1931 (w), 1698 (s), 1476 (vs), 1401 (vs), 1366 (vs), 1337 (s), 1287 (m), 1232 (m), 1180 (w), 1120 (m), 1098 (m), 1035 (w), 909 (w), 880 (w), 841 (w), 773 (w), 764 (w), 748 (w), 704 (m), 690 (m), 677 (m), 536 (w), 509 (m), 481 (w); Raman (1064 nm, 500 mW, 25 °C, cm⁻¹): $\tilde{\nu}$ = 3034 (2), 2970 (14), 2185 (14), 2123 (3), 1473 (100), 1418 (10), 1360 (5), 1232 (3), 1183 (7), 1143 (5), 1123 (2), 1098 (2), 1026 (78), 911 (8), 883 (4), 765 (5), 708 (7), 510 (5), 484 (3), 464 (8), 395 (5), 321 (10), 214 (4); ¹H NMR (DMSO-*d*₆, 25 °C, ppm) δ : 6.40 (s, 4H, NH₂), 4.36 (s, 3H, CH₃); ¹³C NMR (DMSO-*d*₆, 25 °C, ppm) δ : 168.4 (CN₄), 158.7 (C(N₃)₂(NH₂)₂), 40.4 (CH₃); *m/z* (FAB⁺): 86.1 [C(N₃)(NH₂)₂]⁺; *m/z* (FAB⁻): 143.0 [2-MeATNO₂]⁻; EA (C₃H₇N₁₁O₂, 229.16): calcd: C 15.72, H 3.08, N 67.23%; found: C 15.72, H 3.10, N 67.03%; BAM drophammer: 3 J; friction tester: 72 N; ESD: 0.20 J.

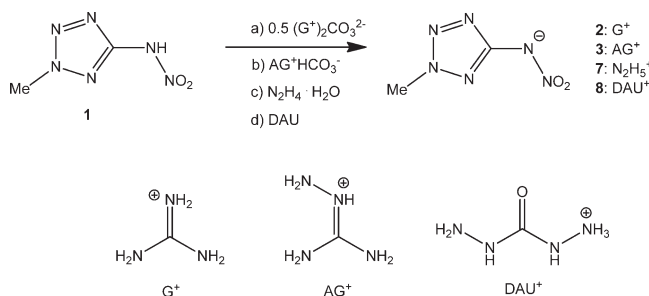
Hydrazinium 2-methyl-5-nitraminotetrazolate (7). 2-Methyl-5-nitraminotetrazole (1.44 g, 10 mmol) is suspended in a few milliliters of water, and hydrazine hydrate (0.50 g, 10 mmol) is added. The mixture is heated to 40 °C, the solvent of the clear solution is removed in vacuum, and the residue then recrystallized from an ethanol/water mixture. Yield: 1.62 g (9.20 mmol, 92%).

DSC (5 °C min⁻¹, °C): 73 °C (m.p.), 208 °C (dec.); IR (KBr, cm⁻¹): $\tilde{\nu}$ = 3407 (m), 3338 (m), 3063 (m), 2764 (w), 2646 (w), 1618 (w), 1532 (w), 1479 (vs), 1419 (m), 1393 (s), 1369 (m), 1355 (s), 1325 (s), 1274 (m), 1208 (m), 1130 (w), 1091 (m), 1044 (m), 1020 (w), 938 (m), 884 (m), 771 (w), 757 (w), 749 (w), 704 (m), 673 (w), 473 (w); Raman (1064 nm, 130 mW, 25 °C, cm⁻¹): $\tilde{\nu}$ = 3280 (3), 3040 (7), 3018 (4), 2962 (15), 2826 (2), 2694 (2), 2329 (3), 1981 (2), 1929 (2), 1628 (5), 1538 (2), 1480 (100), 1463 (11), 1392 (16), 1358 (5), 1217 (8), 1098 (3), 1079 (3), 1053 (6), 1031 (5), 1014 (87), 971 (7), 880 (3), 751 (16), 702 (14), 452 (13), 407 (7); ¹H NMR (DMSO-*d*₆, 25 °C, ppm) δ : 7.10 (s, 5H, NH₂, NH₃), 4.19 (CH₃); ¹³C NMR (DMSO-*d*₆, 25 °C, ppm) δ : 168.5 (CN₄), 39.7 (CH₃); *m/z* (FAB⁺): 33.1 [N₂H₅]⁺; *m/z* (FAB⁻): 143.0 [2-MeATNO₂]⁻; EA (C₂H₈N₈O₂, 176.14): calcd: C 13.64, H 4.58, N 63.62%; found: C 13.75, H 4.61, N 63.23%; BAM drophammer: 7 J; friction tester: 120 N; ESD: 0.1 J.

Diaminouronium 2-Methyl-5-nitriminotetrazolate (8). 2-Methyl-5-nitraminotetrazole (2.88 g, 20 mmol) is suspended in a few milliliters of water, and a solution of diaminourea (1.80 g, 20 mmol) in water is added. The solvent of the clear solution is removed in vacuum, and the residue then recrystallized from an ethanol/water mixture. Yield: 4.40 g (18.8 mmol, 94%).

DSC (5 °C min⁻¹, °C): 131 °C (m.p.), 195 °C (dec.); IR (KBr, cm⁻¹): $\tilde{\nu}$ = 3421 (m), 3324 (s), 3283 (s), 3043 (m), 2659 (w), 1708 (m), 1633 (s), 1465 (s), 1572 (m), 1552 (m), 1493 (vs), 1462 (m), 1430 (s), 1415 (s), 1384 (m), 1327 (s), 1311 (s), 1267 (m), 1209 (m), 1164 (m), 1096 (m), 1059 (m), 1035 (m), 979 (w), 887 (w), 767 (w), 756 (w), 741 (m), 704 (w), 678 (w), 637 (w), 560 (w), 516 (w); Raman (1064 nm, 130 mW, 25 °C, cm⁻¹): $\tilde{\nu}$ = 3325 (3), 3282 (9), 3224 (3), 3044 (9), 3022 (3), 2962 (18), 2839 (3), 1718 (2), 1634 (2), 1494 (100), 1463 (5), 1420 (4), 1368 (8), 1272 (2), 1211 (4), 1098 (2), 1059 (3), 1043 (6), 1014 (32), 889 (2), 758 (3), 742 (2), 702 (4), 455 (4), 407 (2), 223 (3); ¹H NMR (DMSO-*d*₆, 25 °C, ppm) δ : 7.60 (s, br, 7H, NH, NH₂, NH₃⁺), 4.19 (CH₃); ¹³C NMR (DMSO-*d*₆, 25 °C, ppm) δ : 167.8 (CN₄), 159.8 (C(O)(NH₂)₂), 39.8

Scheme 1. Syntheses of Compounds **2**, **3**, **7**, and **8** via Brønsted Acid-Base Reactions



(CH₃); *m/z* (FAB⁺): 90.1 [C(O)(NH₂)₂(NH₂)₂]⁺; *m/z* (FAB⁻): 143.0 [2-MeATNO₂]⁻; EA (C₃H₁₀N₁₀O₃, 223.18): calcd: C 15.39, H 4.30, N 59.81%; found: C 15.41, H 4.16, N 59.51%; BAM drophammer: 5 J; friction tester: 168 N; ESD: 0.5 J.

Urea 2-methyl-5-nitraminotetrazole (9). 2-Methyl-5-nitraminotetrazole (1.44 g, 10 mmol) is suspended in a few milliliters of water, and a solution of urea (0.60 g, 10 mmol) in water is added. The solvent of the clear solution is removed in vacuum, and the residue then recrystallized from an ethanol/water mixture. Yield: 1.95 g (9.55 mmol, 96%).

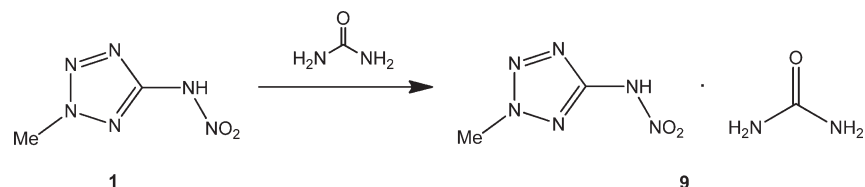
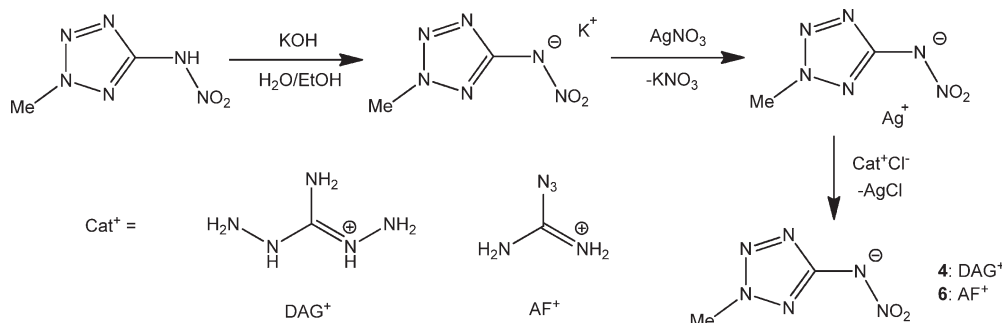
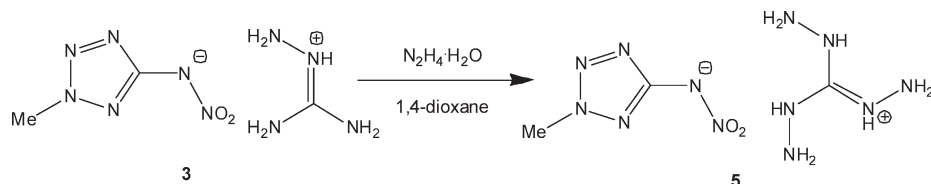
DSC (5 °C min⁻¹, °C): 158 °C (dec 1), 190 °C (dec 2); IR (KBr, cm⁻¹): $\tilde{\nu}$ = 3437 (s, br), 3346 (s, br), 2804 (w), 2642 (w), 2184 (w), 1670 (vs, br), 1465 (s), 1384 (m), 1330 (m), 1279 (m), 1209 (m), 1153 (m), 1050 (m), 1016 (m), 863 (w), 787 (w), 736 (m), 618 (w), 573 (m), 558 (m); Raman (1064 nm, 130 mW, 25 °C, cm⁻¹): $\tilde{\nu}$ = 3437 (2), 3329 (8), 3239 (4), 3124 (2), 2967 (6), 2330 (3), 2130 (1), 1650 (6), 1626 (2), 1538 (11), 1363 (3), 1281 (3), 1176 (5), 1047 (2), 1011 (100), 698 (4), 548 (17), 432 (2), 370 (2), 329 (1), 132 (17), 102 (74), 84 (5); ¹H NMR (DMSO-*d*₆, 25 °C, ppm) δ : 6.99 (s, 1H, NH), 5.78 (s, 4H, NH₂), 4.30 (CH₃); ¹³C NMR (DMSO-*d*₆, 25 °C, ppm) δ : 160.7 (C(O)(NH₂)₂), 158.6 (CN₄), 40.6 (CH₃); *m/z* (FAB⁺): 60.1 [C(O)(NH₂)₂]⁺; *m/z* (FAB⁻): 143.0 [2-MeATNO₂]⁻; EA (C₃H₈N₈O₃, 204.15): calcd: C 17.65, H 3.95, N 54.89%; found: C 17.96, H 4.25, N 54.44%; BAM drophammer: 10 J; friction tester: 288 N; ESD: 0.2 J.

Results and Discussion

Synthesis. The synthesis of 2-methyl-5-aminotetrazole has always been a limiting step in the chemistry dealing with 2-methyl-5-aminotetrazole and 2-methyl-5-nitraminotetrazole because of the very low yield of the methylation reaction of 5-aminotetrazole. Henry et al. reported on a synthesis in 1954 doing the methylation with dimethyl sulfate in aqueous medium.²⁰ This reaction affords 2-methyl-5-aminotetrazole in only 5% yield as a byproduct beside 1-methyl-5-aminotetrazole being the main product. Switching the solvent of the reaction to higher boiling dimethyl formamide allows higher reaction temperatures and therefore the reaction is driven toward the thermodynamic product 2-methyl-5-aminotetrazole, which then can be isolated in up to 29% yield. This makes compounds based on 2-methyl-5-aminotetrazole and especially 2-methyl-5-nitraminotetrazole much more interesting for applications not only as energetic materials but also in coordination chemistry.

Scheme 1 shows the synthesis of the guanidinium (**2**), 1-aminoguanidinium (**3**), hydrazinium (**7**), and diaminouronium salt (**8**) of 2-methyl-5-nitraminotetrazole (**1**). All synthetic routes shown are based on simple Brønsted acid–base reactions. **2** and **3** were formed by reacting the

(20) Henry, R. A.; Finnegan, W. G. *J. Am. Chem. Soc.* **1954**, *76*, 923–926.

Scheme 2. Formation of the Urea Adduct **9****Scheme 3.** Synthetic Routes to **4** and **6** via Silver 2-Methyl-5-nitraminotetrazolate**Scheme 4.** Synthesis of **5** via Hydrazinolysis of **3**

free acid **1** with guanidinium carbonate and aminoguanidinium bicarbonate, respectively, whereas the formation of gaseous CO_2 , which can be expelled from the reaction mixture by moderate warming of the solutions, is utilized. The hydrazinium salt (**7**) and the diaminouronium salt (**8**) are synthesized by the reaction of **1** with the free bases hydrazine and diaminourea (DAU) respectively in aqueous solution.

The basicity of urea is not high enough to deprotonate **1** in aqueous solution; hence, the urea adduct **9** is a cocrystallization product, which was obtained by the reaction of **1** with an aqueous solution of urea. (Scheme 2)

The reaction products 1,3-diaminoguanidinium 2-methyl-5-nitraminotetrazolate (**4**) and azidoformamidinium 2-methyl-5-nitraminotetrazolate (**6**) were obtained by metathesis reactions using silver 2-methyl-5-nitraminotetrazolate as an intermediate. It was prepared from potassium 2-methyl-5-nitraminotetrazolate and silver nitrate in aqueous solution and after being separated from the reaction mixture as poorly soluble white salt, it was further reacted with diaminoguanidinium chloride and azidoformamidinium chloride respectively, which was prepared by the reaction of aminoguanidinium chloride with 1 equiv of NaNO_2 and HCl , followed by a recrystallization from water/ethanol to yield the above-described salts **4** and **6**. The synthetic routes to **4** and **6** are depicted in Scheme 3.

For the synthesis of the triaminoguanidinium 2-methyl-5-nitraminotetrazolate (**5**), the hydrazinolysis reaction of the aminoguanidinium salt **3** was employed. Therefore **3** was heated with hydrazine hydrate in 1,4-dioxane under

the release of ammonia. The reaction procedure is shown in Scheme 4.

Beside from the synthetic routes to the compounds **2–6**, that are shown above, a different way via the potassium salt of **1** and the corresponding guanidinium perchlorates and azidoformamidinium perchlorate, respectively, can be considered, where the reaction is driven by the low solubility of potassium perchlorate. Although this route seems to be more practicable than the syntheses that involve intermediates like silver salts, that have to be isolated first, appropriate safety measures have to be applied because of the high sensitivity of the guanidinium and azidoformamidinium perchlorates used as starting material.

Molecular Structures. To determine the molecular structures of **2–6**, **8**, and **9** in the crystalline state an Oxford Xcalibur3 diffractometer with a Spellman generator (voltage 50 kV, current 40 mA) and a KappaCCD detector were used. The data collection was performed using the CrysAlis CCD software,²¹ and the data reductions were performed with the CrysAlis RED software.²² The solution of all structures were performed using SIR-92,²³ SHELXS-97²⁴ and SHELXL-97²⁵ implemented in the WinGX software

(21) *CrysAlis CCD*, Version 1.171.27p5 beta; Oxford Diffraction Ltd.: Abingdon, U.K.

(22) *CrysAlis RED*, Version 1.171.27p5 beta; Oxford Diffraction Ltd.: Abingdon, U.K.

(23) *SIR-92*; Altomare, A.; Casciarano, G.; Giacovazzo, C.; Guagliardi, A.; *J. Appl. Crystallogr.* **1993**, *26*, 343.

(24) Sheldrick, G. M. *SHELXS-97, Program for Crystal Structure Solution*; University of Göttingen: Göttingen, Germany, 1997.

Table 1. X-ray Data and Parameters

	2	3	4	5	6	8	9
formula	C ₃ H ₉ N ₉ O ₂	C ₃ H ₁₀ N ₁₀ O ₂	C ₃ H ₁₁ N ₁₁ O ₂	C ₃ H ₁₂ N ₁₂ O ₂	C ₃ H ₇ N ₁₁ O ₂	C ₃ H ₁₀ N ₁₀ O ₃	C ₃ H ₈ N ₈ O ₃
fw [g mol ⁻¹]	203.16	218.21	234.24	248.25	229.20	234.21	204.17
space group	<i>P</i> 2 ₁	<i>P</i> $\bar{1}$	<i>P</i> 2 ₁ / <i>c</i>	<i>P</i> $\bar{1}$	<i>P</i> 2 ₁ / <i>n</i>	<i>P</i> 2 ₁ / <i>c</i>	<i>P</i> 2 ₁ / <i>n</i>
<i>a</i> [Å]	3.6562(3)	3.7828(4)	17.4021(14)	6.9170(4)	7.6150(10)	4.1035(3)	7.5867(5)
<i>b</i> [Å]	8.1552(8)	8.5095(8)	8.3403(7)	7.5831(5)	13.7932(14)	27.597(3)	7.3684(7)
<i>c</i> [Å]	13.9458(11)	14.1651(14)	14.7111(13)	11.0147(7)	9.5095(10)	8.1745(5)	15.3282(9)
α [deg]	90	91.281(8)	90	97.315(5)	90	90	90
β [deg]	95.919 (8)	95.299(8)	111.581(9)	106.030(5)	103.988(14)	103.105(7)	95.764(6)
γ [deg]	90	96.743(8)	90	104.979(5)	90	90	90
<i>V</i> [Å ³]	413.61(6)	450.63(8)	1985.5(3)	523.99(6)	969.2(2)	901.61(13)	852.54(11)
<i>Z</i>	2	2	8	2	4	4	4
ρ_{calc} [g cm ⁻³]	1.632	1.608	1.567	1.573	1.571	1.725	1.591
μ [mm ⁻¹]	0.136	0.134	0.065	0.131	0.132	0.148	0.138
<i>F</i> (000)	212	228	488	260	472	488	424
$\lambda_{\text{MoK}\alpha}$ [Å]	0.7107(3)	0.7107(3)	0.7107(3)	0.7107(3)	0.7107(3)	0.7107(3)	0.7107(3)
<i>T</i> [K]	200(2)	173(2)	173(2)	173(2)	173(2)	173(2)	173(2)
θ min-max [deg]	4.41, 28.29	4.34, 32.36	4.24, 33.41	4.20, 32.35	4.26, 28.78	4.5, 27.0	4.17, 28.76
data set	-4:3; -4:10; -17:16	-4:4; -10:8; -16:17	-19:21; -7:10; -15:18	-8:8; -9: 9; -13: 13	-9:5; -15:16; -10:11	-5:4; -13:34; -8:10	-9:6; -9:5; -15:18
refl. coll./ unique	1703/988	3303/1768	5007/1948	5352/2062	3581/1797	3466/1926	3063/1611
<i>R</i> _{int}	0.028	0.024	0.025	0.018	0.027	0.017	0.029
parameters	151	176	189	202	173	185	159
<i>R</i> ₁ (obs)	0.0371	0.0320	0.0328	0.0289	0.0352	0.0539	0.0375
<i>wR</i> ₂ (all data)	0.0767	0.0710	0.0759	0.0773	0.0700	0.1419	0.0856
GoF	0.92	0.83	0.90	1.04	0.82	1.11	0.88
resd. dens. [e/ Å ³]	-0.24, 0.26	-0.22, 0.15	-0.12, 0.08	-0.23, 0.17	-0.21, 0.18	-0.84, 1.03	-0.22, 0.21
CCDC	783134	783137	783138	783135	783139	783140	783136

package,²⁶ and finally checked with the PLATON software.²⁷ In all crystal structures the hydrogen atoms were located and refined. The absorptions were corrected with the SCALE3 ABSPACK multiscan method.²⁸ Selected data and parameter of the X-ray determinations are given in Table 1.

2-Methyl-5-nitraminotetrazole and its crystal structure was recently investigated and published by our research group.¹⁷ Its structure is different compared to the molecular structures of the anions in the investigated 2-methyl-5-nitraminotetrazolate salts. The position of the nitramine group relative to the tetrazole ring plane differs significantly since there are various hydrogen bonds influencing this building block.

Compounds **2**–**6**, **8**, and **9** (Figures 3–10) crystallize in the monoclinic and triclinic space groups *P*2₁ (**2**), *P* $\bar{1}$ (**3** and **5**), *P*2₁/*c* (**4** and **8**), and *P*2₁/*n* (**6** and **9**) with densities lying in a range from 1.567 g cm⁻³ (**4**) to 1.632 g cm⁻³ (**2**). The bond distances between N1, N2, N3, and N4 vary from 1.30 to 1.33 Å, which fits between the bond lengths of a N–N single bond (1.45 Å) and an N=N double bond (1.25 Å).²⁹ The torsion angles C1–N2–N3–N4 are close to 0° (0.3(3)° for **2** to -0.24(14)° for **5**) implying a π -aromatic system. Also, the bond lengths C1–N1 and C1–N4 are located between the bond lengths of a C–N single (1.47 Å) and a C=N double bond (1.22 Å),³⁰

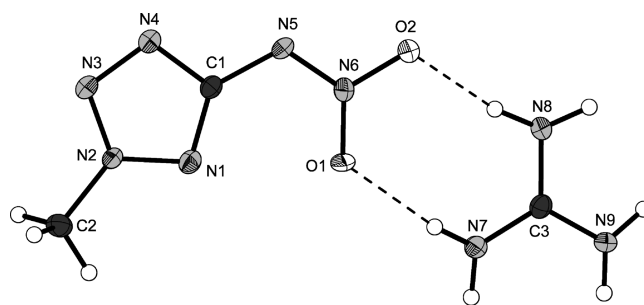


Figure 3. Molecular structure of guanidinium 2-methyl-5-nitraminotetrazolate (**2**). Thermal ellipsoids represent the 50% probability level.

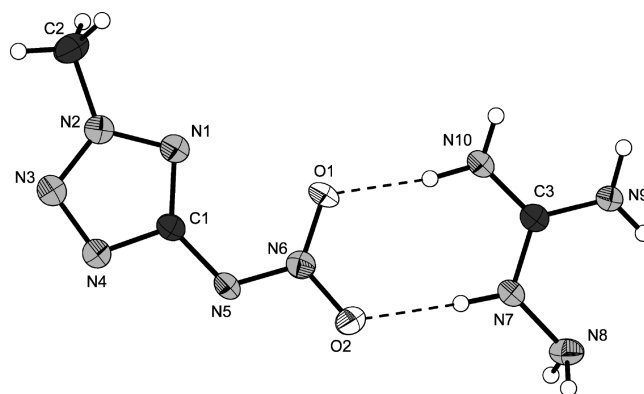


Figure 4. Molecular structure of aminoguanidinium 2-methyl-5-nitraminotetrazolate (**3**). Thermal ellipsoids represent the 50% probability level.

whereas the distance between N2 and the exocyclic carbon atom C2 is in the range of a C–N single bond (1.452(2) (**3**) to 1.462(4) (**2**)). The nitro group of the nitramine unit is more or less strongly twisted out of the tetrazole ring plane indicated by a N1–C1–N5–N6 torsion angle between -1.2(5)° for **2** and up to 30.3(2)° for the triaminoguanidinium salt **5**. The distances between

(25) Sheldrick, G. M. *SHELXL-97, Program for the Refinement of Crystal Structures*; University of Göttingen: Göttingen, Germany, 1994.

(26) Farrugia, L. J. *J. Appl. Crystallogr.* **1999**, *32*, 837–838.

(27) Spek, A. L. *PLATON, A Multipurpose Crystallographic Tool*; Utrecht University: Utrecht, The Netherlands, 1999.

(28) *SCALE3 ABSPACK—An Oxford Diffraction program*; Oxford Diffraction Ltd.: Abingdon, U.K., 2005.

(29) N–N values and N=N values from: International tables for X-ray crystallography; Kluwer Academic Publisher: Dordrecht, The Netherlands, 1992; Vol. C.

(30) Wiberg, N. In *Lehrbuch der Anorganischen Chemie/Holleman-Wiberg*, 101st ed.; Walter de Gruyter: Berlin, Germany, 1995; p 1842.

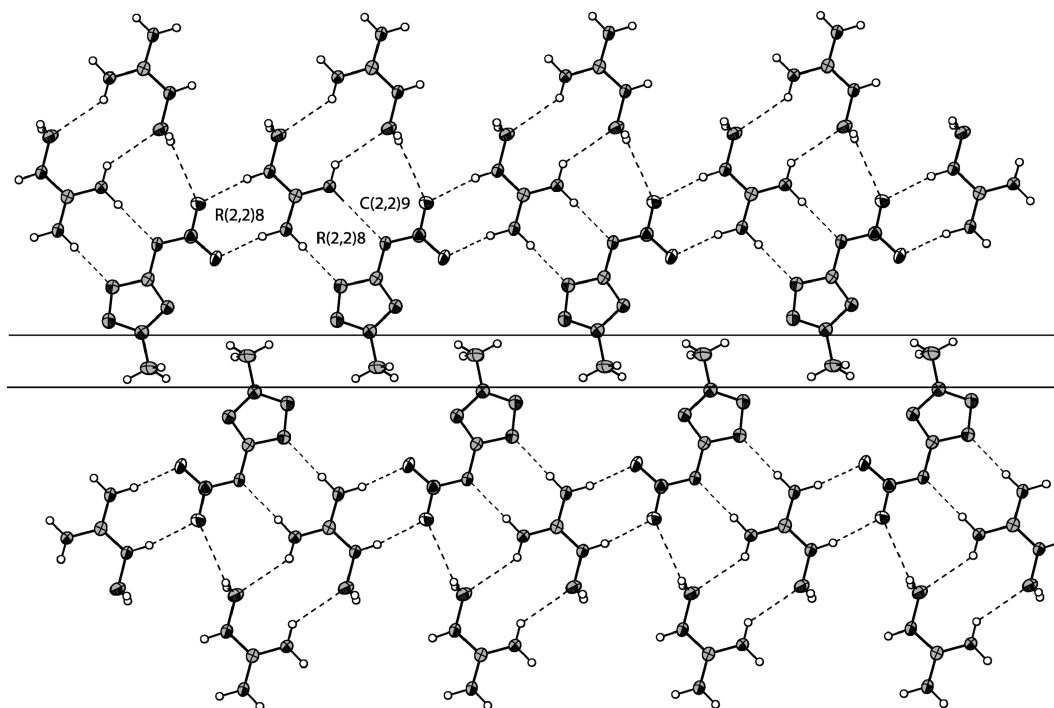


Figure 5. View on the layers in the structure of **3**. A hydrophobic zipper is formed between the lines.

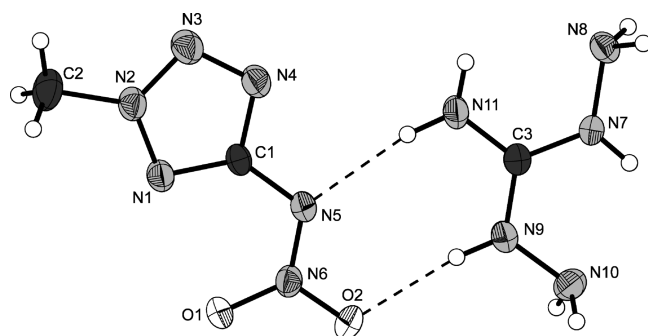


Figure 6. Molecular structure of diaminoguanidinium 2-methyl-5-nitraminotetrazolate (**4**). Thermal ellipsoids represent the 50% probability level.

C1 and N5 are closer to a C–N single bond than to a C=N double bond (1.377(2) Å for **4** to 1.388(2) Å for **3**), which justifies the nomenclature nitraminotetrazolate rather than nitriminotetrazolate. The C–N distances in the cations match the typical values found in literature for guanidinium nitrate³¹ and guanidinium chloride,³² exhibiting a bond order between a single and a double bond. The N–N bond orders of the aminoguanidinium, diaminoguanidinium, and triaminoguanidinium cation are close to a N–N single bond with distances between 1.406(2) Å (**2**) and 1.4191 (17) Å for N9–N10 in **5**. The azidoformamidinium cation is not planar (torsion angle N8–N7–C3–N11 = 16.1(3)°) and angulated (angle N8–N7–C3 = 114.49(15)°), and the bond distances are very similar to those found in azidoformamidinium chloride.³³ The urea moiety in **9** reveals the geometry of urea itself, as it is not protonated but only an adduct, whereas the C–O

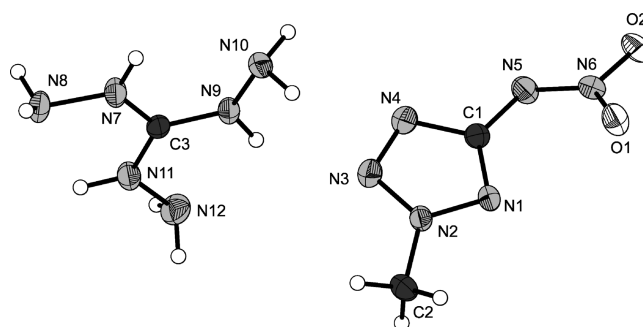


Figure 7. Molecular structure of triaminoguanidinium 2-methyl-5-nitraminotetrazolate (**5**). Thermal ellipsoids represent the 50% probability level.

bond distance is slightly larger (1.225(2) Å) than a classic C=O double bond (1.19 Å)³⁴ because of a very strong H-bond formed between H5 and O3 (1.57(2) Å).

NMR Spectroscopy. All compounds described were investigated using ¹H and ¹³C NMR. In case of **8**, a ¹⁵N NMR (proton coupled) spectrum was recorded additionally. For better comparison, all spectra were measured using *d*₆-DMSO as solvent, and all chemical shifts are given with respect to TMS (¹H, ¹³C) and MeNO₂ (¹⁵N), respectively. For the guanidine derivatives **2**–**6**, the cation proton shifts can be found in a range from 4.50 ppm to 8.62 ppm. The proton signals of the hydrazinium and the diaminouronium salt are shifted to 7.10 ppm and 7.60 ppm, respectively, whereas the proton signal of unprotonated urea in **9** is slightly shifted upfield to 5.78 ppm. Additionally, the proton signals of the methyl group in the methylated nitraminotetrazole are observed in a range from 4.16 ppm to 4.36 ppm for all compounds. For the tetrazole moiety, two signals can be observed in the ¹³C

(31) Akella, A.; Keszler, D. A. *Acta Crystallogr.* **1994**, C50, 1974–1976.

(32) Bryden, J. H. *Acta Crystallogr.* **1957**, 10, 677–680.

(33) Henke, H.; Barnighausen, H. *Acta Crystallogr.* **1972**, B28, 1100.

(34) Wiberg, N. In *Lehrbuch der Anorganischen Chemie/Holleman-Wiberg*, 102nd ed.; Walter de Gruyter: Berlin, Germany, 2007, 2006.

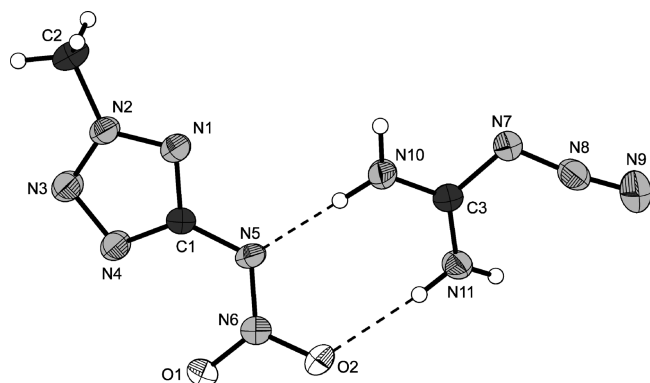


Figure 8. Molecular structure of azidoformamidinium 2-methyl-5-nitramino-tetrazolate (**6**). Thermal ellipsoids represent the 50% probability level.

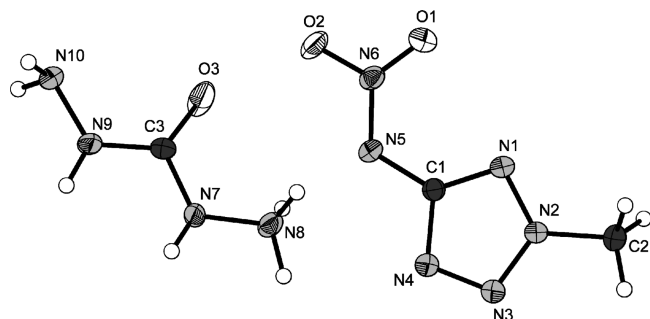


Figure 9. Molecular structure of diaminouronium 2-methyl-5-nitramino-tetrazolate (**8**). Thermal ellipsoids represent the 50% probability level.

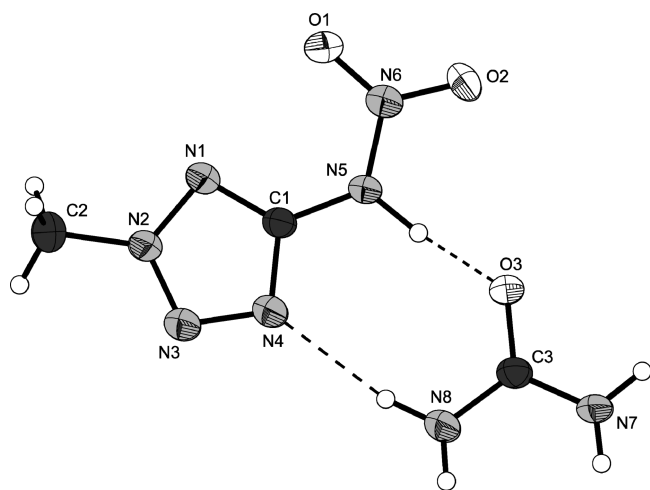


Figure 10. Molecular structure of compound **9**. Thermal ellipsoids represent the 50% probability level.

NMR spectrum whereof the downfield shifted signal of the tetrazole ring carbon atom can reliably be found at 167.8 ppm to 168.8 ppm in the deprotonated species **2–8**. For the still protonated 2-methyl-5-nitraminotetrazole in **9**, the signal is found at 160.7 ppm. Deprotonation of the tetrazole ring does not play such an important role for the NMR shift of the methyl group attached to the ring. It can be observed for all species in a range from 39.6 ppm to 40.6 ppm. The comparison of the observed signals in **2–9** with the proton and carbon atom signals in 1-methyl-5-nitriminotetrazole and its nitrogen-rich salts allows the conclusion, that alkylation at N2, compared to N1, of the

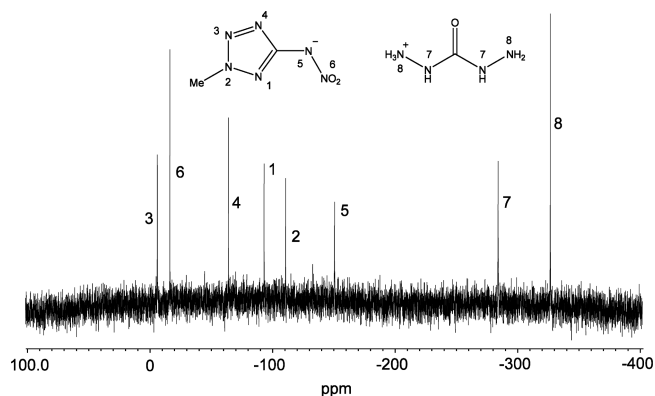


Figure 11. ^{15}N NMR spectrum of **8**: $\delta = -5.8$ (N3, q, $^3J_{\text{NH}} = 1.7$ Hz), -16.2 (N6), -64.1 (N4), -93.0 (N1, q, $^3J_{\text{NH}} = 1.9$ Hz), -110.5 (N2, q, $^2J_{\text{NH}} = 2.2$ Hz), -150.5 (N5), -283.7 (N7), -326.6 (N8).

tetrazole moiety in nitrated aminotetrazoles causes a significant downfield shift of about 10 ppm for the ring carbon atom and about 7 ppm for the methyl group attached to it. The same applies to the signals of the methyl protons, which are shifted by about 0.5 ppm to lower field. In the ^{15}N NMR spectrum of **8**, shown in Figure 11, all signals were assigned by analysis of the ^{15}N - ^1H coupling constants and by comparison with literature.^{17,35}

Vibrational Spectroscopy. Also IR and Raman spectroscopy are suitable for the identification of the described nitraminotetrazolate salts. IR and Raman spectra of all compounds were measured, and the absorptions were assigned according to commonly observed values found in literature.^{16,36–38} All vibrational spectra are mainly determined by C–H-stretching vibrations of the methyl group attached to the tetrazole ring, N–H-stretching vibrations of the cations, stretching vibrations of the nitro group and characteristic stretching and deformation vibrations of the tetrazole ring. The symmetric and asymmetric N–H-stretching vibrations of the amino groups of the cations are assigned to signals observed in the range from 3238 cm^{-1} up to 3484 cm^{-1} . All of the recorded Raman spectra show a significant, however weak, signal of the symmetric C–H-stretching vibration of the methyl group at 2956 cm^{-1} to 2970 cm^{-1} . For the azidoformamidinium salt **6**, the asymmetric and symmetric stretching vibration of the covalent bonded azido group can be observed at 2185 cm^{-1} and 2121 cm^{-1} additionally. The tetrazole ring system itself exhibits stretching and deformation vibrations that can be detected as a set of signals lying in the range from 1011 cm^{-1} to 1026 cm^{-1} , 1031 cm^{-1} to 1043 cm^{-1} , and 1633 cm^{-1} to 1698 cm^{-1} , the latter being a C=N-stretching vibration. Another typical vibration observed is the symmetric stretching vibration of the nitro group, which is found to be in the range of 1473 cm^{-1} to 1494 cm^{-1} for the ionic species **2–8** and slightly shifted to higher energy (1538 cm^{-1}) for the protonated 2-methyl-5-nitraminotetrazole in **9**.

Differential Scanning Calorimetry (DSC). DSC measurements to determine the melt- and decomposition

(35) Karaghiosoff, K.; Klapötke, T. M.; Meyer, P.; Piotrowski, H.; Polborn, K.; Weigand, J. J.; Willer, R. L. *J. Org. Chem.* **2006**, *71*, 1295–1305.

(36) Tremblay, M. *Can. J. Chem.* **1965**, *43*, 1154–1157.

(37) Svetlik, J.; Martvon, A.; Lesko J. *Chem. Papers* **1979**, *33*, 521.

(38) Hesse, M.; Meier, H.; Zeeh, B. *Spektroskopische Methoden in der Organischen Chemie*, 7th ed., Thieme: Stuttgart, Germany, 2005.

temperatures of **2–9** (about 1.5 mg of each energetic material) were performed in covered Al-containers containing a hole (0.1 mm) in the lid for gas release and a nitrogen flow of 20 mL per minute on a Linseis PT 10 DSC³⁹ calibrated by standard pure indium and zinc at a heating rate of 5 °C min⁻¹. The thermal behavior of all energetic materials investigated herein are displayed as DSC plots in a temperature range from 20 to 400 °C in Figure 12. All temperatures are given as onset temperatures. Since all compounds crystallize without crystal water, the first endothermic step in the recorded DSC curves is not due to dehydration but can be assigned to a melting point. Foremost, the melting point depends on ionic and nonionic attractive forces in the solid state and therefore strongly depends on the number and strength of the hydrogen bonds found in the crystal structures. The lowest melting compounds, which are also characterized by X-ray measurements, are the diaminoguanidinium and the azidoformamidinium salts **6** and **4** (114 °C, 138 °C) with only 7 hydrogen bonds (1 non-classical in **6**) followed by the triaminoguanidinium and the aminoguanidinium salts **5** and **3** (143 °C, 146 °C) having 10 or more hydrogen bonds per unit cell (1 non-classical in **3**). Also the hydrogen bond distances play an important role, which can be seen at the guanidinium salt **2** (176 °C) and the urea adduct **9**, which decomposes at 158 °C before melting. Both exhibit only 8 and 6 hydrogen bonds respectively, 1 non-classical in each compound. In contrast to the compounds discussed above, there are two hydrogen bonds with distances below 2 Å in **2** and one very strong hydrogen bond with a distance of only 1.57 Å in **9**. The diaminouronium salt **8** melts at 131 °C despite having a remarkably high number of hydrogen bonds (13, 1 being non-classical). All hydrogen bonds discussed above and the corresponding bond lengths are summarized in Table 2.

The hydrazinium salt **7** stands out with a very high liquidity range of 135 °C between melting and decomposition point, making it suitable for a possible application as melt-castable explosive. Except from the triaminoguanidinium and the azidoformamidinium salt, which decompose at 188 and 148 °C, respectively, because of the high nitrogen content of the cation and the relative thermal instability of covalent bonded azide groups, all other ionic compounds decompose at temperatures close to or even above 200 °C (188 °C–212 °C). The decomposition of the nonionic urea-adduct **9** takes place in two separate processes, which can be observed at 158 and 190 °C belonging to the decomposition of 2-methyl-5-nitraminotetrazole and urea. Compared to the nitrogen-rich 1-methyl-5-nitriminotetrazolate salts, the melting and especially the decomposition temperatures of the 2-methyl-derivatives are lowered by approximately 10 °C.¹⁶

Sensitivities. The impact sensitivity tests were carried out according to the STANAG 4489⁴⁰ modified instruction⁴¹ using a BAM (Bundesanstalt für Materialforschung) drophammer.⁴² The friction sensitivity tests were carried

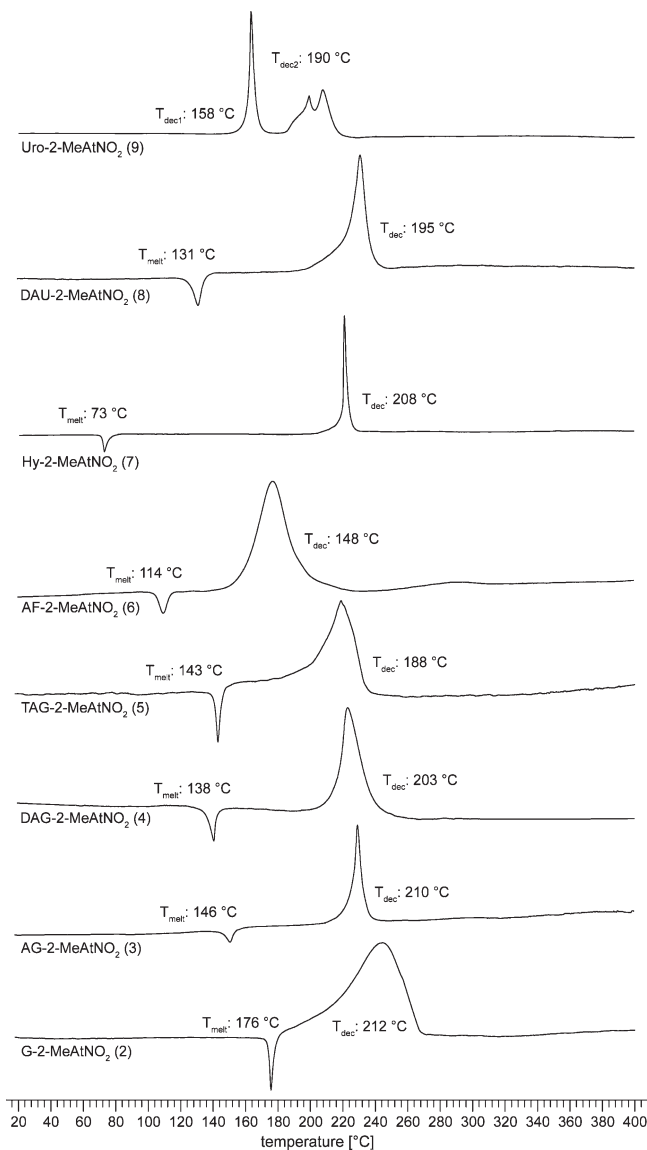


Figure 12. DSC plots (endo down) of compounds **2–9** (5 °C min⁻¹). Melting points, T_{onset} : **2**, 176 °C; **3**, 146 °C; **4**, 138 °C; **5**, 143 °C; **6**, 114 °C; **7**, 73 °C; **8**, 131 °C; decomposition temperatures, T_{onset} : **2**, 212 °C; **3**, 210 °C; **4**, 203 °C; **5**, 188 °C; **6**, 148 °C; **7**, 208 °C; **8**, 195 °C; **9**, 158 °C, 190 °C.

out according to STANAG 4487⁴³ modified instruction⁴⁴ using the BAM friction tester. The classification of the tested compounds results from the “UN Recommendations on the Transport of Dangerous Goods”.⁴⁵ Additionally all compounds were tested upon the sensitivity toward electrical discharge using the Electric Spark Tester ESD 2010 EN.⁴⁶ Beside from the impact sensitivity of **6** (3 J), which has to be classified as very sensitive, the sensitivities of all other compounds **1–5** and **7–9** are in

(43) NATO standardization agreement (STANAG) on explosive, *friction sensitivity tests*, no. 4487, 1st ed., Aug. 22, 2002.

(44) WIWEB-Standardarbeitsanweisung 4-5.1.03, Ermittlung der Explosionsgefährlichkeit oder der Reibeempfindlichkeit mit dem Reibeapparat, Nov. 8, 2002.

(45) Impact: Insensitive > 40 J, less sensitive ≥ 35 J, sensitive ≥ 4 J, very sensitive ≤ 3 J; friction: Insensitive > 360 N, less sensitive = 360 N, sensitive < 360 N a. > 80 N, very sensitive ≤ 80 N, extreme sensitive ≤ 10 N; According to the UN Recommendations on the Transport of Dangerous Goods (+) indicates: not safe for transport.

(46) <http://www.ozm.cz>.

(39) <http://www.linseis.com>.

(40) NATO standardization agreement (STANAG) on explosives, *impact sensitivity tests*, no. 4489, 1st ed., Sept. 17, 1999.

(41) WIWEB-Standardarbeitsanweisung 4-5.1.02, Ermittlung der Explosionsgefährlichkeit, hier der Schlagempfindlichkeit mit dem Fallhammer, Nov. 8, 2002.

(42) <http://www.bam.de>.

Table 2. Hydrogen Bonds and Respective Distances

compound	D—H...A	<i>d</i> (H—A) (Å)	compound	D—H...A	<i>d</i> (H—A) (Å)
2	N7—H7A...N4	2.04(4)	5	N10—H10B...N1	2.305(17)
	N7—H7B...O1	2.06(4)		N11—H11...N8	2.31(2)
	N8—H8A...O2	1.93(3)		N11—H11...O1	2.195(17)
	N8—H8B...O2	1.99(3)		N11—H11...O2	2.53(2)
	N9—H9A...O2	2.30(3)		N12—H12B...O2	2.41(2)
	N9—H9A...N8	2.58(4)		N10—H10A...O1	2.092(19)
	N9—H9B...N5	2.21(4)		N10—H10A...O2	2.48(2)
	C2—H2B...O1	2.57(4)		N10—H10A...N6	2.623(19)
3	N7—H7...O2	2.116(16)	6	N10—H10B...N5	1.92(2)
	N8—H8A...N7	2.58(2)		N11—H11A...N4	1.92(2)
	N8—H8A...O2	2.576(19)		N11—H11B...O2	2.12(2)
	N8—H8B...O2	2.289(19)		C2—H2A...O2	2.59(2)
	N9—H9A...N8	2.385(17)		N7—H7...O2	2.24(4)
	N9—H9A...N8	2.414(17)		N7—H7...O3	2.27(4)
	N9—H9B...N5	2.077(18)		N8—H8A...O3	2.52(4)
	N10—H10A...O1	1.940(17)		N8—H8A...N10	1.92(4)
	N10—H10B...N4	2.056(18)		N8—H8B...O2	1.85(6)
	C2—H2C...O1	2.546(18)		N8—H8B...N5	2.54(5)
	N7—H7...N10	2.296(17)		N8—H8B...N6	2.60(5)
	N8—H8A...O1	2.328(16)		N8—H8C...N5	2.26(5)
4	N8—H8B...N4	2.166(19)	8	N9—H9...O2	1.96(4)
	N9—H9...O2	2.091(17)		N10—H10A...O1	2.47(4)
	N10—H10B...O1	2.143(17)		N10—H10B...N4	2.36(3)
	N11—H11A...N8	2.337(18)		C2—H2A...N1	2.51(3)
	N11—H11B...N5	2.110(19)		C2—H2B...N3	2.57(3)
	N7—H7...N10	2.318(15)		C2—H2C...O1	2.51(4)
	N7—H7...N10	2.45(2)		N5—H5...O3	1.57(2)
	N8—H8A...N4	2.290(18)		N7—H7A...N3	2.36(2)
5	N8—H8B...O2	2.16(2)		N7—H7B...O3	2.02(2)
	N9—H9...N12	2.284(15)		N8—H8A...O1	2.29(2)
	N9—H9...N3	2.220(16)		N8—H8B...N4	2.17(2)
	N10—H10A...O2	2.159(15)		C2—H2C...O1	2.59(2)
	N10—H10B...O1	2.347(15)	9		

the range of 5 to 30 J and therefore have to be classified as sensitive toward impact. The guanidinium salt **2** stands out with a relatively low sensitivity of 30 J. The same classification applies to the friction sensitivities. Again, the azidoformamidinium salt **6** has to be classified as very sensitive with a value of 72 N, whereas the remaining compounds **1–5** and **7–9** are classified as sensitive having values in a range from 120 to 288 N. Concerning the sensitivities toward electrical discharge, the values for all tested materials **1–9** are in the range of 0.1 J–0.5 J, whereas the compounds could not be detonated but started to decompose upon treatment with the specified electrical energy. The explicit sensitivity data can be seen in Tables 3 and 4.

Detonation Parameters. The detonation parameters were calculated using the program EXPLO5 V5.03, as well as with the new version EXPLO5 V5.04.⁴⁷ The program is based on the steady-state model of equilibrium detonation and uses Becker–Kistiakowsky–Wilson equation of state (BKW E.O.S) for gaseous detonation products and Cowan–Fickett EOS for solid carbon.⁴⁸ The calculation of the equilibrium composition of the detonation products is done by applying modified White, Johnson, and Dantzig's free energy minimization technique. The program is designed to enable the calculation of detonation parameters at the CJ point. The BKW equation in the following form was used with the BKWN set of parameters ($\alpha, \beta, \kappa, \theta$) as stated

below the equations and X_i being the mol fraction of i -th gaseous product, k_i is the molar covolume of the i -th gaseous product:⁴⁹

$$pV/RT = 1 + xe^{\beta x} \quad x = (\kappa X_i k_i)/[V(T+\theta)]^\alpha$$

$$\alpha = 0.5, \quad \beta = 0.176, \quad \kappa = 14.71, \quad \theta = 6620$$

The calculations were performed using the maximum densities according to the crystal structures. The most promising compound concerning the detonation velocity and pressure discussed here is the diaminouronium salt **8** with values of $V_{\text{det}} = 8864 \text{ ms}^{-1}$ for the detonation velocity and a detonation pressure of $p_{\text{CJ}} = 307 \text{ kbar}$ since the values are in the range of those of commonly used RDX (royal demolition explosive; $p_{\text{CJ}} = 340 \text{ kbar}$, $V_{\text{det}} = 8882 \text{ m s}^{-1}$). The detonation velocities and pressures of **1–6**, **8**, and **9** are slightly lower than those of RDX ranging from $V_{\text{det}} = 7806 \text{ m s}^{-1}$ (**9**) to $V_{\text{det}} = 8864 \text{ m s}^{-1}$ (**8**). Because of their lower nitrogen content and molar amount of gaseous reaction products, compounds **2–4**, **6**, and **9** do not reach the levels of **5** and **8** in terms of detonation pressure and velocity. However, the molar amount of gaseous reaction products is subject to only small variations (**2**: 844, **3**: 861, **4**: 876, **5**: 888, **6**: 806, **8**: 853, **9**: 822 L kg^{-1}) which are found in the different detonation temperatures

(47) (a) Sućeska, M. *EXPLO5.V2, Computer program for calculation of detonation parameters; Proceedings of 32nd International Annual Conference of ICT*, July 3–6, Karlsruhe, Germany, 2001; pp 110–111. (b) Sućeska, M., *Proceedings of 30th International Annual Conference of ICT*, June 29–July 2, Karlsruhe, Germany, 1999; 50/1.

(48) Sućeska, M. *Propellants, Explos., Pyrotech.* **1991**, 16(4), 197–202.

(49) (a) Sućeska, M. *Mater. Sci. Forum* **2004**, 465–466, 325–330. (b) Sućeska, M. *Propellants, Explos., Pyrotech.* **1999**, 24, 280–285. (c) Hobbs, M. L.; Baer, M. R. *Proceedings of the 10th Symposium (International) on Detonation*, ONR 33395-12, Boston, MA, July 12–16, 1993; p 409.

Table 3. Explosive and Detonation Parameters of **2–5**

	G_2MNAT(2)	AG_2MNAT(3)	DAG_2MNAT(4)	TAG_2MNAT(5)
formula	C ₃ H ₉ N ₉ O ₂	C ₃ H ₁₀ N ₁₀ O ₂	C ₃ H ₁₁ N ₁₁ O ₂	C ₃ H ₁₂ N ₁₂ O ₂
FW/g mol ⁻¹	203.17	218.23	233.11	248.27
IS/J	30	6	10	6
FS/N	192	120	160	120
ESD/J	0.2	0.2	0.16	0.18
N/%	62.1	64.2	66.1	67.72
Ω/%	-66.9	-66.0	-65.2	-64.5
T _{Dec} /°C	212	210	203	188
ρ/g cm ⁻³	1.632	1.608	1.567	1.573
Δ _f H _m ^o /kJ mol ⁻¹	255	366	479	587
Δ _f U ^o /kJ kg ⁻¹	1378	1801	2182	2496
EXPLO5 values: V5.03 (V5.04)				
-Δ _{Ex} U ^o /kJ kg ⁻¹	4148 (4069)	4454 (4367)	4733 (4640)	4959 (4856)
T _{det} /K	2907 (2799)	3039 (2910)	3170 (3014)	3249 (3120)
p _{CJ} /kbar	250 (244)	260 (249)	262 (247)	277 (259)
V _{det} /m s ⁻¹	8300 (8059)	8495 (8169)	8603 (8184)	8827 (8354)
V _o /L kg ⁻¹	844 (812)	861 (825)	876 (837)	888 (847)

Table 4. Explosive and Detonation Parameters of **6, 8, and 9** Compared to RDX

	AF_2MNAT(6)	DAU_2MNAT(8)	Uro_2MNAT(9)	RDX
formula	C ₃ H ₇ N ₁₁ O ₂	C ₃ H ₁₀ N ₁₀ O ₃	C ₃ H ₈ N ₈ O ₃	C ₃ H ₆ N ₆ O ₇
FW/g mol ⁻¹	229.16	234.18	204.19	222.12
IS/J	3	5	10	7.5
FS/N	72	168	288	120
ESD/J	0.2	0.50	0.2	0.1–0.2
N/%	67.23	59.81	54.89	37.8
Ω/%	-52.36	-54.7	-54.9	-21.6
T _{Dec} /°C	148	195	158	210
ρ/g cm ⁻³	1.571	1.73	1.591	1.80
Δ _f H _m ^o /kJ mol ⁻¹	687	345	120	70
Δ _f U ^o /kJ kg ⁻¹	3105	1596	701	417
EXPLO5 values: V5.03 (V5.04)				
-Δ _{Ex} U ^o /kJ kg ⁻¹	5381 (5355)	4948 (4892)	4370 (4353)	6038 (6125)
T _{det} /K	3887 (3700)	3332 (3199)	3179 (3050)	4368 (4236)
p _{CJ} /kbar	258 (252)	307 (305)	224 (227)	341 (349)
V _{det} /m s ⁻¹	8290 (8150)	8864 (8730)	7806 (7800)	8906 (8748)
V _o /L kg ⁻¹	806 (785)	853 (831)	822 (806)	793 (739)

(**2**: 2907, **3**: 3039, **4**: 3170, **5**: 3249, **6**: 3887, **8**: 3332, **9**: 3179 K).

Compared to the nitrogen-rich salts of the 1-methyl-5-nitriminotetrazole, which recently were synthesized in our research group,¹⁶ the detonation velocities and pressures of the 2-methyl-derivatives are slightly higher with larger differences for the guanidinium and aminoguanidinium salts and smaller differences for the diaminoguanidinium and triaminoguanidinium salts. Also the heats of explosion and the explosion temperatures are higher than those of the 1-methyl-derivatives. The molar amount of gaseous products, however, is nearly in the same range because of the same molecular weights.

Conclusions

From the experimental study of N-rich 2-methyl-5-nitraminotetrazolate salts the following conclusions can be drawn:

2-Methyl-5-nitraminotetrazole can be easily deprotonated in aqueous solution using alkali hydroxides forming the corresponding alkali salts in nearly quantitative yields. These form the silver salt by the reaction with AgNO₃ in aqueous solutions.

The nitrogen-rich 2-methyl-5-nitraminotetrazolate salts **2–9** can easily be obtained via Brønsted acid–base reactions using the guanidinium carbonates or metathesis reactions

using silver 2-methyl-5-nitraminotetrazolate and the guanidinium chlorides in aqueous solution with high yields and good purity. The triaminoguanidinium salt **5** was synthesized via the hydrazinolysis of the aminoguanidinium salt **3**. The products can be recrystallized from water/ethanol mixtures resulting in colorless crystals.

The crystal structures of **2–6, 8, and 9** were determined using low temperature single crystal diffraction.

A comprehensive characterization of the physicochemical properties and sensitivities of **2–9** is given. Although the salts are energetic materials with high nitrogen contents, they show good stabilities toward friction and impact and a good thermal stability.

Promising detonation parameters were calculated for **2–9** compared to common explosives like TNT and RDX. The performance (calculated values: p_{CJ} = 307 kbar; V_{det} = 8864 m s⁻¹) of diaminouronium 2-methyl-5-nitraminotetrazolate (**8**) qualifies it for further investigations concerning military applications.

Acknowledgment. Financial support of this work by the Ludwig-Maximilian University of Munich (LMU), the U.S. Army Research Laboratory (ARL), the Armament Research, Development and Engineering Center (ARDEC), the Strategic Environmental Research and Development

Program (SERDP), and the Office of Naval Research (ONR Global, title: "Synthesis and Characterization of New High Energy Dense Oxidizers (HEDO) - NICOP Effort ") under contract nos. W911NF-09-2-0018 (ARL), W911NF-09-1-0120 (ARDEC), W011NF-09-1-0056 (ARDEC), and 10 WPSEED01-002/WP-1765 (SERDP) is gratefully acknowledged. The authors acknowledge collaborations with Dr. Mila Krupka (OZM Research, Czech Republic) in the development of new testing and evaluation methods for energetic materials and with Dr. Muhamed Sucesca (Brodarski Institute, Croatia) in the

development of new computational codes to predict the detonation and propulsion parameters of novel explosives. We are indebted to and thank Drs. Betsy M. Rice and Brad Forch (ARL, Aberdeen, Proving Ground, MD) and Mr. Gary Chen (ARDEC, Picatinny Arsenal, NJ) for many helpful and inspired discussions and support of our work.

Supporting Information Available: Crystallographic data in CIF format. This material is available free of charge via the Internet at <http://pubs.acs.org>.

Calcium 5-Nitriminotetrazolate—A Green Replacement for Lead Azide in Priming Charges

NIKO FISCHER,¹ T. M. KLAPOÖTKE,^{1,2}
and JÖRG STIERSTORFER¹

¹Ludwig-Maximilian University Munich, Energetic
Materials Research, Department of Chemistry and
Biochemistry, Munich, Germany

²Center for Energetic Concepts Development,
CECD, University of Maryland, UMD, Department
of Mechanical Engineering, College Park, Maryland

The new energetic material calcium 5-nitriminotetrazolate (1) is presented. A facile preparative route in combination with an outstanding thermal as well as long-term stability, easy initiation, and low sensitivity make 1 an auspicious green alternative filler in priming charges.

Keywords: nitramines, primary explosives, tetrazoles, X-ray

Introduction

Research on “green” energetic materials is an ongoing project in many research groups worldwide [1–6]. All classes of energetic

Address correspondence to T. M. Klapötke, Ludwig-Maximilian University Munich, Energetic Materials Research, Department of Chemistry and Biochemistry, Butenandtstr. 5-13, Munich D-81377, Germany. E-mail: tmk@cup.uni-muenchen.de

materials (explosives, propellants, pyrotechnics) contain polluting ingredients and decomposition products. Nitrogen-rich derivatives are promising alternatives as energetic materials because the formation of molecular nitrogen as an end-product of propulsion or explosion is highly desirable. These end-products avoid environmental pollution and health risks, as well as reduce plume signatures [7]. In primary explosives, the application of heavy metal salts, for example, lead azide and lead styphnate, should also be strongly reduced. Lead azide is employed as an initiating explosive in blasting caps, because it is reliable, cheap, easy to manufacture, and shows an appropriate thermal stability ($T_{\text{dec.}}$: 320–340°C). When used as a primary charge, it is effective in smaller quantities than mercury fulminate [8]. Primary charges are the secondary component in ignition trains, which are designed to initiate secondary explosives; for example, trinitrotoluene (TNT) or Royal Demolition Explosive (RDX). Next to the high toxicity, lead azide is also decomposed by atmospheric CO_2 and shows high sensitivity toward impact (1–4 J) and friction (0.1–1 N). Several substitutes for lead azide have been suggested over the last decades [9]. Less toxic silver azide ($T_{\text{dec.}}$: 270–275°C) gives a very satisfactory initiation effect that is superior to that of $\text{Pb}(\text{N}_3)_2$. Nevertheless, its practical use is limited, because it is light sensitive and also highly sensitive toward friction. The hardest criteria for new primary explosives are a good thermal stability in combination with great performance. Zhilin et al. presented the two high-energy-capacity complexes tetraammine-*cis*-bis(5-nitro-2*H*-tetrazolato-*N*2)-cobalt(III) perchlorate [10] and tetraammine-bis(1-methyl-5-aminotetrazole-*N*3,*N*4)cobalt(III) perchlorate [11]; the first is presently used in missile manufacture and the mining industry. We also presented several replacements based on copper bis(tetrazole-5-yl)amines [12]. In this work we present our most powerful and qualified replacement for lead azide, calcium 5-nitriminotetrazolate (**1**). A facile synthetic route that can also be performed on larger scales, a comprehensive characterization including safety tests, as well as an initiation experiment are described. It is a further contribution

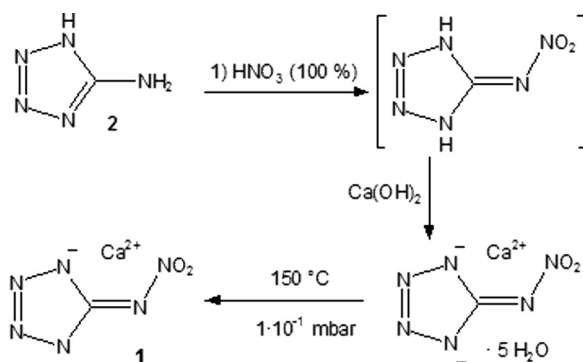
to the promising class of 5-nitriminotetrazoles, which have been extensively described in the literature [13].

Results and Discussion

Calcium 5-nitriminotetrazolate (**1**) is a powerful energetic material that shows sensitivities toward outer stimuli. Proper protective measures (safety glasses, face shield, leather coat, earthened equipment and shoes, Kevlar gloves and earplugs) should be used when handling compound **1**. Extra safety precautions should be taken, especially when 5-nitrimino-1,4*H*-tetrazole is prepared on a larger scale.

The two step, one-pot reaction of **1** is shown in Scheme 1. In the first step 5-amino-1*H*-tetrazole (**2**) is nitrated using 100% nitric acid [14]. After pouring the reaction mixture onto ice, the solution is neutralized by the addition of calcium hydroxide. The precipitate formed is isolated and recrystallized from hot water, yielding calcium 5-nitriminotetrazolate pentahydrate (**1** · 5 H₂O). The last step is dehydration at higher temperatures (150 °C) and lower pressures (10⁻¹ mbar), yielding anhydrous **1** [15].

A thermogravimetric (TG) curve as well as a differential scanning calorimetry (DSC) thermogram are depicted in Fig. 1 [16]. The TG curve shows that the loss of water occurs over two



Scheme 1. Preparative route to calcium 5-nitriminotetrazolate (**1**).

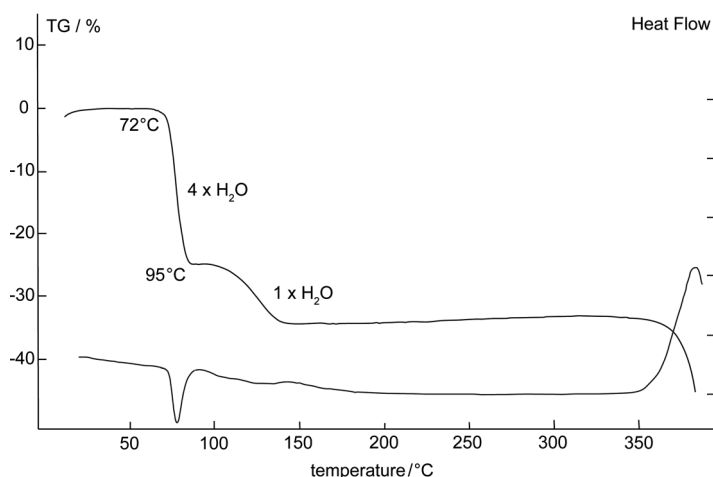


Figure 1. Thermogravimetric plot of compound **1**, showing the loss of mass (left axis, upper curve) and the differential thermal analysis (DTA) curve (right axis, lower curve).

discrete steps, which can be explained by the crystal structure. Four water molecules are lost between 72 and 85°C, which has been calculated by a loss of mass about 27%. The fifth water molecule is removed at temperatures above 92°C. Above 145°C the compound is completely dry (overall loss of mass ~35%). We performed dehydration simply by putting **1** in an oven at 200°C for 48 hr. The DSC plot demonstrates the auspicious thermal stability up to temperatures above 360°C. This decomposition temperature even surpasses that of lead and silver azide.

The structure of **1** · 5 H₂O in the crystalline state was determined by X-ray diffraction. Relevant data and parameters of the X-ray measurements and refinements are given in the references [17]. Further information on the crystal structure determination has been deposited with the Cambridge Crystallographic Data Centre [18] as supplementary publication No. 708342 (**1**·H₂O).

Calcium 5-nitriminetetrazolate pentahydrate crystallizes in the triclinic space group *P*-1 with two molecular moieties in the unit cell. A density of 1.89 g cm⁻³ has been calculated.

$1 \cdot 5\text{H}_2\text{O}$ is best described by the formation of a binuclear complex, which is depicted in Fig. 2. The 5-nitriminotetrazolate dianions coordinate by the atoms N1 and O1 to the calcium cations, forming a bite angle of $67.06(6)^\circ$. In accordance with the TG experiment four molecules of water are μ_1 -coordinated, whereby one is bridging to calcium cations by a μ_2 -coordination.

1 as well as its pentahydrate were investigated by several specific tests determining the energetic behavior. The sensitivities toward impact, friction, and electrical discharge have been explored by the BAM drop hammer and friction tester [19] as well as an ESD 2010EN electric spark tester (OZM Research, Bliznovice 32, Hrochuv Tynec 538 62, Czech Republic) [20]. As with other energetic materials, $1 \cdot 5\text{H}_2\text{O}$ is less sensitive toward impact (75 J) than its anhydrous analogue (5 J). Also, its sensitivity toward friction (**1**:112 N, $1 \cdot 5\text{H}_2\text{O}$: 240 N) and electrical discharge is significantly lower (**1**:0.15 J, $1 \cdot 5\text{H}_2\text{O}$: 1.05 J). The value of the electrical discharge sensitivity is comparable to that of the secondary explosive RDX (ca. 0.2 J) and significantly higher than that of lead azide (0.005 J). The friction and impact sensitivity

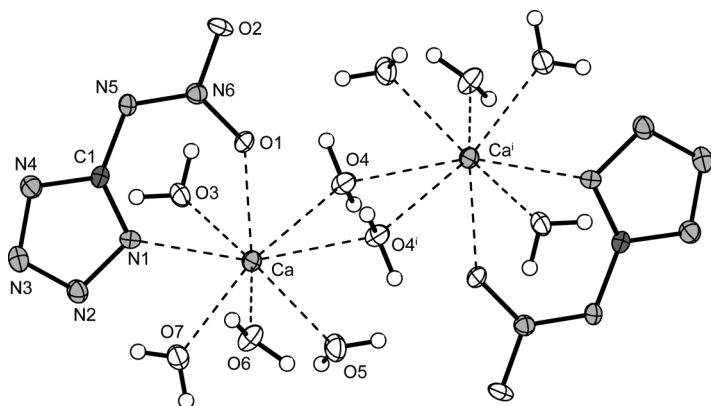


Figure 2. Molecular moiety of $1 \cdot \text{H}_2\text{O}$. Ellipsoids of nonhydrogen atoms are drawn at the 50% probability level. Selected coordination distances (Å): $\text{Ca}-\text{N}_1=2.492(2)$, $\text{Ca}-\text{O}_1=2.413(2)$, $\text{Ca}-\text{O}_3=2.516(2)$, $\text{Ca}-\text{O}_4=2.577(2)$, $\text{Ca}-\text{O}_5=2.3975(2)$, $\text{Ca}-\text{O}_6=2.365(2)$, $\text{Ca}-\text{O}_7=2.397(2)$.

values are lower than those of lead azide (Table 1), where dextrine must be used to reduce the sensitivity response. In order to assess the longevity of **1**, long-term stability tests were performed using a Systag FlexyTSC thermal safety calorimeter in combination with a RADEX V5 oven and the SysGraph Software tool (Systag, Sytem Technik AG, CH-8803, Rüschlikon, Switzerland). The tests were undertaken as long-term isoperibolic runs in glass test vessels at atmospheric pressure with 300 mg of the compound at a temperature of 265°C. Maintaining the salt for 48 hr at this temperature did not yield any decomposition reactions or mass loss.

The heat of formation $\Delta_f H^\circ(\text{s,M})$ of **1** has been calculated by the atomization energy method [5c, 21]:

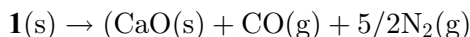
$$\Delta_f H^\circ_{(\text{g,M},298)} = H_{(\text{Molecule},298)} - \sum H^\circ_{(\text{Atoms},298)} + \sum \Delta_f H^\circ_{(\text{Atoms},298)}$$

The enthalpies (H) and free energies (G) were calculated using the complete basis set (CBS) method described by Petersson and coworkers using the Gaussian G03 W (revision B.03) program package [21]. With the calculated gas-phase enthalpies

Table 1
Comparison of **1** with lead azide

	1	1.5H₂O	Pb(N₃)₂
Formula	CCaN ₆ O ₂	CH ₁₀ CaN ₆ O ₇	N ₆ Pb
Form. mass g mol ⁻¹	168.13	258.23	291.23
$\rho_{\text{calc.}}/\text{g cm}^{-3}$	ca. 2.0	1.9	4.8
$\Delta_f H^\circ/\text{kJ kg}^{-1}$	195.1	—	1,638
$\Delta_{\text{Ex}} H^\circ/\text{kJ kg}^{-1}$	-4,632	—	-1,638
Impact sensitivity/J	5	75	2–4
Friction sensitivity/N	112	240	0.1–1 N
ESD/J	0.15	1.05	0.005
Hot plate test	Fulmination	Fulmination	Fulmination
T _{dec.} /°C	360	360	320

(Ca^{2+} : $1,927.3 \text{ kJ mol}^{-1}$, AtNO_2^{2-} : $399.0 \text{ kJ mol}^{-1}$) and the lattice enthalpy (CaAtNO_2 : $2,283.3 \text{ kJ mol}^{-1}$) computed by the Jenkins equation [22], $\Delta_f H^\circ(\text{s}, \text{M})$ has been calculated to be 32.8 kJ mol^{-1} . Using this value the enthalpy of explosion $\Delta_{\text{Ex}} H$ has been calculated according to the following equation and $\Delta_f H^\circ$: $\text{CaO}(\text{s}) = -635.6$; $\Delta_f H^\circ$, $\text{CO}(\text{g}) = -110.5 \text{ kJ mol}^{-1}$ from the literature [23] to have a great value of $-778.9 \text{ kJ mol}^{-1}$.



A comparison of the energetic properties of **1** with those of commonly used lead azide is given in Table 1.

Hexanitrostilbene (HNS) is a secondary explosive with low sensitivities and a high thermal stability ($T_{\text{dec.}} = 318^\circ\text{C}$). It can be used individually but is also manufactured as an additive to cast TNT to improve the fine crystalline structure. However, HNS is hard to initiate, and primary explosives with performances equal to or greater than silver azide are needed. Using the setup shown in Figs. 3a and 3b, we could show that **1** was

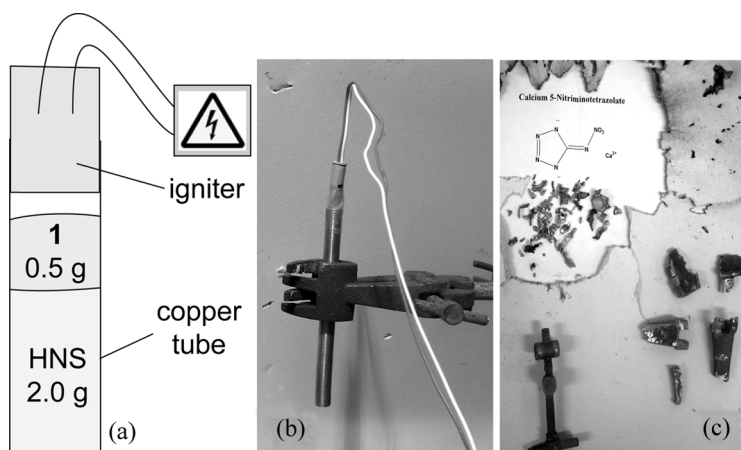


Figure 3. Initiation test of HNS using **1** as the primary explosive. (a) schematic setup; (b) experimental setup; and (c) collected fragments of initiation test.

able to initiate HNS. A standard explosive train [24] was used. A copper tube ($\varnothing = 1.0$ cm) was loaded with 2 g HNS and 0.5 g **1** on the top. As igniter, an Austin Powder Firing Parameter Type I was fixed on top without direct contact to **1**. Immediately after firing the upper igniter, **1** exploded violently and an initiation of the HNS charge could be observed. The entire amount of HNS was detonated in the experiment. Larger collected fragments of the copper tube and clamp are demonstrated in Fig. 3c.

Conclusions

From this combined experimental and theoretical study the following conclusions can be drawn: Calcium 5-nitriminotetrazolate (**1**) is a promising and powerful alternative to commonly used lead azide as a primary explosive. It shows an astonishing thermal stability up to 360°C. Its synthesis can be performed in good yields and larger scales using 5-amino-1*H*-tetrazole as starting material. Compound **1** is less polluting than lead azide because it contains no heavy metals, has a balanced oxygen content to carbon monoxide ($\Omega_{\text{CO}} = 0$) and a low solubility in water and other organic solvents. It can be detonated either by impact or electrical stimulation. The detonation wave has been proved to initiate secondary explosives such as HNS.

Acknowledgments

Financial support of this work by the Ludwig-Maximilian University of Munich (LMU), the Fonds der Chemischen Industrie (FCI), the European Research Office (ERO) of the U.S. Army Research Laboratory (ARL), and the Armament Research, Development and Engineering Center (ARDEC) under contract nos. W911NF-09-2-0018, W911NF-09-1-0120, and W011NF-09-1-0056 is gratefully acknowledged. The authors acknowledge collaborations with Dr. Mila Krupka (OZM Research, Czech Republic) in the development of new testing and evaluation methods for energetic materials and with

Dr. Muhamed Sucesca (Brodarski Institute, Croatia) in the development of new computational codes to predict the detonation and propulsion parameters of novel explosives. We are indebted to and thank Drs. Betsy M. Rice and Brad Forch (ARL, Aberdeen Proving Ground, MD) and Dr. Gary Chen (ARDEC, Picatinny Arsenal, NJ) for many helpful and inspired discussions and support of our work. Furthermore, special thanks to Stefan Huber for determining the sensitivities.

References

- [1] Giles, J. 2004. Green explosives: Collateral damage. *Nature*, 427: 580–581.
- [2] (a) Christe, K. O., W. W. Wilson, J. A. Sheehy, and J. A. Boatz. 1999. N_5^+ : A novel homoleptic polynitrogenion as a high energy density material. *Angewandte Chemie*, 111: 2112–2118. *Angewandte Chemie International Edition*, 38: 2004–2009; (b) Haiges, R., S. Schneider, T. Schroer, and K. O. Christe. 2004. High-energy-density materials: Synthesis and characterization of N_5^+ $[P(N_3)_6]^-$, N_5^+ $[B(N_3)_4]^-$, N_5^+ $[HF_2]_n$, N_5^+ $[BF_4]^-$, N_5^+ $[PF_6]^-$, and N_5^+ $[SO_3F]$. *Angewandte Chemie*, 116: 5027–5032. *Angewandte Chemie International Edition*, 43: 4919–4924; (c) Petrie, M. A., J. A. Sheehy, J. A. Boatz, G. Rasul, G. K. Surya Prakash, G. A. Olah, and K. O. Christe. 1997. Novel high-energy density materials. Synthesis and characterization of triazidocarbenium dinitramide, -perchlorate, and -tetrafluoroborate. *Journal of the American Chemical Society*, 119: 8802–8808.
- [3] (a) Joo, Y.-H., B. Twamley, S. Garg, and J. M. Shreeve. 2008. Energetic nitrogen-rich derivatives of 1,5-diaminotetrazole. *Angewandte Chemie*, 120: 6332–6335; 2008. *Angewandte Chemie International Edition*, 47: 6236–6239; (b) Xue, H., H. Gao, B. Twamley, and J. M. Shreeve. 2007. Energetic salts of 3-Nitro-1,2,4-triazole-5-one, 5-nitroaminotetrazole, and other nitro-substituted azoles. *Chemistry of Materials*, 19: 1731–1739; (c) Guo, Y., H. Gao, B. Twamley, and J. M. Shreeve. 2007. Energetic nitrogen rich salts of N,N-bis[1(2)H-tetrazol-5-yl]amine. *Advance Materials*, 19: 2884–2888; (d) Gao, H., C. Ye, O. D. Gupta, J.-C. Xiao, M. A. Hiskey, B. Twamley, and J. M. Shreeve. 2007. 2,4,5-trinitroimidazole-based energetic salts. *Chemistry – A European Journal*, 13: 3853–3860.

- [4] (a) Chavez, D. E., M. A. Hiskey, D. L. Naud, and D. Parrish. 2008. Synthesis of an energetic nitrate ester. *Angewandte Chemie*, 120: 8431–8433; 2008. *Angewandte Chemie International Edition*, 47: 8307–8309; (b) Huynh, M. H. V., M. A. Hiskey, T. J. Meyer, and M. Wetzler. 2006. Green primaries: Environmentally friendly energetic complexes. *Proceedings of the National Academy of Sciences of the United States of America*, 103: 5409–5412; (c) Huynh, M. H. V., M. A. Hiskey, D. E. Chavez, D. L. Naud, and R. D. Gilardi. 2005. Synthesis, characterization, and energetic properties of diazido heteroaromatic high-nitrogen C–N compound. *Journal of the American Chemical Society*, 127: 12537–12543.
- [5] (a) Klapötke, T. M., J. Stierstorfer, and A. U. Wallek. 2008. Nitrogen-rich salts of 1-methyl-5-nitriminotetrazolate: An auspicious class of thermally stable energetic materials. *Chemistry of Materials*, 20: 4519–4530; (b) Darwich, C., T.M. Klapötke, and C.M. Sabaté. 2008. 1,2,4-triazolium-cation-based energetic salts. *Chemistry – A European Journal*, 14: 5756–5771; (c) Klapötke, T. M. and J. Stierstorfer. 2008. Triaminoguanidinium dinitramide-calculations, synthesis and characterization of a promising energetic compound. *Physical Chemistry Chemical Physics*, 10: 4340–4346; (d) Klapötke, T. M. and C. M. Sabaté. 2008. Nitrogen-rich tetrazolium azotetrazolate salts: A new family of insensitive energetic materials. *Chemistry of Materials*, 20(5): 1750–1763; (e) Klapötke, T. M. and J. Stierstorfer. 2008. The new energetic compounds 1,5-diaminotetrazolium and 5-amino-1-methyltetrazolium dinitramide – synthesis, characterization and testing. *European Journal of Inorganic Chemistry*, 4055–4062; (f) Hiskey, M., A. Hammerl, G. Holl, T. M. Klapötke, K. Polborn, J. Stierstorfer, and J. J. Weigand. 2005. Azidoformamidinium and guanidinium 5,5'-azotetrazolate salts. *Chemistry of Materials*, 17: 3784–3793.
- [6] (a) Vavra, J. and P. Vavra. 2004. Life-cycle-analysis and “green” energetic materials. *New Trends in Research of Energetic Materials, Proceedings of the 7th Seminar*; (b) Nock, L., D. Porada, and G. King. 2002. Green energetic materials (GEM)—A program overview. *CPIA Publication*, Joint Army-Navy-NASA-Air Force (JANNAF) 30th Propellant Development & Characterization Subcommittee Meeting Colorado Springs, Colorado USA, 1–11.

- [7] Singh, R. P., H. Gao, D. T. Meshri, and J. M. Shreeve. 2007. Nitrogen-rich heterocycles. In T. M. Klapötke (ed.), *High Energy Density Materials*, Berlin: Springer.
- [8] Meyer, R., J. Köhler, and A. Homburg. 2007. Lead Azide. In *Explosives*, 6th ed., Weinheim: Wiley-VCH.
- [9] (a) Reddy, G.O. 1992. Co-precipitation studies on lead azide with tetrazole derivatives – a search for lead azide substitute. *Propellants, Explosives, Pyrotechnics*, 17: 241–248; (b) Bates, L.R. 1986. III1–III10, The potential of tetrazoles in initiating explosives systems. In *Proceedings of the 13th Symposium on Explosives and Pyrotechnics*.
- [10] Zhilin, A. Yu., M. A. Ilyushin, I. V. Tselinskii, and A. S. Brykov. 2001. Synthesis of a high-energy-capacity compound, cis-tetraamminebis(5-nitro-2H-tetrazolato- N_2)cobalt(III) perchlorate. *Zh. Prikl. Khim.*, 74: 96–99.
- [11] Zhilin, A. Yu., M. A. Ilyushin, I. V. Tselinskii, A. S. Kozlov, N. E. Kuzmina. 2002. Synthesis and properties of tetraamminebis(1-methyl-5-aminotetrazole- N_3, N_4)cobalt(III) perchlorate. *Russian Journal of Applied Chemistry*, 75: 1849–1851.
- [12] (a) Klapötke, T. M., P. Meyer, K. Polborn, J. Stierstorfer, J. J. Weigand. 2006. 5,5'-Bis-(1H-tetrazolyl)amine (H2BTA): A promising ligand in novel copper based priming charges (PC). In *New Trends in Research of Energetic Materials, Proceedings of the 9th Seminar*; (b) Klapötke, T. M., P. Mayer, K. Polborn, J. Stierstorfer, and J. J. Weigand. 2006. 5,5'-Bis-(1H-tetrazolyl)-amine (H2bta) and 5,5'-bis-(2-methyl-tetrazolyl)amine (Me2bta): Promising ligands in new copper based priming charges (PC). In *37th International Annual Conference of Fraunhofer-Institut für Chemische Technologie (ICT), Karlsruhe, Germany*.
- [13] (a) Gao, H., Y. Huang, C. Ye, B. Twamley, and J. M. Shreeve. 2008. The synthesis of di(aminoguanidine) 5-nitroiminotetrazolate: Some diprotic or monoprotic acids as precursors of energetic salts. *Chemistry – A European Journal*, 14: 5596–5603. (b) Semenov, S. N., A. Yu Rogachev, S. V. Eliseeva, Y. A. Belousov, A. A. Drozdov, and S. I. Troyanov. 2007. 5-Nitroaminotetrazole as a building block for extended network structures: Syntheses and crystal structures of a number of heavy metal derivatives. *Polyhedron*, 26: 4899–4907; (c) Ilyushin, M. A. and I. V. Tselinskii. 2006. The influence of the structure of the salts of azoles upon the processes of their thermal and laser initiation.

- Central European Journal of Energetic Materials*, 3: 39–50; (d) Astakhov, A. M., A. D. Vasiliev, M. S. Molokeev, A. M. Sirotinin, and R. S. Stepanov. 2005. Crystal and molecular structure of nitraminotetrazoles and nitramino-1,2,4-triazoles. V. 5-Nitraminotetrazole methylammonium salt. *Journal of Structural Chemistry*, 46: 517–522; (e) Astakhov, A. M., A. D. Vasiliev, M. S. Molokeev, L. A. Kruglyakova, A. M. Sirotinin, and R. S. Stepanov. 2004. Crystal and molecular structure of nitraminotetrazole and nitramino-1,2,4-triazole. IV. 5-Nitraminotetrazole sodium salt sesquihydrate. *Journal of Structural Chemistry*, 45: 537–540; (f) Vasiliev, A. D., A. M. Astakhov, A. A. Nefedov, and R. S. Stepanov. 2003. Crystal and molecular structure of monoammonium salt of 5-nitroaminotetrazole. *Journal of Structural Chemistry*, 44: 322–325; (g) Astakhov, A. M., A. D. Vasil'ev, M. S. Molokeev, V. A. Revenko, and R. S. Stepanov. 2005. Nitroamines: II. Structure of nitroamino-1,2,4-triazoles. *Russian Journal of Organic Chemistry*, 41: 910–915; (h) Tappan, B. C., C. D. Incarvito, A. L. Rheingold, and T. B. Brill. 2002. Thermal decomposition of energetic materials. 79. Thermal, vibrational, and x-ray structural characterization of metal salts of mono- and di-anionic 5-nitraminotetrazole. *Thermochimica Acta*, 384: 113–120; (i) Astakhov, A. M., R. S. Stepanov, L. A. Kruglyakova, and A. A. Nefedov. 2001. Thermal decomposition of 5-nitraminotetrazole. *Russian Journal of Organic Chemistry*, 37: 577–582.
- [14] Klapötke, T. M. and J. Stierstorfer. 2007. Nitration products of 5-amino-1H-tetrazole and methyl-5-amino-1H-tetrazoles – structures and properties of promising energetic materials. *Helvetica Chimica Acta*, 90: 2132–2150.
- [15] Synthesis starting with **2**: To 5-nitriminotetrazole (2.60 g, 20.0 mmol) dissolved in 20 mL of water, calcium hydroxide (1.48 g, 20.0 mmol) was added and the suspension was heated to 80°C and filtered off. The product was directly recrystallized from water and the crystals filtered off and washed with ethanol/ether to give 4.01 g (15.6 mmol, 78%) of calcium nitriminotetrazolate pentahydrate. DSC (5°C min⁻¹, °C): 72–145°C (loss of crystal water), 360°C (explosion); IR (KBr, cm⁻¹): $\tilde{\nu}$ = 3,532 (m), 3,360 (s), 3,309 (s), 2,167 (w), 1,647 (m), 1,622 (m), 1,559 (w), 1,540 (w), 1,474 (s), 1,412 (s), 1,338 (m), 1,299 (s), 1,158 (m), 1,135 (m), 1,087 (m), 1,042 (w), 1,026 (s), 883 (m), 835 (w), 754 (w), 722 (w), 610 (w), 566 (w); Raman (1,064 nm, 350 mW, 25°C, cm⁻¹): $\tilde{\nu}$ = 1,487 (100), 1,431 (9), 1,406 (6), 1,220 (7), 1,160 (8),

- 1,138 (7), 1,091 (9), 1,047 (7), 1,029 (18), 727 (5), 611 (5), 406 (9); ^1H NMR (DMSO- d_6 , 25°C, ppm) δ : 3.45 (s, H_2O); ^{13}C NMR (DMSO- d_6 , 25°C, ppm) δ : 164.4 (CN_4); m/z (FAB $^-$): 129.1 [HATNO_2] $^-$; EA ($\text{CaCH}_{10}\text{N}_6\text{O}_7$, 258.2): calcd.: C 4.65, H 3.90, N 32.55; found: C 4.66, H 3.65, N 32.54; Sensitivities of the anhydrous compound: IS 5 J; FS > 112 N; ESD > 156 mJ.
- [16] Thermogravimetry was used to investigate the dehydration step and was performed using a Setaram TG-DTA 92-16 (<http://www.setaram.com/>) in a helium atmosphere with a heating rate of 1°C/min to a maximum temperature of 400°C. For the measurement, 4.521 mg of pulverized **1** in a “korund” pan was used.
- [17] Colorless rods, $0.15 \times 0.13 \times 0.05$, triclinic, $P-1$, 6.5227(2), 7.4533(1), 10.380(2) Å, 74.371(2), 72.29(2), 74.660(2)°, 453.68(16) Å 3 , Z : 2, ρ_{calc} : 1.890 g cm $^{-3}$, μ : 0.729 mm $^{-1}$, $F(000)$: 268, $\lambda_{\text{MoK}\alpha}$: 0.71073 Å, T : 200 K, τ (min-max): 3.8, 26.0°, Dataset (h; k; l): -5:8; -7:9; -9:12, Reflect. coll.: 2,373, Independ. refl.: 1,765, R_{int} = 0.019; Reflection obs. = 1,254, No. param.: 176, R_1 (obs): 0.0305, wR_2 (all data): 0.0665, S = 0.91, Resd. Dens. [e Å $^{-3}$]: -0.35, 0.45, Oxford Xcalibur3 CCD, solution: SIR-92, refinement: SHELXL-97, Absorpt. corr.: multiscan.
- [18] Crystallographic data for the structure(s) have been deposited with the Cambridge Crystallographic Data Centre. Copies of the data can be obtained free of charge on application to The Director, CCDC, 12 Union Road, Cambridge CB2 1EZ, UK (Fax: int.code(1223)336-033; e-mail for inquiry: fileserv@ccdc.cam.ac.uk; e-mail for deposition: deposit-@ccdc.cam.ac.uk).
- [19] (a) Sućeska, M. 1995. *Test Methods for Explosives*. New York: Springer, p. 21 (impact), p. 27 (friction). (b) Available at: <http://www.bam.de>; (c) Available at: <http://www.reichel-partner.de/> (accessed Oct 12, 2009)
- [20] (a) Zeman, S., V. Pelikán, and J. Majzlík. 2006. Electric spark sensitivity of nitramines. Part II. A problem of “hot spots.” *Central European Journal of Energetic Materials*, 3: 45–51. (b) Skinner, D., D. Olson, and A. Block-Bolten. 1998. Electrostatic discharge ignition of energetic materials. *Propellants, Explosives, Pyrotechnics*, 23: 34–42. (c) OZM Research, Czech Republic. Available at: <http://www.ozm.cz/testing-instruments/pdf/TI-SmallSpark.pdf>
- [21] (a) Byrd, E. F. and B. M. Rice. 2006. Improved prediction of heats of formation of energetic materials using quantum mechanical calculations. *Journal of Physical Chemistry*, 110: 1005–1013;

- (b) Rice, B. M., S. V. Pai, and J. Hare. 1999. Predicting heats of formation of energetic materials using quantum mechanical calculations. *Combustion and Flame*, 118: 445–458. (c) Frisch, M. J., G. W. Trucks, H. B. Schlegel, P. M. W. Gill, B. G. Johnson, M. A. Robb, J. R. Cheeseman, T. Keith, G. A. Petersson, J. A. Montgomery, K. Raghavachari, M. A. Al-Laham, V. G. Zakrzewski, J. V. Ortiz, J. B. Foresman, C. Y. Peng, P. Y. Ayala, W. Chen, M. W. Wong, J. L. Andres, E. S. Replogle, R. Gomperts, R. L. Martin, D. J. Fox, J. S. Binkley, D. J. Defrees, J. Baker, J. P. Stewart, M. Head-Gordon, C. Gonzalez, J. A. Pople. 1995. Gaussian 94, Revision B. 3. Pittsburgh, PA: Gaussian, Inc.
- [22] (a) Jenkins, H. D. B., H. K. Roobottom, J. Passmore, and L. Glasser. 1999. Relationships among ionic lattice energies, molecular (formula unit) volumes, and thermochemical radii. *Inorganic Chemistry*, 38: 3609–3620; (b) Jenkins, H. D. B., D. Tudela, and L. Glasser. 2002. Lattice potential energy estimation for complex ionic salts from density measurements. *Inorganic Chemistry*, 41: 2364–2367.
- [23] Johnson, D. A. 1982. *Some Thermodynamic Aspects of Inorganic Chemistry*, 2nd ed. Cambridge: Cambridge University Press.
- [24] Meyer, R., J. Köhler, and A. Homburg. 2007. Explosive train. In *Explosives*, 6th ed. Weinheim: Wiley-VCH.

Energetic Nitrogen-Rich Salts of 1-(2-Hydroxyethyl)-5-nitriminotetrazole

Niko Fischer,^[a] Thomas M. Klapötke,^{*[a]} and Jörg Stierstorfer^[a]

Keywords: Nitrogen / Nitrogen heterocycles / Energetic materials / Explosives

1-(2-Hydroxyethyl)-5-nitriminotetrazole (**2**) was formed by the reaction of 5-amino-1-(2-hydroxyethyl)tetrazole (**1**) and 100 % HNO₃. Compound **1** was obtained by alkylation of 5-amino-1*H*-tetrazole with 2-chloroethanol. Nitrogen-rich salts such as the ammonium (**3**), hydroxylammonium (**4**), guanidinium (**5**), aminoguanidinium (**6**), diaminoguanidinium (**7**), triaminoguanidinium (**8**), azidoformamidinium (**9**), and diaminouronium (**10**) 1-(2-hydroxyethyl)-5-nitriminotetrazolate were prepared by deprotonation or metathesis reactions. Compounds **3–10** were fully characterized by single-crystal X-ray diffraction (except for **9** and **10**), vibrational spec-

troscopy (IR and Raman), multinuclear NMR spectroscopy, elemental analysis, and differential scanning calorimetry (DSC) measurements. The heats of formation of **4–10** were calculated by the atomization method based on CBS-4M enthalpies. With these values and the X-ray densities, several detonation parameters such as the detonation pressure, velocity, energy, and temperature were computed using the EXPLO5 code. In addition their sensitivities towards impact, friction, and electrical discharge were tested using a BAM drophammer, a friction tester, and a small-scale electrical discharge device.

Introduction

The design of new energetic materials^[1] often involves nitrogen-rich heterocycles, such as triazoles and tetrazoles. Tetrazole derivatives have the outstanding property of often combining high nitrogen contents and a highly positive heat of formation with acceptable thermal stability and sensitivities owing to their aromatic ring systems. The thermal stability of tetrazole compounds can usually be increased by deprotonation and salt formation. Deprotonation also positively influences the sensitivity. Another way to control sensitivity and performance is the introduction of functional side chains at the nitrogen and/or carbon atoms. Great performances have been accomplished with tetrazoles comprising nitrogen and oxygen-containing functional groups, such as nitro groups (R–NO₂),^[2] nitrate esters (R–ONO₂),^[3] and nitramine functionalities (R–NHNO₂).^[4] In addition, the formation of tetrazolium salts with oxygen-rich counteranions such as NO₃[–]^[5,6] or N(NO₂)₂[–]^[7,8] are in the focus of research because they have balanced oxygen contents. In particular, 5-nitriminotetrazoles, which can be obtained by facile synthetic routes,^[9] and 1-substituted 5-nitriminotetrazoles, such as 1-methyl-5-nitriminotetrazole and 1-ethyl-5-nitriminotetrazole, have been known for some time.^[10] Moreover, various *N*-alkylations of 5-aminotetrazoles, which involve different alkylation reagents such as methyl iodide, dimethyl- and diethyl sulfate, and chloroethanol are known.^[11] Here we report on different salts of 1-(2-

hydroxyethyl)-5-nitriminotetrazole (**2**), which is one of the products obtained by nitration of 5-amino-1-(2-hydroxyethyl)tetrazole (**1**).^[12] The hydroxy group is able to participate in hydrogen bonds and can therefore increase stability. This can be seen by comparing these compounds with their *O*-nitrated analogues, which show much lower decomposition temperatures.^[13]

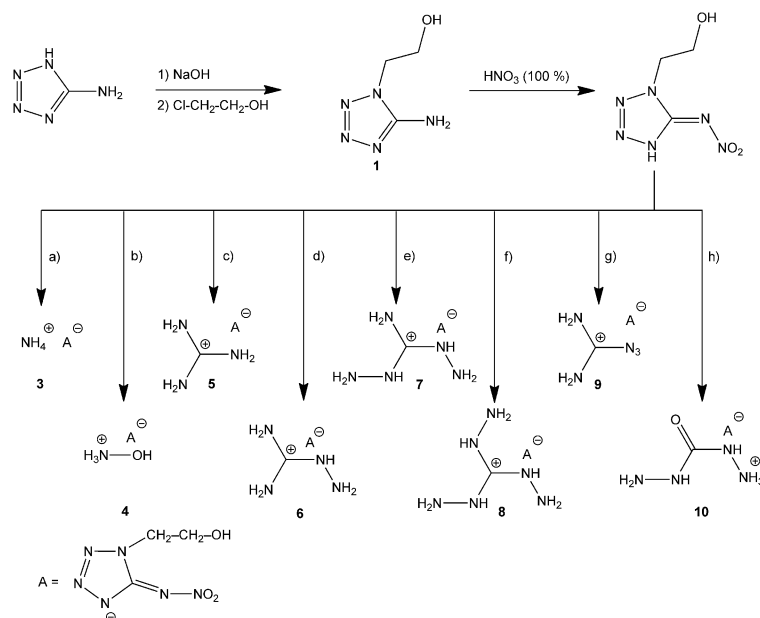
Results and Discussion

Synthesis

5-Amino-1-(2-hydroxyethyl)tetrazole (**1**) was synthesized from the reaction of the sodium salt of 5-amino-1*H*-tetrazole with 2-chloroethanol in aqueous solution under reflux conditions. 5-Amino-2-(2-hydroxyethyl)tetrazole can also be isolated from this reaction.^[12] 1-(2-Hydroxyethyl)-5-nitriminotetrazole (**2**) is obtained by treating **1** with a stoichiometric amount of fuming nitric acid. Using an excess of nitric acid yields the *O*-nitrated species 1-(2-nitratoethyl)-5-nitriminotetrazole. Eight nitrogen-rich salts of **2** were synthesized, which are the ammonium (**3**), hydroxylammonium (**4**), guanidinium (**5**), aminoguanidinium (**6**), diaminoguanidinium (**7**), triaminoguanidinium (**8**), azidoformamidinium (**9**), and diaminouronium (**10**) salt.

The syntheses of the nitrogen-rich salts of **2** are either based on Brønsted acid–base chemistry or metathesis reactions. In the case of **3**, **4**, **8**, and **10**, the free acid **2** was deprotonated by the free bases in aqueous solution. Although diaminourea, ammonia, and hydroxylamine are available as their free bases, triaminoguanidine was prepared by the reaction of a suspension of triaminoguanidin-

[a] Energetic Materials Research, Department of Chemistry, University of Munich (LMU), Butenandtstr. 5–13, 81377 München, Germany
Fax: +49-89-2180-77492
E-mail: tmk@cup.uni-muenchen.de



Scheme 1. Synthesis of nitrogen-rich salts of **2** under different reaction conditions: a) aqueous NH_3 , 50 °C, 5 min; b) aqueous hydroxylamine (50% w/w), 50 °C, 5 min; c) guanidinium carbonate, H_2O , reflux, 5 min; d) aminoguanidinium bicarbonate, H_2O , reflux, 5 min; e) 1. AgNO_3 , H_2O , room temp., 5 min; 2. diaminoguanidinium iodide, H_2O , 30 °C, 30 min; f) triaminoguanidine (free base), 40 °C, 5 min; g) 1. AgNO_3 , H_2O , room temp., 5 min; 2. azidoformamidinium chloride, H_2O , 30 °C, 30 min; h) diaminourea, 50 °C, 5 min.

ium chloride with 1 equiv. of sodium hydroxide in water under N_2 . Triaminoguanidine separates from the reaction mixture as a white solid upon addition of DMF and, after it was isolated in a Schlenk frit, it was kept under N_2 (Scheme 1).

The preparation of triaminoguanidine as a free base facilitated the synthesis of triaminoguanidinium salts as it eliminated the need of hydrazinolysis reactions of the corresponding aminoguanidinium salts or metathesis reactions involving silver nitrate. However, for the preparation of **7** and **9**, a metathesis reaction using silver nitrate in the first step and the corresponding nitrogen-rich halide in a second step remains indispensable as diaminoguanidine or azidoformamidine are still unknown as free bases. Salts **5** and **6** were prepared by reacting **2** with the corresponding carbonate, where carbon dioxide is expelled from the reaction mixture during a short period of heating in aqueous medium.

Molecular Structures

To determine the molecular structures of **3–8** in the crystalline state an Oxford Xcalibur3 diffractometer with a Spellman generator (voltage 50 kV, current 40 mA) and a KappaCCD detector was used. The data collection and reduction were performed using the CRYSLISPRO software.^[14] The structures were solved with SIR-92^[15] or SHELXS-97,^[16] refined with SHELXL-97,^[17] and finally checked using the PLATON software^[18] integrated in the WINGX software suite.^[19] The non-hydrogen atoms were refined anisotropically and the hydrogen atoms were located and freely refined. The absorptions were corrected by a SCALE3 ABSPACK multiscan method.^[20] Selected data

and parameters of the X-ray determinations are given in Tables 1 and 2.

The structure of **2**, which crystallizes in the space group $P\bar{1}$ with a density of 1.733 g cm^{-3} has recently been determined by our group.^[14]

The following ionic compounds contain the 1-(2-hydroxyethyl)-5-nitriminotetrazolate anion. Although showing different arrangements of the hydroxyethyl substituent, the bond lengths of the anion are very similar in all structures. A comparison can be found in Table 2.

Compound **3** crystallizes in the chiral monoclinic space group $P2_1$ with two molecules in the unit cell and a density of 1.617 g cm^{-3} . The molecular structure is shown in Figure 1. The structure of the anion is similar to that observed for neutral **2**. The nitriminotetrazole part is nearly planar, which can be seen by the C1–N5–N6–O1 torsion angle of $-1.8(4)^\circ$. The structure of **3** is stabilized by various H-bonds involving the ammonium cation, which are shown in Figure 2.

Compound **4** crystallizes in the monoclinic space group $P2_1/n$ (Figure 3). Its density of 1.614 g cm^{-3} is equal to that of the ammonium salt. Usually, hydroxylammonium tetrazolates show a significantly higher density (ca. 0.1 g cm^{-3}) than their ammonium homologues.^[21] All *N*- and *O*-bonded hydrogen atoms participate in strong hydrogen bonds, e.g. N7–H7a \cdots O3ⁱ: 0.92(2), 1.82(2), 2.725(2) Å, 169(2)°; N7–H7b \cdots N4ⁱⁱ: 0.98(2), 1.95(2), 2.892(2) Å, 160(2)°; N7–H7c \cdots O1ⁱⁱⁱ: 0.97(2), 2.07(2), 2.977(3) Å, 155.3(19)°; O4–H4 \cdots N3^{iv}: 0.81(2), 2.01(2), 2.818(2) Å, 170(2)°; O3–H3 \cdots O2^v: 0.89(3), 1.99(3), 2.848(2) Å, 162(3)°; symmetry codes: (i) $x, 1 + y, z$; (ii) $-0.5 + x, 1.5 - y, -0.5 + z$; (iii) $0.5 - x, -0.5 + y, 0.5 - z$; (iv) $-0.5 + x, 0.5 - y, -0.5 + z$; (v) $x, -1 + y, z$.

Table 1. X-ray data and parameters for **3–8**.

	3	4	5	6	7	8
Empirical formula	C ₃ H ₉ N ₇ O ₃	C ₃ H ₉ N ₇ O ₄	C ₄ H ₁₁ N ₉ O ₃	C ₄ H ₁₂ N ₁₀ O ₃	C ₄ H ₁₄ N ₁₁ O _{3.5}	C ₄ H ₁₄ N ₁₂ O ₄
<i>FW</i> [g mol ^{−1}]	191.17	207.17	233.22	248.24	544.52	278.27
Crystal system	monoclinic	monoclinic	monoclinic	orthorhombic	triclinic	monoclinic
Space group	<i>P</i> 2 ₁	<i>P</i> 2 ₁ / <i>n</i>	<i>P</i> 2 ₁ / <i>n</i>	<i>Pbca</i>	<i>P</i> $\bar{1}$	<i>P</i> 2 ₁ / <i>n</i>
Color and habit	colorless needle	colorless rod	colorless rod	colorless block	colorless rod	colorless rod
Size [mm]	0.07 × 0.09 × 0.24	0.10 × 0.13 × 0.24	0.18 × 0.26 × 0.28	0.14 × 0.21 × 0.23	0.14 × 0.20 × 0.21	0.10 × 0.15 × 0.25
<i>a</i> [Å]	7.7187(11)	9.6947(15)	11.5414(5)	12.3825(5)	7.0028(5)	11.8798(5)
<i>b</i> [Å]	5.3085(6)	5.3571(8)	5.1839(3)	7.0555(4)	11.5518(8)	6.9453(4)
<i>c</i> [Å]	10.1444(16)	16.597(2)	16.3739(7)	23.8917(10)	14.9190(9)	14.0032(6)
<i>α</i> [°]	90	90	90	90	89.254(5)	90
<i>β</i> [°]	109.216(16)	98.427(13)	103.149(4)	90	76.494(5)	100.430(4)
<i>γ</i> [°]	90	90	90	90	76.641(6)	90
<i>V</i> [Å ³]	392.51(10)	852.7(2)	953.96(8)	2087.29(17)	1140.67(14)	1136.30(10)
<i>Z</i>	2	4	4	8	2	4
<i>ρ</i> _{calcd.} [g cm ^{−3}]	1.617	1.614	1.624	1.580	1.585	1.627
<i>μ</i> [mm ^{−1}]	0.140	0.144	0.137	0.133	0.135	0.136
<i>F</i> (000)	200	432	488	1040	572	584
<i>λ</i> Mo- <i>K</i> _α [Å]	0.71073	0.71073	0.71073	0.71073	0.71073	0.71073
<i>T</i> [K]	173	173	173	173	173	173
<i>θ</i> min., max. [°]	4.3, 33.7	4.3, 26.0	4.3, 26.0	4.4, 26.0	4.2, 26.0	4.2, 26.5
Dataset	−11:11; −8:7; −8:15	−11:8; −6:6; −20:20	−14:14; −4:6; −20:19	−15:11; −8:2; −17:29	−8:8; −14:14; −18:18	−14:13; −8:8; −17:17
Reflections collected	3189	4196	3471	5344	11636	5047
Indep. reflections	1542	1672	1867	2047	4466	2342
<i>R</i> _{int}	0.082	0.037	0.020	0.031	0.043	0.026
Observed reflections	562	995	1285	1411	2561	1639
Parameters	154	163	189	202	446	228
<i>R</i> ₁ (obsd.) ^[a]	0.0440	0.0367	0.0305	0.0340	0.0335	0.0344
<i>wR</i> ₂ (all data) ^[b]	0.0466	0.0834	0.0649	0.0757	0.0571	0.0789
<i>S</i> ^[c]	0.62	0.84	0.88	0.86	0.76	0.91
Resid. density [e/Å ³]	−0.20, 0.22	−0.19, 0.27	−0.20, 0.19	−0.26, 0.19	−0.22, 0.18	−0.20, 0.30
Device type	Oxford Xcalibur3 (CCD)					
Solution	SIR-92	SIR-92	SHELXS-97	SHELXS-97	SHELXS-97	SHELXS-97
Refinement	SHELXL-97					
Absorption correction	multiscan					

[a] $R_1 = \sum |F_o| - |F_c| / \sum |F_o|$. [b] $wR_2 = [\sum (w(F_o^2 - F_c^2)^2) / \sum (w(F_o^2)^2)]^{1/2}$; $w = [\sigma_c^2(F_o^2) + (xP)^2 + yP]^{-1}$ and $P = (F_o^2 + 2F_c^2)/3$. [c] $S = [\sum \{w(F_o^2 - F_c^2)^2\} / (n - p)]^{1/2}$ (n = number of reflections; p = total number of parameters).

Table 2. Anion bond lengths [Å] in the structures of **3–8**.

	3	4	5	6	7	8
O1–N6	1.263(3)	1.2612(18)	1.2500(14)	1.2416(16)	1.2568(17)	1.2566(16)
O2–N6	1.263(3)	1.260(2)	1.2616(15)	1.2654(15)	1.2593(17)	1.2446(17)
N1–N2	1.354(3)	1.345(2)	1.3491(17)	1.3501(16)	1.3495(18)	1.3492(17)
N1–C1	1.340(4)	1.351(2)	1.3538(17)	1.3521(17)	1.3493(19)	1.353(2)
N1–C2	1.484(4)	1.468(2)	1.4619(17)	1.4676(19)	1.469(2)	1.466(2)
N2–N3	1.308(4)	1.297(2)	1.2944(16)	1.2908(17)	1.2970(18)	1.2942(18)
N3–N4	1.374(3)	1.366(2)	1.3710(17)	1.3638(17)	1.3736(18)	1.3599(18)
N4–C1	1.346(4)	1.336(2)	1.3269(17)	1.3234(19)	1.330(2)	1.3374(19)
N5–N6	1.315(4)	1.308(2)	1.3185(16)	1.3232(16)	1.3171(18)	1.3268(19)
N5–C1	1.380(4)	1.365(2)	1.3739(18)	1.3760(18)	1.374(2)	1.3637(18)
C2–C3	1.516(5)	1.506(3)	1.516(2)	1.510(2)	1.510(3)	1.523(3)
O3–C3	1.433(4)	1.396(3)	1.4216(19)	1.427(2)	1.417(2)	1.414(2)

All guanidinium derivatives investigated in this work crystallize in common space groups (**5**, **8**: monoclinic *P*2₁/*n*, **6**: orthorhombic *Pbca*, **7**: triclinic *P* $\bar{1}$). Interestingly, **5** (1.624 g cm^{−3}) and **8** (1.618 g cm^{−3}) have slightly higher densities compared to **6** (1.580 g cm^{−3}) and **7** (1.585 g cm^{−3}). All of the cations show structures that are in agreement with those found in the corresponding guanidinium series of 2-methyl-5-nitriminotetrazolates.^[22] The molecular structure of **5** is shown in Figure 4. The nitro group is slightly

twisted out of the tetrazole ring plane [angle N4–C1–N6–O1: 4.4(2)°]. The structure of **5** is dominated by a strong hydrogen bonded network involving all guanidinium protons as well the hydroxyl hydrogen atom.

The molecular structure of **6** is shown in Figure 5. The packing of **6** can be described as a wavelike layer structure along the *ac* plane. A view of the layers, illustrating the intense hydrogen bond network is shown in Figure 6.

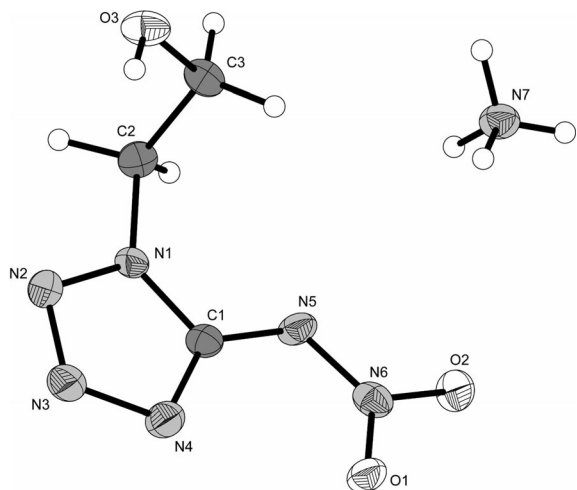


Figure 1. Molecular structure of **3**. Hydrogen atoms shown as spheres of arbitrary radius and ellipsoids are drawn at 50% probability.

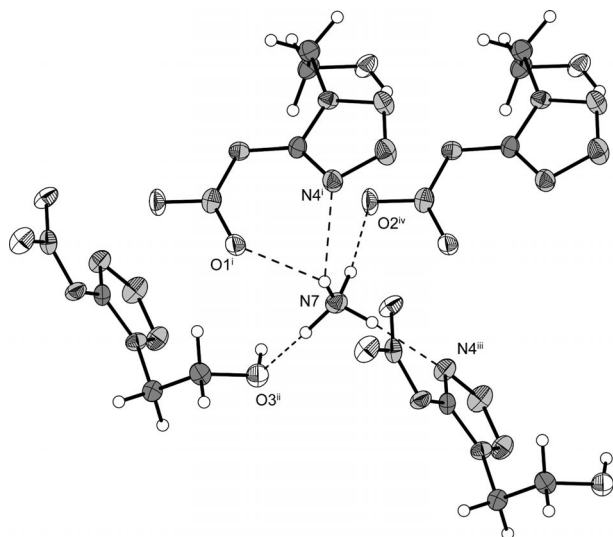


Figure 2. Hydrogen bonding of one ammonium cation in the structure of **3**. Hydrogen bond lengths [Å] and angles: N7–H7a \cdots O1ⁱ 0.83(4), 2.30(4), 2.959(4), 136(4)°; N7–H7c \cdots N4ⁱ 0.83(4), 2.52(4), 3.227(5), 144(4)°; N7–H7b \cdots O3ⁱⁱ 1.05(4), 1.85(4), 2.874(4), 164(3); N7–H7d \cdots N4ⁱⁱⁱ 0.95(4), 2.08(4), 3.018(4), 172(4); N7–H7a \cdots O2^{iv} 1.00(4), 1.96(4), 2.954(4), 169(3); symmetry codes: (i) 1 – x, –0.5 + y, 1 – z; (ii) x, –1 + y, z; (iii) 1 + x, y, z; (iv) 1 – x, 0.5 + y, 1 – z.

Crystalline **7** could only be obtained as its hemihydrate. The molecular structure is depicted in Figure 7.

In contrast to the structure of related triaminoguanidinium 1-(2-nitratoethyl)-5-nitriminotetrazolate,^[13] crystals of which were obtained as its monohydrate, **8** solidified without inclusion of crystal water. The molecular structure of **8** is shown in Figure 8.

The packing of **8** is built by alternating columns along the *c* axis, which is shown in Figure 9. A strong hydrogen bond network can be found within the columns. Alternating moieties consisting of two hydrazinium cations as well as dimeric tetrazolate units are connected by strong classical N–H \cdots N and N–H \cdots O hydrogen bonds.

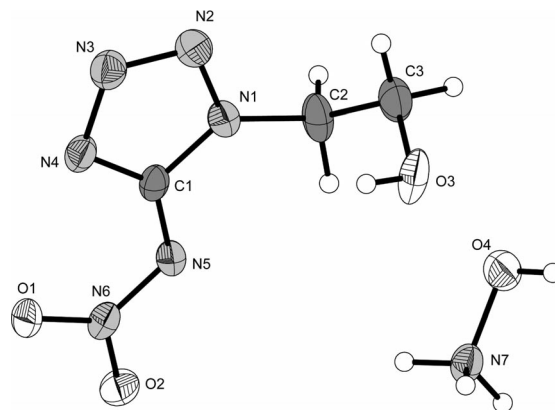


Figure 3. Molecular structure of **4**. Hydrogen atoms shown as spheres of arbitrary radius and thermal displacements set at 50% probability.

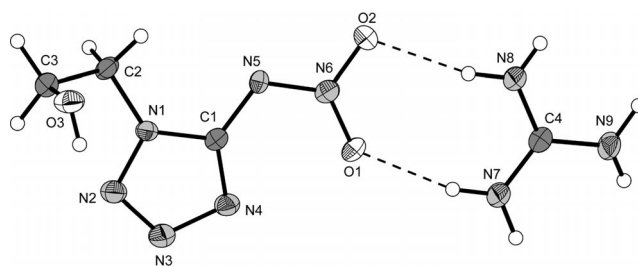


Figure 4. Molecular structure of **5**. Hydrogen atoms shown as spheres of arbitrary radius and thermal displacements set at 50% probability.

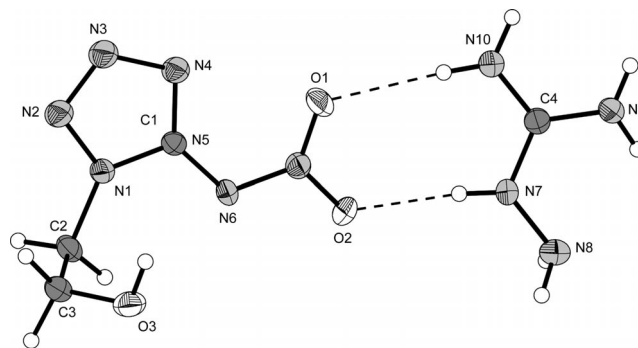


Figure 5. Molecular structure of **6**. Hydrogen atoms shown as spheres of arbitrary radius and thermal displacements set at 50% probability.

NMR Spectroscopy

Compounds **3–10** were investigated by ¹H and ¹³C NMR spectroscopy. Tetramethylsilane (¹H, ¹³C) was used as standard. The spectra were recorded in [D₆]DMSO (for **3–7**, **9**, **10**) and D₂O (for **8**).

The tetrazole carbon atom signals are located in a range from 156.2–157.6 ppm, which is about 7 ppm downfield shifted compared to **2** and can be traced back to the deprotonation of the tetrazole ring system. In contrast, deproton-

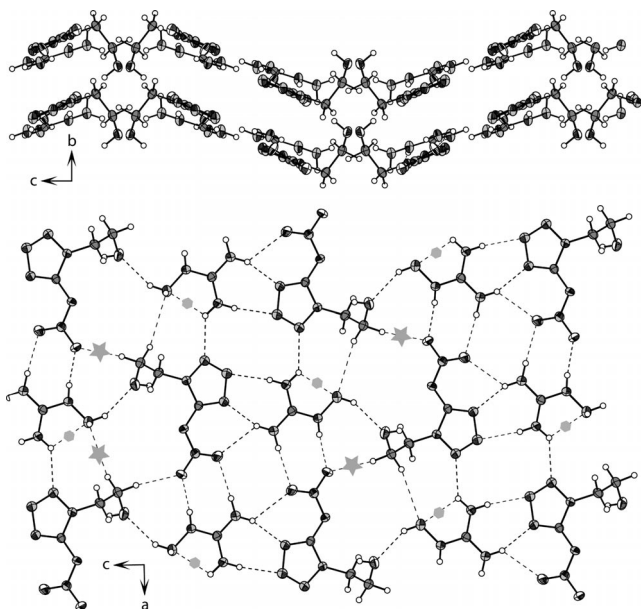


Figure 6. Hydrogen bond network stabilizing the wavelike layer structure of **6**. Nonclassical C–H...O hydrogen bonds are marked with an asterisk, intramolecular hydrogen bonds with a hexagon.

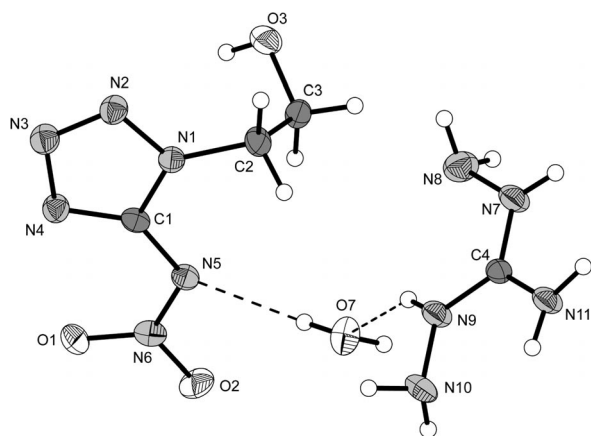


Figure 7. Molecular structure of **7**. Hydrogen atoms shown as spheres of arbitrary radius and thermal displacements set at 50% probability.

ation of the ring system does have a particular impact on the chemical shifts of the carbon atom signals of the aliphatic side chain. The signals are found at 58.1–59.2 ppm and 48.3–50.4 ppm, respectively, however, a final assignment to the hydroxyl- and tetrazole ring-connected methylene moiety remains unclear. The values are very close to those found for **2** (58.1 and 50.4 ppm). Looking at the proton chemical shifts of the anion, there is an indication for the final assignment of the signals, which is the signal of the guanidinium salt at 3.67 ppm; it can be identified as a doublet of triplets due to 3J coupling between the methylene protons and the neighboring hydroxy group. Therefore, the signals located at chemical shifts of 4.03–4.25 ppm can be assigned to the tetrazole-connected methylene unit, whereas the signals shifted to 3.65–3.85 ppm arise from the

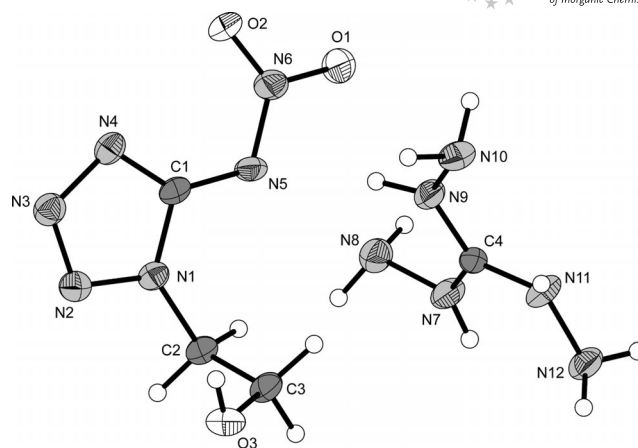


Figure 8. Molecular structure of **8**. Hydrogen atoms shown as spheres of arbitrary radius and thermal displacements set at 50% probability.

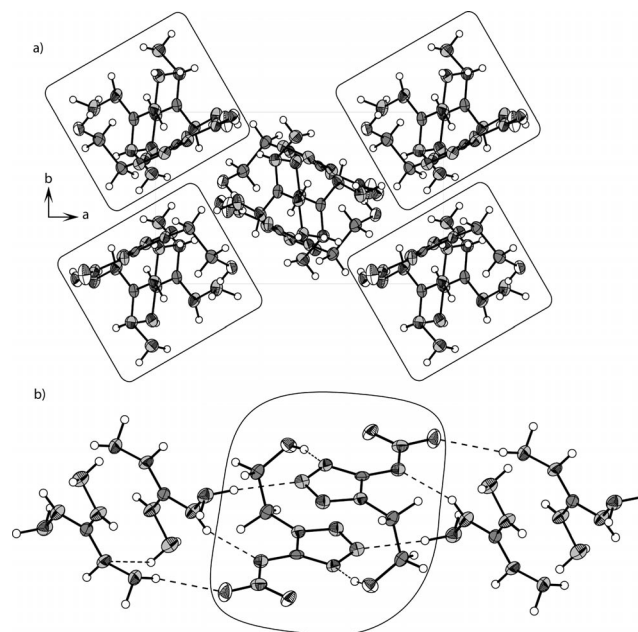


Figure 9. Packing of crystalline **8**. a) View along the columns parallel to the *c* axis; b) hydrogen bonds and dimer formation (marked) within the columns.

hydroxyl-connected methylene unit. Again, the shifts are not strongly affected by the deprotonation of the tetrazole ring, which can be stated after comparison to the values for **2** (4.22 and 3.77 ppm). The carbon and proton chemical shifts of the cations are very similar to those found in literature for nitrogen-rich salts of other nitriminotetrazolate compounds.^[13,22]

Sensitivities and Thermal Stability

Impact sensitivity tests were carried out according to STANAG 4489^[23] modified instruction^[24] using a BAM (German Bundesanstalt für Materialforschung) drophammer.^[25] The friction sensitivity tests were carried out

Table 3. Energetic properties and detonation parameters of **2–10**.

	2	3	4	5	6	7	8	9	10
Formula	C ₃ H ₆ N ₆ O ₃	C ₃ H ₉ N ₇ O ₃	C ₃ H ₉ N ₇ O ₄	C ₄ H ₁₁ N ₉ O ₃	C ₄ H ₁₂ N ₁₀ O ₃	C ₄ H ₁₄ N ₁₁ O _{3.5}	C ₄ H ₁₄ N ₁₂ O ₄	C ₄ H ₉ N ₁₁ O ₃	C ₄ H ₁₂ N ₁₀ O ₄
<i>FW</i> [g mol ^{−1}]	174.14	191.17	207.17	233.22	248.24	272.12	278.27	259.09	264.10
<i>IS</i> [J] ^[a]	6	10	15	>40	10	>40	18	9	40
<i>FS</i> [N] ^[b]	55	144	160	240	192	144	>360	120	288
ESD test [J] ^[c]	–	0.15	0.50	0.25	0.15	0.20	0.80	0.15	0.60
<i>N</i> [%] ^[d]	48.27	51.29	47.33	54.06	56.43	56.60	60.41	59.45	53.01
<i>Ω</i> [%] ^[e]	−55.13	−62.77	−50.20	−72.04	−70.90	−67.58	−69.00	−58.64	−60.55
<i>T</i> _{dec.} [°C] ^[f]	138	205	178	225	225	208	215	154	191
Density [g cm ^{−3}] ^[g]	1.73	1.617	1.614	1.624	1.580	1.585	1.627	1.6 (est.)	1.6 (est.)
<i>Δ_fH_m</i> ^o [kJ mol ^{−1}] ^[h]	110	85	148	47	158	148	370	470	133
<i>Δ_fU</i> ^o [kJ kg ^{−1}] ^[i]	739	569	831	322	759	675	1460	1924	626
Detonation parameters calculated by <i>EXPLO5.04</i>									
− <i>Δ_EU</i> ^o [kJ kg ^{−1}] ^[j]	4827	4541	5497	3699	3984	3319	4428	4839	4459
<i>T_E</i> [K] ^[k]	3314	2989	3542	2601	2714	2558	2869	3357	2986
<i>p_{C-J}</i> [kbar] ^[l]	275	246	268	223	222	202	260	240	238
<i>D</i> [m s ^{−1}] ^[m]	8270	8074	8298	7775	7805	7488	8304	7989	7974
Gas vol. [L kg ^{−1}] ^[n]	768	823	828	803	816	812	836	780	822

[a] Impact sensitivity (BAM drophammer,^[25] 1 of 6). [b] Friction sensitivity (BAM friction tester,^[25] 1 of 6). [c] Electrostatic discharge device (OZM).^[29] [d] Nitrogen content. [e] Oxygen balance. [f] Decomposition temperature from DSC (*β* = 5 °C). [g] From X-ray diffraction. [h] Calculated (CBS-4M) heat of formation. [i] Energy of formation. [j] Energy of explosion. [k] Explosion temperature. [l] Detonation pressure. [m] Detonation velocity. [n] Assuming only gaseous products.

according to STANAG 4487^[26] modified instructions^[27] using a BAM friction tester. The classification of the tested compounds results from the “UN Recommendations on the Transport of Dangerous Goods”.^[28] Additionally all compounds were tested for sensitivity towards electrical discharge using an Electric Spark Tester ESD 2010 EN.^[29] DSC measurements to determine the melt and decomposition temperatures of **2–10** (on about 1.5 mg of each energetic material) were performed in covered Al-containers containing a hole in the lid and a nitrogen flow of 20 mL per minute with a Linseis PT 10 DSC^[30] calibrated with standard pure indium and zinc at a heating rate of 5 °C min^{−1}.

Compared to their 1-(2-nitratoethyl)-substituted sister compounds,^[13] the nitrogen-rich salts of 1-(2-hydroxyethyl)-substituted nitriminotetrazole show excellent thermal stabilities: their decomposition points are above 200 °C with only a few exceptions [**4** (178 °C), **9**, and **10**]. It is a known feature of azidoformamidinium salts that, based on the azido moiety, these compounds decompose at lower temperatures than other nitrogen-rich salts.^[22] Due to the hydroxyethyl substituent, which is located in the 1-position at the tetrazole ring, the thermal stability is increased with respect to unsubstituted nitriminotetrazolates. Not only the thermal stability, but also the sensitivities of the compounds are influenced in a positive manner by hydroxyethyl substitution of the aromatic ring system. Most sensitive, as expected, is **9** with an impact sensitivity of 9 J and a friction sensitivity of 120 N, which is still in the range of commonly used secondary explosives such as RDX (7.5 J, 120 N). The best performing salts, **4** and **8**, show sensitivities that are far below the values found for RDX (**4**: 15 J, 160 N; **8**: 18 J, >360 N). The sensitivities of the remaining compounds are spread over a range between the discussed compounds and range from insensitive towards impact (>40 J for **5** and

7) to sensitive towards impact (10 J for **3** and **6**). The insensitivity of **7** towards impact can be explained by the crystal water included in the structure. The same reasons mentioned for the impact sensitivities apply to the friction sensitivities (144 N for **3** and **7** to 288 N for **10**). Apart from **8**, all compounds are classified as sensitive towards friction. A trend, which has been observed for other nitrogen-rich ionic compounds,^[22] is the relative insensitivity of **5** (>40 J, 240 N). All values for impact and friction sensitivity as well as the sensitivities towards electrical discharge and the decomposition temperatures are summarized in Table 3.

Heat of Formation

Heats of formation were computed theoretically. All calculations were carried out using the Gaussian G09 program package.^[31] The enthalpies (*H*) and free energies (*G*) were calculated using the complete basis set (CBS) method of Petersson and coworkers in order to obtain very accurate energies. The CBS models use the known asymptotic convergence of pair natural orbital expressions to extrapolate using a finite basis set to the estimated complete basis set limit. CBS-4 begins with a HF/3-21G(d) geometry optimization; the zero point energy is computed at the same level. It then uses a large basis set SCF calculation as a base energy, and a MP2/6-31+G calculation with a CBS extrapolation to correct the energy through second order. A MP4(SDQ)/6-31+(d,p) calculation was used to approximate higher order contributions. In this study we applied the modified CBS-4M method (M referring to the use of minimal population localization), which is a reparametrized version of the original CBS-4 method and includes some additional empirical corrections.^[32] The enthalpies of the gas phase species **M** (Table 4) were computed according to the

atomization energy method [Equation (1)]^[33] described in the literature.^[34]

$$\Delta_f H^\circ_{(g,M,298)} = H_{(molecule,298)} - \sum H^\circ_{(atoms,298)} + \sum \Delta_f H^\circ_{(atoms,298)} \quad (1)$$

Table 4. CBS-4M calculation results and molecular volumes taken from X-ray structures.

M	$-H^{298}/\text{a.u.}$	$\Delta_f H^\circ(\text{g,M})/\text{kcal mol}^{-1}$	V_M/nm^3
2	671.089203	41.5	
2 anion	670.586386	−9.5	174.0
NH ₄ ⁺	56.796608	151.9	
NH ₄ O ⁺	131.863249	177.9	
G ⁺	205.453192	136.6	
AG ⁺	260.701802	160.4	
DAG ⁺	315.949896	184.5	
TAG ⁺	371.197775	208.8	
AF ⁺	313.533549	234.9	88.5 ^[a]
DAU ⁺	335.795706	155.6	78.7 ^[b]
3		142.4	196.3
4		168.4	213.2
5		127.1	238.5
6		150.9	260.9
7 (H ₂ O) ^[a]		146.2	285.0
8		199.3	284.1
9		225.4	162.5
10		146.1	252.6

[a] Recalculated from the X-ray structure of azidoformamidinium nitrate. [b] Recalculated from the X-ray structure of diaminouronium nitrate.

Using calculated heats of sublimation for **2** by Trouton's Rule^[35] and lattice enthalpies for the ionic compounds, the gas phase enthalpies of formation (Table 4) were converted into the solid state (standard conditions) enthalpy of formation $\Delta_f H_m^\circ$ (Table 3). Lattice energies (U_L) and lattice enthalpies (ΔH_L) were calculated from the corresponding molecular volumes according to Jenkin's equations.^[36]

Lastly, the molar standard enthalpies of formation (ΔH_m) were used to calculate the molar solid state energies of formation (ΔU_m) according to Equation (2) (Table 4).

$$\Delta U_m = \Delta H_m - \Delta n RT \quad (2)$$

where Δn is the change of mol of gaseous components.

The compound with the highest heat of formation is **9** (470 kJ mol^{−1}) followed by **8** (370 kJ mol^{−1}). The decrease in enthalpy due to water inclusion can be clearly seen by the low value of **7** (148 kJ mol^{−1}). Except for **3** (85 kJ mol^{−1}) and **5** (47 kJ mol^{−1}), all deprotonated nitrogen-rich salts formed are more endothermic than **2** (110 kJ mol^{−1}).

Detonation Parameters

The detonation parameters were calculated using the program EXPLO5 V5.04.^[37] The program is based on the steady-state model of equilibrium detonation and uses Becker–Kistiakowsky–Wilson's equation of state (BKW E.O.S) for gaseous detonation products and Cowan–Fickett E.O.S. for solid carbon. The calculation of the equilibrium composition of the detonation products is performed by applying modified White, Johnson, and Dantzig's free energy minimization technique. The program is designed to enable

the calculation of detonation parameters at the CJ point. The BKW equation in the following form was used with the BKWN set of parameters (α , β , κ , θ) where X_i is the mol fraction of the i^{th} gaseous product and k_i is the molar covolume of the i^{th} gaseous product:

$$pV/RT = 1 + x e^{\beta x}$$

$$x = (\kappa \sum X_i k_i) / [V(T + \theta)]^a$$

$$\alpha = 0.5, \beta = 0.96, \kappa = 17.56, \theta = 4950$$

The calculations were performed using the maximum densities according to the crystal structures. The calculated detonation parameters of **9** and **10** are based on estimated densities of 1.60 g cm^{−3}. For comparison, several commonly used explosives were also calculated with the EXPLO5.04 code. The most important criteria of high explosives are the detonation velocity V_{Det} (TNT: 7253, HNS: 7436, PETN: 8320, RDX: 8747 m s^{−1}), the detonation pressure p_{CJ} (TNT: 216, HNS: 242, PETN: 320, RDX: 348 kbar) and the energy of explosion $\Delta_E U_m^\circ$ (TNT: −5227, HNS: −5476, PETN: −6190, RDX: −6125 kJ kg^{−1}). In terms of detonation velocity, **3–10** hardly reached the level of commonly used secondary explosives such as RDX. Most of the compounds reached calculated detonation velocities of 7700 to 8300 m s^{−1} and are therefore comparable to HNS, a thermally stable polynitrobenzene, and PETN, an aliphatic polynitrate ester, with **8** and **4** being the best performing compounds. A reason for the comparably low detonation velocities and detonation pressures is the highly negative oxygen balance of −50% to −72% arising from the ethyl side chain attached to the tetrazole ring. On the other hand, the tetrazole derivatives are thermally stabilized by the side chain and also show lower sensitivities against impact and friction compared to unsubstituted nitriminotetrazolates.

Conclusions

Several nitrogen-rich salts of 1-(2-hydroxyethyl)-5-nitriminotetrazole (**2**) were synthesized by deprotonation of the free acid **2** or metathesis reactions involving the silver salt of **2** and the corresponding nitrogen rich halides.

The salts **3–8** were characterized by single-crystal X-ray diffraction. They crystallize in the mono- and triclinic space groups $P2_1$ (**3**), $P2_1/n$ (**4**, **5**, **8**), $Pbca$ (**6**), and $P\bar{1}$ (**7**) with densities between 1.580 and 1.627 g cm^{−3}.

Compared to other nitrogen-rich nitriminotetrazolates, the compounds investigated show excellent thermal stabilities up to 225 °C. The impact and friction sensitivities of the nitrogen-rich salts were determined. They are classified as insensitive (**5**, **7**) or sensitive (**3**, **4**, **6**, **8**, **9**, **10**) towards impact and insensitive (**8**) or sensitive (**3–7**, **9**, **10**) towards friction.

Based on the crystal densities and CBS-4M enthalpies, several detonation parameters were calculated. Salts **4** and **8** show the highest values regarding the detonation velocity (**4**: 8298 m s^{−1}, **8**: 8304 m s^{−1}) and the detonation pressure (**4**: 268 kbar, **8**: 260 kbar). They are able to compete with commonly used TNT, however, the performance data for RDX are not reached.

Experimental Section

General: All reagents and solvents were used as received (Sigma–Aldrich, Fluka, Acros Organics) if not stated otherwise. Melting and decomposition points were measured with a Linseis PT10 DSC using a heating rate of $5\text{ }^{\circ}\text{C min}^{-1}$, which were checked with a Büchi melting point B-450 apparatus. ^1H , ^{13}C , and ^{15}N NMR spectra were measured with a JEOL instrument. All chemical shifts are quoted in ppm relative to TMS (^1H , ^{13}C) or nitromethane (^{14}N , ^{15}N). IR spectra were measured with a Perkin–Elmer Spektrum One FTIR instrument. Raman spectra were measured with a Perkin–Elmer Spektrum 2000R NIR FT-Raman instrument equipped with a Nd:YAG laser (1064 nm). Elemental analyses were performed with a Netsch STA 429 simultaneous thermal analyzer. Sensitivity data were determined using a BAM drophammer and a BAM friction tester. The electrostatic sensitivity tests were carried out using an Electric Spark Tester ESD 2010 EN (OZM Research) operating with the “Winspark 1.15” software package.

CAUTION! 1-(2-Hydroxyethyl)-5-nitriminotetrazole (**2**) and its salts **3–10** are all energetic compounds with sensitivity to various stimuli. Although we encountered no issues in the handling of these materials, proper protective measures (face shield, ear protection, body armor, Kevlar gloves, and earthed equipment) should be used at all times.

1-(2-Hydroxyethyl)-5-nitriminotetrazole (2): 5-Amino-1-(2-hydroxyethyl)tetrazole (4.84 g, 37.5 mmol) was added in small portions to fuming nitric acid (7 mL, 10.5 g, 168 mmol) over 60 min at $0\text{--}5\text{ }^{\circ}\text{C}$ in an ice bath. The mixture was stirred for 2 h at $0\text{ }^{\circ}\text{C}$ and overnight at room temp. The mixture was poured into 100 g of ice with stirring and a white solid emerged. After stirring until the ice melted, the mixture was evaporated to dryness under reduced pressure. The product was recrystallized from ethanol/water to yield 6.20 g (35.6 mmol, 95%) of **2**. ^1H NMR ($[\text{D}_6]\text{DMSO}$, $25\text{ }^{\circ}\text{C}$): δ = 4.85 (s, 1 H, OH), 4.22 (t, 2 H, CH_2OH), 3.77 (t, 2 H, NCH_2) ppm. ^{13}C NMR ($[\text{D}_6]\text{DMSO}$, $25\text{ }^{\circ}\text{C}$): δ = 150.9 (CN_4), 58.1 ($\text{CH}_2\text{--N}$), 50.4 ($\text{CH}_2\text{--OH}$) ppm.

Ammonium 1-(2-Hydroxyethyl)-5-nitriminotetrazolate (3): NH_3 (5 mL, 2 M) was added to a solution of 1-(2-hydroxyethyl)-5-nitriminotetrazole (1.74 g, 10 mmol) dissolved in water (10 mL). The clear solution was warmed to $50\text{ }^{\circ}\text{C}$ for 5 min and concentrated with a rotary evaporator. The product was recrystallized from an ethanol/water mixture; yield 82% (1.56 g, 8.17 mmol). DSC ($5\text{ }^{\circ}\text{C min}^{-1}$): $180\text{ }^{\circ}\text{C}$ (m.p.), $205\text{ }^{\circ}\text{C}$ (dec.1), $214\text{ }^{\circ}\text{C}$ (dec.2). IR (KBr): $\tilde{\nu}$ = 3548 (m), 3476 (s), 3413 (vs), 3236 (m), 1637 (w), 1617 (w), 1507 (m), 1454 (m), 1396 (m), 1384 (m), 1336 (s), 1320 (s), 1255 (w), 1105 (w), 1067 (w), 1045 (w), 889 (w), 862 (w), 775 (w), 740 (w), 622 (w), 480 (w) cm^{-1} . Raman (1064 nm, 500 mW, $25\text{ }^{\circ}\text{C}$): $\tilde{\nu}$ = 3013 (15), 2993 (32), 2970 (26), 2937 (4), 2893 (7), 1506 (100), 1330 (14), 1256 (7), 1156 (4), 1107 (5), 1049 (3), 1034 (49), 985 (6), 891 (4), 864 (3), 757 (6), 661 (7) cm^{-1} . ^1H NMR ($[\text{D}_6]\text{DMSO}$, $25\text{ }^{\circ}\text{C}$): δ = 7.12 (t, 4 H, NH_4^+), 4.91 (s, 1 H, OH), 4.03 (t, 2 H, N--CH_2), 3.66 (t, 2 H, $\text{CH}_2\text{--OH}$) ppm. ^{13}C NMR ($[\text{D}_6]\text{DMSO}$, $25\text{ }^{\circ}\text{C}$): δ = 156.9 (CN_4), 58.5 (NCH_2), 48.3 (CH_2OH) ppm. MS (FAB^+): m/z = 18.1 [NH_4^+]; MS (FAB^-): m/z = 173.0 [$\text{C}_3\text{H}_5\text{N}_6\text{O}_3^-$]. $\text{C}_3\text{H}_9\text{N}_7\text{O}_3$ (191.15): calcd. C 18.85, H 4.75, N 51.29; found C 18.78, H 4.76, N 51.29. Impact sensitivity: 10 J. Friction sensitivity: 144 N. ESD: 0.15 J.

Hydroxylammonium 1-(2-Hydroxyethyl)-5-nitriminotetrazolate (4): 1-(2-Hydroxyethyl)-5-nitriminotetrazole (1.74 g, 10 mmol) was dissolved in hot water (20 mL). An aqueous solution of hydroxylamine (50% w/w, 0.66 g, 10 mmol) was added, the mixture heated to $50\text{ }^{\circ}\text{C}$ for 5 min, and the solvent from the resulting clear solution

evaporated in vacuo. A colorless solid formed, which was recrystallized from ethanol to yield **4** as colorless crystals (1.92 g, 9.3 mmol, 93%). DSC [$5\text{ }^{\circ}\text{C min}^{-1}$ ($^{\circ}\text{C}$)]: $133\text{ }^{\circ}\text{C}$ (m.p.), $178\text{ }^{\circ}\text{C}$ (dec. 1), $192\text{ }^{\circ}\text{C}$ (dec. 2). IR (KBr): $\tilde{\nu}$ = 3374 (m), 3135 (m), 3073 (m), 2960 (m), 2933 (m), 2729 (m), 1628 (w), 1546 (m), 1505 (s), 1457 (m), 1431 (m), 1332 (vs), 1265 (m), 1246 (m), 1228 (m), 1163 (w), 1122 (w), 1076 (m), 1037 (m), 1000 (w), 957 (w), 884 (w), 872 (w), 772 (w), 755 (w), 739 (w), 661 (w), 547 (w), 523 (w), 482 (w) cm^{-1} . Raman (1064 nm, 300 mW, $25\text{ }^{\circ}\text{C}$): $\tilde{\nu}$ = 3014 (2), 2969 (9), 2934 (2), 1507 (100), 1392 (3), 1310 (9), 1231 (2), 1125 (11), 1063 (6), 1039 (32), 1002 (9), 886 (2), 872 (4), 758 (7), 661 (3), 283 (2) cm^{-1} . ^1H NMR ($[\text{D}_6]\text{DMSO}$, $25\text{ }^{\circ}\text{C}$): δ = 10.09 (s, 4 H, NH_3OH^+), 4.92 (s, 1 H, OH), 4.08 (t, 2 H, CH_2OH), 3.70 (t, 2 H, NCH_2) ppm. ^{13}C NMR ($[\text{D}_6]\text{DMSO}$, $25\text{ }^{\circ}\text{C}$): δ = 157.4 (CN_4), 59.1 (NCH_2), 48.8 (CH_2OH) ppm. MS (FAB^+): m/z = 34.0 [NH_3OH^+]. MS (FAB^-): m/z = 172.9 [$\text{C}_3\text{H}_5\text{N}_6\text{O}_3^-$]. $\text{C}_3\text{H}_9\text{N}_7\text{O}_4$ (207.15): calcd. C 17.39, H 4.38, N 47.33; found C 17.85, H 4.26, N 46.74. BAM drophammer: 15 J. Friction tester: 160 N. ESD: 0.50 J.

Guanidinium 1-(2-Hydroxyethyl)-5-nitriminotetrazolate (5): 1-(2-Hydroxyethyl)-5-nitriminotetrazole (1.74 g, 10 mmol) was dissolved in water (10 mL) in a 50 mL flask. Guanidinium carbonate (0.90 g, 5 mmol) was added and the mixture was heated to reflux for 5 min. The resulting clear solution was concentrated in a rotary evaporator. The product was recrystallized from ethanol/water in 79% yield (1.84 g, 7.92 mmol). DSC ($5\text{ }^{\circ}\text{C min}^{-1}$): $162\text{ }^{\circ}\text{C}$ (m.p.), $223\text{ }^{\circ}\text{C}$ (dec.). IR (KBr): $\tilde{\nu}$ = 3910 (w), 3426 (vs), 3203 (s), 2947 (m), 2885 (m), 2814 (m), 2388 (w), 2217 (w), 1971 (w), 1934 (w), 1662 (vs), 1572 (m), 1544 (w), 1499 (vs), 1458 (s), 1442 (s), 1434 (s), 1380 (s), 1331 (vs), 1307 (vs), 1269 (s), 1248 (s), 1230 (m), 1157 (m), 1108 (s), 1068 (s), 1039 (s), 989 (m), 949 (w), 892 (m), 867 (m), 770 (w), 736 (w), 603 (m), 547 (m), 537 (w), 516 (w), 487 (w), 469 (w) cm^{-1} . Raman (1064 nm, 500 mW, $25\text{ }^{\circ}\text{C}$): $\tilde{\nu}$ = 3001 (3), 2954 (19), 1501 (100), 1396 (7), 1310 (13), 1111 (5), 1058 (6), 1041 (37), 1010 (15), 868 (3), 757 (3), 435 (1) cm^{-1} . ^1H NMR ($[\text{D}_6]\text{DMSO}$, $25\text{ }^{\circ}\text{C}$): δ = 6.92 [s, 6 H, $\text{C}(\text{NH}_2)_3$], 4.91 (s, 1 H, OH), 4.05 (t, 2 H, N--CH_2), 3.67 (dt, 2 H, $\text{CH}_2\text{--OH}$) ppm. ^{13}C NMR ($[\text{D}_6]\text{DMSO}$, $25\text{ }^{\circ}\text{C}$): δ = 157.9 [$\text{C}(\text{NH}_2)_3$], 156.9 (CN_4), 58.6 (NCH_2), 48.4 (CH_2OH) ppm. MS (FAB^+): m/z = 60.1 [CH_6N_3^+]. MS (FAB^-): m/z = 173.0 [$\text{C}_3\text{H}_5\text{N}_6\text{O}_3^-$]. $\text{C}_4\text{H}_{11}\text{N}_9\text{O}_3$ (233.19): calcd. C 20.60, H 4.75, N 54.06; found C 20.59, H 4.88, N 54.04. Impact sensitivity: > 40 J. Friction sensitivity: 240 N. ESD: 0.25 J.

Aminoguanidinium 1-(2-Hydroxyethyl)-5-nitriminotetrazolate (6): 1-(2-Hydroxyethyl)-5-nitriminotetrazole (1.74 g, 10 mmol) was dissolved in water (10 mL) in a 50 mL flask. Aminoguanidinium hydrogencarbonate (1.36 g, 10 mmol) was added to the solution and the mixture was heated to reflux for 5 min. The resulting clear solution was concentrated with a rotary evaporator. The product was recrystallized from an ethanol/water mixture in 81% yield (2.00 g, 8.07 mmol). DSC ($5\text{ }^{\circ}\text{C min}^{-1}$): $135\text{ }^{\circ}\text{C}$ (m.p.), $225\text{ }^{\circ}\text{C}$ (dec.). IR (KBr): $\tilde{\nu}$ = 3425 (vs), 3387 (vs), 3337 (vs), 3309 (vs), 3188 (s), 3021 (m), 2953 (m), 2901 (m), 2343 (w), 1996 (w), 1688 (vs), 1658 (s), 1596 (w), 1513 (vs), 1471 (m), 1455 (s), 1438 (m), 1423 (m), 1383 (s), 1340 (vs), 1306 (vs), 1270 (s), 1149 (m), 1110 (m), 1060 (m), 1052 (m), 1038 (m), 976 (w), 954 (w), 888 (w), 863 (w), 772 (w), 751 (w), 733 (w), 701 (w), 666 (w), 624 (w), 558 (m), 534 (m), 508 (w), 485 (w) cm^{-1} . Raman (1064 nm, 500 mW, $25\text{ }^{\circ}\text{C}$): $\tilde{\nu}$ = 3339 (3), 3247 (6), 3006 (5), 2982 (20), 2954 (16), 2903 (4), 1507 (100), 1386 (3), 1326 (35), 1113 (9), 1053 (4), 1038 (58), 976 (7), 891 (5), 863 (4), 753 (10), 669 (5), 506 (7), 443 (3) cm^{-1} . ^1H NMR ($[\text{D}_6]\text{DMSO}$, $25\text{ }^{\circ}\text{C}$): δ = 8.54 (s, 1 H, C--NH--NH_2), 7.23 [s, 2 H, (NH_AH_B)], 6.70 [s, 2 H, (NH_AH_B)], 4.89 (s, 1 H, OH), 4.66 (s, 2 H, NH--NH_2), 4.04 (t, 2 H, NCH_2), 3.65 (t, 2 H, CH_2OH) ppm. ^{13}C NMR ($[\text{D}_6]\text{DMSO}$, $25\text{ }^{\circ}\text{C}$): δ = 158.7 [$\text{C}(\text{NH}_2)_2(\text{NHNH}_2)$], 157.0 (CN_4), 58.5

(NCH₂), 48.3 (CH₂OH) ppm. MS (FAB⁺): *m/z* = 75 [CH₇N₄⁺]. MS (FAB⁻): *m/z* = 173.0 [C₃H₅N₆O₃⁻]. C₄H₁₂N₁₀O₃ (248.22): calcd. C 19.36, H 4.87, N 56.43; found C 19.30, H 4.89, N 56.55. Impact sensitivity: 10 J. Friction sensitivity: 192 N. ESD: 0.15 J.

Diaminoguanidinium 1-(2-Hydroxyethyl)-5-nitriminotetrazolate (7): 1-(2-Hydroxyethyl)-5-nitriminotetrazole (2.62 g, 15 mmol) was dissolved in warm water (approx. 20 mL). The clear solution was mixed with a solution of AgNO₃ (2.55 g, 15 mmol) in water (approx. 10 mL). The resulting mixture was stirred for 5 min at room temp. in the darkness. The white precipitate was separated by centrifugation, washed twice with water until free of acid, and resuspended in water (approx. 20 mL). The suspension of silver-1-(2-hydroxyethyl)-5-nitriminotetrazolate was mixed with a solution of diaminoguanidinium iodide (3.26 g, 15 mmol) in warm water (approx. 15 mL). The mixture was stirred for 30 min at 30 °C in darkness. The AgI precipitate was removed by filtration. The clear solution was evaporated to dryness under reduced pressure, and the product was recrystallized from ethanol/water; yield 71% (2.80 g, 10.65 mmol). DSC (5 °C min⁻¹): 110 °C (m.p.), 208 °C (dec.). IR (KBr): $\tilde{\nu}$ = 3441 (s), 3339 (vs), 3289 (vs), 2981 (w), 2955 (w), 2352 (w), 1674 (vs), 1629 (vs), 1556 (w), 1508 (vs), 1455 (s), 1446 (s), 1421 (m), 1344 (vs), 1318 (vs), 1268 (s), 1231 (m), 1174 (m), 1112 (m), 1063 (m), 1049 (m), 1031 (m), 971 (m), 918 (w), 879 (w), 864 (w), 778 (w), 742 (w), 670 (w), 520 (w) cm⁻¹. Raman (1064 nm, 500 mW, 25 °C): $\tilde{\nu}$ = 3340 (3), 3262 (8), 3002 (3), 2984 (15), 2956 (5), 2892 (3), 1505 (100), 1341 (18), 1274 (7), 1177 (3), 1111 (7), 1052 (4), 1033 (30), 992 (8), 936 (5), 865 (5), 748 (7), 671 (4), 489 (3) cm⁻¹. ¹H NMR ([D₆]DMSO, 25 °C): δ = 8.55 [s, 2 H, C(=NH-NH₂)₂], 7.14 (s, 2 H, C=NH₂), 4.93 (s, 1 H, OH), 4.59 [s, 4 H, C(=NH-NH₂)₂], 4.07 (t, 2 H, N-CH₂), 3.70 (t, 2 H, CH₂-OH) ppm. ¹³C NMR ([D₆]DMSO, 25 °C): δ = 160.3 [C(NH-NH₂)₂(NH₂)⁺], 157.6 (CN₄), 59.1 (NCH₂), 48.8 (CH₂OH) ppm. MS (FAB⁺): *m/z* = 90.1 [CH₈N₅⁺]. MS (FAB⁻): *m/z* = 173.0 [C₃H₅N₆O₃⁻]. C₄H₁₃N₁₁O₃ (263.22): calcd. C 18.25, H 4.98, N 58.53; found C 18.17, H 4.87, N 58.07. Impact sensitivity: > 40 J. Friction sensitivity: 144 N. ESD: 0.20 J.

Triaminoguanidinium 1-(2-Hydroxyethyl)-5-nitriminotetrazolate (8): 1-(2-Hydroxyethyl)-5-nitriminotetrazole (1.74 g, 10 mmol) was dissolved in water (10 mL) and triaminoguanidine (1.04 g, 10 mmol) was added under nitrogen. The free base dissolved immediately, the mixture was warmed to 40 °C for 5 min., and the clear solution was evaporated to dryness. Recrystallization of the crude material from ethanol/water affords 2.20 g (7.91 mmol, 79%) of **8** as colorless crystals. DSC (5 °C min⁻¹): 142 °C (m.p.), 215 °C (dec.). IR (KBr): $\tilde{\nu}$ = 3552 (s), 3477 (s), 3414 (vs), 3348 (s), 3213 (s), 1685 (s), 1637 (m), 1617 (s), 1508 (s), 1451 (s), 1423 (m), 1392 (s), 1360 (s), 1337 (s), 1267 (m), 1241 (m), 1227 (m), 1202 (m), 1160 (w), 1128 (m), 1111 (m), 1073 (m), 1054 (w), 1034 (w), 990 (m), 952 (m), 884 (w), 861 (w), 778 (w), 749 (w), 702 (w), 637 (m), 608 (m), 511 (w), 483 (m) cm⁻¹. Raman (1064 nm, 500 mW, 25 °C): $\tilde{\nu}$ = 3345 (13), 3321 (13), 3267 (18), 3007 (7), 2966 (14), 2883 (6), 1687 (3), 1513 (100), 1459 (5), 1423 (7), 1341 (19), 1274 (9), 1110 (12), 1035 (49), 991 (8), 752 (10), 671 (5), 512 (3), 483 (5) cm⁻¹. ¹H NMR (D₂O, 25 °C): δ = 4.67 [s, 10 H, C(=NH-NH₂)₃, -OH], 4.25 (t, 2 H, NCH₂), 3.85 (t, 2 H, CH₂OH) ppm. ¹³C NMR (D₂O, 25 °C): δ = 159.6 [C(=NH-NH₂)₃], 156.2 (CN₄), 59.2 (NCH₂), 48.8 (CH₂OH) ppm. MS (FAB⁺): *m/z* = 105.1 [CH₉N₆⁺]. MS (FAB⁻): *m/z* = 173.0 [C₃H₅N₆O₃⁻]. C₄H₁₄N₁₂O₃ (278.23): calcd. C 17.27, H 5.07, N 60.41; found C 17.13, H 4.88, N 60.27. Impact sensitivity: 18 J. Friction sensitivity: > 360 N. ESD: 0.80 J.

Azidoformamidinium 1-(2-Hydroxyethyl)-5-nitriminotetrazolate (9): 1-(2-Hydroxyethyl)-5-nitriminotetrazole (2.62 g, 15 mmol) was dis-

solved in warm water (approx. 20 mL). The clear solution was mixed with a solution of AgNO₃ (2.55 g, 15 mmol) in water (10 mL). The mixture was stirred for 5 min at room temperature in the darkness. The white precipitate was separated by centrifugation, washed twice with water until free of acid, and finally resuspended in water (approx. 20 mL). This suspension of silver 1-(2-hydroxyethyl)-5-nitriminotetrazolate was mixed with a solution of azidoformamidinium chloride (1.82 g, 15 mmol) in warm water (approx. 15 mL). This mixture was stirred for 30 min at 30 °C in darkness. The AgCl precipitate was removed by filtration. The clear solution was evaporated to dryness under reduced pressure, and the product was recrystallized from ethanol/water to yield 2.88 g (11.1 mmol, 74%) of **9** as very fine needles. Unfortunately no crystals suitable for X-ray crystallography were obtained. DSC (5 °C min⁻¹): 154 °C (dec.). IR (KBr): $\tilde{\nu}$ = 3551 (m), 3474 (s), 3413 (vs), 3236 (w), 2984 (m), 2962 (m), 2643 (w), 2102 (w), 2023 (w), 1911 (w), 1637 (m), 1618 (m), 1578 (vs), 1491 (s), 1454 (m), 1426 (m), 1403 (m), 1364 (m), 1330 (s), 1266 (s), 1222 (m), 1153 (m), 1050 (s), 1033 (s), 991 (m), 949 (m), 887 (m), 871 (m), 862 (m), 777 (w), 724 (m), 684 (w), 668 (w), 583 (m), 523 (m), 485 (w) cm⁻¹. Raman (1064 nm, 500 mW, 25 °C): $\tilde{\nu}$ = 3006 (21), 2988 (46), 2963 (76), 2956 (71), 2903 (16), 1589 (100), 1465 (11), 1450 (9), 1429 (12), 1411 (33), 1404 (41), 1362 (13), 1307 (7), 1258 (8), 1225 (34), 1158 (3), 1043 (18), 995 (13), 952 (4), 874 (11), 863 (11), 778 (3), 762 (17), 724 (3), 670 (10), 524 (9), 488 (7), 449 (5), 327 (3), 278 (11) cm⁻¹. ¹H NMR ([D₆]DMSO, 25 °C): δ = 9.36 [s, 5 H, {C(=NH₂)₂}, -OH], 4.23 (t, 2 H, NCH₂), 3.77 (t, 2 H, CH₂OH) ppm. ¹³C NMR ([D₆]DMSO, 25 °C): δ = 156.8 (CN₄), 150.7 [C(NH₂)₂], 58.1 (NCH₂), 50.4 (CH₂OH) ppm. MS (FAB⁺): *m/z* = 86.1 [CH₄N₅⁺]. MS (FAB⁻): *m/z* = 173.0 [C₃H₅N₆O₃⁻]. C₄H₉N₁₁O₃ (259.19): calcd. C 18.54, H 3.50, N 59.45; found C 19.71, H 3.62, N 49.60. Impact sensitivity: 9 J. Friction sensitivity: 120 N. ESD: 0.15 J.

Diaminouronium 1-(2-Hydroxyethyl)-5-nitriminotetrazolate (10): 1-(2-Hydroxyethyl)-5-nitriminotetrazole (1.74 g, 10 mmol) was dissolved in water (10 mL) and diaminourea (0.90 g, 10 mmol) was added to the clear solution. The free base dissolved immediately, the mixture was warmed to 50 °C for 5 min, and the solution was evaporated to dryness. Recrystallization of the crude material from ethanol/water affords 2.34 g (8.86 mmol, 86%) of **10** as a colorless solid. Unfortunately, no crystals suitable for X-ray crystallography by recrystallization either from water, dimethyl formamide or an ethanol/water mixture were obtained. DSC (5 °C min⁻¹): 136 °C (m.p.), 191 °C (dec.). IR (KBr): $\tilde{\nu}$ = 3460 (m), 3377 (m), 3335 (m), 3295 (m), 3230 (m), 3121 (m), 3024 (w), 2962 (w), 2946 (w), 2896 (w), 2796 (w), 2694 (w), 2379 (w), 2030 (w), 1691 (m), 1624 (m), 1504 (s), 1458 (m), 1430 (m), 1376 (s), 1337 (s), 1311 (vs), 1253 (m), 1234 (m), 1176 (m), 1158 (m), 1117 (m), 1059 (m), 1035 (m), 996 (w), 970 (m), 940 (w), 879 (w), 871 (w), 773 (w), 747 (w), 742 (w), 687 (w), 664 (m), 583 (m), 567 (m), 527 (w) cm⁻¹. Raman (1064 nm, 500 mW, 25 °C): $\tilde{\nu}$ = 3377 (1), 3333 (1), 3298 (2), 3025 (3), 2971 (10), 2898 (2), 1690 (3), 1548 (3), 1502 (100), 1458 (2), 1418 (3), 1375 (7), 1336 (28), 1281 (3), 1231 (2), 1177 (6), 1118 (17), 1052 (7), 1035 (62), 999 (4), 972 (4), 939 (3), 881 (7), 749 (10), 666 (7), 586 (3), 490 (4), 444 (3), 385 (3), 308 (13), 274 (11) cm⁻¹. ¹H NMR ([D₆]DMSO, 25 °C): δ = 7.75 (s, 8 H, -NH-NH₂, NH-NH₃, -OH), 4.08 (t, 2 H, NCH₂), 3.70 (t, 2 H, CH₂OH) ppm. ¹³C NMR ([D₆]DMSO, 25 °C): δ = 159.4 [C(=NH-NH₂)(-NH-NH₃)], 157.3 (CN₄), 59.1 (NCH₂), 48.9 (CH₂OH) ppm. MS (FAB⁺): *m/z* = 91.0 [CH₇N₄O⁺]. MS (FAB⁻): *m/z* = 173.0 [C₃H₅N₆O₃⁻]. C₄H₁₄N₁₀O₄ (264.20): calcd. C 18.18, H 4.58, N 53.01; found C 18.29, H 4.52, N 52.18. Impact sensitivity: 40 J. Friction sensitivity: 288 N. ESD: 0.60 J.

CCDC-819225 (for 3), -819228 (for 4), -819226 (for 5), -819227 (for 6), -815408 (for 7), and -819224 (for 8) contain the supplementary crystallographic data for this paper. These data can be obtained free of charge from The Cambridge Crystallographic Data Centre via www.ccdc.cam.ac.uk/data_request/cif.

Acknowledgments

Financial support by the Ludwig Maximilian University (LMU) of Munich, the U.S. Army Research Laboratory (ARL) (contract number W911NF-09-2-0018), the Armament Research, Development and Engineering Center (ARDEC) (contract numbers W911NF-09-1-0120 and W011NF-09-1-0056), the Strategic Environmental Research and Development Program (SERDP) (contract number 10 WPSEED01-002WP1-765), and the U.S. Office of Naval Research [ONRGlobal, title: Synthesis and Characterization of New High Energy Dense Oxidizers (HEDO) - NICOP Effort] is gratefully acknowledged. The authors acknowledge collaborations with Dr. Mila Krupka (OZM Research, Czech Republic) in the development of new testing and evaluation methods for energetic materials and with Dr. Muhamed Suceska (Brodarski Institute, Croatia) in the development of new computational codes to predict the detonation and propulsion parameters of new explosives. We are indebted to Drs. Betsy M. Rice and Brad Forch (ARL, Aberdeen, Proving Ground, MD) and Mr. Gary Chen (ARDEC, Picatinny Arsenal, NJ) for many helpful and inspired discussions and support of our work. The authors thank Dr. Karina R. Tarantik for the characterization of compound 4. In addition, Mr. Stefan Huber is thanked for performing the sensitivity tests.

- [1] T. M. Klapötke, in: *Chemistry of High-Energy Materials*, De Gruyter, Berlin, **2011**.
- [2] T. M. Klapötke, C. M. Sabaté, J. Stierstorfer, *New J. Chem.* **2009**, 33, 136–147.
- [3] T. M. Klapötke, J. Stierstorfer, K. Tarantik, *Chem. Eur. J.* **2009**, 15, 5775–5792.
- [4] a) T. M. Klapötke, J. Stierstorfer, *Helv. Chim. Acta* **2007**, 90, 2132–2150; b) T. M. Klapötke, J. Stierstorfer, A. U. Wallek, *Chem. Mater.* **2008**, 20, 4519–4530; c) N. Fischer, T. M. Klapötke, J. Stierstorfer, *Z. Anorg. Allg. Chem.* **2009**, 635, 271–281.
- [5] K. Karaghiosoff, T. M. Klapötke, P. Mayer, C. M. Sabate, A. Penger, J. M. Welch, *Inorg. Chem.* **2008**, 47, 1007–1019.
- [6] N. Fischer, T. M. Klapötke, J. Stierstorfer, *Propellants Explos. Pyrotech.* **2011**, 36, 225–232.
- [7] K. O. Christe, W. W. Wilson, M. A. Petrie, H. H. Michels, J. C. Bottaro, R. Gilardi, *Inorg. Chem.* **1996**, 35, 5068–5071.
- [8] a) T. M. Klapötke, J. Stierstorfer, *Phys. Chem. Chem. Phys.* **2008**, 10, 4340–4346; b) T. M. Klapötke, J. Stierstorfer, *Eur. J. Inorg. Chem.* **2008**, 4055–4062.
- [9] E. Lieber, E. Sherman, R. A. Henry, J. Cohen, *J. Am. Chem. Soc.* **1951**, 73, 2327–2329.
- [10] J. A. Garrison, R. M. Herbst, *J. Org. Chem.* **1957**, 22, 278–283.
- [11] R. A. Henry, W. G. Finnegan, *J. Am. Chem. Soc.* **1954**, 76, 923–926.
- [12] N. Fischer, T. M. Klapötke, J. Stierstorfer, K. R. Tarantik, *New Trends in Research of Energetic Materials*, Proceedings of the 13th Seminar, Pardubice, Czech Republic, **2010**, 2, 455–467.
- [13] N. Fischer, T. M. Klapötke, J. Stierstorfer, *Polyhedron*, **2011**, DOI:10.1016/j.poly.2011.05.042.
- [14] *CrysAlisPro*, Oxford Diffraction Ltd., version 171.33.41, **2009**.
- [15] *SIR-92, A program for crystal structure solution*: A. Altomare, G. Casciarano, C. Giacovazzo, A. Guagliardi, *J. Appl. Crystallogr.* **1993**, 26, 343.
- [16] G. M. Sheldrick, *SHELXS-97, Program for Crystal Structure Solution*, University of Göttingen, **1997**.
- [17] G. M. Sheldrick, *SHELXL-97, Program for the Refinement of Crystal Structures*, University of Göttingen, Germany, **1997**.
- [18] A. L. Spek, *PLATON, A Multipurpose Crystallographic Tool*, Utrecht University, The Netherlands, **1999**.
- [19] L. J. Farrugia, *J. Appl. Crystallogr.* **1999**, 32, 837.
- [20] *SCALE3 ABSPACK – An Oxford Diffraction program* (1.0.4, gui: 1.0.3), Oxford Diffraction Ltd., **2005**.
- [21] M. Göbel, K. Karaghiosoff, T. M. Klapötke, D. G. Pierrey, J. Stierstorfer, *J. Am. Chem. Soc.* **2010**, 132, 17216–17226.
- [22] T. Fendt, N. Fischer, T. M. Klapötke, J. Stierstorfer, *Inorg. Chem.* **2011**, 50, 1447–1458.
- [23] *NATO standardization agreement (STANAG) on explosives*, impact sensitivity tests, no. 4489, 1st ed., Sept. 17, **1999**.
- [24] *WIWEB-Standardarbeitsanweisung*, Nr. 4-5.1.02, *Ermittlung der Explosionsgefährlichkeit* (impact sensitivity tests with a drophammer), Nov. 8, **2002**.
- [25] a) <http://www.bam.de>; b) www.reichel&partner.de.
- [26] *NATO standardization agreement (STANAG) on explosive, friction sensitivity tests*, no. 4487, 1st ed., Aug. 22, **2002**.
- [27] *WIWEB-Standardarbeitsanweisung*, Nr. 4-5.1.03, *Ermittlung der Explosionsgefährlichkeit oder der Reibeempfindlichkeit mit dem Reibeapparat*, Nov. 8, **2002**.
- [28] Impact: insensitive > 40 J, less sensitive ≈ 35 J, sensitive ≈ 4 J, very sensitive ≈ 3 J. Friction: insensitive > 360 N, less sensitive ≈ 360 N, sensitive < 360 N, very sensitive ≈ 80 N, extremely sensitive ≈ 10 N. According to the UN Recommendations on the Transport of Dangerous Goods, (+) indicates “Not safe for transport”.
- [29] <http://www.ozm.cz>.
- [30] <http://www.linseis.com>.
- [31] M. J. Frisch, G. W. Trucks, H. B. Schlegel, G. E. Scuseria, M. A. Robb, J. R. Cheeseman, G. Scalmani, V. Barone, B. Mennucci, G. A. Petersson, H. Nakatsuji, M. Caricato, X. Li, H. P. Hratchian, A. F. Izmaylov, J. Bloino, G. Zheng, J. L. Sonnenberg, M. Hada, M. Ehara, K. Toyota, R. Fukuda, J. Hasegawa, M. Ishida, T. Nakajima, Y. Honda, O. Kitao, H. Nakai, T. Vreven, J. A. Montgomery Jr., J. E. Peralta, F. Ogliaro, M. Bearpark, J. J. Heyd, E. Brothers, K. N. Kudin, V. N. Staroverov, R. Kobayashi, J. Normand, K. Raghavachari, A. Rendell, J. C. Burant, S. S. Iyengar, J. Tomasi, M. Cossi, N. Rega, J. M. Millam, M. Klene, J. E. Knox, J. B. Cross, V. Bakken, C. Adamo, J. Jaramillo, R. Gomperts, R. E. Stratmann, O. Yazyev, A. J. Austin, R. Cammi, C. Pomelli, J. W. Ochterski, R. L. Martin, K. Morokuma, V. G. Zakrzewski, G. A. Voth, P. Salvador, J. J. Dannenberg, S. Dapprich, A. D. Daniels, Ö. Farkas, J. B. Foresman, J. V. Ortiz, J. Cioslowski, D. J. Fox, *Gaussian 09*, rev. A.1, Gaussian, Inc., Wallingford CT, **2009**.
- [32] a) J. W. Ochterski, G. A. Petersson, J. A. Montgomery Jr., *J. Chem. Phys.* **1996**, 104, 2598; b) J. A. Montgomery Jr., M. J. Frisch, J. W. Ochterski, G. A. Petersson, *J. Chem. Phys.* **2000**, 112, 6532.
- [33] a) L. A. Curtiss, K. Raghavachari, P. C. Redfern, J. A. Pople, *J. Chem. Phys.* **1997**, 106, 1063; b) E. F. C. Byrd, B. M. Rice, *J. Phys. Chem. A* **2006**, 110, 1005–1013; c) B. M. Rice, S. V. Pai, J. Hare, *Combust. Flame* **1999**, 118, 445–458.
- [34] T. Altenburg, T. M. Klapötke, A. Penger, J. Stierstorfer, *Z. Anorg. Allg. Chem.* **2010**, 636, 463–471.
- [35] a) M. S. Westwell, M. S. Searle, D. J. Wales, D. H. Williams, *J. Am. Chem. Soc.* **1995**, 117, 5013–5015; b) F. Trouton, *Philos. Mag.* **1884**, 18, 54–57.
- [36] a) H. D. B. Jenkins, H. K. Roobottom, J. Passmore, L. Glasser, *Inorg. Chem.* **1999**, 38, 3609–3620; b) H. D. B. Jenkins, D. Tudela, L. Glasser, *Inorg. Chem.* **2002**, 41, 2364–2367.
- [37] M. Sućeska, *EXPLO5.4*, Brodarski institut, Zagreb, Croatia, **2010**.

Received: May 25, 2011

Published Online: ■

Full Paper

Explosives Based on Diaminourea

Niko Fischer, Thomas M. Klapötke,* Jörg Stierstorfer

Energetic Materials Research, Department of Chemistry, University of Munich (LMU), Butenandtstr. 5–13,
D-81377 Munich (Germany)
e-mail: tmk@cup.uni-muenchen.de

Received: January 5, 2011; revised version: February 16, 2011

DOI: 10.1002/prop.201100001

Abstract

Diaminourea (DAU, **1**) is synthesized by the reaction of dimethylcarbonate with hydrazine hydrate. DAU was protonated using nitric as well as perchloric acid yielding diaminouronium nitrate (**2**), diaminouronium dinitrate monohydrate (**3**) and diaminouronium perchlorate (**4**). The bis-perchlorate salt could not be isolated due to its high hygroscopicity. Explosives **2–4** were fully characterized using X-ray diffraction, NMR and vibrational spectroscopy, mass spectrometry and elemental analysis. The thermal properties were determined by differential scanning calorimetry (DSC). The sensitivities towards impact (**2**: 9 J, **3**: > 40 J, **4**: 2 J), friction (**2**: 288 N, **3**: > 360 N, **4**: 5 N) and electrical discharge (**2**: 0.60 J, **3**: 0.50 J, **4**: 0.30 J) were investigated using Bundesanstalt für Materialforschung (BAM) methods and a small scale electrostatic discharge device. The detonation parameters of **2** and **3** were computed using the EXPLO5.04 code with the X-ray densities as well as calculated (CBS-4 M) energies of formation as input values.

Keywords: Crystal Structures, Detonation Parameters, Explosives, Nitrates

1 Introduction

More than 2000 years after first making an appearance, energetic materials continue to expand their scope of application, based on continuous improvement in the underlying chemistry [1]. Energetic materials cover the whole range of explosives, propellants and pyrotechnics, which release their stored energy either by combustion, deflagration or detonation. The ongoing search for new insensitive and environmentally benign but also powerful replacements for secondary explosives such as hexogen (RDX) is exciting on the one hand and very challenging on the other hand [2]. In this work, we report on the mono- and bis-protonated diaminouronium nitrate as well as the perchlorate salt of diaminourea, their synthesis and full characterization. Surprisingly, in contrast to

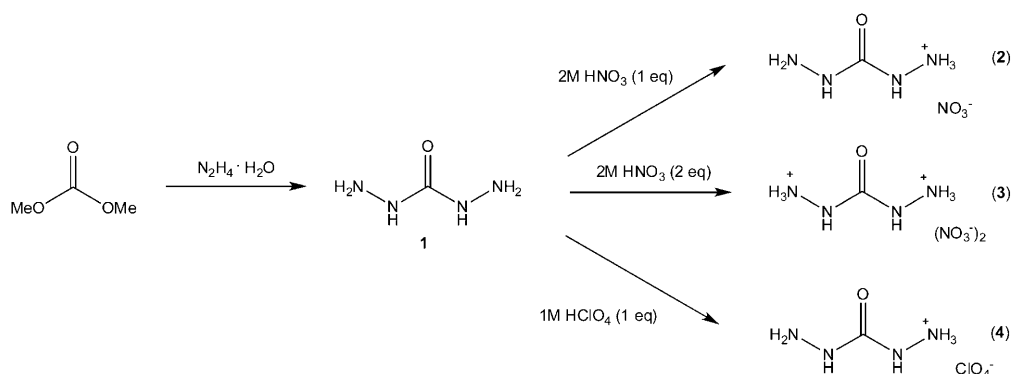
urea- and guanidine chemistry which are rampant in energetic materials' literature [3], diaminourea is rarely described [4].

2 Results and Discussion

2.1 Synthesis

Diaminouronium nitrate (**2**), diaminouronium dinitrate monohydrate (**3**) and diaminouronium perchlorate (**4**) can be synthesized by facile acid–base reaction in aqueous media starting from the base diaminourea. The synthetic routes to **2–4** are shown in Scheme 1.

Diaminourea is synthesized according to literature [5] starting from dimethyl carbonate and hydrazine hydrate in a two step reaction, where both hydrazine moieties are introduced successively. Since the water solubility of diaminourea is very good and it is a fairly strong base, it can be solubilized and protonated by dilute acids such as 2 M nitric or 1 M perchloric acid. After the removal of the water in vacuo, only the perchlorate salt remains as a colourless solid, which can easily be recrystallized. Both nitrate salts, especially the monodeprotonated salt **2**, cause major problems during their isolation since both remain as colourless liquids after the water has been evaporated. **3** crystallizes after the liquid has been taken up in methanol and slowly been evaporated again, whereas **2** solidified after the liquid was taken up in methanol and chilled to -20°C for several days. Scratching the flask with a glass rod after the mixture was allowed to come to room temperature resulted in the crystallization of the product. Regarding the easy synthesis of these compounds it has to be pointed out, that the comparatively cheap starting materials dimethyl carbonate, hydrazine hydrate and dilute nitric acid make compound **2** a very attractive candidate as a replacement for common secondary explosives.



Scheme 1. Synthetic routes to compounds 2–4.

2.2 Crystal Structures

To determine the molecular structures of 2–4 in the crystalline state an Oxford Xcalibur3 diffractometer with a Spellman generator (voltage 50 kV, current 40 mA) and a KappaCCD detector was used. The data collection was performed using the CrysAlis CCD software [6], the data reduction with the CrysAlis RED software [7]. The solution and refinement of all structures were performed using the programs SIR-92 [8], SHELXS-97 [9] and SHELXL-97 [10] implemented in the WinGX software package [11] and finally checked with the PLATON software [12]. In all crystal structures the hydrogen atoms were located and refined. The absorptions were corrected with the SCALE3 ABSPACK multi-scan method [13].

Selected data and parameter of the X-ray determinations are given in Table 1.

The structure of neutral DAU is known in literature and has been even determined at different temperatures [14]. Diaminouronium nitrate (2) crystallizes in the monoclinic space group $P2_1/c$ with four molecular moieties in the unit cell. Its density of 1.782 g cm^{-3} is higher than in most other CHNO nitrates in literature, e.g. morpholinium nitrate (1.444 g cm^{-3}) and glycylglycine nitrate (1.63 g cm^{-3}) [15]. The structure of the DAU cation is in agreement to that of its 5-(4-amino-oxadiazolyl)-tetrazolide salt in the literature [16]. The nitrate anion shows regular D_{3h} symmetry with N–O bond lengths of 125 pm.

The high density can be explained by having a look at the hydrogen bonds within the structure of 2. Its packing is strongly influenced by an intense hydrogen-bond network within discrete layers but also between them. Selected intermolecular and intramolecular H-bonds within a layer are shown in Figure 1. Various graph sets [17] such as the intramolecular S(1,1)5 as well as ring (R) and chain (C) motives can be detected and are partly drawn.

Diaminouronium dinitrate (3) could only be obtained crystalline as its monohydrate, which crystallizes in the orthorhombic space group $Pbca$ with eight cation/anion pairs in the unit cell. The molecular structure is shown in Figure 2. The density of 1.785 g cm^{-3} is slightly higher than that of 2, however, would be even higher without inclusion of crystal water. The structure of the cation is

comparable to that of diaminouronium sulphate described in literature [18].

Figure 3 shows the molecular structure of diaminouronium perchlorate (4), which crystallizes in the monoclinic space group $P2_1/c$. In contrast to the structure of 2, the DAU cation is bent over (C1–N3–N4) forming two intramolecular S(1,1)5 hydrogen bonds. The perchlorate anion shows regular T_d symmetry with Cl–O bond lengths of 143 pm.

2.3 Spectroscopy

2.3.1 NMR spectroscopy

All compounds were investigated using proton and carbon NMR spectroscopy. For the dinitrate salt 3, also a ^{14}N NMR spectrum was recorded. Due to very fast proton exchange for the protonated diaminouronium cation in solution, only a very broad signal at 7.94 ppm (2), 9.79 ppm (3) and 7.59 ppm (4) can be observed. The ^{13}C NMR spectra reveal a singlet at 159.2 ppm for both monoprotonated species 2 and 4 and a singlet, which is slightly shifted upfield to 157.2 ppm for the bis-protonated species 3. This trend is reconfirmed looking at the NMR data of unprotonated diaminourea, where the carbon signal is found at 162.0 ppm. Only for the bis-protonated salt 3 it was worthwhile running a ^{14}N NMR spectrum, because in addition to the nitrate anion at -4.5 ppm , there was a second relatively sharp signal visible at -359.5 ppm belonging to the protonated nitrogen atoms N2 and N4 (see Figure 2) with their comparatively symmetric environment.

2.3.2 Vibrational Spectroscopy

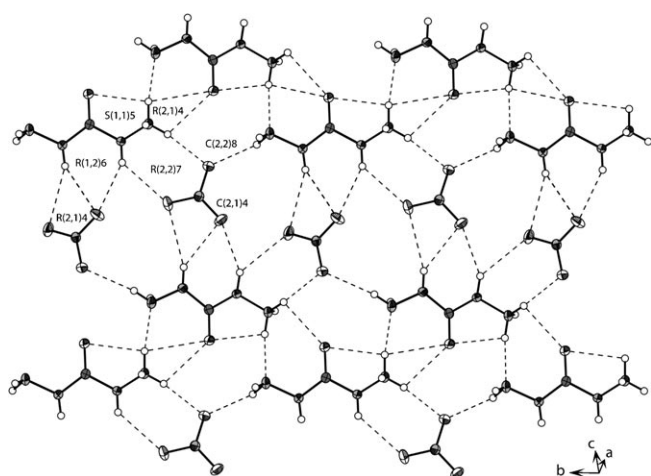
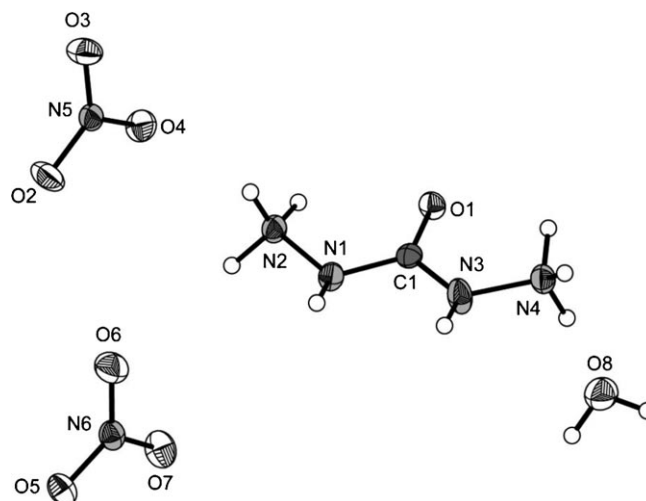
IR as well as Raman spectroscopy were employed for the characterization of 2–4. The most remarkable IR bands and Raman lines respectively belong to the inorganic anions NO_3^- and ClO_4^- . The Raman spectra show lines for the symmetric stretching vibration of the nitrate anion at 1055 cm^{-1} (2) and 1049 cm^{-1} (3) and the symmetric stretching vibration of the perchlorate anion at 939 cm^{-1}

Table 1. X-ray data and parameters.

	2	3	4
Formula	CH ₇ N ₅ O ₄	CH ₉ N ₆ O ₈	CH ₇ ClN ₄ O ₅
Form. Weight (g mol ⁻¹)	153.12	234.15	190.56
Crystal System	Monoclinic	Orthorhombic	Monoclinic
Space Group	<i>P</i> 2 ₁ / <i>c</i> (14)	<i>Pbca</i> (61)	<i>P</i> 2 ₁ / <i>c</i> (14)
Colour/Habit	Colourless Block	Colourless Block	Colourless Plate
Size (mm)	0.14 × 0.15 × 0.17	0.13 × 0.15 × 0.17	0.03 × 0.15 × 0.20
<i>a</i> (pm)	688.79(3)	799.3(5)	109.47(1)
<i>b</i> (pm)	957.01(4)	878.2(5)	712.49(5)
<i>c</i> (pm)	899.32(4)	248.31(5)	909.38(9)
α (°)	90	90	90
β (°)	105.723(5)	90	110.827(11)
γ (°)	90	90	90
<i>V</i> (pm ³)	5706300(500)	17430000(1500)	6629400(1100)
<i>Z</i>	4	8	4
$\rho_{\text{calc.}}$ (g cm ⁻³)	1.782	1.785	1.909
μ (mm ⁻¹)	0.171	0.181	0.564
<i>F</i> (000)	320	976	392
$\lambda_{\text{MoK}\alpha}$ (pm)	71.073	71.073	71.073
<i>T</i> (K)	173	173	173
θ Min–Max (°)	4.3, 26.7	4.2, 26.5	4.5, 26.0
Dataset	–8:8; –12:12; –11:11	–10:10; –11:11; –31:31	–13:13; –6:8; –9:11
Reflections Collected	8632	25007	3339
Independent Reflections	1206	1794	1297
<i>R</i> _{int}	0.023	0.030	0.039
Observed Reflections	1031	1452	946
Parameters	119	176	128
<i>R</i> ₁ (obs)	0.0257	0.0267	0.0328
<i>wR</i> ₂ (All Data)	0.0707	0.0779	0.0746
<i>S</i>	1.04	1.05	0.91
Resd. Dens. (e pm ⁻³)	–0.23 × 10 ⁻⁶ , 0.20 × 10 ⁻⁶	–0.19 × 10 ⁻⁶ , 0.19 × 10 ⁻⁶	–0.43 × 10 ⁻⁶ , 0.25 × 10 ⁻⁶
Device Type	Oxford Xcalibur3 CCD	Oxford Xcalibur3 CCD	Oxford Xcalibur3 CCD
Solution	SIR-92	SIR-92	SHELXS-97
Refinement	SHELXL-97	SHELXL-97	SHELXL-97
Absorption Correction	Multi-scan	Multi-scan	Multi-scan
CCDC	805986	805987	805985

(4). The respective asymmetric stretching vibrations can be observed in the IR spectra at 1385 cm⁻¹ (2), 1384 cm⁻¹ (3) and 1063 cm⁻¹ (4). Additionally, the IR spectra show bands for the C=O stretching vibration of the cation in

the region of 1630 to 1730 cm⁻¹. Also the N–N-stretching vibration of the hydrazine moiety of the cation is visible in bands which are scattered around 1500 cm⁻¹. The N–H


Figure 1. View on selected hydrogen bonds in the structure of 2.

Figure 2. Molecular unit of 3·H₂O. Hydrogen atoms shown as spheres of arbitrary radius and thermal displacements set at 50% probability.

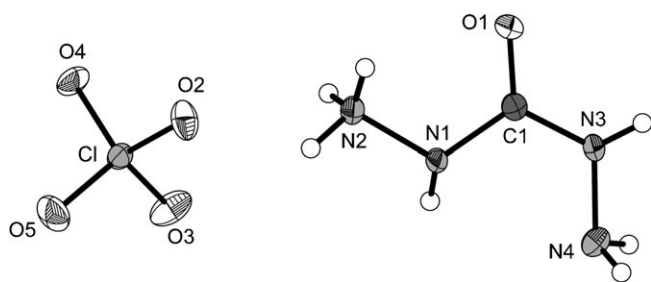


Figure 3. Molecular unit of **4**. Hydrogen atoms shown as spheres of arbitrary radius and thermal displacements set at 50% probability. Selected geometries: bond lengths (pm) N1–C1 136.5(3), N1–N2 142.2(3), N3–C1 133.4(3), N3–N4 140.8(3), O1–C1 123.7(3); bond angles (°) C1–N1–N2 113.8(2), C1–N3–N4 120.5(2), N3–C1–N1 115.5(2), O1–C1–N1 120.7(2), O1–C1–N3 123.8(2).

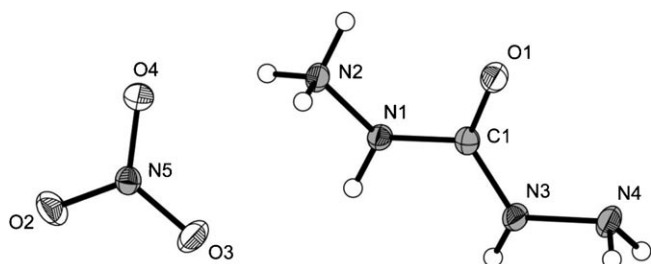


Figure 4. Molecular unit of **2**. Hydrogen atoms shown as spheres of arbitrary radius and thermal displacements set at 50% probability. Selected geometries: bond lengths (pm) N1–C1 139.89(13), N1–N2 142.69(12), N3–C1 134.11(13), N3–N4 141.35(13), O1–C1 122.12(13); bond angles (°) C1–N1–N2 112.75(9), C1–N3–N4 118.01(9), N3–C1–N1 113.67(9), O1–C1–N1 120.68(9), O1–C1–N3 125.63(10).

stretching vibrations at 3300–3440 cm^{-1} are visible in all spectra.

2.3.3 Mass Spectrometry

For detection of the different ions via mass spectrometry, the FAB technique was used. The spectra were recorded using either glycerin (**3**) or 3-nitrobenzyl alcohol (**2,4**) as liquid matrix. In the FAB-spectra the perchlorate (m/z 98.9) as well as the nitrate anion (m/z 62.0) could be detected. Also the mono-protonated DAU $\text{CH}_7\text{N}_4\text{O}^+$ is detected in the FAB+ in all cases (m/z 91.1), whereas the bis-protonated DAU was also detected in the FAB-spec-

trum of **3** as $\text{CH}_8\text{N}_5\text{O}_4^-$ (m/z 154.0), which would correspond to an addition species of $\text{CH}_8\text{N}_4\text{O}^{2+}$ and NO_3^- .

2.4 Thermal Analysis

Differential scanning calorimetry (DSC) measurements to determine the melt- and decomposition temperatures of **2–4** (about 1.5 mg of each energetic material) were performed in covered Al-containers with a hole (0.1 mm) in the lid for gas release and a nitrogen flow of 20 mL min^{-1} on a Linseis PT 10 DSC [19] calibrated by standard pure indium and zinc at a heating rate of 5 $^\circ\text{C min}^{-1}$. The decomposition temperatures are given as onset temperatures. The DSC curves of the compounds show endothermic peaks at 53 $^\circ\text{C}$ (**3**), 86 $^\circ\text{C}$ (**2**) and 158 $^\circ\text{C}$ (**4**), which can be assigned to their melting points. The melting temperatures were additionally determined and confirmed to be correct on a Büchi B-540 melting point apparatus to exclude the possibility of the loss of eventually contained residual solvent. A second endothermic peak in the DSC curve of **3** at 106 $^\circ\text{C}$ indicates the loss of the water molecule, which is included in the molecular unit. The lowest decomposition temperature – indicated by an exothermic peak – is observed at 115 $^\circ\text{C}$ for **3**, the bis-protonated diaminourea compound, which is right after the loss of the water molecule. Both mono-protonated compounds **2** and **4** show very similar decomposition temperatures of 242 $^\circ\text{C}$ (**2**) and 244 $^\circ\text{C}$ (**4**). Therefore, diaminourea has a remarkably high liquidity range of 156 $^\circ\text{C}$, making it a possible candidate for a future melt-cast explosive.

2.5 Energy of Formation

All calculations were carried out using the Gaussian G09 program package [20]. The enthalpies (H) and free energies (G) were calculated using the complete basis set (CBS) method of Petersson and coworkers in order to obtain very accurate energies. The CBS models use the known asymptotic convergence of pair natural orbital expressions to extrapolate from calculations using a finite basis set to the estimated CBS limit. CBS-4 begins with an HF/3-21G(d) geometry optimization; the zero point energy is computed at the same level. It then uses a large basis set SCF calculation as a base energy, and an MP2/6-31+G calculation with a CBS extrapolation to correct the energy through second order. An MP4(SDQ)/6-31+(d,p) calculation is used to approximate higher order contributions. In this study, we applied the modified CBS-

Table 2. Enthalpies of the gas-phase species M.

M	$-H^{298}$ (a.u.)	$\Delta_f H^\circ(\text{g}, \text{M})$ (kJ mol $^{-1}$)	V_M (nm 3)
DAU $^+$	335.781212	+1644	0.079
DAU $^{++}$	335.970629	+1726	0.076
NO_3^-	280.080446	–314	0.064
ClO_4^-	760.171182	–276	0.087
H_2O	76.346181	+534	0.014

Table 3. Explosive and detonation parameters.

	2	3	4	RDX
Formula	CH ₇ N ₅ O ₄	CH ₁₀ N ₆ O ₈	CH ₇ ClN ₄ O ₅	C ₃ H ₆ N ₆ O ₆
FW (g mol ⁻¹)	153.12	234.15	190.56	222.12
IS (J)	9	> 40	2	7.5
FS (N)	288	> 360	5	120
ESD (J)	0.60	0.50	0.30	0.1–0.2
N (%)	45.74	35.90	29.40	37.84
Ω (%)	–15.7	10.3	0.0	–21.6
T _{Dec.} (°C)	242	115	244	210
ρ (g cm ⁻³)	1.782	1.785	1.909	1.80
Δ _f H _m ^o (kJ mol ⁻¹)	–180	–876	–122	70
Δ _f U ^o (kJ kg ⁻¹)	–1048	–3613	–538	417
EXPLO5 values				
–Δ _{Ex} U ^o (kJ kg ⁻¹)	5048	2718	–	6125
T _{det} (K)	3391	2390	–	4236
P _{CJ} (Pa)	3.35 × 10 ¹⁰	2.29 × 10 ¹⁰	–	3.49 × 10 ¹⁰
V _{Det.} (m s ⁻¹)	8903	7577	–	8748
V _o (L kg ⁻¹)	910	889	–	739

4 M method (**M** referring to the use of Minimal Population localization) which is a re-parametrized version of the original CBS-4 method and also includes some additional empirical corrections [21]. The enthalpies of the gas-phase species **M** (Table 2) were computed according to the atomization energy method (Eq. 1) [22] described circumstantially in the literature [23].

$$\Delta_f H_{(g,M,298)}^o = H_{(Molecule,298)} - \sum H_{(Atoms,298)}^o + \sum \Delta_f H_{(Atoms,298)}^o \quad (1)$$

Using calculated lattice enthalpies (Table 2) the gas-phase enthalpies of formation (Table 2) were converted into the solid state (standard conditions) enthalpy of formation $\Delta_f H_m^o$ (Table 3). Lattice energies (U_L) and lattice enthalpies (ΔH_L) were calculated from the corresponding molecular volumes according to Jenkin's equations [24].

Lastly, the molar standard enthalpies of formation (ΔH_m) were used to calculate the molar solid state energies of formation (ΔU_m) according to Eq. (2) (Table 3).

$$\Delta U_m = \Delta H_m - \Delta n RT \quad (2)$$

(Δn being the change of moles of gaseous components)

2.6 Detonation Parameters

The calculation of the detonation parameters was performed with the program package EXPLO5 (version 5.04) [25]. The program is based on the chemical equilibrium, steady-state model of detonation. It uses the Becker–Kistiakowsky–Wilson's equation of state (BKW EOS) for gaseous detonation products and Cowan–Fickett's equation of state for solid carbon. The calculation of the equilibrium composition of the detonation products is done by applying modified White, Johnson and Dantzig's free energy minimization technique. The program is designed to enable the calculation of detonation parameters

at the CJ point. The BKW equation in the following form was used with the BKWN set of parameters (α , β , κ , θ) as stated below the equations and X_i being the mol fraction of i -th gaseous product, k_i is the molar covolume of the i -th gaseous product [26]:

$$pV/RT = 1 + xe^{\beta x} \quad x = (\kappa \sum X_i k_i) / [V(T + \theta)]^a$$

$$\alpha = 0.5, \beta = 0.176, \kappa = 14.71, \theta = 6620.$$

The detonation parameters calculated with the EXPLO5 program (V5.04) of compounds **2** and **3** using the experimentally determined densities (X-ray) are summarized in Table 3 and compared to the values calculated for commonly used RDX.

The detonation velocity and detonation pressure of **2** both ($V_{Det.} = 8903 \text{ m s}^{-1}$, $P_{CJ} = 3.35 \times 10^{10} \text{ Pa}$) are comparable to the values calculated for RDX ($V_{Det.} = 8748 \text{ m s}^{-1}$, $P_{CJ} = 3.49 \times 10^{10} \text{ Pa}$) with the velocity being slightly higher and the pressure being slightly lower, whereas the values for bis-protonated **3** drop rapidly ($V_{Det.} = 7577 \text{ m s}^{-1}$, $P_{CJ} = 2.29 \times 10^{10} \text{ Pa}$) compared to mono-protonated **2**. Since the density of both, **2** and **3**, is almost similar (**2**: $\rho = 1.782 \text{ g cm}^{-3}$, **3**: $\rho = 1.785 \text{ g cm}^{-3}$) and the density of a compound is the most determining factor for the performance data, the influence of other input data e.g. the energy of formation can be discussed very easily. The energy of formation for **3** ($\Delta_f U^o = -3613 \text{ kJ kg}^{-1}$) is much more negative than it is for **2** ($\Delta_f U^o = -1048 \text{ kJ kg}^{-1}$) resulting in a lower detonation energy and, therefore a much lower detonation temperature. The reason for the lower enthalpy of formation is not only the higher lattice enthalpy but also the inclusion of the water molecule into the crystal structure. For the perchlorate salt **4**, no detonation parameters can be determined, since EXPLO5 (V5.04) does not include heteroatoms such as chlorine for the calculation of the performance data as discussed above.

2.7 Sensitivities

The impact sensitivity tests were carried out according to STANAG 4489 [27] modified instruction [28] using a Bundesanstalt für Materialforschung (BAM) drophammer [29]. The friction sensitivity tests were carried out according to STANAG 4487 [30] modified instruction [31] using the BAM friction tester. The classification of the tested compounds results from the 'UN Recommendations on the Transport of Dangerous Goods' [32]. All compounds were tested upon the sensitivity towards electrical discharge using the Electric Spark Tester ESD 2010 EN [33]. Looking at the impact and friction sensitivity of the investigated compounds, a strong differentiation can be observed. Whereas the diaminouronium dinitrate monohydrate (**3**) is insensitive towards impact and friction [>40 J (IS), >360 N (FS)], the diaminouronium nitrate (**2**) is sensitive towards friction and impact with values of 9 J (IS) and 288 N (FS), however being still less sensitive than commonly used RDX [1,3,5-trinitrohexahydro-1,3,5-triazin; 7.5 J (IS), 120 N (FS)]. The perchlorate salt **4** reveals values for the impact sensitivity of 2 J and 5 N for the friction sensitivity and therefore has to be considered as very sensitive towards impact and extremely sensitive towards friction, which is in the expected range for water-free perchlorates. The insensitivity of **3** can be ascribed to the fact that it crystallizes as a monohydrate. The sensitivities towards electrical discharge are in more or less close range. The determined values are 0.60 J (**2**), 0.50 J (**3**) and 0.30 J (**4**). Again the perchlorate salt is most sensitive, whereas the both nitrate salts are very similar in their sensitivity.

3 Experimental Part

All chemicals and solvents were employed as received (Sigma-Aldrich, Fluka, Acros). ^1H and ^{13}C spectra were recorded using a JEOL Eclipse 270, JEOL EX 400 or a JEOL Eclipse 400 instrument. The chemical shifts quoted in ppm in the text refer to typical standards such as tetramethylsilane (^1H , ^{13}C). To determine the melting and decomposition temperatures of the described compounds a Linseis PT 10 DSC (heating rate 5°C min^{-1}) and a Büchi Melting Point B-540 apparatus was used. Infrared spectra were measured using a Perkin Elmer Spectrum One FT-IR spectrometer as KBr pellets. Raman spectra were recorded on a Bruker MultiRAM Raman Sample Compartment D418 equipped with an Nd-YAG-Laser (1064 nm) and an LN-Ge diode as detector. Mass spectra of the described compounds were measured at a JEOL MStation JMS 700 using FAB technique. To measure elemental analyses a Netsch STA 429 simultaneous thermal analyzer was employed.

3.1 Diaminouronium Nitrate (**2**)

Diaminourea (0.90 g, 10 mmol) is dissolved in nitric acid (2 M, 5 mL, 10 mmol) at room temperature. The solvent is removed from the clear solution resulting in a colour-

less oil. Recrystallization from ethanol/water yields **2** as colourless solid (after long standing). Alternatively the compound was crystallized after storage at -20°C under methanol for several days and scratching the flask with a glass rod after the mixture was allowed to come to room temperature. Yield: 1.48 g, 9.7 mmol, 97%.

DSC (5°C min^{-1}): 242°C (dec.); IR (KBr, cm^{-1}): $\tilde{\nu}=3304$ (s), 3227 (s), 3194 (s), 2977 (s), 2914 (s), 2698 (m), 2401 (m), 1764 (w), 1697 (s), 1589 (s), 1544 (s), 1504 (s), 1385 (vs), 1272 (s), 1216 (m), 1101 (m), 1021 (m), 983 (w), 825 (w), 787 (w), 750 (m), 584 (m), 508 (w), 472 (w); Raman (1064 nm, 300 mW, 25°C , cm^{-1}): $\tilde{\nu}=3336$ (6), 3228 (1), 1704 (6), 1647 (2), 1592 (3), 1537 (2), 1488 (1), 1370 (2), 1303 (1), 1268 (3), 1191 (1), 1170 (3), 1055 (100), 984 (7), 726 (4), 714 (5), 520 (4), 378 (2); ^1H NMR (d_6 -DMSO, 25°C): $\delta(\text{ppm})=7.94$ (s, 7H, $\text{H}_2\text{N}-\text{NH}-\text{CO}-\text{NH}-\text{NH}_3^+$); ^{13}C NMR (d_6 -DMSO, 25°C): $\delta(\text{ppm})=159.2$ (C=O); m/z (FAB $^+$): 91.0 ($\text{CH}_7\text{N}_4\text{O}^+$); m/z (FAB $^-$): 62.0 (NO_3^-); EA ($\text{CH}_7\text{N}_5\text{O}_4$, 153.1) calcd.: C 7.85, H 4.61, N 48.74%; Found: C 7.60, H 4.46, N 48.14%; impact sensitivity: 9 J; friction sensitivity: 288 N; ESD: 0.60 J (at grain size 500–1000 μm).

3.2 Diaminouronium Dinitrate Monohydrate (**3**)

Diaminourea (1.00 g, 11.1 mmol) is dissolved in nitric acid (2 M, 11.1 mL, 22.2 mmol) at room temperature. The solvent is removed from the clear solution in vacuo resulting in a colourless oil, which can easily be recrystallized from methanol. **3** crystallizes in colourless blocks in 78% yield (2.03 g, 8.67 mmol).

DSC (5°C min^{-1}): 40°C (m. p.), 115°C (dec.); IR (KBr, cm^{-1}): $\tilde{\nu}=3440$ (m), 2961 (m), 2682 (m), 2426 (w), 1767 (w), 1729 (m), 1541 (m), 1384 (s), 1188 (m), 1091 (m), 1047 (m), 833 (w), 748 (w), 597 (w); Raman (1064 nm, 300 mW, 25°C , cm^{-1}): $\tilde{\nu}=1701$ (3), 1588 (3), 1509 (2), 1400 (1), 1269 (1), 1220 (3), 1049 (100), 980 (12), 722 (9), 506 (4); ^1H NMR (d_6 -DMSO, 25°C): $\delta(\text{ppm})=9.79$ (s, 7H, $\text{H}_2\text{N}-\text{NH}-\text{CO}-\text{NH}-\text{NH}_3^+$); ^{13}C NMR (d_6 -DMSO, 25°C): $\delta(\text{ppm})=157.2$ (C=O); ^{14}N NMR (d_6 -DMSO, 25°C): $\delta(\text{ppm})=-4.5$ (NO_3^-), -359.5 ($-\text{NH}_3^+$); m/z (FAB $^+$): 91.1 ($\text{CH}_7\text{N}_4\text{O}^+$); m/z (FAB $^-$): 62.0 (NO_3^-), 154.0 ($\text{CH}_8\text{N}_5\text{O}_4^-$); EA ($\text{CH}_{10}\text{N}_6\text{O}_8$, 234.13) Calcd.: C 5.13, H 4.31, N 35.90%; Found: C 5.63, H 3.93, N 37.12%; impact sensitivity: >40 J; friction sensitivity: >360 N; ESD: 0.50 J (at grain size 500–1000 μm).

3.3 Diaminouronium Perchlorate (**4**)

Diaminourea (1.70 g, 18.9 mmol) is dissolved in 18.9 mL of 1 M perchloric acid at room temperature. The solvent of the clear solution is removed in vacuo and the white solid residue was recrystallized from an ethanol/water mixture to yield **4** almost quantitatively. (3.50 g, 18.4 mmol, 97%).

DSC (5°C min^{-1}): 158°C (m.p.), 244°C (dec.); IR (ATR, cm^{-1}): $\tilde{\nu}=3556$ (w), 3342 (m), 3200 (m), 3122 (m), 2773 (w), 1701 (m), 1637 (m), 1598 (m), 1572 (m), 1487 (m), 1427 (m), 1353 (w), 1293 (w), 1154 (m), 1063 (vs),

1005 (s), 933 (m), 758 (m), 714 (m); Raman (1064 nm, 400 mW, 25 °C, cm⁻¹): $\tilde{\nu}$ = 3345 (5), 3102 (2), 1687 (2), 1640 (2), 1592 (3), 1424 (7), 1365 (2), 1165 (4), 1123 (8), 939 (100), 681 (2), 630 (19), 583 (7), 470 (15), 453 (24), 259 (2); ¹H NMR (DMSO-*d*₆, 25 °C): δ (ppm) = 7.59 (s, br, 7H, H₂N–NH–CO–NH–NH₃⁺); ¹³C NMR (DMSO-*d*₆, 25 °C): δ (ppm) = 159.2 (C=O); *m/z* (FAB⁺): 91.1 [C(O)(NH)₂(NH₂)(NH₃)⁺]; *m/z* (FAB⁻): 98.9 [ClO₄⁻]; EA (CH₇ClN₄O₅, 190.54): Calc.: C 6.30, H 3.70, N 29.40%; Found: C 6.25, H 3.68, N 29.42%; impact sensitivity: 2 J; friction sensitivity: 5 N; ESD: 0.30 J (at grain size 100–500 μm).

4 Conclusion

From this combined theoretical and experimental study the following conclusions can be drawn:

- (i) Mono-protonated (**2**) and bis-protonated (**3**) diaminouronium nitrate as well as the mono-protonated perchlorate salt (**4**) could be synthesized in good yields and high purity from the corresponding acids and diaminourea.
- (ii) The crystal structures of **2–4** were determined by low-temperature single-crystal X-ray diffraction. The compounds crystallize in the space groups *P*2₁/*c* (**2**, **4**) and *Pbca* (**3**) with densities of 1.782 (**2**) 1.785 (**3**) and 1.909 g cm⁻³ (**4**), respectively. Additionally all compounds were fully characterized by vibrational spectroscopy (IR and Raman) ¹H and ¹³C NMR, mass spectroscopy, and elemental analysis.
- (iii) Thermal stabilities and melting points of **2–4** were investigated by DSC and a melting point apparatus. They melt at 53 °C (**3**), 86 °C (**2**) and 158 °C (**4**) and decompose at 115 °C (**3**), 242 °C (**2**) and 244 °C (**4**), respectively.
- (iv) The sensitivities towards friction, impact and electrostatic discharge were investigated by BAM methods. **2–4** were found to have impact sensitivities of 9 J, >40 J and 2 J respectively, friction sensitivities of 288 N, >360 N and 5 N respectively, and ESD sensitivities of 0.60 J, 0.50 J and 0.30 J, respectively. These are in a range from very sensitive (**4**) to insensitive (**3**).
- (v) Using calculated heats of formation and experimentally obtained crystal densities the detonation parameters (heat of explosion, explosion temperature, detonation pressure and velocity) were calculated. **2** has a detonation velocity of 8903 m s⁻¹ and a detonation pressure of 33.5 GPa. **3** has a detonation velocity of 7577 m s⁻¹ and a detonation pressure of 22.9 GPa.

Symbols and Abbreviations

FW formula weight (g mol⁻¹)
IS impact sensitivity (J)

FS friction sensitivity (N)
ESD electrostatic discharge (J)
N nitrogen content (%)
Ω oxygen balance (%)
*T*_{Dec.} decomposition temperature (°C)
ρ density (g cm⁻³)
Δ_f*H*_m^o heat of formation (kJ mol⁻¹)
Δ_f*U*^o energy of formation (kJ kg⁻¹)
Δ_{Ex}*U*^o energy of explosion (kJ kg⁻¹)
*T*_{det.} detonation temperature (K)
*P*_{Cl} detonation pressure at Chapman Jouguet Point (Pa)
*V*_{Det.} detonation velocity (m s⁻¹)
*V*_o volume of detonation gases (L kg⁻¹)

Acknowledgments

Financial support of this work by the Ludwig-Maximilian University of Munich (LMU), the U.S. Army Research Laboratory (ARL), the Armament Research, Development and Engineering Center (ARDEC), the Strategic Environmental Research and Development Program (SERDP) and the Office of Naval Research (ONR Global, title: “Synthesis and Characterization of New High Energy Dense Oxidizers (HEDO) – NICOP Effort”) under contract nos. W911NF-09-2-0018 (ARL), W911NF-09-1-0120 (ARDEC), W011NF-09-1-0056 (ARDEC) and 10 WPSEED01-002/WP-1765 (SERDP) is gratefully acknowledged. The authors acknowledge collaborations with Dr. Mila Krupka (OZM Research, Czech Republic) in the development of new testing and evaluation methods for energetic materials and with Dr. Muhamed Sucasca (Brodarski Institute, Croatia) in the development of new computational codes to predict the detonation and propulsion parameters of novel explosives. We are indebted to and thank Drs. Betsy M. Rice and Brad Forch (ARL, Aberdeen, Proving Ground, MD) and Mr. Gary Chen (ARDEC, Picatinny Arsenal, NJ) for many helpful and inspired discussions and support of our work.

References

- [1] a) J. P. Agrawal, *High Energy Materials*, Wiley-VCH, Weinheim **2010**; b) T. M. Klapötke, *Chemie der Hochenergetischen Materialien*, de Gruyter, Berlin **2009**; c) T. M. Klapötke, *Chemistry of High-Energy Materials*, de Gruyter, Berlin, **2011**; d) T. M. Klapötke, in: T. M. Klapötke, *High Energy Density Materials*, Springer, Berlin, Heidelberg **2007**, pp. 85–122.
- [2] T. M. Klapötke, J. Stierstorfer, Current Advances in RDX replacements, *Proceedings of the 27th Army Science Conference*, Orlando, FL, USA, November 29–December 2, **2010**.
- [3] a) Y. Guo, H. Gao, B. Twamley, J. M. Shreeve, Energetic Nitrogen Rich Salts of N,N-bis[1(2)H-tetrazol-5-yl]amine, *Adv. Mater.* **2007**, *19*, 2884; b) M. Hiskey, A. Hammerl, G. Holl, T. M. Klapötke, K. Polborn, J. Stierstorfer, J. J. Weigand, Azidoformamidinium and Guanidinium 5,5'-Azotetrazolate Salts, *Chem. Mater.* **2005**, *17*, 3784; c) T. M. Klapötke, J. Stierstorfer, A. U. Wallek, Nitrogen-Rich Salts of 1-Methyl-5-nitriminotetrazolate: An Auspicious Class of Thermally Stable Energetic Materials, *Chem. Mater.* **2008**, *20*, 4519; d) L. Medard, Explosive Properties of Urea Nitrate, Nitrourea, and Guanidine Nitrate, *Mem. d. Poudres* **1951**, *33*, 113.
- [4] a) R. Wang, H. Xu, S. Yong, R. Sa, J. M. Shreeve, Bis[3-(5-nitroimino-1,2,4-triazolate)]-Based Energetic Salts: Synthe-

- sis and Promising Properties of a New Family of High-Density Insensitive Materials, *J. Am. Chem. Soc.* **2010**, *132*, 11904; b) N. Fischer, T. M. Klapötke, D. Piercey, S. Scheut-zow, J. Stierstorfer, Diaminouronium Nitriminotetrazolates – Thermally Stable Explosives, *Z. Anorg. Allg. Chem.* **2010**, *636*, 2357; c) Y. Guo, G.-H. Tao, Z. Zeng, H. Gao, D. Parrish, J. M. Shreeve, Energetic Salts Based on Monoanions of N,N-Bis(1H-tetrazol-5-yl)amine and 5,5'-Bis(tetrazole), *Chem. Eur. J.* **2010**, *16*, 3753; d) A. E. Fogelzang, V. P. Sinditskii, V. Y. Egorshv, V. V. Serushkin, Effect of Structure of Energetic Materials on Burning Rate, *Mater. Res. Soc. Symp. Proc.* **1996**, *418*, 151.
- [5] Z. Li, W. Zhu, J. Yu, X. Ma, Z. Lu, S. Xiao, Green Synthetic Method for 1,5-Disubstituted Carbohydrazones, *Synth. Commun.* **2006**, *36*, 2613.
- [6] *CrysAlis CCD*, Version 1.171.27p5 beta, Oxford Diffraction Ltd.
- [7] *CrysAlis RED*, Version 1.171.27p5 beta, Oxford Diffraction Ltd.
- [8] A. Altomare, G. Casciaro, C. Giacovazzo, A. Guagliardi, Completion and Refinement of Crystal Structures with SIR92, *J. Appl. Crystallogr.* **1993**, *26*, 343.
- [9] G. M. Sheldrick, *SHELXS-97, Program for Crystal Structure Solution*, University of Göttingen, Göttingen, Germany **1997**.
- [10] G. M. Sheldrick, *Shelxl-97, Program for the Refinement of Crystal Structures*, University of Göttingen, Göttingen, Germany **1994**.
- [11] L. J. Farrugia, WinGX Suite for Small-molecule Single-crystal Crystallography, *J. Appl. Crystallogr.* **1999**, *32*, 837.
- [12] A. L. Spek, *PLATON, A Multipurpose Crystallographic Tool*, Utrecht, The Netherlands **1999**.
- [13] SCALE3 ABSPACK-An Oxford Diffraction Program, Oxford Diffraction Ltd., **2005**.
- [14] a) T. Ottersen, H. Hope, The Structure and Electron Deformation Density Distribution of Carbonohydrazide (Carbohydrazide) at 85 K, *Acta Crystallogr.* **1979**, *B35*, 373; b) G. A. Jeffrey, J. R. Ruble, R. G. Nanni, A. M. Turano, J. H. Yates, Neutron Diffraction at 15 K and Ab initio Molecular-orbital Studies of the Molecular Structure of Carbonohydrazide (Carbohydrazide), *Acta Crystallogr.* **1985**, *B41*, 354; c) J. Zhang, T. Thang, K. Yu, The Preparation, Molecular Structure, and Theoretical Study of Carbohydrazide (CHZ), *Struct. Chem.* **2006**, *17*, 249.
- [15] a) S. Swaminathan, G. S. Murthy, Morpholinium Nitrate, *Acta Crystallogr.* **1976**, *B32*, 3140; b) S. Narasinga Rao, R. Parthasarathy, Structure and Conformational Aspects of the Nitrates of Amino Acids and Peptides. I. Crystal Structure of Glycylglycine Nitrate, *Acta Crystallogr.* **1973**, *B29*, 2379.
- [16] R. Wang, Y. Guo, Z. Zeng, B. Twamley, J. M. Shreeve, Furan-functionalized Tetrazolate-based Salts: A New Family of Insensitive Energetic Materials, *Chem. Eur. J.* **2009**, *15*, 2625.
- [17] J. Bernstein, R. E. Davis, L. Shimon, N.-L. Chang, Patterns in Hydrogen Bonding: Functionality and Graph Set Analysis in Crystals, *Angew. Chem., Int. Ed.* **1995**, *34*, 1555.
- [18] A. M. M. Lanfredi, M. A. Pellinghelli, A. Tiripicchio, Crystal and Molecular Structure of Carbonohydrazide Sulfate, *J. Chem. Soc. Perkin Trans.* **1974**, 308.
- [19] <http://www.linseis.com>.
- [20] *Gaussian 09*, Revision A.1, M. J. Frisch, G. W. Trucks, H. B. Schlegel, G. E. Scuseria, M. A. Robb, J. R. Cheeseman, G. Scalmani, V. Barone, B. Mennucci, G. A. Petersson, H. Nakatsuji, M. Caricato, X. Li, H. P. Hratchian, A. F. Izmaylov, J. Bloino, G. Zheng, J. L. Sonnenberg, M. Hada, M. Ehara, K. Toyota, R. Fukuda, J. Hasegawa, M. Ishida, T. Nakajima, Y. Honda, O. Kitao, H. Nakai, T. Vreven, J. A. Montgomery, Jr., J. E. Peralta, F. Ogliaro, M. Bearpark, J. J. Heyd, E. Brothers, K. N. Kudin, V. N. Staroverov, R. Kobayashi, J. Normand, K. Raghavachari, A. Rendell, J. C. Burant, S. S. Iyengar, J. Tomasi, M. Cossi, N. Rega, J. M. Millam, M. Klene, J. E. Knox, J. B. Cross, V. Bakken, C. Adamo, J. Jaramillo, R. Gomperts, R. E. Stratmann, O. Yazyev, A. J. Austin, R. Cammi, C. Pomelli, J. W. Ochterski, R. L. Martin, K. Morokuma, V. G. Zakrzewski, G. A. Voth, P. Salvador, J. J. Dannenberg, S. Dapprich, A. D. Daniels, Ö. Farkas, J. B. Foresman, J. V. Ortiz, J. Cioslowski, D. J. Fox, Gaussian, Inc., Wallingford CT, **2009**.
- [21] a) J. W. Ochterski, G. A. Petersson, J. A. Montgomery, Jr., A Complete Basis Set Model Chemistry. V. Extensions to Six or more Heavy Atoms, *J. Chem. Phys.* **1996**, *104*, 2598; b) J. A. Montgomery, Jr., M. J. Frisch, J. W. Ochterski, G. A. Petersson, A Complete Basis Set Model Chemistry. VII. Use of the Minimum Population Localization Method, *J. Chem. Phys.* **2000**, *112*, 6532.
- [22] a) L. A. Curtiss, K. Raghavachari, P. C. Redfern, J. A. Pople, Assessment of Gaussian-2 and Density Functional Theories for the Computation of Enthalpies of Formation, *J. Chem. Phys.* **1997**, *106*, 1063; b) E. F. C. Byrd, B. M. Rice, Improved Prediction of Heats of Formation of Energetic Materials Using Quantum Mechanical Calculations, *J. Phys. Chem. A* **2006**, *110*, 1005; c) B. M. Rice, S. V. Pai, J. Hare, Predicting Heats of Formation of Energetic Materials Using Quantum Mechanical Calculations, *Combust. Flame* **1999**, *118*, 445.
- [23] T. Altenburg, T. M. Klapötke, A. Penger, J. Stierstorfer, Two Outstanding Explosives Based on 1,2-Dinitroguanidine: Ammonium-dinitroguanidine and 1,7-Diamino-1,7-dinitrimino-2,4,6-trinitro-2,4,6-triazaheptane, *Z. Anorg. Allg. Chem.* **2010**, *636*, 463.
- [24] a) H. D. B. Jenkins, H. K. Roobottom, J. Passmore, L. Glasser, Relationships Among Ionic Lattice Energies, Molecular (Formula Unit) Volumes, and Thermochemical Radii, *Inorg. Chem.* **1999**, *38*, 3609; b) H. D. B. Jenkins, D. Tudela, L. Glasser, Lattice Potential Energy Estimation for Complex Ionic Salts from Density Measurements, *Inorg. Chem.* **2002**, *41*, 2364.
- [25] M. Sućeska, *EXPLO5.04 program*, Zagreb, Croatia, **2010**.
- [26] a) M. Sućeska, Calculation of Detonation Parameters by EXPLO5 Computer Program, *Mater. Sci. Forum* **2004**, *465–466*, 325; b) M. Sućeska, Calculation of the Detonation Properties of C–H–N–O Explosives, *Propellants, Explos., Pyrotech.* **1991**, *16*, 197; c) M. Sućeska, Evaluation of Detonation Energy from EXPLO5 Computer Code Results, *Propellants, Explos., Pyrotech.* **1999**, *24*, 280; d) M. L. Hobbs, M. R. Baer, Calibrating the BKW-EOS with a Large Product Species Data Base and Measured C-J Properties *Proc. of the 10th Symp. (International) on Detonation*, ONR 33395-12, Boston, MA, July 12–16, **1993**, p. 409.
- [27] NATO Standardization Agreement (STANAG) on Explosives, *Impact Sensitivity Tests*, no. 4489, 1st Edn., September 17, **1999**.
- [28] WIWEB-Standardarbeitsanweisung 4-5.1.02, Ermittlung der Explosionsgefährlichkeit, hier der Schlagempfindlichkeit mit dem Fallhammer, November 8, **2002**.
- [29] <http://www.bam.de>.
- [30] NATO Standardization Agreement (STANAG) on Explosives, *Friction Sensitivity Tests*, no. 4487, 1st Edn., August 22, **2002**.
- [31] WIWEB-Standardarbeitsanweisung 4-5.1.03, Ermittlung der Explosionsgefährlichkeit oder der Reibeempfindlichkeit mit dem Reibeapparat, November 8, **2002**.
- [32] Impact: Insensitive >40 J, less sensitive ≥35 J, sensitive ≥4 J, very sensitive ≤3 J; friction: Insensitive >360 N, less sensitive =360 N, sensitive <360 N a. >80 N, very sensitive ≤80 N, extreme sensitive ≤10 N; According to the UN Recommendations on the Transport of Dangerous Goods (+) indicates: not safe for transport.
- [33] <http://www.ozm.cz>.

Hydrazinium Nitrimitotetrazolates

Niko Fischer,^[a] Thomas M. Klapötke,*^[a] and Jörg Stierstorfer^[a]**Keywords:** Tetrazoles; X-ray diffraction; Energetic materials; Sensitivities; IR spectroscopy

Abstract. Hydrazinium 5-nitrimino-1*H*-tetrazolate (**1**) and dihydrazinium nitrimitotetrazolate monohydrate (**2**) were synthesized by the reaction of hydrazine with 5-nitriminotetrazole. The energetic compounds **1** and **2** were characterized by single-crystal X-ray diffraction (only **2**), NMR spectroscopy, IR- and Raman spectroscopy as well

as DSC measurements. The sensitivities towards impact, friction and electrical discharge were determined. In addition, several detonation parameters (e.g. heat of explosion, detonation velocity) were computed by the EXPLO5 computer code based on calculated (CBS-4M) heats of formation and X-ray densities.

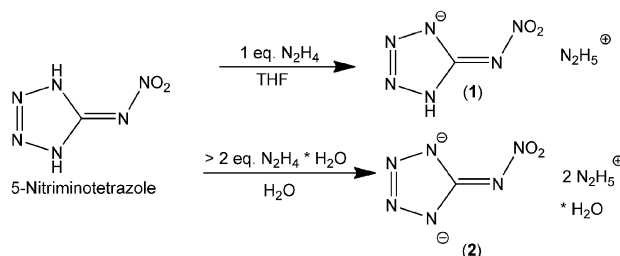
Introduction

The development of new energetic heterocyclic compounds has attracted considerable interest in recent years.^[1] Especially the syntheses and application of energetic nitrogen rich heterocyclic based salts is in the focus of many research programs worldwide.^[2] Energetic materials based on salts often have advantages over non-ionic molecules since these salts tend to exhibit lower vapor pressure and higher densities in comparison to neutral derivatives. Tetrazoles have the outstanding property of often combining high densities, high heats of formation and high nitrogen contents with low sensitivities and good thermal stabilities due to their aromatic rings system. Recently, we described the synthesis and characterization of several highly energetic 5-nitriminotetrazolate salts, such as diaminouronium 5-nitriminotetrazolate,^[3] 1-^[4] and 2-methyl-5-nitriminotetrazolates.^[5] In the present work we continue this series by combining two of the best energetic ionic building blocks. These are the monoprotonated hydrazinium cation in combination with mono- and bis-deprotonated 5-nitriminotetrazolate.

Results and Discussion

The reactions of hydrazine with 5-nitriminotetrazole^[6] are shown in Scheme 1. The monodeprotonated salt **1** was synthesized in THF using a 1M solution of hydrazine in dry THF. The salt precipitated instantly and could be separated by suction filtration. It could be recrystallized from methanol/water, which yielded the hemihydrate, as the elemental analysis showed. The hemihydrate lost its crystal water upon standing for a few days at ambient conditions. Unfortunately, no crystals suitable for X-ray single crystal diffraction could be obtained,

so the density, which is necessary for the calculation of the detonation parameters had to be determined by means of a solvent pycnometer using toluene as solvent. The density of the anhydrous compound was determined to be 1.68 g·cm⁻³.



Scheme 1. Reactions of 5-nitriminotetrazole with different amounts of hydrazine.

2 was synthesized by the reaction of 5-nitriminotetrazole with two equivalents of hydrazine hydrate in aqueous medium. After solvent evaporation, it could be recrystallized from ethanol/water, which unfortunately afforded only the monohydrate (**2**·H₂O), the molecular moiety of which is depicted in Figure 1.

2 crystallizes in the orthorhombic space group *P*2₁2₁2₁ with four molecules in the unit cell (Table 1). The Friedel pairs have been merged. The density of 1.635 g·cm⁻³ is lower than that observed for 5-nitriminotetrazole (1.867 g·cm⁻³)^[6] and 5-nitriminotetrazole monohydrate (1.808 g·cm⁻³).^[7] The planar structure of the bis-deprotonated 5-nitriminotetrazolate anion is comparable to that found in the corresponding copper(II) salt.^[8] The hydrazinium cations show no abnormalities. The hydrazine bond length (both 1.45 Å) is also found in hydrazinium chloride (1.45 Å) in the literature.^[9] The packing is strongly influenced by an intense hydrogen-bond 3-dim network.

Energetic Properties

Heat of formation calculations of compounds **1** and **2** were performed using the atomization method based on CBS-4M

* Prof. Dr. T. M. Klapötke
Fax: + 49-89-2180-77492
E-Mail: tmk@cup.uni-muenchen.de

[a] Department of Chemistry
Ludwig-Maximilian University of Munich
81377 Munich, Germany

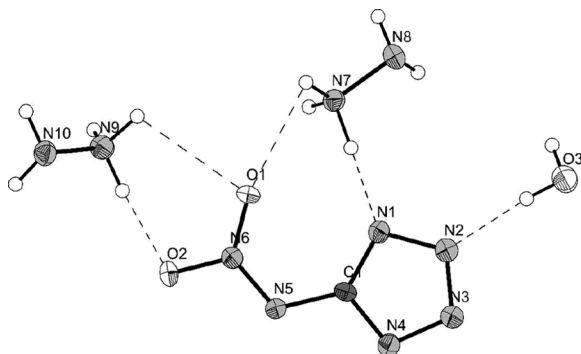


Figure 1. Molecular structure of bis(hydrazinium) 5-nitrimino-tetrazolate monohydrate (**2**). Hydrogen atoms shown as spheres of arbitrary radius and thermal displacements set at 50 % probability. Selected geometries: bond lengths /Å: O1–N6 1.262(3), O2–N6 1.270(3), N1–C1 1.344(3), N1–N2 1.359(3), N2–N3 1.310(3), N3–N4 1.352(3), N4–C1 1.339(3), N5–N6 1.301(3), N5–C1 1.398(3), N7–N8 1.449(3), N9–N10 1.450(3); bond angles /°: C1–N1–N2 103.9(2), N3–N2–N1 110.1(2), N2–N3–N4 109.3(2), C1–N4–N3 104.8(2), N6–N5–C1 117.3(2), O1–N6–O2 118.5(2), O1–N6–N5 124.8(2), O2–N6–N5 116.7(2), N4–C1–N1 112.0(2), N4–C1–N5 115.5(2), N1–C1–N5 132.5(2); torsion angles /°: C1–N1–N2–N3 0.1(3), N6–N5–C1–N1 –5.9(5), C1–N5–N6–O1 –2.1(5), C1–N5–N6–O2 179.0(3).

Table 1. X-ray data and parameters of **2**·H₂O.

	2 ·H ₂ O
Formula	CH ₁₂ N ₁₀ O ₃
Form. weight /g·mol ^{−1}	212.21
Crystal system	Orthorhombic
Space Group	<i>P</i> 2 ₁ 2 ₁ 1 (19)
Color / Habit	colorless plates
Size /mm	0.12 × 0.12 × 0.18
<i>a</i> /Å	3.633(5)
<i>b</i> /Å	12.888(5)
<i>c</i> /Å	18.415(5)
α /°	90
β /°	90
γ /°	90
<i>V</i> /Å ³	862.2(13)
<i>Z</i>	4
$\rho_{\text{calcd.}}$ /g·cm ^{−3}	1.635
μ /mm ^{−1}	0.145
<i>F</i> (000)	448
$\lambda_{\text{Mo-K}\alpha}$ /Å	0.71073
<i>T</i> /K	200
Theta Min-Max /°	4.4, 27.6
Dataset	−3:4; −16:16; −22:23
Reflections collected	4610
Independent reflections	1209
<i>R</i> _{int}	0.056
Observed reflections	1056
No. parameters	127
<i>R</i> ₁ (obs)	0.0467
<i>wR</i> ₂ (all data)	0.0892
<i>S</i>	1.04
Resd. Dens. /e·Å ^{−3}	−0.19, 0.17
Absorption correction	multi-scan
CCDC	819439

enthalpies described recently in detail in the literature (see Equation 1).^[10]

$$\Delta_f H^\circ_{(\text{g}, \text{M}, 298)} = H_{(\text{Molecule}, 298)} - \sum H^\circ_{(\text{Atoms}, 298)} + \sum \Delta_f H^\circ_{(\text{Atoms}, 298)} \quad (1)$$

The results are depicted in Table 2. The gas phase heat of formation ($\Delta_f H^\circ(\text{g}, \text{M})$) was converted into the solid state heat of formation ($\Delta_f H^\circ(\text{s})$) using the Jenkins equations.^[11]

The calculation of the detonation parameters was performed with the program package EXPLO5 (version 5.04)^[12] using the experimentally determined densities (X-ray). The results are summarized in Table 3.

The detonation parameters of **1** are based on the pycnometer density and therefore are related to the anhydrous compound. The detonation velocity of both compounds exceed those of commonly used RDX (cyclic trimethylene trinitramine) (8748 m·s^{−1}) by approximately 200 m·s^{−1} and stay closely below the 9000 m·s^{−1} mark. The influence of the hydrate water in **2** can be seen in the lower explosion energy, the lower detonation temperature and the higher volume of gaseous products compared to **1**. Also the sensitivity data of **1** were determined of the anhydrous compound. The sensitivity data of **1** reveal significantly lower (3 J, 56 N) values compared to the data obtained for the monohydrate **2**, which can be classified as insensitive towards impact (40 N) and less sensitive towards friction (288 N).

Conclusions

From this combined experimentally and theoretically study the following conclusions can be drawn: 5-Nitriminotetrazole can easily be deprotonated by hydrazine in either aqueous or non-aqueous media. The monohydrazinium salt **1** crystallizes (to small for X-ray diffraction) with half a molecule of water per molecular unit as shown by elemental analysis, whereas the bishydrazinium salt **2** crystallizes as monohydrate as shown in the crystal structure. The thermal stability of both, the mono-deprotonated as well as the bis-deprotonated nitrimino-tetrazole lie in the same range at ~ 190 °C. In comparison to neutral 5-nitriminotetrazole (*T*_{dec.} 122 °C) this is a significant increase in thermal stability. In comparison to the corresponding methyl derivatives (*T*_{dec.} >200 °C) it is a slight decrease. The sensitivities of both compounds reach from insensitive for the dihydrazinium salt to very sensitive (belonging to the class of primary explosives) for the monohydrazinium salt following the trend of lower sensitivities observed for bis-deprotonated 5-nitriminotetrazoles compared to mono-deprotonated 5-nitrimino-tetrazoles. Also the inclusion of one molecule of water in the crystal structure of **2** decreases its sensitivities. Last but not least, although **1** offers great performance (better than RDX) and acceptable thermal stability, its high sensitivities will probably retard application of this compound. For applications, a much more promising candidate is diaminouronium 5-nitriminotetrazolate (see Introduction), which is equal in performance but better in thermal stability and sensitivity.

Experimental Section

All chemicals and solvents (analytical grade) were used as supplied by Sigma-Aldrich Inc. ¹H and ¹³C NMR spectra were recorded with a JEOL Eclipse 400 instrument in [D₆]DMSO at or near 25 °C. The chemical shifts are given relative to tetramethylsilane as external stand-

Table 2. Heat of formation calculation of compounds **1** and **2·H₂O**.

	N ₂ H ₅ ⁺	HAtnO ₂ ⁻	AtNO ₂ ²⁻	H ₂ O	1	2·H₂O
−H ²⁹⁸ /a.u.	112.030523	516.973495	516.294886	76.346181		
Δ _f H°(g,M) /kcal·mol ^{−1}	184.9	35.9	95.3	−57.7	220.8	407.4
V _M /nm ³	0.28	0.126	0.136	0.25	0.154	0.2155
ΔH _L / kcal·mol ^{−1}					130.2	355.0
Δ _f H°(s) /kcal·mol ^{−1}					90.7	52.4
Δ _f H°(s) /kJ·mol ^{−1}					379.6	219.3
Δn					8	12.5
M /g·mol ^{−1}					162.15	212.21
Δ _f U°(s) /kJ·kg ^{−1}					2463.5	1179.3

Table 3. Physico-chemical properties of **1** and **2·H₂O**.

	1	2·H₂O
Formula	CH ₆ N ₈ O ₂	CH ₁₂ N ₁₀ O ₃
FW /g·mol ^{−1}	162.21	212.15
Impact sensitivity ^{a)} /J	3	40
Friction sensitivity ^{b)} /N	56	288
ESD-test ^{c)} /J	0.40	0.30
N ^{d)} /%	69.12	66.02
Ω ^{e)} /%	−29.61	−37.7
T _{dec.} ^{f)} /°C	188	192
Density ^{g)} /g·cm ^{−3}	1.680	1.635
Δ _f U° ⁱ⁾ /kJ·mol ^{−1}	2463.5	1179.3
EXPL05 values:		
−Δ _E U _m ^o /kJ·kg ^{−1}	5592	4900
T _E ^{l)} /K	3756	3107
p ^{m)} /kbar	321	303
V _{Det.} ⁿ⁾ /m·s ^{−1}	8926	8890
Gas vol. ^{o)} /L·kg ^{−1}	876	951

a) BAM drophammer; b) BAM friction tester; c) OZM small scall electrostatic discharge device; d) Nitrogen content; e) Oxygen balance; f) Temperature of decomposition by DSC ($\beta = 5^\circ\text{C}\cdot\text{min}^{-1}$); g) estimated from solvent pycnometry (**1**) and X-ray diffraction (**2**); h) Molar heat of formation; i) Energy of formation; j) Energy of Explosion; k) Explosion temperature; l) Detonation pressure; m) Detonation velocity; n) Assuming only gaseous products.

ard. Elemental analyses were performed with a Netsch Simultaneous Thermal Analyzer STA 429. Melting points were determined using a Büchi B-540 apparatus and are uncorrected. Differential Scanning calorimetry was performed with a Linseis PT10 DSC machine. The single-crystal X-ray diffraction data of **2** were collected using an Oxford Xcalibur3 diffractometer with a Spellman generator (voltage 50 kV, current 40 mA) and a KappaCCD detector. The data collection was undertaken using the CRYSLIS CCD software^[13] and the data reduction was performed with the CRYSLIS RED software.^[14] The structure was solved with SIR-92^[15] and refined with SHELXL-97^[16] implemented in the program package WinGX^[17] and finally checked using PLATON.^[18] The hydrogen atoms have been observed and refined. Selected data and parameters from the X-ray data collection and refinement are given in Table 1. Further information regarding the crystal-structure determination have been deposited with the Cambridge Crystallographic Data Centre^[19] as supplementary publication CCDC-819439 (**2**). All quantum chemical calculations were performed with the Gaussian09 software.^[20]

Hydrazinium 5-nitrimino-1H-tetrazolate hemihydrate (1): 5-Nitriminotetrazole (650 mg, 5 mmol) was dissolved in THF (20 mL, dry, over mol. sieves) and a solution of hydrazine in THF (1 M, 5 mL, 5 mmol H₂N–NH₂) was added under vigorous stirring. A thick, color-

less precipitate started to form instantaneously, which was filtered off, washed with diethyl ether and dried. Yield: 480 mg (2.80 mmol, 56 %, calculated as hemihydrate). The product could be recrystallized best from methanol. **DSC** (T_{onset} , $5^\circ\text{C}\cdot\text{min}^{-1}$): 176–180 °C (mp.), 188 °C (dec.). **IR** (KBr): $\tilde{\nu} = 3433$ (s), 3323 (m), 3019 (m), 1621 (w), 1547 (s), 1444 (s), 1351 (s), 1319 (vs), 1225 (m), 1148 (w), 1097 (m), 1059 (m), 1036 (w), 1027 (w), 1000 (w), 983 (w), 865 (w), 775 (w), 743 (w), 697 (w), 512 (w), 419 (w) cm^{−1}; **Raman** (1064 nm, 350 mW, 25 °C): $\tilde{\nu} = 3178$ (3), 1625 (8), 1578 (6), 1530 (100), 1442 (11), 1391 (8), 1375 (13), 1316 (58), 1140 (11), 1104 (9), 1058 (13), 1019 (80), 1008 (48), 981 (17), 869 (10), 753 (17), 690 (3), 478 (18), 417 (19), 377 (13), 256 (16) cm^{−1}. **¹H NMR** ($[D_6]DMSO$, 25 °C): $\delta = 8.20$ (s, H₂N–NH₃⁺). **¹³C NMR** ($[D_6]DMSO$, 25 °C): $\delta = 158.4$; **m/z** (FAB⁺): 33.0 [N₂H₅]⁺; **m/z** (FAB[−]): 129.1 [HAtnO₂][−]; **EA** (CH₆N₈O₂·0.5H₂O, 171.11) calcd.: C 7.02, H 4.12, N 65.48 %; found: C 7.19, H 4.08, N 68.64 %; **impact sensitivity**: 3 J; **friction sensitivity**: 56 N; **ESD**: 0.40 J.

Bis(hydrazinium) 5-nitriminotetrazolate monohydrate (2·H₂O): 5-Nitriminotetrazole (650 mg, 5 mmol) was dissolved in water (10 mL). To this hydrazine hydrate (510 mg, 12 mmol) was added and the obtained solution was evaporated. The residue was recrystallized from MeOH yielding colorless **2·H₂O** (692 mg, 65 % yield). **DSC** (T_{onset} , $5^\circ\text{C}\cdot\text{min}^{-1}$): 192 °C (dec.). **IR** (KBr): $\tilde{\nu} = 3442$ (m), 3350 (m), 3316 (m), 3126 (m), 3058 (m), 2616 (w), 1619 (m), 1545 (m), 1450 (s), 1384 (s), 1363 (s), 1319 (vs), 1117 (s), 1090 (s), 1021 (m), 973 (m), 938 (s), 869 (w), 761 (m), 696 (w) cm^{−1}; **Raman** (1064 nm, 350 mW, 25 °C): $\tilde{\nu} = 3263$ (2), 2878 (2), 1630 (3), 1454 (100), 1403 (4), 1368 (5), 1332 (5), 1221 (12), 1161 (5), 11345 (7), 1086 (5), 1038 (24), 1022 (50), 974 (6), 873 (3), 758 (3), 744 (9), 487 (5), 423 (11), 382 (6), 256 (4) cm^{−1}. **¹H NMR** ($[D_6]DMSO$, 25 °C): $\delta = 6.12$ (s, H₂N–NH₃⁺). **¹³C NMR** ($[D_6]DMSO$, 25 °C): $\delta = 161.3$ (CN₄); **m/z** (FAB⁺): 33.1 [N₂H₅]⁺; **m/z** (FAB[−]): 129.0 [HAtnO₂][−]; **EA** (CH₁₂N₁₀O₃, 212.17) calcd.: C 5.66, H 5.70, N 66.02 %; found C 6.11, H 5.64, N 65.93 %. **impact sensitivity**: 40 J; **friction sensitivity**: 288 N; **ESD**: 0.30 J.

Acknowledgement

Financial support of this work by the Ludwig-Maximilian University of Munich (LMU), the U.S. Army Research Laboratory (ARL), the Armament Research, Development and Engineering Center (ARDEC), the Strategic Environmental Research and Development Program (SERDP) and the Office of Naval Research (ONR Global, title: “Synthesis and Characterization of New High Energy Dense Oxidizers (HEDO) - NICOP Effort”) under contract nos. W911NF-09-2-0018 (ARL), W911NF-09-1-0120 (ARDEC), W011NF-09-1-0056 (ARDEC) and 10 WPSEED01-002 / WP-1765 (SERDP) is gratefully acknowledged. The authors acknowledge collaborations with Dr. Mila Krupka (OZM Research, Czech Republic) in the development of new

testing and evaluation methods for energetic materials and with *Dr. Muhamed Sucesca* (Brodarski Institute, Croatia) in the development of new computational codes to predict the detonation and propulsion parameters of novel explosives. We are indebted to and thank *Drs. Betsy M. Rice* and *Brad Forch* (ARL, Aberdeen, Proving Ground, MD) and *Mr. Gary Chen* (ARDEC, Picatinny Arsenal, NJ) for many helpful and inspired discussions and support of our work. *Mr. Stefan Huber* is thanked for performing the sensitivity tests.

References

- [1] a) T. M. Klapötke, in: *Moderne Anorganische Chemie* (Ed.: E. Riedel), Walter de Gruyter, Berlin, New York, **2007**, vol. 3, pp. 99–104 ; b) R. P. Singh, R. D. Verma, D. T. Meshri, J. M. Shreeve, *Angew. Chem.* **2006**, *118*, 3664; *Angew. Chem. Int. Ed.* **2006**, *45*, 3584; c) T. M. Klapötke, in: *High Energy Density Materials* (Ed.: T. M. Klapötke), Springer, Berlin, Heidelberg, **2007**, pp. 85–122 ; d) B. Rice, E. F. C. Byrd, W. D. Mattson, in: *High Energy Density Materials* (Ed.: T. M. Klapötke), Springer, Berlin, Heidelberg, **2007**, pp. 153–194 .
- [2] a) H. Xue, H. Gao, B. Twamley, J. M. Shreeve, *Chem. Mater.* **2007**, *19*, 1731–1739; b) D. E. Chavez, M. A. Hiskey, R. D. Gilardi, *Org. Lett.* **2004**, *6*, 2889–2891; c) G. W. Drake, T. M. Hawkins, J. Boatz, L. Hall, A. Vij, *Propellants Explos. Pyrotech.* **2005**, *30*, 156–163; d) A. J. Bellamy, P. Golding, *Centr. Eur. J. Energ. Mater.* **2007**, *4*, 33–57; e) K. O. Christe, *Propellants Explos. Pyrotech.* **2007**, *32*, 194–204; f) M. Göbel, K. Karaghiosoff, T. M. Klapötke, D. G. Piercey, J. Stierstorfer, *J. Am. Chem. Soc.* **2010**, *132*, 17216–17226.
- [3] N. Fischer, T. M. Klapötke, J. Stierstorfer, *Propellants Explos. Pyrotech.* **2011**, in press, prep.201100001.
- [4] T. M. Klapötke, J. Stierstorfer, A. U. Wallek, *Chem. Mater.* **2008**, *20*, 4519–4530.
- [5] T. Fendt, N. Fischer, T. M. Klapötke, J. Stierstorfer, *Inorg. Chem.* **2011**, *50*, 1447–1458.
- [6] T. M. Klapötke, J. Stierstorfer, *Helv. Chim. Acta* **2007**, *90*, 2132–2150.
- [7] N. Fischer, T. M. Klapötke, J. Stierstorfer, *Z. Anorg. Allg. Chem.* **2009**, *635*, 271–281.
- [8] T. M. Klapötke, J. Stierstorfer, B. Weber, *Inorg. Chim. Acta* **2009**, *362*, 2311–2320.
- [9] K. Sakurai, Y. Tomiie, *Acta Crystallogr.* **1952**, *5*, 293–294.
- [10] T. Altenburg, T. M. Klapötke, A. Penger, J. Stierstorfer, *Z. Anorg. Allg. Chem.* **2010**, *636*, 463–471.
- [11] a) H. D. B. Jenkins, H. K. Roobottom, J. Passmore, L. Glasser, *Inorg. Chem.* **1999**, *38*, 3609–3620; b) H. D. B. Jenkins, D. Tudela, L. Glasser, *Inorg. Chem.* **2002**, *41*, 2364–2367.
- [12] M. Sućeska, *EXPLO5.4* program, Zagreb, Croatia, **2010**.
- [13] *CrysAlis CCD*, Oxford Diffraction Ltd., Version 1.171.27p5 beta (release 01–04–2005 CrysAlis171.NET).
- [14] *CrysAlis RED*, Oxford Diffraction Ltd., Version 1.171.27p5 beta (release 01–04–2005 CrysAlis171.NET).
- [15] A. Altomare, G. Casciarano, C. Giacovazzo, A. Guagliardi, *J. Appl. Crystallogr.* **1993**, *26*, 343.
- [16] G. M. Sheldrick, *SHELXL-97*, Program for the Refinement of Crystal Structures, University of Göttingen, Germany, **1994**.
- [17] L. Farrugia, *J. Appl. Crystallogr.* **1999**, *32*, 837–838.
- [18] A. L. Spek, *Platon*, A Multipurpose Crystallographic Tool, Utrecht University, Utrecht, The Netherlands, **1999**.
- [19] Crystallographic data for the structures have been deposited with the Cambridge Crystallographic Data Centre. Copies of the data can be obtained free of charge on application to The Director, CCDC, 12 Union Road, Cambridge CB2 1EZ, UK (Fax: +44-1223-336-033; E-Mail for inquiry: fileserv@ccdc.cam.ac.uk; E-Mail for deposition: deposit@ccdc.cam.ac.uk).
- [20] *Gaussian 09, Revision A.1*, M. J. Frisch, G. W. Trucks, H. B. Schlegel, G. E. Scuseria, M. A. Robb, J. R. Cheeseman, G. Scalmani, V. Barone, B. Mennucci, G. A. Petersson, H. Nakatsuji, M. Caricato, X. Li, H. P. Hratchian, A. F. Izmaylov, J. Bloino, G. Zheng, J. L. Sonnenberg, M. Hada, M. Ehara, K. Toyota, R. Fukuda, J. Hasegawa, M. Ishida, T. Nakajima, Y. Honda, O. Kitao, H. Nakai, T. Vreven, J. A. Montgomery Jr., J. E. Peralta, F. Ogliaro, M. Bearpark, J. J. Heyd, E. Brothers, K. N. Kudin, V. N. Staroverov, R. Kobayashi, J. Normand, K. Raghavachari, A. Rendell, J. C. Burant, S. S. Iyengar, J. Tomasi, M. Cossi, N. Rega, J. M. Millam, M. Klene, J. E. Knox, J. B. Cross, V. Bakken, C. Adamo, J. Jaramillo, R. Gomperts, R. E. Stratmann, O. Yazyev, A. J. Austin, R. Cammi, C. Pomelli, J. W. Ochterski, R. L. Martin, K. Morokuma, V. G. Zakrzewski, G. A. Voth, P. Salvador, J. J. Dannenberg, S. Dapprich, A. D. Daniels, Ö. Farkas, J. B. Foresman, J. V. Ortiz, J. Cioslowski, D. J. Fox, Gaussian, Inc., Wallingford CT, **2009**.

Received: March 29, 2011

Published Online: May 10, 2011

Alkaline Earth Metal Salts of 5,5'-Bistetrazole – from Academical Interest to Practical Application

Niko Fischer,^[a] Thomas M. Klapötke,^{*[a]} Kristina Peters,^[a] Magdalena Rusan,^[a] and Jörg Stierstorfer^[a]

In Memory of Professor Kurt Dehnicke

Keywords: Alkaline earth metals; Tetrazoles; Crystal structures; IR spectroscopy; Pyrotechnics

Abstract. The alkaline earth metal salts of 5,5'-BT, [Be(H₂O)₄](5,5'-BT)·H₂O (1), [Mg(H₂O)₆(5,5'-BT)·3H₂O (2), [Ca(H₂O)₄(5,5'-BT)]·H₂O (3), [Sr(H₂O)₄(5,5'-BT)]·2DMF (4), and [Ba(H₂O)₄(5,5'-BT)] (5) were fully characterized by low temperature X-ray diffraction,

vibrational (IR, Raman) and NMR spectroscopy, elemental analysis and differential scanning calorimetry (DSC). A detailed description of the crystal structures is given. In addition, the potential use of 4 and 5 in coloring pyrotechnical compositions was investigated.

Introduction

5,5'-Bistetrazole (5,5'-H₂BT) can be obtained in good yield and high purity from the reaction of sodium azide, sodium cyanide and manganese dioxide in water.^[1] Surprisingly since the determination of the crystal structure of 5,5'-bistetrazole in 1996^[2] only very few examples of ionic compounds containing this heterocycle have been reported. In 2008 a row of rare earth metal salts have been structurally investigated by Klein et al.^[3] Having a nitrogen content of more than 82 %, the 5,5'-bistetrazolate anion is one of the anions with the highest nitrogen contents known, thus it can be considered as a building block for energetic compounds. Hiskey et al. reported on several nitrogen-rich ionic compounds based on 5,5'-bistetrazole and their possible application as high nitrogen fuels in low smoke pyrotechnics in 1999,^[1] however they did not give a complete characterization including the crystal structure of these compounds. The use of alkaline earth metal salts of nitrogen-rich anions in pyrotechnics combines the advantage of a fuel on the one hand and a colorant on the other hand in one compound. Usually calcium, strontium or barium salts are used for red and green flame colors, respectively.

Here we report on the full characterization including the crystal structures of the alkaline earth metal salts beryllium, magnesium, calcium, strontium, and barium 5,5'-bistetrazolate. Of course, the potential use of these compounds decreases within this row. The heavier alkaline earth metal salts can be used in pyrotechnical compositions and have also been tested

towards their behavior in pyrotechnical mixtures together with a vinyl alcohol based binder, magnesium or boron as fuel and ammonium nitrate as oxidizer.

A different approach of this work is the structural determination of the alkaline earth metal salts and a comparison of the different coordination modes found in the structures. Some of the metal centers are coordinated by their hydration shell only, but there are also examples of metal centers in which 5,5'-bistetrazole serves as a bidentate ligand.

Results and Discussion

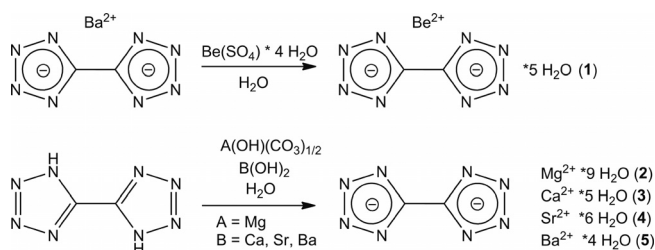
Synthesis

Since 5,5'-bistetrazole, which can be synthesized according to literature,^[1] bears two protons which are readily available in aqueous solution, it can be deprotonated by reaction with the respective metal hydroxide or carbonate. This procedure was used for the preparation of the magnesium (2), calcium (3), strontium (4), and barium (5) 5,5'-bistetrazolate. The solubility of 5,5'-bistetrazole is fairly good in hot water, but poor in cold water. The reactions therefore were carried out under reflux conditions in water, ensuring that the starting material is fully dissolved. Also the choice of the metal source has to depend on the solubility of the respective material. The calcium (3), strontium (4), and barium (5) salt was prepared using the hydroxides since their solubility in water than the respective carbonates is higher by about a factor of 1000. For the preparation of the magnesium salt 2, basic magnesium carbonate was used. For availability reasons, beryllium sulfate was used for the preparation of the beryllium salt 1 via a metathesis reaction using the barium salt of 5,5'-bistetrazole, whereas barium sulfate was filtered off and the beryllium 5,5'-bistetrazolate could be crystallized from the hot aqueous solution. The

* Prof. Dr. T. M. Klapötke
Fax: +49-89-2180-77492

E-Mail: tmk@cup.uni-muenchen.de

[a] Ludwig Maximilian University Munich (LMU)
Department of Chemistry
Energetic Materials Research
Butenandtstr. 5–13 (D)
81377 Munich, Germany



Scheme 1. Synthesis of the alkaline earth metal salts of 5,5'-bistetrazole.

synthetic procedures to compounds **1–5** are summarized in Scheme 1.

Molecular Structures

To determine the molecular structures of **1–5** in the crystal-line state an Oxford Xcalibur3 diffractometer with a Spellman generator (voltage 50 kV, current 40 mA) and a KappaCCD detector was used. The data collections at 173 K were performed using the CrysAlis CCD software,^[4] the data reductions with the CrysAlis RED software.^[5] The solution and refinement of all structures were performed using the programs

SIR-92,^[6] SHELXS-97,^[7] and SHELXL-97^[8] implemented in the WinGX software package^[9] and finally checked with the PLATON software.^[10] In all crystal structures the hydrogen atoms were located and refined. The absorptions were corrected with the SCALE3 ABSPACK multi-scan method.^[11] Selected data and parameters of the X-ray determinations are given in Table 1.

Beryllium 5,5'-bistetrazolate pentahydrate (**1**) (Figure 1) crystallizes in the monoclinic space group $P2_1/c$ with four molecules in the unit cell. The N–N bond lengths in the two C–C linked tetrazolate rings are between N–N single bonds (1.454 Å) and N=N double bonds (1.245 Å). The shortest distance is between the atoms N2–N3 (1.3094(17) Å), the longest between the atoms N1–N2 1.3445(17) Å. The C–C bond length (1.4629(19) Å) is closer to a single bond (1.52 Å) than to a double bond (1.32 Å). In comparison to neutral 5,5'-bistetrazole there are no significant changes regarding the bond lengths (N2–N3 = 1.2976(14) Å, N1–N2 = 1.3439(14) Å, C1–C2 = 1.4535(15) Å). The bond angle in **1** N2–N1–C1 is smaller (104.40(11)°) than in 5,5'-bistetrazole (108.37(9)°),^[12] whereas the angle N1–N2–N3 is larger (109.70(11)°) than in the free acid (106.46(10)°). The five membered 6π electron aromatic tetrazole rings are almost planar for 5,5'-BT (torsion

Table 1. X-ray data and parameters.

	1	2	3	4	5
formula	BeC ₂ H ₁₀ N ₈ O ₅	MgC ₂ H ₁₈ N ₈ O ₉	CaC ₂ H ₁₀ N ₈ O ₅	SrC ₈ H ₂₂ N ₁₀ O ₆	BaC ₂ H ₈ N ₈ O ₄
form. mass /g·mol ^{−1}	235.19	322.55	266.26	441.98	345.49
crystal system	monoclinic	monoclinic	monoclinic	orthorhombic	triclinic
space group	$P2_1/c$ (No. 14)	$P2_1/n$ (No. 14)	$P2_1/c$ (No. 14)	$Pcca$ (No. 54)	$P\bar{1}$ (No. 2)
color / habit	colorless plate	colorless rod	colorless block	colorless plate	colorless rod
size /mm	0.23 × 0.22 × 0.08	0.30 × 0.20 × 0.20	0.25 × 0.20 × 0.10	0.23 × 0.22 × 0.10	0.17 × 0.10 × 0.10
<i>a</i> /Å	11.5764(8)	12.117(4)	6.7848(2)	22.378(5)	7.4679(5)
<i>b</i> /Å	11.8368(7)	6.955(5)	13.6768(3)	5.8533(9)	7.5004(5)
<i>c</i> /Å	7.1908(6)	16.081(6)	10.8009(2)	13.940(3)	9.4148(7)
<i>a</i> /°	90	90	90	90	73.119(6)
<i>β</i> /°	99.035(7)	93.413(5)	91.147(2)	90	70.842(7)
<i>γ</i> /°	90	90	90	90	81.251(5)
<i>V</i> /Å ³	973.11(12)	1352.8(12)	1002.06(4)	1825.9(6)	475.73(6)
<i>Z</i>	4	4	4	4	2
<i>ρ</i> _{calcd.} /g·cm ^{−3}	1.605	1.584	1.765	1.608	2.412
<i>μ</i> /mm ^{−1}	0.145	0.192	0.654	3.000	4.189
<i>F</i> (000)	488	680	552	904	328
<i>λ</i> (Mo- <i>K</i> _α) /Å	0.71073	0.71073	0.71073	0.71073	0.71073
<i>T</i> /K	173	173	173	173	173
<i>θ</i> min-max /°	4.5, 26.0	4.2, 26.0	4.2, 25.7	4.2, 25.0	4.2, 26.0
dataset <i>h</i> ; <i>k</i> ; <i>l</i>	−12:14; −14:14; −8: 7	−14:14; −5:8; −18:19	−8:8; −16:16; −13:13	−17: 26; −6: 6; −16:16	−9: 9; −9: 9; −11:11
reflect. coll.	4876	6818	14722	7853	4862
independ. refl.	1888	2647	1908	1598	1866
<i>R</i> _{int}	0.032	0.027	0.024	0.023	0.041
reflection obs.	295	1996	1678	1245	1648
No. Parameters	185	253	185	134	168
<i>R</i> ₁ (obs)	0.0289	0.0294	0.0202	0.0230	0.0219
<i>wR</i> ₂ (all data)	0.0503	0.0677	0.0566	0.0662	0.0488
<i>S</i>	0.77	0.91	1.03	1.06	0.98
resd. dens. /e·Å ^{−3}	−0.14, 0.19	−0.18, 0.28	−0.23, 0.30	−0.46, 0.35	−0.89, 0.48
device type	Oxford Xcalibur3 CCD	Oxford Xcalibur3 CCD	Oxford Xcalibur3 CCD	Oxford Xcalibur3 CCD	Oxford Xcalibur3 CCD
solution	SHELXS-97	SIR-92	SIR-92	SIR-92	SIR-92
refinement	SHELXL-97	SHELXL-97	SHELXL-97	SHELXL-97	SHELXL-97
absorpt. corr.	multi-scan	multi-scan	multi-scan	multi-scan	multi-scan
CCDC	827503	827502	827501	827504	827500

angle N1–N2–N3–N4 = 0.05(12)) as well as for its alkaline earth metal salts (torsion angle N1–N2–N3–N4 = 0.03(16)°). Exact bond lengths and angles are listed in Table 2. In this structure beryllium is coordinated tetrahedral by four water molecules with bond lengths between 1.60 Å and 1.61 Å and

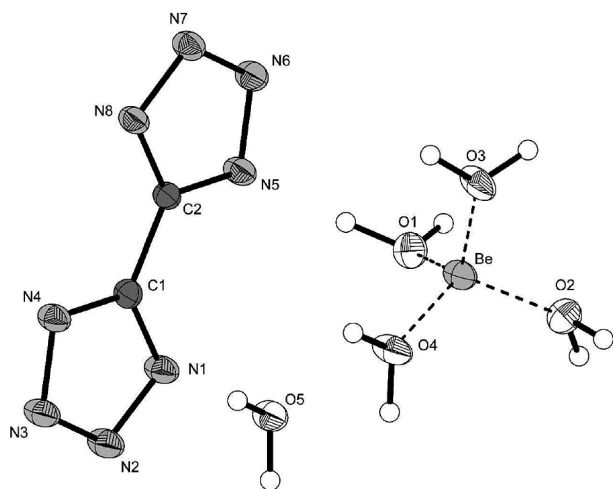


Figure 1. Molecular unit of **1**. Thermal ellipsoids of non-hydrogen atoms represent the 50% probability level.

bond angles between 105.1° and 115.1°. The packing is affected by layers of 5,5'-BT anions connected by strong hydrogen bonds involving all water hydrogen atoms (Figure 2).

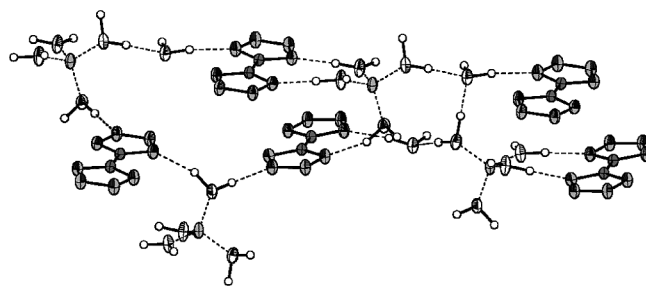


Figure 2. Hydrogen bonding in the structure of **1** forming layers of 5,5'-BT dianions connected by the tetrahedrally solvated beryllium cations.

Basically all of the metal atoms are coordinated by crystal water molecules and partly by the bistetrazolate dianions. The coordination numbers follow an increasing trend by raising the period (CN: Be²⁺ = 4, Mg²⁺ = 6, Ca²⁺ = 6, Sr²⁺ = 8, Ba²⁺ = 9). The densities do not follow a corresponding trend ($\rho(\mathbf{5}) > \rho(\mathbf{3}) > \rho(\mathbf{4}) > \rho(\mathbf{1}) > \rho(\mathbf{2})$), due to the varying water content.

Magnesium 5,5'-bistetrazolate nonahydrate (**2**) crystallizes in the monoclinic space group $P2_1/n$ with four molecular moie-

Table 2. Selected bond lengths /Å, angles /° and torsion angles /° of the anions of compounds **1–5**.

	5,5BT	Be-BT (1)	Mg-BT (2)	Ca-BT (3)	Sr-BT (4)	Ba-BT (5)
Atom 1–2 /Å	<i>d</i> (1–2)	<i>d</i> (1–2)	<i>d</i> (1–2)	<i>d</i> (1–2)	<i>d</i> (1–2)	<i>d</i> (1–2)
N1–N2	1.3439(14)	1.3445(17)	1.343(2)	1.3483(15)	1.349(3)	1.349(5)
N2–N3	1.2976(14)	1.3094(17)	1.315(2)	1.3107(15)	1.313(3)	1.316(4)
N3–N4	1.3583(14)	1.3430(17)	1.343(2)	1.3512(15)	1.352(3)	1.345(4)
N4–C1	1.3178(14)	1.3307(18)	1.332(2)	1.3353(15)	1.329(3)	1.346(5)
N1–C1	1.3289(14)	1.3333(18)	1.336(2)	1.3332(15)	1.331(3)	1.338(5)
C1–C2	1.4535(15)	1.4629(19)	1.461(2)	1.4549(16)	1.465(4)	1.466(5)
N5–C2	1.3178(14)	1.3333(18)	1.332(2)	1.3334(16)		1.331(5)
N5–N6	1.3583(14)	1.3466(17)	1.347(2)	1.3495(15)		1.342(5)
N6–N7	1.2976(14)	1.3032(17)	1.314(2)	1.3126(14)		1.316(4)
N7–N8	1.3439(14)	1.3446(17)	1.346(2)	1.3460(14)		1.342(5)
N8–C2	1.3289(14)	1.3299(18)	1.333(2)	1.3362(15)		1.328(5)
Atoms 1–2–3 /°	<(1–2–3)	<(1–2–3)	<(1–2–3)	<(1–2–3)	<(1–2–3)	<(1–2–3)
N2–N1–C1	108.37(9)	104.40(11)	104.23(12)	104.81(10)	104.02(19)	103.9(3)
N1–N2–N3	106.46(10)	109.70(11)	109.90(12)	109.11(9)	109.7(2)	110.1(3)
N2–N3–N4	110.57(10)	109.28(11)	109.08(12)	109.92(10)	109.3(2)	109.5(3)
N3–N4–C1	105.52(9)	104.80(11)	104.85(12)	104.13(9)	104.16(19)	104.2(3)
N6–N5–C2	105.52(9)	104.50(11)	104.66(12)	103.88(9)		104.9(3)
N5–N6–N7	110.57(10)	109.68(11)	109.24(12)	110.05(9)		108.7(3)
N6–N7–N8	106.46(10)	109.36(11)	109.62(12)	109.22(9)		110.1(3)
N7–N8–C2	108.37(9)	104.89(11)	104.49(12)	104.46(9)		104.2(3)
N1–C1–N4	109.07(10)	111.82(12)	111.94(13)	112.03(10)	112.8(2)	112.3(3)
N4–C1–C2	126.23(10)	124.20(13)	123.94(13)	126.94(11)	124.1(2)	122.1(3)
N1–C1–C2	124.67(9)	123.98(13)	124.10(13)	121.02(10)	123.1(2)	125.4(3)
N5–C2–C1	126.23(10)	124.20(13)	123.63(13)	121.89(10)		124.2(3)
N8–C2–C1	124.67(9)	124.22(13)	124.34(13)	125.69(11)		123.6(3)
N5–C2–N8	109.07(10)	111.58(12)	112.00(13)	112.40(10)		112.2(3)
Atoms 1–2–3–4 /°	<(1–2–3–4)	<(1–2–3–4)	<(1–2–3–4)	<(1–2–3–4)	<(1–2–3–4)	<(1–2–3–4)
N1–C1–C2–N5	–1.94(18)	0.9(2)	–18.9(2)	0.80(18)	0.1(4)	–9.9(6)
N1–C1–C2–N8	–180.00(11)	–179.60(13)	163.35(14)	178.57(11)	178.6(2)	173.6(4)

ties in the unit cell. The magnesium dications are coordinated octahedrally by water molecules, with bond lengths in the range of 2.1 Å (Figure 3). Additionally, there are three free water molecules in each molecular unit. The packing of **2** can be described as a vertical layer structure along the *a* axis, with alternating alignments of octahedrally coordinated Mg^{2+} -cations as well as the 5,5'-BT anions and free water molecules (Figure 4).

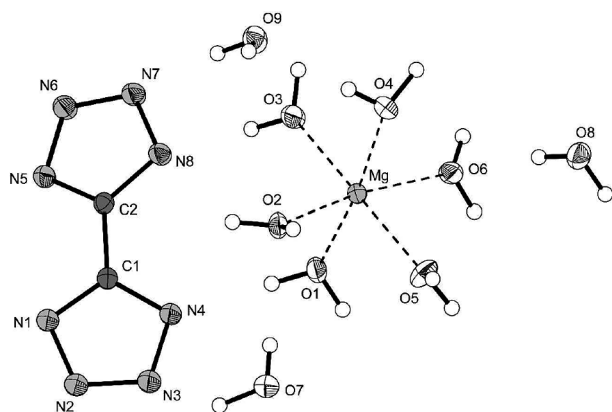


Figure 3. Molecular unit of **2**. Thermal ellipsoids of non-hydrogen atoms represent the 50 % probability level. Coordination distances /Å: Mg–O1 2.067(2), Mg–O2 2.069(2), Mg–O3 2.037(2), Mg–O4 2.089(2), Mg–O5 2.086(2), Mg–O6 2.0745(19).

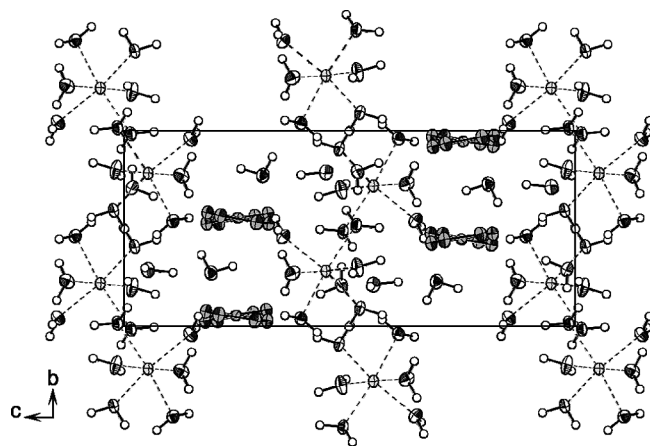


Figure 4. Packing of the magnesium salt **2**, showing the alternating layers within the *a,b* plane.

Calcium 5,5'-bistetrazolate pentahydrate (**3**) crystallizes in the monoclinic space group $P2_1/c$ with four molecular moieties in the unit cell. Calcium is coordinated sixfold by four water molecules, with shorter bond lengths (Ca–O1 = 2.3576(11) Å, Ca–O2 = 2.3955(10) Å, Ca–O3 = 2.3770(10) Å, Ca–O4 = 2.3263(11) Å), and two nitrogen atoms of two different 5,5'-BT anions, with longer bond lengths (Ca–N1 = 2.5049(11) Å, Ca–N6ⁱ = 2.5293(10) Å) (Figure 5). A further contact, indicated in Figure 6, is formed by Ca–N5 with a distance of 2.8739(10) Å, which is slightly above the sum of the *van der Waals* radii. The packing along the *c* axis can be described as a horizontal alternating layer structure between the coordinated cations and the anions with the free water molecules. Within

the *b,c* planes the structure shows alternating vertical layers. The one layer is made up of the 5,5'-BT anions, the calcium cations as well as the free water molecule, while the other one contains just the water coordination sphere of the calcium cation. The packing is affected by several strong hydrogen bonds.

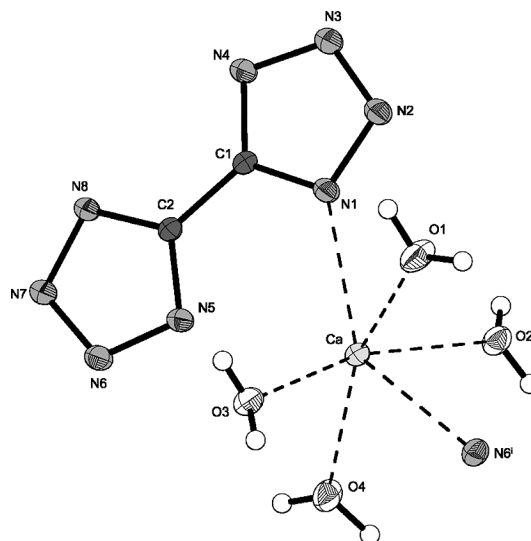


Figure 5. View on the molecular unit of **3** indicating the distorted octahedral coordination sphere of the calcium cations. Thermal ellipsoids represent the 50 % probability level. Symmetry code: (i) *x*, 0.5–*y*, 0.5+*z*.

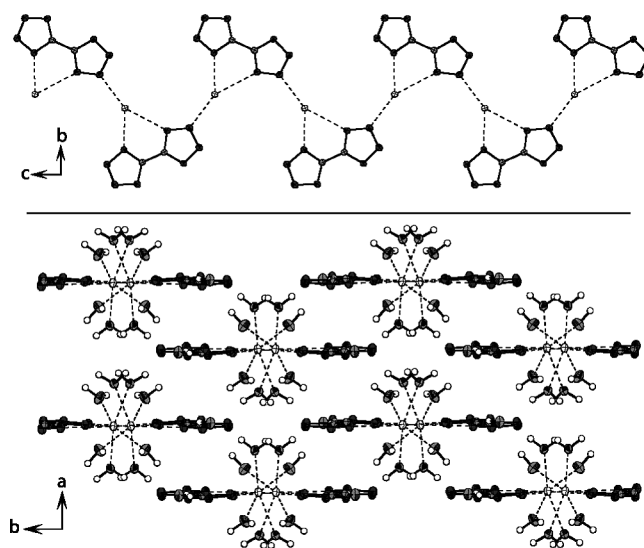


Figure 6. Structural motive within **3**. Top: Strings of Ca^{2+} and 5,5'-BT anions along *c*; bottom: View along *c* axis showing the alternating layers formed by the strings.

Strontium 5,5'-bistetrazolate (**4**) could only be obtained crystalline as its tetrahydrate with two additional DMF molecules per molecular unit. It crystallizes in the orthorhombic space group $Pcca$, with four molecular moieties in its unit cell. The bond lengths and angles in the 5,5'-BT anion are similar to the other alkaline earth metal salts. The strontium cations are coordinated eightfold by two water molecules and two nitrogen atoms of two different 5,5'-bistetrazolate anions. Both

oxygen and nitrogen atoms are doubled by symmetry. The Sr–O bond lengths are shorter (Sr–O1 = 2.579(19) Å, Sr–O2 = 2.594(2) Å) than the Sr–N bond lengths (Sr–N1 = 2.802(2) Å, Sr–N4ⁱ = 2.787(19) Å) (Figure 7). The packing along the *a* axis could be described as a stacking of alternating layers of the strontium 5,5'-bistetrazolate tetrahydrate and the DMF molecules, which are connected by strong hydrogen bonds e.g. O2–H2A•••O3: D–A = 2.688(3), 175(2)°. A view along the *c* axis shows the angulated packing of two 5,5'-bistetrazolate moieties above each other (Figure 8).

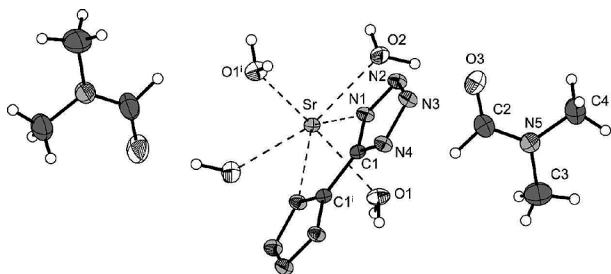


Figure 7. View on the molecular unit of **4**. Thermal ellipsoids represent the 50% probability level. Symmetry code: (i) = 0.5–*x*, 1–*y*, *z*.

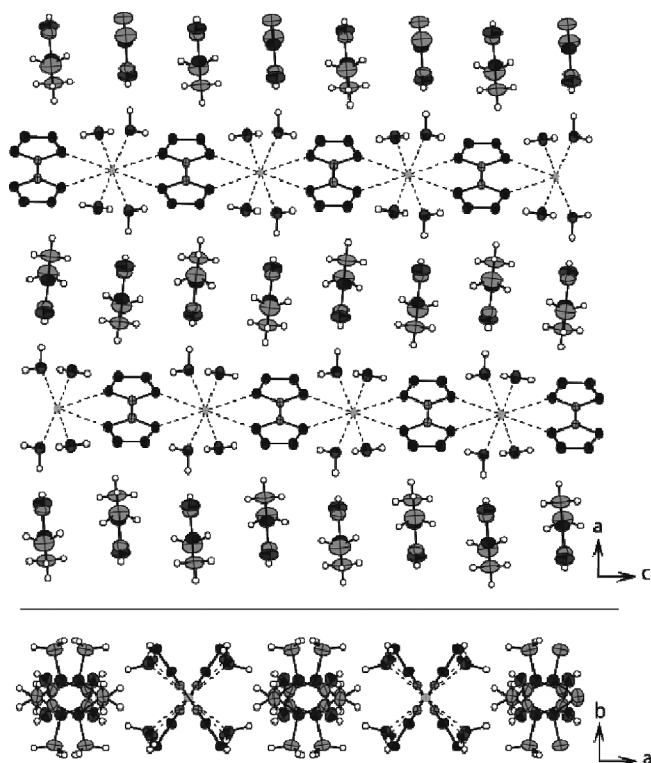


Figure 8. View along the *b*- and *c* axis in the crystal structure of **4** showing the alternating layers.

Barium 5,5'-bistetrazolate tetrahydrate (**5**) crystallizes in the triclinic space group *P* $\bar{1}$ with two molecular moieties in the unit cell. A view on the molecular unit is shown in Figure 9. The bond lengths are in agreement to the previously discussed structures and given in Table 2. The barium atoms are coordinated ninefold, by six oxygen and three nitrogen atoms, as shown in Figure 9 (Ba–O1 = 2.830(3) Å, Ba–O2 = 2.712(4) Å,

Ba–O3 = 2.829(3) Å, Ba–O4 = 2.702(4) Å, Ba–N1 = 2.984(3) Å, Ba–N3ⁱ = 2.975(3) Å, Ba–O3ⁱⁱ = 2.919(3) Å, Ba–Oⁱⁱⁱ = 2.892(3) Å, Ba–N2ⁱⁱⁱ = 2.912(3) Å). The packing along the *c* axis shows an alternating horizontal layer structure between tilted 5,5'-BT anions and barium cations with its water coordination sphere. A view along the *a* axis (Figure 10) presents vertical rows of 5,5'-BT, which are separated from each other through a zig-zag pattern of coordinated barium atoms. Again the structure of **5** is stabilized by various strong hydrogen bonds.

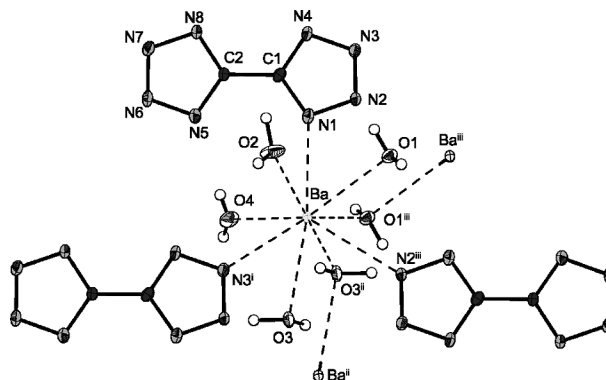


Figure 9. Molecular unit of **5**. Thermal ellipsoids of non-hydrogen atoms represent the 50% probability level. Symmetry codes: (i) *x*, –1+*y*, *z*, (ii) 1–*x*, –*y*, –*z*, (iii) 1–*x*, 1–*y*, –*z*.

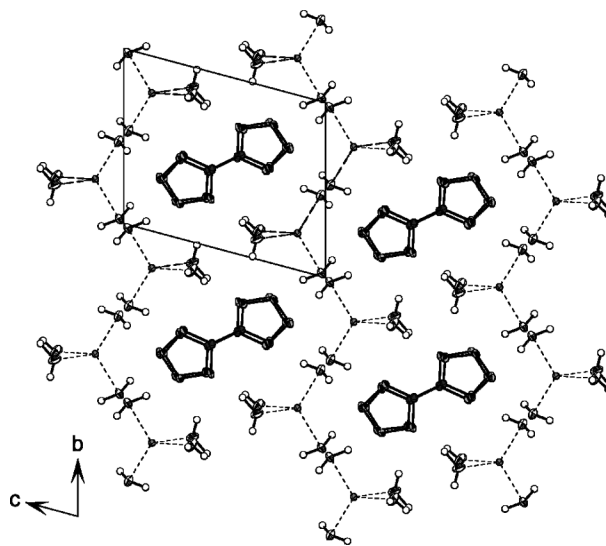


Figure 10. View along the *a* axis showing columns of staggered 5,5'-BT dianions.

Vibrational Spectroscopy

IR- as well as Raman spectroscopy are suitable methods for the detection of the 5,5'-bistetrazolates **1**–**5**. After deprotonation of the free acid, the N–H stretching vibration disappears. The values for the stretching and deformation vibrations in the IR and Raman spectra of the examined substances were compared to values found in literature.^[13–15] The most intensive absorption bands in the raman spectra are the symmetrical

stretching mode between the C–C linked tetrazole rings at around 1576 cm^{-1} and a typical tetrazole ring deformation vibration at around 1143 cm^{-1} . The most intensive absorption bands in the IR spectra can be assigned to asymmetrical $>\text{C}=\text{N}-$ stretching modes of the tetrazole ring system in the range of 1690 and 1640 cm^{-1} . Further, O–H stretching vibrations of the crystal water, which is contained in all compounds, are found in the range of $3600\text{--}3100\text{ cm}^{-1}$. Apart from $>\text{C}=\text{N}-$ stretching modes at 1690 and 1640 cm^{-1} further sets of tetrazole ring stretching and deformation vibrations in a range of $1390\text{--}700\text{ cm}^{-1}$ [$\nu(\text{NCN})$, $\nu(\text{NN})$, $\delta(\text{ring})$, $\delta(\text{NCN})$,] can be identified.

Physico-Chemical Properties

Thermal Behavior

Differential scanning calorimetry (DSC) measurements to determine the melt- and decomposition temperatures of **1–5** (about 1.5 mg of each energetic material) were performed in covered aluminum containers with a hole (0.1 mm) in the lid for gas release and a nitrogen flow of 20 mL per minute with a Linseis PT 10 DSC^[16] calibrated by standard pure indium and zinc at a heating rate of $5\text{ }^{\circ}\text{C}\cdot\text{min}^{-1}$.

In the DSC curves of the salts **1–5** several endothermic peaks between $92\text{ }^{\circ}\text{C}$ and $190\text{ }^{\circ}\text{C}$ can be detected, which can be assigned to the stepwise dehydration of the salts. Except from the strontium salt all compounds show two endothermic peaks, the first one of which is due to the loss of water molecules, which are not coordinated by the metal atoms (**1**: $123\text{ }^{\circ}\text{C}$, **2**: $138\text{ }^{\circ}\text{C}$, **3**: $98\text{ }^{\circ}\text{C}$, **4**: $130\text{ }^{\circ}\text{C}$, **5**: $92\text{ }^{\circ}\text{C}$). The second endothermic peaks, which are observed for **1**, **2**, **3** and **5** can be assigned to the loss of the hydration shells of the metal centers (**1**: $186\text{ }^{\circ}\text{C}$, **2**: $148\text{ }^{\circ}\text{C}$, **3**: $190\text{ }^{\circ}\text{C}$, **5**: $166\text{ }^{\circ}\text{C}$). For the determination of the exact amount of released water thermogravimetric measurements had to be accomplished. Despite the high nitrogen content of the investigated 5,5'-bistetrazolate salts, no exothermic decomposition of any of the compounds could be observed in a temperature range up to $400\text{ }^{\circ}\text{C}$.

Water Solubility

From recrystallization attempts in water and NMR measurements, which were carried out in deuterium oxide, a trend of the water solubility of the salts **1–5** could be observed. For the salts **2** to **5** the water solubility decreases rapidly with increasing molecular weight of the cation just as it also is observed for the alkaline earth metal sulfates. In this context, the beryllium salt plays a special role, since, against expectations from the above mentioned trend, its solubility in water is similar to that of the barium salt. A possible explanation for this behavior could be the same argumentation as it is applied for diagonal relationships in the periodic table saying that lithium salts behave like magnesium salts rather than the other alkali salts or beryllium salts behave like aluminum salts rather than other alkaline earth metal salts because of the similar charge to diameter ratio of the diagonally related ions.

Sensitivities

The impact sensitivity tests were carried out according to STANAG 4489^[17] modified instruction^[18] using a BAM (Bundesanstalt für Materialforschung) drophammer.^[19] The friction sensitivity tests were carried out according to STANAG 4487^[20] modified instruction^[21] using the BAM friction tester. The classification of the tested compounds results from the “UN Recommendations on the Transport of Dangerous Goods”.^[22] All compounds were tested upon the sensitivity towards electrical discharge using the Electric Spark Tester ESD 2010 EN.^[23] Apart from the beryllium salt, the sensitivities of all alkaline earth metal salts were determined. To dehydrate the compounds, all substances were dried at $200\text{ }^{\circ}\text{C}$ previously to sensitivity testing. Also for the sensitivities, a trend from lower to higher molecular weight of the cation can be observed. The impact sensitivities are in a range from 40 J to 30 J with the higher values for the lighter elements (**2**: 40 J , **3**: 40 J , **4**: 35 J , **5**: 30 J). Therefore, the dry magnesium and calcium salts can be considered as insensitive, the strontium salt as less sensitive and the barium salt as sensitive. Also the sensitivity towards electrical discharge shows the same trend. The values reach from 0.30 J for the magnesium salt to 0.15 J for both, the strontium and the barium salt (**2**: 0.30 J , **3**: 0.20 J , **4**: 0.15 J , **5**: 0.15 J). Only the friction sensitivities do not change within the row of the alkaline earth metal salts and were determined to 360 N for all compounds. They can therefore be considered as less sensitive towards friction.

Pyrotechnical Compositions

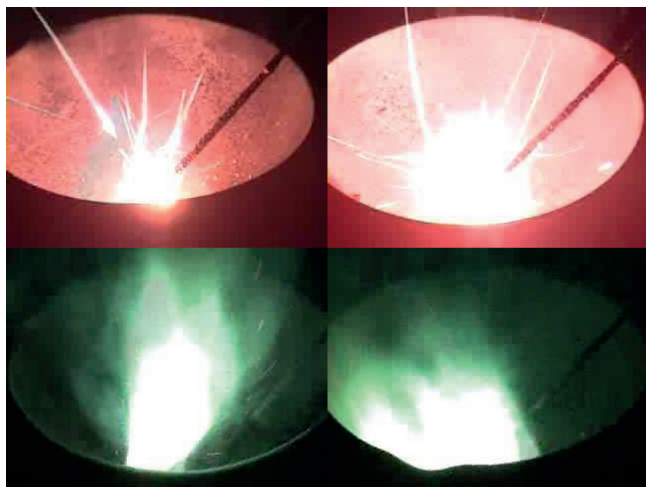
Nitrogen-rich compounds are promising substances in the development of ecologically friendly coloring agents in pyrotechnical formulations. The formation of mainly gaseous products like nitrogen is an important requirement for smokeless combustion, therefore the investigation of nitrogen-rich compounds as coloring substances is focused. For this reason several pyrotechnical formulations with the barium and strontium salts of 5,5'-bistetrazole were tested.

The pyrotechnic mixtures were prepared by mixing all substances, except the binder, in a mortar. Then the binder, a solution of 25% vinyl alcohol acetate resin (VAAR), was added. The mixture was formed by hand and dried under high vacuum for three hours. The controlled burn down was filmed with a digital video camera recorder (SONY, DCR-HC37E). The performance of each composition has been evaluated with respect to color emission (subjective impression), smoke generation and the amount of solid residues. As red and green coloring agents the strontium and barium salts (MBT) were used. In all pyrotechnic formulations ammonium nitrate served as oxidizer. Magnesium and amorphous boron in the case of the formulations with the barium salt were used as fuels. Polyvinyl chloride (PVC) was added to a barium formulation and served as chlorine source for the generation of the green-emitting species BaCl_2 . In Table 3 the content of the compositions (mass percent) is summarized.

Table 3. Composition of pyrotechnical mixtures containing **4** and **5**.

Formulations	Sr-BT_1	Sr-BT_2	Ba-BT_1	Ba-BT_2	Ba-BT_3
MBT /wt.-%	35	39	35	30	40
NH ₄ NO ₃ /wt.-%	40	44	40	35	44
Mg /wt.-%	18	10	–	11	–
B /wt.-%	–	–	18	–	9
PVC /wt.-%	–	–	–	17	–
VAAR /wt.-%	7	7	7	7	7

The pyrotechnic composition Sr-BT_1 consists of 35 % Sr-BT, 40 % NH₄NO₃, 18 % magnesium and 7 % VAAR. The observed flame color is intense red and the combustion occurs fast and smokeless and no residues were observed. Formulation Sr-BT_2 with an increased oxidizer and Sr-BT content of 44 % NH₄NO₃ and 39 % Sr-BT and a decreased amount of 10 % magnesium burned smokeless with an orange-red flame color (Figure 11). The combustion velocity was slower than that of composition Sr-BT_1 and some magnesium sparks and solid residues could be observed.

**Figure 11.** Flame colors of Sr-BT_1 (top left), Sr-BT_2 (top right), Ba-BT_1 (bottom left) and Ba-BT_3 (bottom right).

Both formulations Ba-BT_1 and Ba-BT_3 with 35 % Ba-BT, 40 % NH₄NO₃, 18 % boron, 7 % VAAR and 40 % Ba-BT, 44 % NH₄NO₃, 9 % boron, 7 % VAAR respectively burned fast with an intense green flame color and no residues remained, however a slight generation of smoke was observed for both compositions. The composition Ba-BT_2 containing 30 % Ba-BT, 35 % NH₄NO₃, 11 % magnesium, 17 % PVC and 7 % VAAR combusted fast with an intense white flame color without smoke and no solid residues remained.

Conclusions

5,5'-Bistetrazole was deprotonated in aqueous solution using the alkaline earth metal hydroxides or, in case of the magnesium salt, the basic carbonate to synthesize the corresponding alkaline earth metal salts **2**, **3**, **4**, and **5**. Due to the low solubility of the alkaline earth metal hydroxides in water, the yields of the described reactions are not quantitative. The

beryllium salt **1** of 5,5'-bistetrazole was synthesized in a metathesis reaction using the barium salt of 5,5'-bistetrazole and beryllium sulfate.

The water solubility of the alkaline earth metal salts of 5,5'-bistetrazole in water drops with increasing molecular weight of the cation. As an exception, the solubility of the beryllium salt **1** is almost as low as the solubility of the barium salt **5**.

The salts crystallize in the common mono- and triclinic space groups $P2_1/c$ (**1**, **3**), $P2_1/n$ (**2**), $Pcca$ (**4**) and $P\bar{1}$ (**5**) as tetrahydrate (**4**, **5**), pentahydrate (**1**, **3**) or nonahydrate (**2**). Single crystals of **4** could only be obtained from DMF, where it crystallizes with two molecules of DMF per molecular unit.

All salts can be dehydrated at temperatures between 92 °C and 190 °C. They do not decompose at temperatures lower than 400 °C.

The impact and friction sensitivities were determined of previously dried substances. They reach from 30 J (**5**) to 40 J (**2**, **3**) impact sensitivity. The friction sensitivity of all compounds is 360 N. The salts therefore are comparatively insensitive towards impact and friction.

The strontium (**4**) and the barium salt (**5**) were tested in pyrotechnical compositions as red respectively green colorants. Their color performance for the strontium salt was best in a formulation containing 35 % Sr-BT, 40 % NH₄NO₃, 18 % magnesium and 7 % VAAR. Regarding smokeless combustion, the best performing mixture for the barium salt consists of 40 % Ba-BT, 44 % NH₄NO₃, 9 % boron and 7 % VAAR.

Experimental Section

All chemicals and solvents were employed as received (Sigma-Aldrich, Fluka, Acros). ¹H and ¹³C spectra were recorded using a JEOL Eclipse 270, JEOL EX 400 or a JEOL Eclipse 400 instrument. The chemical shifts quoted in ppm in the text refer to typical standards such as tetramethylsilane (¹H, ¹³C). To determine the melting and decomposition temperatures of the described compounds a Linseis PT 10 DSC (heating rate 5 °C min⁻¹) was used. Infrared spectra were measured using a Perkin-Elmer Spectrum One FT-IR spectrometer as KBr pellets. Raman spectra were recorded with a Bruker MultiRAM Raman Sample Compartment D418 equipped with a Nd-YAG-Laser (1064 nm) and a LN-Ge diode as detector. Mass spectra of the described compounds were measured at a JEOL MStation JMS 700 using FAB technique. To measure elemental analyses a Netsch STA 429 simultaneous thermal analyzer was employed.

Beryllium 5,5'-bistetrazolate pentahydrate (1): Barium bistetrazolate tetrahydrate (2.73 g, 10.0 mmol, 1 equiv.) was dissolved in boiling water (75 mL) and combined with beryllium sulfate tetrahydrate (1.77 g, 10.0 mmol, 1.0 equiv.), which previously was dissolved in hot water (25 mL). Barium sulfate precipitated instantly. Then the mixture was boiled for 20 min and filtered. To remove the remaining barium sulfate, the solution was centrifuged. Lastly, the water was evaporated and the colorless product was recrystallized from ethanol/water in 86 % yield (2.02 g).

DSC (5 °C·min⁻¹): 123 °C (dehydr.), 186 °C (endotherm.), >400 °C (no dec.). **IR** (KBr): $\tilde{\nu}$ = 2931 (s), 2235 (s), 1679 (m), 1593 (m), 1384 (m), 1339 (s), 1319 (m), 1229 (m), 1204 (s), 1167 (m), 1066 (s), 1054 (s), 1038 (vs), 983 (s), 880 (s), 788 (s), 719 (s), 675 (s), 533 (m), 488 (w) cm⁻¹; **Raman** (1064 nm, 200 mW, 25 °C): $\tilde{\nu}$ = 1595 (100), 1231

(15), 1159 (14), 1138 (31), 1101 (16), 782 (3), 540 (1), 489 (3), 426 (5), 392 (11) cm^{-1} . **^1H NMR** (D_2O , 95 °C): δ = 4.78 (H_2O). **^{13}C NMR** (D_2O , 95 °C): δ = 154.8 (CN_4); **m/z (FAB $^-$)** 137.0 [C_2HN_8^-]; **EA** ($\text{C}_2\text{H}_{10}\text{BeN}_8\text{O}_5$, 235.16): calcd.: C 10.21; H 4.29; N 47.65%; found: C 10.69; H 4.11; N 47.72%.

Magnesium 5,5'-bistetrazolate nonahydrate (2): 5,5'-Bistetrazole (1.38 g, 9.99 mmol, 1.0 equiv.) was dissolved in hot water (20 mL) and combined with basic magnesium carbonate ($\text{Mg}(\text{OH})_2 \cdot \text{MgCO}_3$) (0.86 g, 12.06 mmol, 1.21 equiv.). The mixture was boiled for 40 min and filtered hot, to remove remaining basic magnesium carbonate. The product crystallized from the solution at room temperature in 45% yield (1.45 g).

DSC (5 °C \cdot min $^{-1}$): 138 °C (dehydr.), 148 °C (dehydr.), >400 °C (no dec.). **IR** (KBr): $\tilde{\nu}$ = 3553 (s), 3316 (s), 3213 (vs), 2399 (m), 2224 (w), 1876 (w), 1696 (m), 1666 (m), 1384 (w), 1334 (s), 1314 (m), 1300 (m), 1204 (m), 1197 (m), 1161 (m), 1104 (w), 1070 (w), 1053 (w), 1026 (m), 940 (w), 730 (m), 688 (m), 452 (w) cm^{-1} ; **Raman** (1064 nm, 200 mW, 25 °C): $\tilde{\nu}$ = 2859 (1), 1591 (100), 1565 (8), 1221 (6), 1155 (6), 1129 (15), 1091 (9), 783 (3), 486 (2), 428 (2), 391 (4) cm^{-1} . **^1H NMR** (D_2O , 95 °C): δ = 4.83 (H_2O). **^{13}C NMR** (D_2O , 25 °C): δ = 154.7 (CN_4); **m/z (FAB $^-$)** 137.0 [C_2HN_8^-]; **EA** ($\text{C}_2\text{H}_{18}\text{MgN}_8\text{O}_9$, 322.52): calcd.: C 7.45; H 5.63; N 34.74%; found: C 9.57, H 4.13, N 41.49%. **BAM drophammer:** 40 J; **friction tester:** 360 N; **ESD:** 0.30 J (at grain size <100 μm).

Calcium 5,5'-bistetrazolate pentahydrate (3): 5,5'-Bistetrazole (1.38 g, 9.99 mmol, 1 equiv.) was dissolved in hot water (20 mL) and combined with calcium hydroxide (0.89 g, 12.01 mmol, 1.20 equiv.). The mixture was boiled for 40 min and filtered hot. During the following days the product crystallized from the solution at room temperature in light yellowish blocks in 72% yield (1.92 g).

DSC (5 °C \cdot min $^{-1}$): 98 °C (dehydr.), 190 °C (endotherm.), >400 °C (no dec.). **IR** (KBr): $\tilde{\nu}$ = 3468 (s), 3416 (s), 3234 (vs), 2224 (m), 2195 (m), 1685 (m), 1649 (m), 1444 (m), 1384 (m), 1350 (s), 1319 (m), 1220 (m), 1202 (m), 1166 (m), 1154 (m), 1103 (m), 1082 (m), 1062 (m), 1049 (m), 1025 (m), 818 (m), 728 (m), 687 (s), 486 (m) cm^{-1} ; **Raman** (1064 nm, 200 mW, 25 °C): $\tilde{\nu}$ = 3203 (2), 2859 (3), 1604 (100), 1566 (3), 1223 (14), 1148 (5), 1123 (19), 1084 (9), 783 (4), 493 (6), 433 (6) cm^{-1} . **^1H NMR** (D_2O , 25 °C): δ = 4.78 (H_2O). **^{13}C NMR** (D_2O , 25 °C): δ = 154.8 (CN_4); **m/z (FAB $^-$)** 137.0 [C_2HN_8^-]; **EA** ($\text{C}_2\text{H}_{10}\text{N}_8\text{CaO}_5$, 266.23): calcd.: C 9.02; H 3.79; N 42.09%; found: C 9.35; H 3.43; N 41.66%. **BAM drophammer:** 40 J; **friction tester:** 360 N; **ESD:** 0.20 J (at grain size <100 μm).

Strontium 5,5'-bistetrazolate tetrahydrate (4): 5,5'-Bistetrazole (1.38 g, 9.99 mmol, 1 equiv.) was dissolved in hot water (20 mL) and combined with strontium hydroxide octahydrate (3.19 g, 12.00 mmol, 1.20 equiv.). The mixture was boiled for 40 min and filtered hot. After a short period, precipitation of the yellowish product could be observed. Crystals suitable for single-crystal X-ray diffraction could only be obtained by recrystallization from DMF. Yield: 68% after recrystallization of the DMF adduct (3.00 g).

DSC (5 °C \cdot min $^{-1}$): 130 °C (dehydr.), >400 °C (no dec.). **IR** (KBr): $\tilde{\nu}$ = 3614 (s), 3358 (vs), 3178 (s), 2689 (w), 2450 (w), 2430 (w), 2213 (w), 2172 (w), 2125 (w), 1656 (m), 1629 (w), 1590 (w), 1457 (w), 1426 (w), 1384 (w), 1329 (m), 1309 (m), 1208 (w), 1181 (m), 1156 (w), 1128 (w), 1101 (w), 1051 (w), 1022 (w), 1031 (w), 782 (w), 733 (w), 591 (w) cm^{-1} ; **Raman** (1064 nm, 200 mW, 25 °C): $\tilde{\nu}$ = 1590 (100), 1565 (8), 1210 (10), 1181 (1), 1156 (3), 1127 (25), 1083 (19), 1033 (1), 783 (4), 481 (2), 427 (4), 401 (7) cm^{-1} . **^1H NMR** (D_2O ,

25 °C): δ = 4.78 (H_2O). **^{13}C NMR** (D_2O , 25 °C): δ = 154.8 (CN_4); **m/z (FAB $^-$)** 137.0 [C_2HN_8^-]; **EA** ($\text{C}_2\text{H}_8\text{N}_8\text{O}_4\text{Sr}$, 295.76): calcd.: C 8.12; H 2.73; N 37.89%; found: C 8.54; H 2.55; N 37.86%. **BAM drophammer:** 35 J; **friction tester:** 360 N; **ESD:** 0.15 J (at grain size <100 μm).

Barium 5,5'-bistetrazolate tetrahydrate (5): 5,5'-Bistetrazole (1.38 g, 9.99 mmol, 1 equiv.) was dissolved in hot water (20 mL) and combined with barium hydroxide octahydrate (3.78 g, 12.00 mmol, 1.20 equiv.). The mixture was boiled for 40 min and filtered hot. After standing for a few minutes, **5** crystallizes in small colorless blocks in 66% yield (2.28 g).

DSC (5 °C \cdot min $^{-1}$): 92 °C (dehydr.), 166 °C (endotherm.), >400 °C (no dec.). **IR** (KBr): $\tilde{\nu}$ = 3526 (vs), 3386 (s), 3090 (s), 2677 (w), 2195 (w), 1631 (m), 1435 (w), 1384 (w), 1340 (s), 1326 (m), 1310 (s), 1218 (w), 1186 (m), 1151 (w), 1143 (w), 1081 (w), 1047 (w), 1030 (w), 1020 (m), 824 (w), 782 (w), 731 (w), 726 (w), 681 (w), 581 (m), 551 (m), 485 (w) cm^{-1} ; **Raman** (1064 nm, 200 mW, 25 °C): $\tilde{\nu}$ = 1588 (100), 1565 (11), 1219 (5), 1206 (9), 1146 (4), 1125 (24), 1081 (17), 784 (5), 480 (2), 427 (4), 399 (8) cm^{-1} . **^1H NMR** (D_2O , 25 °C): δ = 4.78 (H_2O). **^{13}C NMR** (D_2O , 25 °C): δ = 154.8 (CN_4); **m/z (FAB $^-$)** 137.0 [C_2HN_8^-]; **EA** ($\text{BaC}_2\text{H}_8\text{N}_8\text{O}_4$, 345.46): calcd.: C 6.95; H 2.33; N 32.44%; found: C 7.34; H 2.07; N 32.89%. **BAM drophammer:** 30 J; **friction tester:** 360 N; **ESD:** 0.15 J (at grain size 100–500 μm).

Acknowledgement

Financial support of this work by the Ludwig Maximilian University of Munich (LMU), the U.S. Army Research Laboratory (ARL), the Armament Research, Development and Engineering Center (ARDEC), the Strategic Environmental Research and Development Program (SERDP) and the Office of Naval Research (ONR Global, title: "Synthesis and Characterization of New High Energy Dense Oxidizers (HEDO) - NICOP Effort") under contract nos. W911NF-09-2-0018 (ARL), W911NF-09-1-0120 (ARDEC), W011NF-09-1-0056 (ARDEC) and 10 WPSEED01-002 / WP-1765 (SERDP) is gratefully acknowledged. The authors acknowledge collaborations with Dr. Mila Krupka (OZM Research, Czech Republic) in the development of new testing and evaluation methods for energetic materials and with Dr. Muhamed Sucesca (Brodarski Institute, Croatia) in the development of new computational codes to predict the detonation and propulsion parameters of novel explosives. We are indebted to and thank Drs. Betsy M. Rice and Brad Forch (ARL, Aberdeen, Proving Ground, MD) and Mr. Gary Chen (ARDEC, Picatinny Arsenal, NJ) for many helpful and inspired discussions and support of our work. Mr. Stefan Huber is thanked for performing the sensitivity tests. The Cusanuswerk is gratefully acknowledged for a PhD scholarship (M.R.).

References

- [1] D. E. Chavez, M. A. Hiskey, D. L. Naud, *J. Pyrotech.* **1999**, *10*, 17–36.
- [2] P. J. Steel, *J. Chem. Crystallogr.* **1996**, *26*, 399.
- [3] P. J. Eulgem, A. Klein, N. Maggiora, D. Naumann, P. W. H. Pohl, *Chem. Eur. J.* **2008**, *14*, 3727.
- [4] *CrysAlis CCD*, Version 1.171.27p5 beta; Oxford Diffraction Ltd.
- [5] *CrysAlis RED*, Version 1.171.27p5 beta; Oxford Diffraction Ltd.
- [6] A. Altomare, G. Casciaro, C. Giacovazzo, A. Guagliardi, *J. Appl. Crystallogr.* **1993**, *26*, 343.
- [7] G. M. Sheldrick, *SHELXS-97, Program for Crystal Structure Solution*; University of Göttingen: Göttingen, Germany, **1997**.
- [8] G. M. Sheldrick, *SHELXL-97, Program for the Refinement of*

- Crystal Structures*; University of Göttingen: Göttingen, Germany, **1994**.
- [9] L. J. Farrugia, *WinGX* suite for small-molecule single-crystal crystallography, *J. Appl. Crystallogr.* **1999**, 32, 837–838.
- [10] A. Spek, A. L. *PLATON, A Multipurpose Crystallographic Tool*; Utrecht, The Netherlands, **1999**.
- [11] *SCALE3 ABSPACK*-An Oxford Diffraction program; Oxford Diffraction Ltd., **2005**.
- [12] Personal X-ray redetermination of neutral 5,5'-BT at 173 K.
- [13] T. M. Klapötke, M. Stein, J. Stierstorfer, *Z. Anorg. Allg. Chem.* **2008**, 634, 1711–1723.
- [14] A. Hammerl, G. Holl, T. M. Klapötke, P. Meyer, H. Nöth, H. Piotrowski, M. Warchhold, *Eur. J. Inorg. Chem.* **2002**, 834–845.
- [15] M. Hesse, H. Meier, B. Zeeh, *Spektroskopische Methoden in der organischen Chemie*, Thieme, **2002**, vol. 6, pp. 41–46.
- [16] <http://www.linseis.com>.
- [17] NATO standardization agreement (STANAG) on explosives, *impact sensitivity tests*, no. 4489, 1st ed., Sept. 17, **1999**.
- [18] WIWEB-Standardarbeitsanweisung 4–5.1.02, Ermittlung der Explosionsgefährlichkeit, hier der Schlagempfindlichkeit mit dem Fallhammer, Nov. 8, **2002**.
- [19] <http://www.bam.de>.
- [20] NATO standardization agreement (STANAG) on explosive, *friction sensitivity tests*, no. 4487, 1st ed., Aug. 22, **2002**.
- [21] WIWEB-Standardarbeitsanweisung 4–5.1.03, Ermittlung der Explosionsgefährlichkeit or der Reibeempfindlichkeit mit dem Reibeapparat, Nov. 8, **2002**.
- [22] Impact: Insensitive > 40 J, less sensitive ≥ 35 J, sensitive ≥ 4 J, very sensitive ≤ 3 J; friction: Insensitive > 360 N, less sensitive = 360 N, sensitive < 360 N a. > 80 N, very sensitive ≤ 80 N, extreme sensitive ≤ 10 N; According to the UN Recommendations on the Transport of Dangerous Goods (+) indicates: not safe for transport.
- [23] <http://www.ozm.cz>.

Received: June 14, 2011
Published Online: August 11, 2011



1-Nitratoethyl-5-nitriminotetrazole derivatives – Shaping future high explosives

Niko Fischer, Thomas M. Klapötke*, Jörg Stierstorfer, Carina Wiedemann

Energetic Materials Research, Department of Chemistry, University of Munich (LMU), Butenandtstr. 5-13, D-81377, Germany

ARTICLE INFO

Article history:

Received 31 March 2011

Accepted 31 May 2011

Available online 22 June 2011

Keywords:

1-(2-Nitratoethyl)-5-nitriminotetrazole

High-explosives

Crystal structures

Detonation parameters

ABSTRACT

1-(2-Nitratoethyl)-5-nitriminotetrazole (**2**) was formed by the reaction of 1-(2-hydroxyethyl)-5-aminotetrazole (**1**) and 100% HNO₃. Compound **1** was obtained by alkylation of 5-amino-1H-tetrazole. Next to the known byproduct 1-(2-hydroxyethyl)-5-nitriminotetrazole (**3**), a second one, 1-(2-nitratoethyl)-5-aminotetrazolium nitrate (**4**) was obtained and fully characterized. Nitrogen-rich salts such as the ammonium (**5**), hydroxylammonium (**6**), guanidinium (**7**), aminoguanidinium (**8**), diaminoguanidinium (**9**) and triaminoguanidinium (**10**) 1-(2-nitratoethyl)-5-nitriminotetrazolate were prepared by deprotonation or metathesis reactions. The reaction of **2** and diaminourea yielded 1-(2-nitratoethyl)-5-aminotetrazole (**11**). Compounds **4–11** were fully characterized by single crystal X-ray diffraction, vibrational spectroscopy (IR and Raman), multinuclear NMR spectroscopy, elemental analysis and DSC measurements. The heats of formation of **5–10** were calculated by the atomization method based on CBS-4M enthalpies. Regarding the possible application of these compounds as energetic materials or high explosives, several detonation parameters such as the detonation pressure, velocity, energy and temperature were computed using the EXPLO5 code and the X-ray densities as well as the computed heats of formation. In addition the sensitivities towards impact, friction and electrical discharge were tested using the BAM drophammer, a friction tester as well as a small scale electrical discharge device.

© 2011 Elsevier Ltd. All rights reserved.

1. Introduction

Tetrazoles have the outstanding property of often combining high nitrogen content and high positive heats of formation with good thermal stability, owing to their aromatic ring system. Of particular interest are tetrazoles, which exhibit energetic nitrogen–oxygen-containing functional groups, such as nitro groups (R–NO₂) [1,2], nitrate esters (R–O–NO₂) [3], or nitramine functionalities (R₂N–NO₂) [4–6]. Also, the formation of tetrazolium salts with oxygen-rich counter anions such as NO₃[−] [7,8] or (NO₂)₂[−] [9,10] are the focus of research because these compounds have balanced oxygen contents. 5-Nitriminotetrazoles have been known for a long time, as they can be obtained by facile synthetic routes [11]. 1-Substituted 5-nitriminotetrazoles such as 1-methyl-5-nitriminotetrazole and 1-ethyl-5-nitriminotetrazole were first described in 1957 [12]. Also various N-alkylations of 5-aminotetrazoles, which involve different alkylation reagents such as methyl iodide, dimethyl- and diethyl-sulfate and chloroethanol have been known to literature [13]. The variation of the substituent attached to the tetrazole ring is of major interest, since it becomes possible to control the performance as well as the sensitivities of the energetic compound. 5-Nitriminotetrazole is an appropriate building block during the

synthesis of energetic materials since it has an oxygen balance, which is almost balanced to 0, which means, no oxygen from the atmosphere is necessary to fully oxidize the material. One of the major problems here is the relatively high sensitivity of unsubstituted 5-nitriminotetrazoles. Substitution of the tetrazole ring with an alkyl substituent on the one hand decreases the sensitivity of the compound but on the other hand also lowers the oxygen balance, which disables the compound in its use as energetic material. Therefore the nitration of a hydroxyl group, which is contained in the substituent of the tetrazole ring is necessary to keep up the energetic features of the material, which leads us to nitratoethyl substituted nitriminotetrazoles as a building block for new energetic materials. Here we report on different nitrogen-rich salts of 1-(2-nitratoethyl)-5-nitriminotetrazole, which is one of the products obtained by nitration of 1-hydroxyethyl-5-aminotetrazole [14]. In addition, an unexpected new covalent species, 1-(2-nitratoethyl)-5-aminotetrazole is presented.

2. Results and discussion

2.1. Synthesis

The first step in the synthesis of the nitrogen rich salts of 1-(2-nitratoethyl)-5-nitriminotetrazole is the alkylation of commercially available 5-aminotetrazole, which leads to the starting material **1**: 1-(2-Hydroxyethyl)-5-aminotetrazole (**1**) was synthesized reacting

* Corresponding author.

E-mail addresses: Thomas.M.Klapotke@cup.uni-muenchen.de (T.M. Klapötke), jstsch@cup.uni-muenchen.de (J. Stierstorfer).

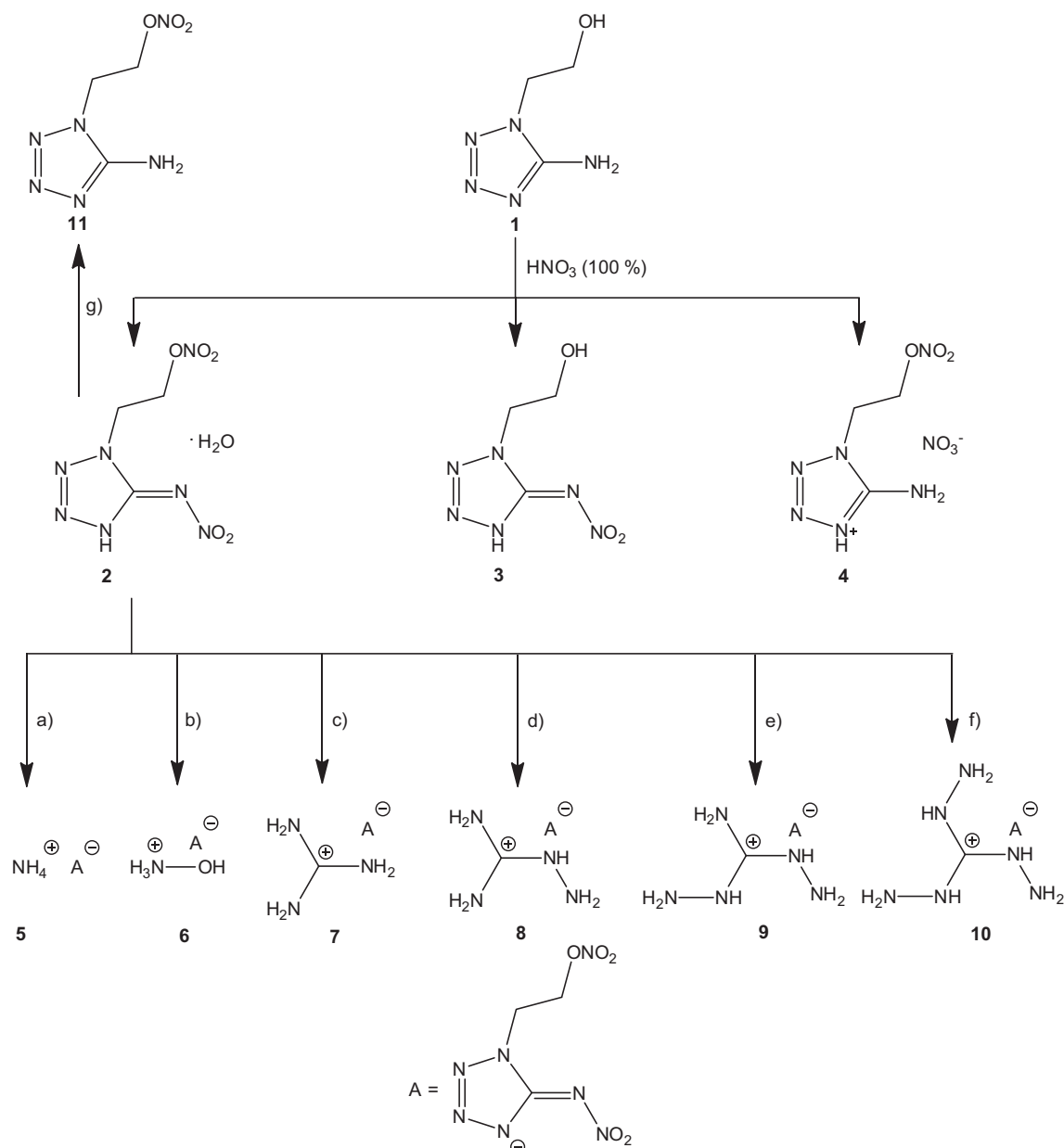
the sodium salt of 5-amino-1*H*-tetrazole with 2-chloroethanol in aqueous solution under reflux conditions. Beside the main product **1**, also 2-(2-hydroxyethyl)-5-aminotetrazole can be isolated from this reaction [13]. Reacting **1** with differently concentrated nitric acid leads to a fairly broad variety of different nitration and protonation products. Using 65% nitric acid, the 5-aminotetrazole moiety is protonated to give 1-(2-hydroxyethyl)-5-amino-tetrazolium nitrate [15]. Using 100% nitric acid, three different products can be observed, since the amino group in **1** can be nitrated as well as the hydroxy group in the side chain (Scheme 1).

Treating **1** with fuming nitric acid at 0 °C overnight affords the O-nitrated compound **3** as well as the double N- and O-nitrated product **2**. They can be separated from each other by recrystallization due to their different solubility in water. The nitrateethyl substituted compound **2** is isolated from the mother liquor first, since it is least soluble in water due to the lack of possible hydrogen bonding in

solution. The hydroxyethyl substituted nitriminotetrazole **3** can be isolated as the second product. Its solubility in water is much better than the solubility of **3** caused by the hydroxyl moiety in the side chain. Even a third product, 1-(2-nitrateethyl)-5-aminotetrazolium nitrate (**4**) could be observed in the reaction mixture and was detected by NMR spectroscopy when less than the required amount of fuming nitric acid was used or the concentration of the nitric acid was decreased by absorption of moisture.

Since the nitration products **2** and **3** are already described in literature [15], we herein concentrate on the synthesis and full characterization of the third nitration product **4** as well as six nitrogen-rich salts of **2**. Also a new covalent species, which was isolated after reducing **2** with 1,3-diaminourea is presented.

Reacting **2** with one equivalent of aqueous ammonia or aqueous hydroxylamine, respectively, yields the ammonium and the hydroxylammonium salts **5** and **6** since **2** is a fairly strong acid



Scheme 1. Different products **2–4** of the nitration of 1-(2-hydroxyethyl)-5-aminotetrazole (**1**). Synthesis of nitrogen-rich salts of 1-nitrateethyl-5-nitriminotetrazole choosing different reaction conditions: (a) aqueous NH₃, 50 °C, 5 min; (b): aqueous NH₂OH, 50 °C, 5 min; (c) guanidinium carbonate, H₂O, 100 °C, 5 min; (d) aminoguanidinium bicarbonate, H₂O, 100 °C, 5 min; (e) 1. AgNO₃, H₂O; 2. diaminoguanidinium iodide, H₂O; (f) triaminoguanidine (free base), H₂O, rt, 5 min; (g) 1,3-diaminourea, H₂O, rt, 5 min.

and therefore can be easily deprotonated by bases like ammonia or hydroxylamine. For the synthesis of the guanidinium (**7**) and the aminoguanidinium (**8**) salt guanidinium carbonate and aminoguanidinium bicarbonate, respectively were used. For expelling the formed carbon dioxide quantitatively, the reaction was carried out at 50 °C. In contrast, the synthesis of the diaminoguanidinium salt **9** requires a metathesis reaction via the silver salt of using diaminoguanidinium chloride since diaminoguanidine is not available as its carbonate and the free base diaminoguanidine is not stable under ambient conditions. The silver salt of can be isolated after addition of silver nitrate to an aqueous solution of **2** by suction filtration due to its very low solubility in water and organic solvents. After the addition of diaminoguanidinium iodide and removal of precipitated silver iodide, the product can be isolated after evaporation of the solvent. The triaminoguanidinium salt **10** cannot be synthesized by treating the aminoguanidinium salt **8** with two equivalents of hydrazine hydrate in dioxane as it was applied for the synthesis of the triaminoguanidinium salt of 1-methyl-5-nitriminotetrazole [**5**]. In our case, the nitrateethyl side chain was reduced by the hydrazine to give the triaminoguanidinium salt of 1-(2-hydroxyethyl)-5-nitriminotetrazole **3**. To also avoid a metathesis reaction, how it was employed for the synthesis of **9**, **2** was reacted with triaminoguanidine, which was isolated as the free base following the described procedure: Triaminoguanidinium chloride is deprotonated with sodium hydroxide in aqueous medium under inert atmosphere. Addition of dimethylformamide to the reaction mixture precipitates triaminoguanidine, which is isolated by suction filtration and has to be stored under nitrogen.

An attempt to synthesize the diaminouronium salt of **2** yielded 1-(2-nitrateethyl)-5-nitriminotetrazole **11**. Diaminourea (carbohydrazide), in contrast to free hydrazine (see synthesis of

the triaminoguanidinium salt), reduced the nitrimino moiety of **2** to an amino group resulting in the isolation of **11**.

2.2. Molecular structures

To determine the molecular structures of **4–11** in the crystalline state an Oxford Xcalibur3 diffractometer with a Spellman generator (voltage 50 kV, current 40 mA) and a KappaCCD detector was used. All datasets were generated using a $\lambda_{\text{Mo K}\alpha}$ radiation wavelength of 0.71073 Å. The data collection and reduction were performed using the CRYSTALISPRO software [16]. The structures were solved with SIR-92 [17] or SHELXS-97 [18], refined with SHELXL-97 [19] and finally checked using the PLATON software [20] integrated in the WINGX software suite [21]. The non-hydrogen atoms were refined anisotropically and the hydrogen atoms were located and freely refined. In the case of the non-centrosymmetric space groups $P2_12_12_1$ (**5**), $Pca2_1$ (**7**) and Cc (**10**) the “Friedel pairs” have been merged. The absorptions were corrected by a SCALE3 ABSPACK multi-scan method [22]. Selected data and parameters of the X-ray determinations are given in Tables 1 and 2.

The structure of 1-(2-nitrateethyl)-5-nitriminotetrazole monohydrate (**2**), which crystallizes in the space group $P-1$ and a density of 1.781 g cm^{-3} has recently been determined in our group [15]. Crystals of 1-(2-nitrateethyl)-5-aminotetrazolium nitrate (**4**) were obtained from the mother liquor of **2**. The molecular unit of **4** is depicted in Fig. 1. The nitrate salt **4** crystallizes in the monoclinic space group $P2_1/c$ with eight anion/cation pairs in the unit cell. The calculated density (1.725 g cm^{-3}) of **3** is slightly lower than the one of **2** (1.781 g cm^{-3}). The bond lengths and angles in **2** and **3** are very similar. However, the packing differs significantly. In **2** alternation layers formed by hydrogen bonds

Table 1
X-ray data and parameters of **4–7**.

	4	5	6	7
Formula	$\text{C}_3\text{H}_7\text{N}_7\text{O}_6$	$\text{C}_3\text{H}_8\text{N}_8\text{O}_5$	$\text{C}_3\text{H}_8\text{N}_8\text{O}_6$	$\text{C}_4\text{H}_{10}\text{N}_{10}\text{O}_5$
Formula weight (g mol^{-1})	237.16	236.17	252.17	278.22
Crystal system	monoclinic	orthorhombic	monoclinic	orthorhombic
Space group	$P2_1/c$	$P2_12_12_1$	$C2/c$	$Pca2_1$
Color/habit	colorless blocks	colorless rods	colorless rods	colorless plates
Size (mm)	0.35 0.25 0.20	0.21 0.23 0.34	0.13 0.14 0.20	0.10 0.15 0.20
<i>Unit cell dimensions</i>				
<i>a</i> (Å)	23.499(2)	5.3372(2)	24.4432(19)	6.4067(4)
<i>b</i> (Å)	5.5543(5)	7.2473(3)	5.3862(4)	14.9629(8)
<i>c</i> (Å)	14.3477(13)	23.9611(8)	14.6227(11)	11.3562(5)
α (°)	90	90	90	90
β (°)	102.769(9)	90	104.300(8)	90
γ (°)	90	90	90	90
<i>V</i> (Å ³)	1826.3(3)	926.82(6)	1865.5(3)	1088.64(10)
<i>Z</i>	8	4	8	4
ρ_{calc} (g cm^{-3})	1.725	1.693	1.796	1.697
μ (mm^{-1})	0.163	0.155	0.168	0.151
<i>F</i> (0 0 0)	976	488	1040	576
<i>T</i> (K)	200(2)	173(2)	173(2)	173(2)
θ Minimum–Maximum (°)	3.8, 28.8	4.2, 26.0	4.2, 26.2	4.2, 26.0
Dataset	–22:28; –6:6; –17:13	–5:6; –8:7; –29:29	–30:30; –6:6; –17:18	–4:7; –18:15; –14:12
Reflections collected	7383	4805	4690	2791
Independent reflections	3561	1094	1872	1117
<i>R</i> _{int}	0.0258	0.034	0.030	0.038
Observed reflections	2270	871	1324	764
Parameters	313	177	186	212
<i>R</i> ₁ (obs.)	0.0345	0.0306	0.0315	0.0320
<i>wR</i> ₂ (all data)	0.0745	0.0696	0.0707	0.0478
<i>S</i>	0.88	0.94	0.89	0.82
Resd. dens. (e/Å^3)	–0.21, 0.21	–0.15, 0.29	–0.25, 0.22	–0.17, 0.16
Device type	Oxford Xcalibur3 CCD	Oxford Xcalibur3 CCD	Oxford Xcalibur3 CCD	Oxford Xcalibur3 CCD
Solution	SIR-92	SIR-92	SHELXS-97	SHELXS-97
Refinement	SHELXL-97	SHELXL-97	SHELXL-97	SHELXL-97
Absorption correction	multi-scan	multi-scan	multi-scan	multi-scan
CCDC	766629	815404	815410	815407

Table 2
X-ray data and parameters of **8–11**.

	8	9	10	11
Formula	C ₄ H ₁₁ N ₁₁ O ₅	C ₄ H ₁₂ N ₁₃ O ₅	C ₄ H ₁₅ N ₁₃ O ₆	C ₃ H ₆ N ₆ O ₃
Formula weight (g mol ^{−1})	293.24	308.26	341.29	236.17
Crystal system	monoclinic	triclinic	monoclinic	monoclinic
Space group	<i>P</i> 2 ₁ / <i>c</i>	<i>P</i> -1	<i>Cc</i>	<i>P</i> 2 ₁ / <i>c</i>
Color/habit	colorless blocks	colorless needle	colorless block	colorless rod
Size (mm)	0.17 0.20 0.28	0.07 0.08 0.30	0.40 0.30 0.25	0.10 0.20 0.30
<i>a</i> (Å)	4.7075(2)	6.6627(18)	12.0111(5)	10.5878(16)
<i>b</i> (Å)	10.7539(4)	10.192(2)	7.0212(3)	5.9447(7)
<i>c</i> (Å)	22.7782(10)	18.355(5)	16.6414(7)	11.7057(17)
α (°)	90	79.79(2)	90	90
β (°)	92.757(4)	88.21(2)	95.896(4)	101.815(15)
γ (°)	90	88.682(19)	90	90
<i>V</i> (Å ³)	1151.79(8)	1225.9(5)	1395.98(10)	721.16(18)
<i>Z</i>	4	4	4	4
ρ_{calc} (g cm ^{−3})	1.691	1.670	1.624	1.604
μ (mm ^{−1})	0.150	0.147	0.145	0.141
<i>F</i> (0 0 0)	608	640	712	360
<i>T</i> (K)	173(2)	173(2)	173(2)	173(2)
θ Minimum–Maximum (°)	4.2, 26.0	4.2, 24.0	4.3, 29.0	4.4, 26.0
Dataset	−5:5; −13:13; −28:26	−6:7; −11:11; −20:19	−16:16; −9:9; −22:22	−13:11; −7:7; −14: 14
Reflections collected	8020	5371	12 498	3504
Independent reflections	2255	3808	1616	1412
<i>R</i> _{int}	0.036	0.067	0.030	0.020
Observed reflections	1470	1460	2450	1088
Parameters	225	346	268	133
<i>R</i> ₁ (obs.)	0.0328	0.0690	0.0304	0.0311
<i>wR</i> ₂ (all data)	0.0679	0.1680	0.0750	0.0791
<i>S</i>	0.84	0.84	1.01	1.01
Resd. dens. (e/Å ³)	−0.22, 0.17	−0.40, 0.44	−0.25, 0.33	−0.26, 0.16
Device type	Oxford Xcalibur3 CCD	Oxford Xcalibur3 CCD	Oxford Xcalibur3 CCD	Oxford Xcalibur3 CCD
Solution	SHELXS-97	SHELXS-97	SHELXS-97	SIR-92
Refinement	SHELXL-97	SHELXL-97	SHELXL-97	SHELXL-97
Absorption correction	multi-scan	multi-scan	multi-scan	multi-scan
CCDC	815405	815771	815406	815409

and alkyl chain interactions and in **3** layers containing the amine and nitrate moieties connected by hydrogen bonds can be distinguished.

All of the following ionic compounds contain the 1-(2-nitratotethyl)-5-nitriminotetrazolate anion. Although showing different arrangements of the nitratotethyl substituent bond lengths of the anions are very similar in all structures. A comparison can be found in Table 3.

The differences in the arrangement of the nitratotethyl moiety within the asymmetric unit can be characterized by the torsion angles C1–N1–C2–C3, N1–C2–C3–O3 and C2–C3–O3–N7. In **7**, **8** and **10** torsion angle C1–N1–C2–C3 is positive (117.9(4)°, 96.61(18)° and 77.4(2)°) and therefore the nitratotethyl moiety lies above the tetrazole ring (if C1 N1 N2 N3 N4 counted clockwise). In contrast for **5**, the same angle is negative (−79.2(3)°) and the nitratotethyl moiety switched to the other side of the tetrazole ring. Combination of the torsion angles N1–C2–C3–O3 = 65.89(18)° and C2–C3–O3–N7 = −90.09(16)° in **8** leads to a geometry, where the nitrate ester is inclined towards the tetrazole ring, which is not the case for **5**, **7** and **10**. The five membered ring of the tetrazole moiety reveals planar geometry indicated e.g. by the torsion angle N1–N2 N3–N4 = 0.09(16)° in **8** and up to 0.6(3)° in **7**. The nitramine unit is slightly twisted out of the tetrazole ring plane in **5** (N4–C1–N5–N6 = 10.2(3)°) and **8** (N4–C1–N5–N6 = −8.9(5)°), whereas it is sitting almost inside the plane in **8** (N4–C1–N5–N6 = −1.8(2)°) and **10** (N4–C1–N5–N6 = 0.3(3)°).

Ammonium 1-(2-nitratotethyl)-5-nitriminotetrazolate (Fig. 2) crystallizes in the non-centrosymmetric space group *P*2₁2₁2₁ forming a density of 1.693 g cm^{−3}. Compound **5** is stabilized by various H-bonds involving the ammonium cation e.g. N8–H8a···

N4, N8–H8a···O1, N8–H8b···N5, N8–H8b···O2, N8–H8c···N3, N8–H8d···N4, N8–H8d···O1.

By adding one oxygen atom to the sum formula of **5** compound **6** is obtained, whose density is significantly higher (1.79 g cm^{−3}) in comparison to that of **5**. This represents also the greatest density of all compounds investigated in this work, which is an important characteristic of a secondary explosive. The hydroxylammonium salt, illustrated in Fig. 3, crystallizes in the space group *C*2/*c* with eight cation/anion pairs in the unit cell.

Also the guanidinium derivatives such as the (7) guanidinium (Fig. 4), aminoguanidinium (**8**) (Fig. 6), diaminoguanidinium (**9**) (Fig. 7) and triaminoguanidinium (**10**) (Fig. 8) crystallize in common space groups listed in Tables 1 and 2. The molecular moieties of **7–10** are depicted in Figs. 5 and 7–9.

The guanidinium salt crystallizes layer-like. Within the layers a strong hydrogen-bond network can be found which is shown in Fig. 5. Several ring graph sets [23] are drawn. The R(2,2)6 hydrogen-bond motive is responsible for the constitution of the nitratotethyl substituent.

The triaminoguanidinium salt is additionally stabilized by hydrogen bonds involving the hydrogen atoms of the crystal water, which are for instance d(H6a–N4ⁱ) = 1.83(4) Å [(i) −1/2 + *x*, 1/2 + *y*, *z*] and d(H6b–O5ⁱⁱ) = 2.16(3) Å [(ii) *x*, −1 + *y*, *z*].

1-Nitratotethyl-5-aminotetrazole (**11**) crystallizes in the monoclinic space group *P*2₁/*c* with four molecules in the unit cell. The molecular unit is shown in Fig. 9. Its density of 1.604 g cm^{−3} is lower than those obtained for **2** (1.781 g cm^{−3}) and **3** (1.733 g cm^{−3}) but higher than that of unnitrated **1** (1.497 g cm^{−3}).

The packing is dominated by the formation of two classical hydrogen bonds (d(N5–H5a···N3ⁱ) = 2.980(2) Å and d(N5–H5b···N4ⁱⁱ) = 3.011(2) Å) as well as three non-classical hydrogen bonds

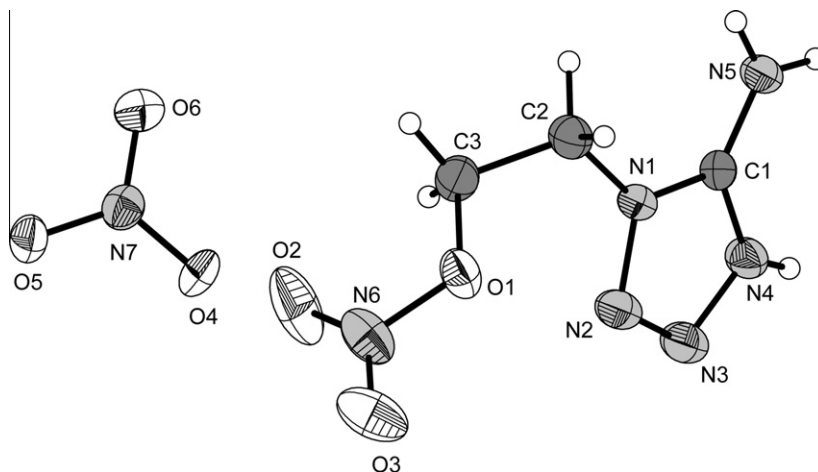


Fig. 1. Molecular unit of **4**. Hydrogen atoms shown as spheres of arbitrary radius and thermal ellipsoids are drawn at a 50% probability level.

Table 3

Anion bond lengths (Å) in the structures of **5–10**.

	5	6	7	8	9	10
N1–N2	1.346(3)	1.3376(17)	1.356(4)	1.3533(17)	1.350(7)	1.351(3)
N1–C1	1.349(3)	1.3589(19)	1.346(4)	1.3535(18)	1.343(8)	1.356(3)
N1–C2	1.459(3)	1.4664(19)	1.462(4)	1.461(2)	1.490(7)	1.459(3)
N2–N3	1.287(3)	1.2983(18)	1.295(4)	1.2928(17)	1.320(7)	1.284(3)
N3–N4	1.365(3)	1.3615(17)	1.372(4)	1.3696(17)	1.377(7)	1.368(3)
N4–C1	1.334(3)	1.3392(19)	1.338(4)	1.3289(19)	1.347(7)	1.326(3)
N5–N6	1.328(3)	1.3034(16)	1.325(4)	1.3232(17)	1.323(7)	1.323(2)
N5–C1	1.366(3)	1.3635(19)	1.370(4)	1.3732(19)	1.352(7)	1.368(2)
C2–C3	1.488(4)	1.503(2)	1.506(5)	1.509(2)	1.518(9)	1.515(3)
O1–N6	1.252(3)	1.2658(15)	1.256(3)	1.2465(16)	1.262(6)	1.239(2)
O2–N6	1.252(3)	1.2666(15)	1.252(4)	1.2654(16)	1.261(6)	1.256(2)
O3–N7	1.382(3)	1.4042(16)	1.384(3)	1.4060(17)	1.412(7)	1.239(2)
O3–C3	1.474(3)	1.4543(19)	1.466(4)	1.4542(19)	1.446(7)	1.456(3)
O4–N7	1.196(3)	1.1997(16)	1.208(3)	1.2054(17)	1.219(8)	1.196(3)
O5–N7	1.210(3)	1.2043(17)	1.212(3)	1.2040(17)	1.214(7)	1.207(3)

($d(\text{C2} \cdots \text{H2b} \cdots \text{N3}^{\text{I}}) = 3.464(2) \text{ \AA}$, $d(\text{C2} \cdots \text{H2a} \cdots \text{O2}^{\text{III}}) = 3.576(2) \text{ \AA}$, $d(\text{C3}^{\text{III}} \cdots \text{H3a}^{\text{III}} \cdots \text{O1}) = 3.472(2) \text{ \AA}$), which are depicted in Fig. 10. Latter one of the classical hydrogen bonds yields to formation of dimers.

2.3. NMR spectroscopy

All discussed compounds were investigated using ^1H as well as ^{13}C NMR spectroscopy. ^{15}N NMR spectra were recorded only of the 1-(2-nitratoethyl)-5-aminotetrazolium nitrate (**4**) as well as of the 1-(2-nitratoethyl)-5-aminotetrazole (**11**), its unprotonated sister compound. Tetramethylsilane (^1H , ^{13}C) and nitromethane (^{15}N) were used as standards.

The assignments of the chemical shifts of the ^{15}N NMR spectra were undertaken using $^3J_{\text{N-H}}$ and $^2J_{\text{N-H}}$ coupling constants and after comparison with literature values [15]. The major part of the signals of the neutral compound is not heavily affected by the protonation of the ring system with nitric acid. The signals of the ring nitrogen N1 are observed at -180.7 (**4**) and -181.6 ppm (**11**), whereas in the spectrum of **11** the signal reveals a triplet with a coupling constant of 2.8 Hz (t, $^3J_{\text{N-H}}$). Also the signals of the ring nitrogen atom N2 are observed as triplets (both t, $^3J_{\text{N-H}} = 1.6 \text{ Hz}$) due to the coupling to the methylene moiety directly attached to the tetrazole ring (-25.5 ppm (**4**), -25.3 ppm (**11**)). The signal of N3 is observed as a singlet since a $^4J_{\text{N-H}}$ coupling cannot be observed (-5.7 ppm (**4**), 3.7 ppm (**11**)). The most remarkable shift of a signal upon protonation is observed for N4 since this is the protonation site of the tetrazole ring. The signal is observed at -94.2 ppm (t, $^3J_{\text{N-H}} = 2.2 \text{ Hz}$)

in the neutral species **11** and is shifted upfield to -116.5 ppm in the protonated species **4**. The signal of the amino group is visible in the upfield region of the spectrum at -332.7 ppm (**4**) and -337.7 ppm (**11**), respectively, however a triplet due to the $^1J_{\text{N-H}}$ coupling to the amino protons could not be resolved. The nitrate ester reveals signals at -43.6 ppm (**4**) and -44.0 ppm (**11**), respectively; both signals are observed as triplets ($^3J_{\text{N-H}} = 3.3 \text{ Hz}$ (**4**), $^3J_{\text{N-H}} = 3.7 \text{ Hz}$ (**11**)). Additionally the nitrate anion shows up as a signal at -14.8 ppm in the spectrum of **4**.

The assignment of the proton and carbon signals of **4–11** was undertaken by comparison to literature [5,15] and to values that have been computed using the GAUSSIAN09 program package [24] ((aug-cc-pvdz)-NMR calculation). The signal of the tetrazole carbon atom can be found at 157.1 – 157.7 ppm in the nitrogen-rich salts **5–10**, which is slightly shifted downfield compared to the neutral compound **2** (151.1 ppm). Also the protonation of the ring system of **11** (152.8 ppm) leads to a downfield shift of the ring carbon atom signal to 167.6 ppm in **4**. The ethylene bridge connecting the nitrate ester with the tetrazole ring is visible in two distinct signals at 70.2 – 70.8 ppm for the nitrate ester connected methylene unit and 43.2 – 43.7 ppm for the tetrazole connected methylene unit in the nitrogen-rich salts **5–10**, whereas in the neutral compound **2** these signals are found upfield shifted to 48.7 and 41.6 ppm, respectively. Neutral **11** reveals two signals in this region at 39.5 and 67.5 ppm, whereas the upfield shifted signal is connected to the tetrazole ring. Protonation of the tetrazole ring (in **4**) leads to a strong downfield shift of the signal at 39.5 – 55.3 ppm, whereas the signal at 67.5 ppm is not so strongly affected and is found at 59.5 ppm in **4**. The signals, which are related to the guanidinium derived cations are in a range of 158.3 – 160.3 ppm.

The same argumentation, that was applied to the shifts of the carbon atoms of the ethylene bridge also applies to the signal of the protons attached to them. A triplet set observed at 4.83 – 4.88 ppm (**2**, **5–10**) can be assigned to the protons of the methylene unit neighbored to the nitrate ester, whereas the triplet set at 3.76 ppm (**2**) and 4.41 – 4.45 ppm (**5–10**) arises from the protons belonging to the tetrazole ring connected methylene moiety. Very similar chemical shifts are observed for the corresponding protons of the aminotetrazole species **4** and **11** at 4.86 ppm (**4**, **11**) and 4.51 ppm (**4**) and 4.50 ppm (**11**), respectively.

2.4. Sensitivities and thermal stability

The impact sensitivity tests were carried out according to STANAG 4489 [25] modified instruction [26] using a BAM (Bundesanstalt für

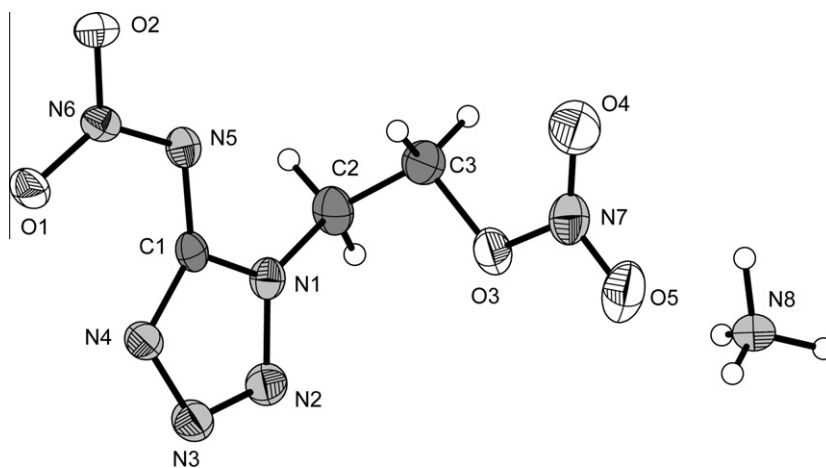


Fig. 2. Molecular unit of **5**. Hydrogen atoms shown as spheres of arbitrary radius and thermal displacements set at 50% probability.

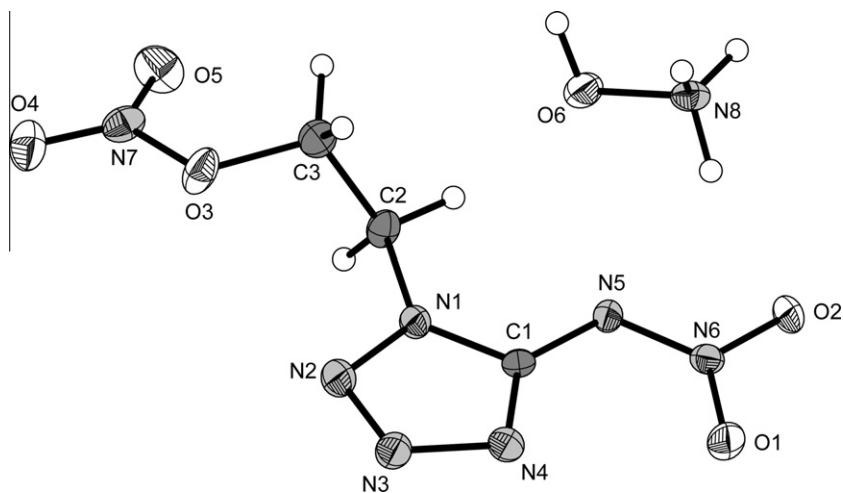


Fig. 3. Molecular unit of **6**. Hydrogen atoms shown as spheres of arbitrary radius and thermal displacements set at 50% probability.

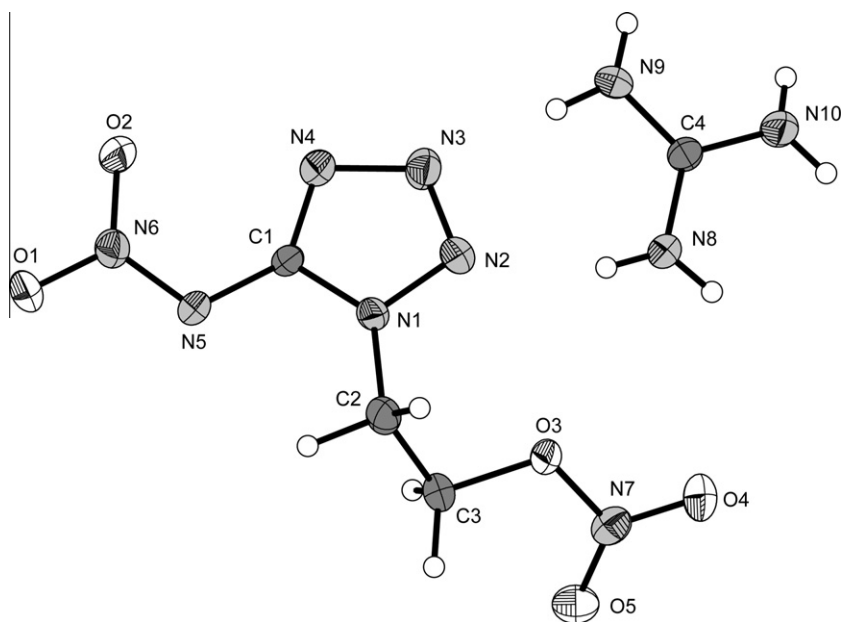


Fig. 4. Molecular unit of **7**. Hydrogen atoms shown as spheres of arbitrary radius and thermal displacements set at 50% probability.

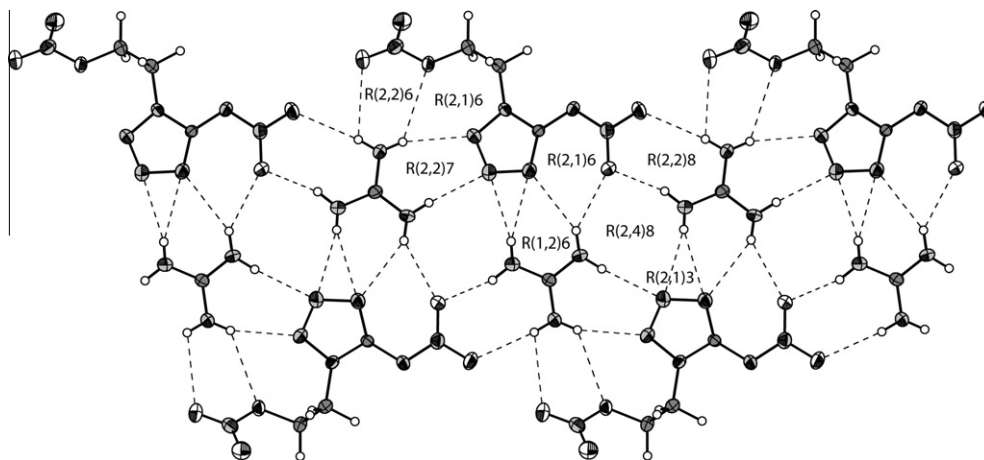


Fig. 5. Hydrogen bonding in the structure of 7.

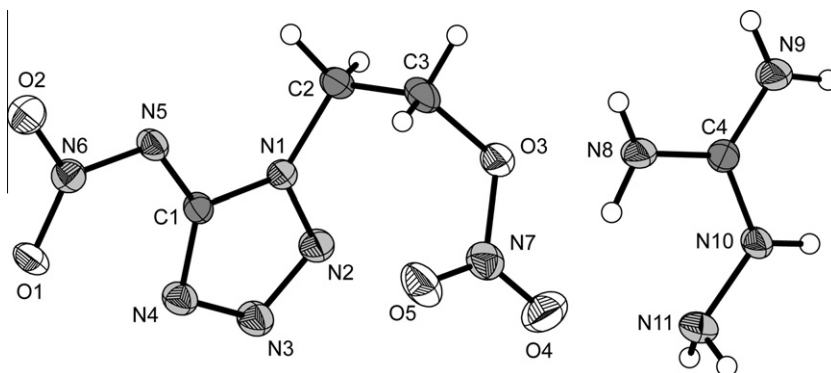


Fig. 6. Molecular unit of 8. Hydrogen atoms shown as spheres of arbitrary radius and thermal displacements set at 50% probability.

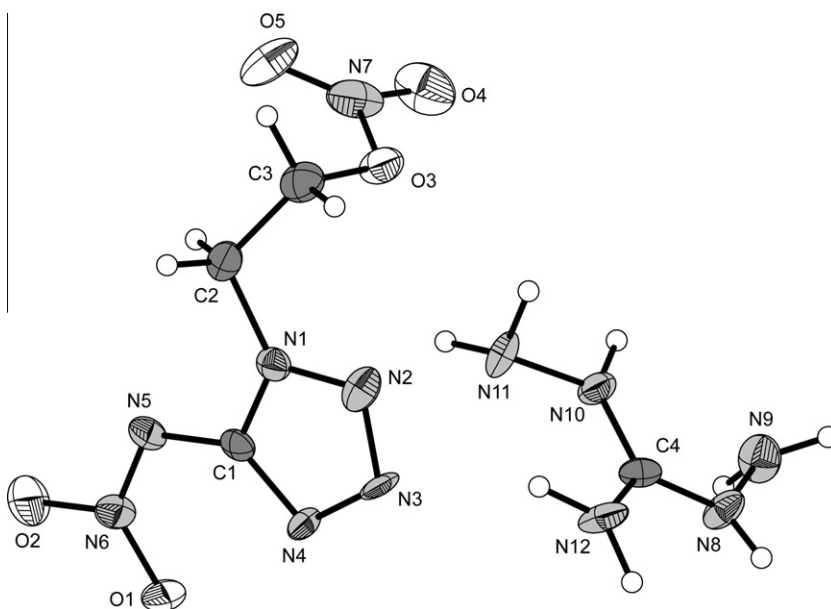


Fig. 7. Molecular unit of 9. Hydrogen atoms shown as spheres of arbitrary radius and thermal displacements set at 50% probability.

Materialforschung) drophammer [27]. The friction sensitivity tests were carried out according to STANAG 4487 [28] modified instruction [29] using the BAM friction tester. The classification of the tested

compounds results from the “UN Recommendations on the Transport of Dangerous Goods” [30]. Additionally all compounds were tested upon the sensitivity towards electrical discharge using the Electric

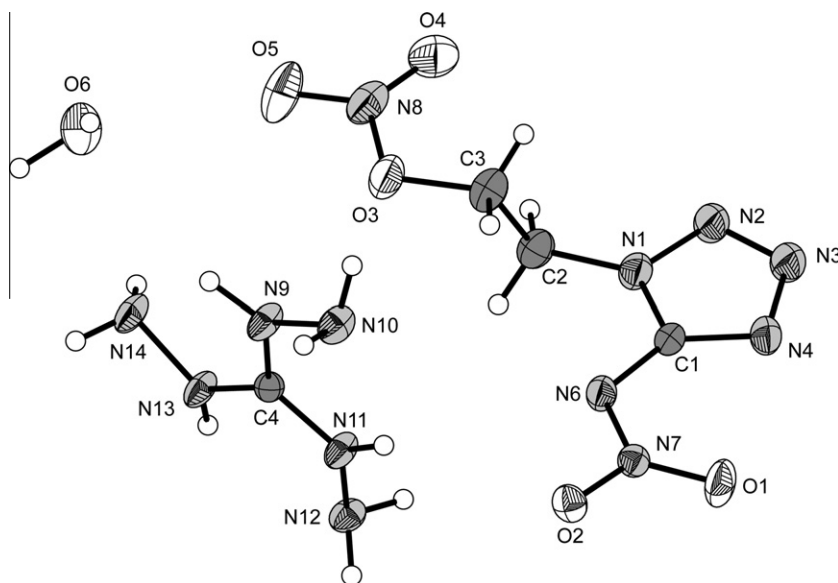


Fig. 8. Molecular unit of **10**. Hydrogen atoms shown as spheres of arbitrary radius and thermal displacements set at 50% probability.

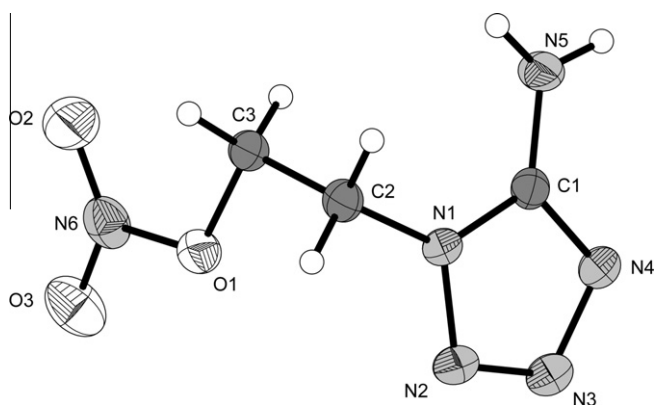


Fig. 9. Molecular unit of **11**. Hydrogen atoms shown as spheres of arbitrary radius and thermal displacements set at 50% probability.

Spark Tester ESD 2010 EN [31]. Differential scanning calorimetry (DSC) measurements to determine the melt- and decomposition temperatures of **4–11** (about 1.5 mg of each energetic material) were performed in covered Al-containers containing a hole in the lid and a nitrogen flow of 20 mL per minute on a Linseis PT 10 DSC [32] calibrated by standard pure indium and zinc at a heating rate of $5\text{ }^{\circ}\text{C min}^{-1}$.

The impact sensitivities of the synthesized compounds **4–11** are mainly determined by the nitrate-moiety in the side chain. Like other nitrate esters such as nitroglycerine, also the nitrateethyl functionalized nitriminotetrazoles show increased sensitivities towards impact and friction. The impact sensitivities of the nitrogen-rich salts **5–9**, all of them are crystallizing as water-free compounds, are in the range of 3–7 J and therefore have to be classified as sensitive (**5**, **7–9**) or very sensitive (**6**). Only the monohydrate **10** shows slightly lower sensitivity with 10 J. Protonation of the ring system, like in **4**, also seems to slightly decrease the impact sensitivity (10 J). Unexpectedly, 1-(2-nitrateethyl)-5-aminotetrazole (**11**) is insensitive towards impact (40 J) and also the neutral compound **2** is rather insensitive (25 J) compared to the nitrogen-rich salts **5–9**, which mainly arises from the included crystal water. The friction sensitivities show the same trend, which is very sensitive for the hydroxylammonium salt **6** (60 N) and sensitive for **5** and

7–10 (96–120 N). Both, the protonated ring compound **4** as well as the aminotetrazole-derivative **11** show slightly decreased sensitivity towards friction (160 N), whereas the neutral compound **2** is insensitive (360 N). In contrast to the impact and friction sensitivity, the sensitivity towards electrostatic discharge strongly depends on the grain size of the material with lower values for smaller grain size. However, they were determined to be in a range of 100–200 mJ for **2** and **5–10** and higher values for **4** and **11**. The sensitivity data of all compounds are summarized in Table 5.

Beside the sensitivity of the compounds, also their thermal stability is influenced by the nitrate-moiety, which is not known to have outstanding thermal stability. The neutral compound **2** decomposes at $122\text{ }^{\circ}\text{C}$ and deprotonation of the tetrazole ring leads to a marginal thermal stabilization of 10–30 $^{\circ}\text{C}$. Therefore, the nitrogen-rich salts **5–10** decompose at temperatures of 130–160 $^{\circ}\text{C}$. Also protonation of the ring system does not lead to any remarkable stabilization, as it is seen for **4** (137 $^{\circ}\text{C}$). The most stable compound, which is discussed, is the neutral aminotetrazole derivative **11** (163 $^{\circ}\text{C}$), however still not thermally stable enough for an application as a high explosive. Additionally, some of the materials show melting points (endothermic peaks in the DSC curve), such as the ammonium salt (81 $^{\circ}\text{C}$), the hydroxylammonium salt (66 $^{\circ}\text{C}$) the diaminoguanidinium salt (103 $^{\circ}\text{C}$) and the aminotetrazole derivative **11** (133 $^{\circ}\text{C}$). Dehydration of the triaminoguanidinium salt **10** takes place at 54 $^{\circ}\text{C}$.

2.5. Heat of formation

The heats formation of **4–10** were computed theoretically. All calculations were carried out using the GAUSSIAN G09 program package [24]. The enthalpies (H) and free energies (G) were calculated using the complete basis set (CBS) method of Petersson and coworkers in order to obtain very accurate energies. The CBS models use the known asymptotic convergence of pair natural orbital expressions to extrapolate from calculations using a finite basis set to the estimated complete basis set limit. CBS-4 begins with a HF/3-21G(d) geometry optimization; the zero point energy is computed at the same level. It then uses a large basis set SCF calculation as a base energy, and a MP2/6-31+G calculation with a CBS extrapolation to correct the energy through second order. A MP4(SDQ)/6-31+(d,p) calculation is used to approximate higher

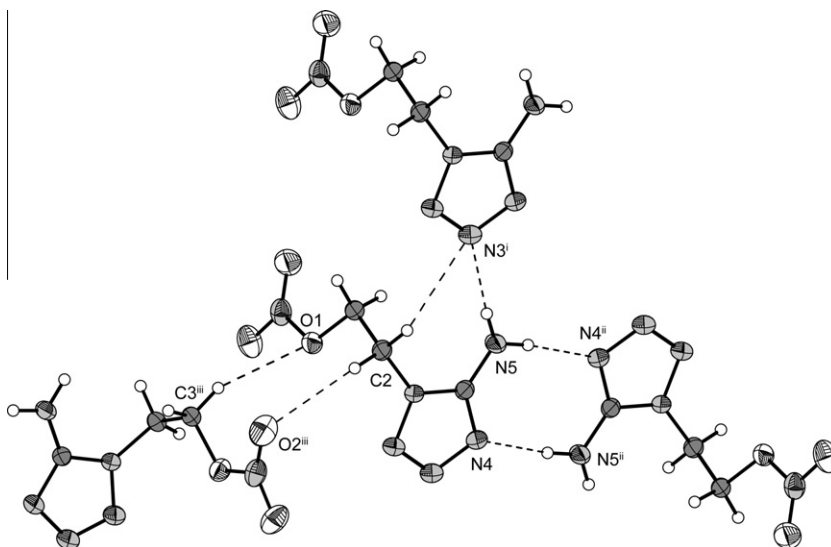


Fig. 10. Hydrogen bonds in the structure of **11**. Symmetry codes: (i): $x, 1 + y, z$; (ii) $H5B-x, -y, 2-z$; (iii) $1-x, -0.5 + y, 1.5-z$.

order contributions. In this study we applied the modified CBS-4M method (**M** referring to the use of Minimal Population localization) which is a re-parametrized version of the original CBS-4 method and also includes some additional empirical corrections [33]. The enthalpies of the gas-phase species **M** (Table 4) were computed according to the atomization energy method (Eq. (1)) [34] described circumstantially in the literature [35].

$$\Delta_f H^\circ(\text{g}, \text{M}, 298) = H_{(\text{Molecule}, 298)} - \sum H_{(\text{Atoms}, 298)}^\circ + \sum \Delta_f H_{(\text{Atoms}, 298)}^\circ \quad (1)$$

Using calculated heat of sublimation for **2** and **11** by the Troutons Rule [36] and lattice enthalpies for the ionic compounds the gas-phase enthalpies of formation (Table 4) were converted into the solid state (standard conditions) enthalpy of formation $\Delta_f H_m^\circ$ (Table 5). Lattice energies (U_L) and lattice enthalpies (ΔH_L) were calculated from the corresponding molecular volumes according to Jenkin's equations [37].

Lastly, the molar standard enthalpies of formation (ΔH_m) were used to calculate the molar solid state energies of formation (ΔU_m) according to Eq. (2).

$$\Delta U_m = \Delta H_m - \Delta n RT$$

(Δn being the change of moles of gaseous components) (2)

Except for **2** as its monohydrate, all compounds are formed endothermically. Comparing the heats of formation in Table 5, it can be seen, that the most endothermic compounds are the hydroxylammonium salt **6** and the diaminoguanidinium derivative **9**. The triaminoguanidinium salt **10** is lower in enthalpy due to the inclusion of one crystal water.

2.6. Detonation parameters

The detonation parameters were calculated using the program EXPLO5 V5.04 [38]. The program is based on the steady-state model of equilibrium detonation and uses Becker–Kistiakowsky–Wilson's equation of state (BKW E.O.S) for gaseous detonation products and Cowan–Fickett E.O.S. for solid carbon [39]. The calculation of the equilibrium composition of the detonation products is done by applying modified White, Johnson and Dantzig's free energy minimization technique. The program is designed to enable

Table 4

CBS-4M calculation results and molecular volumes taken from X-ray solution.

M	$-H^{298}$ (a.u.)	$\Delta_f H^\circ$ (g, M) (kcal mol $^{-1}$)	V_M (nm 3)
2	875.340790	66.1	
2 anion	874.840174	13.8	
NH$_4^+$	56.796608	151.9	
NH$_4\text{O}^+$	131.863249	177.9	
G$^+$	205.453192	136.6	
AG$^+$	260.701802	160.4	
DAG$^+$	315.949896	184.5	
TAG$^+$	371.197775	208.8	
5		165.7	0.232
6		177.9	0.233
7		150.4	0.272
8		174.2	0.288
9		198.3	0.307
10 ($\cdot\text{H}_2\text{O}$)		222.6 (164.9)	0.324 (0.349)
11	671.069048	54.1	

the calculation of detonation parameters at the CJ point. The BKW equation in the following form was used with the BKWN set of parameters ($\alpha, \beta, \kappa, \theta$) as stated below the equations and X_i being the mol fraction of i -th gaseous product, k_i is the molar covolume of the i -th gaseous product [40]:

$$pV/RT = 1 + xe^{\beta x} \quad x = (\kappa \sum X_i k_i) / [V(T + \theta)]^\alpha$$

$$\alpha = 0.5, \beta = 0.176, \kappa = 14.71, \theta = 6620.$$

The calculations were performed using the maximum densities according to the crystal structures.

Since the detonation velocity and the detonation pressure are strongly dependent on the density and energy of formation, the detonation parameters of the hydroxylammonium salt **6** exceed those of the other nitrogen-rich salts by far. It has a density of 1.796 g cm $^{-3}$, which is even higher than the density of the neutral compound **2** (1.781 g cm $^{-3}$). Its energy of formation (1125 kJ kg $^{-1}$) is exceeded only by the energy of formation of **9** (1334 kJ kg $^{-1}$). Its detonation velocity exceeds the benchmark of 9000 m s $^{-1}$, whereas the detonation velocity of the remaining compounds lies between 8300 and 8600 m s $^{-1}$. Due to its low density, the aminotetrazole derivative **11** shows the lowest calculated value and does not even reach the 8000 m s $^{-1}$ level. Compared to commonly used RDX, only

Table 5
Energetic properties and detonation parameters of **4**–**11**.

	2*H ₂ O	4	5	6	7	8	9	10*H ₂ O	11
Formula	C ₃ H ₇ N ₇ O ₆	C ₃ H ₇ N ₇ O ₆	C ₃ H ₈ N ₈ O ₅	C ₃ H ₈ N ₈ O ₆	C ₄ H ₁₀ N ₁₀ O ₅	C ₄ H ₁₁ N ₁₁ O ₅	C ₄ H ₁₂ N ₁₂ O ₅	C ₄ H ₁₅ N ₁₃ O ₆	C ₃ H ₆ N ₆ O ₃
Molecular mass (g mol ⁻¹)	237.13	237.14	236.15	252.15	278.19	293.20	308.22	341.25	174.12
IS (J) ^a	25	10	5	3	7	5	4	10	40
FS (N) ^b	360	160	120	60	120	108	108	96	160
ESD-test (J) ^c	0.10	0.40	0.15	0.15	0.15	0.10	0.20	0.15	0.30
N (%) ^d	41.35	41.35	47.45	44.44	50.35	52.55	54.53	53.36	48.27
Ω (%) ^e	–23.61	–23.61	–33.87	–25.38	–46.01	–46.38	–46.72	–44.54	–55.13
T _{dec.} (°C) ^f	122	137	147	148	160	150	134	130	163
Density (g cm ⁻³) ^g	1.781	1.725	1.692	1.796	1.697	1.691	1.670	1.624	1.604
Δ _f H _m ^o (kJ mol ⁻¹) ^h	–20.9	78.0	204.4	256.5	160.4	266.8	375.2	241.6	151.5
Δ _f U ^o (kJ kg ⁻¹) ⁱ	16.3	433.0	975.5	1125.4	687.9	1023.8	1333.7	831.4	976.5
Detonation parameters calculated by EXPLO5.04									
–Δ _E U ^o (kJ kg ⁻¹) ^j	5498	5896	5780	6349	4953	5134	5293	5159	5044
T _E (K) ^k	3859	4068	3921	4205	3387	3441	3528	3403	3477
p _{C-J} (kbar) ^l	325	316	303	364	274	282	286	270	239
D (m s ⁻¹) ^m	8600	8551	8557	9034	8306	8427	8480	8363	7887
Gas vol. (L kg ⁻¹) ⁿ	769	770	803	787	801	813	823	854	769

^a Impact sensitivity (BAM drophammer [27], 1 of 6).

^b Friction sensitivity (BAM friction tester [27], 1 of 6).

^c Electrostatic discharge device (OZM [23]).

^d Nitrogen content.

^e Oxygen balance.

^f Decomposition temperature from DSC (β = 5 °C).

^g Estimated from X-ray diffraction.

^h Calculated (CBS-4M) heat of formation.

ⁱ Calculated energy of formation.

^j Energy of Explosion.

^k Explosion temperature.

^l Detonation pressure.

^m Detonation velocity.

ⁿ Assuming only gaseous products.

the hydroxylammonium salt **6** is an appropriate alternative as high explosive, regarding only the detonation parameters. Beside the detonation velocity, it is also the only compound with a higher detonation pressure (364 kbar) compared to RDX (349 kbar).

3. Experimental

All reagents and solvents were used as received (Sigma–Aldrich, Fluka, Acros Organics) if not stated otherwise. Melting and decomposition points were measured with a Linseis PT10 DSC using heating rates of 5 °C min⁻¹, which were checked with a Büchi Melting Point B-450 apparatus. ¹H, ¹³C and ¹⁵N NMR spectra were measured with a JEOL instrument. All chemical shifts are quoted in ppm relative to TMS (¹H, ¹³C) or nitromethane (¹⁵N). Infrared spectra were measured with a Perkin–Elmer Spektrum One FT-IR instrument. Raman spectra were measured with a Perkin–Elmer Spektrum 2000R NIR FT-Raman instrument equipped with a Nd:YAG laser (1064 nm). Elemental analyzes were performed with a Netsch STA 429 simultaneous thermal analyzer. Sensitivity data were determined using a BAM drophammer and a BAM friction tester. The electrostatic sensitivity tests were carried out using an Electric Spark Tester ESD 2010 EN (OZM Research) operating with the “Winspark 1.15” software package. 1-(2-Nitrateoethyl)-5-nitriminotetrazole (**2**) was synthesized according to literature [15].

CAUTION! 5-Nitriminotetrazole (**2**), its salts (**5**–**10**) as well as compounds **4** and **11** are all energetic compounds with sensitivity to various stimuli. While we encountered no issues in the handling of these materials, proper protective measures (face shield, ear protection, body armor, Kevlar gloves, and earthened equipment) should be used at all times.

3.1. 1-(2-Nitrateoethyl)-5-aminotetrazolium nitrate (**4**)

This compound was obtained during the reaction of 1-(2-hydroxyethyl)-5-aminotetrazole with nitric acid (100%). It is a

byproduct in the synthesis of 1-(2-nitrateoethyl)-5-nitriminotetrazole monohydrate (**2**) and could be isolated from the mother liquor of the recrystallization of **2**. Yield: 8%.

DSC (5 °C min⁻¹, °C): 137 °C (dec.); IR (ATR, cm⁻¹): $\tilde{\nu}$ = 3347 (m), 3158 (w), 2920 (m), 2853 (w), 2363 (m), 2337 (w), 1690 (m), 1636 (s), 1581 (m), 1548 (w), 1532 (w), 1493 (m), 1447 (m), 1407 (m), 1372 (m), 1341 (m), 1310 (m), 1283 (s), 1241 (m), 1145 (vw), 1060 (w), 1042 (w), 1018 (w), 976 (w), 946 (vw), 894 (w), 871 (w), 852 (w), 843 (w), 778 (vw), 756 (w), 724 (w), 672 (vw), 625 (w); Raman (1064 nm, 200 mW, 25 °C, cm⁻¹): $\tilde{\nu}$ = 3243 (4), 3031 (17), 2982 (41), 2966 (19), 1684 (6), 1638 (9), 1598 (7), 1562 (3), 1503 (10), 1455 (13), 1433 (12), 1380 (14), 1290 (18), 1228 (5), 1144 (5), 1048 (100), 950 (5), 860 (7), 845 (17), 768 (38), 717 (12), 673 (9), 639 (10), 571 (19), 535 (4), 493 (4), 444 (7), 414 (8), 333 (6), 306 (5), 284 (5), 248 (8), 208 (5). ¹H NMR (DMSO-*d*₆, 25 °C, ppm) δ: 8.76 (s, 2H, NH₂), 4.86 (t, ³J = 4.9 Hz, 2H, CH₂ONO₂), 4.51 (t, ³J = 4.9 Hz, 2H, NCH₂). ¹³C NMR (DMSO-*d*₆, 25 °C, ppm) δ: 167.6 (CN₄), 59.5 (CH₂ONO₂), 55.3 (NCH₂). ¹⁴N NMR (DMSO-*d*₆, 25 °C, ppm) δ: –15 (NO₃), –44 (ONO₂). ¹⁵N NMR (DMSO-*d*₆, 25 °C, ppm) δ: –5.7 (N3), –14.8 (NO₃), –25.5 (N2, ³J (¹H, ¹⁵N) = 1.6 Hz), –43.6 (t, ONO₂, ³J (¹H, ¹⁵N) = 3.3 Hz), –116.5 (N4), –180.7 (N1), –332.7 (N5). Anal. Calc. for EA (C₃H₇N₇O₆, 237.13): C, 15.20; H, 2.98; N, 41.35. Found: C, 15.08; H, 3.24; N, 41.32%. BAM drophammer: 10 J; friction tester: 160 N; ESD: 0.40 J (at grain size 100–500 μm).

3.2. Ammonium 1-(2-nitrateoethyl)-5-nitriminotetrazolate (**5**)

1-Nitrateoethyl-5-nitriminotetrazole (1.19 g, 5.0 mmol) is dissolved in 2 M ammonia (2.5 mL, 5.0 mmol). The mixture is filtered off and the solvent of the clear solution is removed in vacuum. The residue is recrystallized from water/ethanol. Yield: 0.96 g (81%, 4.1 mmol).

DSC (5 °C min⁻¹): 81 °C (m.p.), 147 (dec.); IR (KBr, cm⁻¹): $\tilde{\nu}$ = 3412 (m), 3243 (m), 1633 (s), 1505 (s), 1454 (s), 1415 (s),

1384 (s), 1328 (s), 1286 (vs), 1266 (s), 1167 (m), 1107 (m), 1072 (w), 1033 (m), 989 (w), 901 (m), 859 (w), 778 (w), 759 (w), 738 (w), 709 (w), 678 (w), 638 (w) 472 (w); Raman (1064 nm, 500 mW, 25 °C, cm^{-1}): $\tilde{\nu}$ = 3182 (2), 3009 (15), 2973 (20), 2962 (32), 2901 (3), 1653 (1), 1631 (1), 1558 (3), 1504 (100), 1462 (7), 1419 (3), 1384 (8), 1327 (20), 1279 (12), 1249 (1), 1232 (1), 1168 (3), 1109 (10), 1073 (3), 1033 (51), 989 (4), 880 (5), 854 (6), 779 (1), 759 (8), 710 (2), 679 (3), 571 (6), 513 (3), 474 (5), 452 (2), 413 (1); ^1H NMR ($\text{DMSO}-d_6$, 25 °C, ppm) δ : 7.12 (t, 4H, NH_4), 4.87 (t, 3J = 4.9 Hz, 2H, CH_2ONO_2), 4.44 (t, 3J = 4.9 Hz, 2H, NCH_2); ^{13}C NMR ($\text{DMSO}-d_6$, 25 °C, ppm) δ : 157.1 (CN_4), 70.2 (CH_2ONO_2), 43.9 (NCH_2); m/z (FAB^+): 18.0 [NH_4^+]; m/z (FAB^-): 217.9 [$\text{C}_3\text{H}_4\text{N}_7\text{O}_5^-$]; *Anal. Calc.* for EA ($\text{C}_3\text{H}_8\text{N}_8\text{O}_5$, 236.15): C, 15.26; H, 3.41; N, 47.45. Found: C, 14.85; H, 3.30; N, 46.01%; BAM drophammer: 5 J; friction tester: 120 N; ESD: 0.15 J (at grain size 100–500 μm).

3.3. Hydroxylammonium 1-(2-nitratoethyl)-5-nitriminotetrazolate (6)

1-(2-Nitratoethyl)-5-nitriminotetrazole (1.62 g, 6.83 mmol) was dissolved in 20 mL of hot water. An aqueous solution of hydroxylamine (50% w/w, 0.45 g, 6.83 mmol) is added and the solvent from the resulting clear solution is evaporated in vacuum. A colorless oil is formed, which is recrystallized from ethanol to yield **6** as colorless crystals after almost complete evaporation of the solvent (1.59 g, 6.31 mmol, 92%). The crystals were dried afterwards at 50 °C overnight.

DSC (5 °C min^{-1} , °C): 66 °C (m.p.), 148 °C (dec.); IR (KBr, cm^{-1}): $\tilde{\nu}$ = 3413 (m), 3126 (m), 3017 (m), 2934 (m), 2784 (m), 2723 (m), 2380 (w), 1985 (w), 1644 (s), 1635 (s), 1535 (m), 1499 (m), 1455 (m), 1428 (m), 1383 (s), 1343 (vs), 1289 (s), 1251 (m), 1230 (m), 1171 (m), 1123 (m), 1081 (w), 1036 (m), 1014 (m), 985 (m), 904 (m), 881 (m), 853 (m), 771 (w), 741 (m), 679 (m), 627 (w), 527 (w); Raman (1064 nm, 300 mW, 25 °C, cm^{-1}): $\tilde{\nu}$ = 3033 (2), 3017 (2), 2991 (3), 2974 (13), 1636 (3), 1503 (100), 1430 (3), 1380 (7), 1357 (7), 1328 (10), 1279 (15), 1232 (2), 1126 (13), 1037 (23), 1016 (2), 1005 (7), 987 (3), 883 (4), 842 (6), 748 (5), 678 (3), 626 (2), 575 (4), 429 (2), 373 (2), 293 (2), 263 (3); ^1H NMR ($\text{DMSO}-d_6$, 25 °C, ppm) δ : 10.11 (s, 4H, NH_3OH^+), 4.87 (t, 3J = 4.9 Hz, 2H, CH_2ONO_2), 4.45 (t, 3J = 4.9 Hz, 2H, NCH_2); ^{13}C NMR ($\text{DMSO}-d_6$, 25 °C, ppm) δ : 157.6 (CN_4), 70.8 (CH_2ONO_2), 43.7 (NCH_2); m/z (FAB^+): 34.0 [NH_3OH^+]; m/z (FAB^-): 217.8 [$\text{C}_3\text{H}_4\text{N}_7\text{O}_5^-$]; *Anal. Calc.* for EA ($\text{C}_3\text{H}_8\text{N}_8\text{O}_6$, 252.15): C, 14.29; H, 3.20; N, 44.44. Found: C, 14.55; H, 3.00; N, 44.22%; BAM drophammer: 3 J; friction tester: 60 N; ESD: 0.15 J (at grain size 100–500 μm).

3.4. Guanidinium 1-(2-nitratoethyl)-5-nitriminotetrazolate (7)

1-(2-Nitratoethyl)-5-nitriminotetrazole monohydrate (2.37 g, 10 mmol) is suspended in a few milliliters of water and a suspension of guanidinium carbonate (0.90 g, 5 mmol) in water is added slowly. The mixture is heated to 40 °C and then filtrated. The solvent is removed in vacuum and the residue recrystallized from water/ethanol. Yield: 2.10 g (7.55 mmol, 76%).

DSC (5 °C min^{-1} , °C): 160 °C (dec.); IR (KBr, cm^{-1}): $\tilde{\nu}$ = 3552 (s), 3400 (s), 3238 (m), 3169 (s), 2891 (w), 2298 (w), 2049 (m), 1974 (w), 1666 (vs), 1619 (vs), 1496 (s), 1446 (s), 1427 (m), 1373 (s), 1303 (s), 1283 (s), 1265 (s), 1170 (m), 1117 (m), 1040 (m), 1028 (m), 995 (m), 907 (m), 878 (m), 861 (m), 776 (m), 759 (m), 739 (w), 714 (m), 673 (w), 620 (m), 576 (w), 543 (w), 519 (w), 503 (w), 479 (w); Raman (1064 nm, 200 mW, 25 °C, cm^{-1}): $\tilde{\nu}$ = 3009 (4), 2972 (8), 1510 (100), 1373 (3), 1340 (20), 1274 (7), 1162 (4), 1110 (14), 1066 (4), 1034 (49), 993 (6), 974 (7), 895 (4), 845 (6), 745 (12), 629 (5), 582 (8), 506 (4), 489 (3), 439 (4), 385 (3), 258 (9); ^1H NMR ($\text{DMSO}-d_6$, 25 °C, ppm) δ : 6.94 (s, 6H, NH_2), 4.87 (t, 3J = 4.9 Hz, 2H, CH_2ONO_2), 4.45 (t, 3J = 4.9 Hz, 2H, NCH_2); ^{13}C NMR

($\text{DMSO}-d_6$, 25 °C, ppm) δ : 158.4 ($\text{C}(\text{NH}_2)_3$), 157.7 (CN_4), 70.8 (CH_2ONO_2), 43.7 (NCH_2); m/z (FAB^+): 60.1 [$\text{C}(\text{NH}_2)_3^+$]; m/z (FAB^-): 218.0 [$\text{C}_3\text{H}_4\text{N}_7\text{O}_5^-$]; *Anal. Calc.* for EA ($\text{C}_3\text{H}_9\text{N}_9\text{O}_2$, 203.16): C, 17.27; H, 3.62; N, 50.35. Found: C, 17.59; H, 3.81; N, 50.07%; BAM drophammer: 7 J; friction tester: 120 N (at grain size 100–500 μm); ESD: 0.15 J (at grain size <100 μm).

3.5. Aminoguanidinium-1-(2-nitratoethyl)-5-nitriminotetrazolate (8)

1-(2-Nitratoethyl)-5-nitriminotetrazole monohydrate (2.37 g, 10 mmol) is suspended in a few milliliters of water and a suspension of aminoguanidinium bicarbonate (1.36 g, 10 mmol) in water is added slowly. The mixture is heated to 40 °C and then filtrated. The solvent is removed in vacuum and the residue recrystallized from water/ethanol. Yield: 2.25 g (7.68 mmol, 77%).

DSC (5 °C min^{-1} , °C): 150 °C (dec.); IR (KBr, cm^{-1}): $\tilde{\nu}$ = 3930 (w), 3552 (s), 3415 (vs, br), 3168 (s), 3007 (m), 2970 (m), 2893 (m), 2139 (m), 1864 (w), 1777 (m), 1632 (vs), 1545 (m), 1509 (s), 1453 (s), 1428 (s), 1414 (m), 1368 (s), 1338 (s), 1283 (s), 1233 (s), 1108 (s), 1064 (m), 1032 (s), 1011 (s), 935 (m), 895 (m), 877 (s), 844 (s), 773 (m), 742 (m), 704 (w), 676 (s), 607 (s), 488 (s); Raman (1064 nm, 200 mW, 25 °C, cm^{-1}): $\tilde{\nu}$ = 3009 (4), 2972 (8), 1510 (100), 1372 (4), 1341 (20), 1275 (6), 1161 (3), 1111 (14), 1065 (3), 1034 (49), 993 (5), 974 (8), 845 (6), 745 (11), 630 (5), 583 (7), 590 (4), 540 (4), 385 (3), 258 (9), 201 (4); ^1H NMR ($\text{DMSO}-d_6$, 25 °C, ppm) δ : 8.58 (s, 1H, CNH), 7.25 (s, 2H, $\text{C}(\text{NHH})_2$), 6.77 (s, 2H, $\text{C}_{\text{AG}}(\text{NHH})_2$), 4.87 (t, 3J = 4.9 Hz, 2H, CH_2ONO_2), 4.70 (s, 2H, NNH_2), 4.45 (t, 3J = 4.9 Hz, 2H, NCH_2); ^{13}C NMR ($\text{DMSO}-d_6$, 25 °C, ppm) δ : 158.3 ($\text{C}(\text{NH}_2)_2(\text{NH})$), 157.7 (CN_4), 70.8 (CH_2ONO_2), 43.7 (NCH_2); m/z (FAB^+): 75.1 [$\text{C}(\text{NHNH}_2)(\text{NH}_2)_2^+$]; m/z (FAB^-): 217.9 [$\text{C}_3\text{H}_4\text{N}_7\text{O}_5^-$]; *Anal. Calc.* for EA ($\text{C}_3\text{H}_{10}\text{N}_{10}\text{O}_2$, 218.18): C, 16.39; H, 3.78; N, 52.55. Found: C, 16.63; H, 4.00; N, 52.07%; BAM drophammer: 5 J; friction tester: 108 N (at grain size 500–1000 μm); ESD: 0.10 J (at grain size 100–500 μm).

3.6. Diaminoguanidinium 1-(2-nitratoethyl)-5-nitriminotetrazolate (9)

1-(2-Nitratoethyl)-5-nitriminotetrazole (1.65 g, 7.0 mmol) is suspended in a few milliliters of water and an aqueous solution of silver nitrate (1.18 g, 7.0 mmol) is added. The colorless precipitate is filtered off and washed twice with 50 mL water. The residue is suspended in 50 mL water and a solution of diaminoguanidinium iodide (1.52 g, 7.0 mmol) in water is added. The suspension is stirred under exclusion of light for 30 min at 30 °C, filtered off and the solvent of the clear solution is removed in vacuum. The residue is recrystallized from ethanol/water to yield **9** as white crystalline solid (1.65 g, 5.35 mmol, 77%).

DSC (5 °C min^{-1} , °C): 103 °C (m.p.), 134 °C (dec.); IR (KBr, cm^{-1}): $\tilde{\nu}$ = 3552 (s), 3478 (vs), 3412 (vs), 3291 (s), 2381 (w), 2027 (w), 1669 (s), 1638 (vs), 1618 (s), 1506 (s), 1462 (m), 1446 (m), 1432 (m), 1395 (m), 1384 (m), 1347 (s), 1284 (s), 1245 (m), 1172 (m), 1110 (m), 1008 (m), 975 (m), 898 (m), 882 (w), 849 (m), 774 (w), 751 (w), 739 (w), 684 (w), 633 (m), 553 (w), 482 (w); Raman (1064 nm, 300 mW, 25 °C, cm^{-1}): $\tilde{\nu}$ = 3300 (5), 3030 (5), 2985 (9), 1673 (5), 1647 (3), 1507 (100), 1433 (6), 1400 (9), 1310 (16), 1285 (23), 1175 (4), 1112 (7), 1085 (7), 1036 (40), 996 (9), 922 (7), 899 (5), 881 (5), 852 (13), 753 (14), 686 (8), 582 (9), 550 (6), 468 (4), 427 (3); ^1H NMR ($\text{DMSO}-d_6$, 25 °C, ppm) δ : 8.55 (s, 2H, CNH), 7.14 (s, 2H, CNH_2), 4.88 (t, 3J = 4.9 Hz, 2H, CH_2ONO_2), 4.60 (s, 4H, NHNH_2), 4.43 (t, 3J = 4.9 Hz, 2H, NCH_2); ^{13}C NMR ($\text{DMSO}-d_6$, 25 °C, ppm) δ : 160.3 ($\text{C}(\text{NHNH}_2)_2(\text{NH}_2)$), 157.7 (CN_4), 70.8 (CH_2ONO_2), 43.7 (NCH_2); m/z (FAB^+): 90.1 [$\text{C}(\text{NHNH}_2)_2(\text{NH}_2)^+$]; m/z (FAB^-): 218.0 [$\text{C}_3\text{H}_4\text{N}_7\text{O}_5^-$]; *Anal. Calc.* for EA ($\text{C}_4\text{H}_{12}\text{N}_{12}\text{O}_5$, 308.11): C, 15.59; H, 3.92; N, 54.53. Found: C, 15.68; H, 3.87; N,

54.18%; BAM drophammer: 4 J; friction tester: 108 N, ESD: 0.20 J (at grain size 100–500 μm).

3.7. Triaminoguanidinium 1-(2-nitratoethyl)-5-nitriminotetrazolate (**10**)

In a 100 mL Schlenk flask triaminoguanidinium chloride (4.64 g, 33 mmol) is suspended in 6 mL of water under nitrogen. Sodium hydroxide (1.32 g, 33 mmol), previously dissolved in 4 mL of water, is added. After all triaminoguanidinium chloride has been dissolved, 20 mL of *N,N'*-dimethylformamide is added and the mixture is cooled in an ice bath, where triaminoguanidine starts to precipitate. It is isolated in a Schlenk frit and transferred (1.04 g, 10 mmol) to a flask containing a suspension of 1-(2-nitratoethyl)-5-nitriminotetrazole (2.37 g, 10 mmol) as a suspension in 10 mL of water. The mixture is stirred until clear, filtrated and the solvent removed in vacuo. After **10** crystallized from the solution, it was filtered off, washed with cold ethanol and diethyl ether and dried.

DSC (5 °C min⁻¹, °C): 54 °C (dehydr.), 130 °C (dec.); IR (KBr, cm⁻¹): $\tilde{\nu}$ = 3923 (w), 3644 (m), 3340 (s), 3320 (s), 3212 (s), 2348 (w), 1685 (vs), 1636 (s), 1507 (s), 1457 (m), 1433 (m), 1388 (m), 1330 (s), 1281 (s), 1204 (m), 1182 (m), 1129 (m), 1105 (m), 1057 (m), 998 (m), 979 (m), 954 (m), 888 (m), 861 (m), 772 (w), 755 (w), 741 (w), 654 (m), 640 (m), 608 (m), 556 (m); Raman (1064 nm, 500 mW, 25 °C, cm⁻¹): $\tilde{\nu}$ = 3340 (11), 3295 (14), 3244 (14), 3013 (5), 2970 (15), 1685 (4), 1633 (3), 1561 (2), 1505 (100), 1436 (4), 1394 (4), 1339 (19), 1278 (11), 1107 (9), 1060 (8), 1030 (43), 975 (2), 892 (10), 744 (8), 609 (2), 492 (7), 265 (6); ¹H NMR (DMSO-*d*₆, 25 °C, ppm) δ : 8.55 (s, 3H, CNH), 4.83 (t, ³J = 4.9 Hz, 2H, CH₂ONO₂), 4.45 (s, 6H, NNH₂), 4.41 (t, ³J = 4.9 Hz, 2H, NCH₂); ¹³C NMR (DMSO-*d*₆, 25 °C, ppm) δ : 159.1 (C(NHNH₂)₃), 157.2 (CN₄), 70.3 (CH₂ONO₂), 43.2 (NCH₂); *m/z* (FAB⁺): 105.1 [C(NHNH₂)₃⁺]; *m/z* (FAB⁻): 218.0 [C₃H₄N₇O₅⁻]; Anal. Calc. for EA (C₃H₁₀N₁₀O₂, 218.18): C, 14.86; H, 4.05; N, 56.33. Found: C, 14.21; H, 4.25; N, 53.50%; BAM drophammer: 10 J; friction tester: 96 N; ESD: 0.15 J (at grain size 100–500 μm).

3.8. 1-(2-Nitratoethyl)-5-aminotetrazole (**11**)

1-(2-Nitratoethyl)-5-nitriminotetrazole (2.44 g, 10.3 mmol) was suspended in a few milliliter of warm water. 1,3-Diaminourea (0.93 g, 10.3 mmol) was dissolved in a few milliliters of water and both solutions were combined and stirred for five minutes at room temperature. The product crystallizes directly from the reaction mixture as colorless plates in 72% yield (1.29 g, 7.42 mmol).

DSC (5 °C min⁻¹, °C): 133 °C (m.p.), 163 °C (dec); IR (KBr, cm⁻¹): $\tilde{\nu}$ = 3349 (vs), 3152 (s), 1658 (s), 1633 (vs), 1593 (s), 1491 (w), 1452 (w), 1428 (w), 1384 (w), 1365 (w), 1337 (w), 1297 (m), 1287 (m), 1157 (w), 1115 (m), 1057 (w), 1030 (m), 983 (w), 894 (w), 855 (w), 756 (w), 745 (w), 703 (w), 671 (w), 636 (w), 565 (w); Raman (1064 nm, 500 mW, 25 °C, cm⁻¹): $\tilde{\nu}$ = 3321 (4), 3141 (21), 3033 (25), 3008 (24), 2985 (39), 2962 (100), 2894 (4), 2848 (3), 2769 (3), 1675 (4), 1639 (15), 1591 (17), 1483 (9), 1459 (6), 1430 (13), 1391 (13), 1338 (14), 1298 (28), 1273 (21), 1236 (8), 1143 (10), 1030 (4), 982 (11), 879 (2), 849 (24), 776 (43), 703 (6), 666 (5), 565 (23), 486 (9), 463 (7); ¹H NMR (DMSO-*d*₆, 25 °C, ppm) δ : 6.81 (s, 2H, CNH₂), 4.86 (t, ³J = 4.9 Hz, 2H, CH₂ONO₂), 4.50 (t, ³J = 4.9 Hz, 2H, NCH₂); ¹³C NMR (DMSO-*d*₆, 25 °C, ppm) δ : 152.8 (CN₄), 67.5 (CH₂ONO₂), 39.5 (NCH₂); ¹⁵N NMR (*d*₆-DMSO, 25 °C, ppm) δ : 3.7 (s, N3), -25.3 (s, (ONO₂)), -44.0 (t, N4, ³J = 3.7 Hz), -94.2 (s, N2), -181.6 (s, N1), -337.7 (s, br (NH₂)); *m/z* (DEI⁺): 174.1 [M]⁺; Anal. Calc. for EA (C₃H₆N₆O₃, 174.12): C, 20.69; H, 3.47; N, 48.27. Found: C, 20.63; H, 3.32; N, 48.36%; BAM drophammer: 40 (neg.) J; friction tester: 160 N, ESD: 0.30 J (at grain size 100–500 μm).

Acknowledgments

Financial support of this work by the Ludwig-Maximilian University of Munich (LMU), the US Army Research Laboratory (ARL), the Armament Research, Development and Engineering Center (ARDEC), the Strategic Environmental Research and Development Program (SERDP) and the Office of Naval Research (ONR Global, title: "Synthesis and Characterization of New High Energy Dense Oxidizers (HEDO) – NICOP Effort ") under Contract Nos. W911NF-09-2-0018 (ARL), W911NF-09-1-0120 (ARDEC), W011NF-09-1-0056 (ARDEC) and 10 WPSEED01-002/WP-1765 (SERDP) is gratefully acknowledged. The authors acknowledge collaborations with Dr. Mila Krupka (OZM Research, Czech Republic) in the development of new testing and evaluation methods for energetic materials and with Dr. Muhamed Sucasca (Brodarski Institute, Croatia) in the development of new computational codes to predict the detonation and propulsion parameters of novel explosives. We are indebted to and thank Drs. Betsy M. Rice and Brad Forch (ARL, Aberdeen, Proving Ground, MD) and Mr. Gary Chen (ARDEC, Picatinny Arsenal, NJ) for many helpful and inspired discussions and support of our work. The authors are indebted to and thank Dr. Karina R. Tarantik for the characterization of compound **4**. In addition, Mr. Stefan Huber is thanked for performing the sensitivity tests.

Appendix A. Supplementary data

CCDC 766629, 815404, 815410, 815407, 815405, 815771, 815406, 815409 contains the supplementary crystallographic data for **4**, **5**, **6**, **7**, **8**, **9**, **10**, **11**. These data can be obtained free of charge via <http://www.ccdc.cam.ac.uk/conts/retrieving.html>, or from the Cambridge Crystallographic Data Centre, 12 Union Road, Cambridge CB2 1EZ, UK; fax: (+44) 1223 336 033; or e-mail: deposit@ccdc.cam.ac.uk.

References

- [1] (a) T.M. Klapötke, C.M. Sabaté, J. Stierstorfer, New J. Chem. 33 (2009) 136; (b) T.M. Klapötke, C.M. Sabaté, Dalton Trans. 10 (2009) 1835.
- [2] G. Holl, T.M. Klapötke, K. Polborn, C. Rienäcker, Propellants Explos. Pyrotech. 28 (2003) 153.
- [3] K. Karaghiosoff, T.M. Klapötke, A. Michailovski, H. Nöth, M. Suter, Propellants Explos. Pyrotech. 28 (2003) 1.
- [4] (a) T.M. Klapötke, J. Stierstorfer, Helv. Chim. Acta 90 (2007) 213; (b) T.M. Klapötke, J. Stierstorfer, A.U. Wallek, Chem. Mater. 20 (2008) 4519; (c) S. Berger, K. Karaghiosoff, T.M. Klapötke, P. Mayer, H. Piotrowski, K. Polborn, R.L. Willer, J.J. Weigand, J. Org. Chem. 71 (2006) 1295.
- [5] J. Geith, G. Holl, T.M. Klapötke, J.J. Weigand, Combust. Flame 139 (2004) 358.
- [6] J. Geith, T.M. Klapötke, J.J. Weigand, G. Holl, Propellants Explos. Pyrotech. 29 (2004) 3.
- [7] (a) M. von Denffer, T.M. Klapötke, G. Kramer, G. Spiess, J.M. Welch, G. Heeb, Propellants Explos. Pyrotech. 30 (2005) 191; (b) G. Ma, Z. Zhang, J. Zhang, K. Yu, Thermochim. Acta 423 (2004) 137.
- [8] K. Karaghiosoff, T.M. Klapötke, P. Mayer, C.M. Sabaté, A. Penger, J.M. Welch, Inorg. Chem. 47 (2008) 1007.
- [9] K.O. Christe, W.W. Wilson, M.A. Petrie, H.H. Michels, J.C. Bottaro, R. Gilardi, Inorg. Chem. 35 (1996) 5068.
- [10] (a) T.M. Klapötke, J. Stierstorfer, Phys. Chem. Chem. Phys. 10 (2008) 4340; (b) T.M. Klapötke, J. Stierstorfer, Eur. J. Inorg. Chem. 26 (2008) 4055.
- [11] E. Lieber, E. Sherman, R.A. Henry, J. Cohen, J. Am. Chem. Soc. 73 (1951) 2327.
- [12] J.A. Garrison, R.M. Herbst, J. Org. Chem. 22 (1957) 278.
- [13] R.A. Henry, W.G. Finnegan, J. Am. Chem. Soc. 76 (1954) 923.
- [14] N. Fischer, T.M. Klapötke, J. Stierstorfer, K.R. Tarantik, New trends in research of energetic materials, in: Proceedings of the Seminar, 13th, Pardubice, Czech Republic, vol. 2, 2010, pp. 455–467.
- [15] T.M. Klapötke, J. Stierstorfer, K.R. Tarantik, Chem. Eur. J. 15 (2009) 5775.
- [16] CrysAlisPro Oxford Diffraction Ltd., Version 171.33.41, 2009.
- [17] A. Altomare, G. Cascarano, C. Giacovazzo, A. Guagliardi, J. Appl. Cryst. 26 (1993) 343.
- [18] G.M. Sheldrick, SHELXS-97, Program for Crystal Structure Solution, Universität Göttingen, Germany, 1997.
- [19] G.M. Sheldrick, SHELXL-97, Program for the Refinement of Crystal Structures, University of Göttingen, Germany, 1997.
- [20] A.L. Spek, PLATON, A Multipurpose Crystallographic Tool, Utrecht University, Utrecht, The Netherlands, 1999.

- [21] L.J. Farrugia, *J. Appl. Cryst.* 32 (1999) 837.
- [22] SCALE3 ABSPACK – An Oxford Diffraction program (1.0.4.gui:1.0.3) (C). Oxford Diffraction Ltd., 2005.
- [23] J. Bernstein, R.E. Davis, L. Shimon, N.-L. Chang, *Angew. Chem. Int. Ed.* 34 (1995) 1555.
- [24] M.J. Frisch, G.W. Trucks, H.B. Schlegel, G.E. Scuseria, M.A. Robb, J.R. Cheeseman, G. Scalmani, V. Barone, B. Mennucci, G.A. Petersson, H. Nakatsuji, M. Caricato, X. Li, H.P. Hratchian, A.F. Izmaylov, J. Bloino, G. Zheng, J.L. Sonnenberg, M. Hada, M. Ehara, K. Toyota, R. Fukuda, J. Hasegawa, M. Ishida, T. Nakajima, Y. Honda, O. Kitao, H. Nakai, T. Vreven, J.A. Montgomery Jr., J.E. Peralta, F. Ogliaro, M. Bearpark, J.J. Heyd, E. Brothers, K.N. Kudin, V.N. Staroverov, R. Kobayashi, J. Normand, K. Raghavachari, A. Rendell, J.C. Burant, S.S. Iyengar, J. Tomasi, M. Cossi, N. Rega, J.M. Millam, M. Klene, J.E. Knox, J.B. Cross, V. Bakken, C. Adamo, J. Jaramillo, R. Gomperts, R.E. Stratmann, O. Yazyev, A.J. Austin, R. Cammi, C. Pomelli, J.W. Ochterski, R.L. Martin, K. Morokuma, V.G. Zakrzewski, G.A. Voth, P. Salvador, J.J. Dannenberg, S. Dapprich, A.D. Daniels, Ö. Farkas, J.B. Foresman, J.V. Ortiz, J. Cioslowski, D.J. Fox, *GAUSSIAN 09*, Revision A.1, Gaussian, Inc., Wallingford CT, 2009.
- [25] NATO Standardization Agreement (STANAG) on Explosives, Impact Sensitivity Tests, No. 4489, 1st ed., Sept. 17, 1999.
- [26] WIWEB-Standardarbeitsanweisung 4-5.1.02, Ermittlung der Explosionsgefahrlichkeit, hier der Schlagempfindlichkeit mit dem Fallhammer, Nov. 8, 2002.
- [27] (a) <http://www.bam.de>;
(b) www.reichel&partner.de.
- [28] NATO Standardization Agreement (STANAG) on Explosive, Friction Sensitivity Tests, No. 4487, 1st ed., Aug. 22, 2002.
- [29] WIWEB-Standardarbeitsanweisung 4-5.1.03, Ermittlung der Explosionsgefahrlichkeit oder der Reibeempfindlichkeit mit dem Reibeapparat, Nov. 8, 2002.
- [30] Impact: insensitive >40 J, less sensitive >35 J, sensitive >4 J, very sensitive <3 J. Friction: insensitive >360 N, less sensitive = 360 N, sensitive >80 N, very sensitive >10 N, extremely sensitive <10 N. According to the UN Recommendations on the Transport of Dangerous Goods, (+) indicates not safe for transport.
- [31] <http://www.ozm.cz>.
- [32] <http://www.linseis.com>.
- [33] (a) J.W. Ochterski, G.A. Petersson, J.A. Montgomery Jr., *J. Chem. Phys.* 104 (1996) 2598;
(b) J.A. Montgomery Jr., M.J. Frisch, J.W. Ochterski, G.A. Petersson, *J. Chem. Phys.* 112 (2000) 6532.
- [34] (a) L.A. Curtiss, K. Raghavachari, P.C. Redfern, J.A. Pople, *J. Chem. Phys.* 106 (1997) 1063;
(b) E.F.C. Byrd, B.M. Rice, *J. Phys. Chem. A* 110 (2006) 1005;
(c) B.M. Rice, S.V. Pai, J. Hare, *Combust. Flame* 118 (1999) 445.
- [35] T. Altenburg, T.M. Klapötke, A. Penger, J. Stierstorfer, *Z. Anorg. Allg. Chem.* 636 (2010) 463.
- [36] (a) M.S. Westwell, M.S. Searle, D.J. Wales, D.H. Williams, *J. Am. Chem. Soc.* 117 (1995) 5013;
(b) F. Trouton, *Philos. Mag.* 18 (1884) 54.
- [37] (a) H.D.B. Jenkins, H.K. Roobottom, J. Passmore, L. Glasser, *Inorg. Chem.* 38 (1999) 3609;
(b) H.D.B. Jenkins, D. Tudela, L. Glasser, *Inorg. Chem.* 41 (2002) 2364.
- [38] M. Sućeska, *EXPLO5.4* program, Zagreb, Croatia, 2010.
- [39] M. Sućeska, *Propellants Explos. Pyrotech.* 16 (1991) 197.
- [40] (a) M. Sućeska, *Mater. Sci. Forum* 465–466 (2004) 325;
(b) M. Sućeska, *Propellants Explos. Pyrotech.* 24 (1999) 280;
(c) M.L. Hobbs, M.R. Baer, in: *Proceedings of the 10th Symp. (International) on Detonation*, ONR 33395-12, Boston, MA, July 12–16, 1993, pp. 409.

The hydroxylammonium cation in tetrazole based energetic materials

Niko Fischer, Thomas M. Klapötke and Jörg Stierstorfer

Energetic Materials Research, Department of Chemistry,
University of Munich (LMU), Butenandtstr. 5-13, D-81377, Germany

finch@cup.uni-muenchen.de

Abstract:

Due to its basicity, hydroxylamine was used to deprotonate several tetrazole derivatives bearing an acidic proton. Namely, the monodeprotonated 5-nitriminotetrazolate (1), dideprotonated 5-nitriminotetrazolate (2), 1-methyl-5-nitriminotetrazolate (3) and 2-methyl-5-nitraminotetrazolate salt (4) were synthesized. In the series of ethyl substituted 5-nitriminotetrazolates, the 1-hydroxyethyl-5-nitriminotetrazolate (5) and the 1-nitratoethyl-5-nitriminotetrazolate (6) could be isolated. Further, the monodeprotonated (7) and dideprotonated bistetrazolylamine salt (8), a cocrystallization product of (7) with one equivalent of bistetrazolylamine (9) as well as the 5H-tetrazolate (10) and the tetrazole-5-carboxamide salt (11) were synthesized. Additionally the azo-compounds dihydroxylammonium 5,5'-azotetrazolate (12) and the dihydroxylammonium salt of its oxide (13) besides a bistetrazole derivative, the bis-deprotonated 5,5-bistetrazolate (14) and a tetrazole amide oxime (15) were successfully synthesized. All compounds except from 4, 7 and 15 were fully characterized by single crystal X-ray diffraction. Additionally, 1 - 15 were characterized using vibrational spectroscopy (IR and Raman), multinuclear NMR spectroscopy, elemental analysis and DSC measurements. The heats of formation of 1 - 15 were calculated using the atomization method based on CBS-4M enthalpies. With these values and the experimental (X-ray) densities several detonation parameters such as the detonation pressure, velocity, energy and temperature were computed using the EXPLO5 code. In addition, the sensitivities towards impact, friction and electrical discharge were tested using the BAM drophammer, friction tester as well as a small scale electrical discharge device.

Keywords: Hydroxylamine; Energetic Materials; Crystal Structures; Detonation Parameters; Sensitivities

1 Introduction

The design of new energetic materials encompassing all of propellants, explosives, and pyrotechnics is a modern academic and technological challenge.[1] Intense research is focused on the tailoring of new energetic molecules with performances and stability similar to that of RDX (cyclotrimethylenetrinitramine) to replace this widely-used high explosive. For a novel energetic molecule to find practical application as a high explosive it needs to possess high thermal and mechanical stabilities, while at the same time satisfying the increasing demand for higher performing (high detonation velocity, pressure and heat of explosion) materials.[2]

One of the most promising energetic backbones for the tailoring of energetic molecules is the tetrazole ring; the carbon on position 5 of the ring allows the facile attachment of various substituents for energetic tailorability, and the high nitrogen content of the heterocycle leads to high energetic performances.[3] It can be stated that the tetrazole heterocycle occupies the

“middle ground” of the stability vs high performance continuum, where highly stable compounds can be poorly-performing energetics and highly energetic compounds are often unstable. This trend is exemplified in the range of 5-membered azoles from pyrazole to pentazole, where pyrazoles are not used in energetics due to low performance, and the few pentazole derivatives known are highly unstable.[4]

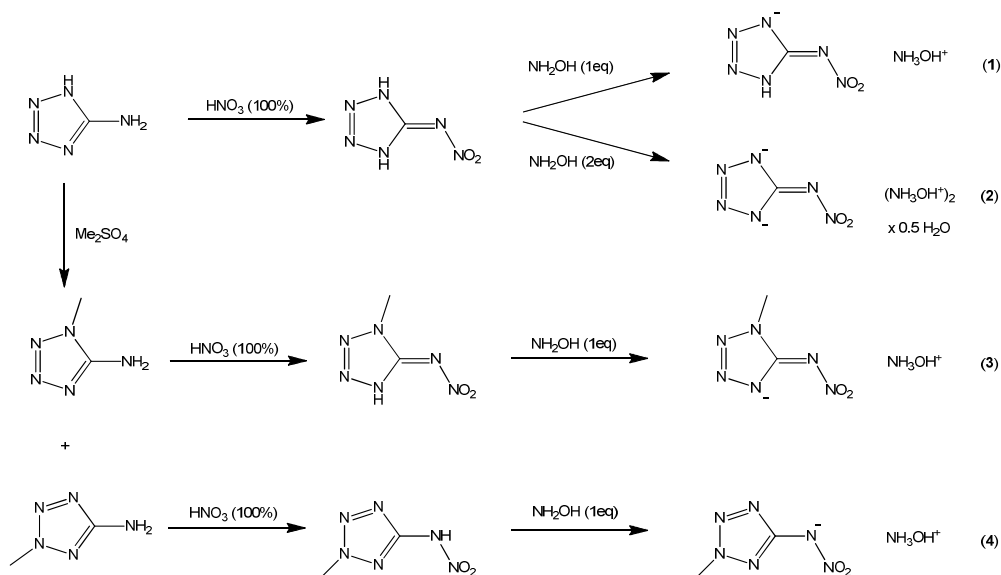
Of the energetic tetrazoles known, nitriminotetrazoles are some of the most promising for practical use as they have some of the highest performances and thermal stabilities. By tailoring substituents and counter-ions, nitriminotetrazoles have been shown to illustrate the entire spectrum of sensitivity from insensitive secondary to sensitive primary explosives,[5,6] while maintaining high thermal stability. High thermal stabilities arise from the aromatic nature of the tetrazole ring, while the high performances arise from the high heats of formation of nitriminotetrazoles, the ring strain of the 5-membered ring, and good oxygen balances.[7]

The oxygen balance is a percentage representation of a compound's ability to oxidize all carbon and hydrogen in the molecule to carbon dioxide and water respectively. When an oxygen balance is at or near zero, explosive performances are high, however deviation into either a negative (fuel rich) or positive (oxygen rich) oxygen balance leads to a loss of performance. For an energetic material containing only CHNO the oxygen balance is easily calculated by the equation $\Omega (\%) = (wO - 2xC - 1/2yH) \cdot 1600/M$ (w : number of oxygen atoms, x : number of carbon atoms, y : number of hydrogen atoms, z : number of sulfur atoms). Unfortunately, while nitriminotetrazole itself has an only slightly negative oxygen balance and as such a high performance, when nitriminotetrazoles are deprotonated forming stable, nitrogen rich, salts of more negative oxygen balances, performances are lost relative to the neutral, acidic, nitriminotetrazole. Our recent efforts pairing nitriminotetrazolate anions with the oxygen-containing diaminouronium cation [8] illustrated the improvement in performances seen when oxygen balances are improved. In our quest for ever higher performances while maintaining thermal stability, we have paired several 5-nitriminotetrazoles (5-nitriminotetrazole, 1-methyl-5-nitriminotetrazole, 2-methyl-5-nitraminotetrazole) and also differently 5-substituted tetrazoles with the hydroxylammonium cation, the synthesis and characterization of which we describe in the following.

2 Results and Discussion

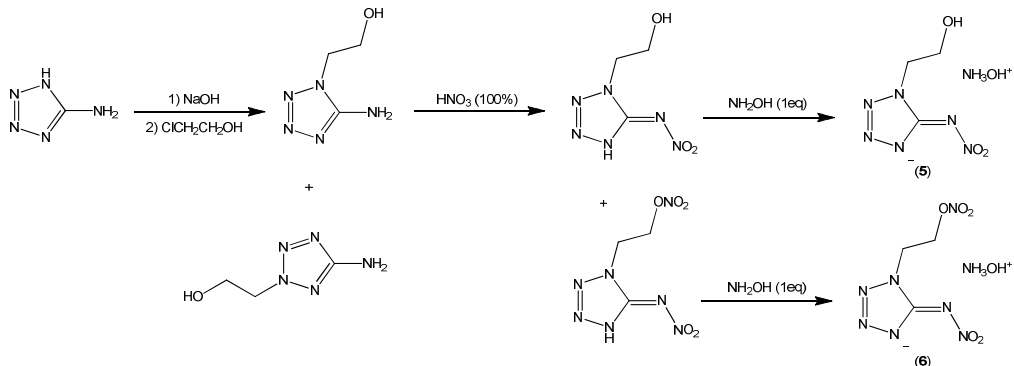
2.1 Synthesis

Several hydroxylammonium tetrazolates were synthesized either from the neutral compounds and an aqueous solution of hydroxylamine or via metathesis reaction using the respective barium salts and hydroxylammonium sulfate. The synthesis of the 5-nitriminotetrazolates **1–4** was achieved using the neutral compounds, which have been deprotonated with an 50% (w/w) aqueous solution of hydroxylamine and is described in Scheme 1. The starting materials 5-nitriminotetrazole as well as the methylated sister compounds 1-methyl-5-nitriminotetrazole and 2-methyl-5-nitraminotetrazole were synthesized according to literature.[9]



Scheme 1. Synthetic routes to the 5-nitriminotetrazolates **1–4**.

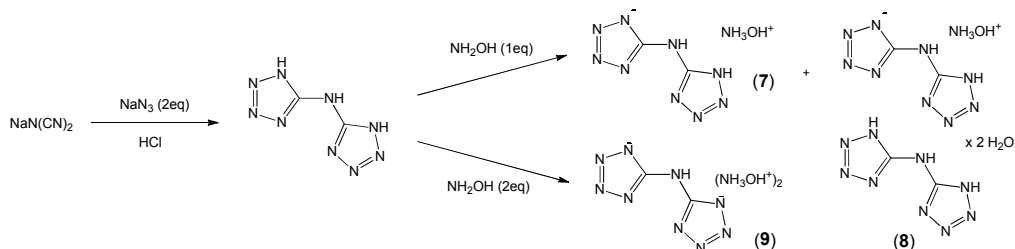
When the sodium salt of 5-aminotetrazole is reacted with 2-chloroethanol, a mixture of 1- and 2-substituted hydroxyethyl-5-aminotetrazoles is obtained.[10] The 1-isomer thereof can be separated by recrystallization from ethanol and further processed by nitration with fuming nitric acid. Depending on the amount of nitric acid used for this reaction two different nitration products are obtained, which is the 1-hydroxyethyl-5-nitriminotetrazole as well as the fully nitrated 1-nitratoethyl-5-nitriminotetrazole.[11] Both compounds bear an acidic proton, which can be abstracted by the addition of aqueous hydroxylamine resulting in the two hydroxylammonium salts **5** and **6**. Their complete synthesis is shown in Scheme 2.



Scheme 2. Full synthesis of the hydroxylammonium 5-nitriminotetrazolates **5** and **6**.

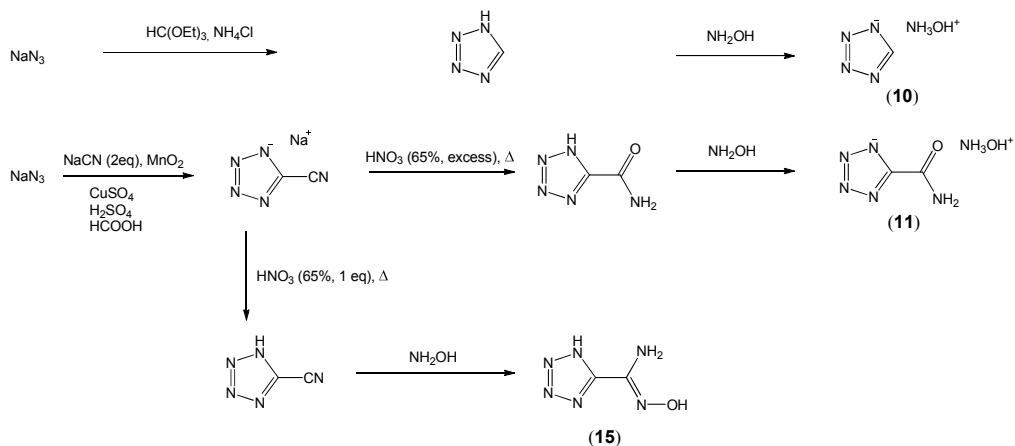
Since the performance data of energetic materials strongly depend on the density of the respective compound, also the synthesis of hydroxylammonium salts of acids, which contain a however-connected bistetrazole unit, was taken into account. Therefore the mono- as well as the bis-deprotonated bistetrazoleamine salt was synthesized starting from bistetrazolamine, which was prepared according to literature.[12] Again the substrate was deprotonated using a

50% (w/w) aqueous solution of hydroxylamine. During the repeated synthesis of the monodeprotonated salt **7** using one equivalent of hydroxylamine, the crystallization of the bisdeprotonated salt **8** was observed first, followed by the crystallization of monodeprotonated **7** which in the crystal structure is accompanied by one equivalent of uncharged bistetrazoleamine. This cocrystallization product **9** was isolated in only minor yields and crystallizes as a dihydrate. Scheme 3 shows the synthetic routes to **7–9** starting from sodium dicyanamide, sodium azide and hydroxylamine.



Scheme 3. Synthesis of the hydroxylammonium salts **7–9**.

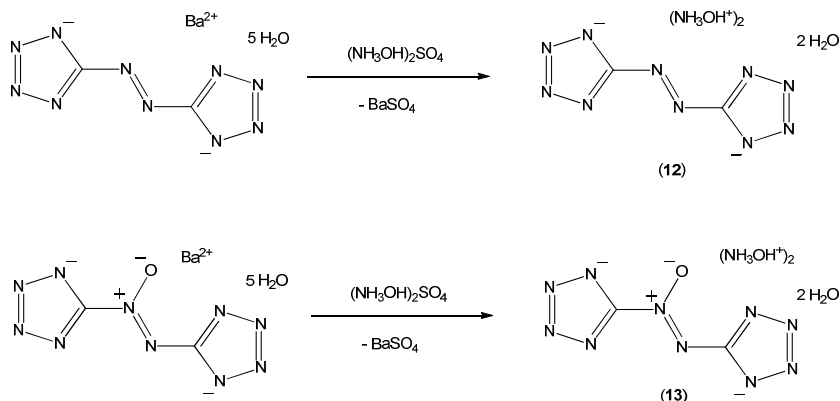
Further tetrazolate salts, which have been synthesized are the *5H*-tetrazolate (**10**) and the tetrazole-5-carboxamide (**11**) (Scheme 4). We have also attempted to synthesize the hydroxylammonium 5-cyanotetrazolate ending in a totally different reaction product which was detected by mass spectrometry as well as NMR spectroscopy and elemental analysis and could be isolated in high yields, namely the tetrazole-5-carboxamide-oxime (**15**).



Scheme 4. Synthesis of the salts **10** and **11** as well as tetrazole-5-carboxamide-oxime (**15**).

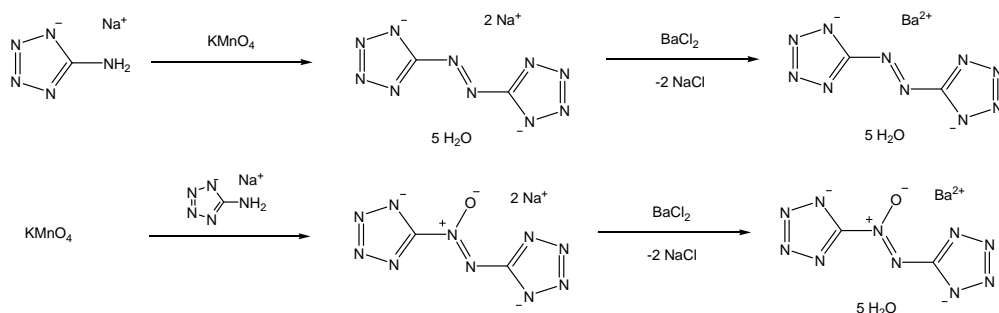
Coming back to the synthesis of anions containing two tetrazole moieties, two important classes of substances of great importance are still missing, which are 5,5'-azotetrazolates and 5,5'-bistetrazolates. Since 5,5'-azotetrazole and its oxidation product 5,5'-azotetrazole-oxide do not exist as free acids, a different route for the synthesis of their hydroxylammonium salts had to be chosen, which is the metathesis reaction starting from their Ba-salts and using hydroxylammonium sulfate as a reagent whereas the very poor solubility of BaSO₄ in aqueous

media is utilized. The synthesis of dihydroxylammonium 5,5'-azotetrazolate (**12**) and dihydroxylammonium diazo-1,2-ditetrizol-5-yl-1-oxide (**13**) is depicted in Scheme 5.



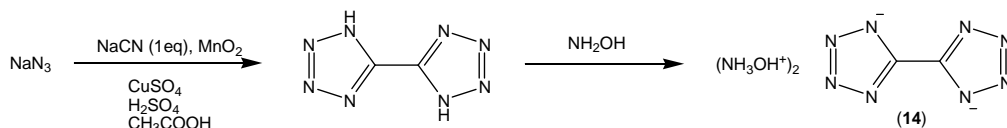
Scheme 5. Synthetic routes to **12** and **13**.

The synthesis of the respective starting materials for **12** and **13** can both be gained from the same precursors in a reaction, that has already been described by Liebig in 1892.[13] Doing the oxidation of 5-aminotetrazole in a reverse order by adding sodium 5-aminotetrazolate to a solution containing excess potassium permanganate results in the formation of the sodium salt of diazo-1,2-ditetrizol-5-yl-1-oxide.[14] Both barium salts are readily available from the respective sodium salts by the addition of barium chloride, which causes the barium salts to precipitate.[15] Scheme 6 shows the synthesis of the precursor molecules for **12** and **13**, which are the barium salts of 5,5'-azotetrazolate and its oxide.



Scheme 6. Synthesis of the precursors for **12** and **13**.

One further promising candidate for a precursor in the synthesis of ionic energetic materials is 5,5'-bistetrazole, which bears two acidic protons. The synthesis of 5,5'-bistetrazole and its dihydroxylammonium salt had already been described by Hiskey *et al.* in 1999 [16] (Scheme 7), however giving only elemental analysis as evidence. We were able to determine the crystal structure of the compound and calculate its performance data with its theoretical maximum density.



Scheme 7. Synthesis of 5,5'-bistetrazole and following deprotonation.

2.2 Crystal Structures

Suitable single crystals of all of the described compounds were picked from the crystallization mixture and mounted in Kel-F oil, transferred to the N₂ stream of an Oxford Xcalibur3 diffractometer with a Spellman generator (voltage 50 kV, current 40 mA) and a KappaCCD detector. The data collection was performed using the CRYSLIS CCD software [17], the data reduction using the CRYSLIS RED software [18]. The structures were solved with SIR-92 [19] and SHELXS-97 [20] refined with SHELXL-97 [21] and finally checked using the PLATON software [22] integrated in the WINGX software suite.[23] The non-hydrogen atoms were refined anisotropically and the hydrogen atoms were located and freely refined. The absorptions were corrected by a SCALE3 ABSPACK multi-scan method.[24]

Hydroxylammonium 5-nitrimino-1*H*-tetrazolate (**1**) crystallizes in the monoclinic space group *P*2₁/*c* with four anion/cation pairs in the unit cell. The asymmetric unit is depicted in Figure 1. Its density of 1.785 g cm⁻³ is quite high in comparison with other tetrazolate salts in literature.[25,26] The hydroxylammonium cations in both structures show equal bond lengths and angles found in literature, e.g. hydroxylammonium perchlorate [27], and hydroxylammonium dinitramide [28]. Latter one is an interesting structure because it contains next to the hydroxylammonium cation the neutral and zwitterionic hydroxylamine moieties.

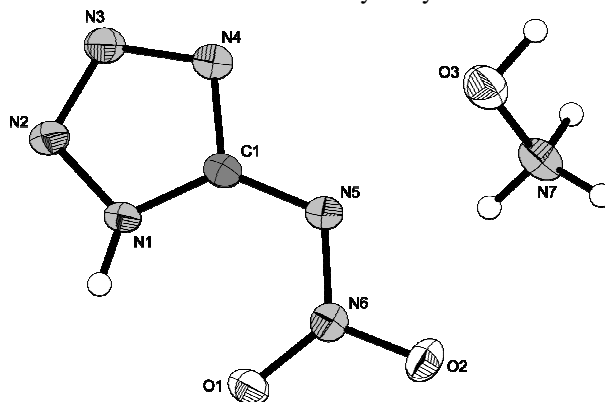


Figure 1. Molecular unit of hydroxylammonium 5-nitriminotetrazolate (**1**). Ellipsoids of non-hydrogen atoms are drawn at the 50 % probability level. Selected bond lengths (Å): O1–N6 1.2493(14), O2–N6 1.2661(14), N1–C1 1.3395(17), N1–N2 1.3436(15), N2–N3 1.2939(17), N3–N4 1.3502(16), N4–C1 1.3342(19), N5–N6 1.3174(17), N5–C1 1.3657(17), O3–N7 1.4145(17); selected bond angles (°): C1–N1–N2 108.95(12), N3–N2–N1 106.47(11), N2–N3–N4 110.92(11), C1–N4–N3 106.12(11), N6–N5–C1 115.88(11), O1–N6–O2 120.47(11), O1–N6–N5 124.70(11), O2–N6–N5 114.82(11), N4–C1–N1 107.55(12), N4–C1–N5 119.74(12), N1–C1–N5 132.69(13).

Compound **1** crystallizes layer-like along the *b*-axis (Figure 2A). The packing is stabilized by several inter- and intramolecular hydrogen bridges within the layers (forming strands) on the one hand. On the other hand, the hydroxylammonium cations act as linkers between two layers by forming strong hydrogen bonds.

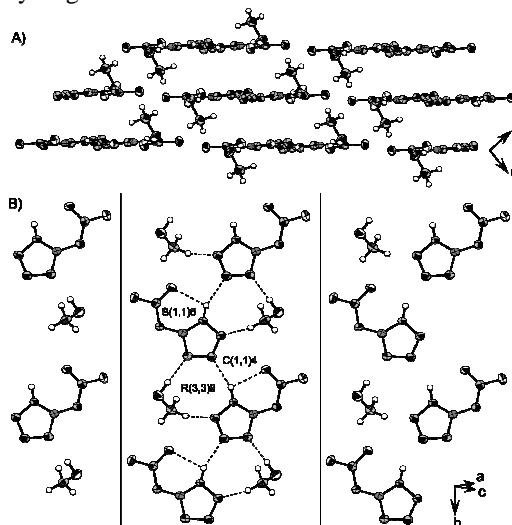


Figure 2. A) View along the *b* axes. B) View on the layers in the structure of **1**. Selected graph sets [29] are drawn.

The dideprotonated salt bis(hydroxylammonium) 5-nitriminotetrazolate (**2**) could only be obtained crystalline as its semihydrate. Compound **2** crystallizes in the monoclinic space group *P2₁/n* with four cation/anion pairs as well as two water molecules in the unit cell. Its density of 1.771 g cm^{-3} is only slightly lower than that of **1**. The structure of the dianion is almost planar, which is in accordance to previously published structures e.g. diammonium 5-nitriminotetrazolate.[30] The molecular unit is depicted in Figure 3.

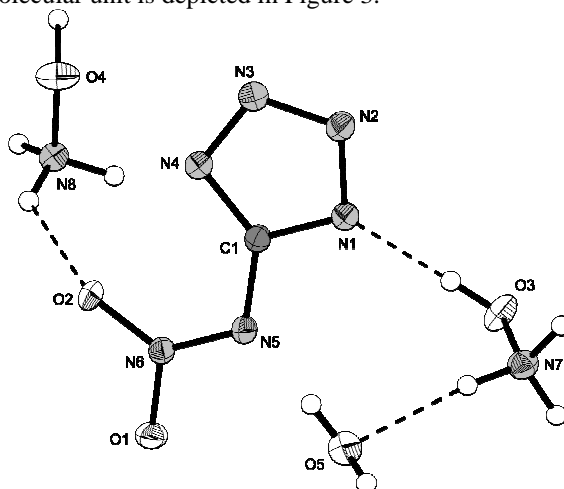


Figure 3. Molecular unit of bis(hydroxylammonium) 5-nitriminotetrazolate monohydrate (**2**). Ellipsoids of non-hydrogen atoms are drawn at the 50 % probability level. Selected bond lengths (Å): N4–C1 1.3381(16), N4–N3 1.3463(15), O2–N6 1.2667(13), O3–N7 1.4101(14), O1–N6 1.2929(13), N1–

N2 1.3368(15), N1–C1 1.3412(16), O4–N8 1.4137(14), N5–N6 1.2873(15), N5–C1 1.3979(16), N2–N3 1.3092(15); selected bond angles ($^{\circ}$): C1–N4–N3 104.30(10), N2–N1–C1 105.70(10), N6–N5–C1 117.49(10), N3–N2–N1 108.67(10), O2–N6–N5 125.54(10), O2–N6–O1 118.22(9), N5–N6–O1 116.23(10), N2–N3–N4 110.41(10), N4–C1–N1 110.91(11), N4–C1–N5 132.35(11), N1–C1–N5 116.74(10).

The packing of **2** is dominated by many strong hydrogen bonds. Exemplarily, the coordination of the crystal water is shown in Figure 4. The water molecules form a tetrahedral coordination sphere, connecting two nitriminotetrazolate anions via the N5 nitrogen atoms.

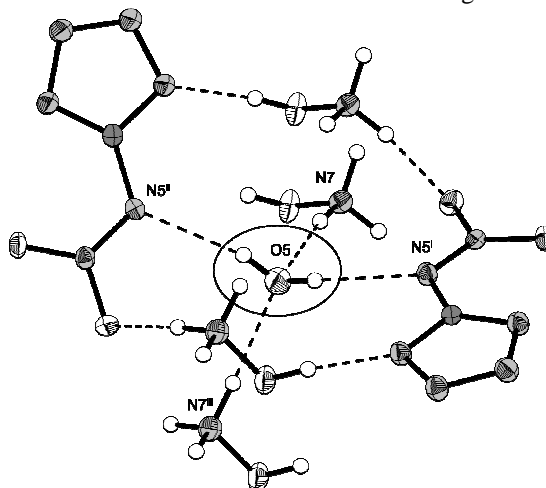


Figure 4: Hydrogen bonds of the crystal water. Symmetry codes: (i) 2.5-x, 1+y, 1.5-z; (ii) -1+x, 1+y, z; (iii) 2.5-x, y, 1.5-z.

Hydroxylammonium 1-methyl-5-nitriminotetrazolate (**3**) crystallizes in the orthorhombic space group *Pbca* with eight anion/cation pairs in the unit cell. The asymmetric unit is shown in Figure 5. Its density of 1.627 g cm⁻³ is significantly lower than that of **3**. Again a strong hydrogen bond network is formed, which is depicted in Figure 6.

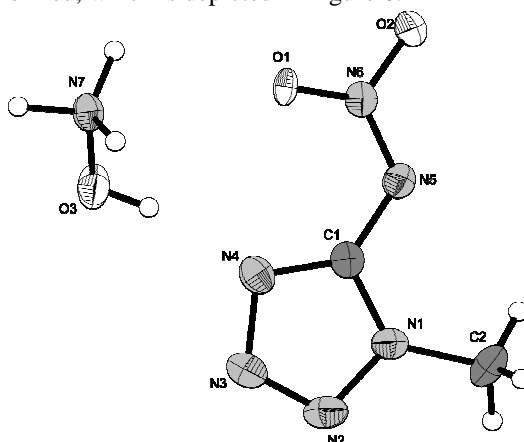


Figure 5. Molecular unit of hydroxylammonium 1-methyl-5-nitriminotetrazolate (**3**). Ellipsoids of non-hydrogen atoms are drawn at the 50 % probability level. Selected bond lengths (\AA): O1–N6 1.234(3), O2–N6 1.279(3), N1–C1 1.335(4), N1–N2 1.352(4), N1–C2 1.466(4), N2–N3 1.288(4), N3–

N4 1.361(4), N4–C1 1.334(4), N5–N6 1.308(3), N5–C1 1.375(4), N7–O3 1.407(3); selected bond angles (°): C1–N1–C2 129.4(3), N2–N1–C2 121.8(3), N3–N2–N1 106.4(2), N2–N3–N4 111.1(3), C1–N4–N3 105.6(3), N6–N5–C1 117.2(3), O1–N6–O2 120.3(3), O1–N6–N5 125.9(2), O2–N6–N5 113.8(2), N4–C1–N1 108.1(3), N4–C1–N5 133.7(3), N1–C1–N5 118.0(3).

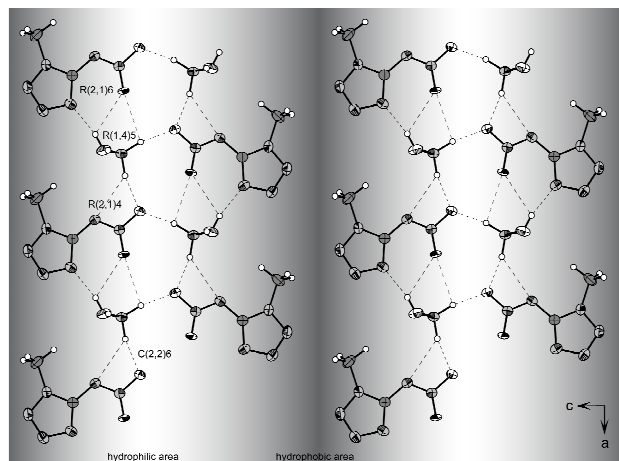


Figure 6. View on the layers in the structure of **3**. Light regions represent hydrophilic parts, dark regions hydrophobic parts.

Hydroxylammonium 1-(2-hydroxyethyl)-5-nitriminotetrazolate (**5**) and hydroxylammonium 1-(2-nitratoethyl)-5-nitriminotetrazolate (**6**), shown in Figure 7 and 8, both crystallize monoclinic (**5**: $P2_1/n$, **6**: $C2/c$). Although showing a similar structure and comparable bond geometries a large difference in the density is observed (**5**: 1.614 g cm^{-3} , **6**: 1.796 g cm^{-3}).

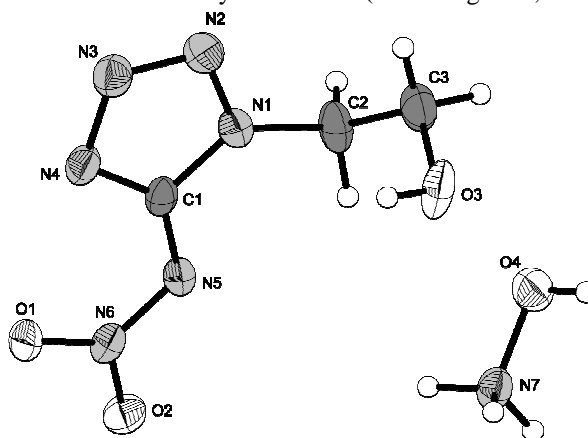


Figure 7. Molecular unit of hydroxylammonium 1-(2-hydroxyethyl)-5-nitriminotetrazolate (**5**). Ellipsoids of non-hydrogen atoms are drawn at the 50 % probability level. Selected bond lengths (Å): O1–N6 1.2612(18), O2–N6 1.260(2), O3–C3 1.396(3), N1–N2 1.345(2), N1–C1 1.351(2), N1–C2 1.468(2), N2–N3 1.297(2), N3–N4 1.366(2), N4–C1 1.336(2), N5–N6 1.308(2), N5–C1 1.365(2), C2–C3 1.506(3), O4–N7 1.413(2); selected bond angles (°): N2–N1–C1 109.07(15), N2–N1–C2 121.71(18), C1–N1–C2 129.18(18), N3–N2–N1 106.06(16), N2–N3–N4 111.69(16), C1–N4–N3 105.15(16), N6–N5–C1 117.31(15), O2–N6–O1 119.41(16), O2–N6–N5 116.00(15), O1–N6–N5 124.60(16), N4–C1–N1 108.01(17), N4–C1–N5 134.59(18), N1–C1–N5 117.38(16), N1–C2–C3 113.3(2), O3–C3–C2 113.4(2).

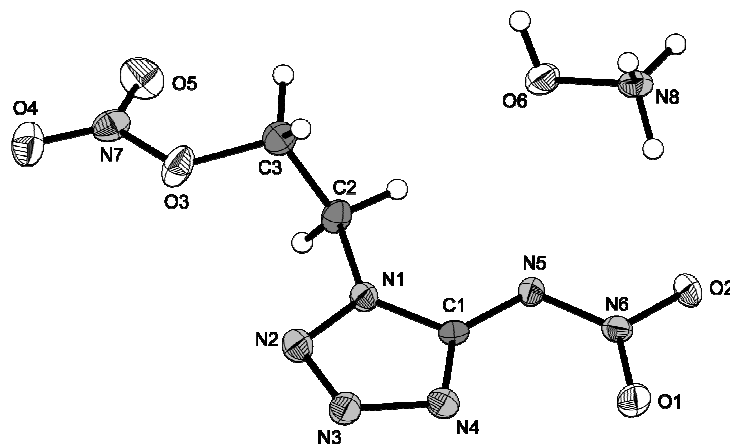


Figure 8. Molecular unit of hydroxylammonium 1-(2-nitratoethyl)-5-nitriminotetrazolate (**6**). Ellipsoids of non-hydrogen atoms are drawn at the 50 % probability level. Selected bond lengths (Å): O1–N6 1.2658(15), O2–N6 1.2666(15), O6–N8 1.4115(17), O3–N7 1.4042(16), O3–C3 1.4543(19), O4–N7 1.1997(16), O5–N7 1.2043(17), N6–N5 1.3034(16), N5–C1 1.3635(19), N1–N2 1.3376(17), N1–C1 1.3589(19), N1–C2 1.4664(19), N4–C1 1.3392(19), N4–N3 1.3615(17), N3–N2 1.2983(18), C2–C3 1.503(2); selected bond angles (°): N7–O3–C3 115.40(12), O1–N6–O2 119.25(11), O1–N6–N5 124.66(12), O2–N6–N5 116.09(11), N6–N5–C1 117.41(12), N2–N1–C1 108.76(12), N2–N1–C2 121.66(12), C1–N1–C2 129.53(13), O4–N7–O5 128.81(14), O4–N7–O3 112.55(12), O5–N7–O3 118.64(13), C1–N4–N3 105.02(12), N2–N3–N4 111.78(12), N3–N2–N1 106.46(11), N1–C2–C3 112.30(13), N4–C1–N1 107.98(13), N4–C1–N5 134.97(14), N1–C1–N5 117.04(13), O3–C3–C2 112.20(13).

Both structures containing the bis(tetrazolyl)amine (BTA) [12] moiety crystallize (**8**: $C2/c$, **9**: $P2_1/c$). The double deprotonated salt, depicted in Figure 9, could be obtained crystalline without inclusion of crystal water resulting in density of 1.733 g cm^{-3} . The BTA dianion is found to be nearly planar and comparable to structures found in the literature, e.g. in the diamine copper(II) complex.[31]

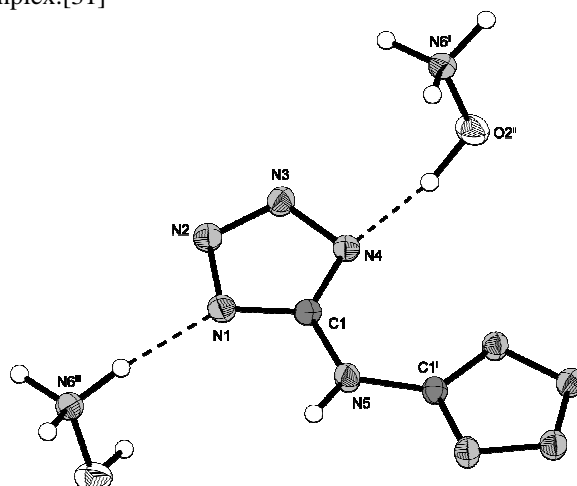


Figure 9. Molecular unit of bis(hydroxylammonium) 5,5'-bis(tetrazolyl)amine (**8**). Ellipsoids of non-hydrogen atoms are drawn at the 50 % probability level. Symmetry codes: (i) $-x, y, 1.5-z$, (ii) $x, 1-y, 0.5+z$, (iii) $x, -1+y, z$. Selected bond lengths (Å): N5–C1 1.380(2), N5–C1 1.380(2), N3–N2 1.303(2), N3–N4 1.362(2), N4–C1 1.325(3), N2–N1 1.352(2), N1–C1 1.339(2), O2–N6 1.420(2); se-

lected bond angles ($^{\circ}$): C1–N5–C1¹ 125.7(3), N2–N3–N4 109.50(16), C1–N4–N3 104.04(16), N3–N2–N1 109.86(16), C1–N1–N2 103.97(17), N4–C1–N1 112.63(18), N4–C1–N5 126.2(2), N1–C1–N5 121.2(2).

The monodeprotonated species (Figure 10) could only be obtained crystalline as cocrystallization product with neutral H₂BTA. The neutral BTA follows the structure described for the monohydrate in the literature.[12]

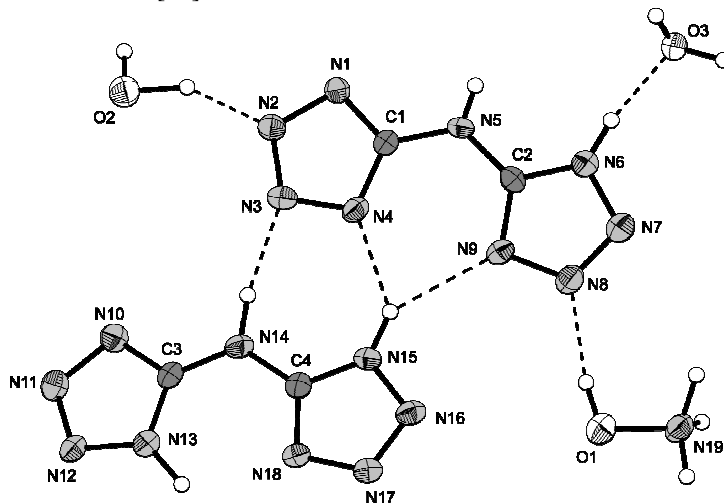


Figure 10. Molecular unit of the cocrystallization product **9**. Ellipsoids of non-hydrogen atoms are drawn at the 50 % probability level. Selected bond lengths (\AA): N13–C3 1.344(3), N13–N12 1.356(3), N1–C1 1.330(3), N1–N2 1.353(3), N5–C2 1.355(3), N5–C1 1.383(3), N15–C4 1.334(3), N15–N16 1.349(3), N14–C3 1.350(3), N14–C4 1.364(3), C3–N10 1.325(3), N4–C1 1.330(3), N4–N3 1.355(3), N9–C2 1.330(3), N9–N8 1.371(3), N6–C2 1.337(3), N6–N7 1.346(3), N11–N12 1.298(3), N11–N10 1.364(3), N17–N16 1.300(3), N17–N18 1.365(3), N2–N3 1.309(2), N18–C4 1.323(3), N7–N8 1.297(3), O1–N19 1.414(3).

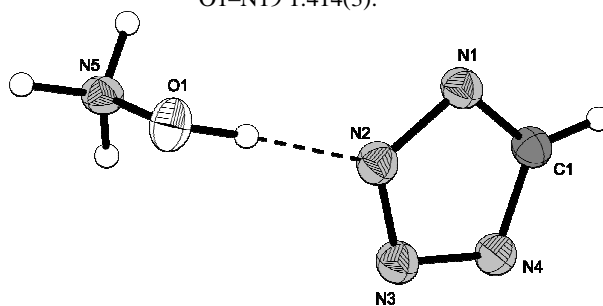


Figure 11. Molecular unit of hydroxylammonium 5*H*-tetrazolate (**10**). Ellipsoids of non-hydrogen atoms are drawn at the 50 % probability level. Selected bond lengths (\AA): O1–N5 1.4223(17), N3–N2 1.3063(15), N3–N4 1.3390(15), N1–C1 1.3239(19), N1–N2 1.3465(16), N4–C1 1.3269(18); selected bond angles ($^{\circ}$): N2–N3–N4 109.14(11), C1–N1–N2 104.12(11), N3–N2–N1 109.75(11), C1–N4–N3 104.77(11), N1–C1–N4 112.21(13).

The molecular moiety of hydroxylammonium 5*H*-tetrazolate (**10**), which crystallizes in the monoclinic space group $P2_1/c$ and a density of 1.557 g cm^{-3} is depicted in Figure 11. The structure of the tetrazolate anion is in agreement to those determined for alkali 5*H*-tetrazolates in the

literature.^[32] The structure of **10** is strongly influenced by several strong classical hydrogen bonds, but also by the weak non-classical $\text{CH}\cdots\text{O}$ hydrogen bond shown in Figure 12.

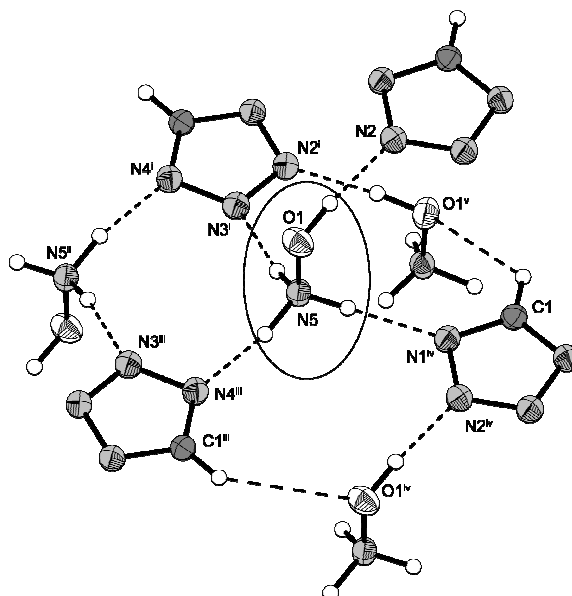


Figure 12: Hydrogen bonding in the structure of **10**. One hydroxylammoniumcation is highlighted. Symmetrie codes: (i) $x, 0.5-y, 0.5+z$, (ii) $1-x, 1-y, 1-z$, (iii) $1-x, 0.5+y, 0.5-z$, (iv) $1+x, y, z$, (v) $x, 0.5-y, 0.5+z$, (vi)

In agreement to the latter discussed structure, also 5-carboxamido-tetrazolate (**11**) crystallizes in the space group $P2_1/c$, illustrated in Figure 13. The anion is planar with common bond lengths for carboxyamido functionalities and consistent with its potassium salt described in the literature.[33]

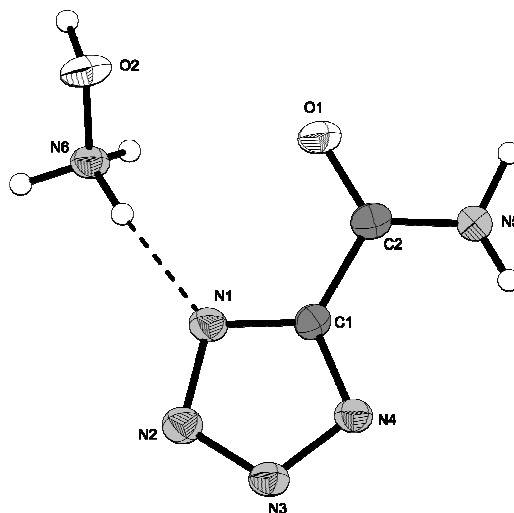


Figure 13. Molecular unit of hydroxylammonium 5-carboxamido-tetrazolate (**11**). Ellipsoids of non-hydrogen atoms are drawn at the 50 % probability level. Selected bond lengths (Å): C1–N4

1.3316(18), C1–N1 1.333(2), C1–C2 1.486(2), N4–N3 1.3404(18), N3–N2 1.3218(17), N2–N1 1.3365(17), N5–C2 1.308(2), C2–O1 1.2481(18), O2–N6 1.4103(17); selected bond angles ($^{\circ}$): N4–C1–N1 112.61(16), N4–C1–C2 126.54(16), N1–C1–C2 120.82(14), C1–N4–N3 103.73(14), N2–N3–N4 110.13(12), N3–N2–N1 108.95(12), C1–N1–N2 104.58(12), O1–C2–N5 122.91(17), O1–C2–C1 118.07(16), N5–C2–C1 119.03(15).

Obtained single crystals of bis(hydroxylammonium) 5,5'-azotetrazolate dihydrate (**12**) follows the structure published by Bentivoglio *et al.*[34] (monoclinic, $C2/c$, $Z=4$, 1.612 g cm^{-3}). The molecular unit is shown in Figure 14.

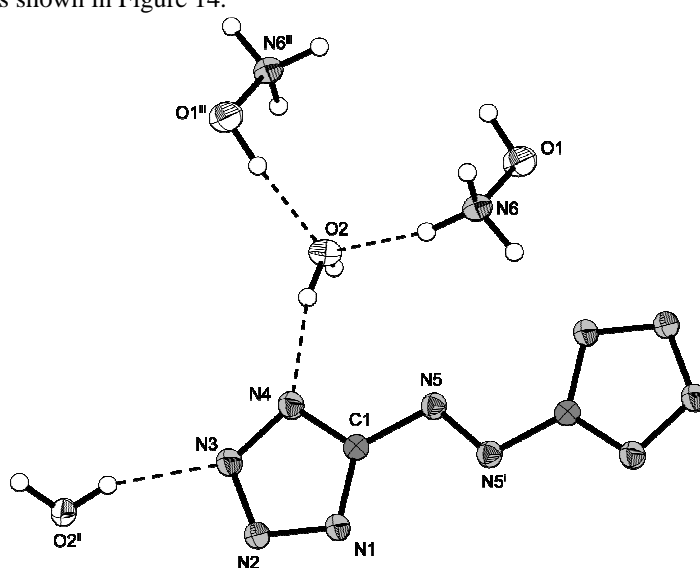


Figure 14. Molecular unit of bis(hydroxylammonium) 5,5'-azotetrazolate dihydrate (**12**). Ellipsoids of non-hydrogen atoms are drawn at the 50 % probability level. Symmetry codes: (i) $1.5-x, 0.5-y, -z$, (ii) $2-x, -1+y, 0.5-z$, (iii) $2-x, 1-y, -z$. Selected bond lengths (\AA): N2–N3 1.3228(14), N2–N1 1.3338(15), O1–N6 1.4145(18), N3–N4 1.3344(16), N4–C1 1.3337(15), N5–N5' 1.2620(18), N5–C1 1.4061(17), N1–C1 1.3318(15); selected bond angles ($^{\circ}$): N3–N2–N1 109.80(10), N2–N3–N4 109.45(9), C1–N4–N3 104.08(9), N5'–N5–C1 112.39(12), C1–N1–N2 103.96(10), N1–C1–N4 112.71(11), N1–C1–N5 127.52(10), N4–C1–N5 119.77(10).

In accordance to the structure of **12**, the corresponding N-oxide **13**, shown in Figure 15, crystallizes also under inclusion of two molecules crystal water in the monoclinic space group $P2_1/c$. N-oxides have been described [35] as promising energetic materials because of increasing densities and thermal stabilities. However, the introduction of an N-oxide to the azo-functionality yields to a decrease in density (**13**: 1.596 g cm^{-3} vs. **12**: 1.612 g cm^{-3}) but increase in thermal stability (**12**: $130 \text{ }^{\circ}\text{C}$ vs. **13**: $175 \text{ }^{\circ}\text{C}$).

Single crystals of bis(hydroxylammonium) 5,5'-bistetrazolate (**14**) solidified triclinic ($P-1$) including one molecular moiety (shown in Figure 16) in the unit cell. Its density of 1.742 g cm^{-3} is comparable to the neutral compound (1.738 g cm^{-3})[36]. The structure of the dianion is in agreement to published structures of 5,5'-bistetrazolates e.g. the erbium(III) salt.[37]

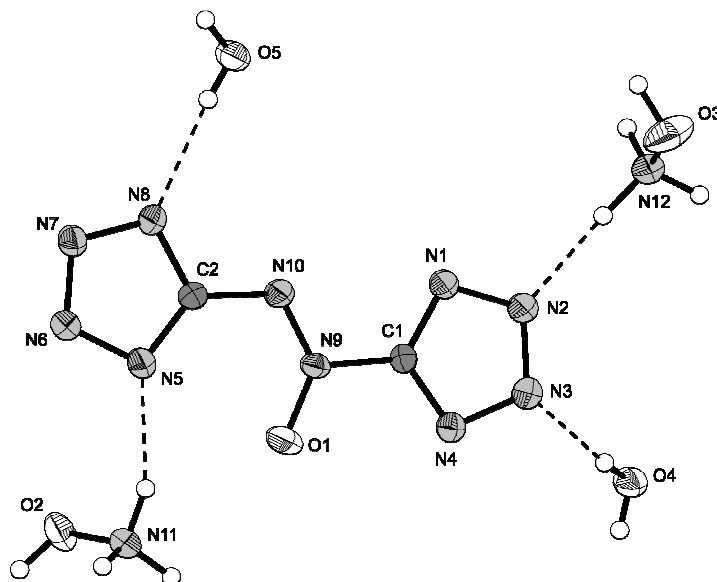


Figure 15. Molecular unit of bis(hydroxylammonium) 5,5'-azotetrazolate-N9-oxide dihydrate (**13**). Ellipsoids of non-hydrogen atoms are drawn at the 50 % probability level. Selected bond lengths (Å): N11–O2 1.410(2), N12–O3 1.408(3), N10–N9 1.273(2), N10–C2 1.396(3), N4–C1 1.318(2), N4–N3 1.341(2), N7–N6 1.316(2), N7–N8 1.334(2), C1–N1 1.320(2), C1–N9 1.440(3), N9–O1 1.253(2), N8–C2 1.341(3), N5–C2 1.336(3), N5–N6 1.346(2), N1–N2 1.340(2), N3–N2 1.324(2); selected bond angles (°): N9–N10–C2 116.93(17), C1–N4–N3 103.50(16), N6–N7–N8 109.52(16), N4–C1–N1 114.19(18), N4–C1–N9 122.30(18), N1–C1–N9 123.50(18), O1–N9–N10 128.99(18), O1–N9–C1 116.56(16), N10–N9–C1 114.44(16), N7–N8–C2 104.37(16), C2–N5–N6 103.51(17), C1–N1–N2 103.54(16), N2–N3–N4 109.42(16), N3–N2–N1 109.35(16), N7–N6–N5 110.15(16), N5–C2–N8 112.44(18), N5–C2–N10 130.69(19), N8–C2–N10 116.87(18).

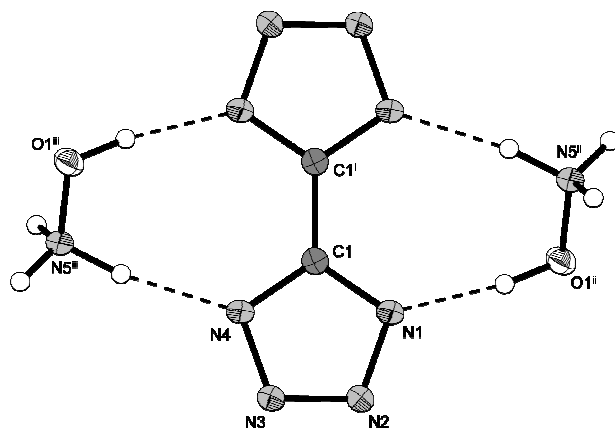


Figure 16. Molecular unit of bis(hydroxylammonium) 5,5'-bistetrazolate (**14**). Ellipsoids of non-hydrogen atoms are drawn at the 50 % probability level. Symmetry codes: (i) 2-x, 1-y, 1-z, (ii) 1+x, y, z, (iii) 1-x, 1-y, 1-z. Selected bond lengths (Å): N3–N2 1.3128(19), N3–N4 1.3452(18), N4–C1 1.333(2), C1–N1 1.336(2), C1–C1ⁱ 1.461(3), N1–N2 1.3443(17), O1–N5 1.4181(16); selected bond angles (°): N2–N3–N4 109.84(12), C1–N4–N3 104.45(13), N4–C1–N1 111.77(13), N4–C1–C1ⁱ 124.02(18), N1–C1–C1ⁱ 124.20(18), C1–N1–N2 104.84(13), N3–N2–N1 109.10(12).

2.3 Energetic properties

2.3.1 Thermal behavior (DSC)

Differential scanning calorimetry (DSC) measurements of **1–15** to determine the melt- and decomposition temperatures (~1.5 mg of each energetic material) were performed in covered Al-containers containing a hole in the lid with a nitrogen flow of 20 mL min⁻¹ on a Linseis PT10 DSC [38] calibrated by standard pure indium and zinc at a heating rate of 5 °C min⁻¹. Compared to nitrogen rich salts such as guanidinium, its aminated derivatives, ammonium or hydrazinium salts, the hydroxylammonium salts show relatively low decomposition temperatures. Since hydroxylamine is a comparatively weak base (Table 1), the thermal stability of the salt is mainly determined by the thermal stability of the free acid, which serves as the respective anion.

Table 1. pK_a and pK_b values of some nitrogen rich corresponding acid-base pairs.[39]

	pK _b	pK _a
NH ₃ /NH ₄ ⁺	4.75	9.25
N ₂ H ₄ /N ₂ H ₅ ⁺	6.07	7.93
NH ₂ OH/NH ₃ OH ⁺	8.20	5.80

When the compound is heated to elevated temperatures, the proton of protonated hydroxylamine is more mobile and tends to be transferred to the deprotonated acid. This phenomenon is more distinctive, the weaker the acid-base combination in a given ionic compound is and has already been seen in the series of salts of 1-amino-3-nitroguanidine, which can only be protonated by strong acids.[40] Their decomposition points are in a range of 80–150°C, whereas free 1-amino-3-nitroguanidine decomposes at 180°C. The decomposition temperatures of the hydroxylammonium salts **1–14** are spread over a very large range from 143°C up to slightly above 200°C depending on the anion. The nitriminotetrazolates are found in the middle range with lower values for unmethylated (**1**) and 2-methylated (**4**) at 180°C and slightly higher values for the 1-methylated compound (**3**, 185°C). The bisdeprotonated nitriminotetrazolate **2** decomposes with a main exothermic peak at 194°C, however there are two smaller exothermic peaks observed at 164°C and 184°C. For the ethyl-substituted nitriminotetrazolates the hydroxyethyl-compound **5** expectedly shows the better thermal stability (178°C) compared to the nitrateethyl substituted heterocycle **6** (148°C). All bistetrazoleamine and bistetrazole compounds (**7**, **8**, **9**, **14**) show comparatively high decomposition points of 200°C, 172°C, 202°C and 200°C respectively, based on the good thermal stability of the free acid bistetrazolamine (260°C) and 5,5'-bistetrazole (252°C) themselves. A very good example of the above stated theory of anion-depending decomposition points are the two presented azotetrazolate salts. Since 5,5'-azotetrazole itself is not stable and decomposes to nitrogen, hydrazoic and formic acid, also its hydroxylammonium salt **12** decomposes at relatively low temperature (130°C). Compared to this, the hydroxylammonium salts of the oxidized form (**13**), which also is not stable as the free acid, but has a lower pK_a-value due to the electron-withdrawing character of the N-oxide moiety and therefore can better stabilize the salt, is stable up to 175°C. The 5*H*-

tetrazolate and its carboxamide substituted sister compound decompose in the lower to middle range of the presented spectrum at 143°C (**10**) and 173°C (**11**). The highest decomposition temperature of the herein presented materials is the covalent tetrazole-5-carboxamide-oxime (**15**) with an onset temperature of decomposition at 244°C.

2.3.2 Sensitivities and detonation parameters

The impact sensitivity tests were carried out according to STANAG 4489 [41] modified instruction [42] using a BAM (Bundesanstalt für Materialforschung) drophammer.[43] The friction sensitivity tests were carried out according to STANAG 4487 [44] modified instruction [45] using the BAM friction tester. The classification of the tested compounds results from the “UN Recommendations on the Transport of Dangerous Goods”.[46] Additionally all compounds were tested upon the sensitivity towards electrical discharge using the Electric Spark Tester ESD 2010 EN [47]. The impact as well as the friction sensitivities of the discussed compounds reach from very sensitive to insensitive. The nitriminotetrazolates **1–4** show increased sensitivity, especially monodeprotonated **1** (2 J, 40 N), which also is the most sensitive compound discussed here. Unlike **1**, the bisdeprotonated salt **2** is less sensitive if nothing else since it crystallizes as a hemihydrate. The same is true for the methylated compounds **3** (8 J, 144 N) and **4** (6 J, 144 N). Like we expected, the salt of the 2-isomer is more sensitive than the salt of the 1-isomer.[7, 48] Except from the bistetrazolylamine cocrystallization product **9**, the tetrazole-5-carboxamide **11** and the neutral oxime **15**, which are insensitive towards impact (>40 J), the rest of the compounds has to be classified as sensitive towards impact with the lower values for the bistetrazolylamine and the 5,5'-bistetrazole salts **7**, **8** and **14** (10 J) and the higher values for the 5H-tetrazolate **10** (22 J) and the azotetrazolates **12** (25 J) and **13** (30 J). The friction sensitivities are mostly geared to the impact sensitivity data. Therefore, **9** is completely insensitive towards friction, whereas the other salts are classified as sensitive with values in a range from 160 N (**13**) to 288 N (**7**, **8**, **10**, **11**). The hydroxyethyl derivative **5** (15 J, 160 N) is less sensitive than the nitrateoethyl derivative **6** (3 J, 60 N), which we expected. The sensitivities towards electrical discharge are strongly depending on the grain size of the material. The values are mostly in a range between 0.15 J and 0.50 J. Only the two bistetrazolylamine salts **7** and **8** stick out with their low values of 0.05 J due to the very fine material that was used for the test.

The detonation parameters were calculated using the program EXPLO5 V5.04.[49] The calculations were performed using the maximum densities according to the crystal structures. Heats of formation were computed theoretically. All calculations were carried out using the Gaussian G09 program package.[50] The enthalpies (H) and free energies (G) were calculated using the complete basis set (CBS) method of Petersson and coworkers in order to obtain very accurate energies. The CBS models use the known asymptotic convergence of pair natural orbital expressions to extrapolate from calculations using a finite basis set to the estimated complete basis set limit. CBS-4 begins with a HF/3-21G(d) geometry optimization; the zero point energy is computed at the same level. It then uses a large basis set SCF calculation as a base energy, and a MP2/6-31+G calculation with a CBS extrapolation to correct the energy through second order. A MP4(SDQ)/6-31+(d,p) calculation is used to approximate higher order contri-

butions. In this study we applied the modified CBS-4M method (**M** referring to the use of Minimal Population localization) which is a re-parametrized version of the original CBS-4 method and also includes some additional empirical corrections.[51] The enthalpies of the gas-phase species **M** were computed according to the atomization energy method (eq. 1) [52] described circumstantially in the literature.[53]

$$\Delta_f H^\circ_{(g, M, 298)} = H_{(Molecule, 298)} - \sum H^\circ_{(Atoms, 298)} + \sum \Delta_f H^\circ_{(Atoms, 298)} \quad (1)$$

Using calculated heat of sublimation by the Troutons rule [54] and lattice enthalpies for the ionic compounds the gas-phase enthalpies of formation were converted into the solid state (standard conditions) enthalpy of formation $\Delta_f H_m^\circ$. Lattice energies (U_L) and lattice enthalpies (ΔH_L) were calculated from the corresponding molecular volumes according to Jenkin's equations.[55]

Lastly, the molar standard enthalpies of formation ($\Delta_f H_m^\circ$) were used to calculate the molar solid state energies of formation ($\Delta_f U_m$) according to equation (2), which then were transformed to kJ kg^{-1} and used as input data for the EXPLO5 code. The values can be found in Tables 2 and 3.

$$\Delta_f U_m = \Delta_f H_m - \Delta n RT \quad (2)$$

(Δn being the change of moles of gaseous components)

Due to the well balanced oxygen content of the hydroxylammonium salts compared to other nitrogen-rich salts of the corresponding acids, the compounds show comparatively good performance data. Compared to commonly used RDX, **6** of the **14** compounds exceed its detonation velocity of 8748 ms^{-1} and **3** of **14** exceed its detonation pressure at the CJ-point of 349 kbar. Due to their high density, which has the most important impact on the detonation velocity, the nitriminotetrazolates **1** and **2** as well as the nitrateoethyl compound **7** even exceed the 9000 ms^{-1} benchmark. For the 2-methyl-5-nitraminotetrazolate **4** the density of the 1-isomer **3** was assumed since we were not able to grow single crystals suitable for X-ray crystallography. The slightly higher heat of formation of the 2-isomer compared to the 1-isomer causes the better performance data of the compound. Also for the monodeprotonated bistetrazolylamine salt **7** we assumed the density to be the average density of the bisdeprotonated salt and bistetrazolylamine monohydrate itself. Another important factor for the good performance data are the highly positive heats of formation, which especially are observed for the monodeprotonated bistetrazolylamine salts **7** and **9**. The low heats of formation of **2**, **12** and **13** arise from the fact, that these compounds crystallize as hemihydrate (**2**) and dihydrates (**12**, **13**) respectively. Also the tetrazolecarboxamide salt **11** has a comparatively low heat of formation due to the thermodynamically very stable carboxamide moiety.

The sensitivity data as well as the decomposition temperatures, the heats of formation and the detonation parameters of the discussed materials are gathered in Tables 2 and 3.

Table 2. Physicochemical properties and detonation parameters of **1–7**.

	1	2	3	4	5	6	7
Formula	CH ₅ N ₇ O ₃	CH ₉ N ₈ O _{4.5}	C ₂ H ₇ N ₇ O ₃	C ₂ H ₇ N ₇ O ₃	C ₃ H ₉ N ₇ O ₄	C ₃ H ₈ N ₈ O ₆	C ₂ H ₆ N ₁₀ O
FW [g mol ⁻¹]	163.13	205.16	177.12	177.12	207.07	252.06	186.14
IS [J] ^a	2	10	8	6	3	15	10
FS [N] ^b	40	80	144	144	160	60	288
ESD-test [J] ^c	0.30	0.30	0.50	0.30	0.50	0.15	0.05
N [%] ^d	60.1	54.6	40.7	40.7	47.3	44.4	75.3
Q [%] ^e	-14.7	-20.3	-55.4	-55.4	-50.2	-25.4	-51.6
T _{dec.} [°C] ^f	180	194	185	180	178	148	200
Density [g cm ⁻³] ^g	1.785	1.771	1.627	1.627*	1.614	1.796	1.714**
Δ _f H _m ^o / kJ mol ⁻¹ h	+290	+80	+331	+352	+133	+490	+680
Δ _f U ^o / kJ kg ⁻¹ i	1895	520	1989	2107	763	1094	3764
EXPLO5 values:							
-Δ _E U ^o [kJ kg ⁻¹] ^j	6113	5459	6095	6210*	5431	6319	5326**
T _E [K] ^k	4219	3567	3949	4000*	3511	4192	3604**
p _{C-J} [kbar] ^l	371	355	297	300*	265	363	319**
D [m s ⁻¹] ^m	9236	9203	865	8690*	8276	9025	8876**
Gas vol. [L kg ⁻¹] ⁿ	853	927	842	842*	828	787	806**

^a impact sensitivity (BAM drophammer^[21], 1 of 6); ^b friction sensitivity (BAM friction tester^[21], 1 of 6); ^c electrostatic discharge device (OZM^[22]); ^d nitrogen content; ^e oxygen balance; ^f decomposition temperature from DSC (β = 5 °C); ^g estimated from X-ray diffraction; ^h calculated (CBS-4M) heat of formation; ⁱ calculated energy of formation; ^j Energy of Explosion; ^k explosion temperature; ^l detonation pressure; ^m detonation velocity; ⁿ assuming only gaseous products.

*assuming the density of hydroxylammonium 1-methyl-5-nitriminotetrazolate (**3**)

assuming an average density of H₂bta*H₂O and Hx₂-bta (8**)

Table 3. Physicochemical properties and detonation parameters of **8–14**.

	8	9	10	11	12	13	14
Formula	C ₂ H ₉ N ₁₁ O ₂	C ₄ H ₁₂ N ₁₉ O ₂	CH ₃ N ₅ O	C ₂ H ₆ N ₆ O ₂	C ₂ H ₁₂ N ₁₂ O ₄	C ₂ H ₁₂ N ₁₂ O ₅	C ₂ H ₈ N ₁₀ O ₂
FW [g mol ⁻¹]	219.17	374.26	103.08	146.11	268.19	284.19	204.15
IS [J] ^a	10	>40	22	>40	25	30	10
FS [N] ^b	288	>360	288	288	192	160	240
ESD-test [J] ^c	0.50	0.50	0.50	0.15	0.30	0.25	0.10
N [%] ^d	70.3	70.9	67.9	57.5	62.7	59.1	68.6
Q [%] ^e	-47.4	-51.0	-54.3	-54.7	-35.8	-28.1	-47.0
T _{dec.} [°C] ^f	172	202	143	173	130	175	200
Density [g cm ⁻³] ^g	1.734	1.719	1.557	1.660	1.615	1.596	1.742
Δ _f H _m ^o / kJ mol ⁻¹ h	+496	+833	+251	+73	+156	+132	+428
Δ _f U ^o / kJ kg ⁻¹ i	2389	2335	2568	617	711	590	2227
EXPLO5 values:							
-Δ _E U ^o [kJ kg ⁻¹] ^j	4888	4534	5228	4088	4502	4906	4841
T _E [K] ^k	3235	3133	3336	2892	3133	3393	3248
p _{C-J} [kbar] ^l	321	296	269	246	262	262	317
D [m s ⁻¹] ^m	8923	8625	8496	8046	8295	8294	8858
Gas vol. [L kg ⁻¹] ⁿ	854	826	873	819	892	893	843

^a impact sensitivity (BAM drophammer^[21], 1 of 6); ^b friction sensitivity (BAM friction tester^[21], 1 of 6); ^c electrostatic discharge device (OZM^[22]); ^d nitrogen content; ^e oxygen balance; ^f decomposition temperature from DSC (β = 5 °C); ^g estimated from X-ray diffraction; ^h calculated (CBS-4M) heat of formation; ⁱ calculated energy of for-

mation; ^j Energy of Explosion; ^k explosion temperature; ^l detonation pressure; ^m detonation velocity; ⁿ assuming only gaseous products.

3 Experimental Part

Caution! The herein described materials as well as their precursors are energetic materials with increased sensitivities towards shock and friction. Therefore, proper safety precautions (safety glass, face shield, earthened equipment and shoes, Kevlar[®] gloves and ear plugs) have to be applied while synthesizing and handling the described compounds.

All chemicals and solvents were employed as received (Sigma-Aldrich, Fluka, Acros). ¹H and ¹³C spectra were recorded using a JEOL Eclipse 270, JEOL EX 400 or a JEOL Eclipse 400 instrument. The chemical shifts quoted in ppm in the text refer to typical standards such as tetramethylsilane (¹H, ¹³C). To determine the melting and decomposition temperatures of the described compounds a Linseis PT 10 DSC (heating rate 5 °C min⁻¹) was used. Infrared spectra were measured using a Perkin Elmer Spectrum One FT-IR spectrometer as KBr pellets. Raman spectra were recorded on a Bruker MultiRAM Raman Sample Compartment D418 equipped with a Nd-YAG-Laser (1064 nm) and a LN-Ge diode as detector. Mass spectra of the described compounds were measured at a JEOL MStation JMS 700 using FAB technique. To measure elemental analyses a Netsch STA 429 simultaneous thermal analyzer was employed.

Hydroxylammonium 5-nitriminotetrazolate (1)

5-Nitriminotetrazole (1.59 g, 12.2 mmol) is dissolved in a few milliliters of water and a solution of silver nitrate (2.07 g, 12.2 mmol) is added. Silver 5-nitriminotetrazolate precipitates instantly as a white solid. It is sucked off and washed with water until free of acid. The white solid is resuspended in 50 mL of warm water and treated with a solution of hydroxylammonium chloride (0.84 g, 13.0 mmol) in 20 mL of water. The mixture is stirred at 30 °C for 1 h in the dark and the formed silver chloride is filtered off. The filtrate is evaporated and the residue was recrystallized from an ethanol/water mixture to yield **1** as a white solid (1.70 g, 10.4 mmol, 85%).

DSC (5 °C min⁻¹, °C): 180 °C (dec.); IR (KBr, cm⁻¹): $\tilde{\nu}$ = 3125 (s), 2958 (s), 2776 (m), 2711 (s), 1617 (m), 1598(m), 1539 (s), 1431 (s), 1383 (m), 1321 (vs), 1244 (m), 1213 (m), 1188 (m), 1153 (m), 1108 (m), 1061 (m), 1039 (m), 1003 (m), 872 (w), 823 (w), 777 (w), 753 (w), 742 (w), 700 (w), 493 (w); Raman (1064 nm, 300 mW, 25 °C, cm⁻¹): $\tilde{\nu}$ = 2715 (1), 1541 (100), 1452 (1), 1433 (1), 1381 (4), 1332 (36), 1158 (7), 1110 (4), 1070 (4), 1036 (22), 1014 (85), 875 (8), 744 (14), 695 (1), 494 (3), 427 (4), 413 (15); ¹H NMR (DMSO-*d*₆, 25 °C, ppm) δ : 10.95 (s); ¹³C NMR (DMSO-*d*₆, 25 °C, ppm) δ : 158.3 (CN₄); m/z (FAB⁺): 34.0 [NH₃OH⁺]; m/z (FAB⁻): 129.1 [HATNO₂⁻]; EA (CH₅N₇O₃, 163.10): calc.: C 7.36, H 3.09, N 60.12 %; found: C 7.38, H 3.17, N 57.40 %; BAM drophammer: 2 J; friction tester: 40 N; ESD: 0.30 J (at grain size 100 - 500 μm).

Dihydroxylammonium nitriminotetrazolate hemihydrate (2)

5-Nitriminotetrazole (2.60 g, 20.0 mmol) is dissolved in 10 mL of cold water and an aqueous solution of hydroxylamine (50% w/w, 2.64 g, 40.0 mmol) is added dropwise. After a few minutes, the product began to crystallize in fine needles, which were isolated. For recovery of

the remaining material the mother liquor was evaporated and the colorless residue was recrystallized from ethanol/water to give **2** in 90% yield (3.69 g, 18.0 mmol).

DSC (5 °C min⁻¹, °C): 166°C (weak exo), 184 °C (weak exo), 194 °C (dec., strong exo); IR (KBr, cm⁻¹): $\tilde{\nu}$ = 3421 (m), 3217 (m), 3101 (s), 2719 (s), 1612 (m), 1523 (m), 1466 (m), 1418 (s), 1384 (vs), 1338 (s), 1310 (s), 1219 (s), 1171 (m), 1146 (m), 1109 (w), 1099 (w), 1039 (w), 1022 (m), 1003 (s), 871 (m), 757 (m), 757 (w), 748 (w), 737 (w), 486 (w); Raman (1064 nm, 300 mW, 25 °C, cm⁻¹): $\tilde{\nu}$ = 1452 (100), 1423 (10), 1395 (3), 1358 (1), 1293 (2), 1236 (6), 1184 (8), 1154 (15), 1109 (3), 1021 (41), 1011 (12), 876 (3), 755 (3), 731 (6), 424 (9), 410 (8); ¹H NMR (DMSO-*d*₆, 25 °C, ppm) δ : 8.83 (s, NH₃OH⁺); ¹³C NMR (DMSO-*d*₆, 25 °C, ppm) δ : 158.4 (CN₄); m/z (FAB⁺): 34.0 [NH₃OH⁺]; m/z (FAB⁻): 129.0 [CHN₆O₂⁻]; EA (CH₈N₈O₄, water-free, 196.13): calc.: C 6.12, H 4.11, N 57.13 %; found: C 6.09, H 3.96, N 57.13 %; BAM drophammer: 10 J; friction tester: 80 N; ESD: 0.30 J (at grain size 500-1000 μ m).

Hydroxylammonium 1-methyl-5-nitriminotetrazolate (**3**)

1-Methyl-5-nitriminotetrazole (1.67 g, 11.6 mmol) is dissolved in a few milliliters of water and a solution of silver nitrate (1.97 g, 11.6 mmol) is added. Silver 1-methyl-5-nitriminotetrazolate precipitates instantly as a white solid. It is sucked off and washed with water until free of acid. The white solid is resuspended in 50 mL of warm water and treated with a solution of hydroxylammonium chloride (0.74 g, 11.5 mmol) in 20 mL of water. The mixture is stirred at 30°C for 1 h in the dark and the formed silver chloride is filtered off. The filtrate is evaporated and the residue was recrystallized from ethanol to yield **3** as a white solid (1.78 g, 10.0 mmol, 86%).

DSC (5 °C min⁻¹, °C): 180°C (m.p.), 185°C (dec.); IR (KBr, cm⁻¹): $\tilde{\nu}$ = 3435 (vs), 3099 (m), 2737 (m), 2375 (w), 1627 (m), 1587 (m), 1515 (m), 1470 (m), 1424 (m), 1396 (m), 1385 (m), 1339 (s), 1303 (m), 1278 (m), 1250 (m), 1205 (m), 1106 (m), 1035 (w), 1011 (w), 987 (w), 890 (w), 831 (w), 774 (w), 753 (w), 733 (w), 689 (w); Raman (1064 nm, 300 mW, 25 °C, cm⁻¹): $\tilde{\nu}$ = 3026 (6), 2960 (53), 2804 (2), 2728 (2), 1585 (3), 1546 (7), 1520 (64), 1471 (35), 1425 (3), 1407 (13), 1342 (10), 1316 (3), 1304 (47), 1254 (4), 1123 (2), 1110 (15), 1037 (100), 1012 (19), 991 (3), 893 (14), 774 (2), 754 (30), 734 (4), 699 (5), 690 (35), 503 (17), 460 (6), 376 (8), 289 (51); ¹H NMR (DMSO-*d*₆, 25 °C, ppm) δ : 10.12 (s, NH₃OH⁺), 3.67 (s, CH₃); ¹³C NMR (DMSO-*d*₆, 25 °C, ppm) δ : 157.5 (CN₄), 33.1 (CH₃); m/z (FAB⁺): 34.0 [NH₃OH⁺]; m/z (FAB⁻): 143.0 [1-MeATNO₂⁻]; EA (C₂H₇N₇O₃, 177.12): calc.: C 13.56, H 3.98, N 55.36 %; found: C 13.70, H 3.73, N 55.08 %; BAM drophammer: 8 J; friction tester: 144 N; ESD: 0.50 J (at grain size 500 - 1000 μ m).

Hydroxylammonium 2-methyl-5-nitraminotetrazolate (**4**)

Ammonium 2-methyl-5-nitraminotetrazolate (4.12 g, 25.6 mmol) was dissolved in 20 mL of water and a solution of silver nitrate (4.34 g, 25.5 mmol) was added. The silver salt of 2-methyl-5-nitraminotetrazolate precipitates as a white solid. After being washed until free of ammonium nitrate it is resuspended in 100 mL of water and a solution of hydroxylammonium chloride (1.61 g, 25.0 mmol) is added. The mixture is stirred for 1 h at 30°C in the dark and the formed silver chloride is filtered off. The filtrate is evaporated and the viscous residue is redissolved in ethanol for recrystallization. **4** crystallizes as a white, fluffy precipitate. Yield: 3.96 g, 22.3 mmol, 87%.

DSC (5 °C min⁻¹, °C): 139°C (m.p.), 180°C (dec.); IR (KBr, cm⁻¹): $\tilde{\nu}$ = 3433 (m), 3116 (s), 3048 (s), 2802 (m), 2724 (s), 1619 (m), 1506 (m), 1483 (s), 1435 (m), 1405 (s), 1384 (s), 1364 (m), 1329 (vs), 1282 (m), 1232 (m), 1212 (m), 1184 (m), 1118 (w), 1101 (m), 1094 (m), 1035 (m), 1013 (w), 1002 (w), 900 (w), 890 (w), 764 (w), 754 (w), 706 (w), 678 (w); Raman (1064 nm, 300 mW, 25 °C, cm⁻¹): $\tilde{\nu}$ = 2965 (17), 2840 (1), 1622 (1), 1603 (1), 1484 (100), 1437 (3), 1420 (3), 1396 (3), 1368 (3), 1290 (1), 1215 (5), 1187 (7), 1119 (3), 1096 (2), 1040 (4), 1030 (47), 1015 (15), 1003 (2), 902 (2), 890 (4), 754 (5), 707 (9), 454 (8), 404 (4); ¹H NMR (DMSO-*d*₆, 25 °C, ppm) δ : 9.90 (s, NH₃OH⁺), 4.20 (s, CH₃); ¹³C NMR (DMSO-*d*₆, 25 °C, ppm) δ : 168.0 (CN₄), 39.7 (CH₃); m/z (FAB⁺): 34.0 [NH₃OH⁺]; m/z (FAB⁻): 143.0 [2-MeATNO₂⁻]; EA (C₂H₇N₇O₃, 177.12): calc.: C 13.56, H 3.98, N 55.36 %; found: C 13.25, H 3.88, N 53.47 %; BAM drophammer: 6 J; friction tester: 144 N; ESD: 0.30 J (at grain size <100 μ m).

Hydroxylammonium 1-hydroxyethyl-5-nitriminotetrazolate (5)

1-(2-Hydroxyethyl)-5-nitriminotetrazole was prepared according to literature.^{Chyba! Zálôžka není definována.} 1-(2-Hydroxyethyl)-5-nitriminotetrazole (1.74 g, 10 mmol) was dissolved in 20 mL of hot water. An aqueous solution of hydroxylamine (50% w/w, 0.66 g, 10 mmol) is added and the solvent from the resulting clear solution is evaporated in vacuum. A colorless solid is formed, which is recrystallized from ethanol to yield **5** as colorless crystals (1.92 g, 9.3 mmol, 93%).

DSC (5 °C min⁻¹, °C): 133°C (m.p.), 178°C (dec. 1), 192°C (dec. 2); IR (KBr, cm⁻¹): $\tilde{\nu}$ = 3374 (m), 3135 (m), 3073 (m), 2960 (m), 2933 (m), 2729 (m), 1628 (w), 1546 (m), 1505 (s), 1457 (m), 1431 (m), 1332 (vs), 1265 (m), 1246 (m), 1228 (m), 1163 (w), 1122 (w), 1076 (m), 1037 (m), 1000 (w), 957 (w), 884 (w), 872 (w), 772 (w), 755 (w), 739 (w), 661 (w), 547 (w), 523 (w), 482 (w); Raman (1064 nm, 300 mW, 25 °C, cm⁻¹): $\tilde{\nu}$ = 3014 (2), 2969 (9), 2934 (2), 1507 (100), 1392 (3), 1310 (9), 1231 (2), 1125 (11), 1063 (6), 1039 (32), 1002 (9), 886 (2), 872 (4), 758 (7), 661 (3), 283 (2); ¹H NMR (DMSO-*d*₆, 25 °C, ppm) δ : 10.09 (s, 4H, NH₃OH⁺), 4.92 (s, 1H, OH), 4.08 (t, 2H, CH₂OH), 3.70 (t, 2H, NCH₂); ¹³C NMR (DMSO-*d*₆, 25 °C, ppm) δ : 157.4 (CN₄), 59.1 (CH₂OH), 48.8 (NCH₂); m/z (FAB⁺): 34.0 [NH₃OH⁺]; m/z (FAB⁻): 172.9 [C₃H₅N₆O₃⁻]; EA (C₃H₅N₇O₄, 207.15): calc.: C 17.39, H 4.38, N 47.33 %; found: C 17.85, H 4.26, N 46.74 %; BAM drophammer: 15 J; friction tester: 160 N; ESD: 0.50 J (at grain size 100-500 μ m).

Hydroxylammonium 1-nitratoethyl-5-nitriminotetrazolate (6)

1-(2-Nitratoethyl)-5-nitriminotetrazole was prepared according to literature.^{Chyba! Zálôžka není definována.} 1-(2-Nitratoethyl)-5-nitriminotetrazole (1.62 g, 6.83 mmol) was dissolved in 20 mL of hot water. An aqueous solution of hydroxylamine (50% w/w, 0.45 g, 6.83 mmol) is added and the solvent from the resulting clear solution is evaporated in vacuum. A colorless oil is formed, which is recrystallized from ethanol to yield **6** as colorless crystals after almost complete evaporation of the solvent (1.59 g, 6.31 mmol, 92%). The crystals were dried afterwards at 50°C overnight.

DSC (5 °C min⁻¹, °C): 66°C (m.p.), 148°C (dec.); IR (KBr, cm⁻¹): $\tilde{\nu}$ = 3413 (m), 3126 (m), 3017 (m), 2934 (m), 2784 (m), 2723 (m), 2380 (w), 1985 (w), 1644 (s), 1635 (s), 1535 (m), 1499 (m), 1455 (m), 1428 (m), 1383 (s), 1343 (vs), 1289 (s), 1251 (m), 1230 (m), 1171 (m),

1123 (m), 1081 (w), 1036 (m), 1014 (m), 985 (m), 904 (m), 881 (m), 853 (m), 771 (w), 741 (m), 679 (m), 627 (w), 527 (w); Raman (1064 nm, 300 mW, 25 °C, cm^{-1}): $\tilde{\nu} = 3033$ (2), 3017 (2), 2991 (3), 2974 (13), 1636 (3), 1503 (100), 1430 (3), 1380 (7), 1357 (7), 1328 (10), 1279 (15), 1232 (2), 1126 (13), 1037 (23), 1016 (2), 1005 (7), 987 (3), 883 (4), 842 (6), 748 (5), 678 (3), 626 (2), 575 (4), 429 (2), 373 (2), 293 (2), 263 (3); ^1H NMR (DMSO- d_6 , 25 °C, ppm) δ : 10.11 (s, 4H, NH_3OH^+), 4.87 (t, 2H, CH_2ONO_2), 4.45 (t, 2H, NCH_2); ^{13}C NMR (DMSO- d_6 , 25 °C, ppm) δ : 157.6 (CN_4), 70.8 (CH_2ONO_2), 43.7 (NCH_2); m/z (FAB^+): 34.0 [NH_3OH^+]; m/z (FAB^-): 217.8 [$\text{C}_3\text{H}_4\text{N}_7\text{O}_5^-$]; EA ($\text{C}_3\text{H}_8\text{N}_8\text{O}_6$, 252.15): calc.: C 14.29, H 3.20, N 44.44 %; found: C 14.55, H 3.00, N 44.22 %; BAM drophammer: 3 J; friction tester: 60 N; ESD: 0.15 J (at grain size 100-500 μm).

Hydroxylammonium bistetrazolylamine (7)

Bistetrazolylamine (1.53 g, 10 mmol) is dispensed in 50 mL of hot water. A solution of hydroxylamine (50% w/w in H_2O , 0.66 g, 10 mmol) is added and the mixture is heated until clear. The resulting clear solution is evaporated under vacuum. The colorless solid residue is recrystallized from ethanol/water to yield 1.73 g (9.3 mmol, 93%) of **7** as a white, amorphous precipitate.

DSC (5 °C min^{-1} , °C): 200°C (dec.); IR (KBr, cm^{-1}): $\tilde{\nu} = 3419$ (m), 3154 (s), 3098 (s), 3002 (s), 2869 (s), 2710 (s), 2070 (w), 1651 (vs), 1562 (m), 1510 (m), 1461 (w), 1436 (m), 1384 (w), 1320 (m), 1254 (w), 1230 (m), 1162 (w), 1140 (w), 1043 (m), 1001 (m), 863 (w), 848 (w), 802 (w), 741 (w), 732 (w), 691 (w), 675 (w), 668 (w), 616 (w); Raman (1064 nm, 300 mW, 25 °C, cm^{-1}): $\tilde{\nu} = 3156$ (6), 2934 (9), 2701 (6), 1684 (5), 1562 (67), 1506 (43), 1436 (9), 1360 (33), 1323 (11), 1258 (11), 1237 (35), 1222 (30), 1142 (45), 1130 (21), 1072 (100), 1028 (19), 1003 (62), 841 (5), 803 (13), 743 (9), 412 (29), 386 (15), 346 (17), 316 (18), 303 (21); ^1H NMR (DMSO- d_6 , 25 °C, ppm) δ : 9.87 (s, 2H, NH), 9.26 (s, 4H, NH_3OH); ^{13}C NMR (DMSO- d_6 , 25 °C, ppm) δ : 156.4 ($(\text{CN}_4)_2$); m/z (FAB^+): 34.0 [NH_3OH^+], 154.0 [$\text{C}_2\text{H}_3\text{N}_9^+$]; m/z (FAB^-): 152.0 [C_2HN_9^-]; EA ($\text{C}_2\text{H}_6\text{N}_{10}\text{O}$, 186.12): calc.: C 12.91, H 3.25, N 75.25 %; found: C 13.39, H 3.18, N 74.24 %; BAM drophammer: 10 J; friction tester: 288 N; ESD: 0.05 J (at grain size <100 μm).

Dihydroxylammonium bistetrazolylamine (8)

Bistetrazolylamine (1.53 g, 10 mmol) is dissolved in 100 mL of boiling water. A solution of hydroxylamine (50% w/w in H_2O , 1.32 g, 20 mmol) is added slowly and the resulting clear solution is evaporated under vacuum. The colorless solid residue is recrystallized from methanol/water to yield 1.82 g (8.3 mmol, 83%) of **8** as colorless needles suitable for X-ray crystallography.

DSC (5 °C min^{-1} , °C): 172°C (dec.); IR (KBr, cm^{-1}): $\tilde{\nu} = 3367$ (s), 2966 (s), 2834 (m), 2726 (s), 2148 (m), 1630 (m), 1609 (vs), 1535 (m), 1486 (m), 1420 (m), 1385 (m), 1290 (m), 1246 (m), 1232 (m), 1171 (w), 1159 (w), 1134 (m), 1128 (m), 1024 (w), 994 (m), 857 (m), 792 (m), 743 (m), 716 (w), 532 (m); Raman (1064 nm, 300 mW, 25 °C, cm^{-1}): $\tilde{\nu} = 3367$ (2), 2963 (4), 2716 (3), 1655 (2), 1529 (100), 1417 (6), 1234 (34), 1163 (3), 1132 (32), 1080 (53), 1024 (12), 998 (44), 787 (3), 749 (6), 554 (2), 521 (2), 407 (15), 379 (7), 345 (8), 327 (25), 255 (17), 228 (21), 159 (13), 132 (29), 122 (29); ^1H NMR (DMSO- d_6 , 25 °C, ppm) δ : 8.56 (s, 9H, NH, NH_3OH); ^{13}C NMR (DMSO- d_6 , 25 °C, ppm) δ : 157.3 ($(\text{CN}_4)_2$); m/z (FAB^+): 34.0 [NH_3OH^+];

m/z (FAB⁻): 152.0 [C₂H₂N₉]; EA (C₂H₉N₁₁O₂, 219.17) calc.: C 10.96, H 4.14, N 70.30 %; found: C 11.42, H 3.92, N 69.98 %; BAM drophammer: 10 J; friction tester: 288 N; ESD: 0.50 J (at grain size 500-1000 μm for IS and FS, <100 μm for ESD).

Hydroxylammonium bistetrazolylamine * bistetrazolylamine dihydrate (9)

Single crystals of **9** were recovered from the mother liquor of a recrystallization of **8** after a small amount of dihydroxylammonium bistetrazolylamine crystals were separated from the liquid phase. The remaining excess bistetrazolylamine in the solution forced the monohydroxylammonium bistetrazolylamine **8** to crystallize as a cocrystallization product with uncharged bistetrazolylamine. **9** was isolated in minor yield, so that only a DSC measurement of the compound was carried out.

DSC (5 °C min⁻¹, °C): 202°C (dec.); BAM drophammer: >40 J (neg.); friction tester: >360 N (neg.); ESD: 0.50 J (at grain size 100-500 μm).

Hydroxylammonium 5H-tetrazolate (10)

5H-Tetrazole (1.05 g, 15 mmol) is dissolved in 20 mL of water. A solution of hydroxylamine (50% w/w, 0.99 g, 15 mmol) was added to the aqueous phase dropwise. The clear solution was evaporated under vacuum and the colorless residue was recrystallized from ethanol/water to give **10** in 82% yield (1.27 g, 12.3 mmol).

DSC (5 °C min⁻¹, °C): 132°C (m. p.), 143°C (dec.); IR (KBr, cm⁻¹): $\tilde{\nu}$ = 3149 (m), 2969 (s), 2871 (s), 2668 (vs), 2543 (s), 2191 (s), 2103 (m), 1848 (m), 1796 (w), 1648 (m), 1556 (m), 1520 (m), 1442 (m), 1426 (m), 1298 (m), 1261 (m), 1203 (s), 1146 (s), 1108 (m), 1030 (m), 1015 (m), 984 (m), 903 (m), 833 (m), 737 (w), 701 (m), 586 (w); Raman (1064 nm, 350 mW, 25 °C, cm⁻¹): $\tilde{\nu}$ = 3150 (25), 2859 (4), 2671 (3), 2195 (3), 1556 (2), 1444 (6), 1428 (15), 1298 (29), 1204 (100), 1152 (13), 1109 (16), 1032 (4), 1017 (7), 985 (32), 739 (2), 703 (4); ¹H NMR (DMSO-*d*₆, 25 °C, ppm) δ : 9.75 (s, 4H, NH₃OH), 8.62 (s, 1H, CH); ¹³C NMR (DMSO-*d*₆, 25 °C, ppm) δ : 147.2 (CN₄); m/z (FAB⁺): 34.0 [NH₃OH⁺]; m/z (FAB⁻): 69.0 [CHN₄⁻], 139.0 [2x CH₂N₄-H⁻], 209.0 [3x CH₂N₄-H⁻]; EA (CH₅N₅O, 103.08) calc.: C 11.65, H 4.89, N 67.94 %; found: C 12.06, H 4.57, N 67.58 %; BAM drophammer: 22 J; friction tester: 288 N; ESD: 0.50 J (at grain size 500-1000 μm).

Hydroxylammonium tetrazole-5-carboxamide (11)

Tetrazole-5-carboxamide (0.71 g, 6.28 mmol) was suspended in 10 mL of water and an aqueous solution of hydroxylamine (0.41 g, 6.28 mmol) was added to the mixture, before it was heated to its boiling point. The solution cleared up and upon cooling the solution to room temperature, the product crystallized as colorless thin needles. Yield: 88% (0.81 g, 5.53 mmol).

DSC (5 °C min⁻¹, °C): 173 (dec.); IR (KBr, cm⁻¹): $\tilde{\nu}$ = 3310 (s), 3201 (m), 2985 (s), 2859 (m), 2741 (vs), 2509 (m), 2178 (w), 2106 (w), 1702 (s), 1671 (s), 1631 (m), 1616 (m), 1587 (m), 1517 (s), 1385 (m), 1334 (m), 1240 (w), 1204 (m), 1173 (m), 1114 (m), 1069 (w), 1050 (w), 1009 (m), 795 (m), 718 (m), 681 (m), 656 (m), 536 (m); Raman (1064 nm, 350 mW, 25 °C, cm⁻¹): $\tilde{\nu}$ = 3139 (4), 2939 (5), 2723 (5), 1637 (5), 1605 (12), 1527 (53), 1395 (2), 1337 (5), 1207 (33), 1175 (26), 1115 (19), 1098 (100), 1071 (47), 1051 (19), 1011 (25), 811 (3), 783 (3), 725 (13), 521 (3), 440 (12), 310 (3), 284 (6), 250 (12), 217 (10); ¹H NMR (DMSO-*d*₆, 25 °C, ppm) δ : 10.06 (s, 4H, NH₃OH), 7.91 (s, 1H, CONH₂), 7.59 (s, 1H, CONH₂); ¹³C NMR

(DMSO-*d*₆, 25 °C, ppm) δ : 163.1 (CONH₂), 157.4 (CN₄); m/z (FAB⁺): 34.0 [NH₃OH⁺]; m/z (FAB⁻): 112.0 [C₂H₂N₅O⁻]; EA (C₂H₆N₆O₂, 146.11): calc.: C 16.44, H 4.14, N 57.52 %; found: C 16.66, H 3.93, N 57.08 %; BAM drophammer: 40 J; friction tester: 288 N; ESD: 0.15 J (at grain size 100-500 μ m).

Dihydroxylammonium 5,5'-azotetrazolate dihydrate (12)

Barium azotetrazolate pentahydrate (1.77 g, 4.52 mmol) is dissolved in 200 mL of boiling water. To the clear solution hydroxylammonium sulfate (0.742 g, 4.52 mmol), previously dissolved in 10 mL of water, is added and a white precipitate forms instantly. Since a slight gas evolution of the hot mixture could be observed, it was cooled in an ice bath and the precipitate was filtered off. The filtrate was evaporated in vacuum at not more than 40°C and the residue recrystallized from water to give **12** as large yellow plates. Yield: 72% (0.87 g, 3.25 mmol).

DSC (5 °C min⁻¹, °C): 130 °C (dec); IR (KBr, cm⁻¹): $\tilde{\nu}$ = 3255 (s), 2978 (vs), 2837 (s), 2715 (vs), 2464 (W9), 2271 (w), 2141 (m), 2098 (m), 2052 (m), 1641 (m), 1625 (m), 1562 (m), 1503 (w), 1477 (w), 1454 (m), 1405 (m), 1385 (m), 1260 (m), 1244 (m), 1203 (m), 1185 (m), 1171 (m), 1087 (w), 1075 (w), 1049 (w), 1000 (m), 829 (m), 774 (m), 737 (m), 664 (m), 629 (m), 561 (m), 492 (w); Raman (1064 nm, 300 mW, 25 °C, cm⁻¹): $\tilde{\nu}$ = 1483 (39), 1426 (12), 1391 (100), 1097 (39), 1081 (29), 1001 (3), 925 (6); ¹H NMR (DMSO-*d*₆, 25 °C, ppm) δ : 8.65 (s, br, NH₃OH); ¹³C NMR (DMSO-*d*₆, 25 °C, ppm) δ : 173.2 (CN₄); m/z (FAB⁺): 34.0 [NH₃OH⁺]; m/z (FAB⁻): 164.9 [C₂HN₁₀⁻]; EA (C₂H₁₂N₁₂O₄, 268.19): calc.: C 8.96, H 4.51, N 62.67 %; found: C 9.29, H 4.26, N 61.83 %; BAM drophammer: 25 J; friction tester: 192 N; ESD: 0.30 J (at grain size 500-1000 μ m).

Dihydroxylammonium diazo-1,2-di(tetrazol-5-yl-1-oxide) (13)

Barium azotetrazolate-oxide pentahydrate (3.41 g, 8.37 mmol) is dissolved in 100 mL of boiling water. To the clear solution hydroxylammonium sulfate (1.37 g, 8.37 mmol), previously dissolved in 10 mL of water, is added and a white precipitate forms instantly. The mixture was centrifuged to remove the BaSO₄ and the supernatant liquid was evaporated in vacuum. The residue was again treated with a few milliliters of water, heated to reflux and filtered to remove residual BaSO₄. The filtrate was left for crystallization. **13** crystallizes in medium sized yellow needles, however not as dark yellow as the azotetrazolate crystals of **8**. Yield: 85% (2.02 g, 7.11 mmol).

DSC (5 °C min⁻¹, °C): 175°C (dec. 1), 225°C (dec. 2); IR (KBr, cm⁻¹): $\tilde{\nu}$ = 3385 (s), 2983 (s), 2739 (vs), 2516 (w), 2133 (w), 2090 (w), 1659 (w), 1618 (m), 1535 (m), 1499 (m), 1476 (m), 1454 (m), 1412 (m), 1384 (m), 1292 (w), 1253 (w), 1215 (w), 1194 (w), 1187 (w), 1166 (w), 1104 (w), 1082 (w), 1068 (w), 1050 (w), 1042 (w), 995 (w), 917 (w), 773 (m), 753 (w), 725 (w), 655 (w), 626 (w), 520 (w); Raman (1064 nm, 300 mW, 25 °C, cm⁻¹): $\tilde{\nu}$ = 1500 (13), 1477 (10), 1453 (100), 1415 (28), 1380 (38), 1294 (3), 1189 (3), 1168 (4), 1105 (68), 1085 (21), 1069 (12), 1052 (5), 997 (5), 919 (2), 758 (1), 402 (2), 266 (4); ¹H NMR (DMSO-*d*₆, 25 °C, ppm) δ : 8.61 (s, br, NH₃OH); ¹³C NMR (DMSO-*d*₆, 25 °C, ppm) δ : 168.2 (N₄C-N), 162.5 (N₄C-N-O); ¹⁴N NMR (DMSO-*d*₆, 25 °C, ppm) δ : -69.8 (N₄C-N-O); m/z (FAB⁺): 34.0 [NH₃OH⁺]; m/z (FAB⁻): 181.0 [C₂HN₁₀O⁻]; EA (C₂H₁₂N₁₂O₅, 284.19): calc.: C 8.45, H 4.26, N

59.14 %; found: C 8.70, H 3.93, N 57.72 %; BAM drophammer: 30 J; friction tester: 160 N; ESD: 0.25 J (at grain size 100 - 500 μm).

Dihydroxylammonium 5,5'-bistetrazolate (14)

5,5'-Bistetrazole (1.38 g, 10 mmol) is dissolved in 20 mL of hot water. A solution of hydroxylamine (50% w/w in H_2O , 1.32 g, 20 mmol) is added slowly and the resulting clear solution is evaporated under vacuum. The colorless solid residue is recrystallized from ethanol/water to yield 1.79 g (8.8 mmol, 88%) of **1** as colorless, fine needles suitable for X-ray crystallography.

DSC (5 $^{\circ}\text{C min}^{-1}$, $^{\circ}\text{C}$): 205 $^{\circ}\text{C}$ (dec.); IR (KBr, cm^{-1}): $\tilde{\nu}$ = 3425 (m), 3030 (vs), 2815 (s), 2744 (s), 2203 (m), 2056 (m), 1987 (m), 1626 (m), 1534 (m), 1385 (w), 1339 (m), 1314 (m), 1247 (s), 1184 (m), 1145 (m), 1095 (w), 1056 (m), 1030 (m), 1000 (m), 769 (m), 725 (m); Raman (1064 nm, 350 mW, 25 $^{\circ}\text{C}$, cm^{-1}): $\tilde{\nu}$ = 2958 (1), 2752 (1), 1591 (100), 1436 (2), 1251 (1), 1205 (17), 1144 (9), 1224 (34), 1093 (17), 1002 (22), 779 (3), 426 (5), 387 (8); ^1H NMR ($\text{DMSO-}d_6$, 25 $^{\circ}\text{C}$, ppm) δ : 10.50 (s, 8H, NH_3OH); ^{13}C NMR ($\text{DMSO-}d_6$, 25 $^{\circ}\text{C}$, ppm) δ : 152.6 ($(\text{CN}_4)_2$); m/z (FAB $^+$): 34.0 [NH_3OH^+]; m/z (FAB $^-$): 137.0 [C_2HN_8]; EA ($\text{C}_2\text{H}_8\text{N}_{10}\text{O}_2$, 204.15) calc.: C 11.77, H 3.95, N 68.61 %; found: C 12.25, H 3.74, N 68.01 %; BAM drophammer: 10 J; friction tester: 240 N; ESD: 0.10 J (at grain size 100-500 μm).

Tetrazole-5-carboxamide-oxime monohydrate (15)

Sodium 5-cyanotetrazolate sesquihydrate was prepared according to literature.⁵⁶ The free acid 5-cyanotetrazole was synthesized by dissolving the sodium salt (3.20 g, 22.2 mmol) in 10 mL of water, adding 1 equivalent of nitric acid (2.15 g, 22.2 mmol, 65%) and heating the solution to reflux for a few minutes. The solution is evaporated in vacuum and the residue is extracted with absolute ethanol. The product crystallizes from the ethanolic solution in colorless crystals.

5-Cyanotetrazole (0.91 g, 9.6 mmol) is dissolved in 15 mL of boiling water and an aqueous solution of hydroxylamine (50%, 0.66 g, 10 mmol) is added. Very thin needles start to crystallize from the aqueous solution and the vessel is stored in a refrigerator for 1 hour for complete crystallization of the product. After isolation of the oxime, it was recrystallized from water. Elemental analysis proved the product to crystallize as a monohydrate.

DSC (5 $^{\circ}\text{C min}^{-1}$, $^{\circ}\text{C}$): 244 $^{\circ}\text{C}$ (dec.); IR (KBr, cm^{-1}): $\tilde{\nu}$ = 3315 (vs), 3128 (s), 3002 (s), 2849 (s), 2745 (s), 2649 (m), 1712 (s), 1650 (m), 1559 (m), 1462 (m), 1394 (m), 1386 (m), 1306 (m), 1199 (w), 1159 (w), 1133 (w), 1121 (w), 1092 (w), 1062 (w), 1047 (w), 1024 (w), 774 (m), 736 (m), 723 (m), 660 (m), 638 (m), 599 (w), 501 (m); Raman (1064 nm, 300 mW, 25 $^{\circ}\text{C}$, cm^{-1}): $\tilde{\nu}$ = 3116 (9), 1648 (9), 1578 (58), 1452 (18), 1400 (6), 1315 (13), 1199 (41), 1161 (31), 1125 (100), 1085 (84), 1062 (59), 1038 (41), 770 (17), 631 (9), 422 (47), 353 (12), 326 (9); ^1H NMR ($\text{DMSO-}d_6$, 25 $^{\circ}\text{C}$, ppm) δ : 10.51 (s, 1H, NOH), 7.09 (s, 2H, NH_2); ^{13}C NMR ($\text{DMSO-}d_6$, 25 $^{\circ}\text{C}$, ppm) δ : 150.7 (CN_4), 144.9 (CNH_2NOH); m/z (FAB $^+$): 129.0 [$\text{M}+\text{H}$] $^+$; m/z (FAB $^-$): 127.0 [$\text{M}-\text{H}$] $^-$; EA ($\text{C}_2\text{H}_6\text{N}_6\text{O}_2$, 146.11) calc.: C 16.44, H 4.14, N 57.52 %; found: C 17.10, H 3.76, N 57.83 %; BAM drophammer: >40 J (neg.); friction tester: 252 N; ESD: 0.08 J (at grain size 100 - 500 μm).

Acknowledgements

Financial support of this work by the Ludwig-Maximilian University of Munich (LMU), the U.S. Army Research Laboratory (ARL), the Armament Research, Development and Engineering Center (ARDEC), the Strategic Environmental Research and Development Program (SERDP) and the Office of Naval Research (ONR Global, title: "Synthesis and Characterization of New High Energy Dense Oxidizers (HEDO) - NICOP Effort ") under contract nos. W911NF-09-2-0018 (ARL), W911NF-09-1-0120 (ARDEC), W011NF-09-1-0056 (ARDEC) and 10 WPSEED01-002 / WP-1765 (SERDP) is gratefully acknowledged. The authors acknowledge collaborations with Dr. Mila Krupka (OZM Research, Czech Republic) in the development of new testing and evaluation methods for energetic materials and with Dr. Muhamed Sucesca (Brodarski Institute, Croatia) in the development of new computational codes to predict the detonation and propulsion parameters of novel explosives. We are indebted to and thank Drs. Betsy M. Rice and Brad Forch (ARL, Aberdeen, Proving Ground, MD) and Mr. Gary Chen (ARDEC, Picatinny Arsenal, NJ) for many helpful and inspired discussions and support of our work. For the measurement of the sensitivity data the authors want to thank Stefan Huber as well as Davin Piercey for the solution of the crystal structure of compound **1**.

4 References

- [1] (a) J. Giles, Collateral Damage, *Nature*, 427, p. 580-581, **2004**; (b) D. Carrington, *New Scientist*, 101, **2001**; (c) T. M. Klapötke, in *Moderne Anorganische Chemie*, Riedel, E. (Hrsg.), 3ed., Walter de Gruyter, Berlin, New York, p. 99-104, **2007**.
- [2] T. M. Klapötke, *High Energy Density Materials*, Springer, **2007**.
- [3] T. M. Klapötke, J. Stierstorfer, The CN_7^- -anion, *J. Am. Chem. Soc.*, 131, p. 1122-1134, **2009**.
- [4] P. Carlqvist, H. Ostmark, T. Brinck, The Stability of Arylpentazoles, *J. Phys. Chem. A*, 108, p. 7463-7467, **2004**.
- [5] T. M. Klapötke, J. Stierstorfer, Calcium 5-nitriminotetrazolate – A green replacement of lead azide, *New Trends in Research of Energetic Materials, Proceedings of the Seminar*, 12th, Pardubice, Czech Republic, 2, p. 825-831, **2009**.
- [6] N. Fischer, T. M. Klapötke, J. Stierstorfer, New Nitriminotetrazoles - Synthesis, Structures and Characterization, *Z. Anorg. Allg. Chem.*, 635, p. 271–281, **2009**.
- [7] T. M. Klapötke, J. Stierstorfer, A. U. Wallek, Nitrogen-Rich Salts of 1-Methyl-5-nitrimino-tetrazolate: An Auspicious Class of Thermally Stable Energetic Materials, *Chem. Mater.*, 20, p. 4519-4530, **2008**.
- [8] N. Fischer, T. M. Klapötke, D. Piercey, S. Scheutzwow, J. Stierstorfer, Diaminouronium Nitriminotetrazolates – Thermally Stable Explosives, *Z. Anorg. Allg. Chem.*, 636, p. 2357-2363, **2010**.
- [9] T. M. Klapötke, J. Stierstorfer, Nitration Products of 5-Amino-1*H*-tetrazole and Methyl-5-amino-1*H*-tetrazoles – Structures and Properties of Promising Energetic Materials, *Helv. Chim. Acta*, 90, p. 2132-2150, **2007**.
- [10] R. A. Henry, W. G. Finnegan, Mono-alkylation of sodium 5-aminotetrazole in aqueous medium, *J. Am. Chem. Soc.*, 76, p. 923-926, **1954**.

- [11] T. M. Klapötke, J. Stierstorfer, K. R. Tarantik, New Energetic Materials: Functionalized 1-Ethyl-5-aminotetrazoles and 1-Ethyl-5-nitriminotetrazoles, *Chem. Eur. J.*, 15, p. 5775-5792, **2009**.
- [12] T. M. Klapötke, P. Mayer, J. Stierstorfer, J. J. Weigand, Bistetrazolylamines - synthesis and characterization *J. Mat. Chem.*, 18, p. 5248-5258, **2008**.
- [13] J. Thiele, *Justus Liebigs Ann. Chem.*, 270, p. 54-63, **1892**; J. Thiele, J. T. Marais, *Justus Liebigs Ann. Chem.*, 273, p. 144-160, **1893**; J. Thiele, *Ber.*, 26, p. 2645-2646, **1893**; J. Thiele, *Justus Liebigs Ann. Chem.*, Azo- and hydrazo-compounds of tetrazole, 303, p. 57-75, **1898**.
- [14] H. Schottenberger, *private communication*, **2009**.
- [15] A. Hammerl, G. Holl, T. M. Klapötke, P. Mayer, H. Noeth, H. Piotrowski, M. Warchhold, *Eur. J. Inorg. Chem.*, Salts of 5,5'-azotetrazolate, 4, p. 834-845, **2002**.
- [16] M. A. Hiskey, D. E. Chavez, D. L. Naud, *Journal of Pyrotechnics*, High-nitrogen fuels for low-smoke pyrotechnics, 10, p. 17-36, **1999**.
- [17] CrysAlis CCD, Oxford Diffraction Ltd., Version 1.171.27p5 beta (release 01-04-2005 CrysAlis171.NET) (compiled Apr 1 2005,17:53:34).
- [18] CrysAlis RED, Oxford Diffraction Ltd., Version 1.171.27p5 beta (release 01-04-2005 CrysAlis171.NET) (compiled Apr 1 2005,17:53:34).
- [19] A. Altomare, G. Casciarano, C. Giacovazzo, A. Guagliardi, SIR-92, 1993, A program for crystal structure solution, *J. Appl. Cryst.*, 26, p. 343, **1993**.
- [20] G. M. Sheldrick SHELXS-97, Program for Crystal Structure Solution, Universität Göttingen, **1997**.
- [21] G. M. Sheldrick, SHELXL-97. Program for the Refinement of Crystal Structures. University of Göttingen, Germany, **1997**.
- [22] A. L. Spek, PLATON, A Multipurpose Crystallographic Tool, Utrecht University, Utrecht, The Netherlands, **1999**.
- [23] L. J. Farrugia, WinGX suite for small molecule single-crystal crystallography, *J. Appl. Cryst.*, 32, p. 837, **1999**.
- [24] SCALE3 ABSPACK - An Oxford Diffraction program (1.0.4,gui:1.0.3) (C), Oxford Diffraction Ltd., **2005**.
- [25] J. Stierstorfer, Energetic materials based on 5-aminotetrazole, *Dissertation*, Ludwig-Maximilians-Universität München, **2009**.
- [26] N. Fischer, T. M. Klapötke, J. Stierstorfer, New nitriminotetrazoles - Synthesis, structures and characterization, *Z. Anorg. Allg. Chem.*, 635, p. 271-281, **2009**.
- [27] B. Dickens, Crystal Structure of Hydroxylammonium Perchlorate at -150 °C, *Acta Crystallogr.*, B25, p. 1875-1882, **1969**.
- [28] R. Gilardi, R. J. Butcher, A new class of flexible energetic salts, part 6: the structures of the hydrazinium and hydroxylammonium salts of dinitramide, *J. Chem. Crystallogr.*, 30(9), p. 599-604, **2000**.
- [29] J. Bernstein, R. E. Davis, L. Shimon, N.-L. Chang, Patterns in hydrogen-bonding: Functionality and graph set analysis in crystals, *Angew. Chem. Int Ed.*, 34, p. 1555-1573, **1995**.
- [30] A. M. Astakhov, A. D. Vasiliev, M. S. Molokeev, A. M. Sirotinin, L. A. Kruglyakova, R. S. Stepanov, Crystal and Molecular Structure of Nitramino Derivatives of Tetrazole and 1,2,4-Triazole. II. 5-Nitraminotetrazole Diammonium Salt, *J. Struct. Chem.*, 45(1), p. 175-180, **2004**.
- [31] M. Friedrich, J. C. Gálvez-Ruiz, T. M. Klapötke, P. Mayer, B. Weber, J. J. Weigand, BTA Transition Metal Complexes – Antiferromagnetic Coupling in a Chain-Type Cop-

- per(II) Complex with a disguised End-to-End Azido Bridge, *Inorg. Chem.*, 44(22), p. 8044 - 8052, **2005**.
- [32] T. M. Klapötke, M. Stein, J. Stierstorfer, Salts of 1*H*-Tetrazole - Synthesis, Characterization and Properties, 634, p. 1711-1723, **2008**.
- [33] G. Herve, G. Jakob, Novel illustrations of the specific reactivity of 1,1-diamino-2,2-dinitroethene (DADNE) leading to new unexpected compounds, *Tetrahedron*, 63, p. 953-959, **2007**.
- [34] G. Bentivoglio, G. Laus, V. Kahlenberg, G. Nauer, H. Schottenberger, Crystal structure of bis(hydroxylammonium)-5,5'-azotetrazolate dihydrate, $(\text{NH}_3\text{OH})_2(\text{C}_2\text{N}_{10}) \times 2\text{H}_2\text{O}$, *Z. Kristallogr. – New Crystal Structures*, 223, p. 425-426, **2008**.
- [35] M. Göbel, K. Karaghiosoff, T. M. Klapötke, D. G. Piercey, J. Stierstorfer, Nitrotetrazolate-2*N*-oxides and the Strategy of *N*-Oxide Introduction, *J. Am. Chem. Soc.*, 132, p. 17216-17226, **2010**.
- [36] P. J. Steel, Heterocyclic tautomerism. XI. Structures of 5,5'-bitetrazole and 1-methyl-5-(2'-pyridyl)tetrazole at 130 K, *J. Chem. Cryst.*, 26, p. 399-402, **1996**.
- [37] P. J. Eulgem, A. Klein, N. Maggiorosa, D. Naumann, R. W. H. Pohl, New rare earth metal complexes with nitrogen-rich ligands: 5,5'-bitetrazolate and 1,3-bis(tetrazol-5-yl)triazenate - on the borderline between coordination and the formation of salt-like compounds, *Chem. Eur. J.*, 14, p. 3727-3736, **2008**.
- [38] <http://www.linseis.com>
- [39] Wiberg, N. in *Lehrbuch der Anorganischen Chemie / Holleman-Wiberg*, 102nd ed., Walter de Gruyter, Berlin, p. 667, 677, 720, **2007**.
- [40] N. Fischer, T. M. Klapötke, F. A. Martin, J. Stierstorfer, Energetic Materials based on 1-Amino-3-nitroguanidine, *New Trends in the Research of Energetic materials, Czech Republic, Proceedings of the Seminar, 13th*, p. 113-129, **2010**.
- [41] NATO standardization agreement (STANAG) on explosives, *impact sensitivity tests*, no. 4489, 1st ed., Sept. 17, **1999**.
- [42] WIWEB-Standardarbeitsanweisung 4-5.1.02, Ermittlung der Explosionsgefährlichkeit, hier der Schlagempfindlichkeit mit dem Fallhammer, Nov. 8, **2002**.
- [43] <http://www.bam.de>
- [44] NATO standardization agreement (STANAG) on explosive, *friction sensitivity tests*, no. 4487, 1st ed., Aug. 22, **2002**.
- [45] WIWEB-Standardarbeitsanweisung 4-5.1.03, Ermittlung der Explosionsgefährlichkeit oder der Reibeempfindlichkeit mit dem Reibeapparat, Nov. 8, **2002**.
- [46] Impact: Insensitive > 40 J, less sensitive ≥ 35 J, sensitive ≥ 4 J, very sensitive ≤ 3 J; friction: Insensitive > 360 N, less sensitive = 360 N, sensitive < 360 N a. > 80 N, very sensitive ≤ 80 N, extreme sensitive ≤ 10 N; According to the UN Recommendations on the Transport of Dangerous Goods (+) indicates: not safe for transport.
- [47] <http://www.ozm.cz>
- [48] T. Fendt, N. Fischer, T. M. Klapötke, J. Stierstorfer, N-rich salts of 2-methyl-5-nitraminotetrazole: Secondary explosives with low sensitivities, *Inorg. Chem.*, 50(4), p. 1447-1458, **2011**.
- [49] M. Sućeska, EXPLO5.4 program, Zagreb, Croatia, **2010**.
- [50] M. J. Frisch, G. W. Trucks, H. B. Schlegel, G. E. Scuseria, M. A. Robb, J. R. Cheeseman, G. Scalmani, V. Barone, B. Mennucci, G. A. Petersson, H. Nakatsuji, M. Caricato, X. Li, H. P. Hratchian, A. F. Izmaylov, J. Bloino, G. Zheng, J. L. Sonnenberg, M. Hada, M. Ehara, K. Toyota, R. Fukuda, J. Hasegawa, M. Ishida, T. Nakajima, Y. Honda, O. Kitao, H. Nakai, T. Vreven, J. A. Montgomery, Jr., J. E. Peralta, F. Ogliaro,

- M. Bearpark, J. J. Heyd, E. Brothers, K. N. Kudin, V. N. Staroverov, R. Kobayashi, J. Normand, K. Raghavachari, A. Rendell, J. C. Burant, S. S. Iyengar, J. Tomasi, M. Cossi, N. Rega, J. M. Millam, M. Klene, J. E. Knox, J. B. Cross, V. Bakken, C. Adamo, J. Jaramillo, R. Gomperts, R. E. Stratmann, O. Yazyev, A. J. Austin, R. Cammi, C. Pomelli, J. W. Ochterski, R. L. Martin, K. Morokuma, V. G. Zakrzewski, G. A. Voth, P. Salvador, J. J. Dannenberg, S. Dapprich, A. D. Daniels, Ö. Farkas, J. B. Foresman, J. V. Ortiz, J. Cioslowski, D. J. Fox, Gaussian 09, Revision A.1, Gaussian, Inc., Wallingford CT, **2009**.
- [51] (a) J. W. Ochterski, G. A. Petersson, and J. A. Montgomery Jr., A complete basis set model chemistry. V. Extensions to six or more heavy atoms, *J. Chem. Phys.*, 104, p. 2598, **1996**; (b) J. A. Montgomery Jr., M. J. Frisch, J. W. Ochterski G. A. Petersson, A complete basis set model chemistry. VII. Use of the minimum population localization method, *J. Chem. Phys.*, 112, p. 6532, **2000**.
- [52] (a) L. A. Curtiss, K. Raghavachari, P. C. Redfern, J. A. Pople, Assessment of Gaussian-2 and density functional theories for the computation of enthalpies of formation, *J. Chem. Phys.*, 106(3), p. 1063, **1997**; (b) E. F. C. Byrd, B. M. Rice, Improved prediction of heats of formation of energetic materials using quantum mechanical calculations, *J. Phys. Chem. A*, 110(3), p. 1005–1013, **2006**; (c) B. M. Rice, S. V. Pai, J. Hare, Predicting heats of formation of energetic materials using quantum mechanical calculations, *Combust. Flame*, 118(3), p. 445–458, **1999**.
- [53] T. Altenburg, T. M. Klapötke, A. Penger, J. Stierstorfer, Two Outstanding Explosives Based on 1,2-Dinitroguanidine: ammonium-dinitroguanidine and 1,7-Diamino-1,7-dinitrimino-2,4,6-trinitro-2,4,6-triazaheptane, *Z. Anorg. Allg. Chem.*, 636, p. 463–471, **2010**.
- [54] (a) M. S. Westwell, M. S. Searle, D. J. Wales, D. H. Williams, Empirical Correlations between Thermodynamic Properties and Intermolecular Forces, *J. Am. Chem. Soc.*, 117, p. 5013–5015, **1995**; (b) F. Trouton, *Philos. Mag.*, 18, p. 54–57, **1884**.
- [55] (a) H. D. B. Jenkins, H. K. Roobottom, J. Passmore, L. Glasser, Relationships among Ionic Lattice Energies, Molecular (Formula Unit) Volumes and Thermochemical Radii, *Inorg. Chem.*, 38(16), p. 3609–3620, **1999**. (b) H. D. B. Jenkins, D. Tudela, L. Glasser, Lattice Potential Energy Estimation for Complex Ionic Salts from Density Measurements, *Inorg. Chem.*, 41(9), p. 2364–2367, **2002**.
- [56] W. Friederich, Cyanotetrazole, ditetrazole, tetrazolecarbamide, tetrazole, and their salts. *German Patent*, DE 940898 19560329, **1956**.

Experimentally determined detonation velocities of new secondary explosives

Manuel Boehm, Niko Fischer, Dennis Fischer, Thomas M. Klapötke, Susanne Scheutzow and Jörg Stierstorfer

Energetic Materials Research, Department of Chemistry,
University of Munich (LMU), Butenandtstr. 5-13, D-81377, Germany

finch@cup.uni-muenchen.de

Abstract:

The detonation velocities of several compounds with possible application as new secondary explosives were experimentally determined in an OZM laboratory detonation chamber (model KV-250) using the fiber optic technique. The investigated explosives are 1-amino-3-nitroguanidine (1), diaminouronium nitrate (2), dihydroxylammonium 5,5-bistetrazolate (3), hydroxylammonium 5-nitriminotetrazolate (4), oxalylhydrazide nitrate (5) and 1,3,5-triaminoguanidinium 1-methyl-5-nitriminotetrazolate (6). The compounds were synthesized on a 20 g scale, loaded into a PE tube and initiated with an electrically ignited detonator. If necessary, PETN or RDX were used as a booster charge. The measured detonation velocity was recorded using the OZM EXPLOMET-FO-2000 system and were compared to the calculated detonation parameters using the EXPLO5 code with the respective loading density of the compound.

Keywords: Booster Charge; Detonation Parameters; Detonation Velocity; Fiber Optic Technique; Secondary Explosives.

1 Introduction

Nitrogen rich compounds play a major role in the development of new energetic materials for the use as (gun-) propellants, explosives and pyrotechnics.[1] A main subject in our research group are secondary explosives and potential RDX replacements. The high demand of versatility is the major challenge that is faced in designing and inventing new nitrogen rich materials. Such materials should feature high thermal and mechanical stabilities and at the same time should be as high performing as possible, regarding the detonation velocity, detonation pressure and heat of explosion. Furthermore, environmental compatibility is a big issue nowadays. Unfortunately, this combination of requirements is rarely achieved.[2,3] Whereas the thermal stability as well as the sensitivity and compatibility of new potential RDX replacements can be determined comparatively easy in laboratory experiments, the only common method for obtaining the performance data is computational calculation. To compare the computational data with real performance, experimentally determined performance tests need to be carried out. In the following, the detonation velocities of several promising new secondary explosives were experimentally determined.

2 Results and Discussion

2.1 Compounds

The detonation velocities of 1-amino-3-nitroguanidine (**1**), diaminouronium nitrate (**2**), dihydroxylammonium 5,5-bistetrazolate (**3**), hydroxylammonium 5-nitriminotetrazolate (**4**), oxalyldihydrazide nitrate (**5**) and 1,3,5-triaminoguanidinium 1-methyl-5-nitriminotetrazolate (**6**), shown in Fig. 1, were experimentally determined and afterwards compared with the values calculated using the EXPLO5 (V5.04) code.

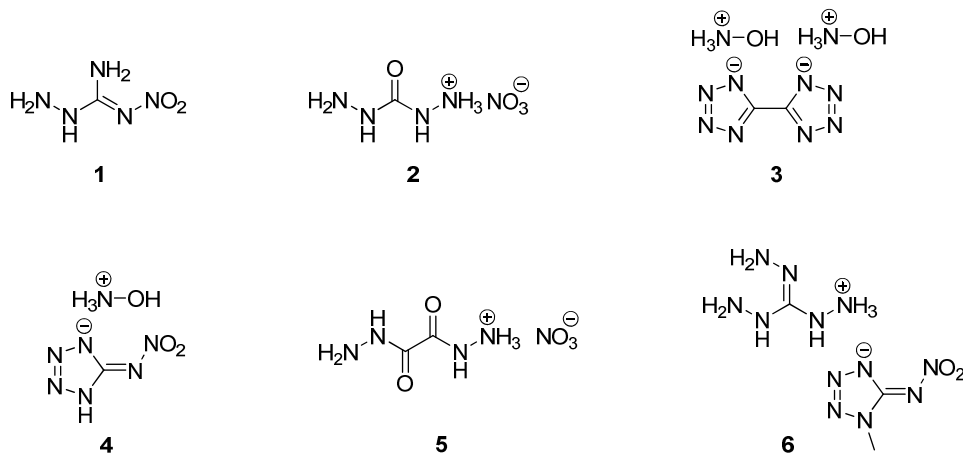


Figure 1: Overview of the investigated compounds 1–6.

Mostly all the investigated compounds meet the high requirements for new secondary explosives, which means, the performance data exceed those or are at least comparable to those of commonly used RDX (Table 1). Apart from **4**, all compounds show mechanical stability towards impact, friction and electrical discharge as well as high decomposition temperatures of higher than 180 °C. The calculated performance data, in particular the detonation velocities, also reveal the potential of the compounds regarding the applicability as new secondary explosives.

Compounds **1**, **2**, **3** and **6** were synthesized according to literature.[4,5,6,7] For the preparation of **4** and **5**, the following procedure was used: Oxalyldihydrazide [8] as well as 5-nitriminotetrazole [9] were prepared according to literature. Hydroxylammonium 5-nitriminotetrazolate (**4**) was prepared by dissolving 5-nitriminotetrazole in water and following addition of aqueous hydroxylamine. Oxalyldihydrazide nitrate (**5**) was prepared by simple protonation of oxalyldihydrazide with dilute nitric acid.[10]

Table 1: Sensivity, stability and performance date of compounds 1–6.

	1	2	3	4	5	6	RDX
Formula	CH ₅ N ₅ O ₂	CH ₇ N ₅ O ₄	C ₂ H ₈ N ₁₀ O ₂	CH ₅ N ₇ O ₃	C ₂ H ₇ N ₅ O ₅	C ₃ H ₁₂ N ₁₂ O ₂	C ₃ H ₆ N ₆ O ₆
FW / g mol ⁻¹	119.08	153.12	204.15	163.13	181.11	248.21	222.12
IS / J	20	9	10	2	11	8	7.5
FS / N	144	288	240	40	>360	240	120
ESD / J	0.15	0.60	0.10	0.30	0.30	0.40	0.1-0.2
N / %	58.81	45.74	68.60	60.12	38.67	67.72	37.80
Ω / %	-33.6	-15.7	-47.0	14.7	-22.1	-64.5	-21.6
T _{Dec.} / °C	184	242	200	180	270	210	210
ρ / g cm ⁻³	1.767	1.782	1.742	1.785	1.840	1.570	1.800
Δ _f H _m ^o / kJ kg ⁻¹	+77	-180	+428	+291	-299	+569	+70
Δ _f U ^o / kJ kg ⁻¹	+770	-1048	+2227	+1895	-1536	+2419	+417
EXPLO5 values:							
-Δ _{Ex} U ^o / kJ kg ⁻¹	4934	5048	4841	6113	4661	4781	6125
T _{det} / K	3436	3391	3248	4219	3275	3091	4236
P _{CJ} / kbar	323	335	317	371	325	255	349
D / m s ⁻¹	8977	8903	8858	9236	8655	8309	8748
V _o / L kg ⁻¹	890	910	843	853	827	847	739

2.2 Experimental setup

The detonation velocities of all compounds were experimentally determined in an OZM laboratory detonation chamber (model KV-250) using the fiber optic technique. This method is based on the autoluminescence of the detonation wave.[11] Since the optical fibre is a capable means of detecting the detonation wave passage and then transporting the signal to the detector station without delay due to the high time resolution, it was the method of choice. For signal detection the OZM detonating velocity measuring system EXPLOMET-FO-2000 was used. The charge was directly loaded and pressed into a PE tube which served as confinement. A density as high as possible, applying this loading method, was aspired. The dimensions of the sleeves were standardized to a depth of 100 mm and 14 mm respectively 20 mm in diameter. Three optical fibres were used for signal detection with an approximate distance of 50 mm to the detonator and a distance of 14 mm between each fibre. For the ignition of the sample only an electrically ignited detonator (ORICA, DYNADET C2-25MS) was used to avoid an eventual influence of the booster on the measured detonation velocities. RDX or PETN, respectively, were used in case the sample was not ignitable only by the detonator cap.

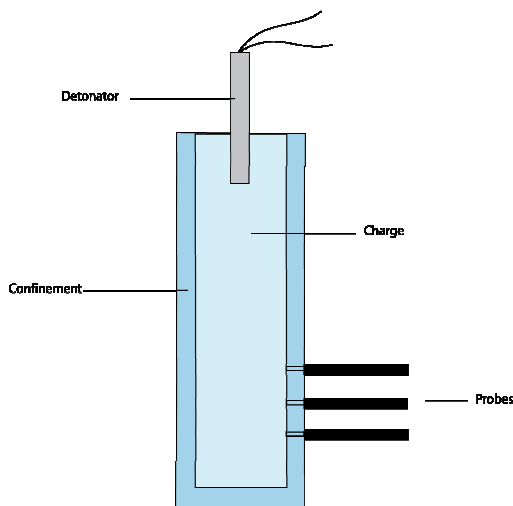


Figure 2: Schematic view of the used setup.

2.3 Experimentally determined velocities

The results of the measurements are shown in Tables 2–7. Conspicuously is that the single detonation velocities of the particular experiments show enormous deviance up to more than thousands of meters per second.

The detonation velocities of 1-amino-3-nitroguanidine (**1**), $D_{1,2}$ in **VOD_1** with 9650 m s^{-1} and $D_{2,3}$ in **VOD_2** with 9493 m s^{-1} (Table 2), exceed the detonation velocities calculated with the crystal density, whereas the other respective detonation velocities diverge from these values extremely.

To ignite the diaminouronium nitrate (**2**), 0.32 g PETN as a booster charge was necessary. The measured individual detonation velocities are approx. 6000 m s^{-1} (Table 3).

Dihydroxylammonium 5,5-bistetrazolate (**3**) could not be ignited above a density of 1.162 g cm^{-3} . The assumption of a higher critical diameter with the increasing density of **3** could not be verified because even increasing the diameter to 20.5 mm in **VOD_3** did not result in the desired detonation (Table 4).

The average detonation velocity of hydroxylammonium 5-nitriminotetrazolate (**4**) is consistent with the computational value, even though the individual detonation velocities differ by 2000 m s^{-1} (Table 5).

Oxalylhydrazide nitrate (**5**) showed extremely different detonation velocities in **VOD_1** and **VOD_2** (Table 6) despite analogue conditions. The average detonation velocities of **VOD_3** - **VOD_5** of compound **5** correspond with the calculated values.

Analogue to compound **3**, 1,3,5-triaminoguanidinium 1-methyl-5-nitriminotetrazolate (**6**) was not ignitable above a density of 1.169 g cm^{-3} , however, at higher densities it could be ignited by using 0.2 g PETN / 0.3 g RDX as booster (Table 7).

Table 2: Experimental detonation velocity data of **1**.

1	VOD_1	VOD_2
\emptyset / mm	14.1	14.1
h_{empty} / mm	100.1	100.2
h_{loaded} / mm	73.9	93.9
m / g	16.1	21.8
ρ / g cm ⁻³	1.387	1.481
m_{Booster} / g	0.3 (PETN)	-
$x_{1,2}$ / mm	15.4	14.7
$x_{2,3}$ / mm	14.3	14.2
$D_{1,2}$ / m s ⁻¹	9650	7726
$D_{2,3}$ / m s ⁻¹	5958	9493
$D_{\text{av.}}$ / m s ⁻¹	7804	8610
$D_{\text{calc.}}$ / m s ⁻¹	7507	7846

Table 3: Experimental detonation velocity data of **2**.

2	VOD_1	VOD_2
\emptyset / mm	14.1	14.1
h_{empty} / mm	100.4	100.2
h_{loaded} / mm	83.7	86.7
m / g	17.0	20.0
ρ / g cm ⁻³	1.305	1.482
m_{Booster} / g	-	0.32 (PETN)
$x_{1,2}$ / mm	14.6	14.2
$x_{2,3}$ / mm	14.3	14.1
$D_{1,2}$ / m s ⁻¹	-	6780
$D_{2,3}$ / m s ⁻¹	-	5862
$D_{\text{av.}}$ / m s ⁻¹	-	6321
$D_{\text{calc.}}$ / m s ⁻¹	7246	7855

Table 4: Experimental detonation velocity data of **3**.

3	VOD_1	VOD_2	VOD_3	VOD_4	VOD_5
\emptyset / mm	14.1	14.0	20.5	14.0	14.0
h_{empty} / mm	100.4	99.9	100.0	99.9	99.9
h_{loaded} / mm	82.2	86.4	92.9	87.8	90.0
m / g	15.0	18.5	40.0	19.0	10.0
ρ / g cm ⁻³	1.162	1.389	1.303	1.401	0.721
m_{Booster} / g	-	-	1.0 (RDX)	0.3 (PETN)	-
$x_{1,2}$ / mm	14.5	14.0	14.8	14.0	14.1
$x_{2,3}$ / mm	13.9	13.9	13.9	14.0	14.0
$D_{1,2}$ / m s ⁻¹	3381	-	-	-	4375
$D_{2,3}$ / m s ⁻¹	5572	-	-	-	3888
$D_{\text{av.}}$ / m s ⁻¹	4477	-	-	-	4132
$D_{\text{calc.}}$ / m s ⁻¹	6387	-	-	-	4695

Table 5: Experimental detonation velocity data of **4**.

4	VOD_1
\emptyset / mm	14.2
h_{empty} / mm	100.4
h_{loaded} / mm	85.8
m / g	15.0
ρ / g cm ⁻³	1.101
m_{Booster} / g	-
$x_{1,2}$ / mm	14.4
$x_{2,3}$ / mm	14.1
$D_{1,2}$ / m s ⁻¹	7220
$D_{2,3}$ / m s ⁻¹	5211
$D_{\text{av.}}$ / m s ⁻¹	6216
$D_{\text{calc.}}$ / m s ⁻¹	6525

Table 6: Experimental detonation velocity data of **5**

5	VOD_1	VOD_2	VOD_3	VOD_4	VOD_5
Ø / mm	14.1	14.0	14.1	20.6	14.0
h _{empty} / mm	100.2	100.0	100.1	100.1	100.1
h _{loaded} / mm	88.8	87.3	88.3	90.0	87.2
m / g	22.0	20.0	18.0	39.9	19.4
ρ / g cm ⁻³	1.577	1.486	1.309	1.331	1.443
m _{Booster} / g	0.3 (PETN)	-	-	-	-
x _{1,2} / mm	14.0	14.0	14.0	13.8	14.1
x _{2,3} / mm	14.1	14.0	14.0	14.1	14.0
D _{1,2} / m s ⁻¹	5048	14020	5600	8088	5620
D _{2,3} / m s ⁻¹	4689	3927	7777	6125	8763
D _{av.} / m s ⁻¹	4869	8974	6689	7107	7192
D _{calc.} / m s ⁻¹	7765	7401	6877	6949	7318

Table 7: Experimental detonation velocity data of **6**.

6	VOD_1	VOD_2	VOD_3	VOD_4
Ø / mm	14.0	14.2	14.2	14.0
h _{empty} / mm	100.2	100.4	100.3	100.0
h _{loaded} / mm	85.8	88.8	85.7	85.5
m / g	22.0	22.0	20.0	15.4
ρ / g cm ⁻³	1.667	1.564	1.473	1.169
m _{Booster} / g	-	0.3 (PETN)	0.8 (PETN)	0.2 (PETN) / 0.3 (RDX)
x _{1,2} / mm	14.3	14.0	14.5	14.0
x _{2,3} / mm	14.1	14.1	14.0	13.9
D _{1,2} / m s ⁻¹	-	-	-	3671
D _{2,3} / m s ⁻¹	-	-	-	3236
D _{av.} / m s ⁻¹	-	-	-	3454
D _{calc.} / m s ⁻¹	8702	8290	7935	6443

2.4 Comparison with calculated values

The calculation of the detonation parameters was performed by using the program EXPLO5 V5.04.[12] The program is based on the steady-state model of equilibrium detonation and uses the Becker-Kistiakowsky-Wilson equation of state (BKW EOS) for gaseous detonation products and the Cowan-Fickett equation of state for solid carbon.[13] The calculation of the equilibrium composition of the detonation products is done by applying the modified White-Johnson-Dantzig free energy minimization technique. The program is designed to enable the calculation of detonation parameters at the Chapman-Jouguet (CJ) point. The BKW equation in the following form was used with the Becker-Kistiakowsky-Wilson-Neumann (BKWN) set of parameters (α , β , κ , θ) as stated below, with X_i being the mol fraction and k_i the molar covolume of the i -th gaseous product.[13,14]

$$pV / RT = 1 + \kappa e^{\beta x} \quad x = (\kappa \sum X_i k_i) / [V(T + \theta)]^\alpha$$

$$\alpha = 0.5, \beta = 0.176, \kappa = 14.71, \theta = 6620.$$

The calculations were performed using the respective density achieved in the particular experiments (Tables 2–7).

The measured detonation velocities between the optical fiber 1 and 2 and between 2 and 3 were averaged and compared to the values computed with the EXPLO5 (version 5.04) code. Although the average values of several measurements of the compounds **1**, **3**, **4** and **5** match the computational values very well, a significant deviation of the measured detonation velocities in each experiment is observed. These circumstances and also the occurrence of measured detonation velocities, which even exceed the values, which were calculated with the theoretical maximum densities, show the complexity of experimentally determined detonation velocities.

2.5 Discussion

Several parameters have an influence on the behavior of detonations. First of all, the density of the substance plays a major role in the experiments concerning detonation velocities. The denser the sample is pressed into the tube, the higher is the detonation velocity, whereas high homogeneity throughout the whole length is aspired. However, directly pressing the loose sample into the tube causes layers of different densities and a density gradient in the tube. This may have a significant effect on the detonation velocity, since the velocity increases in more dense layers, which can be a reason for the variance of the single velocities measured. In addition, the pressure of the shock wave leads to a dynamic compression of the unreacted substance, resulting in a significant temperature and pressure increase, which obviously has different effects depending on the density.

Secondly, air gaps are a main issue concerning detonations and the shock front in particular. Since the shock front travels faster through air gaps than through the explosive material, this leads to an inhomogeneous and faster forwarding of the detonation front, which suggests a higher detonation velocity. To avoid these air gaps a high density was aspired which resulted in the above mentioned inhomogeneous density.

An additional negative effect of high density can be seen in the detonation velocity tests with dihydroxylammonium 5,5-bistetrazolate (**3**), which became unreactive due to the high pressure.

For good detonation velocity measurements, a stable and mainly planar detonation front is required. In the early stages of the detonation, the detonation front expands tapered and becomes planar with increasing propagation. Thus, a preferably long distance between the point of ignition and the first optical fibre is desired. Therefore a large amount of the explosive is required and compromises between the tube length and the amount of material had to be made.

The tube length and the preferably long traveling distance of the detonation front to the first optical fibre also limited the distance between the points of measurement, which leads to a higher error margin. In addition, the diameter of the optical fibre itself, for 1 mm in diameter with a distance of 14 mm to the next optical fibre leads to a higher range of error.

Considering all the above mentioned complex problems, some improvements of the experimental setup have to be made. A good starting point would be a preferably long tube/confinement with an appropriate diameter for the respective substance, to provide a stable and planar detonation front. For a direct loading and pressing of the substance into the tube, a method has to be found to provide homogeneous density. Alternatively, the substance can be pressed outside the tube into pellets prior to use and loaded afterwards. However, with this method an exact fit of the pellet and the tube has to be granted to avoid clear spacing between the pellet and the inner tube surface.

In conclusion, it can be said that the experimental determination of detonation velocities is a very complex task with many parameters and effects to consider, which influence and interfere with each other. Despite the experimentally determined detonation velocities, the tested compounds, e.g. 1-amino-3-nitroguanidine (**1**), dihydroxylammonium 5,5'-bistetrazolate (**3**) or oxalylhydrazide nitrate (**5**) remain promising new secondary explosives since on the one hand they are cheap and easy to synthesize and on the other hand they have very good calculated detonation parameters.

3 Experimental Part

Hydroxylammonium 5-nitriminotetrazolate (4)

5-Nitriminotetrazole (1.59 g, 12.2 mmol) is dissolved in a few millilitres of water and a solution of silver nitrate (2.07 g, 12.2 mmol) is added. Silver 5-nitriminotetrazolate precipitates instantly as a white solid. It is sucked off and washed with water until free of acid. The white solid is resuspended in 50 mL of warm water and treated with a solution of hydroxylammonium chloride (0.84 g, 13.0 mmol) in 20 mL of water. The mixture is stirred at 30°C for 1 h in the dark and the formed silver chloride is filtered off. The filtrate is evaporated and the residue was recrystallized from an ethanol/water mixture to yield **4** as a white solid (1.70 g, 10.4 mmol, 85%).

DSC (5 °C min⁻¹, °C): 180 °C (dec.); IR (KBr, cm⁻¹): $\tilde{\nu}$ = 3125 (s), 2958 (s), 2776 (m), 2711 (s), 1617 (m), 1598(m), 1539 (s), 1431 (s), 1383 (m), 1321 (vs), 1244 (m), 1213 (m), 1188 (m), 1153 (m), 1108 (m), 1061 (m), 1039 (m), 1003 (m), 872 (w), 823 (w), 777 (w), 753 (w), 742 (w), 700 (w), 493 (w); Raman (1064 nm, 300 mW, 25 °C, cm⁻¹): $\tilde{\nu}$ = 2715 (1), 1541 (100), 1452 (1), 1433 (1), 1381 (4), 1332 (36), 1158 (7), 1110 (4), 1070 (4), 1036 (22), 1014 (85), 875 (8), 744 (14), 695 (1), 494 (3), 427 (4), 413 (15); ¹H NMR (DMSO-*d*₆, 25 °C, ppm) δ : 10.95 (s); ¹³C NMR (DMSO-*d*₆, 25 °C, ppm) δ : 158.3 (CN₄); m/z (FAB⁺): 34.0 [NH₃OH⁺]; m/z (FAB⁻): 129.1 [HATNO₂⁻]; EA (CH₅N₇O₃, 163.10): calc.: C 7.36, H 3.09, N 60.12 %; found: C 7.38, H 3.17, N 57.40 %; BAM drophammer: 2 J; friction tester: 40 N; ESD: 0.30 J (at grain size 100 - 500 μ m).

Oxalyldihydrazide nitrate (5)

1.18 g (10 mmol) oxalyldihydrazide was suspended in a mixture of 5.5 mL 2M HNO₃ and 10 mL water. The suspension was heated up while stirring until all oxalyldihydrazide has dissolved and then poured into 20 mL of ethanol. The resulting suspension was cooled to 5 °C, filtered and dried yielding 1.68 g (93%) of colorless crystalline **5**.

DSC (5 °C min⁻¹): 273 °C (dec.); IR (ATR, cm⁻¹): $\tilde{\nu}$ = 3307 (w), 3178 (w), 3028 (w), 2775 (w), 1674 (m), 1531 (m), 1326 (s), 1243 (s), 1152 (w), 1088 (w), 995(m), 802 (m), 709 (m); Raman (1064 nm, 300 mW, 25 °C, cm⁻¹): $\tilde{\nu}$ = 3224 (4), 1735 (9), 1703 (15), 1584 (12), 1553 (28), 1346 (19), 1289 (23), 1206 (9), 1094 (10), 1049 (100), 1003 (4), 938 (15), 812 (2), 719 (7), 510 (5), 400 (5); ¹H NMR (DMSO-*d*₆, 25 °C, ppm) δ : 8.28 ¹³C{¹H} NMR (DMSO-*d*₆, 25 °C, ppm) δ : 157.8; EA (C₂H₇N₅O₅, 181.11): calc.: C 13.26, H 3.90, N 38.67 %; found: C 13.50, H 3.74, N 38.59 %; BAM drophammer: 11 J; friction tester: >360 N; ESD: 0.3 J (at grain size 500-1000 μ m).

Acknowledgment

Financial support of this work by the Ludwig-Maximilian University of Munich (LMU), the U.S. Army Research Laboratory (ARL), the Armament Research, Development and Engineering Center (ARDEC), the Strategic Environmental Research and Development Program (SERDP) and the Office of Naval Research (ONR Global, title: "Synthesis and Characterization of New High Energy Dense Oxidizers (HEDO) - NICOP Effort") under contract nos. W911NF-09-2-0018 (ARL), W911NF-09-1-0120 (ARDEC), W011NF-09-1-0056 (ARDEC) and 10 WPSEED01-002 / WP-1765 (SERDP) is gratefully acknowledged.

The authors acknowledge collaborations with Dr. Mila Krupka (OZM Research, Czech Republic) in the development of new testing and evaluation methods for energetic materials and with Dr. Muhamed Sucasca (Brodarski Institute, Croatia) in the development of new computational codes to predict the detonation and propulsion parameters of novel explosives.

We are indebted to and thank Drs. Betsy M. Rice and Brad Forch (ARL, Aberdeen, Proving Ground, MD) and Mr. Gary Chen (ARDEC, Picatinny Arsenal, NJ) for many helpful and inspired discussions and support of our work.

References

- [1] L. V. De Yong, G. Campanella, A study of blast characteristics of several primary explosives and pyrotechnic compositions, *J. Hazard. Mater.*, 21, p. 125-133, **1989**.
- [2] T. M. Klapötke, J. Stierstorfer, The CN₇-anion, *J. Am. Chem. Soc.*, 131, p. 1122-1134, **2009**.
- [3] A. K. Sikder, N. Sikder, A review of advanced high performance, insensitive and thermally stable energetic materials emerging for military and space applications, *J. Hazard. Mater.*, 112, p. 1-15, **2004**.
- [4] N. Fischer, T. M. Klapötke, F. A. Martin, J. Stierstorfer, Energetic materials based on 1-amino-3-nitroguanidine, *New Trends in Research of Energetic Materials, Proceedings of the Seminar*, 13th, Pardubice, Czech Republic, Apr. 21-23, 1, p. 113-129, **2010**.
- [5] N. Fischer, T. M. Klapötke, J. Stierstorfer, Explosives based on Diaminourea, *Propellants Explos. Pyrotech.*, in press, **2011**.
- [6] M. A. Hiskey, D. E. Chavez, D. L. Naud, High-nitrogen fuels for low-smoke pyrotechnics, *J. Pyrotech.*, 10, p. 17-36, **1999**.
- [7] T. M. Klapötke, J. Stierstorfer, A. U. Wallek, Nitrogen-Rich Salts of 1-Methyl-5-nitrimino-tetrazolate: An Auspicious Class of Thermally Stable Energetic Materials, *Chem. Mater.*, 20, p. 4519-4530, **2008**.
- [8] T. Curtius, K. Hochschwender, Hydrazides and azides of organic acids. XXXI. The hydrazides and azides of oxalic acid, *J. Prakt. Chem.*, 91, p. 415-441, **1915**.
- [9] T. M. Klapötke, J. Stierstorfer, Nitration Products of 5-Amino-1H-tetrazole and Methyl-5-amino-1H-tetrazoles – Structures and Properties of Promising Energetic Materials, *Helv. Chim. Acta*, 90, p. 2132-2150, **2007**.
- [10] D. Fischer, master thesis, Ludwig-Maximilians Universität München, **2010**.
- [11] M. Suceska, *Fragblast: International Journal for Blasting and Fragmentation*, 1, p. 23, **1997**.
- [12] M. Suceska, *EXPLO5.04 program*, Zagreb, Croatia **2010**.
- [13] M. Suceska, Calculation of the detonation properties of C-H-N-O explosives, *Propellants Explos. Pyrotech.*, 16(4), p. 197-202, **1991**.
- [14] a) M. Suceska, Calculation of detonation parameters by EXPLO5 computer program, *Material Science Forum*, p. 465-466, **2004**; b) M. Suceska, Evaluation of detonation energy from EXPLO5 computer code results, *Propellants Explos. Pyrotech.*, 24(5), p. 280-285, **1999**; c) M. L. Hobbs, M. R. Baer, *Proceedings of the 10th Symposium (International) on Detonation*, ONR 33395-12, Boston, MA, July 12-16, 1, **1993**.

Highly sensitive 3,5-diazidotriazole and the binary C_2N_9^- anion

Niko Fischer, Thomas M. Klapötke, Jörg Stierstorfer and Elija N. Wiedemann

Energetic Materials Research, Department of Chemistry,
University of Munich (LMU), Butenandtstr. 5-13, D-81377, Germany

tmk@cup.uni-muenchen.de

Abstract:

3,5-Diazido-1,2,4-triazole (**1**) was yielded by diazotation of 3,5-diaminotriazole followed by the addition of sodium azide. The ammonium (**2**) and hydrazinium (**3**) salts were synthesized by facile deprotonation reactions. Compounds **1** and **2** were characterized by single crystal X-ray diffraction. In addition, a systematic characterization of the chemical and energetic properties was carried out including vibrational and NMR spectroscopy, mass spectrometry and differential scanning calorimetry. The sensitivities were determined with a BAM drophammer, BAM friction tester and a small scale electrostatic discharge device. The detonation parameters of **1** were calculated by the EXPLO5.04 computer code using the X-ray density and the theoretically obtained energy of formation.

Keywords: azides; triazoles; primary explosives; sensitivities.

1 Introduction

The research of “green” primary and secondary explosives is an ongoing project in many research groups. In future primary explosives, the use of toxic heavy metal salts, e.g. lead azide and lead styphnate should be strongly reduced. Nitrogen-rich derivatives with a fast deflagration-to-detonation transition are promising alternatives as primary explosives since the formation of molecular nitrogen as an end-product their decomposition is highly desirable. To obtain suitable sensitivities azide-substituted heterocycles are in the focus. In accordance to recently described 5-azidotetrazoles [1], azidotriazoles (3-azido-1,2,4-triazole [2] and 3,5-diazido-1,2,4-triazole) also show high nitrogen contents.

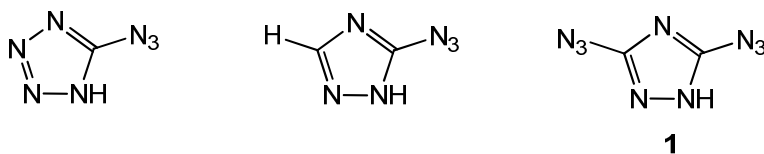


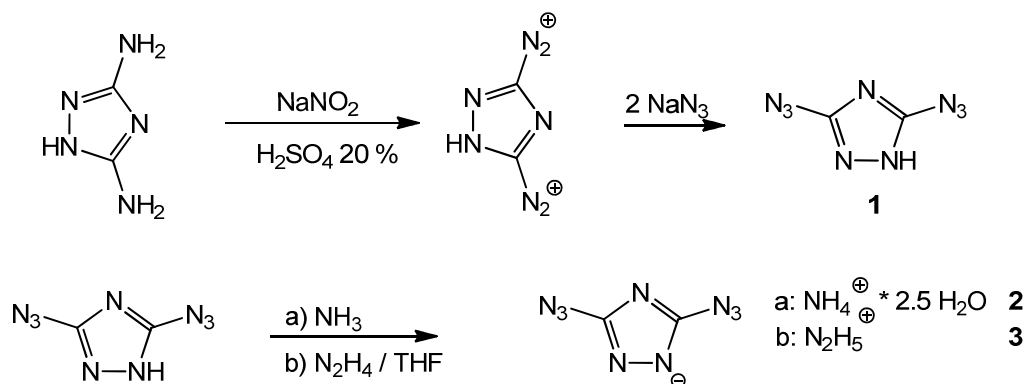
Figure 1: 5-Azidotetrazole, 3-azido-triazole and 3,5-diazidotriazole.

The use of nitrogen rich heterocycles in energetic materials is expedient due to several reasons, e.g. (i) The aromatic ring system mostly yields to stabilized compounds, (ii) the standard heats of formation of the unsubstituted cycles rises with the nitrogen content from imidazole ($\Delta H_f^\circ(\text{cryst.}) = 58.5 \text{ kJ/mol}$) [3] to 1,2,4-triazole ($\Delta H_f^\circ(\text{cryst.}) = 109 \text{ kJ/mol}$) [4] to tetrazole ($\Delta H_f^\circ(\text{cryst.}) = 237.2 \text{ kJ/mol}$). [5] By inserting further nitrogen-containing groups, such as hydrazine or azide to these heterocycles, the heat of formation can be easily multiplied. Replacing one C-H atom by a C-N₃ group ΔH_f° can be increased about $\approx 450 \text{ kJ/mol}$ [5]. 3,5-Diazido-1,2,4-triazole has been described in the literature [6] before. Also its protonation with mineralic acids such as HNO_3 was described. [6] Surprisingly, the deprotonation reaction, which usually leads to an increase in stability, has never been discussed in literature. We now report on 3,5-

diazido-1,2,4-triazole (**1**) including its structure, sensitivities and calculated energetic properties ($\Delta H_f^\circ = 812$ kJ/mol). Deprotonation of **1** has been accomplished by ammonia and hydrazine. Up to now, hydrazinium diazido-1,2,4-triazolate is the triazole with the highest nitrogen content of 84.13 %, including the binary $C_2N_9^-$ anion, which was elucidated by X-ray diffraction for the first time. The ammonium (**2**) and hydrazinium (**3**) salts were characterized to the best of our experimental skills and the influence on thermal stability and sensitivities is discussed.

2 Results and discussion

3,5-Diazidotriazole has been synthesized by a modified procedure analog to the literature.[7] Deprotonation was obtained either by the addition of aqueous ammonia solution or hydrazine solution in THF. The colorless ammonium salt (**2**) was obtained crystalline only with inclusion of two and a half molecules of crystal water per molecular unit by slow evaporation of an aqueous solution. The needle like crystals were stored under Kel-F oil immediately. Salt **3** precipitates quickly after the addition of hydrazine solution to a solution of **1** in THF. Unfortunately, **2** crystallizes in very fine colorless needles too small for single crystal X-ray diffraction. Both compounds decompose to uncharged diazidotriazole and ammonia or hydrazine, respectively, simple standing at ambient conditions. However, the loose of ammonia is much faster than that of hydrazine. Therefore, the ammonia salt must be immediately stored under inert conditions (e.g. under perfluorinated oil) for further characterization. In summary, both salt are not long term stable.



Scheme 1: Synthesis of 3,5-diazidotriazole and its ammonium and hydrazinium salt.

Suitable single crystals of **1** and its ammonium salt **2** were picked from the crystallization mixture and mounted in Kel-F oil, transferred to the N_2 stream of an Oxford Xcalibur3 diffractometer with a Spellman generator (voltage 50 kV, current 40 mA) and a KappaCCD detector. The data collection was performed using the CRYALIS CCD software [8], the data reduction using the CRYALIS RED software [9]. The structures were solved with SIR-92 [10] and SHELXS-97 [11] refined with SHELXL-97 [12] and finally checked using the PLATON software [13] integrated in the WINGX software suite.[14] The non-hydrogen atoms were refined anisotropically and the hydrogen atoms were located and freely refined. The absorptions were corrected by a SCALE3 ABSPACK multi-scan method.[15] Important structural parameters are summarized in Table 1.

Table 1: X-ray data and parameters.

	1	2
Formula	C ₂ HN ₉	C ₂ H ₉ N ₁₀ O _{2.50}
Form. weight [g mol ⁻¹]	151.12	213.19
Crystal system	Monoclinic	Monoclinic
Space group	<i>Cc</i> (No. 9)	<i>P2₁/c</i> (No. 14)
Color / Habit	Colorless rod	Colorless needle
Size, mm	0.06 x 0.14 x 0.17	0.05 x 0.06 x 0.16
<i>a</i> [Å]	12.2017(17)	6.8089(5)
<i>b</i> [Å]	23.3930(15)	14.9301(11)
<i>c</i> [Å]	8.0456(10)	18.7916(15)
α [°]	90	90
β [°]	125.65(2)	95.935(6)
γ [°]	90	90
<i>V</i> [Å ³]	1866.1(6)	1900.1(2)
<i>Z</i>	12	8
$\rho_{\text{calc.}}$ [g cm ⁻³]	1.614	1.490
μ [mm ⁻¹]	0.129	0.129
<i>F</i> (000)	912	888
$\lambda_{\text{MoK}\alpha}$ [Å]	0.71073	0.71073
<i>T</i> [K]	173	173
Theta Min-Max [°]	4.5, 26.5	4.1, 26.0
Dataset	-15;9; -29; 27; -9;10	-8;8; -18;13; -20; 23
Reflections collected	4971	9667
Independent reflections	1921	3710
<i>R</i> _{int}	0.041	0.068
Observed reflections	1263	1549
No. parameters	205	334
<i>R</i> ₁ (obs)	0.0340	0.0441
<i>wR</i> ₂ (all data)	0.0659	0.0763
<i>S</i>	0.87	0.74
Resd. dens. [e Å ⁻³]	-0.18, 0.19	-0.19, 0.32
Device type	Oxford Xcalibur3 CCD	Oxford Xcalibur3 CCD
Solution	SIR-92	SIR-92
Refinement	SHELXL-97	SHELXL-97
Absorption correction	multi-scan	multi-scan

Both compounds **1** and **2** crystallize in monoclinic space groups, the neutral form within the rare space group *Cc* with a density of 1.614 g cm⁻³ and 12 molecules in the unit cell. The asymmetric unit consist of three independent 3,5-diazidotriazole moieties. The molecular structure is shown in Figure 1. Within the structure layers parallel to the *b* axis are formed which are stabilized by hydrogen bonds forming trimers (Figure 2). A molecular structure of the ammonium salt is depicted in Figure 3. It crystallizes with four molecules in the *P2₁/c* symmetry based unit cell showing a lower density of 1.490 g cm⁻³ in comparison to **1**. The ammonium

salt is packed by alternating layers build by the tetrazolate anions as well as the hydrophilic ammonium cations together with the crystal water molecules (Figure 4). The bond lengths and angles of both structures are listed in Tables 2 and 3. However, only slight derivation within the structure geometries could be observed. The largest bond length difference is between the nitrogen atoms C1 and N1, (**1**: 1.311(3) Å vs. **2**: 1.330(3)). The same effect is observed for the bond angles, in which only marginal differences are detected. These small variations were also found for 5-azidotetrazole in comparison to its 5-azidotetrazolate salts.[1]

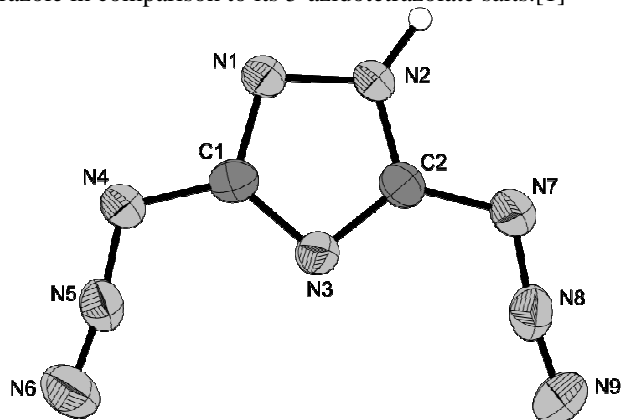


Figure 2: Molecular unit of 3,5-diazo-1,2,4-triazole (**1**). Ellipsoids of non-hydrogen atoms are drawn at the 50 % probability level.

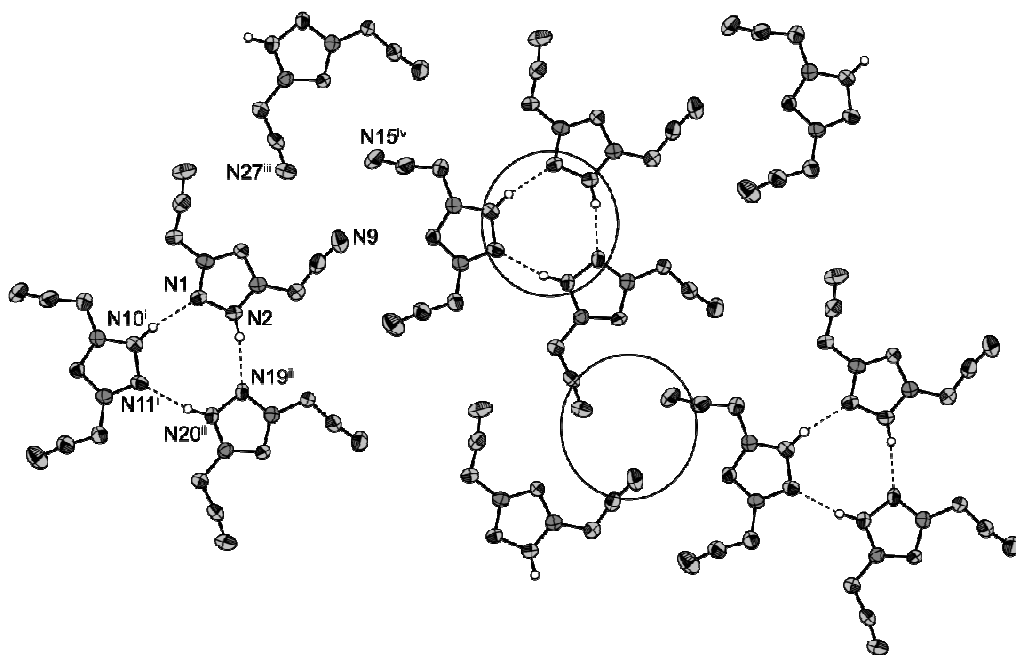


Figure 3: Hydrogen bonding within the layers in the structure of **1** demonstrating the formation of trimers. Symmetrie codes: (i) $x, y, 1+z$; (ii) $0.5+x, 0.5-y, 0.5+z$; (iii) $-0.5+x, 0.5-y, -1.5+z$; (iv) $-0.5+x, 0.5+y, z$.

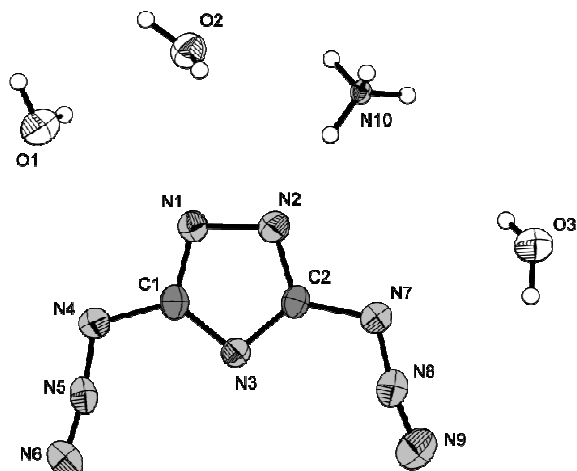


Figure 4: Molecular unit of ammonium 3,5-diazo-1,2,4-triazolate * 2.5 H₂O (**2**). Ellipsoids of non-hydrogen atoms are drawn at the 50 % probability level.

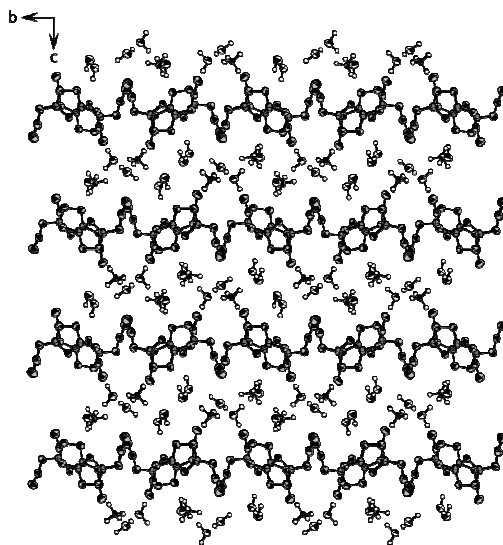


Figure 5: View on a super-cell of **2** along the *a* axis.

Table 2: Bond lengths [Å] of **1** and **2**.

	1	2
C1–N1	1.311(3)	1.330(3)
C1–N3	1.355(1)	1.347(3)
C2–N2	1.321(1)	1.328(3)
C2–N3	1.341(1)	1.334(3)
N1–N2	1.375(3)	1.379(3)
C1–N4	1.397(1)	1.397(3)
N4–N5	1.244(1)	1.248(3)
N5–N6	1.122(1)	1.123(3)
C2–N7	1.396(1)	1.395(3)
N7–N8	1.249(1)	1.246(3)
N8–N9	1.108(1)	1.121(3)

Table 3: Bond angles [°] of **1** and **2**.

	1	2
C1–N1–N2	104.0(2)	103.2(2)
C2–N2–N1	106.6 (1)	106.5(2)
C2–N3–C1	100.5(2)	100.5(2)
N5–N4–C1	115.1(2)	113.2(2)
N6–N5–N4	171.9(2)	172.5(3)
N8–N7–C2	114.8(2)	114.2(2)
N9–N8–N7	171.7(2)	171.0(3)
N1–C1–N3	115.3(1)	115.7(2)
N1–C1–N4	118.4(1)	118.3(2)
N3–C1–N4	126.4(2)	125.9(2)
N2–C2–N3	113.4(2)	114.1(2)
N2–C2–N7	119.3(2)	117.4(2)
N3–C2–N7	127.3(2)	128.4(2)

To investigate the energetic properties, **1–3** were synthesized in a 500 mg scale. The sensitivities were determined by the following methods: Impact sensitivity: BAM drophammer (1 of 6) [16]; Friction sensitivity: BAM friction tester (1 of 6) [16]; Electrostatic Discharge: OZM small scale electrostatic discharge device [17]. The results are summarized in Table 4. According to the *UN recommendations on the transport of dangerous goods* [18] all compounds are classified as “extremely sensitive”. Theoretically, the ammonium and hydrazinium salts should be stabilized by the lattice energy as well as the formation of several strong hydrogen bonds. In addition the crystal water in **2** should decrease the brisance. However, these effects yield only to a marginal decrease in sensitivity.

Table 4: Sensitivity data of **1–4**.

	1	2	3
Formula	C ₂ HN ₉	C ₂ H ₉ N ₁₀ O _{2.5}	C ₂ H ₅ N ₁₁
FW [g mol ⁻¹]	151.12	213.19	183.14
IS [J] ^a	< 1	< 1	< 1
FS [N] ^b	< 5	< 5	< 5
ESD-test [J] ^c	0.005	0.30	0.01
N [%] ^d	83.43	65.71	84.13
Q [%] ^e	-47.64	-45.03	-56.78
T _{dec.} [°C] ^f	122	122	87

^a impact sensitivity; ^b friction sensitivity; ^c electrostatic discharge device; ^d nitrogen content; ^e oxygen balance;

^f decomposition temperature from DSC ($\beta = 5^\circ\text{C}$).

To complete the energetic characterization of **1**, its solid state heat of formation was calculated using the CBS-4M atomization method, described into detail in the literature.[19] The result of the calculation ($\Delta H_f^\circ = 812.2 \text{ kJ mol}^{-1}$) indicates a very strong endothermic character of **1**. In comparison to strongly endothermic 5-azidotetrazole ($\Delta H_f^\circ = 611 \text{ kJ mol}^{-1}$) [20] the value is even higher. With this value and the X-ray density several detonation parameters have been calculated with the EXPLO5.04 computer code.[21]

Table 5: Calculated detonation parameters of 3,5-diazido-triazole.

	$\rho^a / \text{g cm}^{-3}$	$\Delta U_f^b / \text{kJ kg}^{-1}$	$-Q_v^c / \text{kJ kg}^{-1}$	$T_{\text{ex}}^d / \text{K}$	$p_{\text{CJ}}^e / \text{kbar}$	$V_{\text{det}}^f / \text{m s}^{-1}$	$V_0^g / \text{L kg}^{-1}$
1	1.614	5457	5537	4424	260	8157	694

^a estimated from X-ray diffraction; ^b calculated energy of formation; ^c Energy of explosion; ^d explosion temperature; ^e detonation pressure; ^f detonation velocity; ^g assuming only gaseous products.

Although having a superior heat of formation, the performance of **1** is relatively weak in comparison with PETN (nitropenta), RDX (hexogen), and HMX (octogen), which can be traced back to its low density. EXPLO5.04 values: $V_{\text{Det.}} = \mathbf{1}$: 8157, TNT: 7253, PETN: 8320, RDX: 8748 $\text{m}\cdot\text{s}^{-1}$; $p_{\text{CJ}} = \mathbf{1}$: 260, TNT: 216, PETN: 320, RDX: 349 kbar; $Q_v = \mathbf{1}$: -5537, TNT: -5227, PETN: -6190, RDX: -6125 $\text{kJ}\cdot\text{kg}^{-1}$.

3 Conclusions

From this experimental study the following conclusions can be drawn:

- 3,5-Diazidotriazole (**1**) can be synthesized by diazotation of 3,5-diaminotriazole followed by a work-up with sodium azide.
- It can be protonated with mineralic acids as well as deprotonated e.g. with ammonia or hydrazine forming the corresponding salts ammonium (**2**) and hydrazinium 3,5-diazidotriazolate (**3**). At ambient conditions, both salts loose ammonia and hydrazine, respectively, and are therefore not long term stable
- The crystal structures of **1** and its ammonium salt with the inclusion of 2.5 molecules of crystal water per molecular unit was determined by low temperature single crystal X-ray diffraction. Both compounds crystallize in monoclinic space groups (**1**: *Cc*, **2**: *P2₁/c*).
- The sensitivities of **1–3** have been measured. All three compounds are extremely sensitive towards shock and frictions and are classified as primary explosives.
- Deprotonation of **1** does not increase its thermal and outer stimulation stability.

- Detonation parameters of highly endothermic ($\Delta H_f^\circ = 812.2 \text{ kJ mol}^{-1}$) **1** were calculated to be slightly lower than those of PETN.

4 Experimental part

Diazido-1,2,4-triazole (1): To a solution of 3,5-diamino-1,2,4-triazol (0.900 g, 9.08 mmol, 1.00 eq.) in 20 % sulfuric acid (40 mL) cooled with an sodium chloride ice bath to -9°C , sodium nitrite (1.316 g, 19.07 mmol, 2.10 eq.) which was solved in water was added drop wise, so that the temperature did not exceed -6°C . After 1 min stirring urea was added and sodium azide (1.535 g, 23.61 mmol, 2.60 eq.) previously dissolved in water, was added drop wise within 20 min, so that the temperature did not exceed -1°C . The orange solution was stirred further 10 min at -2°C before the ice bath was removed and the reaction mixture was stirred for 2 h while warming up to room temperature. The reaction was then quenched and neutralized with conc. sodium bicarbonate solution or conc. sodium hydroxide solution to $\text{pH} = 5 - 6$. The mixture was extracted with ethyl acetate (4*70 mL) and a red byproduct was separated and washed several times with ethyl acetate. The combined organic layers were dried over magnesium sulfate. The solvent was evaporated and the yellow crude product columned over silica gel with ethyl acetate as eluent. In this way diazido-1,2,4-triazole and azido-amino-triazole can be separated. The yellow side product can be extracted from the silica gel column with ethyl acetate/methanol (v:v, 1:1) or pure methanol. Yield: 0.305 g of diazido-1,2,4-triazole (2.02 mmol, 22 %) as colorless solid and 0.079 g of azido-amino-1,2,4-triazole (0.628 mmol, 7 %) as colorless solid. DSC (5°C min^{-1} , $^\circ\text{C}$): 111°C (m.p.), 122°C (dec.); IR (KBr, cm^{-1}): $\tilde{\nu} = 3416$ (w), 3345 (w), 3161 (s), 3051 (vs), 3002 (vs), 2933 (vs), 2849 (vs), 2715 (vs), 2532 (s), 2428 (s), 2225 (s), 2145 (vs, $-\text{N}_3$), 1574 (vs), 1519 (vs), 1463 (s), 1403 (vs), 1327 (s), 1202 (vs), 1139 (s), 1061 (vs), 1048 (vs), 1011 (s), 837 (vs), 774 (m), 735 (vs), 678 (m), 578 (m), 529 (m), 502 (w), 479 (s); Raman (1064 nm, 220 mW, 25°C , cm^{-1}): $\tilde{\nu} = 2166$ (9), 2137 (32, $-\text{N}_3$), 1578 (56), 1518 (49), 1455 (43), 1407 (70), 1329 (27), 1226 (7), 1159 (9), 1020 (100), 742 (8), 581 (12), 509 (28), 482 (8), 361 (39), 244 (18); ^1H NMR (400 MHz, DMSO- d_6 , 25°C , ppm) δ : 13.91 (s, 1H, NH); ^{13}C NMR (101 MHz, DMSO- d_6 , 25°C , ppm) δ : 156.0, 150.3; ^{14}N NMR (29 MHz, MeOD- d_4 , 25°C , ppm) δ : -138 (N_3), -160 (N_3), -286 (N_3); m/z (DEI): 151.1 [M^+]; BAM drophammer: $< 1 \text{ J}$; friction tester: $< 5 \text{ N}$; ESD: 7 mJ (grain size: 100 – 500 μm).

Ammonium diazido-1,2,4-triazolate (2): Diazido-1,2,4-triazole (0.050 g, 0.33 mmol, 1.0 eq) was dissolved in THF, conc. aqueous ammonia was added. After stirring for 5 h the solvent was evaporated. Yield: Ammonium diazido-1,2,4-triazolate (0.056 g, 0.33 mmol, 100 %) as colorless solid. The ammonium salt loses ammonia within short time and is not shelf stable. DSC (5°C min^{-1} , $^\circ\text{C}$): 94°C (loss of ammonia), 107°C (mp.), 122°C (dec.); BAM drophammer: $< 1 \text{ J}$; friction tester: $< 5 \text{ N}$; ESD: 30 mJ (grain size: 100 – 500 μm).

Hydrazinium diazido-1,2,4-triazolate (3): Diazido-1,2,4-triazole (0.075 g, 0.50 mmol, 1.0 eq.) was dissolved in THF. Hydrazine in THF (0.018 g, 0.55 mmol, 1.0 eq.) was added. The solvent was evaporated and the precipitate washed with small amounts of THF. The obtained salt loses hydrazine within short time and is not shelf stable. Yield: Hydrazinium diazido-1,2,4-triazolate (0.040 g, 0.22 mmol, 44 %) as colorless solid. DSC (5°C min^{-1} , $^\circ\text{C}$): 87°C (dec.); IR (KBr, cm^{-1}): $\tilde{\nu} = 3345$ (m), 3162 (m), 3053 (m), 3002 (m), 2932 (m), 2851 (m), 2766 (m), 2714 (m), 2532 (w), 2428 (w), 2224 (m), 2148 (vs, $-\text{N}_3$), 1633 (m), 1568 (s), 1519 (s), 1457 (m), 1404 (vs), 1261 (m), 1203 (s), 1139 (m), 1095 (m), 1062 (s), 1049 (s), 836 (m), 805 (m), 734 (m), 678 (w), 578 (w), 529 (w), 479 (w); ^1H NMR (400 MHz, DMSO- d_6 , 25°C , ppm) δ : 5.57 (s, 5H, NH); ^{13}C NMR (101 MHz, DMSO- d_6 , 25°C , ppm) δ : 152.9; BAM drophammer: $< 1 \text{ J}$; friction tester: $< 5 \text{ N}$ (grain size: 100 – 500 μm).

Acknowledgements

Financial support of this work by the Ludwig-Maximilian University of Munich (LMU), the U.S. Army Research Laboratory (ARL), the Armament Research, Development and Engineering Center (ARDEC), the Strategic Environmental Research and Development Program (SERDP) and the Office of Naval Research (ONR Global, title: "Synthesis and Characterization of New High Energy Dense Oxidizers (HEDO) - NICOP Effort ") under contract nos. W911NF-09-2-0018 (ARL), W911NF-09-1-0120 (ARDEC), W011NF-09-1-0056 (ARDEC) and 10 WPSEED01-002 / WP-1765 (SERDP) is gratefully acknowledged. The authors acknowledge collaborations with Dr. Mila Krupka (OZM Research, Czech Republic) in the development of new testing and evaluation methods for energetic materials and with Dr. Muhamed Sucesca (Brodarski Institute, Croatia) in the development of new computational codes to predict the detonation and propulsion parameters of novel explosives. We are indebted to and thank Drs. Betsy M. Rice and Brad Forch (ARL, Aberdeen, Proving Ground, MD) and Mr. Gary Chen (ARDEC, Picatinny Arsenal, NJ) for many helpful and inspired discussions and support of our work. For the measurement of the sensitivity Stefan Huber is thanked.

References

- [1] T. M. Klapötke, J. Stierstorfer, The CN_7^- -Anion, *J. Am. Chem. Soc.* **2009**, *131*, 1122–1134.
- [2] Y. Cui, T. L. Zhang, J. G. Zhang, L. Yang, J. Zhang, X. C. Hu, Preparation, molecular structure, and thermal analyses of a novel coordination compound $[\text{Cd}(\text{AZT})_4(\text{H}_2\text{O})_2](\text{PA})_2 \cdot 4\text{H}_2\text{O}$ (AZT = 3-azido-1,2,4-triazole, PA = picrate), *Struct. Chem.* **2008**, *19*, 269–278.
- [3] R. C. Weast, S. M. Selby, *Handbook of Chemistry and Physics*, Vol. 48th ed., The Chemical Rubber Publishing Company, Cleveland **1968**.
- [4] G. Drake, T. Hawkins, A. Brand, L. Hall, V. A. McKay, I. Ismail, Energetic, low-melting salts of simple heterocycles, *Propellants Explos. Pyrotech.* **2003**, *28*, 174–180.
- [5] M. S. Pevzner, T. P. Kofman, I. V. Tselinskii, Energetic 1,2,4-triazoles and tetrazoles synthesis, structure and properties, *Targets Heterocycl. Syst.* **1999**, *3*, 467–526.
- [6] H. Xue, Y. Gao, B. Twamley, J. M. Shreeve, New Energetic Salts Based on Nitrogen-Containing Heterocycles, *Chem. Mater.* **2005**, *17*, 191–198.
- [7] T. P. Kofman, K. N. Krasnov, Reactions of 3-azido-1,2,4-triazole with electrophiles, *Russ. J. Org. Chem.* **2004**, *40*, 1651–1656.
- [8] CrysAlis CCD, Oxford Diffraction Ltd., Version 1.171.27p5 beta (release 01-04-2005 CrysAlis171 .NET) (compiled Apr 1 **2005**, 17:53:34).
- [9] CrysAlis RED, Oxford Diffraction Ltd., Version 1.171.27p5 beta (release 01-04-2005 CrysAlis171 .NET) (compiled Apr 1 **2005**, 17:53:34).
- [10] SIR-92, 1993, A program for crystal structure solution, A. Altomare, G. Cascarano, C. Giacovazzo, A. Guagliardi, *J. Appl. Cryst.* **1993**, *26*, 343.
- [11] G. M. Sheldrick SHELXS-97, Program for Crystal Structure Solution, Universität Göttingen, **1997**.
- [12] G. M. Sheldrick, SHELXL-97. Program for the Refinement of Crystal Structures. University of Göttingen, Germany, **1997**.
- [13] A. L. Spek, PLATON, A Multipurpose Crystallographic Tool, Utrecht University, Utrecht, The Netherlands, **1999**.
- [14] L. J. Farrugia, *J. Appl. Cryst.* **1999**, *32*, 837.

-
- [15] SCALE3 ABSPACK - An Oxford Diffraction program (1.0.4.gui:1.0.3) (C) **2005** Oxford Diffraction Ltd.
- [16] a) <http://www.bam.de>; b) <http://www.reichel-partner.de/>.
- [17] a) OZM research, Czech Republic, <http://www.ozm.cz/testing-instruments/pdf/TI-SmallSpark.pdf>; b) S. Zeman, V. Pelikan, J. Majzlik, Electric spark sensitivity of nitramines. Part II. A problem of "hot spots", *Centr. Eur. J. Energy. Mat.* **2006**, 3, 45–51; c) D. Skinner, D. Olson, A. Block-Bolten, Electrostatic discharge ignition of energetic materials, *Propellants Explos. Pyrotech.* **1997**, 23, 34–42.
- [18] Impact: Insensitive > 40 J, less sensitive ≥ 35 J, sensitive ≥ 4 J, very sensitive ≤ 3 J; friction: Insensitive > 360 N, less sensitive = 360 N, sensitive < 360 N a. > 80 N, very sensitive ≤ 80 N, extreme sensitive ≤ 10 N; According to the UN Recommendations on the Transport of Dangerous Goods (+) indicates: not safe for transport.
- [19] M. Göbel, K. Karaghiosoff, T. M. Klapötke, D. G. Piercey, J. Stierstorfer, Energetic Salts and Chemistry of the Nitrotetrazolate-2N-oxide anion, *New Trends in Research of Energetic Materials, Proceedings of the Seminar*, 14th, Pardubice, Czech Republic, **2011**, in press.
- [20] R. D. Chapman, A. Hammerl, T. M. Klapötke, J. Stierstorfer, 5-Azido-1H-tetrazole – Improved Synthesis, Crystal Structure and Sensitivity Data, *Z. Anorg. Allg. Chem.* **2008**, 634, 1051-1057.
- [21] M. Sućeska, EXPLO5.4 program, Zagreb, Croatia, **2010**.

Nitrogen-Rich 5,5'-Bistetrazolates and their Potential Use in Propellant Systems: A Comprehensive Study

Niko Fischer, Dániel Izsák, Thomas M. Klapötke,* Sebastian Rappenglück, and Jörg Stierstorfer^[a]

Abstract: A large variety of twice-deprotonated nitrogen-rich 5,5'-bistetrazolates, that is, the ammonium (1), hydrazinium (2), hydroxylammonium (3), guanidinium (4), aminoguanidinium (5), diaminoguanidinium (6), triaminoguanidinium (7), and diaminouronium (8) salts, have been synthesized. Energetic compounds 1–8 were fully characterized by single-crystal X-ray diffraction (except 8), NMR spectroscopy, IR

and Raman spectroscopy, and differential scanning calorimetry (DSC) measurements. With respect to their potential use in propellant applications, the sensitivity towards impact, friction, and electrical discharge were determined.

Keywords: energetic materials • nitrogen heterocycles • propellants • sensitivities • X-ray diffraction

Several propulsion and detonation parameters (e.g., heat of explosion, detonation velocity) were computed by using the EXPLO5 computer code based on calculated (CBS-4M) heats of formation and X-ray densities. Additionally, the performance of 1–8 in various formulations was investigated by calculating the specific energy and specific impulse of the compounds under isochoric conditions.

Introduction

Nitrogen-rich materials play an important role in the design of new energetic compounds and their use as propellants, explosives, and pyrotechnics.^[1] The most promising heterocyclic backbone for the preparation of high-performance energetics is considered to be the tetrazole ring.

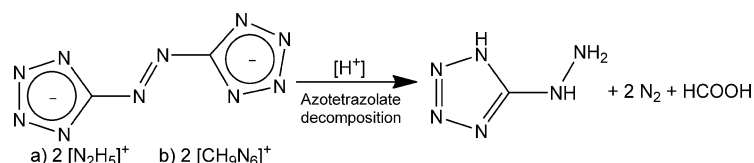
Tetrazole ring systems demonstrate high heats of formation that result from inherently energetic nitrogen–nitrogen and nitrogen–carbon bonds, high ring strain, and high density, and have allowed the preparation of a variety of high-performance primary^[2] and secondary^[3] explosives, which illustrate their dynamic nature. Depending on the ring substituents and anion/cation pairing, tetrazole-based energetic compounds can span the entire spectrum of sensitivity from insensitive to highly sensitive (primary explosives). Since its discovery in the early 20th century,^[4] 5,5'-bistetrazole, which has one of the highest nitrogen contents, and in particular its nitrogen-rich salts have been the focus of research for many decades, which has resulted in a wide variety of applications. However, only very few structurally investigated examples of nitrogen-rich salts of 5,5'-bistetrazole are known to literature.^[5] Owing to its high nitrogen content and high

decomposition temperature, ammonium 5,5'-bistetrazolate was investigated as a gas-generating component in fire-resistant resins and fire-proof adhesives in airbags.^[6] However, Hiskey et al. have reported on the suitability of several nitrogen-rich 5,5'-bistetrazolates for use as low-smoke pyrotechnic fuels.^[7] The above-mentioned properties of thermal stability and high nitrogen content make these molecules appropriate materials for investigation as ingredients in gun or rocket propellant systems, particularly considering barrel erosion problems. Barrel corrosion arises from the formation of iron carbide due to the high carbon contents of currently used propellant mixtures, such as M1 (85 % nitrocellulose, 10 % 2,4-dinitrotoluene, 5 % dibutyl phthalate). An increased N₂/CO ratio in the combustion gases when using nitrogen-rich materials results in the formation of iron nitride in the gun barrel, which has a higher melting point than iron carbide and forms a protective layer on the inside of the gun barrel and helps to increase the lifespan of the equipment by a factor of up to four.^[8] Additionally, the sensitivity of the material used plays an important role for its safe handling; ideally the materials should be less sensitive than RDX (hexogen). Two very interesting additives currently being developed for use in composite modified double base (CMDB) propellant formulations^[9] are hydrazinium 5,5'-azotetrazolate^[10,11] and triaminoguanidinium 5,5'-azotetrazolate.^[12,13] The latter compound is included in the NILE (Navy insensitive low-erosion) propellant mixture, which was developed at NSWC, Indian Head division. The NILE mixture was successfully fielded as a propellant in, for example, the 105 mm Howitzer.^[14]

Unfortunately, 5,5'-azotetrazolates are not stable under mineral-acidic conditions because neutral 5,5'-azotetrazole decomposes into 5-hydrazinotetrazole, dinitrogen, and

[a] N. Fischer, D. Izsák, Prof. Dr. T. M. Klapötke, S. Rappenglück, Dr. J. Stierstorfer
Department of Chemistry
Energetic Materials Research
Ludwig Maximilian University
Butenandtstr. 5–13 (D)
81377 München (Germany)
Fax: (+49)89-2180-77492
E-mail: tmk@cup.uni-muenchen.de

formic acid (see Scheme 1).^[15] The corresponding salts of 5,5'-bistetrazole reported herein are stable in acidic media and show performance similar to 5,5'-azotetrazolates. The parent compound, 5,5'-bistetrazole, is easily accessible in high quantities and unlike 5,5'-azotetrazole is stable in acidic media.



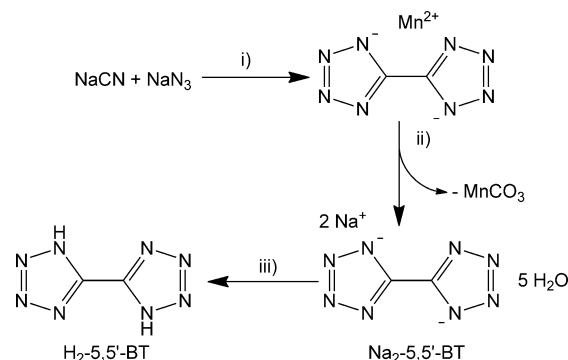
Scheme 1. Hydrazinium (a) and 1,3,5-triaminoguanidinium 5,5'-azotetrazolate (b) and their decomposition reaction in mineralic acids.

Results and Discussion

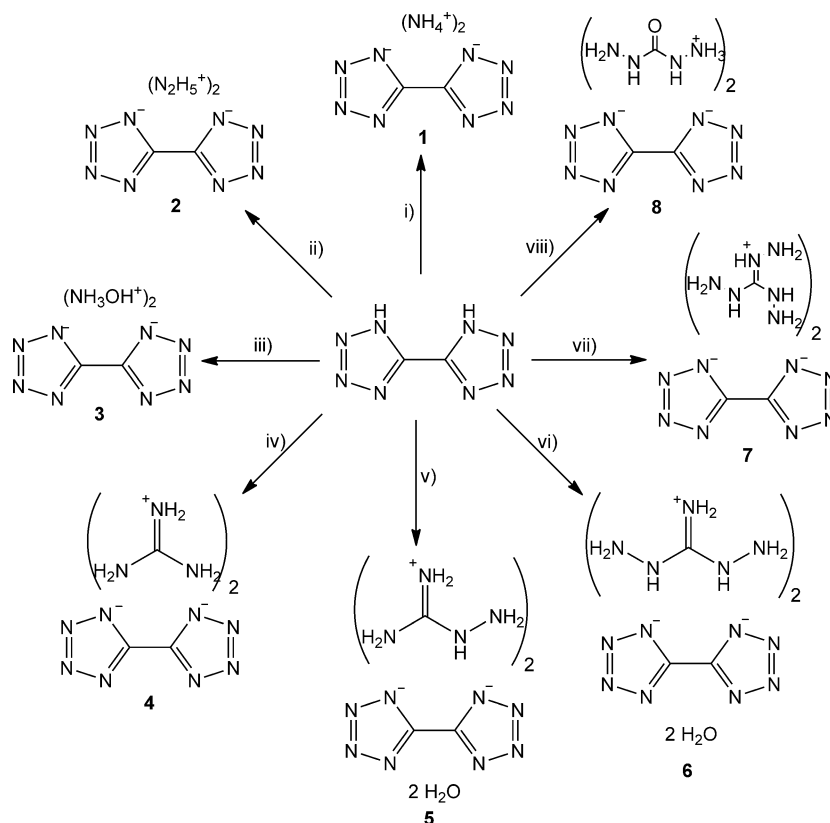
Synthesis: The synthesis of 5,5'-bistetrazole (H_2 -5,5'-BT) has already been described in the literature;^[4,7] the basic principle is a ring-closure reaction in a [2+3] dipolar cycloaddition reaction starting from cyanogen. Depending on the literature source, cyanogen can either be prepared and isolated in an additional step and treated with either sodium azide or hydrazoic acid or it can be generated in situ from sodium cyanide and manganese dioxide as the oxidizing agent under acidic conditions and be further treated with sodium azide. Herein, we chose the latter synthetic route because it is the more convenient strategy (Scheme 2).

The workup involves two further steps because the manganese(II) salt of 5,5'-bistetrazole is formed in the first synthetic step. It is treated with sodium carbonate to form the less soluble $MnCO_3$ and the sodium salt of 5,5'-BT, which stays in solution. The free acid H_2 -5,5'-BT can be precipitated by adding excess concentrated HCl to the mixture. After further recrystallization, the product can be treated with the respective bases to give compounds **1–8** through Brønsted acid–base chemistry or metathesis reactions (Scheme 3).

For compounds **1–3**, **7**, and **8**, the free bases were reacted with an aqueous solution of 5,5'-bistetrazole, whereas for **4** and **5** an aqueous acidic solution of 5,5'-BT was heated to reflux with a suspension of the corresponding carbonates. Diaminoguanidinium salt **6** had to be prepared by a metathesis reaction, in which 5,5'-BT was first converted into the sodium salt. After addition of barium



Scheme 2. Synthesis of 5,5'-bistetrazole according to Hiskey et al.^[7] Conditions: i) MnO_2 , $90^\circ C$, 3 h, H_2SO_4 , CH_3COOH , $CuSO_4 \cdot 5H_2O$; ii) Na_2CO_3 ; iii) concd HCl.



Scheme 3. Synthesis of the nitrogen-rich salts **1–8**. Conditions: i) NH_3 , H_2O , reflux, 5 min; ii) $N_2H_4 \cdot H_2O$, H_2O , reflux, 5 min; iii) NH_2OH , H_2O , reflux, 5 min; iv) G_2CO_3 , H_2O , reflux, 10 min; v) $AG^+HCO_3^-$, H_2O , reflux, 10 min; vi) $NaOH$, H_2O , RT, then $BaCl_2$, H_2O , RT, then DAG_2SO_4 , reflux, 5 min; vii) TAG , RT; viii) DAU , RT. G = guanidinium, AG = aminoguanidinium, DAG = diaminoguanidinium, TAG = triaminoguanidinium, DAU = diaminouronium.

chloride, the barium salt precipitates and can be isolated and further treated with diaminoguanidinium sulfate to obtain **6**. The solubility of nitrogen-rich 5,5'-bistetrazolates **1–7** is only moderate in water, so crystals of **1–7** suitable for X-ray single-crystal analysis were obtained after filtration and slow evaporation of the aqueous mother liquors.

Crystal structures: Suitable single crystals of the described compounds (**1–7**) were selected from the crystallization mixture and mounted in Kel-F oil, transferred to the N₂ stream of an Oxford Xcalibur3 diffractometer equipped with a Spellman generator (voltage 50 kV, current 40 mA) and a KappaCCD detector (MoK α radiation, $\lambda = 0.71073$ Å). All structures were measured at -100°C . The data collection and data reduction was carried out by using the CrysAlisPro software.^[16] The structures were solved by using Sir-92^[17] or Sir-97,^[17] refined with Shelxl-97,^[18] and finally checked using the Platon software^[19] integrated in the WinGX software suite.^[20] The non-hydrogen atoms were refined anisotropically and the hydrogen atoms were located and freely re-

fined. The absorptions were corrected by using a SCALE3 ABSPACK multi-scan method.^[21] Important data and parameters are listed in Table 1.

Compound **1** crystallizes in the monoclinic space group *C2m* with two formula units in the unit cell and a calculated density of 1.590 g cm^{-3} . The asymmetric unit contains only one quarter of the molecular unit (Figure 1). Therefore, the anion consists of two identical tetrazolate rings. The structure of the bistetrazolate dianion is in agreement with corresponding structures of, for example, the erbium(III) salt described in the literature.^[22] The N–N bond lengths lie between N–N single bonds (1.48 Å) and N=N double bonds (1.20 Å), and the C–N bonds lie between C–N single (1.47 Å) and C=N double bonds (1.22 Å).^[23] Both are comparable to other tetrazolates, for example, alkali 5-aminotetrazolates.^[24] The torsion angles N1–N2–N2ⁱ–N1ⁱ ($0.0(1)^\circ$) and N1–C1–N1ⁱ–N2ⁱ ($0.2(1)^\circ$) indicate a completely planar ring, which together with the bond lengths leads to the assumption of a 6π aromatic system. The C1–C1ⁱⁱ bond (1.46 Å) is slightly longer than in the neutral 5,5'-bistetrazole.^[25] How-

Table 1. X-ray data and parameters.^[a]

	1	2	3	4	5	6	7
formula	C ₂ H ₈ N ₁₀	C ₂ H ₁₀ N ₁₂	C ₂ H ₈ N ₁₀ O ₂	C ₄ H ₁₂ N ₁₄	C ₄ H ₁₈ N ₁₆ O ₂	C ₄ H ₂₀ N ₁₈ O ₂	C ₄ H ₁₈ N ₂₀
<i>M_r</i> [g mol ⁻¹]	172.18	202.18	204.18	256.28	322.34	352.38	346.38
crystal system	monoclinic	monoclinic	monoclinic	monoclinic	monoclinic	triclinic	monoclinic
space group	<i>C2/m</i> (No. 12)	<i>P</i> $\bar{1}$ (No. 2)	<i>P</i> $\bar{1}$ (No. 2)	<i>P2₁/c</i> (No. 14)	<i>P2₁/n</i> (No. 14)	<i>P</i> $\bar{1}$ (No. 2)	<i>P2₁/n</i> (No. 14)
color, habit	colorless, block	colorless, needle	colorless, block	colorless, rod	colorless, rod	colorless, needle	colorless, rod
size [mm]	0.30 × 0.20 × 0.08	0.30 × 0.05 × 0.05	0.15 × 0.23 × 0.31	0.11 × 0.14 × 0.20	0.18 × 0.22 × 0.23	0.13 × 0.14 × 0.30	0.10 × 0.11 × 0.28
<i>a</i> [Å]	8.8511(8)	3.6096(5)	3.6736(3)	3.588(4)	11.8344(11)	7.3878(6)	10.417(5)
<i>b</i> [Å]	11.1956(9)	7.9134(12)	7.3455(7)	15.014(5)	3.8684(4)	7.5263(8)	3.929(5)
<i>c</i> [Å]	3.6809(4)	8.2992(16)	7.4908(8)	10.048(6)	14.9914(14)	8.1937(8)	18.660(5)
α [°]	90	72.058(15)	102.666(9)	90	90	83.689(8)	90
β [°]	99.608(9)	79.051(14)	95.283(8)	97.362(5)	95.741(9)	70.034(8)	101.092(5)
γ [°]	90	79.132(13)	96.302(8)	90	90	64.158(9)	90
<i>V</i> [Å ³]	359.64(6)	219.27(6)	194.61(3)	536.8(7)	682.87(11)	384.98(7)	749.5(10)
<i>Z</i>	2	1	1	2	2	1	2
ρ_{calcd} [g cm ⁻³]	1.590	1.531	1.742	1.586	1.568	1.520	1.535
μ [mm ⁻¹]	0.125	0.121	0.148	0.122	0.128	0.124	0.120
<i>F</i> (000)	180	106	106	268	340	186	364
λ (MoK α) [Å]	0.71073	0.71073	0.71073	0.71073	0.71073	0.71073	0.71073
<i>T</i> [K]	173	173	173	173	173	173	173
θ range [°]	4.7–27.0	4.3–26.0	4.5–26.5	4.3–26.0	4.3–26.2	4.8–26.0	4.2–26.5
dataset (<i>h</i> , <i>k</i> , <i>l</i>)	$-6 \leq h \leq 11$ $-14 \leq k \leq 12$ $-4 \leq l \leq 3$	$-4 \leq h \leq 4$ $-6 \leq k \leq 9$ $-9 \leq l \leq 10$	$-4 \leq h \leq 4$ $-9 \leq k \leq 9$ $-9 \leq l \leq 9$	$-4 \leq h \leq 4$ $-18 \leq k \leq 18$ $-12 \leq l \leq 12$	$-14 \leq h \leq 14$ $-4 \leq k \leq 4$ $-18 \leq l \leq 11$	$-9 \leq h \leq 9$ $-9 \leq k \leq 9$ $-10 \leq l \leq 10$	$-10 \leq h \leq 13$ $-4 \leq k \leq 4$ $-23 \leq l \leq 23$
reflns. collected	1026	1152	2302	5201	3275	3896	3786
independent reflns.	416	868	806	1061	1372	1507	1536
<i>R</i> _{int}	0.027	0.020	0.029	0.048	0.034	0.029	0.032
observed reflns	343	580	595	740	1012	1143	1027
parameters	38	84	80	106	136	149	145
<i>R</i> ₁ (obsd)	0.0320	0.0362	0.0333	0.0356	0.0350	0.0329	0.0325
<i>wR</i> ₂ (all data)	0.0803	0.0883	0.0782	0.0885	0.0900	0.0815	0.0752
<i>S</i>	1.05	0.88	0.94	0.91	0.97	0.95	0.87
residual density [e Å ⁻³]	−0.29, 0.17	−0.17, 0.21	−0.20, 0.21	−0.17, 0.20	−0.17, 0.20	−0.21, 0.17	−0.15, 0.20
solution	SIR-97	SIR-97	SIR-92	SIR-92	SIR-92	SIR-92	SIR-92
refinement	SHELXL-97	SHELXL-97	SHELXL-97	SHELXL-97	SHELXL-97	SHELXL-97	SHELXL-97
absorption	multi-scan	multi-scan	multi-scan	multi-scan	multi-scan	multi-scan	multi-scan
correction							

[a] CCDC-854127 (**1**), -854128 (**2**), -854126 (**3**), -854129 (**4**), -854132 (**5**), -854131 (**6**), and -854130 (**7**) contain the supplementary crystallographic data for this paper. These data can be obtained free of charge from The Cambridge Crystallographic Data Centre via www.ccdc.cam.ac.uk/data_request/cif.

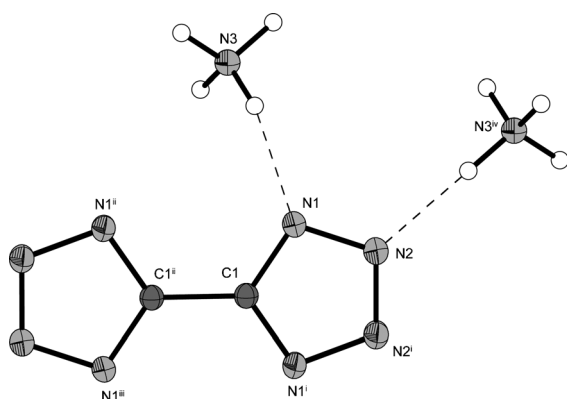


Figure 1. Molecular unit of diammonium 5,5'-bistetrazolate (**1**). Ellipsoids of non-hydrogen atoms are drawn at the 50% probability level. Bond lengths [Å]: N1–C1 1.334(1), N1–N2 1.342(1), N2–N2ⁱ 1.314(1), C1–C1ⁱⁱ 1.461(2); bond angles [°]: N1–C1–N1ⁱ 112.1(1), N2–N1–C1 104.4(1), N1–N2–N2ⁱ 109.6(1), N1–C1–C1ⁱⁱ 123.9(1); torsion angles [°]: N1–N2–N2ⁱ–N1ⁱ 0.0(1), N1–C1–N1ⁱ–N2ⁱ 0.2(1), N1–C1–C1ⁱⁱ–N1ⁱⁱⁱ –180.0(1), N1–C1–C1ⁱⁱ–N1ⁱⁱⁱ –0.9(2); symmetry codes: i: $x, -y, z$; ii: $-x, y, 2-z$; iii: $-x, -y, 2-z$; iv: $0.5-x, 0.5-y, 1-z$.

ever, the C–C bonds of all structures observed in this work are significantly shorter (mean value 1.46 Å) than typical C–C single bonds of approximately 1.54 Å.^[23] The N1–C1–C1ⁱⁱ–N1ⁱⁱ torsion angle is –180.0(1)°, which shows the complete planarity of the whole anion. In the crystal structure, layers comprised of infinite parallel chains of longitudinal bistetrazolate anions are stacked with ammonium cations between the layers (Figure 2). One ammonium is coordinated by four bistetrazolates, two from each layer above and below the cation, through two crystallographically independent

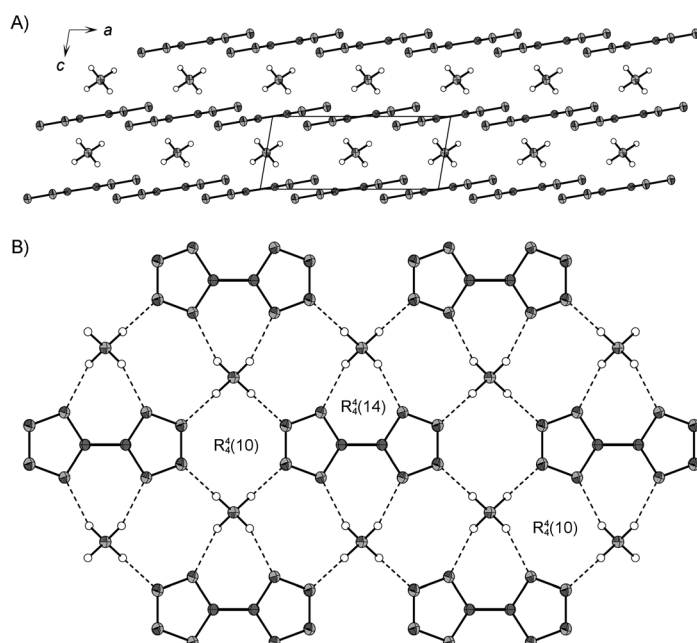


Figure 2. A) Layer structure of **1** (view along [010]); B) hydrogen-bonding network with the three most characteristic graph-set descriptors (view along [001]).

ent hydrogen bonds. The resulting hydrogen-bonding network consists of multiple ring patterns, of which $R_4^1(14)$ and $R_4^1(10)$ are the most characteristic.

Suitable single crystals of **2** were directly obtained from the mother liquor in the form of fine needles. The compound crystallizes in the triclinic space group $P\bar{1}$ with one formula unit in the unit cell and a calculated density of 1.531 g cm^{–3}. Due to the lower symmetry of the space group, the asymmetric unit contains one half of the molecular unit shown in Figure 3. The bond lengths and angles are never-

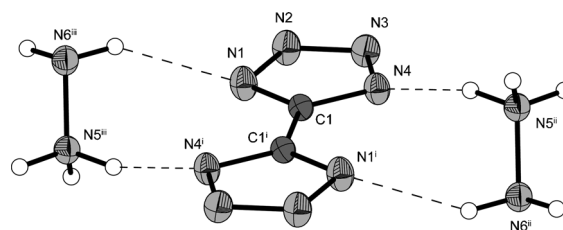


Figure 3. Molecular unit of dihydrazinium 5,5'-bistetrazolate (**2**). Ellipsoids of non-hydrogen atoms are drawn at the 50% probability level. Bond lengths [Å]: N1–C1 1.332(2), N1–N2 1.346(2), N2–N3 1.314(2), N3–N4 1.347(2), N4–C1 1.338(2), C1–C1ⁱ 1.460(2), N5–N6 1.454(2); bond angles [°]: N1–C1–N4 112.1(1), N2–N1–C1 104.4(1), N1–N2–N3 109.7(1), N2–N3–N4 109.5(1), N3–N4–C1 104.4(1), N1–C1–C1ⁱ 124.2(1), N4–C1–C1ⁱ 123.7(1); torsion angles [°]: N1–N2–N3–N4 –0.0(2), N1–C1–N4–N3 0.1(2), N2–N1–C1–N4 –0.1(2), N1–C1–C1–N1 180.0(2), N1–C1–C1–N4 –0.7(3); symmetry codes: i: $1-x, 1-y, -1-z$; ii: $x, y, -1+z$; iii: $1-x, 1-y, -z$.

theless almost identical to those in **1**, and so are also the torsion angles. The N5–N6 bond of the hydrazinium is in the range of a N–N single bond and is comparable to the bond in other hydrazinium compounds, such as hydrazinium 5-aminotetrazolate^[3] or hydrazinium tetrafluoroborate.^[26] The geometry of the hydrogen atoms is staggered. The hydrazinium cation is coordinated by one other cation and three anions, which leads to all hydrogen atoms being involved in the formation of hydrogen bonds (Figure 4). The longest N–H bond and shortest H⋯A contact is observed in the hydrogen bond involving the two hydrazinium cations, which results in $C_1^1(3)$ chains.

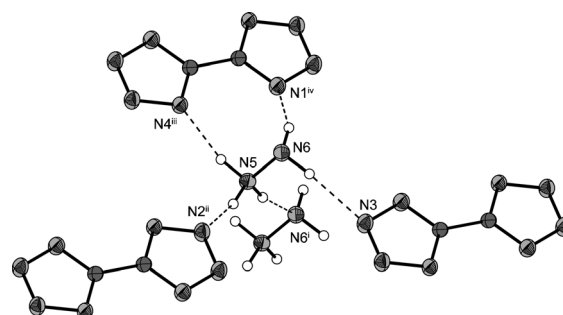


Figure 4. Coordination sphere of the hydrazinium cation in **2**. Ellipsoids of non-hydrogen atoms are drawn at the 50% probability level. Symmetry codes: i: $-1+x, y, z$; ii: $2-x, -y, -z$; iii: $x, y, 1+z$; iv: $1-x, 1-y, -z$.

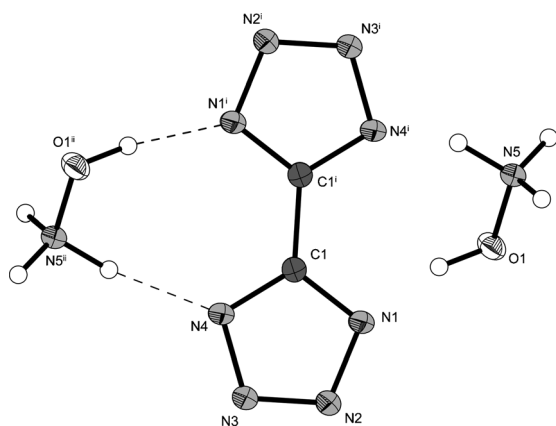


Figure 5. Molecular unit of di(hydroxylammonium) 5,5'-bistetrazolate (**3**). Ellipsoids of non-hydrogen atoms are drawn at the 50% probability level. Selected bond lengths [Å]: N3–N2 1.3128(19), N3–N4 1.3452(18), N4–C1 1.333(2), C1–N1 1.336(2), C1–C1' 1.461(3), N1–N2 1.3443(17), O1–N5 1.4181(16); selected bond angles [°]: N2–N3–N4 109.84(12), C1–N4–N3 104.45(13), N4–C1–N1 111.77(13), N4–C1–C1' 124.02(18), N1–C1–C1' 124.20(18), C1–N1–N2 104.84(13), N3–N2–N1 109.10(12); symmetry codes: i: 2–x, 1–y, 1–z, ii: 1–x, 1–y, 1–z.

Single crystals of di(hydroxylammonium) 5,5'-bistetrazolate (**3**) crystallized in the triclinic ($P\bar{1}$) space group with one molecular moiety (Figure 5) in the unit cell. Its density of 1.742 g cm^{-3} is the highest of the salts investigated herein and is comparable to the neutral compound (1.738 g cm^{-3}).^[25] The structure of the dianion is in agreement with those of **1** and **2**.

Compounds **4** and **5** (Figures 6 and 7) crystallize in the monoclinic space groups $P2_1/c$ (**4**) and $P2_1/n$ (**5**) with two

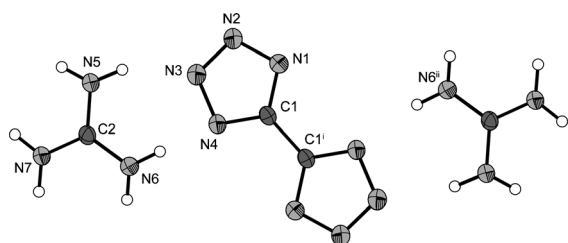


Figure 6. Molecular unit of bis(guanidinium) 5,5'-bistetrazolate (**4**). Ellipsoids of non-hydrogen atoms are drawn at the 50% probability level. Symmetry codes: i: 2–x, –y, 2–z; ii: 1–x, –y, 2–z.

formula units per unit cell and densities of 1.586 g cm^{-3} (**4**) and 1.568 g cm^{-3} (**5**). Diaminoguanidinium salt dihydrate **6** (Figure 8) crystallizes in the triclinic space group $P\bar{1}$ with a density of 1.520 g cm^{-3} , which is the lowest density observed herein. Triaminoguanidinium salt **7** (Figure 9) crystallizes in the monoclinic space group $P2_1/n$ and has a density of 1.535 g cm^{-3} . Crystals of compound **8** were also obtained by recrystallization from water and measured by XRD. However, the refinement could not be finished due to a twinning problem along the c axis. The cell volume of 606.68 Å^3 was used to calculate a density of 1.742 g cm^{-3} , which is equal to that observed for **3**. Of guanidines **4–7**, compounds **5** and **6**

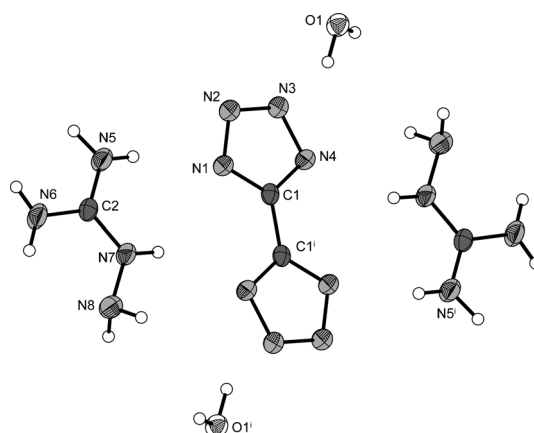


Figure 7. Molecular unit of bis(aminoguanidinium) 5,5'-bistetrazolate (**5**). Ellipsoids of non-hydrogen atoms are drawn at the 50% probability level. Symmetry code: i: 1–x, 1–y, 1–z.

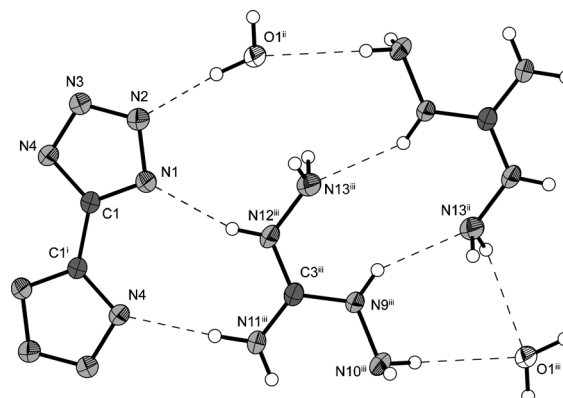


Figure 8. Molecular unit of bis(diaminoguanidinium) 5,5'-bistetrazolate (**6**). Ellipsoids of non-hydrogen atoms are drawn at the 50% probability level. Symmetry codes: i: 1–x, 1–y, –z; ii: 1–x, 1–y, –z; iii: –x, 1–y, –z.

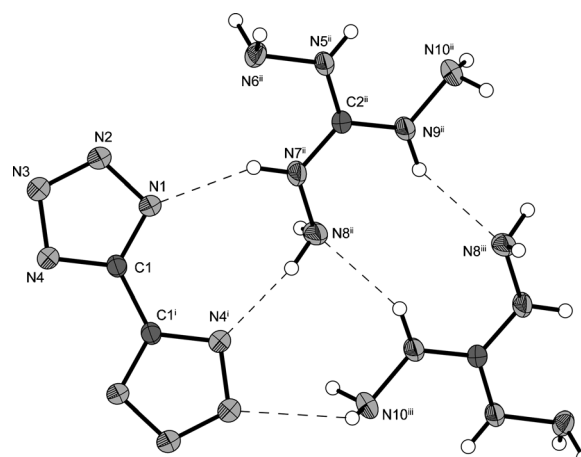


Figure 9. Molecular unit of bis(triaminoguanidinium) 5,5'-bistetrazolate (**7**). Ellipsoids of non-hydrogen atoms are drawn at the 50% probability level. Symmetry codes: i: 2–x, –y, 1–z; ii: 1.5–x, –0.5+y, 0.5–z; iii: 2.5–x, 0.5+y, 0.5–z.

crystallized as dihydrates, whereas **4** and **7** were obtained as solvent-free crystals. The structures of the guanidines are in agreement with those observed for other guanidinium tetrazolates in the literature,^[27] which participate strongly in many classical hydrogen bonds. Regarding the structure of the dianions, all compounds show planar geometries comparable to that discussed in detail for compound **1**.

Spectroscopy: All compounds described were investigated by using ¹H and ¹³C NMR spectroscopy. Additionally a ¹⁴N NMR spectrum was recorded for ammonium salt **1**. For better comparison all spectra (except for **1** and **7**) were measured in [D₆]DMSO as the solvent and all chemical shifts are given with respect to TMS (¹H, ¹³C).

Proton signals for the C-NH₂ protons of the guanidinium derivatives can be found at δ = 7.73 (**4**, **5**) and 7.76 ppm (**6**). Due to the presence of both NH and NH₂ groups in **5**, **6**, and **7**, additional resonances at δ = 4.63–4.77 (NHNH₂) and 9.61–9.65 ppm (NH) are observed. Due to the poor solubility of **1** and **7** in DMSO, D₂O was used instead and thus only one singlet is observed in both proton spectra due to fast proton exchange. Because of fast proton exchange in the protonated 1,3-diaminouronium cation of **8**, only a broad signal at δ = 7.22 ppm is observed for all protons. The measured ¹³C NMR spectra of all guanidine derivatives reveal a single resonance at δ = 154.6–155.1 ppm, which can be assigned to the bistetrazolate ring carbon atom. The guanidine carbon atom signal is found at δ = 158.9–160.6 ppm for **4**, **5**, and **6**, but not for **7**, the NMR spectrum of which was measured in D₂O. The ¹³C NMR spectrum of **8** reveals two single resonances at δ = 150.1 ppm for the bistetrazolate ring carbon and at δ = 161.1 ppm for the urea carbonyl group of the cation. Unfortunately no ¹H or ¹³C NMR spectrum could be recorded for ammonium salt **1** in DMSO due to its low solubility in this solvent, however the spectra recorded in D₂O show the expected signals. The ¹⁴N NMR spectrum reveals a sharp singlet for the ammonium cation at δ = –356 ppm and two singlets at δ = –66 and 3 ppm assigned to the two nonequivalent nitrogen atoms in the 5,5'-bistetrazolate anion. In the proton spectrum of the hydrazinium (**2**) and hydroxylammonium (**3**) salt, a singlet at δ = 7.20 (**2**) and 10.50 ppm (**3**) is observed, which nicely demonstrates the lower pK_a value of protonated hydroxylamine compared to the hydrazinium monocation, which is shown by the downfield shift in the spectrum of **3** compared to **2**. The bistetrazole carbon atom signals are found at δ = 152.6 (**3**) and 154.5 ppm (**2**), respectively, which is the same region as observed for the guanidinium derivatives.

IR and Raman spectroscopy were used for the identification of structural elements and functional groups in all compounds. Absorptions were assigned according to values reported in the literature.^[28,29] The characteristic vibrations of the bistetrazole system were observed in all IR spectra, including the bistetrazole framework vibrations at 1011 to 1184 cm^{–1}, the asymmetric and symmetric stretching vibrations of the N1-C1-N4 fragment^[30] in the range of 1299 to 1335 cm^{–1} and the stretching vibration of the cyclic C=N

bond at 1650 to 1890 cm^{–1}. The latter is in the same range as the C=N stretching vibration of the guanidine derivatives. Due to the presence of amino groups, N–H and NH₂ wagging absorptions can be observed between 603 and 781 cm^{–1} and the corresponding bending vibrations appear in the range of 1536 to 1614 cm^{–1}. In compound **8**, N–H and NH₂ bending vibrations are in the same range as the C=O stretching vibration of 1,3-diaminourea. N–H stretching vibrations are partly shifted to lower frequencies by H-bonding effects, and can be found between 3092 and 3470 cm^{–1}. In the spectra of **4**, **5**, and **8**, two well-defined sharp characteristic absorptions due to the asymmetric and symmetric N–H stretching vibrations of the primary amino groups appear at 3350 to 3449 cm^{–1} (**4**), 3345 to 3409 cm^{–1} (**5**), and 3185 to 3296 cm^{–1} (**8**). All Raman spectra show the characteristic and very intense signal of the 5,5'-bistetrazole C–C bond at 1582 to 1591 cm^{–1}, which has a partial double-bond character, as can be seen from the bond lengths discussed above in the X-ray crystallography section, and very weak N–H vibrations at 3166 to 3429 cm^{–1}. However, bistetrazole framework vibrations are visible in all Raman spectra in the range of 1013 to 1207 cm^{–1}. The measured IR and Raman spectra correspond very well and verify the structural elements in all investigated compounds.

Sensitivities and thermal behavior: The impact sensitivity tests were carried out according to STANAG 4489^[31] modified instructions^[32] by using a BAM (Bundesanstalt für Materialforschung) drop hammer.^[33] The friction sensitivity tests were carried out according to STANAG 4487^[34] modified instructions^[35] by using the BAM friction tester. The classification of the tested compounds results from the “UN Recommendations on the Transport of Dangerous Goods”.^[36] All compounds were tested for sensitivity towards electrical discharge by using the Electric Spark Tester ESD 2010 EN.^[37] Generally, all investigated materials showed surprisingly low sensitivities towards both impact and friction despite their high nitrogen contents. Compounds **1**, **2**, **4**, **5**, and **8** are classified as less sensitive towards impact (**2**, **4**, **5**: 40 J; **1**, **8**: 35 J), whereas **3**, **6**, and **7** are classified as sensitive (**3**: 10 J; **6**: 30 J; **7**: 15 J). As expected, the hydroxylammonium and the triaminoguanidinium salt are the most sensitive towards impact, which is partly due to the low carbon content of the cation and, therefore, the highest nitrogen content for the ionic compounds, and partly due to the fact that both species crystallize without the inclusion of crystal water. This trend is also observed for the friction sensitivity. The hydroxylammonium (**3**: 240 N), the aminoguanidinium (**5**: 324 N), and the triaminoguanidinium (**7**: 285 N) salts are classified as sensitive towards friction, whereas **2**, **6**, and **8** are less sensitive (**2**, **6**, **8**: 360 N). The ammonium and the guanidinium salts did not show any response and are, therefore, classified as insensitive (**1**, **4**: >360 N). The inclusion of water, as in the case of **5** and **6**, usually also plays a role, but because the materials are comparatively insensitive no obvious trend for the desensitization of **5** and **6** was observed. The sensitivity to-

wards electrostatic discharge for most of the substances is low, with values between 0.50 for **8** and 1.0 J for **4** and **5**. However, the hydrazinium (**2**: 0.23 J) and the hydroxylammonium (**3**: 0.10 J) salts do not follow this trend. The observed results of the impact sensitivity testing are comparable to the results observed by Hiskey et al. They also determined the impact sensitivities of the diammonium, the dihydrazinium, and the dihydroxylammonium salt by using a different method, and stated that those fuels are fairly insensitive when not mixed with an oxidizer, such as ammonium perchlorate.^[7]

Differential scanning calorimetry (DSC) measurements to determine the melting and decomposition temperatures of **1–8** (about 1.5 mg of each energetic material) were performed in covered Al-containers with a hole (0.1 mm) in the lid for gas release and a nitrogen flow of 20 mL min^{−1} on a Linseis PT 10 DSC^[38] calibrated by standard pure indium and zinc at a heating rate of 5 °C min^{−1}. The decomposition temperatures are given as absolute onset temperatures. It is very remarkable that despite their very high nitrogen content, except for **2** and **8**, none of the compounds show any decomposition at temperatures below 200 °C. Even the hydroxylammonium (**3**) and triaminoguanidinium salts (**7**) decompose at temperatures of 205 (**3**) and 207 °C (**7**), which is in the same range as observed for RDX (hexogen), whereas the ammonium (**1**) and guanidinium salts (**4**) reach decomposition temperatures as high as 312 (**1**) and 316 °C (**4**), which is comparable to the melting- and decomposition point of HNS (hexanitrostilbene, a highly thermally stable explosive). The remaining compounds fill the range between these extreme values, with the lowest temperature being recorded for **6** (208 °C) up to 234 and 237 °C for **2** and **8** and 251 °C for **5**. The ammonium (**1**), hydroxylammonium (**3**), and triaminoguanidinium salts (**7**) do not show any endothermic steps in their DSC curve before decomposition, whereas the guanidinium (**4**), aminoguanidinium (**5**), and diaminoguanidinium salts (**6**) melt directly before they decompose, as indicated by endothermic steps observed prior to their exothermic decomposition peaks. Two salts, namely, the hydrazinium (**2**) and the diaminouronium salts (**8**), show one or more endothermic peaks in their respective DSC curves at 165, 185, and 217 °C (**2**), and at 175 °C (**8**). These observations are in accordance with results published by Hiskey et al.,^[7] who found that the dihydrazinium salt loses

hydrazine at temperatures starting from 130 °C in a thermogravimetric analysis experiment. The lower temperature compared to 165 °C as observed in our case can be explained by the lower heating rate used by Hiskey et al. (0.1 °C min^{−1}). The same could be true for the diaminouronium salt because the cation in **8** is also a hydrazine derivative, however, a thermogravimetric analysis would be necessary to support this assumption.

Theoretical calculations

Heats of formation: Usually energetic materials tend to explode in bomb calorimetric measurements and consequently doubtful combustion energies are obtained. Therefore, the heats of formation of energetic materials are mostly calculated theoretically. In our group, we combine the atomization energy method [Eq. (1)] with CBS-4M electronic ener-

Table 2. CBS-4M results and gas-phase enthalpies.

	Formula	$-H^{298}$ [a.u.]	$\Delta_f H(g)$ [kJ mol ^{−1}]
BT ^{2−}	C ₂ N ₈ ^{2−}	513.511502	596.7
NH ₄ ⁺	NH ₄ ⁺	56.796608	635.8
N ₂ H ₅ ⁺	N ₂ H ₅ ⁺	112.030523	774.1
Hx ⁺	H ₄ NO ⁺	131.863229	687.2
G ⁺	CH ₆ N ₃ ⁺	205.453192	571.9
AG ⁺	CH ₇ N ₄ ⁺	260.701802	671.6
DAG ⁺	CH ₈ N ₅ ⁺	315.949896	772.7
TAG ⁺	CH ₉ N ₆ ⁺	371.197775	874.3
DAU ⁺	CH ₇ N ₄ O ⁺	335.795706	651.3

gies (Table 2), which has been shown to be suitable in many recently published studies.^[39] CBS-4M energies of the atoms, cations, and anions were calculated by using the Gaussian 09 (revision A1) software package^[42] and checked for imaginary frequencies. Values for $\Delta_f H^\circ$ (atoms) were taken from the NIST database.^[43]

$$\Delta_f H^\circ_{(g, M, 298)} = H_{(M, 298)} - \sum H^\circ_{(Atoms, 298)} + \sum \Delta_f H^\circ_{(Atoms, 298)} \quad (1)$$

For calculation of the solid-state energy of formation (Table 3) of **4–8**, the lattice energy (U_L) and lattice enthalpy (ΔH_L) were calculated from the corresponding molecular volumes (obtained from X-ray elucidations) according to

Table 3. Solid-state energies of formation ($\Delta_f U^\circ$).

	Formula	$\Delta_f H^\circ(g)$ [kJ mol ^{−1}]	V_M [nm ³]	U_L [kJ mol ^{−1}]	ΔH_L [kJ mol ^{−1}]	$\Delta_f H^\circ(s)$ [kJ mol ^{−1}]	Δn	$\Delta_f U^\circ(s)$ [kJ mol ^{−1}]	M [g mol ^{−1}]	$\Delta_f U^\circ(s)$ [kJ kg ^{−1}]
1	C ₂ H ₈ N ₁₀	1868.3	0.180	1578.4	1589.3	279.0	9	301.4	172.18	1750.0
2	C ₂ H ₁₀ N ₁₂	2144.9	0.219	1465.9	1476.9	668.1	11	695.3	202.18	3438.2
3	C ₂ H ₈ N ₁₀ O ₂	1971.1	0.195	1532.7	1543.6	427.5	10	452.3	204.18	2215.0
4	C ₄ H ₁₂ N ₁₄	1740.5	0.268	1358.8	1369.7	370.8	13	403.0	256.28	1572.5
5	C ₄ H ₁₈ N ₁₆ O ₂	1459.2 ^[a]	0.291	1317.2	1328.1	131.1	18	175.7	322.34	545.1
6	C ₄ H ₂₀ N ₁₈ O ₂	1661.3 ^[a]	0.335	1249.2	1260.2	401.2	20	450.8	352.38	1279.1
7	C ₄ H ₁₈ N ₂₀	2345.2	0.374	1196.9	1207.8	1137.4	19	1184.5	346.38	3419.2
8	C ₄ H ₁₄ N ₁₆ O ₂	1899.3	0.300	1302.8	1313.7	585.6	16	625.3	318.34	1964.2

[a] Value has been corrected (−483.4 kJ mol^{−1}) due to dihydrate formation.

Table 4. Composition of the calculated gun propellant charges.

Formulation	Components	Ratio [wt %]
M1	NC (13.25)/2,4-DNT ^[a] /DBP ^[b] /DPA ^[c]	86/10/3/1
EX-99	RDX/CAB ^[d] /BDNPA/F ^[e] /NC (13.25)	76/12/8/4
HN-1	RDX/TAGzT/CAB ^[d] /BDNPA/F ^[e] /NC (13.25)	56/20/12/8/4
HN-2	RDX/TAGzT/FOX-12 ^[f] /CAB ^[d] /BDNPA/F ^[e] /NC (13.25)	40/20/16/12/8/4
HN-1-1-4; 7; 8	RDX/1-4; 7; 8/CAB ^[d] /BDNPA/F ^[e] /NC (13.25)	56/20/12/8/4
HN-2-1-4; 7; 8	RDX/1-4; 7; 8/FOX-12 ^[f] /CAB ^[d] /BDNPA/F ^[e] /NC (13.25)	40/20/16/12/8/4

[a] 2,4-Dinitrotoluene. [b] Dibutyl phthalate. [c] Diphenyl amine. [d] Cellulose acetate butyrate. [e] 1:1 mixture of bis(2,2-dinitroprop-1-yl)acetal and -formal. [f] 1,1-Dinitro-2,2-diaminoethylene.

the equations provided by Jenkins et al.^[42] With the calculated lattice enthalpy (Table 3), the gas-phase enthalpy of formation was converted into the solid-state (standard conditions) enthalpy of formation. These molar standard enthalpies of formation (ΔH_m) were used to calculate the molar solid-state energies of formation (ΔU_m , see Table 4) according to Equation (2):

$$\Delta U_m = \Delta H_m - \Delta nRT \quad (2)$$

in which Δn is the change in moles of gaseous components.

Gun propellant evaluations: The most important parameters for gun propellant formulations are the specific energy f_E ($[J\ g^{-1}]$, $f_E = nRT_c$), the combustion temperature T_c [K], the co-volume b_E [$cm^3\ g^{-1}$], and the pressure p_{max} [bar, 3000–4000 bar] while assuming isochoric combustion. These parameters and furthermore the N_2/CO ratio can be calculated with the program package EXPLO5 (v. 5.04),^[43] with an error of usually less than 5% (loading densities ca. $0.2\ g\ cm^{-3}$) when the maximum pressure, the specific energy, and the co-volume are considered.

Table 4 contains the compositions of the calculated gun propellant charges. M1 is a typical single-base propellant based on nitrocellulose (NC), used for large caliber artillery guns.^[44] The drawbacks of this formulation are the relatively low performance and the toxicity of almost all ingredients.^[45] EX-99 is a typical formulation for large naval guns and contains high amounts of the highly energetic RDX.^[46] The formulations herein referred to as High-Nitrogen 1 and 2 (HN-1 and HN-2, respectively) are two erosion-reduced formulations derived from EX-99, which contain the nitrogen-rich compound bis(triaminoguanidinium) 5,5'-azobistetrazolate (TAGzT, 82% nitrogen). Synthesized compounds **1–8** (except for **5** and **6** due to the formation of hydrates) were calculated in formulations based on HN-1 and HN-2, in which they replace the TAGzT. The heats of formation were either taken from the EXPLO5 database, from the literature (BDNPA/F),^[47] or calculated in this study.

The combustion parameters of the formulations were calculated assuming isochoric conditions by using the virial

Table 5. Calculated performance of the gun propellant charges.

	T_c [K]	p_{max} [bar]	f_E [$kJ\ g^{-1}$]	b_E [$cm^3\ g^{-1}$]	N_2/CO [w/w]
M1	2834	2591	1.005	1.125	0.23
EX-99	3406	3249	1.257	1.129	0.71
HN-1	2922	3042	1.161	1.185	0.95
HN-2	2735	2848	1.088	1.181	1.05
1 HN-1	2798	2890	1.103	1.181	0.95
1 HN-2	2610	2691	1.030	1.174	1.06
2 HN-1	2975	3109	1.186	1.187	0.96
2 HN-2	2783	2910	1.111	1.183	1.06
3 HN-1	3130	3157	1.211	1.164	0.87
3 HN-2	2928	2964	1.138	1.163	0.96
4 HN-1	2737	2830	1.080	1.183	0.90
4 HN-2	2556	2635	1.008	1.175	1.01
7 HN-1	2942	3091	1.178	1.190	0.93
7 HN-2	2756	2896	1.105	1.185	1.03
8 HN-1	2960	3037	1.161	1.176	0.87
8 HN-2	2770	2845	1.089	1.172	0.96

equation of state with a loading density of $0.2\ g\ cm^{-3}$; the results are compiled in Table 5.

As expected from the ingredients, the M1 and EX-99 formulations have the worst N_2/CO ratios, but EX-99 also has the highest performance. The formulations based on HN-1 have generally higher performance than those based on HN-2, due to the higher content of RDX, but also have higher combustion temperatures (T_c) and N_2/CO ratios that are lower by about 0.1. The most promising compound is the hydrazinium salt **2**, which outperforms HN-2 itself, with an f_E of $1.111\ kJ\ g^{-1}$, a p_{max} of 2910 bar, and, together with **1**, the best N_2/CO ratio of 1.06. The T_c value of 2783 K is comparable to the triaminoguanidinium-based formulations HN-2 ($T_c = 2735\ K$) and **7** HN-2 ($T_c = 2756\ K$). Guanidinium salt formulation **4** HN-2 has the lowest T_c value of 2556 K, but also the lowest general performance. Figure 10 illustrates the calculated performances of M1, EX-99, HN-2, and the HN-2 analogues of **1**, **2**, **4**, and **7**. As expected, the formulations with **3** and **8** show the worst N_2/CO ratios due to the higher oxygen content at the expense of the nitrogen content. Additionally, compound **3** has the highest specific energy in both HN-1 and HN-2 formulations, outperforming the original formulations.

Detonation parameters and specific impulse: Although compounds **1–8** show promise as alternative additives in gun propellants, they nevertheless detonate when stimulated by using a primary explosive in combination with a booster charge. All compounds show better detonation behavior than TNT (trinitrotoluene), compound **3** is even better than RDX (hexogen). Table 6 shows the detonation values of **1–8** calculated by using the EXPLO5.04 software, the heats of formation, and X-ray densities. In addition, the specific impulse of the pure compounds when used as monopropellants was calculated assuming rocket propellant conditions (isobaric combustion with a chamber pressure of 60 bar).

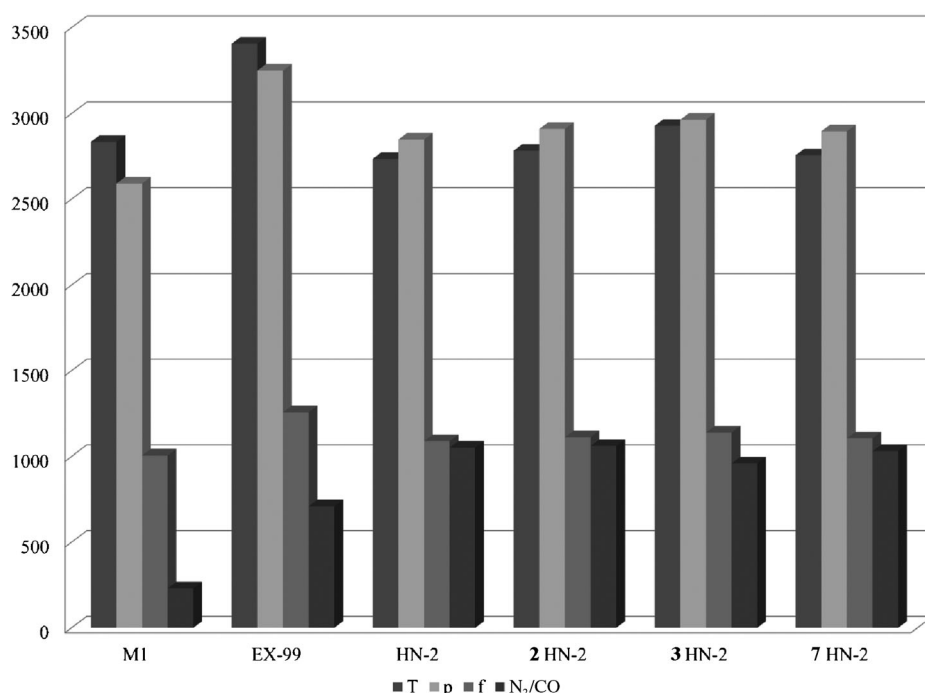


Figure 10. Comparison of the calculated performances of M1, EX-99, HN-2, 2 HN-2, 3 HN-2 and 7 HN-2. For each formulation, column 1: T_c [K], column 2: p_{max} [bar], column 3: f_E [J g⁻¹], column 4: $N_2/CO/0.001$.

Table 6. Calculated specific impulses, nitrogen contents, oxygen balances, and detonation parameters of 1–8.

	I_{sp} [s ⁻¹] ^[a]	N [%] ^[b]	Ω [%] ^[c]	ρ [g cm ⁻³] ^[d]	$-\Delta_E U^\circ$ [kJ kg ⁻¹] ^[e]	T_E [K] ^[f]	p_{C-J} [kbar] ^[g]	$V_{Det.}$ [m s ⁻¹] ^[h]	V_0 [L kg ⁻¹] ^[i]
1	172.3	81.36	-74.34	1.590	2415	1976	189	7417	826
2	225.2	83.13	-71.21	1.531	4126	2744	236	8265	853
3	227.9	68.61	-47.02	1.742	4829	3243	317	8854	843
4	165.8	76.53	-87.41	1.586	2239	1869	176	7199	790
5	174.6	69.54	-74.46	1.568	2656	2049	193	7504	859
6	190.1	71.56	-72.65	1.520	3284	2320	205	7711	872
7	224.1	80.89	-78.53	1.535	4129	2698	238	8181	846
8	204.8	70.42	-65.35	1.742	3893	2676	288	8562	824

[a] Specific impulse. [b] Nitrogen content. [c] Oxygen balance.^[48] [d] Density calculated from X-ray structure. [e] Energy of explosion. [f] Explosion temperature. [g] Detonation pressure. [h] Detonation velocity. [i] Volume of detonation gases.

Conclusion

From this combined theoretical and experimental study, several conclusions can be drawn. Deprotonation of 5,5'-bistetrazole with nitrogen-rich bases leads to a variety of compounds, namely, the diammonium salt (1), the dihydrazinium salt (2), the di(hydroxylammonium) salt (3), the bis(guanidinium) salt (4), the bis(aminoguanidinium) salt (5), the bis(diaminoguanidinium) salt (6), the bis(triaminoguanidinium) salt (7), and the bis(diaminouronium) salt (8), which were prepared in high yields and good purity. Only the double-deprotonated 5,5'-bistetrazolates could be isolated even when using stoichiometric amounts (1.0 equiv) of the

corresponding bases. The crystal structures of 1–7 were determined by low-temperature single-crystal X-ray diffraction. The compounds crystallize in the space groups $P\bar{1}$ (2, 3, 6), $C2/m$ (1), $P2_1/c$ (4), and $P2_1/n$ (5, 7) with densities between 1.520 (for the bis(aminoguanidinium) salt dihydrate) and 1.742 g cm⁻³ (for the di(hydroxylammonium) salt). Additionally, all compounds were fully characterized by using vibrational spectroscopy (IR and Raman), ¹H and ¹³C NMR spectroscopy, mass spectrometry, and elemental analysis. The thermal stabilities of 1–8 were investigated by DSC. All compounds decompose at temperatures higher than 200 °C, with the guanidinium salt being the most thermally stable salt (316 °C).

The sensitivity of compounds 1–8 towards friction, impact, and electrostatic discharge were investigated by BAM methods.

Compounds 1–8 were found to have impact sensitivities between 10 (3, sensitive) and 40 J (2, 4, 5, less sensitive), friction sensitivities of between 240 (3, sensitive) and >360 N (1, 4, insensitive), and ESD sensitivities of between 0.1 (3) and 1.0 J (4, 5). Therefore, the hydroxylammonium salt 3 is the most sensitive, whereas the guanidinium salt 4 is the least sensitive compound. However, all materials are less sensitive than commonly used high explosives, such as RDX.

By using calculated heats of formation and loading densities of 0.2 g cm⁻³, the isochoric combustion parameters (specific energy, combustion temperature, pressure, co-volume, and N_2/CO ratios) for formulations of 1–4, 7, and 8 were calculated with the EPXLO5 program and compared to common formulations found in the literature. The most promising compound for gun propellant formulations is 2, which has a specific energy of 1.111 kJ g⁻¹, a pressure of 2910 bar, a combustion temperature of 2783 K, and an N_2/CO ratio of 1.06. Formulations with 1, 3, 4, 7, and 8 are similar in performance to formulations reported in the literature.

Experimental Section

Caution! 5,5'-Bistetrazole and its salts are energetic materials with increased sensitivities towards shock and friction. Therefore, proper safety

precautions (safety glass, face shield, earthed equipment and shoes, Kevlar gloves, and ear plugs) have to be applied while synthesizing and handling the described compounds.

All chemicals and solvents were employed as received (Sigma–Aldrich, Fluka, Acros). ^1H and ^{13}C NMR spectra were recorded by using a JEOL Eclipse 270, JEOL EX 400 or a JEOL Eclipse 400 instrument. The chemical shifts are quoted in ppm and refer to typical standards, such as tetramethylsilane (^1H , ^{13}C) and nitromethane (^{14}N). To determine the melting and decomposition temperatures of the described compounds, a Linseis PT 10 DSC instrument (heating rate 5°Cmin^{-1}) was used. Infrared spectra were measured as KBr pellets by using a Perkin–Elmer Spectrum One FT-IR spectrometer. Raman spectra were recorded by using a Bruker MultiRAM Raman Sample Compartment D418 equipped with a Nd-YAG laser ($\lambda = 1064\text{ nm}$) and a LN-Ge diode as the detector. Mass spectra of the described compounds were measured by using a JEOL MStation JMS 700 spectrometer and the FAB technique. To record elemental analyses, a Netsch STA 429 simultaneous thermal analyzer was used. 5,5'-Bistetrazole was synthesized according to a literature procedure.¹⁷

Diammonium 5,5'-bistetrazolate (1): 5,5'-Bistetrazole (5.52 g, 40.0 mmol) was dissolved in warm water (20 mL) and aqueous half-concentrated ammonia (100 mL) was added. Water was added to the reaction mixture, which was heated to reflux, until a clear solution was obtained (40 mL). After heating to reflux for 20 min, the reaction mixture was cooled to RT and then stored for 20 h at 4°C . The precipitate was filtered off, washed with a small amount of water and plentiful ethanol, and dried in medium vacuum to give the title compound as colorless needles (yield: 5.25 g, 30.5 mmol, 76%). DSC (5°Cmin^{-1}): 312°C (decomp.); ^1H NMR (D_2O , 60°C): $\delta = 4.80\text{ ppm}$ (s, NH_4^+ , H_2O); ^{13}C NMR ($[\text{D}_6]\text{DMSO}$, 25°C): $\delta = 155.2\text{ ppm}$ ($\text{N}_4\text{C-CN}_4$); ^{14}N NMR ($[\text{D}_6]\text{DMSO}$, 25°C): $\delta = -356$ (NH_4^+), -66 (CN_4), 3 ppm (CN_4); IR (ATR): $\tilde{\nu} = 3170$ (w), 2984 (w), 2875 (w), 2360 (w), 2341 (w), 2140 (w), 1880 (w), 1722 (w), 1692 (m), 1680 (m), 1432 (s), 1327 (s), 1302 (s), 1184 (s), 1147 (s), 1084 (m), 1051 (m), 1016 (s), 732 cm^{-1} (w); Raman (1064 nm , 250 mW , 25°C): $\tilde{\nu} = 3005$ (8), 1588 (100), 1568 (9), 1208 (22), 1144 (8), 1116 (33), 1109 (8), 1074 (26), 784 cm^{-1} (5); MS (FAB^+): m/z : 18.0 [NH_4^+]; MS (FAB^-): m/z : 137.0 [C_2HN_8^-]; elemental analysis calcd (%) for $\text{C}_2\text{H}_8\text{N}_{10}\text{O}$ (172.15): C 13.95, H 4.68, N 81.36; found: C 14.36, H 4.46, N 81.36; BAM drophammer: 35 J ; friction tester: $>360\text{ N}$; ESD: 0.60 J (at grain size $500\text{--}1000\text{ }\mu\text{m}$).

Dihydrazinium 5,5'-bistetrazolate (2): 5,5'-Bistetrazole (2.76 g, 20.0 mmol) was suspended in warm water (5 mL) and hydrazine hydrate (5.01 g, 100 mmol, 5.00 equiv) was added. The reaction mixture was heated to reflux for 20 min, then cooled to RT and stored at 4°C for 5 h. The resulting precipitate was filtered off and washed with a small amount of water, ethanol, and diethyl ether to give the title compound as colorless, fine needles (yield: 0.50 g, 2.47 mmol, 12%). DSC (5°Cmin^{-1}): 234°C (decomp.); ^1H NMR ($[\text{D}_6]\text{DMSO}$, 25°C): $\delta = 7.20\text{ ppm}$ (brs, NH_2NH_3^+); ^{13}C NMR ($[\text{D}_6]\text{DMSO}$, 25°C): $\delta = 154.5\text{ ppm}$ ($\text{N}_4\text{C-CN}_4$); IR (ATR): $\tilde{\nu} = 3235$ (m), 3142 (m), 2883 (m, br), 2574 (s, br), 2350 (m), 2248 (m, br), 1613 (m, br), 1549 (m), 1529 (m), 1328 (s), 1306 (m), 1185 (m), 1167 (m), 1120 (vs), 1079 (s), 1051 (s), 968 (vs), 728 cm^{-1} (m); Raman (1064 nm , 250 mW , 25°C): $\tilde{\nu} = 3151$ (6), 1586 (100), 1563 (10), 1210 (16), 1141 (8), 1113 (27), 1078 (18), 971 (11), 782 cm^{-1} (6); MS (FAB^+): m/z : 33.0 [N_2H_5^+]; MS (FAB^-): m/z : 137.0 [C_2HN_8^-]; elemental analysis calcd (%) for $\text{C}_2\text{H}_{10}\text{N}_{12}$ (202.18): C 11.88, H 4.99, N 81.13; found: C 12.30, H 4.62, N 81.15; BAM drophammer: 40 J ; friction tester: 360 N ; ESD: 0.23 J (at grain size $100\text{--}500\text{ }\mu\text{m}$).

Dihydroxylammonium 5,5'-bistetrazolate (3): 5,5'-Bistetrazole (1.38 g, 10 mmol) was dissolved in hot water (20 mL). A solution of hydroxylamine (50% w/w in H_2O , 1.32 g, 20 mmol, 2.00 equiv) was added slowly and the resulting clear solution was evaporated under vacuum. The colorless solid residue was recrystallized from ethanol/water to give **3** as colorless, fine needles suitable for X-ray crystallography (yield: 1.79 g, 8.8 mmol, 88%). Alternatively, single crystals could be obtained by slow evaporation of the mother liquor. DSC (5°Cmin^{-1}): 205°C (decomp.); ^1H NMR ($[\text{D}_6]\text{DMSO}$, 25°C): $\delta = 10.50\text{ ppm}$ (s, 8H; NH_2OH); ^{13}C NMR ($[\text{D}_6]\text{DMSO}$, 25°C): $\delta = 152.6\text{ ppm}$ ($\text{N}_4\text{C-CN}_4$); IR (KBr): $\tilde{\nu} = 3425$ (m), 3030 (vs), 2815 (s), 2744 (s), 2203 (m), 2056 (m), 1987 (m), 1626 (m),

1534 (m), 1385 (w), 1339 (m), 1314 (m), 1247 (s), 1184 (m), 1145 (m), 1095 (w), 1056 (m), 1030 (m), 1000 (m), 769 (m), 725 cm^{-1} (m); Raman (1064 nm , 350 mW , 25°C): $\tilde{\nu} = 2958$ (1), 2752 (1), 1591 (100), 1436 (2), 1251 (1), 1205 (17), 1144 (9), 1224 (34), 1093 (17), 1002 (22), 779 (3), 426 (5), 387 cm^{-1} (8); MS (FAB^+): m/z : 34.0 [NH_3OH^+]; MS (FAB^-): m/z : 137.0 [C_2HN_8^-]; elemental analysis calcd (%) for $\text{C}_2\text{H}_8\text{N}_{10}\text{O}_2$ (204.15): C 11.77, H 3.95, N 68.61; found: C 12.25, H 3.74, N 68.01; BAM drophammer: 10 J ; friction tester: 240 N (neg.); ESD: 0.10 J (at grain size $100\text{--}500\text{ }\mu\text{m}$).

Bis(guanidinium) 5,5'-bistetrazolate (4): A solution of guanidine carbonate (1.80 g, 9.99 mmol, 1.00 equiv) in H_2O (10 mL) was added to a solution of 5,5'-bistetrazole (1.38 g, 9.99 mmol, 1.00 equiv) in H_2O (15 mL). The resulting solution was heated until all solids were dissolved, then filtered. Slow evaporation of the solvent gave colorless crystals of compound **4** that were suitable for X-ray diffraction (yield: 1.88 g, 7.34 mmol, 73%). DSC (5°Cmin^{-1}): 316 (m.p.), 319°C (decomp.); ^1H NMR ($[\text{D}_6]\text{DMSO}$, 25°C): $\delta = 7.73\text{ ppm}$ (s, 6H; NH_2); ^{13}C NMR ($[\text{D}_6]\text{DMSO}$, 25°C): $\delta = 158.9$ ($\text{C}(\text{NH}_2)_3$), 154.9 ppm ($\text{N}_4\text{C-CN}_4$); IR (KBr): $\tilde{\nu} = 3449$ (vs), 3350 (s), 3092 (s), 2194 (w), 1707 (m), 1650 (vs), 1584 (m), 1384 (m), 1327 (m), 1308 (m), 1183 (m), 1142 (m), 1088 (w), 1044 (w), 1017 (w), 726 (w), 603 (m), 543 cm^{-1} (m); Raman (1064 nm , 300 mW , 25°C): $\tilde{\nu} = 3177$ (2), 1592 (100), 1563 (3), 1207 (7), 1139 (4), 1123 (20), 1073 (26), 1014 (50), 780 (4), 542 (20), 483 (3), 421 (4), 382 (7), 167 (13), 156 (5), 131 (5), 115 (68), 107 (12), 70 cm^{-1} (6); MS (FAB^+): m/z : 60.1 [CH_5N_3^+]; MS (FAB^-): m/z : 137.0 [C_2HN_8^-]; elemental analysis calcd (%) for $\text{C}_4\text{H}_{12}\text{N}_{14}$ (256.23): C 18.75, H 4.72, N 76.53; found: C 19.06, H 4.46, N 75.24; BAM drophammer: 40 J ; friction tester: $>360\text{ N}$; ESD: 1.0 J (at grain size $100\text{--}500\text{ }\mu\text{m}$).

Bis(aminoguanidinium) 5,5'-bistetrazolate dihydrate (5): A suspension of aminoguanidine bicarbonate (2.73 g, 20.1 mmol, 2.00 equiv) in H_2O (30 mL) was added to a solution of 5,5'-bistetrazole (1.38 g, 9.99 mmol, 1.00 equiv) in H_2O (15 mL). The resulting suspension was diluted with H_2O (45 mL) and heated to reflux until all solids were dissolved. Slow evaporation of the solvent gave colorless crystals of compound **5** that were suitable for X-ray diffraction (yield: 1.72 g, 6.01 mmol, 60%). DSC (5°Cmin^{-1}): 247 (m.p.), 251°C (decomp.); ^1H NMR ($[\text{D}_6]\text{DMSO}$, 25°C): $\delta = 9.65$ (brs, 1H; NH), 7.73 (brs, 4H; $\text{C}(\text{NH}_2)_2$), 4.73 ppm (s, 2H; NHNH_2); ^{13}C NMR ($[\text{D}_6]\text{DMSO}$, 25°C): $\delta = 159.7$ ($\text{C}(\text{NHNH}_2)(\text{NH})\text{NH}_2$), 155.1 ppm ($\text{N}_4\text{C-CN}_4$); IR (KBr): $\tilde{\nu} = 3409$ (vs), 3345 (vs), 3162 (vs), 2994 (s), 2891 (s), 2175 (w), 1690 (vs), 1668 (vs), 1553 (w), 1463 (m), 1384 (w), 1327 (s), 1299 (m), 1223 (w), 1169 (m), 1145 (m), 1079 (w), 1042 (w), 1015 (m), 983 (m), 957 (m), 758 (w), 728 (w), 687 (m), 607 (m), 511 (w), 463 cm^{-1} (w); Raman (1064 nm , 300 mW , 25°C): $\tilde{\nu} = 3347$ (2), 3279 (5), 3166 (1), 1670 (3), 1587 (100), 1564 (10), 1423 (2), 1194 (8), 1142 (5), 1108 (32), 1073 (19), 973 (11), 783 (4), 626 (3), 512 (7), 480 (1), 424 (9), 394 (6), 329 (2), 133 (39), 100 (7), 70 cm^{-1} (13); MS (FAB^+): m/z : 75.0 [CH_7N_4^+]; MS (FAB^-): m/z : 136.9 [C_2HN_8^-]; elemental analysis calcd (%) for $\text{C}_4\text{H}_{18}\text{N}_{16}\text{O}_2$ (322.29): C 14.91, H 5.63, N 69.54; found: C 15.21, H 5.56, N 69.42; BAM drophammer: 40 J ; friction tester: 324 N ; ESD: 1.0 J (at grain size $500\text{--}1000\text{ }\mu\text{m}$).

Bis(diaminoguanidinium) 5,5'-bistetrazolate dihydrate (6): A solution of bis(diaminoguanidinium) sulfate (1.26 g, 4.56 mmol, 1.00 equiv) in H_2O (10 mL) was added to a solution of barium 5,5'-bistetrazolate tetrahydrate (1.58 g, 4.57 mmol, 1.00 equiv) in H_2O (40 mL). Filtration and slow evaporation of the solvent gave colorless crystals of compound **6** that were suitable for X-ray diffraction (yield: 1.23 g, 3.49 mmol, 77%). DSC (5°Cmin^{-1}): 97 (H_2O), 204 (m.p.), 208°C (decomp.); ^1H NMR ($[\text{D}_6]\text{DMSO}$, 25°C): $\delta = 9.61$ (brs 2H; NH), 7.64 (s, 2H; C-NH_2), 4.63 ppm (s, 4H; NHNH_2); ^{13}C NMR ($[\text{D}_6]\text{DMSO}$, 25°C): $\delta = 160.6$ ($\text{C}(\text{NHNH}_2)_2$), 155.1 ppm ($\text{N}_4\text{C-CN}_4$); IR (KBr): $\tilde{\nu} = 3470$ (s), 3435 (s), 3341 (vs), 3329 (vs), 3195 (vs), 2906 (s), 2252 (w), 2185 (w), 1672 (vs), 1590 (m), 1416 (m), 1384 (m), 1325 (s), 1302 (m), 1205 (m), 1184 (s), 1146 (w), 1081 (w), 1043 (w), 1018 (s), 986 (m), 781 (w), 742 (w), 663 (m), 593 (m), 473 cm^{-1} (w); Raman (1064 nm , 300 mW , 25°C): $\tilde{\nu} = 3330$ (3), 3219 (6), 1670 (2), 1585 (100), 1565 (5), 1417 (2), 1206 (17), 1185 (2), 1146 (3), 1129 (4), 1109 (29), 1072 (18), 922 (12), 783 (3), 655 (2), 547 (4), 471 (1), 425 (8), 402 (5), 366 (3), 282 (3), 224 cm^{-1} (3); MS (FAB^+): m/z : 90.1 [CH_8N_5^+]; MS (FAB^-): m/z : 137.0 [C_2HN_8^-]; elemental analysis

calcd (%) for $C_4H_{20}N_{18}O_2$ (352.32): C 13.64, H 5.72, N 71.56; found: C 14.22, H 5.46, N 71.16; BAM drophammer: 30 J; friction tester: 360 N; ESD: 0.70 J (at grain size 100–500 μm).

Bis(triaminoguanidinium) 5,5'-bistetrazolate (7): Triaminoguanidine (1.04 g, 9.99 mmol, 1.00 equiv) was added to a solution of 5,5'-bistetrazole (1.45 g, 10.5 mmol, 1.05 equiv) in H_2O (25 mL). Filtration and slow evaporation of the solvent gave slightly purple crystals of **7** that were suitable for X-ray diffraction (yield: 1.42 g, 4.10 mmol, 82%). DSC (5°Cmin^{-1}): 207°C (decomp.); ^1H NMR (D_2O , 25°C): $\delta = 4.77$ ppm (s, 6H; NH_2); ^{13}C NMR (D_2O , 25°C): $\delta = 154.6$ ppm (N_4C-CN_4); IR (KBr): $\tilde{\nu} = 3340$ (m), 3320 (s), 3289 (m), 3211 (vs), 3139 (s), 2178 (w), 1685 (vs), 1614 (m), 1451 (w), 1383 (w), 1335 (m), 1322 (m), 1303 (m), 1224 (w), 1177 (w), 1171 (w), 1157 (m), 1128 (s), 1078 (w), 1043 (w), 1017 (m), 1011 (m), 952 (s), 764 (w), 732 (w), 638 (w), 611 (m), 566 cm^{-1} (w); Raman (1064 nm, 300 mW, 25°C): $\tilde{\nu} = 3340$ (5), 3292 (2), 3240 (2), 3195 (11), 1686 (4), 1664 (1), 1582 (100), 1564 (7), 1457 (2), 1423 (2), 1339 (3), 1198 (26), 1158 (4), 1137 (5), 1111 (38), 1073 (27), 1026 (2), 885 (12), 783 (4), 650 (1), 608 (2), 478 (2), 431 (8), 393 (4), 295 (3), 265 cm^{-1} (2); MS (FAB⁺): m/z : 105.1 [$CH_9N_6^+$]; MS (FAB[−]): m/z : 137.0 [$C_2HN_8^-$]; elemental analysis calcd (%) for $C_4H_{18}N_{20}$ (346.32): C 13.87, H 5.24, N 80.89; found: C 14.02, H 4.87, N 79.21; BAM drophammer: 15 J; friction tester: 285 N; ESD: 0.70 J (at grain size 100–500 μm).

Bis(diaminouronium) 5,5'-bistetrazolate dihydrate (8): Diaminourrea (1.81 g, 20.1 mmol, 2.00 equiv) in H_2O (25 mL) was added to a solution of 5,5'-bistetrazole (1.39 g, 10.1 mmol, 1.00 equiv) in H_2O (30 mL). The solvent was removed under reduced pressure and the residue was recrystallized from EtOH/ H_2O (1:4) to give colorless crystals of compound **8** (yield: 2.84 g, 8.92 mmol, 88%). DSC (5°Cmin^{-1}): 174 (m.p.), 237°C (decomp.); ^1H NMR ($[D_6]DMSO$, 25°C): $\delta = 7.22$ ppm (brs, 7H); ^{13}C NMR ($[D_6]DMSO$, 25°C): $\delta = 161.1$ (C=O), 150.1 ppm (N_4C-CN_4); IR (KBr): $\tilde{\nu} = 3296$ (vs), 3185 (vs), 2996 (vs), 2718 (vs), 2490 (vs), 2225 (s), 2083 (s), 1739 (w), 1681 (s), 1646 (vs), 1621 (vs), 1590 (vs), 1560 (vs), 1536 (vs), 1384 (m), 1335 (vs), 1306 (vs), 1251 (m), 1225 (s), 1183 (s), 1144 (s), 1122 (vs), 1092 (s), 1056 (m), 1015 (s), 977 (m), 817 (m), 727 (s), 702 (s), 534 (w), 504 cm^{-1} (w); Raman (1064 nm, 300 mW, 25°C): $\tilde{\nu} = 3297$ (1), 3184 (4), 1679 (2), 1588 (100), 1560 (6), 1432 (2), 1340 (2), 1325 (5), 1226 (2), 1204 (22), 1143 (9), 1119 (28), 1092 (19), 1017 (5), 975 (9), 780 (4), 512 (7), 426 (12), 385 (9), 365 (3), 192 (7), 161 (3), 144 (34), 126 (9), 107 (42), 90 (27), 67 cm^{-1} (3); MS (FAB⁺): m/z : 91.0 [$CH_5N_4O^+$]; MS (FAB[−]): m/z : 137.0 [$C_2HN_8^-$]; elemental analysis calcd (%) for $C_4H_{18}N_{16}O_4$ (318.26): C 15.10, H 4.43, N 70.42; found: C 15.46, H 4.10, N 69.48; BAM drophammer: 35 J; friction tester: 360 N; ESD: 0.50 J (at grain size 100–500 μm).

Acknowledgements

Financial support of this work by the Ludwig Maximilian University of Munich (LMU), the U.S. Army Research Laboratory (ARL), the Armament Research, Development and Engineering Center (ARDEC), the Strategic Environmental Research and Development Program (SERDP), and the Office of Naval Research (ONR Global, title: "Synthesis and Characterization of New High Energy Dense Oxidizers (HEDO) - NICOP Effort") under contract nos. W911NF-09-2-0018 (ARL), W911NF-09-1-0120 (ARDEC), W011NF-09-1-0056 (ARDEC), and 10 WPSEED01-002/WP-1765 (SERDP) is gratefully acknowledged. The authors acknowledge collaborations with Dr. Mila Krupka (OZM Research, Czech Republic) for the development of new testing and evaluation methods for energetic materials and Dr. Muhamed Sucasca (Brodarski Institute, Croatia) for the development of new computational codes to predict the detonation and propulsion parameters of novel explosives. We are indebted to and thank Drs. Betsy M. Rice and Brad Forch (ARL, Aberdeen, Proving Ground, MD) and Mr. Gary Chen (ARDEC, Picatinny Arsenal, NJ) for many helpful and inspired discussions and support of our work. Mr. Stefan Huber is thanked for performing the sensitivity tests.

- [1] L. V. De Yong, G. Campanella, *J. Hazard. Mater.* **1989**, *21*, 125.
- [2] M. H. V. Huynh, M. A. Hiskey, T. J. Meyer, M. Wetzler, *Proc. Natl. Acad. Sci. USA* **2006**, *103*, 5409–5412.
- [3] N. Fischer, T. M. Klapötke, S. Scheutzw, J. Stierstorfer, *Cent. Eur. J. Energ. Mater.* **2008**, *5*, 3–18.
- [4] E. Oliveri-Mandala, T. Passalacqua, *Gazz. Chim. Ital.* **1914**, *43(II)*, 465–475.
- [5] a) Y. Guo, G.-H. Tao, Z. Zeng, H. Gao, D. A. Parrish, J. M. Shreeve, *Chem. Eur. J.* **2010**, *16*, 3753–3762.
- [6] S. Hachiya, M. Sato (Jpn. Kokai Tokkyo) JP 2006096860A 20060413, **2006**.
- [7] D. E. Chavez, M. A. Hiskey, D. L. Naud, *J. Pyrotech.* **1999**, *10*, 17–36.
- [8] T. M. Klapötke in *Chemistry of High-Energy Materials*, de Gruyter, Berlin, **2011**, 90–91.
- [9] R. Sivabalan, N. Senthikumar, B. Kavitha, S. N. Asthana, *J. Therm. Anal. Calorim.* **2004**, *78*, 781–792.
- [10] R. Sivabalan, M. Anniyappan, S. J. Pawar, M. B. Talawar, G. M. Gore, S. Venugopalan, B. R. Gandhe, *J. Hazard. Mater.* **2006**, *137*, 672–680.
- [11] A. Hammerl, T. M. Klapötke, H. Nöth, M. Warchhold, *Inorg. Chem.* **2001**, *40*, 3570–3575.
- [12] a) M. Tremblay, *Can. J. Chem.* **1965**, *43*, 1230; b) M. A. Hiskey, N. Goldman, J. R. Stine, *J. Energ. Mater.* **1998**, *16*, 119; c) A. Hammerl, M. A. Hiskey, G. Holl, T. M. Klapötke, K. Polborn, J. Stierstorfer, J. J. Weigand, *Chem. Mater.* **2005**, *17*, 3784–3793.
- [13] B. C. Tappan, A. N. Ali, S. F. Son, T. B. Brill, *Propellants Explos. Pyrotech.* **2006**, *31*, 163–168.
- [14] C. M. Michienzi, C. J. Campagnuolo, E. G. Tersine, C. D. Knott, NDIA IM/EM Symposium October 11–14, 2010, Munich, Germany, <http://www.imemg.org/>.
- [15] A. Hammerl, G. Holl, M. Kaiser, T. M. Klapötke, P. Mayer, H. Nöth, H. Piotrowski, M. Warchhold, *Eur. J. Inorg. Chem.* **2002**, 834–845.
- [16] CrysAlisPro Oxford Diffraction Ltd., Version 171.33.41, **2009**.
- [17] a) SIR92: A. Altomare, G. Cascarano, C. Giacovazzo, A. Guagliardi, *J. Appl. Crystallogr.* **1993**, *26*, 343; b) SIR97: A. Altomare, M. C. Burla, M. Camalli, G. L. Cascarano, C. Giacovazzo, A. Guagliardi, A. G. Moliterni, G. Polidori, R. Spagna, *J. Appl. Crystallogr.* **1999**, *32*, 115–119.
- [18] G. M. Sheldrick SHELXS-97, Program for Crystal Structure Solution, Universität Göttingen, **1997**.
- [19] PLATON, Utrecht University, Utrecht, The Netherlands, A. L. Spek, **1998**.
- [20] L. J. Farrugia, *J. Appl. Crystallogr.* **1999**, *32*, 837–838.
- [21] Empirical absorption correction using spherical harmonics, implemented in SCALE3 ABSPACK scaling algorithm (CrysAlisPro Oxford Diffraction, v. 171.33.41, **2009**).
- [22] P. J. Eulgem, A. Klein, N. Maggiora, D. Naumann, R. W. H. Pohl, *Chem. Eur. J.* **2008**, *14*, 3727–3736.
- [23] A. F. Holleman, E. Wiberg, N. Wiberg, *Lehrbuch der Anorganischen Chemie*, 102. Auflage, Walter de Gruyter, Berlin, **2007**.
- [24] V. Ernst, T. M. Klapötke, J. Stierstorfer, *Z. Anorg. Allg. Chem.* **2007**, *633*, 879–887.
- [25] P. J. Steel, *J. Chem. Crystallogr.* **1996**, *26*, 399–402.
- [26] M. Kowalewski, P. Mayer, A. Schulz, A. Villinger, *Acta Crystallogr. Sect. E* **2006**, *62*, i248–i249.
- [27] T. Fendt, N. Fischer, T. M. Klapötke, J. Stierstorfer, *Inorg. Chem.* **2011**, *50*, 1447–1458.
- [28] M. Hesse, H. Meier, B. Zeeh, *Spektroskopische Methoden in der Organischen Chemie*, 7th ed., Thieme, Stuttgart, Germany, **2005**.
- [29] G. Socrates, *Infrared and Raman Characteristics Group Frequencies*, 3rd ed., John Wiley & Sons, Chichester, **2004**.
- [30] T. M. Klapötke, P. Mayer, C. Miro Sabate, J. M. Welch, N. Wiegand, *Inorg. Chem.* **2008**, *47*, 6014–6027.
- [31] NATO standardization agreement (STANAG) on explosives, *Impact Sensitivity Tests*, no. 4489, 1st ed., Sept. 17, **1999**.

- [32] WIWEB-Standardarbeitsanweisung 4-5.1.02, Ermittlung der Explosionsgefährlichkeit, hier der Schlagempfindlichkeit mit dem Fallhammer, Nov. 8, **2002**.
- [33] <http://www.bam.de>.
- [34] NATO standardization agreement (STANAG) on explosives, *Friction Sensitivity Tests*, no. 4487, 1st ed., Aug. 22, **2002**.
- [35] WIWEB-Standardarbeitsanweisung 4-5.1.03, Ermittlung der Explosionsgefährlichkeit oder der Reibeempfindlichkeit mit dem Reibeapparat, Nov. 8, **2002**.
- [36] Impact: insensitive >40 J, less sensitive ≥ 35 J, sensitive ≥ 4 J, very sensitive ≤ 3 J; friction: insensitive >360 N, less sensitive =360 N, sensitive 360–80 N, very sensitive ≤ 80 N, extreme sensitive ≤ 10 N. According to the UN Recommendations on the Transport of Dangerous Goods (+) indicates not safe for transport.
- [37] <http://www.ozm.cz>.
- [38] <http://www.linseis.com>.
- [39] T. Altenburg, T. M. Klapötke, A. Penger, J. Stierstorfer, *Z. Anorg. Allg. Chem.* **2010**, 636, 463–471.
- [40] Gaussian 09, Revision A.1, M. J. Frisch, G. W. Trucks, H. B. Schlegel, G. E. Scuseria, M. A. Robb, J. R. Cheeseman, G. Scalmani, V. Barone, B. Mennucci, G. A. Petersson, H. Nakatsuji, M. Caricato, X. Li, H. P. Hratchian, A. F. Izmaylov, J. Bloino, G. Zheng, J. L. Sonnenberg, M. Hada, M. Ehara, K. Toyota, R. Fukuda, J. Hasegawa, M. Ishida, T. Nakajima, Y. Honda, O. Kitao, H. Nakai, T. Vreven, J. A. Montgomery, Jr., J. E. Peralta, F. Ogliaro, M. Bearpark, J. J. Heyd, E. Brothers, K. N. Kudin, V. N. Staroverov, R. Kobayashi, J. Normand, K. Raghavachari, A. Rendell, J. C. Burant, S. S. Iyengar, J. Tomasi, M. Cossi, N. Rega, J. M. Millam, M. Klene, J. E. Knox, J. B. Cross, V. Bakken, C. Adamo, J. Jaramillo, R. Gomperts, R. E. Stratmann, O. Yazyev, A. J. Austin, R. Cammi, C. Pomelli, J. W. Ochterski, R. L. Martin, K. Morokuma, V. G. Zakrzewski, G. A. Voth, P. Salvador, J. J. Dannenberg, S. Dapprich, A. D. Daniels, Ö. Farkas, J. B. Foresman, J. V. Ortiz, J. Cioslowski, and D. J. Fox, Gaussian, Inc., Wallingford CT, **2009**.
- [41] *NIST Chemistry WebBook, NIST Standard Reference Database Number 69* (Eds.: P. J. Linstrom, W. G. Mallard), National Institute of Standards and Technology, Gaithersburg MD, 20899, <http://webbook.nist.gov>, (retrieved October 27, **2011**).
- [42] a) H. D. B. Jenkins, H. K. Roobottom, J. Passmore, L. Glasser, *Inorg. Chem.* **1999**, 38, 3609–3620; b) H. D. B. Jenkins, D. Tudela, L. Glasser, *Inorg. Chem.* **2002**, 41, 2364–2367.
- [43] M. Sućeska, EXPLO5.04 program, Zagreb, Croatia, **2010**.
- [44] K. M. Dontsova, J. C. Pennington, C. Hayes, J. Šimunek, C. W. Williford, *Chemosphere* **2009**, 77, 597–603.
- [45] United States Environmental Protection Agency, <http://www.epa.gov/>.
- [46] C. M. Walsh, C. D. Knott, C. S. Leveritt, *Reduced Erosion Additive for a Propelling Charge*, US 6984275 B1, **2006**.
- [47] F. Volk, H. Bathelt, *Propellants Explos. Pyrotech.* **1997**, 22, 120–124.
- [48] Calculation of oxygen balance: $\Omega [\%] = (wO - 2xC - 1/2yH - 2zS)/1600/M$. (w : number of oxygen atoms, x : number of carbon atoms, y : number of hydrogen atoms, z : number of sulfur atoms, M : molecular weight).

Received: November 28, 2011
Published online: February 24, 2012

Hydroxylammonium 5-Nitriminotetrazolates

Niko Fischer,^[a] Thomas M. Klapötke,^{*[a]} Davin G. Piercey,^[a] and Jörg Stierstorfer^[a]

Keywords: Tetrazoles; Explosives; X-ray diffraction; Detonation parameters; Sensitivities

Abstract. The hydroxylammonium salts of monodeprotonated 5-nitriminotetrazole (**4**), double deprotonated 5-nitriminotetrazole (**5**), 1-methyl-5-nitriminotetrazole (**6**), and 2-methyl-5-nitraminotetrazole (**7**) have been prepared in high yield from the corresponding 5-nitriminotetrazoles as free acids and an aqueous solution of hydroxylamine or the metathesis reactions of hydroxylammonium hydrochloride with the silver salt of the corresponding nitriminotetrazole, respectively. The

energetic salts **4–7** were fully characterized by single-crystal X-ray diffraction (**4–6**), NMR spectroscopy, IR- and Raman spectroscopy as well as DSC measurements. The sensitivities towards impact, friction and electrical discharge were determined. In addition, several detonation parameters (e.g. heat of explosion, detonation velocity) were computed by the EXPLO5.04 computer code based on calculated (CBS-4M) heats of formation and X-ray densities.

Introduction

The design of new energetic materials encompassing all of propellants, explosives, and pyrotechnics is a modern academic and technological challenge.^[1–3] Intense research is focused on the tailoring of new energetic molecules with performances and stability similar to that of RDX (cyclotrimethylenetrinitramine) to replace this widely-used high explosive. For a novel energetic molecule to find practical application as a high explosive it needs to possess high thermal and mechanical stabilities, while at the same time satisfying the increasing demand for higher performing (high detonation velocity, pressure and heat of explosion) materials.^[4]

One of the most promising energetic backbones for the tailoring of energetic molecules is the tetrazole ring; the carbon on position 5 of the ring allows the facile attachment of various substituents for energetic tailorability, and the high nitrogen content of the heterocycle leads to high energetic performances.^[5] It can be stated that the tetrazole heterocycle occupies the “middle ground” of the stability vs. high performance continuum, where highly stable compounds can be poorly-performing energetics and highly energetic compounds are often unstable. This trend is exemplified in the range of five-membered azoles from pyrazole to pentazole, where pyrazoles are not used in energetics due to low performance, and the few pentazole derivatives known are highly unstable.^[6]

Of the energetic tetrazoles known, nitriminotetrazoles are some of the most promising for practical use as they have some of the highest performances and thermal stabilities. By tailoring substituents and counterions, nitriminotetrazoles have

been shown to illustrate the entire spectrum of sensitivity from insensitive secondary to sensitive primary explosives,^[7,8] while maintaining high thermal stability. High thermal stabilities arise from the aromatic nature of the tetrazole ring, whereas the high performances arise from the high heats of formation of nitriminotetrazoles, the ring strain of the five-membered ring, and good oxygen balances.^[9]

The oxygen balance is a percentage representation of a compound's ability to oxidize all carbon and hydrogen in the molecule to carbon dioxide and water, respectively. When an oxygen balance is at or near zero, explosive performances are high, however deviation into either a negative (fuel rich) or positive (oxygen rich) oxygen balance leads to a loss of performance. For an energetic material containing only CHNO the oxygen balance is easily calculated by the equation $\Omega (\%) = (wO - 2xC - 1/2yH) \cdot 1600/M$ (w : number of oxygen atoms, x : number of carbon atoms, y : number of hydrogen atoms, z : number of sulfur atoms). Nitriminotetrazole itself has an only slightly negative oxygen balance and hence, shows very good detonation performance data. When nitriminotetrazoles are deprotonated to form stable, nitrogen rich salts, the oxygen balance decreases and also the performance compared to the neutral, acidic form. Our recent efforts pairing nitriminotetrazolate anions with the oxygen-containing diaminouronium cation^[10] illustrated the improvement in performances seen when oxygen balances are improved. In our quest for ever higher performances while maintaining thermal stability, we have paired three nitriminotetrazoles (5-nitriminotetrazole, 1-methyl-5-nitriminotetrazole, 2-methyl-5-nitraminotetrazole) with the hydroxylammonium cation, the synthesis and characterization of which we describe in the following.

Results and Discussion

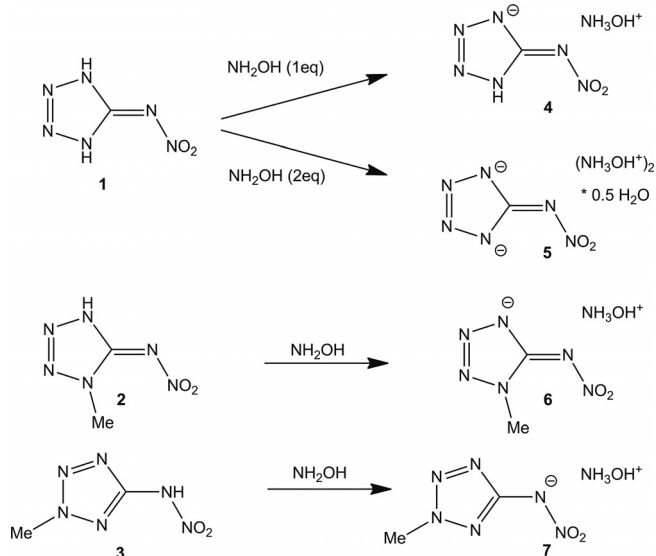
Synthesis

Hydroxylammonium 5-nitriminotetrazolates can be synthesized most easily either from the neutral 5-nitriminotetrazol-

* Prof. Dr. T. M. Klapötke
Fax: +49-89-2180-77492
E-Mail: tmk@cup.uni-muenchen.de

[a] Energetic Materials Research
Department Chemie
Ludwigs-Maximilians Universität München
Butenandtstr. 5–13
81377 München, Germany

ates and an aqueous solution of hydroxylamine or via metathesis reaction using the respective silver salts and hydroxylammonium chloride. The synthesis of the 5-nitriminotetrazolates **4–7** was achieved employing both synthetic routes; the first one is using the neutral compounds, which have been deprotonated with an 50% (w/w) aqueous solution of hydroxylamine as described in Scheme 1. The second route using the silver salts of the corresponding 5-nitriminotetrazoles and hydroxylammonium chloride is working with yields, that are almost as high (80–90%), but the use of expensive starting materials (AgNO_3) and the isolation of the highly friction and impact sensitive silver 5-nitriminotetrazolates make this route disadvantageous compared to the first route described here. Unexpectedly, the solubility of the monodeprotonated 5-nitriminotetrazolate salts **5–7** is very good in water and to a small extend, the salts are even soluble in lower aliphatic alcohols such as methanol. Therefore, they have to be recrystallized from mixtures containing methanol or ethanol and small amounts of water to obtain crystals suitable for X-ray single crystal measurements. In contrast, the solubility of the double deprotonated salt **4** is comparatively low in water, which means, that single crystals for the structure determination have to be grown directly from the aqueous reaction mixture after the addition of hydroxylamine to the free acid. The starting materials 5-nitriminotetrazole as well as the methylated compounds



Scheme 1. Synthesis via Brønsted acid-base reactions of the target molecules presented in this work: hydroxylammonium 5-nitriminotetrazolate (**4**), bishydroxylammonium 5-nitriminotetrazolate semihydrate (**5**), hydroxylammonium 1-methyl-5-nitriminotetrazolate (**6**), hydroxylammonium 2-methyl-5-nitriminotetrazolate (**7**).

1-methyl-5-nitriminotetrazole and 2-methyl-5-nitriminotetrazole were synthesized according to literature.^[11]

Table 1. X-ray data and parameters.

	4	5	6
Formula	$\text{CH}_3\text{N}_7\text{O}_3$	$\text{CH}_6\text{N}_8\text{O}_{4.5}$	$\text{C}_2\text{H}_7\text{N}_7\text{O}_3$
FW / $\text{g}\cdot\text{mol}^{-1}$	163.12	205.16	177.15
Crystal system	monoclinic	monoclinic	orthorhombic
Space Group	$P2_1/c$ (14)	$P2_1/n$ (13)	$Pbca$ (61)
Color / Habit	colorless rod	colorless block	colorless block
Size /mm	$0.12 \times 0.20 \times 0.24$	$0.32 \times 0.34 \times 0.40$	$0.06 \times 0.07 \times 0.13$
a /Å	8.6228(5)	14.7405(10)	7.6060(17)
b /Å	9.2014(5)	3.6447(2)	6.5593(12)
c /Å	7.6673(5)	15.2973(9)	28.995(7)
α /°	90	90	90
β /°	93.768(5)	110.602(7)	90
γ /°	90	90	90
V /Å ³	607.02(6)	769.28(9)	1446.6(5)
Z	4	2	8
$\rho_{\text{calcd.}}$ / $\text{g}\cdot\text{cm}^{-3}$	1.785	1.771	1.627
μ / mm^{-1}	0.164	0.166	0.145
$F(000)$	336	428	736
$\lambda_{\text{Mo-K}\alpha}$ /Å	0.71073	4.8, 26.0	0.71073
T /K	173	173	173
$\theta_{\text{Min-Max}}$ /°	4.3, 26.2	4.8, 26.0	4.2, 26.0
Dataset hkl	−10:10; −11:11; −9: 9	−15:18; −4:4; −18:18	−9:9; −8:8; −35:26
Reflections collected	8996	3633	6409
Independent reflections	1219	1516	1366
R_{int}	0.036	0.019	0.083
Observed reflections	951	1275	720
Parameters	120	160	126
R_1 (obs)	0.0277	0.0285	0.0520
wR_2 (all data)	0.0760	0.0771	0.1191
GooF	0.98	1.03	0.86
Resd. Dens. / $\text{e}\cdot\text{Å}^{-3}$	−0.19, 0.17	−0.20, 0.20	−0.22, 0.40
Device type	Oxford Xcalibur 3	Oxford Xcalibur 3	Oxford Xcalibur 3
Solution	SIR-92	SIR-92	SHELXS-97
Refinement	SHELXL-97	SHELXL-97	SHELXL-97
Absorption correction	semiempirical	semiempirical	semiempirical
CCDC	790986	851203	790987

Crystal Structures

Relevant data and parameters of the crystal structure elucidations are listed in Table 1. Bond lengths and angles are listed in Table 2.

Table 2. Bond lengths and bond angles of **4**, **5** and **6**.

atoms	4	5	6
	<i>d</i> / Å	<i>d</i> / Å	<i>d</i> / Å
O1–N6	1.2493(15)	1.2930(14)	1.234(3)
O2–N6	1.2661(15)	1.2668(14)	1.279(3)
N5–N6	1.3175(16)	1.2873(14)	1.308(3)
N5–C1	1.3657(17)	1.3980(16)	1.375(4)
N1–C1	1.3396(17)	1.3412(15)	1.335(4)
N4–C1	1.3342(19)	1.3382(17)	1.334(4)
N1–N2	1.3436(16)	1.3368(16)	1.352(4)
N2–N3	1.2939(16)	1.3093(16)	1.288(4)
N3–N4	1.3502(16)	1.3463(15)	1.361(4)
N1(N2)–C2			1.466(4)
O3–N7	1.4145(18)	1.4100(17)	1.407(3)
O4–N8		1.4138(16)	
	∠ / °	∠ / °	∠ / °
O1–N6–O2	120.48(11)	118.22(10)	120.3(3)
O2–N6–N5	114.81(11)	125.54(11)	113.8(2)
O1–N6–N5	124.70(11)	116.23(10)	125.9(2)
N6–N5–C1	115.88(11)	117.49(11)	117.2(3)
N3–N4–C1	106.11(11)	104.30(10)	105.6(3)
N2–N1–C1	108.95(11)	105.70(10)	108.8(3)
N1–N2–N3	106.46(11)	108.68(10)	106.4(2)
N2–N3–N4	110.92(11)	110.41(11)	111.1(3)
N4–C1–N5	119.75(12)	132.35(11)	133.7(3)
N1–C1–N4	107.55(11)	110.91(10)	108.1(3)
N1–C1–N5	132.69(13)	116.75(11)	118.0(3)
C1–N1–C2			129.4(3)
N2–N1–C2			121.8(3)

Hydroxylammonium 5-nitriminotetrazolate (**4**) crystallizes in the monoclinic space group $P2_1/c$ with four anion/cation pairs in the unit cell. The asymmetric unit is depicted in Figure 1. Its density of 1.785 g cm^{-3} is quite high in comparison with other tetrazolate salts in literature.^[12,13] The hydroxylammonium cations in all structures described here show equal bond lengths and angles comparable to those found in literature, e.g. for hydroxylammonium azotetrazolate monohydrate.^[14]

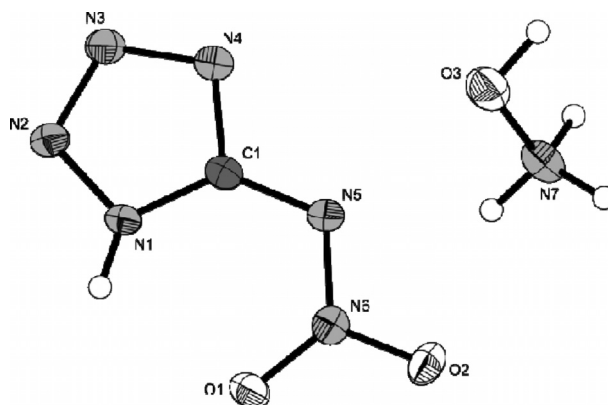


Figure 1. Molecular unit of hydroxylammonium 5-nitriminotetrazolate (**4**). Ellipsoids of non-hydrogen atoms are drawn at the 50% probability level.

Compound **4** crystallizes layer-like along the *b*-axes (Figure 2A). The packing is stabilized by several inter- and intra-

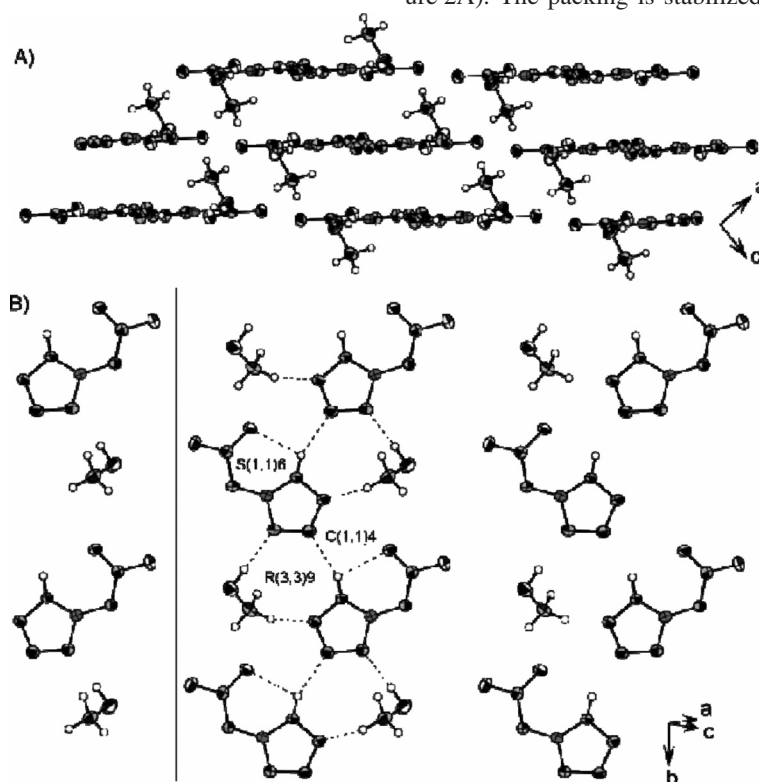


Figure 2. A) View along the *b* axes. B) View on the layers in the structure of **4**. Selected graph sets^[15] are drawn.

molecular hydrogen bridges within the layers (forming strands) on the one hand. On the other hand, the hydroxylammonium cations act as linkers between two layers by forming strong hydrogen bonds.

The double deprotonated salt bis(hydroxylammonium) 5-nitriminotetrazolate (**5**) could only be obtained crystalline as its hemihydrate. Compound **5** crystallizes in the monoclinic space group *P2₁/n* with four cation/anion pairs as well as two water molecules in the unit cell. Its density of 1.771 g·cm⁻³ is only slightly lower than that of **4**. The structure of the dianion is almost planar, which is in accordance with previously published structures e.g. diammonium 5-nitrimino-tetrazolate.^[16] The molecular unit is depicted in Figure 3.

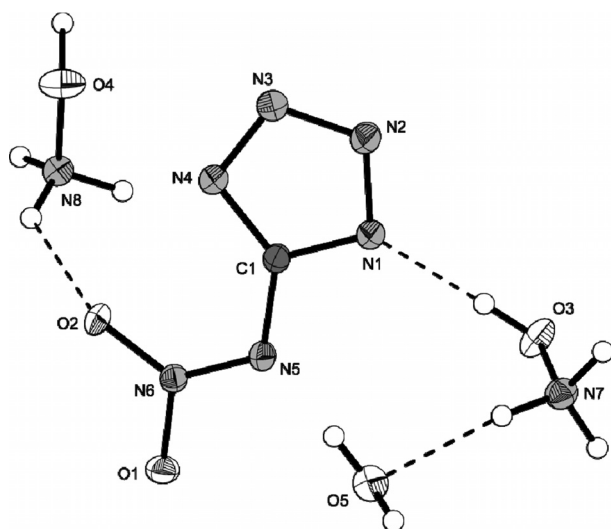


Figure 3. Molecular unit of bis(hydroxylammonium) 5-nitriminotetrazolate semihydrate (**5**). Ellipsoids of non-hydrogen atoms are drawn at the 50 % probability level.

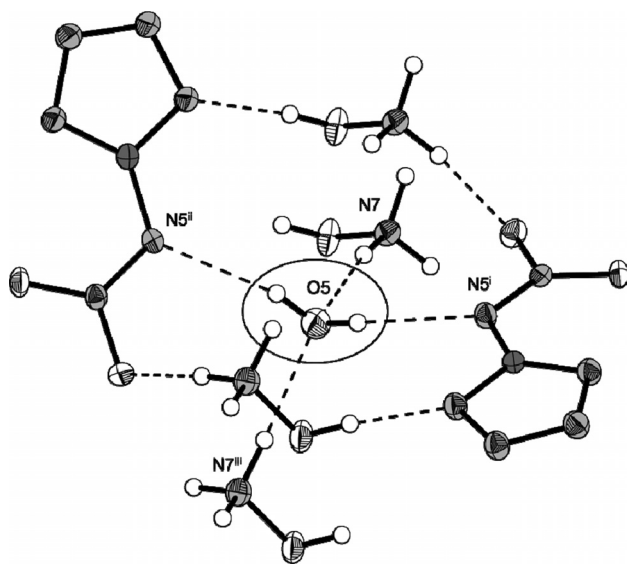


Figure 4. Hydrogen bonds of the crystal water. Symmetry codes: (i) 2.5-x, 1+y, 1.5-z; (ii) -1+x, 1+y, z; (iii) 2.5-x, y, 1.5-z.

The packing of **5** is dominated by several strong hydrogen bonds. Exemplarily, the coordination of the crystal water is

shown in Figure 4. The water molecules form a tetrahedral coordination sphere, connecting two nitriminotetrazolate anions via the N5 nitrogen atoms.

Hydroxylammonium 1-methyl-5-nitriminotetrazolate (**6**) crystallizes in the orthorhombic space group *Pbca* with eight anion/cation pairs in the unit cell. The asymmetric unit is shown in Figure 5. Its density of 1.627 g·cm⁻³ is significantly lower than that of **4** and **5**. Again a strong hydrogen bond network is formed, which is depicted in Figure 6.

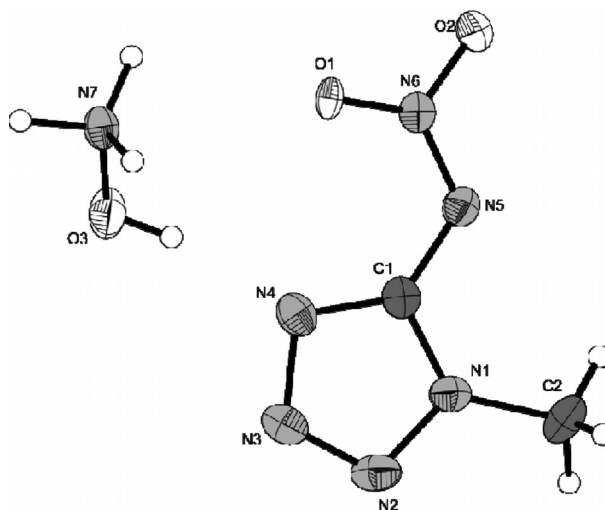


Figure 5. Molecular unit of hydroxylammonium 1-methyl-5-nitriminotetrazolate (**6**). Ellipsoids of non-hydrogen atoms are drawn at the 50 % probability level.

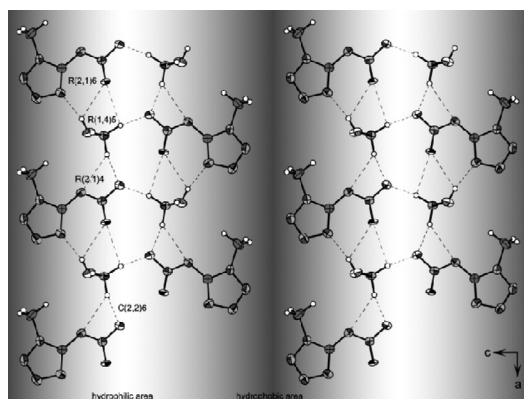


Figure 6. View on the layers in the structure of **6**. Bright regions represent hydrophilic parts, dark regions hydrophobic parts.

Heats of Formation

Usually energetic materials tend to explode in bomb calorimetric measurements. Consequently doubtful combustion energies are obtained. Therefore heats of formation of energetic materials mostly are calculated theoretically. In our group we combine the atomization energy method (Equation (1)) with CBS-4M electronic energies which has been shown suitable in many recently published studies.^[17] CBS-4M energies of the atoms, cations, and anions were calculated with the

Gaussian09 (revision A1) software package^[18] and checked for imaginary frequencies. Values for $\Delta_f H^\circ$ (atoms) were taken from the NIST database.^[19]

$$\Delta_f H^\circ_{(g, M, 298)} = H_{(Molecule, 298)} - \sum H^\circ_{(Atoms, 298)} + \sum \Delta_f H^\circ_{(Atoms, 298)} \quad (1)$$

For calculation of the solid state energy of formation (Table 4) of **4–7**, the lattice energies (U_L) and lattice enthalpies (ΔH_L) were calculated from the corresponding molecular volumes (obtained from X-ray elucidations) according to the equations provided by Jenkins et al.^[20] With the calculated lattice enthalpy (Table 4), the CBS-4M based gas-phase enthalpy of formation (Table 3) was converted into the solid state (standard conditions) enthalpy of formation. These molar standard enthalpies of formation (ΔH_m) were used to calculate the molar solid state energies of formation (ΔU_m) according to Equation (2) (Table 4).

$$\Delta U_m = \Delta H_m - \Delta n RT \quad (2)$$

(Δn being the change of moles of gaseous components)

Compounds **4–7** are all formed endothermically. The 2-methyl derivative **7** has the highest value of 352.2 kJ·mol^{−1}. The significantly lower value (63.3 kJ·mol^{−1}) of compound **5**

Table 3. CBS-4M results and gas phase enthalpies.

M	$-H^{298}$ /a.u.	$\Delta_f H$ (g) /kJ·mol ^{−1}
H ₄ NO ⁺ (in 4–7)	131.863229	687.0
CHN ₆ O ₂ [−] (in 4)	516.973495	150.5
CN ₆ O ₂ ^{2−} (in 5)	516.294886	399.0
C ₂ H ₃ N ₆ [−] (in 6)	556.194636	166.3
C ₂ H ₃ N ₆ [−] (in 7)	556.186685	187.2

is based on the inclusion of crystal water on the one hand and the higher lattice enthalpy of a 2:1 salt on the other hand.

Detonation Parameters

The detonation parameters calculated with the EXPLO5 V5.04 computer code^[21] using the experimentally determined densities (X-ray) are summarized in Table 5.

Especially the detonation parameters of compound **4** and **5** show promising values, much higher than those of trinitrotoluene (**TNT**), pentaerythrityl tetranitrate (**PETN**) and hexogen (**RDX**). The most powerful compound in terms of all calculated detonation parameters is the monodeprotonated salt **4**, which has also the highest density. Also compound **5** and **6** exceed the values of **TNT** and **PETN**. The most important criteria of high explosives are their detonation velocity (V_{det}).

Table 4. Calculation of solid state energies of formation ($\Delta_f U^\circ$).

	$\Delta_f H$ (g) /kJ·mol ^{−1}	V_M / nm ³	U_L /kJ·mol ^{−1}	ΔH_L /kJ·mol ^{−1}	$\Delta_f H^\circ$ (s) /kJ·mol ^{−1}	Δn	$\Delta_f U^\circ$ (s) /kJ·mol ^{−1}	M /g·mol ^{−1}	$\Delta_f U^\circ$ (s) /kJ·kg ^{−1}
4	837.7	151.8	543.6	547.1	290.5	7.5	309.1	163.13	1895.1
5	1652.6*	179.8	1578.4	1589.3	63.3	10.75	90.0	205.16	438.6
6	853.5	180.8	518.7	522.2	331.3	8.5	352.4	177.16	1989.0
7	874.4	180.8	518.7	522.2	352.2	8.5	373.3	177.16	2106.9

*Value has been corrected (−120 kJ·mol^{−1}) to hemihydrate formation.

Table 5. Physico-chemical properties of **4–7** in comparison with trinitrotoluene (**TNT**), nitropenta (**PETN**) and hexogen (**RDX**).

	4	5	6	7	TNT*	PETN*	RDX*
Formula	CH ₅ N ₇ O ₃	CH ₉ N ₈ O _{4.5}	C ₂ H ₇ N ₇ O ₃	C ₂ H ₇ N ₇ O ₃	C ₇ H ₅ N ₃ O ₆	C ₅ H ₈ N ₄ O ₁₂	C ₃ H ₆ N ₆ O ₇
FW /g·mol ^{−1}	163.13	205.16	177.12	177.12	227.13	316.14	222.12
IS /J ^{a)}	2	10	8	6	15	3	7.5
FS /N ^{b)}	40	80	144	144	353	60	120
ESD-test /J	0.30	0.30	0.50	0.30	---	---	0.1–0.2
N % ^{c)}	60.1	54.6	40.7	40.7	18.50	17.72	37.8
O % ^{d)}	−14.7	−20.3	−55.4	−55.4	−73.96	−10.1	−21.6
T_{dec} /°C ^{e)}	172	166	185	180	>160	202	210
ρ /g·cm ^{−3} ^{f)}	1.785	1.771	1.627	1.627*	1.654	1.778	1.800
$\Delta_f H_m^\circ$ /kJ·mol ^{−1} ^{g)}	+290	+80	+331	+352	−59	−539	+70
$\Delta_f U^\circ$ /kJ·kg ^{−1} ^{h)}	1895	520	1989	2107	−185	−1612	417
EXPLO5 values:							
$-\Delta_E U^\circ$ /kJ·kg ^{−1} ⁱ⁾	6113	5678	6095	6210	5227	6190	6125
T_E /K ^{j)}	4219	3715	3949	4000	3657	4306	4236
p_{C-J} /kbar ^{k)}	371	360	297	300	216	320	349
V_{Det} /m·s ^{−1} ^{l)}	9236	9214	8651	8690	7253	8320	8748
Gas vol. /L·kg ^{−1} ^{m)}	853	923	842	842	574	688	739

a) Impact sensitivity measured by the BAM drophammer, grain size (75–150 µm); b) Impact sensitivity measured by the BAM friction tester, grain size (75–150 µm); c) Nitrogen content; d) Oxygen balance;^[22] e) Temperature of decomposition by DSC ($\beta = 5^\circ\text{C}$); f) Density from X-ray structure; g) Molar enthalpy of formation; h) Energy of formation; i) Energy of explosion; j) Explosion temperature; k) Detonation pressure; l) Detonation velocity; m) Assuming only gaseous products; *Values based on Ref.^[23] and the EXPLO5 database; #: estimated to be equal than **6**.

= **4**: 9236, **5**: 9214, **6**: 8651, **7**: 8690, TNT: 7253, PETN: 8320, RDX: 8748 $\text{m}\cdot\text{s}^{-1}$), detonation pressure (p_{C-J} = **4**: 371, **5**: 360; **6**: 297, **7**: 300, TNT: 216, PETN: 320, RDX: 349 kbar) and energy of explosion ($\Delta_E U^\circ$ = **4**: -6113, **5**: -5678, **6**: -6095, **7**: -6210, TNT: -5227, PETN: -6190, RDX: -6125 $\text{kJ}\cdot\text{kg}^{-1}$).

Sensitivity Testing

For application of new energetic compounds important values for safety, handling and processing are the sensitivity data. The values for friction and impact sensitivity were determined according to BAM standard methods described in the NATO STANAG 4487, 4489 and 4490 specifications for energetic materials.^[24–30] The sensitivities towards electrical discharge were determined on a small scale electrostatic discharge device.^[31] According to the UN Recommendations on the Transport of Dangerous Goods compound **4** is regarded very sensitive towards impact (2 J), whereas compounds **5–7** are classified as sensitive towards impact (**5**: 10 J, **6**: 8 J, **7**: 6 J).^[32] Also the friction sensitivities vary between very sensitive for **4** and **5** (**4**: 40 N, **5**: 80 N) and sensitive for **6** and **7** (both 144 N). A general trend towards higher sensitivity for the 2-methylated compound compared to the 1-methylated compound, which has also been shown for other nitrogen-rich salts of both nitriminotetrazoles^[9,33] is reconfirmed in this case, if the sensitivity data of **6** and **7** are compared. The sensitivities towards electrostatic discharge are relatively similar being in a range between 0.30 J (**4**, **5**, **7**) and 0.50 J (**6**).

Thermal Stabilities

Thermostability of energetic compounds is considered important especially in processing and storing the material. Because of the diverse use of energetic materials e.g. under extreme climatic conditions like in desserts, for oil drilling or military ammunition high temperature stability is desired. Three of the four introduced compounds (**4–6**) decompose in a two or even three step mechanism, whereas the decomposition of **7** involves only a single step. For a safe handling of the material, certainly the first decomposition step is of major importance. In the following, all decomposition temperatures are given as absolute onset temperatures. For the monodeprotonated salt **4**, a first decomposition at 172 °C is observed and a following at 204 °C. It decomposes without previous melting, which is not the case for compounds **5–7**, indicated by an endothermic step before decomposition. For the double deprotonated salt **5** a more complex decomposition mechanism can be proposed since it involves three exothermic steps at 166 °C, 184 °C and 194 °C, respectively, however for a detailed investigation of the mechanism a thermogravimetric measurement would be necessary. It furthermore loses its crystal water and melts before decomposition indicated by two endothermic steps at 129 °C and 162 °C, respectively. Also the 1-methyl-5-nitriminotetrazolate **6** melts at 180 °C right before it decomposes at 185 °C followed by a second decomposition step at 193 °C. Compound **7**, which has its methyl group in position 2 at the tetrazole ring differs in that it has a significantly lower

melting point 139 °C and a relatively large liquidity range before it decomposes at 180 °C. All DSC plots are depicted in Figure 7.

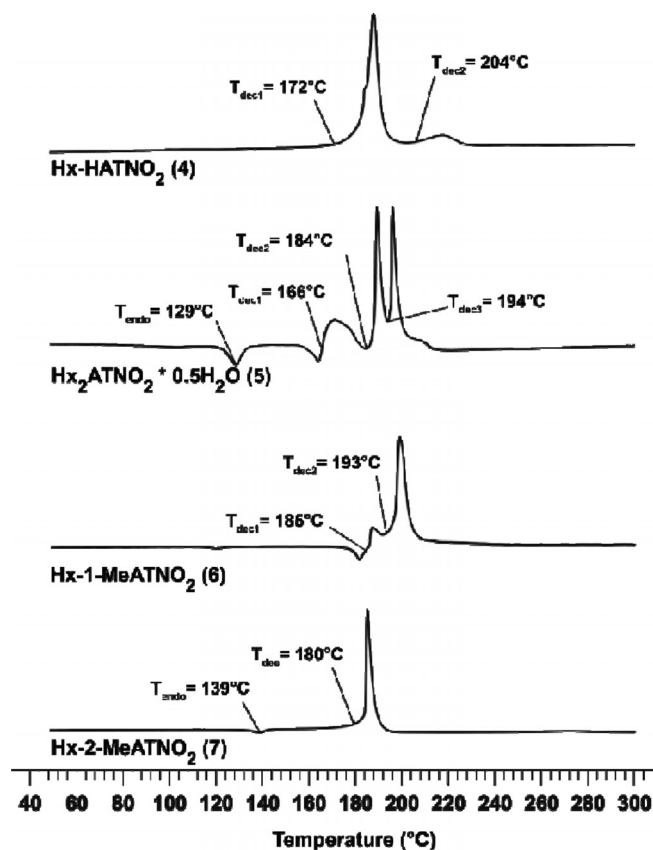


Figure 7. DSC-plots of compounds **4–7** at a heating rate of 5 $\text{K}\cdot\text{min}^{-1}$. Exothermic = \uparrow , endothermic = \downarrow .

Conclusions

From this combined experimental and theoretical study the following conclusions can be drawn: Four different hydroxylammonium 5-nitriminotetrazolates, namely hydroxylammonium 5-nitriminotetrazolate (**4**), bishydroxylammonium 5-nitriminotetrazolate semihydrate (**5**), hydroxylammonium 1-methyl-5-nitriminotetrazolate (**6**) and hydroxylammonium 2-methyl-5-nitraminotetrazolate (**7**), were synthesized from the corresponding 5-nitriminotetrazoles and aqueous hydroxylamine or via the corresponding silver 5-nitriminotetrazolates and hydroxylammonium chloride in high yields and good purity. All compounds were fully characterized including the structural determination of **4–6**. The detonation performance of these high energy density materials was calculated based on the crystal density and CBS-4M based heats of formation. Unfortunately, the monodeprotonated salt hydroxylammonium 5-nitriminotetrazolate (**4**), which shows the best performance reveals sensitivity data comparable to primary explosives (IS: 2 J, FS: 40 N), whereas the double deprotonated salt **5**, which is less sensitive towards impact and friction (IS: 10 J, FS: 80 N) reveals a poor thermal stability of 166 °C. Both

methyated compounds **6** and **7** show a higher thermal stability whereas having a lower detonation performance. The above mentioned findings again confirm the fact, that highly stable compounds can be poorly-performing energetics and highly energetic compounds are often unstable, which is one of the greatest challenges when synthesizing new high explosives.

Experimental Section

Caution! Nitriminotetrazoles and their salts are highly energetic materials with increased sensitivities towards shock and friction. Therefore, proper security precautions (safety glass, face shield, earthened equipment and shoes, Kevlar® gloves and ear plugs) have to be applied while synthesizing and handling the herein described compounds.

All reagents and solvents were used as received (Sigma–Aldrich, Fluka, Acros Organics) if not stated otherwise. Melting and decomposition points were measured with a Linseis PT10 DSC using heating rates of $5\text{ K}\cdot\text{min}^{-1}$, which were checked with a Büchi Melting Point B-450 apparatus. ^1H , ^{13}C and ^{15}N NMR spectra were measured with a JEOL instrument. All chemical shifts are quoted in ppm relative to TMS (^1H , ^{13}C) or nitromethane (^{15}N). Infrared spectra were measured with a Perkin–Elmer Spektrum One FT-IR instrument. Raman spectra were measured with a Perkin–Elmer Spektrum 2000R NIR FT-Raman instrument equipped with a Nd:YAG laser (1064 nm). Elemental analyses were performed with a Netsch STA 429 simultaneous thermal analyzer. Sensitivity data were determined using a BAM drophammer and a BAM friction tester. The electrostatic sensitivity tests were carried out using an Electric Spark Tester ESD 2010 EN (OZM Research). The X-ray structure determinations were performed on a Oxford Xcalibur3 diffractometer with a Spellman generator (voltage 50 kV, current 40 mA) and a KappaCCD detector using a $\lambda_{\text{Mo-K}\alpha}$ radiation wavelength of 71.073 pm. All structures were measured at -100°C . Suitable single crystals of the compounds (**4**–**7**) were picked from the crystallization mixture and mounted in Kel-F oil on a glass fiber on top of the goniometer head. The data collection and data reduction was carried out with the CrysAlisPro software.^[34] The structures were solved with SIR-92^[35] or SHELXS-97^[36] refined with SHELXL-97^[37] and finally checked using the PLATON software^[38] integrated in the WINGX software suite.^[39] The non-hydrogen atoms were refined anisotropically and the hydrogen atoms were located and freely refined. The absorptions were corrected by a SCALE3 ABSPACK multi-scan method.^[40]

Hydroxylammonium 5-Nitriminotetrazolate (**4**)

5-Nitriminotetrazole (1.30 g, 10.0 mmol) was dissolved in cold water (10 mL) and an aqueous solution of hydroxylamine (50 % w/w, 1.32 g, 20.0 mmol) was added dropwise. The solvent was removed with a rotary evaporator and the residue was recrystallized from ethanol/water. Yield: 88 % (1.44 g, 8.82 mmol).

Alternative route: 5-Nitriminotetrazole (1.59 g, 12.2 mmol) was dissolved in water (a few mL) and a solution of silver nitrate (2.07 g, 12.2 mmol) was added. Silver 5-nitriminotetrazolate precipitated instantly as a colorless solid. It was sucked off and washed with water until free of acid. The colorless solid was resuspended in warm water (50 mL) and treated with a solution of hydroxylammonium chloride (0.84 g, 13.0 mmol) in water (20 mL). The mixture was stirred at 30°C for 1 h in the dark and the formed silver chloride was filtered off. The filtrate was evaporated and the residue was recrystallized from an

ethanol/water mixture to yield **5** as a colorless solid (1.70 g, 10.4 mmol, 85 %).

DSC ($5\text{ K}\cdot\text{min}^{-1}$): 172°C (dec.). **IR** (KBr, cm^{-1}): $\tilde{\nu} = 3125$ (s), 2958 (s), 2776 (m), 2711 (s), 1617 (m), 1598(m), 1539 (s), 1431 (s), 1383 (m), 1321 (vs), 1244 (m), 1213 (m), 1188 (m), 1153 (m), 1108 (m), 1061 (m), 1039 (m), 1003 (m), 872 (w), 823 (w), 777 (w), 753 (w), 742 (w), 700 (w), 493 (w); **Raman** (1064 nm, 300 mW, 25°C , cm^{-1}): $\tilde{\nu} = 2715$ (1), 1541 (100), 1452 (1), 1433 (1), 1381 (4), 1332 (36), 1158 (7), 1110 (4), 1070 (4), 1036 (22), 1014 (85), 875 (8), 744 (14), 695 (1), 494 (3), 427 (4), 413 (15). **^1H NMR** ($[\text{D}_6]\text{DMSO}$, 25°C , ppm): $\delta = 10.95$ (s). **^{13}C NMR** ($[\text{D}_6]\text{DMSO}$, 25°C , ppm): $\delta = 158.3$ (CN_4); m/z (FAB⁺): 34.0 [NH_3OH^+]; m/z (FAB[−]): 129.1 [HATNO_2^-]; **EA** ($\text{CH}_5\text{N}_7\text{O}_3$, 163.10): calcd.: C 7.36, H 3.09, N 60.12 %; found: C 7.38, H 3.17, N 57.40 %; BAM drophammer: 2 J; friction tester: 40 N; ESD: 0.30 J (at grain size 100–500 μm).

Dihydroxylammonium 5-Nitriminotetrazolate Hemihydrate (**5**)

5-Nitriminotetrazole (2.60 g, 20.0 mmol) was dissolved in cold water (10 mL) and an aqueous solution of hydroxylamine (50 % w/w, 2.64 g, 40.0 mmol) was added. After a few minutes, the product began to crystallize in fine needles, which were isolated. For recovery of the remaining material the mother liquor was evaporated and the colorless residue was recrystallized from ethanol/water to give **4** in 90 % overall-yield (3.69 g, 18.0 mmol).

DSC ($5\text{ K}\cdot\text{min}^{-1}$): 166°C (weak exo), 184°C (weak exo), 194°C (dec., strong exo). **IR** (KBr, cm^{-1}): $\tilde{\nu} = 3421$ (m), 3217 (m), 3101 (s), 2719 (s), 1612 (m), 1523 (m), 1466 (m), 1418 (s), 1384 (vs), 1338 (s), 1310 (s), 1219 (s), 1171 (m), 1146 (m), 1109 (w), 1099 (w), 1039 (w), 1022 (m), 1003 (s), 871 (m), 757 (m), 757 (w), 748 (w), 737 (w), 486 (w); **Raman** (1064 nm, 300 mW, 25°C , cm^{-1}): $\tilde{\nu} = 1452$ (100), 1423 (10), 1395 (3), 1358 (1), 1293 (2), 1236 (6), 1184 (8), 1154 (15), 1109 (3), 1021 (41), 1011 (12), 876 (3), 755 (3), 731 (6), 424 (9), 410 (8). **^1H NMR** ($[\text{D}_6]\text{DMSO}$, 25°C , ppm): $\delta = 8.83$ (s, NH_3OH). **^{13}C NMR** ($[\text{D}_6]\text{DMSO}$, 25°C , ppm): $\delta = 158.4$ (CN_4); m/z (FAB⁺): 34.0 [NH_3OH^+]; m/z (FAB[−]): 129.0 [CHN_6O_2^-]; **EA** ($\text{CH}_8\text{N}_8\text{O}_4$, water-free, 196.13): calcd.: C 6.12, H 4.11, N 57.13 %; found: C 6.09, H 3.96, N 57.13 %; BAM drophammer: 10 J; friction tester: 80 N; ESD: 0.30 J (at grain size 500–1000 μm).

Hydroxylammonium 1-Methyl-5-nitriminotetrazolate (**6**)

1-Methyl-5-nitriminotetrazole (1.44 g, 10.0 mmol) was dissolved in cold water (20 mL) and an aqueous solution of hydroxylamine (50 % w/w, 0.66 g, 10.0 mmol) was added dropwise. The solvent was removed on a rotary evaporator and the residue was recrystallized from ethanol/water. Yield: 88 % (1.56 g, 8.81 mmol).

Alternative route: 1-Methyl-5-nitriminotetrazole (1.67 g, 11.6 mmol) was dissolved in water (a few mL) and a solution of silver nitrate (1.97 g, 11.6 mmol) was added. Silver 1-methyl-5-nitriminotetrazolate precipitated instantly as a white solid. It was sucked off and washed with water until free of acid. The white solid was resuspended in warm water (50 mL) and treated with a solution of hydroxylammonium chloride (0.74 g, 11.5 mmol) in water (20 mL). The mixture was stirred at 30°C for 1 h in the dark and the formed silver chloride was filtered off. The filtrate was evaporated and the residue was recrystallized from ethanol to yield **6** as a colorless solid (1.78 g, 10.0 mmol, 86 %).

DSC ($5\text{ K}\cdot\text{min}^{-1}$): 180°C (m.p.), 185°C (dec.). **IR** (KBr, cm^{-1}): $\tilde{\nu} = 3435$ (vs), 3099 (m), 2737 (m), 2375 (w), 1627 (m), 1587 (m), 1515

(m), 1470 (m), 1424 (m), 1396 (m), 1385 (m), 1339 (s), 1303 (m), 1278 (m), 1250 (m), 1205 (m), 1106 (m), 1035 (w), 1011 (w), 987 (w), 890 (w), 831 (w), 774 (w), 753 (w), 733 (w), 689 (w); **Raman** (1064 nm, 300 mW, 25 °C, cm^{-1}): $\tilde{\nu}$ = 3026 (6), 2960 (53), 2804 (2), 2728 (2), 1585 (3), 1546 (7), 1520 (64), 1471 (35), 1425 (3), 1407 (13), 1342 (10), 1316 (3), 1304 (47), 1254 (4), 1123 (2), 1110 (15), 1037 (100), 1012 (19), 991 (3), 893 (14), 774 (2), 754 (30), 734 (4), 699 (5), 690 (35), 503 (17), 460 (6), 376 (8), 289 (51). **^1H NMR** ($[\text{D}_6]\text{DMSO}$, 25 °C, ppm): δ = 10.12 (s, NH_3OH^+), 3.67 (s, CH_3). **^{13}C NMR** ($[\text{D}_6]\text{DMSO}$, 25 °C, ppm): δ = 157.5 (CN_4), 33.1 (CH_3); m/z (FAB^+): 34.0 [NH_3OH^+]; m/z (FAB^-): 143.0 [1-MeATNO_2^-]; **EA** ($\text{C}_2\text{H}_7\text{N}_7\text{O}_3$, 177.12): calcd.: C 13.56, H 3.98, N 55.36%; found: C 13.70, H 3.73, N 55.08%; BAM drop hammer: 8 J; friction tester: 144 N; ESD: 0.50 J (at grain size 500–1000 μm).

Hydroxylammonium 2-Methyl-5-nitraminotetrazolate (7)

2-Methyl-5-nitraminotetrazole (1.44 g, 10.0 mmol) is dissolved in 20 mL of cold water and an aqueous solution of hydroxylamine (50% w/w, 0.66 g, 10.0 mmol) is added dropwise. The solvent was removed on a rotary evaporator and the residue recrystallized from ethanol/water. Yield: 82% (1.45 g, 8.20 mmol).

Alternative route: Ammonium 2-methyl-5-nitraminotetrazolate (4.12 g, 25.6 mmol) was dissolved in 20 mL of water and a solution of silver nitrate (4.34 g, 25.5 mmol) was added. The silver salt of 2-methyl-5-nitraminotetrazolate precipitates as a colorless solid. After being washed until free of ammonium nitrate it is resuspended in 100 mL of water and a solution of hydroxylammonium chloride (1.61 g, 25.0 mmol) is added. The mixture is stirred for 1 h at 30 °C in the dark and the formed silver chloride is filtered off. The filtrate is evaporated and the viscous residue is redissolved in ethanol for recrystallization. **7** crystallizes as a colorless, fluffy precipitate. Yield: 3.96 g, 22.3 mmol, 87%.

DSC (5 $\text{K} \cdot \text{min}^{-1}$): 139 °C (m.p.), 180 °C (dec.). **IR** (KBr, cm^{-1}): $\tilde{\nu}$ = 3433 (m), 3116 (s), 3048 (s), 2802 (m), 2724 (s), 1619 (m), 1506 (m), 1483 (s), 1435 (m), 1405 (s), 1384 (s), 1364 (m), 1329 (vs), 1282 (m), 1232 (m), 1212 (m), 1184 (m), 1118 (w), 1101 (m), 1094 (m), 1035 (m), 1013 (w), 1002 (w), 900 (w), 890 (w), 764 (w), 754 (w), 706 (w), 678 (w); **Raman** (1064 nm, 300 mW, 25 °C, cm^{-1}): $\tilde{\nu}$ = 2965 (17), 2840 (1), 1622 (1), 1603 (1), 1484 (100), 1437 (3), 1420 (3), 1396 (3), 1368 (3), 1290 (1), 1215 (5), 1187 (7), 1119 (3), 1096 (2), 1040 (4), 1030 (47), 1015 (15), 1003 (2), 902 (2), 890 (4), 754 (5), 707 (9), 454 (8), 404 (4). **^1H NMR** ($[\text{D}_6]\text{DMSO}$, 25 °C, ppm): δ = 9.90 (s, NH_3OH^+), 4.20 (s, CH_3). **^{13}C NMR** ($[\text{D}_6]\text{DMSO}$, 25 °C, ppm): δ = 168.0 (CN_4), 39.7 (CH_3); m/z (FAB^+): 34.0 [NH_3OH^+]; m/z (FAB^-): 143.0 [2-MeATNO_2^-]; **EA** ($\text{C}_2\text{H}_7\text{N}_7\text{O}_3$, 177.12): calcd.: C 13.56, H 3.98, N 55.36%; found: C 13.25, H 3.88, N 53.47%; BAM drop hammer: 6 J; friction tester: 144 N; ESD: 0.30 J (at grain size <100 μm).

Acknowledgments

Financial support of this work by the Ludwig-Maximilian University of Munich (LMU), the U.S. Army Research Laboratory (ARL), the Armament Research, Development and Engineering Center (ARDEC), the Strategic Environmental Research and Development Program (SERDP) and the Office of Naval Research (ONR Global, title: "Synthesis and Characterization of New High Energy Dense Oxidizers (HEDO) – NICOP Effort") under contract nos. W911NF-09-2-0018 (ARL), W911NF-09-1-0120 (ARDEC), W011NF-09-1-0056

(ARDEC) and 10 WPSEED01-002 / WP-1765 (SERDP) is gratefully acknowledged. The authors acknowledge collaborations with *Dr. Mila Krupka* (OZM Research, Czech Republic) in the development of new testing and evaluation methods for energetic materials and with *Dr. Muhamed Sucesca* (Brodarski Institute, Croatia) in the development of new computational codes to predict the detonation and propulsion parameters of novel explosives. We are indebted to and thank *Drs. Betsy M. Rice* and *Brad Forch* (ARL, Aberdeen, Proving Ground, MD) and *Mr. Gary Chen* (ARDEC, Picatinny Arsenal, NJ) for many helpful and inspired discussions and support of our work.

References

- [1] J. Giles, *Nature* **2004**, 427, 580.
- [2] D. Carrington, *New Scientist* **2001**, 101.
- [3] T. M. Klapötke, *Tin Moderne Anorganische Chemie* (Ed.: E. Riedel), 3ed., Walter de Gruyter, Berlin, New York, **2007**, pp. 99–104.
- [4] T. M. Klapötke, *High Energy Density Materials*, Springer, **2007**.
- [5] T. M. Klapötke, J. Stierstorfer, *J. Am. Chem. Soc.* **2009**, 131, 1122.
- [6] P. Carlqvist, H. Ostmark, T. Brinck, *J. Phys. Chem. A* **2004**, 108, 7463.
- [7] T. M. Klapötke, J. Stierstorfer, *New Trends in the Research of Energetic Materials*, 12th Seminar, Pardubice, Czech Republic, **2009**.
- [8] N. Fischer, T. M. Klapötke, J. Stierstorfer, *Z. Anorg. Allg. Chem.* **2009**, 635, 271.
- [9] T. M. Klapötke, J. Stierstorfer, A. U. Wallek, *Chem. Mater.* **2008**, 20, 4519.
- [10] N. Fischer, T. M. Klapötke, D. G. Piercey, S. Scheutzw, J. Stierstorfer, *Z. Anorg. Allg. Chem.* **2010**, 636, 2357.
- [11] T. M. Klapötke, J. Stierstorfer, *Helv. Chim. Acta* **2007**, 90, 2132.
- [12] J. Stierstorfer, Dissertation, Ludwig-Maximilians-Universität München, **2009**.
- [13] N. Fischer, T. M. Klapötke, J. Stierstorfer, *Z. Anorg. Allg. Chem.* **2009**, 635, 271.
- [14] G. Bentivoglio, G. Laus, V. Kahlenberg, G. Nauer, H. Schottenberger, *Z. Kristallogr.* **2008**, 223, 425.
- [15] J. Bernstein, R. E. Davis, L. Shimoni, N.-L. Chang, *Angew. Chem. Int. Ed. Engl.* **1995**, 34, 1555.
- [16] A. M. Astakhov, A. D. Vasiliev, M. S. Molokeev, A. M. Sirotnin, L. A. Kruglyakova, R. S. Stepanov, *J. Struct. Chem.* **2004**, 45, 175.
- [17] T. Altenburg, T. M. Klapötke, A. Penger, J. Stierstorfer, *Z. Anorg. Allg. Chem.* **2010**, 636, 463.
- [18] *Gaussian 09, Revision A.1*, M. J. Frisch, G. W. Trucks, H. B. Schlegel, G. E. Scuseria, M. A. Robb, J. R. Cheeseman, G. Scalmani, V. Barone, B. Mennucci, G. A. Petersson, H. Nakatsuji, M. Caricato, X. Li, H. P. Hratchian, A. F. Izmaylov, J. Bloino, G. Zheng, J. L. Sonnenberg, M. Hada, M. Ehara, K. Toyota, R. Fukuda, J. Hasegawa, M. Ishida, T. Nakajima, Y. Honda, O. Kitao, H. Nakai, T. Vreven, J. A. Montgomery Jr., J. E. Peralta, F. Ogliaro, M. Bearpark, J. J. Heyd, E. Brothers, K. N. Kudin, V. N. Staroverov, R. Kobayashi, J. Normand, K. Raghavachari, A. Rendell, J. C. Burant, S. S. Iyengar, J. Tomasi, M. Cossi, N. Rega, J. M. Millam, M. Klene, J. E. Knox, J. B. Cross, V. Bakken, C. Adamo, J. Jaramillo, R. Gomperts, R. E. Stratmann, O. Yazyev, A. J. Austin, R. Cammi, C. Pomelli, J. W. Ochterski, R. L. Martin, K. Morokuma, V. G. Zakrzewski, G. A. Voth, P. Salvador, J. J. Dannenberg, S. Dapprich, A. D. Daniels, Ö. Farkas, J. B. Foresman, J. V. Ortiz, J. Cioslowski, D. J. Fox, Gaussian, Inc., Wallingford CT, **2009**.
- [19] *NIST Chemistry WebBook*, NIST Standard Reference Database Number 69 (Eds.: P. J. Linstrom, W. G. Mallard), National Institute of Standards and Technology, Gaithersburg MD, 20899, <http://webbook.nist.gov>, October 27, **2011**.
- [20] a) H. D. B. Jenkins, H. K. Roobottom, J. Passmore, L. Glasser,

- Inorg. Chem.* **1999**, 38, 3609; b) H. D. B. Jenkins, D. Tudela, L. Glasser, *Inorg. Chem.* **2002**, 41, 2364.
- [21] a) M. Sućeska, *EXPLO5.3* program, Zagreb, Croatia, **2009**; b) M. Sućeska, *EXPLO5.4* program, Zagreb, Croatia, **2010**.
- [22] Calculation of oxygen balance: Ω (%) = $(wO - 2xC - 1/2yH - 2zS)/1600/M$. (w : number of oxygen atoms, x : number of carbon atoms, y : number of hydrogen atoms, z : number of sulfur atoms, M : molecular weight).
- [23] J. Köhler, R. Meyer, in: *Explosivstoffe*, 9th Ed., Wiley-VCH, Weinheim, **1998**.
- [24] *NATO standardization agreement (STANAG) on explosives, impact sensitivity tests*, no. 4489, 1st ed., Sept. 17, **1999**.
- [25] *NATO standardization agreement (STANAG) on explosive, friction sensitivity tests*, no. 4487, 1st ed., Aug. 22, **2002**.
- [26] *NATO standardization agreement (STANAG) on explosive, electrostatic discharge sensitivity tests*, no. 4490, 1st ed., Feb. 19, **2001**.
- [27] *WIWEB-Standardarbeitsanweisung 4–5.1.02*, Ermittlung der Explosionsgefährlichkeit, hier der Schlagempfindlichkeit mit dem Fallhammer, Nov. 8, **2002**.
- [28] *WIWEB-Standardarbeitsanweisung 4–5.1.03*, Ermittlung der Explosionsgefährlichkeit or der Reibeempfindlichkeit mit dem Reibeapparat, Nov. 8, **2002**.
- [29] <http://www.bam.de>.
- [30] Impact: Insensitive > 40 J, less sensitive \geq 35 J, sensitive \geq 4 J, very sensitive \leq 3 J; friction: Insensitive > 360 N, less sensitive = 360 N, sensitive < 360 N a. > 80 N, very sensitive \leq 80 N, extreme sensitive \leq 10 N; According to the UN Recommendations on the Transport of Dangerous Goods (+) indicates: not safe for transport.
- [31] a) <http://www.ozm.cz/testing-instruments/small-scale-electrostatic-discharge-tester.htm>; b) V. Pelikán, OZM research, Czech Republic, private communication.
- [32] a) *REICHELTE & PARTNER GmbH*, <http://www.reichelt-partner.de>; b) Test methods according to the *UN Recommendations on the Transport of Dangerous Goods, Manual of Test and Criteria*, fourth revised edition, United Nations Publication, New York and Geneva, **2003**, ISBN 92–1–139087–7, Sales No. E.03.VIII.2; 13.4.2 Test 3a (ii) BAM Fallhammer.
- [33] T. Fendt, N. Fischer, T. M. Klapötke, J. Stierstorfer, *Inorg. Chem.* **2011**, 50, 1447.
- [34] *CrysAlisPro*, Agilent Technologies, Version 1.171.35.11, **2011**.
- [35] *SIR-92*, 1993, A Program for Crystal Structure Solution, A. Altomare, G. Cascarano, C. Giacovazzo, A. Guagliardi, *J. Appl. Crystallogr.* **1993**, 26, 343.
- [36] G. M. Sheldrick *SHELXS-97*, Program for Crystal Structure Solution, Universität Göttingen, **1997**.
- [37] G. M. Sheldrick, *SHELXL-97*, Program for the Refinement of Crystal Structures. University of Göttingen, Germany, **1997**.
- [38] A. L. Spek, *PLATON*, A Multipurpose Crystallographic Tool, Utrecht University, Utrecht, The Netherlands, **1999**.
- [39] L. J. Farrugia, *J. Appl. Crystallogr.* **1999**, 32, 837.
- [40] *SCALE3 ABSPACK* - An Oxford Diffraction Program (1.0.4.gui:1.0.3), Oxford Diffraction Ltd, **2005**.

Received: November 2, 2011
Published Online: January 9, 2012

Sensitivities of Some Imidazole-1-sulfonyl Azide Salts

Niko Fischer,[†] Ethan D. Goddard-Borger,[‡] Robert Greiner,[†] Thomas M. Klapötke,^{*,†} Brian W. Skelton,[§] and Jörg Stierstorfer[†]

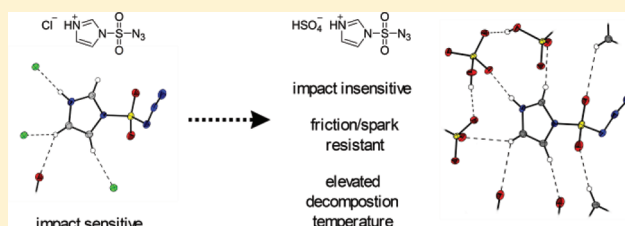
[†]Energetic Materials Research, Department of Chemistry, University of Munich (LMU), Butenandtstrasse 5-13, D-81377, Germany

[‡]Department of Chemistry, University of British Columbia, 2036 Main Mall, Vancouver, British Columbia V6T 1Z1, Canada

[§]School of Biomedical, Biomolecular and Chemical Sciences, The University of Western Australia, Crawley, WA 6009, Australia

Supporting Information

ABSTRACT: Imidazole-1-sulfonyl azide hydrochloride, an inexpensive and effective diazotransfer reagent, was recently found to be impact sensitive. To identify safer-to-handle forms of this reagent, several different salts of imidazole-1-sulfonyl azide were prepared, and their sensitivity to heat, impact, friction, and electrostatic discharge was quantitatively determined. A number of these salts exhibited improved properties and can be considered safer than the aforementioned hydrochloride. The solid-state structures of the chloride and less sensitive hydrogen sulfate were determined by single-crystal X-ray diffraction in an effort to provide some insight into the different properties of the materials.



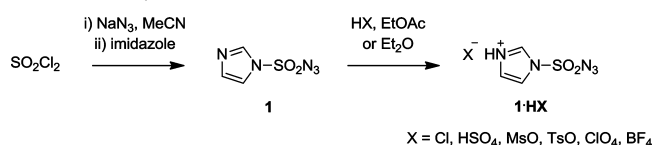
INTRODUCTION

In recent times, organic azides have attracted considerable attention because of the facile reactions that these high energy, kinetically stable molecules undergo.¹ Their use in dipolar cycloadditions, investigated in detail by Huisgen and co-workers in the 1960s² and popularized in the past decade by the revelation that such reactions are catalyzed by various metals,³ is particularly noteworthy. As a consequence of this popularity, there is a considerable interest in synthetic methodologies for the preparation of organic azides. The diazo-transfer reaction is one such method and involves the conversion of a primary amine into an organic azide by the action of a powerful diazo donor (most commonly a sulfonyl azide). For the reaction to proceed in a facile manner, the sulfonyl azide must be adjoined to a strong electron-withdrawing group; trifluoromethanesulfonyl azide is most commonly used because arylsulfonyl azides are, for the most part, simply not reactive enough. To circumvent the problems of high cost and instability associated with using trifluoromethanesulfonyl azide, imidazole-1-sulfonyl azide hydrochloride **1·HCl** was developed as an inexpensive and shelf-stable alternative diazo-transfer reagent with comparable efficacy.⁴ The shock sensitivity and thermal stability of activated, low-molecular weight azides has always been cause for concern,^{1,5,6} and after hearing of an explosion that occurred during the synthesis of **1·HCl**⁴ we sought to quantify the sensitivity of **1** and a number of its salts toward impact, friction, and electrostatic discharge to provide a rational assessment of the relative safety of these compounds. It was anticipated that the sensitivity of reagent **1** to various stimuli could be “tuned”, for better or worse, by crystallization with different acids.

RESULTS AND DISCUSSION

Imidazole-1-sulfonyl azide **1** is easily prepared by the addition of 2 molar equiv of imidazole to chlorosulfonyl azide preformed in situ by the reaction of equimolar quantities of sodium azide and sulfonyl chloride in acetonitrile (Scheme 1).⁴ This product

Scheme 1. Synthesis of Different Salts of **1**



can be precipitated from the crude solution as the pure hydrochloride salt **1·HCl** by treatment with ethanolic hydrogen chloride. Partitioning **1·HCl** between an organic solvent and aqueous sodium bicarbonate proved to be a convenient method for obtaining organic solutions of pure **1**. Solutions of **1** in ethyl acetate were treated with sulphuric acid, toluenesulfonic acid, perchloric acid, or tetrafluoroboric acid to precipitate the corresponding salts **1·H₂SO₄**, **1·TsOH**, **1·HClO₄**, and **1·HBF₄**, respectively. Similarly, treatment of a solution of **1** in diethyl ether with methanesulfonic acid provided the corresponding salt **1·MsOH**.

The ability of these salts to act as diazo donors was confirmed by the conversion of 4-aminobenzoic acid into 4-azidobenzoic acid under standard diazo-transfer reaction conditions (Table 1).⁴ All of the reactions provided product in

Received: November 9, 2011

Published: January 23, 2012

Table 1. Different Anions Do Not Significantly Affect the Efficacy of Reagent 1

<chem>Nc1ccc(cc1)C(=O)O</chem> $\xrightarrow[\text{K}_2\text{CO}_3, \text{MeOH}]{\text{1}\cdot\text{HX}, \text{CuSO}_4\cdot 5\text{H}_2\text{O}}$ <chem>[N+]#Cc1ccc(cc1)C(=O)O</chem>		1·HCl	1·H ₂ SO ₄	1·MsOH	1·TsOH	1·HClO ₄	1·HBF ₄
yield (%)		63	63	61	70	57	64

comparable isolated yield, demonstrating that the different anions do not significantly affect the efficacy of the reagent.

Differential scanning calorimetry (DSC) was performed on 1 and all of its salts to determine their melting points and decomposition onset temperatures. The thermal behavior of these materials is displayed as DSC plots in a temperature range from 20 to 400 °C in Figure 1. Since none of the compounds

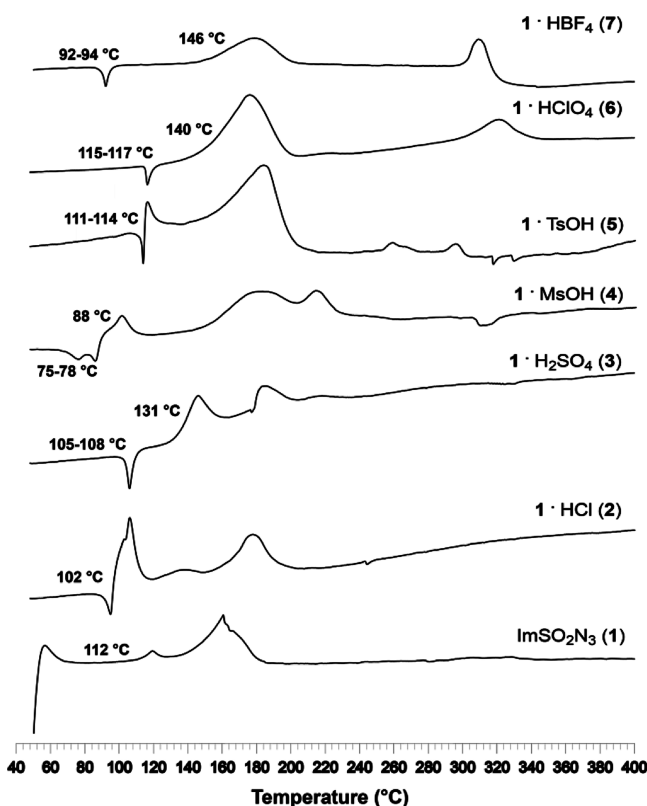


Figure 1. DSC plots of compound 1 and its various salts (exothermic = ↑, endothermic = ↓).

crystallized as hydrates or with included solvent, as indicated by elemental analyses, the small endothermic peaks of each DSC curve can be assigned as the melting point for each salt, while the exothermic peaks can be ascribed to decomposition. Decomposition temperatures for each compound are defined by the lowest onset temperature of the exotherms.

Interestingly, the temperature at which decomposition commences varies considerably; from the low value of 88 °C for 1·MsOH, to the parent compound 1 at 112 °C, up to 146 °C, as observed for 1·HBF₄. The only salt with a relatively large liquid range (>50 °C) was 1·HBF₄, which melted at 92–94 °C but did not begin to decompose until it reached a temperature of 146 °C. From the DSC data, it is evident that all of the materials can be used at a temperature less than 88 °C and

some even higher. However, in practice, when drying samples, using or storing the materials, it is advisable to use temperatures less than 60 °C. This provides a particularly large margin for error for the more thermostable salts like 1·HBF₄ and 1·H₂SO₄.

The sensitivities of each substance to mechanical stimuli were assessed. Impact sensitivity tests were carried out according to STANAG 4489⁷ modified instructions⁸ using a BAM (Bundesanstalt für Materialforschung) drophammer,⁹ while friction sensitivity tests were carried out according to STANAG 4487¹⁰ modified instructions¹¹ using the BAM friction tester. The sensitivity of each compound toward electrical discharge was also determined using the electric spark tester ESD 2010 EN.¹² These data, together with decomposition temperatures and nitrogen content (percentage by weight) of each material, are presented in Table 2. When interpreting the data presented

Table 2. Sensitivity Data for 1 and Its Salts^a

compd	sensitivity			percentage nitrogen (w/w, %)	dec temp (°C)
	impact (J)	friction (N)	ESD (J)		
1	<1	72		40.5	112
1·HCl	6	240	0.50	33.4	102
1·H ₂ SO ₄	40	240	0.30	25.8	131
1·MsOH	40	192	0.10	26.0	88
1·TsOH	30	>360	0.70	20.3	114
1·HClO ₄	<1	<5	0.15	25.6	140
1·HBF ₄	40	240	0.50	26.8	146

^aESD is an acronym for electrostatic discharge. The technique used to determine these values cannot be applied to 1 because it is a liquid under standard conditions.

in Table 2, one should note that the larger a value is for a given test, the less sensitive that material is to that given form of stimulus. Further, subsequent descriptions of materials as “insensitive”, “less sensitive”, “sensitive”, “very sensitive”, or “extremely sensitive” are based on the UN Recommendations on the Transport of Dangerous Goods.¹³

What is quite remarkable about the data in Table 2 is that the properties of the materials vary significantly, ranging from extremely sensitive to insensitive, even though they all contain the same energetic species. The parent compound 1, as well as the perchlorate 1·HClO₄, is *very sensitive* toward impact, as one would expect. The previously reported chloride 1·HCl and the tosylate 1·TsOH are *sensitive* to impact and should be handled with care. The hydrogen sulfate 1·H₂SO₄, mesylate 1·MsOH, and tetrafluoroborate 1·HBF₄ are *insensitive* to impact. A similar trend is observed for the friction sensitivity of the compounds. The parent sulfonyl azide 1 and its perchlorate salt 1·HClO₄ are again of concern: classified as *very sensitive* and *extremely sensitive*, respectively. The other salts have higher values and are only considered *sensitive* to friction, except for the tosylate 1·TsOH, which is *insensitive* to friction. Values determined for electrostatic discharge (ESD) are strongly dependent on the grain size of the crystalline material, thus differing between batches of each material and for technical reasons cannot be determined for a liquid like 1. Nevertheless, all of the salts returned values in the range of 0.10–0.70 J, indicating that none were particularly sensitive toward electrostatic discharge.

From these results, several recommendations can be made. The parent compound 1, as a neat liquid, should be handled with extreme caution and ideally would never be isolated but

instead prepared and used only in solution. As expected, the perchlorate $1 \cdot \text{HClO}_4$ is even more hazardous than **1** and should not be prepared by those without expertise in handling energetic materials. The hydrochloride salt $1 \cdot \text{HCl}$ has comparable impact sensitivity (not to be confused with energetic yield) to RDX (cyclotrimethylenetrinitramine), a commonly used high explosive, and must be handled with caution. On the other hand, the relatively high decomposition temperature, impact insensitivity, low friction, and ESD sensitivities of the hydrogensulfate $1 \cdot \text{H}_2\text{SO}_4$ and the tetrafluoroborate $1 \cdot \text{HBF}_4$ make these two materials safe to manipulate, although all the usual precautions taken when handling energetic laboratory reagents should still be observed.

Another issue worthy of consideration, especially if these reagents are to be kept in bulk, is the question of shelf stability. If not stored with desiccation, the hygroscopic hydrochloride $1 \cdot \text{HCl}$ discolors and liquefies over the course of a few weeks, producing a brown oil that smells of hydrazoic acid. The hydrogensulfate $1 \cdot \text{H}_2\text{SO}_4$ is less hygroscopic, remaining unchanged after storage for several months under ambient conditions. However, after more than one year, this salt also discolored and liquefied with the liberation of hydrazoic acid. Only the tetrafluoroborate $1 \cdot \text{HBF}_4$ remained unaffected by storage under ambient conditions for one year. Thus, one can conclude that $1 \cdot \text{HBF}_4$ has the most favorable characteristics of all the salts investigated but that $1 \cdot \text{H}_2\text{SO}_4$ is a less expensive, viable alternative if stored with the exclusion of moisture.

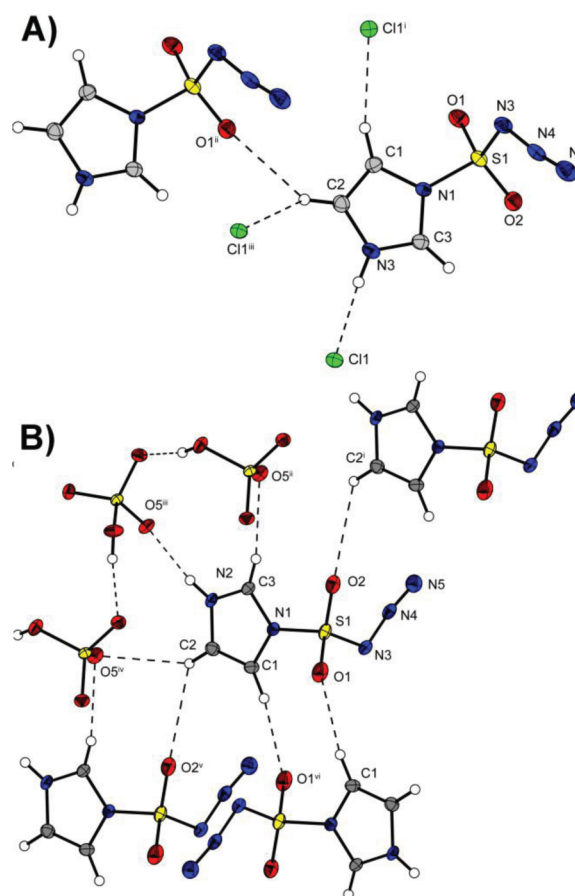
The solid-state structures of $1 \cdot \text{HCl}$ and $1 \cdot \text{H}_2\text{SO}_4$, two salts with quite different sensitivities, were determined by single-crystal X-ray diffraction to see if some insight might be gained into why the former salt is more sensitive to mechanical stimuli than the latter. The structures of both materials were solved (see the Experimental Section for details) and found to crystallize in the monoclinic space group $P2_1/c$ with four molecules to each unit cell. The molecular moiety of each solid is depicted in the Supporting Information (Figure S1). The bond lengths and angles associated with both imidazole moieties and counterions are commensurate with literature values,¹⁴ while those associated with the sulfonyl azide moiety did not differ significantly between structures.

The main difference between these materials lies in their molar volumes, density and the number of intermolecular hydrogen bonding contacts made (Table 3, Figure 2). The more

Table 3. Molar Volume, Density, And Hydrogen Bonding in $1 \cdot \text{HCl}$ and $1 \cdot \text{H}_2\text{SO}_4$

	V_M ($\text{cm}^3 \text{mol}^{-1}$)	ρ (g cm^{-3})	classical H-bonds per molecule	nonclassical H- bonds per molecule
$1 \cdot \text{HCl}$	122.4	1.713	1	3
$1 \cdot \text{H}_2\text{SO}_4$	144.8	1.873	2	4

sensitive salt, $1 \cdot \text{HCl}$, has a smaller molar volume, lower density, and fewer hydrogen bonds than the less sensitive salt, $1 \cdot \text{H}_2\text{SO}_4$. The greater molar volume of $1 \cdot \text{H}_2\text{SO}_4$ leads to a lower calculated lattice enthalpy (according to Jenkins' equation^{15,16} $\Delta_L H (1 \cdot \text{H}_2\text{SO}_4) = 484.5 \text{ kJ mol}^{-1}$, $\Delta_L H (1 \cdot \text{HCl}) = 506.4 \text{ kJ mol}^{-1}$) but translates to fewer high energy azide groups per unit volume in the solid. Its greater density and more extensive network of hydrogen bonds may act as an energy sink to suppress decomposition.



very sensitive and have to be handled with great care. Plastic suction filters and spatulas are recommended for the isolation of the crystalline materials described. Mother liquors and other waste, which may contain the highly explosive sulfonyl diazide, should be treated with excess sodium nitrite and acidified to destroy azide-containing species.

Imidazole-1-sulfonyl azide (**1**) as well as its hydrochloride (**2**) was prepared according to literature procedures.⁴ Unfortunately, all described compounds suffer from partial decomposition during the NMR experiments in DMSO-*d*₆, so that in all cases remaining undecomposed material besides a decomposition product can be observed. Presumably from the 3-azidosulfonyl-3*H*-imidazol-1-ium cation the azidosulfonyl moiety is cleaved off resulting in the respective 1,3*H*-imidazol-1-ium salts. Because of the polar character of the described compounds and resulting solubility problems, it was not possible to gain NMR data from different solvents such as CDCl₃, CD₃OD, or acetone-*d*₆. The NMR signals of the decomposition product can be identified in all recorded spectra and are marked with an asterisk in the experimental procedures.

3-Azidosulfonyl-3*H*-imidazol-1-ium Hydrogen Sulfate (1·H₂SO₄). Sulfuric acid (3.9 g, 39.85 mmol; in 20 mL EtOAc) was added slowly to a solution of imidazole-1-sulfonyl azide **1** (6.9 g, 39.85 mmol; in 20 mL EtOAc) at 0 °C. The reaction mixture was stirred for 1 h at rt. The precipitate was filtered, washed, and dried in vacuo to give 9.3 g (29.52 mmol, 74%) of **1·H₂SO₄** as a white, crystalline powder. DSC (5 °C min⁻¹, °C): 105–108 °C (mp), 131 °C (dec). IR (KBr, cm⁻¹): 3110 (s), 3084 (s), 2969 (s), 2864 (s), 2177 (s), 1586 (m), 1516 (m), 1460 (w), 1431 (s), 1302 (m), 1233 (vs), 1191 (s), 1152 (vs), 1127 (vs), 1100 (vs), 1067 (s), 1018 (s), 983 (m), 872 (m), 834 (m), 774 (s), 740 (m); Raman (1064 nm, 400 mW, 25 °C, cm⁻¹): 3187 (13), 3157 (23), 3113 (13), 2174 (100), 1588 (20), 1518 (23), 1462 (70), 1426 (26), 1329 (19), 1304 (44), 1236 (24), 1192 (35), 1146 (12), 1129 (18), 1103 (13), 1071 (48), 1021 (83), 984 (41), 899 (24), 780 (67), 646 (15), 617 (18), 599 (19), 585 (90), 486 (36), 467 (55), 430 (15), 411 (26), 372 (71), 362 (48), 322 (25), 203 (26). ¹H NMR (DMSO-*d*₆, 25 °C, ppm): δ = 14.30 (s, br, NH⁺), 12.42 (s, br, HSO₄⁻), 9.06* (t, CH, *J* = 1.1 Hz), 8.69 (dd, CH, *J*₁ = 0.8 Hz, *J*₂ = 1.5 Hz), 7.98 (dd, CH, *J*_{1/2} = 1.5 Hz), 7.66* (d, CH, *J* = 1.2 Hz), 7.37 (dd, CH, *J*₁ = 0.9 Hz, *J*₂ = 1.7 Hz). ¹³C NMR (DMSO-*d*₆, 25 °C, ppm): δ = 138.3, 134.9*, 130.6, 119.8*, 119.5. *m/z* (FAB⁺): 174.0 [HImSO₂N₃⁺]. *m/z* (FAB⁻): 96.9 [HSO₄⁻]. Anal. Calcd for C₃H₃N₅O₆S₂: C, 13.28; H, 1.86; N, 25.82; S, 23.64. Found: C, 13.61; H, 2.03; N, 26.11; S, 23.29. BAM drophammer: >40 J; friction tester: >240 N; ESD: 0.3 J.

3-Azidosulfonyl-3*H*-imidazol-1-ium Methanesulfonate (1·MsOH). Imidazole-1-sulfonyl azide **1** (8.66 g, 50 mmol) was diluted with 10 mL of Et₂O. Then methanesulfonic acid (4.81 g, 50 mmol) was added dropwise under stirring at 0 °C. The precipitate was filtered off, washed with EtOH and Et₂O, and dried in vacuo, yielding 11.50 g (42.7 mmol, 85%) of **1·MsOH** as a white powder. DSC (5 °C min⁻¹, °C): 75–78 °C (mp), 88 °C (dec). IR (KBr, cm⁻¹): 3439 (br), 3107 (s), 3058 (s), 2908 (s), 2761 (s), 2704 (s), 2661 (s), 2577 (m), 2173 (vs), 1629 (w), 1580 (m), 1508 (m), 1449 (m), 1428 (vs), 1322 (m), 1195 (vs), 1161 (vs), 1135 (vs), 1103 (m), 1059 (vs), 981 (w), 834 (s), 780 (vs), 638 (s), 584 (s), 562 (s), 535 (m). Raman (1064 nm, 400 mW, 25 °C, cm⁻¹): 3178 (17), 3120 (28), 3035 (49), 3020 (41), 2947 (100), 2179 (100), 1582 (10), 1514 (10), 1471 (66), 1444 (32), 1424 (21), 1321 (25), 1302 (24), 1244 (11), 1189 (28), 1124 (12), 1058 (26), 1031 (59), 981 (30), 966 (12), 785 (96), 769 (25), 581 (60), 555 (22), 546 (21), 523 (12), 482 (22), 467 (28), 375 (29), 357 (36), 343 (24), 320 (11). ¹H NMR (DMSO-*d*₆, 25 °C, ppm): δ = 14.88 (s, br, MeSO₃H), 14.28 (s, br, NH), 9.03* (t, CH, *J* = 1.2 Hz), 8.76 (dd, CH, *J*₁ = 0.8 Hz, *J*₂ = 1.6 Hz), 7.99 (dd, CH, *J*_{1/2} = 1.6 Hz), 7.63* (d, CH, *J* = 1.4 Hz), 7.39 (dd, CH, *J*₁ = 0.8 Hz, *J*₂ = 1.6 Hz), 2.46 (s, CH₃SO₃⁻). ¹³C NMR (DMSO-*d*₆, 25 °C, ppm): δ = 138.4, 134.9*, 129.9, 119.8*, 119.6, 40.9 (CH₃SO₃⁻). *m/z* (FAB⁺): 174.1 [HImSO₂N₃⁺]. *m/z* (FAB⁻): 95.0 [MeSO₃⁻]. Anal. Calcd for C₄H₄N₅O₅S₂: C, 17.84; H, 2.62; N, 26.01. Found: C, 17.46; H, 2.76; N, 25.88. BAM drophammer: >40 J; friction tester: >192 N; ESD: >0.1 J.

3-Azidosulfonyl-3*H*-imidazol-1-ium 4-Toluenesulfonate (1·TsOH). Imidazole-1-sulfonyl azide hydrochloride **1** (4.19 g, 20 mmol) was suspended in EtOAc (50 mL). Under stirring, a saturated solution of NaHCO₃ (50 mL) was added. After **1** dissolved under gas evolution, the phases were separated. The organic phase was dried over MgSO₄ and subsequently treated with a solution of *p*-toluenesulfonic acid monohydrate (3.8 g, 20 mmol) in EtOAc (35 mL). Then the reaction mixture was cooled with an ice bath, and a small amount of hexane was added. The precipitate was filtered off and washed with Et₂O to give 3.29 g (9.53 mmol, 48%) of **1·TsOH** as a white powder. DSC (5 °C min⁻¹, °C): 111–114 °C (mp); 114 °C (dec 1); 155 °C (dec 2). IR (KBr, cm⁻¹): 3440 (br), 3157 (s), 3086 (s), 3058 (s), 2969 (m), 2554 (m), 2418 (m), 2305 (m), 2172 (vs), 1584 (m), 1495 (m), 1438 (vs), 1226 (vs), 1173 (vs), 1119 (vs), 1057 (s), 1011 (vs), 874 (m), 817 (m), 778 (vs), 682 (vs), 644 (vs), 566 (vs). Raman (1064 nm, 400 mW, 25 °C, cm⁻¹): 3185 (12), 3158 (11), 3065 (100), 2984 (16), 2924 (53), 2872 (13), 2177 (58), 1601 (45), 1496 (18), 1450 (28), 1383 (22), 1318 (16), 1244 (10), 1213 (41), 1182 (20), 1123 (72), 1086 (27), 1060 (18), 1035 (27), 1014 (34), 982 (42), 803 (98), 777 (40), 685 (24), 651 (13), 637 (27), 605 (13), 584 (36), 483 (30), 466 (33), 402 (27), 363 (79), 318 (26), 293 (84), 232 (37). ¹H NMR (DMSO-*d*₆, 25 °C, ppm): δ = 14.28 (s, br, NH), 9.08* (t, CH, *J* = 1.2 Hz), 8.73 (dd, CH, *J*₁ = 0.9 Hz, *J*₂ = 1.7 Hz), 8.00 (dd, CH, *J*_{1/2} = 1.1 Hz), 7.67* (d, CH, *J* = 1.4 Hz), 7.51 (d, CH (p-TolSO₃⁻), *J* = 8.0 Hz), 7.39 (dd, CH, *J*₁ = 0.9 Hz, *J*₂ = 1.7 Hz), 7.14 (d, CH, (p-TolSO₃⁻), *J* = 8.0 Hz), 2.29 (s, CH₃). ¹³C NMR (DMSO-*d*₆, 25 °C, ppm): δ = 145.4 (C₁, p-TolSO₃⁻), 138.8 (C₄, p-TolSO₃⁻), 138.4, 134.9*, 130.5, 128.8 (C_{3/5}, p-TolSO₃⁻), 126.1 (C_{2/6}, p-TolSO₃⁻), 119.9*, 119.5, 21.3 (CH₃). *m/z* (FAB⁺): 174.2 [HImSO₂N₃⁺]. *m/z* (FAB⁻): 171.1 [C₇H₇SO₃⁻]. Anal. Calcd for C₁₀H₁₁N₅O₅S₂: C, 34.78; H, 3.21; N, 20.28; S, 18.57. Found: C, 34.62; H, 3.34; N, 20.14; S, 18.81. BAM drophammer: >30 J; friction tester: >360 N; ESD: 0.7 J.

3-Azidosulfonyl-3*H*-imidazol-1-ium Perchlorate (1·HClO₄). Imidazole-1-sulfonyl azide (**1**) (13.8 g, 79.7 mmol) and perchloric acid (60%, 5.2 mL, 79.7 mmol) were dissolved in 30 mL of EtOAc each. Then the perchloric acid solution was slowly added to the imidazole-1-sulfonyl azide solution at 0 °C. After the reaction mixture was stirred for 1 h at rt, the white precipitate was filtered off and dried in vacuo to give 3.9 g (14.25 mmol, 18%) of **1·HClO₄** as a white powder. DSC (5 °C min⁻¹, °C): 115–117 °C (mp); 140 °C (dec). IR (KBr, cm⁻¹): 3168 (s), 2172 (s), 1581 (m), 1512 (m), 1446 (s), 1327 (m), 1284 (m), 1222 (m), 1197 (s), 1157 (s), 1121 (s), 1083 (vs), 1059 (vs), 981 (m), 888 (w), 779 (vs), 746 (m). Raman (1064 nm, 400 mW, 25 °C, cm⁻¹): 3183 (9), 3170 (8), 2171 (47), 1580 (5), 1512 (8), 1444 (42), 1328 (14), 1286 (15), 1224 (23), 1196 (16), 1156 (7), 1134 (9), 1113 (17), 1078 (14), 983 (32), 938 (101), 930 (43), 910 (11), 788 (49), 627 (28), 590 (59), 485 (24), 462 (46), 365 (35), 359 (48), 330 (20), 210 (16). ¹H NMR (DMSO-*d*₆, 25 °C, ppm): δ = 14.52 (s, br, HClO₄), 14.27 (s, br, NH), 9.04* (CH), 8.76 (CH), 8.00 (CH), 7.66* (s, CH), 7.41 (CH). ¹³C NMR (DMSO-*d*₆, 25 °C, ppm): δ = 138.4, 134.8*, 130.4, 119.8*, 119.6. *m/z* (FAB⁺): 174.0 [HImSO₂N₃⁺]. *m/z* (FAB⁻): 98.9 [ClO₄⁻]. Anal. Calcd for C₃H₄ClN₅O₆S: C, 13.17; H, 1.47; N, 25.60; S, 11.72. Found: C, 13.11; H, 1.53; N, 25.55; S, 11.47. BAM drophammer: <1 J (!); friction tester: <5 N (!); ESD: 0.15 J.

3-Azidosulfonyl-3*H*-imidazol-1-ium Tetrafluoroborate (1·HBF₄). At 0 °C, a solution of 54% fluoroboric acid in Et₂O (3.25 g, 20 mmol) was slowly added to a solution of imidazole-1-sulfonyl azide (**1**) in 25 mL of EtOAc (3.46 g, 20 mmol). A white precipitate instantly formed. It was filtered off and washed with Et₂O to give 3.20 g (12.3 mmol, 61%) of **1·HBF₄** as a white powder. DSC (5 °C min⁻¹, °C): 92–94 °C (mp); 146 °C (dec). IR (KBr, cm⁻¹): 3426 (s), 3168 (m), 3059 (m), 2167 (s), 1629 (w), 1580 (m), 1509 (w), 1438 (s), 1322 (w), 1294 (m), 1195 (vs), 1124 (vs), 1105 (vs), 1083 (vs), 1064 (vs), 1036 (vs), 834 (vw), 778 (s), 640 (s), 601 (m), 584 (m). Raman (1064 nm, 400 mW, 25 °C, cm⁻¹): 3198 (15), 3173 (11), 3132 (10), 2166 (83), 1586 (11), 1446 (63), 1432 (29), 1324 (15), 1287 (14), 1230 (23), 1198 (20), 1143 (11), 1068 (16), 976 (31), 783 (64), 771 (51), 649 (21), 597 (102), 483 (34), 465 (42), 361 (71), 325 (30). ¹H NMR (DMSO-*d*₆, 25 °C, ppm): δ = 14.21 (s, br, NH), 9.04* (t, CH, *J* = 1.2 Hz), 8.80 (dd, CH, *J*₁ = 1.1 Hz,

$J_2 = 2.2$ Hz), 8.02 (dd, CH, $J_{1/2} = 1.3$ Hz), 7.66* (d, CH, $J = 1.5$ Hz), 7.43 (dd, CH, $J_1 = 1.1$ Hz, $J_2 = 2.1$ Hz). ^{13}C NMR (DMSO- d_6 , 25 °C, ppm): $\delta = 138.4, 134.9^*, 130.0, 119.8^*, 119.6$. m/z (FAB $^+$): 174.1 [HImSO $_2$ N $_3^+$]. m/z (FAB $^-$): 87.0 [BF $_4^-$]. Anal. Calcd for C $_3$ H $_4$ BF $_4$ N $_3$ O $_3$ S: C, 13.81; H, 1.54; N, 26.84; S, 12.29. Found: C, 13.78; H, 1.77; N, 26.43; S, 12.59. BAM drophammer: >40 J; friction tester: >240 N; ESD: 0.5 J.

■ ASSOCIATED CONTENT

■ Supporting Information

Crystal structures (discussion, ORTEP figure of molecular unit, and crystallographic data and parameters) of 1·HCl and 1·H $_2$ SO $_4$. ^1H and ^{13}C NMR spectra of 1·H $_2$ SO $_4$, 1·MsOH, 1·TsOH, 1·HClO $_4$, and 1·HBF $_4$. This material is available free of charge via the Internet at <http://pubs.acs.org/>.

■ AUTHOR INFORMATION

Corresponding Author

*E-mail: tmk@cup.uni-muenchen.de.

■ ACKNOWLEDGMENTS

Financial support of this work by the Ludwig-Maximilian University of Munich (LMU), the U.S. Army Research Laboratory (ARL), the Armament Research, Development and Engineering Center (ARDEC), the Strategic Environmental Research and Development Program (SERDP), and the Office of Naval Research (ONR Global, title: "Synthesis and Characterization of New High Energy Dense Oxidizers (HEDO) - NICOP Effort") under contract nos. W911NF-09-2-0018 (ARL), W911NF-09-1-0120 (ARDEC), W011NF-09-1-0056 (ARDEC), and 10 WPSEED01-002/WP-1765 (SERDP) is gratefully acknowledged. We acknowledge collaborations with Dr. Mila Krupka (OZM Research, Czech Republic) in the development of new testing and evaluation methods for energetic materials and with Dr. Muhamed Sucasca (Brodarski Institute, Croatia) in the development of new computational codes to predict the detonation and propulsion parameters of novel explosives. We are indebted to and thank Drs. Betsy M. Rice and Brad Forch (ARL, Aberdeen, Proving Ground, MD) and Mr. Gary Chen (ARDEC, Picatinny Arsenal, NJ) for many helpful and inspired discussions and support of our work. Mr. Stefan Huber is thanked for performing the sensitivity tests.

■ REFERENCES

- (1) Bräse, S.; Gil, C.; Knepper, K.; Zimmermann, V. *Angew. Chem.* **2005**, *117*, 5320–5374.
- (2) (a) Huisgen, R. *Angew. Chem., Int. Ed. Engl.* **1963**, *2*, 565–598. (b) Huisgen, R. *Angew. Chem., Int. Ed. Engl.* **1963**, *2*, 633–645.
- (3) (a) Tornøe, C. W.; Christensen, C.; Meldal, M. *J. Org. Chem.* **2002**, *67*, 3057–3064. (b) Rostovtsev, V. V.; Green, L. G.; Fokin, V. V.; Sharpless, K. B. *Angew. Chem., Int. Ed.* **2002**, *41*, 2596–2599. (c) Kuang, G.-C.; Guha, P. M.; Brotherton, W. S.; Simmons, J. T.; Stanke, L. A.; Nguyen, B. T.; Clark, R. J.; Zhu, L. *J. Am. Chem. Soc.* **2011**, *133*, 13984–14001. (d) Donnelly, P. S.; Zannatta, S. D.; Zammit, S. C.; White, J. M.; Williams, S. J. *Chem. Commun.* **2008**, 2459–2461. (e) Zhang, L.; Chen, X.; Xue, P.; Sun, H. H. Y.; Williams, I. D.; Sharpless, K. B.; Fokin, V. V.; Jia, G. *J. Am. Chem. Soc.* **2005**, *127*, 15998–15999.
- (4) Goddard-Borger, E. D.; Stick, R. V. *Org. Lett.* **2007**, *9*, 3797–3800.
- (5) (a) Tuma, L. D. *Thermochim. Acta* **1994**, *243*, 161–167. (b) Cavender, C. J.; Shiner, V. J. *J. Org. Chem.* **1972**, *37*, 3567–3569.
- (6) (a) Smith, P. A. S. *Open-Chain Nitrogen Compounds*; Benjamin: New York, 1966; Vol. 2, pp 211–256. (b) Boyer, J. H.; Moriarty, R.; de B. Darwent, B.; Smith, P. A. S. *Chem. Eng. News* **1964**, *42* (31), 6.
- (7) NATO standardization agreement (STANAG) on explosives, impact sensitivity tests, no. 4489, 1st ed., Sep 17, 1999.
- (8) WIWEB-Standardarbeitsanweisung 4-5.1.02, Ermittlung der Explosionsgefährlichkeit, hier der Schlagempfindlichkeit mit dem Fallhammer, Nov 8, 2002.
- (9) <http://www.bam.de>, accessed February 7, 2012.
- (10) NATO standardization agreement (STANAG) on explosive, friction sensitivity tests, no. 4487, 1st ed., Aug 22, 2002.
- (11) WIWEB-Standardarbeitsanweisung 4-5.1.03, Ermittlung der Explosionsgefährlichkeit oder der Reibeempfindlichkeit mit dem Reibeapparat, Nov 8, 2002.
- (12) <http://www.ozm.cz>, accessed February 7, 2012.
- (13) Impact: insensitive >40 J, less sensitive ≥ 35 J, sensitive ≥ 4 J, very sensitive ≤ 3 J; friction: Insensitive >360 N, less sensitive = 360 N, sensitive <360 N a. > 80 N, very sensitive ≤ 80 N, extreme sensitive ≤ 10 N. According to the UN Recommendations on the Transport of Dangerous Goods (+) indicates: not safe for transport.
- (14) Quick, A.; Williams, D. J. *Can. J. Chem.* **1976**, *54*, 2465–2469.
- (15) Jenkins, H. D. B.; Roobottom, H. K.; Passmore, J.; Glasser, L. *Inorg. Chem.* **1999**, *38*, 3609–3620.
- (16) Jenkins, H. D. B.; Tudela, D.; Glasser, L. *Inorg. Chem.* **2002**, *41*, 2364–2367.
- (17) (a) Depernet, D.; François, B. WO 02/057210 A1, PCT/FR02/00189, US 2002/0107416; *Chem. Abstr.* **2002**, *137*, 109123. (b) Ozanne, A.; Pouységu, L.; Depernet, D.; François, B.; Quideau, S. *Org. Lett.* **2003**, *5* (16), 2903–2906.

Cite this: *Dalton Trans.*, 2012, **41**, 11201

www.rsc.org/dalton

PAPER

5,5'-Azoxytetrazolates – a new nitrogen-rich dianion and its comparison to 5,5'-azotetrazolate†

Niko Fischer,^a Katharina Hüll,^a Thomas M. Klapötke,^{*a} Jörg Stierstorfer,^a Gerhard Laus,^b Michael Hummel,^b Carmen Froschauer,^b Klaus Wurst^b and Herwig Schottenberger^b

Received 6th June 2012, Accepted 13th July 2012

DOI: 10.1039/c2dt31217d

A modification of the synthesis of sodium 5,5'-azotetrazolate pentahydrate, described by Thiele in 1898, yields the unknown and unexpected corresponding 5N-oxido derivative sodium 5,5'-azoxybistetrazolate pentahydrate ($\text{Na}_2\text{zTO} \cdot 5\text{H}_2\text{O}$, **1**). Purification was achieved by recrystallization based on the better solubility of $\text{Na}_2\text{zTO} \cdot 5\text{H}_2\text{O}$ in water. Different nitrogen-rich salts, such as the diammonium (**3**), the dihydroxylammonium (**4**), the bis-diaminoguanidinium (**5**), the bis-triaminoguanidinium (**6**) and the diaminouronium salt (**7**), have been prepared using metathesis reactions starting from barium 5,5'-azoxybistetrazolate pentahydrate (**2**) and ammonium, hydroxylammonium, diaminoguanidinium or diaminouronium sulfate and triaminoguanidinium chloride, respectively. The nitrogen rich azoxy-derivatives **3–7** were characterized using NMR, IR and Raman spectroscopy, mass spectrometry and elemental analysis. Additionally the solid state structures of **3**, **4**, **5** and **7** were determined by single crystal X-ray diffraction. The heats of formation of **3** and **4** and their corresponding azo-tetrazolate derivatives were calculated by the atomization method based on CBS-4M enthalpies. With these values and the crystal densities, several detonation parameters such as the detonation velocity, detonation pressure and specific impulse were calculated (EXPLO5) and compared. The sensitivities towards shock (BAM drophammer), friction (BAM friction tester) and electrostatic discharge of the described compounds were determined.

Introduction

The azo-coupling of nitrogen-rich heterocycles such as 5-amino-tetrazole under alkaline conditions leads to sodium 5,5'-azotetrazolate.¹ In the literature, a broad variety of metal and non-metal 5,5'-azotetrazolates has been described including their structural determination by X-ray single crystal diffraction. At the moment more than 68 entries for azotetrazolates can be found only in the CCDC database. More than 200 references are listed in the SCIFINDER database containing the azotetrazolate dianion (zT^{2-}). 123 years after their discovery by Thiele,¹ salts of 5,5'-azotetrazolate have found various applications mainly in the energetic materials sector including, due to their high nitrogen content, the use as gas generating agents in propellant systems. For example, the bis(triaminoguanidinium) salt² (Fig. 1) finds application as a nitrogen-rich additive in the NILE-propellant (Navy Insensitive Low-Erosion Propellant).³

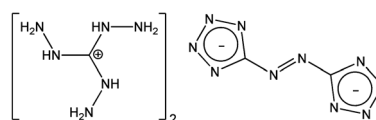


Fig. 1 Bis(triaminoguanidinium) 5,5'-azotetrazolate (TAG_2zT), a nitrogen-rich energetic material of great interest.

Tetraamine copper 5,5'-azobis(tetrazolate) dihydrate was recently described as being a “green” additive in solid rockets as a low-smoke propellants ingredient.⁴ Even several lanthanoid complexes have been published by Austrian coworkers in 2009.⁵ They claimed luminescent or nonlinear optic properties of potential interest. Very recently we also described the silver amine azotetrazolate complex as a new primary explosive.⁶ Unfortunately, 5,5'-azotetrazolates are not stable under mineral-acidic conditions since neutral 5,5'-azotetrazole decomposes into 5-hydrazinotetrazol, dinitrogen and formic acid.⁷

By a small variation in the synthesis of 5,5'-azotetrazole, which is a change of the order of mixing the reagents, sodium 5,5'-azoxybistetrazolate pentahydrate could be isolated. N-oxides are getting more and more popular in the development of new energetic materials.⁸ The N-oxide formation at one of the azo-bridge nitrogen atoms changes the properties of the isolated species notably. Not only that the crystal density, which is a very important parameter when calculating the detonation

^aEnergetic Materials Research, Department of Chemistry, University of Munich (LMU), Butenandtstr. 5-13, 81377 Munich, Germany. E-mail: tmk@cup.uni-muenchen.de; Fax: +49-89-2180-77492

^bFaculty of Chemistry and Pharmacy, University of Innsbruck, 6020 Innsbruck, Austria

†Electronic supplementary information (ESI) available. CCDC 881227–881231 and 881233. For ESI and crystallographic data in CIF or other electronic format see DOI: 10.1039/c2dt31217d

performance of a new material, is dramatically affected by further possibilities to form hydrogen-bonds in the solid state, but also the increased oxygen content makes the materials suitable alternatives to 5,5'-azotetrazolates when residue-free combustion of the compound is desired. Further we expect a change in the melting- and decomposition temperatures of these materials. In the following, the synthesis and characterization of five nitrogen-rich salts including the diammonium (3), the dihydroxylammonium (4), the bis-diaminoguanidinium (5), the bis-triaminoguanidinium (6) and the bis-diaminouronium (7) salt are described, whereas the main attention is directed to the comparison of their physicochemical properties to those of selected respective 5,5'-azotetrazolates.

Results and discussion

Synthesis

Sodium 5,5'-azotetrazolate pentahydrate, as described by Thiele in 1898,¹ can be easily prepared in a one step reaction starting from 5-aminotetrazole *via* oxidation with potassium permanganate. By using the same reagents, but reacting them in a different order, sodium 5,5'-azoxybistetrazolate pentahydrate ($\text{Na}_2\text{zTO} \cdot 5\text{H}_2\text{O}$) could be isolated in 16% yield (not optimized protocol). The difference compared to the synthesis of sodium 5,5'-azotetrazolate is that 5-aminotetrazole is added to the oxidizing agent potassium permanganate. A proposed mechanism of the formation of 5,5'-azoxybistetrazolate in comparison to the formation of 5,5'-azotetrazolate is depicted in Scheme 1. A similar process was already observed for the formation of azoxybenzene from solutions of phenyl-hydroxylamine upon air oxidation to nitrosobenzene and following condensation with phenylhydroxylamine to form azoxybenzene.⁹ Here, 5-aminotetrazole is oxidized to 5-hydroxylaminotetrazole and partially further oxidized

to 5-nitrosotetrazole, which together with 5-hydroxylaminotetrazole condensates to 5,5'-azoxy-bistetrazolate.

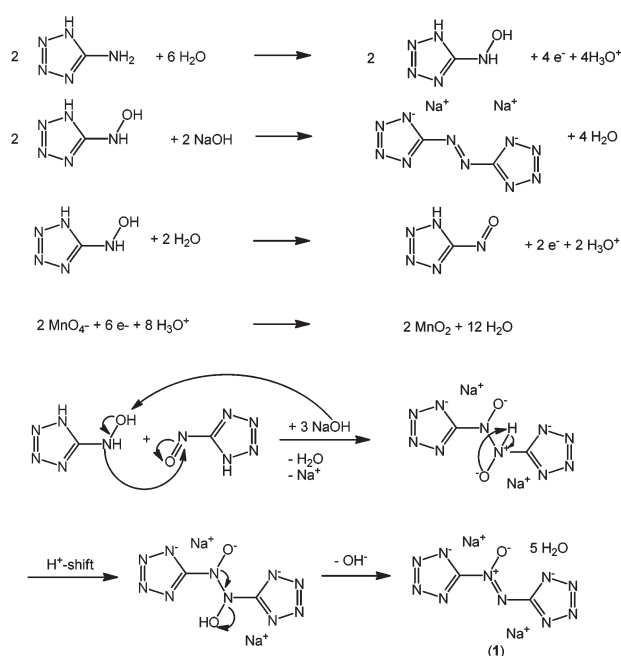
The excess of potassium permanganate firstly ensures the oxidation of 5-hydroxylaminotetrazole to 5-nitrosotetrazole and makes it impossible for the hydroxylaminotetrazole to self-condensate, which would result in the formation of 5,5'-azotetrazolate. This is the case if the oxidizing agent potassium permanganate is added to an excess of 5-aminotetrazole under alkaline conditions as described by Thiele.¹ In a further study we tested the influence of the addition of sodium hydroxide to the reaction mixture. For the formation of the azoxy-derivative **1** it is only of minor importance whether sodium hydroxide is added at the beginning of the reaction, which supposedly should facilitate the formation of the redox products 5-hydroxylaminotetrazole and 5-nitrosotetrazole, or towards the end of the reaction, where it catalyses the condensation reaction as shown in Scheme 1, indicated by only a small difference in the yields of both synthetic protocols. Instead of 16% yield, we observed 14% yield, when sodium hydroxide is added stoichiometrically at the beginning of the reaction. Therefore, only the protocol, in which sodium hydroxide is added towards the end of the reaction, is described in the experimental part.

For the transformation into the nitrogen rich 5,5'-azoxybistetrazolates, metathesis reactions using the sodium or the barium salt were utilized. The poorly soluble barium salt can be prepared by reacting the sodium salt with 1 equiv. of barium chloride. The barium salt **2** precipitates readily from the aqueous solution and can be filtered off (Scheme 2).

The barium salt **2** was further reacted with the respective nitrogen-rich sulfates, which are ammonium sulfate, hydroxylammonium sulfate, diaminoguanidinium sulfate and diaminouronium sulfate. The triaminoguanidinium salt was prepared starting from the sodium salt using triaminoguanidinium chloride.

Except from the triaminoguanidinium salt **6**, single crystals suitable for X-ray diffraction of all the remaining compounds **3–5** and **7** were obtained after recrystallization from either water or an ethanol–water mixture. The analytical data in the Experimental section of compound **7** were taken from the compound as isolated from the synthesis without recrystallization, namely bis-diaminouronium 5,5'-azoxybistetrazolate (**7a**). Recrystallization from EtOH–H₂O however afforded a compound with 1 equiv. of double protonated diaminourea, 2 equiv. of monoprotonated 5,5'-azoxybistetrazolate and four molecules of water per molecular unit, as shown in Scheme 3.

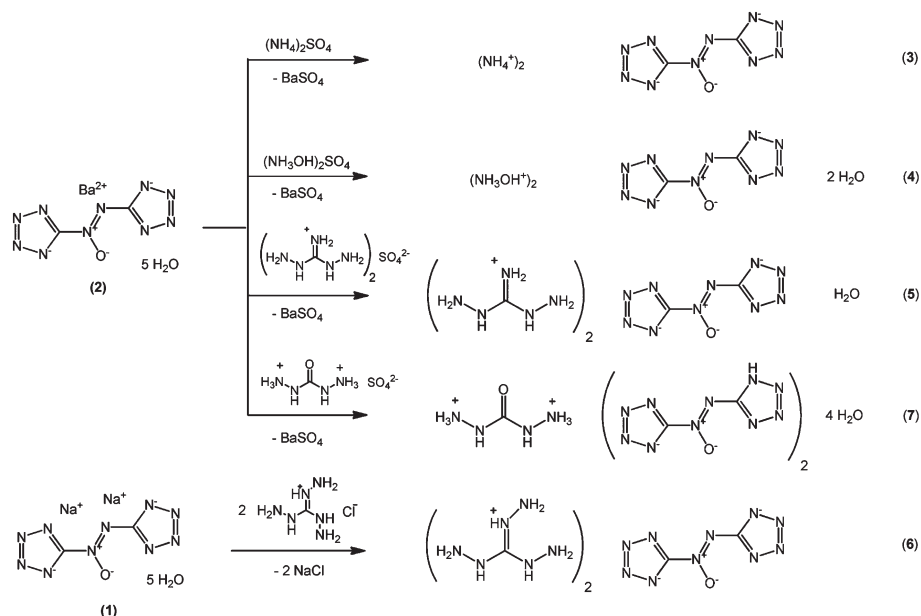
The sulfates, which were used for the metathesis reactions, were obtained from commercial sources (ammonium sulfate, hydroxylammonium sulfate) or prepared as follows. Diaminoguanidinium sulfate was obtained after ion exchange from commercially available diaminoguanidinium chloride. Triaminoguanidinium chloride was prepared from commercially available



Scheme 1 Mechanism for the formation of 5,5'-azotetrazolate and **1**.



Scheme 2 Formation of barium azoxy-5,5'-bistetrazolate (**2**).



Scheme 3 Metathesis reactions leading to the nitrogen rich salts 3–7.

aminoguanidinium bicarbonate after acidification with hydrochloric acid to obtain aminoguanidinium chloride and following a hydrazinolysis reaction with hydrazine hydrate in dioxane. Diaminouronium sulfate was obtained after combining solutions of diaminourea (=carbonyldihydrazide) and 1 mol L⁻¹ sulfuric acid.

Behavior in acidic media

The chemical stability of the 5,5'-azoxybistetrazolate anion in acidic media compared to the stability of 5,5'-azotetrazolate was tested in 4 experiments by treating both disodium salts with either 0.5 or 1.0 equiv. of 0.01 molar hydrochloric acid on a very small scale (0.33 mmol) after dissolving the salts in 3 mL of water. All four solutions showed gas evolution after a short time, whereas the two solutions containing 5,5'-azotetrazolate showed enhanced gas evolution and also turned red after one day. The two experiments with 5,5'-azoxybistetrazolate stayed yellow even after several days. However a difference between the experiments using 0.5 and 1.0 equiv. of acid could be observed. The solutions using 1.0 equiv. discolored to some extent due to their faster decomposition as compared to the experiments using 0.5 equiv. of acid. The higher stability of the 5,5'-azoxybistetrazolate anion compared to 5,5'-azotetrazolate towards acidic media was already assumed after the solution of the crystal structure of monoprotonated 5,5'-azoxybistetrazolate 7. To date, no example of a monoprotonated 5,5'-azotetrazolate has been described in the literature.

Single crystal X-ray structure analysis

Compounds 1–5, as well as 7 were investigated by low temperature single crystal X-ray diffraction. Selected data and parameters of the X-ray determinations are given in the ESI (Table S1†). Cif

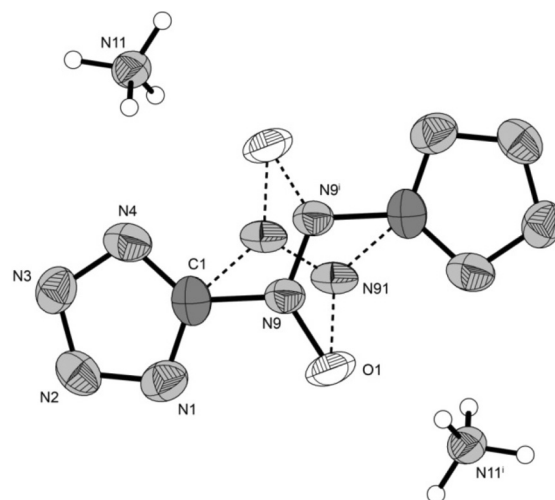


Fig. 2 Molecular unit of diammonium 5,5'-azoxybistetrazolate (3). Ellipsoids of non-hydrogen atoms are drawn at the 50% probability level. Dashed bonds show the crystallographic disorder of the azoxy group. Symmetry code: (i) 1 - x, -y, 1 - z.

files for the structures have been deposited with the Cambridge Crystallographic Data Centre.¹⁰

The molecular structure of diammonium 5,5'-azoxybistetrazolate (3) revealing the disordered azoxy moiety is shown in Fig. 2. This kind of disorder can be found in most of our investigated azoxy-structures. In comparison to ammonium 5,5'-azotetrazolate ((NH₄)₂zT)¹¹ with a density of 1.562 g cm⁻³ (both crystallize in the triclinic space group *P* $\bar{1}$) 3 shows a slightly higher density of 1.592 g cm⁻³. The bond length and angles of the tetrazolate rings are between typical C–N/N–N single and C=N/N=N double bonds¹² due to the aromaticity. The azoxybistetrazolate dianion is shaped (nearly) planar. The diazene-bond length N9–N9ⁱ is 1.27(1) Å which is similar in (NH₄)₂zT

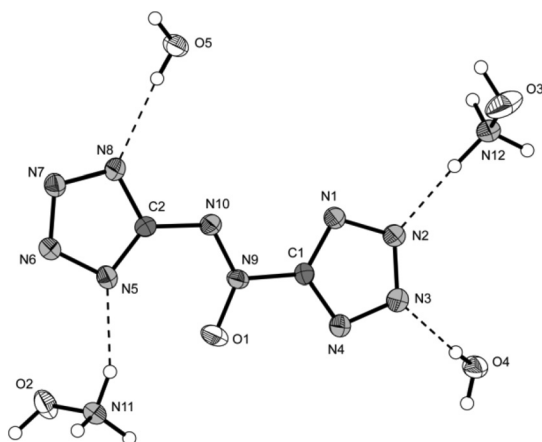


Fig. 3 Molecular unit of dihydroxylammonium 5,5'-azoxybistetrazolate dihydrate (**4**). Ellipsoids of non-hydrogen atoms are drawn at the 50% probability level. Selected bond lengths (Å): N11–O2 1.410(2), N12–O3 1.408(3), N10–N9 1.273(2), N10–C2 1.396(3), N4–C1 1.318(2), N4–N3 1.341(2), N7–N6 1.316(2), N7–N8 1.334(2), C1–N1 1.320(2), C1–N9 1.440(3), N9–O1 1.253(2), N8–C2 1.341(3), N5–C2 1.336(3), N5–N6 1.346(2), N1–N2 1.340(2), N3–N2 1.324(2); selected bond angles (°): N9–N10–C2 116.93(17), C1–N4–N3 103.50(16), N6–N7–N8 109.52(16), N4–C1–N1 114.19(18), N4–C1–N9 122.30(18), N1–C1–N9 123.50(18), O1–N9–N10 128.99(18), O1–N9–C1 116.56(16), N10–N9–C1 114.44(16), N7–N8–C2 104.37(16), C2–N5–N6 103.51(17), C1–N1–N2 103.54(16), N2–N3–N4 109.42(16), N3–N2–N1 109.35(16), N7–N6–N5 110.15(16), N5–C2–N8 112.44(18), N5–C2–N10 130.69(19), N8–C2–N10 116.87(18).

(1.36(1) Å) and slightly longer than a typical N=N double bond (1.20 Å). The N–O bond length is 1.316(8) Å which is between a typical N–O single (1.45 Å) and N=O double (1.17 Å) bond. In the structure of **3** there is no difference between the two C1–N9 bonds due to the symmetry centre caused by the disorder.

In accordance with the structure of hydroxylammonium 5,5'-azotetrazolate dihydrate¹³ (monoclinic, $C2/c$, $Z = 4$, $\rho = 1.612 \text{ g cm}^{-3}$), the corresponding N-oxide **4**, shown in Fig. 3, crystallizes also under inclusion of two molecules of crystal water in the monoclinic space group $P2_1/c$. As mentioned before, N-oxides have been described¹⁴ as promising energetic materials because of increasing densities and thermal stabilities. However, comparison of the hydroxylammonium structures shows a lower density for the N-oxide (**4**: 1.596 g cm^{-3}) but an increase in thermal stability ($(\text{Hx})_2\text{zT}$: 130°C vs. **4**: 175°C). The molecular structures of the dianions in **4** are similar to those observed for **3**. However, the dianions are not disordered in this structure. Therefore the influence of the N-bonded oxygen atom can be seen by the elongation ($\sim 0.05 \text{ Å}$) of the C1–N9 bond of 1.440(3) Å in comparison to the distance of C2–N10 (1.396(3) Å). Again the diazo distance N9=N10 is 1.273(2) Å.

Recrystallization of the residue of the 1 : 1 reaction of barium 5,5'-azoxybistetrazolate and diaminouronium sulfate from 40% hydrofluoric acid yielded the monoprotonated 5,5'-azoxybistetrazolate with a twice positively charged diaminouronium cation and inclusion of four crystal water molecules (Fig. 4). It is the first example of a structurally determined monoprotonated derivative of 5,5'-azotetrazolate, whose existence can be rationalized by the formation of the intramolecular hydrogen bridges

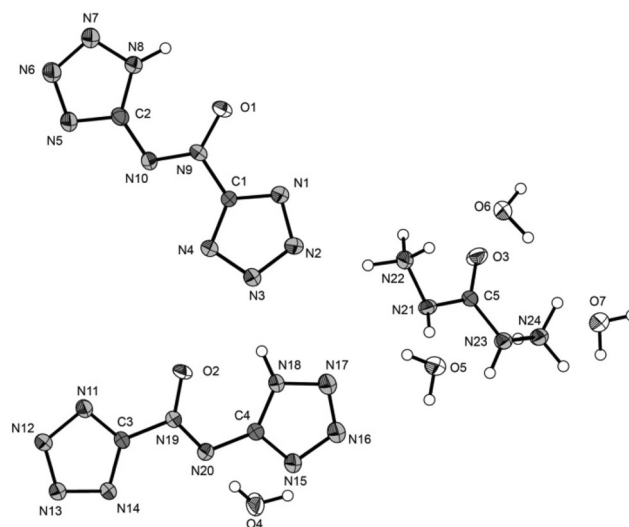


Fig. 4 Molecular unit of diaminouronium bis(5,5'-azoxybistetrazolate) tetrahydrate (**7**). Ellipsoids of non-hydrogen atoms are drawn at the 50% probability level. Selected bond lengths (Å): N21–C5 1.367(3), N23–C5 1.364(3), O3–C5 1.219(3), N21–N22 1.420(3), N23–N24 1.430(3); selected bond angles (°): O3–C5–N23 123.3(2), O3–C5–N21 122.7(2), N22–N21–C5 113.59(18), N24–N23–C5 113.58(18).

(graph set S1,1(6)) N8–H8...O1 (0.92(3), 2.17(3), 2.604(3) Å, $107.8(19)^\circ$) and N18–H18...O2 (0.92(3), 2.18(3), 2.562(2) Å, $104(2)^\circ$). The compound crystallizes in the monoclinic space group $P2_1/c$ with four cation/anion pairs in the unit cell and a calculated density of 1.650 g cm^{-3} which is the highest one of the metal-free compounds investigated in this work. The bond lengths (Table S1†) of the ring atoms are not influenced by the observed protonation. However, the diazene distances N9(19)=N10(20) are slightly elongated in comparison to the structures discussed previously. The diaminouronium cation is not planar showing a torsion angle N22–N21–N23–24 of $\sim 59.1^\circ$ (Fig. 4).

The structure of disodium 5,5'-azotetrazolate ($\text{Na}_2\text{zT} \cdot 5\text{H}_2\text{O}$) pentahydrate has been described in the literature twice.^{7,15} The structure of the sodium salt **1** is quite similar also crystallizing with inclusion of five molecules of crystal water in the triclinic space group $P\bar{1}$. Its density of 1.720 g cm^{-3} is slightly higher than in $\text{Na}_2\text{zT} \cdot 5\text{H}_2\text{O}$ (1.684 g cm^{-3}). The NaI cations are distortedly octahedrally coordinated. Sodium 1 is surrounded by the five water oxygen atoms O2, O3, O4, O5ⁱ, O4ⁱⁱ and nitrogen atom N3 with distances between 2.38 and 2.46 Å. Sodium 2 shows a larger coordination sphere with longer distances. It is surrounded by the atoms O6, O5 and O6ⁱ with similar distances of $\sim 2.42 \text{ Å}$ and by the atoms N10, O1A, O3ⁱ, O1Aⁱ and N4ⁱ ($\sim 2.58\text{--}2.7 \text{ Å}$) in larger distances. Symmetry codes: (i) $-x, 2 - y, 1 - z$; (ii) $1 - x, 2 - y, -z$. Due to the described coordination alternating azoxybis-tetrazolate layers and water layers are formed (Fig. 5 and 6).

NMR spectroscopy

^1H and ^{13}C NMR spectroscopy was applied to all of the investigated compounds **1–7**. Additionally a $^{15}\text{N}\{^1\text{H}\}$ NMR spectrum was recorded of the diammonium salt of 5,5'-azoxy-tetrazole (**3**) and for a comparison, a second one of the respective literature known non-oxide compound diammonium 5,5'-azotetrazolate.

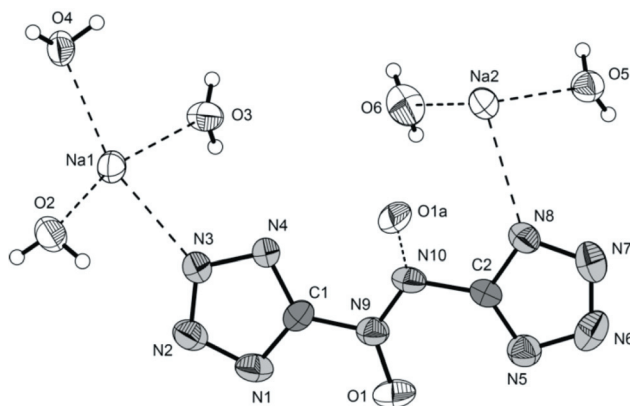


Fig. 5 Molecular unit of disodium 5,5'-azoxybistetrazolate pentahydrate (**1**). Ellipsoids of non-hydrogen atoms are drawn at the 50% probability level. Selected bond lengths (Å): Na1–O4 2.389(2), Na1–O2 2.393(2), Na1–O3 2.468(2), Na1–N3 2.457(2), Na2–O5 2.417(2), Na2–O6 2.420(3), Na2–N8 2.613(2).

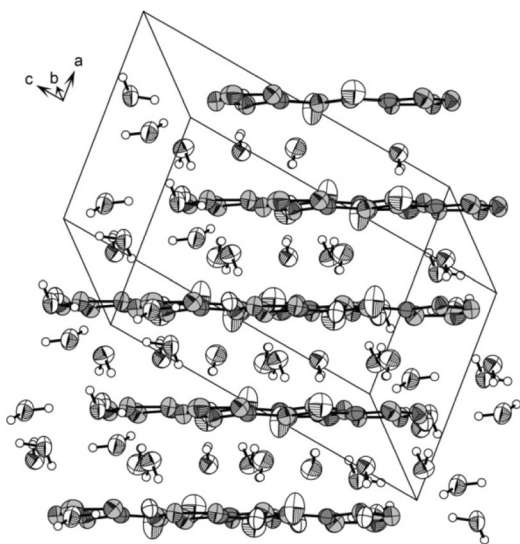


Fig. 6 View on the layer packing in the structure of **1**.

The proton NMR spectra of the metal salts **1** and **2** reveal only crystal water signals at 3.40 ppm (**1**) and 3.36 ppm (**2**), which is also true for the hydrated compound **5** (3.40 ppm). The protons of the ammonium cation of **3** appear as a broad signal at 3.70 ppm, whereas the signal of the protons of the hydroxyl-ammonium cation in **4** is downfield shifted to 8.61 ppm (s, br). The aminated guanidinium derivatives **5** and **6** show proton signals at 8.02 (**5**, NH) and 8.60 ppm (**6**, NH) in their spectra and additional upfield shifted signals at 4.60 (**5**) and 4.51 ppm (**6**), which can be assigned to the C- and N-amino groups of their cations. A similar pattern is observed for the diammonium salt **7** with signals at 7.82 ppm (NH) and 6.82 ppm (NNH₃⁺, NNH₂).

In the carbon NMR spectra of **1–7** two signals at chemical shifts of 168.2–168.5 and 162.5–164.3 ppm can be observed, whereas a final assignment to the two chemically inequivalent carbon atoms cannot be made without further investigations.

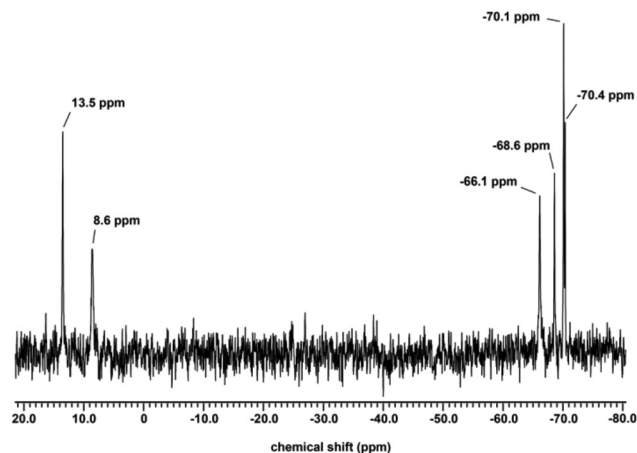


Fig. 7 ¹⁵N{¹H} NMR spectrum of diammonium 5,5'-azoxybistetrazolate (**3**) in the region between 20 and –80 ppm revealing the six signals observed for the 5,5'-azoxybistetrazolate dianion.

Compared to the carbon atom shift of the signal of 5,5'-azotetrazolates (around 173.2 ppm¹⁶), the signals of the azoxy-derivatives are somewhat shifted upfield indicating a lower shielding of the carbon atom cores.

The ¹⁵N{¹H} NMR spectrum of diammonium 5,5'-azotetrazolate reveals, due to its symmetry (*D*_{2h}) and the possible free rotation around the N_{azo}–C_{tetrazole}-bond, a set of 3 signals, which can be assigned to the anion, and one additional signal for the ammonium cation. The assignments were carried out after comparison to literature known values of the same anion.¹⁶ The signal of the ammonium cation is visible in the upfield region of the spectrum as a singlet at –358.5 ppm. Two signals are observed for both tetrazole rings at 12.8 ppm (N_β) and –66.3 ppm (N_α). The azo-bridge nitrogen atoms reveal a signal at 106.6 ppm. The addition of an oxygen atom to the azo-bridge changes the symmetry of the anion to lower symmetry (*C*_s) resulting in a larger number of observed signals in its ¹⁵N{¹H} NMR spectrum. Here 6 signals of the anion and one additional signal of the cation are observed. A partial assignment was undertaken according to a GIAO NMR calculation with Gaussian09.³⁶ Two signals in the downfield region at 13.5 and 8.6 ppm can be assigned to the N_β atoms of both tetrazole rings. The exact assignment of the remaining four signals to the two azoxy-bridge nitrogen atoms, as well as the two N_α atoms of the tetrazole rings is comparatively difficult since all signals are observed within a range of 4.3 ppm, whereas two of them differ only by 0.3 ppm (–66.1, –68.6, –70.1 and –70.4 ppm). The remaining signal in the upfield region of the spectrum at –358.8 ppm can again clearly be assigned to the ammonium cation. Fig. 7 shows the ¹⁵N{¹H} NMR spectrum of the anion of **3**, the signals of which are observed in the region between 20 and –80 ppm.

If the ¹⁵N{¹H} NMR spectra of both above discussed compounds are compared, it can be stated that N-oxidation at the azo-bridge of the anion mainly affects the chemical shifts of the nitrogen atoms in the azo-bridge itself. The signals are strongly shifted upfield from 106.6 ppm for the azo-bridge N atoms to signals in the vicinity of –68 ppm for the azoxy bridge. Neither the N_α (12.8 ppm for the azo compound vs. 13.5/8.6 ppm for **3**)

nor the N_{β} (−66.3 ppm for the azo compound vs. signals at −66.1 to −70.4 ppm for **3**) atoms of the tetrazole rings are shifted significantly to higher or lower field.

Vibrational spectroscopy

Also Raman and IR spectroscopy were applied for the identification of **1–8**. Generally, the crystal water containing compounds **1**, **2**, **4** and **5** show absorptions in the region between 3030 and 3422 cm^{-1} in their IR spectra due to O–H valence vibrations. Additionally, N–H valence vibration absorptions of all nitrogen-rich cation (ammonium, hydroxylammonium, diaminoguanidinium, triaminoguanidinium and diaminouronium) containing compounds **3–7** are observed in the region 3171–3388 cm^{-1} .

Further characteristic absorption bands, which are observed for azoxybistetrazolates, are based on the $C_{\text{tetrazole}}-N_{\text{azoxy}}$ -valence vibration at 1390–1412 cm^{-1} and the $N=N$ -azoxy valence vibration at 1499–1504 cm^{-1} . The guanidinium derived cations in **5** and **6** reveal absorption bands of the C–N stretching vibration at 1685 cm^{-1} (**6**) and 1684/1667 cm^{-1} (**5**). The ammonium salt **3** additionally can be identified by the deformation vibration of its cation visible in a strong absorption band at 1430 cm^{-1} . Although the mentioned absorption bands prove the identity of the synthesized compounds, due to a large number of combination modes, especially in the IR spectra, not all absorption bands could be assigned.

Thermal behavior

Differential scanning calorimetry (DSC) measurements to determine the melt- and decomposition temperatures of **1–8** (about 1.5 mg of each energetic material) were performed in covered Al-containers with a hole (0.1 mm) in the lid for gas release and a nitrogen flow of 20 mL min^{-1} at a heating rate of 5 $^{\circ}\text{C min}^{-1}$. The decomposition temperatures are given as onset temperatures and are within a range from 160 $^{\circ}\text{C}$ (**7a**) to 222 $^{\circ}\text{C}$ (**1** and **3**). The sodium salt **1** loses its hydrate water, indicated by an endothermic peak in the DSC trace at 80–130 $^{\circ}\text{C}$, which is also true for the barium salt **2** at 100–130 $^{\circ}\text{C}$. However, the barium salt decomposes earlier (188 $^{\circ}\text{C}$) compared to the sodium salt (222 $^{\circ}\text{C}$). If comparing the two metal salts to their 5,5'-azotetrazolate analogues, the decomposition temperatures of the 5,5'-azotetrazolates are somewhat higher ($\text{Na}_2\text{zT}\cdot 5\text{H}_2\text{O}$: 248 $^{\circ}\text{C}$; $\text{Ba}_2\text{zT}\cdot 5\text{H}_2\text{O}$: 211 $^{\circ}\text{C}$ ⁷). The opposite trend is observed if comparing the ammonium and the hydroxylammonium (Hx^-) salts of both anions. Both ammonium salts crystallize water free with decomposition temperatures of 222 $^{\circ}\text{C}$ for the 5,5'-azoxybistetrazolate (**3**) and only 195 $^{\circ}\text{C}$ for the corresponding 5,5'-azotetrazolate. Both hydroxylammonium salts crystallize as dihydrate and decompose much earlier at 175 $^{\circ}\text{C}$ (**4**) and 130 $^{\circ}\text{C}$ (corresponding 5,5'-azotetrazolate). They lose their crystal water at 60–150 $^{\circ}\text{C}$ (**4**) and 105–125 $^{\circ}\text{C}$ (5,5'-azotetrazolate) respectively. Fig. 8 clearly shows the observed trend of higher decomposition temperatures of the ammonium salts compared to their corresponding hydroxylammonium salts as well as the observed trend of higher decomposition temperatures of the azoxy-derivatives **3** and **4** compared to their non-oxide analogs $(\text{NH}_4)_2\text{zT}$ and Hx_2zT , which, astonishingly, is not true for the sodium and the barium

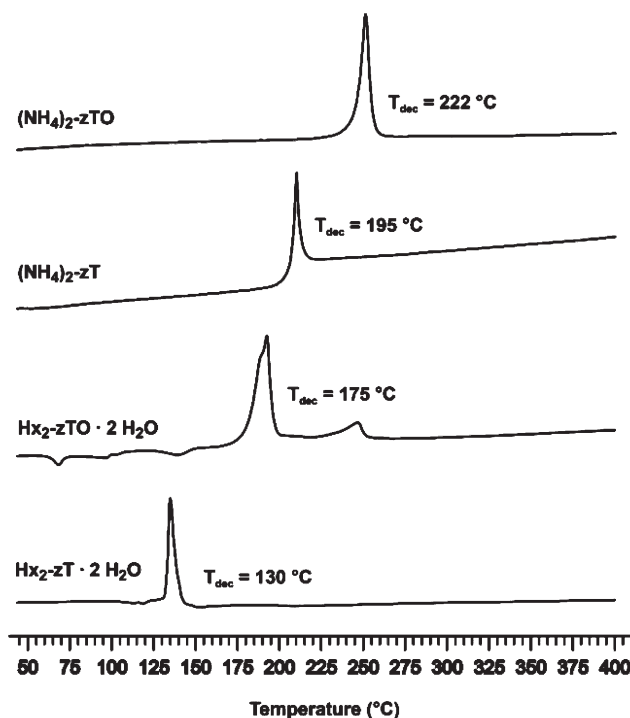


Fig. 8 DSC curves of **3** ($(\text{NH}_4)_2\text{zTO}$) and **4** (Hx_2zTO) and their corresponding non-oxide dihydroxylammonium 5,5'-azotetrazolate (Hx_2zT) and diammonium 5,5'-azotetrazolate ($(\text{NH}_4)_2\text{zT}$).

salts of these anions as described above. All decomposition temperatures are summarized in Table 3.

Sensitivity testing

For application of new energetic compounds important values for safety, handling and processing are the sensitivity data. The values for friction and impact sensitivity were determined according to BAM (Bundesanstalt für Materialforschung) standard methods described in the NATO STANAG 4487, 4489 and 4490 specifications for energetic materials using a BAM friction tester and a BAM drophammer.^{17–24} The sensitivities towards electrical discharge were determined on a small scale electrostatic discharge device.²⁵

According to the UN recommendations on the transport of dangerous goods, the sodium salt **1** can be regarded as less sensitive towards impact with a value of 40 J, whereas the barium salt, although being a pentahydrate, is much more sensitive (7 J). The same trend is observed for the friction sensitivity of both salts (**1**: 324 N; **2**: 160 N). The comparatively low sensitivity of the sodium salt can mainly be explained by the formation of the pentahydrate, since contained crystal water usually desensitizes a compound. The remaining nitrogen-rich salts **3–7** need to be classified as sensitive (**4–7**) or very sensitive (**3**) towards impact, however there are still large differences in their impact sensitivity data. Whereas the dihydroxylammonium salt **4** reveals an impact sensitivity of 30 J, which again can be explained by the formation of a dihydrate, the bis-diaminoguanidinium salt **5** (as its monohydrate) has a value of only 15 J and both the bis-

triaminoguanidinium salt **6** and the bis-diaminouronium salt **7** are already close to being classified as very sensitive towards impact (**6**: 4 J; **7**: 3.5 J), which is true for the diammonium salt **3** with an impact sensitivity of only 1 J (!). The friction sensitivities of the above discussed compounds **4–7** are in a range between 120 N for **6** and 324 N for **5**, whereas both kinds of sensitivity data do not seem to be directly related to each other as evidenced by the bis-diaminouronium salt **7**, which is rather sensitive towards impact (3.5 J) but on the other hand shows only a moderate value for the friction sensitivity (240 N). The ammonium salt again shows the highest sensitivity amongst the discussed compounds (40 N). The sensitivities towards electrostatic discharge are in a range between 0.2 J (**1**) and 0.50 J (**5**, **7**). Through normal activities, the human body can generate up to 25 mJ of static electricity, which can easily set off the most sensitive explosives. All compounds presented herein have electrostatic sensitivities higher than the one possibly being generated by the human body, allowing safety during handling. Only the value of **6** (90 mJ) is noticeably low, but the non-crystallinity of **6** can be a possible reason for this result, since the sensitivity towards electrostatic discharge is also dependent on the grain size of the investigated material.

Heats of formation

The heats of formation of water-free **3** and (NH₄)₂zT as well as of **4** and Hx₂zT·2H₂O for comparison were calculated with the atomization method (eqn (1)) using CBS-4M enthalpies and summarized in Table 1.^{26,27} Heats of formation of the other hydrated compounds and of the triaminoguanidinium salt, of which the density could not be determined by XRD, were neglected. The gas phase enthalpies of formation $\Delta_f H^\circ$ (g, M) were converted into the solid state enthalpies of formation ($\Delta_f H^\circ$ (s, M))

Table 1 Gas phase enthalpies of formation based on CBS-4M calculations

M	Formula	$-H_{(M, 298)}^a$ /a.u.	$\Delta_f H^\circ$ ^b (g, M)/kJ mol ⁻¹
zTO ²⁻	C ₂ N ₁₀ O ²⁻	697.959163	711.2
zT ²⁻	C ₂ N ₁₀ ²⁻	622.850742	769.6
NH ₄ ⁺	NH ₄ ⁺	56.796608	635.8
Hx ⁺	NH ₃ OH ⁺	131.863229	687.2

^a Electronic enthalpies in Hartree. ^b Calculated gas phase heat of formation of the involved anions and cations.

by using the Jenkins' equations for X₂Y salts²⁸ (for ionic derivatives).

$$\Delta_f H^\circ_{(g,M,298)} = H_{(M,298)} - \sum H^\circ_{(Atoms,298)} + \sum \Delta_f H^\circ_{(Atoms,298)} \quad (1)$$

Lastly, the molar standard enthalpies of formation (ΔH_m) were used to calculate the molar solid state energies of formation (ΔU_m) according to eqn (2) (Table 2).

$$\Delta U_m = \Delta H_m - \Delta n RT \quad (2)$$

(Δn being the change of moles of gaseous components).

A more positive heat of formation for the solid state was calculated for (NH₄)₂zT (547 kJ mol⁻¹) (which was expected) in comparison to the N-oxide **3** (519 kJ mol⁻¹).

Detonation parameters

In order to explore the performance of the highly energetic backbone 5,5'-azoxybistetrazolate, several detonation parameters of its diammonium and dihydroxylammonium salts **3** and **4** were calculated with the EXPLO5.05²⁹ software code and compared to those for diammonium and dihydroxylammonium 5,5'-azotetrazolate (Table 3). In the case of the ammonium salts, which crystallize water free, also the calculated specific impulse under isobaric conditions is discussed. The program EXPLO5 is based on the steady-state model of equilibrium detonation and uses Becker–Kistiakowsky–Wilson's equation of state (BKW E.O.S.) for gaseous detonation products and Cowan–Fickett's E.O.S. for solid carbon.³⁰ The calculation of the equilibrium composition of the detonation products is done by applying the modified White, Johnson and Dantzig's free energy minimization technique. The program is designed to enable the calculation of detonation parameters at the Chapman–Jouguet point. The BKW equation in the following form was used with the BKWN set of parameters (α , β , κ , θ) as stated below the equations and X_i being the mole fraction of the i -th gaseous product, k_i is the molar covolume of the i -th gaseous product:³¹

$$pV/RT = 1 + x e^{\beta x}$$

$$x = (\kappa \sum X_i k_i) / [V(T + \theta)]^\alpha, \quad \alpha = 0.5, \quad \beta = 0.176, \quad \kappa = 14.71, \quad \theta = 6620.$$

In terms of performance **3** is superior to the corresponding non-N-oxide (NH₄)₂zT. Due to the higher oxygen content a

Table 2 Lattice energies and enthalpies as well as solid state enthalpies and energies of formation ($\Delta_f U^\circ$)

	Formula	M /g mol ⁻¹	$\Delta_f H^\circ$ ^a (g)/kJ mol ⁻¹	V_M ^b /nm ³	U_L ^c /kJ mol ⁻¹	ΔH_L ^d /kJ mol ⁻¹	$\Delta_f H^\circ$ ^e (s)/kJ mol ⁻¹	Δn	$\Delta_f U^\circ$ ^f (s)/kJ mol ⁻¹
(NH ₄) ₂ zT	C ₂ H ₈ N ₁₂	200.2	2041.3	0.213	1482.4	1489.9	551.4	10	576.2
3	C ₂ H ₈ N ₁₂ O	216.2	1982.9	0.225	1451.9	1459.3	523.6	10.5	549.6
(Hx) ₂ zT·2H ₂ O	C ₂ H ₁₂ N ₁₂ O ₄	268.11	1660.9	0.227	1554.9	1567.3	93.6	14	128.3
4	C ₂ H ₁₂ N ₁₂ O ₅	284.1	1602.5	0.247	1510.5	1522.9	79.5	14.5	115.5

^a Calculated gas phase heat of formation of the ionic compounds. ^b Molecular volumes calculated from the X-ray structures (V/Z). ^c Lattice energy.

^d Lattice enthalpy. ^e Calculated heat of formation of the ionic compounds in the solid state. ^f Calculated energy of formation of the ionic compounds in the solid state.

Table 3 Energetic properties and detonation parameters of **3**, **4**, (NH₄)₂zT and Hx₂zT·2H₂O

	3	(NH ₄) ₂ zT	4	Hx ₂ zT·2H ₂ O
Formula	C ₂ H ₈ N ₁₂ O	C ₂ H ₈ N ₁₂	C ₂ H ₁₂ N ₁₂ O ₅	C ₂ H ₁₂ N ₁₂ O ₄
MW [g mol ⁻¹]	216.2	200.2	284.1	268.11
IS ^a [J]	1	3	30	25
FS ^b [N]	40	42	160	192
ESD-test ^c [J]	0.30	0.035	0.25	0.30
N ^d [%]	77.8	84.0	59.1	62.7
Ω ^e [%]	-51.8	-63.9	-28.2	-35.8
T _{dec.} ^f [°C]	222	195	175	130
Density ^g [g cm ⁻³]	1.592	1.562	1.596	1.615
Δ _f H _m ^{o,h} [kJ mol ⁻¹]	+524	+551	+80	+94
Δ _f U ^{o,i} [kJ kg ⁻¹]	+2542	+2878	+406	+478
EXPLO5.05 values				
I _{sp} ^j [s]	215	207	234	218
-Δ _E U ^{o,k} [kJ kg ⁻¹]	4039	3437	4723	4271
T _E ^l [K]	2935	2565	3309	3020
p _{C-J} ^m [kbar]	240	216	258	254
D ⁿ [m s ⁻¹]	8054	7788	8224	8200
V _o ^o [L kg ⁻¹]	831	824	893	892

^a Impact sensitivity (BAM drophammer, method 1 of 6). ^b Friction sensitivity (BAM friction tester, method 1 of 6). ^c Small-scale electrostatic discharge device (OZM). ^d Nitrogen content. ^e Oxygen balance. ^f Decomposition temperature from DSC (β = 5 °C). ^g Estimated from X-ray diffraction. ^h Calculated (CBS-4M) heat of formation. ⁱ Calculated energy of formation. ^j Specific impulse (isobaric combustion with a chamber pressure of 60 bar). ^k Energy of explosion. ^l Explosion temperature. ^m Detonation pressure. ⁿ Detonation velocity. ^o Volume of detonation products assuming only gaseous products.

higher energy of detonation (4039 kJ mol⁻¹) was computed. Because of its slightly higher density (1.592 g cm⁻³ (**3**) vs. 1.562 g cm⁻³ ((NH₄)₂zT) also the detonation pressure (240 kbar) and velocity (8054 m s⁻¹) are higher. Basically latter detonation values are greater than those observed for TNT but smaller than that of PETN (pentaerythriol tetranitrate) or RDX (hexogen).³² In addition, the specific impulse of the pure compounds when used as monopropellants was calculated assuming rocket propellant conditions (isobaric combustion with a chamber pressure of 60 bar). Also the calculated specific impulse of **3** is better than that of (NH₄)₂zT. The same trend can be proposed for the hydrazinium and triaminoguanidinium salts whose azotetrazolates showed promise as propellant ingredients (see Introduction).

In the case of the two dihydroxylammonium salts dihydrates **4** and Hx₂zT·2H₂O (against expectations) we observe a slightly lower density of the azoxy compound. Again the heat of formation is slightly decreased by the introduction of the N-oxide. However, the less negative oxygen balance of the azoxy compound (-28.2% vs. -35.8%) in combination with its slightly higher gas volume (893 L vs. 892 L) compensates for both, the slightly lower density and the lower heat of formation, so that the calculated detonation parameters of both salts are almost equal with 258 (**4**) and 254 kbar for both calculated detonation pressures and 8224 ms⁻¹ (**4**) and 8200 ms⁻¹ (Hx₂zT·2H₂O) for the detonation velocities. If comparing the explosion energy and the detonation temperature, one notices a stronger influence of the N-oxidation on these parameters for **4** and Hx₂zT·2H₂O. Also the calculated specific impulse of **4** (234 s) is higher than that of Hx₂zT·2H₂O (218 s).

Conclusions

From this combined theoretical and experimental study the following conclusions can be drawn:

- Sodium 5,5'-azoxybistetrazolate pentahydrate can be isolated from the oxidation of 5-aminotetrazole with potassium permanganate, when 5-aminotetrazole is added to a stirred solution of the oxidizing agent KMnO₄.

- A proposed mechanism for the formation of 5,5'-azoxybistetrazolate is formulated *via* the condensation of 5-hydroxylamino-tetrazole and 5-nitrosotetrazole.

- Bearing a numerous amount of inherently energetic C–N and N–N bonds, sodium 5,5'-azoxybistetrazolate was subjected to various metathesis reactions leading to the isolation and full characterization, including the X-ray single crystal measurements of a variety of nitrogen rich salts of this previously undescribed anion.

- Compared to 5,5'-azotetrazolates, 5,5'-azoxybistetrazolates show a comparable or even higher density due to better possibilities to form hydrogen bonds in the solid state.

- The calculated (CBS-4M) heats of formation of the partially oxidized N-oxides are, however, insignificantly lower compared to the respective 5,5'-azotetrazolates.

- The difference in thermal behaviour between 5,5'-azotetrazolates and 5,5'-azoxybistetrazolates is varying from compound to compound. The disodium and barium salt of 5,5'-azoxybistetrazole were found to be less thermally stable than the respective 5,5'-azotetrazolates, whereas the nitrogen-rich diammonium and dihydroxylammonium salts are thermally more stable than their respective 5,5'-azotetrazolate counterparts.

- If comparing the ammonium salt **3** to (NH₄)₂zT, it can be stated that based on its higher density, it reveals improved detonation performance, *i.e.* detonation velocity, detonation pressure, detonation temperature and explosion energy.

Experimental part

General procedures

All reagents and solvents were used as received (Sigma-Aldrich, Fluka, Acros Organics) if not stated otherwise. Melting and decomposition points were measured with a Linseis PT10 DSC using a heating rate of 5 °C min⁻¹, which were checked with a Büchi Melting Point B-450 apparatus. ¹H, ¹³C and ¹⁵N NMR spectra were measured with a JEOL Eclipse 400 ECX instrument. All chemical shifts are quoted in ppm relative to TMS (¹H, ¹³C) and nitromethane (¹⁵N). Infrared spectra were measured as KBr-pellets on a Perkin-Elmer Spektrum One FT-IR instrument. Raman spectra were recorded on a Bruker MultiRAM FT-Raman fitted with a liquid nitrogen cooled germanium detector and a Nd:YAG laser (λ = 1064 nm). Elemental analyses were performed with a Netsch STA 429 simultaneous thermal analyzer. Melting points were determined in capillaries with a Büchi Melting Point B-540 instrument and are uncorrected. Decomposition points were determined by differential scanning calorimetry (DSC) measurements with a Linseis DSC-PT10 DSC,³³ calibrated by standard pure indium and zinc using a heating rate of 5 °C min⁻¹. Pycnometric measurements were carried out with a Quantachrome helium gas pycnometer.

Sensitivity data (impact and friction) were performed using a drophammer and friction tester analog to BAM standards (Bundesanstalt für Materialforschung und prüfung).^{17–24,34} Electrostatic sensitivities were measured with an OZM small scale electrostatic discharge tester.³⁵ Quantum chemical calculations were performed with the Gaussian09 software.³⁶ The crystal structures of **1**, **2** and **3** were measured at $-65\text{ }^{\circ}\text{C}$ on a Nonius KappaCCD instrument. XRD of **4**, **5** as well as **7** and **8** was performed on an Oxford Xcalibur3 diffractometer with a Spellman generator (voltage 50 kV, current 40 mA) and a KappaCCD detector using Mo-K α radiation ($\lambda = 0.71073\text{ }\text{\AA}$). The data collection and reduction was carried out using the CRYSLISPRO software.³⁷ The structures were solved either with SHELXS-97³⁸ or SIR-92,³⁹ refined with SHELXL-97⁴⁰ and finally checked using the PLATON⁴¹ software integrated in the WINGX⁴² software suite. The absorptions of **4**, **5** as well as **7** and **8** were corrected with a Scale3 Abspack multi-scan method.⁴³

Sodium 5,5'-azoxybistetrazolate pentahydrate (1). Potassium permanganate (17.1 g, 108 mmol, 1.00 equiv.) was dissolved in water (150 mL) and 5-aminotetrazole (12.4 g, 146 mmol, 1.35 equiv.) was added in small portions at $0\text{ }^{\circ}\text{C}$. The brown reaction mixture was stirred at $0\text{ }^{\circ}\text{C}$ (1 h), room temperature (1 h) and $50\text{ }^{\circ}\text{C}$ (3 h). Ethanol (30 mL, 514 mmol, 4.76 equiv.) and an aqueous solution of sodium hydroxide (15%, 150 mL, 562 mmol, 5.20 equiv.) were added and the thick, brown slurry was stirred at $90\text{ }^{\circ}\text{C}$ (3 h). The still hot mixture was filtered over diatomaceous earth and washed with boiling water as long as the filtrate was still yellow. The solvent was removed by rotary evaporation and the remaining light yellow solid was extracted with hot ethanol. Ethanol was removed by rotary evaporation and the remaining yellow solid was twice recrystallized from EtOH–H₂O. Sodium 5,5'-azoxybistetrazolate pentahydrate (2.80 g, 8.80 mmol, 16%) was obtained as clear, yellow crystals.

DSC (T_{onset} , $5\text{ }^{\circ}\text{C min}^{-1}$): $222\text{ }^{\circ}\text{C}$ (dec.); IR (KBr, cm^{-1}): $\tilde{\nu} = 3835$ (w), 3422 (vs), 1632 (m), 1500 (m), 1473 (vw), 1450 (m), 1396 (m), 1275 (w), 1207 (w), 1160 (w), 1061 (w), 1034 (w), 913 (w), 768 (m), 559 (w); Raman (1064 nm, 300 mW, $25\text{ }^{\circ}\text{C}$, cm^{-1}): $\tilde{\nu} = 1532$ (7), 1503 (64), 1458 (26), 1448 (100), 1401 (49), 1387 (69), 1373 (70), 1282 (4), 1208 (7), 1164 (4), 1100 (40), 1082 (32), 1063 (69), 1050 (29), 924 (4), 754 (3), 401 (4), 252 (8), 89 (36); ^1H NMR (d_6 -DMSO, $25\text{ }^{\circ}\text{C}$, ppm): $\delta = 3.40$ (H_2O); ^{13}C NMR (d_6 -DMSO, $25\text{ }^{\circ}\text{C}$, ppm): $\delta = 168.4$ (CN_4), 164.0 (CN_4); m/z (FAB^+): 23.0 [Na^+]; m/z (FAB^-): 181.1 [$\text{C}_2\text{HN}_{10}\text{O}^-$]; EA ($\text{C}_2\text{H}_{10}\text{N}_{10}\text{O}_6\text{Na}_2$, 316.14) calcd: N 44.30, C 7.60, H 3.10; found: N 43.57, C 7.78, H 3.06; impact sensitivity: 40 J; friction sensitivity: 324 N; ESD: 0.2 J (at grain size 500–1000 μm).

Barium 5,5'-azoxybistetrazolate pentahydrate (2). Sodium 5,5'-azoxybistetrazolate pentahydrate (2.80 g, 8.80 mmol, 1.00 equiv.) was dissolved in hot water (8 mL) and a hot solution of barium chloride dihydrate (2.15 g, 8.80 mmol, 1.00 equiv.) was added and shortly heated. The solution was allowed to cool down and the resulting yellow precipitate was filtered, recrystallized from EtOH–H₂O and dried to obtain barium azoxy-5,5'-bistetrazolate pentahydrate (3.50 g, 8.60 mmol, 98%).

DSC (T_{onset} , $5\text{ }^{\circ}\text{C min}^{-1}$): $188\text{ }^{\circ}\text{C}$ (dec.); IR (KBr, cm^{-1}): $\tilde{\nu} = 3414$ (vs), 1623 (m), 1504 (s), 1473 (w), 1445 (m), 1394 (s),

1286 (w), 1204 (w), 1168 (w), 1071 (w), 1037 (w), 921 (m); 764 (m), 735 (w), 647 (w), 562 (w), 529 (w); Raman (1064 nm, 300 mW, $25\text{ }^{\circ}\text{C}$, cm^{-1}): $\tilde{\nu} = 1506$ (66), 1484 (18), 1456 (62), 1395 (100), 1376 (66), 1287 (5), 1206 (3), 1191 (2), 1171 (3), 1099 (47), 1079 (66), 1053 (17), 924 (4), 755 (2), 403 (3), 258 (3); ^1H NMR (d_6 -DMSO, $25\text{ }^{\circ}\text{C}$, ppm): $\delta = 3.36$ (H_2O); ^{13}C NMR (d_6 -DMSO, $25\text{ }^{\circ}\text{C}$, ppm): $\delta = 168.4$ (CN_4), 163.6 (CN_4); m/z (FAB^-): 181.1 [$\text{C}_2\text{HN}_{10}\text{O}^-$]; EA ($\text{C}_2\text{H}_{10}\text{BaN}_{10}\text{O}_6$, 407.49) calcd: N 34.37, C 5.89, H 2.47; found: N 34.30, C 5.91, H 2.51%; impact sensitivity: 7 J; friction sensitivity: 160 N; ESD: 0.60 J (at grain size 500–1000 μm).

Diammonium 5,5'-azoxybistetrazolate (3). Barium 5,5'-azoxybistetrazolate pentahydrate (3.54 g, 8.69 mmol) was suspended in 100 mL of water and a solution of ammonium sulphate (1.15 g, 8.69 mmol) in 20 mL of water was added. The mixture was heated to reflux for 5 min and further stirred at room temperature overnight. BaSO₄ was removed by filtration over diatomaceous earth and the filtrate was concentrated in a rotary evaporator. From the concentrated solution, the diammonium salt crystallized in yellow blocks, which were isolated by filtration, washed with the mother liquor several times and dried in air. Yield: 65% (1.73 g, 5.65 mmol).

DSC (T_{onset} , $5\text{ }^{\circ}\text{C min}^{-1}$): $222\text{ }^{\circ}\text{C}$ (dec.); IR (KBr, cm^{-1}): $\tilde{\nu} = 3173$ (m), 3002 (m), 2856 (m), 1692 (m), 1503 (m), 1430 (vs), 1390 (s), 1368 (m), 1276 (w), 1200 (m), 1185 (m), 1163 (m), 1070 (m), 1035 (w), 914 (m), 782 (s), 755 (m), 746 (m), 731 (m), 655 (w), 519 (m); Raman (1064 nm, 300 mW, $25\text{ }^{\circ}\text{C}$, cm^{-1}): $\tilde{\nu} = 1530$ (10), 1506 (50), 1490 (26), 1441 (100), 1394 (78), 1382 (56), 1371 (77), 1279 (7), 1203 (4), 1168 (5), 1090 (53), 1075 (95), 1047 (21), 918 (5), 757 (3), 402 (2), 256 (6), 183 (4); ^1H NMR (d_6 -DMSO, $25\text{ }^{\circ}\text{C}$, ppm): $\delta = 3.70$ (s, br, NH_4^+); ^{13}C NMR (d_6 -DMSO, $25\text{ }^{\circ}\text{C}$, ppm): $\delta = 168.4$ (CN_4), 164.3 (CN_4); m/z (FAB^+): 110.1 [$\text{NH}_3 + \text{matrix}^+$]; m/z (FAB^-): 181.1 [$\text{C}_2\text{HN}_{10}\text{O}^-$]; EA ($\text{C}_2\text{H}_8\text{N}_{12}\text{O}$, 216.16) calcd: N 77.76, C 11.11, H 3.73; found: N 77.35, C 11.69, H 3.53%; impact sensitivity: 1 J; friction sensitivity: 40 N; ESD: 0.30 J (at grain size 100–500 μm).

Dihydroxylammonium 5,5'-azoxybistetrazolate dihydrate (4). Barium 5,5'-azoxybistetrazolate pentahydrate (3.41 g, 8.37 mmol) was dissolved in the smallest possible volume of water (*ca.* 100 mL). A solution of hydroxylammonium sulfate (1.37 g, 8.37 mmol) was added. The instantaneously formed precipitate of BaSO₄ was removed after centrifugation of the mixture. The supernatant liquid was evaporated to almost dryness, the residue was again slurried in a little water and the mixture was filtered again to remove the remaining BaSO₄. The aqueous filtrate was left for crystallization. Yield: 72% (6.04 mmol, 1.50 g).

DSC (T_{onset} , $5\text{ }^{\circ}\text{C min}^{-1}$): $175\text{ }^{\circ}\text{C}$ (dec.); IR (KBr, cm^{-1}): $\tilde{\nu} = 3385$ (s), 2983 (s), 2739 (vs), 2133 (w), 2090 (w), 1659 (w), 1618 (m), 1535 (m), 1499 (m), 1476 (m), 1454 (m), 1412 (m), 1384 (m), 1292 (w), 1253 (w), 1215 (w), 1194 (w), 1187 (w), 1166 (w), 1104 (w), 1082 (w), 1068 (w), 1050 (w), 1042 (w), 995 (w), 917 (w), 773 (m), 753 (m), 725 (w), 655 (w), 626 (w), 520 (w); Raman (1064 nm, 300 mW, $25\text{ }^{\circ}\text{C}$, cm^{-1}): $\tilde{\nu} = 1500$ (16), 1477 (10), 1453 (100), 1415 (28), 1380 (38), 1294 (3), 1189 (3), 1168 (4), 1105 (68), 1085 (21), 1069 (12), 1052 (5), 997 (5), 919 (2), 758 (1), 402 (2), 266 (4); ^1H NMR (d_6 -DMSO, $25\text{ }^{\circ}\text{C}$,

ppm): δ = 8.61 (s, br, NH, OH); ^{13}C NMR (d_6 -DMSO, 25 °C, ppm): δ = 168.2 (CN_4), 162.5 (CN_4); m/z (FAB^+): 34.0 [NH_3OH^+]; m/z (FAB^-): 181.0 [$\text{C}_2\text{HN}_{10}\text{O}^-$]; EA ($\text{C}_2\text{H}_{12}\text{N}_{12}\text{O}_5$, 284.19) calcd: N 59.14, C 8.45, H 4.26; found: N 57.72, C 8.70, H 3.93%; impact sensitivity: 30 J; friction sensitivity: 160 N; ESD: 0.25 J (at grain size 100–500 μm).

Bis-diaminoguanidinium 5,5'-azoxybistetrazolate monohydrate (5). Barium 5,5'-azoxybistetrazolate pentahydrate (0.445 g, 1.09 mmol, 1.00 equiv.) was dissolved in boiling water and added to, previously dissolved in hot water, diaminoguanidinium sulphate (0.304 g, 1.10 mmol, 1.01 equiv.). The mixture was heated (5 min) and the precipitating barium sulphate was filtered off (diatomaceous earth). The light yellow solution was left to crystallize and diaminoguanidinium azoxy-5,5'-bistetrazolate monohydrate (0.260 g, 0.722 mmol, 66%) was obtained as ochre crystals.

DSC (T_{onset} , 5 °C min^{-1}): 179 °C (dec.); IR (KBr, cm^{-1}): $\tilde{\nu}$ = 3388 (vs), 3336 (vs), 2257 (vw), 1684 (vs), 1667 (vs), 1504 (m), 1541 (w), 1395 (s), 1274 (w), 1173 (m), 1033 (vw), 974 (m), 915 (w), 770 (m), 751 (w), 742 (w), 655 (w), 538 (m); Raman (1064 nm, 300 mW, 25 °C, cm^{-1}): $\tilde{\nu}$ = 3335 (4), 1676 (5), 1639 (3), 1506 (69), 1472 (11), 1450 (16), 1429 (83), 1402 (25), 1368 (78), 1275 (5), 1201 (5), 1179 (9), 1166 (8), 1069 (100), 1038 (19), 930 (12), 767 (3), 664 (2), 549 (9), 396 (5), 376 (5), 282 (3), 252 (6), 122 (52), 95 (47), 83 (39); ^1H NMR (d_6 -DMSO, 25 °C, ppm): δ = 8.02 (s, br, NH), 4.60 (s, CNH_2 , NNH_2), 3.40 (s, H_2O); ^{13}C NMR (d_6 -DMSO, 25 °C, ppm): δ = 168.4 (CN_4), 163.8 (CN_4), 160.3 ($\text{C}=\text{NH}_2$); m/z (FAB^+): 90.1 [CH_8N_5^+]; m/z (FAB^-): 181.1 [$\text{C}_2\text{HN}_{10}\text{O}^-$]; EA ($\text{C}_4\text{H}_{18}\text{N}_{20}\text{O}_2$, 378.32) calcd: N 74.05, C 12.70, H 4.80; found: N 73.96, C 13.48, H 4.60%; impact sensitivity: 15 J; friction sensitivity: 324 N; ESD: 0.5 J (at grain size 100–500 μm).

Bis-triaminoguanidinium 5,5'-azoxybistetrazolate (6). Sodium 5,5'-azoxybistetrazolate (0.650 g, 2.06 mmol, 1.00 equiv.) and triaminoguanidinium chloride (0.580 g, 4.13 mmol, 2.00 equiv.) were each dissolved in just enough boiling water, combined and brought to the boil. The crude product precipitated during night and was then filtered and washed with a few drops of ice water and ethanol. Triaminoguanidinium 5,5'-azoxybistetrazolate (0.611 g, 1.57 mmol, 76%) was obtained as light yellow thin needles.

DSC (T_{onset} , 5 °C min^{-1}): 190 °C (dec.); IR (KBr, cm^{-1}): $\tilde{\nu}$ = 3320 (m), 3211 (s), 3030 (m); 2868 (m), 1685 (s), 1503 (m), 1437 (s), 1394 (s), 1369 (m); 1277 (w), 1201 (w), 1129 (w), 1071 (w), 1035 (w), 952 (w), 915 (w), 763 (w), 608 (w), 519 (w), 401 (w), 336 (w); Raman (1064 nm, 300 mW, 25 °C, cm^{-1}): $\tilde{\nu}$ = 3337 (2), 3240 (3), 1681 (2), 1531 (6), 1494 (48), 1474 (18), 1434 (101), 1396 (37), 1371 (42), 1362 (65), 1277 (5), 1197 (10), 1162 (3), 1079 (27), 1063 (16), 1047 (81), 919 (5), 885 (6), 641 (1), 402 (5), 246 (5), 141 (12), 93 (23); ^1H NMR (d_6 -DMSO, 25 °C, ppm): δ = 8.60 (s, NH), 4.51 (s, NH_2); ^{13}C NMR (d_6 -DMSO, 25 °C, ppm): δ = 168.5 (CN_4), 164.0 (CN_4), 159.6 ($\text{C}(\text{NHNH}_2)_3^+$); m/z (FAB^+): 105.1 [CH_9N_6^+]; m/z (FAB^-): 181.1 [$\text{C}_2\text{HN}_{10}\text{O}^-$]; EA ($\text{C}_4\text{H}_{18}\text{N}_{22}\text{O}$, 390.2) calcd: N 78.94, C 12.31, H 4.65; found: N 76.16, C 13.17, H 4.80%; impact sensitivity: 4 J; friction sensitivity: 120 N; ESD: 90 mJ (at grain size 100–500 μm).

Bis-diaminouronium 5,5'-azoxybistetrazolate (7a). Barium 5,5'-azoxybistetrazolate pentahydrate (2.04 g, 5.00 mmol, 1.00 equiv.) and diaminouronium sulphate (0.940 g, 5.00 mmol, 1.00 equiv.) were both dissolved in boiling water (30 mL each) as well. The two solutions were combined and diaminouraea (0.433 g, 5.00 mmol, 1.00 equiv.) was added. After gas evolution stopped and the mixture was cooled down, the precipitated barium sulphate was filtered off over diatomaceous earth and the filtrate was left to crystallize under a slight nitrogen stream. Bis-diaminouronium 5,5'-azoxybistetrazolate (1.23 g, 3.40 mmol, 68%) was obtained as a light yellow solid. Recrystallization from ethanol–water however afforded diaminouronium 5,5'-azoxybistetrazolate tetrahydrate (7).

DSC (T_{onset} , 5 °C min^{-1}): 160 °C (dec.); IR (KBr, cm^{-1}): $\tilde{\nu}$ = 3346 (vs), 3166 (s), 2654 (m), 1701 (vs), 1627 (m), 1527 (m), 1447 (m), 1403 (m), 1348 (s), 1263 (w), 1189 (s), 1155 (w), 1106 (vw), 1039 (vw), 967 (w), 907 (vw), 765 (m), 730 (vw), 637 (vw), 571 (w), 549 (w); Raman (1064 nm, 300 mW, 25 °C, cm^{-1}): $\tilde{\nu}$ = 3343 (1), 1697 (2), 1601 (2), 1582 (2), 1530 (6), 1493 (20), 1476 (27), 1453 (81), 1402 (52), 1376 (73), 1281 (8), 1191 (4), 1176 (4), 1157 (3), 1139 (3), 1138 (3), 1076 (101), 1059 (53), 969 (3), 944 (2), 915 (3), 766 (3), 746 (1), 723 (1), 582 (2), 180 (6), 405 (2), 371 (1), 285 (1), 180 (6), 120 (29), 89 (17), 66 (12); ^1H NMR (d_6 -DMSO, 25 °C, ppm): δ = 7.82 (s, br), 6.20 (s, br); ^{13}C NMR (d_6 -DMSO, 25 °C, ppm): δ = 168.3 (CN_4), 164.0 (CN_4), 160.5 ($\text{C}=\text{O}$); m/z (FAB^+): 90.1 [$\text{CH}_7\text{N}_4\text{O}^+$]; m/z (FAB^-): 181.1 [$\text{C}_2\text{HN}_{10}\text{O}^-$]; EA ($\text{C}_4\text{H}_{14}\text{N}_{18}\text{O}_3$, 362.15) calcd: N 69.59, C 13.26, H 3.90; found: N 68.54, C 13.69, H 3.76%; impact sensitivity: 3.5 J; friction sensitivity: 240 N; ESD: 0.5 J (at grain size <100 μm).

Acknowledgements

Financial support of this work by the Ludwig-Maximilian University of Munich (LMU), the U.S. Army Research Laboratory (ARL) under grant no. W911NF-09-2-0018, the Armament Research, Development and Engineering Center (ARDEC) under grant no. R&D 1558-TA-01, and the Office of Naval Research (ONR) under grant nos. ONR.N00014-10-1-0535 and ONR.N00014-12-1-0538 is gratefully acknowledged. The authors acknowledge collaborations with Dr Mila Krupka (OZM Research, Czech Republic) in the development of new testing and evaluation methods for energetic materials and with Dr Muhamed Suceca (Brodarski Institute, Croatia) in the development of new computational codes to predict the detonation and propulsion parameters of novel explosives. We are indebted to and thank Drs Betsy M. Rice and Brad Forch (ARL, Aberdeen, Proving Ground, MD). Last but not least the authors thank Mr St. Huber for sensitivity measurements.

Notes and references

- 1 J. Thiele, *Justus Liebigs Ann. Chem.*, 1989, **303**, 57–75.
- 2 (a) M. Tremblay, *Can. J. Chem.*, 1965, **43**, 1230; (b) M. A. Hiskey, N. Goldman and J. R. Stine, *J. Energ. Mater.*, 1998, **16**, 119; (c) M. A. Hiskey, A. Hammerl, G. Holl, T. M. Klapötke, K. Polborn, J. Stierstorfer and J. J. Weigand, *Chem. Mater.*, 2005, **17**, 3784–3793; (d) B. C. Tappan, A. N. Ali, S. F. Son and T. B. Brill, *Propellants, Explos., Pyrotech.*, 2006, **31**, 163–168.

- 3 C. M. Michienzi, C. J. Campagnuolo, E. G. Tersine and C. D. Knott, NDIA IM/EM Symposium, October 11–14, 2010, Munich, Germany, <http://www.imemg.org>
- 4 G.-H. Tao, B. Twamley and J. M. Shreeve, *Inorg. Chem.*, 2009, **48**, 9918–9923.
- 5 G. Steinhäuser, G. Giester, N. Leopold, C. Wagner and M. Villa, *Helv. Chim. Acta*, 2009, **92**, 2038–2051.
- 6 G. Laus, V. Kahlenberg, K. Wurst, H. Schottenberger, N. Fischer, J. Stierstorfer and T. M. Klapötke, *Crystals*, 2012, **2**, 127–136.
- 7 A. Hammerl, G. Holl, M. Kaiser, T. M. Klapötke, P. Mayer, H. Nöth, H. Piotrowski and M. Warchhold, *Eur. J. Inorg. Chem.*, 2002, **4**, 834–845.
- 8 T. M. Klapötke, D. Piercey and J. Stierstorfer, *Chem.–Eur. J.*, 2011, **17**, 5775–5792.
- 9 E. Bamberger, *Chem. Ber.*, 1894, **27**, 1548–1557.
- 10 Crystallographic data for the structure(s) have been deposited with the Cambridge Crystallographic Data Centre.
- 11 A. Hammerl, G. Holl, M. Kaiser, T. M. Klapötke, P. Mayer, H. Piotrowski and M. Vogt, *Z. Naturforsch., B: Chem. Sci.*, 2001, **56B**, 847.
- 12 A. F. Holleman and E. Wiberg, *Lehrbuch der anorganischen Chemie*, de Gruyter, Berlin, 2007, 102nd edn, 2006.
- 13 G. Bentivoglio, G. Laus, V. Kahlenberg, G. Nauer and H. Schottenberger, *Z. Kristallogr. - New Cryst. Struct.*, 2008, **223**, 425–426.
- 14 M. Göbel, K. Karaghiosoff, T. M. Klapötke, D. G. Piercey and J. Stierstorfer, *J. Am. Chem. Soc.*, 2010, **132**, 17216–17226.
- 15 G. Singh, R. Prajapati and R. Frohlich, *J. Hazard. Mater.*, 2005, **118**, 75.
- 16 T. M. Klapötke and C. M. Sabaté, *Chem. Mater.*, 2008, **20**, 1750–1763.
- 17 NATO standardization agreement (STANAG) on explosives, impact sensitivity tests, no. 4489, 1st ed., Sept. 17, 1999.
- 18 NATO standardization agreement (STANAG) on explosive, friction sensitivity tests, no. 4487, 1st ed., Aug. 22, 2002.
- 19 NATO standardization agreement (STANAG) on explosive, electrostatic discharge sensitivity tests, no. 4490, 1st ed., Feb. 19, 2001.
- 20 WIWEB-Standardarbeitsanweisung 4-5.1.02, Ermittlung der Explosionsgefährlichkeit, hier der Schlagempfindlichkeit mit dem Fallhammer, Nov. 8, 2002.
- 21 WIWEB-Standardarbeitsanweisung 4-5.1.03, Ermittlung der Explosionsgefährlichkeit oder der Reibeempfindlichkeit mit dem Reibeapparat, Nov. 8, 2002.
- 22 <http://www.bam.de>
- 23 Impact: insensitive > 40 J, less sensitive ≥ 35 J, sensitive ≥ 4 J, very sensitive ≤ 3 J; friction: insensitive > 360 N, less sensitive = 360 N, sensitive < 360 N a. > 80 N, very sensitive ≤ 80 N, extreme sensitive ≤ 10 N; According to the UN Recommendations on the Transport of Dangerous Goods (+) indicates: not safe for transport.
- 24 (a) REICHEL & PARTNER GmbH, <http://www.reichelt-partner.de>; (b) Test methods according to the UN Recommendations on the Transport of Dangerous Goods, Manual of Test and Criteria, fourth revised edition, United Nations Publication, New York and Geneva, 2003, ISBN 92-1-139087-7, Sales No. E.03.VIII.2; 13.4.2 Test 3(a) (ii) BAM Fallhammer.
- 25 (a) <http://www.ozm.cz/testing-instruments/small-scale-electrostatic-discharge-tester.htm>; (b) V. Pelikán, OZM research, Czech Republic, private communication.
- 26 (a) J. W. Ochterski, G. A. Petersson and J. A. Montgomery Jr., *J. Chem. Phys.*, 1996, **104**, 2598; (b) J. A. Montgomery Jr., M. J. Frisch, J. W. Ochterski and G. A. Petersson, *J. Chem. Phys.*, 2000, **112**, 6532.
- 27 (a) L. A. Curtiss, K. Raghavachari, P. C. Redfern and J. A. Pople, *J. Chem. Phys.*, 1997, **106**, 1063; (b) E. F. C. Byrd and B. M. Rice, *J. Phys. Chem. A*, 2006, **110**, 1005–1013; (c) B. M. Rice, S. V. Pai and J. Hare, *Combust. Flame*, 1999, **118**, 445–458.
- 28 (a) H. D. B. Jenkins, H. K. Roobottom, J. Passmore and L. Glasser, *Inorg. Chem.*, 1999, **38**, 3609–3620; (b) H. D. B. Jenkins, D. Tudela and L. Glasser, *Inorg. Chem.*, 2002, **41**, 2364–2367.
- 29 M. Sućeska, *EXPLO5.4 program*, Zagreb, Croatia, 2010.
- 30 M. Sućeska, *Propellants, Explos., Pyrotech.*, 1991, **16**, 197–202.
- 31 (a) M. Sućeska, *Mater. Sci. Forum*, 2004, **465–466**, 325–330; (b) M. Sućeska, *Propellants, Explos., Pyrotech.*, 1999, **24**, 280–285; (c) M. L. Hobbs and M. R. Baer, Proceedings of the 10th Symp. (International) on Detonation, ONR 33395-12, Boston, MA, July 12–16, 1993, 409.
- 32 R. Mayer, J. Köhler and A. Homburg, *Explosives*, Wiley VCH, Weinheim, 5th edn, 2002.
- 33 <http://www.linseis.com>
- 34 (a) M. Sućeska and M. Test, *Methods for Explosives*, Springer, New York, 1995; p 21 (impact), p 27 (friction); (b) www.bam.de; (c) NATO standardization agreement (STANAG) on explosives, *impact sensitivity tests*, no. 4489, Ed. 1, Sept. 17, 1999; (d) WIWEB-Standardarbeitsanweisung 4-5.1.02, Ermittlung der Explosionsgefährlichkeit, hier der Schlagempfindlichkeit mit dem Fallhammer, Nov. 8, 2002; (e) <http://www.reichel-partner.de>; (f) NATO standardization agreement (STANAG) on explosives, *friction sensitivity tests*, no. 4487, Ed. 1, Aug. 22, 2002.
- 35 <http://www.ozm.cz/testinginstruments/small-scale-electrostatic-discharge-tester.htm>
- 36 M. J. Frisch, G. W. Trucks, H. B. Schlegel, G. E. Scuseria, M. A. Robb, J. R. Cheeseman, G. Scalmani, V. Barone, B. Mennucci, G. A. Petersson, H. Nakatsuji, M. Caricato, X. Li, H. P. Hratchian, A. F. Izmaylov, J. Bloino, G. Zheng, J. L. Sonnenberg, M. Hada, M. Ehara, K. Toyota, R. Fukuda, J. Hasegawa, M. Ishida, T. Nakajima, Y. Honda, O. Kitao, H. Nakai, T. Vreven, J. A. Montgomery, Jr., J. E. Peralta, F. Ogliaro, M. Bearpark, J. J. Heyd, E. Brothers, K. N. Kudin, V. N. Staroverov, R. Kobayashi, J. Normand, K. Raghavachari, A. Rendell, J. C. Burant, S. S. Iyengar, J. Tomasi, M. Cossi, N. Rega, J. M. Millam, M. Klene, J. E. Knox, J. B. Cross, V. Bakken, C. Adamo, J. Jaramillo, R. Gomperts, R. E. Stratmann, O. Yazyev, A. J. Austin, R. Cammi, C. Pomelli, J. W. Ochterski, R. L. Martin, K. Morokuma, V. G. Zakrzewski, G. A. Voth, P. Salvador, J. J. Dannenberg, S. Dapprich, A. D. Daniels, Ö. Farkas, J. B. Foresman, J. V. Ortiz, J. Cioslowski and D. J. Fox, *GAUSSIAN 09 (Revision A.02)*, Gaussian, Inc., Wallingford CT, 2009.
- 37 CrysAlisPro, Agilent Technologies, Version 1.171.35.11, 2011.
- 38 G. M. Sheldrick, *SHELXS-97, Program for Crystal Structure Solution*, Universität Göttingen, 1997.
- 39 A. Altomare, G. Cascarano, C. Giacovazzo and A. Guagliardi, *J. Appl. Crystallogr.*, 1993, **26**, 343.
- 40 G. M. Sheldrick, *Shelxl-97, Program for the Refinement of Crystal Structures*, University of Göttingen, Germany, 1994.
- 41 A. L. Spek and A. Platon, *Multipurpose Crystallographic Tool*, Utrecht University, Utrecht, The Netherlands, 1999.
- 42 L. Farrugia, *J. Appl. Crystallogr.*, 1999, **32**, 837–838.
- 43 Empirical absorption correction using spherical harmonics, implemented in SCALE3 ABSPACK scaling algorithm (CrysAlisPro Oxford Diffraction Ltd., Version 171.33.41, 2009).

Pushing the limits of energetic materials – the synthesis and characterization of dihydroxylammonium 5,5'-bistetrazole-1,1'-diolate†

Niko Fischer, Dennis Fischer, Thomas M. Klapötke,* Davin G. Piercey and Jörg Stierstorfer

Received 6th June 2012, Accepted 9th August 2012

DOI: 10.1039/c2jm33646d

The safe preparation and characterization (XRD, NMR and vibrational spectroscopy, DSC, mass spectrometry, sensitivities) of a new explosive dihydroxylammonium 5,5'-bistetrazole-1,1'-diolate (TKX-50) that outperforms all other commonly used explosive materials is detailed. While much publicized high-performing explosives, such as octanitrocubane and CL-20, have been at the forefront of public awareness, this compound differs in that it is simple and cheap to prepare from commonly available chemicals. TKX-50 expands upon the newly exploited field of tetrazole oxide chemistry to produce a material that not only is easily prepared and exceedingly powerful, but also possesses the required thermal insensitivity, low toxicity, and safety of handling to replace the most commonly used military explosive, RDX (1,3,5-trinitro-1,3,5-triazacyclohexane). In addition, the crystal structures of the intermediates 5,5'-bistetrazole-1,1'-diol dihydrate, 5,5'-bistetrazole-1,1'-diol dimethanolate and dimethylammonium 5,5'-bistetrazole-1,1'-diolate were determined and presented.

Introduction

The rational design of new energetic materials is a rapidly exploding field^{1–7} with a long traditional rooting in the chemical sciences^{8,9} and a complexity that rivals that of the drug design. While the field has come a long way since the days of Liebig, Berzelius and Gay-Lussac, and the concept of isomerism being determined from explosive silver fulminate and non-explosive silver cyanate,¹⁰ current work in this field still follows the trend of its historic beginnings; that of simultaneous academic and practical interest and advances. In the quest for higher-performing, safer, cheaper, greener, explosive materials, energetic materials chemistry must push the boundaries of the energy

capacity of compounds, which requires new classes of compounds,^{2,11} new synthetic strategies,¹² and advanced computational techniques. For example, the high nitrogen content of many advanced explosives has led to the preparation of new nitrogen–nitrogen bond forming reactions¹² and new heterocyclic systems¹³ in the quest for even higher performance.

In both civilian and military circles, the highest performing explosives make use of the same strategy: cyclic and caged nitramines. Belonging to the oldest class of explosives, those derive their energy from the oxidation of a carbon backbone by containing the oxidizer in the same molecule; RDX (1,3,5-trinitro-1,3,5-triazacyclohexane), HMX (1,3,5,7-tetranitro-1,3,5,7-tetraazacyclooctane) and CL-20 (2,4,6,8,10,12-hexanitro-2,4,6,8,10,12-hexaza-isowurtzitane) all have fatal flaws that mandate replacement with modern explosives. Advanced energetic strategies allow for retention or improvement of the explosive performance, while avoiding the multitude of downsides present in these compounds: toxicity to living organisms (all), difficult and expensive synthesis (HMX, CL-20), high sensitivity to mechanical stimuli (all), and spontaneous changing of properties (CL-20).² New strategies in the design of energetic materials include those with ring or cage strain, high heat of formation compounds, and compounds containing strong dipoles or zwitterionic structures.¹⁴

Unfortunately, the known materials with the highest detonation energy are often highly sensitive due to their unprecedented energy content,⁵ and are made *via* long and expensive pathways with a multitude of steps, making industrial scale-up infeasible. For example, both DDF (dinitroazofuroxane) and ONC (octanitrocubane) possess detonation velocities at the limit of known performances (around 10 000 m s^{−1}), however both are highly

Energetic Materials Research, Department of Chemistry, University of Munich (LMU), Butenandstr. 5-13, D-81377, Germany. E-mail: tmk@cup.uni-muenchen.de; Fax: +49 (0)89 2180 77492; Tel: +49 (0)89 2180 77491

† Electronic supplementary information (ESI) available: 1. Materials and methods; 1.1. NMR spectroscopy; 1.2. vibrational spectroscopy; 1.3. mass spectrometry and elemental analysis; 1.4. differential scanning calorimetry; 1.5. sensitivity testing; 2. experimental work; 2.1. synthesis *via* oxidation of 5,5'-bistetrazole with potassium peroxymonosulfate; 2.2. synthesis *via* cyclization of diazidoglyoxime; 2.3. safer synthesis including a multi-step one pot reaction; 3. X-ray diffraction; 3.1. instrument and refinement software; 3.2. crystallographic data and refinement parameters; 3.3. bond lengths, bond angles and hydrogen bonding of TKX-50; 3.4. crystal structures of 5,5'-bistetrazole-1,1'-diol; 3.5. crystal structure of dimethylammonium 5,5'-bistetrazole-1,1'-diolate; 4. explosive performance; 4.1. heat of formation calculations; 4.2. small scale shock reactivity test; 4.3. flame test; 4.4. hot plate test; 5. toxicity assessment; 6. Fast Cook-Off test. cif files. CCDC 872230, 872231, 872232, 884559, 884560 and 884561. For ESI and crystallographic data in CIF or other electronic format see DOI: 10.1039/c2jm33646d

sensitive and have more than 10 synthetic steps with exotic, expensive reagents used.¹⁵

A very promising explosophoric moiety in the design of new energetic materials is the tetrazole ring; the carbon on position 5 of the ring allows the facile attachment of various substituents for energetic tailorability, and the high nitrogen content and heat of formation of the heterocycle lead to high energetic performances. In order to improve the energetic properties of tetrazoles, several recently published studies showed that introduction of N-oxides yields compounds with even higher densities and stabilities, lower sensitivities and better oxygen balances.^{2,7,11} Combining these principles with practical considerations in mind, a simple and secure synthetic pathway to the high performing energetic material dihydroxylammonium 5,5'-bistetrazole-1,1'-diolate (TKX-50) was devised.

Results and discussion

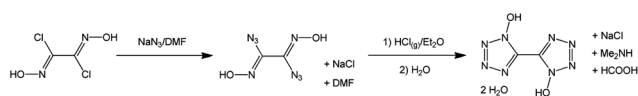
Synthesis (simple and scalable)

There are two major routes (A and B) to the 5,5'-bistetrazole-1,1'-diol (1,1-BTO) moiety (Scheme 1). The first (A) of which, the oxidation of the parent heterocycle with aqueous potassium peroxydisulfate only leads to 1,1-BTO in poor yield (11%). The oxidation of the 5,5'-bistetrazolate anion with peroxydisulfate was carried out in a manner similar to that we have previously reported for 5-nitro- and 5-azidotetrazoles.^{2,7} Unfortunately, this reaction was found to produce the 2,2' isomer as the major product, with only traces of the 1,1' isomer which crystallized upon adding aqueous hydroxylamine.

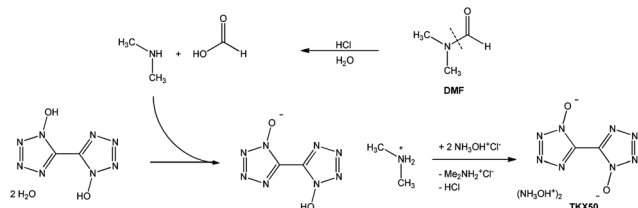
After discovering the outstanding characteristics of TKX-50 as a high explosive, a different route to the precursor 5,5'-bistetrazole-1,1'-diol was necessitated. Tselinskii *et al.*¹⁶ reported on the synthesis of the mentioned precursor 1,1-BTO from the cyclization of diazidoglyoxime under acidic conditions for the first time. Diazidoglyoxime is prepared from dichloroglyoxime in a chloro-azido exchange reaction in DMF with more than 80 % yield, whereas dichloroglyoxime is prepared from glyoxime *via* chlorination in ethanol in high yield.

The problematic step here is the isolation of the highly friction and impact sensitive compound diazidoglyoxime, mandating a revised procedure before industrial-scaled use. The problem was overcome by a procedure combining the formation and cyclization of diazidoglyoxime in one step in solution. Starting from commercially available glyoxal, the reaction process was transformed into a five step, four pot synthesis to isolate TKX-50.

The prepared solution of diazidoglyoxime in DMF (impure with sodium chloride) is directly poured into diethylether and



Scheme 2 Synthesis of 5,5'-bistetrazole-1,1'-diol in a one pot reaction from dichloroglyoxime.



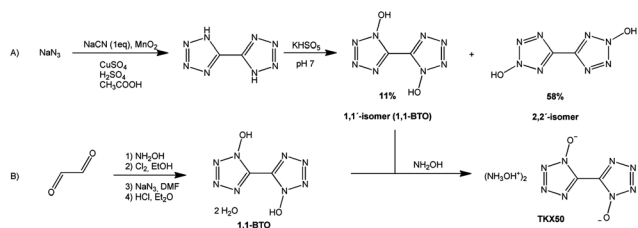
Scheme 3 Synthesis of TKX-50 from 5,5'-bistetrazole-1,1'-diol isolated from the one pot reaction described in Scheme 2. DMF is cleaved under the acidic conditions to form the dimethylammonium salt of 5,5'-bistetrazole-1,1'-diol, which is then converted into TKX-50.

HCl gas is bubbled through (Scheme 2). After cyclization of the azidooxime in the acidic medium the dimethylammonium salt of 5,5'-bistetrazole-1,1'-diol is formed by a reaction with dimethylamine (formed by hydrolysis of DMF). After isolation and recrystallization of dimethylammonium 5,5'-bistetrazole-1,1'-diolate, it is dissolved in a sufficient amount of boiling water and combined with a solution of hydroxylammonium chloride, from which TKX-50 crystallizes first (Scheme 3).

An alternative procedure using NMP (*N*-methyl-2-pyrrolidone) instead of DMF for the chloro-azido exchange, followed by the same treatment, leads to the free acid 5,5'-bistetrazole-1,1'-diol which is then isolated as its sodium salt tetrahydrate upon the addition of aqueous sodium hydroxide and subsequently treated with hydroxylammonium chloride in water. Starting from dichloroglyoxime, the overall yields of both procedures are very high with 72 % (DMF-route) and 85 % (NMP-route) for the synthesis of TKX-50. For a detailed description of all synthetic routes yielding TKX-50 and for all analytical data please refer to the ESI.†

X-ray diffraction

The crystal structure of TKX-50 was determined at three temperatures (100 K, 173 K, 298 K) in order to detect potential low temperature phase transitions and obtain precise densities (for explosive performance calculations). In addition the crystal structures of the intermediates 5,5'-bistetrazole-1,1'-diol dihydrate (recryst. from either water, MeCN, EtOH or glacial acetic acid), 5,5'-bistetrazole-1,1'-diol dimethanolate (recryst. from methanol) and dimethylammonium 5,5'-bistetrazole-1,1'-diolate (crystallized from H₂O) were determined and are presented in the ESI.† Detailed crystallographic data and parameters of the measurements and solutions are given in Table S1.† The lack of observed phase transitions between 100 K and 298 K is advantageous for energetic materials use as constant properties upon temperature changes result. The density follows the expected trend of decreasing with increased temperature (100 K: 1.918 g cm⁻³ > 173 K: 1.915 g cm⁻³ > 298 K: 1.877 g cm⁻³). TKX-50 crystallizes in the monoclinic space group *P*2₁/*c* with two anion-cation moieties in the unit cell. The molecular moiety of



Scheme 1 Synthesis of TKX-50 *via* oxidation of 5,5'-bistetrazole (A) and *via* cyclization of diazidoglyoxime (B).

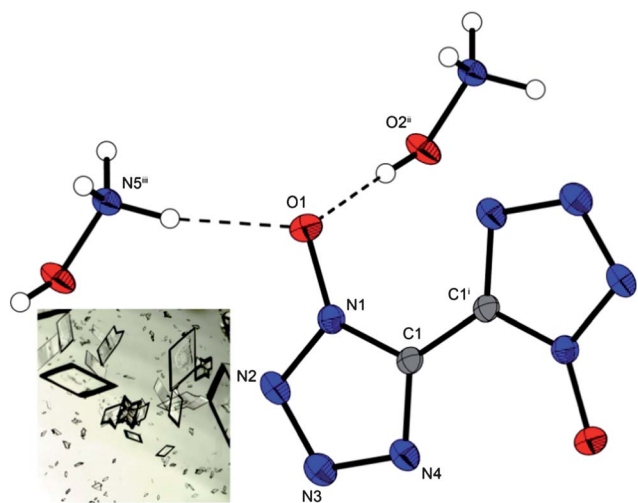


Fig. 1 Representation of the solid state molecular structure of TKX-50 at 100 K. Thermal ellipsoids are drawn at the 50% probability level; symmetry codes: (i) $2 - x, -y, 2 - z$; (ii) $x, 0.5 - y, -0.5 + z$; and (iii) $-1 + x, 0.5 - y, -0.5 + z$.

TKX-50 at 100 K is depicted in Fig. S1.† Its density of 1.918 g cm^{-3} is significantly higher than that of non-oxide dihydroxylammonium 5,5'-bistetrazolate (1.742 g cm^{-3}) recently published.¹⁷ The reason for this may be the strong hydrogen bond network (involving all four hydrogen atoms of the hydroxylammonium cations) (Fig. 1).

Energetic performance

The performance data (Table 1) were calculated with the computer code EXPLO5.05 (latest version). EXPLO5.05 is based on the chemical equilibrium, a steady state model of detonation.

It uses Becker–Kistiakowsky–Wilson's equation of state (BKW EOS) for gaseous detonation products and Cowan–Fickett's equation of state for solid carbon (see ESI†). The input is based on the sum formula, calculated heats of formation (see ESI†) and the maximum densities according to their crystal structures (ESI, Table S1†).

With respect to the detonation velocity (Table 1), TKX-50 shows higher calculated values than all other mass-produced and used explosives like 2,4,6-trinitrotoluene (TNT), RDX, HMX and CL-20. Looking at the detonation pressure, TKX-50 exceeds the values calculated for TNT and RDX and is comparable to HMX, but is slightly lower than for CL-20. Also in terms of potential use as a propellant mixture ingredient TKX-50 shows promising values due to its high nitrogen content. The calculated specific impulse using 60 bar isobaric rocket conditions is 261 seconds, which is slightly better than those of the other compounds in Table 1.

To assess the explosive performance of TKX-50 on a small laboratory scale, a small-scale reactivity test (SSRT) was carried out (see ESI†) in comparison to CL-20 and RDX. Here, a defined volume of the explosive is pressed into a perforated steel block, which is topped with a commercially available detonator (Orica, DYNADET-C2-0ms). Initiation of the tested explosive results in denting a separate aluminium block, which is placed right underneath the steel block (Fig. 2). From measuring the volumes of the dents ($\text{CL-20} \geq \text{TKX-50} \gg \text{RDX}$) (Table 2 in the ESI†), it can be concluded that the small scale explosive performance of TKX-50 exceeds the performance of commonly used RDX and is comparable to that of CL-20.

The performance and safety characteristics for shipping of an explosive can be related to the data obtained from the Koenen test.^{18,19} The explosive is placed in an open-ended, flanged steel tube, which is locked up with a closing plate with variable orifice (0–10 mm), through which gaseous decomposition products are

Table 1 Energetic properties and detonation parameters of prominent high explosives in comparison to TKX-50

	2,4,6-TNT	RDX	β -HMX	ε -CL-20	TKX-50
Formula	$\text{C}_7\text{H}_5\text{N}_3\text{O}_6$	$\text{C}_3\text{H}_6\text{N}_6\text{O}_6$	$\text{C}_4\text{H}_8\text{N}_8\text{O}_8$	$\text{C}_6\text{H}_6\text{N}_{12}\text{O}_{12}$	$\text{C}_2\text{H}_8\text{N}_{10}\text{O}_4$
Molecular mass [g mol^{-1}]	227.13	222.12	296.16	438.19	236.15
IS [J] ^a	15 ²¹	7.5 ²¹	7 ²¹	4 ²¹	20
FS [N] ^b	353	120 ²¹	112 ²¹	48 ²¹	120
ESD-test [J] ^c	—	0.20	0.20	0.13	0.10
N [%] ^d	18.50	37.84	37.84	38.3	59.3
Q [%] ^e	−73.96	−21.61	−21.61	−10.95	−27.10
T_m [$^\circ\text{C}$] ^f	81	205 ²²	275 ²⁴	—	—
T_{dec} [$^\circ\text{C}$] ^f	290	210 ²⁴	279 ²⁴	215 ²³	221
Density [g cm^{-3}] ^g	1.713 (100 K) ²⁴ 1.648 (298 K) ²⁵	1.858 (90 K) ²⁶ 1.806 (298 K) ²⁷	1.944 (100 K) ²⁸ 1.904 (298 K) ²⁸	2.083 (100 K) ²⁹ 2.035 (298 K) ²⁹	1.918 (100 K) ³⁰ 1.877 (298 K) ³⁰
Theor. $\Delta_f H^\circ$ [kJ mol^{-1}] ^h	−55.5	86.3	116.1	365.4	446.6
Theor. $\Delta_f U^\circ$ [kJ kg^{-1}] ⁱ	−168.0	489.0	492.5	918.7	2006.4
<i>EXPLO5.05 values</i>					
− $\Delta_f U^\circ$ [kJ kg^{-1}] ^j	5258	6190	6185	6406	6025
T_E [K] ^k	3663	4232	4185	4616	3954
p_{C-J} [kbar] ^l	235	380	415	467	424
D [m s^{-1}] ^m	7459	8983	9221	9455	9698
Gas vol. [L kg^{-1}] ⁿ	569	734	729	666	846
I_S [s] ^o	205	258	258	251	261

^a Impact sensitivity (BAM drophammer (1 of 6)). ^b Friction sensitivity (BAM friction tester (1 of 6)). ^c Electrostatic discharge device (OZM research). ^d Nitrogen content. ^e Oxygen balance ($Q = (xO - 2yC - 1/2zH)M/1600$). ^f Decomposition temperature from DSC ($\beta = 5^\circ\text{C min}^{-1}$). ^g From X-ray diffraction. ^h Calculated (CBS-4M method) enthalpy of formation. ⁱ Calculated energy of formation. ^j Energy of explosion. ^k Explosion temperature. ^l Detonation pressure. ^m Detonation velocity. ⁿ Volume of detonation gases (assuming only gaseous products). ^o Specific impulse using isobaric (60 bar) conditions.

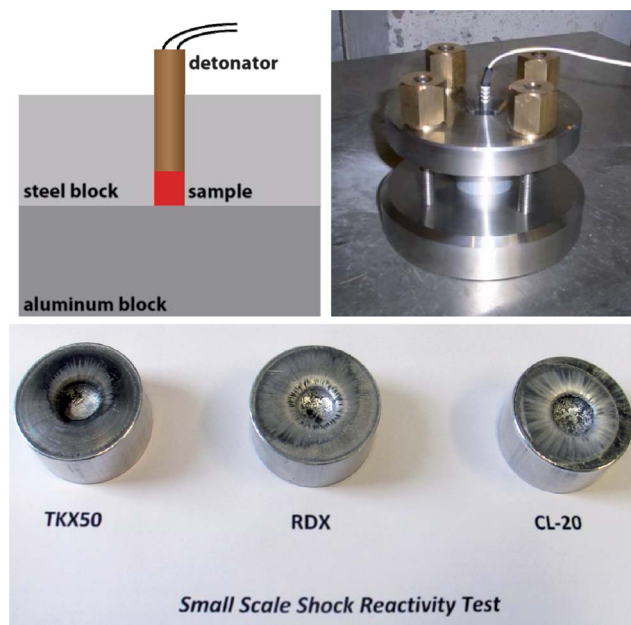


Fig. 2 Small-scale reactivity test of TKX-50, RDX and CL-20. Above pictures: test setup for the SSRT. Below: dented aluminium blocks after initiation of the explosive with a commercial detonator.

vented. A defined volume of 25 mL of the compound is loaded into the flanged steel tube and a threaded collar is slipped onto the tube from below. The closing plate is fitted over the flanged tube and secured with a nut. The decomposition is initiated *via* thermal ignition using four Bunsen burners, which are ignited simultaneously. The test is completed when either rupture of the tube or no reaction is observed after heating the tube for a minimal time period of at least 5 min. In the case of the tube's rupture, the fragments are collected and weighed. The reaction is evaluated as an explosion if the tube is destroyed into three or more pieces. The Koenen test was performed with 23.0 g of TKX-50 using a closing plate with an orifice of 10 mm and caused the rupture of the steel tube into approximately 100 pieces, the size of which reached down to smaller than 1 mm from 40 mm (Fig. 3).

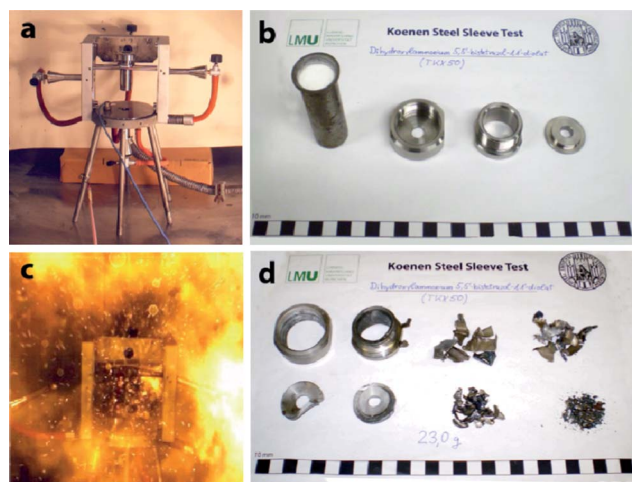


Fig. 3 a) Koenen test experimental setup. (b) Parts of the Koenen steel sleeve before and (d) after the test. (c) Moment of detonation.

TNT destroys the steel tube up to an orifice width of 6 mm, RDX even up to 8 mm.²⁰ In order to get an “Interim Hazard Classification” also a “Fast Cook-Off test” (UN test 3d) was performed in which TKX-50 underwent controlled deflagration (no explosion occurred).

High safety – low sensitivity

Impact sensitivity is a high priority in explosive devices used in the military due to the range of stresses devices may be exposed to. The impact sensitivity of TKX-50 is 20 J which is much lower than those for RDX, HMX and CL-20, which range from 4 to 7.5 J, and all three of which need desensitizing components added for practical use. The low impact sensitivity of TKX-50 shows that it can be used without desensitization.

Friction sensitivity is more important in the manufacturing context, where TKX-50 with 120 N is of comparable or lower sensitivity than any of RDX, HMX or CL-20, increasing the margin of safety in the industrial context. Both the impact and friction sensitivities of TKX-50 as compared to 2,4,6-trinitrotoluene (TNT), RDX, HMX and CL-20 are presented in Table 1.

The human body can generate up to 25 mJ of static electricity, which can easily set off the most sensitive explosives such as lead azide or silver fulminate. TKX-50 has an electrostatic sensitivity of 0.100 J, which is far higher than the human body can generate, allowing a comparable margin of safety when handling, comparable to RDX or HMX.

Thermal stability is important for any explosive in practical use as demanding military requirements need explosives that can withstand high temperatures. For example, a munition sitting in the desert can exceed 100 °C and for general use a component explosive must be stable above 200 °C. TKX-50 with a decomposition onset of 222 °C easily surpasses this requirement (Fig. 4, inset). This stability has been confirmed using a long-term stability test, where the sample is heated in an open glass vessel to a temperature of 75 °C over 48 h to ensure safe handling of the material even at elevated temperatures (Fig. 4, outer curve). The lack of exothermic or endothermic events in the sample temperature or heat flow curve implies that the compound is stable.

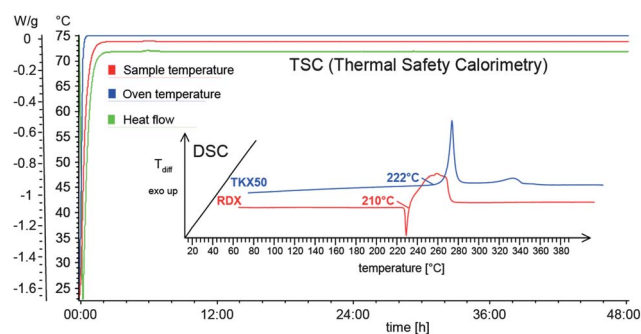


Fig. 4 Outer curve: long term stability (TSC plot) of TKX-50 at a temperature of 75 °C over a period of 48 h. Inner plot: thermal stability of TKX-50 and RDX shown in the DSC plot (heating rate 5 °C min⁻¹).

Toxicity – environmentally friendly

One of the major aims in our search for new “green” energetic materials is the low toxicity of the newly investigated compound

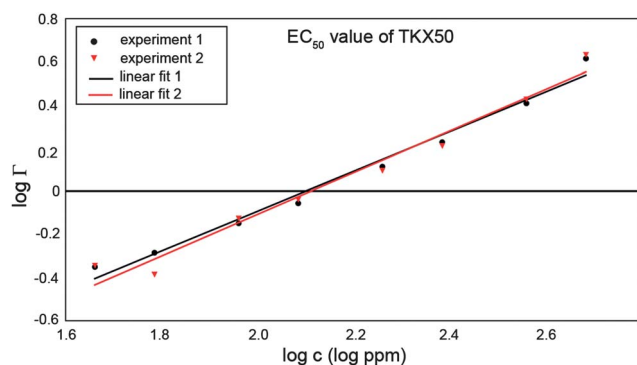


Fig. 5 Toxicity assessment of TKX-50 using a luminescent bacteria inhibition test. Plot of $\log I$ against $\log c$ for determination of the EC_{50} value.

itself, and of its degradation and decomposition products. In recent times the toxicity of energetic materials is a growing concern due to new understandings of the fate of explosives in the environment. The nitramine content of the ubiquitous RDX as well as less used HMX and CL-20 has been shown to be toxic to vital organisms at the base of the food chain, and in addition RDX is a probable human carcinogen. To assess the toxicity of TKX-50 to aquatic life, diluted aqueous solutions of the high explosive were subjected to the luminescent marine bacterium *Vibrio fischeri* using the commercially available bioassay system LUMISTox®. *Vibrio fischeri* is a representative species for other aquatic life and therefore a useful indicator when it comes to groundwater pollution. Being the most important toxicological parameter, the EC_{50} value of the sample was determined. EC_{50} is the effective concentration of the examined compound, at which the bioluminescence of the strain *Vibrio fischeri* is decreased by 50% after a defined period of exposure as compared to the original bioluminescence of the sample before being treated with the differently diluted solutions of the test compound. For RDX we observe an EC_{50} value of 91 ppm after an incubation time of 30 minutes. The herein determined EC_{50} value of TKX-50 of 130 ppm (Fig. 5 and ESI†) lies significantly above the EC_{50} value found for RDX indicating a lower toxicity to *Vibrio fischeri*, and as such, other aquatic life.

Conclusions

We have detailed the preparation of a new explosive, TKX-50 or dihydroxylammonium 5,5'-bistetrazole-1,1'-diolate. This material has exemplified the utility of the tetrazole N-oxide chemistry by providing a new explosive material that is of very high performance (as calculated and demonstrated by SSRT testing), pushing the limits towards the most powerful explosives known, and synthesized in an industrially viable process. Additionally, TKX-50 is of lower sensitivity (mechanically and thermally) than its contemporaries in currently used explosives such as RDX, HMX and CL-20, making increased margins of safety when applied in practical use and devices. Finally, we have demonstrated the lower toxicity of TKX-50 compared to the nitramine RDX, as determined by the EC_{50} value for the decrease in luminescence of *Vibrio fischeri*. All of the characteristics of TKX-50 make it appropriate and exemplary to not just fulfill the long-standing goal of a "green" RDX replacement, but also to replace it with a material of superior performance.

Acknowledgements

Financial support of this work by the Ludwig-Maximilian University of Munich (LMU), the U.S. Army Research Laboratory (ARL), the Armament Research, Development and Engineering Center (ARDEC), the Strategic Environmental Research and Development Program (SERDP) and the Office of Naval Research (ONR) is acknowledged. Furthermore, the authors acknowledge the contributions of Stefan Huber, Susanne Scheutzw, Dr Karin Lux, Sebastian Rest, Marius Reymann and Fabian Wehnkamp.

Notes and references

- 1 M. Göbel, B. H. Tchitchanov, J. S. Murray, P. Politzer and T. M. Klapötke, *Nat. Chem.*, 2009, **1**, 229–235.
- 2 M. Göbel, K. Karaghiosoff, T. M. Klapötke, D. G. Piercey and J. Stierstorfer, *J. Am. Chem. Soc.*, 2010, **132**, 17216–17226.
- 3 H. Gao and J. M. Shreeve, *Chem. Rev.*, 2011, **111**, 7377–7436.
- 4 Y.-C. Li, C. Qi, S.-H. Li, H.-J. Zhang, C.-H. Sun, Y.-Z. Yu and S.-P. Pang, *J. Am. Chem. Soc.*, 2010, **132**, 12172–12173.
- 5 T. M. Klapötke and D. G. Piercey, *Inorg. Chem.*, 2011, **50**, 2732–2734.
- 6 V. Thottempudi and J. M. Shreeve, *J. Am. Chem. Soc.*, 2011, **133**, 19982–19992.
- 7 T. M. Klapötke, D. G. Piercey and J. Stierstorfer, *Chem.–Eur. J.*, 2011, **17**, 13068–13077.
- 8 J. L. Gay-Lussac, *Ann. Chem. Phys.*, 1824, **27**, 199.
- 9 J. Berzelius, *Justus Liebigs Ann. Chem.*, 1844, **50**, 426–429.
- 10 J. L. Gay-Lussac and J. Liebig, *Kastners Archiv.*, 1824, **II**, 58–91.
- 11 A. M. Churakov and V. A. Tartakovsky, *Chem. Rev.*, 2004, **104**, 2601–2616.
- 12 A. M. Churakov, O. Y. Smirnov, S. L. Ioffe, Y. A. Strelenko and V. A. Tartakovsky, *Eur. J. Org. Chem.*, 2002, 2342–2349.
- 13 L. A. Burke and P. J. Fazen, *Int. J. Quantum Chem.*, 2009, **109**, 3613–3618.
- 14 R. A. Carboni, J. C. Kauer, J. E. Castle and H. E. Simmons, *J. Am. Chem. Soc.*, 1967, **89**, 2618–2625.
- 15 M.-X. Zhang, P. E. Eaton and R. Gilardi, *Angew. Chem., Int. Ed.*, 2000, **39**, 401–404.
- 16 I. V. Tselinskii, S. F. Mel'nikova and T. V. Romanova, *Russ. J. Org. Chem.*, 2001, **37**, 430–436.
- 17 N. Fischer, D. Izsák, T. M. Klapötke, S. Rappenglück and J. Stierstorfer, *Chem.–Eur. J.*, 2012, **18**, 4051–4062.
- 18 R. C. West and S. M. Selby, *Handbook of Chemistry and Physics*, The Chemical Rubber Co., Cleveland, 48th edn, 1967, pp. D22–D51.
- 19 V. A. Ostrovskii, M. S. Pevzner, T. P. Kofman and I. V. Tselinskii, *Targets Heterocycl. Syst.*, 1999, **3**, 467–526.
- 20 J. Köhler and R. Meyer, *Explosivstoffe*, Wiley-VCH, Weinheim, 9th edn, 1998, pp. 166–168.
- 21 R. Mayer, J. Köhler and A. Homburg, *Explosives*, Wiley-VCH, Weinheim, 5th edn, 2002.
- 22 J. P. Agrawal, *High Energy Materials*, Wiley-VCH, Weinheim, 1st edn, 2010, p. 189.
- 23 R. Turcotte, M. Vachon, Q. S. M. Kwok, R. Wang and D. E. G. Jones, *Thermochim. Acta*, 2005, **433**, 105–115.
- 24 R. M. Vrcelj, J. N. Sherwood, A. R. Kennedy, H. G. Gallagher and T. Gelbrich, *Cryst. Growth Des.*, 2003, **3**, 1027–1032.
- 25 N. I. Golovina, A. N. Titkov, A. V. Raevskii and L. O. Atovmyan, *J. Solid State Chem.*, 1994, **113**, 229–238.
- 26 P. Hakey, W. Ouellette, J. Zubieta and T. Korter, *Acta Crystallogr., Sect. E: Struct. Rep. Online*, 2008, **64**(8), o1428.
- 27 C. S. Choi and E. Prince, *Acta Crystallogr., Sect. B: Struct. Crystallogr. Cryst. Chem.*, 1972, **28**, 2857.
- 28 J. R. Deschamps, M. Frisch and D. Parrish, *J. Chem. Crystallogr.*, 2011, **41**, 966–970.
- 29 N. B. Bolotina, J. M. Hardie, R. L. Speer Jr and A. A. Pinkerton, *J. Appl. Crystallogr.*, 2004, **37**, 808–814.
- 30 X-ray density (for details see CCDC 872231 and 872232).

1-Amino-3-nitroguanidine (ANQ) in High-performance Ionic Energetic Materials

Niko Fischer, Thomas M. Klapötke and Jörg Stierstorfer

Department of Chemistry, Energetic Materials Research, Ludwig-Maximilian University of Munich, Butenandtstr. 5–13 (Haus D), D-81377 Munich, Germany

Reprint requests to Prof. Dr. Thomas M. Klapötke. Fax: (+49-(0)89-2180 77492).

E-mail: tmk@cup.uni-muenchen.de

Z. Naturforsch. **2012**, *67b*, 573–588 / DOI: 10.5560/ZNB.2012-0066

Received March 5, 2012 / revised April 3, 2012

Dedicated to Professor Wolfgang Beck on the occasion of his 80th birthday

1-Amino-3-nitroguanidine (ANQ, **2**) was synthesized *via* hydrazinolysis of nitroguanidine (**1**). An appropriate Lewis structure of ANQ is drawn based on VB calculations. Due to its basicity, it can be protonated by strong mineral acids or acidic heterocycles. In order to synthesize new energetic materials the nitrate (**3**) and perchlorate (**4**) salts of 1-amino-3-nitroguanidine were synthesized by protonation of **2** with 40% nitric acid and 60% perchloric acid, respectively. 5-Nitrimino-1,4*H*-tetrazole obtained by reacting 5-amino-1*H*-tetrazole with 100% HNO₃ was used to synthesize the nitriminotetrazolate salt **5**. Furthermore, the dinitramide salt **6** of 1-amino-3-nitroguanidine was synthesized by metathesis reaction of silver dinitramide and 1-amino-3-nitroguanidinium chloride. The dinitroguanidinate salt **7** was synthesized by protonation of **2** with 1,3-dinitroguanidine, which was prepared from nitroguanidine in anhydrous nitric acid/N₂O₅. All compounds were fully characterized by single-crystal X-ray diffraction, vibrational spectroscopy (IR and Raman), multinuclear NMR spectroscopy, mass spectrometry, elemental analysis, and DSC measurements. The heats of formation of **2–7** were calculated using the atomization method based on CBS-4M enthalpies. With these values and the experimental (X-ray) densities several detonation parameters such as the detonation pressure, velocity, energy, and temperature were computed using the EXPLO5 code. In addition, the sensitivities towards impact, friction and electrical discharge were tested using the BAM drophammer, friction tester as well as a small-scale electrical discharge device. A Koenen test with 1-amino-3-nitroguanidinium nitrate (**3**) was carried out in order to evaluate its explosive performance and shipping classification.

Key words: Nitroguanidine, Energetic Materials, Crystal Structure, Sensitivity

Introduction

The guanidine building block is one of the first structural moieties that has been known to the chemical and biological community and was discovered as early as 1866, when the first guanidine derivative was prepared by Hofmann [1]. Since then, guanidine chemistry has evolved into an extremely wide ranging field of applications starting from bioorganic chemistry and biochemistry [2] to inorganic chemistry, which most importantly can be traced back to a vast variability of derivatization of the guanidine moiety itself. If focusing on the field of inorganic chemistry, principally amination and nitration products of guanidine and the guanidinium cation are of major interest. Whereas the full series of amination

products of the guanidinium cation (amino-, diamino- and triaminoguanidinium cation) is known [3], only mononitro- [4] and dinitroguanidine [5] as the respective nitration analogs have been discovered. On the one hand, amination of one of the amino groups in the guanidine moiety is achieved in a hydrazinolysis reaction, which can be applied up to three times leading to triaminoguanidine [3]. On the other hand, nitration is performed by treating guanidinium nitrate with conc. sulfuric acid. Nitroguanidine (**1**), HN=C(NH₂)NHNO₂, was first prepared in larger quantities by Jousselin [4] using the aforementioned synthetic pathway, when the compound separated upon dilution with water. However, for the preparation of dinitroguanidine, harsher conditions using N₂O₅ as nitration reagent are required [5]. (Mono)nitroguanidine

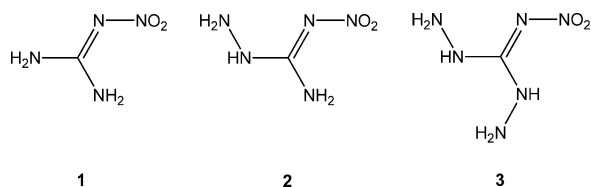


Fig. 1. Formula structures of amino-nitroguanidines: **1**: 1-nitroguanidine (NQ), **2**: 1-amino-3-nitroguanidine (ANQ), **3**: 1,3-diamino-5-nitroguanidine (DANQ) (not known yet).

is used principally as an ingredient in explosive and propellant formulations [6]. In this work, we mainly focus on a mixed amination/nitration product, which is aminonitroguanidine (**2**) and ionic materials, which utilize the aminonitroguanidinium cation as the respective protonated species. To date, only very little correspondence on aminonitroguanidine [7–9], especially if it comes to its structural investigation, is found in the literature. The next step in the preparation of mixed aminonitroguanidines could be the synthesis of diaminonitroguanidine (**3**), which still is a completely unknown field (Fig. 1).

To tie in with the application of nitroguanidine as an energetic material, the possible advantage resulting from introducing one further amino group to nitroguanidine is the generation of a larger gas volume when the compound is burned, which mainly is desired if the material is used in propellant systems. Apart from that, we also expect a higher heat of formation, which is a desirable feature if the compound should find application as a high explosive. Since one of the main topics in this work is the preparation of energetic aminonitroguanidinium salts, from the chemical point of view it is necessary to look at the acid base properties of mixed aminonitroguanidines. The introduction of one further amino group to nitroguanidine through a hydrazinolysis reaction has on the one hand the advantage of lowering the pK_B value of nitroguanidine so that it can be protonated in aqueous solution and therefore utilized as an energetic cation. However, we found that strong acids are required to protonate it. On the other hand, a second reason which makes 1-amino-3-nitroguanidine a suitable precursor in the synthesis of ionic energetic materials is its higher oxygen content compared to amino-substituted guanidine derivatives such as aminoguanidine or triaminoguanidine. It therefore combines the advantages of ease of protonation of the amino-substituted guanidine derivatives and good oxygen balances and high densities of

the nitro-substituted guanidine derivatives. Here we report on the synthesis and characterization of energetic salts of 1-amino-3-nitroguanidine such as the nitrate (**3**), the perchlorate (**4**), the nitriminotetrazolate (**5**), the dinitramide (**6**), and the dinitroguanidinate (**7**).

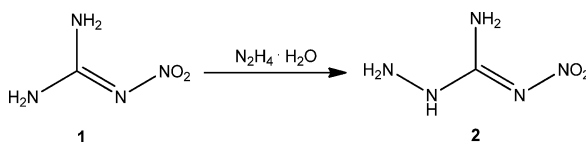
Results and Discussion

Synthesis

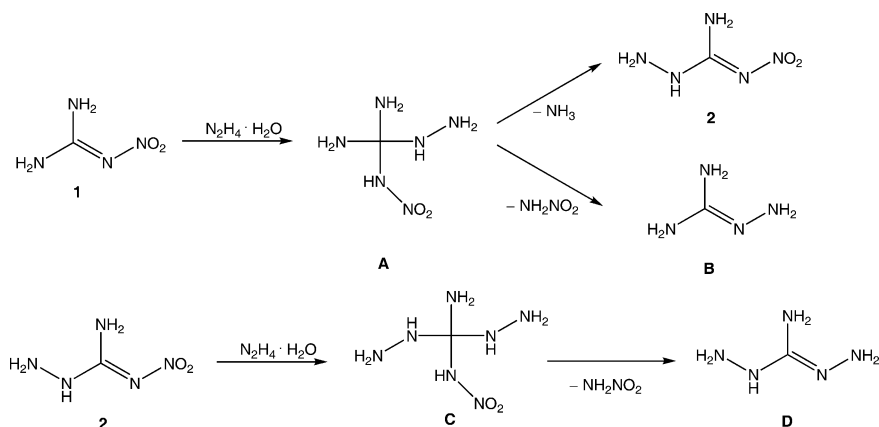
Aminonitroguanidine (**2**) was synthesized in aqueous solution employing a hydrazinolysis reaction of commercially available nitroguanidine (**1**), whereas it is important to control the temperature accurately (Scheme 1) [7]. The product itself shows fairly poor solubility in water and therefore can be recrystallized from hot water.

Considering that the yield is only 45%, there still is the question about the remaining starting material. Henry, Lewis and Smith [8], when reinvestigating the hydrazinolysis of nitroguanidine found two by-products of the reaction to be aminoguanidine and diaminoguanidine. Assuming an addition-elimination mechanism, nitroguanidine reacts with hydrazine to form an intermediate containing a tetrasubstituted carbon atom (**A**), which under the elimination of ammonia converts into **2**. However, the elimination of nitramine (which decomposes to N_2O and H_2O) leads to aminoguanidine **B**. The formation of diaminoguanidine as the second by-product can be explained by a further reaction of **2** with an additional equivalent of hydrazine to form species **C**, which under the elimination of nitramine forms diaminoguanidine **D** (Scheme 2) [10]. These findings are also corroborated by an experiment using a larger excess of hydrazine hydrate (2.2 eq.) in order to form diaminonitroguanidine, which only resulted in the isolation of **2** in minor yields (23%).

For the synthesis of the ionic compounds, ANQ can be protonated by strong mineral acids such as hydrochloric acid, nitric acid and perchloric acid in excess at elevated temperatures (60 °C). During the syn-



Scheme 1. Hydrazinolysis of nitroguanidine. Reaction conditions: stirring, 55 °C, 15 min.



Scheme 2. Possible formation of the reaction by-products **B** and **D** assuming an addition-elimination mechanism.

thesis and crystallization of the nitrate (**3**) and the perchlorate (**4**) salt it is necessary to use acids of concentrations not lower than 40% to avoid the precipitation of the poorly water soluble unprotonated ANQ. Once ANQ is dissolved in the corresponding acid, the nitrate or perchlorate salt will crystallize from the aqueous solution in large colorless blocks. Also the acidity of 5-nitriminotetrazole [11] is high enough to protonate aminonitroguanidine. The experiment was carried out under the same conditions using the sister compounds 1-methyl-5-nitriminotetrazole [11] and 2-methyl-5-nitriminotetrazole [11]. Both compounds failed to react, so that only aminonitroguanidine and the free acids could be isolated afterwards. The acidity of 5-nitriminotetrazole drops by adding an alkyl side chain to the heterocycle in such a way, that it is not sufficiently acidic any more to protonate aminonitroguanidine in aqueous solutions. For the preparation of the dinitramide a metathesis reaction using silver dinitramide [12] and the aminonitroguanidine hydrochloride salt is necessary. Aminonitroguanidinium chloride was synthesized by simple protonation of the ANQ unit with half-concentrated hydrochloric acid (20% w/v).

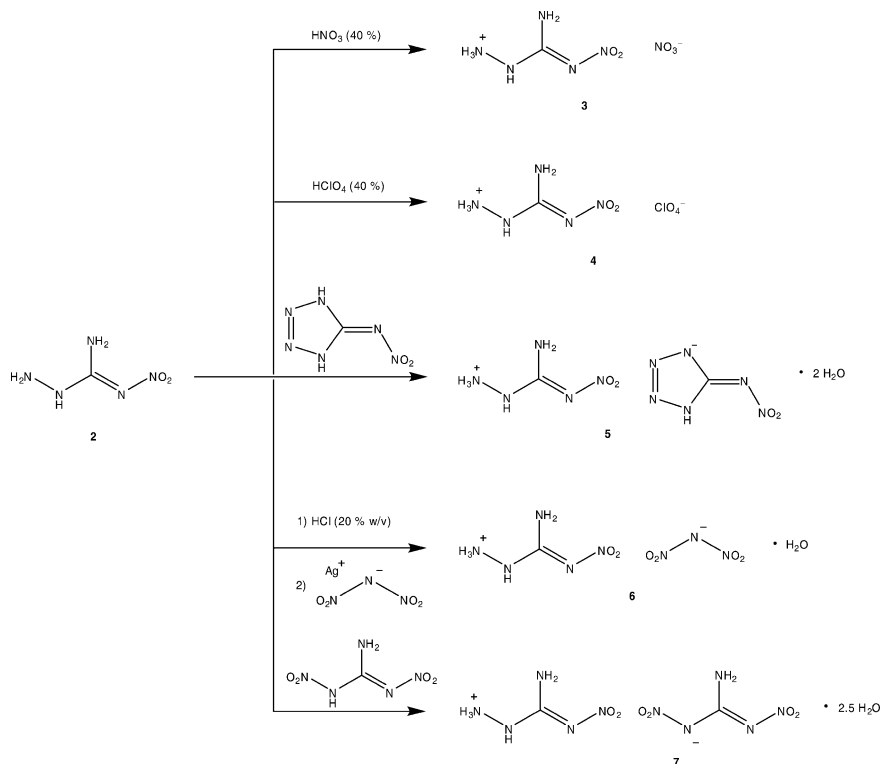
The silver dinitramide was prepared according to the literature [12] as acetonitrile adduct, dissolved in very little acetonitrile and then added to an aqueous solution of aminonitroguanidinium chloride. To avoid the inclusion of one equivalent of silver coordinated to aminonitroguanidine, both, the hydrochloride and the silver dinitramide were reacted in equimolar amounts, whereas the silver dinitramide, dissolved in acetonitrile, was added dropwise to the solution of the hy-

drochloride in water. To ensure the completeness of the reaction, the mixture was further heated to 35 °C for 2 h under the exclusion of light resulting in the formation of **6** before being filtered off. From a facile Brønsted acid base reaction of an aqueous solution of **2** with an aqueous solution of dinitroguanidine the ionic product **7** could be isolated. It crystallizes directly from the reaction mixture with two and a half molecules of water per molecular unit. Dinitroguanidine was synthesized according to literature [5]. Interestingly, the exchange of one amino group in **2** by a nitro group lowers the pK_a value of the compound by a step which is just large enough to protonate **2** in aqueous solution. All reaction pathways are gathered in Scheme 3.

Single-crystal X-ray structure analyses

Experimental details

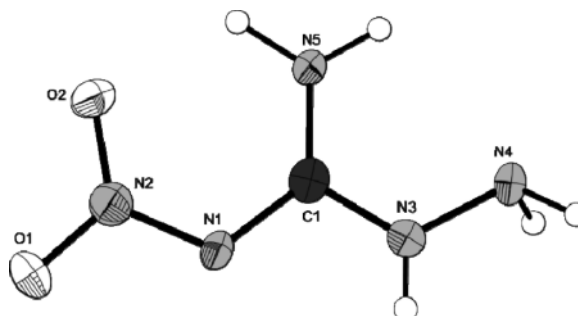
The low temperature (173 K) determination of the crystal structures of **2–7** was performed on an Oxford Xcalibur3 diffractometer with a Spellman generator (voltage 50 kV, current 40 mA) and a KappaCCD detector with a wavelength of 0.71073 Å. The data collection and reduction was carried out using the CRYSTALISPRO software [13]. The structures were solved either with SHELXS-97 [14a] or SIR-92 [14b], refined with SHELXL-97 [15] and finally checked using the PLATON [16] software integrated in the WINGX [17] software suite. The non-hydrogen atoms were refined anisotropically, and the hydrogen atoms were located and freely refined. The absorptions were corrected with a Scale3 Abspack multi-scan method. Selected

Scheme 3. Formation of aminonitroguanidinium salts **3**–**7**.

data and parameters of the X-ray determinations are given in Table 1. Crystallographic data have been deposited with The Cambridge Crystallographic Data Centre [18].

Structural details

Although compound **2** has been known for a long time, its crystal structure has never been published. Naidu *et al.* [19] claimed that ANQ belongs to a tetragonal crystal system which could not be confirmed in our study. Suitable single crystals of **2** were obtained from acidic aqueous media (40% HF in H_2O). Compound **2** crystallizes in the monoclinic space group $P2_1/c$ with four molecules in the unit cell. The structure could sufficiently be refined using a merohedral twinning matrix. Fig. 2 represents the asymmetric unit. The bond lengths of neutral **2** and its protonated species **3**–**7** are listed in Table 2. Protonation always takes place at the outer hydrazine nitrogen atom N4, which does not influence the molecular structures (bond lengths and angles). All of the C–N bonds are

Fig. 2. Molecular structure of compound **2**. Ellipsoids are drawn at the 50% probability level.

significantly shorter than C–N single bonds. Except for **2**, in all structures investigated in this work the C1–N5 distances are found to have the shortest values within the ANQ moieties. Also both N–N distances (N1–N2 and N3–N5) are between N–N single (1.48 Å) and N=N double (1.30 Å) bonds.

The relatively high density of 1.72 g cm^{-3} is a consequence of several strong N–H \cdots N and N–H \cdots O hy-

Table 1. Crystal structure data for compounds 2–7.

	2	3	4	5	6	7
Formula	CH ₂ N ₅ O ₂	CH ₆ N ₆ O ₅	CH ₆ N ₅ ClO ₆	C ₂ H ₁₁ N ₁₁ O ₆	CH ₈ N ₈ O ₇	C ₂ H ₁₃ N ₁₀ O _{8.5}
<i>M_r</i>	119.08	182.10	219.54	285.18	244.12	313.19
Cryst. size, mm ³	0.08 × 0.12 × 0.22	0.18 × 0.19 × 0.20	0.13 × 0.16 × 0.20	0.19 × 0.20 × 0.29	0.09 × 0.17 × 0.18	0.16 × 0.19 × 0.32
Crystal system	monoclinic	triclinic	triclinic	monoclinic	monoclinic	triclinic
Space group	<i>P</i> 2 ₁ / <i>c</i>	<i>P</i> $\bar{1}$	<i>P</i> $\bar{1}$	<i>P</i> 2 ₁ / <i>c</i>	<i>P</i> 2 ₁ / <i>c</i>	<i>P</i> $\bar{1}$
<i>a</i> , Å	6.8301(9)	7.1184(5)	7.1838(6)	9.3828(6)	7.3698(4)	7.2535(6)
<i>b</i> , Å	9.4491(14)	7.1485(6)	7.7952(8)	6.4467(4)	13.7548(8)	8.4153(7)
<i>c</i> , Å	7.1192(14)	7.8285(7)	7.9723(8)	18.7233(11)	8.6857(5)	11.0683(9)
α , deg	90	64.908(7)	73.897(9)	90	90	76.326(7)
β , deg	90.000(5)	65.418(8)	69.213(9)	104.242(7)	95.266(6)	79.414(7)
γ , deg	90	67.476(9)	63.009(10)	90	90	69.246(7)
<i>V</i> , Å ³	459.46(13)	317.57(5)	368.28(7)	1097.73(12)	876.75(9)	610.14(9)
<i>Z</i>	4	2	2	4	4	2
<i>D</i> _{calcd.} , g cm ^{−3}	1.72	1.91	1.98	1.73	1.85	1.71
μ (MoK α), cm ^{−1}	0.2	0.2	0.5	0.2	0.2	0.2
<i>F</i> (000), e	248	188	224	592	504	326
<i>hkl</i> range	−8 ≤ <i>h</i> ≤ 8; −12 ≤ <i>k</i> ≤ 8; −6 ≤ <i>l</i> ≤ 9	−8 ≤ <i>h</i> ≤ 7; −8 ≤ <i>k</i> ≤ 7; −9 ≤ <i>l</i> ≤ 9	−8 ≤ <i>h</i> ≤ 8; −9 ≤ <i>k</i> ≤ 9; −9 ≤ <i>l</i> ≤ 9	−11 ≤ <i>h</i> ≤ 10; −8 ≤ <i>k</i> ≤ 7; −23 ≤ <i>l</i> ≤ 23	−9 ≤ <i>h</i> ≤ 8; −16 ≤ <i>k</i> ≤ 10; −6 ≤ <i>l</i> ≤ 10	−9 ≤ <i>h</i> ≤ 7; −10 ≤ <i>k</i> ≤ 9; −13 ≤ <i>l</i> ≤ 13
((sin θ)/ λ) _{max} , Å ^{−1}	27.0	26.5	26.0	26.5	26.0	26.5
Ref. meas./unique/ <i>R</i> _{int}	2578/998/0.039	1879/1276/0.012	2805/1444/0.023	8692/2258/0.032	3807/1718/0.022	4257/2510/0.025
Param. refined	94	134	142	130	177	250
<i>R</i> 1 (obs) ^a	0.0358	0.0303	0.0323	0.0355	0.0319	0.0350
<i>wR</i> 2 (all data) ^b	0.0801	0.0855	0.0773	0.0967	0.0783	0.0639
GoF (<i>F</i> ²) ^c	1.02	1.07	1.01	1.04	0.95	0.84
$\Delta\rho_{\text{fin}}$ (min/max), e Å ^{−3}	−0.21/0.20	−0.26/0.27	−0.53/0.24	−0.45/0.38	−0.35/0.18	−0.26/0.19

^a $R1 = \sum ||F_o| - |F_c|| / \sum |F_o|$; ^b $wR2 = [\sum w(F_o^2 - F_c^2)^2 / \sum w(F_o^2)^2]^{1/2}$, $w = [\sigma^2(F_o^2) + (AP)^2 + BP]^{-1}$, where $P = (\text{Max}(F_o^2, 0) + 2F_c^2)/3$ and A and B are constants adjusted by the program; ^c GoF = $S = [\sum w(F_o^2 - F_c^2)^2 / (n_{\text{obs}} - n_{\text{param}})]^{1/2}$, where n_{obs} is the number of data and n_{param} the number of refined parameters.

Atoms A–B	2	3	4	5	6	7
O1–N2	1.245(2)	1.239(1)	1.247(2)	1.235(2)	1.252(2)	1.247(2)
O2–N2	1.254(2)	1.236(1)	1.239(2)	1.240(2)	1.230(2)	1.243(2)
N1–N2	1.336(2)	1.348(2)	1.338(2)	1.345(2)	1.348(2)	1.343(2)
N3–N4	1.414(2)	1.411(2)	1.408(2)	1.414(2)	1.415(2)	1.421(2)
N1–C1	1.374(2)	1.346(2)	1.348(3)	1.354(2)	1.350(2)	1.355(2)
N3–C1	1.334(2)	1.348(2)	1.355(3)	1.356(2)	1.354(2)	1.351(2)
N5–C1	1.319(3)	1.320(2)	1.306(3)	1.314(2)	1.306(2)	1.312(2)

Table 2. Selected bond lengths (Å) of compounds 2–7.

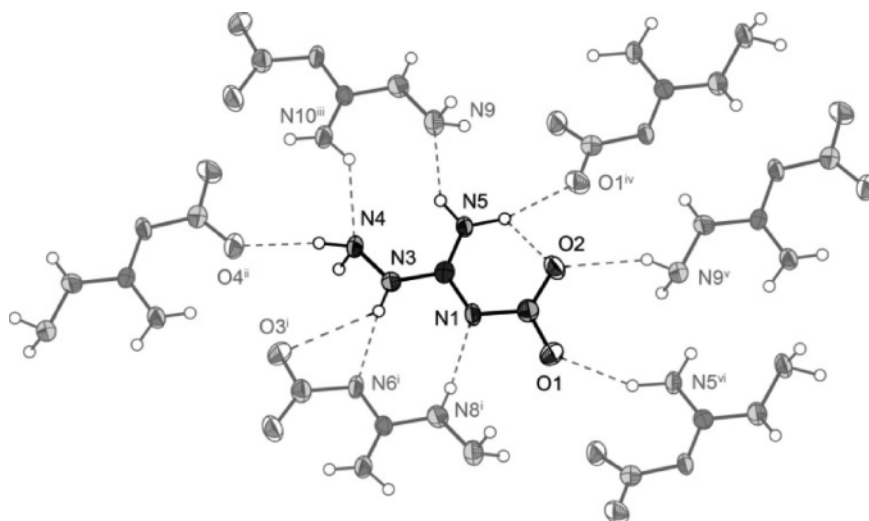
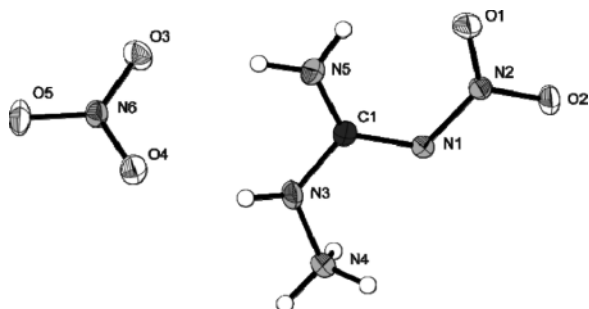
Fig. 3. Hydrogen bonding of one aminonitroguanidine molecule. Symmetry codes: (i) $1-x, 1-y, 1-z$; (ii) $1+x, 0.5-y, 0.5+z$; (iii) $1-x, -y, 1-z$; (iv) $1-x, -0.5+y, 0.5-z$; (v) $x, 0.5-y, -0.5+z$; (vi) $1-x, 0.5+y, 0.5-z$.

Fig. 4. Molecular structure of compound 3. Ellipsoids are drawn at the 50% probability level.

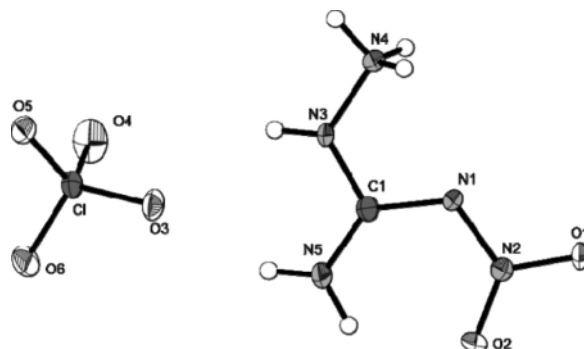


Fig. 5. Molecular structure of compound 4. Ellipsoids are drawn at the 50% probability level.

drogen bonds. **2** crystallizes in a layer-like structure, in which the layers are formed by the H-bond modes depicted in Fig. 3.

This constitution is observed for all ANQ salts presented in this work and is therefore probably caused by the protonation of nitrogen atom N4. The cations of compound **3** are arranged parallel and are connected by the nitrate anions which follow the direction of the hydrazinium proton H4c (not within the cation's plane). Fig. 4 shows the molecular moiety of compound **3**.

The perchlorate salt **4** crystallizes triclinically with the highest density (1.98 g cm^{-3}) of the investigated compounds (Fig. 5). The Cl–O bond lengths in the ClO_4^- anion lie between 1.41 and 1.44 Å, which is a commonly observed bond length and can also be found in other perchlorate structures [20].

Single crystals of **5** were obtained from a water/ethanol mixture. Salt **5** holding monodeprotonated 5-nitriminotetrazolate as the counter anion could only

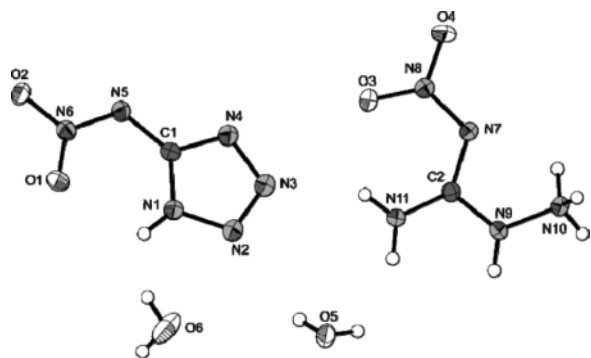


Fig. 6. Molecular structure of compound **5**. Ellipsoids are drawn at the 50% probability level. Selected bond lengths of the nitriminotetrazolate anion (Å): O1–N6 1.245(2), O2–N6 1.269(2), N1–C1 1.340(2), N1–N2 1.349(2), N2–N3 1.294(2), N3–N4 1.354(2), N4–C1 1.332(2), N5–N6 1.318(2), N5–C1 1.376(2).

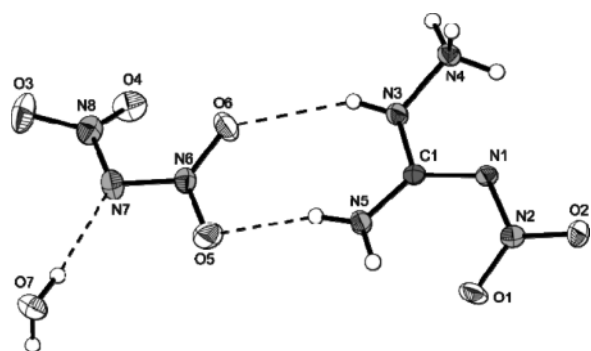


Fig. 7. Molecular structure of compound **6**. Ellipsoids are drawn at the 50% probability level. Bond lengths of the dinitramide anion (Å): O3–N8 1.2317(17), O4–N8 1.2172(17), O5–N6 1.2541(16), O6–N6 1.2287(16), N6–N7 1.3423(17), N7–N8 1.3926(18).

be obtained in crystalline form (monoclinic space group $P2_1/c$) with the inclusion of two molecules of crystal water (Fig. 6). The planar structure of the anion, fixed by the intramolecular hydrogen bond N1–H1...O1 (graph set R1,1(6)), is in agreement with several examples published in the literature [21, 22] bearing this anion. The packing is best described by a wave-like arrangement along the c axis.

Amino-nitroguanidinium dinitramide monohydrate (**6**) crystallizes also in the monoclinic space group $P2_1/c$ with $Z = 4$ and a high density of 1.85 g cm^{-3} . The dinitramide anion participating in several strong hydrogen bonds is significantly twisted (bent angle $\sim 59.5^\circ$) (Fig. 7). Again a wave-like arrangement along the b axis can be detected.

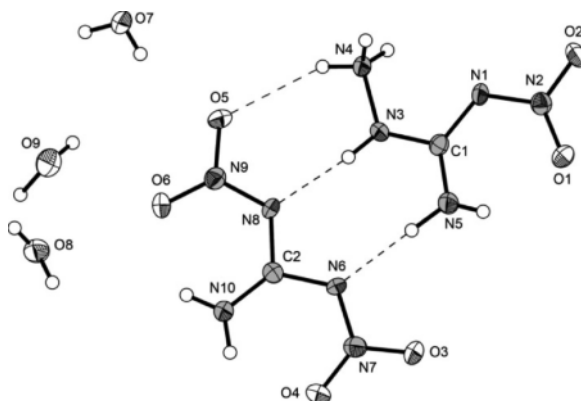


Fig. 8. Molecular structure of compound **7**. Ellipsoids are drawn at the 50% probability level. Selected bond lengths of the DNQ anion (Å): O3–N7 1.2422(18), O4–N7 1.2430(17), O5–N9 1.2544(17), O6–N9 1.2491(18), N6–N7 1.3426(19), N6–C2 1.363(2), N8–N9 1.3316(19), N8–C2 1.376(2), N10–C2 1.309(2).

The combination of two different nitroguanidines in compound **7** leads to the inclusion of two and a half crystal water molecules in the crystalline state (Fig. 8). The compound crystallizes in the triclinic space group $P\bar{1}$ with the lowest density of 1.705 g cm^{-3} observed in this work. The dinitroguanidinate anion follows the structure described for its ammonium salt [23]. In the packing layers are formed by the cations and anions. The parallel layers are exclusively connected by hydrogen bonds involving the crystal water molecules between the layers.

NMR spectroscopy

^1H as well as ^{13}C and ^{14}N NMR spectroscopy were applied to identify 1-amino-3-nitroguanidine and its salts. Additionally a ^{15}N NMR spectrum of **2** was recorded. For better comparison all spectra were measured using $[\text{D}_6]\text{DMSO}$ as solvent, and all chemical shifts are given with respect to TMS (^1H , ^{13}C) and nitromethane ($^{14}\text{N}/^{15}\text{N}$). The proton spectrum of the neutral compound **2** reveals 4 singlets corresponding to the protons of the NH and of both NH_2 groups. The signal of the hydrazine NH_2 group appears at 4.64 ppm at highest field. For the two protons of the C-bonded amino group two distinct signals at 8.22 and 7.52 ppm are observed. This indicates hindered rotation around the C–N bond due to partial double bond character. The signal of the NH proton is found at 9.29 ppm and thus

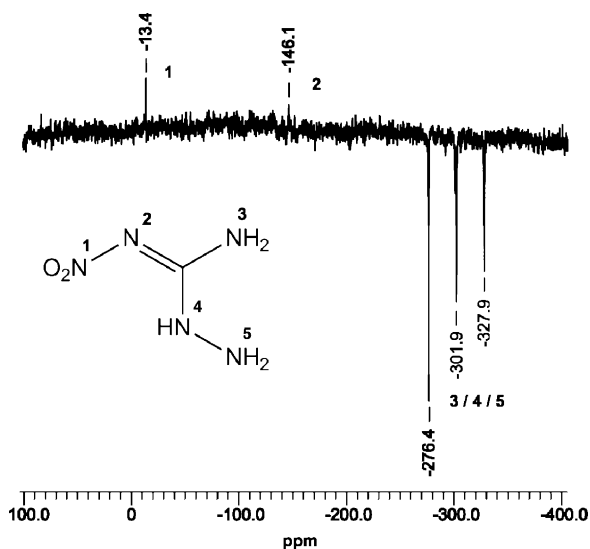


Fig. 9. $^{15}\text{N}\{^1\text{H}\}$ NMR spectrum of 1-amino-3-nitroguanidine (2).

at lowest field. The ^{13}C NMR spectrum shows a clear singlet at 161.5 ppm for the carbon atom, whereas the ^{14}N NMR spectrum reveals a singlet (line width at half height 17 Hz) at -13 ppm for the nitro group contained. The signals of the other nitrogen atoms are broad and difficult to locate in the ^{14}N NMR spectrum. However, they are clearly observed in the $^{15}\text{N}\{^1\text{H}\}$ NMR spectrum, which is shown in Fig. 9. Due to the nuclear Overhauser effect, the three nitrogen atoms having directly bonded protons display negative signals in the high-field region of the spectrum at -276.4 , -301.8 and -327.9 ppm (NH/NH_2). In accordance with literature values of other primary nitramines [24], the signal at -146.3 ppm is assigned to the remaining nitrogen atom ($\text{N}-\text{NO}_2$) of the nitramine moiety.

All ionic compounds **3–7** show two broad singlets in their proton NMR spectra: one between 8.14 and 9.53 ppm for NH and a second between 6.90 and 8.38 ppm for $-\text{NH}_2/-\text{NH}_3^+$. In contrast to compound **2** only one signal is observed for the protons of the C-bonded amino group. In the carbon NMR spectra of compounds **3–7** one signal at 159.0 to 160.7 ppm can be assigned to the protonated aminonitroguanidine, and an additional signal at 154.7 ppm for deprotonated 5-nitriminotetrazole is observed in the spectrum of **5**. The ^{14}N NMR spectra show the signals of the nitro group of the aminonitroguanidinium cation at -15 ppm. Further nitro groups are observed

in the spectrum of **3** (NO_3^- , -7 ppm), **5** (NNO_2 , -8 ppm), **6** ($\text{N}(\text{NO}_2)_2^-$, -10 ppm) and **7** ($(\text{NNO}_2)_2$, -19 ppm). Also the protonated terminal amino groups of the cation can be detected as sharp signals at high field [-354 (**4**), -353 (**5**), -360 (**7**)].

Sensitivities and thermal stability

The impact sensitivity tests were carried out according to STANAG 4489 [25] modified instruction [26] using a BAM (Bundesanstalt für Materialforschung) drophammer [27]. The friction sensitivity tests were carried out according to STANAG 4487 [28] modified instruction [29] using the BAM friction tester. The classification of the tested compounds results from the “UN Recommendations on the Transport of Dangerous Goods” [30]. Additionally all compounds were tested for their sensitivity towards electrical discharge using the Electric Spark Tester ESD 2010 EN [31]. All sensitivities of compounds **2–7** were determined by the above described procedures. Expectedly, the perchlorate salt **4** is the most sensitive compound with values of 1 J (IS) and 20 N (FS), which has to be classified as very sensitive. Also the 5-nitriminotetrazolate **5** shows enhanced impact sensitivity (5 J) and friction sensitivity (96 N). The same applies to the friction sensitivity of the dinitramide **6** (40 N). Astonishingly, the impact sensitivity of **6** (10 J) is very similar to that of the nitrate salt **3** (10 J) and the dinitroguanidinate salt **7** (12 J). Regarding the impact sensitivity, the least sensitive compound within the investigated group is the unprotonated aminonitroguanidine itself. Apparently, protonation of the molecule leads to a certain destabilization by lowering the C–N bond order of the hydrazine moiety in aminonitroguanidine. The sensitivities towards electrical discharge are in a range between 0.10 J (**6**) and 0.50 J (**3**). These values depend strongly on the crystal size of the corresponding compound. The nitrate salt **3** crystallizes in large blocks, thus its sensitivity towards electrical discharge is comparatively low. The sensitivities as well as the decomposition and dehydration temperatures of all investigated compounds are gathered in Table 3.

Differential scanning calorimetry (DSC) measurements to determine the melting and decomposition temperatures of **2–7** (about 1.5 mg of each energetic material) were performed in covered Al containers with a hole in the lid at a nitrogen flow of 20 mL

Table 3. Sensitivities and thermal behavior of compounds **2–7**.

	IS (J)	FS (N)	ESD (J)	T_{dec} (°C)	T_{dehydr} (°C)
2	20	144	0.15	184	–
3	10	120	0.50	130	–
4	1	20	0.15	108	–
5	5	96	0.40	136	76
6	10	40	0.10	108	66
7	12	288	0.20	118	79

per minute on a Linseis PT 10 DSC [32] calibrated by standard pure indium and zinc at a heating rate of 5 °C min^{-1} . The most temperature-stable of the described energetic materials is the free base ANQ itself. It decomposes in a two step mechanism, which could be due to the loss of an amino group in a first step at 184 °C and then to the decomposition of the remaining nitroguanidine in a second step starting at 200 °C . For the ionic species **3–7** decomposition temperatures are significantly lower ranging from 108 °C (**4**, **6**) to 136 °C (**5**). The same arguments as for the sensitivities of the protonated aminonitroguanidine compounds can be applied to their thermal stability, which is the lowering of the C–N bond order resulting in an earlier decomposition. Additionally, the loss of crystal water in compounds **5–7** can be observed in the DSC curves as endothermic peaks between 66 °C (**6**) and 79 °C (**7**).

Heat of formation and detonation parameters

Heats and corresponding energies of formation were calculated with the atomization energy method (Eq. 1) using CBS-4M electronic energies (Table 4). Values obtained by this method have been shown to be suitable in several recently published studies [23].

Table 4. CBS-4M results and gas phase enthalpies.

	Formula	$-H^{298}$ (a.u.)	$\Delta_f H$ (g) (kJ mol^{-1})
ANQ	$\text{CH}_5\text{N}_5\text{O}_2$	464.602726	161.7
ANQ^+	$\text{CH}_6\text{N}_5\text{O}_2^+$	464.914496	877.0
NO_3^-	NO_3^-	280.080446	–313.6
ClO_4^-	ClO_4^-	760.171182	–277.6
HAAtNO_2^-	CHN_6O_2^-	516.973495	150.4
DN^-	N_3O_4^-	464.499549	–124.0
DNQ^-	$\text{CH}_2\text{N}_5\text{O}_4^-$	613.123393	–101.9

CBS-4M energies of the atoms (C,H,N,O), ANQ, the ANQ^+ cation, and the anions were calculated with the GAUSSIAN09 (revision A1) software package [33] and checked for imaginary frequencies. Values for $\Delta_f H^\circ$ (atoms) were taken from the NIST database [34].

$$\Delta_f H_{(\text{g, M}, 298)}^\circ = H_{(\text{Molecule}, 298)} - \sum H_{(\text{Atoms}, 298)}^\circ + \sum \Delta_f H_{(\text{Atoms}, 298)}^\circ \quad (1)$$

For calculation of the solid-state energy of formation (Table 5) of **3–7**, the lattice energy (U_L) and lattice enthalpy (ΔH_L) were calculated from the corresponding molecular volumes (obtained from X-ray elucidations) according to the equations provided by Jenkins *et al.* [35]. With the calculated lattice enthalpy (Table 5) the gas-phase enthalpy of formation was converted into the solid-state (standard conditions) enthalpy of formation. These molar standard enthalpies of formation (ΔH_m) were used to calculate the molar solid state energies of formation (ΔU_m) according to Eq. 2 (Table 5):

$$\Delta U_m = \Delta H_m - \Delta n RT \quad (2)$$

with Δn being the change of moles of gaseous components.

Table 5. Solid state energies of formation ($\Delta_f U^\circ$) of compounds **2–7**.

	$\Delta_f H$ (g) (kJ mol^{-1})	V_M (nm^3)	U_L (kJ mol^{-1})	ΔH_L (kJ mol^{-1})	$\Delta_f H^\circ$ (s) (kJ mol^{-1})	Δn	$\Delta_f U^\circ$ (s) (kJ mol^{-1})	M (g mol^{-1})	$\Delta_f U^\circ$ (s) (kJ kg^{-1})
2	161.7	–	–	85.9 ^a	76.9	6	91.8	119.1	770.4
3	563.4	0.158	537.8	541.2	22.2	8.5	43.3	182.1	237.5
4	599.4	0.184	591.3	594.8	4.6	8	24.5	219.6	111.4
5	544.3 ^b	0.224	489.8	493.3	51.0	14	85.7	285.2	300.4
6	511.4	0.194	508.9	512.4	–0.2	11.5	27.5	244.1	112.7
7	40.9	0.243	480.0	484.4	–312.3	15.75	–273.3	313.09	–872.8

^a Sublimation enthalpy calculated by Trouton's rule [36] ($188 \cdot T_m$ (K); $T_m = 457$ K); ^b values are corrected for hydrate water (-241 kJ mol^{-1} per water molecule).

Table 6. Energetic characteristics and calculated explosive performance parameters of compounds **2–7** using the EXPLO5 code.

	2	3	4	5	6	7
Formula	CH ₅ N ₅ O ₂	CH ₆ N ₆ O ₅	CH ₆ N ₅ O ₆ Cl	C ₂ H ₁₁ N ₁₁ O ₆	CH ₈ N ₈ O ₇	C ₂ H ₁₃ N ₁₀ O _{8.5}
FW, g mol ⁻¹	119.08	182.10	219.54	285.18	244.12	313.19
N, % ^a	58.8	46.2	31.90	54.4	45.9	44.7
Ω, % ^b	-33.59	0.0	+10.93	-19.63	+6.55	-10.22
ρ, g cm ⁻³ ^c	1.722	1.905	1.980	1.726	1.850	1.705
EXPLO5.04 values:						
-Δ _{Ex} U ^o , kJ kg ⁻¹ ^d	4915	6191	–	5236	5636	5313
T _{det} , K ^e	3310	4196	–	3607	3949	3612
P _{CJ} , kbar ^f	307	427	–	317	377	311
V _{det} , m s ⁻¹ ^g	8729	9551	–	8753	9175	8656
V _o , L kg ⁻¹ ^h	878	857	–	880	871	890

^a Nitrogen content; ^b oxygen balance [38]; ^c density from X-ray diffraction; ^d energy of explosion; ^e explosion temperature; ^f detonation pressure; ^g detonation velocity; ^h volume of detonation gases assuming only gaseous products.

The detonation parameters were calculated using the program EXPLO5 V5.04 [37]. The program is based on the steady-state model of equilibrium detonation and uses Becker-Kistiakowsky-Wilson's equation of state (BKW E. O. S.) for gaseous detonation products and Cowan-Fickett E. O. S. for solid carbon.

The calculations for **2–7** were performed using the maximum densities according to the crystal structures. Additionally the explosion performance parameters of the water-free dinitramide were calculated assuming the same density as for the monohydrate. Except for **6** and **7**, all calculated heats of formation are positive with values ranging from only slightly positive (**4**: 4.6 kJ mol⁻¹) to more endothermic (**2**: 76.9 kJ mol⁻¹). All calculated values for the heats and energies of formation can be found in Table 5.

Having a look at the explosive performance parameters shown in Table 6, the nitrate salt **3** and the dinitramide salt **6** stand out with their very high detonation velocities and pressures of 9551 m s⁻¹ and 427 kbar (**3**) and 9175 m s⁻¹ and 377 kbar (**6**), which are caused by their high densities of 1.91 g cm⁻³ (**3**) and 1.85 g cm⁻³ (**6**). The perchlorate salt **4** and dinitramide salt **6** reveal an even positive oxygen balance which is a desirable feature for oxidizers in propellant formulations. Compound **3** is an example of an energetic compound having a balanced oxygen content, which is found very rarely in the literature. Its combustion equation can be formulated ideally to be CH₆N₆O₅ → CO₂ + 3 H₂O + 3 N₂. Also **2** shows a detonation velocity in the vicinity of 9000 m s⁻¹ which is higher than commonly used RDX.

Valence bond (VB) calculations

In order to elucidate the bonding situation based on valence bond (VB) theory and to determine the most relevant Lewis-type structure(s), various calculations were performed using the VB2000 [version 2.5(R1)] code [39]. The input structure was taken from a fully optimized (within C_s symmetry) MP2/aug-cc-pVDZ calculation (NIMAG = 0) where all atoms involved in π bonding (O1, N2, O3, N4, C5, N6, N7) were placed into the xy plane (see Fig. 10), and the corresponding seven p_z orbitals were used as VB orbitals to accommodate the ten π electrons. In all VB calculations we used strictly localized p_z-π orbitals (BRILLMASK function in VB2000). For clarity, the π electrons are shown as dots (·) whereas the σ backbone (HF treatment) is shown as solid bonds (–) (Fig. 10).

Initially we carried out a CASVB(10,7)/D95 calculation using Dunning/Huzinaga's full double-zeta basis set and invoking resonance between all possible 196 π structures (NOROT option to disable any σ – π mixing). The calculation clearly showed that only the seven structures (**I–VII**) shown in Fig. 10 contribute significantly to the resonance scheme (Hiberty weights > 0.01) (Table 7).

In a subsequent VB(10)/D95 calculation we only included the seven structures **I–VII** into the resonance scheme (Table 7). It is apparent that only structures **I–III** and **VI** have significant weight, whereas structures **IV**, **V** and **VII** are not significant contributors to the resonance scheme.

The above VB calculations reveal that resonance structures **I–III** and **VI** (Fig. 10) are the most rele-

	$-E$ (a.u.)	I	II	III	IV	V	VI	VII
CASVB(10,7)/D95	461.471657	0.04	0.29	0.05	0.02	0.01	0.07	0.06
VB(10)/D95	461.338488	0.07	0.70	0.07	0.02	0.01	0.11	0.02

Table 7. VB energies and Hibtory weights for resonance structures **I–VII** (see Fig. 10).

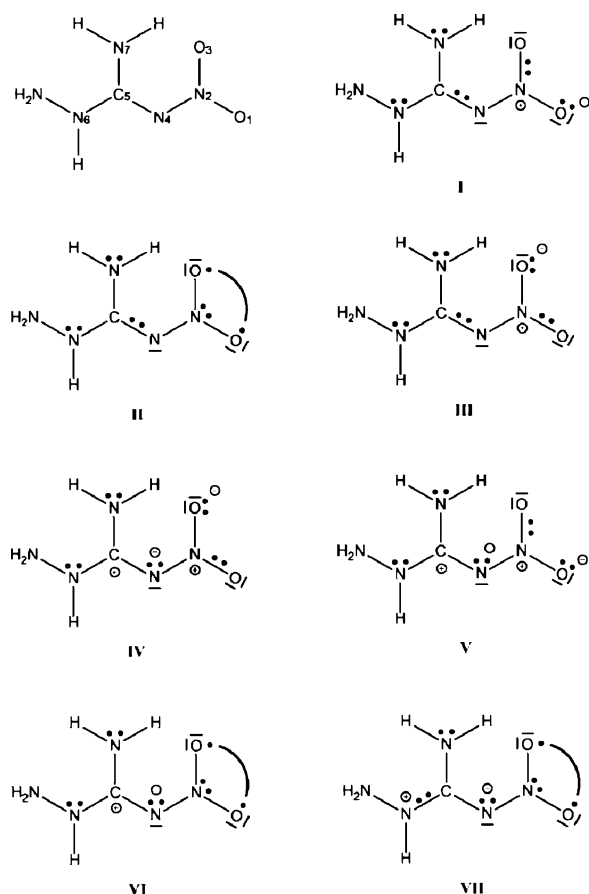


Fig. 10. Atomic numbering and resonance structures **I–VII** for the π resonance scheme of **2**.

vant individual structures for describing the π electron distribution of **2**. Whereas the Kekulé-type structures **I** and **III** have two π bonds each, the Kekulé-/Dewar-type structure **II** also with two π bonds (one Kekulé- and one Dewar-type bond) is by far the most important individual resonance structure for **2** since it does not carry any formal charge [40].

In addition, we also carried out an NBO analysis [41] and calculated the natural Lewis structure which is shown in Fig. 11. Taking into account that there is only one strong hyperconjugative interaction (LP (3) O3 \rightarrow BD*(2) O1–N2) which essentially delocalizes the π bond between O1–N2 and O3–N2, both

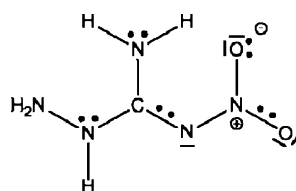


Fig. 11. Natural Lewis structure of ANQ (**2**).

pictures (VB and NBO) agree with a N4=C5 double bond and a strongly π -bound nitro ($-\text{NO}_2$) unit. It has to be stressed, however, that the natural Lewis structure is *not* a classical Lewis structure in the London-Heitler picture, and that the resonance structure **II** (see above) with one long (or Dewar-type) bond accounts best for maximizing the bond order and simultaneously reducing the number of formal charges.

Koenen Test of 1-amino-3-nitroguanidinium nitrate (**3**)

Due to its cheap and comparatively easy synthesis, 1-amino-3-nitroguanidinium nitrate (**3**) was investigated regarding its explosion performance under confinement using a “Koenen test” steel sleeve apparatus [42, 43]. The performance of an explosive can be related to the data obtained from the Koenen test. Also the shipping classification of the substance can be determined, and the degree of venting required to avoid an explosion during processing operations can be evaluated. The explosive is placed in a non-reusable open-ended flanged steel tube, which is locked up with a closing plate with variable orifice (0–10 mm), through which gaseous decomposition products are vented. A defined volume of 25 mL of the compound is loaded into the flanged steel tube, and a threaded collar is slipped onto the tube from below. The closing plate is fitted over the flanged tube and secured with a nut. The explosion is initiated *via* thermal ignition using four Bunsen burners, which are lighted simultaneously. The test is completed when either rupture of the tube or no reaction is observed after heating the tube for a time period of at least 5 min. In case of the tube’s rupture the fragments are collected and weighed. The reaction is evaluated as an explosion if the tube is destroyed into three or more pieces. The

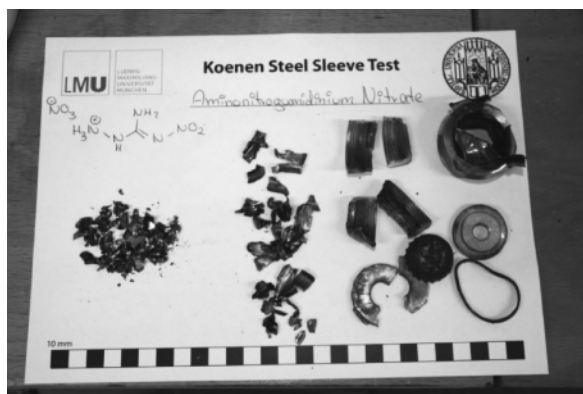


Fig. 12. Fragments of the steel sleeve after the ignition of 32.5 g 1-amino-3-nitroguanidinium nitrate (**3**).

Koenen test was performed with 32.5 g of 1-amino-3-nitroguanidinium nitrate (**3**) using a closing plate with an orifice of 10 mm. The first trial was successful as indicated by the rupture of the steel tube into approximately 100 pieces, the sizes of which are reaching from 40 mm down to smaller than 1 mm (Fig. 12). TNT destroys the steel tube up to an orifice width of 6 mm, RDX even up to 8 mm [44]. Compared to these commonly used secondary explosives, the detonation performance of **3** is apparently better, which is already indicated by the calculated performance data.

Conclusion

From the experimental study of energetic materials based on 1-amino-3-nitroguanidine the following conclusions can be drawn:

- 3-Amino-1-nitroguanidine can be easily prepared by the reaction of 1-nitroguanidine and hydrazine hydrate.
- 1-Amino-3-nitroguanidine can be protonated using moderate to strong “Brønsted acids” such as nitric acid, hydrochloric acid, perchloric acid, dinitroguanidine, or 5-nitriminotetrazole.
- The hydrochloride of 1-amino-3-nitroguanidine can be utilized in metathesis reactions with silver salts of nitrogen/oxygen-rich anions. The metathesis was used for the synthesis of 1-amino-3-nitroguanidinium dinitramide.
- The crystal structures of compounds **2–7** were determined using low-temperature single-crystal X-ray diffraction.

- A comprehensive characterization of the physico-chemical properties and sensitivities of compounds **2–7** is given. Promising detonation parameters were calculated especially for **3** compared to common explosives like TNT and RDX. The outstanding performance (calculated values: $p_{CJ} = 427$ kbar; $D = 9551 \text{ m s}^{-1}$) qualifies it for further investigations concerning special military applications. Unfortunately the decomposition temperatures of the protonated species are low compared to the free base 1-amino-3-nitroguanidine. This causes major restrictions for the investigated compounds with respect to their application as secondary explosives.

Experimental Section

Caution! ANQ and its salts are highly energetic materials with increased sensitivities towards shock and friction. Therefore, proper safety precautions (safety glass, face shield, earthed equipment and shoes, Kevlar® gloves and ear plugs) have to be applied while synthesizing and handling the described compounds.

All chemicals and solvents were employed as received (Sigma-Aldrich, Fluka, Acros). ^1H and ^{13}C spectra were recorded using Jeol Eclipse 270, Jeol EX 400 or Jeol Eclipse 400 instruments. The chemical shifts quoted in ppm in the text refer to typical standards such as tetramethylsilane (^1H , ^{13}C) or nitromethane ($^{14}\text{N}/^{15}\text{N}$). To determine the melting and decomposition temperatures of the described compounds a Linseis PT 10 DSC (heating rate 5°C min^{-1}) was used. Infrared spectra were measured using a Perkin Elmer Spectrum One FT-IR spectrometer as KBr pellets. Raman spectra were recorded on a Bruker MultiRAM Raman Sample Compartment D418 equipped with an Nd-YAG Laser (1064 nm) and an LN-Ge diode as detector. Mass spectra of the described compounds were measured at a Jeol MStation JMS 700 using FAB technique. To measure elemental analyses, a Netsch STA 429 simultaneous thermal analyzer was employed.

1-Amino-3-nitroguanidine (**2**)

Commercially available nitroguanidine (25 g, 192 mmol) is dispensed in 250 mL of water, and the mixture is heated to 55°C . Hydrazine hydrate (10.5 mL, 216 mmol) is added dropwise over a period of 15 min, and the temperature is kept at 55°C for further 15 min under constant stirring. After the mixture has turned to a clear, orange solution, it is cooled to room temperature in an ice bath, and the reaction is quenched with conc. hydrochloric acid ($\text{pH} = 7$). 1-Amino-3-nitroguanidine starts to precipitate after the solution has been cooled to 4°C overnight. The product is separated by suction filtration and recrystallized from hot water. Yield: 10.3 g (86 mmol, 45%). – DSC (5°C min^{-1}):

184 °C (dec. 1), 200 °C (dec. 2). – IR (KBr, cm^{-1}): $\tilde{\nu}$ = 3551 (s), 3411 (s), 3234 (s), 2025 (w), 1692 (m), 1637 (s), 1616 (vs), 1545 (m), 1502 (m), 1443 (m), 1384 (m), 1329 (m), 1134 (m), 1108 (m), 1088 (m), 1031 (m), 1005 (w), 963 (w), 870 (w), 772 (w), 745 (w), 696 (w), 622 (m), 571 (w), 482 (m). – Raman (1064 nm, 200 mW, 25 °C, cm^{-1}): $\tilde{\nu}$ = 3319 (4), 3255 (13), 1659 (5), 1616 (4), 1580 (32), 1381 (13), 1287 (32), 1190 (5), 1111 (39), 1019 (5), 961 (100), 770 (27), 483 (30), 419 (33), 378 (10), 248 (13). – ^1H NMR ($[\text{D}_6]\text{DMSO}$, 25 °C, ppm): δ = 9.29 (s, 1 H, NH), 8.23 (s, 1H, C-NH_AH_B), 7.52 (s, 1H, C-NH_AH_B), 4.64 (s, 2H, N-NH₂). – ^{13}C NMR ($[\text{D}_6]\text{DMSO}$, 25 °C, ppm): δ = 161.5 (C(NNO₂)(N₂H₄)(NH₂)). – ^{15}N NMR ($[\text{D}_6]\text{DMSO}$, 25 °C, ppm): δ = -13.3 (NO₂), -146.3 (NNO₂), -276.4 (NH/NH₂), -301.8 (NH/NH₂), -327.9 (NH/NH₂). – MS ((-)-FAB): m/z = 117.99 [M-H]⁻. – CH₅N₅O₂ (119.08): calcd. C 10.09, H 4.23, N 58.81 %; found C 10.51, H 4.32, N 58.90 %. – BAM drophammer: 20 J. – Friction tester: 144 N. – ESD: 0.15 J (at grain size 100–500 μm).

1-Amino-3-nitroguanidinium nitrate (3)

2 (5.00 g, 42.0 mmol) is dissolved in warm nitric acid (40 %, 12.71 g, 84.0 mmol). The yellowish, clear solution is left for crystallization. **3** crystallizes in large, colorless blocks after a few hours (yield: 7.12 g, 39.1 mmol, 93 %). – DSC (5 °C min⁻¹): 130 °C (dec.). – IR (KBr, cm^{-1}): $\tilde{\nu}$ = 3397 (m), 3293 (m), 3090 (m), 1648 (s), 1581 (s), 1470 (s), 1384 (vs), 1281 (vs), 1215 (s), 1166 (m), 1112 (m), 1050 (w), 1014 (w), 913 (w), 823 (w), 785 (w), 708 (w), 625 (w), 568 (w). – Raman (1064 nm, 500 mW, 25 °C, cm^{-1}): $\tilde{\nu}$ = 3319 (2), 3046 (2), 1623 (8), 1578 (11), 1494 (6), 1373 (4), 1263 (37), 1218 (9), 1168 (7), 1053 (100), 1010 (6), 921 (12), 803 (20), 788 (4), 735 (4), 712 (4), 626 (20), 440 (9), 358 (18), 256 (14), 173 (16), 112 (9). – ^1H NMR ($[\text{D}_6]\text{DMSO}$, 25 °C, ppm): δ = 9.53 (s, 5 H, NH₂), 8.38 (s, 1H, NH-NH₂). – ^{13}C NMR ($[\text{D}_6]\text{DMSO}$, 25 °C, ppm): δ = 159.3 (C(NNO₂)(N₂H₄⁺)(NH₂)). – ^{14}N NMR ($[\text{D}_6]\text{DMSO}$, 25 °C, ppm): δ = -7 (NO₂), -15 (NO₃). – MS ((+)-FAB): m/z = 120 [C(NNO₂)(NH₂)(NHNH₃)]⁺. – MS ((-)-FAB): m/z = 62 [NO₃]⁻. – CH₆N₆O₅ (182.04): calcd. C 6.60, H 3.32, N 46.15 %; found C 6.49, H 3.30, N 45.82 %. – BAM drophammer: 10 J. – Friction tester: 120 N (neg.). – ESD: 0.5 J (at grain size 500–1000 μm).

1-Amino-3-nitroguanidinium perchlorate (4)

2 (1.19 g, 10 mmol) is dissolved in 1M HClO₄ (20 mL, 20 mmol) under moderate heating to 60 °C. **4** crystallizes from the clear solution in colorless blocks. Yield: 4.16 g, 18.9 mmol, 95 %. – DSC (5 °C min⁻¹): 108 °C (dec.). – IR (ATR, cm^{-1}): $\tilde{\nu}$ = 3387 (m), 3293 (m), 3084 (m, br), 3008 (m, br), 2891 (m, br), 2753 (m, br), 2686 (m, br), 2168 (w), 1705 (m), 1634 (m), 1559 (m), 1484 (m), 1450 (m), 1373

(m, br), 1270 (m, br), 1089 (vs, br), 1019 (s, br), 930 (s), 785 (m), 687 (w). – Raman (1064 nm, 400 mW, 25 °C, cm^{-1}): $\tilde{\nu}$ = 3336 (3), 1623 (6), 1572 (10), 1491 (14), 1264 (28), 1159 (9), 1107 (10), 1038 (4), 1001 (11), 933 (100), 799 (25), 634 (35), 472 (15), 453 (17), 436 (8), 359 (32), 285 (9). – ^1H NMR ($[\text{D}_6]\text{DMSO}$, 25 °C, ppm): δ = 9.03 (s, NH-NH₃⁺), 8.37 (s, NH₂). – ^{13}C NMR ($[\text{D}_6]\text{DMSO}$, 25 °C, ppm): δ = 159.0 (C(NNO₂)(N₂H₄⁺)(NH₂)). – MS ((+)-FAB): m/z = 120.1 [C(NNO₂)(N₂H₃)(NH₂)+H]⁺. – MS ((-)-FAB): m/z = 98.9 [ClO₄]⁻. – CH₆ClN₅O₆ (219.54): calcd. C 5.47, H 2.75, N 31.90 %; found C 5.70, H 2.80, N 31.28 %. – BAM drophammer: 1 J. – Friction tester: 20 N. – ESD: 0.15 J (at grain size 100–500 μm).

1-Amino-3-nitroguanidinium 5-nitriminotetrazolate dihydrate (5)

2 (1.19 g, 10 mmol) is dissolved in a few milliliters of boiling water. The solution is cooled to 70 °C, and then a solution of 5-nitriminotetrazole (1.63 g, 11 mmol) is added slowly. The solvent is removed *in vacuo* and the residue recrystallized from an ethanol/water mixture. Yield: 2.17 g (7.6 mmol, 76 %). – DSC (5 °C min⁻¹): 136 °C (dec.). – IR (KBr, cm^{-1}): $\tilde{\nu}$ = 3358 (vs), 3126 (s), 2939 (s), 2736 (s, br), 1658 (s), 1591 (s), 1531 (s), 1489 (s), 1436 (s), 1384 (s), 1313 (s), 1267 (s), 1210 (s), 1167 (m), 1144 (m), 1117 (m), 1087 (m), 1042 (s), 918 (w), 870 (w), 789 (w), 738 (w), 638 (m), 489 (w), 457 (w). – Raman (1064 nm, 300 mW, 25 °C, cm^{-1}): $\tilde{\nu}$ = 3908 (2), 3701 (2), 3355 (3), 3106 (3), 1581 (2), 1534 (100), 1437 (2), 1382 (3), 1315 (25), 1272 (6), 1144 (5), 1030 (34), 1010 (16), 925 (5), 874 (4), 799 (5), 757 (3), 630 (5), 457 (3), 415 (3), 376 (2), 251 (3), 113 (4), 85 (31). – ^1H NMR ($[\text{D}_6]\text{DMSO}$, 25 °C, ppm): δ = 8.15 (s, NH), 7.13 (NH₂). – ^{13}C NMR ($[\text{D}_6]\text{DMSO}$, 25 °C, ppm): δ = 160.7 (C(NNO₂)(N₂H₄⁺)(NH₂)), 154.7 (CN₄). – MS ((+)-FAB): m/z = 120.2 [C(NNO₂)(N₂H₄)(NH₂)]⁺. – MS ((-)-FAB): m/z = 129.1 [HATNO₂]⁻. – C₂H₁₁N₁₁O₆ (281.15): calcd. C 8.42, H 3.89, N 54.03 %; found C 8.51, H 3.85, N 54.01 %. – BAM drophammer: 5 J. – Friction tester: 96 N. – ESD: 0.4 J (at grain size 100–500 μm).

1-Amino-3-nitroguanidinium dinitramide monohydrate (6)

10 mmol of silver dinitramide acetonitrile adduct was prepared according to the literature [9]. 1-Amino-3-nitroguanidinium chloride (1.47 g, 9.4 mmol) is dissolved in 10 mL of boiling water. After cooling the solution to about 60 °C, the silver dinitramide acetonitrile adduct, dissolved in 5 mL of acetonitrile is added dropwise to the solution. After complete addition, the mixture is stirred under the exclusion of light at 35 °C for further 2 h. The mixture is cooled to 5 °C in a refrigerator and then filtered. **6** crystallizes from the clear filtrate in colorless blocks. Yield: 1.34 g (5.5 mmol, 59 %). – DSC (5 °C min⁻¹): 66 °C (dehydr.), 108 °C (dec.). – IR

(ATR, cm^{-1}): $\tilde{\nu}$ = 3535 (w), 3413 (m), 3296 (m), 3121 (m), 2736 (m), 1633 (m), 1579 (m), 1508 (m), 1467 (m), 1429 (m), 1387 (m), 1324 (w), 1265 (m), 1167 (s), 1037 (m), 994 (m), 905 (m), 823 (w), 783 (w), 760 (m), 740 (w). – Raman (1064 nm, 400 mW, 25 °C, cm^{-1}): $\tilde{\nu}$ = 3333 (4), 3133 (4), 1574 (24), 1528 (20), 1491 (27), 1426 (17), 1397 (23), 1340 (90), 1331 (84), 1320 (100), 1258 (78), 1199 (19), 1182 (22), 1161 (21), 1105 (6), 1035 (45), 993 (11), 964 (31), 920 (40), 826 (95), 805 (54), 762 (12), 622 (43), 497 (44), 442 (23), 362 (21), 316 (12), 298 (16), 252 (7). – ^1H NMR ($[\text{D}_6]\text{DMSO}$, 25 °C, ppm): δ = 8.37 (s, 1H, NH), 6.90 (s, 5H, $-\text{NH}_2$, $-\text{NH}_3^+$). – ^{13}C NMR ($[\text{D}_6]\text{DMSO}$, 25 °C, ppm): δ = 159.2 (C(NNO₂)(N₂H₄⁺)(NH₂)). – ^{14}N NMR ($[\text{D}_6]\text{DMSO}$, 25 °C, ppm): δ = –10 (N(NO₂)₂), –15 (N-NO₂). – MS ((+)-FAB): m/z = 119.9 [C(NNO₂)(N₂H₃)(NH₂)+H]⁺. – MS ((–)-FAB): m/z = 106.1 [N(NO₂)₂][–]. – CH₈N₈O₇(244.12): calcd. C 4.92, H 3.30, N 45.90%; found C 4.74, H 3.23, N 44.40%. – BAM drophammer: 10 J. – Friction tester: 40 N. – ESD: 0.10 J (at grain size 500–1000 μm).

1-Amino-3-nitroguanidinium dinitroguanidinate pentahemihydrate (7)

Dinitroguanidine (1.49 g, 10 mmol) is dissolved in 10 mL of hot water and poured onto neat **2** (1.19 g, 10 mmol). The suspension is heated until no precipitate is observed any more and then filtered. The filtrate shows evolution of gas and turns to light yellow. A yellow, amorphous precipitate starts to form, which is filtered off again. From the mother liquor, **7** precipitates in colorless blocks on standing for a few minutes. Yield: 1.85 g (5.9 mmol, 59%). – DSC

(5 °C min^{–1}): 79 °C (dehydr.), 118 °C (dec.). – IR (KBr, cm^{-1}): $\tilde{\nu}$ = 3605 (m), 3409 (s), 3377 (s), 3205 (m), 2672 (m), 1619 (s), 1492 (m), 1384 (m), 1357 (m), 1259 (vs), 1218 (vs), 1150 (m), 1112 (m), 1063 (m), 974 (w), 915 (w), 785 (m), 764 (w), 720 (w), 680 (m), 636 (m), 589 (w), 550 (w). – Raman (1064 nm, 500 mW, 25 °C, cm^{-1}): $\tilde{\nu}$ = 3440 (5), 3199 (9), 1609 (15), 1578 (15), 1456 (22), 1370 (38), 1310 (5), 1254 (19), 1191 (35), 1154 (100), 1060 (24), 977 (54), 917 (8), 792 (32), 631 (14), 553 (22), 554 (6), 352 (24), 231 (13). – ^1H NMR ($[\text{D}_6]\text{DMSO}$, 25 °C, ppm): δ = 9.74 (s), 9.52 (s), 8.59 (s), 8.14 (s), 5.30 (s). – ^{13}C NMR ($[\text{D}_6]\text{DMSO}$, 25 °C, ppm): δ = 161.4 (C(NNO₂)(N₂H₃)(NH₂)), 160.3 (C(NNO₂)(N₂H₄⁺)(NH₂)), 159.5 (C(NH₂)(N-NO₂)₂). – ^{14}N NMR ($[\text{D}_6]\text{DMSO}$, 25 °C, ppm): δ = –15 (CNNO₂), –19 (CNNO₂)₂. – MS ((+)-FAB): m/z = 120.1 [C(NNO₂)(N₂H₄)(NH₂)⁺]. – MS ((–)-FAB): m/z = 147.9 [C(NH₂)(N-NO₂)₂][–]. – C₂H₁₃N₁₀O_{8.5}(313.09): calcd. C 7.67, H 4.18, N 44.72%; found C 7.90, H 4.20, N 45.43%. – BAM drophammer: 12 J. – Friction tester: 288 N. – ESD: 0.20 J (at grain size 100–500 μm).

Acknowledgement

Financial support of this work by the Ludwig-Maximilian University of Munich (LMU), the US Army Research Laboratory (ARL), the Armament Research, Development and Engineering Center (ARDEC), the Strategic Environmental Research and Development Program (SERDP), and the Office of Naval Research (ONR). Mr. S. Huber is thanked for the sensitivity measurements. The authors also thank Prof. Dr. K. Karaghiosoff for help with the NMR spectra and Dr. K. Lux for crystallographic support.

- [1] A. W. Hofmann, *J. Chem. Soc. Trans.* **1866**, 19, 249–255.
- [2] a) R. G. S. Berlinck, A. C. B. Burtoloso, A. E. Trindade-Silva, S. Romminger, R. P. Morais, K. Bandeira, C. M. Mizuno, *Nat. Prod. Rep.* **2010**, 27, 1871–1907; b) F. Saczewski, L. Balewski, *Expert Opin. Ther. Pat.* **2009**, 19, 1417–1448.
- [3] T. E. O'Connor, K. Horgan and J. Reilly, *J. Appl. Chem.* **1951**, 1, 91–92.
- [4] a) L. Jousselin, *Compt. Rend.* **1879**, 88, 1086; b) G. Pellizzari, *Gazz. Chim. Ital.* **1891**, 21, 405–409.
- [5] A. A. Astrat'yev, D. V. Dashko, L. L. Kuznetsov, *Russ. J. Org. Chem.* **2003**, 3, 501–512.
- [6] C. Gonzalez, G. Ballester, M. A. Rodriguez, 40th International Annual Conference of ICT (Energetic Materials), **2009**, 44/1–44/11.
- [7] J. A. Castillo-Meléndez, B. T. Golding, *Synthesis* **2004**, 10, 1655–1663.
- [8] R. A. Henry, H. D. Lewis, G. B. L. Smith, *J. Am. Chem. Soc.* **1950**, 72, 2015.
- [9] R. Phillips, J. F. Williams, *J. Am. Chem. Soc.* **1928**, 50, 2465.
- [10] A. F. McKay, *Chem. Rev.* **1952**, 51, 301–346.
- [11] J. Stierstorfer, T. M. Klapötke, *Helv. Chim. Acta* **2007**, 90, 2132–2150.
- [12] T. M. Klapötke, B. Krumm, M. Scherr, *Dalton Trans.* **2008**, 43, 5876–5878.
- [13] CRYSLISPRO (version 1.171.35.11), Agilent Technologies, Loveland, Colorado (USA) **2011**.
- [14] a) G. M. Sheldrick, SHELXS-97, Program for the Solution of Crystal Structures, University of Göttingen, Göttingen (Germany) **1997**. See also: G. M. Sheldrick, *Acta Crystallogr.* **1990**, A46, 467–473; b) A. Altomare, G. Cascarano, C. Giacovazzo, A. Gugliardi, M. C. Burla, G. Polidori, M. Camalli, SIR92, A Program for Automatic Solution of Crystal Structures

- by Direct Methods; see: A. Altomare, G. Cascarano, C. Giacovazzo, A. Guagliardi, M. C. Burla, G. Polidori, M. Camalli, *J. Appl. Crystallogr.* **1994**, 27, 435; A. Altomare, G. Cascarano, C. Giacovazzo, A. Guagliardi, *J. Appl. Crystallogr.* **1993**, 26, 343–350.
- [15] G. M. Sheldrick, SHELXL-97, Program for the Refinement of Crystal Structures, University of Göttingen, Göttingen (Germany) **1997**. See also: G. M. Sheldrick, *Acta Crystallogr.* **2008**, A64, 112–122.
- [16] A. L. Spek, PLATON, A Multipurpose Crystallographic Tool, Utrecht University, Utrecht (The Netherlands) **2010**. See also: A. L. Spek, *J. Appl. Crystallogr.* **2009**, D65, 148–155.
- [17] L. J. Farrugia, WINGX, A MS-Windows System of Programs for Solving, Refining and Analysing Single Crystal X-ray Diffraction Data for Small Molecules, University of Glasgow, Glasgow, Scotland (UK) **2005**. See also: L. J. Farrugia, *J. Appl. Crystallogr.* **1999**, 32, 837–838.
- [18] CCDC 831494 (2), 831496 (3), 831492 (4), 831491 (5), 831493 (6), and 831495 (7) contain the supplementary crystallographic data for this paper. These data can be obtained free of charge from The Cambridge Crystallographic Data Centre via www.ccdc.cam.ac.uk/data_request/cif.
- [19] S. R. Naidu, N. M. Bhide, K. V. Prabhakaran, E. M. Kurian, *J. Thermal Anal.* **1995**, 44, 1449–1462.
- [20] A. Martin, A. A. Pinkerton, *Acta Crystallogr.* **1996**, C52, 1048–1052.
- [21] N. Fischer, T. M. Klapötke, D. Piercey, S. Scheutzw, J. Stierstorfer, *Z. Anorg. Allg. Chem.* **2010**, 636, 2357–2363.
- [22] T. M. Klapötke, J. Stierstorfer, B. Weber, *Inorg. Chim. Acta* **2009**, 362, 2311–2320.
- [23] T. Altenburg, T. M. Klapötke, A. Penger, J. Stierstorfer, *Z. Anorg. Allg. Chem.* **2010**, 636, 463–471.
- [24] J. Stierstorfer, T. M. Klapötke, A. U. Wallek, *Chem. Mater.* **2008**, 20, 4519–4530.
- [25] NATO standardization agreement (STANAG) on explosives, impact sensitivity tests, no. 4489, 1st ed., September 17, **1999**.
- [26] WIWEB-Standardarbeitsanweisung 4–5.1.02, Ermittlung der Explosionsgefährlichkeit, hier der Schlagempfindlichkeit mit dem Fallhammer, Nov. 8, **2002**.
- [27] <http://www.bam.de> (retrieved April 2, **2012**).
- [28] NATO standardization agreement (STANAG) on explosive, friction sensitivity tests, no. 4487, 1st ed., Aug. 22, **2002**.
- [29] WIWEB-Standardarbeitsanweisung 4–5.1.03, Ermittlung der Explosionsgefährlichkeit oder der Reibempfindlichkeit mit dem Reibeapparat, Nov. 8, **2002**.
- [30] Impact: insensitive > 40 J, less sensitive > 35 J, sensitive > 4 J, very sensitive < 3 J. Friction: insensitive > 360 N, less sensitive = 360 N, sensitive < 360 N and > 80 N, very sensitive < 80 N, extremely sensitive < 10 N. According to the UN Recommendations on the Transport of Dangerous Goods, (+) indicates not safe for transport.
- [31] <http://www.ozm.cz> (retrieved April 2, **2012**).
- [32] <http://www.linseis.com> (retrieved April 2, **2012**).
- [33] M. J. Frisch, G. W. Trucks, H. B. Schlegel, G. E. Scuseria, M. A. Robb, J. R. Cheeseman, G. Scalmani, V. Barone, B. Mennucci, G. A. Petersson, H. Nakatsuji, M. Caricato, X. Li, H. P. Hratchian, A. F. Izmaylov, J. Bloino, G. Zheng, J. L. Sonnenberg, M. Hada, M. Ehara, K. Toyota, R. Fukuda, J. Hasegawa, M. Ishida, T. Nakajima, Y. Honda, O. Kitao, H. Nakai, T. Vreven, J. A. Montgomery Jr., J. E. Peralta, F. Ogliaro, M. Bearpark, J. J. Heyd, E. Brothers, K. N. Kudin, V. N. Staroverov, R. Kobayashi, J. Normand, K. Raghavachari, A. Rendell, J. C. Burant, S. S. Iyengar, J. Tomasi, M. Cossi, N. Rega, J. M. Millam, M. Klene, J. E. Knox, J. B. Cross, V. Bakken, C. Adamo, J. Jaramillo, R. Gomperts, R. E. Stratmann, O. Yazyev, A. J. Austin, R. Cammi, C. Pomelli, J. W. Ochterski, R. L. Martin, K. Morokuma, V. G. Zakrzewski, G. A. Voth, P. Salvador, J. J. Dannenberg, S. Dapprich, A. D. Daniels, Ö. Farkas, J. B. Foresman, J. V. Ortiz, J. Cioslowski, D. J. Fox, GAUSSIAN 09 (revision A.1), Gaussian, Inc., Wallingford CT (USA) **2009**.
- [34] P. J. Linstrom, W. G. Mallard (Eds.), *NIST Chemistry WebBook*, NIST Standard Reference Database Number 69, National Institute of Standards and Technology, Gaithersburg MD, **2005**; <http://webbook.nist.gov> (retrieved October 27, **2011**).
- [35] a) H. D. B. Jenkins, H. K. Roobottom, J. Passmore, L. Glasser, *Inorg. Chem.* **1999**, 38, 3609–3620; b) H. D. B. Jenkins, D. Tudela, L. Glasser, *Inorg. Chem.* **2002**, 41, 2364–2367.
- [36] a) M. S. Westwell, M. S. Searle, D. J. Wales, D. H. Williams, *J. Am. Chem. Soc.* **1995**, 117, 5013–5015; b) F. Trouton, *Philos. Mag.* **1884**, 18, 54–57.
- [37] M. Sueska, EXPLO5.04 program, Zagreb (Croatia) **2010**.
- [38] Calculation of oxygen balance: $\Omega(\%) = (wO - 2xC - 1/2yH - 2zS) \cdot 1600/M$ (w : number of oxygen atoms, x : number of carbon atoms, y : number of hydrogen atoms, z : number of sulfur atoms).
- [39] J. Li, B. Duke, R. McWeeny, VB2000 (version 2.1), SciNet Technologies, San Diego, CA (USA) **2011**; <http://www.scinetec.com/> (retrieved April 2, **2012**). See also: J. Li, R. McWeeny, *Int. J. Quantum Chem.* **2002**, 89, 208–216.
- [40] a) R. D. Harcourt, T. M. Klapötke, *Research Trends Inorg. Chem.* **2006**, 9, 11–22; and references therein;

- b) R. D. Harcourt, *Qualitative Valence-Bond Descriptions of Electron-Rich Molecules: Pauling "3-Electron Bonds" and "Increased-Valence Theory"*, Lecture Notes in Chemistry, Vol. 30, Springer, Berlin, Heidelberg, New York, **1982**; c) R. D. Harcourt, *Eur. J. Inorg. Chem.* **2000**, 1901–1916; d) T. M. Klapötke, A. Schulz with an invited chapter by R. D. Harcourt, *Quantum Chemical Methods in Main-Group Chemistry*, J. Wiley, Chichester, **1998**; e) T. M. Klapötke, Nichtmetallchemie, in *Moderne Anorganische Chemie*, (Ed.: E. Riedel), 3rd ed., Walter de Gruyter, Berlin, New York, **2007**.
- [41] a) J. E. Carpenter, F. Weinhold, *J. Mol. Struct. (Theochem.)* **1988**, 169, 41; b) J. P. Foster, F. Weinhold, *J. Am. Chem. Soc.* **1980**, 102, 7211; c) A. E. Reed, F. Weinhold, *J. Chem. Phys.* **1983**, 78, 4066; d) A. E. Reed, F. Weinhold, *J. Chem. Phys.* **1983**, 1736; e) A. E. Reed, R. B. Weinstock, F. Weinhold, *J. Chem. Phys.* **1985**, 83, 735; f) A. E. Reed, L. A. Curtiss, F. Weinhold, *Chem. Rev.* **1988**, 88, 899; g) F. Weinhold, J. E. Carpenter, *Plenum* **1988**, 227.
- [42] R. C. West, S. M. Selby, *Handbook of Chemistry and Physics*, 48th ed., The Chemical Rubber Co., Cleveland, **1967**, pp. D22–D51.
- [43] V. A. Ostrovskii, M. S. Pevzner, T. P. Kofman, I. V. Tselinskii, *Targets Heterocycl. Syst.* **1999**, 3, 467.
- [44] J. Köhler, R. Meyer, *Explosivstoffe*, 9th ed., Wiley-VCH, Weinheim, **1998**, pp. 166–168.

Article

Synthesis and Crystal Structures of New 5,5'-Azotetrazolates

Gerhard Laus¹, Volker Kahlenberg², Klaus Wurst¹, Herwig Schottenberger¹, Niko Fischer³, Jörg Stierstorfer³ and Thomas M. Klapötke^{3,*}

¹ Faculty of Chemistry and Pharmacy, University of Innsbruck, 6020 Innsbruck, Austria;
E-Mails: gerhard.laus@uibk.ac.at (G.L.); klaus.wurst@uibk.ac.at (K.W.);
herwig.schottenberger@uibk.ac.at (H.S.)

² Institute of Mineralogy and Petrography, University of Innsbruck, 6020 Innsbruck, Austria;
E-Mail: volker.kahlenberg@uibk.ac.at (V.K.)

³ Department of Chemistry, University of Munich (LMU), 81377 Munich, Germany;
E-Mails: finch@cup.uni-muenchen.de (N.F.); jstch@cup.uni-muenchen.de (J.S.)

* Author to whom correspondence should be addressed; E-Mail: tmk@cup.uni-muenchen.de;
Tel.: +49-89-2180-77491; Fax: +49-89-2180-77492 (T.M.K.).

Received: 27 December 2011; in revised form: 21 February 2012 / Accepted: 29 February 2012 /
Published: 15 March 2012

Abstract: Five new 5,5'-azotetrazolate salts (amminsilver, trimethylsulfonium, tetramethyl-phosphonium, trimethylsulfoxonium, 2-(hydroxyethyl)trimethylammonium) were prepared and characterized. The crystal structures were determined by X-ray diffraction. Interactions between the ions are identified and discussed. The sensitivities of the highly energetic silver salt were measured by BAM (Bundesanstalt für Materialforschung und-prüfung) methods.

Keywords: azotetrazolate; cholin; phosphonium; silver; sulfonium; sulfoxonium

1. Introduction

Nitrogen-rich “energetic salts” have received considerable attention as propellants or gas generators [1,2]. These salts typically contain cations such as hydrazinium [3–5], ammonium and guanidinium [6], triazolium [7–10], tetrazolium [11,12], or tetraaminopiperazinium [13], sometimes involving additional azido groups [6,10]. Preferred anions are—beside azide, nitrate, perchlorate and picrate—dinitramide [7], nitroazolates [7,10,14,15], dianions such as 5,5'-bis(tetrazolate) [16] and, in

particular, 5,5'-azotetrazolate [3–6,11,12,16]. The synthesis of 5,5'-azotetrazolates was first reported by Thiele [17]. Beyond the much acclaimed use as explosives, nitrogen-rich heterocycles are also of interest as ligands in coordination chemistry. With respect to their performance as potential explosives or propellants powerful materials are obtained when nitrogen-rich cations (e.g., hydrazinium, guanidinium) are used. When ions with lower nitrogen and higher carbon content are employed, the resulting less energetic materials are still relevant. Due to their electrochemical or optical properties, technical applications such as molecular electronics are envisioned [18]. They also have potential as precursors of functional materials, for example in the synthesis of low-density, nanoporous metal foams [19].

Numerous crystal structures of 5,5'-azotetrazolate salts [3–8,11–13,16,20,21] have been reported, including a series of metal salts; specifically, alkali and alkaline earth metals [22,23], lanthanoids [24–26], Pb [27], Tl [28], Mn [29], Fe [30], Cu and Cd [31] form crystalline salts.

In the present work 5,5'-azotetrazolate salts comprising cations based on sulfur or phosphorus are reported. A not yet described salt of choline and a new energetic silver complex are also disclosed, the latter one showing high sensitivities belonging to the class of primary explosives.

2. Results and Discussion

The silver complex was prepared by slow diffusion of the components. The incorporated ammonia molecule has a phlegmatizing effect causing the product to be less sensitive than the pure silver salt. The other salts were synthesized by two metathetical steps (the $\text{Ag}_2\text{SO}_4/\text{Ba}$ azotetrazolate method) starting from the respective halogenides. Satisfactory crystals could be obtained with little effort by slow evaporation of solutions in water or methanol. The structures reported herein are centrosymmetric. In all cases the asymmetric unit contained one half of the planar azotetrazolate ion which is completed by inversion. The crystallographic data and structure refinement parameters of all structures **1–5** are gathered in Table 1.

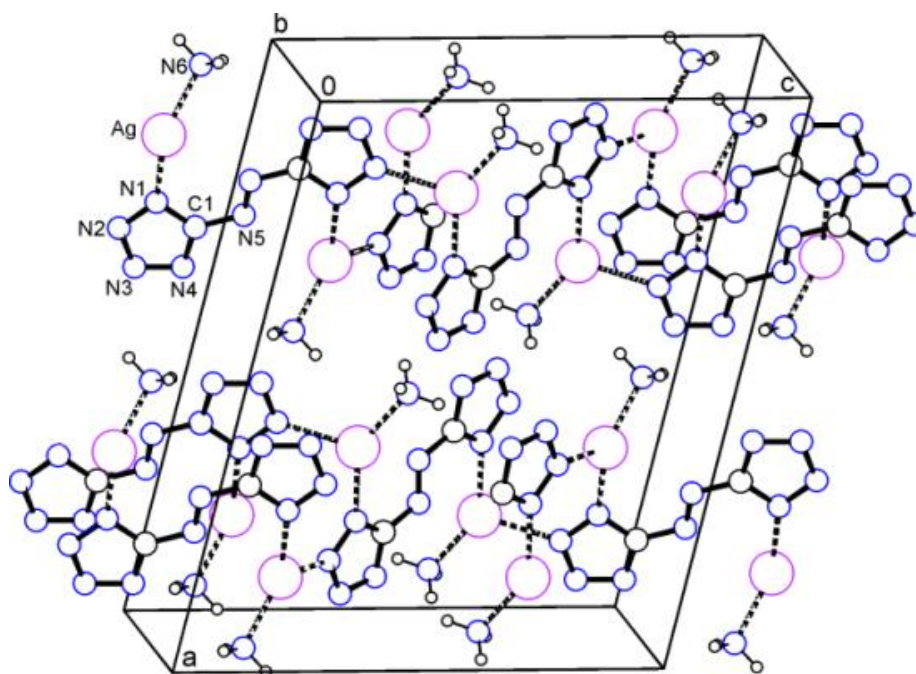
Table 1. Crystal data and structure refinement details for compounds **1–5**.

Compound	1	2	3	4	5
CCDC no.	846911	846912	846913	846914	846915
Chemical formula	Ag ₂ (NH ₃) ₂ (C ₂ N ₁₀)	(C ₃ H ₉ S) ₂ (C ₂ N ₁₀)	(C ₄ H ₁₂ P) ₂ (C ₂ N ₁₀)	(C ₃ H ₉ OS) ₂ (C ₂ N ₁₀)	(C ₃ H ₁₄ NO) ₂ (C ₂ N ₁₀)
<i>M_r</i>	413.89	318.43	346.31	350.42	372.43
Crystal shape, color	plate, orange	prism, yellow	plate, orange	fragment, yellow	fragment, yellow
Crystal size/mm ³	0.1 × 0.1 × 0.06	0.44 × 0.36 × 0.24	0.36 × 0.32 × 0.12	0.2 × 0.2 × 0.2	0.40 × 0.24 × 0.24
Crystal system	monoclinic	triclinic	monoclinic	monoclinic	triclinic
Space group	<i>C</i> 2/ <i>c</i>	<i>P</i> $\bar{1}$	<i>P</i> 2 ₁ / <i>c</i>	<i>P</i> 2 ₁ / <i>n</i>	<i>P</i> $\bar{1}$
<i>a</i> /Å	18.0338(7)	5.9032(7)	5.9035(9)	5.2452(2)	5.4900(4)
<i>b</i> /Å	3.601(2)	7.4591(8)	13.388(2)	14.0290(4)	8.4206(6)
<i>c</i> /Å	14.906(3)	9.2538(8)	11.3173(19)	10.7735(4)	10.3003(6)
α /°	90	113.598(9)	90	90	78.564(5)
β /°	91.94(1)	98.370(8)	93.941(17)	102.036(3)	85.796(6)
γ /°	90	99.017(9)	90	90	81.876(6)
<i>V</i> /Å ³	967.4(6)	358.88(7)	892.4 (2)	775.34 (5)	461.53(6)
<i>Z</i>	8	2	4	4	2
<i>D_x</i> /g cm ^{−3}	2.84	1.47	1.29	1.50	1.34
μ /mm ^{−1}	4.04	0.38	0.26	0.37	0.10
<i>F</i> (000)/e	784	168	368	368	200
Diffractometer	Nonius KappaCCD	Gemini Ultra	Gemini-R Ultra	Gemini-R Ultra	Gemini-R Ultra
Data collection method	φ and ω scans	ω scans	ω scans	Ω scans	ω scans
Temperature/K	233	173	173	173	173
θ_{\max} /°	24	25.4	25	28	25
<i>h, k, l</i> range	−19 ≤ <i>h</i> ≤ 20 −4 ≤ <i>k</i> ≤ 3 −16 ≤ <i>l</i> ≤ 17	−6 ≤ <i>h</i> ≤ 7 −8 ≤ <i>k</i> ≤ 5 −10 ≤ <i>l</i> ≤ 11	−5 ≤ <i>h</i> ≤ 7 −14 ≤ <i>k</i> ≤ 16 −15 ≤ <i>l</i> ≤ 13	−6 ≤ <i>h</i> ≤ 6 −18 ≤ <i>k</i> ≤ 17 −13 ≤ <i>l</i> ≤ 13	−6 ≤ <i>h</i> ≤ 5 −10 ≤ <i>k</i> ≤ 10 −12 ≤ <i>l</i> ≤ 10
Absorption correction	none	multi-scan	multi-scan	multi-scan	none
Measured reflections	1927	2168	3626	6332	3070
Independent reflections (<i>R</i> _{int})	739 (0.028)	1288 (0.024)	1760 (0.021)	1723 (0.021)	1686 (0.030)
Observed reflections [<i>I</i> ≥ 2σ(<i>I</i>)]	620	1162	1461	1573	1449
Restraints / parameters	0/75	0/94	0/104	0/103	0/123
<i>R</i> ₁ / <i>wR</i> ₂ [<i>I</i> ≥ 2σ(<i>I</i>)]	0.037/0.097	0.030/0.070	0.030/0.079	0.028/0.070	0.035/0.095
<i>R</i> ₁ / <i>wR</i> ₂ (all data)	0.046/0.104	0.035/0.073	0.039/0.082	0.031/0.072	0.042/0.098
Goodness of fit	1.09	1.06	1.08	1.05	1.03
$\Delta\rho_{\max/\min}$ /e Å ^{−3}	1.38/−0.81	0.24/−0.25	0.27/−0.24	0.34/0.31	0.19/−0.17

2.1. Bis(amminsilver(I)) 5,5'-Azotetrazolate (1)

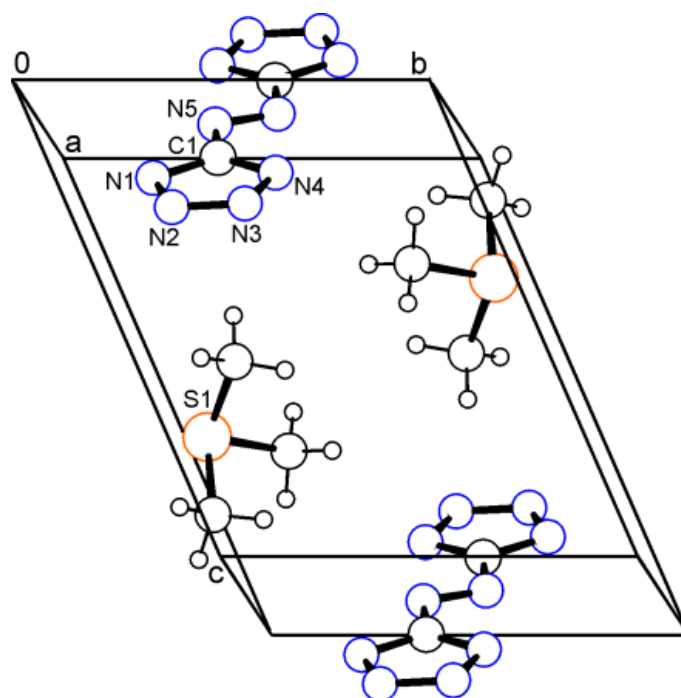
The silver ion in compound **1** coordinates to two nitrogen atoms of two azotetrazolate anions and to the ammonia molecule. Short contacts observed are Ag...N1 (2.255(5) Å), Ag...N2ⁱ (2.342(5) Å), and Ag...N6 (2.205(6) Å), respectively (Figure 1). Symmetry operation *i*: $1/2 - x, 1/2 + y, 1/2 - z$. These interionic contacts assemble a layer structure parallel to the *bc*-plane.

Figure 1. Packing diagram of Ag salt **1**. Dashed lines represent the Ag...N interactions. Layers are arranged parallel to the *bc*-plane.



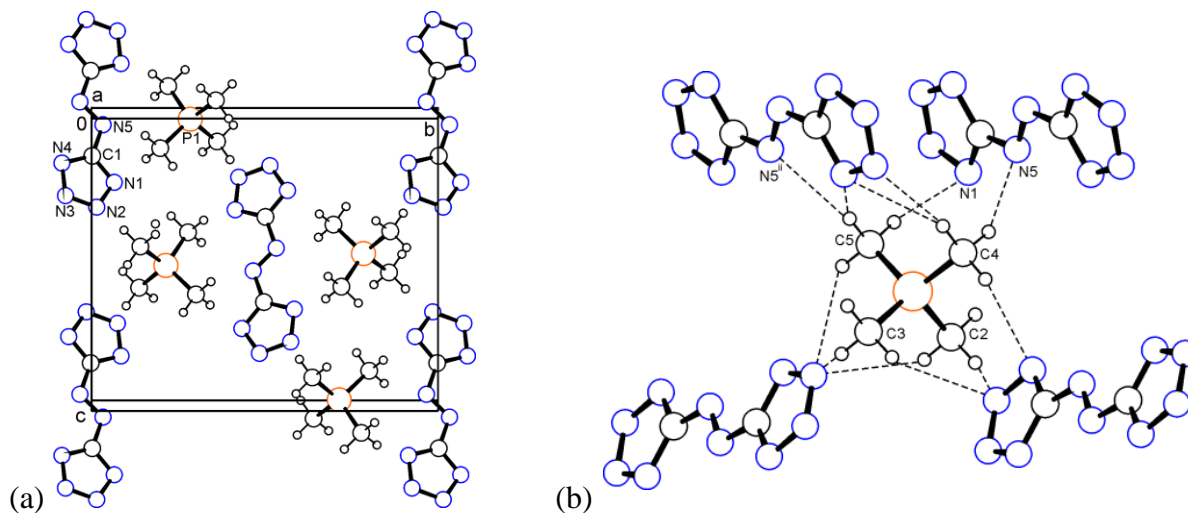
2.2. Bis(trimethylsulfonium) 5,5'-Azotetrazolate (2)

In contrast, no directional interactions are found in salt **2**. This aggregate consists of discrete ions and is predominantly stabilized by electrostatic forces. The $(\text{CH}_3)_3\text{S}^+$ cation is pyramidal and exhibits approximately $3m$ symmetry as found in other trimethylsulfonium salts in the literature [32]. The C–S bond lengths are equal within the experimental error (1.782(2) Å), and the C–S–C angles differ only slightly (100.3, 101.6 and 102.4°). As discussed previously [33], the electron lone pair is not a structure-determining factor. The shortest distance between neighbouring S atoms is 3.742 Å. The unit cell is shown in Figure 2.

Figure 2. Packing diagram of trimethylsulfonium salt **2**.

2.3. Bis(tetramethylphosphonium) 5,5'-Azotetrazolate (**3**)

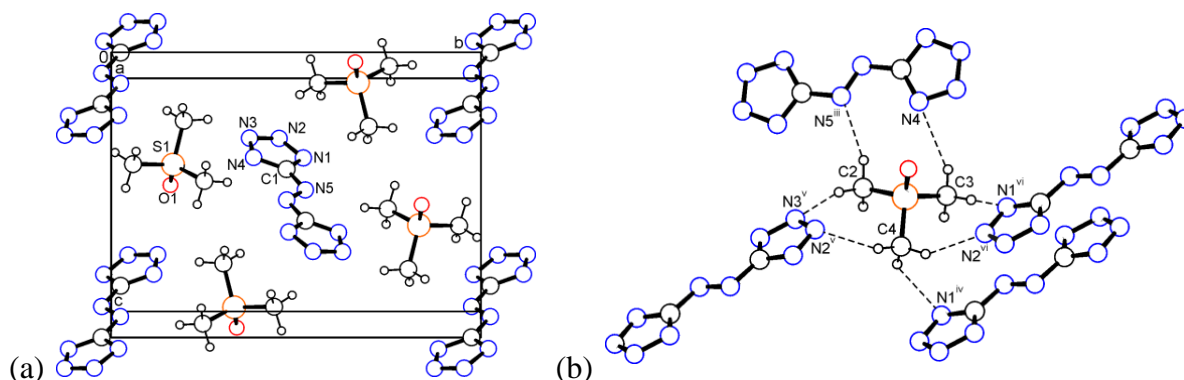
The $(\text{CH}_3)_4\text{P}^+$ cation in **3** shows only small deviations from ideal tetrahedral geometry. The C–P bond lengths range from 1.772 to 1.777 Å, and the C–P–C angles from 107.9 to 110.4°. The shortest distance between neighbouring P atoms is 5.736 Å. The crystal packing is shown in Figure 3a. There is a number of weak C–H \cdots N contacts in this structure with three of them being considerably shorter than the sum of van der Waals radii. Thus, C4–H \cdots N5 ($d(\text{H}\cdots\text{A}) = 2.494$ and $d(\text{D}\cdots\text{A}) = 3.404$ Å, $\angle(\text{D–H}\cdots\text{A}) = 154.4^\circ$), C5–H \cdots N1 (2.566 and 3.540 Å, 172.4°), and C5–H \cdots N5ⁱⁱ (2.517 and 3.403 Å, 150.2°) are the major interactions (Figure 3b). Symmetry operation ii: $-1 + x, y, z$.

Figure 3. (a) Packing diagram of tetramethylphosphonium salt **3**. (b) Dashed lines represent the C–H \cdots N contacts. Only N atoms engaged in major interactions are numbered.

2.4. Bis(trimethylsulfoxonium) 5,5'-Azotetrazolate (**4**)

The $(\text{CH}_3)_3\text{SO}$ cation in **4** again adopts a pyramidal geometry. It has neither a mirror plane nor a rotation axis. Nevertheless, the $3m$ symmetry is approximately fulfilled in good agreement with known trimethylsulfoxonium salts [34]. The shortest S–S distance is 5.245 Å. The packing is presented in Figure 4a. Probably due to the enhanced dipolar character of this cation, it participates in a series of significant C–H \cdots N interactions with the anion. All nitrogen atoms of the anion serve as acceptors building a three-dimensional network (Figure 4b): C3–H \cdots N4 (2.477 and 3.289 Å, 140.0°), C2–H \cdots N5ⁱⁱⁱ (2.411 and 3.352 Å, 160.8°), C4–H \cdots N1^{iv} (2.634 and 3.407 Å, 136.1°), C2–H \cdots N3^v (2.497 and 3.428 Å, 158.6°), C4–H \cdots N2^v (2.563 and 3.499 Å, 159.8°), C3–H \cdots N1^{vi} (2.435 and 3.334 Å, 152.3°), C4–H \cdots N2^{vi} (2.446 and 3.320 Å, 148.4°). Symmetry codes iii: $1 - x, 1 - y, 1 - z$; iv: $1/2 - x, -1/2 + y, 1/2 - z$; v: $-1/2 + x, 1/2 - y, 1/2 + z$; vi: $3/2 - x, -1/2 + y, 1/2 - z$.

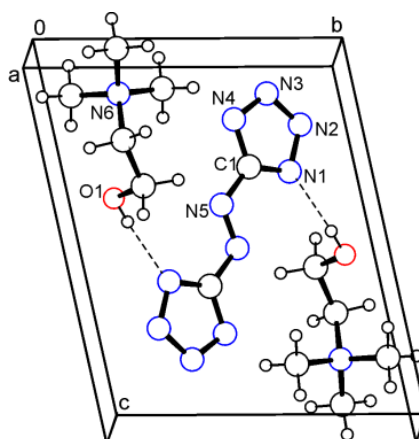
Figure 4. (a) Packing diagram of trimethylsulfoxonium salt **4**. (b) Dashed lines represent the short C–H \cdots N contacts (for symmetry operators see text).



2.5. Bis(2-(hydroxyethyl)trimethylammonium) 5,5'-azotetrazolate (**5**)

In the structure of **5**, a strong hydrogen bond with the parameters O1–H \cdots N1 (1.984 and 2.791 Å, 160.8°) between the cation and the dianion is observed. Figure 5 shows the unit cell of **5**.

Figure 5. Packing diagram of cholinium salt **5**. Dashed lines represent the strong inter-molecular O–H \cdots N hydrogen bonds.



3. Experimental Section

The starting materials were obtained from Sigma-Aldrich and used as received. The NMR spectra were recorded with a Bruker AC 300 spectrometer. IR spectra were obtained with a Nicolet 5700 FT instrument in ATR mode. The impact and friction sensitivity of silver salt **1** was determined by the BAM drophammer (method 1 of 6) [35–37] and BAM friction tester [35–37] respectively. The sensitivity towards electrostatic discharge was measured using an OZM small scale electrostatic discharge device [38]. X-Ray diffraction data were collected on Oxford Diffraction Gemini-R Ultra and Nonius Kappa CCD diffractometers using Mo- $K\alpha$ radiation. The structures were solved by direct methods and refined by full-matrix least-squares methods on F^2 [39,40]. CCDC 846911-846915 contain the supplementary crystallographic data for this paper. These data can be obtained free of charge from The Cambridge Crystallographic Data Centre.

3.1. *Bis(amminsilver(I)) 5,5'-Azotetrazolate (1)*

Caution: this compound is a primary explosive with extremely high sensitivities towards friction and also electrostatic discharge when dry. Proper protective measures (safety glasses, face shield, leather coat, earthened equipment and shoes, Kevlar® gloves and ear plugs) should be used during the handling of this compound. Concentrated NH_3 (2 mL) was layered over a solution of AgNO_3 (51 mg, 0.30 mmol) in H_2O (2 mL) and concentrated NH_3 (1 mL). A solution of sodium azotetrazolate pentahydrate (45 mg, 0.15 mmol) in H_2O (5 mL) and concentrated NH_3 (1 mL) was added cautiously on top of the mixture. The mixture was set aside, and orange-red crystals grew overnight at 20 °C. Yield: 10 mg (16%). No melting below 230 °C (dec). No NMR spectra could be recorded due to insolubility in common solvents. IR (neat, cm^{-1}): 1396 (s), 1214 (w), 1184 (m), 1168 (m), 1049 (w), 1032 (w), 765 (m), 737 (s), 719 (m). BAM drophammer: 2 J. BAM friction tester (<5 N). ESD: 5 mJ.

3.2. *Preparation of 5,5'-Azotetrazolates (2–5) (General Procedure)*

Ag_2SO_4 (78 mg, 0.25 mmol) was added to a solution of the respective organic halide (0.50 mmol) in H_2O (10 mL). The mixture was stirred at 50 °C for 10 min and ultrasonicated for 5 min. Subsequently, the precipitate was removed by centrifugation. Barium azotetrazolate pentahydrate (94 mg, 0.24 mmol) was added to the supernatant, and the mixture was again stirred at 50 °C for 10 min and ultrasonicated for 5 min. After centrifugation, the supernatant solution was brought to dryness in a rotary evaporator, the temperature not exceeding 50 °C. The yellow residue was recrystallized from MeOH, collected by filtration and vacuum-dried.

3.3. *Bis(trimethylsulfonium) 5,5'-Azotetrazolate (2)*

Yield: 61 mg (80%), m.p. 155 °C (dec.). ^1H NMR (DMSO-d_6 , 300 MHz): δ 2.90 (s). ^{13}C NMR (DMSO-d_6 , 75 MHz): δ 26.2 (3C), 173.3. IR (neat): ν 2992 (m), 2976 (m), 1417 (w), 1401 (s), 1196 (w), 1163 (w), 1039 (s), 773 (m), 739 (s), 733 (s) cm^{-1} .

3.4. Bis(tetramethylphosphonium) 5,5'-Azotetrazolate (**3**)

Yield: 70 mg (84%), m.p. 215 °C (dec.). ^1H NMR (DMSO- d_6 , 300 MHz, ppm): δ 1.85 (d, $J_{\text{H-P}} = 15.4$ Hz). ^{13}C NMR (DMSO- d_6 , 75 MHz, ppm): δ 8.9 (d, $J_{\text{C-P}} = 55$ Hz, 4C), 173.4. IR (neat, cm^{-1}): ν 2985 (m), 2915 (w), 1434 (m), 1374 (m), 1289 (m), 1174 (w), 1149 (w), 1015 (m), 973 (s), 772 (m), 725 (m).

3.5. Bis(trimethylsulfoxonium) 5,5'-Azotetrazolate (**4**)

Yield: 75 mg (89%), m.p. 192–193 °C (dec.). ^1H NMR (DMSO- d_6 , 300 MHz, ppm): δ 3.92 (s). ^{13}C NMR (DMSO- d_6 , 75 MHz, ppm): δ 39.2 (3C), 173.2. IR (neat, cm^{-1}): ν 2959 (s), 2878 (m), 1403 (s), 1225 (s), 1036 (s), 950 (s), 756 (m), 741 (m).

3.6. Bis(2-(hydroxyethyl)trimethylammonium) 5,5'-Azotetrazolate (**5**)

Yield: 65 mg (73%), m.p. 126–129 °C. ^1H NMR (DMSO- d_6 , 300 MHz, ppm): δ 3.15 (s, 9H), 3.45 (m, 2H), 3.82 (m, 2H), 5.76 (s, 1H). ^{13}C NMR (DMSO- d_6 , 75 MHz, ppm): δ 53.2 (3C), 55.1, 66.9, 173.3. IR (neat, cm^{-1}): ν 3177 (w), 3028 (w), 2902 (w), 1471 (m), 1384 (s), 1338 (w), 1179 (w), 1146 (w), 1095 (s), 1028 (w), 950 (s), 875 (m), 722 (m).

4. Conclusions

A large number of crystalline azotetrazolates is known today and can also be found in a recently published review article [41]. This versatile dianion grants access to an almost unlimited diversity of intriguing structures. Certainly, the five new salts presented in this work will be succeeded by others in due course, stimulating both materials science and crystallography. Silver salt **1** was characterized to be a thermally stable primary explosive which detonates in flame. The sensitivities towards outer stimuli are in the range of those observed for lead azide.

References and Notes

1. Singh, R.P.; Verma, R.D.; Meshri, D.T.; Shreeve, J.M. Energetic Nitrogen-Rich Salts and Ionic Liquids. *Angew. Chem. Int. Ed.* **2006**, *45*, 3584–3601.
2. Steinhauser, G.; Klapötke, T.M. “Green” Pyrotechnics: A Chemists’ Challenge. *Angew. Chem. Int. Ed.* **2008**, *47*, 3330–3347.
3. Hammerl, A.; Holl, G.; Kaiser, M.; Klapötke, T.M.; Mayer, P.; Piotrowski, H.; Vogt, M. Methylated Ammonium and Hydrazinium Salts of 5,5'-Azotetrazolate. *Z. Naturforsch.* **2001**, *56b*, 847–856.
4. Hammerl, A.; Holl, G.; Kaiser, M.; Klapötke, T.M.; Mayer, P.; Nöth, H.; Piotrowski, H.; Suter, M. New Hydrazinium Salts of 5,5'-Azotetrazolate. *Z. Naturforsch.* **2001**, *56b*, 857–870.
5. Hammerl, A.; Klapötke, T.M.; Nöth, H.; Warchhold, M.; Holl, G.; Kaiser, M.; Ticmanis, U. $[\text{N}_2\text{H}_5]^+{}_2[\text{N}_4\text{C-N=N-CN}_4]^{2-}$: A New High-Nitrogen High-Energetic Material. *Inorg. Chem.* **2001**, *40*, 3570–3575.

6. Hammerl, A.; Hiskey, M.A.; Holl, G.; Klapötke, T.M.; Polborn, K.; Stierstorfer, J.; Weigand, J.J. Azidoformamidinium and Guanidinium 5,5'-Azotetrazolate Salts. *Chem. Mater.* **2005**, *17*, 3784–3793.
7. Darwich, C.; Klapötke, T.M.; Sabaté C.M. 1,2,4-Triazolium-Cation-Based Energetic Salts. *Chem. Eur. J.* **2008**, *14*, 5756–5771.
8. Klapötke, T.M.; Sabaté C.M. Bistetrazoles: Nitrogen-Rich, High-Performing, Insensitive Energetic Compounds. *Chem. Mater.* **2008**, *20*, 3629–3637.
9. Xue, H.; Arritt, S.W.; Twamley, B.; Shreeve, J.M. Energetic Salts from N-Aminoazoles. *Inorg. Chem.* **2004**, *43*, 7972–7977.
10. Xue, H.; Shreeve, J.M. Energetic Ionic Liquids from Azido Derivatives of 1,2,4-Triazole. *Adv. Mater.* **2005**, *17*, 2142–2146.
11. Klapötke, T.M.; Sabaté C.M. New energetic compounds based on the nitrogen-rich 5,5'-azotetrazolate anion ($[\text{C}_2\text{N}_{10}]^{2-}$). *New J. Chem.* **2009**, *33*, 1605–1617.
12. Klapötke, T.M.; Sabaté C.M. Nitrogen-Rich Tetrazolium Azotetrazolate Salts: A New Family of Insensitive Energetic Materials. *Chem. Mater.* **2008**, *20*, 1750–1763.
13. Gao, H.; Huang, Y.; Twamley, B.; Ye, C.; Shreeve, J.M. Energetic N,N,N',N'-Tetraaminopiperazinium Salts. *ChemSusChem* **2008**, *2*, 222–227.
14. Katritzky, A.R.; Singh, S.; Kirichenko, K.; Holbrey, J.D.; Smiglak, M.; Reichert, W.M.; Rogers, R.D. 1-Butyl-3-methylimidazolium 3,5-dinitro-1,2,4-triazolate: a novel ionic liquid containing a rigid, planar energetic anion. *Chem. Commun.* **2005**, 868–870.
15. Gao, H.; Ye, C.; Gupta, O.D.; Xiao, J.C.; Hiskey, M.A.; Twamley, B.; Shreeve, J.M. 2,4,5-Trinitroimidazole-Based Energetic Salts. *Chem. Eur. J.* **2007**, *13*, 3853–3860.
16. Ye, C.; Xiao, J.-C.; Twamley, B.; Shreeve, J.M. Energetic salts of azotetrazolate, iminobis(5-tetrazolate) and 5,5'-bis(tetrazolate). *Chem. Commun.* **2005**, 2750–2752.
17. Thiele, J. Ueber Azo- und Hydrazoverbindungen des Tetrazols. *Ann. Chem.* **1898**, *303*, 57–75.
18. Weibel, N.; Grunder, S.; Mayor, M. Functional molecules in electronic circuits. *Org. Biomol. Chem.* **2007**, *5*, 2343–2353.
19. Tappan, B.C.; Huynh, M.H.; Hiskey, M.A.; Chavez, D.E.; Luther, E.P.; Mang, J.T.; Son, S.F. Ultralow-Density Nanostructured Metal Foams: Combustion Synthesis, Morphology, and Composition. *J. Am. Chem. Soc.* **2006**, *128*, 6589–6594.
20. Bentivoglio, G.; Laus, G.; Kahlenberg, V.; Nauer, G.; Schottenberger, H. Crystal structure of bis(hydroxylammonium) 5,5'-azotetrazolate dihydrate, $(\text{NH}_3\text{OH})_2(\text{C}_2\text{N}_{10}) \cdot 2\text{H}_2\text{O}$. *Z. Kristallogr. NCS* **2008**, *223*, 425–426.
21. Pan, W.-L.; Chena, X.-Y.; Hu, C.-W. Bis(amantadinium) 5,5'-diazenediyliditetrazolate dihydrate. *Acta Crystallogr.* **2007**, *E63*, o1606–o1608.
22. Hammerl, A.; Holl, G.; Klapötke, T.M.; Mayer, P.; Nöth, H.; Piotrowski, H.; Warchhold, M. Salts of 5,5'-Azotetrazolate. *Eur. J. Inorg. Chem.* **2002**, 834–845.
23. Meng, Y. Poly[1-(5,5'-diazenediyliditetrazolido)dicaesium]. *Acta Crystallogr.* **2011**, *E67*, m453.
24. Steinhauser, G.; Giester, G.; Leopold, N.; Wagner, C.; Villa, M. Nitrogen-Rich Compounds of the Lanthanoids: The 5,5'-Azobis[1H-tetrazol-1-ides] of the Light Rare Earths (Ce, Pr, Nd, Sm, Eu, Gd). *Helv. Chim. Acta* **2009**, *92*, 2038–2051.

25. Steinhäuser, G.; Giester, G.; Wagner, C.; Leopold, N.; Sterba, J.H.; Lendl, B.; Bichler, M. Nitrogen-Rich Compounds of the Lanthanoids: The 5,5'-Azobis[1H-tetrazol-1-ides] of some Yttric Earths (Tb, Dy, Ho, Er, Tm, Yb, and Lu). *Helv. Chim. Acta* **2009**, *92*, 1371–1384.
26. Steinhäuser, G.; Giester, G.; Leopold, N.; Wagner, C.; Villa, M.; Musilek, A. Nitrogen-Rich Compounds of the Lanthanoids: Highlights and Summary. *Helv. Chim. Acta* **2010**, *93*, 183–202.
27. Pierce-Butler, M.A. Structure of Bis[hydroxolead(II)] 5,5'-Azotetrazole diide. *Acta Crystallogr.* **1982**, *B38*, 2681–2683.
28. Bhandari, S.; Mahon, M.F.; Molloy, K.C.; Palmer, J.S.; Sayers, S.F. Thallium(I)- and organothallium(III)-substituted mono-, bis- and tris-tetrazoles: synthesis and supramolecular structures. *J. Chem. Soc. Dalton Trans.* **2000**, 1053–1060.
29. Jiao, B.; Chen, S.; Zhao, F.; Hu, R.; Gao, S. A new high-nitrogen compound [Mn(ATZ)(H₂O)₄] 2H₂O: Synthesis and characterization. *J. Hazard. Mater.* **2007**, *142*, 550–554.
30. Jiao, B.; Yan, Z.; Fan, G.; Chen, S.; Gao, S. *catena*-Poly[[[tetraaquairon(II)]- μ -5,5'-diazenediyl di-tetrazolido] dihydrate]. *Acta Crystallogr.* **2010**, *E66*, m1374.
31. Tao, G.-H.; Twamley, B.; Shreeve, J.M. Energetic Nitrogen-Rich Cu(II) and Cd(II) 5,5'-Azobis(tetrazolate) Complexes. *Inorg. Chem.* **2009**, *48*, 9918–9923.
32. Jannin, M.; Puget, R.; de Brauer, C.; Perret, R. Structures of Trimethylsulfonium Salts. I. Refinement of the Structure of the Iodide (CH₃)₃SI. *Acta Cryst.* **1991**, *C47*, 982–984.
33. Knop, O.; Linden, A.; Vincent, B.R.; Choi, S.C.; Cameron, T.S.; Boyd, R.J. The lone electron pair and crystal packing: observations on pyramidal YEL₃ species, *ab initio* calculations, and the crystal structures of Me₃SOI, Et₃SI, (Me₃S)₂SnCl₆, (Me₃SO)₂SnCl₆, and (Et₃S)₂SnCl₆. *Can. J. Chem.* **1989**, *67*, 1984–2008.
34. Jannin, M.; Puget, R.; de Brauer, C.; Perret, R. Structures of Trimethyloxosulfonium Salts. I. The Iodide and the Bromide. *Acta Cryst.* **1991**, *C47*, 1687–1689.
35. Available online: www.bam.de (accessed on 4 March 2012)
36. Available online: www.reichel-partner.de (accessed on 4 March 2012)
37. Impact: insensitive > 40 J, less sensitive > 35 J, sensitive > 4 J, very sensitive < 3 J. Friction: insensitive > 360 N, less sensitive = 360 N, sensitive < 360 N and > 80 N, very sensitive < 80 N, extremely sensitive < 10 N. According to the UN Recommendations on the Transport of Dangerous Goods, (+) indicates not safe for transport.
38. Available online: <http://www.ozm.cz/en/sensitivity-tests/esd-2008a-small-scale-electrostatic-spark-sensitivity-test/> (accessed on 4 March 2012)
39. Burla, M.C.; Carrozzini, B.; Cascarano, G.L.; Giacovazzo, C.; Polidori, G. More power for direct methods: SIR2002. *Z. Kristallogr.* **2002**, *217*, 629–635.
40. Sheldrick, G.M. A short history of SHELX. *Acta Crystallogr.* **2008**, *A64*, 112–122.
41. Gao, H.; Shreeve, J.M. Azole-Based Energetic Salts. *Chem. Rev.* **2011**, *111*, 7377–7436.

Article

Inorganic Amino-Nitro-Guanidinium Derivatives

Niko Fischer, Thomas M. Klapötke *, Karin Lux, Franz A. Martin and Jörg Stierstorfer

Energetic Materials Research, Department of Chemistry, University of Munich (LMU),
Butenandtstrasse 5-13, Munich D-81377, Germany; E-Mails: finch@cup.uni-muenchen.de (N.F.);
kluch@cup.uni-muenchen.de (K.L.); fmach@cup.uni-muenchen.de (F.A.M.);
jstch@cup.uni-muenchen.de (J.S.)

* Author to whom correspondence should be addressed; E-Mail: tmk@cup.uni-muenchen.de;
Tel.: +49-89-2180-77491; Fax: +49-89-2180-77492.

Received: 2 May 2012; in revised form: 6 June 2012 / Accepted: 7 June 2012 /

Published: 18 June 2012

Abstract: 1-Amino-3-nitroguanidine (ANQ, **1**) was synthesized by hydrazinolysis of nitroguanidine (NQ) with hydrazine hydrate. Four different amino-nitroguanidinium salts (chloride (**2**), bromide (**3**), iodide (**4**) and sulfate (**5**)) were synthesized and structurally characterized by low-temperature X-ray diffraction. The halides **2–4** could only be obtained crystalline as monohydrates. In addition, they were characterized by NMR and vibrational spectroscopy, elemental analysis and the sensitivities towards impact, friction and electrostatic discharge were determined. The compounds can be used in silver (AgX, X = Cl, Br, I) and barium (BaSO₄) based metathesis reactions in order to form more complex salts of 1-amino-nitroguanidine.

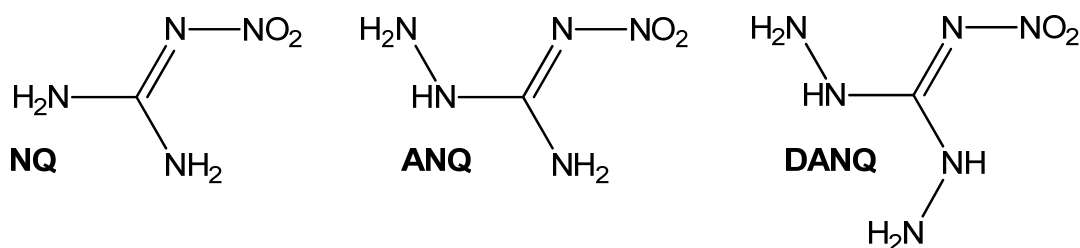
Keywords: nitroguanidine; crystal structures; halides; sulfates

1. Introduction

1-Amino-3-nitroguanidine (**1**, ANQ) can be described as the aminated sister compound of the famous 1-nitroguanidine (NQ) [1]. The next step in the preparation of mixed aminonitroguanidines would be the synthesis of 1,3-diamino-5-nitroguanidine (DANQ), which is completely unknown yet (Figure 1). Nitroguanidine is used in airbags and many other double- and triple- based propellant applications [2]. Interestingly, only very little correspondence on aminonitroguanidine is found in the literature [3–5]. We recently investigated the use of ANQ in energetic materials in its neutral as well as

protonated form [6]. For example, highly energetic 1-amino-3-nitroguanidinium dinitramide has been described [6]. Because dinitraminic acid ($\text{HN}(\text{NO}_2)_2$) and concentrated aqueous solutions can explode spontaneously, the reaction pathway using a metathesis reaction of amino-nitroguanidinium chloride with silver dinitramide was chosen. This example shows the utility of the herein described compounds as precursor materials for the synthesis of ionic energetic materials containing the 1-amino-3-nitroguanidinium cation when using metathesis reaction protocols to precipitate low soluble silver halides in case of reacting the ANQ halides with the corresponding silver salts of the used acids or to precipitate BaSO_4 in case the corresponding Ba-salts are reacted with the herein described sulfate salt of ANQ. Here we present the synthesis and characterization of three amino-nitroguanidinium halides and bis(amino-nitroguanidinium) sulfate.

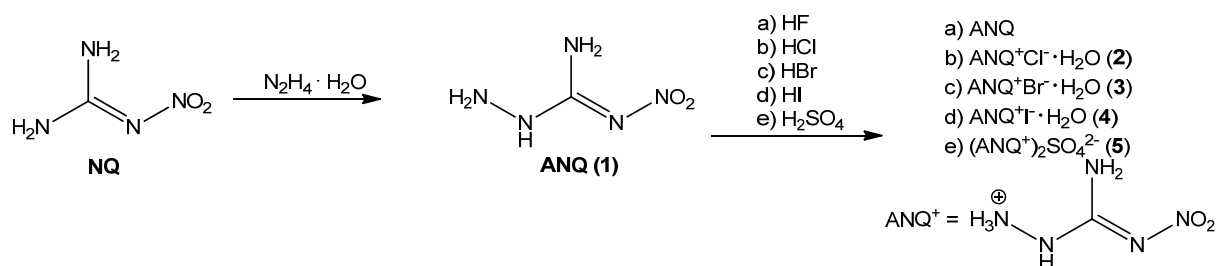
Figure 1. Chemical structures of amino-nitroguanidines: **NQ**: 1-nitroguanidine, **ANQ**: 1-amino-3-nitroguanidine, **DANQ**: 1,3-Diamino-5-nitroguanidine (not known yet).



2. Results and Discussion

2.1. Synthesis

The synthesis of 1-amino-3-nitroguanidine (**1**: ANQ) was achieved starting from commercially available nitroguanidine (NQ) by treatment with hydrazine hydrate. In a hydrazinolysis reaction, the aminated nitroguanidine is formed after the elimination of ammonia [5]. Unprotonated ANQ shows rather poor solubility in water, so that it can be isolated from the reaction mixture after neutralization by suction filtration. Unlike in water or buffered neutral solutions, in acidic media ANQ is dissolved comparatively easily upon the formation of the protonated ANQ^+ species. Therefore, the halides as well as the sulfate salt can be prepared by dissolving ANQ in dilute aqueous solutions of the respective mineral acids HCl , HBr , HI and H_2SO_4 . To fully synthesize and characterize all halides (F^- , Cl^- , Br^- , I^-) of ANQ, it was also dissolved in 40% aqueous HF . Unfortunately it was only possible to isolate unprotonated ANQ from this reaction mixture (Scheme 1). The reason for this behavior is easily found in the pK_a values of the used mineral acids. ANQ, due to the presence of the electron withdrawing character of the nitro group, is a comparatively weak base and requires strong mineral acids for protonation in aqueous media. Since the acidic strength of the hydrohalides in aqueous solution decreases in the order $\text{HI} > \text{HBr} > \text{HCl} > \text{HF}$, the latter one is not able to protonate ANQ in aqueous solution any more. However, 40% aqueous HF proved to be an excellent solvent for the recrystallization of the poorly water soluble ANQ, especially if single crystals, e.g., for single crystal X-ray diffraction, are needed.

Scheme 1. Synthesis of **1** (ANQ) and investigated amino-nitroguanidinium salts **2–5**.

The storage stability of the halides decreases with increasing molecular weight of the anion. Whereas the hydrochloride remains a colorless crystalline material even after several months, the hydrobromide discolors slightly and the hydroiodide turns completely dark after the release of I₂ indicating a decomposition of the material.

2.2. Single Crystal X-ray Structure Analysis

The low temperature determination of the crystal structures of **2–5** was performed on an Oxford Xcalibur3 diffractometer with a Spellman generator (voltage 50 kV, current 40 mA) and a KappaCCD detector. The data collection and reduction was carried out using the CRYALISPRO software [7]. The structures were solved either with SHELXS-97 [8] or SIR-92 [9], refined with SHELXL-97 [10] and finally checked using the PLATON [11] software integrated in the WINGX [12] software suite. The non-hydrogen atoms were refined anisotropically and the hydrogen atoms were located and freely refined. The absorptions were corrected with a Scale3 Abspack multi-scan method [13]. Selected data and parameters of the X-ray determinations are given in Table 1. Crystallographic data for the structures have been deposited with the Cambridge Crystallographic Data Centre [14].

Table 1. X-ray data and parameters of **2–5**.

	2	3	4	5
Formula	CH ₆ N ₅ O ₂ , H ₂ O, Cl	CH ₆ N ₅ O ₂ , H ₂ O, Br	CH ₆ N ₅ O ₂ , H ₂ O, I	2(CH ₆ N ₅ O ₂), SO ₄
FW [g mol ⁻¹]	173.56	218.03	265.02	336.29
Crystal system	Monoclinic	Monoclinic	Triclinic	Orthorhombic
Space Group	<i>P</i> 2 ₁ / <i>n</i>	<i>P</i> 2 ₁ / <i>c</i>	<i>P</i> -1	<i>F</i> dd2
Color/Habit	Colorless block	Colorless plate	Colorless block	Colorless block
Size [mm]	0.37 × 0.44 × 0.49	0.04 × 0.21 × 0.50	0.38 × 0.42 × 0.50	0.14 × 0.22 × 0.26
<i>a</i> [Å]	7.6616(6)	8.0261(5)	6.6931(3)	11.0638(8)
<i>b</i> [Å]	12.7248(7)	12.7412(7)	7.0540(4)	30.380(2)
<i>c</i> [Å]	7.8116(8)	7.9296(5)	9.1359(5)	6.7531(5)
<i>α</i> [°]	90	90	97.754(5)	90
<i>β</i> [°]	119.012(11)	118.051(9)	96.942(4)	90
<i>γ</i> [°]	90	90	115.961(5)	90
<i>V</i> [Å ³]	666.01(12)	715.64(7)	376.35(4)	2269.8(3)
<i>Z</i>	4	4	2	8
<i>ρ</i> _{calc.} [g cm ⁻³]	1.731	2.024	2.339	1.968
<i>μ</i> [mm ⁻¹]	0.535	5.708	4.221	0.359
<i>F</i> (000)	360	432	252	1392

Table 1. Cont.

	2	3	4	5
$\lambda_{\text{MoK}\alpha}$ [Å]	0.71073	0.71073	0.71073	0.71073
T [K]	173	173	173	173
θ Min–Max [°]	4.4, 28.6	4.3, 33.6	4.4, 32.4	4.6, 30.1
Dataset	–10:7; –17:9; –8:9	–9:9; –15:10; –9:9	–9:9; –10:10; –13:13	–15:15; –42:42; –9:9
Reflections collected	2525	5748	5175	10,853
Independent refl.	1437	2172	2457	1670
R_{int}	0.017	0.047	0.023	0.055
Observed reflections	1298	1395	2286	1392
Parameters	116	123	116	120
R_1 (obs)	0.0292	0.0411	0.0220	0.0283
wR_2 (all data)	0.0807	0.0697	0.0554	0.0607
S (GooF)	1.09	1.04	1.08	0.95
Resd. Dens. [e Å ^{–3}]	–0.38, 0.43	–0.77, 0.68	–1.56, 0.76	–0.35, 0.25
Device type	Oxford Xcalibur3	Oxford Xcalibur3	Oxford Xcalibur3	Oxford Xcalibur3
	CCD	CCD	CCD	CCD
Solution	SIR-92	SHELXS-97	SIR-92	SHELXS-97
Refinement	SHELXL-97	SHELXL-97	SHELXL-97	SHELXL-97
CCDC	858928	858930	858931	858929

The structure of the 1-amino-3-nitroguanidinium cation is similar in all four structures investigated in this work. The cation is almost planar, controlled by the intramolecular hydrogen bond N5–H5 \cdots O1 (D \cdots A: 2.589(2) Å–2.605(3) Å) [graph set [15]: R₁¹(6)] but also by the strong angulated (~90°) hydrogen bond N4–H4x \cdots N1 (D \cdots A: 2.547(5) Å–2.576(7) Å) [graph set: R₁¹(5)]. The C–N bond distances are between typical C–N single and C=N double bonds showing the delocalization of the positive charge. However, in all structures the bond length between C1 and N5 is observed to be the shortest one. Also the bonds N2–O1, N2–O2 and N1–N2 are significantly shorter than single bonds. These structural details are in agreement with our previously described investigations of this cation in the literature [6]. Selected bond lengths and angles of the cation of all structurally investigated compounds **2–5** are gathered in Table 2. The halides, which were obtained crystalline under their monohydrated form, crystallize in common space groups (**2**: $P2_1/n$, **3**: $P2_1/c$, **4**: $P-1$) and follow the trend of rising densities (**2**: $1.73 < \mathbf{3}$: $2.02 < \mathbf{4}$: 2.34 g cm^{-3}). All three structures are dominated by many hydrogen bonds [16–18] involving the crystal water molecules. Figure 2 shows the molecular structure of **2**.

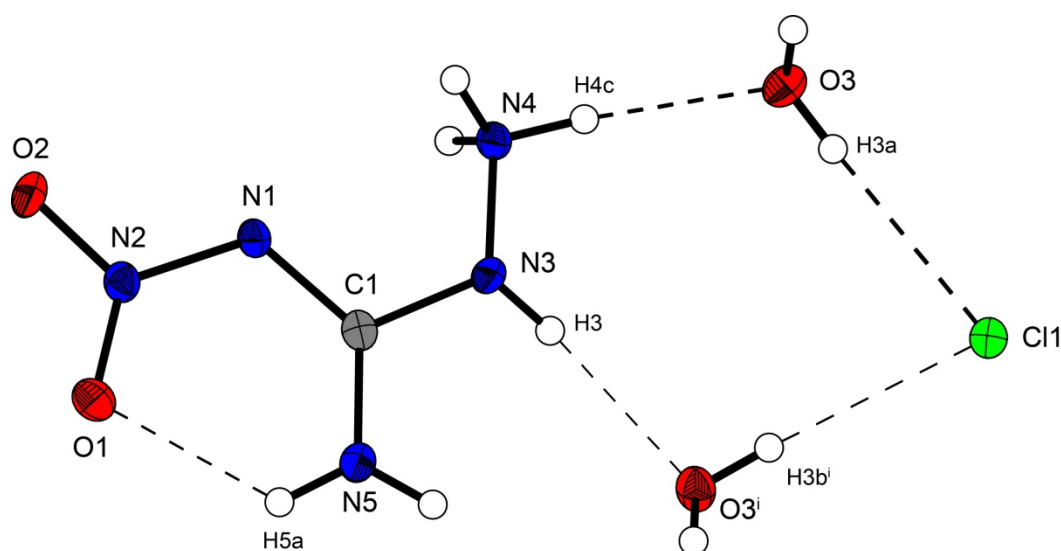
Table 2. Selected bond lengths [Å] of compounds **2–5**.

bond lengths [Å]	2	3	4	5
O1–N2	1.235(2)	1.241(4)	1.236(3)	1.239(2)
O2–N2	1.234(2)	1.229(4)	1.242(3)	1.255(2)
N1–N2	1.361(2)	1.366(4)	1.345(3)	1.330(2)
N3–N4	1.423(2)	1.433(4)	1.419(3)	1.417(2)
N1–C1	1.339(2)	1.337(4)	1.348(3)	1.356(3)
N3–C1	1.368(2)	1.374(4)	1.355(4)	1.349(3)
N5–C1	1.317(2)	1.318(4)	1.315(3)	1.311(2)

Table 2. Cont.

bond angles [°]	2	3	4	5
C1–N1–N2	117.7(1)	117.5(3)	118.0(2)	117.5(1)
C1–N3–N4	117.8(1)	116.6(3)	118.1(2)	119.4(2)
O2–N2–O1	121.8(1)	121.8(3)	121.2(2)	120.7(1)
O2–N2–N1	114.2(1)	114.3(3)	114.4(2)	115.7(1)
O1–N2–N1	124.0(2)	123.8(3)	124.5(2)	123.6(1)
N5–C1–N1	130.5(2)	130.9(3)	130.6(2)	130.0(2)
N5–C1–N3	116.0(1)	115.1(3)	116.7(2)	118.0(2)
N1–C1–N3	113.5(1)	114.0(3)	112.7(2)	111.8(2)
Torsion angles [°]	2	4	5	
N2–N1–C1–N5	0.5(2)	−0.8(5)	4.6(3)	10.9(3)
N4–N3–C1–N5	171.1(1)	174.0(3)	−177.1(2)	−174.0(2)

Figure 2. Molecular structure of amino-nitro-guanidinium chloride monohydrate (**2**). Ellipsoids are drawn at the 50% probability level. Symmetry code: (i) $0.5 + x$, $0.5 - y$, $0.5 + z$.



In the crystal structure the ions are held together by a three dimensional network of moderate N–H···O ($d(\text{N}–\text{O}) \sim 2.83\text{--}3.04 \text{ \AA}$), N–H···Cl ($d(\text{N}–\text{Cl}) \sim 3.24\text{--}3.30 \text{ \AA}$) and O–H···Cl ($d(\text{O}–\text{Cl}) \sim 3.08\text{--}3.14 \text{ \AA}$) hydrogen bonds. The distorted pseudo-octahedral coordination sphere of the chloride anions is shown in Figure 3. The chloride anion is coordinated by two water molecules and four cations (two times by the amine group and two times by the ammonium group). The bond lengths and angles of selected hydrogen bonds are listed in Tables 3 and 4. The water molecules bridge between the chloride anions and 1-amino-3-nitroguanidinium cation, and act both as acceptor and donor. The cations build a chain via the hydrogen bridge $\text{N3}^{\text{vi}}\text{--H3}^{\text{vi}}\cdots\text{O2}$ along the b-axis [graph set: C(6)]. Two cations build dimers via the hydrogen bridge $\text{N4}^{\text{ii}}\text{--H4c}^{\text{ii}}\cdots\text{O2}$ parallel to the c-axis [graph set: $\text{R}_2^2(14)$]. The oxygen atom (O2) of the nitro group acts as bifurcated acceptor.

Figure 3. Coordination sphere of one chloride anion in **2**. Symmetry codes: (i) $0.5 + x, 0.5 - y, 0.5 + z$; (ii) $1.5 - x, 0.5 + y, 1.5 - z$; (iii) $-0.5 + x, 0.5 - y, 0.5 + z$; (iv) $0.5 - x, 0.5 + y, 0.5 - z$; (v) $-0.5 + x, 0.5 - y, -0.5 + z$.

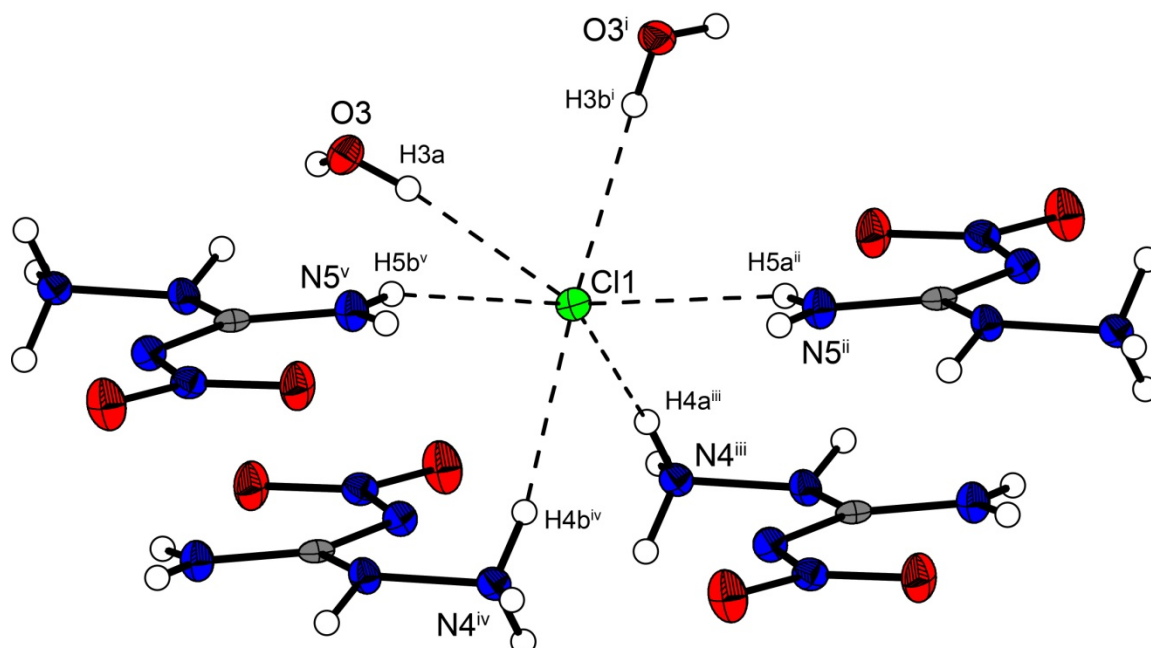


Table 3. Selected hydrogen bonds in the structure of **2**. Symmetry codes: (vi) $1.5 - x, -0.5 + y, 0.5 - z$; (vii) $1 - x, -y, -z$.

D–H···A	d(D–H)	d(H···A)	d(D···A)	<(D–H···A)	<(H···A–X)
N3 ^{vi} –H3 ^{vi} ···O2	0.83(2)	2.57(2)	3.043(2)	117.5(15)	150.7(5)
N4 ^{vii} –H4c ^{vii} ···O2	0.89(2)	2.417(18)	2.881(2)	112.6(14)	126.9(5)

Table 4. Selected hydrogen bonds in the structure of **2**. Symmetry codes: (i) $0.5 + x, 0.5 - y, 0.5 + z$; (ii) $1.5 - x, 0.5 + y, 1.5 - z$; (iii) $-0.5 + x, 0.5 - y, 0.5 + z$; (iv) $0.5 - x, 0.5 + y, 0.5 - z$; (v) $-0.5 + x, 0.5 - y, -0.5 + z$.

D–H···A	d(D–H)	d(H···A)	d(D···A)	<(D–H···A)
N4 ⁱⁱⁱ –H4a ⁱⁱⁱ ···Cl1	0.88(2)	2.42(2)	3.279(1)	168.8(2)
N4 ^{iv} –H4b ^{iv} ···Cl1	0.88(2)	2.37(2)	3.242(1)	159.1(2)
N5 ⁱⁱ –H5a ⁱⁱ ···Cl1	0.85(2)	2.59(2)	3.291(1)	141.2(2)
N5 ^v –H5b ^v ···Cl1	0.82(2)	2.54(2)	3.299(1)	155.5(2)
O3–H3a···Cl1	0.78(2)	2.34(2)	3.084(1)	160(2)
O3 ⁱ –H3b ⁱ ···Cl1	0.80(2)	2.33(2)	3.135(1)	175(2)

Figure 4 shows the molecular moiety of **3** while Figure 5 shows the same pseudo-octahedral coordination sphere of the bromide anion as we could observe in the chloride structure. The bond lengths and angles of selected hydrogen bonds are listed in Tables 5,6. Also in this structure the ions are held together by a three dimensional network of moderate N–H···O ($d(\text{N–O}) \sim 2.82\text{--}3.08 \text{ \AA}$), N–H···Cl ($d(\text{N–Br}) \sim 3.36\text{--}3.49 \text{ \AA}$) and O–H···Cl ($d(\text{O–Cl}) \sim 3.20\text{--}3.28 \text{ \AA}$) hydrogen bonds. The crystal packing is identical to the chloride structure **2**. The N–Br and O–Br hydrogen bonds are approximately 0.15 \AA longer than those in the chloride structure **2**.

Figure 4. Molecular structure of amino-nitro-guanidinium bromide monohydrate (**3**). Ellipsoids are drawn at the 50% probability level.

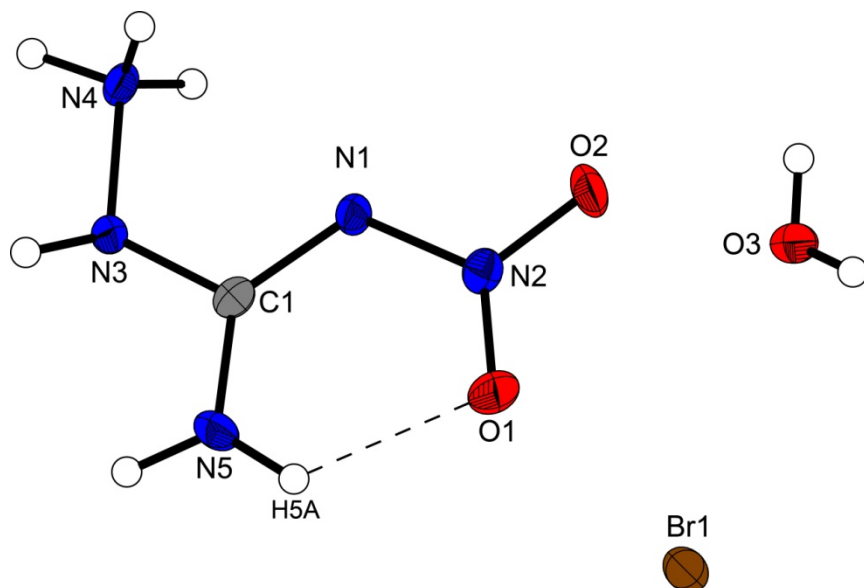


Figure 5. Coordination sphere of one bromide anion in **3**. Symmetry codes: (i) $-1 + x, 0.5 - y, -0.5 + z$; (ii) $-1 + x, y, z$; (iii) $x, 0.5 - y, 0.5 + z$; (iv) $1 - x, 0.5 + y, 1.5 - z$; (v) $x, 0.5 - y, -0.5 + z$; (vi) $-x, 0.5 + y, 0.5 - z$.

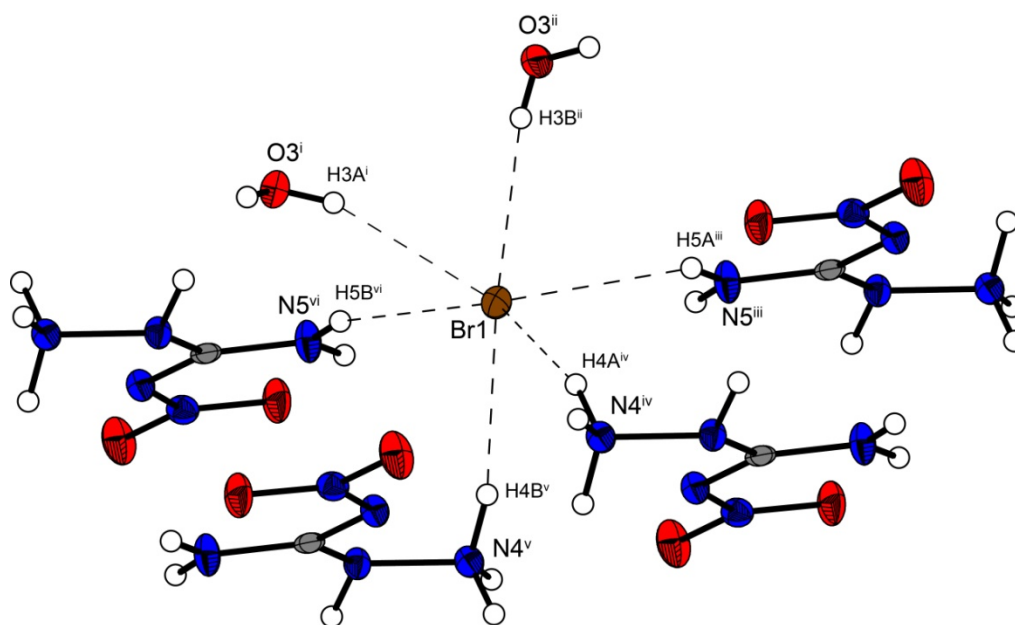


Table 5. Selected hydrogen bonds in the structure of **3**. Symmetry codes: (vi) $1 - x, 0.5 + y, 1.5 - z$; (vii) $1 - x, -y, 2 - z$.

D–H···A	d(D–H)	d(H···A)	d(D···A)	<(D–H···A)	<(H···A–X)
N3 ^{vi} –H3 ^{vi} ···O2	0.89(1)	2.52(4)	3.075(4)	121(3)	151.1(7)
N4 ^{vii} –H4 ^c ···O2	0.90(4)	2.40(4)	2.871(4)	113(3)	128.0(10)

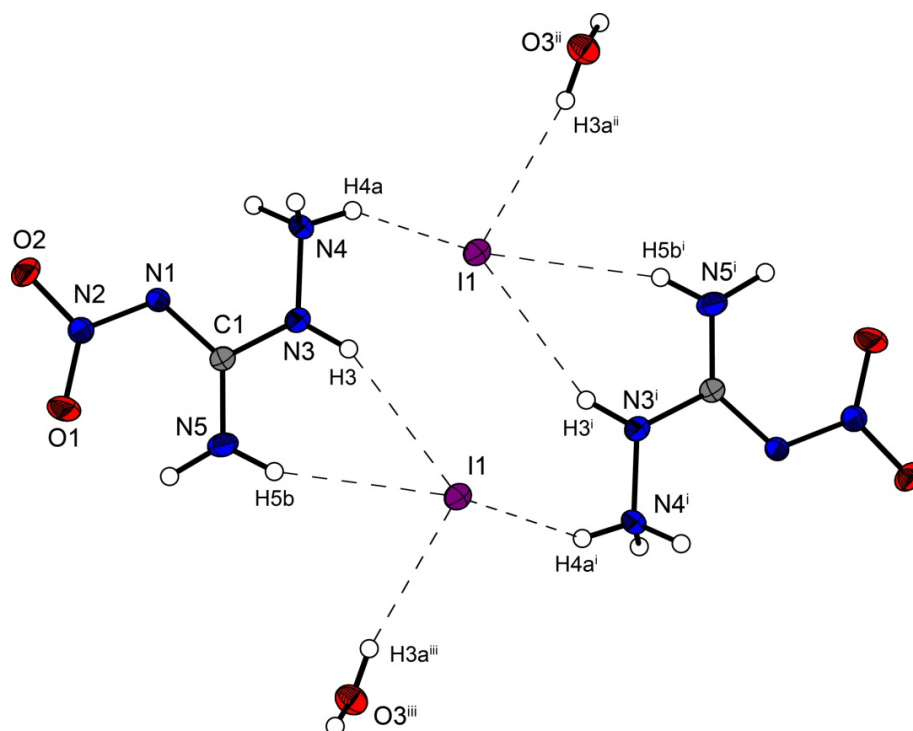
Table 6. Selected hydrogen bonds in the structure of **3**.

D–H···A	d(D–H)	d(H···A)	d(D···A)	<(D–H···A)
N4 ^{iv} –H4a ^{iv} ···Br1	0.91(4)	2.57(4)	3.427(3)	156(3)
N4 ^v –H4b ^v ···Br1	0.92(4)	2.47(4)	3.360(3)	163(3)
N5 ⁱⁱⁱ –H5a ⁱⁱⁱ ···Br1	0.90(1)	2.71(3)	3.428(3)	138(3)
N5 ^{vi} –H5b ^{vi} ···Br1	0.90(1)	2.65(2)	3.493(3)	156(3)
O3 ⁱ –H3a ⁱ ···Br1	0.78(4)	2.48(5)	3.203(3)	156(4)
O3 ⁱⁱ –H3b ⁱⁱ ···Br1	0.78(4)	2.50(4)	3.275(3)	172(4)

However the iodine structure **4** crystallizes in the triclinic space group $P\bar{1}$ with two formula units in the unit cell. The crystal packing is different from the described chloride (**2**) and bromide (**3**) structure. Two molecular moieties of **4** connected to dimers are depicted in Figure 6. These dimers are packed in layers which are linked by the water molecules.

The iodide anions participate in four hydrogen bonds listed in Table 7. The N···I and O···I distances observed reveal ordinary values comparable to those found in 3-Cyano-anilinium iodide monohydrate [19].

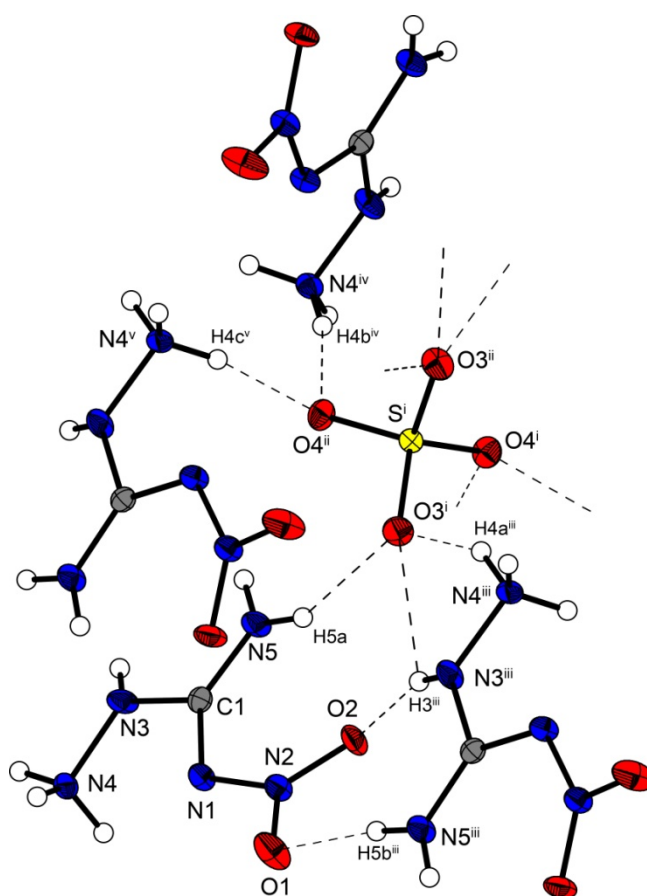
Figure 6. Molecular structure of amino-nitro-guanidinium iodide monohydrate (**4**). Ellipsoids are drawn at the 50% probability level. Symmetry codes: (i) $2 - x, 1 - y, 1 - z$; (ii) $1 + x, y, z$; (iii) $1 - x, 1 - y, 1 - z$.

**Table 7.** Selected hydrogen bonds in the structure of **4**.

D–H···A	d(D–H)	d(H···A)	d(D···A)	<(D–H···A)
N3 ⁱ –H3 ⁱ ···I1	0.90(3)	2.80(3)	3.635(2)	156(3)
N4–H4a···I1	0.87(3)	2.78(3)	3.501(2)	141(3)
N5 ⁱ –H5b ⁱ ···I1	0.88(3)	2.83(3)	3.669(2)	160(3)
O3 ⁱⁱ –H3a ⁱⁱ ···I1	0.84(4)	2.71(4)	3.540(2)	169(3)

Bis(amino-nitroguanidinium) sulfate crystallizes in the non-centrosymmetric orthorhombic space group *Fdd2* with eight formula units in the unit cell. The density of 1.97 g cm^{-3} is slightly lower than that of the bromide structure **3** but higher than that of **2**. The molecular structure of **5** is depicted in Figure 7. The sulfur atoms lie on the special position $\frac{1}{2}, 0, z$. The S–O bonds are uniform with a length of 1.48 \AA , which is in agreement to many sulfate structures in the literature, e.g., that of potassium sulfate [20].

Figure 7. Molecular structure of bis(amino-nitro-guanidinium) sulfate (**5**). Ellipsoids are drawn at the 50% probability level. Symmetry codes: (i) $0.75 - x, 0.25 + y, 0.75 + z$; (ii) $-0.25 + x, 0.25 - y, 0.75 + z$; (iii) $0.25 + x, 0.25 - y, -0.75 + z$; (iv) $0.25 - x, 0.25 + y, 0.25 + z$; (v) $-0.25 + x, 0.25 - y, -0.25 + z$.



In the crystal structure of **5**, the amino-nitro-guanidinium cations and the sulfate anion are held together by a three dimensional network of moderate N–H···O ($d(\text{N} \cdots \text{O}) \sim 2.60\text{--}3.08 \text{ \AA}$) hydrogen bonds. Selected bond lengths and angles of the hydrogen bonds are listed in Table 8. In the crystal structure there are two layers of cations which twisted around $\sim 60^\circ$ against each other. The layers are connected via hydrogen bonds with the sulfate anions. The oxygen atoms of the sulfate anions act as bifurcated acceptors. The oxygen atom O4 bridges two cations via the hydrogen bonds $\text{N4}^{\text{iv}}\text{--H4b}^{\text{iv}} \cdots \text{O4}^{\text{ii}}$ and $\text{N4}^{\text{v}}\text{--H4c}^{\text{v}} \cdots \text{O4}^{\text{ii}}$, which form zig-zag chains along the *c*-axis [graph set: $\text{C}_2^1(4)$]. Also the oxygen atom O3 bridges two cations via the hydrogen bonds $\text{N5}\text{--H5a} \cdots \text{O3}^{\text{i}}$, $\text{N4}^{\text{iii}}\text{--H4a}^{\text{iii}} \cdots \text{O3}^{\text{i}}$ and $\text{N3}^{\text{iii}}\text{--H3}^{\text{iii}} \cdots \text{O3}^{\text{i}}$. This hydrogen bonding pattern forms a “chain of rings” along the *ab*-diagonal [graph set: $\text{C}_3^2(7)[\text{R}_2^1(5)]$]. However this chain is also held together by the hydrogen

bonds $\text{N3}^{\text{iii}}-\text{H3}^{\text{iii}}\cdots\text{O2}$ and $\text{N5}^{\text{iii}}-\text{H5b}^{\text{iii}}\cdots\text{O1}$ of the nitrate group [graph set: $\text{C}_2^2(6)[\text{R}_2^2(8)]$]. In the crystal structure one observes a short $\text{O}\cdots\text{O}$ contact ($\text{O1}\cdots\text{O4}$: 2.733(2) Å), which is generated by the existing hydrogen bonds. Such a short $\text{O}\cdots\text{O}$ contact has also been observed in the literature [21,22].

Table 8. Selected hydrogen bonds in the structure of **5**.

D–H \cdots A	d(D–H)	d(H \cdots A)	d(D \cdots A)	<(D–H \cdots A)
$\text{N5}^{\text{iii}}-\text{H5a}^{\text{iii}}\cdots\text{O3}^{\text{i}}$	0.89(3)	2.17(2)	2.979(2)	152(2)
$\text{N4}^{\text{iii}}-\text{H4a}^{\text{iii}}\cdots\text{O3}^{\text{i}}$	0.88(2)	1.95(2)	2.731(2)	149(2)
$\text{N3}^{\text{iii}}-\text{H3}^{\text{iii}}\cdots\text{O3}^{\text{i}}$	0.74(2)	2.57(2)	2.964(2)	115(2)
$\text{N3}^{\text{iii}}-\text{H3}^{\text{iii}}\cdots\text{O2}$	0.74(2)	2.15(2)	2.869(2)	163(2)
$\text{N5}^{\text{iii}}-\text{H5b}^{\text{iii}}\cdots\text{O1}$	0.83(2)	2.09(2)	2.916(2)	173(2)
$\text{N4}^{\text{iv}}-\text{H4b}^{\text{iv}}\cdots\text{O4}^{\text{ii}}$	0.87(3)	2.23(3)	3.081(2)	167(2)
$\text{N4}^{\text{v}}-\text{H4c}^{\text{v}}\cdots\text{O4}^{\text{ii}}$	0.89(2)	1.81(2)	2.688(2)	168(2)

2.3. Analytical Characterization

All investigated compounds were characterized using vibrational (IR and Raman) and NMR (^1H , ^{13}C) spectroscopy. Also mass spectrometry and elemental analysis were employed to identify the corresponding materials. For analytical details of the respective compounds see the *Experimental Section*. The decomposition temperatures were determined by differential scanning calorimetry on a Linseis PT 10 DSC [23].

2.3.1. Infrared Spectroscopy

The strongest observed absorptions in the IR spectra of the ANQ^+ -species are the symmetric N–H-valence vibrations of the $-\text{NH}_3^+$ functionality at 3379–3414 cm^{-1} . In the IR spectrum of neutral ANQ, an additional strong absorption at 3551 cm^{-1} is observed. Here, the symmetric N–H-valence vibrations are found at higher energy since the amine group is not protonated. Further strong absorptions indicate the presence of the nitramine moiety found in all investigated compounds, which reveals the antisymmetric N–O-valence vibration of the nitro group at 1632–1639 cm^{-1} and the symmetric N–O-valence vibration at 1278–1280 cm^{-1} . The IR spectrum of the sulfate salt additionally shows the strong antisymmetric S–O-valence vibration of the sulfate anion at 1065 cm^{-1} .

2.3.2. Differential Scanning Calorimetry

Unlike unprotonated ANQ, which decomposes at 180 °C, the protonated ANQ^+ salts show thermal stabilities, which are far below that value. The halides decompose at 80 °C (**2**, **3**) and 86 °C (**4**) respectively, whereas the sulfate salt **5** is stable up to 144 °C.

2.3.3. Sensitivity Testing

Since 1-amino-3-nitroguanidinium salts show enhanced sensitivity towards outer stimuli such as impact and friction, the impact and friction sensitivities were determined and carried out according to STANAG 4489 [24] and 4487 [25] modified instructions [26,27] using a BAM (Bundesanstalt für Materialforschung) drophammer [28–30] and a BAM friction tester [28–30]. Regarding the

sensitivities of the salts, a large difference between the halides **2–4** and the sulfate salt **5** is also observed. Whereas the halides reveal sensitivities of 25 J (impact sensitivity) and 288 N (friction sensitivity), the sulfate salt **5** is much more sensitive, having 6 J (impact sensitivity) and 120 N (friction sensitivity). This can primarily be explained by the formation of monohydrates, which is true for all halides **2–4**, whereas the sulfate salt **5** crystallizes water-free. The determined values imply a classification [25] of the tested materials as “sensitive” towards both impact and friction. The higher sensitivities of the protonated species discussed herein compared to the neutral compound ANQ can be correlated to a lowered C–N bond order of the hydrazine moiety of the molecule, which appears upon protonation of the molecule as it was found during the structural investigation of neutral ANQ and its protonated species in reference 4. The same argumentation can also be applied to the thermal stabilities of the compounds, whereas a weaker C–N bond of the hydrazine moiety facilitates the loss of the hydrazine moiety and thus, decomposition of the material.

3. Experimental Section

All reagents and solvents were used as received (Sigma-Aldrich, Fluka, Acros Organics) unless stated otherwise. Melting and decomposition points were measured with a Linseis PT10 DSC using a heating rate of 5 °C min^{−1}, which were checked with a Büchi Melting Point B-450 apparatus. ¹H and ¹³C NMR spectra were measured with a JEOL instrument. All chemical shifts are quoted in ppm relative to TMS (¹H, ¹³C). Infrared spectra were measured with a Perkin-Elmer Spektrum One FT-IR instrument. Raman spectra were measured with a Perkin-Elmer Spektrum 2000R NIR FT-Raman instrument equipped with a Nd:YAG laser (1064 nm). Elemental analyses were performed with a Netsch STA 429 simultaneous thermal analyzer. Friction and Impact sensitivity data were determined using a BAM drophammer and a BAM friction tester [25]. The electrostatic sensitivity tests were carried out using an Electric Spark Tester ESD 2010 EN (OZM Research) operating with the “Winspark 1.15” software package [31].

3.1. 1-Amino-3-nitroguanidinium Chloride Monohydrate (**2**)

1 (2.38 g, 20.0 mmol) was suspended in 2 M HCl (24 mL, 48 mmol), the mixture was heated to 60 °C and the water was removed in vacuum. The residue was recrystallized from ethanol/water to yield 2.80 g (16.1 mmol, 81%) of **2** as a white powder. Alternatively, the compound can be crystallized by slow evaporation of the water in an open dish in slightly lower yields.

DSC (5 °C min^{−1}, °C): 80 °C (dec. 1); IR (KBr, cm^{−1}): $\tilde{\nu}$ = 3549 (s), 3414 (vs), 3236 (s), 2964 (m), 2719 (m), 2675 (m), 2109 (w), 1636 (s), 1618 (s), 1561 (m), 1488 (m), 1384 (m), 1278 (s), 1223 (m), 1195 (m), 908 (w), 783 (w), 621 (w), 483 (w); Raman (1064 nm, 200 mW, 25 °C, cm^{−1}): $\tilde{\nu}$ = 3335 (14), 3250 (27), 3159 (6), 2965 (16), 1625 (7), 1584 (6), 1565 (18), 1551 (5), 1478 (15), 1402 (10), 1258 (98), 1194 (16), 992 (12), 913 (26), 800 (32), 616 (30), 432 (7), 345 (15); ¹H NMR (DMSO-*d*₆, 25 °C, ppm) δ : 8.44 (s, 1H, NH), 6.24 (s, 5H, −NH₃⁺, −NH₂); ¹³C NMR (DMSO-*d*₆, 25 °C, ppm) δ : 159.5 (C(NNO₂)(N₂H₄⁺)(NH₂)); *m/z* (FAB⁺): 120.1 [CH₆N₅O₂⁺]; *m/z* (FAB[−]): 35.0 [Cl[−]]; EA (CH₅N₅O₂·H₂O·HCl, 173.56) calc.: C 6.92, H 4.65, N 40.35%; found: C 6.82, H 4.51, N 39.82%; BAM drophammer: 40 J; friction tester: 288 N; ESD: 0.15 J (at grain size 100–500 μ m).

3.2. 1-Amino-3-nitroguanidinium Bromide Monohydrate (3)

1 (2.38 g, 20.0 mmol) was suspended in 20 mL of water and an aqueous HBr-solution (48% (w/v), 5.0 mL, 44.0 mmol) was added. The mixture was heated to 60 °C until a clear solution is obtained and the water was slowly evaporated in an open dish. **3** crystallizes in colorless blocks in 86% yield (3.73 g, 17.1 mmol).

DSC (5 °C min⁻¹, °C): 80 °C (dec.); IR (KBr, cm⁻¹): $\tilde{\nu}$ = 3379 (vs), 2996 (s), 2681 (m), 2375 (w), 2086 (w), 1633 (s), 1586 (s), 1557 (m), 1538 (m), 1490 (m), 1475 (m), 1399 (m), 1383 (m), 1323 (m), 1279 (s), 1223 (s), 1190 (m), 1155 (m), 1121 (m), 1096 (m), 1037 (w), 908 (w), 783 (w), 662 (w), 581 (w), 532 (w), 473 (w); Raman (1064 nm, 300 mW, 25 °C, cm⁻¹): $\tilde{\nu}$ = 3318 (1), 3254 (8), 2974 (11), 1609 (8), 1580 (3), 1567 (2), 1556 (15), 1533 (2), 1485 (10), 1406 (7), 1255 (100), 1186 (13), 1155 (4), 1094 (5), 994 (15), 913 (24), 800 (45), 720 (2), 614 (37), 587 (2), 519 (2), 467 (1), 431 (8); ¹H NMR (DMSO-*d*₆, 25 °C, ppm) δ : 9.64 (s, 1H, -NHH), 9.17 (s, 1H, -NHH), 6.31 (s, 4H, NHNH₃⁺); ¹³C NMR (DMSO-*d*₆, 25 °C, ppm) δ : 160.8 (C(NNO₂)(N₂H₃)(NH₂)), 161.0 (C(NNO₂)(N₂H₄⁺)(NH₂)); *m/z* (FAB⁺): 120.1 [CH₆N₅O₂⁺]; *m/z* (FAB⁻): 78.9 [⁷⁹Br⁻], 80.9 [⁸¹Br⁻]; EA (CH₅N₅O₂·H₂O·HBr, 218.01) calc.: C 5.51, H 3.70, N 32.12%; found: C 5.43, H 3.57, N 31.76 %; BAM drophammer: 25 J; friction tester: 288 N; ESD: 0.20 J (at grain size 500–1000 μm).

3.3. 1-Amino-3-nitroguanidinium Iodide Monohydrate (4)

1 (2.38 g, 20.0 mmol) was suspended in 20 mL of water and an aqueous HI-solution (57% (w/v), 5.8 mL, 44.0 mmol) was added. The mixture was heated to 60 °C until a clear solution is obtained and the water was slowly evaporated in an open dish. **4** crystallizes in large colorless blocks in 86% yield (3.73 g, 17.1 mmol), which tend to turn yellowish after a few days upon the release of molecular I₂.

DSC (5 °C min⁻¹, °C): 86 °C (dec.); IR (KBr, cm⁻¹): $\tilde{\nu}$ = 3384 (vs), 3278 (s), 3224 (s), 2927 (m), 2732 (m), 2371 (w), 1632 (vs), 1587 (s), 1475 (s), 1458 (m), 1369 (m), 1278 (vs), 1122 (m), 1099 (m), 1037 (w), 1000 (w), 913 (w), 835 (w), 783 (w), 701 (w), 618 (w), 581 (w); Raman (1064 nm, 300 mW, 25 °C, cm⁻¹): $\tilde{\nu}$ = 3393 (2), 3235 (7), 2978 (2), 1629 (7), 1604 (1), 1563 (44), 1531 (8), 1489 (19), 1456 (2), 1383 (24), 1264 (100), 1162 (21), 1110 (3), 999 (21), 921 (38), 797 (69), 699 (5), 620 (37), 571 (2), 433 (32); ¹H NMR (DMSO-*d*₆, 25 °C, ppm) δ : 8.30 (s, 3H, NH, NH₂), 6.47 (s, 3H, -NH₃⁺); ¹³C NMR (DMSO-*d*₆, 25 °C, ppm) δ : 159.3 (C(NNO₂)(N₂H₄⁺)(NH₂)); *m/z* (FAB⁺): 120.1 [CH₆N₅O₂⁺]; *m/z* (FAB⁻): 126.9 [I⁻]; EA (CH₅N₅O₂·H₂O·HI, 265.01) calc.: C 4.53, H 3.04, N 26.43 %; found: C 4.87, H 2.92, N 26.46%; BAM drophammer: 25 J; friction tester: 288 N; ESD: 0.20 J (at grain size 500–1000 μm).

3.4. Bis(1-amino-3-nitroguanidinium) Sulfate (5)

1 (2.38 g, 20.0 mmol) was suspended in 20 mL of water and 1 M H₂SO₄ (11 mL, 11 mmol) was added. The mixture was heated to 60 °C and the water was removed in vacuum. The residue was again recrystallized from water to yield 2.93 g (8.71 mmol, 87%) of **5** as colorless crystals.

DSC (5 °C min⁻¹, °C): 144 °C (dec.); IR (KBr, cm⁻¹): $\tilde{\nu}$ = 3401 (s), 3307 (vs), 3153 (s), 2923 (m), 2647 (m), 2060 (w), 1684 (m), 1659 (m), 1639 (m), 1566 (m), 1485 (m), 1459 (m), 1384 (m), 1280 (s), 1256 (s), 1161 (m), 1124 (m), 1091 (m), 1065 (s), 1009 (m), 976 (m), 924 (w), 788 (w), 728 (w),

647 (w), 614 (m), 457 (w); Raman (1064 nm, 200 mW, 25 °C, cm^{-1}): $\tilde{\nu} = 3238$ (4), 3165 (4), 1643 (10), 1580 (9), 1543 (8), 1485 (11), 1414 (5), 1280 (23), 1161 (19), 1131 (13), 1091 (7), 982 (100), 935 (35), 802 (31), 635 (28), 604 (10), 476 (11), 458 (15), 435 (12), 356 (30), 248 (14), 196 (30), 178 (29), 136 (44), 116 (43); ^1H NMR (DMSO- d_6 , 25 °C, ppm) δ : 8.17 (s, NH), 7.64 (s, 5H, $-\text{NH}_3^+$, $-\text{NH}_2$); ^{13}C NMR (DMSO- d_6 , 25 °C, ppm) δ : 160.5 (C(NNO $_2$)(N $_2$ H $_4^+$)(NH $_2$)); m/z (FAB $^+$): 120.1 [CH $_6$ N $_5$ O $_2^+$]; m/z (FAB $^-$): 96.9 [HSO $_4^-$]; EA (C $_2$ H $_{12}$ N $_{10}$ O $_8$ S, 336.24) calc.: C 7.14, H 3.60, N 41.66%; found: C 7.47, H 3.44, N 41.35%; BAM drophammer: 6 J; friction tester: 120 N; ESD: 0.30 J (at grain size 500–1000 μm).

4. Conclusions

From this experimental study the following conclusions can be drawn:

- 1-Amino-3-nitro-guanidine (**1**) can be protonated with strong acids ($\text{pKs} < 1$). Protonation was accomplished with hydrochloric, hydrobromic, hydroiodic and sulfuric acid. No protonation could be observed with aqueous hydrofluoric acid (40%).
- The structures of the crystalline state of amino-nitroguanidinium chloride monohydrate (**2**), amino-nitroguanidinium bromide monohydrate (**3**), amino-nitroguanidinium iodide monohydrate (**4**) and bis(amino-nitroguanidinium) sulfate (**5**) were determined by low temperature X-ray diffraction. The salts crystallize in common space group (**2**: $P2_1/n$, **3**: $P2_1/c$, **4**: $P-1$, **5**: $Fdd2$).
- The good solubility and availability of **2–5** allows the metathesis reaction with different silver and barium salts under precipitation of low-soluble AgCl, AgBr, AgI or BaSO $_4$ for the synthesis of a variety of amino-nitroguanidinium salts as exemplarily shown for 1-amino-3-nitroguanidinium dinitramide [4].

Acknowledgments

Financial support of this work by the Ludwig-Maximilian University of Munich (LMU), the U.S. Army Research Laboratory (ARL), the Armament Research, Development and Engineering Center (ARDEC), the Strategic Environmental Research and Development Program (SERDP) and the Office of Naval Research (ONR).

Conflict of Interest

The authors declare no “conflict of interest”.

References and Notes

1. McKay, A.F. Nitroguanidines. *Chem. Rev.* **1952**, *51*, 301–346.
2. Klapötke, T.M. *Chemistry of High-Energy Materials*, 1st ed.; Walter de Gruyter GmbH & Co. KG: Berlin, Germany; New York, NY, USA, 2011; p. 4 and 38.
3. Henry, R.A.; Lewis, H.D.; Smith, G.B.L. Hydrazinolysis of nitroguanidine and alkylnitroguanidines. *J. Am. Chem. Soc.* **1950**, *72*, 2015–2018.
4. Phillips, R.; Williams, J.F. Nitroaminoguanidine. *J. Am. Chem. Soc.* **1928**, *50*, 2465–2470.

5. Castillo-Meléndez, J.A.; Golding, B.T. Optimization of the synthesis of guanidines from amines via nitroguanidines using 3,5-dimethyl-N-nitro-1*H*-pyrazole-1-carboxamidine. *Synthesis* **2004**, *10*, 1655–1663.
6. Fischer, N.; Klapötke, T.M.; Stierstorfer, J. 1-Amino-3-nitroguanidine (ANQ) in high performing energetic materials. *Z. Naturforsch. B* **2012**, in press.
7. *CrysAlisPro*, Agilent Technologies, Version 1.171.35.11; Agilent Technologies: UK: Yarnton, UK, 2011.
8. Sheldrick, G.M. *SHELXS-97, Program for Crystal Structure Solution*; University of Göttingen: Göttingen, Germany, 1997.
9. Altomare, A.; Cascarano, G.; Giacovazzo, C.; Guagliardi, A. Completion and refinement of crystal structures with SIR92. *Appl. Cryst.* **1993**, *26*, 343–350.
10. Sheldrick, G.M. *SHELXL-97, Program for the Refinement of Crystal Structures*; University of Göttingen: Göttingen, Germany, 1994.
11. Spek, A.L. *Platon, A Multipurpose Crystallographic Tool*; Utrecht University: Utrecht, The Netherlands, 1999.
12. Farrugia, L. WinGX suite for small-molecule single crystal crystallography. *J. Appl. Cryst.* **1999**, *32*, 837–838.
13. *Empirical Absorption Correction Using Spherical Harmonics, Implemented in Scale3 Abspack Scaling Algorithm*, Version 171.33.41; CrysAlisPro Oxford Diffraction Ltd.: Yarnton, UK, 2009.
14. Crystallographic data for the structure(s) have been deposited with the Cambridge Crystallographic Data Centre. Copies of the data can be obtained free of charge on application to The Director, CCDC, 12 Union Road, Cambridge CB2 1EZ, UK (Fax: int.code_(1223)336-033; e-mail for inquiry: fileserv@ccdc.cam.ac.uk; e-mail for deposition: deposit-@ccdc.cam.ac.uk).
15. Bernstein, J.; Davis, R.E.; Shimon, L.; Chang, N.-L. Patterns in hydrogen bonding: Functionality and graph set analysis in crystals. *Angew. Chem. Int. Ed.* **1995**, *34*, 1555–1573.
16. Kollman, P.A.; Allen, L.C. Theory of hydrogen bond. *Chem. Rev.* **1972**, *72*, 283–303.
17. Arunan, E.; Desiraju, G.R.; Klein, R.A.; Sadlej, J.; Scheiner, S.; Alkorta, I.; Clary, D.C.; Crabtree, R.H.; Dannenberg, J.J.; Hobza, P.; *et al.* Definition of the hydrogen bond (IUPAC Recommendations 2011). *Pure Appl. Chem.* **2011**, *83*, 1637–1641.
18. Desiraju, G.R.; Steiner, T. *The Weak Hydrogen Bond in Structural Chemistry and Biology*; Oxford University Press: Oxford, UK, 1999.
19. Dai, J.; Chen, X.-Y. 3-Cyanoanilinium iodide monohydrate. *Acta Cryst.* **2010**, *E66*, o3295.
20. McGinnety, J.A. Redetermination of the structures of potassium sulfate and potassium chromate. Effect of electrostatic crystal forces upon observed bond lengths. *Acta Cryst.* **1972**, *B28*, 2845–2852.
21. Ramesh, P.; Subbiahpandi, A.; Manikannan, R.; Muthusubramanian, S.; Ponnuswamy, M.N. 3-Cyclohexylsulfanyl-2-(4-methylphenyl)-5,7-dinitro-1*H*-indole. *Acta Cryst.* **2008**, *E64*, o1890.
22. Yu, Z.; Kuroda-Sowa, T.; Nabei, A.; Maekawa, M.; Okubo, T. {6,6'-Dimethoxy-2,2'-[naphthalene-2,3-diylbis(nitrilomethylidyne)]diphenolato}thiocyanatocobalt(III) diethyl ether dichloromethane solvate. *Acta Cryst.* **2009**, *E65*, m257–m258.
23. Linseis. Available online: <http://www.linseis.com> (accessed on 26 March 2012).

24. NATO. *Standardization Agreement (STANAG) on Explosives, Impact Sensitivity Tests*, No. 4489, 1st ed.; NATO: Brussels, Belgium, 1999.
25. NATO. *Standardization Agreement (STANAG) on Explosive, Friction Sensitivity Tests*, No. 4487, 1st ed.; NATO: Brussels, Belgium, 2002.
26. *WIWEB-Standardarbeitsanweisung, Nr. 4-5.1.02, Ermittlung der Explosionsgefährlichkeit (Impact Sensitivity Tests with a Drophammer)*; WIWEB: Erding, Germany, 2002.
27. *WIWEB-Standardarbeitsanweisung, Nr. 4-5.1.03, Ermittlung der Explosionsgefährlichkeit oder der Reibeempfindlichkeit mit dem Reibeapparat*; WIWEB: Erding, Germany, 2002.
28. Bundesanstalt für Materialforschung und -prüfung. Available online: <http://www.bam.de> (accessed on 26 March 2012).
29. Reichel & Partner GmbH. Available online: <http://www.reichel-partner.de> (accessed on 26 March 2012).
30. Impact: insensitive > 40 J, less sensitive > 35 J, sensitive > 4 J, very sensitive < 3 J. Friction: insensitive > 360 N, less sensitive = 360 N, sensitive < 360 N and > 80 N, very sensitive < 80 N, extremely sensitive < 10 N. According to the UN Recommendations on the Transport of Dangerous Goods, (+) indicates not safe for transport.
31. ESD 2008A small-scale electrostatic spark sensitivity test, Available online: <http://ozm.cz/en/sensitivity-tests/esd-2008a-small-scale-electrostatic-spark-sensitivity-test/> (accessed on 26 March 2012).

© 2012 by the authors; licensee MDPI, Basel, Switzerland. This article is an open access article distributed under the terms and conditions of the Creative Commons Attribution license (<http://creativecommons.org/licenses/by/3.0/>).

TKX50 – The revolution in RDX-replacements

Niko Fischer*, Thomas M. Klapötke and Jörg Stierstorfer

Energetic Materials Research, Department of Chemistry,
University of Munich (LMU), Butenandtstr. 5-13, D-81377, Germany

finch@cup.uni-muenchen.de

Abstract:

The new high performing secondary explosive based on 5,5'-bistetrazole-1,1'-dioxide, namely TKX50 has been synthesized in excellent yields in large quantities. It was completely characterized with respect to its chemical and energetic properties. Its calculated (EXPLO5.05) detonation performances exceed the performance of HMX and CL-20 (V_{det} (TKX50) = 9698 ms⁻¹). Nevertheless, it shows excellent thermal stability (T_{dec} (TKX50) = 221 °C) as well as compatibility in mixtures while being significantly less sensitive (IS/FS (TKX50) = 20 J/120 N) than commonly used explosives such as hexogen (RDX) and octogen (HMX). To study the initiation properties of TKX50, a small scale shock reactivity test (SSRT) was performed. Here we observed performance (as evidenced by denting an aluminum block) after initiation of TKX50 comparable to HMX and superior to RDX.

Keywords: 5,5'-bistetrazole-1,1'-dioxide; crystal density; detonation parameters; RDX replacement; sensitivities; thermal stability;

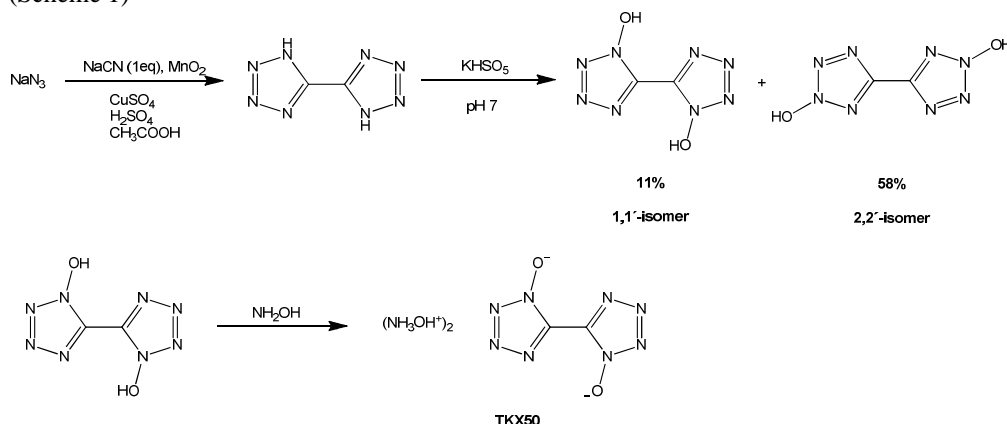
1 Introduction

The design of new energetic materials encompassing all of propellants, explosives, and pyrotechnics is a modern academic and technological challenge.[1] Intense research is focused on the tailoring of new energetic molecules with performances and stability similar to that of RDX (cyclotrimethylenetrinitramine) to replace this widely-used high explosive. For a novel energetic molecule to find practical application as a high explosive it needs to possess high thermal and mechanical stabilities, while at the same time satisfying the increasing demand for higher performing (high detonation velocity, pressure and heat of explosion) materials.[2] A very promising explosophoric moiety in the design of new energetic materials is the tetrazole ring; the carbon on position 5 of the ring allows the facile attachment of various substituents for energetic tailorability, and the high nitrogen content and heat of formation of the heterocycle leads to high energetic performances. It can be stated that the tetrazole heterocycle occupies the “middle ground” of the stability vs. high performance continuum, where highly stable compounds can be poorly-performing energetics and highly energetic compounds are often unstable.[3,4] In order to improve the already application-viable tetrazoles, several recently published studies showed that introduction of N-oxides yield compounds with even higher densities and stabilities, lower sensitivities and better oxygen balances.[5,6,7] Combining these principles with practical considerations in mind, we have devised a simple synthetic pathway to the high performing energetic material hydroxylammonium salt of 5,5'-bistetrazole-1,1'-dioxide (TKX50) (in honor of Thomas Klapötke's 50th birthday).

2 Results and Discussion

2.1 Synthesis

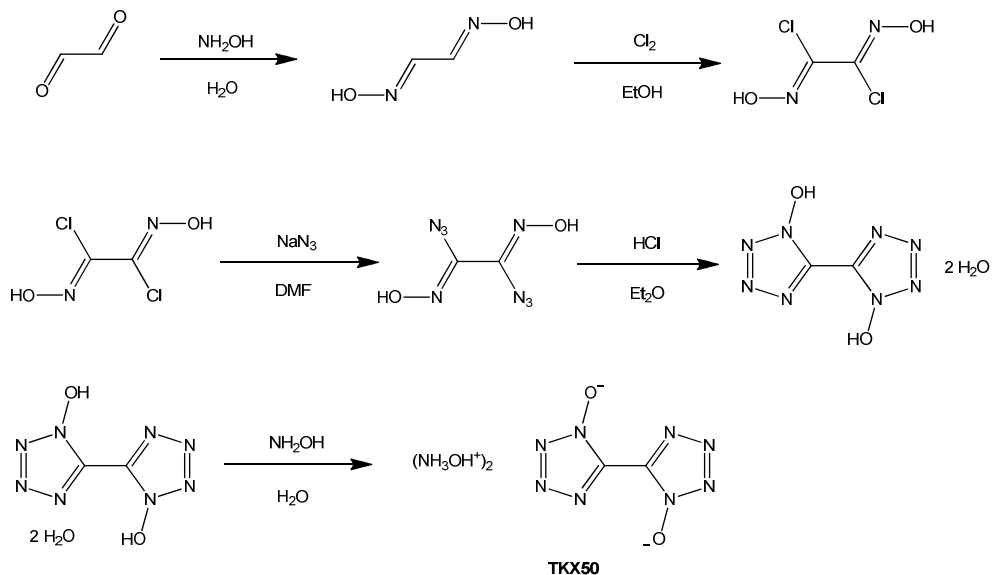
There are two major routes to the 5,5'-bistetrazole-1,1'-dioxide moiety that forms the backbone of TKX50. The first of which, the oxidation of the parent heterocycle with aqueous potassium peroxymonosulfate, was the method by which we prepared this new material first. The oxidation of the 5,5'-bistetrazolate anion with peroxymonosulfate was carried out in a manner similar to that we have previously reported for 5-nitro and 5-azidotetrazoles.[5,6] Unfortunately, this reaction was found to produce the 2,2' isomer as major product, with only traces of the 1,1' which crystallized upon adding aqueous hydroxylamine as a result of lower solubility. However, the downside of this method is the low yield (~11%) of the 1,1'-isomer. (Scheme 1)



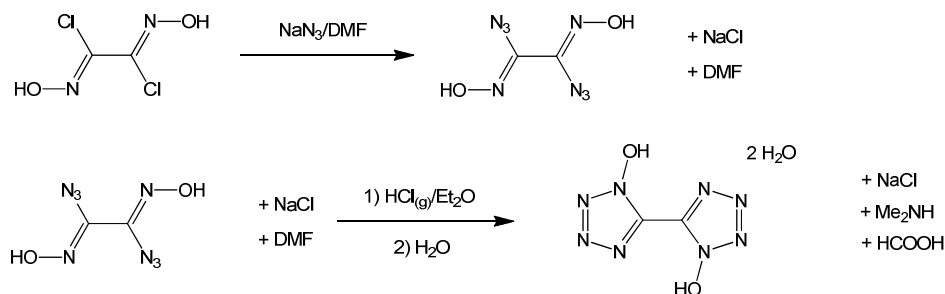
Scheme 1. Synthesis of TKX50 via oxidation of 5,5'-bistetrazole using peroxymonosulfate.

To achieve a higher yield of the 1,1'-isomer, a different route for the synthesis of this precursor had to be chosen, which is the cyclization of diazidoglyoxime under acidic conditions (HCl gas in diethyl ether) as reported by Tselinskii et al. [8]. Here, diazidoglyoxime was prepared from dichloroglyoxime and sodium azide in DMF. After isolation of the precursor 5,5'-bistetrazol-1,1'-diol dihydrate it can be treated with an aqueous solution of hydroxylamine forcing TKX50, which shows a water solubility of only 3 g/L H_2O at 20°C , to precipitate (Scheme 2).

To overcome the problem of isolating the highly sensitive diazidoglyoxime, the whole reaction process was transformed into a multi-step one pot reaction starting from dichloroglyoxime involving the chloro-azido exchange in DMF and subsequent cyclization, whereas the whole mixture is poured onto diethyl ether and HCl gas is bubbled through it affording the dimethylammonium salt of 5,5'-bistetrazole-1,1'-dioxide (Scheme 3). The dimethylammonium salt, after recrystallization, can be treated with hydroxylammonium chloride resulting in a precipitate of TKX50.



Scheme 2. Synthesis of TKX50 via cyclization of diazidoglyoxime.



Scheme 3. Synthesis of 5,5'-bistetrazole-1,1'-diol in a one pot reaction starting from dichloroglyoxime.

2.2 Crystal Structure

A suitable single crystal of TKX50 was picked from the crystallization mixture and mounted in Kel-F oil, transferred to the N_2 stream of an Oxford Xcalibur3 diffractometer with a Spellman generator (voltage 50 kV, current 40 mA) and a KappaCCD detector. The data collection was performed using the CRYSLIS CCD software [9], the data reduction using the CRYSLIS RED software [10]. The structure was solved with SIR-92 [11], refined with SHELXL-97 [12] and finally checked using the PLATON software [13] integrated in the WINGX software suite.[14] The non-hydrogen atoms were refined anisotropically and the hydrogen atoms were located and freely refined. The absorptions were corrected by a SCALE3 ABSPACK multi-scan method.[15]

TKX50 crystallizes in the monoclinic space group $P2_1/c$ with two anion/cation moieties in the unit cell. Its density of 1.918 g cm^{-3} is significantly higher than that of bishydroxylammonium 5,5'-bistetrazolate (1.742 g cm^{-3}) recently published.[16] The structure is strongly influ-

enced by several strong hydrogen bonds involving all four hydrogen atoms of the hydroxylammonium cations. The molecular moiety of TKX50 is depicted in Figure 1.

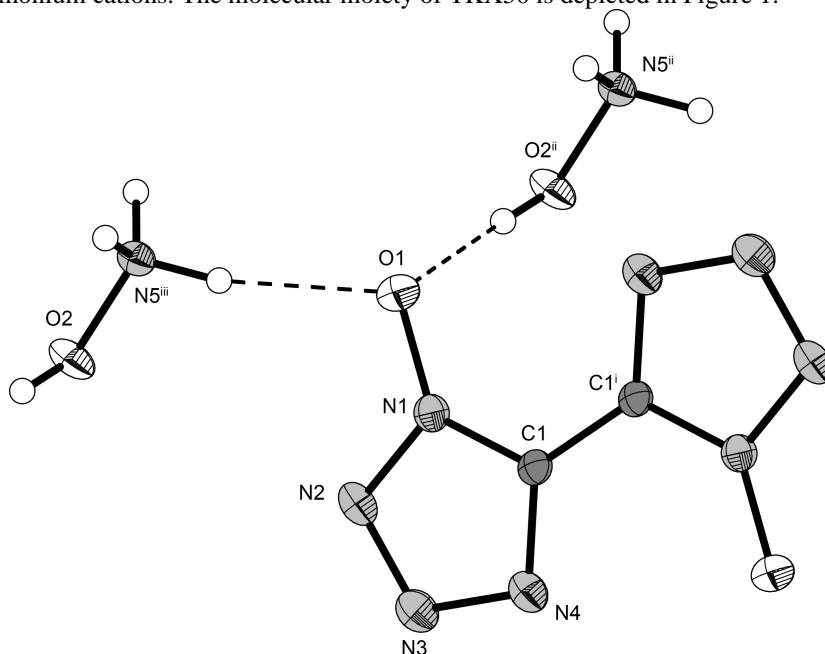


Figure 1: Representation of the solid state molecular structure of **TKX50** (hydroxylammonium 5,5'-bistetrazole-1,1'-dioxide). Thermal ellipsoids are drawn at the 50% probability level. Selected X-ray parameters: $\text{C}_2\text{H}_8\text{N}_{10}\text{O}_4$, 236.18 g mol⁻¹, monoclinic, $P2_1/c$, $a = 5.4872(8)$ Å, $b = 11.5472(15)$ Å, $c = 6.4833(9)$ Å, $\beta = 95.402(12)^\circ$, $V = 408.97(10)$ Å³, $Z = 2$, $\rho = 1.918$ g cm⁻³, 100 K, $\theta_{\text{min-max}} = 4.7, 27.2$, $hkl = -6:7; -11:14; -4:8$, $R_1 = 0.0342$, $wR_2 = 0.0895$, $S = 1.06$, Resd. Dens. (min/max) = $-0.31/0.24$. Selected bond lengths (Å): O1–N1 1.3280(15), N1–N2 1.3424(17), N1–C1 1.3451(18), N2–N3 1.3128(17), N3–N4 1.3513(18), N4–C1 1.3358(19), C1–C1' 1.445(3), O2–N5 1.4152(15). Selected bond angles ($^\circ$): O1–N1–N2 122.09(11), O1–N1–C1 129.25(12), N2–N1–C1 108.65(12), N3–N2–N1 106.16(12), N2–N3–N4 111.24(11), C1–N4–N3 105.43(11), N4–C1–N1 108.52(13), N4–C1–C1' 127.46(16), N1–C1–C1' 124.02(16). Symmetry codes: (i) $2-x, -y, 2-z$; (ii) $x, 0.5-y, -0.5+z$; (iii) $-1+x, 0.5-y, -0.5+z$.

2.3 Energetic properties

2.3.1 Thermal behavior (DSC)

Differential scanning calorimetry (DSC) measurements of **1–15** to determine the melt- and decomposition temperatures (~ 1.5 mg of each energetic material) were performed in covered Al-containers containing a hole in the lid with a nitrogen flow of 20 mL min⁻¹ on a Linseis PT10 DSC [17] calibrated by standard pure indium and zinc at a heating rate of 5 °C min⁻¹. Thermal stability is important for any explosive in practical use as demanding military requirements require explosives that can withstand high temperatures. For example, a munition sitting in the desert can exceed 100 °C and for general use a component explosive must be stable above 200 °C. TKX50 with a decomposition onset of 221 °C easily surpasses this requirement. The DSC plot of TKX50 in comparison to that of RDX is shown in Figure 2.

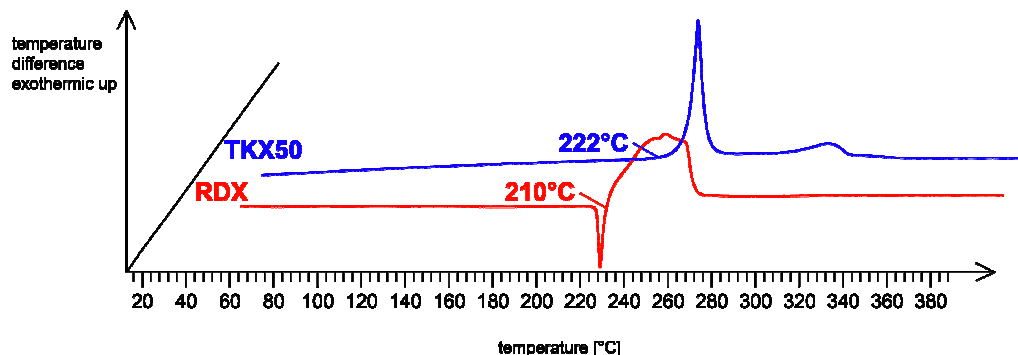


Figure 2: DSC plot of both TKX50 and RDX at a heating rate of $5^{\circ}\text{C min}^{-1}$.

2.3.2 Sensitivities and detonation parameters

The impact sensitivity tests were carried out according to STANAG 4489 [18] modified instruction [19] using a BAM (Bundesanstalt für Materialforschung) drophammer.[20] The friction sensitivity tests were carried out according to STANAG 4487 [21] modified instruction [22] using the BAM friction tester. The classification of the tested compounds results from the “UN Recommendations on the Transport of Dangerous Goods”.[23] Additionally all compounds were tested upon the sensitivity towards electrical discharge using the Electric Spark Tester ESD 2010 EN [24].

The impact sensitivity of TKX50 is 20 J, much higher than those for RDX, HMX and CL-20, which range from 4 to 7.5 J, and all three of which need desensitizing components added for practical use. The low impact sensitivity of TKX50 means it can be used without desensitization, resulting in higher explosive content per volume, and as such higher explosive performance. Impact sensitivity is a high priority in explosive devices used in the military due to the range of stresses devices must be under. This is in contrast to the friction sensitivity which is less important in physical explosive devices as the explosive is contained within and protected from friction. Friction sensitivity is more important in the manufacturing context, where TKX50 with 120 N is of comparable or lower sensitivity than any of RDX, HMX or CL-20, increasing the margin of safety in the industrial context. Through normal activities, the human body can generate up to 25 mJ of static electricity, which can easily set off the most sensitive explosives. Like RDX, CL-20, and HMX, TKX50 has electrostatic sensitivities higher than that is capable of being generated by the human body, allowing safety during handling.

The detonation parameters were calculated using the program EXPLO5 V5.05.[25] The calculations were performed using the maximum densities according to the crystal structures. Heats of formation were computed theoretically. All calculations were carried out using the Gaussian G09 program package.[26] The enthalpies (H) and free energies (G) were calculated using the complete basis set (CBS) method of Petersson and coworkers in order to obtain very accurate energies. The sensitivity data as well as the decomposition temperatures, the heats of formation and the detonation parameters of TKX50 are compared to those of TNT, RDX, HMX and CL-20 in Table 1. Due to its high heat of formation, TKX50 outperforms even CL-20 in terms of detonation velocity, however, the detonation pressure is slightly lower as compared to CL-20.

Table 1: Physicochemical properties and detonation parameters of selected high explosives.

	TNT	RDX	HMX	CL-20	TKX50
Formula	$C_7H_5N_3O_6$	$C_3H_6N_6O_6$	$C_4H_8N_8O_8$	$C_6H_6N_{12}O_{12}$	$C_2H_8N_{10}O_4$
FW [g mol ⁻¹]	227.13	222.12	296.16	438.19	236.15
IS [J] ^a	15 ^[27]	7.5 ^[27]	7 ^[27]	4 ^[27]	20
FS [N] ^b	353	120 ^[27]	112 ^[27]	48 ^[27]	120
ESD-test [J] ^c	---	0.2	0.2	---	0.1
N [%] ^d	18.50	37.84	37.84	38.36	59.31
O [%] ^e	-73.96	-21.61	-21.61	-10.95	-27.10
T _m [°C] ^f	81	205 ^[28]	275 ^[28]	---	---
T _{dec} [°C] ^f	290	210 ^[28]	279 ^[28]	215 ^[29]	221
Density [g cm ⁻³] ^g	1.713 ^[30]	1.858 ^[31]	1.944 ^[32]	2.083 ^[33]	1.918
Δ _f H° / kJ mol ⁻¹ ^h	-55.5	86.3	116.1	365.4	446.6
Δ _f U° / kJ kg ⁻¹ ⁱ	-168.0	489.0	492.5	918.7	2006.4
EXPLO5.05 values:					
-Δ _E U° [kJ kg ⁻¹] ^j	5258	6190	6185	6406	6025
T _E [K] ^k	3663	4232	4185	4616	3954
p _{C-J} [kbar] ^l	235	380	415	467	424
D [m s ⁻¹] ^m	7459	8983	9221	9455	9698
Gas vol. [L kg ⁻¹] ⁿ	569	734	729	666	846

^a impact sensitivity (BAM drophammer^[20], 1 of 6); ^b friction sensitivity (BAM friction tester^[20], 1 of 6); ^c electrostatic discharge device (OZM^[24]); ^d nitrogen content; ^e oxygen balance; ^f melt- and decomposition temperature from DSC (β = 5 °C); ^g estimated from X-ray diffraction, measurement at 100 K for TNT, HMX, CL-20 and TKX50 and 90 K for RDX; ^h calculated (CBS-4M) heat of formation; ⁱ calculated energy of formation; ^j Energy of Explosion; ^k explosion temperature; ^l detonation pressure; ^m detonation velocity; ⁿ assuming only gaseous products.

2.3.3 Small-Scale Shock Reactivity Test

The Small-Scale Shock Reactivity Test (SSRT) [34] was introduced by researchers at IHDIV, DSWC (Indian Head Division, Naval Surface Warfare Center). The SSRT measures the shock reactivity (explosiveness) of energetic materials, often well-below critical diameter, without requiring a transition to detonation. The test setup combines the benefits from a lead block test [35] and a gap test [36]. In comparison to gap tests, the advantage is the use of a smaller sample size of the tested explosive (ca. 500 mg). The sample volume V_s is recommended to be 0.284 mL (284 mm³). For our test setup, shown in Figure 3, no possible attenuator (between detonator and sample) and air gap (between sample and aluminum block) was used. The used sample weight m_s was calculated by the formula $V_s \times \rho_{Xray} \times 0.95$. Several tests with commonly used explosives such as TNT, PETN, RDX, HMX and also CL-20 were performed in order to obtain different dents in the aluminum plate. The dent sizes were measured by filling them with fine quartz sand and calculating the volume from the corresponding SiO₂ mass.

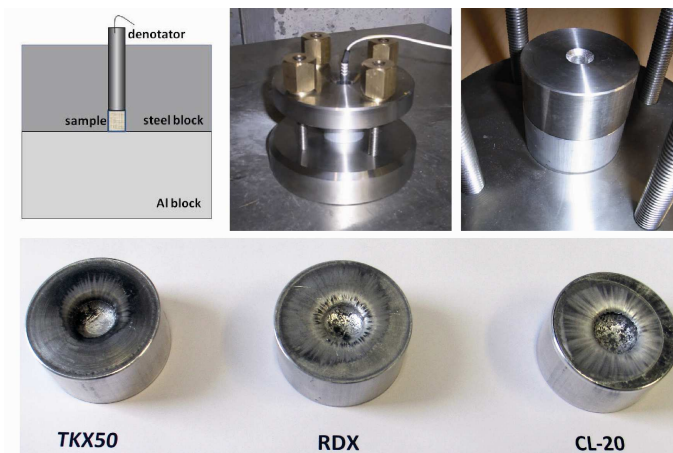


Figure 3: Small Scale Shock Reactivity Test (SSRT). Upper line: Test setup. Lower line: Test results.

As it can also be seen from Figure 3, the dent resulted from **TKX50** is significantly larger than that of **RDX** and in the same range of that observed for **CL-20**. Quantitative values have been summarized in Table 2. Therefore it can be concluded that the explosive performance of TKX50 is in the range of that of CL-20.

Table 2: Results of the Small Scale Shock Reactivity Test (SSRT).

<i>Explosive</i>	<i>weight [mg]</i>	<i>dent [mg SiO₂]</i>
<i>RDX</i>	<i>504</i>	<i>589</i>
<i>CL-20</i>	<i>550</i>	<i>947</i>
<i>TKX50</i>	<i>509</i>	<i>857</i>

3 Experimental Part

Caution! The herein described materials as well as their precursors are energetic materials with increased sensitivities towards shock and friction. Therefore, proper safety precautions (safety glass, face shield, earthened equipment and shoes, Kevlar[®] gloves and ear plugs) have to be applied while synthesizing and handling the described compounds.

All chemicals and solvents were employed as received (Sigma-Aldrich, Fluka, Acros). ¹H and ¹³C spectra were recorded using a JEOL Eclipse 270, JEOL EX 400 or a JEOL Eclipse 400 instrument. The chemical shifts quoted in ppm in the text refer to typical standards such as tetramethylsilane (¹H, ¹³C). To determine the melting and decomposition temperatures of the described compounds a Linseis PT 10 DSC (heating rate 5°C min⁻¹) was used. Infrared spectra were measured using a Perkin Elmer Spectrum One FT-IR spectrometer as KBr pellets. Raman spectra were recorded on a Bruker MultiRAM Raman Sample Compartment D418 equipped with a Nd-YAG-Laser (1064 nm) and a LN-Ge diode as detector. Mass spectra of the described compounds were measured at a JEOL MStation JMS 700 using FAB technique. To measure elemental analyses a Netsch STA 429 simultaneous thermal analyzer was employed.

Dihydroxylammonium 5,5'-bistetrazole-1,1'-dioxide (TKX50) via oxidation of 5,5'-bistetrazole with peroxymonosulfate

5,5'-Bistetrazole (3.00 g, 21.7 mmol) was dissolved in 200 mL of water. Oxone (80.0 g, 109 mmol, 5 eq.) was added to the clear solution and the resulting solution was buffered with trisodium phosphate to pH 7. The mixture turned to a pink color, as soon as the pH exceeds a certain value. The mixture is stirred at room temperature for 5 h, is then acidified with conc. sulfuric acid and extracted into ether. Evaporation of the solvent gave the raw product as a slightly yellow solid, which can be recrystallized from methanol to remove remaining sulfates or phosphates. The reaction yields a mixture of the 1,1'-isomer, the 2,2'-isomer and the 1,2'-isomer in overall 71% yield (2.60 g, 15.3 mmol) with the 2,2'-isomer being the main product. The isomer mixture (1.70 g, 10 mmol) is dissolved in 20 mL of hot water. An aqueous solution of hydroxylamine (50% w/w, 1.32 g, 20 mmol) is added and a colorless precipitate forms instantly. The precipitate is redissolved by warming the mixture and the product, which is the dihydroxylammonium salt of the 1,1'-isomer starts to precipitate again. It can be filtered off and recrystallized from water to remove the salt of the remaining 2,2'-isomer, which shows better solubility in water. Due to the predominant formation of the 2,2'-isomer via the oxidation with oxone, the dihydroxylammonium salt of the 1,1'-isomer could only be obtained in minor yields (0.31 g, 1.3 mmol, 13%).

Dihydroxylammonium 5,5'-bistetrazole-1,1'-dioxide (TKX50) via cyclization of diazidoglyoxime

Glyoxime

27.5 g (0.69 mol) of NaOH were dissolved in 75 mL of water and the solution is cooled to 0 °C in a salt-ice bath. Hydroxylammonium chloride (69.5 g, 1.00 mol) is added while stirring. To the obtained solution glyoxal (72.5 g, 0.50 mol, 40% w/w in H₂O) is added, while the temperature is kept below 10 °C. After complete addition of the glyoxal the solution is further chilled in the salt-ice bath until glyoxime precipitates. The solid is removed by suction filtration and washed with only little ice-water to remove remaining sodium chloride.

Dichloroglyoxime

17.6 g (200 mmol) of glyoxime were suspended in 200 mL of ethanol. Chlorine was bubbled through the suspension at -20 °C until the green suspension turned into a yellowish solution. The solution was allowed to warm up slowly to room temperature meanwhile releasing dissolved chlorine. Then the solvent was removed under vacuum and the remaining solid was resuspended in 50 mL of chloroform, stirred for 15 min at room temperature and filtered yielding 26.6 g (85 %) of the colorless product.

¹H NMR (DMSO-*d*₆, 25 °C, ppm) δ: 13.10 ¹³C{¹H} NMR (DMSO-*d*₆, 25 °C, ppm) δ: 131.2; EA (C₂H₂Cl₂N₂O₂, 156.96): calc.: C 15.30, H 1.28, N 17.85 %; found: C 15.65, H 1.25, N 17.49 %;

Diazidoglyoxime

784 mg (5 mmol) of dichloroglyoxime were dissolved in 10 mL of dimethyl formamide. At 0 °C 841 mg (12.93 mmol) sodium azide were added. The suspension was stirred for 20 min at 0 °C and 100 mL of water were added. The precipitate was filtered, washed with 20 mL of water and air dried yielding 713 mg (84%) of the colorless product.

DSC (5 °C min⁻¹): 170 °C (dec.); IR (atr, cm⁻¹): $\tilde{\nu}$ = 3209 (w), 2170 (w), 2123 (w), 1622 (w), 1400 (w), 1361 (w), 1286 (m), 1013 (vs), 930 (m), 920 (s), 855 (s), 731 (s); Raman (1064 nm, 300 mW, 25 °C, cm⁻¹): $\tilde{\nu}$ = 2166 (8), 2129 (5), 2091 (3), 1621 (100), 1457 (14), 1390 (12), 1216 (19), 1034 (3), 882 (20), 672 (3), 442 (6); ¹H NMR (DMSO-*d*₆, 25 °C, ppm) δ:

12.08; $^{13}\text{C}\{^1\text{H}\}$ NMR (DMSO- d_6 , 25 °C, ppm) δ : 136.5; EA (C₂H₂N₈O₂, 170.09): calc.: C 14.12, H 1.19, N 65.88 %; found: C 14.38, H 1.46, N 66.01 %; BAM drophammer: 1.5 J; friction tester: <5 N; ESD: 7 mJ.

5,5'-Bistetrazole-1,1'-diol dihydrate

850 mg (5 mmol) of diazidoglyoxime were suspended in 40 mL of diethyl ether. Gaseous HCl was bubbled through the reaction mixture at 0 to 5 °C while stirring for 2 hours and then the flask was sealed and stirred at room temperature over night. The solution was allowed to stand for crystallization yielding 760 mg (73 %) of 5,5'-bis(1-hydroxy)tetrazole dihydrate as pale yellow crystals.

DSC (5 °C min⁻¹): 214 °C (dec.); IR (atr, cm⁻¹): $\tilde{\nu}$ = 3229 (m), 1665 (m), 1411 (w), 1375 (w), 1302 (w), 1208 (w), 1144 (m), 995 (s), 714 (w), 662 (w); Raman (1064 nm, 300 mW, 25 °C, cm⁻¹): $\tilde{\nu}$ = 1608 (100), 1270 (26), 1157 (46), 1133 (38), 1019 (22), 766 (31), 738 (13), 693 (4), 597 (6), 402 (29); ^1H NMR (DMSO- d_6 , 25 °C, ppm) δ : 6.80; $^{13}\text{C}\{^1\text{H}\}$ NMR (DMSO- d_6 , 25 °C, ppm) δ : 135.8; EA (206.12): calc.: C 11.65, H 2.93, N 54.36 %; found: C 12.18, H 2.81, N 54.04 %; BAM drophammer: >40 J; friction tester: 216 N; ESD: 0.5 J.

Dihydroxylammonium 5,5'-bistetrazole-1,1'-dioxide (TKX50)

5,5'-bistetrazole-1,1'-diol dihydrate (2.06 g, 10 mmol) is dissolved in 50 mL of warm water. Hydroxylamine (1.32 g, 20 mmol, 50% w/w in H₂O) is added. Cooling down the solution to room temperature forces the dihydroxylammonium salt to crystallize. It can be isolated by suction filtration and air dried. (Yield: 82%)

DSC (5 °C min⁻¹, °C): 221 °C (dec.); IR (KBr, cm⁻¹): $\tilde{\nu}$ = 3425 (m), 3219 (s), 3081 (s), 3050 (s), 2936 (s), 2689 (s), 2513 (m), 1599 (m), 1577 (m), 1527 (s), 1426 (s), 1413 (s), 1389 (m), 1352 (m), 1338 (m), 1316 (w), 1236 (vs), 1174 (m), 1145 (w), 1095 (w), 1046 (w), 1029 (w), 1011 (m), m997 (m), 800 (m), 723 (m), 676 (w), 612 (w), 579 (w), 539 (w), 498 (w); Raman (1064 nm, 300 mW, 25 °C, cm⁻¹): $\tilde{\nu}$ = 1616 (100), 1469 (3), 1278 (2), 1239 (25), 1173 (2), 1143 (6), 1116 (10), 1014 (7), 1004 (12), 763 (4), 612 (3), 409 (4), 335 (2), 257 (2), 199 (2); ^1H NMR (DMSO- d_6 , 25 °C, ppm) δ : 9.66 (s, 8H, NH₃OH); ^{13}C NMR (DMSO- d_6 , 25 °C, ppm) δ : 135.5 ((CN₄)₂); m/z (FAB⁺): 34.0 [NH₃OH⁺]; m/z (FAB⁻): 169.1 [C₂HN₈O₂⁻]; EA (C₂H₈N₁₀O₄, 236.15) calc.: C 10.17, H 3.41, N 59.31 %; found: C 10.60, H 3.63, N 59.31 %; BAM drophammer: 20 J; friction tester: 120 N; ESD: 0.11 J (at grain size <100 μm).

Dihydroxylammonium 5,5'-bistetrazole-1,1'-dioxide (TKX50) via improved synthesis

Dichloroglyoxime (785 mg, 5 mmol) is dissolved in 10 mL of DMF at room temperature. The solution is cooled to 0 °C and NaN₃ (715 mg, 11 mmol) is added. The mixture is stirred for 40 min at 0 °C. NaCl precipitates, whereas the diazidoglyoxime stays in solution. The mixture is transferred to a flask containing 100 mL of diethyl ether, which is cooled to 0 °C in a salt-ice bath. HCl is bubbled through the suspension maintaining the temperature below 20 °C, until saturation of the diethyl ether indicated by a drop of the temperature back to 0-5 °C is reached. A precipitate, which is formed during the reaction first agglomerates and then is resuspended, once the mixture is saturated with HCl. The flask is stoppered tightly and the reaction mixture is stirred overnight at room temperature under a slight overpressure of HCl, which forms upon warming the mixture to room temperature. The pressure is released and the mixture is poured into an open dish for evaporation either overnight at room temperature or in 1-2 h at 50 °C. After most of the diethyl ether has evaporated, 50 mL of water are added resulting in a clear solution. The water is evaporated on a rotary evaporator and the remaining DMF is removed under high vacuum, yielding crude dimethylammonium 5,5'-bistetrazole-1,1'-dioxide as a colorless solid. The solid is dissolved in the smallest possible volume of boiling water (ca. 10 mL) and

hydroxylammonium chloride (750 mg, 10.8 mmol, 2.16 eq.) as a concentrated aqueous solution is added. TKX50 precipitates from the solution in 74.6 % yield (882 mg, 3.73 mmol), which can be isolated by suction filtration, washed with cold water and air dried.

Acknowledgements

Financial support of this work by the Ludwig-Maximilian University of Munich (LMU), the U.S. Army Research Laboratory (ARL), the Armament Research, Development and Engineering Center (ARDEC), the Strategic Environmental Research and Development Program (SERDP) and the Office of Naval Research (ONR Global, title: "Synthesis and Characterization of New High Energy Dense Oxidizers (HEDO) - NICOP Effort ") under contract nos. W911NF-09-2-0018 (ARL), W911NF-09-1-0120 (ARDEC), W011NF-09-1-0056 (ARDEC) and 10 WPSEED01-002 / WP-1765 (SERDP) is gratefully acknowledged. The authors acknowledge collaborations with Dr. Mila Krupka (OZM Research, Czech Republic) in the development of new testing and evaluation methods for energetic materials and with Dr. Muhamed Sucesca (Brodarski Institute, Croatia) in the development of new computational codes to predict the detonation and propulsion parameters of novel explosives. We are indebted to and thank Drs. Betsy M. Rice and Brad Forch (ARL, Aberdeen, Proving Ground, MD) and Mr. Gary Chen (ARDEC, Picatinny Arsenal, NJ) for many helpful and inspired discussions and support of our work. For the measurement of the sensitivity data the authors want to thank Stefan Huber. We also would like to thank Davin G. Piercey, Dennis Fischer and Marius Reimann for their support.

References

- [1] (a) J. Giles, Collateral Damage, *Nature*, 427, p. 580-581, **2004**; (b) D. Carrington, *New Scientist*, 101, **2001**; (c) T. M. Klapötke, in *Moderne Anorganische Chemie*, Riedel, E. (Hrsg.), 3rd ed., Walter de Gruyter, Berlin, New York, p. 99-104, **2007**.
- [2] T. M. Klapötke, *High Energy Density Materials*, Springer, **2007**.
- [3] T. M. Klapötke, D. G. Piercey, 1,1'-Azobis(tetrazole): A Highly Energetic Nitrogen-Rich Compound with a N₁₀ Chain, *Inorg. Chem.*, 50, p. 2732-2734, **2011**.
- [4] L. A. Burke, P. J. Fazen, Correlation Analysis of the interconversion and nitrogen loss reactions of aryl pentazenes and pentazoles derived from aryl diazonium and azide ions, *Int. J. Quantum. Chem.*, 109, p. 3613-3618, **2009**.
- [5] M. Göbel, K. Karaghiosoff, T. M. Klapötke, D. G. Piercey, J. Stierstorfer, Nitrotetrazolate-2N-oxides and the Strategy of N-Oxide Introduction, *J. Am. Chem. Soc.*, 132, p. 17216-17226, **2010**.
- [6] T. M. Klapötke, D. G. Piercey, J. Stierstorfer, The Taming of CN₇⁻: The azidotetrazolate 2-Oxide Anion, *Chem. Eur. J.*, 17, p. 13068-13077, **2011**.
- [7] A. M. Churakov, V. A. Tartakovsky, Progress in 1,2,3,4-tetrazine chemistry, *Chem. Rev.* 104, p. 2601-2616, **2004**.
- [8] I. V. Tselinskii, S. F. Mel'nikova, T. V. Romanova, *Russ. J. Org. Chem.*, 37, p. 430- 436, **2001**.
- [9] CrysAlis CCD, Oxford Diffraction Ltd., Version 1.171.27p5 beta (release 01-04-2005 CrysAlis171.NET) (compiled Apr 1 2005, 17:53:34).
- [10] CrysAlis RED, Oxford Diffraction Ltd., Version 1.171.27p5 beta (release 01-04-2005 CrysAlis171.NET) (compiled Apr 1 2005, 17:53:34).
- [11] A. Altomare, G. Cascarano, C. Giacovazzo, A. Guagliardi, SIR-92, 1993, A program for crystal structure solution, *J. Appl. Cryst.*, 26, p. 343, **1993**.
- [12] G. M. Sheldrick, SHELXL-97. Program for the Refinement of Crystal Structures. University of Göttingen, Germany, **1997**.

- [13] A. L. Spek, PLATON, A Multipurpose Crystallographic Tool, Utrecht University, Utrecht, The Netherlands, **1999**.
- [14] L. J. Farrugia, WinGX suite for small molecule single-crystal crystallography, *J. Appl. Cryst.*, 32, p. 837, **1999**.
- [15] SCALE3 ABSPACK - An Oxford Diffraction program (1.0.4,gui:1.0.3) (C), Oxford Diffraction Ltd., **2005**.
- [16] N. Fischer, D. Izsák, T. M. Klapötke, S. Rappenglück, J. Stierstorfer, Nitrogen-Rich 5,5'-Bistetrazolates and their Potential Use in Propellant Systems: A Comprehensive Study, *Chem. Eur. J.* **2012**, in press, DOI: 10.1002/chem.201103737.
- [17] <http://www.linseis.com>
- [18] NATO standardization agreement (STANAG) on explosives, *impact sensitivity tests*, no. 4489, 1st ed., Sept. 17, **1999**.
- [19] WIWEB-Standardarbeitsanweisung 4-5.1.02, Ermittlung der Explosionsgefährlichkeit, hier der Schlagempfindlichkeit mit dem Fallhammer, Nov. 8, **2002**.
- [20] <http://www.bam.de>
- [21] NATO standardization agreement (STANAG) on explosive, *friction sensitivity tests*, no. 4487, 1st ed., Aug. 22, **2002**.
- [22] WIWEB-Standardarbeitsanweisung 4-5.1.03, Ermittlung der Explosionsgefährlichkeit oder der Reibeempfindlichkeit mit dem Reibeapparat, Nov. 8, **2002**.
- [23] Impact: Insensitive > 40 J, less sensitive ≥ 35 J, sensitive ≥ 4 J, very sensitive ≤ 3 J; friction: Insensitive > 360 N, less sensitive = 360 N, sensitive < 360 N a. > 80 N, very sensitive ≤ 80 N, extreme sensitive ≤ 10 N; According to the UN Recommendations on the Transport of Dangerous Goods (+) indicates: not safe for transport.
- [24] <http://www.ozm.cz>
- [25] M. Sućeska, EXPLO5.5 program, Zagreb, Croatia, **2010**.
- [26] M. J. Frisch, G. W. Trucks, H. B. Schlegel, G. E. Scuseria, M. A. Robb, J. R. Cheeseman, G. Scalmani, V. Barone, B. Mennucci, G. A. Petersson, H. Nakatsuji, M. Caricato, X. Li, H. P. Hratchian, A. F. Izmaylov, J. Bloino, G. Zheng, J. L. Sonnenberg, M. Hada, M. Ehara, K. Toyota, R. Fukuda, J. Hasegawa, M. Ishida, T. Nakajima, Y. Honda, O. Kitao, H. Nakai, T. Vreven, J. A. Montgomery, Jr., J. E. Peralta, F. Ogliaro, M. Bearpark, J. J. Heyd, E. Brothers, K. N. Kudin, V. N. Staroverov, R. Kobayashi, J. Normand, K. Raghavachari, A. Rendell, J. C. Burant, S. S. Iyengar, J. Tomasi, M. Cossi, N. Rega, J. M. Millam, M. Klene, J. E. Knox, J. B. Cross, V. Bakken, C. Adamo, J. Jaramillo, R. Gomperts, R. E. Stratmann, O. Yazyev, A. J. Austin, R. Cammi, C. Pomelli, J. W. Ochterski, R. L. Martin, K. Morokuma, V. G. Zakrzewski, G. A. Voth, P. Salvador, J. J. Dannenberg, S. Dapprich, A. D. Daniels, Ö. Farkas, J. B. Foresman, J. V. Ortiz, J. Cioslowski, D. J. Fox, Gaussian 09, Revision A.1, Gaussian, Inc., Wallingford CT, **2009**.
- [27] R. Mayer, J. Köhler, A. Homburg, Explosives, 5th ed., Wiley VCH, Weinheim, **2002**.
- [28] J. P. Agrawal, in High Energy Materials, 1st ed., Wiley-VCH, Weinheim, p. 189, **2010**.
- [29] R. Turcotte, M. Vachon, Q. S. M. Kwok, R. Wang, D. E. G. Jones, *Thermochimica Acta*, 433, p. 105-115, **2005**.
- [30] R. M. Vrcelj, J. N. Sherwood, A. R. Kennedy, H. G. Gallagher, T. Gelbrich, *Cryst. Growth Des.*, 3, p. 1027, **2003**.
- [31] P. Hakey, W. Ouellette, J. Zubietta, T. Korter, *Acta Crystallogr.*, E64, p. 1428, **2008**.
- [32] J. R. Deschamps, M. Frisch, D. Parrish, Thermal Expansion of HMX, *J. Chem. Crystallogr.*, 41, p. 966-970, **2011**.

-
- [33] N. B. Bolotina, M. J. Hardie, R. L. Speer Jr., A. A. Pinkerton, *J. Appl. Cryst.*, 37, p. 808-814, **2004**.
- [34] a) J. E. Felts, H. W. Sandusky and R. H. Granholm, Development of the small scale shock sensitivity test (SSST), *AIP Conf. Proc.*, 1195, p. 233, **2009**; b) H. W. Sandusky, R. H. Granholm, D. G. Bohl, "Small-Scale Shock Reactivity Test (SSRT)", IHTR 2701, Naval Surface Warfare Center, Indian Head, MD, 12 Aug 2005.
- [35] R. Mayer, J. Köhler, A. Homburg, *Explosives*, 5th ed., Wiley VCH, Weinheim, **2002**, p. 197-200.
- [36] R. Mayer, J. Köhler, A. Homburg, *Explosives*, 5th ed., Wiley VCH, Weinheim, **2002**, p. 148.



The Reactivity of 5-Cyanotetrazole towards Water and Hydroxylamine

Niko Fischer, Thomas M. Klapötke,* Sebastian Rappenglück, and Jörg Stierstorfer^[a]

Sodium 5-cyanotetrazolate sesquihydrate (**1**) was prepared from sodium azide and two equivalents of sodium cyanide under acidic conditions. Its hydrolysis, when treated with an excess of 6 M nitric acid yields tetrazole-5-carboxamide (**4**), whereas stoichiometric amounts of 2 M nitric acid yields the free acid 5-cyanotetrazole (**2**). 5-Cyanotetrazole readily reacts with hydroxylammonium chloride to form the oxime of tetrazole-5-carboxamide (**6**). Both compounds, the tetrazole-5-carboxamide (**4**) and its oxime (**6**), bear an acidic proton, which can be abstracted with bases such as aqueous ammonia or hydroxylamine, to form the respective hydroxylammonium (**5**, **7**) or ammonium salts (**8**). Also the guanidinium (**9**) and the triaminoguanidinium salt (**10**) were prepared using guanidinium

and triaminoguanidinium chloride, respectively. All mentioned compounds, including the silver salt of 5-cyanotetrazole (**3**), were structurally characterized by low-temperature single-crystal X-ray analysis. In addition, the materials were characterized using NMR and vibrational (IR, Raman) spectroscopy as well as mass spectrometry and elemental analysis. The thermal behavior was studied from DSC measurements and the sensitivities of the compounds towards shock, friction, and electrostatic discharge were determined. Moreover, the heats of formation were calculated (atomization method, CBS-4M enthalpies) and several detonation/propulsion parameters computed with the EXPLO5 code.

Introduction

Since their discovery, the spectrum of different applications of tetrazoles has extended over a very large field during the last century and especially in the last decades, reaching from pharmaceutical compounds^[1] up to energetic materials,^[2] where they are used because of their high nitrogen content and comparatively high thermal stability, which traces back to their stable 6 π -aromatic system. Their preparation utilizes the 1,3-dipolar cycloaddition of inorganic,^[3] organic,^[4,5] silyl,^[6] and complexed metal azides^[7] with nitriles, whereas electron withdrawing groups attached to the nitrile enhance their reactivity towards 1,3-dipoles such as the azide moiety.^[3] This might be a probable reason for the early discovery of 5-cyanotetrazole from a dipolar cycloaddition of cyanogen, which has a very electron-poor environment, with hydrazoic acid generated in situ.^[8] Although the first synthetic route is accomplished in aqueous media, also the preparation employing SO₂ (l) as the solvent was reported recently.^[9] Because the nitrile group in 5-cyanotetrazole is a versatile electrophilic moiety, which additional to its hydrolysis also can react with a variety of different nucleophiles, 5-cyanotetrazole can be regarded as an intermediate in variable syntheses for future applications, which do not only include the above-mentioned sectors of pharmaceutical compounds and energetic materials. Here, the product of the reaction of 5-cyanotetrazole and hydroxylamine, namely tetrazole-5-carboxamide oxime, is introduced and characterized as an example of a transformation of the nitrile moiety into a further useful intermediate for organic synthesis. Polanc and co-workers^[10] report on the use of carboxamide oximes as precursors for the synthesis of pyrimidine N-oxides, while pointing out the use of N-oxides as intermediates or auxiliary

agents in the synthesis, as protecting groups, oxidants, ligands in metal complexes, as catalysts, pharmaceuticals, and agrochemicals.^[10]

Along with the hydrolysis product of 5-cyanotetrazole, tetrazole-5-carboxamide, herein we want to concentrate on the energetic character of tetrazole-5-carboxamide oxime and the nitrogen-rich salts thereof, the synthesis and analytical characterization of which we report in the following.

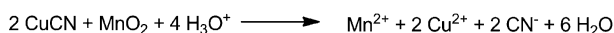
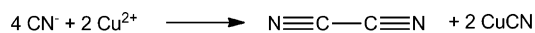
Results and Discussion

Synthesis

The sodium salt of 5-cyanotetrazole, which has been known since the early 20th century,^[8] is here prepared from a slightly modified procedure in a 2,3-dipolar cycloaddition (Huisgen reaction), starting from sodium azide and two equivalents of sodium cyanide under acidic conditions, using Cu²⁺ as a catalyst and MnO₂ as the oxidizing agent. Here, the cyanide anion is oxidized to cyanogen by Cu²⁺, which is reoxidized by MnO₂ afterwards as depicted in Scheme 1.

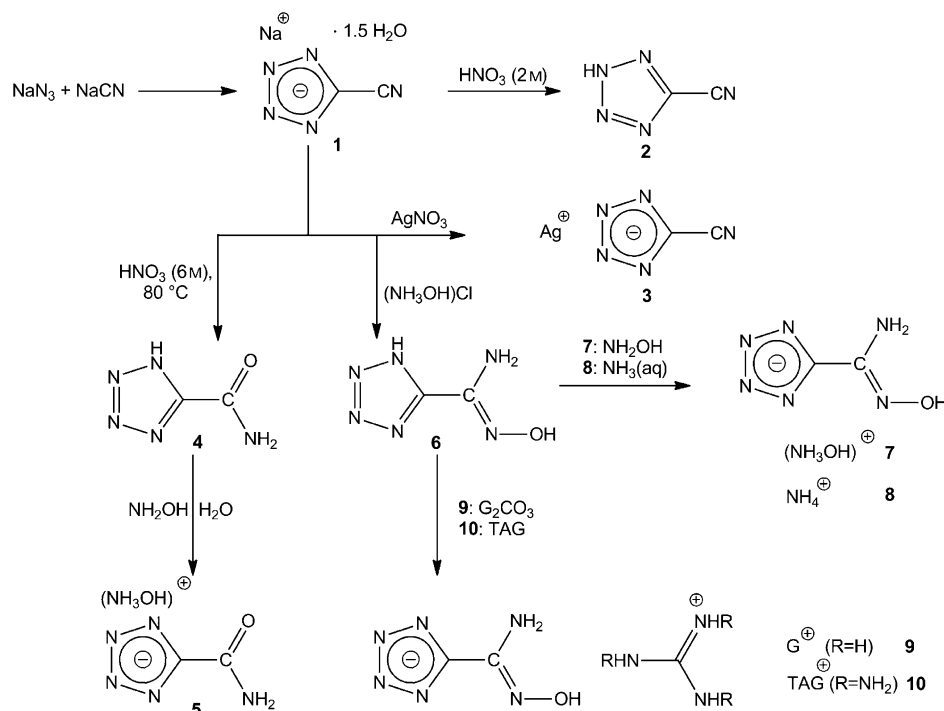
[a] N. Fischer, Prof. Dr. T. M. Klapötke, S. Rappenglück, J. Stierstorfer
Department of Chemistry
Ludwig-Maximilian University of Munich
81377 Munich (Germany)
Fax: (+49) 89-2180-77492
E-mail: tmk@cup.uni-muenchen.de

Supporting information for this article is available on the WWW under <http://dx.doi.org/10.1002/cplu.201200136>.



Scheme 1. Generation of cyanogen in situ.

The cyanogen generated in situ cyclizes with hydrazoic acid to 5-cyanotetrazole. To remove remaining MnO_2 , the reaction mixture is filtrated and the filtrate is treated with Na_2CO_3 to remove Mn^{2+} as its poorly soluble carbonate by filtration and to obtain the sodium salt of 5-cyanotetrazole, which can be extracted with boiling acetone and recrystallized from ethanol/ethyl acetate (2:1; Scheme 2).



Scheme 2. Synthesis of sodium 5-cyanotetrazolate (1), the free acid 2 and the silver salt 3 as well as the tetrazole-5-carboxamide (4), its salt 5 and the tetrazole-5-carboxamide oxime (6), and the salts 7–10 thereof.

The treatment of sodium 5-cyanotetrazolate with different concentrations of nitric acid, such as 2 M and 6 M HNO_3 , yields two different reaction products, which first is the free acid 5-cyanotetrazole (2) in the case of 2 M HNO_3 and second the hydrolysis product tetrazole-5-carboxamide (4) in the case of using 6 M HNO_3 at elevated temperature. Silver 5-cyanotetrazolate (3) can be isolated after combining a silver nitrate solution with a solution of 1. It precipitates instantly owing to its very low water solubility, but nevertheless, it was possible to obtain single crystals of 3 from slowly cooling down a hot solution of 3 in *N,N'*-dimethylformamide (DMF). Silver salt 3 is a primary explosive with high sensitivities towards shock, friction, and electrostatic discharge!

The electrophilic reactivity of nitriles can be used in reactions with hydroxylamine leading to the respective carboxamide oxime.^[11] Based on 5-cyanotetrazole, tetrazole-5-carboxamide oxime (6) can be isolated in yields up to 70%. Alternatively, hydroxylammonium chloride and 1, instead of hydroxylamine and 2, can be used. Here, the hydroxylammonium cation is partially deprotonated in the reaction mixture by the tetrazole moiety, resulting in a higher nucleophilicity of the amine moiety, which is necessary for the reaction with the cyano group of 1. Tetrazole-5-carboxamide oxime (6) again can be deprotonated at the tetrazole ring using nitrogen-rich bases such as hydroxylamine, ammonia, guanidinium carbonate, or triaminoguanidine, resulting in the respective salts hydroxylammonium tetrazole-5-carboxamide oxime (7), ammonium tetrazole-5-carboxamide oxime (8), guanidinium tetrazole-

5-carboxamide oxime (9), and 1,3,5-triaminoguanidinium tetrazole-5-carboxamide oxime (10), respectively. Beside 7, also the hydroxylammonium salt of tetrazole-5-carboxamide was isolated after deprotonation of 4 in aqueous solution. Single crystals of all described compounds, except for the tetrazole-5-carboxamide oxime (6), the corresponding free acid could be obtained after recrystallization from ethanol/ethyl acetate (2:1; 1), ethanol (2), *N,N'*-dimethylformamide (3), water (4), or ethanol/water (ca. 10:1 to 20:1; 5, 7–10), respectively.

Crystal structures

The crystal structures of compounds 2–5 as well as 7–10 were determined by low-temperature X-ray analysis. Different parameters regarding the measurements and solutions are gathered in Table 1 and Table 2. Although the crystal structure of

ammonium, sodium, potassium, and guanidinium salt were described,^[9] the structure of the parent compound is still unknown. 5-Cyanotetrazole (2) crystallizes in the monoclinic space group $P2_1/m$ with two molecules in the unit cell. Its density of 1.635 g cm^{-3} is in agreement to other neutral tetrazole compounds reported in the literature, for example, 5-oxotetrazole (1.699 g cm^{-3}).^[12] The proton connected to the ring nitrogen atom N2 participates in two hydrogen bonds forming a planar structure shown in Figure 1.

The highly sensitive silver salt 3 crystallizes in the monoclinic space group $P2_1/n$ with a density of 3.245 g cm^{-3} , which is slightly higher than that of silver 1-methyl-5-nitriminotetrazolate (2.948 g cm^{-3}).^[13] The coordination sphere of the silver

Table 1. X-ray diffraction data and parameters.

	2	3	4	5	7	8	9	10
formula	C ₂ H ₅ N ₅	C ₂ AgN ₅	C ₂ H ₃ N ₅ O	C ₂ H ₆ N ₆ O ₂	C ₂ H ₃ N ₅ O ₂	C ₂ H ₃ N ₅ O	C ₃ H ₉ N ₉ O	C ₃ H ₁₂ N ₁₂ O
<i>M_r</i> [g mol ⁻¹]	95.08	201.94	113.09	146.13	161.15	145.15	187.19	232.25
crystal system	monoclinic	monoclinic	monoclinic	monoclinic	monoclinic	monoclinic	orthorhombic	monoclinic
space group	<i>P</i> ₂ ₁ / <i>m</i>	<i>P</i> ₂ ₁ / <i>n</i>	<i>P</i> ₂ ₁ / <i>m</i>	<i>P</i> ₂ ₁ / <i>c</i>	<i>P</i> ₂ ₁ / <i>n</i>	<i>C</i> ₂ / <i>c</i>	<i>Pca</i> ₂	<i>P</i> ₂ ₁ / <i>n</i>
color/habit	colorless platelet	colorless block	colorless platelet	colorless block	colorless block	colorless block	colorless rod	colorless block
size [mm]	0.04 × 0.22 × 0.27	0.10 × 0.14 × 0.21	0.10 × 0.23 × 0.30	0.18 × 0.20 × 0.21	0.18 × 0.19 × 0.28	0.18 × 0.18 × 0.20	0.10 × 0.10 × 0.20	0.20 × 0.22 × 0.28
<i>a</i> [Å]	5.085(3)	6.8789(4)	4.9867(3)	10.5123(9)	3.6131(4)	25.578(3)	12.7861(9)	8.5050(11)
<i>b</i> [Å]	6.103(2)	7.6299(5)	6.1274(4)	8.3076(5)	13.1996(17)	3.6503(4)	8.6469(5)	7.1498(12)
<i>c</i> [Å]	6.294(2)	7.9473(4)	7.2221(4)	6.8496(6)	13.4657(14)	13.4265(15)	7.4790(5)	16.028(2)
α [°]	90	90	90	90	90	90	90	90
β [°]	98.54(4)	97.657(5)	100.421(5)	102.185(8)	93.827(11)	103.357(12)	90	101.821(14)
γ [°]	90	90	90	90	90	90	90	90
<i>V</i> [Å ³]	193.16(15)	413.40(4)	217.04(2)	584.71(8)	640.77(13)	1219.7(2)	826.88(9)	954.0(2)
<i>Z</i>	2	4	2	4	4	8	4	4
ρ_{calc} [g cm ⁻³]	1.635	3.245	1.730	1.660	1.670	1.581	1.504	1.617
μ [mm ⁻¹]	0.126	4.723	0.143	0.143	0.143	0.129	0.120	0.130
<i>F</i> (000)	96	376	116	304	336	608	392	488
$\lambda_{\text{MoK}\alpha}$ [Å]	0.71073	0.71073	0.71073	0.71073	0.71073	0.71073	0.71073	0.71073
<i>T</i> [K]	173	173	173	173	173	173	173	173
θ min, max [°]	4.7, 27.5	4.2, 26.0	4.2, 28.2	4.7, 26.5	4.3, 25.0	4.9, 26.0	4.2, 26.7	4.1, 26.4
dataset	–6.6; –7.5; –8.8	–8.8; –8.9; –9.6	–6.6; –7.8; –9.7	–13.13; –10.10; –8.8	–4.4; –15.10; –15.15	–18.30; –4.4; –16.16	–14.16; –10.10; –9.7	–10.10; –8.8; –20.10
reflections collected	1121	1449	1321	5947	2981	2965	4298	4877
independent reflections	487	810	580	1210	1122	1204	949	1934
<i>R</i> _{int}	0.058	0.025	0.033	0.056	0.039	0.042	0.036	0.044
observed reflections	376	639	415	762	782	886	861	1445
reflections								
parameters	47	73	58	115	100	119	154	193
<i>R</i> ₁ (obs)	0.0537	0.0263	0.0324	0.0322	0.0419	0.0391	0.0287	0.0412
<i>wR</i> ₂ (all data)	0.1438	0.0505	0.0841	0.0626	0.1037	0.0882	0.0673	0.1029
<i>S</i> ^a	1.13	0.92	0.94	0.80	0.93	1.01	1.08	1.07
$\Delta\rho_{\text{max}}$, $\Delta\rho_{\text{min}}$ [e Å ⁻³]	–0.26, 0.31	–0.66, 0.58	–0.19, 0.24	–0.16, 0.25	–0.24, 0.37	–0.21, 0.22	–0.16, 0.16	–0.25, 0.22
device type	Oxford Xcalibur3 CCD	Oxford Xcalibur3 CCD	Oxford Xcalibur3 CCD	Oxford Xcalibur3 CCD	Oxford Xcalibur3 CCD	Oxford Xcalibur3 CCD	Oxford Xcalibur3 CCD	Oxford Xcalibur3 CCD
solution	SIR-92	SIR-92	SHELXS-97	SIR-92	SIR-92	SIR-92	SHELXS-97	SIR-92
refinement	SHELXL-97	SHELXL-97	SHELXL-97	SHELXL-97	SHELXL-97	SHELXL-97	SHELXL-97	SHELXL-97
absorption correction	multiscan	multiscan	multiscan	multiscan	multiscan	multiscan	multiscan	multiscan
CCDC	867191	867194	867192	867195	867196	867198	867199	867197

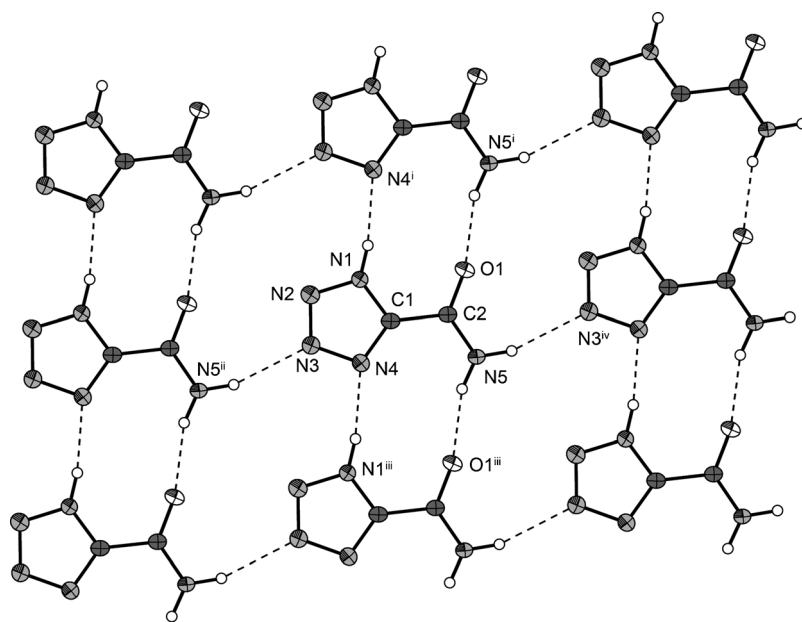


Figure 3. Hydrogen bonding in the structure of 1*H*-tetrazole-5-carboxamide (**4**). Thermal ellipsoids represent the 50% probability level. Selected bond lengths [Å]: N1–C1 1.334(2), N1–N2 1.337(2), N5–C2 1.322(2), O1–C2 1.2306(19), N4–C1 1.324(2), N4–N3 1.365(2), N2–N3 1.298(2), C2–C1 1.488(2); selected bond angles [°]: C1–N1–N2 109.35(14), C1–N4–N3 105.64(13), N3–N2–N1 106.27(14), N2–N3–N4 110.57(13), O1–C2–N5 124.70(15), O1–C2–C1 117.39(14), N5–C2–C1 117.92(14), N4–C1–N1 108.18(15), N4–C1–C2 131.67(15), N1–C1–C2 120.15(14); hydrogen bonds [D–H...A, d(D–H), d(H...A), d(D–A), <(D–H...A)]: N1–H1...N4ⁱ 0.90(3) Å, 1.96(3) Å, 2.845(2) Å, 171(3)°; N5–H51...O1ⁱⁱⁱ 0.91(3) Å, 1.92(3) Å, 2.804(2) Å, 163(2)°, N5–H52...N3^{iv} 0.92(2) Å, 2.24(2) Å, 3.121(2) Å, 162.4(18)°; symmetry codes: i) $-1+x, y, z$; ii) $x, y, -1+z$; iii) $1+x, y, z$; iv) $x, y, 1+z$.

The proton NMR spectrum of **2** shows one singlet at 13.02 ppm, that can be assigned to the relatively acidic proton at the tetrazole ring, which is slightly shifted upfield in the spectrum of the less acidic compound **6** (δ = 10.51 ppm). In addition, the comparatively sharp signal of the oxime proton is visible at δ = 7.09 ppm, whereas the amino group can only be assigned to a broad elevation of the baseline at around δ = 6.30 ppm. The hydrolysis product **4** reveals two distinct singlets in its proton NMR spectrum, which can be assigned to the amino protons of the amide functionality at δ = 8.57 and 8.19 ppm, which show hindered rotation owing to the amide resonance.

The tetrazole carbon atom of **2** is visible as a signal at $\delta = 139.3$ ppm, which is strongly shifted downfield upon hydroly-

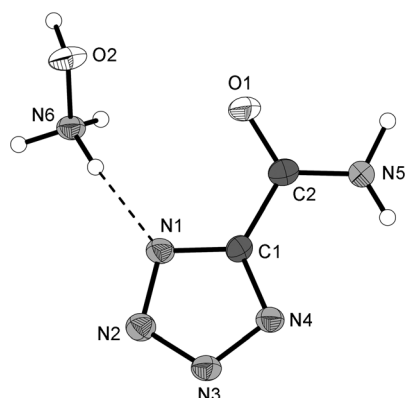


Figure 4. Molecular unit of hydroxylammonium 5-carboxamido-tetrazolate (5). Ellipsoids of nonhydrogen atoms are drawn at the 50% probability level. Selected bond lengths (Å): C1–N4 1.3316(18), C1–N1 1.333(2), C1–C2 1.486(2), N4–N3 1.3404(18), N3–N2 1.3218(17), N2–N1 1.3365(17), N5–C2 1.308(2), C2–O1 1.2481(18), O2–N6 1.4103(17); selected bond angles (°): N4–C1–N1 112.61(16), N4–C1–C2 126.54(16), N1–C1–C2 120.82(14), C1–N4–N3 103.73(14), N2–N3–N4 110.13(12), N3–N2–N1 108.95(12), C1–N1–N2 104.58(12), O1–C2–N5 122.91(17), O1–C2–C1 118.07(16), N5–C2–C1 119.03(15).

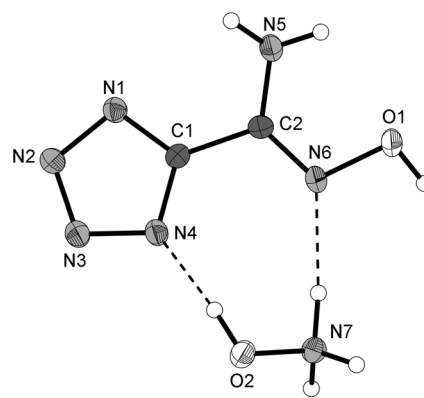


Figure 5. Molecular unit of hydroxylammonium 5-(*N*-hydroxy-carboximide)-tetrazolate (7). Thermal ellipsoids represent the 50% probability level. Selected bond lengths [Å]: O1–N6 1.414(2), N1–C1 1.331(3), N1–N2 1.346(3), N2–N3 1.313(3), N3–N4 1.341(2), N4–C1 1.330(3), N5–C2 1.347(3), N6–C2 1.285(3), C1–C2 1.474(3), O2–N7 1.416(2).

sis (**4**: $\delta = 152.0$ ppm, **6**: $\delta = 150.7$ ppm). The same applies also to the nitrile carbon atom, which is shifted from $\delta = 112.3$ ppm in **2** to 157.2 ppm in **4**, and 144.9 ppm in **6**.

The hydroxylammonium salt of **4** (**5**), in addition to the amide proton signals, reveals the signal of the protons of the hydroxylammonium cation at $\delta = 10.06$ ppm in the proton NMR spectrum and slightly changed chemical shifts for the carbon atoms as compared to **4** in its ^{13}C NMR spectrum. Both signals are shifted downfield to $\delta = 163.1$ and 157.4 ppm, respectively.

NMR spectroscopy

All compounds **1–10** were investigated using ^1H and ^{13}C NMR spectroscopy. The chemical shifts are related to tetramethylsilane as standard. Here, an interesting comparison between the spectra of 5-cyanotetrazole and its hydrolysis products tetrazole-5-carboxamide and tetrazole-5-carboxamide oxime seems appropriate.

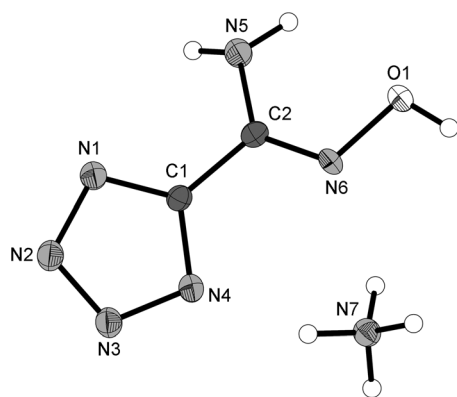


Figure 6. Molecular unit of ammonium 5-(*N*-hydroxy-carboximidamide)-tetrazolate (**8**). Thermal ellipsoids represent the 50% probability level. Selected bond lengths [Å]: O1–N6 1.421(2), N1–C1 1.336(2), N1–N2 1.352(2), N2–N3 1.323(2), N3–N4 1.345(2), N4–C1 1.344(2), N5–C2 1.362(2), N6–C2 1.290(2), C1–C2 1.474(3).

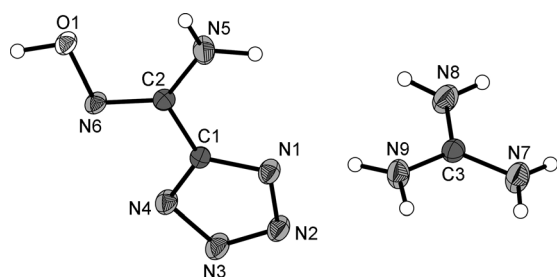


Figure 7. Molecular unit of Guanidinium 5-(*N*-hydroxy-carboximidamide)-tetrazolate (**9**). Thermal ellipsoids represent the 50% probability level. Selected bond lengths [Å]: O1–N6 1.431(2), N1–C1 1.333(3), N1–N2 1.358(3), N2–N3 1.317(3), N3–N4 1.346(3), N4–C1 1.343(3), N5–C2 1.341(3), N6–C2 1.293(3), C1–C2 1.473(3), N7–C3 1.326(3), N8–C3 1.326(3), N9–C3 1.318(3).

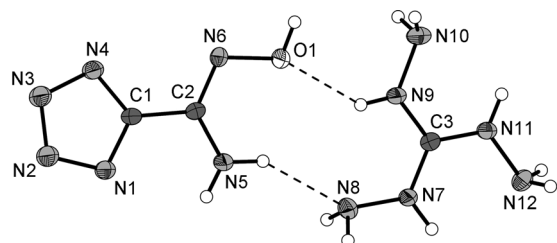


Figure 8. Molecular unit of 1,3,5-triaminoguanidinium 5-(*N*-hydroxy-carboximidamide)-tetrazolate (**10**). Thermal ellipsoids represent the 50% probability level. Selected bond lengths [Å]: O1–N6 1.4345(18), N8–N7 1.417(2), N7–C3 1.322(2), N10–N9 1.406(2), N11–C3 1.322(2), N11–N12 1.406(2), N2–N3 1.318(2), N2–N1 1.345(2), N6–C2 1.294(2), N5–C2 1.343(2), N3–N4 1.353(2), N4–C1 1.337(2), N1–C1 1.334(2), N9–C3 1.332(2), C2–C1 1.474(2).

The proton NMR spectrum of the hydroxylammonium salt of **6** (**7**) shows two broad signals at $\delta=12.31$ and 8.47 ppm, which can be assigned to the hydroxylammonium protons and the protons of the carboxamide-oxime functionality, whereas a definite assignment is not possible. For the ammonium salt **8**, three broad singlets at $\delta=7.35$, 5.59 , and 3.49 ppm are observed, which belong to the oxime-OH, NH_2 , and the ammonium cation, respectively. The spectrum of the guanidinium salt

9, in addition to a broad singlet at $\delta=6.61$ ppm (NH_2/OH), shows the guanidinium cation protons in a sharp singlet at $\delta=5.72$ ppm, whereas the proton NMR spectrum of the triaminoguanidinium salt shows a set of four singlets at $\delta=9.44$ (OH), 8.67 (NH, 1,2,3-triaminoguanidinium), 5.51 (NH_2), and 4.54 ppm (NH_2 , 1,2,3-triaminoguanidinium).

Also the carbon atom signals of the anion of the aforementioned salts are slightly shifted downfield upon deprotonation compared to the neutral compound **6** as already observed for **4**. Signals at $\delta=146.5$ – 148.2 ppm are observed for the carbon atom of the carboxamide-oxime moiety and signals at $\delta=156.2$ – 156.5 ppm for the tetrazole carbon atom. The carbon atoms of the guanidinium and triaminoguanidinium cation are visible as signals at $\delta=158.7$ and 159.6 ppm, respectively.

Vibrational spectroscopy

Additional to NMR spectroscopy, IR, and Raman spectroscopy were used for the identification of structural elements and functional groups. Absorptions were assigned according to values reported in the literature and exemplarily discussed for selected compounds in the following.^[16,17] The characteristic vibrations of the tetrazole ring system can be observed in all IR/Raman spectra of **1**–**10**. The tetrazole framework vibrations at $\nu=1001$ – 1209 cm^{-1} , the asymmetric and symmetric stretching vibrations of the N1–C1–N4 fragment^[18] in the range from $\nu=1372$ – 1394 cm^{-1} and the stretching vibration of the cyclic C=N bond are observed. Latter occurs in the same region as the C=N stretching vibration of the oxime subunit and the in-plane scissoring absorption of the NH_2 group **6**–**10**. The mentioned C=N and N–H vibrations appear in a range from $\nu=1542$ – 1712 cm^{-1} , which complicates a clear assignment without quantum chemical calculations. As the IR spectrum of **2** shows a medium absorption at $\nu=1686\text{ cm}^{-1}$, which can be definitely assigned to the cyclic C=N bond, it is to assume, that the corresponding absorption bands at $\nu=1682\text{ cm}^{-1}$ in **6** and $\nu=1712\text{ cm}^{-1}$ in **8** correspond to the cyclic C=N stretching vibration as well. Because most oximes reported in the literature show weak IR and strong Raman absorptions in the range of $\nu=1620$ – 1690 cm^{-1} ,^[16] it is suggested, that the absorptions at $\nu=1650\text{ cm}^{-1}$ in the spectrum of **6** and at $\nu=1643\text{ cm}^{-1}$ in the spectrum of **8** are caused by the exocyclic C=N vibration of the oxime subunit. This finding corresponds with a strong Raman absorption at $\nu=1665\text{ cm}^{-1}$, which is found for carboxamide oxime **6**. Thus the remaining absorptions at $\nu=1559\text{ cm}^{-1}$ (**6**) and $\nu=1542\text{ cm}^{-1}$ (**8**), can be assigned to in-plane scissoring motions of the NH_2 group. Further characteristic NH_2 bands occur in the range of $\nu=638$ – 856 cm^{-1} and result by out-of-plane wagging motions, which can be identified without doubts in the spectra of **6**–**10**. The nitrile functionality in the Raman and IR spectra of **1** and **2** can be clearly identified as strong absorptions at $\nu=2260\text{ cm}^{-1}$ (**1**) and $\nu=2280\text{ cm}^{-1}$ (**2**). Furthermore, N–H and O–H valence vibrations can be observed in the region of $\nu=2744$ – 3461 cm^{-1} . In case of **8**, two well defined sharp absorptions corresponding to asymmetric and symmetric N–H stretching vibrations of the primary amino group appear at $\nu=3454\text{ cm}^{-1}$ and $\nu=$

3366 cm^{-1} . In the spectrum of **6**, dominating crystal water absorptions avoided such a well-defined separation of the absorption bands. The IR/Raman spectra of tetrazole-5-carboxamide (**4**) and its hydroxylammonium salt **5** nicely show the C=O stretching vibration of the amide moiety in an absorption band at $\nu=1671\text{ cm}^{-1}$ (**5**) and $\nu=1688\text{ cm}^{-1}$ (**4**). Also the N–H stretching modes are visible as absorption bands at $\nu=3250\text{ cm}^{-1}$ in the Raman spectrum of **4** and at $\nu=3201\text{ cm}^{-1}$ in the IR spectrum of **5**.

Sensitivities and thermal stability

The impact sensitivity tests were carried out according to STANAG 4489^[19] modified instruction,^[20] using a BAM (Bundesanstalt für Materialforschung) drop hammer.^[21] The friction sensitivity tests were carried out according to STANAG 4487^[22] modified instruction,^[23] using the BAM friction tester. The classification of the tested compounds results from the "UN Recommendations on the Transport of Dangerous Goods" (Impact: Insensitive $>40\text{ J}$, less sensitive $\geq 35\text{ J}$, sensitive $\geq 4\text{ J}$, very sensitive $\leq 3\text{ J}$; friction: Insensitive $>360\text{ N}$, less sensitive $=360\text{ N}$, sensitive $<360\text{ N}$ a. $>80\text{ N}$, very sensitive $\leq 80\text{ N}$, extreme sensitive $\leq 10\text{ N}$. According to the UN Recommendations on the Transport of Dangerous Goods (+) indicates: not safe for transport.). Compounds **1**, **3**, and **5–10** were also tested upon the sensitivity towards electrical discharge,^[24] using the Electric Spark Tester ESD 2010 EN.^[25] The starting material sodium 5-cyanotetrazolate shows no impact sensitivity ($>40\text{ J}$), however, it was tested positive in the friction tester (160 N , sensitive). This could be a reason of the inclusion of 1.5 equivalents of crystal water. On the other hand, its silver salt **3** is highly sensitive towards both, impact ($<1\text{ J}$) and friction ($<5\text{ N}$).

Tetrazole-5-carboxamide oxime as well as its ammonium and guanidinium salt can be classified as less sensitive towards impact (40 J), whereas the hydroxylammonium (**7**) and the triaminoguanidinium salt (**10**) are more sensitive towards impact (**7**: 10 J , **10**: 15 J), which is a trend, that already has been observed for other nitrogen-rich salts of tetrazole derivatives.^[26] Looking at their friction sensitivity, no definite trend can be observed, however **7**, **9**, and **10** can be classified as less sensitive towards friction (360 N), **6** and **8** need to be classified as sensitive (**6**: 252 N , **8**: 288 N). Also the hydroxylammonium salt of tetrazole-5-carboxamide is less sensitive towards impact (40 J) and shows no enhanced friction sensitivity (288 N), which leads to the assumption, that also tetrazole-5-carboxamide is only less sensitive towards impact and friction, however, these sensitivities have not been tested yet. Also the sensitivities of neutral 5-cyanotetrazole have only be roughly determined. Owing to its electron deficiency in the tetrazole ring it must be also categorized as at least sensitive towards both, impact and friction.

The values for the sensitivities towards electrostatic discharge are spread over a large range from 1 mJ (**3**) to 1 J (**9**, **10**). Not surprisingly, the silver salt of 5-cyanotetrazole shows the highest sensitivity here, but for the other compounds, the values also strongly depend on the grain size of the material,

whereas powderlike materials are more sensitive and larger crystals show lower sensitivities.

Differential scanning calorimetry (DSC) measurements to determine the melt and decomposition temperatures of **1**, **3**, and **5–10** (about 1.5 mg of each energetic material) were performed in covered aluminum-containers with a hole (0.1 mm) in the lid for gas release and a nitrogen flow of 20 mL per minute on a Linseis PT 10 DSC^[27] calibrated by standard pure indium and zinc at a heating rate of 5°C min^{-1} . The decomposition temperatures are given as absolute onset temperatures. The highest thermal stabilities among the investigated materials were observed for both 5-cyanotetrazolate salts **1** (263°C) and **3** (284°C). Also the tetrazole-5-carboxamide oxime (**6**) has a surprisingly high thermal stability of 244°C . Here the dehydration of the compound, which precipitates as a monohydrate as evidenced by elemental analysis, is indicated by an endothermic step in the DSC curve at 120°C . Looking at the thermal stabilities of the ionic compounds **5–10**, again the hydroxylammonium and the triaminoguanidinium salts have the lowest thermal stability (**5**: 173°C , **7**: 171°C , **10**: 160°C), whereas the ammonium and guanidinium salts decompose not below 200°C (**8**: 202°C , **9**: 206°C).

Calculations

Several energetic parameters such as the detonation pressure, detonation velocity, and heat of explosion of **5** as well as **7–10** were calculated by the EXPLO5.05 computer code.^[28] The program is based on the input of the energy of formation (kJ kg^{-1}), density (g cm^{-3}) and the sum formula.

The heats of formation of **5** and **7–10** were also computed theoretically by using the atomization method Equation (1) in combination with CBS-4M electronic enthalpies.^[29] The CBS models use the known asymptotic convergence of pair natural orbital expressions to extrapolate from calculations using a finite basis set to the estimated complete basis set limit. CBS-4 begins with a HF/3-21G(d) geometry optimization; the zero-point energy is computed at the same level. It then uses a large basis set self-consistent-field (SCF) calculation as a base energy, and a MP2/6-31+G calculation with a CBS extrapolation to correct the energy through second order. A MP4(SDQ)/6-31+(d,p) calculation is used to approximate higher-order contributions. In this study we applied the modified CBS-4M method (**M** referring to the use of Minimal Population localization) which is a reparametrized version of the original CBS-4 method and also includes some additional empirical corrections.^[30] This method was shown to be suitable for energetic compounds in different recent publications.^[31] The quantum chemical calculations were carried out using the Gaussian G09 program package.^[32] Coordinates of the optimized structures can be found in the Supporting Information.

$$\Delta_f H^\circ_{(\text{g}, \text{M}, 298)} = H_{(\text{Molecule}, 298)} - \sum H^\circ_{(\text{Atoms}, 298)} + \sum \Delta_f H_{(\text{Atoms}, 298)} \quad (1)$$

For the ionic compounds the gas-phase enthalpies of forma-

Table 3. Energetic properties and detonation parameters of **5** and **7–10**.

	5	7	8	9	10	2,4,6-TNT	RDX
formula	C ₂ H ₆ N ₆ O ₂	C ₂ H ₇ N ₇ O ₂	C ₂ H ₇ N ₇ O	C ₃ H ₉ N ₉ O	C ₃ H ₁₂ N ₁₂ O	C ₇ H ₅ N ₃ O ₆	C ₃ H ₆ N ₆ O ₆
<i>M_r</i> [g mol ^{−1}]	146.11	161.12	145.12	187.16	232.21	227.13	222.12
IS [J] ^[a]	40	10	40	40	15	15 ^[21]	7.5 ^[21]
FS [N] ^[b]	288	> 360	288	360	360	353	120 ^[21]
ESD-test [J] ^[c]	0.15	0.30	0.75	1.0	1.0	0.8	0.2
<i>N</i> [%] ^[d]	57.52	60.85	67.56	67.35	72.38	18.50	37.84
<i>Q</i> [%] ^[e]	−54.75	−54.61	−71.65	−81.20	−75.78	−73.96	−21.61
<i>T</i> _{decomp} [°C] ^[f]	173	171	202	206	160	81 (m.p.), 290 (decomp)	205 (m.p.), 210 (decomp)
density [g cm ^{−3}] ^[g]	1.660	1.670	1.581	1.504	1.617	1.713 (100 K) ^[41]	1.858 (90 K) ^[42]
Δ _f <i>H</i> _m ^o [kJ mol ^{−1}] ^[h]	74.7	294.4	235.9	214.4	535.2	−55.5	86.3
Δ _f <i>U</i> ^o [kJ kg ^{−1}] ^[i]	929.9	1950.1	1753.3	1270.8	2837.7	−168.0	489.0
EXPLO5 values							
−Δ _f <i>U</i> ^o [kJ kg ^{−1}] ^[j]	4395	5168	3875	3078	4444	5258	6190
<i>T</i> _E [K] ^[k]	3036	3349	2674	2297	2827	3663	4232
<i>p</i> _{C-J} [kbar] ^[l]	258	294	230	180	271	235	380
<i>D</i> [m s ^{−1}] ^[m]	8180	8643	7962	7254	8508	7459	8983
gas vol. [L kg ^{−1}] ^[n]	819	837	827	802	841	569	734
<i>I</i> _s [s ^{−1}] ^[o]	206	230	202	182	223	205	258

[a] Impact sensitivity (BAM drophammer, method 1 of 6). [b] Friction sensitivity (BAM friction tester, method 1 of 6). [c] Electrostatic discharge device (OZM). [d] Nitrogen content. [e] Oxygen balance. [f] Decomposition temperature from DSC ($\beta = 5^\circ\text{C}$). [g] Estimated from X-ray analysis. [h] Calculated (CBS-4M) heat of formation. [i] Calculated energy of formation. [j] Energy of explosion. [k] Explosion temperature. [l] Detonation pressure. [m] Detonation velocity. [n] Assuming only gaseous products. [o] Specific impulse (isobaric conditions, chamber pressure of 60 bar).

tion (Table 2) were converted into the solid-state (standard conditions) enthalpy of formation $\Delta_f H_m$ (Table 3) by subtraction of lattice enthalpies. These lattice energies (U_L) and lattice enthalpies (ΔH_L) were calculated from the corresponding molecular volumes (from XRD) according to Jenkin's equations.^[33]

Lastly, the molar standard enthalpies of formation ($\Delta_f H_m$) were used to calculate the solid state energies of formation (ΔU) per kilo according to Equation (1), where Δn is the change of moles of gaseous components.

$$\Delta_f U = (\Delta_f H_m - \Delta n \times RT) \times 1000/M \quad (2)$$

All compounds are formed endothermically in the solid state (Table 3). Triaminoguanidinium salt **10** shows the highest value of 535 kJ mol^{−1}, which is caused mainly by the three N–N bonds within the cation. The lowest heat of formation of 75 kJ mol^{−1} is observed for **5**, which can be explained by the formal addition of one exothermically formed water molecule.

The detonation parameters and specific impulse were calculated using the latest version of the EXPLO5 code (V5.05). EXPLO5 is based on the steady-state model of equilibrium detonation and uses the Becker–Kistiakowsky–Wilson equation of state (BKW E.O.S) for gaseous detonation products and Cowan–Fickett E.O.S. for solid carbon. The calculation of the equilibrium composition of the detonation products is done by applying modified White, Johnson, and Dantzig's free energy minimization technique. The program is designed to enable the calculation of detonation parameters at the Chapman–Jouget (CJ) point.

For all compounds their maximum X-ray densities at -173 K were used for the EXPLO5 computations. In addition, the specific impulse of the pure compounds when used as monopropellants

was calculated assuming rocket propellant conditions (isobaric combustion with a chamber pressure of 60 bar). The calculations were performed using the maximum densities according to the crystal structures and the results are gathered in Table 3. With respect to desired detonation performance compound **7** has the best calculated values regarding the most important values: detonation pressure ($p_{CJ} = 294\text{ kbar}$), velocity ($D = 8643\text{ m s}^{-1}$), and heat of detonation ($\Delta_f U = -5168\text{ kJ kg}^{-1}$). It has also the highest calculated specific impulse ($I_s = 230\text{ s}$). However, modern low-corrosive propellant mixtures demand low deflagration temperatures, which is ensured better by compound **10**. The detonation parameters of all investigated compounds are lower as compared to those of commonly used high explosives such as RDX (hexogen, Table 3) or HMX (octogen). However, in the case of **7** and **10**, the calculated detonation performance is significantly better than that of for example, PETN (pentaerythritol tetranitrate) and largely better than those of TNT (trinitrotoluene), which are listed in Table 3.

Conclusion

From this initial study the following conclusions can be drawn:

- Sodium 5-cyanotetrazolate sesquihydrate (**1**) was protonated with 2 M HCl to give the free acid 5-cyanotetrazole (**2**). The silver salt of **2** was prepared by treating **1** with AgNO₃.
- The hydrolysis product of **1**, tetrazole-5-carboxamide (**4**) was obtained after treating **1** with an excess of 6 M HNO₃ at 80 °C. It was deprotonated with hydroxylamine to give the hydroxylammonium salt **5**.

- Sodium 5-cyanotetrazolate sesquihydrate (**1**) can be converted into tetrazole-5-carboxamide oxime (**6**) by treatment with hydroxylammonium chloride and gave 60% yield. Treatment of 5-cyanotetrazole (**2**) with hydroxylamine yielded the same compound in 74% yield.
- Four nitrogen-rich salts of **6**, the hydroxylammonium (**7**), ammonium (**8**), guanidinium (**9**), and triaminoguanidinium tetrazole-5-carboxamide oxime (**10**) were prepared and fully characterized.
- The crystal structures of **2–5** and **7–10** were determined using low-temperature single-crystal X-ray analysis. They crystallize in the common space groups $P2_1/m^{-1}$ (**2**, **4**), $P2_1/n$ (**3**, **7**, **10**), $P2_1/c$ (**5**), $C2/c$ (**8**), and $Pca2_1$ (**9**) with densities between 1.504 g cm^{-3} (**9**), and 1.730 g cm^{-3} (**4**) for the CHNO compounds and 3.245 g cm^{-3} for the silver salt **3**.
- The sensitivities towards impact, friction, and electrostatic discharge were determined of **1**, **3**, and **5–10**. They reach from very sensitive (IS: $<1\text{ J}$, FS: $<5\text{ N}$, ESD: 1 mJ) for the silver salt **3** to insensitive for the guanidinium salt **9** (IS: 40 J , FS: 360 N , ESD: 1.0 J).
- The thermal stabilities of **1**, **3**, and **5–10** were determined by DSC measurements. Here, the sodium (263°C) and the silver salt (284°C) of **2** reached the highest thermal stabilities, whereas the triaminoguanidinium salt of **6** (160°C) and the hydroxylammonium salts of **4** (173°C) and **6** (171°C) decompose below 180°C .
- With the calculated heats of formation (CBS-4M) and the X-ray densities, several detonation parameters of **2**, **4**, **5**, and **7–10** were calculated (EXPLO5.05). Their detonation velocities reach from 7254 (**9**) to 8643 ms^{-1} (**7**), while having detonation pressures that reach from 180 (**9**) to 294 kbar (**7**). Therefore, the detonation parameters of all investigated compounds are lower compared to those of military high explosives such as RDX or HMX. However, in the case of **7** and **10**, the detonation performance is slightly better than that of PETN (pentaerythritol tetranitrate) and largely better than those of TNT.

Experimental Section

Experimental details

CAUTION! 5-Cyanotetrazole, tetrazole-5-carboxamide and tetrazole-5-carboxamide oxime and the salts thereof are energetic materials with increased sensitivities towards shock and friction. Therefore, proper safety precautions (safety glass, face shield, earthed equipment and shoes, Kevlar gloves, and ear plugs) have to be applied while synthesizing and handling the described compounds.

All chemicals and solvents were used as received (Sigma–Aldrich, Fluka, Acros). ^1H and ^{13}C spectra were recorded using a JEOL Eclipse 270, JEOL EX 400, or a JEOL Eclipse 400 instrument. The chemical shifts quoted in ppm in the text refer to typical standards such as tetramethylsilane (^1H , ^{13}C). To determine the melting and decomposition temperatures of the described compounds a Linseis PT 10 DSC (heating rate 5°C min^{-1}) was used. Infrared spectra were measured using a PerkinElmer Spectrum One FT-IR spectrom-

eter as KBr pellets. Raman spectra were recorded on a Bruker MultiRAM Raman Sample Compartment D418 equipped with a Nd-YAG-Laser (1064 nm) and a LN-Ge diode as detector. Mass spectra of the described compounds were measured at a JEOL MStation JMS 700 using either FAB, DEI, or DCI technique. To measure elemental analyses a Netsch STA 429 simultaneous thermal analyzer was employed.

The crystal structures of compounds **2–5** as well as **7–10** were determined by low-temperature X-ray analysis on an Oxford Xcalibur3 diffractometer with a Spellman generator (voltage 50 kV , current 40 mA) and a KappaCCD detector. The data collection and reduction was carried out using the CrysAlisPro software.^[34] The structures were solved either with Shelxs-97^[35] or Sir-92,^[36] refined with Shelxl-97^[37] and finally checked using the Platon^[38] software integrated in the WinGX^[39] software suite. The absorptions were corrected with a Scale3 Abspack multiscan method. Selected data and parameter of the X-ray determinations are given in Table 1. Further crystallographic data for the structures have been deposited with the Cambridge Crystallographic Data Centre.^[40]

The detonation parameters were calculated using the program EXPLO5V5.05. The program is based on the steady-state model of equilibrium detonation and uses Becker–Kistiakowsky–Wilson equation of state (BKW E.O.S) for gaseous detonation products and Cowan–Fickett E.O.S. for solid carbon. The calculation of the equilibrium composition of the detonation products is done by applying modified White, Johnson, and Dantzig's free energy minimization technique. The program is designed to enable the calculation of detonation parameters at the CJ point.

Triaminoguanidine (free base) was synthesized by dissolving triaminoguanidinium chloride in aqueous sodium hydroxide under N_2 and addition of DMF to the mixture. Subsequently precipitated triaminoguanidine was filtered off with a Schlenk frit. Triaminoguanidinium chloride was isolated after treating aminoguanidinium bicarbonate with HCl and following reaction of the chloride with 2 equivalents of hydrazine hydrate in 1,4-dioxane under reflux conditions.

Synthesis

Sodium 5-cyanotetrazolate sesquihydrate (1**):** To a solution of sodium cyanide (50.0 g , 1.02 mol , 2.00 equiv) and sodium azide (32.5 g , 500 mmol , 1.00 equiv) in H_2O (400 mL) was added MnO_2 (50.0 g , 575 mmol , 1.15 equiv). To the resulting dark brown suspension was added dropwise a mixture of H_2SO_4 (100 mL of a 50% solution in H_2O , 936 mmol , 1.87 equiv), formic acid (60.0 g , 1.11 mol , 2.22 equiv) and $\text{CuSO}_4 \cdot 5\text{ H}_2\text{O}$ (1.00 g , 4.01 mmol , $8.02 \times 10^{-3}\text{ equiv}$) within 30 min . During this period of time the temperature was kept between 38 and 43°C by cooling the reaction mixture with an ice bath. Afterwards the mixture was heated to 60°C for 2 h before it was cooled to RT. The resulting brown slurry was filtered off and the filtrate was adjusted to pH 10 by addition of Na_2CO_3 (106 g , 1.00 mol , 2.00 equiv). The solution was diluted with H_2O (300 mL), the thus formed manganese formate was filtered off and the filtrate was neutralized with formic acid (7.00 mL). The solvent was removed under reduced pressure and the resulting residue was extracted with boiling acetone. Removal of the solvent under reduced pressure and recrystallization from ethanol/ethyl acetate yielded slightly yellow/ocher crystals of **1** (19.5 g , 135 mmol , 27%). DSC (5°C min^{-1}): m.p = 255°C , decomp = 263°C ; ^1H NMR (270 MHz , $[\text{D}_6]\text{DMSO}$, 25°C , TMS): $\delta = 3.48\text{ ppm}$ (s, 2H ; H_2O); ^{13}C NMR (68 MHz , $[\text{D}_6]\text{DMSO}$, 25°C , TMS): $\delta = 138.3$ (CN_4), 115.6 ppm (CN); ^{14}N NMR (29 MHz , $[\text{D}_6]\text{DMSO}$, 25°C , CH_3NO_2): $\delta = 17.5$ (s, 2N ; N(1)-

$N(2)=N(3)$, -47.7 (s, 2N); $N(1)-C(5)=N(4)$, -119 ppm (s, 1N; C-CN); IR (KBr): $\tilde{\nu}=3520$ (s), 3414 (vs), 3298 (s), 2863 (w), 2836 (w), 2474 (w), 2460 (w), 2260 (m), 2180 (w), 2142 (w), 2102 (w), 2087 (w), 1704 (m), 1670 (w), 1619 (s), 1471 (w), 1422 (w), 1380 (m), 1369 (w), 1196 (w), 1150 (w), 1055 (w), 1047 (w), 877 (w), 753 (w), 738 (w), 728 (w), 671 (w), 660 (w), 602 (w), 549 (m), 533 (m), 499 cm^{-1} (w); Raman (1064 nm, 300 mW, 25 °C): $\tilde{\nu}=3359$ (1), 2266 (100), 1420 (59), 1200 (8), 1161 (5), 1095 (10), 1084 (6), 1060 (18), 737 (2), 608 (8), 495 (9), 226 cm^{-1} (5); MS (DCI⁺): m/z calcd for $\text{C}_2\text{H}_3\text{N}_5\text{O}^+$: 113.0 [M^+]; found: 113.1; elemental analysis calcd (%) for $\text{NaC}_2\text{H}_3\text{N}_5\text{O}_{1.5}$: C 16.67, H 2.10, N 48.61; found: C 16.13, H 2.02, N 46.71; BAM drophammer: 40 J; friction tester: 160 N; ESD: 380 mJ (at grain size 100–500 μm).

5-Cyanotetrazole (2): Sodium-5-cyanotetrazolate sesquihydrate (1; 3.27 g, 22.7 mmol, 1.00 equiv) was dissolved in 2 M HNO_3 (11.4 mL, 22.7 mmol, 1.00 equiv) at RT and the solvent was carefully removed under reduced pressure at a maximum temperature of 40 °C. The residue was dried under high vacuum and suspended in dry EtOH (30 mL). Filtration and slow evaporation of the mother liquor yielded slightly greenish crystals of compound **2** (1.20 g, 12.6 mmol, 56%). After almost complete evaporation of the mother liquor further green/brown crystals of **2** (0.960 g, 10.1 mmol, 44%) were obtained. ^1H NMR (400 MHz, $[\text{D}_6]\text{DMSO}$, 25 °C, TMS): $\delta=14.80$ ppm (s, 1H; NH); ^{13}C NMR (101 MHz, $[\text{D}_6]\text{DMSO}$, 25 °C, TMS): $\delta=139.2$ (CN_4), 113.3 (CN) ppm; IR (KBr): $\tilde{\nu}=3461$ (w), 3158 (m), 2979 (w), 2881 (w), 2781 (w), 2680 (w), 2548 (w), 2278 (w), 2266 (w), 2153 (w), 1947 (w), 1788 (w), 1686 (m), 1560 (w), 1513 (w), 1466 (w), 1438 (w), 1414 (w), 1393 (w), 1372 (w), 1323 (m), 1294 (s), 1222 (w), 1209 (w), 1184 (w), 1170 (m), 1112 (m), 1044 (s), 1022 (s), 976 (w), 871 (w), 834 (s), 741 (m), 697 cm^{-1} (w); Raman (1064 nm, 300 mW, 25 °C): $\tilde{\nu}=3165$ (2), 2280 (100), 1468 (14), 1439 (14), 1413 (34), 1386 (3), 1297 (4), 1221 (7), 1173 (10), 1110 (26), 1068 (15), 1024 (10), 744 (4), 725 (3), 608 (13), 542 (4), 494 (15), 214 cm^{-1} (23); MS (DEI⁺): m/z calcd for C_2HN_5^+ : 95.0 [M^+]; found: 95.0; elemental analysis calcd (%) for C_2HN_5 : C 25.27, H 1.06, N 73.67; found: C 25.41, H 1.03, N 72.44.

Silver 5-cyanotetrazolate (3): Compound **1** (432 mg, 3.00 mmol, 1.00 equiv) was dissolved in H_2O (10 mL) at RT. Afterwards an aqueous solution of AgNO_3 (10 mL, 510 mg, 3.00 mmol, 1.00 equiv) was added. A thick, white precipitate started to form immediately, which was stirred for further 15 min under the exclusion of light. The precipitate was filtered off, washed with water to remove residual NaNO_3 and air-dried. Yield: 595 mg (2.95 mmol, 98%). DSC (5 °C min^{-1}): decomp=284 °C; elemental analysis calcd (%) for C_2AgN_5 : C 11.90, N 34.68; found: C 11.99, N 34.37; BAM drophammer: <1 J; friction tester: <5 N; ESD: 1 mJ (!; at grain size <100 μm).

Tetrazole-5-carboxamide (4): Compound **1** (3.20 g, 22.2 mmol) was dissolved in 6 M HNO_3 (10 mL) and the solution was heated to 80 °C for 15 min. The solvent was removed under reduced pressure and the residue was extracted with boiling ethanol (3×100 mL). After the solvent was removed from the combined extracts, the residue was recrystallized from boiling water. Yield: 1.74 g (15.4 mmol, 69%). ^1H NMR (400 MHz, $[\text{D}_6]\text{DMSO}$, 25 °C, TMS): $\delta=8.57$ (s, 1H; CONH_2), 8.19 ppm (s, 1H; CONH_2); ^{13}C NMR (101 MHz, $[\text{D}_6]\text{DMSO}$, 25 °C, TMS): $\delta=157.2$ (CONH_2), 152.0 ppm (CN_4); Raman (1064 nm, 300 mW, 25 °C): $\tilde{\nu}=3361$ (3), 3250 (10), 3192 (5), 2808 (2), 1688 (42), 1649 (6), 1604 (31), 1571 (64), 1442 (38), 1298 (20), 1229 (100), 1108 (82), 1090 (79), 1059 (35), 997 (7), 804 (13), 759 (2), 696 (30), 630 (2), 511 (6), 415 (58), 241 (46), 221 cm^{-1} (24); ele-

mental analysis calcd (%) for $\text{C}_2\text{H}_3\text{N}_5\text{O}$: C 21.24, H 2.67, N 61.93; found: C 18.29, H 2.30, N 62.25.

Hydroxylammonium 5-carboxamide tetrazolate (5): Compound **4** (0.710 g, 6.28 mmol, 1.00 equiv) was dissolved in H_2O (10 mL) and hydroxylamine (0.39 mL of a 50% w/v solution in H_2O , 0.420 g, 6.36 mmol, 1.01 equiv) was added. After cooling down the solution to 2 °C, **5** crystallized from the mother liquor in 88% yield (0.810 g, 5.54 mmol). DSC (5 °C min^{-1}): decomp=173 °C; ^1H NMR (400 MHz, $[\text{D}_6]\text{DMSO}$, 25 °C, TMS) $\delta=10.06$ (s, 4H; NH_3OH), 7.91 (s, 1H; CONH_2), 7.59 (s, 1H; CONH_2); ^{13}C NMR (101 MHz, $[\text{D}_6]\text{DMSO}$, 25 °C, TMS) $\delta=163.1$ (CONH_2), 157.4 ppm (CN_4); IR (KBr): $\tilde{\nu}=3310$ (s), 3201 (m), 2985 (s), 2859 (m), 2741 (vs), 2509 (m), 2178 (w), 2106 (w), 1702 (s), 1671 (s), 1631 (m), 1616 (m), 1587 (m), 1517 (s), 1385 (m), 1334 (m), 1240 (w), 1204 (m), 1173 (m), 1114 (m), 1069 (w), 1050 (w), 1009 (m), 795 (m), 718 (m), 681 (m), 656 (m), 536 cm^{-1} (m); Raman (1064 nm, 350 mW, 25 °C): $\tilde{\nu}=3139$ (4), 2939 (5), 2723 (5), 1637 (5), 1605 (12), 1527 (53), 1395 (2), 1337 (5), 1207 (33), 1175 (26), 1115 (19), 1098 (100), 1071 (47), 1051 (19), 1011 (25), 811 (3), 783 (3), 725 (13), 521 (3), 440 (12), 310 (3), 284 (6), 250 (12), 217 cm^{-1} (10); MS (FAB⁺): m/z calcd for NH_4O^+ : 34.0 [M^+]; found: 34.0; MS (FAB⁻): m/z calcd for $\text{C}_2\text{H}_2\text{N}_5\text{O}^-$: 112.0 [M^-]; found: 112.0; elemental analysis calcd (%) for $\text{C}_2\text{H}_6\text{N}_6\text{O}_2$: C 16.44, H 4.14, N 57.52; found: C 16.66, H 3.93, N 57.08; BAM drophammer: 40 J; friction tester: 288 N; ESD: 0.15 J (at grain size 100–500 μm).

Tetrazole-5-carboxamide oxime monohydrate (6): To a solution of 5-cyanotetrazole (**2**) (1.66 g, 17.5 mmol, 1.00 equiv) in H_2O (30 mL) was added hydroxylamine (1.07 mL of a 50% w/v solution in H_2O , 1.15 g, 17.5 mmol, 1.00 equiv) at RT. Crystallization started immediately after addition and yielded **6** (1.89 g, 12.9 mmol, 74%) as colorless precipitate.

Alternatively, a solution of **1** (11.5 g; 80.0 mmol; 1.00 equiv) in water (30 mL) was treated with an aqueous solution of hydroxylammonium chloride (20 mL, 5.91 g; 85.0 mmol, 1.04 equiv). The solution was heated at reflux for 10 min, until precipitation of **6** started. The crude product was filtered off and recrystallized from hot water. The filtrate was left to stand for a few more days to improve the yield. **6** (7.01 g; 48.0 mmol; 60%) was gained as colorless solid. DSC (5 °C min^{-1}): 120 °C (H_2O), decomp=244 °C; ^1H NMR (270 MHz, $[\text{D}_6]\text{DMSO}$, 25 °C, TMS): $\delta=10.51$ (br. s, 1H; NH), 7.09 ppm (s, 2H; C-NH₂); ^{13}C NMR (68 MHz, $[\text{D}_6]\text{DMSO}$, 25 °C, TMS): $\delta=150.7$ (CN_4), 144.9 ppm ($\text{C}(\text{NH}_2)\text{NOH}$); IR (KBr): $\tilde{\nu}=3315$ (vs), 3128 (vs), 3002 (vs), 2849 (vs), 2745 (vs), 2649 (s), 2250 (w), 2211 (w), 2141 (w), 2117 (w), 1814 (w), 1801 (w), 1712 (vs), 1650 (s), 1559 (m), 1500 (w), 1462 (m), 1394 (s), 1386 (s), 1306 (m), 1199 (w), 1173 (w), 1159 (w), 1133 (w), 1121 (w), 1092 (w), 1062 (w), 1047 (w), 1024 (w), 977 (w), 774 (s), 736 (s), 723 (s), 668 (m), 660 (m), 638 (s), 599 (m), 525 (w), 501 cm^{-1} (m); Raman (1064 nm, 300 mW, 25 °C): $\tilde{\nu}=3116$ (9), 1648 (9), 1578 (58), 1452 (18), 1400 (6), 1315 (13), 1199 (41), 1161 (30), 1125 (100), 1085 (84), 1062 (59), 1038 (41), 770 (17), 631 (8), 422 (47), 353 (12), 326 (9), 192 (10), 157 cm^{-1} (28); MS (FAB⁺): m/z calcd for $\text{C}_2\text{H}_4\text{N}_6\text{O}^+$: 128.0 [M^+]; found: 128.0; elemental analysis calcd (%) for $\text{C}_2\text{H}_6\text{N}_6\text{O}_2$: C 16.44, H 4.14, N 57.52; found: C 17.10, H 3.76, N 57.83; BAM drophammer: 40 J; friction tester: 252 N; ESD: 80 mJ (at grain size 100–500 μm).

Hydroxylammonium 5-carboxamide-oxime tetrazolate (7): To a suspension of **6** (0.713 g, 4.88 mmol, 1.00 equiv) in H_2O (40 mL) was added hydroxylamine (0.5 mL of a 50% (w/v) solution in H_2O , 0.539 g, 8.16 mmol, 1.67 equiv) and the resulting mixture was stirred at RT until everything was dissolved. Rapidly beginning crystallization yielded small colorless crystal needles of compound **7** (435 mg, 2.69 mmol, 55%). Crystals suitable for X-ray diffraction

were obtained by slow evaporation of a solution of **7** in DMF/H₂O (1:4). DSC (5 °C min⁻¹): decomp = 171 °C; ¹H NMR (400 MHz, [D₆]DMSO, 25 °C, TMS): δ = 12.31 (br. s, 3H; H₃N-OH), 8.47 ppm (s, 2H; C-NH₂); ¹³C NMR (101 MHz, [D₆]DMSO, 25 °C, TMS): δ = 156.5 (CN₄), 148.2 ppm (CNH₂NOH); ¹⁴N NMR (29 MHz, [D₆]DMSO, 25 °C, CH₃NO₂): δ = -68.8 ppm (s, 1N; C=N-OH); IR (KBr): ν̄ = 3454 (s), 3366 (s), 3197 (m), 3118 (m), 3005 (m), 2906 (m), 2744 (m), 1682 (m), 1643 (m), 1542 (m), 1469 (m), 1385 (s), 1309 (m), 1273 (m), 1207 (w), 1152 (m), 1116 (m), 1045 (w), 1001 (w), 970 (m), 856 (w), 808 (m), 765 (w), 732 (w), 696 (w), 502 cm⁻¹ (w); Raman (1064 nm, 300 mW, 25 °C): ν̄ = 3358 (3), 1666 (38), 1604 (3), 1551 (100), 1472 (1), 1393 (3), 1315 (2), 1264 (2), 1208 (30), 1153 (18), 1118 (8), 1085 (36), 1062 (3), 1047 (3), 1002 (19), 967 (13), 818 (4), 766 (8), 654 (1), 518 (2), 444 (12), 422 (2), 362 (13), 285 (1), 217 (4), 187 (3), 146 (2), 131 (29), 120 (9), 106 (28), 95 (14), 78 cm⁻¹ (81); MS (FAB⁺): *m/z* calcd for NH₄O⁺: 34.0 [*M*⁺]; found: 34.0; MS (FAB⁻): *m/z* calcd for C₂H₃N₆O⁻: 127.0 [*M*⁻]; found: 127.0; elemental analysis calcd (%) for C₂H₇N₇O₂: C 14.91, H 4.38, N 60.85; found: C 15.42, H 4.05, N 59.98; BAM drophammer: 10 J; friction tester: > 360 N, ESD: 300 mJ (at grain size 100–500 μm).

Ammonium 5-carboxamide-oxime tetrazolate (8): Compound **6** (1.47 g; 10.1 mmol; 1.00 equiv) was suspended in boiling water (25 mL) and ammonia (32%; 0.5 mL; 26.7 mmol; 2.64 equiv) was added. The suspension was heated until the reaction mixture became clear and then cooled down. The solvent was removed by rotary evaporation and **8** (1.37 g; 9.44 mmol; 93%) was afforded as colorless solid. DSC (5 °C min⁻¹): decomp = 202 °C; ¹H NMR (400 MHz, [D₆]DMSO, 25 °C, TMS): δ = 7.3 (br. s, 1H; OH), 5.6 (br. s, 2H; NH₂), 3.5 ppm (br. s, 4H; NH₄⁺); ¹³C NMR (101 MHz, [D₆]DMSO, 25 °C, TMS): δ = 156.3 (CN₄), 145.1 ppm (CNH₂NOH); ¹⁴N NMR (29 MHz, [D₆]DMSO, 25 °C, CH₃NO₂): δ = -353.4 ppm (NH₄⁺); IR (KBr): ν̄ = 3449 (s), 3339 (vs), 3178 (vs), 3058 (vs), 2883 (s), 2165 (vw), 1907 (w), 1679 (s), 1597 (m), 1537 (w), 1447 (s), 1384 (s), 1294 (m), 1196 (w), 1144 (w), 1103 (w), 1039 (w), 962 (s), 808 (s), 690 (m), 582 (w), 495 (w) cm⁻¹; Raman (1064 nm, 300 mW, 25 °C): ν̄ = 3450 (2), 3328 (5), 3242 (2), 3189 (2), 3033 (7), 2869 (3), 1913 (2), 1663 (32), 1603 (3), 1542 (100), 1452 (2), 1378 (2), 1309 (4), 1200 (34), 1144 (17), 1119 (7), 1102 (12), 1061 (43), 1039 (4), 957 (36), 819 (6), 769 (11), 662 (2), 515 (3), 430 (13), 367 (7), 325 (11), 216 cm⁻¹ (19); MS (FAB⁺): *m/z* calcd for NH₄⁺: 18.0 [*M*⁺]; found: 18.0; MS (FAB⁻): *m/z* calcd for C₂H₃N₆O⁻: 127.0 [*M*⁻]; found: 127.0; elemental analysis calcd (%) for C₂H₇N₇O: C 16.55, H 4.86, N 67.56; found: C 16.97, H 4.67, N 67.03; BAM drophammer: 40 J; friction tester: 288 N; ESD: 0.75 J (at grain size 100–500 μm).

Guanidinium 5-carboxamide-oxime tetrazolate (9): Compound **6** (1.47 g, 10.1 mmol, 2.00 equiv) was suspended in H₂O (50 mL), the suspension was brought to reflux and guanidinium carbonate was added (0.900 g, 5.00 mmol, 1.00 equiv). After boiling the suspension for 5 min, it became a clear solution. The solvent was removed under reduced pressure and the residue was recrystallized from ethanol/water to give 1.59 g (8.50 mmol, 85%) of **9** as colorless crystals. DSC (5 °C min⁻¹): m.p. = 160 °C, decomp = 206 °C; ¹H NMR (400 MHz, [D₆]DMSO, 25 °C, TMS): δ = 6.61 (s, 3H; NH₂, OH), 5.72 ppm (s, 6H; C(NH₂)₃); ¹³C NMR (101 MHz, [D₆]DMSO, 25 °C, TMS): δ = 158.7 (C(NH₂)₃), 156.2 (CN₄), 146.5 ppm (CNH₂NOH); IR (KBr): ν̄ = 3472 (s), 3428 (s), 3351 (s), 3269 (s), 3230 (s), 3174 (vs), 2785 (m), 1673 (vs), 1655 (vs), 1605 (m), 1563 (m), 1530 (w), 1412 (w), 1389 (m), 1292 (w), 1187 (w), 1139 (w), 1082 (w), 1061 (w), 1031 (w), 934 (m), 877 (w), 807 (m), 661 (w), 571 (w), 520 cm⁻¹ (w); Raman (1064 nm, 500 mW, 25 °C): ν̄ = 3240 (4), 3175 (5), 1659 (14), 1607 (11), 1537 (100), 1390 (3), 1189 (37), 1140 (17), 1085 (27), 1064 (26), 1032 (5), 1011 (53), 940 (27), 806 (5), 770 (6), 663 (3), 529 (7),

490 (3), 431 (11), 341 (8), 124 (79), 110 (95), 99 (112), 75 cm⁻¹ (68); MS (FAB⁺): *m/z* calcd for CH₆N₃⁺: 60.0 [*M*⁺]; found: 60.0; MS (FAB⁻): *m/z* calcd for C₂H₃N₆O⁻: 127.0 [*M*⁻]; found: 127.1; elemental analysis calcd (%) for C₃H₉N₉O: C 19.25, H 4.85, N 67.35; found: C 19.77, H 4.77, N 66.41. BAM drophammer: 40 J; friction tester: 360 N; ESD: 1.0 J (at grain size 500–1000 μm).

Triaminoguanidinium 5-carboxamide-oxime tetrazolate (10): Compound **6** (2.56 g; 20.0 mmol; 1.00 equiv) was suspended in boiling water and triaminoguanidine (2.08 g; 20.0 mmol; 1.00 equiv) was added under nitrogen atmosphere. The solution turned red and became clear. After a short time of heating, the solution became light orange and then colorless, was filtrated and left to crystallize. **10** (3.32 g; 14.3 mmol; 72%) was afforded as orange-brown crystals. DSC (5 °C min⁻¹): decomp = 160 °C; ¹H NMR (400 MHz, [D₆]DMSO, 25 °C, TMS): δ = 9.4 (s, 1H; OH), 8.7 (s, 3H; NH-NH₂), 5.5 (s, 2H; C-NH₂), 4.5 ppm (s, 6H; NH-NH₂); ¹³C NMR (101 MHz, [D₆]DMSO, 25 °C, TMS): δ = 159.6 (C(NHNH₂)₃), 156.5 (CN₄), 145.7 ppm (CNH₂NOH); IR (KBr): ν̄ = 3851 (vw), 3319 (vs), 3211 (vs), 3104 (s), 2903 (m), 1684 (s), 1613 (s) 1536 (w), 1476 (w), 1425 (w), 1381 (m), 1334 (s), 1292 (m), 1188 (vw), 1128 (s), 1031 (w), 952 (vs), 800 (w), 770 (vw), 737 (vw), 703 (vw), 638 (m), 607 (s), 489 cm⁻¹ (vw); Raman (1064 nm, 300 mW, 25 °C): ν̄ = 3431 (2), 3352 (4), 3297 (6), 3297 (6), 3264 (5), 3179 (2), 1658 (28), 1611 (11), 1526 (100), 1371 (7), 1299 (2), 1181 (32), 1152 (5), 1125 (16) 1080 (31), 1048 (18), 938 (28), 881 (21), 804 (4), 770 (7), 643 (5), 485 (2), 426 (26), 409 (8), 347 (11), 294 (2), 261 (10), 199 (15), 189 (15), 148 cm⁻¹ (14); MS (FAB⁺): *m/z* calcd for CH₉N₆⁺: 105.1 [*M*⁺]; found: 105.1; MS (FAB⁻): *m/z* calcd for C₂H₃N₆O⁻: 127.0 [*M*⁻]; found: 127.2; elemental analysis calcd (%) for C₃H₁₂N₁₂O: C 15.52, H 5.21, N 72.15; found: C 16.09, H 5.01, N 72.15; BAM drophammer: 15 J; friction tester: 360 N; ESD: 1.0 J (at grain size 500–1000 μm).

Acknowledgements

Financial support of this study from the Ludwig-Maximilian University of Munich (LMU), the U.S. Army Research Laboratory (ARL) under grant no. W911NF-09-2-0018, the Armament Research, Development and Engineering Center (ARDEC), and the Office of Naval Research (ONR) under grant no. N00014-10-1-0535 is gratefully acknowledged. We acknowledge collaborations with Dr. Mila Krupka (OZM Research, Czech Republic) in the development of new testing and evaluation methods for energetic materials and with Dr. Muhamed Sucasca (Brodarski Institute, Croatia) in the development of new computational codes to predict the detonation and propulsion parameters of novel explosives. We are indebted to and thank Drs. Betsy M. Rice and Brad Forch (ARL, Aberdeen, Proving Ground, MD). We also thank Stefan Huber for sensitivity measurements.

Keywords: calculations • energetic materials • heterocycles • tetrazoles • X-ray diffraction

- [1] P. B. Mohite, V. H. Bhaskar, *Int. J. PharmTech Res.* **2011**, *3*, 1557–1566.
- [2] R. P. Singh, R. D. Verma, D. T. Meshri, J. M. Shreeve, *Angew. Chem.* **2006**, *118*, 3664–3682; *Angew. Chem. Int. Ed.* **2006**, *45*, 3584–3601.
- [3] W. G. Finnegan, R. A. Henry, R. Lofquist, *J. Am. Chem. Soc.* **1958**, *80*, 3908–3911.
- [4] L. A. Lazukina, V. P. Khuzar, *Zh. Org. Khim.* **1979**, *15*, 2216–2217.
- [5] A. A. Melnikov, M. M. Sokolova, M. A. Pervozvanskaya, V. V. Melnikov, *Zh. Org. Khim.* **1979**, *15*, 1861–1866.

- [6] S. S. Washburne, W. R. Peterson Jr., *J. Organomet. Chem.* **1970**, *21*, 427–430.
- [7] W. Beck, W. P. Fehlhammer, *Angew. Chem.* **1967**, *79*, 146–147; *Angew. Chem. Int. Ed. Engl.* **1967**, *6*, 169–170.
- [8] E. Oliveri-Mandala, T. Passalacqua, *Gazz. Chim. Ital.* **1912**, *41*, 430–435.
- [9] M.-J. Crawford, T. M. Klapötke, F. A. Martin, C. M. Sabate, M. Rusan, *Chem. Eur. J.* **2011**, *17*, 1683–1695.
- [10] B. Mlakar, B. Stefane, M. Kocevar, S. Polanc, *Tetrahedron* **1998**, *54*, 4387–4396.
- [11] B. A. Bovenzi, G. A. Pearse, G. A. Pearse Jr., *J. Chem. Soc., Dalton Trans.* **1997**, 2793–2797.
- [12] Y. Ohno, Y. Akutsu, M. Arai, M. Tamura, T. Matsunaga, M. Iida, *Acta Crystallogr. Sect. C* **1998**, *54*, 1160–1162.
- [13] T. M. Klapötke, J. Stierstorfer, A. U. Wallek, *Chem. Mater.* **2008**, *20*, 4519–4530.
- [14] J. Stierstorfer, T. M. Klapötke, A. Hammerl, R. D. Chapman, *Z. Anorg. Allg. Chem.* **2008**, *634*, 1051–1057.
- [15] G. Hervé, G. Jacob, *Tetrahedron* **2006**, *63*, 953–959.
- [16] M. Hesse, H. Meier, B. Zeeh, *Spektroskopische Methoden in der Organischen Chemie*, 7th ed., Thieme, Stuttgart, **2005**.
- [17] G. Socrates, *Infrared and Raman Characteristics Group Frequencies*, 3rd ed, Wiley, Chichester, **2004**.
- [18] T. M. Klapötke, P. Mayer, C. Miro Sabate, J. M. Welch, N. Wiegand, *Inorg. Chem.* **2008**, *47*, 6014–6027.
- [19] NATO standardization agreement (STANAG) on explosives, *Impact Sensitivity Tests*, 1st ed., no. 4489, September 17, **1999**.
- [20] WIWEB-Standardarbeitsanweisung 4–5.1.02, Ermittlung der Explosionsgefährlichkeit, hier der Schlagempfindlichkeit mit dem Fallhammer, Nov. 8, **2002**.
- [21] <http://www.bam.de>.
- [22] NATO standardization agreement (STANAG) on explosive, *Friction Sensitivity Tests*, 1st ed., no. 4487, August 22, **2002**.
- [23] WIWEB-Standardarbeitsanweisung 4–5.1.03, Ermittlung der Explosionsgefährlichkeit oder der Reibeempfindlichkeit mit dem Reibeapparat, Nov. 8, **2002**.
- [24] a) S. Zeman, V. Pelikán, J. Majzlík, J. Koei, *Cent. Eur. J. Energetic Mater.* **2006**, *3*, 45–51; b) D. Skinner, D. Olson, A. Block-Bolten, *Propellants Explos. Pyrotech.* **1998**, *23*, 34–42.
- [25] <http://www.ozm.cz/en/sensitivity-tests/esd-2008a-small-scale-electrostatic-spark-sensitivity-test/>.
- [26] N. Fischer, D. Izsak, T. M. Klapötke, S. Rappenglück, J. Stierstorfer, *Chem. Eur. J.* **2012**, *18*, 4051–4062.
- [27] <http://www.linseis.com>.
- [28] a) M. Sućeska, EXPLO5.5 program, Zagreb, Croatia, **2011**; b) M. Sućeska, *Propellants, Explos. Pyrotech.* **1999**, *24*, 280–285.
- [29] a) E. F. C. Byrd, B. M. Rice, *J. Phys. Chem. A* **2006**, *110*, 1005–1013; b) B. M. Rice, S. V. Pai, J. Hare, *Comb. Flame* **1999**, *118*, 445–458.
- [30] a) J. W. Ochterski, G. A. Petersson, J. A. Montgomery Jr., *J. Chem. Phys.* **1996**, *104*, 2598–2619; b) J. A. Montgomery Jr., M. J. Frisch, J. W. Ochterski, G. A. Petersson, *J. Chem. Phys.* **2000**, *112*, 6532–6542.
- [31] T. Altenburg, T. M. Klapötke, A. Penger, J. Stierstorfer, *Z. Anorg. Allg. Chem.* **2010**, *636*, 463–471.
- [32] Gaussian 09, Revision A.1, M. J. Frisch, et al. Gaussian, Inc., Wallingford CT, **2009**. See the Supporting Information for the full citation.
- [33] a) H. D. B. Jenkins, H. K. Roobottom, J. Passmore, L. Glasser, *Inorg. Chem.* **1999**, *38*, 3609–3620; b) H. D. B. Jenkins, D. Tudela, L. Glasser, *Inorg. Chem.* **2002**, *41*, 2364–2367.
- [34] CrysAlisPro, Agilent Technologies, Version 1.171.35.11, **2011**.
- [35] G. M. Sheldrick, SHELXS-97, Program for Crystal Structure Solution, Universität Göttingen, Göttingen (Germany), **1997**.
- [36] A. Altomare, G. Cascarano, C. Giacovazzo, A. Guagliardi, *Appl. Crystallogr.* **1993**, *26*, 343–350.
- [37] G. M. Sheldrick, SHELXL-97, Program for the Refinement of Crystal Structures, University of Göttingen, Göttingen (Germany), **1994**.
- [38] A. L. Spek, Platon, A Multipurpose Crystallographic Tool, Utrecht University, Utrecht (The Netherlands), **1999**.
- [39] L. Farrugia, *J. Appl. Crystallogr.* **1999**, *32*, 837–838.
- [40] CCDC 867191 (2), 867194 (3), 867192 (4), 867195 (5), 867196 (7), 867198 (8), 867199 (9), and 867197 (10) contain the supplementary crystallographic data for this paper. These data can be obtained free of charge from The Cambridge Crystallographic Data Centre via www.ccdc.cam.ac.uk/data_request/cif.
- [41] R. M. Vrcelj, J. N. Sherwood, A. R. Kennedy, H. G. Gallagher, T. Gelbrich, *Cryst. Growth Des.* **2003**, *3*, 1027–1032.
- [42] P. Hakey, W. Ouellette, J. Zubietta, T. Korter, *Acta Crystallogr.* **2008**, *E64*, o1428.

Received: May 31, 2012

Published online on July 20, 2012

Month 2012 Synthesis and Characterization of the New Heterocycle 5-(4-Amino-1,2,4-triazol-3-on-5'-yl)-1H-tetrazole and Some Ionic Nitrogen-rich Derivatives

1

Niko Fischer Katharina Hüll Thomas M. Klapötke* and Jörg Stierstorfer

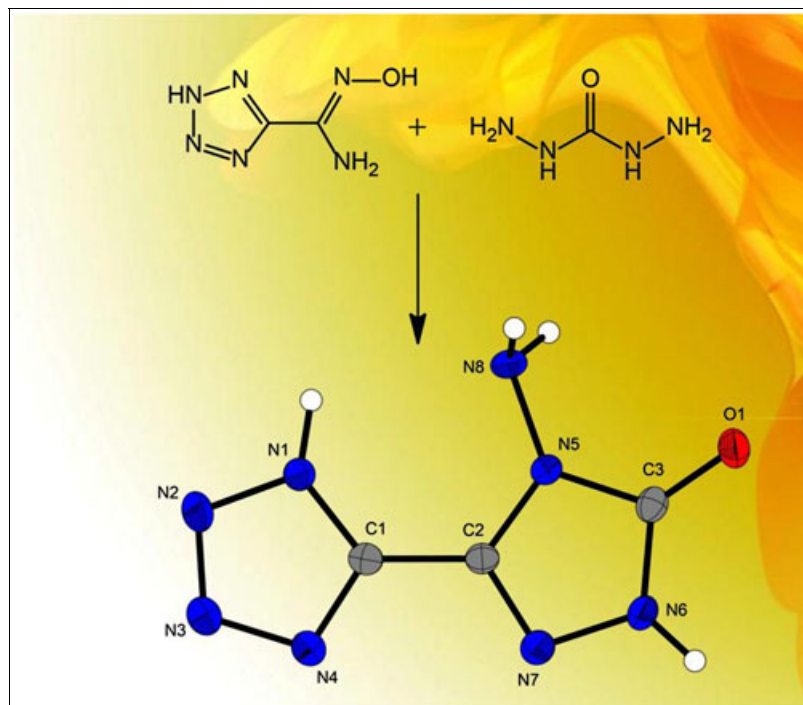
Energetic Materials Research, Department of Chemistry, University of Munich (LMU), Butenandtstr. 5-13D-81377, Germany

*E-mail: tmk@cup.uni-muenchen.de

Received August 13, 2012;2012

DOI 10.1002/jhet.1877

Published online 00 Month 2012 in Wiley Online Library (wileyonlinelibrary.com).



A new heterocycle consisting of a tetrazole ring attached to an amino-triazolone ring, namely 5-(4-amino-1,2,4-triazol-3-on-5'-yl)-1H-tetrazole (**3**) as well as its ammonium salt (**2**), hydroxylammonium (**3**), and sodium (**4**), is introduced. Its ammonium salt (**2**) is formed starting from tetrazole-5-carboxamide oxime (**1**), which is reacted with diaminourea (carbonyldihydrazide) in aqueous media. All compounds **2–5** were structurally characterized by single crystal X-ray diffraction. The thermal behavior was investigated using differential scanning calorimetry, and the sensitivities towards impact, friction, and electrostatic discharge were determined. Furthermore, several detonation parameters were calculated with the program EXPLO5 to determine the potential use of these compounds as highly energetic materials.

J. Heterocyclic Chem., **00**, 00 (2012).

INTRODUCTION

Besides their use as energetic materials, especially in the field of primary [1] and secondary [2] explosives as well as gas generating agents [3] or as pyrotechnic fuels [4], tetrazoles cover a wide range of applications also including pharmaceutically active compounds [5] because of their extraordinary stability under metabolic conditions. Furthermore, the considerable amount of local electron density at the nitrogen atoms of tetrazoles leads to a variety of metal and molecular complexes [6] with these nitrogen-rich molecules, which resulted in an increasing interest of the scientific community in this class of heterocycles over the last decades. Also the development of a facile synthesis of 5-substituted tetrazoles, which was possible after the

detailed investigation of [2+3]-dipolar cycloadditions by Huisgen and coworkers in the 1960s [7], helped to promote their recent importance in diverse areas of research.

However, the combination of tetrazoles and triazoles still remained an only rarely described field. During the synthesis of nitrogen-rich salts of tetrazole-5-carboxamide oxime (**1**), which the authors reported recently [8], a new class of heterocyclic compounds consisting of a tetrazole ring connected to a triazole was discovered. Here, diaminourea (DAU) was reacted with tetrazole-5-carboxamide oxime to form the ammonium salt of 5-(4-amino-1,2,4-triazol-3-on-5'-yl)-1H-tetrazole. Besides the ammonium salt, also the hydroxylammonium salt of the mentioned tetrazole-triazole anion as well as the free acid was synthesized. The main focus of this work, however, is the investigation of the

energetic properties of these materials, as it has been a long tradition in our research group, because of their high nitrogen content and their high thermal stability.

RESULTS AND DISCUSSION

Synthesis. The mechanism for the synthesis of the starting material **1** (Scheme 1) is the nucleophilic attack of hydroxylamine to 5-cyanotetrazole. Cheaper and also more convenient is the reaction of sodium 5-cyanotetrazolate, which is the product of the reaction of sodium azide and sodium cyanide with hydroxylammonium chloride. The hydroxylammonium cation partially is deprotonated by the tetrazole ring resulting in an enhanced nucleophilicity for the addition to the nitrile group of 5-cyanotetrazole.

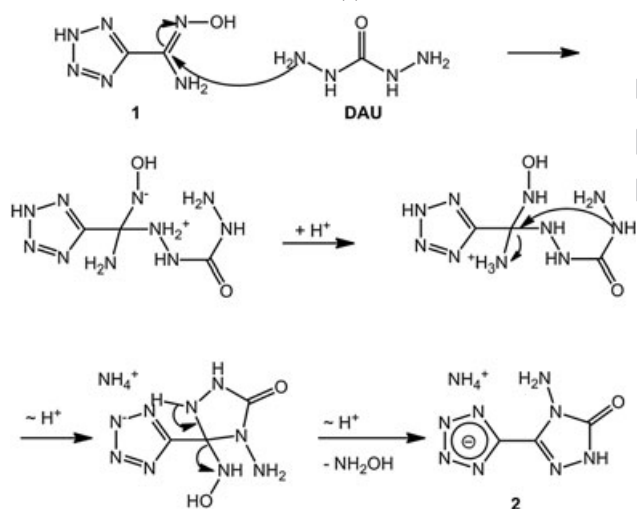
For the formation of the 5-(4-amino-1,2,4-triazol-3-yl)-1*H*-tetrazole heterocycle, **1** is dissolved in hot water, and DAU is added. The formation of the triazole ring starts with a nucleophilic attack of the amino group of DAU to the electrophilic carbon atom of the carboxamide oxime moiety of

1 (Scheme 2). A second nucleophilic attack of the α -N atom of DAU to the now sp^3 hybridized carbon atom of the former carboxamide oxime moiety under the release of ammonia closes the five-membered triazole ring. Finally, after proton transfer, also one mole of hydroxylamine is released into the reaction mixture. Because of its higher basicity compared with hydroxylamine, the released ammonia deprotonates the tetrazole ring resulting in the formation of the ammonium salt **2**. Because the reaction is acid-catalyzed, also an E1 instead of an E2 mechanism can be considered.

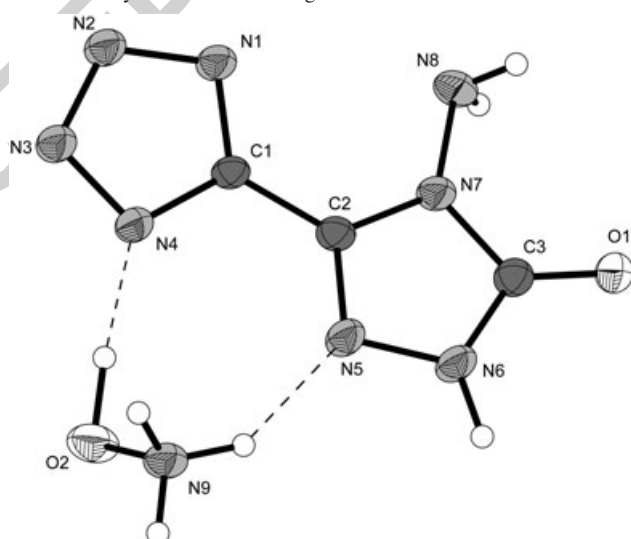
A different approach for the synthesis of the aminotriazolone ring could be the reaction of DAU with 5-cyanotetrazole itself utilizing the strongly electrophilic character of the nitrile moiety in 5-cyanotetrazole, which has been shown to be successful for other nitrile containing molecules [9].

Starting from the ammonium salt **2**, the hydroxylammonium salt **3** can be isolated after treatment with excess hydroxylamine under reflux conditions, which expels the partially formed ammonia because of its higher volatility

Scheme 1. Synthetic steps to the starting material tetrazol-5-carboxamide oxime (**1**).



Scheme 3. Synthesis of **2–5** starting from tetrazol-5-carboxamide oxime **1**. [Q1]



Scheme 2. Proposed mechanism for the cyclization of **1** with 1,3-diaminourea (DAU = carbonyldihydrazide).

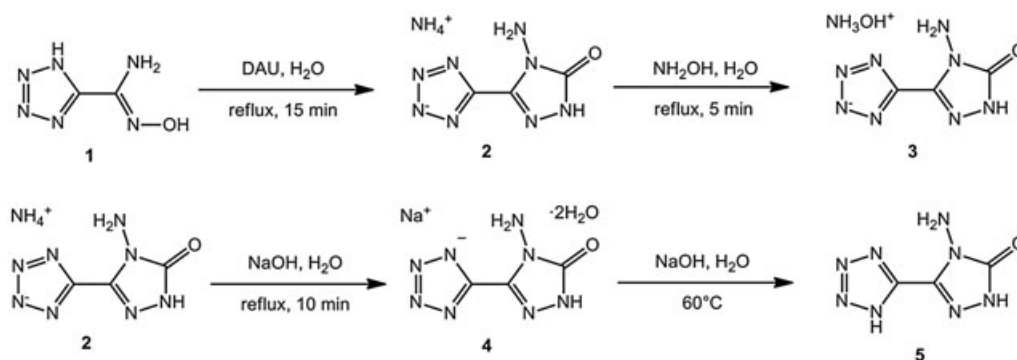


Table 1
XRD data and parameters.

	2	2.2 H ₂ O	3	4.2 H ₂ O	5
Formula	C ₃ H ₁₂ N ₉ O	C ₃ H ₁₁ N ₉ O ₃	C ₃ H ₇ N ₉ O ₂	C ₃ H ₇ N ₈ NaO ₃	C ₃ H ₄ N ₈ O
FW (g mol ⁻¹)	185.18	221.21	201.18	226.16	168.14
Crystal system	triclinic	triclinic	monoclinic	orthorhombic	monoclinic
Space group	<i>P</i> -1 (No. 2)	<i>P</i> -1 (No. 2)	<i>P</i> ₂ / <i>n</i> (No. 14)	<i>Cmca</i> (No. 64)	<i>P</i> ₂ / <i>n</i> (No. 14)
Color/Habit	Colorless needle	Colorless rod	Colorless block	Colorless block	Colorless platelet
Size (mm)	0.10 × 0.20 × 0.41	0.16 × 0.19 × 0.30	0.18 × 0.20 × 0.26	0.20 × 0.24 × 0.30	0.04 × 0.13 × 0.15
<i>a</i> (Å)	6.9987(11)	6.484(4)	7.633(2)	6.431(3)	12.4740(9)
<i>b</i> (Å)	114.350(14)	8.3585	7.026(3)	17.248(6)	6.8484(4)
<i>c</i> (Å)	8.3241(11)	9.239(6)	14.383(3)	15.629(6)	16.3826(12)
α (°)	99.385(12)	105.857(4)	90	90	90
β (°)	114.350(14)	107.246(5)	92.990(18)	90	111.830(9)
γ (°)	94.470(12)	94.060(6)	90	90	90
<i>V</i> (Å ³)	378.49(11)	453.4(5)	770.3(4)	1733.6(12)	1299.16(17)
<i>Z</i>	2	2	4	8	8
$\rho_{\text{calc.}}$ (g cm ⁻³)	1.625	1.620	1.735	1.733	1.719
μ (mm ⁻¹)	0.131	0.139	0.146	0.189	0.139
<i>F</i> (000)	192	232	416	928	688
$\lambda_{\text{MoK}\alpha}$ (Å)	0.71073	0.71073	0.71073	0.71073	0.71073
<i>T</i> (K)	173	173	173	173	173
θ min-max (°)	4.3, 26.0	4.4, 27.5	4.1, 26.5	4.3, 26.0	4.4, 25.8
Dataset	–8.8; –9.7; –10:10	–8.8; –7.10; –11:11	–8.9; –7.8; –11:18	–7.7; –18.21; –19:18	–15.15; –8.8; –20:20
Reflections collected	2863	2671	3914	4279	18134
Independent reflections	1476	2051	1563	923	2493
<i>R</i> _{int}	0.024	0.015	0.040	0.061	0.043
Observed reflections	1212	1611	1131	679	2155
Parameters	146	2051	155	85	249
<i>R</i> ₁ (obs)	0.0401	0.0418	0.0412	0.0446	0.0352
<i>wR</i> ₂ (all data)	0.1120	0.1051	0.0997	0.1205	0.0930
<i>S</i> ^c	1.04	1.04	1.00	1.02	1.07
Resd. dens. (e Å ⁻³)	–0.21, 0.49	–0.22, 0.21	–0.24, 0.22	–0.37, 0.48	–0.28, 0.32
Device type	Oxford Xcalibur3 CCD	Oxford Xcalibur3 CCD	Oxford Xcalibur3 CCD	Oxford Xcalibur3 CCD	Oxford Xcalibur3 CCD
Solution	SIR-92	SIR-92	SIR-92	SIR-92	SIR-92
Refinement	SHELXL-97	SHELXL-97	SHELXL-97	SHELXL-97	SHELXL-97
Absorption correction	multi-scan	multi-scan	multi-scan	multi-scan	multi-scan
CCDC	884791	884792	884793	884794	884795

compared with hydroxylamine, which, on the other hand, also possesses the lower basicity. To prepare the free acid **5**, the ammonium salt **2**, first, is converted into the sodium salt **4** after treatment with 2 M aqueous NaOH under reflux conditions to expel ammonia followed by acidification of the previously isolated sodium salt with excess 2 M hydrochloric acid. The synthetic pathways to **2–5** are depicted in

S3 Scheme 3.

Despite all efforts, it was not possible to abstract the second proton located at the triazole ring, even if excess base (NH₃, NH₂OH, NaOH) was used, implying a higher pK_a value (lower acidity) for this proton. Stronger bases (e.g., NaH) under anhydrous conditions may have to be applied to form the dianion of **5**.

Q2 **Crystal structures.** Single crystals of **2–5** suitable for structure determination by X-ray single crystal diffraction were obtained after crystallization from the aqueous reaction mixtures in the cases of **2**, **4**, and **5**. Compound **3** was isolated as crude material from the aqueous mother liquor and recrystallized from an ethanol/water mixture. Compounds **3** and **5** crystallize as crystal water free, whereas the sodium salt crystallizes as a dihydrate. Of the ammonium salt, two different crystal structures were obtained depending on the recrystallization conditions. Compound **2** crystallizes water free after slower crystallization and as a dihydrate, when the mother liquor is cooled down more rapidly resulting in faster crystallization. Different parameters regarding the measurements and solutions are gathered in Table 1.

Compound **2** and 2·2 H₂O crystallize in the triclinic space group *P*–1 with two cation/anion pairs in the unit cell. The water-free structure shows only a slightly higher density (1.625 g cm^{–3}) in comparison with the dihydrate (1.620 g cm^{–3}). The bond lengths and angles of the tetrazolyl moiety (listed in Table 2) are in accordance with those reported in literature [10]. The C1–C2 bond length is shorter than a C–C single bond (1.54 Å) and longer than a C=C double bond (1.33 Å). In addition, the tetrazole as well as triazole ring systems are nearly coplanar in all investigated structures. The largest anomaly was observed in the structure of **3** (<N1–C1–C2–C5 = 167.98(2)°).

The planarity of the heterocycle and the fact that all C–N and N–N bonds in the triazolone ring structure are in between the lengths for single and double bonds is consistent with the assumption that the mesomeric resonance is distributed across the whole molecule. Compared with compounds **3** and **4**, the C=O double bond in 2·2 H₂O is slightly longer (1.246(5) Å), also longer than a typical C=O double bond (1.19 Å) is. This is explained by the comparatively strong hydrogen bonds between the oxygen atom of the carbonyl group and the hydrogen atoms of the ammonium cation (Figs 1 and 2).

Hydroxylammonium 5-(4-amino-1,2,4-triazol-3-on-5'-yl)-1*H*-tetrazolate (**3**) crystallizes without inclusion of crystal water in the monoclinic space group *P*2₁/*n*. The bond lengths and geometry of the anion are comparable with those observed for **2** and 2·2 H₂O, except for the C=O double

Table 2

Bond lengths (Å–B), bond angles (Å–B–C), and torsion angles (Å–B–C–D).

	2	2·2 H ₂ O	3	4	5a	5b
A–B	(Å)	(Å)	(Å)	(Å)	(Å)	(Å)
O1–C3	1.246(2)	1.241(2)	1.238(2)	1.232(2)	1.2368(18)	1.244(2)
N1–C1	1.337(2)	1.340(2)	1.331(2)	1.324(2)	1.339(2)	1.337(2)
N1–N2	1.342(2)	1.344(2)	1.350(2)	1.343(2)	1.3489(18)	1.343(2)
N2–N3	1.320(2)	1.313(2)	1.313(2)	1.325(2)	1.3004(19)	1.300(2)
N3–N4	1.348(2)	1.347(2)	1.344(2)	1.341(2)	1.3601(18)	1.365(2)
N4–C1	1.337(2)	1.335(2)	1.337(2)	1.342(2)	1.3199(19)	1.323(2)
N5–C2	1.305(2)	1.307(2)	1.310(3)	1.315(2)	1.3041(19)	1.368(2)
N5–N6	1.386(2)	1.378(2)	1.375(2)	1.364(2)	1.3759(18)	1.377(2)
N6–C3	1.345(2)	1.349(2)	1.345(2)	1.365(2)	1.350(2)	1.346(2)
N7–C2	1.370(2)	1.375(2)	1.364(2)	1.363(2)	1.3651(19)	1.368(2)
N7–C3	1.379(2)	1.376(2)	1.372(2)	1.369(2)	1.3854(19)	1.372(2)
N7–N8	1.402(2)	1.413(2)	1.411(2)	1.340(2)	1.4005(17)	1.399(2)
C1–C2	1.465(2)	1.460(2)	1.457(3)	1.466(2)	1.452(2)	1.452(2)
A–B–C	(°)	(°)	(°)	(°)	(°)	(°)
N1–C1–N4	112.3(2)	111.9(1)	111.87(2)	112.8(1)	109.4(1)	109.3(1)
N5–C2–C1	123.6(2)	123.2(2)	122.74(2)	124.3(1)	121.8(1)	123.9(1)
O1–C3–N6	130.5(2)	129.8(2)	128.48(2)	127.2(1)	129.6(1)	129.8(1)
O1–C3–N7	125.7(2)	126.5(2)	127.17(2)	129.4(1)	127.1(1)	127.1(1)
C2–N7–N8	127.1(1)	127.4(1)	126.57(2)	129.1(1)	124.4(1)	124.0(1)
N6–C3–N7	103.8(2)	103.7(1)	104.34(2)	103.4(1)	103.3(1)	103.1(1)
A–B–C–D	(°)	(°)	(°)	(°)	(°)	(°)
N1–C1–C2–N5	–175.98(2)	2.1(2)	167.98(2)	180.0(1)	177.2(1)	172.7(2)
N8–N7–C3–O1	–3.4(3)	–2.4(3)	7.2(3)	0.0(1)	5.9(2)	0.8(3)

bond which is slightly shorter. The structure is dominated by several strong hydrogen bonds (Fig. 3).

Sodium salt **4** crystallizes in the orthorhombic space group *Cmca* with eight molecules per unit cell. All Na-O distances (exact values in the caption of Fig. 4) are within 2.37–2.44 Å, which are typical values for coordinative bonds. The sodium cations are distorted octahedrally coordinated by two anions and four molecules of crystal water. A comparable arrangement can be found in sodium 5-tetrazolate [10]. In the structure of **4**, chains along the α axis can be found (Fig. 4).

Neutral 5-(4-amino-1,2,4-triazol-3-on-5'-yl)-1H-tetrazole (**5**) crystallizes in the monoclinic space group *P2₁/c*. Only half of the asymmetric unit (one molecule) is depicted in Figure 5. Its density (1.719 g cm⁻³) is slightly

lower than that of **3** and **4**. Protonation of the tetrazole ring takes place at the nitrogen atom N1 that is mostly observed for electron withdrawing groups connected to the carbon atom of the tetrazole ring.

NMR spectroscopy. All compounds **2–5** were investigated using ¹H and ¹³C NMR spectroscopy. The chemical shifts are related to tetramethylsilane as standard.

In all proton NMR spectra of the salts **2–4**, the NH proton of the triazole ring appears as a signal at 11.63–11.69 ppm in the low field region. The two NH protons of the free acid **5**, however, are not separated into two signals because of fast proton exchange. Also, the position of the signal assigned to the amine functionality of the triazole ring differs from the deprotonated species **2–4** (5.50–5.59 ppm) to the free acid **5** (6.87 ppm). In the spectra of the ammonium

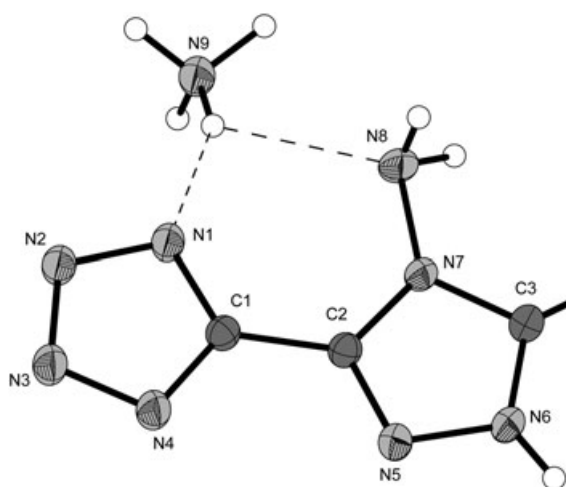


Figure 1. Molecular unit of ammonium 5-(4-amino-1,2,4-triazol-3-on-5'-yl)-1H-tetrazolate (**2**). Ellipsoids of nonhydrogen atoms are drawn at the 50% probability level.

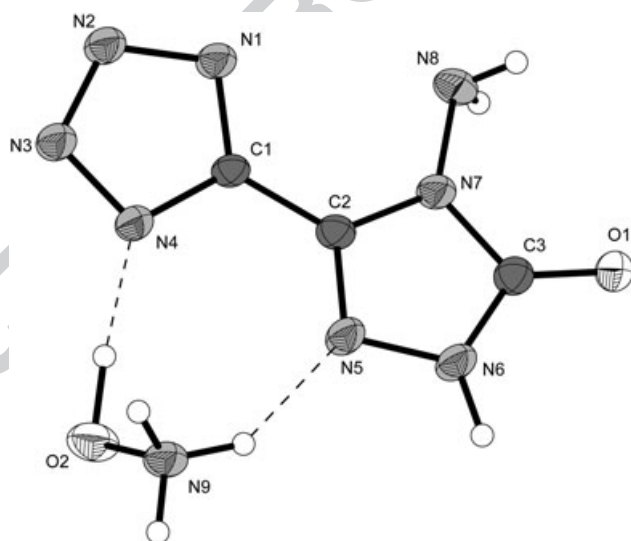


Figure 3. Molecular unit of hydroxylammonium 5-(4-amino-1,2,4-triazol-3-on-5'-yl)-1H-tetrazolate (**3**). Ellipsoids of nonhydrogen atoms are drawn at the 50% probability level.

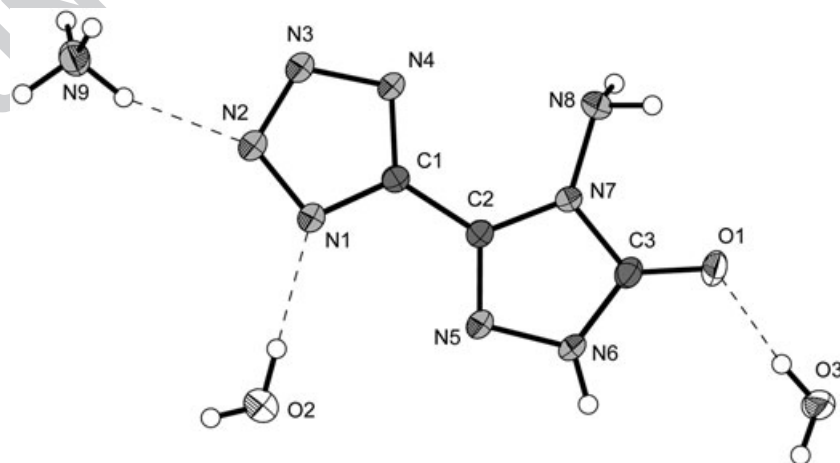


Figure 2. Molecular unit of ammonium 5-(4-amino-1,2,4-triazol-3-on-5'-yl)-1H-tetrazolate dihydrate (2·2 H₂O) showing the atom-labeling scheme. Ellipsoids of nonhydrogen atoms are drawn at the 50% probability level.

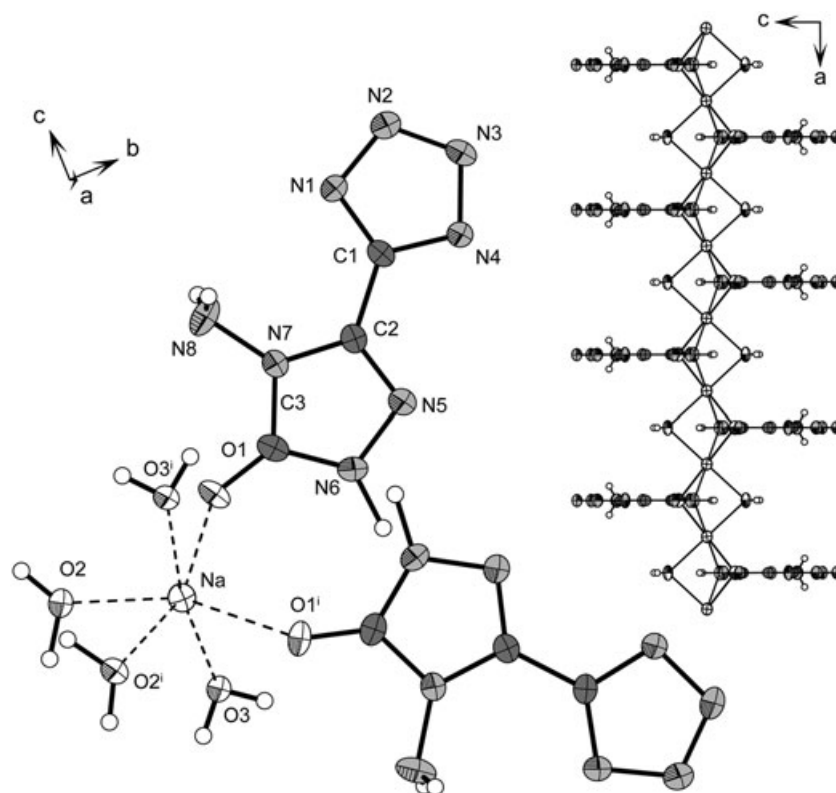


Figure 4. Depictions of the crystal structure of sodium 5-(4-amino-1,2,4-triazol-3-on-5'-yl)-1H-tetrazolate dihydrate (4·2 H₂O). View along the *a* and *b* axis. Ellipsoids of nonhydrogen atoms are drawn at the 50% probability level. Coordination distances (Å): Na–O3 2.3714, Na–O2 2.3994(12), Na–O1 2.4401(18). Coordination angles (°): O3–Na–O2 77.10(3), O3–Na–O1 83.36(6), O2–Na–O1 79.76(5). Symmetry code: (i) 0.5 + *x*, *y*, 0.5 – *z*.

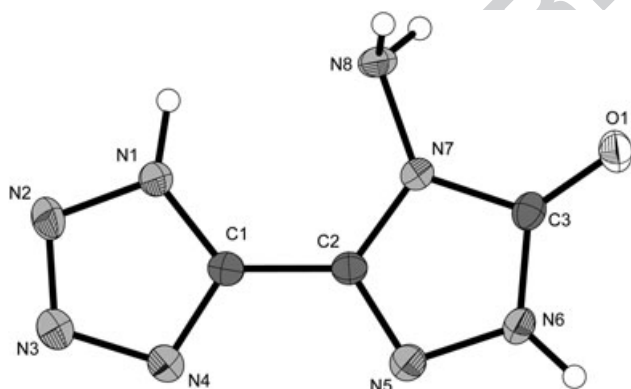


Figure 5. Molecular unit of 5-(4-amino-1,2,4-triazol-3-on-5'-yl)-1H-tetrazole (**5**). Ellipsoids of nonhydrogen atoms are drawn at the 50% probability level.

and the hydroxylammonium salts, additionally, the signals of the cationic protons are observed at 7.23 ppm (**2**) and 7.25 ppm (**3**).

The carbon NMR spectra show three signals according to the three carbon atoms of the triazole-tetrazole heterocycle, the chemical shifts of which are almost similar in all ionic compounds but differ significantly for the free acid. One signal at lowest field (**2–4**: 154.1–154.2 ppm) is least

affected by deprotonation (**5**: 154.6 ppm) and is therefore assigned to the carbonyl C-atom of the triazole ring. The two remaining signals at 151.6–151.8 ppm and 141.3–141.5 ppm (**2–4**) are assigned to the tetrazole carbon atom (lower field) and the triazole carbon atom C5 (higher field) for two reasons: The electron deficient tetrazole ring causes the higher downfield shift of the carbon atom signal as compared with the electron richer amino-substituted triazole ring. The second reason for the assignment is the comparison to the carbon NMR spectrum of the starting material **1**, which also shows the tetrazole ring carbon atom at lower field (150.7 ppm) and the carboxamide oxime carbon atom signal (145.1 ppm) at slightly higher field [8]. Also, the two mentioned signals of the tetrazol-triazolone anion are subjected to larger shifts upon deprotonation of the heterocycle as evidenced by the signals found for the free acid **5** (146.5 and 136.9 ppm).

Sensitivities and thermal stability. The impact and friction sensitivities of the ionic compounds **2–4** as well as of the free acid **5** were determined on a BAM (Bundesanstalt für Materialforschung) drop hammer and a BAM friction tester, respectively. The sensitivity towards electrostatic discharge was determined using a small-scale electrostatic-sensitive device. For references, see Experimental part.

The impact sensitivities of the ionic compounds were determined to be 40 J (less sensitive), whereas the free acid has to be classified as sensitive (20 J), a trend that is often observed for sensitivities of neutral and deprotonated tetrazole derivatives [11]. The friction sensitivities of all investigated materials **2–5** were determined to be 360 N, which means that they are equally less sensitive towards friction. Also, the sensitivities towards electrostatic discharge are in a range of static electricity (0.30–1.50 J); the human body is not capable to generate, which allows a safe handling. All sensitivity data (impact, friction, and electrostatic discharge) are gathered in Table 4.

F6 Figure 6 displays the differential scanning calorimetry (DSC) plots of **2–5** as well as of the dihydrate of **2** and its dehydration product in a temperature range of 60–400°C at a heating rate of 5°C min⁻¹. The given decomposition temperatures are absolute onset temperatures. Uncommonly observed is a comparatively high decomposition temperature of the free acid **5** ($T_{\text{dec}} = 268^\circ\text{C}$) compared with the deprotonated species. It decomposes right after melting, indicated by a small endothermic peak starting at 260°C. The endothermic peaks in the plots of **4** and the dihydrate of **2** are due to the loss of crystal water at 140–150°C. After dehydration, the sodium salt **4** still withstands temperatures of 330°C. The

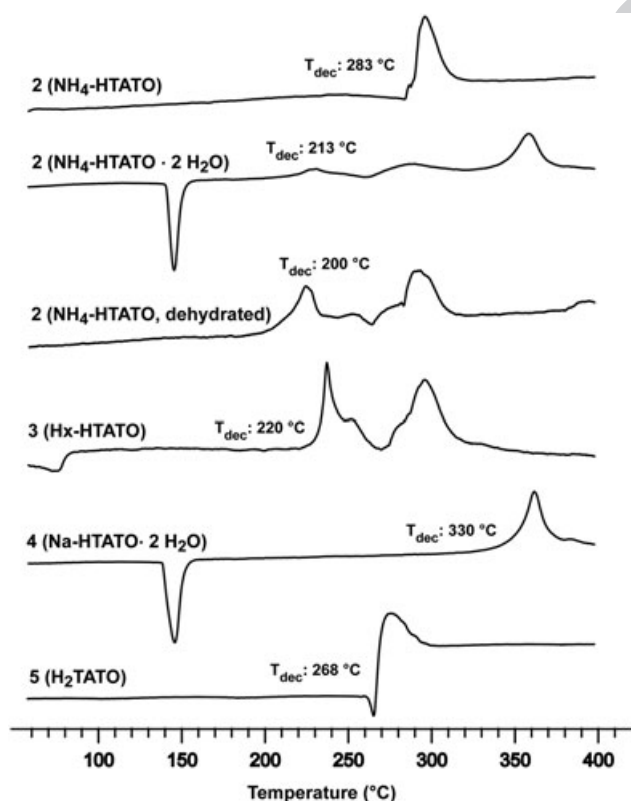


Figure 6. DSC plots of **2–5** as well as of the dihydrate of **2** and its dehydration product in a temperature range of 60–400°C. Exothermic events in the upper direction. HTATO = monodeprotonated 5-(4-amino-1,2,4-triazol-3-on-5'-yl)-1H-tetrazole.

hydroxylammonium salt **3** ($T_{\text{dec}} = 220^\circ\text{C}$) is less thermally stable than the corresponding crystal water-free ammonium salt **2** ($T_{\text{dec}} = 283^\circ\text{C}$), which is also observed for ionic species containing these cations in combination with other anions [4]. Also, noteworthy is the comparison between the ammonium salt **2**, which crystallizes crystal water free as well as containing two moles of crystal water depending on the recrystallization conditions. The compound, which crystallizes water free itself, shows a much better thermal stability ($T_{\text{dec}} = 283^\circ\text{C}$) compared with the material, which was gained after dehydration of the dihydrate at 160°C for 24 h ($T_{\text{dec}} = 200^\circ\text{C}$). Its decomposition temperature is in about the same range, which is observed for the dihydrate, that has lost its crystal water during the DSC experiment ($T_{\text{dec}} = 213^\circ\text{C}$). The reason for the lower decomposition temperature of dehydrated compounds as compared with their originally crystal water-free analogs might be the formation of crystal defects in their structures after removal of the water molecules and thus a destabilization of the structure because of reduced hydrogen bonding.

Calculations. Heats of formation. The heats of formation of **2**, **3**, and **5** were computed by using the atomization method (eq 1) in combination with CBS-4M electronic enthalpies [12,13]. This method has been proved to be suitable for energetic nitrogen-rich compounds in many recent publications [14,15].

$$\Delta_f H^\circ_{(\text{g}, \text{M}, 298)} = H_{(\text{Molecule}, 298)} - \sum H^\circ_{(\text{Atoms}, 298)} + \sum \Delta_f H^\circ_{(\text{Atoms}, 298)} \quad (1)$$

For the ionic compounds, the gas-phase enthalpies of formation (Table 3) were converted into the solid state (standard conditions) enthalpy of formation $\Delta_f H_m^\circ$ (Table 4) by subtraction of lattice enthalpies. The lattice energies (U_L) and lattice enthalpies (ΔH_L) were calculated from the corresponding molecular volumes (from XRD) according to Jenkin's equations for 1:1 salts [16]. For neutral **5**, the sublimation enthalpy was calculated by the Trouton's rule [17].

Lastly, the molar standard enthalpies of formation ($\Delta_f H_m$) were used to calculate the solid state energies of formation (ΔU) per kilo according to eq 2.

$$\Delta_f U = (\Delta_f H_m - \Delta n RT) \cdot 1000 / M \quad (2)$$

(Δn being the change of moles of gaseous components).

Generally, the heat of formation ($\Delta_f H_m$) in nitrogen-rich compounds increases with the number of N–N/N–O single and N=N double bonds. 5-(4-Amino-1,2,4-triazol-3-on-5'-yl)-1H-tetrazole (**5**) is an endothermically formed compound with a heat of formation at 314 kJ mol⁻¹. The hydroxylammonium salt has an even more positive heat of formation at 369 kJ mol⁻¹. Compound **2** shows the lowest heat of formation at 316 kJ mol⁻¹ because of a lower gas phase enthalpy of formation of the ammonium cation in comparison with the hydroxylammonium cation.

Table 3

CBS-4M calculation results, molecular volumes taken from X-ray solution, and calculated lattice enthalpy.

M	$-H^{298}/\text{a.u.}$	$\Delta_f H^\circ(\text{g}, \text{M})/\text{kJ mol}^{-1}$	V_{M}/nm^3	$\Delta H_{\text{L}}(2,3); \Delta H_{\text{sub}}(5)/\text{kJ mol}^{-1}$	Δn
5	629.061835	415.5		101.7	6.5
5 anion	628.560921	197.2			
NH ₄ ⁺	56.796608	635.8			
NH ₄ O ⁺	131.863249	687.2			
2		833.0	0.189	517.4	8.5
3		884.4	0.193	515.0	9

Table 4

Energetic properties and detonation parameters of **2**, **3**, and **5** in comparison with TNT, PETN, and RDX.

	2	3	5	2,4,6-TNT	PETN	RDX
Formula	C ₃ H ₇ N ₉ O	C ₃ H ₇ N ₉ O ₂	C ₃ H ₄ N ₈ O	C ₇ H ₅ N ₃ O ₆	C ₅ H ₈ N ₄ O ₁₂	C ₃ H ₆ N ₆ O ₆
MW (g mol ⁻¹)	185.15	201.15	168.12	227.13	316.1	222.12
IS (J) ^a	40	40	20	15	4	7.5
FS (N) ^b	360	360	—	353	80	120
ESD-test (J) ^c	1.50	0.50	—	0.8	0.1	0.2
N (%) ^d	68.09	62.67	66.65	18.50	17.72	37.84
Ω (%) ^e	−73.45	−59.65	−66.61	−73.96	−10.12	−21.61
T _{dec.} (°C) ^f	283	220	268	81 (mp), 290 (dec)	141	205 (mp), 210 (dec)
Density (g cm ⁻³) ^g	1.625 (173 K)	1.735 (173 K)	1.719 (173 K)	1.713 (100 K) [20]	1.845 (100 K) [21]	1.858 (90 K) [22]
$\Delta_f H_m^\circ/\text{kJ mol}^{-1}$ ^h	315.6	369.4	313.8	−55.5	−481.4	86.3
$\Delta_f U^\circ/\text{kJ kg}^{-1}$ ⁱ	1818.1	1947.0	1961.9	−168.0	−1428.4	489.0
EXPLO5.05 values						
− $\Delta_f U^\circ$ (kJ kg ⁻¹) ^j	3480	4522	3544	5258	6351	6190
T _E (K) ^k	2591	3144	2804	3663	4391	4232
p _{C-J} (kbar) ^l	218	285	230	235	353	380
D (m s ⁻¹) ^m	7702	8445	7726	7459	8561	8983
Gas vol. (L kg ⁻¹) ⁿ	769	782	712	569	681	734
I _{sp} (L kg ⁻¹) ^o	193	215	194	205	250	258

^aImpact sensitivity (BAM drop hammer, method 1 of 6).^bFriction sensitivity (BAM friction tester, method 1 of 6).^cElectrostatic discharge device (OZM).^dNitrogen content.^eOxygen balance.^fDecomposition temperature from DSC ($\beta=5^\circ\text{C}$).^gEstimated from X-ray diffraction.^hCalculated (CBS-4M) heat of formation.ⁱCalculated energy of formation.^jEnergy of explosion.^kExplosion temperature.^lDetonation pressure.^mDetonation velocity.ⁿAssuming only gaseous products.^oSpecific impulse (isobaric conditions, 60 bar chamber pressure).

Detonation and propulsion parameters. Several energetic parameters such as the detonation pressure, detonation velocity, and heat of explosion of **2**, **3**, and **5** were calculated with the EXPLO5.05 computer code [18]. The program is based on the input of the energy of formation (kJ kg⁻¹), density (g cm⁻³), and the sum formula. For all calculations, the maximum X-ray densities of the respective compounds at −173 K were used. In addition, the specific impulse of the pure compounds when used as monopropellants was calculated assuming rocket propellant conditions (isobaric combustion with a chamber

pressure of 60 bar). The calculations were performed using the maximum densities according to the crystal structures, and the results are gathered in Table 4. The detonation parameters and specific impulses were calculated using the latest version of the EXPLO5 code (V5.05). EXPLO5 is based on the steady-state model of equilibrium detonation and uses Becker–Kistiakowsky–Wilson's equation of state (BKW E.O.S) for gaseous detonation products and Cowan–Fickett E.O.S. for solid carbon. The calculation of the equilibrium composition of the detonation products is carried out by applying modified White, Johnson,

and Dantzig's free energy minimization technique. The program is designed to enable the calculation of detonation parameters at the Chapman–Jouguet point.

The comparison of **2**, **3**, and **5** (Table 4) affords that only the hydroxylammonium salt **3** could be of potential use for energetic applications. Because it reveals the highest density and the highest positive heat of formation among the investigated compounds, its detonation velocity can be compared with this of pentaerythritol tetranitrate (PETN) at the same time being less sensitive, whereas the detonation velocities of the ammonium salt **2** and the free acid **5** are in a range between those of 2,4,6-trinitrotoluene (TNT) and PETN. The calculated detonation pressures of all three species are comparatively low in a range between TNT and PETN (**3**) or even lower than that of PETN (**2**, **5**). The specific impulse of **2**, **3**, and **5** at isobaric conditions is comparatively low in comparison with other recently described compounds with a higher nitrogen and lower carbon content [22].

CONCLUSIONS

From this initial study, the following conclusions can be drawn:

- The reaction of tetrazole-5-carboxamide oxime (**1**) with DAU leads to a new heterocycle, namely the ammonium salt of 5-(4-amino-1,2,4-triazol-3-on-5'-yl)-1H-tetrazole (**2**).
- Starting from **2**, the hydroxylammonium (**3**) and the sodium salt (**4**) as well as the free acid (**5**) can be synthesized after reaction with hydroxylamine (**3**), sodium hydroxide (**4**), or sodium hydroxide followed by hydrochloric acid (**5**), respectively.
- All materials show a very good thermal stability with decomposition temperatures of 200°C and above. Except the free acid **5**, which proved to be somewhat impact sensitive (20 J); all compounds were classified as less sensitive towards both impact (40 J) and friction (360 N).
- In summary, it can be stated that the calculated detonation velocity of the hydroxylammonium salt **3** is comparable with that of PETN, a commonly used high explosive, whereas **2** and **5** show performances comparable with that of TNT.

EXPERIMENTAL

Caution! 5-(4-Amino-1,2,4-triazol-3-on-5'-yl)-1H-tetrazole and its nitrogen-rich ionic derivatives and starting materials are energetic materials with increased sensitivities towards shock and friction. Although we had no problems during syntheses and characterization, proper safety precautions (safety glass, face shield, earthed equipment and shoes, Kevlar gloves, and ear plugs) have to be applied while synthesizing and handling the described compounds.

All chemicals and solvents were used as received (Sigma-Aldrich, Fluka, Acros). ^1H and ^{13}C NMR spectra were recorded using a JEOL Eclipse 270, JEOL EX 400, or a JEOL Eclipse 400 instrument. The chemical shifts quoted in ppm in the text refer to typical standards such as tetramethylsilane (^1H , ^{13}C). To determine the melting and decomposition temperatures of the described compounds, a Linseis PT 10 DSC (heating rate 5°C min^{-1}) was used. Infrared spectra were measured using a Perkin Elmer Spectrum One FTIR spectrometer as KBr pellets. Raman spectra were recorded on a Bruker MultiRAM Raman Sample Compartment D418 equipped with a Nd-YAG-Laser (1064 nm) and an LN-Ge diode as detector. Mass spectra of the described compounds were measured at a JEOL MStation JMS 700 using either FAB, DEI, or DCI technique. To measure elemental analyses, a Netsch STA 429 simultaneous thermal analyzer was used.

The crystal structures of compounds **2–5** were determined by low temperature X-ray diffraction on an Oxford Xcalibur3 diffractometer with a Spellman generator (voltage 50 kV, current 40 mA) and a KappaCCD detector. The data collection and reduction was carried out using the CRYSTALISPRO software [23]. The structures were solved either with SHELXS-97 [24] or SIR-92 [25], refined with SHELXL-97 [26], and finally checked using the PLATON [27] software integrated in the WINGX [28] software suite. The absorptions were corrected with a Scale3 Abspack multi-scan method. Selected data and parameters of the X-ray determinations are given in Tables 1 and 2. Further crystallographic data for the structures have been deposited with the Cambridge Crystallographic Data Centre [29].

All quantum chemical calculations were carried out using the Gaussian G09 program package [30]. The detonation parameters were calculated using the program EXPLO5 V5.05. The program is based on the steady-state model of equilibrium detonation and uses Becker–Kistiakowsky–Wilson's equation of state (BKW E.O.S) for gaseous detonation products and Cowan–Fickett E.O.S. for solid carbon. The calculation of the equilibrium composition of the detonation products is carried out by applying modified White, Johnson, and Dantzig's free energy minimization technique. The program is designed to enable the calculation of detonation parameters at the CJ point.

The impact sensitivity tests were carried out according to STANAG 4489 [31] modified instruction [32] using a BAM drop hammer [33]. The friction sensitivity tests were carried out according to STANAG 4487 [34] modified instruction [35] using the BAM friction tester. The classification of the tested compounds results from the "UN Recommendations on the Transport of Dangerous Goods" [36]. Compounds **2–5** were also tested upon the sensitivity towards electrical discharge using the Electric Spark Tester ESD 2010 EN [37].

Differential scanning calorimetry measurements to determine the melt and decomposition temperatures of **2–5** (about 1.5 mg of each energetic material) were performed in covered Al containers with a hole (0.1 mm) in the lid for gas release and a nitrogen flow of 20 mL min^{-1} on a Linseis PT 10 DSC [38] calibrated by standard pure indium and zinc at a heating rate of 5°C min^{-1} . The decomposition temperatures are given as absolute onset temperatures.

Tetrazole-5-carboxamide oxime monohydrate (1) To a solution of 5-cyanotetrazole [8] (1.66 g, 17.5 mmol) in H_2O (30 mL) was added hydroxylamine (1.07 mL of a 50% w/v solution in H_2O , 1.15 g, 17.5 mmol) at room temperature. Crystallization started immediately after addition and yielded **1** (1.89 g, 12.9 mmol, 74%) as colorless precipitate.

Alternatively, a solution of sodium 5-cyanotetrazolate [8] (11.5 g; 80.0 mmol) in water (30 mL) was treated with an aqueous solution of hydroxylammonium chloride (20 mL, 5.91 g; 85.0 mmol). The solution was heated to reflux for 10 min, until precipitation of **1** started. The crude product was filtered off and recrystallized from hot water. The filtrate was left to stand for a few more days to improve the yield. Compound **1** (7.01 g; 48.0 mmol; 60%) was isolated as a colorless solid.

IR (KBr, cm^{-1}): ν = 3315 (vs), 3128 (vs), 3002 (vs), 2849 (vs), 2745 (vs), 2649 (s), 2250 (w), 2211 (w), 2141 (w), 2117 (w), 1814 (w), 1801 (w), 1712 (vs), 1650 (s), 1559 (m), 1500 (w), 1462 (m), 1394 (s), 1386 (s), 1306 (m), 1199 (w), 1173 (w), 1159 (w), 1133 (w), 1121 (w), 1092 (w), 1062 (w), 1047 (w), 1024 (w), 977 (w), 774 (s), 736 (s), 723 (s), 668 (m), 660 (m), 638 (s), 599 (m), 525 (w), 501 (m) cm^{-1} ; Raman (1064 nm, 300 mW, 25°C): ν = 3116 (9), 1648 (9), 1578 (58), 1452 (18), 1400 (6), 1315 (13), 1199 (41), 1161 (30), 1125 (100), 1085 (84), 1062 (59), 1038 (41), 770 (17), 631 (8), 422 (47), 353 (12), 326 (9), 192 (10), 157 (28) cm^{-1} ; ^1H NMR (DMSO- d_6 , 25°C, ppm): δ = 10.51 (br. s, 1H; NH), 7.09 (s, 2H; C-NH₂) ppm; ^{13}C NMR (DMSO- d_6 , 25°C, ppm): δ = 150.7 (CN₄), 144.9 (C(NH₂)NOH) ppm; MS (FAB⁺): m/z = 128.0 [C₂H₄N₆O⁺]; EA (C₂H₆N₆O₂, 146.11): Calcd: C 16.44, H 4.14, N 57.52; found: C 17.10, H 3.76, N 57.83%.

Ammonium 5-(4-amino-1,2,4-triazol-3-on-5'-yl)-1H-tetrazolate (2). Tetrazole-5-carboxamide-oxime monohydrate [8] (1.46 g; 10.0 mmol) was suspended in hot water, and DAU [39] (0.901 g; 10.0 mmol) was added. Hydrochloric acid (37%; 0.15 mL; 4.88 mmol) was added and the suspension was refluxed for 15 min during which the reaction mixture turned from a colorless suspension to a clear and red solution. The solution was filtered, left for crystallization, and **2** (1.23 g; 6.65 mmol; 67%) was isolated as light yellow crystals.

DSC (T_{onset} , 5°C, min⁻¹): 283°C (dec.); IR (KBr, cm^{-1}): ν = 3395 (s), 3310 (s), 3204 (s), 3022 (s), 2850 (s), 2794 (s), 1743 (m), 1693 (s), 1634 (s), 1595 (m), 1527 (w), 1445 (m), 1407 (s), 1384 (m), 1365 (m), 1276 (vw), 1232 (w), 1193 (m), 1154 (w), 1107 (vw), 1058 (vw), 1041 (w), 1019 (w), 954 (m), 807 (m), 714 (s); Raman (1064 nm, 300 mW, 25°C, cm^{-1}): ν = 3206 (4), 3017 (4), 2794 (4), 1628 (19), 1597 (100), 1522 (7), 1476 (3), 1461 (3), 1350 (3), 1283 (4), 1236 (12), 1193 (21), 1156 (4), 1107 (24), 1041 (4), 965 (2), 811 (15), 761 (6), 716 (11), 677 (2), 625 (3), 422 (6), 404 (4), 381 (4), 338 (4), 295 (3), 233 (4), 203 (4), 166 (5), 103 (40), 75 (24); ^1H NMR (DMSO- d_6 , 25°C, ppm): δ = 11.7 (s, NH, 1H), 7.2 (s, br, NH₄⁺, 4H), 5.6 (s, br, NH₂, 2H); ^{13}C NMR (DMSO- d_6 , 25°C, ppm): δ = 154.1 (C=O), 151.7 (N₄C-CN₃HNNH₂O), 141.5 (N₄C-CN₃HNNH₂O); MS (FAB⁺): m/z = 167.1 [C₃H₃N₈O⁺]; EA (C₃H₇N₉O, 185.15) Calcd: N 68.09, C 19.46, H 3.81; found: N 67.31, C 19.87, H 3.62%; impact sensitivity: 40 J; friction sensitivity: >360 N; ESD: 1.5 J (at grain size 100–500 μm).

Hydroxylammonium 5-(4-amino-1,2,4-triazol-3-on-5'-yl)-1H-tetrazolate (3). Ammonium salt **2** (0.377 g; 2.03 mmol) was dissolved in hot water, and an aqueous solution of hydroxylamine (50% w/v, 0.134 g; 4.06 mmol) was added. The solution was heated to reflux for 5 min and allowed to slowly cool down. The precipitated crude material was recrystallized from EtOH/H₂O, and **3** (0.213 g; 1.16 mmol; 57%) was isolated as colorless crystals.

DSC (T_{onset} , 5°C, min⁻¹): 220°C (dec.); IR (KBr, cm^{-1}): ν = 3415 (vs), 2802 (m), 1746 (m), 1704 (m), 1639 (m), 1521 (w), 1384 (vs), 1274 (w), 1233 (w), 1192 (w), 1103 (w), 1044

(w), 965 (w), 906 (vw), 807 (m), 712 (m); Raman (1064 nm, 300 mW, 25°C, cm^{-1}): ν = 3205 (2), 1642 (5), 1597 (101), 1526 (5), 1460 (2), 1370 (4), 1233 (10), 1194 (22), 1150 (4), 1112 (18), 1038 (3), 810 (12), 760 (5), 714 (9), 671 (2), 624 (3), 410 (6), 380 (3), 291 (3), 105 (26); ^1H NMR (DMSO- d_6 , 25°C, ppm): δ = 11.7 (s, br, NH, 1H); ^{13}C NMR (DMSO- d_6 , 25°C, ppm): δ = 154.2 (C=O), 151.6 (N₄C-CN₃HNNH₂O), 141.3 (N₄C-CN₃HNNH₂O); EA (C₃H₇N₆O₂, 201.15) Calcd: N 62.67, C 17.91, H 3.51; found: N 62.44, C 18.19, H 3.46%; impact sensitivity: 40 J; friction sensitivity: 360 N; ESD: 0.3 J (at grain size 100–500 μm).

Sodium 5-(4-amino-1,2,4-triazol-3-on-5'-yl)-1H-tetrazolate dihydrate (4). The ammonium salt **2** (1.85 g, 10.0 mmol) was dissolved in 20 mL of water, and sodium hydroxide solution (7 mL, 2 mol/L) was added. The mixture was refluxed for 10 min to expel ammonia, and the resulting aqueous solution was left for crystallization for a day. Compound **4** crystallizes in colorless blocks in 71% yield (1.61 g, 7.12 mmol).

DSC (T_{onset} , 5°C, min⁻¹): 330°C (dec.); IR (KBr, cm^{-1}): ν = 3420 (s), 3065 (w), 3021 (w), 2950 (w), 2857 (w), 2795 (w), 2373 (w), 2285 (w), 1743 (m), 1704 (m), 1621 (m), 1596 (m), 1459 (w), 1368 (w), 1275 (vw), 1231 (w), 1196 (w), 1152 (vw), 1116 (w), 1102 (w), 1070 (vw), 1042 (vw), 984 (w), 943 (w), 908 (w), 810 (m), 709 (m), 653 (m); Raman (1064 nm, 300 mW, 25°C, cm^{-1}): ν = 3205 (2), 1642 (5), 1597 (100), 1525 (5), 1460 (2), 1370 (4), 1194 (22), 1151 (4), 1112 (18), 1038 (3), 810 (12), 760 (5), 714 (9), 671 (2), 624 (3), 410 (6), 380 (3), 291 (3); ^1H NMR (DMSO- d_6 , 25°C, ppm): δ = 11.6 (s, NH, 1H), 5.6 (s, NH₂, 2H); ^{13}C NMR (DMSO- d_6 , 25°C, ppm): δ = 154.1 (C=O), 151.9 (N₄C-CN₃HNNH₂O), 141.6 (N₄C-CN₃HNNH₂O); EA (C₃H₇N₈NaO₃, 226.13) Calcd: N 49.55, C 15.93, H 3.12; found: N 49.54, C 16.49, H 3.04%; impact sensitivity: 40 J; friction sensitivity: 360 N; ESD: 0.3 J (at grain size 500–1000 μm).

5-(4-Amino-1,2,4-triazol-3-on-5'-yl)-1H-tetrazole (5). Compound **4** (94 mg, 0.46 mmol) is dissolved in 7 mL of hot water, and HCl (5 mL, 2 mol/L) is added. The free acid **5** crystallizes from the solution in colorless blocks (437 mg, 0.26 mmol, 57%).

DSC (T_{onset} , 5°C, min⁻¹): 268°C (dec.); IR (KBr, cm^{-1}): ν = 3353 (s), 3262 (s), 3080 (s), 2950 (s), 2818 (m), 2752 (m), 1715 (vs), 1686 (vs), 1633 (s), 1602 (m), 1543 (m), 1458 (w), 1412 (m), 1395 (m), 1347 (m), 1318 (m), 1277 (w), 1233 (m), 1225 (m), 1095 (m), 1082 (m), 1049 (s), 998 (m), 989 (m), 914 (m), 874 (m), 816 (m), 787 (m), 746 (w), 732 (m), 709 (m), 670 (m), 622 (m); Raman (1064 nm, 300 mW, 25°C, cm^{-1}): ν = 3266 (2), 1731 (2), 1633 (100), 1609 (63), 1424 (9), 1393 (19), 1318 (3), 1234 (25), 1226 (36), 1115 (27), 1075 (5), 987 (6), 812 (14), 747 (4), 711 (7), 620 (3), 397 (7), 386 (7), 371 (9), 310 (3), 289 (5), 227 (2); ^1H NMR (DMSO- d_6 , 25°C, ppm): δ = 12.42 (s, NH, 1H), 6.87 (s, NH₂, 2H); ^{13}C NMR (DMSO- d_6 , 25°C, ppm): δ = 154.6 (C=O), 146.5 (N₄C-CN₃HNNH₂O), 136.9 (N₄C-CN₃HNNH₂O); MS (DEI⁺): m/z = 168.2 [C₃H₄N₈O⁺]; EA (C₃H₄N₈O, 168.12) Calcd: N 66.65, C 21.43, H 2.40; found: N 66.27, C 21.79, H 2.38%; impact sensitivity: 20 J; friction sensitivity: 360 N; ESD: 0.80 J (at grain size 500–1000 μm).

Acknowledgments. Financial support of this work by the Ludwig-Maximilian University of Munich (LMU), the US Army Research Laboratory (ARL) under grant no. W911NF-09-2-0018, the Armament Research, Development and Engineering Center (ARDEC) under grant no. R&D 1558-TA-01, and the Office of Naval Research (ONR) under grant nos. ONR.N00014-10-1-0535

and ONR.N00014-12-1-0538 is gratefully acknowledged. The authors acknowledge collaboration with Dr. Muhamed Sućeska (Brodarski Institute, Croatia) in the development of new computational codes to predict the detonation and propulsion parameters of novel explosives. We are indebted to and thank Drs. Betsy M. Rice and Brad Forch (ARL, Aberdeen, Proving Ground, MD). Last but not least, the authors thank Mr. St. Huber for sensitivity measurements.

REFERENCES AND NOTES

- [1] Huynh, M. H. V.; Hiskey, M. A.; Meyer, T. J.; Wetzler, M. *Proc Natl Acad Sci USA* 2006, 103, 5409.
- [2] Gao, H.; Shreeve, J. M. *Chem Rev* 2011, 111, 7377.
- [3] Hachiya, S.; Sato, M. *Jpn Kokai Tokkyo, JP* 2006096860A 20060413, 2006.
- [4] Chavez, D. E.; Hiskey, M. A.; Naud, D. L. *J Pyrotech* 1999, 10, 17.
- [5] Singh, H.; Chawla, A. S.; Kapoor, V. K.; Paul D.; Malhotra R. K. *Progress in Medicinal Chemistry*; Ellis, G. P.; West, G. P. Ed.; Biomedical Press: 1980; Vol. 17, p. 631.
- [6] Butler R. N.; *Adv Heterocycl Chem* 1977, 21, 323.
- [7] (a) Huisgen, R. *Angew Chem Int Ed Engl* 1963, 2, 565; (b) Huisgen, R. *Angew Chem Int Ed Engl* 1963, 2, 633.
- [8] Fischer, N.; Klapötke, T. M.; Rappenglück, S.; Stierstorfer, J. *ChemPlusChem* 2012, DOI: 10.1002/cplu.200.
- [9] Koenig, K.; Mueller, K. H.; Rohe, L. *Eur Pat Appl* 1990, EP403889 A1 19901227.
- [10] Klapötke, T. M.; Stein, M.; Stierstorfer, J. *Z. Anorg Allg Chem* 2008, 634, 1711.
- [11] Fendt, T.; Fischer, N.; Klapötke, T. M.; Stierstorfer, J. *Inorg Chem* 2011, 50(4), 1447.
- [12] Byrd, E. F. C.; Rice, B. M. *J Phys Chem A* 2006, 110(3), 1005.
- [13] Rice, B. M.; Pai, S. V.; Hare, J. *Comb Flame* 1999, 118(3), 445.
- [14] Pan, Y.; Li, J.; Cheng, B.; Zhu, W.; Xiao, H. *Comput Theor Chem* 2012, 992, 110.
- [15] Thottempudi, V.; Forohor, F.; Parrish, D. A.; Shreeve, J. M. *Angew Chem.* 2012, 51(39), 9881.
- [16] (a) Jenkins, H. D. B.; Roobottom, H. K.; Passmore, J.; Glasser, L. *Inorg Chem* 1999, 38, 3609; (b) Jenkins, H. D. B.; Tudela, D.; Glasser, L. *Inorg Chem* 2002, 41, 2364.
- [17] (a) Westwell, M. S.; Searle, M. S.; Wales, D. J.; Williams, D. H. *J Am Chem Soc* 1995, 117, 5013; (b) Trouton, F. *Philos Mag* 1884, 18, 54.
- [18] (a) Sućeska, M. *EXPLO5.5* program, Zagreb, Croatia, 2011; (b) Sućeska, M. *Propellants Explos Pyrotech* 1999, 24, 280.
- [19] Vrcelj, R. M.; Sherwood, J. N.; Kennedy, A. R.; Gallagher, H. G.; Gelbrich, T. *Cryst Growth Des* 2003, 3, 1027.
- [20] Zhurova, E. A.; Stash, A. I.; Tsirelson, V. G.; Zhurov, V. V.; Bartashevich, E. V.; Potemkin, V. A.; Pinkerton, A. A. *J Am Chem Soc* 2006, 128(45), 14728.
- [21] Hakey, P.; Ouellette, W.; Zubieta, J.; Korter, T. *Acta Crystallogr* 2008, E64(8), o1428.
- [22] Fischer, N.; Izsak, D.; Klapötke, T. M.; Rappenglück, S.; Stierstorfer, J. *Chem Eur J* 2012, 18(13), 4051.
- [23] CrysAlisPro, Agilent Technologies, Version 1.171.35.11, 2011.
- [24] Sheldrick, G. M. *SHELXS-97*, Program for Crystal Structure Solution, Universität Göttingen, 1997.
- [25] Altomare, A.; Casciarano, G.; Giacovazzo, C.; Guagliardi, A. *Appl Cryst* 1993, 26, 343.
- [26] Sheldrick, G. M. *SHELXL-97*, Program for the Refinement of Crystal Structures, University of Göttingen, Germany, 1994.
- [27] Spek, A. L. *Platon*, A Multipurpose Crystallographic Tool, Utrecht University, Utrecht, The Netherlands, 1999.
- [28] Farrugia, L. J. *Appl Cryst* 1999, 32, 837.
- [29] Crystallographic data for the structures have been deposited with the Cambridge Crystallographic Data Centre. Copies of the data can be obtained free of charge on application to The Director, CCDC, 12 Union Road, Cambridge CB2 1EZ, UK (Fax: int.code_(1223)336-033; e-mail for inquiry: fileserv@ccdc.cam.ac.uk; e-mail for deposition: deposit@ccdc.cam.ac.uk).
- [30] Frisch, M. J.; Trucks, G. W.; Schlegel, H. B.; Scuseria, G. E.; Robb, M. A.; Cheeseman, J. R.; Scalmani, G.; Barone, V.; Mennucci, B.; Petersson, G. A.; Nakatsuji, H.; Caricato, M.; Li, X.; Hratchian, H. P.; Izmaylov, A. F.; Bloino, J.; Zheng, G.; Sonnenberg, J. L.; Hada, M.; Ehara, M.; Toyota, K.; Fukuda, R.; Hasegawa, J.; Ishida, M.; Nakajima, T.; Honda, Y.; Kitao, O.; Nakai, H.; Vreven, T.; Montgomery, Jr. J. A.; Peralta, J. E.; Ogliaro, F.; Bearpark, M.; Heyd, J. J.; Brothers, E.; Kudin, K. N.; Staroverov, V. N.; Kobayashi, R.; Normand, J.; Raghavachari, K.; Rendell, A.; Burant, J. C.; Iyengar, S. S.; Tomasi, J.; Cossi, M.; Rega, N.; Millam, J. M.; Klene, M.; Knox, J. E.; Cross, J. B.; Bakken, V.; Adamo, C.; Jaramillo, J.; Gomperts, R.; Stratmann, R. E.; Yazyev, O.; Austin, A. J.; Cammi, R.; Pomelli, C.; Ochterski, J. W.; Martin, R. L.; Morokuma, K.; Zakrzewski, V. G.; Voth, G. A.; Salvador, P.; Dannenberg, J. J.; Dapprich, S.; Daniels, A. D.; Farkas, Ö.; Foresman, J. B.; Ortiz, J. V.; Cioslowski, J.; Fox, D. J. *Gaussian 09*, Revision A.1, Gaussian, Inc., Wallingford CT, 2009.
- [31] NATO standardization agreement (STANAG) on explosives, impact sensitivity tests, no. 4489, 1st ed., Sept. 17, 1999.
- [32] WIWEB-Standardarbeitsanweisung 4-5.1.02, Ermittlung der Explosionsgefährlichkeit, hier der Schlagempfindlichkeit mit dem Fallhammer, Nov. 8, 2002.
- [33] <http://www.bam.de>
- [34] NATO standardization agreement (STANAG) on explosive, friction sensitivity tests, no. 4487, 1st ed., Aug. 22, 2002.
- [35] WIWEB-Standardarbeitsanweisung 4-5.1.03, Ermittlung der Explosionsgefährlichkeit oder der Reibeempfindlichkeit mit dem Reibeapparat, Nov. 8, 2002.
- [36] Impact: Insensitive >40 J, less sensitive ≥35 J, sensitive ≥4 J, very sensitive ≤3 J; friction: Insensitive >360 N, less sensitive = 360 N, sensitive <360 N a. >80 N, very sensitive ≤80 N, extreme sensitive ≤10 N; According to the UN Recommendations on the Transport of Dangerous Goods (+) indicates: not safe for transport.
- [37] <http://www.ozm.cz>
- [38] <http://www.linseis.com>
- [39] Li, Z. *et al.*, *Synth Commun.* 2006, 36, 2613.

Nitrogen-Rich Salts of 5,5'-Bis(1-hydroxytetrazole) – Energetic Materials Combining Low Sensitivities with High Thermal Stability


Niko Fischer,^[a] Thomas M. Klapötke,^{*[a]} Marius Reymann^[a] and Jörg Stierstorfer^[a]

Keywords: Energetic Materials / Tetrazoles / N-oxide / Crystal Structure / Sensitivities

5,5'-Bis(1-hydroxytetrazole) was synthesized starting from glyoxal, which is converted to glyoxime after the reaction with hydroxylamine. Chlorination of glyoxime with Cl₂ gas in ethanol and following chloro-azido exchange yields diazidoglyoxime, which is cyclized under acidic conditions (HCl gas in diethyl ether) to give 5,5'-bis(1-hydroxytetrazole) dihydrate (**1**). A large variety of nitrogen rich salts of **1** such as the diammonium (**2**), the dihydrazinium (**3**), the bis-guanidinium (**4**), the bis-aminoguanidinium (**5**), the diaminoguanidinium salt monohydrate (**6**), the triaminoguanidinium salt monohydrate (**7**), the 1-amino-3-nitroguanidinium salt dihydrate (**8**), the diaminouronium salt monohydrate (**9**), the bis-oxalyldihydrazidinium (**10**), the oxalyldihydrazidinium salt dihydrate (**11**), the 3,6-dihydrazino-1,2,4,5-tetrazinium (**12**), the 5-aminotetrazolium (**13**), the bis-1-methyl-5-aminotetrazolium salt (**14**), the bis-2-methyl-5-aminotetrazole adduct (**15**) and the 1,5-diaminotetrazolium salt (**16**) were synthesized via Bronsted acid base or metathesis reactions.

All compounds were fully characterized by vibrational spectroscopy (IR and Raman), multinuclear NMR spectroscopy, elemental analysis and DSC measurements. The crystal structures of **1–16** could be determined using single crystal X-ray diffraction. The heats of formation of **1–16** were calculated using the atomization method based on CBS-4M enthalpies. Regarding their potential use as RDX or HNS replacements, several detonation parameters such as the detonation pressure, detonation velocity, explosion energy and explosion temperature were computed using the EXPLO5 code based on the experimental (X-ray) densities and calculated heats of formation. In addition, the sensitivities towards impact, friction and electrical discharge were tested using the BAM drop hammer, a friction tester as well as a small scale electrical discharge device.

[a] Niko Fischer, Prof. Dr. Thomas M. Klapötke, * Marius Reymann, Dr. Jörg Stierstorfer
Department of Chemistry
Energetic Materials Research
Ludwig Maximilian University
Butenandtstr. 5–13 (D)
81377 München (Germany)
Fax: +49 89 2180 77492
E-Mail: tmk@cup.uni-muenchen.de

 Supporting information for this article is available on the WWW under <http://www.chemeurj.org/> or from the author.

Introduction

From an early 21st century point of view the practical design of new energetic materials has a long tradition in the materials chemists community. Reaching back at least to the end of the 19th century^[1], when the energetic character of nitrogen-rich materials was first recognized, the development of energetic materials in the 20th century was mainly determined by efforts in synthesizing cyclic and caged nitramines, as the most prominent examples thereof, RDX^[2], HMX^[3] and CL-20^[4], which cover a wide range of civil and military applications, show. Recent concerns about the environmental impact of energetic materials nowadays have caused a renaissance in the synthesis of so called green energetic materials^[5], which are based on a high nitrogen content releasing mainly environmentally benign N₂ after decomposition or degradation. While cyclic and caged nitramines decompose into a significant amount of toxic reaction products such as nitro- and nitrosoamines^[6] after degradation, the use of nitrogen-rich azoles such as

triazole- and tetrazole derivatives circumvents the drawbacks, which are related to the use of the above mentioned nitramines. Not only, that the high nitrogen content of triazoles and, especially, tetrazoles brings the environmental benefit of releasing mainly N₂ after decomposition, it also increases the heat of formation of the compound due to inherently energetic C–N and N–N bonds contained in the molecule. Along with a high heat of formation, also a high density, high thermal stability and low sensitivities towards impact, friction and electrical discharge of a new material are amongst the most desirable features, when it comes to the synthesis of new energetic compounds with improved detonation performance such as the detonation pressure and the detonation velocity, which both strongly depend on the characteristic values of ρ and $\Delta_f H^\circ$.^[7,8]

The authors recently reported on the synthesis and energetic characterization of a series of nitrogen-rich 5,5'-bistetrazolates.^[9] These molecules showed to have excellent thermal stabilities, while being comparatively insensitive, despite their very high nitrogen contents of up to 83%. A further improvement of the energetic character of tetrazole containing compounds was demonstrated by the introduction of N-oxides^[10,11,12], in that the density is increased by further possibilities to form hydrogen bonds in the solid state and also the oxygen content of the molecule is better balanced ensuring a maximum energy output, when the compound decomposes to low heat of formation products such as CO₂, H₂O and N₂.

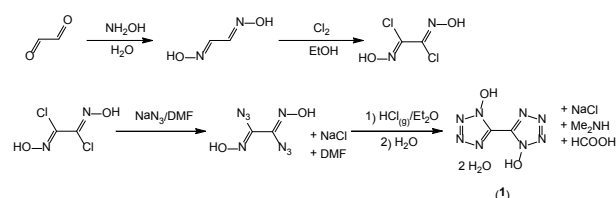
A very promising candidate, which fulfils a variety of the aforementioned desirable properties is 5,5'-bis(1-hydroxytetrazole). This dihydroxylated bistetrazole is strongly acidic bearing two protons, which can be easily abstracted by nitrogen-rich bases such

as ammonia, guanidine or even other tetrazole derivatives. We recently described the energetic properties of its dihydroxylammonium salt, which shows extremely promising for use as an explosive filler in the future.^[13] Scheme 2 gives an overview about the herein discussed 5,5'-bis(tetrazole-1-oxide)s, all of which were structurally characterized by low temperature single crystal X-ray diffraction.

Results and Discussion

Synthesis

The synthesis of the nitrogen rich salts **1–16** necessarily needs to start with the synthesis of the free acid 5,5'-bis(1-hydroxytetrazole) (**1**), which is depicted in scheme 1. Oxidation of 5,5'-bistetrazole using oxone or hypofluoric acid yield mixtures of the 1,1'-, 1,2'- and favored 2,2'-dihydroxy derivatives. Tselinskii et al.^[14] reported about the formation of this dihydroxylated heterocycle in 2001 upon cyclization of diazidoglyoxime, which itself is synthesized starting from commercially available glyoxal. Glyoxal is reacted with hydroxylamine to form glyoxime. Chlorination of glyoxime with Cl₂ gas in ethanol and following chloro-azido exchange with sodium azide in N,N-dimethylformamide affords the desired diazidoglyoxime. After isolation of the covalent diazide, it is slurried in diethyl ether and HCl gas is bubbled through the suspension. After the diethyl ether phase is saturated with HCl, the mixture further needs to be stirred overnight in a closed flask. The cyclized product can then be isolated after evaporation of the solvent and recrystallization from hot water. Although this route is very simple we recently investigated a one-pot synthesis route (from dichloroglyoxime to **1**) to avoid isolation of highly sensitive diazidoglyoxime.^[13]

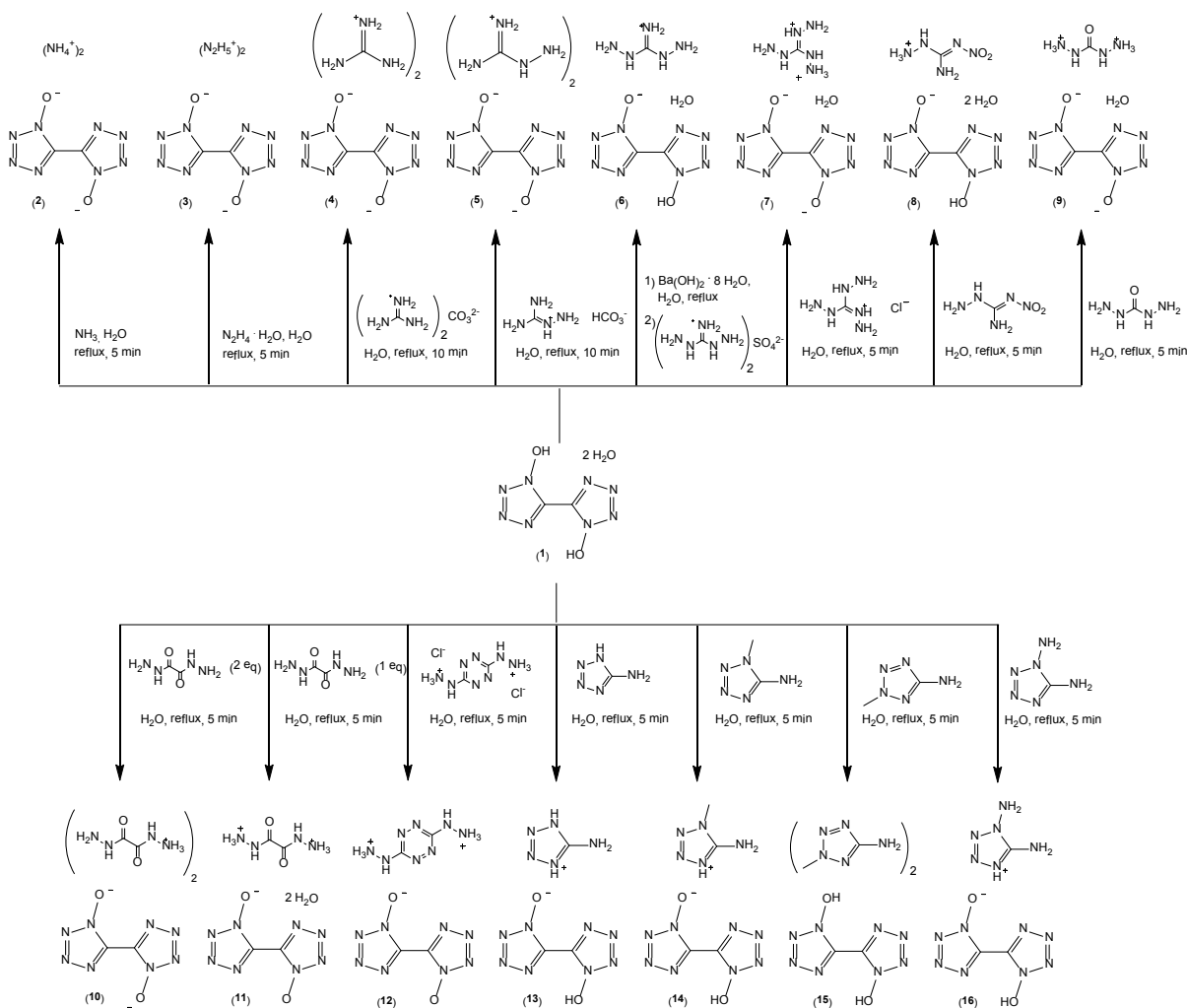


Scheme 1. Synthesis of 5,5'-bis(1-hydroxytetrazole) following the procedure to diazidoglyoxime described by Tselinskii et al..

Starting from 5,5'-bis(1-hydroxytetrazole) (**1**), all compounds except the diamino-, the triaminoguanidinium and the 3,6-dihydrazino-1,2,4,5-tetrazinium salt **6**, **7** and **12** were

synthesized after reacting **1** with the stoichiometric amounts of the respective free base or, in case of the guanidinium and the aminoguanidinium salt **4** and **5**, the respective carbonate (**4**) and bicarbonate (**5**). An overview is depicted in Scheme 2. The diaminoguanidinium salt **6** was isolated from a reaction mixture containing the barium salt of **1** and diaminoguanidinium sulfate after filtering off the poorly soluble barium sulfate. The triaminoguanidinium salt **7** crystallized from a mixture containing the free acid **1** and triaminoguanidinium chloride and also for the 3,6-dihydrazinium-1,2,4,5-tetrazine salt **12** the respective chloride salt was reacted with **1**. Regarding the stoichiometries used in the different reaction mixtures, we anticipated to isolate 2:1 compounds so that also 2:1 stoichiometries were used in the respective reactions except for **8**, where, due to its low water solubility, only one equivalent of 1-amino-3-nitroguanidine was used to avoid precipitation of the base, and except for **12**, since the tetrazine derivative was used as its dihydrochloride. However, what we observed was the crystallization of compounds having a 2:1 stoichiometry in the cases of **1-4**, **10** and **15** and, unexpectedly, a 1:1 stoichiometry in the cases of **5-8**, **11-14** and **16**, with even double protonated cations in the cases of **7**, **9**, **11** and **12**.

Aminoguanidinium chloride was synthesized from aminoguanidinium bicarbonate by acidification with HCl. The resulting aminoguanidinium chloride is reacted with two equivalents hydrazine hydrate in 1,4-dioxane under N₂ forming the triaminoguanidinium synthon. Diaminoguanidinium sulphate was obtained from commercially available diaminoguanidinium chloride after ion exchange.^[15] Diaminourea^[16] and oxalyldihydrazide^[17] were obtained from the reaction of hydrazine hydrate with dimethylcarbonate or diethylmalonate respectively. The first step in the synthesis of 3,6-dihydrazino-1,2,4,5-tetrazinium dichloride monohydrate is the reaction of triaminoguanidinium chloride with pentane-2,4-dione to form 3,6-bis((3,5-dimethyl)pyrazol-1-yl)-1,2-dihydro-1,2,4,5-tetrazine,^[18,19] which is subjected to a hydrazinolysis reaction to form 3,6-dihydrazino-1,2,4,5-tetrazine. Further reaction with hydrochloric acid in methanol yields the dichloride. The methylated 5-aminotetrazoles 1-methyl- and 2-methyl-5-aminotetrazole were obtained by methylation of commercially available 5-aminotetrazole.^[20] 1,5-Diaminotetrazole was prepared by the reaction of thiosemicarbazide and sodium azide in the presence of lead(II)oxide and ammonium chloride^[21] and 1-amino-3-nitroguanidine was gained from a hydrazinolysis reaction of nitroguanidine.^[22,23]



Scheme 2. Synthesis of the nitrogen-rich salts 2–16.

The solubility of 5,5'-bis(1-hydroxytetrazole) **1** and its nitrogen-rich salts 2–16 is only moderate in water, so that crystals of **1**–**16** suitable for X-ray single crystal measurements were obtained after filtration and slow evaporation of the aqueous mother liquors. Efforts to crystallize **1** without crystal water resulted in the formation of a methanol adduct^[13] when being recrystallized from dry methanol or the dihydrate **1** when being recrystallized from glacial acetic acid or acetonitrile, respectively.

Crystal Structures

Suitable single crystals of the described compounds (**1**–**16**) were picked from the crystallization mixture and mounted in Kel-F oil, transferred to the N_2 stream of an Oxford Xcalibur3 diffractometer with a Spellman generator (voltage 50 kV, current 40 mA) and a KappaCCD detector using a $\lambda_{\text{MoK}\alpha}$ radiation wavelength of 0.71073 Å. All structures were measured at -100°C . The data collection and data reduction was carried out with the CRYSLISPRO software^[24]. The structures were solved with SIR-92^[25], SIR-97^[26] or SHELXS-97^[27], refined with SHELXL-97^[28] and finally checked using the PLATON software^[29] integrated in the WINGX software suite.^[30] The non-hydrogen atoms were refined anisotropically and the hydrogen atoms were located and freely refined. The absorptions were corrected by a SCALE3 ABSPACK multi-scan method.^[31] Data and parameters of the measurements and refinements are gathered in

Tables S1, S2 and S3 in the Supplementary Information. Exact bond lengths, angles and selected hydrogen bonds are also given in the Supplementary Information in Table S3–S12. Cif files have been deposited within the Cambridge Crystallographic Data Centre using the CCDC Nos. 884561 (**1**), 895972 (**2**), 895963 (**3**), 895965 (**4**), 895973 (**5**), 895969 (**6**), 895970 (**7**), 895977 (**8**), 895964 (**9**), 895967 (**10**), 895975 (**11**), 895974 (**12**), 895966 (**13**), 895976 (**14**), 895971 (**15**), and 895968 (**16**).

5,5'-Bis(1-hydroxytetrazole) (**1**) crystallizes as a dihydrate in the monoclinic space group $C2/m$ with two molecular units per unit cell and a density of 1.811 g cm^{-3} . The two planar tetrazole rings are not distorted as it is also observed in all ionic structures. The N–N and C–N bond lengths of the tetrazole rings vary between the lengths typically observed for N–N single and N=N double bonds as well as C–N single and C=N double bonds. Also the C–C bond connecting the two tetrazole moieties as well as the N–O bonds are between a C–C single and a C=C double bond ($d(\text{C1}–\text{C1}') = 1.454(2)\text{ Å}$) and a N–O single and N=O double bond ($d(\text{N1}–\text{O1}) = 1.340(3)\text{ Å}$), respectively. The acidic proton is involved in hydrogen bonding to the oxygen atom of the water molecule, which stabilizes the structure and makes it difficult to crystallize the material solvent free (which was not possible despite all efforts). Upon deprotonation, the N–O bond length is slightly shortened, whereas the C–N and N–

N bond lengths of the tetrazole rings are subject to only marginal variations.

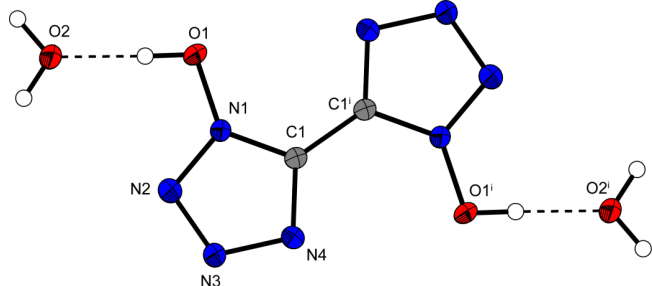


Figure 1 Representation of the molecular unit with the labeling scheme of **1** as its dihydrate. Ellipsoids are shown at the 50 % probability level. Symmetry code: (i) $1-x, y, -z$.

The crystal structure of diammonium 5,5'-bis(tetrazole-1-oxide) (**2**) is highly disordered and crystallizes in the orthorhombic face-centered space group $I222$ with four molecules in the unit cell and a density of 1.800 g cm^{-3} . The strongest H-bonds are located between $\text{O1}\cdots\text{H5A}/\text{O1}^i\cdots\text{H5A}^i$ ($1.956(29) \text{ \AA}$), weaker hydrogen bonds between $\text{O1}\cdots\text{H5B}^{ii}/\text{O1}^i\cdots\text{H5B}^{iii}$ ($2.257(31) \text{ \AA}$).

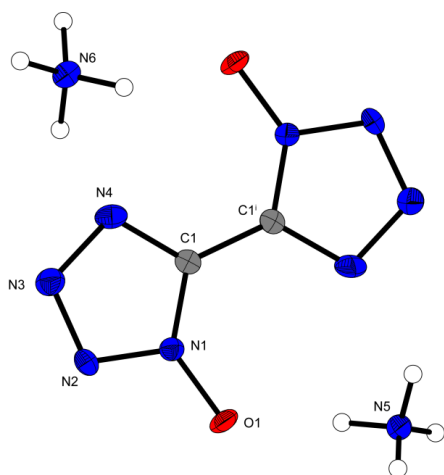


Figure 2 Molecular unit of crystalline **2** with its labelling scheme. Ellipsoids are shown at the 50 % probability level.

Having two different 5,5'-bis(tetrazole-1-oxide) anionic moieties in the asymmetric unit, dihydrazinium-5,5'-bis(tetrazole-1-oxide) (**3**) crystallizes in the triclinic space group $P\bar{1}$ with two molecules in the unit cell and a density of 1.725 g cm^{-3} . The two asymmetric anionic moieties differ in their coordination geometry, whereas the first one is coordinated by six hydrazinium cations forming eight hydrogen bonds and the second one is coordinated by eight hydrazinium cations forming twelve hydrogen bonds. Both anions are connected to each other by bridging hydrazinium cations which form H-bonds between $\text{N7}\cdots\text{N10B}^{iii}$ with a length of $2.263(20) \text{ \AA}$ and between $\text{O1}\cdots\text{H9C}^{iii}$ with a strong interaction of $1.926(19) \text{ \AA}$ distance.

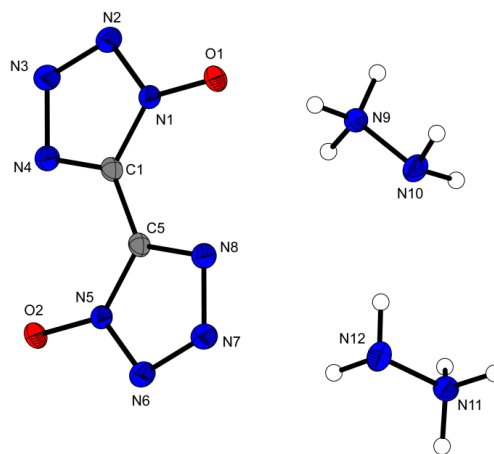


Figure 3 Molecular unit of crystalline **3** with its labelling scheme. Ellipsoids are shown at the 50 % probability level...

Bis(guanidinium)-5,5'-bis(tetrazole-1-oxide) (**4**) crystallizes without inclusion of crystal water in the monoclinic space group $P2_1/c$ with two molecules in the unit cell and a density of 1.639 g cm^{-3} . The aromatic bis(tetrazole-1-oxide) ring system is coordinated by four guanidinium cations where each of them forms two hydrogen bonds. Showing lengths of $1.952(20) \text{ \AA}$ ($\text{O1}\cdots\text{H5A}$) and $1.980(19) \text{ \AA}$ ($\text{O1}\cdots\text{H7A}^{ii}$) these interactions are in the range of strong hydrogen bonds.

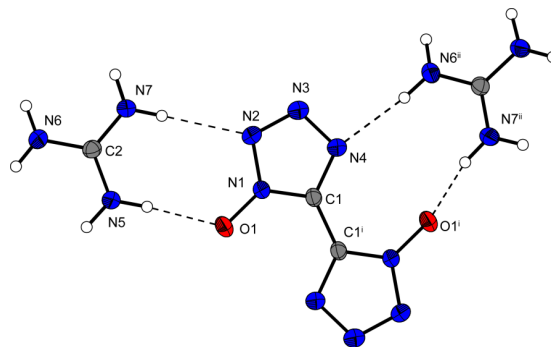


Figure 4 Molecular unit of crystalline **4** with its labelling scheme. Ellipsoids are shown at the 50 % probability level. Symmetry codes: (i) $1-x, -y, -z$; (ii) $1-x, -0.5+y, 0.5-z$.

Bis(aminoguanidinium)-5,5'-bis(tetrazole-1-oxide) (**5**) crystallizes also anhydrously in the monoclinic space group $C2/m$ with two molecules in the unit cell and a comparatively low density of 1.596 g cm^{-3} . One bis(tetrazole-1-oxide) anion, the packing of which is affected by several strong hydrogen bonds, is coordinated by four further aminoguanidinium cations. Stronger hydrogen bonds between $\text{O1}\cdots\text{H5B-N5}$ ($2.072(51) \text{ \AA}$) and $\text{N2}\cdots\text{H6B-N6}$ ($2.061(48) \text{ \AA}$) are also observed.

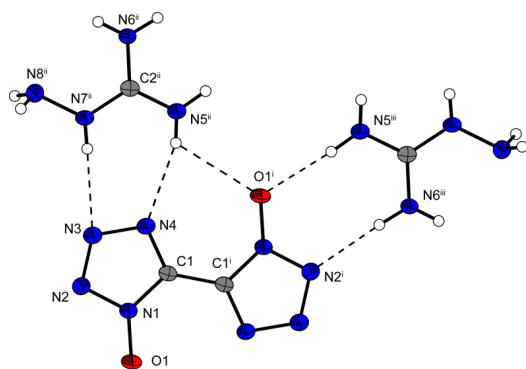


Figure 5 Molecular unit of crystalline **5** with its labeling scheme. Ellipsoids are shown at the 50 % probability level.

Despite a reaction stoichiometry of 2:1, diaminoguanidinium-5,5'-bis(tetrazole-1-oxide) monohydrate (**6**) was only obtained as its mono-deprotonated 5-(1-hydroxytetrazole)-5'-(tetrazole-1'-oxide) salt (stoichiometry 1:1) with inclusion of one molecule of crystal water per molecular unit. Compound **6** crystallizes in the triclinic space group $P\bar{1}$ with two molecules in the unit cell and a density of 1.729 g cm^{-3} . In the structure of **6**, the mono-deprotonated anions build long chains along the a -axis by formation of very strong hydrogen bonds $\text{H1}^i \cdots \text{O2}$ and $\text{H1} \cdots \text{O2}^{ii}$ which are nearly symmetric and similar to those observed in the HF_2^- anion.

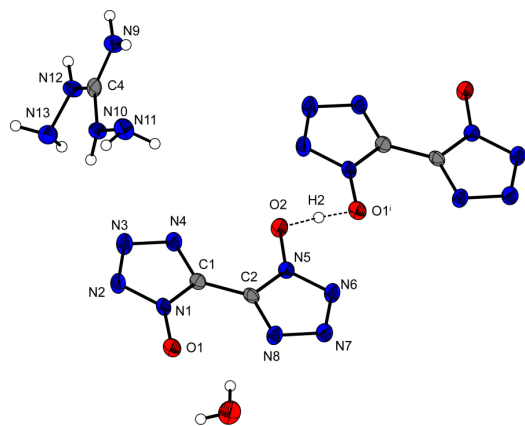


Figure 6 View to a selected detail of the crystal structure of **6** showing the nearly symmetric hydrogen bridge $\text{O2-H2} \cdots \text{O1}^i$. Ellipsoids are shown at the 50 % probability level. Symmetry code: (i) $-1+x, y, z$.

In agreement to **6**, triaminoguanidinium-5,5'-bis(tetrazole-1-oxide) (**7**) could only be obtained crystalline with one molecule of crystal water as a compound with 1:1 stoichiometry. It crystallizes in the triclinic space group $P\bar{1}$ with two molecules in the unit cell and a comparatively high density of 1.749 g cm^{-3} , which could be explained by the stronger attractive ionic forces between the twice positively/negatively charged ions. The coordination geometry of a single anion consists of interactions with four triaminoguanidinium cations and two hydrate water molecules.

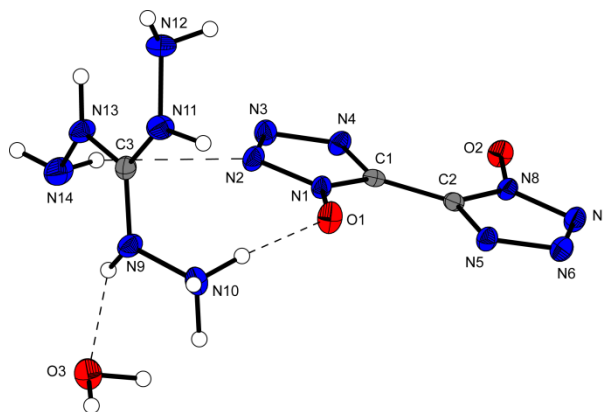


Figure 7 Molecular unit of crystalline **7** with its labeling scheme. Ellipsoids are shown at the 50 % probability level.

1-Amino-3-nitroguanidinium 5-(1-hydroxytetrazole)-5'-(tetrazole-1'-oxide) (**8**) crystallizes as a dihydrate in the monoclinic space group $P2_1/n$ with a density of 1.778 g cm^{-3} and four molecular moieties in the unit cell. Comparable to **6**, also in the structure of **8** the anions are connected to each other in a chain-like arrangement via a strong hydrogen bond $\text{O2-H2} \cdots \text{O1}$ with a distance $\text{H2} \cdots \text{O1}$ of $1.24(2) \text{ \AA}$. Also the hydrate water molecules strongly contribute to a tight hydrogen bond network (e.g. $\text{O6-H6A} \cdots \text{O5}$: $1.86(3) \text{ \AA}$, $\text{N13-H13A} \cdots \text{O6}$: $1.790(19) \text{ \AA}$, $\text{N13-H13B} \cdots \text{O5}$: $1.77(2) \text{ \AA}$).

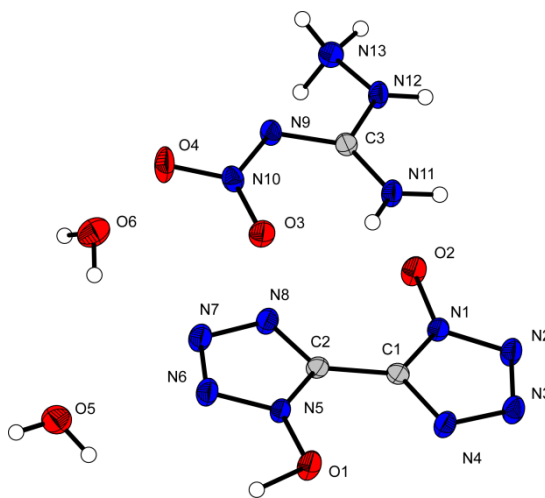


Figure 8 Molecular unit of crystalline **8** with its labelling scheme. Ellipsoids are shown at the 50 % probability level.

Diaminouronium-5,5'-bis(tetrazole-1-oxide) (**9**) is a 1:1 compound that could only be crystallized as its monohydrate. It crystallizes in the monoclinic space group $P2_1/c$ with four molecules in the unit cell and a high density of 1.800 g cm^{-3} . Both cation and anion are charged twice, whereas the positive charges are localized at the NH_3 -ends N10 and N12 of the diaminouronium cation. Both hydrazide moieties show torsion angles OCNH of more than 20° indicating no mesomeric stabilization.

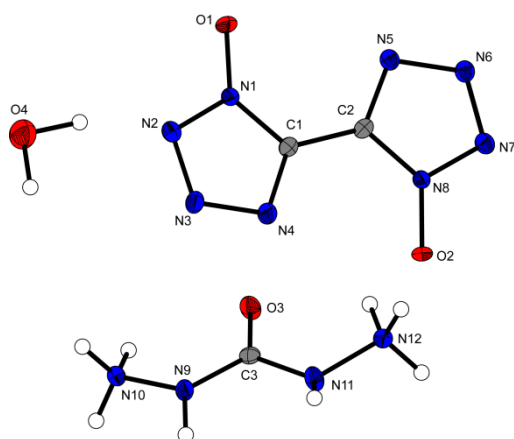
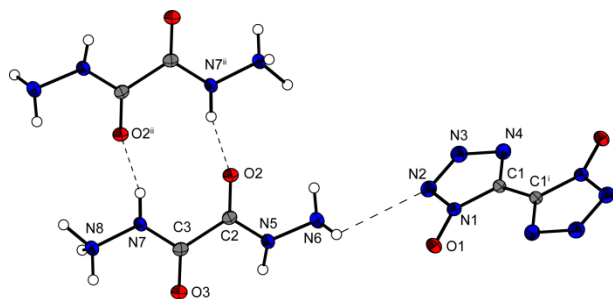


Figure 9 Molecular unit of crystalline **9** with its labeling scheme. Ellipsoids are shown at the 50 % probability level.

Bis(oxalyldihydrazinium)-5,5'-bis(tetrazole-1-oxide) (**10**) crystallizes anhydrously in the monoclinic space group $P2_1/c$ with two molecules in the unit cell and a density of 1.828 g cm^{-3} . The compound has a 2:1 stoichiometry with a twice deprotonated anion and two single positively charged oxalyldihydrazinium cations, whereas this positive charge is localized at N8 and N8ⁱ. The mesomeric stabilization of the carbohydrazide moiety is evidenced by the torsion angle H7–N7–C3–O3 of $180.00(144)^\circ$. However the second carbonylhydrazide unit has a minor torsion of 8.52° at O2–C2–N5–H5. The bond lengths C2–N5 ($1.320(3) \text{ \AA}$) and C3–N7 ($1.340(3) \text{ \AA}$) are located between a C=N double and a C–N single bond which is typical for a peptide-like stabilization, too.



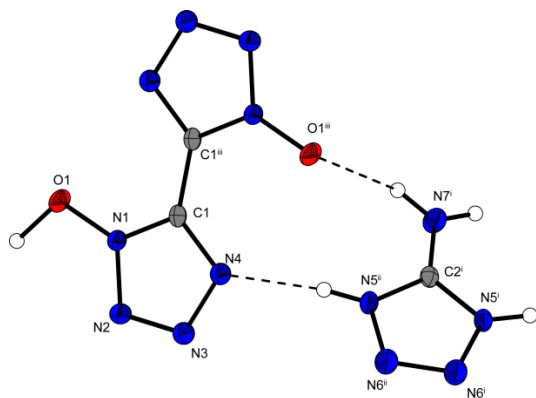


Figure 13 Molecular unit of crystalline **13** with its labeling scheme. Ellipsoids are shown at the 50 % probability level. Symmetry codes: (i) $1+x, y, z$; (ii) $1-x, y, 0.5-z$; (iii) $1-x, -y, -z$.

1-Methyl-5-aminotetrazolium 5,5'-bis(tetrazole-1-oxide) crystallizes in the triclinic space group $P\bar{1}$ with two molecular moieties per unit cell and a density of 1.762 g cm^{-3} . Except by the strong hydrogen bond $\text{O1-H1}\cdots\text{O2}$ ($1.33(3) \text{ \AA}$), which connects the anions, the structure is also stabilized by a strong hydrogen bond $\text{N12-H12}\cdots\text{N4}$ ($1.90(2) \text{ \AA}$).

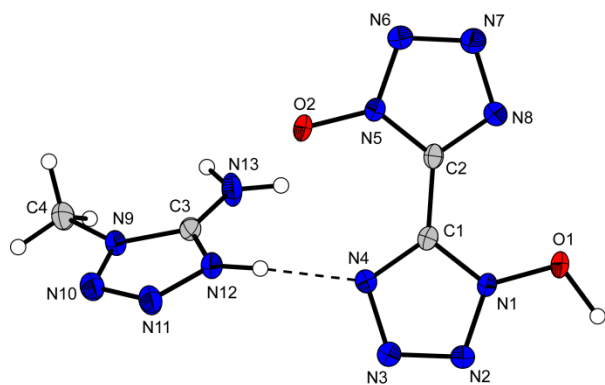


Figure 14 Molecular unit of crystalline **14** with its labeling scheme. Ellipsoids are shown at the 50 % probability level.

In the structure of **15**, no proton transfer between 5,5'-bis(1-hydroxytetrazole) as the acid and 2-methyl-5-aminotetrazole as the base is observed. It must be described as a cocrystallization product between the two mentioned species. The fact that 2-methyl-5-aminotetrazole is a weaker base compared to 1-methyl-5-aminotetrazole has been demonstrated in similar crystal structures before.^[32] **15** crystallizes in the monoclinic space group $C2/c$ with four molecules in the unit cell and a density of 1.608 g cm^{-3} , which is remarkably lower as compared to **14** due to the lack of ionic attractive forces although the structure is stabilized by strong hydrogen bonds. The most important, since the shortest hydrogen bond, is found between $\text{O1}^i\cdots\text{N8}^{ii}$ with a distance of $1.32(19) \text{ \AA}$. This is only slightly longer than the O-H bond length in the 5,5'-bis(1-hydroxytetrazole) molecule ($1.192(19) \text{ \AA}$). Unlike in all ionic structures described in this work the two tetrazole moieties in the 5,5'-(1-hydroxytetrazole) molecule are distorted as evidenced by the torsion angle ($\text{N1-C1-C1}^i\text{-N1}^i$) of $-122.98(16)^\circ$.

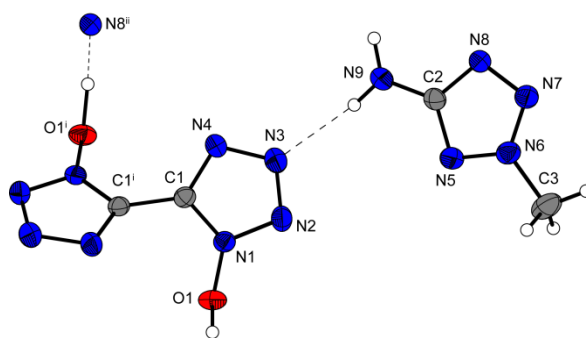


Figure 15 Molecular unit of crystalline **15** with its labeling scheme. Ellipsoids are shown at the 50 % probability level. Symmetry codes: (i) $-x, y, 0.5-z$; (ii) $-x, y, 0.5-z$.

In contrast to **13**, diaminotetrazolium 5,5'-bis(tetrazole-1-oxide) (**16**) crystallizes in the triclinic space group $P\bar{1}$ with only two molecules in the unit cell and a similar density of 1.828 g cm^{-3} . The N9-N13 bond length is in the range of a typical N-N single bond, however, even slightly longer ($1.394(9) \text{ \AA}$). The diaminotetrazolium ring itself is planar and the protons of the carbon linked amino group H14A/H14B are in the plane of the ring, which is not the case for the protons at N13 . For the anion, a moderate torsion angle of the two tetrazole-oxide rings at N5-C2-C1-N4 of $5.18(23)^\circ$ has been detected. Again, chains of the anions are formed after continuous H-bond formation between $\text{H1}^i\cdots\text{O2}$ and $\text{H1}\cdots\text{O2}^{ii}$ ($1.296(22) \text{ \AA}$), a motif, that often has been observed for the structures discussed before.

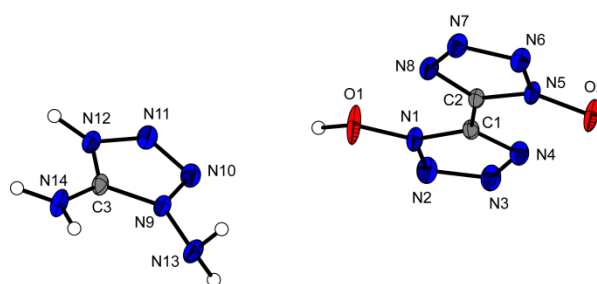


Figure 16 Molecular unit of crystalline **16** with its labeling scheme. Ellipsoids are shown at the 50 % probability level.

Spectroscopy

NMR spectroscopy: All compounds **1-16** were investigated using ^1H and ^{13}C NMR spectroscopy. Additionally, ^{15}N NMR spectra of **1** as well as of its ammonium salt **2** were recorded. For better comparison all spectra were measured using d_6 -DMSO as solvent and all chemical shifts are given with respect to TMS (^1H , ^{13}C) or nitromethane (^{15}N).

In the proton NMR spectra of **2, 3, 10, 11, 13, 14** and **15** all N connected protons contained in the cation are visible as only one singlet, which appears between 7.07 and 8.72 ppm. For the 5-aminotetrazolium salt **13**, an exceptionally high value of 11.90 ppm is observed. Except for the ammonium salt **2**, a fast proton exchange causes the coincidence of the signals of the chemically inequivalent protons. For the guanidinium derivatives **4-8**, the signals of chemically non-equivalent protons can be distinguished well. The NH_2 protons of **4** are visible as a singlet at 7.10 ppm, whereas two singlets appear for the protons of **7** and **8** for NH_2 (4.46

ppm (7), 7.03 (8)) and NH (8.62 ppm (7), 8.27 ppm (8)). The amino- and diaminoguanidinium salts **5** and **6** reveal three separated signals for CNHNH_2 (4.60 ppm, **5**; 5.15 ppm, **6**), CNH_2 (7.01 ppm, **5**; 7.10 ppm, **6**) and CNHNH_2 (8.89 ppm, **5**; 8.50 ppm, **6**). In contrast to the hydrazinium salt **3**, in the spectra of the hydrazino moiety containing compounds **9** and **12** the signals for NH (8.31 ppm (**9**), 9.57 ppm (**12**)) can be distinguished from the signals for NH_3^+ (7.80 ppm (**9**), 6.38 ppm (**12**)). Furthermore the existence of the methyl groups in the cations of **14** and **15** is evidenced by resonances at 3.67 (**14**) and 4.07 ppm (**15**). For the anionic species in **2–16** a single resonance at 134.5–135.8 ppm in the ^{13}C NMR spectrum is observed, which does not significantly differ from the signal of the neutral species **1** (135.8 ppm). However, this signal differs significantly from the signals observed for the precursor molecules glyoxime (145.9 ppm), dichloroglyoxime (131.2 ppm) and diazidoglyoxime (136.5 ppm), which makes NMR spectroscopy the analytical procedure of choice to monitor the completeness of these reactions. A second signal of the cation is visible in each carbon NMR spectrum in the range of 158.6–160.2 ppm for the guanidine derivatives **4–8**, in the range of 157.8–159.6 for the carbohydrazide derivatives **9–11**, 162.5 ppm for **12** and 154.2–167.7 ppm for the substituted tetrazolium cations in **13–16** respectively.

In the ^{15}N NMR spectrum of the free acid **1**, a set of four signals according to the four chemically inequivalent nitrogen atoms of the two tetrazole moieties (C_i symmetry of the 5,5'-bis(tetrazole-1-oxide) molecule) can be found (Figure 17). A partial assignment was undertaken according to a GIAO NMR calculation with Gaussian09^[33], which gave the relative NMR shifts of both **1** and **2** in good accordance. Thereafter, the β -nitrogen atoms N3 and N2 are shifted to the lowest field. For unsubstituted 5,5'-bistetrazole, two signals at 3 ppm and –66 ppm are observed^[9], according to the β - (3 ppm) and the α -nitrogen atoms (–66 ppm). In the spectra of **1** and **2**, N3 is assigned to signals at –2.0 ppm (**1**, **2**) and N2 to signals at –18.7 (**1**) and –19.8 ppm (**2**). A larger difference, however, is observed for the chemical shifts of the α -nitrogen atoms of **1** and **2**, since unlike N4, N1 is hydroxyl-substituted. For N4, signals at –52.3 (**1**) and –53.6 ppm (**2**) are observed, which is comparable to the chemical shift of the α -nitrogen atoms in unsubstituted 5,5'-bistetrazole (–66 ppm), whereas the signal for the hydroxylated N1 are found at –110.5 (**1**) and –107.5 ppm (**2**) respectively. In the spectrum of **2**, an additional signal at –359.7 ppm for the ammonium cation is visible as a triplet due to NH coupling ($^1J_{\text{NH}} = 70.7$ Hz).

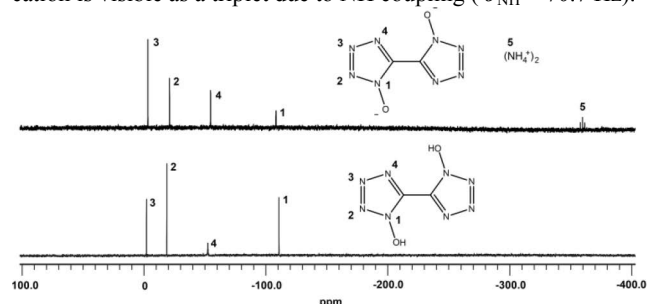


Figure 17 ^{15}N NMR of **1** and **2**. Chemical shifts are given with respect to MeNO_2 .

Vibrational spectroscopy: The assignments of the observed absorption bands to the corresponding functional groups was undertaken based on values found in literature.^[34] The Raman and IR spectra of all investigated compounds show absorptions of the aromatic ring system of the 5,5'-bis(tetrazole-1-oxide) anion at 1350–1550 cm^{-1} and 700–1350 cm^{-1} [$\nu(\text{NN})$, $\nu(\text{NCN})$, $\gamma(\text{CN})$, δ (aromatic tetrazole-oxide ring)], which partially are in the

fingerprint region. Furthermore the N-O^- vibration can hardly be observed in a range of 1550–1600 cm^{-1} . In all cases hydroxyl groups, which are involved in hydrogen bonding, can be detected as absorptions in the range of 3209–3454 cm^{-1} [$\nu(\text{O-H})$].

In the Raman spectrum of the ammonium salt **2** an absorption at 3075 cm^{-1} [$\nu_{\text{sym}}(\text{NH}_4^+)$] can be observed whereas the IR spectrum exhibits several signals in the range of 3047–3180 cm^{-1} referring to the asymmetric valence vibrations of the ammonium cation.

Vibrations of the hydrazinium cation in **3** as well as those of the hydrazino groups of diaminourea in compound **9** and the hydrazine moiety in the cation of **12** can be observed in the range of 3059–3434 cm^{-1} [$\nu_{\text{asym}}(\text{NH}_2/\text{NH}_3^+)$] and also in the range of 1535–1620 cm^{-1} [$\delta_{\text{sym}}(\text{NH}_2/\text{NH}_3^+)$, $\delta_{\text{asym}}(\text{NH}_2/\text{NH}_3^+)$]. Furthermore the carbonyl moiety of the diaminourea cation of **9** reveals a sharp absorption band at 1702 cm^{-1} , whereas the stretching and deformation vibrations of the tetrazine ring (in **12**) are located in the same region as those of the bistetrazole-dioxide ring system discussed above.

The spectra of the guanidine derivatives **4–8** show absorption bands of valence vibrations of the amino groups at 3000–3500 cm^{-1} [$\nu_{\text{sym}}(\text{NH}_2)$, $\nu_{\text{asym}}(\text{NH}_2)$]. Furthermore deformation vibrations of the amino groups can be found at 1577–1690 cm^{-1} [$\delta_{\text{sym}}(\text{NH}_2)$, $\delta_{\text{asym}}(\text{NH}_2)$]. Moreover valence vibrations of the C–N double bonds in the guanidine part of the cations appear at 1680–1470 cm^{-1} [$\nu(\text{C=N})$]. Another characteristic absorption band of the nitro-amine in the cation of **8** is observed at 1262 cm^{-1} in the IR spectrum.

The spectra of both compounds **10** and **11** show the symmetric deformation vibration of the protonated hydrazino groups, the absorption bands of which are located at 1615 cm^{-1} [$\delta_{\text{sym}}(\text{NH}_3^+)$] and are clearly visible in the Raman spectra. A further strong absorption at 1677 cm^{-1} [$\delta_{\text{asym}}(\text{NH}_3^+)$] can be assigned to the C=O valence vibration of the carbohydrazide moiety in both compounds. Moreover the asymmetric valence vibrations of the NH group of the hydrazino moieties is observed at 3029 cm^{-1} [$\nu_{\text{asym}}(\text{NH})$, **10**] and at 3074 cm^{-1} [$\nu_{\text{asym}}(\text{NH})$, **11**]. The asymmetric C–H valence vibration of the methyl group in the IR spectra as well as the symmetric one in the Raman spectra of compounds **14** and **15** can be observed at 2960 and 2966 cm^{-1} [$\nu_{\text{sym}}(\text{CH}_3)$] and at 2850–2960 cm^{-1} [$\nu_{\text{asym}}(\text{CH}_3)$]. Also the $-\text{CH}_3$ deformation vibration is visible in absorptions at 1439 cm^{-1} [$\delta_{\text{asym}}(\text{CH}_3)$] and 1390 cm^{-1} [$\delta_{\text{sym}}(\text{CH}_3)$] in the spectra of **15**.

In contrast to the aminotetrazolium salts **13–15**, which have their very sharp absorption bands at 1703 (**13**), 1693 (**14**) and 1659 cm^{-1} (**15**) [$\delta_{\text{asym}}(\text{NH}_2)$] and 1624 (**13**), 1616 (**14**) and 1627 cm^{-1} (**15**) [$\delta_{\text{sym}}(\text{NH}_2)$] the diaminosubstituted cation in **16** exhibits a broadened signal at 1577–1731 cm^{-1} [$\delta_{\text{sym}}(\text{NH}_2)$, $\delta_{\text{asym}}(\text{NH}_2)$] because of the existence of two amino groups.

Thermal Behavior and Sensitivities

Differential scanning calorimetry (DSC) measurements to determine the melt- and decomposition temperatures as well as the dehydration temperature of crystal water containing salts of **1–16** (about 1.5 mg of each energetic material) were performed in covered Al-containers with a hole (0.1 mm) in the lid for gas release and a nitrogen flow of 20 mL per minute on a Linseis PT 10 DSC^[35] calibrated by standard pure indium and zinc at a heating rate of 5 $^\circ\text{C min}^{-1}$. The decomposition temperatures are given as absolute onset temperatures.

Except for the 1-amino-3-nitroguanidinium salt **8**, the non ionic compound **15** and the 1,5-diaminotetrazolium salt **16**, the decomposition temperatures for all remaining salts are at or even above 180 $^\circ\text{C}$, which is a necessary requirement for possible RDX replacements, which itself decomposes at about 210 $^\circ\text{C}$. The low

decomposition temperature of the 1-amino-3-nitroguanidinium salt **8** is in agreement to other energetic compounds based on this cation in the literature.^[23] Also the low decomposition temperature of **16** is in agreement to other 1,5-diaminotetrazolium based materials.^[36] This is in contrast to the 5-aminotetrazolium salt **13**, which is stable up to 224 °C. A potential reason for the low decomposition temperature of **15** (155 °C) possibly is the lack of ionic attractive forces in the solid state, which nicely can be compared to the ionic structure of **14**, the sister compound, which is methylated at position 1 of the tetrazole ring and is thermally stable up to 192 °C. The highest decomposition temperature is observed for the ammonium salt **2** (290 °C), however, the hydrazinium salt **3** as well as the other hydrazino moiety containing compounds **9–12** decompose significantly earlier at 220–224 °C (**3**, **9–11**) and 180 °C (**12**). A comparison between the guanidinium salts **4–7** shows, that **4** reveals by far the highest decomposition temperature of 274 °C, whereas **5–7** decompose at 204–210 °C. The loss of crystal water in the hydrated compounds **6–9** and **11** can be observed as endothermic steps in the cases of **6** (160 °C), **8** (140 °C, immediately before decomposition) and **11** (110 °C). In **6**, the hydrate water seems to be comparatively strong bonded by H-bonds as it cannot be removed before 160 °C. Also melting points are observed in the DSC traces of **5**, **6**, and **14–16** as evidenced by (additional) endothermic steps. In the cases of **5**, **6**, **14** and **16**, the materials melt right before decomposition, whereas the adduct **15** has a melting point, which is somewhat below its decomposition temperature ($T_m = 125$ °C). For the free acid **1**, which crystallizes as a dihydrate, a decomposition temperature of 214 °C and a dehydration temperature of 115 °C was recorded. By heating the compound to 140 °C for 24 h, the crystal water could completely be removed as evidenced by elemental analysis.

The impact sensitivity tests of compounds **1–16** were carried out according to STANAG 4489^[37] modified instruction^[38] using a BAM (Bundesanstalt für Materialforschung und -prüfung) drophammer.^[39] The friction sensitivity tests were carried out according to STANAG 4487^[40] modified instruction^[41] using the BAM friction tester. The classification of the tested compounds results from the “UN Recommendations on the Transport of Dangerous Goods”^[42]. Additionally all compounds were tested upon the sensitivity towards electrical discharge using the Electric Spark Tester ESD 2010 EN^[43].

First it has to be mentioned, that the precursor material diazidoglyoxime, as one would expect for a covalent diazide, was determined to be very impact and extremely friction sensitive (IS: 1.5 J, FS: <5N) requiring extreme caution when being handled. In contrast, cyclized **1**, proved to be impact insensitive (>40J) and only moderately sensitive towards friction (216 N), which cannot be explained only by the inclusion of two molecules of crystal water. However, the free acid **1**, which was dried at 140 °C for 24 h revealed sensitivities of 4 J (IS) and 10 N (FS) and therefore needs to be handled with greater care.

Due to their impact sensitivity of more than 35–40 J compounds **2**, **5**, **11** and **12** can be classified as less sensitive, which in the case of **11** probably can be explained by a dihydrate formation. The guanidinium salt **4** is even insensitive towards impact with a value of more than 40 J. **3**, **6–10** show sensitivities in the range of 9–20 J and therefore can be classified as sensitive towards impact. Expectedly the protonated tetrazolium salts **13**, **14** and **16** as well as the hydrogen bond stabilized adduct with 2-methyl-5-aminotetrazole (**15**) reveal the lowest values for impact sensitivity and therefore are classified as sensitive (**14**, **15**) or very sensitive towards impact (**13**,

16). Except for **11**, no apparent desensitization of the materials is observed, when hydrate water is included as it is the case for **6–9**.

For the friction sensitivity the same trends as for the impact sensitivity was observed. However a few exceptions have been observed, e.g. bishydrazinotetrazinium salt **12**, which is friction sensitive (80 N) while being insensitive towards impact (40 J). The opposite behavior is observed for **15**, which is insensitive towards friction (360 N) while being impact sensitive (8 J). Furthermore again the guanidinium salt **4** is the least sensitive compound (>360 N) and also **2**, **10** and **15** can be classified as less sensitive. The remaining compounds fill the space between being less sensitive (360 N) and being very sensitive (80–10 N) with the 5-aminotetrazolium salt (**13**, 72 N) as the most sensitive compound.

The sensitivity towards electrical discharge next to the compound's design also depends on the grain size of the material, whereas larger crystals tend to be less sensitive and powders show enhanced sensitivity. For this reason, the grain size of the materials is given in the experimental part. Regardless the grain size, the guanidinium (**4**) as well as the 1-methyl-5-aminotetrazolium salt **14** were determined to be the least sensitive compounds and the hydrazinium salt **9** (0.10 J) as well as the 1-amino-3-nitroguanidinium (**8**) and the 3,6-dihydrazino-1,2,4,5-tetrazinium salt **12** (both 0.08 J) to be the most sensitive, whereas it has to be mentioned, that through normal activities, the human body can generate up to 25 mJ of static electricity, which can easily set off the most sensitive explosives, but is well below the value found for the most sensitive compounds presented here.

Theoretical Calculations

Heats of formation

Usually energetic materials tend to explode in bomb calorimetric measurements. Consequently doubtful combustion energies are obtained. Therefore heats of formation of energetic materials mostly are calculated theoretically. In our group we combine the atomization energy method (eq. 1) with CBS-4M electronic enthalpies (Table 1) which has been shown suitable in many recently published studies.^[44] CBS-4M energies of the atoms, cations, and anions were calculated with the Gaussian 09 (revision A1) software package^[33] and checked for imaginary frequencies. Values for $\Delta_f H^\circ$ (atoms) were taken from the NIST database.^[45]

$$\Delta_f H^\circ_{(g, M, 298)} = H_{(Molecule, 298)} - \sum H^\circ_{(Atoms, 298)} + \sum \Delta_f H^\circ_{(Atoms, 298)} \quad (1)$$

Table 1. CBS-4M results and gas phase enthalpies

	Formula	$-H^{298a}$ / a.u.	$\Delta_f H$ (g) ^b / kJ mol ⁻¹
1	C₂H₂N₈O₂	664.816722	689.1
BTO⁻	C₂HN₈O₂⁻	664.334858	420.7
BTO²⁻	C₂N₈O₂²⁻	663.687267	587.7
NH₄⁺	NH₄⁺	56.796608	635.8
N₂H₅⁺	N₂H₅⁺	112.030523	774.1
G⁺	CH₆N₃⁺	205.453192	571.9
AG⁺	CH₇N₄⁺	260.701802	671.6
DAG⁺	CH₈N₅⁺	315.949896	772.7
TAG²⁺	CH₁₀N₆⁺	371.348640	2012.3
ANQ⁺	CH₆N₅O₂⁺	464.914496	877.0
DAU²⁺	CH₇N₄O⁺	335.970626	1726.2
Oxahy⁺	C₂H₇N₄O₂⁺	448.979375	550.6
Oxahy²⁺	C₂H₈N₄O₂²⁺	449.181787	1553.2
BHT²⁺	C₂H₈N₈²⁺	517.532665	2307.0
5-AT⁺	CH₄N₅⁺	313.534215	981.8
1-Me-5-AT⁺	C₂H₆N₅⁺	352.779155	935.2

2-Me-5-AT	C₂H₅N₅	352.445333	277.8
1,5-DAT⁺	CH₅N₆⁺	368.793548	1053.4

^a CBS-4M enthalpy at room temperature; ^b calculated gas phase heat of formation by the atomization equation.

For calculation of the solid state energy of formation (Table 2) of **1–16**, the lattice energy (U_L) and lattice enthalpy (ΔH_L) were calculated from the corresponding molecular volumes (obtained from X-ray elucidations) according to the equations provided by Jenkins and Glasser.^[46] With the calculated lattice enthalpy (Table 3) the gas-phase enthalpy of formation was converted into the solid state (standard conditions) enthalpy of formation. In the case of the neutral compounds **1** and **15**, their sublimation enthalpy was calculated with the Troutons' rule^{''} ($\Delta H_{sub} [\text{kJ mol}^{-1}] = 188 \cdot T_m [\text{K}]$).^[47] These molar standard enthalpies of formation (ΔH_m) were used to calculate the molar solid state energies of formation (ΔU_m) according to equation 2 (Tables 3 and 4).

$$\Delta U_m = \Delta H_m - \Delta n RT \quad (2)$$

(Δn being the change of moles of gaseous components)

The solid state energies of formation reach from highly positive values ($>3000 \text{ kJ kg}^{-1}$) for the hydrazinium salt (**3**) as well as the bishydrazinotetrazinium (**12**) and the tetrazolium derivatives (**13–16**) to even negative energies of formation for the oxalyldihydrazidinium salt **11** (-1363 kJ kg^{-1}). Beside **11**, also the diaminouonium salt **9** reveals a comparatively low value of 42 kJ kg^{-1} , which in both cases is due to their high lattice enthalpy (both are 1:1 compounds with twice charged an-/cations) and hydrate formation. The highest energies of formation are found for the tetrazolium derivatives, which have a large number of inherently energetic N–N single and double bonds in combination with a solvent free crystallization as for the 5-amino- and 1,5-diaminotetrazolium derivatives **13** (3667 kJ kg^{-1}) and **16** (3767 kJ kg^{-1}).

Detonation Parameters

The detonation parameters of **1–16** (Tables 3 and 4) were calculated using the program EXPLO5 V5.05^[48]. The program is based on the steady-state model of equilibrium detonation and uses Becker-Kistiakowsky-Wilson's equation of state (BKW E.O.S) for gaseous detonation products and Cowan-Fickett E.O.S. for solid carbon^[49]. The program is designed to enable the calculation of detonation parameters at the Chapman-Jouguet point. The calculations were performed using the maximum densities according to the crystal structures at low temperatures as well as the solid state energies of formation and the sum formula of the respective compound.

The calculated detonation parameters are compared to two prominent secondary explosives which are widely used, namely RDX (1,3,5-trinitro-1,3,5-triazacyclohexane) and HMX (1,3,5,7-tetranitro-1,3,5,7-tetraazacyclooctane). For consistence also the low temperature densities of RDX and HMX were used. The detonation velocities reach from 7917 m s^{-1} (**4**) to 9160 m s^{-1} (**16**), whereas apart from three compounds (**3**, **13**, **16**), the bigger part does not reach the detonation velocity calculated for RDX (8983 m s^{-1}) and even the best performing material in terms of its detonation velocity (**16**) does not reach the value calculated for HMX (9221 m s^{-1}). The same argumentation applies to the detonation pressures, where we find values reaching from 233 (**4**) up to 361 kbar (**16**), which is below the values calculated for RDX as well as HMX. If a material should reveal detonation parameters exceeding those of RDX or even HMX it is advantageous to have a combination of a high crystal density and at the same time a high energy of formation. Unfortunately in this study on the one hand the densest materials do not have the highest energies of formation and on the other hand the compounds with the highest energies of formation do not reveal the highest densities.

Table 2. Solid state energies of formation ($\Delta_f U^\circ$)

	$\Delta_f H^\circ (\text{g})^a /$ kJ mol^{-1}	$V_M^b /$ nm^3	$U_L^c /$ kJ mol^{-1}	$\Delta H_L^d /$ kJ mol^{-1}	$\Delta_f H^\circ (\text{s})^e /$ kJ mol^{-1}	Δn^f	$\Delta_f U^\circ (\text{s})^g /$ kJ mol^{-1}	Formula	$M /$ g mol^{-1}	$\Delta_f U^\circ (\text{s})^h /$ kJ kg^{-1}
1	205.9			91.58 [#]	114.3	9	136.6	C ₂ H ₆ N ₈ O ₄	206.12	662.8
2	1859.4	0.188	1551.4	1558.9	300.5	10	325.3	C ₂ H ₈ N ₁₀ O ₂	204.15	1592.9
3	2136.0	0.225	1450.9	1458.3	677.7	12	707.4	C ₂ H ₁₀ N ₁₂ O ₂	234.18	3020.2
4	1731.5	0.292	1316.2	1323.5	408.0	14	442.7	C ₄ H ₁₂ N ₁₄ O ₂	288.28	1535.5
5	1930.9	0.331	1254.8	1262.3	668.6	16	708.3	C ₄ H ₁₄ N ₁₆ O ₂	318.31	2225.0
6	951.8 [*]	0.242	538.7	542.1	409.6	13.5	443.1	C ₃ H ₁₁ N ₁₃ O ₃	277.27	1598.2
7	2358.5 [*]	0.253	2029.4	2041.8	316.7	14.5	352.6	C ₃ H ₁₂ N ₁₄ O ₃	292.27	1206.5
8	814.5 [*]	0.255	582.5	592.4	222.1	15	259.3	C ₃ H ₁₁ N ₁₃ O ₆	325.10	797.4
9	2072.3 [*]	0.232	2080.6	2093.0	-20.7	13	11.6	C ₃ H ₁₀ N ₁₂ O ₄	278.23	41.6
10	1688.8	0.365	1208.5	1216.0	472.9	18	517.5	C ₆ H ₁₄ N ₁₆ O ₆	406.33	1273.5
11	1657.7 [*]	0.237	2122.1	2136.9	-479.2	15	-442.0	C ₆ H ₁₂ N ₁₂ O ₆	324.26	-1363.3
12	2894.7	0.290	1896.9	1906.8	987.9	13	1020.1	C ₄ H ₈ N ₁₆ O ₂	202.18	3266.7
13	1402.5	0.230	486.5	491.4	911.1	10	935.9	C ₃ H ₅ N ₁₃ O ₂	255.20	3667.0
14	1355.8	0.254	474.4	479.3	876.5	11	903.8	C ₄ H ₇ N ₁₅ O ₂	269.18	3356.8
15	1244.7			80.5 [#]	1164.2	16	1203.8	C ₆ H ₁₂ N ₁₈ O ₂	368.34	3268.1
16	1474.0	0.246	478.5	483.4	990.6	11	1017.9	C ₃ H ₆ N ₁₄ O ₂	270.22	3766.8

^a Gas phase enthalpies of formation (those of the ionic compounds are taken as the respective sums of the non-interacting component ions); ^{*} gas phase enthalpy of included water has been subtracted; [#] sublimation enthalpy calculated by the Trouton rule; ^b molecular volume of the molecular moiety in the crystal structure; ^c lattice energy calculated by Jenkins and Glasser equations; ^d lattice enthalpy calculated by Jenkins and Glasser equations; ^e solid state molar heat of formation; ^f change of moles of gaseous components; ^g molar energy of formation; ^h energy of formation (mass dependent).

Table 3 Energetic properties and detonation parameters of 1–8.

	1	2	3	4	5	6	7	8
Formula	C ₂ H ₆ N ₈ O ₄	C ₂ H ₈ N ₁₀ O ₂	C ₂ H ₁₀ N ₁₂ O ₂	C ₄ H ₁₂ N ₁₄ O ₂	C ₄ H ₁₄ N ₁₆ O ₂	C ₃ H ₁₁ N ₁₃ O ₃	C ₃ H ₁₂ N ₁₄ O ₃	C ₃ H ₁₁ N ₁₃ O ₆
FW [g mol ⁻¹]	206.12	204.18	234.18	288.28	318.31	277.27	292.27	325.10
IS [J] ^a	> 40	35	9	>40	40	12	15	10
FS [N] ^b	216	360	252	>360	324	168	120	192
ESD-test [J] ^c	0.50	0.25	0.10	0.50	0.25	0.25	0.25	0.08
N [%] ^d	54.4	68.6	71.8	68.0	70.4	65.7	67.1	56.0
Ω [%] ^e	-23.28	-47.02	-47.82	-66.60	-65.35	-49.06	-49.27	-27.06
T _{dec} [°C] ^f	214	290	220	274	228	204	210	140
Density [g cm ⁻³] ^g	1.811	1.800	1.725	1.639	1.596	1.729	1.749	1.778
Δ _f H _m ^o [kJ mol ⁻¹] ^h	114.3	300.5	677.7	408.0	668.6	409.6	316.7	222.1
Δ _f U ^o [kJ kg ⁻¹] ⁱ	662.8	1592.9	3020.2	1535.5	2225.0	1598.2	222.1	797.4
<i>Detonation parameters calculated with EXPLO5.05:</i>								
-Δ _E U ^o [kJ kg ⁻¹] ^j	5043	4213	5415	3581	4160	4439	2981	5118
T _E [K] ^k	3625	2939	3433	2606	2852	3072	2342	3599
p _{CJ} [kbar] ^l	331	316	340	233	243	294	246	325
D [m s ⁻¹] ^m	8764	8817	9159	7917	8111	8598	8028	8796
Gas vol. [L kg ⁻¹] ⁿ	810	843	863	806	825	837	844	840
I _{sp} [s] ^o	240	211	246	194	212	215	179	241

^a impact sensitivity (BAM drophammer, 1 of 6); ^b friction sensitivity (BAM friction tester, 1 of 6); ^c electrostatic discharge device (OZM); ^d nitrogen content; ^e oxygen balance^[50]; ^f decomposition temperature from DSC (β = 5 °C); ^g estimated from X-ray diffraction; ^h calculated (CBS-4M) heat of formation; ⁱ calculated energy of formation; ^j Energy of explosion; ^k explosion temperature; ^l detonation pressure; ^m detonation velocity; ⁿ assuming only gaseous products; ^o specific impulse calculated at isobaric (60 bar) rocket conditions.

Table 4. Energetic properties and detonation parameters of 9–16.

	9	10	11	12	13	14	15	16	RDX	HMX
Formula	C ₃ H ₁₀ N ₁₂ O ₄	C ₆ H ₁₄ N ₁₆ O ₆	C ₄ H ₁₂ N ₁₂ O ₆	C ₄ H ₈ N ₁₆ O ₂	C ₃ H ₅ N ₁₃ O ₂	C ₄ H ₇ N ₁₃ O ₂	C ₆ H ₁₂ N ₁₈ O ₂	C ₃ H ₆ N ₁₄ O ₂	C ₃ H ₆ N ₆ O ₆	C ₄ H ₈ N ₈ O ₈
FW [g mol ⁻¹]	278.23	406.33	324.26	202.18	255.20	269.18	368.34	270.22	222.12	296.16
IS [J] ^a	20	20	40	40	4	6	8	2	7.5 ^[51]	7 ^[51]
FS [N] ^b	240	360	288	80	72	240	360	160	120 ^[51]	112 ^[51]
ESD-test [J] ^c	0.40	0.40	0.35	0.08	0.30	0.50	0.40	0.35	0.2	0.2
N [%] ^d	64.6	55.2	51.8	71.8	71.4	67.6	68.5	65.4	37.84	37.84
Ω [%] ^e	-40.26	-51.19	-39.48	-51.24	-40.75	-56.46	-69.50	-41.45	-21.61	-21.61
T _{dec} [°C] ^f	220	224	222	180	224	192	155	170	205	275
Density [g cm ⁻³] ^g	1.800	1.847	1.885	1.787	1.839	1.762	1.608	1.828	1.858 (90 K) ^[52]	1.944 (100K) ^[53]
Δ _f H _m ^o [kJ mol ⁻¹] ^h	-20.7	472.9	-479.2	987.9	911.1	903.8	1164.2	990.6	86.3	116.1
Δ _f U ^o [kJ kg ⁻¹] ⁱ	41.6	1273.5	-1363.3	3266.7	3667.0	3356.8	3268.1	3766.8	489.0	492.5
<i>Detonation parameters calculated with EXPLO5.05:</i>										
-Δ _E U ^o [kJ kg ⁻¹] ^j	3595	4868	3072	4961	5576	5264	4828	5625	6190	6185
T _E [K] ^k	2743	3303	2452	3527	4009	3665	3325	3970	4232	4185
p _{CJ} [kbar] ^l	277	333	275	320	358	313	249	361	380	415
D [m s ⁻¹] ^m	8306	8878	8203	8788	9097	8718	8090	9160	8983	9221
Gas vol. [L kg ⁻¹] ⁿ	832	789	826	767	760	751	756	774	734	729
I _{sp} [s] ^o	191	217	175	236	250	240	232	252	258	258

^a impact sensitivity (BAM drophammer, 1 of 6); ^b friction sensitivity (BAM friction tester, 1 of 6); ^c electrostatic discharge device (OZM); ^d nitrogen content; ^e oxygen balance; ^f decomposition temperature from DSC (β = 5 °C); ^g estimated from X-ray diffraction; ^h calculated (CBS-4M) heat of formation; ⁱ calculated energy of formation; ^j Energy of explosion; ^k explosion temperature; ^l detonation pressure; ^m detonation velocity; ⁿ assuming only gaseous products; ^o specific impulse calculated at isobaric (60 bar) rocket conditions.

Conclusion

From this combined theoretical and experimental study the following conclusions can be drawn:

- For smaller scales 5,5'-bis(1-hydroxytetrazole) (**1**) is synthesized easiest by cyclization of isolated diazidoglyoxime, which is prepared from glyoxal via glyoxime and dichloroglyoxim.

- **1** can be used in Bronsted acid-base reactions or metathesis reactions to isolate the diammonium (**2**), dihydrazinium (**3**), bis-guanidinium (**4**), bis-aminoguanidinium (**5**), diaminoguanidinium (**6**), triaminoguanidinium (**7**), 1-amino-3-nitroguanidinium (**8**), diaminouronium (**9**), bis-oxalyldihydrazidinium (**10**), oxalyldihydrazidinium (**11**), 3,6-dihydrazino-1,2,4,5-tetrazinium (**12**), 5-aminotetrazolium (**13**), 1-methyl-5-aminotetrazolium (**14**), 1,5-diaminotetrazolium (**16**) salt and a bis-2-methyl-5-aminotetrazole adduct (**15**). In the cases of **5**, **7**, **11** and **12** a 1:1 stoichiometry of the salts is observed with twice protonated cations and twice deprotonated bis(tetrazole-1-oxide). For **2–5** and **10** a cation/anion ratio of 2:1 was observed, whereas in the cases of **6**, **8**, **13** and **14** a 1:1 stoichiometry with monodeprotonated anions occurs. **15** is an adduct of **1** and 2-methyl-5-aminotetrazole, which is stabilized by strong hydrogen bonds.

- The crystal structures of **1–16** were determined by low-temperature single-crystal X-ray diffraction. The compounds crystallize in the space groups *P*-1 (**3**, **6**, **7**, **12**, **14**, **16**), *P*₂/c (**4**, **9–11**), *P*_n (**8**), *C*₂/c (**13**, **15**), *C*₂/m (**1**, **5**) and *I*222 (**2**) with densities between 1.596 g cm⁻³ for the bis-aminoguanidinium salt **5** and 1.885 g cm⁻³ for the oxalyldihydrazidinium salt **11**. Additionally, all compounds were fully characterized by vibrational spectroscopy (IR and Raman) ¹H and ¹³C NMR, mass spectrometry and elemental analysis. - Thermal stabilities of **1–16** were investigated by DSC at a heating rate of 5 °C min⁻¹. Except for the 1-amino-3-nitroguanidinium salt **8** (140 °C) and the adduct **15** (155 °C) all compounds withstand temperatures of 180 °C or more. Here, the diammonium salt **2** reveals the highest thermal stability (290 °C).

- The sensitivities of towards friction, impact and electrostatic discharge were investigated by BAM methods. All investigated compounds can be categorized starting from insensitive (>40 J: **1**, **4**) to less sensitive (35–40 J: **2**, **5**, **11**, **12**), sensitive (4–35 J: **3**, **6–10**, **13–15**) and very sensitive (0–3 J: **16**) towards impact and insensitive (>360 N: **4**) less sensitive (=360 N: **2**, **10**, **15**), sensitive (80–360 N: **1**, **3**, **5–9**, **11**, **12**, **14**, **16**) and very sensitive (<80 N: **13**) towards friction. The sensitivities towards electrostatic discharge vary from 0.08 J (**8**, **12**) to 0.50 J (**1**, **4**, **14**). With sensitivities of 1.5 J (IS), <5 N (FS) and 0.007 J (ESD), the precursor diazidoglyoxime is by far more sensitive than the salts **2–16** or the free acid 5,5'-bis(1-hydroxytetrazole) dihydrate **1**.

- Using calculated heats of formation and low temperature X-ray densities detonation parameters such as the detonation velocity *D* and pressure *p*_{CJ} as well the specific impulse *I*_{sp} at 60 bar (isobaric conditions) were calculated with the EPXLO5 program. The most promising compounds in terms of explosive performance are the hydrazinium salt **3** (*D* = 9159 m s⁻¹, *p*_{CJ} = 340 kbar, *I*_{sp} = 246 s), the 5-aminotetrazolium salt **13** (*D* = 9097 m s⁻¹, *p*_{CJ} = 358 kbar, *I*_{sp} = 250 s) and the 1,5-diaminotetrazolium salt **16** (*D* = 9160 m s⁻¹, *p*_{CJ} = 361 kbar, *I*_{sp} = 252 s).

Experimental Section

Caution! 5,5'-Bis(1-hydroxytetrazole) and its salts are energetic materials with increased sensitivities towards shock and friction. Therefore, proper safety precautions (safety glass, face shield, earthed equipment and shoes, Kevlar® gloves and ear plugs) have to be applied while synthesizing and handling the described compounds.

All chemicals and solvents were employed as received (Sigma-Aldrich, Fluka, Acros). ¹H, ¹³C and ¹⁵N NMR spectra were recorded using a JEOL Eclipse 270, JEOL EX 400 or a JEOL Eclipse 400 instrument. The chemical shifts quoted in ppm in the text refer to typical standards such as tetramethylsilane (¹H, ¹³C) or nitromethane (¹⁵N). To determine the melting and decomposition temperatures of the described compounds a Linseis PT 10 DSC (heating rate 5 °C min⁻¹) was used. Infrared spectra were measured using a Perkin Elmer Spectrum One FT-IR spectrometer as KBr pellets. Raman spectra were recorded on a Bruker MultiRAM Raman Sample Compartment D418 equipped with a Nd-YAG-Laser (1064 nm) and a LN-Ge diode as detector. Mass spectra of the described compounds were measured at a JEOL MStation JMS 700 using FAB technique. To measure elemental analyses a Netsch STA 429 simultaneous thermal analyzer was employed. 5,5'-Bis(1-hydroxytetrazole) was synthesized according to a modified literature procedure.^[13]

5,5'-bis(1-hydroxytetrazole) dihydrate (**1**)

Glyoxime: 27.5 g (0.69 mol) of NaOH were dissolved in 75 mL of water and the solution is cooled to 0 °C in a salt-ice bath. Hydroxylammonium chloride (69.5 g, 1.00 mol) is added while stirring. To the obtained solution glyoxal (72.5 g, 0.50 mol, 40% w/w in H₂O) is added, while the temperature is kept below 10 °C. After complete addition of the glyoxal the solution is further chilled in the salt-ice bath until glyoxime precipitates. The solid is removed by suction filtration and washed with only little ice-water to remove remaining sodium chloride.

Dichloroglyoxime: 17.6 g (200 mmol) of glyoxime were suspended in 200 mL of ethanol. Cl₂ gas was bubbled through the suspension at -20 °C until the green suspension turned into a yellowish solution. The solution was allowed to warm up slowly to room temperature meanwhile releasing dissolved chlorine. Then the solvent was removed under vacuum and the remaining solid was resuspended in 50 mL of chloroform, stirred for 15 min at room temperature and filtered yielding 26.6 g (85 %) of the colorless product.

¹H NMR (DMSO-d₆, 25 °C, ppm) δ: 13.10; ¹³C NMR (DMSO-d₆, 25 °C, ppm) δ: 131.2; EA (C₂H₂Cl₂N₂O₂, 156.96): calc.: C 15.30, H 1.28, N 17.85 %; found: C 15.65, H 1.25, N 17.49 %.

Diazidoglyoxime: 3.13 g (20 mmol) of dichloroglyoxime were dissolved in 40 mL of dimethyl formamide. At 0 °C 2.93 g (45 mmol) of sodium azide were added. The suspension was stirred for 20 min at 0 °C and 100 mL of water were added. The precipitate was filtered, washed with 100 mL of water and air dried yielding 2.85 g (84%) of the colorless product.

DSC (5 °C min⁻¹): 170 °C (dec.); IR (atr, cm⁻¹): ν = 3209 (w), 2170 (w), 2123 (w), 1622 (w), 1400 (w), 1361 (w), 1286 (m), 1013 (vs), 930 (m), 920 (s), 855 (s), 731 (s); Raman (1064 nm, 300 mW, 25 °C, cm⁻¹): ν = 2166 (8), 2129 (5), 2091 (3), 1621 (100), 1457 (14), 1390 (12), 1216 (19), 1034 (3), 882 (20), 672 (3), 442 (6); ¹H NMR (DMSO-d₆, 25 °C, ppm) δ: 12.08; ¹³C NMR (DMSO-d₆, 25 °C, ppm) δ: 136.5; EA (C₂H₂N₄O₂, 170.09): calc.: C 14.12, H 1.19, N 65.88 %; found: C 14.38, H 1.46, N 66.01 %; BAM drophammer: 1.5 J; friction tester: <5 N; ESD: 7 mJ.

5,5'-Bis(1-hydroxytetrazole) dihydrate (**1**): 1.70 g (10 mmol) of diazidoglyoxime were suspended in 100 mL of diethyl ether which is cooled to 0 °C in a salt-ice bath. HCl is bubbled through the suspension maintaining the temperature below 20 °C, until saturation of the diethyl ether indicated by a drop of the temperature back to 0–5 °C is reached. The flask is stoppered tightly and the reaction mixture is stirred overnight at room temperature under a slight overpressure of HCl, which forms upon warming the mixture to room temperature. The HCl overpressure is released carefully and the mixture is evaporated either overnight at room temperature in an open dish or in 1–2 h at 50 °C. After most of the diethyl ether has evaporated, 20 mL of water is added resulting in a clear solution. A remaining colorless precipitate indicates uncompleted conversion of diazidoglyoxime to 5,5'-bis(1-hydroxytetrazole). The water is again evaporated on a rotary evaporator to remove remaining HCl and diethyl ether yielding crude 5,5'-bis(1-hydroxytetrazole) dihydrate as a colorless solid, which can be further purified by recrystallization from hot water. Yield: 1.90 g (9.2 mmol, 92 %).

DSC (5 °C min⁻¹): 115 °C (dehydr.), 214 °C (dec.); IR (KBr, cm⁻¹): ν = 3229 (m), 1665 (m), 1411 (w), 1375 (w), 1302 (w), 1208 (w), 1144 (m), 995 (s), 714 (w), 662 (w); Raman (1064 nm, 300 mW, 25 °C, cm⁻¹): ν = 1608 (100), 1270 (26), 1157 (46), 1133 (38), 1019 (22), 766 (31), 738 (13), 693 (4), 597 (6), 402 (29); ¹H NMR (DMSO-d₆, 25 °C, ppm) δ: 6.80; ¹³C NMR (DMSO-d₆, 25 °C, ppm) δ: 135.8; ¹⁵N NMR

(DMSO- d_6 , 25 °C, ppm) δ : -2.0 (N3), -18.7 (N2), -52.3 (N4), -110.5 (N1); EA (206.12): calc.: C 11.65, H 2.93, N 54.36 %; found: C 12.18, H 2.81, N 54.04 %; BAM drophammer: >40 J; friction tester: 216 N; ESD: 0.5 J.

Diammonium-5,5'-bis(tetrazole-1-oxide) (2)

5,5'-Bis(1-hydroxytetrazole) dihydrate (2.06 g, 10 mmol) is suspended in aqueous ammonia (2 mol/L, 10 mL). The mixture is heated after adding 90 mL of water. After boiling, the mixture turns into a clear solution. The solution is cooled down to room temperature and the colorless crystalline residue is filtrated whereas 1.14 g (5.57 mmol, 56 % yield) are obtained.

DSC (5 °C min⁻¹, °C): 290 °C (dec.); IR (KBr, cm⁻¹): ν = 3180 (s), 3047 (s), 2851 (s), 2150 (w), 1817 (w), 1668 (w), 1433 (s), 1400 (vs), 1352 (s), 1231 (s), 1165 (s), 1046 (m), 997 (m), 727 (m), 501 (m); Raman (1064 nm, 300 mW, 25 °C, cm⁻¹): ν = 3075 (1), 1605 (100), 1463 (3), 1278 (2), 1245 (23), 1118 (8), 1000 (7), 774 (8), 740 (3), 616 (3), 408 (4), 281 (3), 120 (14), 102 (18), 81 (16); ¹H NMR (DMSO- d_6 , 25 °C, ppm) δ : 7.07 (s, NH₄⁺); ¹³C NMR (DMSO- d_6 , 25 °C, ppm) δ : 134.8 (CN₄O); ¹⁵N NMR (DMSO- d_6 , 25 °C, ppm) δ : -2.0 (N3), -19.8 (N2), -53.6 (N4), -107.5 (N1); m/z (FAB⁺): 169.0 [C₂N₈O₂]⁺; m/z (FAB⁻): 18.1 [NH₄⁺]; EA (C₂H₈N₁₀O₂, 204.15): calc.: C 11.77, H 3.95, N 68.61 %; found: C 12.14, H 3.69, N 68.18 %; BAM drophammer: 35 J; friction tester: 360 N; ESD: 0.25 J.

Dihydrazinium 5,5'-bis(tetrazole-1-oxide) (3)

5,5'-Bis(1-hydroxytetrazole) dihydrate (2.06 g, 10 mmol) is suspended in a few milliliters of water and hydrazine hydrate (1.00 g, 20 mmol) is added to the clear solution. The mixture is heated and filtrated. Dihydrazinium 5,5'-bis(tetrazole-1-oxide) is gained as small colorless crystalline needles to yield 0.95 g (4.05 mmol, 41 %).

DSC (5 °C min⁻¹, °C): 220 °C (dec.); IR (KBr, cm⁻¹): ν = 3434 (w), 3322 (s), 3294 (s), 3189 (s), 2958 (s), 2864 (s), 2743 (s), 2642 (s), 2133 (m), 1832 (w), 1620 (s), 1578 (m), 1529 (m), 1511 (m), 1420 (s), 1408 (s), 1347 (m), 1232 (s), 1170 (s), 1117 (s), 1096 (s), 1046 (w), 1038 (w), 998 (m), 970 (vs), 732 (m), 712 (w), 523 (w), 495 (w); Raman (1064 nm, 300 mW, 25 °C, cm⁻¹): ν = 3294 (1), 3196 (2), 2006 (1), 1605 (100), 1476 (1), 1458 (2), 1399 (2), 1241 (21), 1139 (7), 1109 (8), 1007 (7), 974 (6), 782 (9), 739 (3), 613 (3), 406 (6); ¹H NMR (DMSO- d_6 , 25 °C, ppm) δ : 7.20 (s, NH₂NH₃⁺); ¹³C NMR (DMSO- d_6 , 25 °C, ppm) δ : 134.9 (CN₄O); m/z (FAB⁺): 33.1 [N₂H₂⁺]; m/z (FAB⁻): 169.0 [C₂HN₈O₂]⁻; EA (C₂H₁₀N₁₂O₂, 234.18): calc.: C 10.26, H 4.30, N 71.77 %; found: C 10.71, H 3.97, N 71.17 %; BAM drophammer: 9 J; friction tester: 252 N; ESD: 0.1 J.

Bis(guanidinium) 5,5'-bis(tetrazole-1-oxide) (4)

5,5'-Bis(1-hydroxytetrazole) dihydrate (2.06 g, 10 mmol) is suspended in a few milliliters of water and guanidinium carbonate (1.08 g, 12 mmol) is added. The mixture is heated to reflux for 10 minutes and filtrated. After cooling the filtrate down to room temperature 4 precipitates as colorless crystalline needles. Yield: 2.00 g (6.94 mmol, 69 %).

DSC (5 °C min⁻¹, °C): 274 °C (dec.); IR (KBr, cm⁻¹): ν = 3454 (s), 3376 (s), 3089 (s), 2192 (w), 1652 (vs), 1583 (m), 1424 (s), 1385 (m), 1347 (m), 1289 (w), 1234 (m), 1169 (m), 1139 (m), 1068 (m), 1014 (w), 999 (m), 744 (m), 595 (w), 543 (w), 530 (w), 513 (m), 490 (w); Raman (1064 nm, 300 mW, 25 °C, cm⁻¹): ν = 3197 (2), 1603 (100), 1458 (4), 1233 (17), 1152 (12), 1120 (6), 1017 (33), 791 (9), 739 (2), 621 (2), 545 (5), 422 (3), 409 (4), 292 (6), 179 (4), 128 (18), 100 (18); ¹H NMR (DMSO- d_6 , 25 °C, ppm) δ : 7.10 (s, C(NH₂)₃); ¹³C NMR (DMSO- d_6 , 25 °C, ppm) δ : 158.6 (C(NH₂)₃), 134.6 (CN₄O); m/z (FAB⁺): 60.1 [CH₅N₅]⁺; m/z (FAB⁻): 169.0 [C₂HN₈O₂]⁻; EA (C₄H₁₂N₁₄O₂, 288.23): calc.: C 16.67, H 4.20, N 68.03 %; found: C 16.95, H 3.94, N 67.45 %; BAM drophammer: > 40 J; friction tester: > 360 N; ESD: 0.5 J.

Bis(aminoguanidinium) 5,5'-bis(tetrazole-1-oxide) (5)

5,5'-Bis(1-hydroxytetrazole) dihydrate (2.06 g, 10 mmol) is suspended in a few milliliters of water. After two equivalents of aminoguanidinium bicarbonate (2.72 g, 20 mmol) are added, the mixture is heated until boiling for 10 minutes and the hot solution is filtrated. The solvent is slowly evaporated from the filtrate to yield 1.94 g (6.09 mmol, 61 %) of 5 as colorless crystals.

DSC (5 °C min⁻¹, °C): 208 °C (m.p.), 228 °C (dec.); IR (KBr, cm⁻¹): ν = 3432 (s), 3308 (s), 3180 (s), 2344 (w), 1678 (vs), 1416 (m), 1424 (s), 1384 (m), 1352 (w), 1234 (m), 1208 (w), 1176 (w), 1101 (w), 994 (m), 957 (w), 730 (w), 712 (w), 677 (w), 643 (w), 515 (w), 494 (w); Raman (1064 nm, 300 mW, 25 °C, cm⁻¹): ν = 3302 (2), 3245 (3), 3184 (4), 1673 (2), 1613 (100), 1590 (32), 1452 (2), 1292 (2), 1241 (23), 1214 (2), 1147 (10), 1133 (6), 1114 (9), 1009 (7), 968 (10), 778 (10), 736 (2), 637 (1),

612 (4), 512 (4), 423 (2), 339 (1), 289 (11), 177 (10), 145 (10), 95 (23); ¹H NMR (DMSO- d_6 , 25 °C, ppm) δ : 8.89 (s, 1H, CNHNH₂), 7.01 (s, 4H, C(NH₂)₃), 4.60 (s, 2H, NHNH₂); ¹³C NMR (DMSO- d_6 , 25 °C, ppm) δ : 159.4 (C(NH₂)₃NHNH₂), 134.7 (CN₄O); m/z (FAB⁺): 75.1 [CH₃N₄⁺]; m/z (FAB⁻): 169.0 [C₂HN₈O₂]⁻; EA (C₄H₁₄N₁₆O₂, 318.26): calc.: C 15.10, H 4.43, N 70.42 %; found: C 15.41, H 4.24, N 69.46 %; BAM drophammer: 40 J; friction tester: 324 N; ESD: 0.25 J.

Diaminoguanidinium-5,5'-bis(tetrazole-1-oxide) monohydrate (6)

5,5'-Bis(1-hydroxytetrazole) dihydrate (2.06 g, 10 mmol) is suspended in a few milliliters of water. Ba(OH)₂ x 8 H₂O (3.16 g, 10 mmol) is added to the clear solution and the mixture is heated until boiling to obtain a white, poorly soluble deposit. The white barium 5,5'-bis(tetrazole-1-oxide) is filtrated in vacuum and dried. The substance was proved to be anhydrous by elemental analysis. Afterwards, the white powder is suspended in water to mix it with diaminoguanidinium sulphate (5.72 g, 20 mmol). BaSO₄ is filtered off and 6 precipitates from the filtrate as clear crystalline agglomerates to yield 1.52 g (5.48 mmol, 55%).

DSC (5 °C min⁻¹, °C): 160 °C (dehydr.), 200 °C (m.p.), 204 °C (dec.); IR (KBr, cm⁻¹): ν = 3437 (s), 3338 (vs), 3301 (s), 2302 (w), 1690 (s), 1670 (s), 1628 (m), 1602 (m), 1458 (w), 1408 (w), 1369 (s), 1340 (w), 1269 (m), 1179 (s), 1148 (s), 1085 (s), 1022 (s), 867 (s), 758 (s), 710 (m), 692 (m), 631 (s), 491 (w); Raman (1064 nm, 300 mW, 25 °C, cm⁻¹): ν = 3338 (3), 3290 (2), 3237 (2), 1615 (100), 1469 (2), 1250 (33), 1180 (2), 1122 (9), 1150 (15), 1132 (16), 1009 (6), 924 (5), 763 (3), 739 (3), 695 (2), 540 (3), 411 (5); ¹H NMR (DMSO- d_6 , 25 °C, ppm) δ : 8.50 (s, 2H, C(NH)₂), 7.10 (s, 2H, C=NH₂⁺), 5.15 (s, 4H, (NHNH₂)₂); ¹³C NMR (DMSO- d_6 , 25 °C, ppm) δ : 160.2 (C=NH₂⁺), 135.7 (CN₄O); m/z (FAB⁺): 90.1 [CH₃N₅]⁺; m/z (FAB⁻): 169.0 [C₂HN₈O₂]⁻; EA (C₃H₁₁N₁₃O₃, 277.20): calc.: C 13.00, H 4.00, N 65.69%; found: C 13.79, H 3.31, N 67.46 %; BAM drophammer: 12 J; friction tester: 168 N; ESD: 0.25 J.

Triaminoguanidinium 5,5'-bis(tetrazole-1-oxide) monohydrate (7)

5,5'-Bis(1-hydroxytetrazole) dihydrate (2.06 g, 10 mmol) is suspended in a few milliliters of water and triaminoguanidinium chloride (2.81 g, 20 mmol) is added to the clear solution. The mixture is shortly heated to reflux and filtrated. From the filtrate, 7 crystallizes as small crystalline needles to give 2.43 g (8.32 mmol, 83 %).

DSC (5 °C min⁻¹, °C): 210 °C (dec.); IR (KBr, cm⁻¹): ν = 3364 (m), 3320 (s), 3209 (s), 2994 (m), 1683 (vs), 1615 (m), 1585 (m), 1508 (w), 1410 (s), 1384 (m), 1338 (m), 1235 (m), 1202 (m), 1150 (m), 1128 (m), 1057 (m), 1013 (m), 989 (m), 949 (m), 779 (w), 733 (m), 638 (m), 567 (m), 496 (w); Raman (1064 nm, 300 mW, 25 °C, cm⁻¹): ν = 3362 (3), 3270 (7), 3171 (7), 1680 (5), 1657 (5), 1602 (100), 1456 (4), 1374 (2), 1232 (25), 1171 (2), 1135 (13), 1110 (14), 1002 (8), 890 (11), 779 (14), 740 (4), 646 (3), 613 (5), 424 (9), 406 (6), 289 (6), 143 (24), 118 (15), 100 (41), 83 (34); ¹H NMR (DMSO- d_6 , 25 °C, ppm) δ : 8.62 (s, 3H, C(NH)₃), 4.46 (s, 6H, C(NHNH₂)₃); ¹³C NMR (DMSO- d_6 , 25 °C, ppm) δ : 159.7 (C(NHNH₂)₃), 134.5 (CN₄O); m/z (FAB⁺): 105.1 [CH₅N₆⁺]; m/z (FAB⁻): 169.0 [C₂HN₈O₂]⁻; EA (C₃H₁₂N₁₄O₃, 292.22): calc.: C 12.33, H 4.14, N 67.10 %; found: C 13.17, H 4.51, N 73.36 %; BAM drophammer: 15 J; friction tester: 120 N; ESD: 0.25 J.

1-Amino-3-nitroguanidinium 5,5'-bis(tetrazole-1-oxide) dihydrate (8)

5,5'-Bis(1-hydroxytetrazole) dihydrate (0.59 g, 2.87 mmol) is dissolved in 5 mL of warm water and a solution of 1-amino-3-nitroguanidine (0.34 g, 2.87 mmol) in 10 mL of hot water is added. After boiling and stirring the mixture for a few minutes, 8 precipitates as thin, colorless plates upon cooling the solution to room temperature. Single crystals suitable for X-ray crystallography in this case were grown from a 40% aqueous solution of HF.

DSC (5 °C min⁻¹, °C): 138 °C (dehydr.), 140 °C (dec.); IR (KBr, cm⁻¹): ν = 3494 (m), 3373 (s), 3285 (m), 3197 (m), 3097 (s), 2677 (m), 1644 (m), 1577 (m), 1469 (m), 1377 (s), 1262 (vs), 1248 (s), 1166 (w), 1153 (w), 1116 (m), 1074 (m), 1024 (w), 1002 (w), 910 (w), 820 (m), 763 (s), 729 (m), 646 (s), 460 (w); Raman (1075 nm, 300 mW, 25 °C, cm⁻¹): ν = 3092 (1), 1628 (100), 1491 (3), 1475 (2), 1392 (2), 1257 (30), 1152 (13), 1015 (5), 913 (9), 799 (7), 738 (3), 621 (7), 445 (3), 404 (4), 361 (7), 282 (7); ¹H NMR (DMSO- d_6 , 25 °C, ppm) δ : 9.34 (s, 1H, CN₄OH), 8.27 (s, 1H, NHNH₂), 7.03 (s, 4H, NHNH₂, NH₂); ¹³C NMR (DMSO- d_6 , 25 °C, ppm) δ : 160.0 (C(NH₂)(NHNH₂)(NNO₂), 135.7 (CN₄O); m/z (FAB⁺): 120.1 [CH₆N₉O₂⁺]; m/z (FAB⁻): 169.0 [C₂HN₈O₂]⁻; EA (C₃H₁₁N₁₃O₆, 325.20): calc.: C 11.08, H 3.41, N 55.99 %; found: C 11.54, H 3.27, N 55.96 %; BAM drophammer: 10 J; friction tester: 192 N; ESD: 0.08 J (at grain size 100–500 μ m).

Diaminouronium-5,5'-bis(tetrazole-1-oxide) monohydrate (9)

5,5'-Bis(1-hydroxytetrazole) dihydrate (2.06 g, 10 mmol) is suspended in a few milliliters of water. Diaminouraea (1.81 g, 20 mmol) is added to the clear solution. The

mixture is shortly heated to reflux and filtrated. After cooling down to room temperature **9** precipitates as crystalline needles. Yield: 2.56 g (9.20 mmol, 92 %).

DSC (5 °C min⁻¹, °C): 220 °C (dec.); IR (KBr, cm⁻¹): ν = 3617 (m), 3545 (m), 3274 (s), 2964 (s), 2659 (s), 2126 (w), 2049 (w), 1702 (m), 1608 (s), 1535 (vs), 1427 (s), 1413 (s), 1385 (m), 1356 (w), 1269 (w), 1233 (s), 1171 (s), 1048 (m), 1006 (w), 996 (w), 978 (w), 729 (m), 565 (w), 504 (w); Raman (1064 nm, 300 mW, 25 °C, cm⁻¹): ν = 1709 (2), 1616 (100), 1474 (5), 1289 (2), 1246 (18), 1202 (4), 1144 (11), 1122 (9), 1008 (7), 1000 (4), 980 (4), 778 (8), 744 (3), 614 (4), 411 (3); ¹H NMR (DMSO-d₆, 25 °C, ppm) δ : 8.31 (s, C(NHNH₂)₂), 7.80 (s, C(NHNH₂)₂); ¹³C NMR (DMSO-d₆, 25 °C, ppm) δ : 135.7 (CN₄O), 159.6 (C(NHNH₂)₂); m/z (FAB⁺): 91.1 [CH₂N₄⁺]; m/z (FAB⁻): 169.0 [C₂HN₈O₂⁻]; EA (C₃H₁₀N₁₂O₄ 278.19): calc.: C 12.95, H 3.62, N 60.42 %; found: C 13.29, H 3.28, N 60.21 %; BAM drophammer: 20 J; friction tester: 240 N; ESD: 0.4 J.

Bis(oxalyldihydrazidinium) 5,5'-bis(tetrazole-1-oxide) (**10**)

5,5'-Bis(1-hydroxytetrazole) dihydrate (2.06 g, 10 mmol) is suspended in a few milliliters of water and oxalyldihydrazide (2.36 g, 20 mmol) is added. The mixture is shortly heated to reflux and filtrated. After cooling down to room temperature **10** precipitates as small crystalline needles to yield 3.57 g (8.79 mmol, 88 %).

DSC (5 °C min⁻¹, °C): 224 °C (dec.); IR (KBr, cm⁻¹): ν = 3423 (m), 3316 (m), 3269 (s), 3029 (s), 2340 (w), 1677 (vs), 1607 (s), 1579 (s), 1512 (s), 1429 (s), 1412 (s), 1348 (m), 1290 (m), 1256 (m), 1239 (s), 1175 (m), 1148 (m), 1077 (m), 971 (m), 927 (m), 831 (m), 780 (w), 730 (m), 712 (w), 636 (w), 536 (m), 498 (m), 479 (m); Raman (1064 nm, 300 mW, 25 °C, cm⁻¹): ν = 3318 (1), 3259 (2), 2017 (1), 1715 (4), 1674 (2), 1615 (100), 1542 (9), 1471 (2), 1320 (12), 1285 (4), 1245 (13), 1211 (2), 1139 (12), 1119 (8), 1071 (1), 1003 (4), 977 (3), 932 (6), 776 (5), 744 (4), 617 (1), 525 (1), 503 (1), 433 (2), 407 (5), 363 (2), 327 (2), 296 (3), 271 (3), 158 (38), 98 (11), 67 (6); ¹H NMR (DMSO-d₆, 25 °C, ppm) δ : 7.74 (s); ¹³C NMR (DMSO-d₆, 25 °C, ppm) δ : 135.7 (CN₄O), 158.1 (C=O); m/z (DEI⁺): 118.1 [C₂H₆N₄O₂⁺]; m/z (FAB⁻): 169.1 [C₂HN₈O₂⁻]; EA (C₆H₁₄N₁₆O₆, 406.28): calc.: C 17.74, H 3.47, N 55.16 %; found: C 17.80, H 3.24, N 54.41 %; BAM drophammer: 20 J; friction tester: 360 N; ESD: 0.4 J.

Oxalyldihydrazidinium 5,5'-bis(tetrazole-1-oxide) dihydrate (**11**)

5,5'-Bis(1-hydroxytetrazole) dihydrate (1.03 g, 5 mmol) is suspended in a few milliliters of water and oxalyldihydrazide (0.59 g, 5 mmol) is added. The mixture is shortly heated to reflux and filtrated. After cooling down to room temperature **11** was obtained as small crystalline needles to give 1.41 g (4.35 mmol, 87 %).

DSC (5 °C min⁻¹, °C): 110 °C (dehydr.), 222 °C (dec.); IR (KBr, cm⁻¹): ν = 3871 (w), 3428 (s), 3074 (s), 2837 (s), 2730 (s), 2043 (m), 1676 (vs), 1585 (m), 1523 (s), 1431 (s), 1415 (s), 1358 (m), 1265 (m), 1241 (s), 1209 (m), 1173 (m), 1040 (m), 1000 (m), 811 (m), 735 (m), 715 (w), 616 (w), 532 (m), 471 (w); Raman (1064 nm, 300 mW, 25 °C, cm⁻¹): ν = 1706 (5), 1660 (2), 1615 (100), 1591 (4), 1555 (2), 1478 (2), 1334 (3), 1287 (1), 1248 (18), 1216 (3), 1139 (6), 1116 (9), 1008 (5), 929 (5), 779 (4), 744 (3), 631 (2), 520 (2), 416 (4), 397 (3), 322 (1), 287 (4), 266 (2), 162 (12), 151 (15), 124 (20), 88 (17), 66 (5); ¹H NMR (DMSO-d₆, 25 °C, ppm) δ : 7.53 (s, (NHNH₃)₂); ¹³C NMR (DMSO-d₆, 25 °C, ppm) δ : 157.8 (C=O), 135.7 (CN₄O); m/z (DEI⁺): 118.1 [C₂H₆N₄O₂⁺]; m/z (DCI⁺): 119.14 [C₂H₇N₄O₂⁺]; m/z (FAB⁻): 169.1 [C₂HN₈O₂⁻]; EA (C₄H₁₂N₁₂O₆, 324.21): calc.: C 14.82, H 3.73, N 51.84 %; found: C 15.14, H 3.52, N 51.32 %; BAM drophammer: 40 J; friction tester: 288 N; ESD: 0.35 J.

3,6-Bishydrazino-1,2,4,5-tetrazinium 5,5'-bis(tetrazole-1-oxide) (**12**)

5,5'-Bis(1-hydroxytetrazole) dihydrate (0.37 g, 1.8 mmol) is suspended in a few milliliters of water and 3,6-Bishydrazino-1,2,4,5-tetrazinium dichloride monohydrate (0.41 g, 1.8 mmol), previously dissolved in a few milliliters of water is added. The mixture is heated until boiling to obtain a clear solution. After cooling down to 10 °C **12** precipitates as a red flaky deposit, which is filtrated and washed with little cold water. 0.36 g (1.15 mmol, 64 %) of small, orange crystals are obtained.

DSC (5 °C min⁻¹, °C): 180 °C (dec.); IR (KBr, cm⁻¹): ν = 3424 (m), 3259 (s), 3059 (m), 2923 (m), 2857 (m), 2657 (m), 2005 (w), 1620 (m), 1573 (m), 1535 (s), 1495 (s), 1426 (vs), 1359 (w), 1327 (w), 1242 (s), 1175 (m), 1159 (m), 1098 (w), 1053 (m), 1000 (w), 939 (m), 856 (m), 730 (m), 706 (m), 595 (m), 508 (w), 464 (w); Raman (1064 nm, 300 mW, 25 °C, cm⁻¹): ν = 3260 (2), 1907 (1), 1615 (100), 1550 (2), 1515 (3), 1490 (7), 1314 (3), 1286 (2), 1247 (21), 1221 (2), 1165 (2), 1141 (10), 1115 (8), 1077 (2), 1008 (7), 876 (8), 816 (2), 777 (7), 740 (3), 702 (1), 671 (3), 613 (4), 467 (4), 435 (3), 415 (3), 293 (9), 198 (3), 157 (7), 127 (18), 115 (47), 105 (54), 90 (34); ¹H NMR (DMSO-d₆, 25 °C, ppm) δ : 9.57 (s, 2H, NHNH₃⁺), 6.38 (s, 6H, NHNH₃⁺); ¹³C NMR (DMSO-d₆, 25 °C, ppm) δ : 162.5 (C₂N₄), 135.7 (CN₄O); m/z (FAB⁻): 169.1 [C₂HN₈O₂⁻]; EA (C₄H₈N₁₆O₆ 312.21): calc.: C 15.39, H 2.58, N 71.78 %; found: C 15.79, H 2.49, N 70.58 %; BAM drophammer: 40 J; friction tester: 80 N; ESD: 0.08 J.

5-Aminotetrazolium 5,5'-bis(tetrazole-1-oxide) (**13**)

5,5'-Bis(1-hydroxytetrazole) dihydrate (2.06 g, 10 mmol) is suspended in a few milliliters of water and 5-aminotetrazole (1.70 g, 20 mmol) is added. The mixture is shortly heated to reflux and filtrated. After cooling down to room temperature **13** crystallizes as colorless needles. Yield: 2.31 g (9.05 mmol, 91 %).

DSC (5 °C min⁻¹, °C): 224 °C (dec.); IR (KBr, cm⁻¹): ν = 3407 (s), 3325 (s), 3281 (m), 3167 (m), 2965 (m), 2837 (m), 2720 (s), 2565 (m), 2508 (m), 1703 (vs), 1594 (m), 1489 (m), 1451 (w), 1407 (w), 1370 (m), 1322 (m), 1281 (m), 1140 (m), 1080 (m), 1056 (m), 999 (s), 809 (s), 522 (m), 456 (w); Raman (1064 nm, 300 mW, 25 °C, cm⁻¹): ν = 1698 (1), 1624 (100), 1592 (3), 1496 (17), 1322 (3), 1297 (1), 1260 (26), 1143 (6), 1130 (11), 1063 (10), 1018 (3), 819 (1), 787 (2), 743 (8), 653 (1), 411 (3), 403 (2), 295 (5), 173 (9), 129 (18), 121 (18), 111 (15), 97 (45), 77 (25); ¹H NMR (DMSO-d₆, 25 °C, ppm) δ : 11.90 (s, CNH₂, (NH₂)₂⁺); ¹³C NMR (DMSO-d₆, 25 °C, ppm) δ : 155.7 (CH₄N₅⁺), 135.8 (CN₄O); m/z (FAB⁺): 86.1 [CH₄N₅⁺]; m/z (FAB⁻): 169.0 [C₂HN₈O₂⁻]; EA (C₃H₅N₁₃O₂, 255.16): calc.: C 14.12, H 1.98, N 71.36 %; found: C 14.50, H 1.91, N 70.90 %; BAM drophammer: 4 J; friction tester: 72 N; ESD: 0.3 J.

1-Methyl-5-aminotetrazolium 5,5'-bis(tetrazole-1-oxide) (**14**)

5,5'-Bis(1-hydroxytetrazole) (2.06 g, 10 mmol) is suspended in a few milliliters of water and 1-methyl-5-aminotetrazole (1.98 g, 20 mmol) is added. The mixture is heated and filtrated. After cooling down to room temperature **14** crystallizes as colorless blocks to yield 1.07 g (3.98 mmol, 40 %).

DSC (5 °C min⁻¹, °C): 188 °C (m.p.), 192 °C (dec.); IR (KBr, cm⁻¹): ν = 3496 (m), 3398 (s), 3296 (m), 3126 (m), 3061 (m), 2950 (m), 2850 (m), 2752 (m), 2676 (m), 1693 (vs), 1514 (w), 1465 (w), 1424 (w), 1367 (m), 1273 (m), 1240 (w), 1138 (m), 1116 (m), 1084 (m), 1042 (m), 1007 (w), 963 (m), 847 (m), 779 (w), 759 (m), 713 (m), 661 (w), 621 (m); Raman (1075 nm, 300 mW, 25 °C, cm⁻¹): ν = 3032 (4), 3012 (2), 2960 (9), 2822 (2), 1712 (1), 1616 (100), 1513 (1), 1464 (2), 1422 (4), 1366 (2), 1275 (5), 1252 (34), 1131 (15), 1112 (10), 1063 (1), 1039 (5), 1013 (4), 969 (2), 781 (25), 741 (5), 671 (5), 623 (1), 475 (2), 412 (4), 314 (5), 292 (5), 231 (6); ¹H NMR (DMSO-d₆, 25 °C, ppm) δ : 8.72 (s, br, NH, NH₂, OH), 3.67 (s, CH₃); ¹³C NMR (DMSO-d₆, 25 °C, ppm) δ : 155.6 (CN₄), 135.8 (CN₄O), 32.2 (CH₃); m/z (FAB⁺): 100.0 [C₂H₆N₅⁺]; m/z (FAB⁻): 169.0 [C₂HN₈O₂⁻]; EA (C₄H₇N₁₃O₂, 269.08): calc.: C 17.85, H 2.62, N 67.64 %; found: C 18.27, H 2.60, N 67.09 %; BAM drophammer: 6 J; friction tester: 240 N; ESD: 0.50 J (at grain size 500–1000 μ m).

Bis(2-methyl-5-aminotetrazole) 5,5'-bis(tetrazole-1-oxide) (**15**)

5,5'-Bis(1-hydroxytetrazole) dihydrate (2.06 g, 10 mmol) is suspended in a few milliliters of water and 2-methyl-5-aminotetrazole (1.98 g, 20 mmol) is added. The mixture is shortly heated to reflux and filtrated. After cooling down to room temperature **15** precipitates as clear crystals to yield 0.98 g (2.66 mmol, 27 %).

DSC (5 °C min⁻¹, °C): 125 °C (m.p.), 155 °C (dec.); IR (KBr, cm⁻¹): ν = 3403 (s), 3344 (s), 3212 (m), 2743 (w), 2400 (w), 1659 (vs), 1596 (s), 1439 (m), 1287 (m), 1159 (s), 1130 (m), 1064 (m), 896 (m), 781 (m), 748 (m), 710 (m), 653 (m), 487 (m); Raman (1064 nm, 300 mW, 25 °C, cm⁻¹): ν = 3220 (7), 3047 (9), 3029 (14), 2966 (49), 1847 (4), 1771 (4), 1714 (4), 1671 (7), 1627 (100), 1438 (18), 1414 (8), 1390 (16), 1328 (4), 1268 (27), 1150 (18), 1091 (10), 1065 (11), 1015 (24), 807 (5), 768 (18), 724 (10), 647 (51), 562 (10), 493 (18), 409 (19), 324 (15), 305 (6), 276 (7), 207 (21), 138 (71); ¹H NMR (DMSO-d₆, 25 °C, ppm) δ : 7.26 (s, 2H, CNH₂), 4.07 (s, 3H, NCH₃); ¹³C NMR (DMSO-d₆, 25 °C, ppm) δ : 167.7 (CNH₂), 135.8 (CN₄O), 39.4 (NCH₃); m/z (FAB⁺): 100.1 [C₂H₆N₅⁺]; m/z (FAB⁻): 169.1 [C₂HN₈O₂⁻]; EA (C₆H₁₂N₁₈O₂, 368.28): calc.: C 19.57, H 3.28, N 68.46 %; found: C 20.08, H 3.24, N 68.50 %; BAM drophammer: 8 J; friction tester: 360 N; ESD: 0.4 J.

1,5-Diaminotetrazolium 5,5'-bis(tetrazole-1-oxide) (**16**)

5,5'-Bis(1-hydroxytetrazole) dihydrate (2.06 g, 10 mmol) is suspended in a few milliliters of water and 1,5-diaminotetrazole (2.04 g, 20 mmol) is added. The mixture is heated and filtrated. After cooling down to room temperature **16** crystallizes from the aqueous solution to give 2.60 g (9.62 mmol, 96 %) of **16**.

DSC (5 °C min⁻¹, °C): 160 °C (m.p.), 170 °C (dec.); IR (KBr, cm⁻¹): ν = 3322 (s), 3325 (s), 3225 (s), 3153 (s), 2791 (w), 2692 (w), 2439 (w), 2241 (w), 1731 (m), 1655 (vs), 1577 (m), 1487 (w), 1470 (w), 1368 (w), 1329 (s), 1134 (w), 1109 (m), 1077 (m), 1002 (m), 931 (m), 745 (m), 687 (m), 605 (m), 486 (w); Raman (1064 nm, 300 mW, 25 °C, cm⁻¹): ν = 3322 (7), 3247 (8), 3157 (9), 1671 (8), 1618 (20), 1547 (30), 1498 (6), 1328 (23), 1306 (32), 1250 (5), 1135 (6), 1106 (26), 1079 (10), 1000 (4), 957 (3), 792 (100), 698 (20), 497 (2), 322 (34), 231 (16), 138 (22), 105 (44), 92 (37), 78 (62); ¹H NMR (DMSO-d₆, 25 °C, ppm) δ : 7.87 (s, CNH₂, N(NH₂), NH⁺); ¹³C NMR (DMSO-d₆, 25 °C, ppm) δ : 154.2 (CH₃N₆⁺), 135.8 (CN₄O); m/z (FAB⁺): 101.1

[CH₅N₆⁺]; m/z (FAB⁺): 169.1 [C₂H₈N₆O₂⁺]; EA (C₃H₆N₁₄O₂, 270.17): calc.: C 13.34, H 2.24, N 72.58 %; found: C 13.95, H 2.23, N 75.97 %; BAM drophammer: 2 J; friction tester: 160 N; ESD: 0.35 J.

Acknowledgements

Financial support of this work by the Ludwig-Maximilian University of Munich (LMU), the U.S. Army Research Laboratory (ARL) under grant no. W911NF-09-2-0018, the Armament Research, Development and Engineering Center (ARDEC) under grant no. R&D 1558-TA-01, and the Office of Naval Research (ONR) under grant nos. ONR.N00014-10-1-0535 and ONR.N00014-12-1-0538 is gratefully acknowledged. The authors acknowledge collaborations with Dr. Mila Krupka (OZM Research, Czech Republic) in the development of new testing and evaluation methods for energetic materials and with Dr. Muhamed Sucesca (Brodarski Institute, Croatia) in the development of new computational codes to predict the detonation and propulsion parameters of novel explosives. We are indebted to and thank Drs. Betsy M. Rice and Brad Forch (ARL, Aberdeen, Proving Ground, MD). Stefan Huber is acknowledged for measuring the sensitivities of all compounds. Furthermore the authors thank Mr. Dennis Fischer for many helpful discussions as well as Mr. Andreas Preimesser for supplying 3,6-bishydrazino-1,2,4,5-tetrazinium dichloride monohydrate.

- [1] J. Thiele, *Liebigs Ann. Chem.* **1898**, 203, 57–75.
- [2] W. E. Bachmann, J. C. Sheehan, *J. Am. Chem. Soc.* **1949**, 71, 1842–1845.
- [3] H. Fischer, *Chem. Ber.* **1949**, 82, 192–193.
- [4] A. T. Nielsen, A. P. Chafin, S. L. Christian, D. W. Moore, M. P. Nadler, R. A. Nissan, D. J. Vanderah, R. D. Gilardi, C. F. George, J. L. Flippen-Anderson, *Tetrahedron* **1998**, 54(39), 11793–11812.
- [5] (a) H. Gao, J. M. Shreeve, *Chem. Rev.* **2011**, 111, 7377–7436; (b) R. Haiges, S. Schneider, T. Schroer, K. O. Christe, *Angew. Chem. Int. Ed.*, **2004**, 43, 4919–4924; (c) D. E. Chavez, M. A. Hiskey, D. L. Naud, D. Parrish, *Angew. Chem. Int. Ed.* **2008**, 47, 8307–8309; (d) M. B. Talawar, R. Sivabalan, T. Mukundan, H. Muthurajan, A. K. Sikder, B. R. Gandhe, A. Subhananda Rao, *J. Hazard. Mater.* **2009**, 161(2–3), 589–607; (e) O. S. Bushuyev, P. Brown, A. Maiti, R. H. Gee, G. R. Peterson, B. L. Weeks, L. J. Hope-Weeks, *J. Am. Chem. Soc.* **2012**, 134 1422–1425.
- [6] S. A. Meyer, A. J. Marchand, J. L. Hight, G. H. Roberts, L. B. Escalon, L. S. Inouye, D. K. MacMillan, *J. Appl. Toxicol.* **2005**, 25(5), 427–434.
- [7] T. M. Klapötke, in *High Energy Density Materials*, Springer, Berlin, Heidelberg, **2007**.
- [8] D. E. Chavez, M. A. Hiskey, R. D. Gilardi, *Angew. Chem. Int. Ed.* **2000**, 39(10), 1791–1793.
- [9] N. Fischer, D. Iszak, T. M. Klapötke, S. Rappenglück, J. Stierstorfer, *Chem. Eur. J.* **2012**, 18(13), 4051–4062.
- [10] M. Göbel, K. Karaghiosoff, T. M. Klapötke, D. G. Piercey, J. Stierstorfer, *J. Am. Chem. Soc.* **2010**, 132, 17216–17226.
- [11] T. M. Klapötke, D. G. Piercey, J. Stierstorfer, *Chem. Eur. J.* **2011**, 17, 13068–13077.
- [12] A. M. Churakov, V. A. Tartakovsky, *Chem. Rev.* **2004**, 104, 2601–2616.
- [13] N. Fischer, D. Fischer, T. M. Klapötke, D. Piercey, J. Stierstorfer, *J. Mater. Chem.* **2012**, 22, 20418–20422.
- [14] I. V. Tselinskii, S. F. Mel'nikova, T. V. Romanova, *Russ. J. Org. Chem.* **2001**, 37, 430–436.
- [15] T. M. Klapötke, P. Mayer, J. Stierstorfer, *Phosphorus, Sulfur Silicon Relat. Elem.* **2009**, 184, 2393–2407.
- [16] Z. Li, W. Zhu, J. Yu, X. Ma, Z. Lu, S. Xiao, *Synth. Commun.* **2006**, 36, 2613–2619.
- [17] T. Curtius, K. Hochschwender, *J. Prakt. Chem.* **1915**, 91, 415–441.
- [18] K. Y. Lee, M. D. Coburn, *US 4733610*, **1988**, 28, 1–2.
- [19] M. D. Coburn, G. A. Buntain, B. W. Harris, *J. Heterocyclic Chem.*, **1991**, 28, 2049–2050.
- [20] R. A. Henry, W. G. Finnegan, *J. Am. Chem. Soc.* **1954**, 76, 923–926.
- [21] P. N. Gaponik, V. P. Karavai, *Chem. Heterocycl. Compd.* **1984**, 1683–1686.
- [22] J. A. Castillo-Melendez, B. T. Golding, *Synthesis* **2004**, 10, 1655–1663.
- [23] N. Fischer, T. M. Klapötke, J. Stierstorfer, *Z. Naturforsch.* **2012**, 67b, 573–588.
- [24] CrysAlisPro Oxford Diffraction Ltd., Version 171.33.41, **2009**.
- [25] A. Altomare, G. Cascarano, C. Giacovazzo, A. Guagliardi, *J. Appl. Cryst.* **1993**, 26, 343.
- [26] A. Altomare, M. C. Burla, M. Camalli, G. L. Cascarano, C. Giacovazzo, A. Guagliardi, A. G. G. Moliterni, G. Polidori, R. Spagna, *J. Appl. Cryst.* **1999**, 32, 115–119.
- [27] G. M. Sheldrick, SHELXS-97, Program for Crystal Structure Solution, Universität Göttingen, **1997**.
- [28] G. M. Sheldrick, SHELXL-97, Program for the Refinement of Crystal Structures, University of Göttingen, Germany, **1997**.
- [29] A. L. Spek, PLATON, A Multipurpose Crystallographic Tool, Utrecht University, Utrecht, The Netherlands, **1998**.
- [30] L. J. Farrugia, *J. Appl. Cryst.* **1999**, 32, 837–838.
- [31] Empirical absorption correction using spherical harmonics, implemented in SCALE3 ABSPACK scaling algorithm (CrysAlisPro Oxford Diffraction Ltd., Version 171.33.41, **2009**).
- [32] N. Fischer, T. M. Klapötke, J. Stierstorfer, *Z. Anorg. Allg. Chem.* **2009**, 635, 271–281.
- [33] Gaussian 09, Revision A.1, M. J. Frisch, G. W. Trucks, H. B. Schlegel, G. E. Scuseria, M. A. Robb, J. R. Cheeseman, G. Scalmani, V. Barone, B. Mennucci, G. A. Petersson, H. Nakatsuji, M. Caricato, X. Li, H. P. Hratchian, A. F. Izmaylov, J. Bloino, G. Zheng, J. L. Sonnenberg, M. Hada, M. Ehara, K. Toyota, R. Fukuda, J. Hasegawa, M. Ishida, T. Nakajima, Y. Honda, O. Kitao, H. Nakai, T. Vreven, J. A. Montgomery, Jr., J. E. Peralta, F. Ogliaro, M. Bearpark, J. J. Heyd, E. Brothers, K. N. Kudin, V. N. Staroverov, R. Kobayashi, J. Normand, K. Raghavachari, A. Rendell, J. C. Burant, S. S. Iyengar, J. Tomasi, M. Cossi, N. Rega, J. M. Millam, M. Klene, J. E. Knox, J. B. Cross, V. Bakken, C. Adamo, J. Jaramillo, R. Gomperts, R. E. Stratmann, O. Yazyev, A. J. Austin, R. Cammi, C. Pomelli, J. W. Ochterski, R. L. Martin, K. Morokuma, V. G. Zakrzewski, G. A. Voth, P. Salvador, J. J. Dannenberg, S. Dapprich, A. D. Daniels, Ö. Farkas, J. B. Foresman, J. V. Ortiz, J. Cioslowski, and D. J. Fox, Gaussian, Inc., Wallingford CT, 2009.
- [34] M. Hesse, H. Meier, B. Zeeh, in *Spektroskopische Methoden in der organischen Chemie*, Vol. 6, Thieme, Stuttgart, New York, **2002**.
- [35] <http://www.linseis.com>
- [36] T. M. Klapötke, F. A. Martin, J. Stierstorfer, *Chem. Eur. J.* **2012**, 18(5), 1487–1501.
- [37] NATO standardization agreement (STANAG) on explosives, impact sensitivity tests, no. 4489, 1st ed., Sept. 17, **1999**.
- [38] WIWEB-Standardarbeitsanweisung 4-5.1.02, Ermittlung der Explosionsgefährlichkeit, hier der Schlagempfindlichkeit mit dem Fallhammer, Nov. 8, **2002**.
- [39] a) <http://www.bam.de>; b) www.reichel&partner.de
- [40] NATO standardization agreement (STANAG) on explosive, friction sensitivity tests, no. 4487, 1st ed., Aug. 22, **2002**.
- [41] WIWEB-Standardarbeitsanweisung 4-5.1.03, Ermittlung der Explosionsgefährlichkeit oder der Reibeempfindlichkeit mit dem Reibeapparat, Nov. 8, **2002**.
- [42] Impact: insensitive > 40 J, less sensitive > 35 J, sensitive > 4 J, very sensitive < 3 J. Friction: insensitive > 360 N, less sensitive = 360 N, sensitive > 80 N, very sensitive > 10 N, extremely sensitive < 10 N. According to the UN Recommendations on the Transport of Dangerous Goods, (+) indicates not safe for transport.
- [43] <http://www.ozm.cz>
- [44] E. F. C. Byrd, B. M. Rice, *J. Phys. Chem. A* **2006**, 110, 1005–1013.

- [45] P. J. Linstrom, W. G. Mallard, (Eds.), in *NIST Chemistry WebBook*, NIST Standard Reference Database Number 69, National Institute of Standards and Technology, Gaithersburg MD, 20899, <http://webbook.nist.gov>, (retrieved October 27, **2011**).
- [46] (a) H. D. B. Jenkins, H. K. Roobottom, J. Passmore, L. Glasser, *Inorg. Chem.* **1999**, *38*(16), 3609–3620. (b) H. D. B. Jenkins, D. Tudela, L. Glasser, *Inorg. Chem.* **2002**, *41*(9), 2364–2367.
- [47] M. S. Westwell, M. S. Searle, D. J. Wales, D. H. Williams, *J. Am. Chem. Soc.* **1995**, *117*, 5013–5015; (b) F. Trouton, *Philos. Mag.* **1884**, *18*, 54–57.
- [48] M. Sućeska, EXPLO5.05 program, Zagreb, Croatia, **2012**.
- [49] M. Sućeska, *Propellants Explos. Pyrotech.* **1991**, *16*, 197–202.
- [50] Calculation of oxygen balance: $\Omega (\%) = (wO - 2xC - 1/2yH - 2zS)/1600/M$. (w: number of oxygen atoms, x: number of carbon atoms, y: number of hydrogen atoms, z: number of sulfur atoms, M: molecular weight).
- [51] R. Mayer, J. Köhler, A. Homburg, in *Explosives*, Vol. 5, WILEY-VCH, Weinheim, **2002**.
- [52] P. Hakey, W. Ouellette, J. Zubieta, T. Korter, *Acta Crystallogr.* **2008**, *E64*(8), o1428/1–o1428/6.
- [53] J. R. Deschamps, M. Frisch, D. Parrish, *J. Chem. Crystallogr.* **2011**, *41*, 966–970.

Received: ((will be filled in by the editorial staff))
Published online: ((will be filled in by the editorial staff))

Transition metal complexes of 3-amino-1-nitroguanidine as laser ignitable primary explosives – structures and properties

Niko Fischer,^[a] Manuel Joas,^[a] Thomas M. Klapötke^{*,[a]}, Jörg Stierstorfer^[a] and Tobias Stürzer^[a]

^[a] Energetic Materials Research, Department of Chemistry,
University of Munich (LMU), Butenandtstr. 5–13, D-81377, Germany

Abstract:

3-Amino-1-nitroguanidine (ANQ, **1**) was synthesized via hydrazinolysis of nitroguanidine. By dissolving **1** in solutions containing transition metal salts, several complexes $M^{2+}(ANQ)_2X_2(H_2O)_y$ with $M^{2+} = Co, Ni, Cu, Zn$ as well as $M(ANQ)_2X(H_2O)_y$ with $M = Ag$ could be isolated. In these cases, nitrate as well as perchlorate and chloride served as the respective anions X. Additionally, the ANQ complexes of Co, Ni and Ag with dinitramide as the anion were synthesized from ANQ and silver dinitramide and by reacting the cobalt and nickel ANQ perchlorate complexes with ammonium dinitramide. The crystal structures of all described complexes were determined by low temperature single crystal X-ray diffraction. Additionally, they were characterized using IR spectroscopy and elemental analysis. The decomposition temperatures were determined by differential scanning calorimetry and the sensitivities towards impact and friction were assessed using a BAM drophammer and a BAM friction tester (BAM = Bundesanstalt für Materialforschung und –prüfung). Additionally, the sensitivity towards electrostatic discharge was determined on a small scale ESD device. The potential use of the nitrate, dinitramide and perchlorate containing species as primary explosives was investigated in a laser ignition test.

Keywords: 3-Amino-1-nitroguanidine; Crystal Structures; Laser Ignition; Primary Explosives; Sensitivities.

1 INTRODUCTION

In the continuous research towards new energetic materials high-energy capacity transition metal complexes became more and more popular.^{1,2,3} These materials mostly combine facile syntheses, good thermal stabilities with energetic properties similar to that of the prominent primary explosive lead azide which should be replaced due to its high toxicity. For the synthesis of energetic complexes especially nitrogen-rich heterocycles⁴ or guanidine based ligands can be used.

The guanidine building block is one of the first structural moieties that has been known to the chemical and biological community and was discovered as early as 1866, when the first

guanidine derivative was prepared by Hofmann.⁵ Since then, guanidine chemistry has evolved into an extremely wide ranging field of applications starting from bioorganic chemistry and biochemistry⁶ to inorganic chemistry, which most importantly can be traced back to a vast variability of derivatization of the guanidine moiety itself. Whereas a lot of correspondence can be found dealing with either aminated or nitrated guanidines such as aminoguanidine⁷ or nitroguanidine,⁸ only very few sources report on the synthesis⁹ and use of the mixed 3-amino-1-nitroguanidine (ANQ), which is the only today known guanidine derivative containing both, an amine and a nitro substituent. Nevertheless, it has found application as a useful intermediate for cyclization reactions yielding bis-nitraminotriazoles,¹⁰ for the synthesis of 5-nitriminotetrazole, which proceeds via a diazotization reaction and following cyclization of nitroguanyl azide,¹¹ or as a cationic species in ionic energetic materials.¹²

Due to the considerable amount of electron density at its amine and nitramine substituent, it expectedly shows fairly good characteristics as a ligand in transition metals complexes, which have not been described in literature before. Furthermore, while amine substituted guanidine derivatives are subject to oxidative decomposition in air, ANQ is stable under ambient conditions.

Ilyushin et al. report on the synthesis of a cobalt(III) complex bearing tetrazole as a ligand and perchlorate as the counterion and its use as nontoxic initiating explosive.¹³ Bearing this in mind, the choice of counterions was directed to anions such as the nitrate, dinitramide or perchlorate anion, which frequently have been reported as counterions in ionic energetic materials.^{14,15} The first reported synthesis of a dinitramide compound was that of its ammonium salt.¹⁶ To overcome the problems, which nowadays are discussed regarding the safe handling of commonly used primary explosives such as lead azide, which beside from being toxic, has a high impact and friction sensitivity, a new class of initiating charges, which are laser-ignitable primary explosives, are investigated.¹⁷ If insensitive towards impact and friction, these materials can easily be ignited by a short, but highly energetic laser pulse with a specific wave length. This considerably reduces the probability of being accidentally ignited, which oftentimes happened while handling the commonly used impact and friction sensitive primary explosives. Here, the use of transition metal complexes has already been discussed, whereas the exact mechanism, by which transition metal containing complexes are ignited upon laser irradiation, is still under investigation.

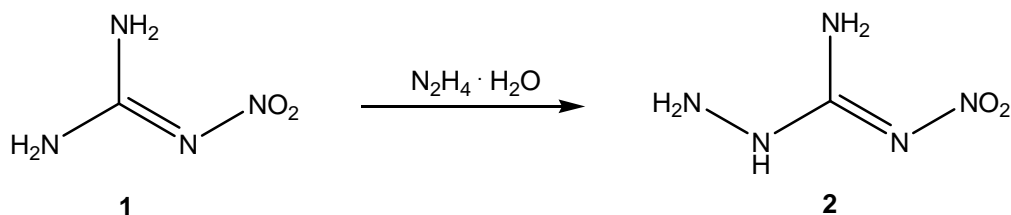
As possible candidates for laser ignitable primary explosives, the ANQ complexes of Co^{2+} , Ni^{2+} , Cu^{2+} , Zn^{2+} and Ag^+ with a choice of counterions (NO_3^- , $\text{N}(\text{NO}_2)_2^-$, ClO_4^- , Cl^-) were investigated including their synthesis and structure determination.

2 RESULTS AND DISCUSSION

2.1 Synthesis

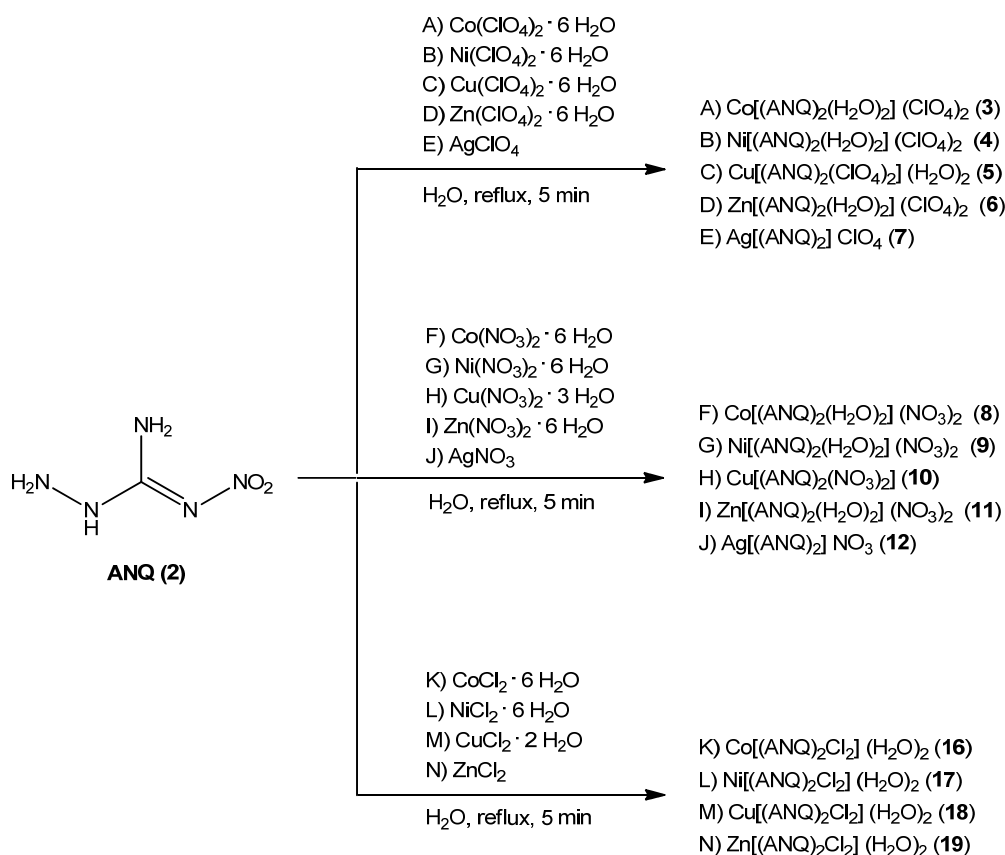
3-Amino-1-nitroguanidine (ANQ, **2**) was synthesized in aqueous solution employing a hydrazinolysis reaction of commercially available nitroguanidine (**1**), whereas it is important to

control the temperature accurately.¹⁸ The product itself shows fairly poor solubility in water and therefore can be recrystallized from hot water.



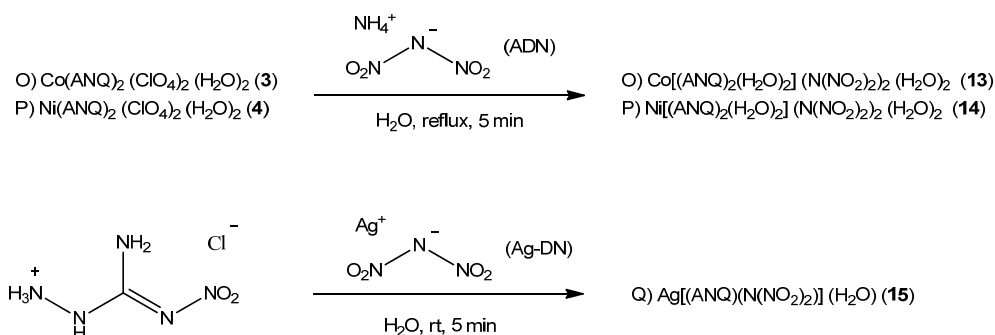
Scheme 1. Hydrazinolysis of nitroguanidine. Reaction conditions: stirring, 55 °C, 15 min.

The formation of the perchlorate, nitrate, and chloride based 3-amino-1-nitroguanidinium complexes **3–7**, **8–12** and **16–19** proceeds after dissolving the respective Co^{2+} , Ni^{2+} , Cu^{2+} , Zn^{2+} and Ag^+ perchlorates, nitrates or chlorides, as indicated in Scheme 2, in a boiling solution of ANQ. The stoichiometry of the reaction of ANQ: metal salt was chosen to be 1:1 instead of 2:1 (which is the stoichiometry found in the crystalline products), since poorly water soluble ANQ tends to precipitate from the mixture upon cooling down. In some cases precipitated ANQ indeed had to be filtered off from the mixture, before crystals of the complex began to grow, which especially was observed for the zinc(II) complexes. The yields of the described reactions were determined only of the first isolated fraction of crystals and lie between <10% and 49 %, which presumably can be optimized by further evaporation of the mother liquors.



Scheme 2. Formation of perchlorate, nitrate and chloride based 3-amino-1-nitroguanidinium complexes **3–7**, **8–12** and **16–19**.

The ANQ complexes bearing a dinitramide counterion in the cases of the cobalt and nickel complexes **13** and **14** were synthesized from the respective metal perchlorate containing solutions after addition of ammonium dinitramide in a stoichiometric ratio of metal perchlorate: ADN = 1:2. The advantage of the perchlorate containing solutions as starting material over the nitrate or chloride containing solutions is the better solubility of the metal-ANQ perchlorates as compared to the nitrates or chlorides, so that they do not precipitate before the dinitramides were isolated from the mother liquors. Using potassium dinitramide instead is disadvantageous because of the simultaneous precipitation of both potassium perchlorate and the metal-ANQ dinitramides. The silver complex was formed after combining solutions of 3-amino-1-nitroguanidinium chloride¹⁹ and acetonitrile stabilized silver dinitramide²⁰ in a 1:1 stoichiometric ratio. After filtering off AgCl, the silver-ANQ dinitramide monohydrate crystallizes from the mother liquor in colorless needles.



Scheme 3. Formation of dinitramide based 3-amino-1-nitroguanidinium complexes **13–15**.

2.2 Single Crystal X-ray structure analysis

The low temperature determination of the crystal structures of **3–19** were performed on a Oxford Xcalibur3 diffractometer with a Spellman generator (voltage 50 kV, current 40 mA) and a KappaCCD detector. The data collection and reduction were carried out using the CrysAlisPro software.²¹ The structures were solved either with SIR-92²² or SHELXS-97,²³ refined with SHELXL-97²⁴ and finally checked using the PLATON²⁵ software integrated in the WinGX²⁶ software suite. The absorptions were corrected by a Scale3 Abspack multi-scan method.²⁷ Selected data and parameter of the X-ray determinations are given in the Supplementary Information in Tables S1–S3. Cif files have been deposited within the Cambridge Crystallographic Data Centre using the CCDC Nos. 900148 (**3**), 900144 (**4**), 900147 (**5**), 900149 (**6**), 900143 (**7**), 900142 (**8**), 900139 (**9**), 900141 (**10**), 900146 (**11**), 900140 (**12**), 900155 (**13**), 900154 (**14**), 900138 (**15**), 900152 (**16**), 900153 (**17**), 900151 (**18**) and 900156 (**19**).

The ANQ ligand shows a similar structure in all investigated complexes in this work. Recently we published the structure of neutral ANQ as well as some inorganic salts.^{12,19} The ligand is almost planar. The C–N bonds are significantly shorter than C–N single bonds, with lengths between 1.28 and 1.38 Å. Coordination to the metal centres take place by the outer hydrazine nitrogen atom N4 and nitrogen atom N1. The coordination angles N1–M–N4 approximately increase with the following order. Ag (ca. 68°) < Zn = Co < Ni < Cu (ca. 80°).

[Co(ANQ)₂(H₂O)₂](ClO₄)₂ (**3**) crystallizes in the monoclinic space group *P*2₁/*c* with two formula units in the unit cell. The molecular moiety is depicted in Figure 1. A similar coordination sphere has been described for diaqua-tetrakis-picoline cobalt(II) diperchlorate.²⁸

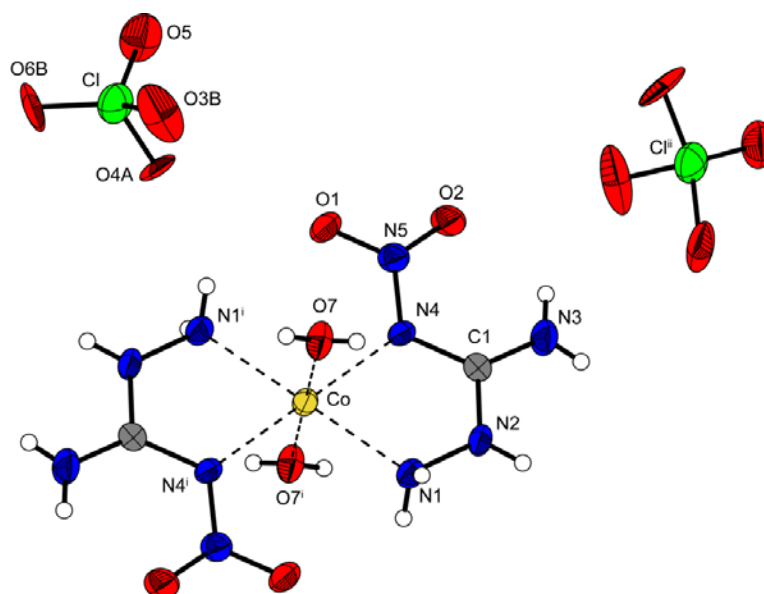


Figure 1 Molecular moiety of **3**. Thermal displacements of non-hydrogen atoms were set at 50 % probability. Hydrogen atoms are shown as spheres of arbitrary radius. Perchlorate anions are strongly disordered. Only selected split positions are depicted. Selected coordination distances (Å): Co–O7 2.088(3), Co–N4 2.108(3), Co–N1 2.130(3); angles (°): O7–Co–N4 89.24(11), O7–Co–N1 90.69(13), N4–Co–N1 75.76(11). Symmetry codes: (i) 1–x, –y, –z; (ii) 1–x, 0.5+y, 0.5–z.

The corresponding nickel complex $[\text{Ni}(\text{ANQ})_2(\text{H}_2\text{O})_2](\text{ClO}_4)_2$ (**4**) crystallizes in the orthorhombic space group $Pca2_1$ with four formula units in the unit cell. The molecular moiety is depicted in Figure 2. With the exception of the copper salt the densities of the perchlorates increase with rising atomic numbers (ρ [g cm^{–3}]: **3** (2.068) < **5** (2.128) < **4** (2.159) < **6** (2.193) < **7** (2.316)).

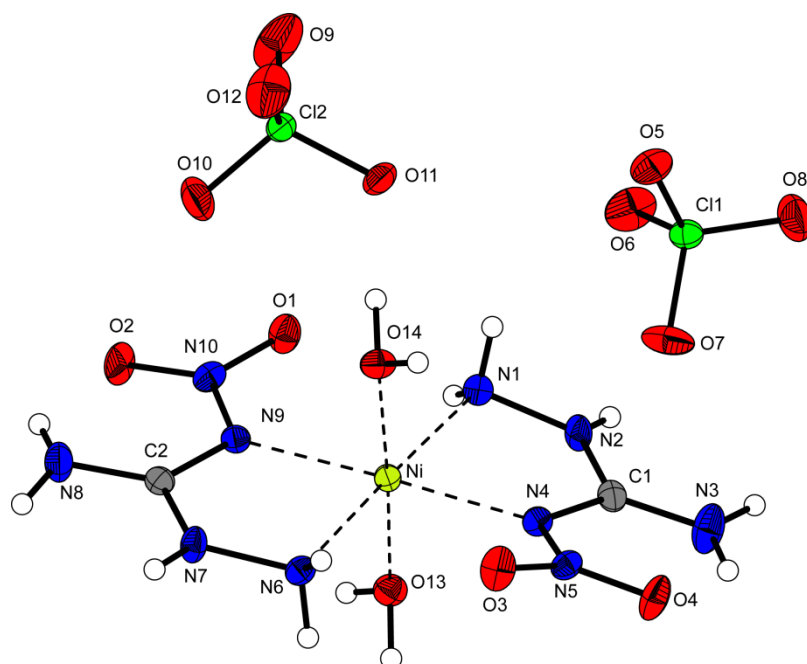


Figure 2 Molecular moiety of **4**. Thermal displacements of non-hydrogen atoms were set at 50 % probability. Hydrogen atoms are shown as spheres of arbitrary radius. Selected coordination distances (Å): Ni–N4 2.0692, Ni–O14 2.0764, Ni–N6 2.0821, Ni–N9 2.0877, Ni–N1 2.0891, Ni–O13 2.125; angles (°): N4–Ni–O14 94.8, N4–Ni–N6 101.9, O14–Ni–N6 86.6, O14–Ni–N9 87.0, N6–Ni–N9 77.5, N4–Ni–N1 76.7, O14–Ni–N1 95.0, N4–Ni–O13 88.4, N6–Ni–O13 93.9, N9–Ni–O13 89.8, N1–Ni–O13 84.5.

In agreement to all copper complexes investigated in this work, also $[\text{Cu}(\text{ANQ})_2(\text{ClO}_4)_2](\text{H}_2\text{O})_2$ (**5**) shows a Jahn-Teller²⁹ distorted octahedral coordination sphere due to the d^9 electron configuration. The elongation of the octahedron is due to longer Cu–OCIO₃ coordination bonds in comparison to the Cu–N coordination bonds which is similar described for dimethylethylenediamine bis-perchlorate.³⁰ The water molecules do not participate in metal coordination. The triclinic unit cell ($P\bar{1}$) contains one molecular moiety.

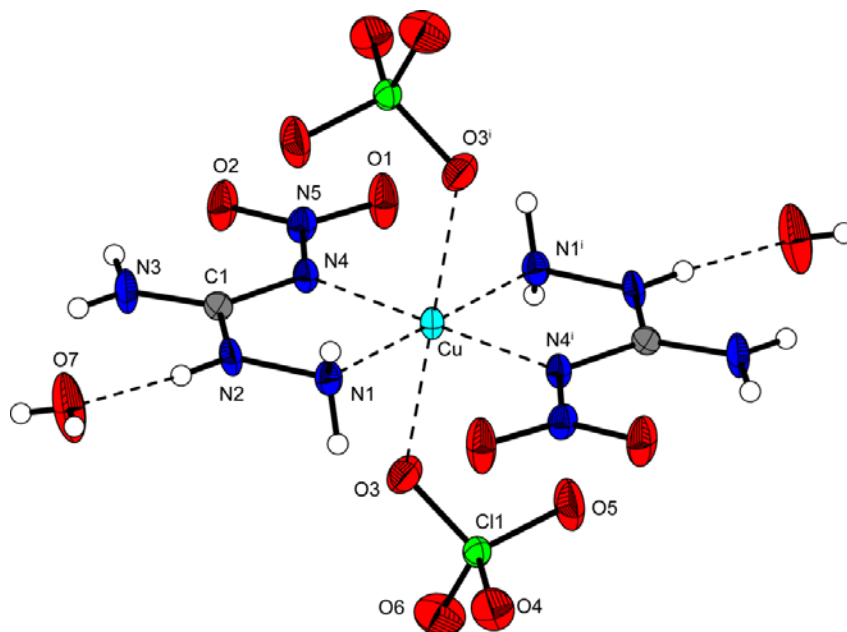


Figure 3 Molecular moiety of **5**. Thermal displacements of non-hydrogen atoms were set at 50 % probability. Hydrogen atoms are shown as spheres of arbitrary radius. Selected coordination distances (Å): Cu–N1 1.982(2), Cu–N4 2.032(2), Cu–O3 2.4364(19), angles (°): N1–Cu–N4 79.58(9), N1–Cu–O3 85.41(10), N4–Cu–O3 83.44(8). Symmetry codes: (i) $-x, 1-y, -z$.

The molecular structure of $[\text{Zn}(\text{ANQ})_2(\text{H}_2\text{O})_2](\text{ClO}_4)_2$ (**6**) is shown in Figure 4. The zinc(II) cations in **6**, which crystallizes in the monoclinic space group $P2_1/c$, have a centrosymmetric sixfold coordination sphere.

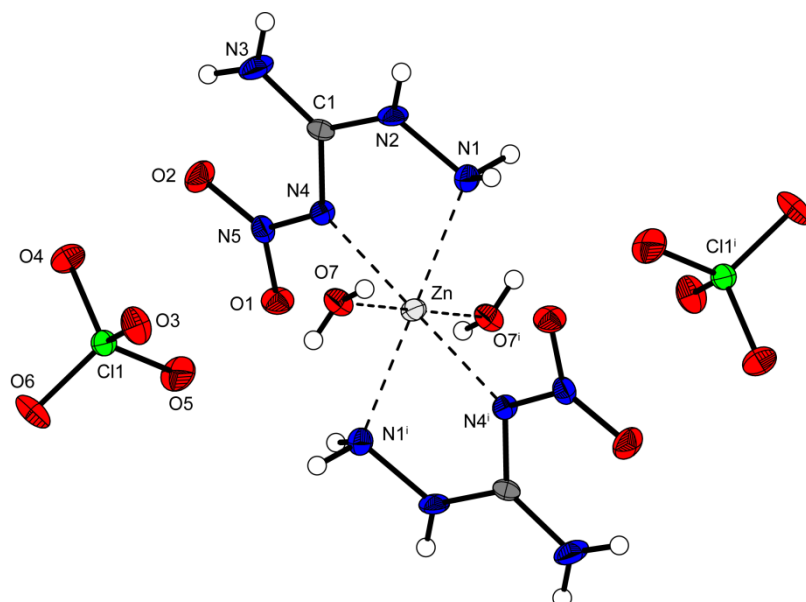


Figure 4 Molecular moiety of **6**. Thermal displacements of non-hydrogen atoms were set at 50 % probability. Hydrogen atoms are shown as spheres of arbitrary radius. Selected coordination distances (Å): Zn–N4 2.106(2), Zn–N1 2.148(2), Zn–O7 2.164(2); angles (°): N4–Zn–N1 74.70(8), N4–Zn–O7 88.51(8), N1–Zn–O7 84.43(10); . Symmetry codes: (i) $-x, 1-y, -z$.

The molecular moiety of $[\text{Ag}(\text{ANQ})_2]\text{ClO}_4$ (**7**), which crystallizes in the triclinic space group $P\bar{1}$, is depicted in Figure 5. The silver cations are coordinated by four nitrogen atoms in square planar arrangement.

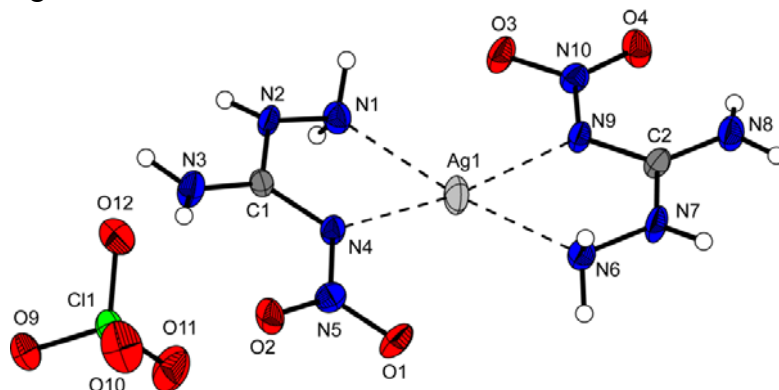


Figure 5 Molecular moiety of **7**. Thermal displacements of non-hydrogen atoms were set at 50 % probability. Hydrogen atoms are shown as spheres of arbitrary radius. Selected coordination distances (Å): Ag1–N4 2.346(3), Ag1–N9 2.359(3), Ag1–N1 2.374(3), Ag1–N6 2.396(3); angles (°): N4–Ag1–N9 175.12(8), N4–Ag1–N1 68.55(10), N9–Ag1–N1 116.31(10), N4–Ag1–N6 107.47(10), N9–Ag1–N6 67.88(10), N1–Ag1–N6 167.67(15).

One formula unit of $[\text{Co}(\text{ANQ})_2(\text{H}_2\text{O})_2](\text{NO}_3)_2$ (**8**) shown in Figure 6 is incorporated in the centrosymmetric triclinic unit cell. The nitrate anions do not participate in the coordination of the Co^{2+} centres.

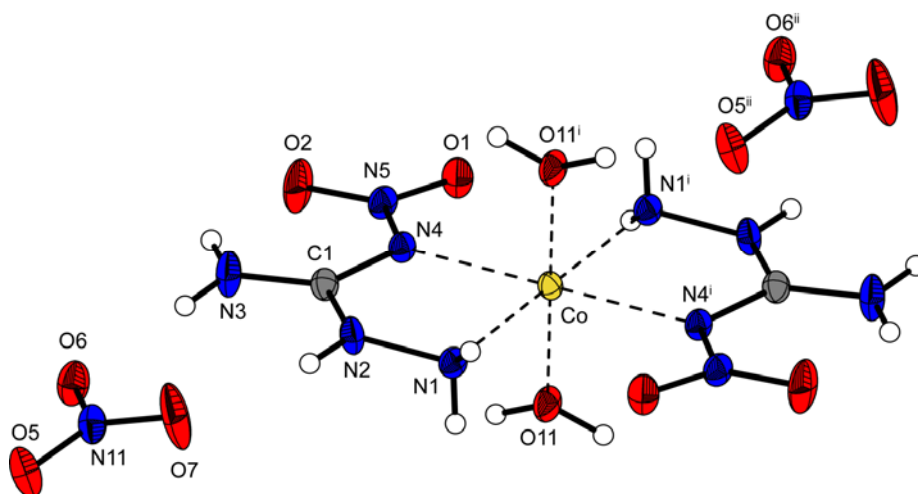


Figure 6 Molecular moiety of **8**. Thermal displacements of non-hydrogen atoms were set at 50 % probability. Hydrogen atoms are shown as spheres of arbitrary radius. Selected coordination distances (Å): Co–O11 2.0623(11), Co–N1 2.1307(14), Co–N4 2.1543(13); angles (°): O11–Co–N1 90.93(5), O11–Co–N4 88.74(5), N1–Co–N4 74.77(5). Symmetry codes: (i) $1-x, 1-y, -z$; (ii) $1-x, 1-y, -z$.

Figure 7 is used exemplarily for the molecular structures of $[\text{Ni}(\text{ANQ})_2(\text{H}_2\text{O})_2](\text{NO}_3)_2$ (**9**) and $[\text{Zn}(\text{ANQ})_2(\text{H}_2\text{O})_2](\text{NO}_3)_2$ (**11**). The complexes are crystallizing isotypically in the triclinic space group $P\bar{1}$ showing almost the same unit cell dimensions (Table S2) and densities (ρ [g cm^{-3}]: **9** (2.011), **11** (1.992).

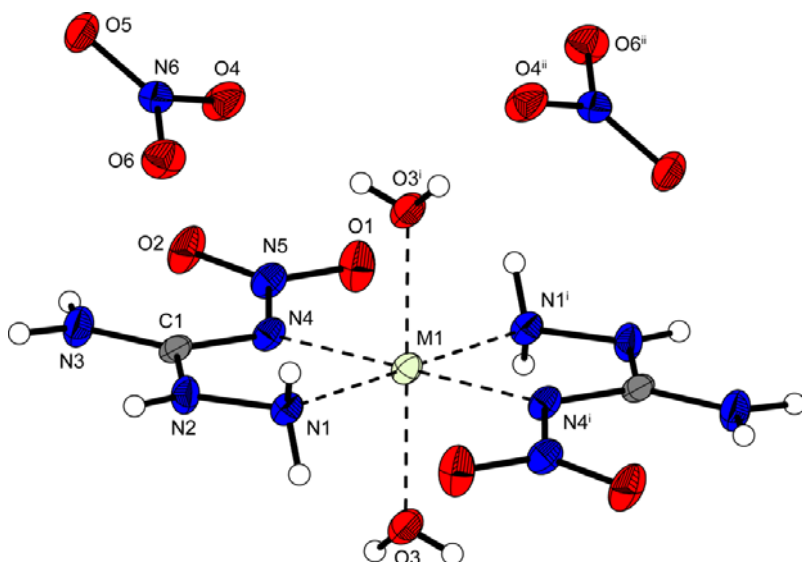


Figure 7 Molecular moiety of **9** (M1 = Ni) and **11** (M1 = Zn). Thermal displacements of non-hydrogen atoms were set at 50 % probability. Hydrogen atoms are shown as spheres of arbitrary radius. Selected coordination distances (Å): **9**: Ni–N1 2.0587(19), Ni–O3 2.0805(18), Ni–N4 2.1023(19); **11**: Zn–N1 2.1144(17), Zn–O3 2.1315(15), Zn–N4 2.1650(15); angles (°) **9**: N1–Ni–O3 86.99(8), N1–Ni–N4 77.27(7), O3–Ni–N4 92.03(8); **11**: N1–Zn–O6 91.33(7), N1–Zn–N4 75.66(6), O6–Zn–N4 87.98(7). Symmetry codes: (i) 2–x, 1–y, 1–z; (ii) 1–x, 1–y, 1–z.

The copper complex [Cu(ANQ)₂(NO₃)₂] (**10**) is shown in Figure 8. It crystallizes in the monoclinic space group *C2/c* with a density of 2.171 g cm^{–3}. The Cu²⁺ cations reveal a distorted octahedral coordination sphere. This is indicated by the Cu–O bond lengths, which significantly differ from each other and the O5–Cu–O8 angle of ~160°.

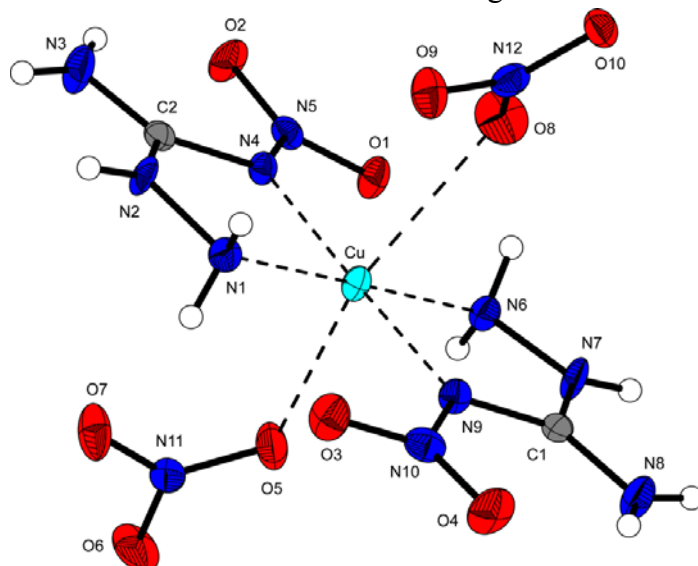


Figure 8 Molecular moiety of **10**. Thermal displacements of non-hydrogen atoms were set at 50 % probability. Hydrogen atoms are shown as spheres of arbitrary radius. Selected coordination distances (Å): Cu–N6 1.982(2), Cu–N1 1.989(2), Cu–N4 2.0326(19), Cu–N9 2.0370(19), Cu–O5 2.3382(19); Cu–O8 2.586(2); angles (°): N6–Cu–N1 178.8(1), N6–Cu–N4

99.67(8), N1–Cu–N4 79.69(8), N6–Cu–N9 79.02(9), N1–Cu–N9 101.65(9), N4–Cu–N9 178.13(8), N6–Cu–O5 84.27(9), N1–Cu–O5 94.70(9), N4–Cu–O5 94.28(7), N9–Cu–O5 86.93(8), O5–Cu–O8 160.18(7).

The density of complex [Ag(ANQ)₂NO₃] (**11**) is considerably smaller (2.235 g cm⁻³) than that observed for silver(I) nitrate (4.35 g cm⁻³).³¹ The silver cations in the structure of **11**, which crystallizes in the orthorhombic space group *Pbca*, are distorted tetrahedrally coordinated by only nitrogen atoms.

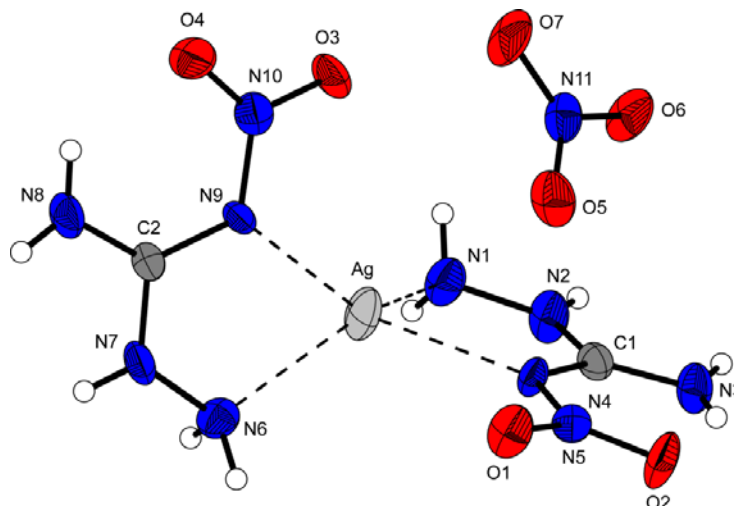


Figure 9 Molecular moiety of **12**. Thermal displacements of non-hydrogen atoms were set at 50 % probability. Hydrogen atoms are shown as spheres of arbitrary radius. Selected coordination distances (Å): Ag–N6 2.344(4), Ag–N1 2.328(3), Ag–N9 2.301(3), Ag–N4 2.318(2); angles (°): N9–Ag–N4 145.28(10), N9–Ag–N1 130.40(12), N4–Ag–N1 69.55(11), N9–Ag–N6 69.33(11), N4–Ag–N6 122.72(11), N1–Ag–N6 131.09(16).

The dinitramide complexes **13** and **14** crystallize isotypically as tetrahydrates in the monoclinic crystal system within the space group *P2₁/c*. Two water molecules participate in the coordination sphere, while the others are connected to the dinitramide anions by formation of hydrogen bonds (see Figure 10). The density of the cobalt complex **13** is slightly lower (1.964 g cm⁻³) than that of nickel complex **14** (1.982 g cm⁻³). The dinitramide anions are not planar and follow the twisted structure observed for e.g. lithium and potassium dinitramide.³²

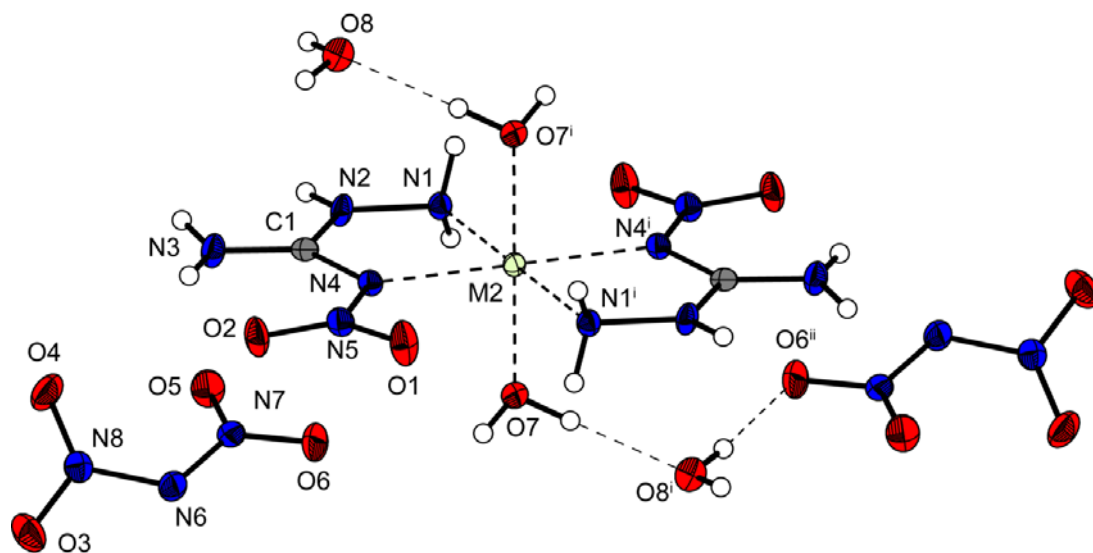


Figure 10 Molecular moiety of **13** ($M2 = \text{Co}$) and **14** ($M2 = \text{Ni}$). Thermal displacements of non-hydrogen atoms were set at 50 % probability. Hydrogen atoms are shown as spheres of arbitrary radius. Selected coordination distances (\AA): **13**: $\text{Co}-\text{O}7$ 2.0998(12), $\text{Co}-\text{N}1$ 2.1128(14), $\text{Co}-\text{N}4$ 2.1413(13); **14**: $\text{Ni}-\text{N}1$ 2.0652(13), $\text{Ni}-\text{O}7$ 2.0877(11), $\text{Ni}-\text{N}4$ 2.1024(12); angles ($^\circ$) **13**: $\text{O}7-\text{Co}-\text{N}1$ 89.87(6), $\text{O}7-\text{Co}-\text{N}4$ 90.67(5), $\text{N}1-\text{Co}-\text{N}4$ 76.44(5); **14**: $\text{N}1-\text{Ni}-\text{O}7$ 90.76(5), $\text{N}1-\text{Ni}-\text{N}4$ 78.19(5), $\text{O}7-\text{Ni}-\text{N}4$ 89.47(5). Symmetry codes: (i) $1-x$, $1-y$, $1-z$.

The silver complex **15** could only be obtained crystalline (monoclinic, $P2_1/c$) as a monohydrate. The molecular motif is shown in Figure 11. The density of 2.456 g cm^{-3} is the highest observed in this work and is similar to that (2.488 g cm^{-3}) of silver dinitramide as its acetonitrile adduct.³³

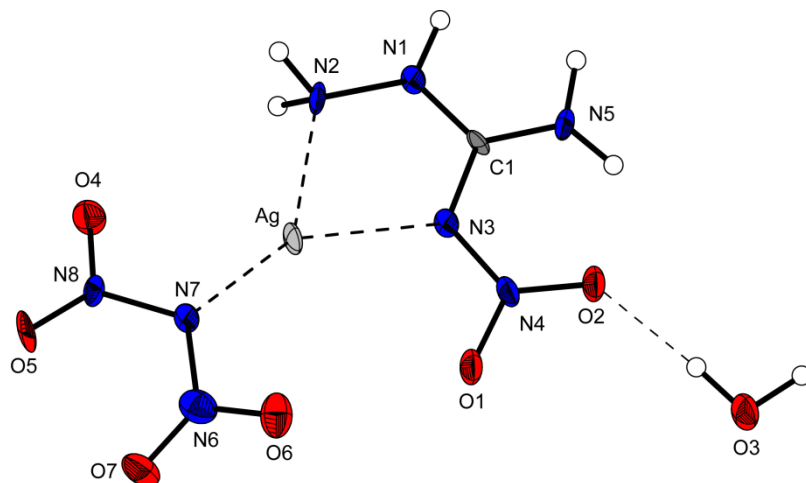


Figure 11 Molecular moiety of **15**. Thermal displacements of non-hydrogen atoms were set at 50 % probability. Hydrogen atoms are shown as spheres of arbitrary radius. Selected coordination distances (\AA): $\text{Ag}-\text{N}7$ 2.147(9), $\text{Ag}-\text{N}3$ 2.260(9), $\text{Ag}-\text{N}2$ 2.340(10); angles ($^\circ$): $\text{N}7-\text{Ag}-\text{N}3$ 147.4(4), $\text{N}7-\text{Ag}-\text{N}2$ 142.3(3), $\text{N}3-\text{Ag}-\text{N}2$ 70.1(3).

Remarkably, the chlorido complexes $[\text{M}(\text{ANQ})\text{Cl}_2](\text{H}_2\text{O})_2$ (**16** ($\text{M}=\text{Co}^{2+}$), **17** ($\text{M}=\text{Ni}^{2+}$) and **19** ($\text{M}=\text{Zn}^{2+}$)) investigated in this work crystallize isotypically in the monoclinic space group $P2_1/n$. Also **18** shows very similar unit cell dimensions, however for the space group $P2_1/c$.

The molecular unit for **16**, **17** and **19** is depicted in Figure 12. In contrast to the crystal water molecules the chlorido anions are enclosed in coordination. The densities of **16** (1.927 g cm^{-3}), **17** (1.950 g cm^{-3}), **18** (1.945 g cm^{-3}) and **19** (1.944 g cm^{-3}) are similar and in total the lowest observed in this work.

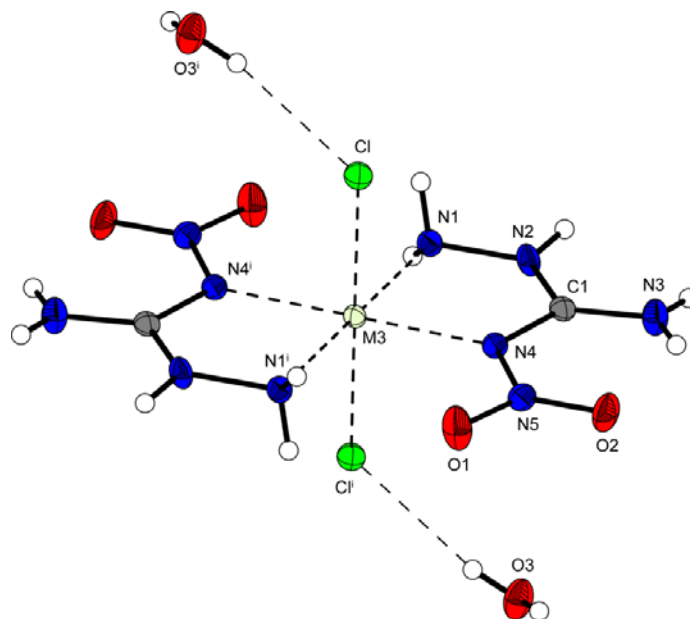


Figure 12 Molecular moiety of **16** ($M3 = \text{Co}$), **17** ($M3 = \text{Ni}$), and **19** ($M3 = \text{Zn}$). Thermal displacements of non-hydrogen atoms were set at 50 % probability. Hydrogen atoms are shown as spheres of arbitrary radius. Selected coordination distances (\AA): **16**: Co-N1 2.1212(14), Co-N4 2.1305(13), Co-Cl 2.4810(4); **17**: Ni-N1 2.0651(13), Ni-N4 2.0949(12), Ni-Cl 2.4600(4); **18**: Cu-N1 1.997(2), Cu-N4 2.053(2), Cu-Cl 2.7155(7); **19**: Zn-N1 2.1071(15), Zn-N4 2.1439(14), Zn-Cl 2.5473(4); angles ($^\circ$) **16**: N1-Co-N4 75.69(5), N1-Co-Cl 90.66(4), N4-Co-Cl 90.61(4); **17**: N1-Ni-N4 77.66(5), N1-Ni-Cl 89.71(4), N4-Ni-Cl 89.46(3); **18**: N1-Cu-N4 79.14(8), N1-Cu-Cl 89.11(7), N4-Cu-Cl 89.90(6); **19**: N1-Zn-N4 76.18(6), N1-Zn-Cl 89.24(5), N4-Zn-Cl 89.41(4). Symmetry codes: (i) $1-x, -y, 1-z$.

As already observed for the coordination sphere of the cations in **16**, **17** and **19**, the copper cations in **18** possess an elongated octahedral coordination sphere due to the Jahn Teller effect. The copper chlorine coordination bonds are much longer ($\sim 2.71 \text{ \AA}$) than the Cu-O bonds in the previously described complexes **5** and **10**. This is in agreement to the recently published structure of dichlorido-tetrakis-1,2,4-triazole copper(II) where the Cu-Cl bonds are even longer (2.83 \AA).³⁴

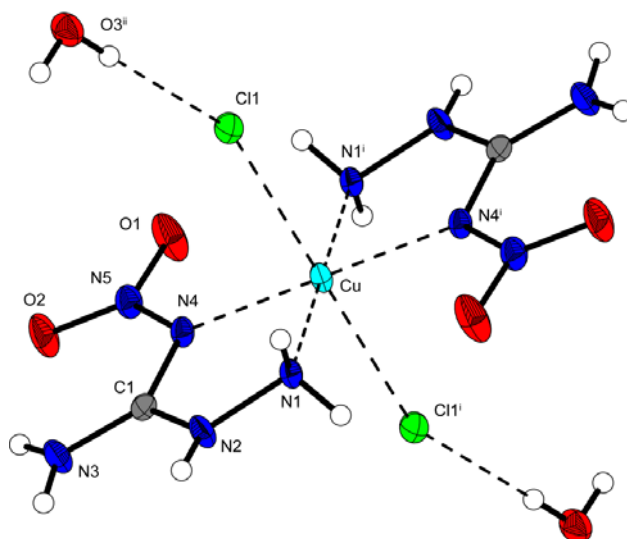


Figure 13 Molecular moiety of **18**. Thermal displacements of non-hydrogen atoms were set at 50 % probability. Hydrogen atoms are shown as spheres of arbitrary radius. Selected coordination distances (Å): Cu–N1 1.997(2), Cu–N4 2.053(2), Cu–Cl 2.7155(7); angles (°): N1–Cu–N4 79.14(8), N1–Cu–Cl 89.11(7), N4–Cu–Cl 89.90(6); Symmetry codes: (i) $-x, -y, 2-z$; (ii) $-x, -0.5+y, 0.5-z$.

2.3. IR spectroscopy

The assignments of absorptions were undertaken referring to values reported in literature.^{14,35} Strong absorptions are observed in all spectra in the region above 3000 cm^{-1} , indicating N–H and O–H valence vibrations. Here, the N–H valence vibration of the hydrazine moiety of the ligand is visible as a relatively sharp absorption band at $3430\text{--}3378\text{ cm}^{-1}$. This is in contrast to the absorptions of O–H valence vibrations at around $3300\text{--}3200\text{ cm}^{-1}$ of the crystal water containing complexes, which are broadened due to hydrogen bond formation. In comparison to the IR absorptions of neutral, uncomplexed ANQ, the N–H valence vibrations are observed at somewhat lower energies if complexed (3551 cm^{-1} in ANQ). Other important absorptions are the anti-symmetric and the symmetric N–O valence vibration of the nitramine moiety both of which are present as strong absorptions in all spectra at $1687\text{--}1651\text{ cm}^{-1}$ (asym) and $1297\text{--}1275\text{ cm}^{-1}$ (sym). For both absorptions again lower wave numbers are observed as compared to uncomplexed ANQ, which reveals values of 1692 cm^{-1} and 1329 cm^{-1} for the absorptions of the aforementioned vibrations. A relatively strong absorption at $1245\text{--}1203\text{ cm}^{-1}$ can be assigned to the N–N valence vibration of the nitramine moiety, whereas a second absorption, however at slightly lower energy ($1139\text{--}1097\text{ cm}^{-1}$) attributes to the N–N valence vibration of the hydrazine moiety of the ligand. Furthermore, the characteristic absorptions of the nitrate and the perchlorate anion at $1385\text{--}1382$ and $1097\text{--}1083\text{ cm}^{-1}$ are observed in the respective IR spectra. The dinitramide anion can be detected by strong absorptions at $1539\text{--}1529\text{ cm}^{-1}$ (asymmetric in phase N–O valence vibration) and $1434\text{--}1431\text{ cm}^{-1}$ (asymmetric out of phase N–O valence vibration).

2.4. Sensitivities and thermal stability

The impact sensitivity tests were carried out according to STANAG 4489³⁶ modified instruction³⁷ using a BAM (Bundesanstalt für Materialforschung) drophammer.³⁸ The friction sensitivity tests were carried out according to STANAG 4487³⁹ modified instruction⁴⁰ using the BAM friction tester. The classification of the tested compounds results from the “UN Recommendations on the Transport of Dangerous Goods”.⁴¹ Additionally all compounds were tested upon the sensitivity towards electrical discharge using the Electric Spark Tester ESD 2010 EN.⁴² Since the described complexes are transition metal complexes with an energetic ligand together with energetic counterions such as nitrate, perchlorate and dinitramide, we expect enhanced sensitivities towards outer stimuli. The perchlorates **3–7** are very sensitive towards impact, some of them (**5**, **7**) even bearing values of less than 1 J, which in the case of the silver complex is not least due to fact, that it crystallizes water free. Also the friction sensitivities are in a range between very sensitive (**3–6**) and extremely sensitive (**7**). The complexes bearing a nitrate counterion (**8–12**) at an average are less sensitive towards impact and friction than the perchlorate containing compounds, however they are still sensitive towards impact with two exceptions, the copper (**10**) and the silver (**12**) complex, which crystallize water free, again are very sensitive towards impact, a trend, which already has been observed for the perchlorate containing compounds **5** and **7**. Almost the same argumentation can be applied to the friction sensitivities of the nitrates. Interestingly, the dinitramides **13–15**, while still being comparatively sensitive, do not reach the high sensitivity levels of e.g. **7**, **10** and **12** in terms of impact as well as friction sensitivity, presumably due to the inclusion of four (**13,14**) and one (**15**) molecule of crystal water per formula unit, respectively. Holding no energetic anion, the four chloride complexes **16**, **17** and **19** show moderate impact sensitivity and are less sensitive towards friction. Unfortunately, the yields of **18** allowed no determination of sensitivities..

Differential scanning calorimetry (DSC) measurements to determine the dehydration- and decomposition temperatures of **3–17** and **19** (about 1.5 mg of each energetic material) were performed in covered Al-containers containing a hole in the lid and a nitrogen flow of 20 mL per minute on a Linseis PT 10 DSC⁴³ calibrated by standard pure indium and zinc at a heating rate of 5 °C min⁻¹. All decomposition temperatures are given as absolute onset temperatures, whereas dehydration temperatures are set at the minimum of the endothermic peak in the DSC curve.

Several interesting trends can be observed while comparing the decomposition temperatures of the complexes **3–17** and **19**. The nickel complexes reveal the highest decomposition temperatures if compounds bearing the same anion are compared to each other (e.g. **4**: 230 °C). For the perchlorates and nitrates, the zinc complexes follow the nickel complexes (e.g. **6**: 198 °C) having the second highest decomposition temperatures again followed by the cobalt complexes (e.g. **3**: 176 °C). The silver and especially the copper complexes decompose at relatively low temperatures oftentimes even below 100 °C (e.g. **5**: 134 °C, **10**: 77 °C). Comparing complexes with the same metal ion, the perchlorates have higher decomposition temperatures as the nitrates (e.g. **7**: 148 °C, **12**: 142 °C). Most of the chlorides show decomposition at even higher temperatures as the perchlorates except for the zinc complex (**19**: 172 °C). The dinitramides expectedly decompose at relatively low temperatures (**13**: 118 °C, **14**: 142 °C), whereas the trend of higher decomposition temperatures of the nickel complexes

is again confirmed. A detailed list of all decomposition and dehydration temperatures as well as the sensitivities towards impact, friction and electrostatic discharge can be found in Table 1. Most of the crystal water containing complexes can be dehydrated after heating (**4**, **6**, **11**, **13**, **14–16**, **19**) indicated by an endothermic peak in the DSC curve, which is well separated from the exothermic decomposition event. Some of the complexes decompose immediately after they start to lose their crystal water (**3**, **5**, **9**, **14**), whereas for **8** no endothermic event before decomposition can be observed although it crystallizes as a dihydrate.

Table 1. Sensitivities and thermal behaviour of **3–19**.

	IS (J)	FS (N)	ESD (J)	T _{dehydr} (°C)	T _{dec} (°C)
3	3	10	0.03	170 ^a	176
4	3	10	0.04	162	230
5	<1	16	0.50	120 ^a	134
6	3	28	0.30	108, 154	198
7	<1	<5	0.01	- ^b	148
8	9	80	0.70	- ^c	139
9	4	120	0.08	160 ^a	186
10	<1	<5	0.50	- ^b	77
11	5	120	0.50	119	181
12	<1	<5	0.01	- ^b	142
13	5	80	0.70	85	118
14	3	80	0.60	138 ^a	142
15	2	7	0.10	71	108
16	10	360	0.70	144	186
17	10	360	0.70	150	250
19	10	360	0.70	104	172

^a decomposition (exothermic) occurs immediately after dehydration (endothermic)

^b no crystal water contained

^c no dehydration (endothermic event) observed before decomposition (exothermic event)

2.5. UV-Vis-NIR spectroscopy and laser ignition tests

Further, the synthesized metal complexes **3**, **4**, **5** and **7** were investigated upon their behavior towards single pulsed laser irradiation at a wavelength of 940 nm and a pulse length of 100 μs. The cobalt(II) complex **3**, copper(II) complex **5** and also the silver(I) complex **7** could be initiated by a single pulse laser beam and led to detonation of samples, which previously to the experiment were pressed into pellets of approximately 8 mm diameter and 2 mm thickness. The nickel(II) complex **4** and all corresponding nitrate complexes **8–12** as well as even the complexes holding the highly energetic dinitramide anion **13–15** did not show any response to laser irradiation. The laser initiation mechanism (electronically, thermally, etc.) of transition state metal complexes is still unknown. Related to that, the UV-Vis-NIR reflectance of the solid samples **3** (Co[(ANQ)₂(H₂O)₂](ClO₄)₂), **4** (Ni[(ANQ)₂(H₂O)₂](ClO₄)₂), **5** (Cu[(ANQ)₂(ClO₄)₂](H₂O)₂) and **7** (Ag[(ANQ)₂](ClO₄)) were measured on a *Varian Cary 500* spectrometer in a wavelength range of 350–1300 nm. The measured diffuse reflectance *R* [%]

was transformed after applying the KUBELKA–MUNK equation (1) to give the absorption function $F(R)$ (no unit).⁴⁴

$$\frac{K}{S} = \frac{(1-R_{\infty})^2}{2R_{\infty}} \quad (1)$$

K : absorption component

S : scattering component

R_{∞} : reflectance of an infinite thick sample

The step in the absorption intensity $F(R)$ at 800 nm in Figure 14 is caused by a detector change. The spectra have only qualitative character. Due to technical limits no quantitative information about the absorption intensity can be obtained from the spectra. Commonly, R_{∞} is technically approximated by a sample layer thick enough that the measuring instrument cannot detect differences in the thickness-dependent diffuse reflectance. However, not all samples could be coated on the object plate thick enough that there were no differences detectable anymore.

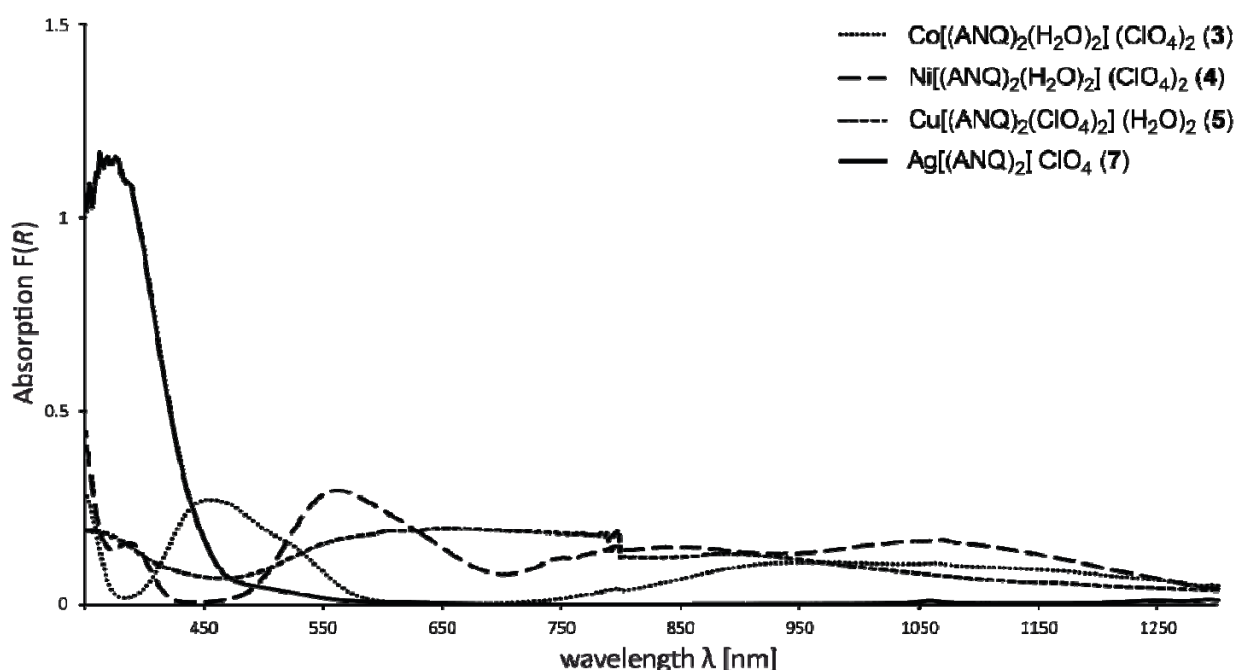


Figure 14. UV-Vis-NIR spectra of complexes **3–5** and **7**. The absorption function $F(R)$ is obtained after applying the Kubelka-Munk equation.

The information obtained from the UV-Vis-NIR spectra essentially is, that the four samples considerably differ in their absorption only at wavelengths in the visible and near UV region of the electromagnetic spectrum, what we would expect of four obviously differently colored samples. However in the NIR region, the samples **3–5** equally absorb radiation, especially at 940 nm, which is the wavelength of the laser beam used for laser initiation experiments. However, the silver complex shows no absorption at this wavelength.

Considering, that all metal perchlorates **3–5** except the silver(I) complex **7** were light absorbing at 940 nm together with the initiation results it seems that there is no relation

between optical absorption properties and the photosensitivity towards pulsed laser irradiation which is in agreement with the laser initiation experiments made by Ilyushin *et al.*^{13,45} The fact that only perchlorate compounds and no nitrates could be initiated fits to the literature claimed initiation mechanism where an active perchlorate radical is formed by a one-electron transfer from the perchlorate anion to the metal cation induced by the laser beam.⁴⁵

Consequently, it seems, that the initiation of energetic materials by a short pulsed laser beam rather is an electronic process than a thermal one, especially when comparing the decomposition temperatures of the samples with their laser ignitability. For example, Cu[(ANQ)₂(NO₃)₂] (**10**) could not be initiated by the laser beam but shows the lowest thermal stability ($T_{\text{dec.}} = 77\text{ }^{\circ}\text{C}$) of the investigated compounds.

The role of the nature of the ligand in the laser initiation process is not yet fully understood and therefore under current investigation.

3 CONCLUSION

From the experimental study of energetic complexes based on 3-amino-1-nitroguanidine the following conclusions can be drawn:

- Combining boiling solutions of 3-amino-1-nitroguanidine (ANQ) and a transition metal (M = Co, Ni, Cu, Zn, Ag) perchlorate (X = ClO₄) or nitrate (X = NO₃) affords complexes M²⁺(ANQ)₂(X⁻)₂(H₂O)_n (n = 0, 2) in the case of Co, Ni, Cu and Zn or M⁺(ANQ)₂(X⁻) in the case of Ag, which readily crystallize from their aqueous mother liquors, however in minor yields. For Co, Ni, Cu and Zn, also the respective chlorides M²⁺(ANQ)₂(X⁻)₂(H₂O)₂ were isolated following the same procedure.
- Complexes M²⁺(ANQ)₂(X⁻)₂(H₂O)₄ with X = (N(NO₂)₂)₂ were isolated in the case of M = Co and Ni starting from the respective perchlorate containing complexes upon addition of ammonium dinitramide to the solutions. Ag(ANQ)₂(N(NO₂)₂)(H₂O) crystallized after combining solutions of silver dinitramide and 3-amino-1-nitroguanidinium chloride (ANQ⁺Cl⁻).
- The complexes crystallize in the space groups *P*-1 (**5**, **7–9**, **11**), *P*2₁/*c* (**3**, **6**, **13–15**, **18**), *P*2₁/*n* (**16**, **17**, **19**), *C*2/*c* (**10**), *Pca*2₁ (**4**) and *Pbca* (**12**) with densities between 1.927 (**16**) and 2.456 (**15**), whereas perchlorates, if hydrated, reveal higher densities than nitrates and chlorides. The highest densities are observed for the silver complexes.
- All perchlorate, nitrate and chloride containing complexes crystallize as dihydrates, except for the silver complexes **7** and **12** and the copper complex **10**, which crystallize water free. The dinitramides crystallize as tetrahydrates (**13**, **14**) and monohydrate (**15**) respectively. Most of the crystal water containing complexes can be dehydrated (**4**, **6**, **11**, **13**, **15–19**) without decomposition.
- Nickel complexes generally show the highest decomposition temperatures (**17**: 250 °C), whereas copper and silver complexes decompose at relatively low temperatures (**10**: 77 °C). Also a trend of higher decomposition temperatures for chlorides and perchlorates as compared to nitrates and dinitramides is observed.

- All complexes bearing energetic counterions show enhanced sensitivities towards impact and friction, which especially applies to the solvate water free silver and copper complexes **7**, **10** and **12** with values of <1 J (IS) and <5 N (FS).
- All perchlorate, nitrate and dinitramide containing complexes were tested upon their laser ignitability with a 100 μ s laser pulse at 940 nm. Only the perchlorate containing complexes **3**, **5** and **7** could successfully be initiated.
- UV-Vis-NIR spectra of the perchlorate containing complexes **3–5** and **7** were recorded and show, that there is no relationship between their absorption behavior at the designated wavelength of the laser beam (940 nm) and their initiation properties.

4 EXPERIMENTAL PART

Caution! The herein described metal complexes of ANQ are energetic materials with increased sensitivities towards shock and friction. Therefore, proper safety precautions (safety glass, face shield, earthed equipment and shoes, Kevlar[®] gloves and ear plugs) have to be applied while synthesizing and handling the described compounds. All chemicals and solvents were employed as received (Sigma-Aldrich, Fluka, Acros). ¹H and ¹³C and ¹⁵N NMR spectra were recorded using a JEOL Eclipse 270, JEOL EX 400 or a JEOL Eclipse 400 instrument. The chemical shifts quoted in ppm in the text refer to typical standards such as tetramethylsilane (¹H, ¹³C) or nitromethane (¹⁵N). To determine the melting and decomposition temperatures of the described compounds a Linseis PT 10 DSC (heating rate 5 °C min⁻¹) was used. Infrared spectra were measured using a Perkin Elmer Spectrum One FT-IR spectrometer as KBr pellets. Raman spectra were recorded on a Bruker MultiRAM Raman Sample Compartment D418 equipped with a Nd-YAG-Laser (1064 nm) and a LN-Ge diode as detector. Mass spectra of the described compounds were measured at a JEOL MStation JMS 700 using FAB technique. To measure elemental analyses a Netsch STA 429 simultaneous thermal analyzer was employed.

3-Amino-1-nitroguanidine (**2**)

Commercially available nitroguanidine (20 % H₂O, 25 g, 192 mmol) is dispensed in 250 mL of water and the mixture is heated to 55 °C. Hydrazine hydrate (10.5 mL, 216 mmol) is added dropwise over a period of 15 min and the temperature is kept at 55°C for further 15 min under constant stirring. After the mixture turned to a clear, orange solution, it is cooled down to room temperature in an ice bath and the reaction is quenched with conc. hydrochloric acid (pH 7). 3-amino-1-nitroguanidine starts to precipitate after the solution has been cooled down to 4 °C overnight. The product is separated by filtration and recrystallized from hot water. Yield: 10.3 g (86 mmol, 45%).

DSC (5 °C min⁻¹, °C): 184°C (dec. 1), 200°C (dec.2); IR (KBr, cm⁻¹): $\tilde{\nu}$ = 3551 (s), 3411 (s), 3234 (s), 2025 (w), 1692 (m), 1637 (s), 1616 (vs), 1545 (m), 1502 (m), 1443 (m), 1384 (m), 1329 (m), 1134 (m), 1108 (m), 1088 (m), 1031 (m), 1005 (w), 963 (w), 870 (w), 772 (w), 745 (w), 696 (w), 622 (m), 571 (w), 482 (m); Raman (1064 nm, 200 mW, 25 °C, cm⁻¹): $\tilde{\nu}$ = 3319 (4), 3255 (13), 1659 (5), 1616 (4), 1580 (32), 1381 (13), 1287 (32), 1190 (5), 1111 (39), 1019 (5), 961 (100), 770 (27), 483 (30), 419 (33), 378 (10), 248 (13); ¹H NMR (DMSO-*d*₆, 25 °C, ppm) δ : 9.29 (s, 1H, NH), 8.23 (s, 1H, C–NH_AH_B), 7.52 (s, 1H, C–NH_AH_B), 4.64 (s, 2H,

N-NH₂); ¹³C NMR (DMSO-*d*₆, 25 °C, ppm) δ: 161.5 (C(NNO₂)(N₂H₄)(NH₂)); ¹⁵N NMR (DMSO-*d*₆, 25 °C, ppm) δ: -13.3 (NO₂), -146.3 (NNO₂), -276.4 (NH/NH₂), -301.8 (NH/NH₂), -327.9 (NH/NH₂); MS (FAB⁻): *m/z* = 117.99 [M-H]⁻; EA (CH₅N₅O₂, 119.08) calc.: C 10.09, H 4.23, N 58.81 %; found: C 10.51, H 4.32, N 58.90 %; BAM drophammer: 20 J; friction tester: 144 N; ESD: 0.15 J (at grain size 100–500 μm).

bis-(3-amino-1-nitroguanidine) cobalt(II) perchlorate dihydrate (3)

3-amino-1-nitroguanidine (0.50 g, 4.23 mmol) is dissolved in 20 mL of boiling water. Cobalt(II) perchlorate hexahydrate (1.548 g, 4.23 mmol) is added and the mixture is boiled until a clear solution results. The clear solution is filtered and slowly cooled down to room temperature. After a few days the product starts to crystallize as red blocks. Yield: 35% (788 mg, 1.48 mmol). The crystal density is 2.068 g cm⁻³.

DSC (5 °C min⁻¹, °C): 176 °C (dec.); IR (KBr, cm⁻¹): $\tilde{\nu}$ = 3548 (m), 3407 (s), 3321 (s), 3303 (s), 2964 (w), 2615 (w), 2231 (w), 2135 (w), 2059 (w), 1660 (s), 1579 (w), 1508 (m), 1480 (m), 1424 (m), 1385 (m), 1278 (s), 1211 (s), 1097 (vs), 938 (m), 820 (w), 808 (w), 779 (m), 717 (w), 671 (w), 663 (w), 627 (m), 599 (m), 520 (m); EA (C₂H₁₄Cl₂N₁₀O₁₄Co, 532.03): calcd: C 4.52, H 2.65, N 26.33%; found: C 3.96, H 2.60, N 23.03%. BAM drophammer: 3 J; friction tester: 10 N; ESD: 0.03 J (at grain size 500–1000 μm).

bis-(3-amino-1-nitroguanidine) nickel(II) perchlorate dihydrate (4)

3-amino-1-nitroguanidine (0.50 g, 4.23 mmol) is dissolved in 20 mL of boiling water. Nickel(II) perchlorate hexahydrate (1.547 g, 4.23 mmol) is added and the mixture is boiled until a clear solution results. The clear solution is filtered and slowly cooled down to room temperature. After a few days the product starts to crystallize as light purple blocks. Yield: 21% (467 mg, 0.88 mmol).

DSC (5 °C min⁻¹, °C): 230 °C (dec.); IR (KBr, cm⁻¹): $\tilde{\nu}$ = 3527 (m), 3439 (s), 3401 (s), 3307 (s), 3247 (s), 2774 (w), 2626 (w), 2510 (w), 2219 (w), 2219 (w), 2054 (w), 2021 (w), 1657 (s), 1613 (s), 1569 (m), 1511 (s), 1492 (m), 1459 (m), 1412 (m), 1390 (m), 1283 (s), 1207 (s), 1108 (vs), 1083 (s), 938 (m), 814 (w), 776 (m), 716 (m), 672 (m), 625 (m), 600 (m), 515 (m); EA (C₂H₁₄Cl₂N₁₀O₁₄Ni, 531.79): calcd: C 4.52, H 2.65, N 26.34%; found: C 4.72, H 2.50, N 25.98%. BAM drophammer: 3 J; friction tester: 10 N; ESD: 0.04 J (at grain size 500–1000 μm).

bis-(3-amino-1-nitroguanidine) copper(II) perchlorate dihydrate (5)

3-amino-1-nitroguanidine (0.50 g, 4.23 mmol) is dissolved in 20 mL of boiling water. Copper(II) perchlorate hexahydrate (1.567 g, 4.23 mmol) is added and the mixture is boiled until a clear solution results. The clear solution is filtered and slowly cooled down to room temperature. After one hour the product starts to crystallize in blue blocks. Yield: 6.5% (137 mg, 0.27 mmol).

DSC (5 °C min⁻¹, °C): 134 °C (dec.); IR (KBr, cm⁻¹): $\tilde{\nu}$ = 3500 (m), 3406 (s), 3285 (m), 3203 (m), 3076 (m), 1651 (s), 1610 (m), 1558 (w), 1511 (m), 1495 (s), 1432 (w), 1385 (m), 1322 (m), 1281 (s), 1212 (s), 1135 (s), 1108 (vs), 1083 (vs), 935 (m), 820 (w), 773 (w), 735 (w), 707 (w), 653 (w), 622 (m), 606 (m), 521 (m); EA (C₂H₁₄Cl₂N₁₀O₁₄Cu, 536.64): calcd: C

4.48, H 2.63, N 26.10%; found: C 4.73, H 2.50, N 25.85%. BAM drophammer: 1 J; friction tester: 16 N; ESD: 0.50 J (at grain size 100–500 μm).

bis-(3-amino-1-nitroguanidine) zinc(II) perchlorate dihydrate (6)

3-amino-1-nitroguanidine (0.50 g, 4.23 mmol) is dissolved in 20 mL of boiling water. Zinc(II) perchlorate hexahydrate (1.575 g, 4.23 mmol) is added and the mixture is boiled until a clear solution results. The clear solution is filtered and slowly cooled down to room temperature. Slow evaporation of the solvent affords **5** as colorless crystals. Yield: 21% (441 mg, 0.82 mmol).

DSC (5 $^{\circ}\text{C min}^{-1}$, $^{\circ}\text{C}$): 198 $^{\circ}\text{C}$ (dec.); IR (KBr, cm^{-1}): $\tilde{\nu}$ = 3531 (m), 3487 (m), 3430 (s), 3338 (s), 3312 (s), 1655 (s), 1630 (m), 1576 (m), 1519 (m), 1495 (m), 1413 (m), 1384 (m), 1288 (s), 1217 (m), 1139 (s), 1090 (vs), 936 (m), 815 (w), 778 (m), 720 (w), 636 (m), 626 (m), 592 (w), 544 (w), 468 (w); EA ($\text{C}_2\text{H}_{14}\text{Cl}_2\text{N}_{10}\text{O}_{14}\text{Zn}$, 538.49): calcd: C 4.46, H 2.62, N 26.01%; found: C 4.48, H 2.67, N 24.33%. BAM drophammer: 3 J; friction tester: 28 N; ESD: 0.30 J (at grain size 100–500 μm).

bis-(3-amino-1-nitroguanidine) silver(I) perchlorate (7)

3-amino-1-nitroguanidine (0.50 g, 4.23 mmol) is dissolved in 20 mL of boiling water. Silver(I) perchlorate (0.877 g, 4.23 mmol) is added and the mixture is boiled until a clear solution results. The clear solution is filtered and slowly cooled down to room temperature. A fine grey precipitate, which forms upon standing of the solution after several hours is removed by filtration, whereafter light yellow fascicular crystals began to grow. Slow evaporation of the solvent affords **6** in 22% yield (407 mg, 0.91 mmol).

DSC (5 $^{\circ}\text{C min}^{-1}$, $^{\circ}\text{C}$): 148 $^{\circ}\text{C}$ (dec.); IR (KBr, cm^{-1}): $\tilde{\nu}$ = 3400 (s), 3305 (s), 3228 (s), 1656 (s), 1623 (s), 1583 (m), 1504 (m), 1460 (m), 1401 (m), 1291 (s), 1203 (m), 1095 (vs), 1023 (m), 1001 (m), 923 (m), 801 (w), 774 (w), 704 (w), 624 (m), 584 (m), 485 (w); EA ($\text{C}_2\text{H}_{10}\text{ClN}_{10}\text{O}_8\text{Ag}$, 445.48): calcd: C 5.39, H 2.26, N 31.44%; found: C 5.68, H 2.94, N 31.31%. BAM drophammer: <1 J; friction tester: <5 N; ESD: 0.01 J (at grain size 100–500 μm).

bis-(3-amino-1-nitroguanidine) cobalt(II) nitrate dihydrate (8)

3-amino-1-nitroguanidine (0.50 g, 4.23 mmol) is dissolved in 20 mL of boiling water. Cobalt(II) perchlorate hexahydrate (1.231 g, 4.23 mmol) is added and the mixture is boiled until a clear solution results. The clear solution is filtered and slowly cooled down to room temperature. **7** starts to crystallize in red blocklike crystals after 30 minutes. Yield 47% (910 mg, 1.99 mmol).

DSC (5 $^{\circ}\text{C min}^{-1}$, $^{\circ}\text{C}$): 139 $^{\circ}\text{C}$ (dec.); IR (KBr, cm^{-1}): $\tilde{\nu}$ = 3409 (s), 3329 (m), 3273 (s), 3237 (m), 3196 (m), 1666 (s), 1638 (m), 1588 (m), 1524 (s), 1486 (s), 1384 (vs), 1340 (s), 1315 (m), 1275 (s), 1219 (s), 1111 (s), 1044 (m), 1028 (m), 937 (m), 825 (w), 814 (w), 780 (m), 694 (m), 647 (w), 616 (w), 597 (w), 523 (m); EA ($\text{C}_2\text{H}_{14}\text{N}_{12}\text{O}_{12}\text{Co}$, 457.14): calcd: C 5.25, H 3.09, N 36.77%; found: C 5.59, H 2.94, N 36.51%. BAM drophammer: 7 J; friction tester: 240 N; ESD: 0.50 J (at grain size 500–1000 μm).

bis-(3-amino-1-nitroguanidine) nickel(II) nitrate dihydrate (9)

3-amino-1-nitroguanidine (0.50 g, 4.23 mmol) is dissolved in 20 mL of boiling water. Nickel(II) nitrate hexahydrate (1.230 g, 4.23 mmol) is added and the mixture is boiled until a clear solution results. The clear solution is filtered and slowly cooled down to room temperature. After a few minutes the product starts to crystallize as light purple plates. Yield: 49% (950 mg, 2.08 mmol).

DSC (5 °C min⁻¹, °C): 186 °C (dec.); IR (KBr, cm⁻¹): $\tilde{\nu}$ = 3412 (s), 3274 (s), 2637 (w), 2417 (w), 2296 (w), 2225 (w), 2142 (w), 2060 (w), 1972 (w), 1766 (m), 1662 (s), 1635 (s), 1522 (m), 1489 (s), 1385 (vs), 1278 (s), 1220 (s), 1111 (s), 1031 (m), 938 (m), 825 (w), 817 (w), 776 (m), 688 (m), 647 (w), 598 (w), 532 (m); EA (C₂H₁₄N₁₂O₁₂Ni, 456.90): calcd: C 5.26, H 3.09, N 36.79%; found: C 5.57, H 2.94, N 36.07%. BAM drophammer: 4 J; friction tester: 120 N; ESD: 0.08 J (at grain size 500–1000 µm).

bis-(3-amino-1-nitroguanidine) copper(II) nitrate (10)

3-amino-1-nitroguanidine (0.50 g, 4.23 mmol) is dissolved in 20 mL of boiling water. Copper(II) nitrate trihydrate (1.022 g, 4.23 mmol) is added and the mixture is boiled until a clear solution results. The clear solution is filtered and slowly cooled down to room temperature. After one hour the product starts to crystallize as deep blue, blocklike crystals. Yield: 15% (274 mg, 0.64 mmol).

DSC (5 °C min⁻¹, °C): 77 °C (dec.); IR (KBr, cm⁻¹): $\tilde{\nu}$ = 3439 (m), 3412 (m), 3280 (m), 3126 (m), 1665 (s), 1629 (m), 1500 (m), 1382 (vs), 1281 (s), 1212 (s), 1141 (m), 1111 (m), 1045 (w), 943 (w), 820 (w), 773 (w), 724 (w), 705 (w), 653 (w), 603 (w), 565 (w), 480 (w); EA (C₂H₁₀N₁₂O₁₀Cu, 425.72): calcd: C 5.64, H 2.37, N 39.48%; found: C 6.00, H 2.24, N 37.98%. BAM drophammer: <1 J; friction tester: <5 N; ESD: 0.50 J (at grain size 100–500 µm).

bis-(3-amino-1-nitroguanidine) zinc(II) nitrate dihydrate (11)

3-amino-1-nitroguanidine (0.50 g, 4.23 mmol) is dissolved in 20 mL of boiling water. Zinc(II) nitrate hexahydrate (1.258 g, 4.23 mmol) is added and the mixture is boiled until a clear solution results. The clear solution is filtered and slowly cooled down to room temperature. Slow evaporation of the solvent affords **10** as colorless crystals. Yield: 25% (492 mg, 1.06 mmol).

DSC (5 °C min⁻¹, °C): 181 °C (dec.); IR (KBr, cm⁻¹): $\tilde{\nu}$ = 3414 (s), 3272 (s), 3240 (s), 3176 (s), 2763 (w), 2643 (w), 2426 (w), 2295 (w), 2223 (w), 2147 (w), 2064 (w), 1766 (w), 1663 (s), 1590 (m), 1526 (m), 1487 (s), 1384 (vs), 1280 (s), 1221 (s), 1114 (s), 1044 (m), 1030 (m), 935 (m), 827 (w), 813 (w), 780 (m), 745 (w), 696 (m), 638 (w), 584 (w), 527 (m); EA (C₂H₁₄N₁₂O₁₂Zn, 463.60): calcd: C 5.18, H 3.04, N 36.26%; found: C 5.48, H 2.83, N 36.09%. BAM drophammer: 5 J; friction tester: 120 N; ESD: 0.50 J (at grain size 100–500 µm).

bis-(3-amino-1-nitroguanidine) silver(I) nitrate (12)

3-amino-1-nitroguanidine (0.50 g, 4.23 mmol) is dissolved in 20 mL of boiling water. Silver(I) nitrate (0.719 g, 4.23 mmol) is added and the mixture is boiled until a clear solution results. The clear solution is filtered and slowly cooled down to room temperature. After 15

minutes the product starts to crystallize as colorless blocks, which turn grey after several hours if not isolated and dried. Yield: 26% (448 mg, 1.10 mmol).

DSC ($5\text{ }^{\circ}\text{C min}^{-1}$, $^{\circ}\text{C}$): $142\text{ }^{\circ}\text{C}$ (dec.); IR (KBr, cm^{-1}): $\tilde{\nu} = 3432$ (s), 3401 (s), 3313 (s), 3219 (s), 3104 (m), 3010 (m), 2923 (m), 1665 (s), 1618 (s), 1580 (m), 1522 (m), 1473 (s), 1382 (s), 1355 (vs), 1292 (vs), 1245 (s), 1179 (s), 1108 (m), 1028 (m), 960 (m), 919 (m), 831 (w), 820 (w), 795 (w), 776 (w), 735 (w), 696 (m), 600 (m), 578 (m), 540 (m), 482 (w); EA ($\text{C}_2\text{H}_{10}\text{N}_{11}\text{O}_7\text{Ag}$, 408.04): calcd: C 5.89, H 2.47, N 37.76%; found: C 6.25, H 2.28, N 37.30%. BAM drophammer: 1 J; friction tester: $<5\text{ N}$; ESD: 0.01 J (at grain size $<100\text{ }\mu\text{m}$).

bis-(3-amino-1-nitroguanidine) cobalt(II) dinitramide tetrahydrate (13)

3-amino-1-nitroguanidine (0.50 g, 4.23 mmol) is dissolved in 15 mL of boiling water. Cobalt(II) perchlorate hexahydrate (1.55 g, 4.23 mmol) is added and the mixture is boiled until a clear solution results. Ammonium dinitramide (1.05 g, 8.46 mmol) is added to the solution and dissolved. The resulting solution is allowed to slowly cool down to room temperature. The product crystallizes in flat orange prisms in 46% yield (1.13 g, 1.94 mmol).

DSC ($5\text{ }^{\circ}\text{C min}^{-1}$, $^{\circ}\text{C}$): $118\text{ }^{\circ}\text{C}$ (dec.); IR (KBr, cm^{-1}): $\tilde{\nu} = 3597$ (m), 3406 (s), 3302 (s), 3244 (s), 1658 (s), 1630 (m), 1612 (m), 1529 (s), 1512 (s), 1454 (s), 1434 (s), 1390 (m), 1344 (m), 1281 (s), 1204 (vs), 1178 (s), 1123 (m), 1099 (s), 1031 (s), 952 (m), 936 (m), 827 (w), 808 (w), 778 (w), 761 (w), 732 (m), 688 (w), 640 (w), 594 (w), 507 (m); EA ($\text{C}_2\text{H}_{18}\text{N}_{16}\text{O}_{16}\text{Co}$, 581.20): calcd: C 4.13, H 3.12, N 38.56%; found: C 4.65, H 2.78, N 38.68%. BAM drophammer: 5 J; friction tester: 80 N; ESD: 0.70 J (at grain size $100\text{--}500\text{ }\mu\text{m}$).

bis-(3-amino-1-nitroguanidine) nickel(II) dinitramide tetrahydrate (14)

3-amino-1-nitroguanidine (0.50 g, 4.23 mmol) is dissolved in 15 mL of boiling water. Nickel(II) perchlorate hexahydrate (1.55 g, 4.23 mmol) is added and the mixture is boiled until a clear solution results. Ammonium dinitramide (1.05 g, 8.46 mmol) is added to the solution and dissolved. The resulting solution is allowed to slowly cool down to room temperature. The product crystallizes in light purple plates in 36% yield (0.888 g, 1.53 mmol).

DSC ($5\text{ }^{\circ}\text{C min}^{-1}$, $^{\circ}\text{C}$): $142\text{ }^{\circ}\text{C}$ (dec.); IR (KBr, cm^{-1}): $\tilde{\nu} = 3405$ (s), 3302 (s), 3243 (s), 1658 (s), 1612 (m), 1539 (s), 1512 (s), 1454 (s), 1434 (s), 1388 (m), 1344 (m), 1283 (s), 1205 (vs), 1178 (s), 1122 (m), 1099 (s), 1022 (s), 952 (w), 936 (m), 827 (w), 808 (w), 778 (w), 761 (m), 749 (w), 732 (m), 688 (m), 640 (w), 593 (w), 509 (m); EA ($\text{C}_2\text{H}_{18}\text{N}_{16}\text{O}_{16}\text{Ni}$, 580.96): calcd: C 4.13, H 3.12, N 38.58%; found: C 4.57, H 2.99, N 38.09%. BAM drophammer: 3 J; friction tester: 80 N; ESD: 0.60 J (at grain size $100\text{--}500\text{ }\mu\text{m}$).

(3-amino-1-nitroguanidine) silver(I) dinitramide monohydrate (15)

10 mmol of silver dinitramide acetonitrile adduct was prepared according to literature.²⁰ 1-amino-3-nitroguanidinium chloride¹⁹ (1.00 g, 6.4 mmol) was dissolved in 10 mL of boiling water. After cooling down the solution to about 60°C , the silver dinitramide acetonitrile adduct, dissolved in 5 mL of acetonitrile was added to the solution. After which the mixture was stirred under the exclusion of light at 35°C for further 2 h. The mixture was filtrated and **15** crystallizes from the clear filtrate in colorless needles. Yield: 0.61 g (2.50 mmol, 39%).

DSC (5 °C min⁻¹, °C): 71°C (dehydr.), 108°C (dec.); IR (KBr, cm⁻¹): $\tilde{\nu}$ = 3398 (m), 3304 (m), 3218 (m), 1671 (m), 1622 (m), 1580 (m), 1539 (s), 1431 (s), 1344 (m), 1297 (s), 1205 (vs), 1176 (vs), 1108 (w), 1031 (s), 951 (w), 827 (w), 761 (w), 732 (w), 706 (w), 594 (w), 484 (w), 470 (w); ¹H NMR (DMSO-*d*₆, 25 °C, ppm) δ : 9.31 (s, 1H, NH), 8.19 (s, 1H, C–NH₄H_B), 7.69 (s, 1H, C–NH_AH_B), 4.76 (s, 2H, N–NH₂), 3.36 (s, 2H, H₂O); ¹³C NMR (DMSO-*d*₆, 25 °C, ppm) δ : 160.9 (C(NNO₂)(N₂H₄)(NH₂)); ¹⁴N NMR (DMSO-*d*₆, 25 °C, ppm) δ : –11.0 (NO₂), –14.5 (NNO₂); m/z (FAB⁺): 120.1 [C(NNO₂)(N₂H₃)(NH₂)+H⁺], 107.0 [Ag⁺]; m/z (FAB[–]): 106.0 [N(NO₂)₂[–]]; EA (AgCH₇N₈O₇, 244.12): calc.: C 3.42, H 2.01, N 31.93 %; found: C 3.31, H 1.80, N 31.61 %; BAM drophammer: 2 J; friction tester: 7 N; ESD: 0.10 J.

bis-(3-amino-1-nitroguanidine) cobalt(II) chloride dihydrate (16)

3-amino-1-nitroguanidine (0.50 g, 4.23 mmol) is dissolved in 15 mL of boiling water. Cobalt(II) chloride hexahydrate (1.006 g, 4.23 mmol) is added and the mixture is boiled until a clear solution results. The solution is allowed to slowly cool down to room temperature. The product starts to crystallize in red blocklike crystals in 32% yield (0.555 g, 1.37 mmol).

DSC (5 °C min⁻¹, °C): 186 °C (dec.); IR (KBr, cm⁻¹): $\tilde{\nu}$ = 3457 (s), 3393 (vs), 3295 (s), 3245 (s), 3029 (m), 2963 (m), 1667 (s), 1626 (s), 1577 (m), 1521 (m), 1491 (s), 1430 (m), 1384 (m), 1277 (vs), 1217 (s), 1106 (s), 1015 (w), 931 (m), 777 (w), 748 (w), 705 (m), 594 (m); EA (C₂H₁₄Cl₂N₁₀O₆Co, 404.04): calcd: C 5.95, H 3.49, N 34.67%; found: C 5.93, H 3.47, N 34.42%. BAM drophammer: 10 J; friction tester: 360 N; ESD: 0.70 J (at grain size 100–500 μ m).

bis-(3-amino-1-nitroguanidine) nickel(II) chloride dihydrate (17)

3-amino-1-nitroguanidine (0.50 g, 4.23 mmol) is dissolved in 15 mL of boiling water. Nickel(II) chloride hexahydrate (1.005 g, 4.23 mmol) is added and the mixture is boiled until a clear solution results. The solution is allowed to slowly cool down to room temperature. The product starts to crystallize in light blue blocklike crystals in 42% yield (0.722 g, 1.79 mmol).

DSC (5 °C min⁻¹, °C): 250 °C (dec.); IR (KBr, cm⁻¹): $\tilde{\nu}$ = 3378 (s), 3303 (s), 3245 (s), 2963 (m), 2923 (m), 2549 (m), 2457 (m), 1687 (vs), 1626 (m), 1519 (w), 1494 (m), 1432 (w), 1379 (m), 1277 (m), 1217 (m), 1196 (m), 1120 (m), 1094 (m), 1037 (m), 975 (m), 935 (m), 775 (w), 746 (w), 728 (w), 705 (w), 562 (m), 537 (m); EA (C₂H₁₄Cl₂N₁₀O₆Ni, 403.80): calcd: C 5.95, H 3.49, N 34.69%; found: C 6.04, H 3.28, N 34.91%. BAM drophammer: 10 J; friction tester: 360 N; ESD: 0.70 J (at grain size <100 μ m).

bis-(3-amino-1-nitroguanidine) copper(II) chloride dihydrate (18)

3-amino-1-nitroguanidine (0.50 g, 4.23 mmol) is dissolved in 15 mL of boiling water. Copper(II) chloride dihydrate (0.721 g, 4.23 mmol) is added and the mixture is boiled until a clear solution results. The solution is allowed to slowly cool down to room temperature. Eventually precipitating 3-amino-1-nitroguanidine is filtered off. The product starts to crystallize in deep blue blocklike crystals in minor yield. Unfortunately, no analytical data except the crystal structure could be obtained, since ANQ started to precipitate immediately after the isolation of a single crystal of **18**.

bis-(3-amino-1-nitroguanidine) zinc(II) chloride dihydrate (19)

3-amino-1-nitroguanidine (0.50 g, 4.23 mmol) is dissolved in 15 mL of boiling water. Zinc(II) chloride (0.577 g, 4.23 mmol) is added and the mixture is boiled until a clear solution results. The solution is allowed to slowly cool down to room temperature. 3-amino-1-nitroguanidine precipitates as a colorless solid first, which is filtered off. The product starts to crystallize after several days in colorless blocks in minor yield.

DSC (5 °C min⁻¹, °C): 172 °C (dec.); IR (KBr, cm⁻¹): $\tilde{\nu}$ = 3388 (s), 3244 (s), 3030 (m), 2961 (m), 1665 (s), 1628 (s), 1580 (m), 1521 (m), 1494 (s), 1432 (m), 1284 (vs), 1219 (s), 1111 (s), 1017 (w), 931 (m), 778 (m), 752 (w), 706 (m), 598 (m); EA (C₂H₁₄Cl₂N₁₀O₆Zn, 410.48): calcd: C 5.85, H 3.44, N 34.12%; found: C 6.02, H 3.27, N 33.49%. BAM drophammer: 10 J; friction tester: 360 N; ESD: 0.70 J (at grain size <100 µm).

Acknowledgment

Financial support of this work by the Ludwig-Maximilian University of Munich (LMU), the European Research Office (ERO) of the U.S. Army Research Laboratory (ARL), the Armament Research, Development and Engineering Center (ARDEC) and the Strategic Environmental Research and Development Program (SERDP) under contract nos. W911NF-09-2-0018 (ARL), W911NF-09-1-0120 (ARDEC), W011NF-09-1-0056 (ARDEC) and 10 WPSEED01-002 / WP-1765 (SERDP) is gratefully acknowledged. The authors acknowledge collaborations with Dr. Mila Krupka (OZM Research, Czech Republic) in the development of new testing and evaluation methods for energetic materials and with Dr. Muhamed Sucasca (Brodarski Institute, Croatia) in the development of new computational codes to predict the detonation and propulsion parameters of novel explosives. We are indebted to and thank Drs. Betsy M. Rice and Brad Forch (ARL, Aberdeen, Proving Ground, MD) and Mr. Gary Chen (ARDEC, Picatinny Arsenal, NJ) for many helpful and inspired discussions and support of our work. The authors thank Mr. Stefan Huber for the sensitivity measurements.

5 REFERENCES

- (1) a) Tao, G.-H.; Parrish, D. A.; Shreeve J. M. *Inorg. Chem.* **2012**, *51*, 5305–5312; b) Tao, G.-H.; Twamley, B.; Shreeve J. M. *Inorg. Chem.* **2009**, *48*–9918–9923.
- (2) Tappan, B. C.; Huynh, M. H.; Hiskey, M. A.; Chavez, D. E.; Luther, E. P.; Mang, J. T.; Son, S. F. *J. Am. Chem. Soc.* **2006**, *128*, 6589–6594.
- (3) Zhao, H.; Qu, Z. R.; Ye, H. Y.; Xiong, R. G. *Chem. Soc. Rev.* **2008**, *37*, 84–100.
- (4) Singh, R.P.; Verma, R.D. Meshri, D.T., Shreeve, J.M. *Angew. Chem. Int. Ed.* **2006**, *45*, 3584–3601.
- (5) Hofmann, A. W. *J. Chem. Soc. Trans.* **1866**, *19*, 249–255.
- (6) (a) Berlinck, R. G. S.; Burtoloso, A. C. B.; Trindade-Silva, A. E.; Romminger, S.; Morais, R. P.; Bandeira, K.; Mizuno, C. M. *Nat. Prod. Rep.* **2010**, *27*(12), 1871–1907. (b) Saczewski, F.; Balewski, L. *Expert Opin. Ther. Pat.* **2009**, *19*(10), 1417–1448.
- (7) Neumann, F. W.; Shriner, R. L. *Org. Synth.* **1946**, *26*, 7–8.
- (8) Davis, T. L. *Org. Synth.* **1927**, *7*, 68–69.

- (9) (a) Jousselin, L. *Compt. Rend.* **1879**, 88, 1086. (b) Pellizzari, G. *Gazz. chim. ital.* **1891**, 21, 405–409.
- (10) Metelkina, E. L.; Novakova, T. A.; Berdonosova, S. N.; Berdonosov, D. Yu. *Russ. J. Org. Chem.* **2005**, 41(3), 440–443.
- (11) O'Connor, T. E.; Fleming, G.; Reilly, J. J. *J. Soc. Chem. Ind. London*, **1949**, 68, 309–310.
- (12) Fischer, N.; Klapötke, T. M.; Stierstorfer, J. *Z. Naturforsch. B* **2012**, 67(6), 573–588.
- (13) Zhilin, A. Y.; Ilyushin, M. A.; Tselinskii, I. V.; Kozlov, A. S.; Lisker, I. S. *Russ. J. Appl. Chem.* **2003**, 76(4), 572–576.
- (14) Christe, K. O.; Wilson, W. W.; Petrie, M. A.; Michels, H. H.; Bottaro, J. C.; Gilardi, R. *Inorg. Chem.* **1996**, 35(17), 5068–5071.
- (15) Gao, Y.; Gao, H.; Piekarski, C.; Shreeve, J. M. *Eur. J. Inorg. Chem.* **2007**, 31, 4965–4972.
- (16) Bottaro, J. C.; Penwell, P.E.; Schmitt, R. J. *J. Am. Chem. Soc.* **1997**, 119, 9405–9410.
- (17) Hafenrichter, E. S.; Marshall Jr., B.; Fleming, K. J. *Proceedings of the International Pyrotechnics Seminar* **2002**, 29th, 787–793.
- (18) Castillo-Meléndez, J. A.; Golding, B. T. *Synthesis* **2004**, 10, 1655–1663.
- (19) Fischer, N.; Klapötke, T. M.; Lux, K.; Martin, F. A.; Stierstorfer, J. *Crystals* **2012**, 2, 675–689.
- (20) Ang, H.-G.; Fraenk, W.; Karaghiosoff, K.; Klapötke, T. M.; Mayer, P.; Nöth, H.; Sprott, J.; Warchhold, M. *Z. Anorg. Allg. Chem.* **2002**, 628, 2894–2900.
- (21) CrysAlisPro Oxford Diffraction Ltd., Version 171.33.41, **2009**.
- (22) Altomare, A.; Cascarano, G.; Giacovazzo, C.; Guagliardi, A. *J. Appl. Cryst.* **1993**, 26, 343.
- (23) Sheldrick, G. M. *SHELXS-97, Program for Crystal Structure Solution*, University of Göttingen, Germany, **1997**.
- (24) Sheldrick, G. M. *SHELXL-97, Program for the Refinement of Crystal Structures*, University of Göttingen, Germany, **1997**.
- (25) Spek, A. L. *PLATON, A Multipurpose Crystallographic Tool*, Utrecht University, Utrecht, The Netherlands, **1998**.
- (26) Farrugia, L. J. *J. Appl. Cryst.* **1999**, 32, 837–838.
- (27) Empirical absorption correction using spherical harmonics, implemented in SCALE3 ABSPACK scaling algorithm (CrysAlisPro Oxford Diffraction Ltd., Version 171.33.41, **2009**).
- (28) Hu, S.; Barton, R.J.; Johnson, K.E.; Robertson B.E. *Acta Crystallogr.* 1981, A37, 229–238.
- (29) Jahn, H. A.; Teller, E.; *Proc. Royal Soc. Lon. A*, **1937**, 161, 220–235.
- (30) Akitsu, T.; Einaga, Y. *Acta Crystallogr.* **2004**, E60, m234–m236.
- (31) Lindley, P. F.; Woodward, P., *J. Chem. Soc. A* **1966**, 123–126.
- (32) Gilardi, R.; Flippen-Anderson, J.; George, C.; Butcher, R. J. *J. Am. Chem. Soc.* **1997**, 119, 9411–9416.
- (33) Ang, H.-G.; Fraenk, W.; Karaghiosoff, K.; Klapötke, T.M.; Mayer, P.; Nöth, H. Sprott, J.; Warchhold, M.; *Z. Anorg. Allg. Chem.* **2002**, 628, 2894–2900.
- (34) Vidmar, M.; Kobal, T.; Kozlevcar, B.; Segedin, P.; Golobic, A.; *Acta Crystallogr.* **2012**, E68, m375–376.

- (35) Hesse, M.; Meier, H.; Zeeh, B. in *Spektroskopische Methoden in der Organischen Chemie*, 8th ed., Thieme, Stuttgart, Germany, **2012**.
- (36) NATO standardization agreement (STANAG) on explosives, impact sensitivity tests, no. 4489, 1st ed., Sept. 17, **1999**.
- (37) WIWEB-Standardarbeitsanweisung 4-5.1.02, Ermittlung der Explosionsgefährlichkeit, hier der Schlagempfindlichkeit mit dem Fallhammer, Nov. 8, **2002**.
- (38) <http://www.bam.de>.
- (39) NATO standardization agreement (STANAG) on explosive, friction sensitivity tests, no. 4487, 1st ed., Aug. 22, **2002**.
- (40) WIWEB-Standardarbeitsanweisung 4-5.1.03, Ermittlung der Explosionsgefährlichkeit oder der Reibeempfindlichkeit mit dem Reibeapparat, Nov. 8, **2002**.
- (41) Impact: insensitive > 40 J, less sensitive g 35 J, sensitive g 4 J, very sensitive e 3 J. Friction: insensitive > 360 N, less sensitive) 360 N, sensitive < 360 N a.> 80 N, very sensitive e 80 N, extremely sensitive e 10 N. According to the UN Recommendations on the Transport of Dangerous Goods, (+) indicates not safe for transport.
- (42) <http://www.ozm.cz>.
- (43) <http://www.linseis.com>.
- (44) Kubelka, P.; Munk, F. *Zeitschrift für technische Physik* **1931**, *1*, 593–601.
- (45) Ugryumov, I. A.; Ilyushin, M. A.; Tselinskii, I. V.; Kozlov, A. S. *Russ. J. Appl. Chem.* **2003**, *76*(3), 439–441.

Energetic Salts of 5,5'-Bis(tetrazole-2-oxide) in a Comparison to 5,5'-Bis(tetrazole-1-oxide) Derivatives

Niko Fischer,[†] Li Gao,[†] Thomas M. Klapötke,^{†‡} Jörg Stierstorfer[†]*

[†] Department of Chemistry and Biochemistry, Energetic Materials Research, Ludwig-Maximilian University of Munich, Butenandstr. 5-13, D-81377 Munich, Germany.

[‡] Center for Energetic Concepts Development, CECD, University of Maryland, UMD, Department of Mechanical Engineering, College Park, MD 20742, USA

Corresponding author: * Prof. Dr. Thomas M Klapötke,
tmk@cup.uni-muenchen.de, FAX: +49 89 2180 77492

Abstract

The preparation and isolation of 5,5'-bis(2-hydroxytetrazole) by oxidation of 5,5'-bistetrazole using commercially available oxone is described. The nitrogen-rich salts including ammonium, hydroxylammonium, guanidinium, aminoguanidinium, triaminoguanidinium, 5-aminotetrazolium and aminonitroguanidinium have been prepared, characterized (XRD, NMR and vibrational spectroscopy, DSC, mass spectrometry) and compared to their 5,5'-bis(tetrazole-1-oxide) analogues. The impact, friction and electrical spark sensitivities of all compounds were measured and several detonation parameters such as the detonation velocities and detonation pressures were also calculated with the EXPLO5 code based on calculated heats of formation (CBS-4M) and the X-ray densities.

Keywords: Energetic Materials, Tetrazoles, N-oxides, Sensitivities, Crystal Structures

1 Introduction

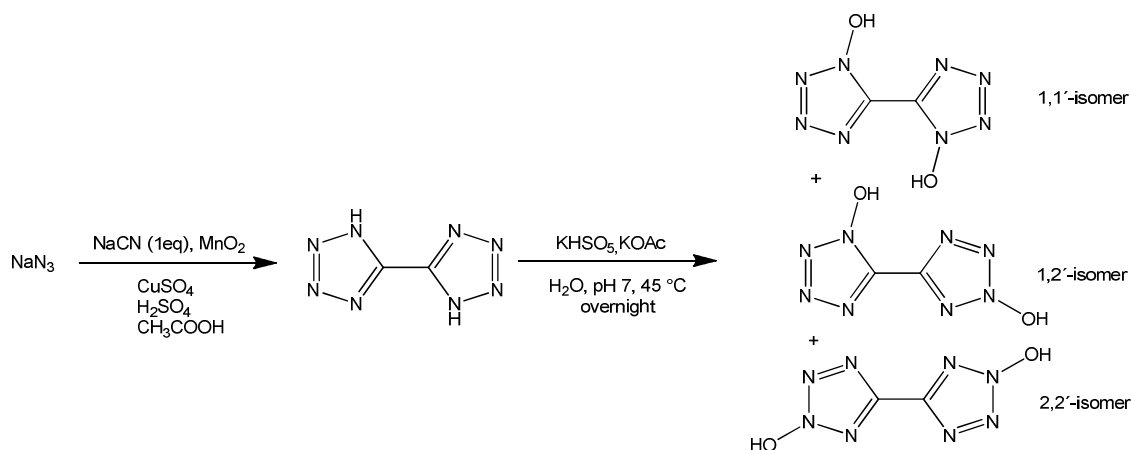
The research in the field of energetic materials has come a long way since Alfred Nobel introduced nitroglycerine as an explosive in the form of dynamite in 1866 [1]. Since then, the development of new energetic materials has become a very versatile and competitive field comparable to that of modern drug design. Looking at currently used explosives such as TNT and RDX, the combination of fuel and oxidizer in the same molecule is inevitable to achieve high performance. However with regard to the aforementioned explosives, that derive most of their energy from oxidizing their carbon backbone, conventional C/H/N/O explosives based on nitrocarbons seem to have reached their limits and are thus long obsolete [2]. In addition to the design of more powerful explosives, the requirement of new energetic materials to be

“greener” is nowadays a major concern in the energetic materials community. New approaches in the design of energetic materials include high heat of formation compounds [3], nitrogen-rich materials [4], compounds with ring [5] or cage strain [6] as well as combinations of all these [7]. Unfortunately most energetic materials with high performances are highly sensitive at the same time [8]. Vice versa those compounds with acceptable sensitivities simply cannot match the energetic values of current standards. Finding the perfect balance between these two attributes makes the research for new energetic materials a challenge that requires new synthetic pathways [6,9] and improved computational methods. Taking the row of azoles into consideration as a basis for new energetic materials, the tetrazole ring seems to be a good compromise between high performance and low sensitivities, since pyrazoles, due to their low nitrogen content, on the one hand reveal only low heats of formation and pentazoles are highly unstable and hence, sensitive. In addition the carbon atom on position 5 of the tetrazole ring offers the introduction of oxygen-rich substituents, such as nitro- or nitramine groups to compensate the naturally low oxygen balance of tetrazoles. Another approach to increase the oxygen content is the introduction of N-oxides, which not only results in a better oxygen balance but also affords compounds with higher densities and lower sensitivities. Despite their advantages, only little correspondence on tetrazole-oxides can be found in literature i.e. only a handful of compounds for 1*N*-oxides [10,11,12] and even less for 2*N*-oxides [13,14]. In the following we will give a report about the preparation and isolation of 5,5'-bis-(2-hydroxytetrazole), the characterization of some energetic nitrogen-rich salts and a comparison to their 5,5'-bis-(tetrazole-1-oxide) analogues.

2 Results and Discussion

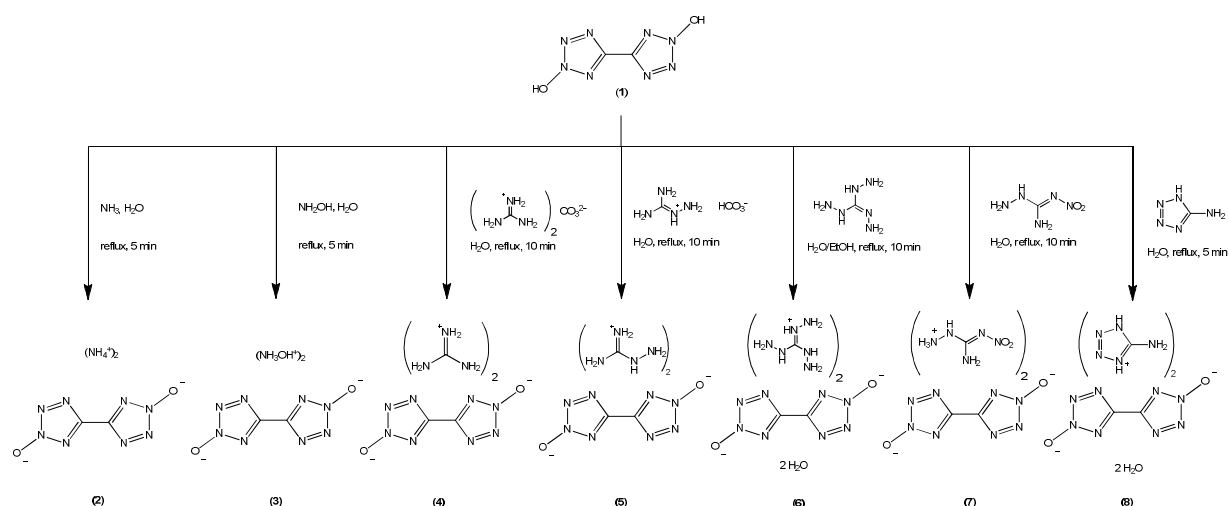
2.1. Synthesis

The preparation of 5,5'-bis(tetrazole-2-oxide) was performed in a way similar to that we recently reported on for other tetrazole *N*-oxides [10,13]. The successful *N*-oxidation of 5,5'-bistetrazole to exclusively obtain 5,5'-bis(tetrazole-2-oxide) in a buffered oxone suspension depends on several parameters. First of all the starting material 5,5'-bistetrazole [15] needs to be of high purity, which was achieved by recrystallization from 2M hydrochloric acid prior to use in the oxidation reaction. Since the preparation of 5,5'-bistetrazole involves Cu-catalysis, these heavy metal impurities need to be removed. We have observed that the use of impure 5,5'-bistetrazole caused the formation of different side-products such as mono-oxidized 5,5'-bistetrazole, which are hard to separate from the desired product. Secondly an excess (6 equivalents) of oxone was used in order to push the equilibrium to the product side. The oxidation was not successful when using only equimolar amounts or a slight excess of oxone. A third important parameter is the reaction temperature. Different isomers of 5,5'-bistetrazole-oxides such as 5,5'-bis-(1-hydroxytetrazole) or the mixed 2-hydroxytetrazol-5-yl-1-hydroxytetrazole were obtained at a reaction temperature of 35 °C (Scheme 1). Increasing the temperature to 45 °C favors the formation of 5,5'-bis-(2-hydroxytetrazole). However, to avoid decomposition of oxone, the temperature should not exceed 47 °C.



Scheme 1 Oxidation products of 5,5'-bistetrazole with potassium peroxomonosulfate at pH 7.

The buffer system plays an important role as well. After discovering that using trisodium phosphate as a buffer yielded 5,5'-bis-(2-hydroxytetrazole) with traces of the 1,1'- and 1,2'-isomer as well as the mono-oxidized product, a different buffer was necessitated. Also, after work-up, the isolated product was sticky and stayed wet due to remaining phosphoric acid, which cannot easily be removed. Despite giving less yield (39 % compared to 69 %, when using the trisodium phosphate buffer), potassium acetate was used, since it turned out, that 5,5'-bis(2-hydroxytetrazole) could be isolated in a very high purity. The isolation of 5,5'-bis(2-hydroxytetrazole) was achieved by stepwise acidification and subsequent extraction of the aqueous reaction mixture into diethyl ether. The aqueous suspension needs to be acidified to protonate the product. Concentrated HCl proved to be the best protonating agent, since conc. H_2SO_4 and conc. H_3PO_4 could not be removed from the isolated product anymore and conc. nitric acid led to the formation of nitrous gases, when concentrating the organic phases under reduced pressure. To avoid oxidation of HCl to Cl_2 by remaining excess of oxone, the reaction mixture was treated with sodium sulfite first. The acidification was done stepwise, since the pK_A value of 5,5'-bistetrazole-2,2'-diole is presumably lower than those of other isomers. Thus the aqueous suspension was acidified to pH 0 first, a small excess of conc. hydrochloric acid was added (10 mL) to make sure that the acetate as well as side products with lower acidity than 5,5'-bis(2-hydroxytetrazole) are protonated and extracted into the organic phase. Water was added to the aqueous layer until a clear solution was obtained, which then was extracted into diethyl ether giving mainly acetic acid. The aqueous layer was treated with a large excess of conc. hydrochloric acid (100 mL), in order to protonate 5,5'-bis(tetrazole-2-oxide), and again extracted into diethyl ether. Residues of acetic acid can be removed azeotropically on a rotary evaporator after repeated addition of benzene and removing the solvent. We have noticed that low pressures (< 150 mbar) and water bath temperatures higher than 40 °C led to minor formation of nitrous gases, supposedly by decomposition of the product. 5,5'-bis(2-hydroxytetrazole) can then carefully be isolated from the benzene suspension. To improve the yield, the acidification/extraction process can be repeated several times. Starting from the free acid 5,5'-bis(2-hydroxytetrazole), all nitrogen rich salts **2–8** were synthesized after reacting **1** with the necessary amount of the respective free base or, in case of the guanidinium and aminoguanidinium salt, the respective carbonate, as it is depicted in Scheme 2.



Scheme 2 Synthesis of the nitrogen-rich 5,5'-bis(tetrazole-2-oxide)s **2–8**.

2.2. Spectroscopy

Compounds **1–8** can easily be identified by ^1H and ^{13}C NMR spectroscopy. Additionally a ^{15}N NMR spectrum of **1** and its ammonium salt **2** were recorded. For better comparison all spectra were measured using d_6 -DMSO as solvent and all chemical shifts are given with respect to TMS (^1H , ^{13}C) or nitromethane (^{15}N). Since the ^1H and ^{13}C NMR shifts of the cations of **1–8** have already been described in various publications [10], here we concentrate on the ^{13}C and ^{15}N NMR spectra of **1** and the changes in its NMR spectrum, which occur upon deprotonation as exemplified in the ^{13}C and ^{15}N NMR spectra of **1** and the ammonium salt **2**. The carbon atom signal of the free acid is visible at 151.6 ppm and is only slightly shifted upfield to around 150 ppm (**2**: 150.2 ppm) after deprotonation. Compared to the signal of the carbon atoms in 5,5'-bis(1-hydroxytetrazole), [10] which is visible at 135.8 ppm, here we observe a remarkable downfield shift, when 5,5'-bistetrazole is oxidized at N2 instead of N1 in the ^{13}C NMR spectrum of **1**.

The ^{15}N NMR spectrum of the free acid **1** expectedly shows four signals, which can be assigned to the four chemically inequivalent nitrogen atoms of the 5,5'-bis(1-hydroxytetrazole) heterocycle (Figure 1). We have to mention that the assignments have been done according our long experience and are not in total agreement to the corresponding DFT calculations. The chemical shifts were calculated using Gaussian09 [17] (GIAO NMR method, B3LYP/6-31G(d,p)).

Since the spectrum of **1** was measured proton coupled, N2 reveals a broader signal due to NH coupling to the hydrogen atom of the hydroxyl group at -64.6 ppm. The signal of N2 at the same time is subject to the largest shift to lower field upon deprotonation and is found at -41.0 ppm in the spectrum of **2**, which can be explained by the Lewis structure B of the anion of **2** depicted in Figure 1, where N2 carries a positive charge. Since firstly, N3 and N1 both carry a negative charge in the Lewis structure B and secondly, they are both directly connected to N2, we expect the same effect to the signals of these nitrogen atoms after

deprotonation. Indeed, what we observe, is that the signals of N3 and N1 are both equally shifted to higher field after deprotonation by approximately 10 ppm (**1**: –24.7 ppm (N3), –68.6 ppm (N1); **2**: –37.3 ppm (N3), –78.0 ppm (N1)). The signal found at lowest field in both spectra is assigned to N3, which also is in agreement to ^{15}N NMR shifts of β -nitrogen atoms found in other differently substituted tetrazole rings [16]. The same argumentation applies to the assignment of nitrogen atom N4, which in both spectra is found at highest field (**1**: –92.2 ppm, **2**: –98.0 ppm). Additionally, the signal of N4 is least affected by deprotonation of the heterocycle, which is also reasonable if comparing the Lewis structures of the neutral species **1** and both Lewis structures A and B of deprotonated **2**. Furthermore N5 (NH_4^+) in the spectrum of **2** is assigned to a signal found at –359.4 ppm.

Table 1 ^{15}N chemical shifts (ppm) of compounds **1** and **2** given with respect to MeNO_2 as an external standard.

	N1	N2	N3	N4
1 (calc.)	–93.0	–75.0	–23.9	–44.0
1 (exp.)	–68.6	–64.6	–24.7	–92.2
2 (calc.)	–95.	–21.6	–39.0	–76.1
2 (exp.)	–78.0	–41.0	–37.3	–98.0

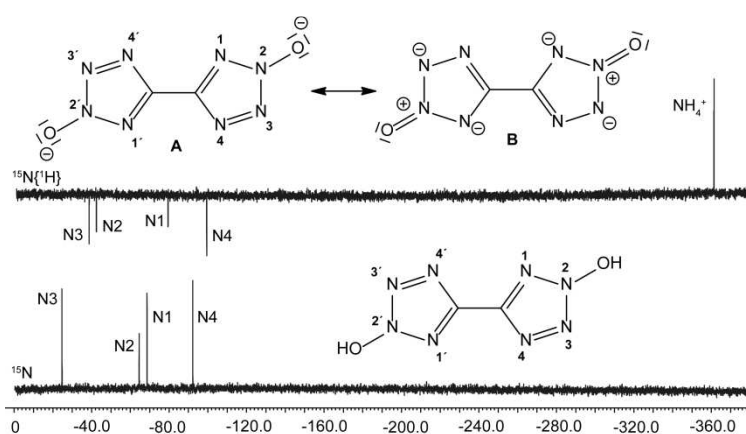


Figure 1 ^{15}N Spectroscopy of **1** and **2** with potential assignments.

IR and Raman spectroscopy were used for the identification of structural elements and functional groups in all compounds. Absorptions were assigned according to values reported in the literature [18]. Characteristic vibrations of the aromatic 5,5'-bis(tetrazole-2-oxide) anion of compounds **1–8** are visible in all spectra, such as the bistetrazole framework vibrations, the asymmetric and symmetric N–C–N stretching vibrations, stretching vibrations of N–N and out of plane vibration of the cyclic C=N bond at 1500–1350 cm^{-1} and 1350–700 cm^{-1} . All Raman spectra show the characteristic valence vibration of the C–C bond in the 5,5'-bis(tetrazole-2-oxide) anion at 1633–1590 cm^{-1} as a strong absorption. Additionally the N–O valence vibration of the N-oxide moiety can be seen in all Raman spectra at 1080–1034 cm^{-1} . The IR spectra of compounds **1** and **3** show characteristic O–H stretching vibrations the hydroxyl groups, which are involved in hydrogen bonding at 3452–3425 cm^{-1} . Also

absorption bands of the O–H deformation vibrations can be seen at 1391–1360 cm⁻¹. A broad absorption band in the IR spectrum of the ammonium salt **2** at 3197 cm⁻¹ shows the asymmetric stretching vibrations of the ammonium cation. Furthermore an absorption band at 1399 cm⁻¹ can be assigned to the deformation vibrations of the ammonium cation. Compounds **4–8** show strong absorption of the N–H stretching vibrations of the amino groups in the guanidine and 5-aminotetrazole based cations at 3500–3329 cm⁻¹, as well as N–H deformation vibrations ranging from 1566–1699 cm⁻¹. C=N stretching vibration of the guanidinium derivatives can be assigned to absorptions at 1678–1639 cm⁻¹. Also the characteristic absorption band of the nitro-amine in the cation of **8** is observed at 1271 cm⁻¹ in its IR spectrum.

2.3. X-ray diffraction

XRD was performed on an Oxford Xcalibur3 diffractometer with a Spellman generator (voltage 50 kV, current 40 mA) and a KappaCCD detector using Mo-*K*_α radiation ($\lambda = 0.71073$ Å). The data collection and reduction was carried out using the CRYSLISPRO software [19]. The structures were solved either with SHELXS-97 [20] or SIR-92 [21], refined with SHELXL-97 [22] and finally checked using the PLATON [23] software integrated in the WINGX [24] software suite. All hydrogen atoms were found and freely refined. Friedel pairs of non-centrosymmetric space groups have been merged using the MERG3 command. The absorptions were corrected with a Scale3 Abspack multi-scan method [25]. Except for **1** (173 K), all structures were measured at room temperature with a X-ray wavelength of 0.71073. Data and parameters of the measurements and refinements are gathered in Table S1 and S2. Exact bond lengths and angles are given in Table S3. Cif files have been deposited within the Cambridge Crystallographic Data Centre using the CCDC Nos. 904648 (**1**), 904652 (**2**), 904653 (**3**), 904655 (**4**), 904650 (**5**), 904651 (**6**), 904649 (**7**) and 904654 (**8**).

Neutral **1** crystallizes with a very high density of 1.953 g cm⁻³ in the monoclinic space group *P*2₁/*c*. Its structure is similar to the structure of corresponding 5,5'-bis(1-hydroxytetrazole) recently published [26]. Both tetrazole rings are coplanar and connected by the C1–C1ⁱ bond (1.45 Å) which is significantly shorter than a C–C single bond (1.54 Å). The same value is observed for 5,5'-bistetrazole [27]. Within the planar tetrazole rings bond lengths between typical C–N/N–N single and C=N/N=N double bonds are observed. The hydroxyl group is bond to the nitrogen atom N2 with a distance of 1.34 Å, which is longer than in the deprotonated oxides **2–8** (mean value 1.30 Å). The N–O bond lengths are shorter than a typical N–O single bond (1.45 Å) but still longer than N=O double bonds (1.17 Å). The other bond lengths and angles are hardly influenced by deprotonation of the hydroxyl group (see Table S3). In comparison to neutral 5,5'-bistetrazole [27], which shows also a planar geometry) the N2–N3 bond is slightly elongated. In the structure of **1**, the hydrogen atoms do not follow the planar geometry and are bent ($\angle \text{N1–N2–O1–H1} = -112^\circ$) because of a strong hydrogen bond interaction (O1–H1 \cdots N4ⁱⁱ, D–H 1.07, H \cdots A 1.58, D \cdots A 2.65, D–H \cdots A 175°, (ii) $x, 1/2 - y, 1/2 + z$). Due to this, a 3-dimensional network of nearly orthogonal bistetrazole moieties is observed.

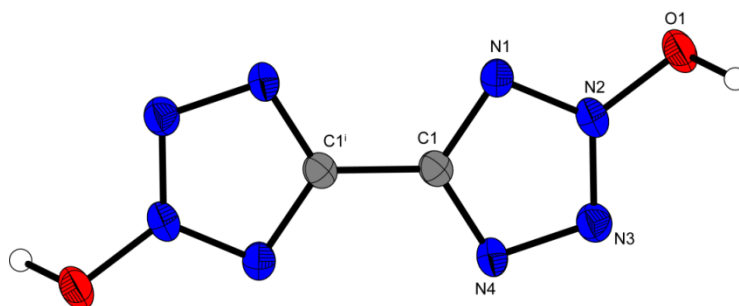


Figure 2 Molecular unit of **1** showing the labeling scheme. Ellipsoids are drawn at the 50 % probability level. Symmetry code: (i) $2-x, 1-y, -z$.

Except for **5** and **7** ($P-1$) all structures investigated in this work crystallize in the monoclinic space groups $P2_1/c$ and $P2_1/n$, respectively. In agreement to **1**, also in all ionic compounds (**2–8**) both tetrazole-oxide rings are coplanar to each other. Except for the ammonium salt **2**, all dianions show a centre of symmetry at the middle of the C–C bond. With respect to the X-ray densities of the energetic salts, **3** (1.832 g cm^{-3}) and **7** (1.822 g cm^{-3}) show the highest values. The lowest one was observed for the triaminoguanidinium salt **6** (1.600 g cm^{-3}). The molecular units are shown in the following Figures 2(**1**), 3(**2**), 4(**3**), 5(**4**), 6(**5**), 7(**6**), 8(**7**) and 9(**8**).

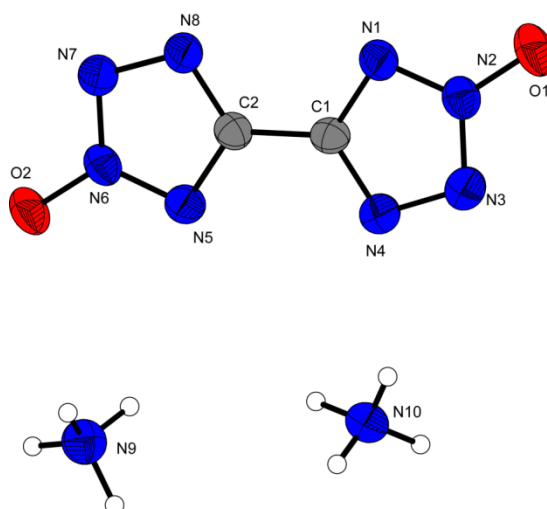


Figure 3 Molecular unit of **2** showing the labeling scheme. Ellipsoids are drawn at the 50 % probability level.

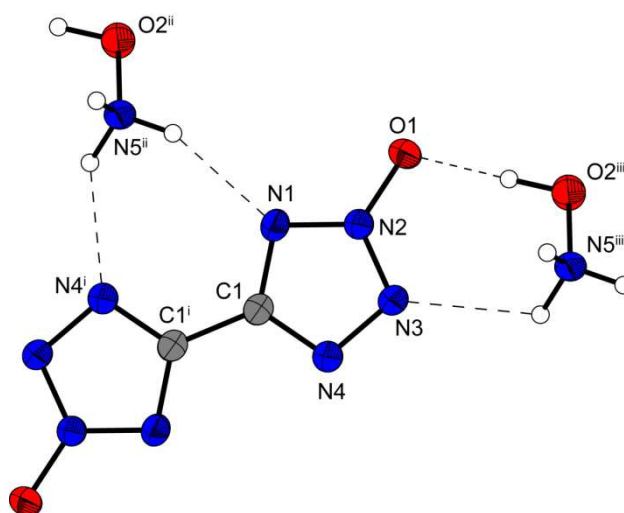


Figure 4 Molecular unit of **3** showing the labeling scheme. Ellipsoids are drawn at the 50 % probability level. Symmetry codes: (i) $-x, -y, -z$; (ii) $-x, -0.5+y, 0.5-z$; (iii) $1-x, 0.5+y, 0.5-z$.

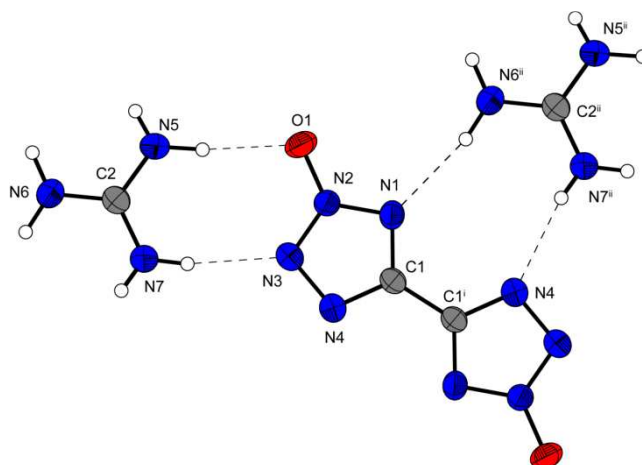


Figure 5 Molecular unit of **4** showing the labeling scheme. Ellipsoids are drawn at the 50 % probability level. Symmetry codes: (i) $2-x, -y, -z$; (ii) $x, y, -1+z$.

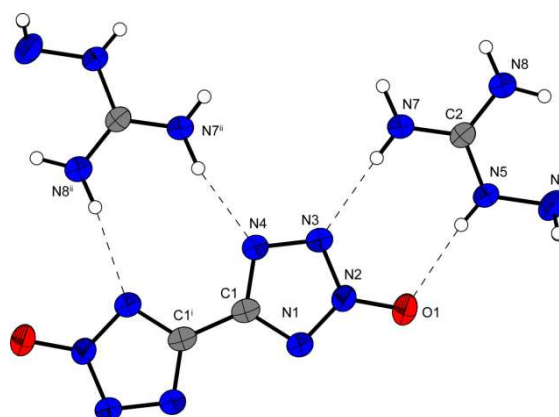


Figure 6 Molecular unit of **5** showing the labeling scheme. Ellipsoids are drawn at the 50 % probability level. Symmetry codes: (i) $-x, -y, 1-z$; (ii) $-x, 1-y, 1-z$.

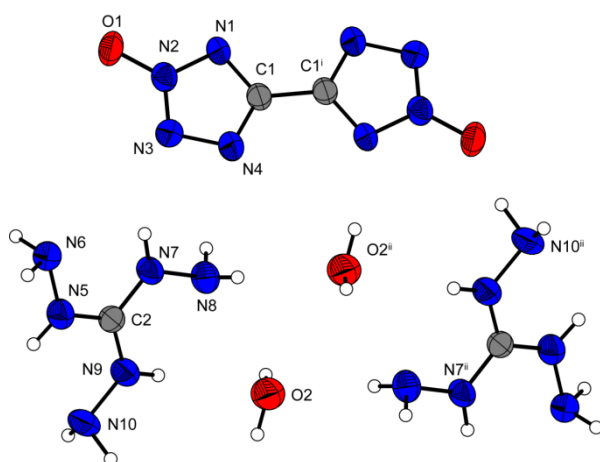


Figure 7 Molecular unit of **6** showing the labeling scheme. Ellipsoids are drawn at the 50 % probability level. Symmetry codes: (i) $-x, 2-y, -z$; (ii) $1-x, 2-y, -z$.

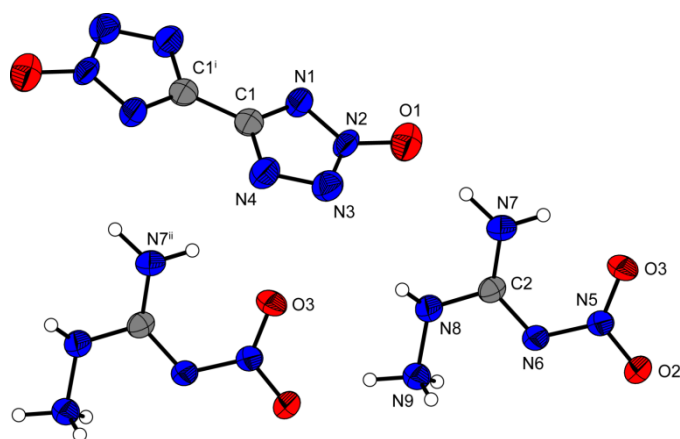


Figure 8 Molecular unit of **7** showing the labeling scheme. Ellipsoids are drawn at the 50 % probability level. Symmetry codes: (i) $-x, 1-y, -z$; (ii) $-1+x, y, z$.

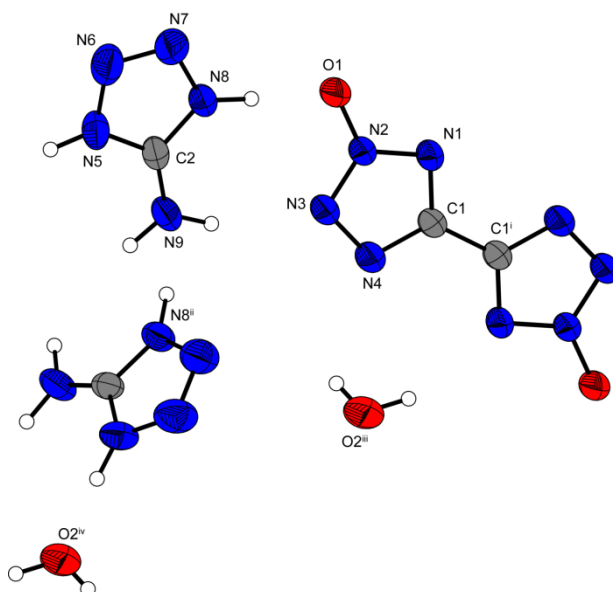


Figure 9 Molecular unit of **8** showing the labeling scheme. Ellipsoids are drawn at the 50 % probability level. Symmetry codes: (i) $2-x, -y, -z$; (ii) $x, 0.5-y, -0.5+z$; (iii) $1-x, -y, -z$; (iv) $-1+x, y, -1+z$.

2.4. Heats of formation

Usually energetic materials tend to explode in bomb calorimetric measurements. Consequently doubtful combustion energies are obtained. Therefore heats of formation of energetic materials mostly are calculated theoretically. Details on the heat of formation calculations are given in the Supporting Materials.

All investigated compounds are formed endothermically (Tables 2 and 3). The highest heat of formation was calculated for the 3-amino-1-nitroguanidinium salt **7** (1044 kJ / mol) followed by the aminoguanidinium salt **5** (608 kJ mol⁻¹), which is in the range of neutral 5,5'-bis(2-hydroxytetrazole) (560 kJ mol⁻¹). In comparison to the 1-oxide derivatives [26] the herein described compounds have lower heats of formation for the neutral as well as the deprotonated forms. This can be seen very well on the gas phase enthalpies of formation $\Delta_f H^\circ$ (g) for 5,5'-bis(2-hydroxytetrazole) (642 kJ mol⁻¹) and 5,5'-bis(1-hydroxytetrazole) (689 kJ mol⁻¹) or 5,5'-bis(tetrazole-2-oxide) (500 kJ mol⁻¹) and 5,5'-bis(tetrazole-1-oxide) (587.7 kJ mol⁻¹) respectively.

2.5. Detonation parameters

The detonation parameters were calculated using the program EXPLO5 V5.05 [28] (for details, see Supplementary Information). The results are gathered in Tables 2 and 3.

Table 2. Explosive and detonation parameters of **1** and its energetic salts **2–5**.

	1	2	3	4	5
Formula	C ₂ H ₂ N ₈ O ₂	C ₂ H ₈ N ₁₀ O ₂	C ₂ H ₈ N ₁₀ O ₄	C ₄ H ₁₂ N ₁₄ O ₂	C ₄ H ₁₄ N ₁₆ O ₂
FW / g mol ⁻¹	170.09	204.15	236.15	288.23	318.26
IS / J ^a	3	10	3	> 40	30
FS / N ^b	5	360	60	> 360	> 360
ESD / J ^c	0.03	0.75	0.26	0.15	0.20
N / % ^d	65.88	68.61	59.31	68.03	70.42
Ω / % ^e	-28.22	-47.02	-27.10	-66.60	-65.35
T _{Dec.} / °C ^f	165	265	172	331	255
ρ / g cm ⁻³ ^g	1.953	1.664	1.822	1.633	1.637
Δ _f H _m ^o / kJ mol ⁻¹ ^h	559.7	257.3	390.7	322.0	568.7
Δ _f U ^o / kJ kg ⁻¹ ⁱ	3377.3	1381.6	1769.7	1237.2	1911.1
EXPLO5 values:					
V5.05					
-Δ _{Ex} U ^o / kJ kg ⁻¹ ^j	5854	4006	5790	3288	3851
T _{det} / K ^k	4396	2903	3869	2481	2698
P _{CJ} / kbar ^l	409	258	372	221	247
V _{Det.} / m s ⁻¹ ^m	9364	8212	9264	7752	8137
V _o / L kg ⁻¹ ⁿ	721	843	847	805	824
I _S / s ^o	254	205	256	186	203

a impact sensitivity (BAM drophammer (1 of 6)); b friction sensitivity (BAM friction tester (1 of 6)); c electrostatic discharge device (OZM research); d nitrogen content; e oxygen balance ($\Omega = (xO - 2yC - 1/2zH)M/1600$); f decomposition temperature from DSC ($\beta = 5$ °C); g from X-ray diffraction; h calculated enthalpy of formation; i calculated energy of formation; j energy of explosion; k explosion temperature; l detonation pressure; m detonation velocity; n volume of detonation gases (assuming only gaseous products); o specific impulse using isobaric (60 bar) conditions.

Table 3. Explosive and detonation parameters of **6–8** in comparison to RDX and HMX..

	6	7	8	RDX	HMX
Formula	C ₄ H ₂₂ N ₂₀ O ₄	C ₄ H ₁₂ N ₁₈ O ₆	C ₄ H ₁₂ N ₁₈ O ₄	C ₃ H ₆ N ₆ O ₆	C ₄ H ₈ N ₈ O ₈
FW / g mol ⁻¹	414.35	408.26	376.26	222.12	296.16
IS / J ^a	15	10	5	7.5 [29]	7 [29]
FS / N ^b	324	48	360	120 [29] ^{Fehler!} Textmarke nicht definiert.	112 [29]
ESD / J ^c	0.5	1.5	1.0	0.2	0.2
N / % ^d	67.61	61.76	67.01	37.84	37.84
Ω / % ^e	-57.91	-31.35	-42.52	-21.61	-21.61
T _{Dec.} / °C ^f	217	163	188	205	275
ρ / g cm ⁻³ ^g	1.600	1.832	1.633	1.858 (90 K) [30]	1.944 (100K) [31]
Δ _f H _m ^o / kJ mol ⁻¹ ^h	454.9	1043.8	608.1	86.3	116.1
Δ _f U ^o / kJ kg ⁻¹ ⁱ	1235.3	2665.6	1727.9	489.0	492.5
EXPLO5 values:					
V5.05					
-Δ _{Ex} U ^o / kJ kg ⁻¹ ^j	4024	6135	4420	6190	6185
T _{det} / K ^k	2711	4129	3249	4232	4185
P _{CJ} / kbar ^l	251	382	252	380	415
V _{Det.} / m s ⁻¹ ^m	8256	9350	8094	8983	9221
V _o / L kg ⁻¹ ⁿ	885	816	815	734	729
I _S / s ^o	206	261	215	258	258

a impact sensitivity (BAM drophammer (1 of 6)); b friction sensitivity (BAM friction tester (1 of 6)); c electrostatic discharge device (OZM research); d nitrogen content; e oxygen balance ($\Omega = (xO - 2yC - 1/2zH)M/1600$); f decomposition temperature from DSC ($\beta = 5$ °C); g from X-ray diffraction; h calculated enthalpy of formation; i calculated energy of formation; j energy of explosion; k explosion temperature; l detonation pressure; m detonation velocity; n volume of detonation gases (assuming only gaseous products); o specific impulse using isobaric (60 bar) conditions.

The free acid **1**, since revealing the highest density as well as a comparatively high heat of formation, shows the best detonation performance as exemplified by the highest detonation velocity (9364 ms⁻¹) and the highest detonation pressure (409 kbar). Other candidates, which have detonation parameters comparable or higher than those of HMX (1,3,5,7-tetranitro-1,3,5,7-tetraazacyclooctane, a commonly used high explosive), are the hydroxylammonium salt **3** as well as the 3-amino-1-nitroguanidinium salt **7**, whereas the reason herefore again is a high density in combination with comparatively high heats of formation. An interesting comparison between the guanidinium salt **4** and the triaminoguanidinium salt **6** shows, that, if looking at the sum formulas of both compounds, a lower carbon content and therefore a higher nitrogen and hydrogen content also increases the detonation velocity and the detonation pressure, here by around 500 ms⁻¹ and 80 kbar respectively, since both salts have comparable densities and almost the same heats of formation. Unfortunately, all compounds exceeding a detonation velocity of 9000 ms⁻¹ (**1**, **3**, **7**) decompose at temperatures, which do not qualify them as suitable replacements for the commonly used high explosives RDX (1,3,5-tetranitro-1-3-5-tetraazacyclohexane) and HMX.

2.6. Thermal stability and sensitivities

Melting and decomposition temperatures of **1** and the nitrogen-rich salts thereof were determined on a Linseis PT10 DSC [32], calibrated by standard pure indium and zinc, using ~ 1.5 mg of each energetic material in sealed Al-containers with a hole (0.1 mm) for gas release and a nitrogen flow of 20 mL min⁻¹ at a heating rate of 5 °C min⁻¹. The decomposition temperatures are given as absolute onset temperatures. None of the prepared compounds

shows any sign of melting before decomposition, indicated by endothermic steps in their DSC curves. Decomposition temperatures range from 160 to over 300 °C, with the lowest being that of the 3-amino-1-nitroguanidium salt **7** (163 °C) followed by the free acid **1** (165 °C) and the hydroxylammonium salt **3** (172 °C). The low decomposition temperature of the aminonitroguanidine salt **7** is a trend, that has been seen for all compounds bearing the protonated 3-amino-1-nitroguanidine cation and presumably is due to the lowering of the C–N bond order in this cation upon protonation [33]. Since **3** and **7** decompose below 180 °C they are no suitable replacements for the commonly used RDX despite their good performances. The other compounds all decompose above 180 °C with the highest decomposition temperature observed for the guanidinium salt **4** (331 °C), surpassing that of HNS (hexanitrostilbene, a highly thermally stable explosive). This indicates that, if paired with the right cation, the 5,5'-bis(tetrazole-2-oxide) anion forms compounds with thermal stabilities, that are equally comparable to the corresponding salts of 5,5'-bis(1-hydroxytetrazole) [26]. The substituted guanidinium salts **5** (255 °C) and **6** (217 °C) show decreasing thermal stability with an increasing nitrogen content. The ammonium salt **2** (265 °C) reveals the better thermal stability as compared to the dihydroxylammonium salt and the 5-amino-1-H-tetrazolium salt **8** decomposes at 188 °C. Dehydration of the hydrated compounds **6** and **8** can be observed as endothermic steps in the cases of **6** (80 °C) and **8** (70 °C). Since the difference between dehydration and decomposition temperature of these compounds is higher than 100 °C, they can be dehydrated at 140 °C without decomposition. A comparison of **2–8** to the corresponding nitrogen-rich salts of 5,5'-bis(1-hydroxytetrazole) [26] shows, that some of the salts (**4–7**) have higher decomposition temperatures, whereas **2**, **3** and **8** have lower decomposition temperatures. Hence, there is no observable trend of lower decomposition temperatures for the nitrogen-rich salts of 5,5'-bis(2-hydroxytetrazole) compared to the salts of 5,5'-bis(1-hydroxytetrazole), although the thermal stability of neutral 5,5'-bis(2-hydroxytetrazole, 165 °C) is much lower than that of 5,5'-bis(1-hydroxytetrazole, 214 °C). The impact sensitivity tests of compounds **1–8** were carried out according to STANAG 4489 [34] modified instruction [35] using a BAM (Bundesanstalt für Materialforschung) drophammer [36]. The friction sensitivity tests were carried out according to STANAG 4487 [37] modified instruction [38] using the BAM friction tester. The classification of the tested compounds results from the “UN Recommendations on the Transport of Dangerous Goods” [39]. Additionally all compounds were tested upon the sensitivity towards electrical discharge using the Electric Spark Tester ESD 2010 EN [40]. All compounds except the guanidinium salt **4** (> 40 J) are impact sensitive. The free acid **1** and the hydroxylammonium salt **3** even need to be classified as very sensitive due to their impact sensitivity of 3 J each. The 5-amino-1-H-tetrazolium salt **8** and the triaminoguanidinium salt **6** are also sensitive (**4**: 15 J, **8**: 5 J) despite the fact that both species crystallize with the inclusion of two moles of crystal water, which usually reduces the sensitivity considerably. Regarding the friction sensitivity some compounds seem to follow the trends observed for the impact sensitivities, some do not. For example the guanidinium salt **5** is again insensitive (> 360 N), the free acid **1** is extremely sensitive (< 5 N) and the hydroxylammonium salt **3** and the aminonitroguanidinium salt **7** are very sensitive (**2**: 60 N, **7**: 48 N). The triaminoguanidinium salt **4** is regarded as sensitive (324 N). Although being sensitive to friction, the remaining salts **2**, **4** and **8** are less sensitive (360 N). The sensitivities towards electrical discharge cover a large range. This is also due to the varying crystallinity of the compounds, which has a great influence on these results, thus

grain sizes of the examined materials are given in the experimental part. Nonetheless the free acid is regarded as very sensitive (0.03 J), which is the only compound, that has to be handled with care regarding electrical, since it can also be set off by the human body, which can generate up to 25 mJ of static electricity through normal activities. All decomposition temperatures as well as sensitivities are summarized in Table 5.

3. Conclusions

- Starting from 5,5'-bistetrazole, 5,5'-bis(2-hydroxytetrazole) can be synthesized via oxidation with oxone[®] (KHSO₅ as oxidizing agent) in high purities and moderate yields in a potassium acetate buffered aqueous suspension at 45 °C overnight.
- Bearing two highly acidic protons, it can be deprotonated with various selected bases to form a series of nitrogen rich ionic energetic materials.
- The crystal structures of the free acid (**1**) as well as of its ammonium (**2**), hydroxylammonium (**3**), guanidinium (**4**), aminoguanidinium (**5**), triaminoguanidinium (**6**), 3-amino-1-nitroguanidinium (**7**) and 5-amino-1-H-tetrazolium salt were determined. They crystallize in the common space groups *P*-1 (**5**, **7**), *P*2₁/*c* (**1**, **3**, **8**) and *P*2₁/*n* (**2**, **4**, **6**) with densities ranging from 1.953 g cm⁻³ for the free acid **1** and 1.600 g cm⁻³ for its triaminoguanidinium salt dihydrate **6**.
- All ionic compounds except the 3-amino-1-nitroguanidinium salt **8** and the hydroxylammonium salt **3** are thermally stable up to more than 180 °C with the highest decomposition temperature of 331 °C for the guanidinium salt **4**. Deprotonation of the free acid (*T*_{dec} = 165 °C) leads to a thermal stabilization.
- The sensitivities of **1-8** vary from very sensitive towards impact (**1**, **3**: 3 J) to insensitive (**4**: >40 J). The same is observed for the friction sensitivities, which reach from extremely sensitive (free acid **1**) to insensitive (**4**, **5**: >360 N). In summary, the nitrogen rich salts of 5,5'-bis(2-hydroxytetrazole) are more sensitive than the salts of 5,5'-bis(1-hydroxytetrazole).
- Regarding the explosive performance of the ionic compounds **2-8**, **3** and **7** show most promising as suitable RDX replacements with detonation velocities of 9264 ms⁻¹ (**3**) and 9350 ms⁻¹ (**7**) and detonation pressures of 372 kbar (**3**) and 382 kbar (**7**). However, their thermal stabilities and sensitivities do not reach the values observed for RDX (*T*_{dec} = 220 °C, IS = 7.5 J, FS = 120 N).

4. Experimental Part

Caution! 5,5'-bis(2-hydroxytetrazole) and its salts are energetic materials with increased sensitivities towards shock and friction. Therefore, proper safety precautions (safety glass, face shield, earthed equipment and shoes, Kevlar[®] gloves and ear plugs) have to be applied while synthesizing and handling the described compounds.

All chemicals and solvents were employed as received (Sigma-Aldrich, Fluka, Acros). ¹H, ¹³C and ¹⁵N NMR spectra were recorded using a JEOL Eclipse 270, JEOL EX 400 or a JEOL Eclipse 400 instrument. The chemical shifts quoted in ppm in the text refer to typical standards such as tetramethylsilane (¹H, ¹³C) or nitromethane (¹⁵N). To determine the melting and decomposition temperatures of the described compounds a Linseis PT 10 DSC (heating

rate 5 °C min⁻¹) was used. Infrared spectra were measured using a Perkin Elmer Spectrum One FT-IR spectrometer as KBr pellets. Raman spectra were recorded on a Bruker MultiRAM Raman Sample Compartment D418 equipped with a Nd-YAG-Laser (1064 nm) and a LN-Ge diode as detector. Mass spectra of the described compounds were measured at a JEOL MStation JMS 700 using FAB technique. To measure elemental analyses a Netsch STA 429 simultaneous thermal analyzer was employed.

5,5'-Bis(2-hydroxytetrazole) (1)

80.0 g (0.13 mol) oxone[®] (KHSO₅ · KHSO₄ · 2 K₂SO₄) was suspended in 150 mL of water and the suspension was buffered to pH 5 with potassium acetate. A solution of 5,5'-bistetrazole (3.00 g, 21.7 mmol) in 30 mL of 2M NaOH was added. Further 20 mL of water was added and the slightly pink mixture was stirred for 15 h at 45 °C. To quench the reaction by destroying remaining KHSO₅, 0.50 g of sodium sulfite was added. The mixture was then brought to pH 0 with HCl conc. and an additional 10 mL portion of HCl conc. was added. Water was added until a colorless clear solution resulted. The solution was then extracted with diethyl ether (4 x 200 mL) and the combined organic layers were dried over MgSO₄, filtered and the solvent was removed on a rotary evaporator, whereas in the first fraction mostly acetic acid was isolated. 100 mL of concentrated HCl was added to the aqueous layer which again was extracted with diethyl ether (4 x 200 mL). The combined organic layers were dried, filtered and the solvent was removed on a rotary evaporator. To azeotropically remove traces of acetic acid the crude product was repeatedly treated with benzene (3 x 30 mL) which each time was evaporated under reduced pressure again. To avoid decomposition of the product while evaporating the solvent, the temperature of the water bath must not exceed 40 °C and the pressure must not be lower than 150 mbar. The slightly yellowish product was suspended in 20 mL benzene and isolated by filtration. Acidification and extraction of the aqueous layer with diethylether was repeated three times resulting in 1.44 g (8.48 mmol, 39 %) of the combined fractions of **1**.

DSC (5 °C min⁻¹): 165 °C (dec.); IR (KBR, cm⁻¹): $\tilde{\nu}$ = 3425 (s), 2950 (w), 2532 (w), 1626 (w), 1360 (m), 796 (w); Raman (1064 nm, 300 mW, 25 °C, cm⁻¹): $\tilde{\nu}$ = 1633 (100), 1562 (15), 1359 (11), 1251 (16), 1107 (9), 1038 (75), 770 (8); ¹H NMR (DMSO-*d*₆, 25 °C, ppm) δ : 4.69; ¹³C NMR (DMSO-*d*₆, 25 °C, ppm) δ : 151.6; MS(FAB⁺): *m/z* = 171.1 [M+H⁺]; MS (FAB⁻): *m/z* = 169.2 [M-H⁺]; EA (C₂H₂N₈O₂, 170.09 g mol⁻¹): calc.: C 14.12, H 1.19, N 65.88 %; found: C 14.19, H 1.33, N 65.59 %; BAM drophammer: 3 J; friction tester: <5 N; ESD: 0.3 J (grain size 100–500 μ m).

Diammonium 5,5'-bis(tetrazole-2-oxide) (2)

5,5'-Bis(2-hydroxytetrazole) (538 mg, 3.16 mmol) was dissolved in aqueous ammonia (2 mol/L, 3.16 mL). The mixture was heated up for a short time and filtrated. The solution was cooled down to room temperature and **2** precipitated as small colorless needles. Yield: 511 mg (2.50 mmol, 79 %).

DSC (5 °C min⁻¹): 265 °C (dec.); IR (KBr, cm⁻¹): $\tilde{\nu}$ = 3421 (s), 3197 (s), 1399 (vs), 1300 (s), 1214 (m), 1000 (w), 760 (m), 714 (m), 546 (w); Raman (1064 nm, 300 mW, 25 °C, cm⁻¹): $\tilde{\nu}$ = 1601 (100), 1373 (3), 1230 (6), 1146 (9), 1076 (7), 1023 (44), 795 (4), 765 (4); ¹H NMR (DMSO-*d*₆, 25 °C, ppm) δ : 7.28 (t, J = 50 Hz); ¹³C NMR (DMSO-*d*₆, 25 °C, ppm) δ : 150.2; MS (FAB⁺): m/z = 18.1 [NH₄⁺]; MS (FAB⁻): m/z = 169.2 [C₂HN₈O₂⁻]; EA (C₂H₈N₁₀O₂, 204.15 g mol⁻¹): calc.: C 11.77, H 3.95, N 68.61 %; found: C 11.74, H 3.71, N 67.87 %; BAM drophammer: 10 J; friction tester: 360 N; ESD: 0.75 J (grain size 100–500 μ m).

Dihydroxylammonium 5,5'-bis(tetrazole-2-oxide) (3)

5,5'-Bis(2-hydroxytetrazole) (300 mg, 1.76 mmol) was dissolved in 1 mL water and a solution of hydroxylamine (233 mg, 3.53 mmol) was added to the clear yellowish solution. The mixture was boiled up for a short time and filtrated. Crystallization gave **3** as colorless small needles. Yield: 201 mg (0.85 mmol, 48 %).

DSC (5 °C min⁻¹): 172 °C (dec.); IR (KBr, cm⁻¹): $\tilde{\nu}$ = 3452 (vs), 2694 (m), 1632 (m), 1304 (w), 1219 (w), 1050 (w), 760 (w), 712 (w), 562 (w); Raman (1064 nm, 300 mW, 25 °C, cm⁻¹): $\tilde{\nu}$ = 1600 (100), 1371 (4), 1155 (8), 1075 (6), 1040 (41), 1014 (10); ¹H NMR (DMSO-*d*₆, 25 °C, ppm) δ : 10.24; ¹³C NMR (DMSO-*d*₆, 25 °C, ppm) δ : 150.0; MS (FAB⁺): m/z = 126.1 [Matrix⁺+33], MS (FAB⁻) m/z = 169.1 [C₂HN₈O₂⁻]; EA (C₂H₈N₁₀O₄, 236.15 g mol⁻¹): calc.: C 10.17, H 3.41, N 59.31 %; found: C 10.75, H 3.32, N 58.79 %; BAM drophammer: 3 J; friction tester: 60 N; ESD: 0.26 J (grain size 100–500 μ m).

Bis(guanidinium) 5,5'-bis(tetrazole-2-oxide) (4)

5,5'-Bis(2-hydroxytetrazole) (554 mg, 3.26 mmol) was dissolved in 1 mL water and guanidinium carbonate (587 mg, 3.26 mmol) was added to the clear yellowish solution. The mixture was heated to reflux after adding 75 mL water. The clear solution was boiled down to 25 mL and filtrated. After cooling the filtrate down to room temperature **4** precipitated as small colorless crystalline needles. Yield: 665 mg (2.31 mmol, 71 %).

DSC (5 °C min⁻¹): 331 °C (dec.); IR (KBr, cm⁻¹): $\tilde{\nu}$ = 3422 (vs), 1647 (m), 1384 (w), 1314 (w), 1217 (w), 769 (w), 713 (w), 602 (w); Raman (1064 nm, 300 mW, 25 °C, cm⁻¹): $\tilde{\nu}$ = 3259 (3), 1599 (100), 1575 (5), 1236 (6), 1138 (11), 1077 (10), 1035 (63), 1011 (24), 803 (9), 548 (10); ¹H NMR (DMSO-*d*₆, 25 °C, ppm) δ : 7.00; ¹³C NMR (DMSO-*d*₆, 25 °C, ppm) δ : 158.5 (CH₆N₃⁺), 149.7 (C₂N₈O₂²⁻); MS (FAB⁺): m/z = 60 [CH₆N₃⁺]; MS (FAB⁻): m/z = 169.0 [C₂HN₈O₂⁻]; EA (C₄H₁₂N₁₄O₂, 288.23 g mol⁻¹): calc.: C 16.67, H 4.20, N 68.03 %; found: C 17.09, H 4.21, N 67.20 %; BAM drophammer: 40 J; friction tester: 360 N; ESD: 0.15 J (grain size 100–500 μ m).

Bis(aminoguanidinium) 5,5'-bis(tetrazole-2-oxide) (5)

5,5'-Bis(2-hydroxytetrazole) (490 mg, 2.88 mmol) was dissolved in 1 mL water and aminoguanidinium bicarbonate (784 mg, 5.76 mmol) was added to the clear yellowish solution. The mixture was heated to reflux after adding 13 mL water. The clear solution was

boiled down to 10 mL and filtrated. **5** precipitated as thin, colorless plates upon cooling the solution to room temperature. Yield: 820 mg (2.58 mmol, 89 %).

DSC (5 °C min⁻¹): 255 °C (dec.); IR (KBr, cm⁻¹): $\tilde{\nu}$ = 3433 (vs), 1678 (s), 1465(w), 1385 (m), 1313 (m), 1212 (w), 1001 (w), 767 (w), 600 (w); Raman (1064 nm, 300 mW, 25 °C, cm⁻¹): $\tilde{\nu}$ = 3251 (2), 1601 (100), 1137 (11), 1076 (7), 1032 (55), 963 (11), 802 (12), 522 (6); ¹H NMR (DMSO-*d*₆, 25 °C, ppm) δ : 8.75 (NHNH₂), 7.28 (NH₂), 6.93 (NH₂), 4.66 (NHNH₂); ¹³C NMR (DMSO-*d*₆, 25 °C, ppm) δ : 159.4 (CH₇N₄⁺), 149.7 (C₂N₈O₂²⁻); MS (FAB⁺): *m/z* = 75.0 [CH₇N₄⁺]; MS (FAB⁻): *m/z* = 169.1 [C₂HN₈O₂⁻]; EA (C₄H₁₄N₁₆O₂, 318.26 g mol⁻¹): calc.: C 15.10, H 4.43, N 70.42 %; found: C 15.55, H 4.32, N 69.54 %; BAM drophammer: 30 J; friction tester: 360 N; ESD: 0.2 J (grain size 100–500 μm).

Bis(triaminoguanidinium) 5,5'-bis(tetrazole-2-oxide) dihydrate (6)

5,5'-Bis(2-hydroxytetrazole) (545 mg, 3.20mmol) was dissolved in 1 mL water and triaminoguanidine (667 mg, 6.41 mmol) was added to the clear yellowish solution. The mixture was heated after adding 50 mL of water. After boiling, the mixture turned into a clear solution. The water was removed at a rotary evaporator. The residue was recrystallized out of ethanol/water to give **6** as small colorless needles. Yield: 530 mg (1.40 mmol, 44 %).

DSC (5 °C min⁻¹): 80 °C (dehydr.), 217 °C (dec.); IR (KBr, cm⁻¹): $\tilde{\nu}$ = 3455 (vs), 3318 (vs), 3213 (vs), 1685 (s), 1615 (m), 1384 (m), 1312 (w), 1128 (w), 925 (s), 773 (w), 605 (m); Raman (1064 nm, 300 mW, 25 °C, cm⁻¹): $\tilde{\nu}$ = 3223 (4), 1591 (100), 1125 (14), 1069 (4), 1030 (34), 891 (5), 801 (6); ¹H NMR (DMSO-*d*₆, 25 °C, ppm) δ : 8.56 (–NHNH₂), 4.46 (–NHNH₂); ¹³C NMR (DMSO-*d*₆, 25 °C, ppm) δ : 159.6 (CH₉N₆⁺), 149.8 (C₂N₈O₂²⁻); MS (FAB⁺): *m/z* = 105.1 [CH₉N₆⁺]; MS (FAB⁻): *m/z* = 169.3 [C₂HN₈O₂⁻]; EA (C₄H₂₂N₂₀O₄, 414.35 g mol⁻¹): calc.: C 11.59, H 5.35, N 67.61 %; found: C 12.11, H 5.15, N 66.89 %; BAM drophammer: 15 J; friction tester: 324 N; ESD: 0.5 J (grain size 100–500 μm).

Bis(3-amino-1-nitroguanidinium) 5,5'-bis(tetrazole-2-oxide) (7)

5,5'-Bis(2-hydroxytetrazole) (475 mg, 2.79 mmol) was dissolved in 1 mL water and 1-amino-3-nitroguanidine (665 mg, 5.59 mmol) in 13 mL water was added. The solution was heated up and boiled down to half the volume. After cooling the filtrate down to room temperature **7** precipitated as yellowish crystalline needles to give 816 mg (2.00 mmol, 72 %).

DSC (5 °C min⁻¹): 163 °C (dec.); IR (KBr, cm⁻¹): $\tilde{\nu}$ = 3362 (vs), 2986 (m), 2038 (w), 1639 (s), 1412 (s), 1271 (vs), 914 (w), 778 (m), 717 (w), 616 (w); Raman (1064 nm, 300 mW, 25 °C, cm⁻¹): $\tilde{\nu}$ = 1595 (100), 1377 (6), 1264 (13), 1132 (16), 1038 (33), 923 (8), 801 (9), 634 (8), 366 (9); ¹H NMR (DMSO-*d*₆, 25 °C, ppm) δ : 9.30 (NHNH₂), 8.00 (NH₂), 4.49 (NHNH₂); ¹³C NMR (DMSO-*d*₆, 25 °C, ppm) δ : 161.4 (CH₆N₅O₂⁺), 151.3 (C₂N₈O₂²⁻); MS (FAB⁺): *m/z* = 120.0 [CH₆N₅O₂⁺]; MS (FAB⁻): *m/z* = 169.1 [C₂HN₈O₂⁻]; EA (C₄H₁₂N₁₈O₄, 408.26 g mol⁻¹): calc.: C 11.77, H 2.96, N 61.76 %; found: C 12.21, H 2.93, N 60.96 %; BAM drophammer: >10 J; friction tester: 48 N; ESD: 1.5 J (grain size 500–1000 μm).

Bis(5-amino-1-H-tetrazolium) 5,5'-bis(tetrazole-2-oxide) dihydrate (8)

5,5'-Bis(2-hydroxytetrazole) (499 mg, 2.93 mmol) was dissolved in 1 mL water and 5-aminotetrazole (499 mg, 5.87 mmol) in 13 mL water was added. The solution was heated up and boiled down to one fourth the volume. After cooling down to room temperature **8** crystallized as colorless crystalline needles. Yield: 283 mg (0.83 mmol, 28%).

DSC (5 °C min⁻¹): 70 °C (dehydr.), 188 °C (dec.); IR (KBr, cm⁻¹): $\tilde{\nu}$ = 3503 (s), 3329 (s), 2501 (m), 1699 (m), 1383 (m), 1298 (m), 1119 (w), 1052 (w), 975 (w), 767 (w), 589 (w); Raman (1064 nm, 300 mW, 25 °C, cm⁻¹): $\tilde{\nu}$ = 1595 (100), 1527 (3), 1234 (8), 1156 (8), 1072 (5), 1035 (32), 764 (5), 745 (6), 446 (4); ¹H NMR (DMSO-*d*₆, 25 °C, ppm) δ : 8.00 (br); ¹³C NMR (DMSO-*d*₆, 25 °C, ppm) δ : 157.0 (CH₄N₅⁺), 151.5 (C₂N₈O₂²⁻); MS (FAB⁺): *m/z* = 86.0 [CH₄N₅⁺]; MS (FAB⁻): *m/z* = 169.3 [C₂HN₈O₂⁻]; EA (C₄H₁₂N₁₈O₄, 376.26): calc.: C 12.77, H 3.21, N 67.01 %; found: C 13.46, H 2.37, N 67.43 %; BAM drophammer: 5 J; friction tester: 360 N; ESD: 1.0 J (grain size 500–1000 μ m).

Acknowledgements

Financial support of this work by the Ludwig-Maximilian University of Munich (LMU), the U.S. Army Research Laboratory (ARL) under grant no. W911NF-09-2-0018, the Armament Research, Development and Engineering Center (ARDEC) under grant no. R&D 1558-TA-01, and the Office of Naval Research (ONR) under grant nos. ONR.N00014-10-1-0535 and ONR.N00014-12-1-0538 is gratefully acknowledged. The authors acknowledge collaborations with Dr. Mila Krupka (OZM Research, Czech Republic) in the development of new testing and evaluation methods for energetic materials and with Dr. Muhamed Sucesca (Brodarski Institute, Croatia) in the development of new computational codes to predict the detonation and propulsion parameters of novel explosives. We are indebted to and thank Drs. Betsy M. Rice and Brad Forch (ARL, Aberdeen, Proving Ground, MD) for many helpful discussions. Last but not least the authors thank Mr. St. Huber for sensitivity measurements.

5. References

- [1] A. Nobel, Improved Explosive Compound, *United States Patent Office*, US57175 (A) (1866).
- [2] T.M. Klapötke, *Chemistry Of High-Energy Materials*, second ed., de Gruyter, Berlin, 2011.
- [3] R. Haiges, M. Rahm, D.A. Dixon, E.B. Garner, K.O. Christe, *Inorg. Chem.* 51 (2012) 1127–1141.
- [4] Mehilal, N. Sikder, A.K. Sikder, J.P. Agrawal, *Indian J. of Eng. & Mater. Sci.* 11 (2004) 516–520.
- [5] D. Klasovity, S. Zeman, *Univ. of Pardubice*, CZ 302068 (2010).

- [6] O. Bolton, L.R. Simke, P.F. Pagoria, A.J. Matzger, *Cryst. Growth Des.* 12 (2012) 4311–4314.
- [7] V. Thottempudi, F. Forohor, D.A. Parrish, J.M. Shreeve, *Angew. Chem., Int. Ed.* 39 (2012) 9881–9885.
- [8] P.W. Leonard, C.J. Pollard, D.E. Chavez, B.M. Rice, D. A. Parrish, *Synlett* 14 (2011) 2097–2099.
- [9] R.G. Sarawadekar, J.P. Agrawal, *Nanomaterials in pyrotechnics*, *Def. Sci. J.* 58 (2008) 486–495.
- [10] N. Fischer, D. Fischer, T.M. Klapötke, D.G. Piercey, J. Stierstorfer, *J. Mater. Chem.* 22 (2012) 20418–20422.
- [11] J. Plenkiewicz, A. Roszkiewicz, *Pol. J. Chem.* 67 (1993) 1767–1778.
- [12] A.J. Liepa, D.A. Jones, T.D. McCarthy, R.H. Nearn, *Aust. J. Chem.* 53 (2000) 619–622.
- [13] M. Göbel, K. Karaghiosoff, T.M. Klapötke, D.G. Piercey, J. Stierstorfer, *J. Am. Chem. Soc.* 132 (2010) 17216–17226.
- [14] T. Harel, S.J. Rozen, *J. Org. Chem.* 75 (2010) 3141–3143.
- [15] D.E. Chavez, M.A. Hiskey, D.L. Naud, *J. Pyrotech.* 10 (1999) 17–36.
- [16] N. Fischer, D. Izsák, T.M. Klapötke, S. Rappenglück, J. Stierstorfer *Chem. Eur. J.* 18(13) (2012) 4051–4062.
- [17] Gaussian 09, Revision A.1, M.J. Frisch, G.W. Trucks, H.B. Schlegel, G.E. Scuseria, M.A. Robb, J.R. Cheeseman, G. Scalmani, V. Barone, B. Mennucci, G.A. Petersson, H. Nakatsuji, M. Caricato, X. Li, H.P. Hratchian, A.F. Izmaylov, J. Bloino, G. Zheng, J.L. Sonnenberg, M. Hada, M. Ehara, K. Toyota, R. Fukuda, J. Hasegawa, M. Ishida, T. Nakajima, Y. Honda, O. Kitao, H. Nakai, T. Vreven, J.A. Montgomery, Jr., J.E. Peralta, F. Ogliaro, M. Bearpark, J.J. Heyd, E. Brothers, K.N. Kudin, V.N. Staroverov, R. Kobayashi, J. Normand, K. Raghavachari, A. Rendell, J.C. Burant, S.S. Iyengar, J. Tomasi, M. Cossi, N. Rega, J.M. Millam, M. Klene, J.E. Knox, J.B. Cross, V. Bakken, C. Adamo, J. Jaramillo, R. Gomperts, R.E. Stratmann, O. Yazyev, A.J. Austin, R. Cammi, C. Pomelli, J.W. Ochterski, R.L. Martin, K. Morokuma, V.G. Zakrzewski, G.A. Voth, P. Salvador, J.J. Dannenberg, S. Dapprich, A.D. Daniels, Ö. Farkas, J.B. Foresman, J.V. Ortiz, J. Cioslowski, D.J. Fox, Gaussian, Inc., Wallingford CT, 2009.
- [18] M. Hesse, H. Meier, B. Zeeh, *Spektroskopische Methoden in der Organischen Chemie*, 8th ed., Thieme, Stuttgart, Germany, 2012.
- [19] CrysAlisPro, Agilent Technologies, Version 1.171.35.11, 2011.
- [20] G.M. Sheldrick, SHELXS-97, Program for Crystal Structure Solution, Universität Göttingen, 1997.

- [21] A. Altomare, G. Cascarano, C. Giacovazzo, A. Guagliardi, *Appl. Cryst.* 26 (1993) 343–50.
- [22] G.M. Sheldrick, SHELXL-97, Program for the Refinement of Crystal Structures, University of Göttingen, Germany, 1994.
- [23] A.L. Spek, Platon, A Multipurpose Crystallographic Tool, Utrecht University, Utrecht, The Netherlands, 1999.
- [24] L. Farrugia, WinGX suite for small-molecule single-crystal crystallography, *J. Appl. Crystallogr.* 32 (1999) 837–838.
- [25] Empirical absorption correction using spherical harmonics, implemented in SCALE3 ABSPACK scaling algorithm (CrysAlisPro Oxford Diffraction Ltd., Version 171.33.41, 2009).
- [26] N. Fischer, T.M. Klapötke, M. Reymann, J. Stierstorfer, *Eur. J. Inorg. Chem.* (2012) submitted.
- [27] P.J. Steel, *Chem. J. Cryst.* 26 (1996) 399–402.
- [28] M. Sućeska, *Materials Science Forum* (2004) 465–466, 325–330
- [29] R. Mayer, J. Köhler, A. Homburg, *Explosives*, 5th ed., Wiley VCH, Weinheim, 2002.
- [30] P. Hakey, W. Ouellette, J. Zubietta, T. Korter, *Acta Crystallogr.* E64(8), (2008), 1428.
- [31] J. R. Deschamps, M. Frisch, D. Parrish, *J. Chem. Crystallogr.*, 31 (2011), 966–970.
- [32] <http://www.linseis.com>
- [33] N. Fischer, T.M. Klapötke, J. Stierstorfer, *Z. Naturforsch. B* 67 (2012) 573–588.
- [34] NATO standardization agreement (STANAG) on explosives, impact sensitivity tests, no. 4489, 1st ed., Sept. 17, 1999.
- [35] WIWEB-Standardarbeitsanweisung 4-5.1.02, Ermittlung der Explosionsgefährlichkeit, hier der Schlagempfindlichkeit mit dem Fallhammer, Nov. 8, 2002.
- [36] a) <http://www.bam.de>; b) www.reichel&partner.de
- [37] NATO standardization agreement (STANAG) on explosive, friction sensitivity tests, no. 4487, 1st ed., Aug. 22, 2002.
- [38] WIWEB-Standardarbeitsanweisung 4-5.1.03, Ermittlung der Explosionsgefährlichkeit oder der Reibeempfindlichkeit mit dem Reibeapparat, Nov. 8, 2002.
- [39] Impact: insensitive > 40 J, less sensitive > 35 J, sensitive > 4 J, very sensitive < 3 J. Friction: insensitive > 360 N, less sensitive = 360 N, sensitive > 80 N, very sensitive

>10 N, extremely sensitive < 10 N. According to the UN Recommendations on the Transport of Dangerous Goods, (+) indicates not safe for transport.

[40] <http://www.ozm.cz>

Full Paper

DOI: 10.1002/prop.201((full DOI will be filled in by the editorial staff))

A Selection of Alkali and Alkaline Earth Metal Salts of 5,5'-Bis(1-hydroxytetrazole) in Pyrotechnic Compositions

Niko Fischer^[a], Thomas M. Klapötke^{*[a]}, Stefan Marchner^[a], Magdalena Rusan^[a], Susanne Scheutzwow^[a] and Jörg Stierstorfer^[a]

Abstract: The dilithium (1), disodium (2), dipotassium (3) and dicesium (4) salt as well as the calcium (5), strontium (6) and barium (7) salt of 5,5'-bis(1-hydroxytetrazole) were prepared and characterized including NMR-, IR- and Raman spectroscopy, mass spectrometry, elemental analysis and differential scanning calorimetry. The crystal structures of 1, 2 and 4–6 additionally were determined by single crystal X-ray diffraction. The sensitivities of the salts towards impact, friction and electrostatic discharge were determined by means of BAM (Bundesanstalt für Materialforschung- und prüfung) methods. The potential use of 1, 6 and 7 as coloring agents in pyrotechnical mixtures as well as the utilization of 3 and 4 as additives in near infrared (NIR) emitting pyrotechnical formulations was examined.

Keywords: 5,5'-Bis(tetrazole-1-oxide), Crystal Structures, NIR Flares, Pyrotechnics, Sensitivities

1 Introduction

The research in the various classes of energetic materials is an ongoing project of interest. Recently several strong achievements were described in the field of high explosives [1,2] as well as pyrotechnics [3,4]. Due to an increase in environmental awareness, today's research in the field of high explosives however is more and more based on the interest of synthesizing so called green energetic materials [5,6]. This trend progressively is also observed for the examination of new materials for pyrotechnic applications [7]. The concept of these compounds rests upon a high nitrogen content in order to promote the release of environmentally benign N₂ after decomposition or degradation. Nitrogen-rich azoles [8] such as triazole- and tetrazole derivatives especially in their ionic forms [9] benefit from a high-nitrogen content to release the desirable N₂. In contrast cyclic and caged nitramines mainly decompose into toxic reaction products like nitro- and nitroso-amines [10]. Next to only releasing N₂, the heat of formation of these compounds is fairly high due to a large number of inherently energetic C–N and N–N bonds. Beside a high heat of formation, a high density, high thermal stability and low sensitivities towards impact, friction and electrical discharge are further goals of interest. An energetic building block which fulfills a multitude of the desired features is 5,5'-bis(1-hydroxytetrazole) [11,12]. After abstracting both highly acidic protons of the dihydroxylated bistetrazole an anion for different energetic salts for applications in the high explosives sector as well as for pyrotechnic compositions is created. The tetrazole N-oxide [13,14] not only reveals a high thermal stability, it also leads to a higher density compared to non-oxidized tetrazoles because of further possibilities to form hydrogen bonds. In this context alkali metal and alkaline earth metal salts of the aforementioned anion are further investigated for applications in the fields of “green

pyrotechnics” or primary explosives. Whereas the disodium salt has also been described as an intermediate in the synthesis of dihydroxylammonium 5,5'-bis(tetrazole-1-oxide) (TKX50) [11], the use of dilithium as well as of the alkaline earth metal salts strontium and barium 5,5'-bis(tetrazole-1-oxide) as coloring agents in pyrotechnical mixtures [15] is investigated. Furthermore the dipotassium and dicesium salt are possible additives [16] in pyrotechnical compositions emitting in the near infrared region (NIR) of the electromagnetic spectrum and thus their utilization as ingredient in NIR flares is examined.

Here we report on the full characterization including the crystal structures of most of the alkali metal salts dilithium (1), disodium (2), dipotassium (3) and dicesium (4) as well as the alkaline earth metal salts calcium (5), strontium (6) and barium (7) 5,5'-bis(tetrazol-1-oxide).

2 Results and Discussion

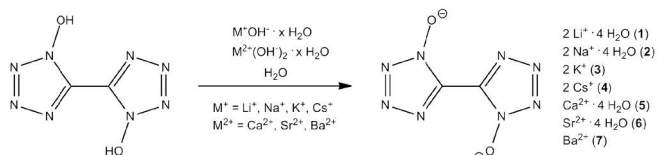
2.1 Synthesis

The starting material 5,5'-bis(1-hydroxytetrazole) was synthesized according to literature [11] and further converted into the various metal salts by adding the respective metal hydroxides to the aqueous solution of 5,5'-bis(1-hydroxytetrazole), which is a divalent acid bearing two highly acidic protons.

The solubility of 5,5'-bis(1-hydroxytetrazole) is fairly good in

[a] Niko Fischer, Stefan Marchner, Prof. Dr. Thomas M. Klapötke*, Magdalena Rusan, Susanne Scheutzwow, Dr. Jörg Stierstorfer
Department Chemie
LMU München
Butenandtstr. 5-13, 81377 München
Fax: (+) 49 89 2180 77492
E-mail: tmk@cup.uni-muenchen.de

hot water but poor in cold water. Regarding this, all reactions were carried out under reflux conditions to make sure that all starting material is entirely dissolved. Due to the lower solubility of the alkaline earth metal hydroxides compared to the alkali metal hydroxides in water, an excess of 1.2 equivalents relative to 5,5'-bis(1-hydroxytetrazole) of the respective alkaline earth metal hydroxide were used in order to achieve better yields. After addition of the base, all batches were filtered hot and slowly cooled down to room temperature. Faster crystallization in the cases of the better soluble alkali metal salts could be achieved by reducing the mother liquors under reduced pressure. The synthetic procedure to compounds **1–7** is summarized in Scheme 1.



Scheme 1. Synthesis of the alkali metal and alkaline earth metal salts of 5,5'-bis(tetrazole-1-oxide).

The dilithium (**1**), the disodium (**2**) as well as the calcium (**5**) and the strontium salt (**6**) crystallize as tetrahydrate as evidenced by single crystal X-ray diffraction. Unfortunately, no single crystals of the potassium (**3**) and the barium salt (**7**) suitable for X-ray diffraction could be obtained, so that the assumption of a crystal water free compound is only based on elemental analysis. The dicesium salt (**4**) crystallizes water free.

2.2 Single Crystal X-ray structure analysis

Selected data and parameter of the X-ray determinations are given in Table 1. In the crystal structures of **1**, **2** and **4–6** the 5,5'-bis(tetrazole-1-oxide) anion reveals similar structural properties. Due to the torsion angles N4ⁱ–C1ⁱ–C1–N1 close varying from 0.3–1.2 ° the dianion can be considered planar and also the tetrazole rings show no distortion. The N–N and C–N bond lengths of the tetrazole rings vary between the lengths typically observed for N–N single and N=N double bonds as well as C–N single and C=N double bonds. Also the C–C bond connecting the two tetrazole moieties as well as the N–O bonds are between a C–C single and a C=C double bond and a N–O single and N=O double bond respectively.

Dilithium 5,5'-bis(tetrazole-1-oxide) tetrahydrate (**1**) crystallizes in the triclinic space group *P*–1 with only one molecular unit (shown in Figure 1) in the unit cell. With an ionic radius of 76 pm, the lithium cations have coordinative bonds to the oxygen atom O1 of the anion (Li1–O1 214.3(2) pm) and also to the nitrogen atoms of the anion (Li1–N4ⁱ 218.7(2) pm). The lithium cations in the structure of **1** are similarly coordinated by four hydrate water molecules revealing different bond lengths each. The anion is coordinated by eight hydrate water molecules which are stabilized by hydrogen bond formation.

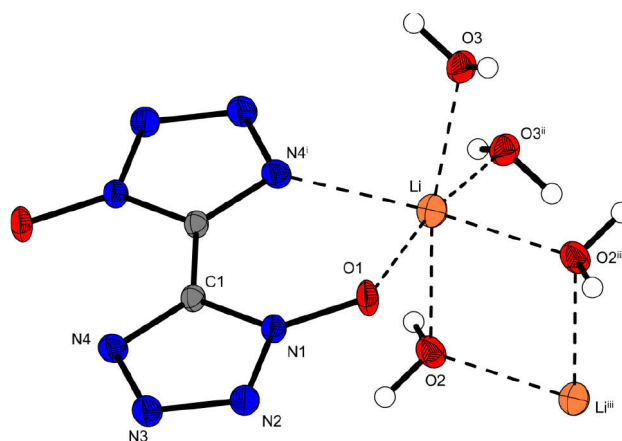


Figure 1. Molecular structure of dilithium 5,5'-bis(tetrazole-1-oxide) tetrahydrate (**1**). Ellipsoids are drawn at the 50 % probability level. Coordination distances [pm]: Li–O1 214.3(2), Li–N4ⁱ 218.7(2), Li–O2 224.1(2), Li–O3 204.7(2), Li–O3ⁱⁱ 232.6(3), Li–O2ⁱⁱⁱ 211.6(3). Symmetry codes: (i) –x, –y, –z; (ii) –x, 1–y, 1–z; (iii) 1–x, 1–y, 1–z.

Disodium 5,5'-bis(tetrazole-1-oxide) tetrahydrate (**2**) (Figure 2) crystallizes in the triclinic space group *P*–1 with two molecular units per unit cell and a density of 1.767 g cm^{–3}. Each sodium ion is coordinated sixfold by four oxygen atoms of hydrate water molecules and one oxygen as well as one nitrogen atom of the anion. The coordination sphere can be described as a distorted octahedron. A view onto the *a/c* plane reveals alternating layers of the dianions and the sodium cations including their coordination sphere. Chains of 5,5'-bis(tetrazole-1-oxide) anions, sodium cations and hydrate water are detected in a view onto the *b/c* plane.

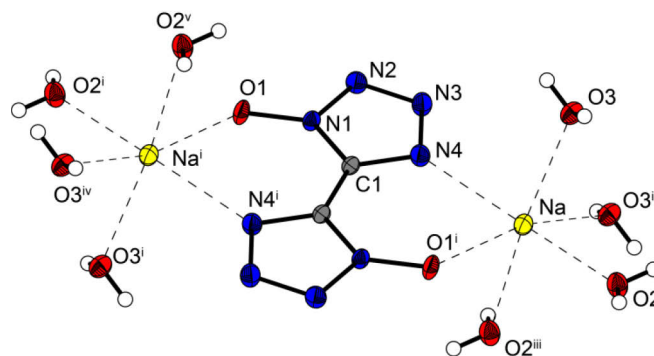


Figure 2. Extended molecular structure of disodium 5,5'-bis(tetrazole-1-oxide) tetrahydrate (**2**). Ellipsoids are drawn at the 50 % probability level. Coordination distances [pm]: Na–O2 235.88(15), Na–O3 234.82(15), Na–N4 241.44(15), Na–O1ⁱ 235.96(14), Na–O3ⁱⁱ 241.40(14), Na–O2ⁱⁱⁱ 249.41(17). (Symmetry codes: (i) –x, –y, –z; (ii) –x, 1–y, 1–z; (iii) 1–x, 1–y, 1–z, (iv); x, –1+y, –1+z, (v); –1+x, –1+y, –1+z.)

Dicesium-5,5'-bis(tetrazole-1-oxide) (**4**) (Figure 3) crystallizes in the orthorhombic space group *Pbca* with a density of 3.285 g cm^{–3}. The unit cell contains eight molecular units. Each cesium atom is coordinated eightfold by four oxygen atoms and four nitrogen atoms. The coordination sphere can be described as a distorted cube. A view along the *c* axis presents alternating layers of the

dianions and cesium cations, which are arranged in a zig-zag pattern.

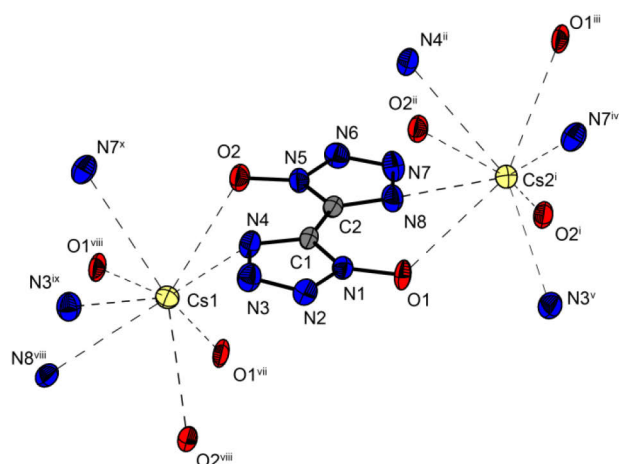


Figure 3. Extended molecular structure of dicesium-5,5'-bis(tetrazole-1-oxide) (**4**). Ellipsoids are drawn at the 50 % probability level. Coordination distances [pm]: Cs1–O1^{viii} 308.3(3), Cs1–O1^{vii} 314.6(3), Cs1–O2 305.1(3), Cs1–O2^{viii} 315.5(3), Cs1–N3^{ix} 327.4(4), Cs1–N4 328.4(4), Cs1–N7^x 339.5(4), Cs1–N8^{viii} 332.4(4), Cs2ⁱ–O1 313.1(4), Cs2ⁱ–O1ⁱⁱⁱ 326.0(4), Cs2ⁱ–O2ⁱⁱ 312.5(3), Cs2ⁱ–N8 331.2(4), Cs2ⁱ–N3^v 331.1(4), Cs2ⁱ–N4ⁱⁱ 331.7(4), Cs2ⁱ–N7^{iv} 327.5(4), Cs2ⁱ–O2³ 323.3(3). Symmetry codes: (i) 0.5–x, 1–y, –0.5+z; (ii) 1–x, 1–y, –z; (iii) 1–x, 0.5+y, –0.5–z; (iv) 0.5+x, y, –0.5–z; (v) x, 0.5–y, –0.5+z; (vi) –0.5+x, 0.5–y, –z; (vii) 0.5–x, –0.5+y, z; (viii) x, 0.5–y, 0.5+z; (ix) –0.5+x, y, 0.5–z; (x) 0.5–x, 1–y, 0.5+z.

Calcium 5,5'-bis(tetrazole-1-oxide) tetrahydrate **5** (Figure 4) crystallizes in the monoclinic space group *C2/c* with four molecular units per unit cell and a density of 1.953 g cm^{–3}. Calcium is coordinated eightfold by four water molecules as well as two oxygen atoms and two nitrogen atoms of two different 5,5'-bis(tetrazole-1-oxide) anions each which all together form a distorted dodecahedron. The packing parallel to the *a/b* planes can be described as alternating layers of calcium, water and the dianions. Along the *c* axis chains of calcium and water molecules are formed.

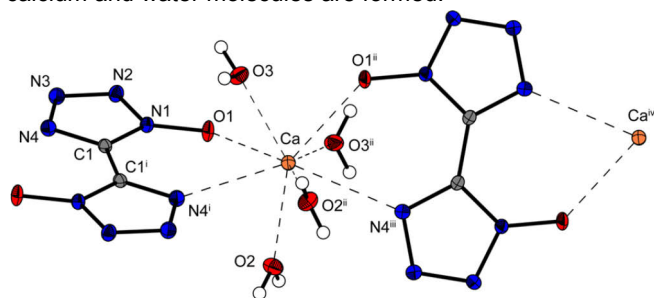


Figure 4. Extended molecular structure of calcium 5,5'-bis(tetrazole-1-oxide) tetrahydrate (**5**). Ellipsoids are drawn at the 50 % probability level. Coordination distances [pm]: Ca–O1 247.91(12), Ca–O2 236.97(14), Ca–O3 239.96(13), Ca–N4ⁱ

266.45(14). Symmetry codes: (i) 1.5–x, 0.5–y, –z; (ii) 2–x, y, 0.5–z; (iii) 0.5+x, 0.5–y, 0.5+z; (iv) 2.5–x, 0.5–y, 1–z.

Strontium 5,5'-bis(tetrazole-1-oxide) tetrahydrate **6** (Figure 5) crystallizes very similar to **5** also in the monoclinic space group *C2/c* with four formula units in the unit cell. Compared to the ionic interaction in the structure of **5**, the different sizes of the ions and also the minor difference of the electronegativity (EN) of the strontium ion lead to collectively larger ionic interactions between Sr and N as well as Sr and O.

Comparing the coordination geometry of **5** with that of **6** one can see that both cations exhibit a highly distorted octahedral coordination sphere consisting of four hydrate water molecules and two further oxygen atoms of the anions.

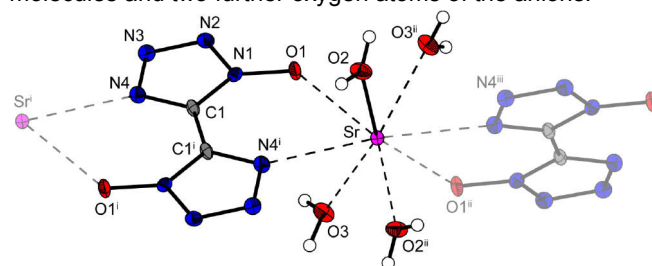


Figure 5. Extended molecular structure of strontium 5,5'-bis(tetrazole-1-oxide) tetrahydrate (**6**). Ellipsoids are drawn at the 50 % probability level. Coordination distances [pm]: Sr1–N4ⁱ 275.1(4), Sr1–O1 257.6(2), Sr1–O2/Sr1–O2ⁱ 252.2(2), Sr1–O3/Sr1–O3ⁱⁱ 254.3(2). Symmetry codes: (i) –x, 2–y, –z; (ii) –x, y, 0.5–z; (iii) x, 2–y, 0.5+z.

IR spectroscopy

Both IR- and Raman spectroscopy can be consulted for the identification of the 5,5'-bis(tetrazole-1-oxide) salts **1–7**. The assignment of absorptions to the different functional groups are based on the values given in literature [17]. The most intensive absorption band in the Raman spectra is the symmetrical stretching mode between the C–C linked tetrazole rings at around 1627–1586 cm^{–1}. The typical ring vibrations of the 5,5'-bis(tetrazole-1-oxide) anion are observed at around 1690–1640 cm^{–1} [ν (CN)] and 1440–700 cm^{–1} [ν (NN), ν (NCN), δ (aromatic tetrazole-oxide ring), δ (NCN)], which partially are in the fingerprint region. Further absorptions based on the N–O valence vibration are visible in the range of 1250–1230 cm^{–1}. All IR spectra additionally show O–H stretching vibrations in the range of 3600–3100 cm^{–1} indicating the presence of the crystal water or moisture.

Table 1. X-ray data and parameters of **3–8**.

	1	2	4	5	6
Formula	C ₂ H ₈ Li ₂ N ₈ O ₆	C ₂ H ₈ N ₈ Na ₂ O ₆	C ₂ Cs ₂ N ₈ O ₂	C ₂ CaH ₈ N ₈ O ₆	C ₂ H ₈ N ₈ O ₆ Sr
FW [g mol ⁻¹]	254.04	286.14	433.92	280.24	327.78
Crystal system	triclinic	triclinic	orthorhombic	monoclinic	monoclinic
Space Group	<i>P</i> -1	<i>P</i> -1	<i>Pbca</i>	<i>C2/c</i>	<i>C2/c</i>
Color / Habit	colorless block	colorless block	colorless rod	colorless block	colorless block
Size [mm]	0.30 x 0.30 x 0.10	0.17 x 0.22 x 0.34	0.09 x 0.10 x 0.18	0.18 x 0.21 x 0.23	0.17 x 0.18 x 0.19
<i>a</i> [pm]	528.96(5)	564.23(6)	1148.69(3)	1164.97(15)	1193.80(8)
<i>b</i> [pm]	637.41(7)	644.12(8)	1157.51(4)	567.03(4)	574.26(3)
<i>c</i> [pm]	825.52(9)	829.25(10)	1319.72(4)	1619.2(2)	1545.6(1)
α [°]	105.928(9)	100.108(10)	90	90	90
β [°]	98.073(9)	96.877(10)	90	116.988(17)	107.484(7)
γ [°]	111.86(1)	112.214(11)	90	90	90
<i>V</i> [pm ³]	2390500(500)	2688900(600)	17547300(900)	953100(200)	10106400(1100)
<i>Z</i>	1	1	8	4	4
$\rho_{\text{calc.}}$ [g cm ⁻³]	1.765	1.767	3.285	1.953	2.154
μ [mm ⁻¹]	0.161	0.228	8.300	0.701	5.375
<i>F</i> (000)	130	146	1552	576	648
$\lambda_{\text{MoK}\alpha}$ [pm]	71.073	71.073	71.073	71.073	71.073
<i>T</i> [K]	173	173	298	173	173
θ Min–Max [°]	4.3, 26.5	4.3, 26.0	4.2, 25.0	4.4, 26.2	4.4, 25.5
Dataset	–6:6; –7:7; –10:10	–6:6; –7:7; –10:10	–13:8; –12:13; –15:14	–12:14; –7:7; –20:20	–14:10; –6:6; –18:18
Reflections collected	2516	2694	7700	2364	2352
Independent refl.	987	1046	1536	950	926
<i>R</i> _{int}	0.024	0.029	0.037	0.022	0.040
Observed reflections	791	803	1242	809	825
Parameters	98	98	128	94	89
<i>R</i> ₁ (obs) ^a	0.0272	0.0284	0.0225	0.0246	0.0248
<i>wR</i> ₂ (all data) ^b	0.0703	0.0715	0.0526	0.0661	0.0488
GooF ^c	1.01	0.94	1.08	1.03	0.94
Resd. Dens. [e pm ⁻³]	–0.24 x 10 ⁻⁶ , 0.19 x 10 ⁻⁶	–0.27 x 10 ⁻⁶ , 0.23 x 10 ⁻⁶	–0.66 x 10 ⁻⁶ , 1.24 x 10 ⁻⁶	–0.22 x 10 ⁻⁶ , 0.29 x 10 ⁻⁶	–0.39 x 10 ⁻⁶ , 0.66 x 10 ⁻⁶
Device type	Oxford Xcalibur3 CCD	Oxford Xcalibur3 CCD	Oxford Xcalibur3 CCD	Oxford Xcalibur3 CCD	Oxford Xcalibur3 CCD
Solution	SIR-92	SIR-92	SIR-92	SIR-92	SIR-92
Refinement	SHELXL-97	SHELXL-97	SHELXL-97	SHELXL-97	SHELXL-97
Absorption correction	multi-scan	multi-scan	multi-scan	multi-scan	multi-scan
CCDC	906341	906342	906343	906339	906340

^a $R_1 = \sum ||F_o| - |F_c|| / \sum |F_o|$; ^b $wR_2 = \{\sum [w(F_o^2 - F_c^2)^2] / \sum [w(F_o^2)]\}^{1/2}$; $w = [\sigma_c^2(F_o^2) + (xP)^2 + yP]^{-1}$ and $P = (F_o^2 + 2F_c^2)/3$; ^c GooF = $\{\sum [w(F_o^2 - F_c^2)^2] / (n-p)\}^{1/2}$ (*n* = number of reflections; *p* = total number of parameters).

Sensitivities and thermal stability

With impact sensitivities of 27–40 J compounds **1**, **5** and **6** can be classified as less sensitive. The sodium salt **2** can be even considered as insensitive towards impact with a value higher than 40 J. These low sensitivities can be attributed probably to the presence of crystal water. The determined values of 2 J (**3**, **4**) and 12 J (**7**) indicate, that these salts are regarded as very sensitive (**3**, **4**) or sensitive towards impact (**7**) respectively, which presumably is due to the fact, that these salts crystallize solvent free.

For the friction sensitivity nearly the same trends as for the impact sensitivity can be observed.

Therefore the sodium (**2**) and strontium (**6**) salt can be considered as less sensitive with regard to their friction sensitivities of 360 N. Compound **1** is regarded as sensitive (324 N) towards friction. Surprisingly the

calcium salt **5** is fairly friction sensitive (56 N) although it is less sensitive towards impact comparable to **1** and **6**. The potassium (**3**), cesium (**4**) and barium salt (**7**) however follow the observed trend, like the friction sensitivities (2, 2 and 12 N) show. Therefore **3–4** have to be classified as very sensitive and **7** as sensitive towards friction.

Except compounds **5** (0.2 J) and **7** (0.1 J) all values for the sensitivity towards electrical discharge (ESD) reach from 0.5 J for the strontium salt **6** to 1 J for the lithium salt **1** (**1**: 1.0, **2**: 0.7, **3**: 0.7, **4**: 0.7, **6**: 0.5) implying only low ESD sensitivities.

In order to determine the melt- and decomposition temperatures as well as the dehydration temperatures of the partially crystal water containing salts of **1–7** differential scanning calorimetry measurements (DSC) were carried out. All experiments were performed in covered aluminium containers (about 1.5 mg of each

energetic material) with a hole (0.1 mm) in the lid for gas release and a nitrogen flow of 20 mL per minute with a Linseis PT 10 DSC [18] calibrated by standard pure indium and zinc at a heating rate of 5 °C min⁻¹. The decomposition temperatures are given as absolute onset temperatures.

The decomposition temperatures of the investigated alkali salts **1-4** (**1**: 225 °C, **2**: 330 °C, **3**: 335 °C, **4**: 314 °C) as well as the alkaline earth metal salts **5-7** (**5**: 300 °C, **6**: 300 °C, **7**: 290 °C) lie in the vicinity of 300 °C except for the dilithium salt **1**, which already decomposes at 225 °C.

The hydrated compounds **1**, **2**, **5** and **6** also show endothermic steps based on the loss of crystal water. Dependent on the geometrical parameters of the crystal structure and its coordination of water the loss is either single or multi stage. In the cases of **5** (144 °C) and **6** (132 °C) the dehydration can be observed as single step, whereas compounds **1** (104, 178 °C) and **2** (124, 154, 180 °C) show two and three endothermic signals indicating a stepwise dehydration of the salt. The barium salt **7** shows no endothermic signal in its DSC curve although the low sensitivity towards impact and friction indicates inclusion of crystal water. This finding however was proved by elemental analysis, which rather indicates a crystal water free structure. Unfortunately also no X-ray structure of the compound could be obtained to ascertain the inclusion or the lack of crystal water molecules in this compound.

In order to determine the exact amount of released crystal water in any of the salts, thermogravimetric measurements had to be accomplished.

Table 2. Sensitivities and thermal behaviour of **1-7**.

	IS (J)	FS (N)	ESD (J)	T _{dehydr} (°C)	T _{dec} (°C)
1	40	324	1.00	104, 178	225
2	>40	360	0.70	124, 154, 180	330
3	2	20	0.70	-	335
4	2	60	0.70	-*	314
5	27	56	0.20	144	300
6	30	360	0.50	132	300
7	12	216	0.50	-	290

* no crystal water contained

Dipotassium (**3**) and dicesium 5,5'-bis(tetrazole-1-oxide) (**4**) as additives in near infrared (NIR) pyrotechnic compositions

For the development of night vision devices new pyrotechnic formulations emitting in the NIR region of the electromagnetic spectrum are of major interest.

The mainly used spectral region for night vision detection is in the range of 700 to 1000 nm [19]. NIR pyrotechnics find therefore their applications in clandestine night operations and are used for instance as hand-held signal flares or parachute flares to illuminate large areas or aiding in emergency landings of aircrafts. IR illuminants are specified by *radiometric* measurements. Important radiometric parameters are the 'radiant intensity' and the introduced 'concealment index'.

The concealment index χ gives the ratio of the emitted NIR radiation to the emitted visible light (equation 1).

$$\chi = \frac{I_{NIR}}{I_{VIS}} \quad (1)$$

with λ_{NIR} = 700–1000 nm and λ_{VIS} = 400–700 nm. It is favored to obtain a high concealment index χ , which means a high NIR emission, and low emission in the visible area. A commonly known disadvantage of many conventional compositions is the high emission of visible light which leads by mischance to a low concealment index. Therefore, compounds which burn with a invisible diffuse flame and furthermore produce large amounts of nitrogen to disseminate condensed reaction products are favored additives in NIR formulations.

For pyrotechnic formulations the following compounds were used: Epon 828 (70 %), Epicure 3140 (30 %) (binder system) and silicon (mesh 250). Hexamine, potassium nitrate and cesium nitrate were received from Sigma-Aldrich, pulverized separately in a ball mill from HARBOR FREIGHT TOOLS for several hours, sieved and dried at 60 °C for at least 12 h prior to use. All compounds were mixed in a mortar and prepared as 50 g (5 x 10 g) batches according to the respective weight percentages of the formulations given in table 2. 10 g of the composition was pressed with 2–3 t in a 54PM250 hydraulic press using a corresponding 20 mm die set from MAASSEN GmbH.

Radiometric emissive properties of the formulations were characterized using a HR2000+ES spectrometer with an ILX511B linear silicon CCD-array detector and included software from OCEAN OPTICS. The spectrometer comprises a wavelength region from 200–1100 nm, in which the measurements for NIR calculations were in the range of 400–1100 nm. The standard integration time was 100 ms and the average scan time 35 s. Radiometric data obtained from the spectrometer were normally given in counts and converted to Watts per steradian (W/sr) and Candela (Cd) with an in-house MATLAB program. The distance between detector and NIR pellet was 1 m. To assess the utility of **3** and **4** as ingredients in NIR pyrotechnic compositions, two formulations BTO1 and BTO2 were prepared and the radiometric emissive properties

measured and compared to reference compositions 1 and 2, which are currently used compositions [19] containing cesium and/or potassium nitrate as oxidizer.

Table 3. Composition of pyrotechnic formulations containing dipotassium and dicesium 5,5'-bis(tetrazole-1-oxide) **3** and **4** as well as the reference compositions 1 and 2.

[wt%] in form.	Ref. 1	Ref. 2	BTO1	BTO2
KNO ₃	70	30	70	30
CsNO ₃	-	40	-	40
Hexamine	16	16	11	15
3	-	-	5	-
4	-	-	-	1
Silicon	10	10	10	10
Binder	4	4	4	4

The average weight of the BTO1 pellets was 9.9 g at a density of 1.68 g cm⁻¹ and for BTO2 pellets 9.8 g at a density of 1.71 g cm⁻¹, respectively. Both compositions are insensitive against friction, impact, and electric discharge (360 N, 40 J, 1.5 J). Due to the surprisingly poor burning behavior, only two compositions were tested whereas the amount of **4** in composition 2 was reduced to 1 %. The size of the observed flame for BTO1 and 2 was diminutive compared to the flame surface of both references. The maximum intensity of 20 g of reference 1 was about 13 W/sr with a concealment index of 34 and a burning time of 25 s to 30 s. The maximum intensity of reference 2 was about 12 W/sr for 20 g of the composition, a concealment index of around 60 and a burning time of 30 s. The maximum intensities of BTO1 (20 g flare) was around 5 W/sr with a concealment index of 25 and a burning time of larger than 30 s, and for BTO2 around 15 W/sr (20 g), a concealment index of 33 and a burning time of 33 s, respectively (Figure 1).

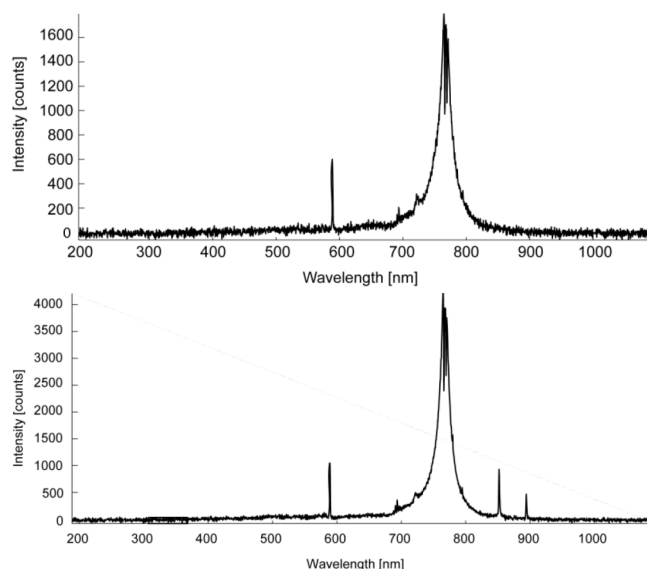


Figure 4. Intensity plots of formulations BTO1 (20 g) and BTO2 (10 g).

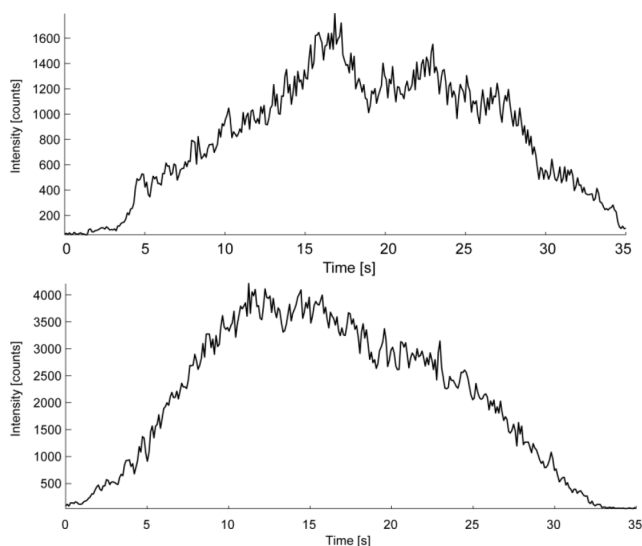


Figure 5. Burn time plots of formulations BTO1 (20 g) and BTO2 (10 g).

Although the burn times of both formulations are high, the maximum intensity values in BTO1 containing 5 % of **3** are very low. The value for the formulation BTO2 containing only 1 % of **4** are slightly better than the values obtained for reference 2.

Pyrotechnic compositions using strontium (6) and barium 5,5'-bis(tetrazole-1-oxide) (7) as coloring agents

In order to obtain pyrotechnics with a high color brilliance it is necessary to avoid the generation of smoke during the combustion. Therefore compounds with a high nitrogen content are suitable as coloring agents [20,21]. Due to the formation of nitrogen as main decomposition product these compounds are additionally promising substances in the development

of ecologically friendly pyrotechnic. Therefore investigations of several pyrotechnical mixtures with strontium and barium 5,5'-bis(tetrazole-1-oxide) were performed.

Several pyrotechnic formulations of **6** and **7** were investigated (Table 4). The pyrotechnical compositions were prepared by mixing all substances, except the binder, in a mortar. Then the binder, a solution of 25 % vinyl alcohol acetate resin (VAAR), was added. The mixture was formed by hand and dried under high vacuum for three hours. The controlled burn down was filmed with a digital video camera recorder (SONY, DCR-HC37E). The performance of each composition has been evaluated with respect to color emission (subjective impression), smoke generation and the amount of solid residues. **6** and **7** were used as red and green coloring agents. Ammonium nitrate and magnesium or boron were used as oxidizer and fuel respectively. In table 4 the content of the compositions (mass percent) is summarized.

Table 4. Composition of pyrotechnical formulations containing **6** and **7** as coloring agents.

[wt%]	Sr-BTO_1	Sr-BTO_2	Ba-BTO_1	Ba-BTO_2	Ba-BTO_3
MBTO	40	43	40	43	35
NH ₄ NO ₃	45	42	45	42	45
Mg	8	8	-	-	-
B	-	-	8	8	13
VAAR	7	7	7	7	7

The formulations Sr-BTO_1 and Sr-BTO_2 consist of 40 % and 43 % of the metal salt, 45% and 42 % of NH₄NO₃ and in both formulations 8 % of magnesium and 7 % of binder. Both Sr-BTO formulations burned fast with an intense red flame color (Fig. 6). While the combustion of composition Sr-BTO_1 produced some smoke, the burning of Sr-BTO_2 was smokeless. Some residues could be observed for both compositions.



Figure 6. From left to right: Flame colors of Sr-BTO_1, Sr-BTO_2, Ba-BTO_1, Ba-BTO_2 and Ba-BTO_3.

The compositions Ba-BTO_1 and Ba-BTO_2 with 40% and 43 % of the barium salt, 45 % and 42 % of ammonium nitrate as oxidizer, 8 % of amorphous boron as fuel and 7 % of binder showed a fast combustion with a green flame color. Mixture Ba-BTO_1 burned smokeless whereas formulation Ba-BTO_2 revealed some smoke and in both cases some residues remained. The third investigated formulation Ba-BTO_3 with 35 % of the metal salt, 45 % of oxidizer, 13 % of fuel and 7 % of binder showed a faster combustion velocity than the other Ba-BTO compositions. A green flame color with lots of sparks could be observed and some solid residues remained (Fig. 6).

3 Experimental Part

Caution! The herein described alkali and alkaline earth metal salts are energetic materials and show increased sensitivities towards shock and friction,

especially if crystal water free or dehydrated. Therefore, proper safety precautions (safety glass, face shield, earthed equipment and shoes, Kevlar® gloves and ear plugs) have to be applied while synthesizing and handling the described compounds.

All chemicals and solvents were employed as received (Sigma-Aldrich, Fluka, Acros). ¹H and ¹³C NMR spectra were recorded using a JEOL Eclipse 270, JEOL EX 400 or a JEOL Eclipse 400 instrument. The chemical shifts quoted in ppm in the text refer to typical standards such as tetramethylsilane (¹H, ¹³C). To determine the melting and decomposition temperatures of the described compounds a Linseis PT 10 DSC (heating rate 5 °C min⁻¹) was used. Infrared spectra were measured using a Perkin Elmer Spectrum One FT-IR spectrometer as KBr pellets. Raman spectra were recorded on a Bruker MultiRAM Raman Sample Compartment D418 equipped with a Nd-YAG-Laser (1064 nm) and a LN-Ge diode as

detector. Mass spectra of the described compounds were measured at a JEOL MStation JMS 700 using FAB technique. To measure elemental analyses a Netsch STA 429 simultaneous thermal analyzer was employed.

The low temperature determination of the crystal structures of **1**, **2** and **4–6** were performed on a Oxford Xcalibur3 diffractometer with a Spellman generator (voltage 50 kV, current 40 mA) and a KappaCCD detector. The data collection and reduction were carried out using the CrysAlisPro software [22]. The structures were solved either with SIR-92 [23] or SHELXS-97 [24], refined with SHELXL-97 [25] and finally checked using the PLATON [26] software integrated in the WinGX [27] software suite. The non-hydrogen atoms were refined anisotropically and the hydrogen atoms were located and freely refined. The absorptions were corrected by a Scale3 Abspack multi-scan method [28].

The impact sensitivity tests were carried out according to STANAG 4489 [29] modified instruction [30] using a BAM (Bundesanstalt für Materialforschung) drophammer [31]. The friction sensitivity tests were carried out according to STANAG 4487 [32] modified instruction [33] using the BAM friction tester. The classification of the tested compounds results from the "UN Recommendations on the Transport of Dangerous Goods" [34]. Additionally all compounds were tested upon the sensitivity towards electrical discharge using the Electric Spark Tester ESD 2010 EN [35].

General procedure for alkali metal salts

10 mmol (2.06 g) of 5,5'-bis(1-hydroxytetrazole) dihydrate was suspended in 80 mL of water. The mixture is heated to reflux to obtain a clear solution. 20 mmol of the alkali metal hydroxide was added and the solution was cooled down to room temperature causing the precipitation of the salts, all of which only show moderate water solubility. In some cases the mother liquors had to be concentrated on a rotary evaporator to app. 60 % of their original volume to initiate precipitation of the products.

Dilithium 5,5'-bis(tetrazole-1-oxide) tetrahydrate (**1**)

The colorless crystalline precipitate was filtrated and 2.11 g of **1** (8.31 mmol, 83%) was obtained.

DSC (5 °C min⁻¹): 104, 178 °C (dehydr.), 225 °C (dec.); IR (KBr, cm⁻¹): $\tilde{\nu}$ = 3538 (s), 3311 (vs), 2725 (w), 2187 (w), 2021 (w), 1669 (s), 1434 (s), 1368 (m), 1243 (s), 1181 (m), 1064 (m), 1009 (m), 757 (m), 704 (m), 618 (m), 509 (w); Raman (1064 nm, 300 mW, 25 °C, cm⁻¹): $\tilde{\nu}$ = 1627 (100), 1603 (4), 1481 (2), 1248 (15), 1150 (11), 1130 (7), 1019 (5), 791 (2), 745 (1), 620 (1),

423 (2), 411 (2); ¹H NMR (DMSO-*d*₆, 25 °C, ppm) δ : 4.56; ¹³C NMR (DMSO-*d*₆, 25 °C, ppm) δ : 135.5; MS (FAB⁻) *m/z* = 169.1 (C₂HN₈O₂⁻); EA (C₂H₈N₈O₆Li₂, MW 254.02): calc.: C 9.46, H 3.17, N 44.11 %; found: C 9.97, H 2.99, N 44.42 %; BAM drophammer: 40 J; friction tester: 324 N; ESD: 1.0 J.

Disodium 5,5'-bis(tetrazole-1-oxide) tetrahydrate (**2**)

Filtration of the colorless crystalline precipitate yielded 2.30 g (8.04 mmol, 80%) of **2**.

DSC (5 °C min⁻¹): 124, 154, 180 °C (dehydr.), 330 °C (dec.); IR (KBr, cm⁻¹): $\tilde{\nu}$ = 3496 (vs), 3404 (vs), 3308 (s), 3269 (s), 2192 (w), 1672 (m), 1423 (s), 1382 (w), 1359 (w), 1239 (s), 1178 (m), 1149 (w), 1067 (m), 1007 (m), 755 (m), 718 (w), 656 (m), 620 (m), 501 (m); Raman (1064 nm, 300 mW, 25 °C, cm⁻¹): $\tilde{\nu}$ = 1605 (100), 1581 (3), 1468 (2), 1248 (13), 1154 (11), 1131 (4), 1016 (4), 791 (3), 614 (1), 410 (2); ¹H NMR (DMSO-*d*₆, 25 °C, ppm) δ : 3.43; ¹³C NMR (DMSO-*d*₆, 25 °C, ppm) δ : 134.7; EA (C₂H₈N₈O₆Na₂, MW 286.11): calc.: C 8.40, H 2.82, N 39.16 %; found: C 8.99, H 2.76, N 38.79 %; BAM drophammer: >40 J; friction tester: 360 N; ESD: 0.7 J.

Dipotassium 5,5'-bis(tetrazole-1-oxide) (**3**)

The precipitate was filtrated to yield 2.15 g (8.73 mmol, 87%) of **3** as slightly yellow octahedral cystals.

DSC (5 °C min⁻¹): 335 °C (dec.); IR (KBr, cm⁻¹): $\tilde{\nu}$ = 3496 (s), 3407 (s), 3252 (m), 2165 (w), 1663 (w), 1637 (w), 1510 (w), 1409 (s), 1356 (m), 1234 (vs), 1164 (s), 1058 (m), 997 (m), 732 (m), 713 (w), 614 (w), 502 (m); Raman (1064 nm, 300 mW, 25 °C, cm⁻¹): $\tilde{\nu}$ = 2012 (1), 1605 (100), 1458 (5), 1240 (27), 1142 (6), 1131 (9), 1118 (17), 1000 (11), 781 (27), 741 (2), 620 (8); 434 (4), 411 (6), 285 (7); ¹H NMR (DMSO-*d*₆, 25 °C, ppm) δ : 4.67; ¹³C NMR (DMSO-*d*₆, 25 °C, ppm) δ : 140.0; MS (FAB⁻): *m/z* = 169.0 (C₂HN₈O₂⁻); EA (C₂N₈O₂K₂, MW 246.27): calc.: C 9.75, N 45.50 %; found: C 10.19, N 45.21 %; BAM drophammer: 2 J; friction tester: 20 N; ESD: 0.7 J.

Dicesium 5,5'-bis(tetrazole-1-oxide) (**4**)

After filtration of the precipitate 3.92 g (9.03 mmol, 90%) of **4** as colorless crystals could be isolated.

DSC (5 °C min⁻¹): 314 °C (dec.); IR (KBr, cm⁻¹): $\tilde{\nu}$ = 3495 (vs), 3407 (vs), 2163 (w), 1663 (w), 1409 (s), 1382 (m), 1355 (m), 1234 (m), 1163 (w), 1057 (w), 997 (w), 732 (w), 501 (w), 488 (w); Raman (1064 nm, 300 mW, 25 °C, cm⁻¹): $\tilde{\nu}$ = 3162 (1), 1981 (1), 1586 (100), 1447 (3), 1285 (1), 1229 (22), 1187 (1), 1138 (8), 1100 (11), 997 (6), 755 (9), 739 (2), 702 (1), 609 (4), 416

(5); ^1H NMR (DMSO- d_6 , 25 °C, ppm) δ : 4.67; ^{13}C NMR (DMSO- d_6 , 25 °C, ppm) δ : 134.0; MS (FAB $^-$): m/z = 169.0 ($\text{C}_2\text{HN}_8\text{O}_2^-$); EA ($\text{C}_2\text{N}_8\text{O}_2\text{Cs}_2$, MW 206.12): calc.: C 5.54, N 25.83 %; found: C 5.48, H 0.34, N 23.33 %; BAM drophammer: 2 J; friction tester: 60 N; ESD: 0.7 J.

General procedure of Alkaline earth metal salts

10 mmol (2.06 g) of 5,5'-bis(1-hydroxytetrazole) dihydrate was suspended in 80 mL of water. The mixture is heated to reflux in order to dissolve the acid. After obtaining a clear solution 24 mmol of the alkaline earth metal hydroxide was added. The solution was kept boiling for 5 min. followed by filtration of the hot solution. The filtrate was then cooled down to room temperature and the alkali earth metal salts precipitated within a few minutes.

Calcium 5,5'-bis(tetrazole-1-oxide) tetrahydrate (5)

After filtration of the colorless crystalline precipitate 2.11 g (7.53 mmol, 75%) of **5** were obtained.

DSC (5 °C min $^{-1}$): 144 °C (dehydr.), 300 °C (dec.); IR (KBr, cm $^{-1}$): $\tilde{\nu}$ = 3477 (vs), 3360 (s), 3241 (s), 2207 (w), 2032 (w), 1678 (w), 1640 (m), 1424 (s), 1414 (s), 1358 (w), 1242 (s), 1189 (m), 1152 (w), 1073 (m), 1010 (m), 746 (m), 591 (w), 506 (w); Raman (1064 nm, 300 mW, 25 °C, cm $^{-1}$): $\tilde{\nu}$ = 2032 (1), 1614 (100), 1590 (3), 1469 (2), 1296 (1), 1257 (13), 1158 (9), 1141 (6), 1019 (4), 790 (4), 742 (1), 704 (1), 422 (2), 294 (1), 183 (2), 119 (10); EA ($\text{C}_2\text{H}_8\text{N}_8\text{O}_6\text{Ca}$, MW 280.21): calc.: C 8.57, H 2.88, N 39.99 %; found: C 8.98, H 2.75, N 39.92 %; BAM drophammer: 27 J; friction tester: 56 N; ESD: 0.2 J.

Strontium 5,5'-bis(tetrazole-1-oxide) tetrahydrate (6)

The colorless crystalline precipitate was filtrated yielding 2.33 g (7.11 mmol, 71%) of **6**.

DSC (5 °C min $^{-1}$): 132 °C (dehydr.), 300 °C (dec.); IR (KBr, cm $^{-1}$): $\tilde{\nu}$ = 3495 (vs), 3387 (s), 2703 (w), 2198 (w), 2027 (w), 1672 (w), 1627 (m), 1535 (w), 1421 (m), 1412 (s), 1242 (s), 1184 (m), 1069 (m), 1008 (m), 747 (m), 573 (w), 499 (w); Raman (1064 nm, 300 mW, 25 °C, cm $^{-1}$): $\tilde{\nu}$ = 1603 (100), 1466 (3), 1295 (1), 1256 (15), 1154 (10), 1135 (6), 1017 (4), 791 (4), 741 (1), 703 (1); 418 (2); MS (FAB $^-$): m/z = 169.0 ($\text{C}_2\text{HN}_8\text{O}_2^-$); EA ($\text{C}_2\text{H}_8\text{N}_8\text{O}_6\text{Sr}$, MW 327.75): calc.: C 7.33, H 2.46, N 34.19 %; found: C 7.66, H 2.27, N 34.18 %; BAM drophammer: 30 J; friction tester: 360 N; ESD: 0.5 J.

Barium 5,5'-bis(tetrazole-1-oxide) hydrate (7)

The precipitate was filtrated to yield 2.39 g (7.83 mmol, 78%) of **7** as a slightly yellow solid.

DSC (5 °C min $^{-1}$): 290 °C (dec.); IR (KBr, cm $^{-1}$): $\tilde{\nu}$ = 3435 (s), 3280 (m), 2010 (w), 1652 (m), 1515 (w), 1425 (s), 1414 (s), 1358 (m), 1236 (vs), 1173 (s), 1050 (m), 1004 (m), 734 (m), 716 (w), 597 (w), 506 (m); Raman (1064 nm, 300 mW, 25 °C, cm $^{-1}$): $\tilde{\nu}$ = 3219 (1), 1613 (100), 1590 (3), 1476 (2), 1464 (1), 1291 (1), 1243 (18), 1143 (6), 1125 (6), 1011 (6), 783 (8), 742 (1), 623 (3), 427 (1), 410 (3); EA ($\text{C}_2\text{H}_8\text{N}_8\text{O}_6\text{Ba}$, MW 206.12): calc.: C 7.87, N 36.69 %; found: C 7.32, N 32.83 %; BAM drophammer: >40 J; friction tester: 216 N; ESD: 0.5 J.

4 Conclusion

From the experimental study of alkali and alkaline earth metal salts of 5,5'-bis(1-hydroxytetrazole) the following conclusions can be drawn:

- By reacting aqueous solutions of 5,5'-bis(1-hydroxytetrazole) with alkali and alkaline earth metal hydroxides, the dilithium (**1**), disodium (**2**), dipotassium (**3**), dicesium (**4**), calcium (**5**) strontium (**6**) and barium (**7**) 5,5'-bis(tetrazole-1-oxide) can be isolated. Due to their only moderate (**1–4**) or poor (**5–7**) water solubility they either crystallize from their original aqueous mother liquors or after reducing the volume of the mother liquor to approximately 60 %.
- The salts studied crystallize in the space groups *P*-1 (**1**, **2**), *Pbca* (**4**) and *C2/c* (**5**, **6**) with densities between 1.765 g cm $^{-3}$ for the dilithium salt **1** and 3.285 g cm $^{-3}$ for the dicesium salt **4** either as tetrahydrates (**1**, **2**, **5**, **6**) or water free (**4**). No crystal structures of **3** and **7** were measured, however, their elemental analyses indicate a solvent free crystallization of these salts.
- All salts decompose at temperatures higher than 200 °C (**1**: 225 °C, **5**, **6**: 300 °C, **7**: 290 °C) or higher than 300 °C (**2**: 330 °C, **3**: 335 °C, **4**: 314 °C). The (stepwise) loss of crystal water is observed in their DSC curves at 104 and 178 °C (**1**), 124, 154 and 180 °C (**2**), 144 °C (**5**) and 132 °C (**6**) as endothermic events.
- If crystal water free (**3**, **4**) they are highly sensitive towards impact and friction (IS: 2 J; FS 20 N (**3**), 60 N (**4**)). If hydrated the sensitivities are moderate to low (IS: 40 J (**1**, **2**), 12 J (**7**), 30 J (**6**), 27 J (**5**); FS: 360 N (**2**, **6**), 324 N (**1**), 216 (**7**), 56 N (**5**)).
- If used as additives in pyrotechnic formulations for NIR flares, compositions containing **3** (BTO1: 5 W/sr, χ = 25) and **4** (BTO2: 15 W/sr, χ = 33) do not reach the radiant intensities and concealment indices observed for the commonly used reference

formulations 1 (Ref1: 13 W/sr, $\chi = 34$) and 2 (Ref2: 12 W/sr, $\chi = 60$).

- The strontium (6) and the barium salt (7) were tested in pyrotechnical compositions as red respectively green colorants. The color performance of both formulations containing 6 shows no noteworthy difference. Both mixtures burned with less smoke and some residues remained. Among the formulations containing the barium salt 7, the composition Ba-BTO_2 with the highest content of the metal salt showed the most intense green flame color and no sparks. Only the Ba-BTO_1 mixture revealed no smoke during the combustion, but residues were observable.

Acknowledgment

Financial support of this work by the Ludwig-Maximilian University of Munich (LMU), the European Research Office (ERO) of the U.S. Army Research Laboratory (ARL), the Armament Research, Development and Engineering Center (ARDEC) and the Strategic Environmental Research and Development Program (SERDP) under contract nos. W911NF-09-2-0018 (ARL), W911NF-09-1-0120 (ARDEC), W011NF-09-1-0056 (ARDEC) and 10 WPSEED01-002 / WP-1765 (SERDP) is gratefully acknowledged. The authors acknowledge collaborations with Dr. Mila Krupka (OZM Research, Czech Republic) in the development of new testing and evaluation methods for energetic materials and with Dr. Muhamed Sucasca (Brodarski Institute, Croatia) in the development of new computational codes to predict the detonation and propulsion parameters of novel explosives. We are indebted to and thank Drs. Betsy M. Rice and Brad Forch (ARL, Aberdeen, Proving Ground, MD) and Mr. Gary Chen (ARDEC, Picatinny Arsenal, NJ) for many helpful and inspired discussions and support of our work. The authors thank Mr. Stefan Huber for the sensitivity measurements.

Symbols and Abbreviations

BAM	Bundesanstalt für Materialforschung und -prüfung
BTO	5,5'-bis(tetrazole-1-oxide)
CCDC	Cambridge crystallographic data centre
DSC	differential scanning calorimetry
FW	formula weight (g/mol)
IS	impact sensitivity (J)
FS	friction sensitivity (N)
ESD	electrostatic discharge (J)
EN	electronegativity
GoF	goodness of fit

IR	infrared
$\lambda_{\text{MoK}\alpha}$	X-ray laser wavelength
MS	mass spectrometry
N	nitrogen content (%)
NIR	near infrared
NMR	nuclear magnetic resonance
ρ	density (g/cm ³)
STANAG	standardization agreement
$T_{\text{dec.}}$	decomposition temperature (°C)
$T_{\text{dehydr.}}$	dehydration temperature
χ	concealment index
VAAR	vinyl alcohol acetate resin
Z	number of molecular units per unit cell

References

- [1] V. Thottempudi, F. Forohor, D. A. Parrish, J. M. Shreeve, Tris(triazolo)benzene and Its Derivatives: High-Density Energetic Materials, *Angew. Chem. Int. Ed.* **2012**, 39, 9881–9885.
- [2] L. Liang, H. Huang, K. Wang, C. Bian, S. Chengming; L. Jinhong; L. Ling, Z. Liming; F. Zhao, Z. Zhou, Oxy-bridged bis(1H-tetrazol-5-yl)furan and its energetic salts paired with nitrogen-rich cations: highly thermally stable energetic materials with low sensitivity, *J. Mater. Chem.* **2012**, 22, 21954–21964.
- [3] E.-C. Koch, V. Weiser, E. Roth, 2,4,6-Trinitrotoluene: A Surprisingly Insensitive Energetic Fuel and Binder in Melt-Cast Decoy Flare Compositions, *Angew. Chem. Int. Ed.* **2012**, 51, 10038–10040.
- [4] E.-C. Koch, A. Hahma, Metal-Fluorocarbon Pyrolants. XIV: High Density-High Performance Decoy Flare Compositions Based on Ytterbium/Polytetrafluoroethylene/Viton®, *Z. Anorg. Allg. Chem.* **2012**, 638, (5), 721–724.
- [5] P. Pagoria, M. Z. A. DeHope, G. Lee, A. Mitchell, P. Leonard, “Green” energetic materials synthesis at LLNL, New Trends in Research of Energetic Materials, Proceedings of the Seminar, 15th, Pardubice, Czech Republic, Apr. 18-20, **2012**, 1, 55-65.
- [6] M. B. Talawar, R. Sivabalan, T. Mukundan, H. Muthurajan, A. K. Sikder, B. R. Gandhe, A. Subhananda Rao, Environmentally compatible next generation green energetic materials (GEMs), *J. Hazard. Mater.* **2009**, 161(2–3), 589–607.
- [7] G. Steinhäuser, T. M. Klapötke, “Green” Pyrotechnics: A Chemists’ Challenge, *Angew. Chem. Int. Ed.* **2008**, 47, 3330–3347.

- [8] H. Gao, J. M. Shreeve, Azole-Based Energetic Salts, *Chem Rev.* **2011** 111, 7377–7436.
- [9] R. P. Singh, R. D. Verma, D. T. Meshri, J. M. Shreeve, Energetic Nitrogen-Rich Salts and Ionic Liquids, *Angew. Chem. Int. Ed.* **2006**, 45, 3584 – 3601.
- [10] S. A. Meyer, A. J. Marchand, J. L. Hight, G. H. Roberts, L. B. Escalon, L. S. Inouye, D. K. MacMillan, Up- and down-procedure (UDP) determinations of acute oral toxicity of nitroso degradation products of hexahydro-1,3,5-trinitro-1,3,5-triazine (RDX), *J. Appl. Toxicol.* **2005**, 25(5), 427–434.
- [11] N. Fischer, D. Fischer, T. M. Klapötke, D. Piercey, J. Stierstorfer, Pushing the limits of energetic materials – the synthesis and characterization of dihydroxylammonium 5,5'-bistetrazole-1,1'-diolate, *J. Mater. Chem.* **2012**, 22, 20418–20422.
- [12] I. V. Tselinskii, S. F. Mel'nikova and T. V. Romanova, Synthesis and reactivity of carbohydroximoyl azides: I. Aliphatic and aromatic carbohydroximoyl azides and 5-substituted 1-hydroxytetrazoles based thereon, *Russ. J. Org. Chem.* **2001**, 37, 430–436.
- [13] M. Göbel, K. Karaghiosoff, T. M. Klapötke, D. G. Piercey, J. Stierstorfer, Nitrotetrazolate-2N-oxides and the strategy of N-oxide introduction, *J. Am. Chem. Soc.* **2010**, 132(48), 17216–17226.
- [14] A. M. Churakov, V. A. Tartakovsky, Progress in 1,2,3,4-Tetrazine Chemistry, *Chem. Rev.* **2004**, 104, 2601–2616.
- [15] E.-C. Koch, Special materials in Pyrotechnics: III. Application of lithium and its compounds in energetic systems, *Propellants Explos. Pyrotech.* **2004**, 29(2), 67–80.
- [16] P. A. Jemmett, K. Patel, Enhanced near infrared illuminating compositions, *Proceedings of the International Pyrotechnics Seminar*, 36th, August 23rd -29th **2009**, Rotterdam, The Netherlands, pp. 73–86.
- [17] M. Hesse, H. Meier, B. Zehe, S. Bienz, L. Bigler, T. Fox, in *Spektroskopische Methoden in der organischen Chemie*, Vol. 8, Thieme, Stuttgart, New York, **2012**.
- [18] <http://www.linseis.com>
- [19] E.-C. Koch, Survey on State-of-the-art Near-Infrared Emitting Compositions for Flares and Tracers, NATO-MSIAC, Belgium, **2009**, and literature therein.
- [20] D. E. Chavez, M. A. Hiskey, D. L. Naud, High-Nitrogen Fuels for Low-Smoke Pyrotechnics, *J. Pyrotech.* **1999**, 10, 17–36.
- [21] D. E. Chavez, M. A. Hiskey, High-Nitrogen Pyrotechnic Compositions, *J. Pyrotech.* **1998**, 7, 11–14.
- [22] CrysAlisPro Oxford Diffraction Ltd., Version 171.33.41, **2009**.
- [23] A. Altomare, G. Cascarano, C. Giacovazzo, A. Guagliardi, Completion and refinement of crystal structures with SIR92, *J. Appl. Cryst.* **1993**, 26, 343.
- [24] G. M. Sheldrick, *SHELXS-97, Program for Crystal Structure Solution*, University of Göttingen, Germany, **1997**.
- [25] G. M. Sheldrick, *SHELXL-97, Program for the Refinement of Crystal Structures*, University of Göttingen, Germany, **1997**.
- [26] A. L. Spek, *PLATON, A Multipurpose Crystallographic Tool*, Utrecht University, Utrecht, The Netherlands, **1998**.
- [27] L. J. Farrugia, WinGX suite for small-molecule single-crystal crystallography, *J. Appl. Cryst.* **1999**, 32, 837–838.
- [28] Empirical absorption correction using spherical harmonics, implemented in SCALE3 ABSPACK scaling algorithm (CrysAlisPro Oxford Diffraction Ltd., Version 171.33.41, **2009**).
- [29] NATO standardization agreement (STANAG) on explosives, impact sensitivity tests, no. 4489, 1st ed., Sept. 17, **1999**.
- [30] WIWEB-Standardarbeitsanweisung 4-5.1.02, Ermittlung der Explosionsgefährlichkeit, hier der Schlagempfindlichkeit mit dem Fallhammer, Nov. 8, **2002**.
- [31] <http://www.bam.de>
- [32] NATO standardization agreement (STANAG) on explosive, friction sensitivity tests, no. 4487, 1st ed., Aug. 22, **2002**.
- [33] WIWEB-Standardarbeitsanweisung 4-5.1.03, Ermittlung der Explosionsgefährlichkeit oder der Reibeempfindlichkeit mit dem Reibeapparat, Nov. 8, **2002**.
- [34] Impact: insensitive > 40 J, less sensitive 35 J, sensitive 4 J, very sensitive 3 J. Friction: insensitive > 360 N, less sensitive = 360 N, sensitive < 360 N, > 80 N, very sensitive < 80 N, extremely sensitive < 10 N. According to the UN

Recommendations on the Transport of Dangerous Goods, (+) indicates not safe for transport.

[35] <http://www.ozm.cz>

Bibliography

Publications

1. N. Fischer, T. M. Klapötke, S. Scheutzow, J. Stierstorfer, Hydrazinium 5-Aminotetrazolate: An Insensitive Energetic Material Containing 83.72% Nitrogen, *Cent. Eur. J. Energetic Mater.* **2008**, 5 (3–4), 3-18.
2. N. Fischer, T. M. Klapötke, J. Stierstorfer, New Nitriminotetrazoles – Synthesis, Structures and Characterization, *Z. Anorg. Allg. Chem.* **2009**, 635, 271–281.
3. N. Fischer, K. Karaghiosoff, T. M. Klapötke, J. Stierstorfer, New Energetic Materials featuring Tetrazoles and Nitramines – Synthesis, Characterization and Properties, *Z. Anorg. Allg. Chem.* **2010**, 636, 735–749.
4. N. Fischer, T. M. Klapötke, D. Piercey, S. Scheutzow, J. Stierstorfer, Diaminouronium Nitriminotetrazolates – Thermally Stable Explosives, *Z. Anorg. Allg. Chem.* **2010**, 636, 2357–2363.
5. N. Fischer, T. M. Klapötke, F. Martin, J. Stierstorfer, Energetic Materials based on 1-Amino-3-nitroguanidine, *New Trends in Research of Energetic Materials, Proceedings of the Seminar*, 13th, Pardubice, Czech Republic, **2010**, 1, 113–129.
6. N. Fischer, T. M. Klapötke, J. Stierstorfer, K. R. Tarantik, 1-Nitratoethyl-5-nitriminotetrazole Derivatives - Shaping Future High Explosives, *New Trends in Research of Energetic Materials, Proceedings of the Seminar*, 13th, Pardubice, Czech Republic, **2010**, 2, 455–467.
7. N. Fischer, T. M. Klapötke, J. Stierstorfer, Salts of 2-methyl-5-nitraminotetrazole – Secondary Explosives with Low Sensitivities, *New Trends in Research of Energetic Materials, Proceedings of the Seminar*, 13th, Pardubice, Czech Republic, **2010**, 2, 684–698.
8. T. Fendt, N. Fischer, T. M. Klapötke, J. Stierstorfer, N-Rich Salts of 2-Methyl-5-nitraminotetrazole: Secondary Explosives with Low Sensitivities, *Inorg. Chem.* **2011**, 50, 1447–1458.
9. N. Fischer, T. M. Klapötke, J. Stierstorfer, Calcium 5-nitriminotetrazolate – A Green Replacement for Lead Azide in Priming Charges, *J. Energetic Mater.* **2011**, 29(1), 61–74.
10. N. Fischer, T. M. Klapötke, J. Stierstorfer, Energetic Nitrogen-Rich Salts of 1-(2-Hydroxyethyl)-5-nitriminotetrazole, *Eur. J. Inorg. Chem.* **2011**, 4471–4480.

11. N. Fischer, T. M. Klapötke, J. Stierstorfer, Explosives Based on Diaminourea, *Propellants Explos. Pyrotech.* **2011**, 36, 225–232.
12. N. Fischer, T. M. Klapötke, J. Stierstorfer, Hydrazinium Nitriminotetrazolates, *Z. Anorg. Allg. Chem.* **2011**, 637, 1273–1276.
13. N. Fischer, T. M. Klapötke, Kristina Peters, Magdalena Rusan, J. Stierstorfer, Alkaline Earth Metal Salts of 5,5'-Bistetrazole – from Academical Interest to Practical Application, *Z. Anorg. Allg. Chem.* **2011**, 637, 1693–1701.
14. N. Fischer, T. M. Klapötke, J. Stierstorfer, C. Wiedemann, 1-Nitratoethyl-5-nitriminotetrazole derivatives – Shaping future high explosives, *Polyhedron* **2011**, 30(14), 2374–2386.
15. N. Fischer, T. M. Klapötke, J. Stierstorfer, The Hydroxylammonium Cation in Tetrazole based Energetic Materials, *New Trends in Research of Energetic Materials, Proceedings of the Seminar, 14th*, Pardubice, Czech Republic **2011**, 1, 127–155.
16. M. Boehm, D. Fischer, N. Fischer, T. M. Klapötke, S. Scheutzow, J. Stierstorfer, Experimentally determined Detonation Velocities of new Secondary Explosives, *New Trends in Research of Energetic Materials, Proceedings of the Seminar, 14th*, Pardubice, Czech Republic **2011**, 2, 512–520.
17. N. Fischer, T. M. Klapötke, J. Stierstorfer, E. N. Wiedemann, Highly sensitive 3,5-diazidotriazole and the binary $C_2N_9^-$ anion, *New Trends in Research of Energetic Materials, Proceedings of the Seminar, 14th*, Pardubice, Czech Republic **2011**, 2, 636–645.
18. N. Fischer, D. Izsak, T. M. Klapötke, S. Rappenglück, J. Stierstorfer, Nitrogen-Rich 5,5'-Bistetrazolates and their Potential Use in Propellant Systems: A Comprehensive Study, *Chem. Eur. J.* **2012**, 18(13), 4051–4062.
19. N. Fischer, T. M. Klapötke, D. Piercey, J. Stierstorfer, Hydroxylammonium 5-Nitriminotetrazolates, *Z. Anorg. Allg. Chem.* **2012**, 638, 302–310.
20. N. Fischer, E. D. Goddard-Borger, R. Greiner, T. M. Klapötke, B. W. Skelton, J. Stierstorfer, Sensitivities of Some Imidazole-1-sulfonyl Azide Salts, *J. Org. Chem.* **2012**, 77, 1760–1764.
21. N. Fischer, K. Hüll, T. M. Klapötke, J. Stierstorfer, G. Laus, M. Hummel, C. Froschauer, K. Wurst, H. Schottenberger, 5,5'-Azoxytetrazolates – a new nitrogen-rich dianion and its comparison to 5,5'-azotetrazolate, *Dalton Trans.* **2012**, 41(36), 11201–11211.
22. N. Fischer, D. Fischer, T. M. Klapötke, D. G. Piercey, J. Stierstorfer, Pushing the limits of energetic materials – the synthesis and characterization of dihydroxylammonium 5,5'-bistetrazole-1,1'-diolate, *J. Mater. Chem.* **2012**, 22, 20418–20422.

23. N. Fischer, T. M. Klapötke, J. Stierstorfer, 1-Amino-3-nitroguanidine (ANQ) in High performance Ionic Energetic Materials, *Z. Naturforsch. B* **2012**, 67(6), 573–588.
24. N. Fischer, T. M. Klapötke, J. Stierstorfer, V. Kahlenberg, G. Laus, H. Schottenberger, K. Wurst, Synthesis and Crystal Structures of New 5,5'-azotetrazolates, *Crystals* **2012**, 2, 127–136.
25. N. Fischer, T. M. Klapötke, K. Lux, F. A. Martin, J. Stierstorfer, Inorganic Amino-Nitro-Guanidinium Derivatives, *Crystals* **2012**, 2, 675–689.
26. N. Fischer, T. M. Klapötke, J. Stierstorfer, TKX50 – The revolution in RDX-replacements, *New Trends in Research of Energetic Materials, Proceedings of the Seminar*, 15th, Pardubice, Czech Republic **2012**, 1, 130–141.
27. N. Fischer, T. M. Klapötke, S. Rappenglück, J. Stierstorfer, The Reactivity of 5-Cyanotetrazole towards Water and Hydroxylamine, *Chempluschem* **2012**, 77(10), 877–888.
28. N. Fischer, K. Hüll, T. M. Klapötke, J. Stierstorfer, Synthesis and Characterization of the New Heterocycle 5-(4-Amino-1,2,4-triazol-3-on-5'-yl)-1*H*-tetrazole and Some Ionic Nitrogen-rich Derivatives, *J. Heterocycl. Chem.* **2012**, in press.
29. N. Fischer, T. M. Klapötke, M. Reymann, J. Stierstorfer, Nitrogen-Rich Salts of 5,5'-Bis(1-hydroxytetrazole) – Energetic Materials Combining Low Sensitivities with High Thermal Stability, *Eur. J. Inorg. Chem.* **2012**, in press.
30. N. Fischer, M. Joas, T. M. Klapötke, J. Stierstorfer, T. Stürzer, Transition metal complexes of 3-amino-1-nitroguanidine as laser ignitable primary explosives – structures and properties, *Inorg. Chem.* **2012**, submitted.
31. N. Fischer, L. Gao, T. M. Klapötke, J. Stierstorfer, Nitrogen-rich Salts of 5,5'-Bis(tetrazole-2-oxide) in a Comparison to 5,5'-Bis(tetrazole-1-oxide) Derivatives, *Polyhedron* **2012**, submitted.
32. N. Fischer, T. M. Klapötke, S. Marchner, M. Rusan, S. Scheutzwow, J. Stierstorfer, A Selection of Alkali and Alkaline Earth Metal Salts of 5,5'-Bis(1-hydroxytetrazole)le in Pyrotechnic Compositions, *Propellants Explos. Pyrotech.* **2012**, in press.

Oral Presentations

1. N. Fischer, Energetic Materials based on 1-amino-3-nitroguanidine, 13th NTREM conference, Pardubice, Czech Republic, **2010**.
2. N. Fischer, The Hydroxylammonium Cation in Tetrazole based Energetic Materials, 14th NTREM conference, Pardubice, Czech Republic, **2011**.

3. N. Fischer, TKX50 – The Revolution in RDX Replacements ? , 15th NTREM conference, Pardubice, Czech Republic, **2012**.

Poster Presentations

1. N. Fischer, T. M. Klapötke, J. Stierstorfer, Salts of 2-methyl-5-nitraminotetrazole, 13th NTREM Conference, Pardubice, Czech Republic, **2010**.
2. N. Fischer, T. M. Klapötke, J. Stierstorfer, K. R. Tarantik, 1-Nitratoethyl-5-nitriminotetrazole Derivatives - Shaping Future High Explosives, 13th NTREM Conference, Pardubice, Czech Republic, **2010**.
3. M. Boehm, N. Fischer, D. Fischer, T. M. Klapötke, S. Scheutzow, J. Stierstorfer, Experimentally determined Detonation Velocities of new Secondary Explosives, 14th NTREM Conference, Pardubice, Czech Republic, **2011**.
4. N. Fischer, T. M. Klapötke, J. Stierstorfer, E. N. Wiedemann, Highly sensitive 3,5-Diazidotriazole and the binary $C_2N_9^-$ anion, 14th NTREM Conference, Pardubice, Czech Republic, **2011**.

Awards

1. Award for great oral presentation, 13th conference in Pardubice, Czech Republic, *New Trends in Research of Energetic Materials*, **2010**.
2. Römer price of the “Dr. Klaus Römer foundation” at the Ludwig-Maximilian University Munich for excellent scientific results in chemistry and biochemistry, **2010**.

Patents

1. N. Fischer, D. Fischer, T. M. Klapötke, D. G. Piercey, M. Reymann, J. Stierstorfer, Patentanmeldung, DE 10 2011 081 254.7, Energetische Wirkmasse umfassend ein Dihydroxylammoniumsalz oder Diammoniumsalz des 5,5'-Bistetrazole-1,1'-diols, 5,5'-Bistetrazole-2,2'-diols, 5,5'-Bistetrazole-1,2'-diols oder einer Mischung daraus.